Symposium 7: Protein and Cellular Mechanics

1097-Symp
How Mechanical Forces Can Switch On and Off Protein and Cell Binding Sites
Viola Vogel.
Inst Bio Oriented Mat, Zurich, Switzerland.
How do cells sense whether proteins are stretched or relaxed? While mounting evidence exists that cells and tissues sense mechanical stimuli and convert them into biochemical signals, knowledge about the underpinning mechanisms is sparse. A multitude of structural mechanisms have evolved among extracellular and cytoplasmic proteins that are part of force-bearing protein networks, each enabling distinct modes of mechano-chemical signal conversion. The structural motives include designs by which force can destroy recognitions sites, or alternatively open up cryptic sites that can then recruit other proteins in a force-upregulated manner. Here we will discuss how the stretching of fibronectin fibers, which form the most extensible protein fibers known so far, can activate or destroy protein and cell binding sites over a wide range of mechanical strains. Stretching of fibronectin fibers thus not only increases their Young's moduli, over orders of magnitude until they rupture when stretched to a few MPa, but their biochemical display is altered in intricate ways as well. Deciphering the underlying engineering design principles by which extracellular matrix proteins can serve as mechano-chemical signalling switches is not only essential to learn how cells sense and respond to mechanical forces, and probe the physical properties of their environments. It has far reaching implications in tissue engineering, systems biology and medicine.

1098-Symp
Nanoscale Protein Architecture of Focal Adhesions
Pakorn Kanchanawong[1], Gleb Shtengle[2], Erika B. Ramko[3], Michael W. Davidson[3], Harald F. Hess[2], **Clare Waterman[1]**.
[1]NHLBI, NIH, Bethesda, MD, USA, [2]Janelia Farm HHMI, Ashburn, VA, USA, [3]National High Magnetic Field Laboratory, The Florida State University, Talahassee, FL, USA.
Focal adhesions (FAs) mediate cell interactions with their extracellular matrices (ECMs) and consist of integrin ECM receptors linked to the actin cytoskeleton via plasma-membrane-associated protein plaques. Despite their fundamental importance in multicellular organisms, the three-dimensional organization of proteins within FAs is unknown. Here we determine FA molecular architecture by using 3D superresolution microscopy (interferometric Photo-Activated Localization Microscopy) to map nanoscale protein organization. We find that the FAs consist of partially overlapping proteinspecific vertical layers of 15-50 nm thickness, with integrins and actin separated by a 30-50 nm FA core which is spanned by talin tethers. This reveals a structural basis for FA function whereby a multilaminar core architecture mediates the interdependent cell processes of adhesion, signaling, force transduction, and actin cytoskeletal regulation.

1099-Symp
Force Probing the Molecular Mechanics of Cell Rounding
Daniel J. Mueller[1], Martin P. Stewart[2], Jonne Helenius[2], Yusuke Toyoda[3], Subramaniam P. Rmanathan[2], Anthony A. Hyman[3].
[1]Biotec Der TU Dresen, Dresden, Germany, [2]Biotechnology Center, TU Dresen, Dresden, Germany, [3]Max-Planck-Institute of Molecular Cell Biology and Genetics, Dresden, Germany.
During mitosis tissue culture cells undergo a dramatic shape change, from essentially flat to nearly spherical. The forces and mechanisms that drive this shape change remain unexplained. Here we use assays based on atomic force microscopy to measure the height and rounding force of single mitotic cells. We show that under our conditions, human cells exert forces approaching 100 nN when they round up. The force depends not only on the actomyosin cortex but also on trans-membrane ion gradients. In further experiments we demonstrate which membrane proteins are coupled to and regulated by the actomyosin cortex to establish a hydrostatic pressure that rounds up the cell. By using single-molecule force spectroscopy we look inside these individual membrane proteins to quantify by which interactions and mechanisms they are functionally regulated. Based on these results we introduce an advanced model of cell rounding in which a hydrostatic outward pressure, and contractile actomyosin cortex forces govern shape.

1100-Symp
Regulation of Mechanical Equilibrium in Multicellular Arrangements
Qingzong Tseng[1], Alexandre Deshieres[2], Hervé Guillou[3], Odile Filhol-Cochet[2], **Manuel Thery[1]**.
[1]Physics of the Cytoskeleton and Morphogenesis / iRTSV / CEA, Grenoble, France, [2]Signal Transduction / iRTSV / CEA, Grenoble, France, [3]Institut Neel, Grenoble, France.
We investigated the physical laws governing the mechanical equilibrium of multi-cellular arrangements. Breaking and maintaining this equilibrium are the fundamental basis for embryonic morphogenesis and tissue homeostasis. It notably plays a key role in epithelium-mesenchymal transition (EMT) during normal development and tumor transformation. Since multi-cellular equilibrium relies on a spatial regulation of the force balance between cell-cell and cell-extra cellular matrix (ECM) adhesions, we studied human epithelial cell pairs confined on defined ECM micro-patterns geometries. We developed an automated tracking method to quantify the cell movements in high throughput time-lapse acquisitions. We found that cell pairs could adopt different behaviors depending on pattern geometries. A complete survey over many different geometries showed that cells adopted all graded phenotypes from continuous cell migration to static mechanical equilibrium. After induced EMT the stability of cell pair configuration was affected.
We used cytoskeleton observations and physical modeling to identify the physical parameters implicated in the establishment of mechanical equilibrium. Current physical models of multi-cellular equilibrium, which consider a constant line tension along the perimeter, surface tension of the membrane and adhesion energies could not account for spatial arrangements we observed. Immuno-fluorescent labellings and in vivo expression of actin marker revealed three types of actin cables: cables above adhesive regions connecting two ECM adhesion sites and cables above non adhesive regions connecting either two ECM adhesion sites or one ECM and one cell-cell adhesion site. Preliminary nano-ablation experiments to severe actin cables suggested that tension could vary in each type of cable. It seems that cells develop an anisotropic distribution of line tension in response to local adhesiveness. We currently investigate with experimental and numerical approaches whether anisotropic distribution of tension could be the regulator of the spatial arrangement we observed in various microenvironment geometries.

Symposium 8: Structure and Dynamics of Membrane Transporters

1101-Symp
A Dynamical View of Membrane Transporter Function at Sub-Angstrom Resolution
Emad Tajkhorshid.
University of Illinois at Urbana-Champaign, Urbana, IL, USA.
Membrane transporters provide the main mechanism for active exchange of materials between the cytoplasm and a cell's environment in a highly selective manner. These complex molecular machines present a structurally diverse group of pumps evolved to efficiently couple various sources of cellular energy to the selective transport of different molecules. Depending on the source of energy used and the type of the substrate transported, different protein architectures and, thus, different mechanisms are employed by membrane transporters. Active transporters undergo various degrees of protein conformational changes (induced, e.g., by ATP hydrolysis or by binding of the substrate and the co-transported ions) during their transport cycle. In other words, they adopt distinct conformational states during their function. Due to the difficulties associated with structure determination of membrane proteins, however, for the majority of structurally-known transporters only one of the major functional states has been structurally characterized. Substrate binding and translocation along the transport pathway in membrane transporters are closely coupled to numerous stepwise protein conformational changes of various magnitudes and forms that are induced by and/or coordinated with the energy-providing mechanisms. A detailed description of the mechanism of membrane transporters, therefore, relies on high-resolution methodologies that can describe the dynamics of the process at an atomic level. In this talk, latest results of molecular dynamics simulations performed on a number of membrane transporters with diverse mechanisms, and the molecular events involved in their function revealed by these simulations will be presented.

1102-Symp
Ion Transport by the Sodium Pump
Hanne Poulsen.
University of Aarhus, Aarhus C, Denmark.
The first crystal structure of the Na^+,K^+-ATPase revealed the potassium-bound form of the pig kidney enzyme at 3.5 Å resolution. This large membrane protein complex consists of an alpha subunit similar to the Ca^{2+}-ATPase, a heavily glycosylated beta subunit and a small regulatory gamma subunit (also known as FXYD2). The electrogenic transport performed by the Na^+,K^+-ATPase causes extrusion of three sodium ions and uptake of two potassium ions per ATP split. The gradients thus formed are of fundamental importance in physiology as they

control ionic conditions in the cell and energise osmotic potentials, secondary transport schemes and ionotropic signalling.
A surprising finding from the Na+,K+-ATPase structure was the docking of two conserved tyrosine residues at the C-terminus of the alpha subunit into the transmembrane domain, hinting that this was a previously unidentified regulatory element. Several mutations causing human neurological syndromes have subsequently been mapped to the C-terminal structure element, also clearly indicating that conservation of the structure is important for pump function.
Mutational analysis confirmed this and prompted our further analysis by electrophysiology and molecular dynamics simulations, which have shown a profound effect of the C-terminus on the electrogenic transport properties. We further propose that the C-terminal region forms a binding pocket that can be exploited for pharmacological intervention in cardiovascular and neurological disease.

1103-Symp
Alternating Access Mechanism of Glutamate Transporters
Olga Boudker.
Weill Cornell Med Coll, New York, NY, USA.
In the central nervous system, glutamate transporters are responsible for the glutamate clearance following rounds of neurotransmission. They are molecular pumps, which utilizes the energy of pre-existing electrochemical gradients of ions to drive substrate uptake against steep concentration gradients. Sodium coupled aspartate transporter from Pyrococcus horikoshii, GltPh, is a homologue of the mammalian transporters and has served as a model system, within which to understand the molecular details of transport. The previously determined crystal structures of GltPh revealed the substrate and sodium binding sites located near the extracellular solution leaving the question of how they reach the cytoplasm unanswered. Recently, we have determined the crystal structure of a double cysteine mutant of GltPh, captured by cross-linking in a novel conformational state. In this state the substrate-binding sites are near the cytoplasmic surface of the protein. These findings suggest a novel and unexpected mechanism, by which GltPh and, by analogy mammalian glutamate transporters catalyze trans-membrane transport of their substrates.

1104-Symp
Alternating Access of the Maltose Transporter
Jue Chen.
Purdue Univ, West Lafayette, IN, USA.
No Abstract.

Platform R: Channel Regulation & Modulation

1105-Plat
Photopharmacology: Controlling Native Voltage-Gated Ion Channels with Light
Alexandre Mourot[1], Timm Fehrentz[1], Michael Kienzler[2], Ivan Tochitsky[1], Matthew R. Banghart[3], Dirk Trauner[2], Richard H. Kramer[1].
[1]University of California Berkeley, Berkeley, CA, USA, [2]University of Munich, Munich, Germany, [3]Harvard Medical Schoo, Boston, MA, USA.
Optical control of proteins provides critical advantages for studying cell signaling and offers great promise in biotechnology and biomedical research. We have developed a series of photochromic ligands (PCLs) that target voltage-gated ion channels. They possess an azobenzene photoswitch connected on one side to a quaternary ammonium ligand (internal blocker for potassium, sodium and calcium channels) and on the other side to a variety of chemical groups. The azobenzene photoisomerizes between cis and trans configurations using different wavelengths of light, thereby repetitively turning on and off ion flow.
Alteration of the R group makes our approach very modular. First, increasing hydrophobicity allows better membrane penetration and therefore greater potency of the PCL. Second, PCLs with a charged R group require hydrophilic pathways to cross cell membranes and can be specifically targeted to cells expressing entry-route proteins. Third, selectivity for certain ion channels can be attained, allowing a more precise control over cellular excitability. Fourth, some PCLs act as cis blockers, offering the advantage of being silent in the dark. Finally, modifying the R group can be used to tune the spectral characteristics of the PCL, with potential interest for vision restoration.

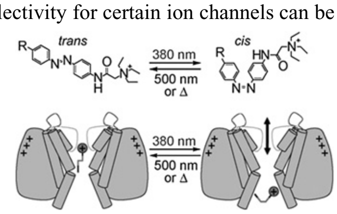

1106-Plat
Receptor and Subunit Specificity in AKAP79/150 Actions On M-Type(KCNQ) K^+ Channels
Jie Zhang, Oleg Zaika, Manjot Bal, Mark Shapiro.
UTHSCSA, San Antonio, TX, USA.
A-kinase-anchoring protein (AKAP)79/150 mediated PKC phosphorylation of M-type (KCNQ) channels is involved in M current (I_M) suppression by muscarinic M_1, but not bradykinin B_2 receptors (Hoshi *et al.* Nat. Cell Biol. 7:1066-73). In this study, we first explored the involvement of AKAP79/150 in muscarinic suppression of KCNQ currents by co-transfecting AKAP79 with KCNQ1-5 subunits in CHO cells stably expressing M_1 receptors. Expression of AKAP79 sensitized KCNQ2-5 and KCNQ2/3, but not KCNQ1, channels to suppression by the M_1 receptor agonist oxotremorine (oxo-M). Mutation of the PKC phosphorylation site on KCNQ4 (T553A) eliminated the effect of AKAP79, confirming the role of PKC. Co-transfection of wild-type, but not dominant negative, calmodulin abolished the effect of AKAP79 on KCNQ2/3 channels. We asked if purinergic and angiotensin suppression of I_M in superior cervical ganglion (SCG) sympathetic neurons involves AKAP79/150, since purinergic P2Y receptors depress I_M in SCG neurons via a similar mechanism to that of bradykinin, involving IP_3-mediated Ca^{2+} signals, whereas angiotensin AT_1 receptors depress I_M via a similar mechanism as M_1 receptors, by depletion of PIP_2. Transfection of ΔA-AKAP79, which lacks the A-domain necessary for PKC binding, did not affect I_M suppression by the purinergic agonist UTP (2 μM), nor by bradykinin (100 nM), but did reduce I_M suppression by oxo-M (1 μM) and angiotensin II (500 nM). We also tested association of AKAP79 with M_1, B_2, $P2Y_6$ and AT_1 receptors via FRET experiments on CHO cells under TIRF microscopy, which revealed weaker FRET between AKAP79 and $P2Y_6$ or B_2 receptors than for M_1 and AT_1 receptors. Our data suggest AKAP79/150 action generalizes to KCNQ2-5 subtypes, is disrupted by calmodulin, and is involved in angiotensin, but not in purinergic, suppression of neuronal M current. Supported by NIH grants R01 NS043394 and R01 NS065138.

1107-Plat
Potassium Channel Modulation by A Toxin Domain in Matrix Metalloprotease 23
Srikant Rangaraju[1], Keith Khoo[2], Zhiping Feng[2], George Crossley[3], Daniel Nugent[4], Ilya Khaytin[4], Michael Pennington[4], Raymond Norton[5], **K. George Chandy**[1].
[1]University of California Irvine, Irvine, CA, USA, [2]Walter and Eliza Hall Institute of Medical Research, Parkville, Victoria, Australia, Parkville, Australia, [3]Bachem Bioscience Inc., 3700 Horizon Dr., King of Prussia, PA, USA, [4]Bachem Bioscience Inc., King of Prussia, PA, USA, [5]Walter and Eliza Hall Institute of Medical Research, Parkville, Australia.
Peptide toxins found in a wide array of venoms block K+ channels causing profound physiological and pathological effects. Here, we describe the first functional K+ channel-blocking toxin domain in a mammalian protein. Matrix metalloprotease 23 (MMP23) contains a domain (MMP23TxD) that is evolutionarily related to peptide toxins from sea anemones. MMP23TxD shows close structural similarity to the sea anemone toxins BgK and ShK, and the domain blocks K+ channels in the nanomolar to low micromolar range (Kv1.6 > Kv1.3 > Kv1.1 = Kv3.2 > Kv1.4 in decreasing order of potency), while sparing other K+ channels (Kv1.2, Kv1.5, Kv1.7, KCa3.1). Full-length MMP23 suppresses K+ channels with a pattern of inhibition consistent with MMP23TxD activity. Our results provide clues to the structure and function of the vast family of proteins that contain domains related to sea anemone toxins. Evolutionary pressure to maintain a channel-modulatory function may contribute to the conservation of this domain throughout the plant and animal kingdom.

1108-Plat
Differential Redox Regulation of ORAI Channels: A Mechanism to Tune T-Cell Responses
Ivan Bogeski[1], Carsten Kummerow[1], Dalia Al-Ansary[1], Richard Koehler[1], Eva C. Schwarz[1], Daisuke Kozai[2], Nobuaki Takahashi[2], Christine Peinelt[1], Desiree Griesemer[1], Monika Bozem[1], Yasuo Mori[2], Markus Hoth[1], Barbara A. Niemeyer[1].
[1]Biophysics, Homburg, Germany, [2]Synthetic Chemistry and Biological Chemistry, Kyoto, Japan.
Phagocytes play an essential role in host defence against pathogens by generating reactive oxygen species (ROS). Effector T helper (Th) cells migrating to sites of infection will be exposed to this highly oxidative environment. Here we show how Th-cells respond and adapt to ROS. Oxidation affects different Ca^{2+}-signalling pathways essential for T-cell function. ORAI1 channels are inhibited with an IC_{50} of ~40 μM H_2O_2, but ORAI3 channels are insensitive. We identify cysteine (C195) of ORAI1, absent in ORAI3, as the major redox

sensor. A reduced sensitivity of effector Th-cells towards oxidation is due to upregulation of Orai3 and of cytosolic antioxidants. The differential redox regulation of ORAI channels is a novel mechanism to tune Th-cell based immune responses during clonal expansion and inflammation.

1109-Plat

Comparative Analysis of Cholesterol Sensitivity of Kir Channels: Role of the Cytoplasmic Domain

Avia Rosenhouse-Dantsker[1], Edgar Leal-Pinto[2], Diomedes E. Logothetis[2], Irena Levitan[1].
[1]University of Illinois at Chicago, Chicago, IL, USA, [2]Virginia Commonwealth University, Richmond, VA, USA.

Kir channels are important in setting the resting membrane potential and modulating membrane excitability. A common feature of Kir2 channels and several other ion channels that has emerged in recent years is that they are regulated by cholesterol, a major lipid component of the plasma membrane whose excess is associated with multiple pathological conditions. Yet, the mechanism by which cholesterol affects channel function is not clear.
Here we show that in addition to Kir2 channels, members of other Kir subfamilies are also regulated by cholesterol. Interestingly, while similarly to Kir2 channels, several Kir channels are suppressed by an increase in membrane cholesterol, the function of others is enhanced following cholesterol enrichment. Furthermore, similarly to Kir2.1, and independent of the impact of cholesterol on channel function, we find that mutation of residues in the CD loop affect cholesterol sensitivity of Kir channels.
Among Kir2.1 CD loop residues, we have recently shown that the L222I mutation has the strongest effect on cholesterol sensitivity. This result is surprising since Kir2.2, which is as cholesterol sensitive as Kir2.1, already has an isoleucine at the corresponding position. Here we obtain further insight regarding the role of the cytosolic domain of Kir2 channels by examining mutations in adjacent cytosolic regions that also lead to loss of cholesterol sensitivity. In addition, we trace the source of the difference between Kir2.1 and Kir2.2 to a residue in the EF loop, N251, whose mutation to an aspartate reverses the effect of the L222I residue, and restores cholesterol sensitivity.
These findings suggest an indirect role of the cytosolic domain of Kir channels in regulating the effect of cholesterol on channel function and provide insight into the structural determinants of their gating mechanism.

1110-Plat

Molecular Mapping of An I_{KS} Channel Opener Reveals Crucial Interactions Between KCNE1 and the Kv7.1 Voltage Sensor Paddle

Yoni Haitin, Nataly Menaker, Simona Shats, Asher Peretz, **Bernard Attali**.
Sackler Medical School, Tel Aviv University, TelAviv, Israel.

Voltage-gated K^+ channels co-assemble with accessory subunits to form macromolecular complexes. In heart, assembly of Kv7.1 pore-forming subunits with KCNE1 auxiliary subunits generates the repolarizing K^+ current I_{KS}. We and others, recently suggested a strategic location of KCNE1 wedged close to helices S1 and S4 of two adjacent Kv7.1 voltage sensing domains (VSD) and nearby helix S6 of another Kv7.1 subunit. Here we show that the I_{KS} channel opener, diisothiocyanostilbene-2',2'-disulfonic acid (DIDS) acts on I_{KS} as a gating-modifier, thereby converting the time- and voltage-dependent channels into almost voltage- and time-independent currents. While DIDS activates Kv7.1, it does not affect Kv7.2. The two isothiocyanate functionalities are crucial for the potent activating effect of DIDS on $I_{KS,}$ since 4'-acetamido-4'-isothiocyanostilbene-2',2'-disulfonic acid (SITS) that has only one of these groups and 4,4'-dinitrostilbene-2,2'-disulfonic acid (DNDS), which lacks isothiocyanate groups and thus cannot form covalent bonds with amino acids, do not activate I_{KS} currents. Mutagenesis and modeling data indicate that DIDS activates I_{KS} by docking to an externally-accessible pocket, formed at the interface between the superficial N-terminal boundary of the KCNE1 transmembrane segment and the VSD paddle motif of Kv7.1. DIDS does not activate the channel complex formed by co-expression of KCNE1 and a chimeric Kv7.1 endowed with a Kv7.2 VSD paddle. DIDS binding at the Kv7.1 VSD-KCNE1 interface reveals that two lysine residues, K41 in KCNE1 and K218 in Kv7.1 S3-S4 linker are distant to about 10 [[Unable to Display Character: Å]]. Thus, KCNE1 affects Kv7.1 channel gating by closely interacting with the VSD paddle motif.

1111-Plat

Kv Channel Modulation: Closed State Block of Benzocaine But Not of Bupivacaine

Johanna Nilsson[1], Michael Madeja[2], Kristoffer Sahlholm[3], Peter Arhem[1].
[1]Dept of Neurosci., Karolinska Institutet, Stockholm, Sweden, [2]Dept of Physiol, Munster University, Munster, Germany, [3]Dept. of Neurosci., Karolinska Institutet, Stockholm, Sweden.

Local anaesthetics (LAs) block action potentials mainly by blocking Na channels. They are generally assumed to preferentially bind to channels in inactivated and/or open state. Recently it has been suggested that they mainly bind to channels in intermediate closed states. This is based on the finding that LAs affect the currents time and voltage-dependently in voltage clamped channels; that they reduce the peak current more at low voltage steps than at high.
In previous studies on inactivating K channels we have concluded that LAs preferentially bind to channels in open state. In the present study we have reanalysed the effects of LAs on K channels with special reference to the new findings of closed state binding. We analysed the effects of bupivacaine and benzocaine on Kv3.1 and Shaker channels expressed in Xenopus oocytes. As shown previously bupivacaine induces a peaked current in both channel types. In accordance with the results on the Na currents bupivacaine reduced the peak less at +60 mV than at lower potentials. Nevertheless, a modelling analysis suggested that the results are explained by binding preferentially to open channels. In contrast, benzocaine did not induce a peak at any potential, but the early current was reduced more at low potentials than at high. The modelling analysis suggested that the effect is caused by binding to closed and open channels.
We thus conclude that bupivacaine and benzocaine blocks K channels differently; bupivaciane open state-dependently and benzocaine both open and closed state-dependently. We also conclude that a time and voltage-dependent block, similar to that reported for Na channels, with less inhibition of the peak current at high potentials than at low potentials, does not necessarily imply binding of channels in a closed state.

1112-Plat

Introducing Drug Action into Single-Cell Cardiac Models

Louise Dyson, Denis Noble, David Gavaghan, Anna Sher.
University of Oxford, Oxford, United Kingdom.

Drug development failures due to adverse cardiac effects cost the drugs industry millions of dollars every year. Many of these failures may be predicted through mathematical modelling of drug actions. In order to achieve this it is necessary to investigate the effectiveness of different ways of incorporating drug action into models. Five different single-cell cardiac models are studied with and without drug action. These comprise two rabbit models (Mahajan *et al.*, 2008; Shannon *et al.*, 2004) and three other species (ten Tusscher and Panfilov, 2006; Hinch *et al.*, 2004; Faber *et al.*, 2007). The L-type calcium channel regulation properties of the different models are compared, and their calcium-dependent and voltage-dependent inactivation properties are considered. It is found that the different models respond in very different ways to the introduction of drug action through a simple pore block with none of the models successfully reproducing experimental results for both drugs that are considered. It is therefore concluded that the kinetics of drug action on active and inactive channels must be included to better model the drug action. The differing responses of the models at different pacing frequencies and drug doses indicate that it is necessary to perform experiments at a range of frequencies and drug concentrations.

Platform S: Imaging & Optical Microscopy I

1113-Plat

Telomeres Diffusion Study Implies on A Self-Organization Mechanism of the Genome in the Nucleus

Irena Bronshtein[1], Yonatan Israel[1], Eldad Kepten[1], Sabine Mai[2], Yaron Shav-Tal[3], Eli Barkai[1], **Yuval Garini**[1].
[1]Physics Department, Bar Ilan University, Ramat Gan, Israel, [2]Manitoba Institute of Cell Biology, CancerCare Manitoba, University of Manitoba, Winnipeg, MB, Canada, [3]The Mina & Everard Goodman Faculty of Life Sciences, Bar Ilan University, Ramat Gan, Israel.

The human genome contains tens of thousands of genes that are organized in chromosomes and packed in the nucleus of the cell. How can the chromosomes and DNA stay organized in territories without any compartmentalization? This order is sustained throughout the life cycle of a cell, a property that emerges as a key contributor to genome function, though its full extent is not yet known.
To address this question, we studied fluorescently-labeled telomeres diffusion in a broad time range of 10^{-2} - 10^{4} seconds by combining a few microscopy methods followed by comprehensive diffusion analysis [1]. We found that the telomeres follow a complex diffusion pattern never reported before. The diffusion of the telomeres was found to be anomalous (subdiffusive) at short time scales and it changes to normal diffusion at longer times.
The transient diffusion indicates that telomeres are subject to a local binding mechanism with a wide but finite time distribution.
We therefore suggest that local temporal binding mechanism leads to the maintenance of structures and positions in the nucleus without the need for actual

compartments. Such a mechanism has another advantage by providing flexibility. If telomere binding is switched off (e.g., by shortening the binding time), this will allow the nucleus to undergo architectural changes.

[1] I. Bronstein, Y. Israel, E. Kepten, S. Mai, Y. Shav-Tal, E. Barkai and Y. Garini, Transient anomalous diffusion of telomeres in the nucleus of mammalian cells. Physical Review Letters **103**, 018102 (2009).

1114-Plat
Mapping Neuronal Connectivity Using Stochastic Optical Reconstruction Microscopy (Storm): The Brainstorm Project

Melike Lakadamyali, Mark Bates, Hazen Babcock, Jeff Lichtman, Xiaowei Zhuang.
Harvard University, Cambridge, MA, USA.

The human brain is a highly sophisticated circuit consisting of hundreds of billions of neurons that are interconnected by an even larger number of synapses. This dense network of neurons and their connections holds key information to understanding normal brain function and perhaps what underlies its disorders. Obtaining a physical map of the brain's connectivity, however, is highly challenging due to the small size and high density of neuronal processes within a given volume. Therefore, in order to generate a map of neuronal connectivity a technique that can provide high spatial resolution and molecular specificity is needed.

We are using 3D multi-color stochastic optical reconstruction microscopy (STORM) in order to trace neuronal networks in culture at high spatial resolution. In order to capture an entire network of connections, we are using an automated, motorized piezo stage to image large areas in x-y ($\geq$ 120x120 μm) as well as in z ($\geq$ 2 μm). With this technique we can not only outline neuronal morphology at 30 μm lateral and 50 μm axial resolution, but we can also image synaptic content with high molecular specificity and identify synaptic connections. These techniques will be greatly useful for generating connectional maps of neurons in the mammalian brain and help obtain a physical understanding behind brain function.

1115-Plat
Monitoring the [ATP]/[ADP] Ratio in Beta-Cells During Glucose Stimulated Insulin Secretion Using the Genetically Encoded Fluorescent Reporter Perceval

Gert-Jan Kremers, Amicia D. Elliott, W. Steven Head, David W. Piston.
Vanderbilt University Medical Center, Nashville, TN, USA.

Pancreatic beta-cells secrete insulin in response to elevated blood glucose levels. Glucose stimulated insulin secretion depends on glucose metabolism that produces ATP. The resulting increase in [ATP]/[ADP] ratio closes ATP-sensitive potassium (KATP) channels, which leads to membrane depolarization and opening of voltage-dependent $Ca2+$ channels. This causes an elevation of intracellular free $Ca2+$ and insulin exocytosis. Insulin is secreted in a pulsatile manner, which is thought to be regulated in part by oscillations in glucose metabolism. Such metabolic oscillations would also lead to oscillations in the [ATP]/[ADP] ratio and hence regulate KATP channel activity.

Oscillations in [ATP]/[ADP] ratio have been demonstrated using biochemical and luciferase assays, but neither approach allows measurements of such oscillations in single cells. Perceval is a recently developed fluorescent protein biosensor for [ATP]/[ADP] ratio, and it permits direct measurement of [ATP]/[ADP] ratios inside living cells. We use Perceval in combination with quantitative confocal and two-photon excitation microscopy for direct measurement of the [ATP]/[ADP] ratio in beta-cells during glucose stimulated insulin secretion. For this purpose we have developed an adenoviral vector to express Perceval specifically in the beta-cells of intact mouse islets. Dynamic changes in [ATP]/[ADP] ratio can be correlated with glucose metabolism (by simultaneous imaging of Perceval fluorescence and NAD(P)H autofluorescence) and with intracellular free $Ca2+$ levels (by simultaneous imaging of Perceval fluorescence and the calcium sensor, FuraRed). This data allows us to test hypotheses regarding the role of localized subcellular signaling complexes and putative microdomains of glucose metabolism, [ATP]/[ADP] ratio, and $Ca2+$ dynamics in the regulation of glucose stimulated insulin secretion.

1116-Plat
Multiple Components Mapping of Live Tissue by Phasor Analysis of Fluorescence Lifetime Imaging

Chiara Stringari, Michelle Digman, Peter Donovan, Enrico Gratton.
University California Irvine, Irvine, CA, USA.

In fluorescence lifetime microscopy (FLIM) of live tissues a major issue is the assignment of autofluorescence to specific molecular components and their interactions within the physiological context. Here we use the phasor approach to fluorescence lifetime imaging to analyze complex decays in a live tissue. The tissues used were seminiferous tubules from the testes of wild type mice or mice expressing GFP from an Oct4 transgene. Lifetime images were acquired in the time domain and analytically transformed in the phasor representation. By examination of the clustering of the phasors we identified different molecular components: auto fluorescence, GFP, collagen and retinol. Each chemical species was identified and categorized by its specific location in the phasor plot. This phasor fingerprint reduces the importance of knowing the exact lifetime distribution of the fluorophores and emphasizes the contribution of the species to the signal. To better identify specific tissue components we also used spectral imaging and second harmonic generation microscopy. Linear combinations in the same pixel of molecular species were recognized and their relative fraction was calculated and mapped. The analysis of the fluorescence decay with higher harmonics of the phasor plot separates different molecular components that have the same location in the phasor plot at one harmonic but arise from different lifetime distributions. The phasor approach to lifetime imaging in live tissue provides a unique and straightforward method for interpreting complex decays in terms of molecular features by identifying fluorophores and obtaining functional maps of their relative concentration. This method has the potential to become a non invasive tool to characterize the local microenvironment and monitor differentiation and diseases in label-free live tissues. Work supported by NIH-P41 P41-RRO3155 and P50-GM076516, NIH RO1 HD49488, NIH PO1 HD47675, CIRM RC1-00110 PD.

1117-Plat
Ultra-High Resolution Imaging of the Dynamic Nature of Post-Synaptic Molecules

Deepak Nair, **Jean-Baptiste Sibarita**, Daniel Choquet.
Institut François Magendie - Université Bordeaux 2, Bordeaux, France.

The spatial and temporal regulation in the composition of the postsynaptic membrane of synapses participates in the different forms of synaptic plasticity that trigger the cellular processes of memory formation, consolidation, and retrieval. Neurotransmitter receptors move rapidly in and out of synapses by lateral diffusion. This mobility is crucial to control the number of receptors present at a given synapse. Thus, the equilibrium between the synaptic and extra synaptic AMPA receptor number is crucial in controlling basal transmission and synaptic plasticity. This balance is regulated by the subunit composition of these receptors and by the interaction of intracellular scaffold proteins. However, how the trafficking of receptors and the scaffolding molecules in and out synapse is controlled remains unknown. Here we attempt to determine the relative distribution and trafficking properties of AMPA receptors and various scaffold proteins at unprecedented spatial (< 40nm) and temporal resolution (>50 Hz) using a variety of novel ultra-high resolution fluorescence imaging approaches. We combine Single Particle Tracking (SPT) and Photo Activation Localization Microscopy (PALM) to map trajectories at the level of individual molecules. Here we describe the implementation of a multimodal microscope along with the development of a new dedicated analysis for single molecule segmentation and tracking. Furthermore we will discuss the application of SPT-PALM experiments on living neurons. With this novel approach, we expect to comprehend the motilities of receptors or scaffolding proteins when they traffic between the submicron sized molecular zones of dendritic spines. The combination of this type of detection and analysis will provide the information from thousands of discrete trajectories from a single cell with which it would be possible to appreciate finer details of versatile molecular mechanisms pertinent in the functioning of an excitatory synapse.

1118-Plat
Optical Recording of Electrical Activity of Cortical Layer 2/3 Pyramidal Neurons Using A Genetically-Encoded Voltage Probe

Walther Akemann, Hiroki Mutoh, Reiko Yoshida, Tomomi Shimogori, Thomas Knopfel.
RIKEN Brain Science Institute, Wako City, Japan.

Voltage-Sensitive Fluorescent Protein 2.3, VSFP2.3, is a genetically-encoded probe of membrane voltage using fluorescence resonance energy transfer (FRET) between a pair of cyan (CFP) and yellow (YFP) fluorescent proteins to convert voltage-activated motions of a voltage sensor domain from *Ciona intestinalis* voltage-sensitive phosphatase (Ci-VSP) into a differential voltage dependent fluorescence signal. To evaluate the utility of VSFP2.3 as a probe of electrical activity of neurons in intact brain tissue, we performed targeted whole cell current clamp and simultaneous optical recordings from L2/3 pyramidal

cells of the mouse cerebral cortex in acute brain slices. VSFP2.3 expression in neocortical cells was achieved by *in-utero* electroporation into the cortical ventricular zone at embryonic age 15.5 of a plasmid vector containing VSFP2.3 under the CAG hybrid promoter. This procedure resulted in strong VSFP2.3 fluorescence at postnatal age (up to day 30 tested) from a restricted cortical area, mostly within somato-sensory cortex, with the fluorescence originating from a clustered population of pyramidal neurons with cell bodies in layer 2/3. Electric current injection into VSFP2.3-positive cells (postnatal day 16-22) revealed an optical response signal to sub-threshold slow depolarization of the somatic membrane that could be resolved in single trials. While the optical signal in response to fast action potentials was noisy in single trials, S/N above two was obtained by event-triggered averaging over a few (5-10) action potentials. We also tested for the optical response to synaptically evoked EPSPs which were reliably detected at near threshold amplitudes in single trials. Our results provide the first demonstration of an optical readout of neuronal activity at cellular resolution using a genetically-targetable voltage probe in intact brain tissue *in-vitro*.

1119-Plat

Functional and Structural Characterization of A New Monomeric Far-Red Fluorescent Protein

Michael Z. Lin[1], Michael R. McKeown[2], Ho Leung Ng[3], Tom Alber[3], Roger Y. Tsien[2].

[1]Stanford University, Palo Alto, CA, USA, [2]University of California, San Diego, La Jolla, CA, USA, [3]University of California, Berkeley, Berkeley, CA, USA.

Fluorescent proteins have become valuable tools for biomedical research as protein tags, reporters of gene expression, biosensor components, and cell lineage tracers. However, applications of fluorescent proteins for deep tissue imaging have been constrained by the opacity of tissues to excitation light below 600 nm, due to absorbance by hemoglobin. Fluorescent proteins that excite efficiently in the "optical window" above 600 nm are therefore highly desirable. We report here the evolution of a far-red fluorescent protein with peak excitation at 600 nm and peak emission at 650 nm. This, Neptune, performs well in imaging deep tissues in living mice. The crystal structure of Neptune reveals novel mechanisms for red-shifting, including the acquisition of a new hydrogen bond with the chromophore. Neptune may serve as the basis for fluorescent indicators or FRET reporters that are more compatible with deep tissue imaging.

1120-Plat

Adaptive Phase Modulation for Multiphoton Microscopy

Rebecca M. Williams, Warren R. Zipfel.

Cornell University, Ithaca, NY, USA.

Tissue structures present index mismatches at a variety of spatial scales that can aberrate the focal volume and thus blur cellularly resolved multiphoton images acquired within biological tissues and live animals. We are investigating the extent to which adaptive phase modulation can be used to reconstruct the point-spread-function (PSF) and enable deeper and clearer multiphoton imaging into biological tissues. To do this, a Ti:Sapphire beam is reflected off of a reflective spatial light modulator conjugate to the objective pupil plane. The excitation PSF is directly imaged with a separate objective mounted perpendicular to the optic axis. We find that the fluorescence signal increases with increasing size of the scattering structures. Resolution degradation, however, reaches a maximum with scatterer spatial frequencies at one tenth of the maximal frequency allowed by the focusing objective NA. PSF aberrations from tissue structures can be somewhat compensated by modulating the phase at the back aperture using Zernike polynomials as a basis set for increasing overall image brightness. In this scheme two fitness measurements are required for each Zernike order. Initial results through tissue sections show that spherical aberration is a problem, but not the only problem. (Research supported by NIH/NCI R01 CA116583.)

Platform T: Muscle: Fiber & Molecular Mechanics & Structure II

1121-Plat

Relay Loop Stabilizes the Force-Generating Region in Myosin

Yuri E. Nesmelov[1], Roman V. Agafonov[2], Igor V. Negrashov[2], Sarah Blakely[2], Margaret A. Titus[2], David D. Thomas[2].

[1]University of North Carolina, Charlotte, NC, USA, [2]University of Minnesota, Minneapolis, MN, USA.

We have used transient time-resolved FRET (TR^2FRET) to monitor the conformation of the relay helix in a myosin II functional mutant during the recovery stroke in real time. Myosin was perturbed with the F506A mutation (*Dictyostelium discoideum* sequence), located within the relay loop in the force-generating region. F506 is a highly conserved residue in myosin II and is a hypertrophic cardiomyopathy mutation site. Previous studies [Tsiavaliaris, EMBO Rep, 2002, 3(11), 1099] showed a significant effect of the F506A mutation on myosin function. Actin affinity in the presence of ATP was increased, and the mutant did not move actin filaments in *in vitro* motility assays. A small decrease in intrinsic fluorescence was observed upon addition of excess ATP, but ATP binding and hydrolysis were not affected by the mutation. It was proposed that the F506A disrupts the communication between the active site and the lever arm. We engineered a double-Cys myosin mutant (A639C:K498C) in the Cys-less background with the F506A functional mutation, and labeled the mutant with optical probes. We used TR-FRET to determine the interprobe distance, and TR^2FRET measurements after rapid mixing with ATP revealed changes in the relay helix conformation during the recovery stroke in real time. The mutation induced significant disorder of the relay helix in the force-generating region, but myosin still produces a recovery stroke, changing the relay helix conformation from straight to bent. We conclude that (a) the relay helix is disordered in myosin functional mutant F506A, which demonstrates the importance of the relay loop - relay helix interaction in the relay helix stabilization, and (b) the relay helix is the major structural element in the force-generating region of myosin, responsible for communication from the active site to the converter domain and the lever arm.

1122-Plat

Converter Domain Residue R759 Interaction with Relay Loop Residue N509 in Drosophila Muscle Myosin is Critical for Motor Function, Myofibril Stability and Flight Ability

Girish C. Melkani, William A. Kronert, Anju Melkani, Sanford I. Bernstein.

Department of Biology, Molecular Biology and SDSU Heart Institute, San Diego State University, San Diego, CA, USA.

We used an integrative approach to probe the significance of the interaction between the relay loop and converter domain of Drosophila melanogaster skeletal muscle myosin. We generated a transgenic line expressing myosin with a mutation in the converter domain (R759E) at the relay loop interaction site. The mutation depresses calcium, basal or actin-activated MgATPase values (Vmax) by ~60% and actin sliding velocity ~35% compared to wild-type myosin. Ultrastructure of two-day-old adult fibers shows cracking and frayed myofibrils with some disruption of the myofilament lattice which becomes more severe in one-week-old adults. Flight ability is reduced in two-day-old flies compared to controls and is absent in 1-week-old adults. Thus appropriate interaction between the relay loop and converter domain is essential for normal motor function, myofibril stability and locomotion. To examine the specificity of this interaction, we used a compensatory mutational approach to attempt to restore the function of the R759E mutant myosin. Our modeling indicates that relay loop residues N509 and D511 interact with converter domain residue R759. To verify our model, we generated two transgenic lines that express R759E and either the N509K or D511K mutations. Interestingly, calcium, basal, and actin stimulated ATPase values are restored to 70% and actin sliding velocity is restored to 90% in N509K/R759E but not in D511K/R759E. Structurally fibers from 2-day or one-week -old adults appear morphologically normal in N509K/R759E and their flight ability is like wild type. However, D511K/R759E myofibrils do not show any improvement compared to R759E and flight ability is worse than R759E. Overall, our results reveal the critical interaction between the converter domain with relay loop residues and their role in myosin motor function and myofibril assembly/stability.

1123-Plat

Familial Hypertrophic Cardiomyopathy Mutations of the Myosin Regulatory Light Chain Remove Myosin Load Sensitivity

Michael J. Greenberg[1], Katarzyna Kazmierczak[2], Danuta Szczesna-Cordary[2], Jeffrey R. Moore[1].

[1]Boston University, Boston, MA, USA, [2]University of Miami Miller School of Medicine, Miami, FL, USA.

The myosin head domain consists of a globular head and an elongated alpha-helical neck region, the "lever arm", which undergoes large conformational changes during the ATPase cycle. This lever arm has been proposed to be part of the communication pathway transmitting external loads to the active site. Since the regulatory light chain (RLC) supports and imparts stiffness to the myosin lever arm, we hypothesized that alterations in the structure of the myosin heavy chain-RLC interaction could alter myosin load-dependent biochemistry.

Using modifications to the *in vitro* motility assay under unloaded and loaded conditions, we examined the biochemical properties of two RLC mutations that have been implicated in causing familial hypertrophic cardiomyopathy, N47K and R58Q. Myosin was purified from porcine ventricles carrying beta-MHC, and the native RLC was replaced with recombinant human wild type (WT) or mutant RLC. Our data show that under unloaded conditions, there are no differences between the mutant myosins and the WT. On the other hand, consistent with skinned fiber studies, we saw significant changes under loaded conditions, with both mutants showing reductions in isometric force, power output, and the load at which peak power occurs. We also see that both ATP and ADP affinity are load-dependent in the WT. Interestingly, our data suggests that cardiac myosin undergoes a load-dependent isomerization in the ADP bound state, similar to other "load sensing" myosins. Furthermore, we show that whereas WT shows a reduction in affinity for exogenously added ADP under loaded conditions, the mutants are relatively insensitive to load. Taken together these data demonstrate that mutations of the RLC change the load dependent kinetics of cardiac myosin, suggesting a role for the RLC in tuning load-dependent myosin mechanochemistry.

1124-Plat

Gravitational Force Spectroscopy Reveals Separation of Myosin Heads at the S1/S2 Hinge

James Dunn, Kathy Wang, Irene Cai, Nakiuda Hall, **Douglas D. Root**.
University of North Texas, Denton, TX, USA.

In order for striated muscle myosin to interact productively with thin filaments, it must both span the gap between thin and thick filaments and possess sufficient degrees of freedom to align its actin binding site with protomers of various helical orientations. This flexibility requires extensions and rotations of the coiled coil S2 domain of myosin including the S1/S2 hinge. To examine the ability of the coiled coil to separate, a novel gravitational force spectrometer was created that can apply femtonewton to piconewton forces with high accuracy to regions of a single myosin molecule defined by site-specific antibodies. Force-distance curves indicate that when the piconewton forces are applied perpendicular to the long axis of the S2 coiled coil at the S1/S2 hinge, the strands separate readily in a force dependent manner. However when similar levels of force are applied parallel to the long axis of the S2 coiled coil, there is much less extension. Computational force spectroscopy simulations on the atomic model of human S2 provided confirming results and with atomic resolution detail. As a control, simulations on scallop myosin S2 indicated that its coiled coil separates with less force than human S2 which is consistent with previously published reports. Furthermore, several familial hypertrophic cardiomyopathy causing mutations in the S1/S2 hinge were introduced into the human S2 simulations and resulted in further destabilization of its nanomechanical properties. These results indicate that the myosin S2 has intrinsic structural functions that may be independent of its interactions with other proteins. It is possible that interactions with myosin binding proteins may modulate these properties. (Supported by NSF 084273 ARRA)

1125-Plat

Three-Dimensional Structure of the Relaxed State of Calcium-Regulated Myosin Filaments

John L. Woodhead, Fa-Qing Zhao, **Roger Craig**.
UMass Medical School, Worcester, MA, USA.

Myosin filaments of muscle are regulated either by phosphorylation of their regulatory light chains or Ca^{2+}-binding to the essential light chains, contributing to on-off switching or modulation of contraction. Phosphorylation-regulated filaments in the relaxed state are characterized by an asymmetric interaction between the "blocked" and "free" heads of each myosin, inhibiting actin-binding or ATPase activity (Wendt et al., 2001; Woodhead et al., 2005). We have tested whether a similar interaction occurs in Ca^{2+}-regulated filaments. Filaments were purified from scallop striated adductor muscle and imaged by cryo-electron microscopy. 3D reconstruction was carried out by single particle methods. Reconstructions showed a 7-fold symmetric, helical array of myosin head-pair motifs lying above the filament surface. Fitting of the motif with a myosin head atomic model revealed that the heads interact in a similar way to phosphorylation-regulated filaments. However, the 2-headed motif was more tilted and higher above the filament surface in the Ca^{2+}-regulated filaments. Subfragment 2 of the myosin tail emerged from the motif near the blocked head and connected the motif to the filament backbone, which comprised a 7-fold array of comma-shaped subfilaments. This structure reveals new detail compared with a previous cryo-EM study (Vibert, 1992) and demonstrates that the interpretation of head organization in a negative stain reconstruction of scallop filaments (AL-Khayat et al., 2009) is incorrect. We conclude that the relaxed state of Ca^{2+}-regulated filaments is achieved in a similar way to phosphorylation-regulated filaments, confirming that head-head interaction is a widely used motif (Woodhead et al., 2005). In the scallop filament, the pairs of myosin heads are much closer together azimuthally and the subfilaments have a different structure compared with phosphorylation-regulated filaments, implying that general models for thick filament structure (Squire, 1973) need modification. Supported by NIH grant AR34711.

1126-Plat

Electron Tomography of Cryofixed, Isometrically Contracting Insect Flight Muscle Reveals Novel Actin-Myosin Interactions

Shenping Wu[1], Jun Liu[1], Mary C. Reedy[2], Hanspeter Winkler[1], Richard T. Tregear[3], Carmen Lucaveche[2], Clara Franzini-Armstrong[4], Hiroyuki Sasaki[5], Yale E. Goldman[4], Michael K. Reedy[2], **Kenneth A. Taylor[1]**.
[1]Florida State University, Tallahassee, FL, USA, [2]Duke University Medical Center, Durham, NC, USA, [3]MRC Laboratory of Molecular Biology, Cambridge, United Kingdom, [4]University of Pennsylvania, Philadelphia, PA, USA, [5]Jikei University School of Medicine, Tokyo, Japan.

We have applied multivariate data analysis to 38.7 nm repeat segments obtained from electron tomograms of isometrically contracting insect flight muscle fibers, mechanically monitored, rapidly frozen, freeze-substituted and thin sectioned. Improved resolution reveals for the first time the helix of F-actin subunits in the thin filament with sufficient clarity that an atomic model can be built into the density independent of the myosin cross-bridges, thereby providing an objective method for identifying weak and strong actin-myosin attachments. The tomogram shows strong binding myosin attachments on only four F-actin subunits midway between successive troponin complexes; these actin subunits comprise the "target zone" of active contraction. Improved quantitation facilitates a more detailed description of weak and strong myosin attachments all along the thin filament including for the first time myosin heads contacting the thin filament on troponin. Most strong binding actin attachments consist of single myosin heads but 28% of bound heads are 2-headed myosin attachments. Strong binding attachments show an axial lever arm range of 77° sweeping out a distance of 12.9 nm. The azimuthal range for the lever arm of strong binding attachments is 127° with a distribution nearly completely to one side of the initial crystallographic structures used for the fitting. There is no apparent coupling between axial angle, representing progress through the power stroke of myosin, and the azimuthal lever arm angle. Two types of weak actin attachments are observed. One type, which is found exclusively on target zone actin subunits, appears to represent prepowerstroke intermediates. The other, which appears to have a different function, is positioned on the M-ward side of the target zone, i.e. the direction toward which filaments slide during sarcomere shortening. Its motor domain contacts tropomyosin rather than actin. Supported by NIH.

1127-Plat

Microscopic Measurement of Periodic Cross-Bridge Formation in Skeletal Myofibril

Madoka Suzuki[1,2], Shin'ichi Ishiwata[3,2].
[1]Comprehensive Research Organization, Waseda University, Tokyo, Japan, [2]Waseda Bioscience Research Institute in Singapore, Waseda University, Tokyo, Japan, [3]Department of Physics, Faculty of Science and Engineering, Waseda University, Tokyo, Japan.

Electron microscopy and X-ray diffraction studies have been usually used for the examination of the interactions between actin and myosin, i.e., cross-bridge formation, in muscle fibers. These studies suggested the existence of "target zones [regions]" in actin (thin) filament, which are composed of three to four actin monomers that myosin heads in myosin thick filament can form cross-bridges. Direct evidence for the target zones, however, has been missing in myofibrils. Here we studied the interaction between a single actin filament and the thick filaments of rabbit skeletal myofibril under optical microscope. Single bead-tailed actin filament was manipulated by optical tweezers to make rigor cross-bridges on the outer surface of myofibril, and rupturing events were directly detected. We found the periodic cross-bridge formation, and frequently observed gaps, which are probably due to the incommensurate helical pitches between the thin and the thick filaments.

1128-Plat

The First Millisecond of the Myosin Working Stroke Under Constant Load

Marco Capitanio[1], Monica Canepari[2], Manuela Maffei[2], Diego Beneventi[1], Roberto Bottinelli[2], Francesco Pavone[1].
[1]LENS, Firenze, Italy, [2]Università di Pavia, Pavia, Italy.

Myosin II is the motor protein that drives muscle contraction through cyclical interactions with an actin filament. The working stroke produced by a single myosin head has been previously measured in isolated myosin molecules, but the effects of the high loads acting on the myosin molecule during muscle contraction could not be investigated. In fact, current single molecule techniques apply force with a delay of few milliseconds after actin-myosin binding, when the working stroke of skeletal muscle myosin has already been completed.

Here, we developed a novel single molecule technique in which the delay between myosin binding and force application is abolished. This method is capable of resolving the development of the myosin working stroke under different loads with a very high time resolution and detecting events as short as 100 μs. We found that under loads in the range 1 to 10 pN myosin can follow two distinct pathways in its interaction with actin. In the first pathway myosin detaches from actin before producing any movement (weak binding state); these events are very fast (240 ± 23 μs), their duration does not depend on ATP concentration, and is not significantly affected by force. In the second pathway myosin steps and remains bound to actin for a longer time (strong binding state). At low forces ($|F| < 2$ pN) the lifetime of this second population of events linearly decreases with ATP concentration in the range 5-50 μM. At higher forces this relation becomes non-linear due to premature unbinding of myosin from actin.

The working stroke is produced in two steps and its mean amplitude is found to be smaller at increasing loads and vanishes at the isometric force (5.7 ± 0.6 pN).

Platform U: Membrane Active Peptides

1129-Plat

Effect of Molecular Organization in Micelles and Bilayers on Binding and Conformation of Biologically Active Peptides

Shirley Schreier.
Institute of Chemistry, University of São Paulo, São Paulo, Brazil.

Amphiphiles form different types of aggregates, such as micelles and bilayers, depending on their shape and hydrophilic-hydrophobic balance. While bilayers form vesicles containing an inner aqueous compartment, micelles are smaller, approximately spherically-shaped, and have no internal aqueous compartment. Thus, molecular packing and mobility vary in these aggregates, and EPR spectra of spin probes can be used to examine these properties. EPR spectra evince tighter molecular packing and slower rate of motion in bilayers than in micelles. Such differences affect binding of peptides, both qualitatively and quantitatively. Fluorescence, CD, and EPR were employed to investigate interactions of micelles and vesicles with antimicrobial peptides, as well as fragments of GPCR and cytolytic toxins. EPR was also used for peptide analogues containing the paramagnetic amino acid TOAC. Two-component spectra indicated slow exchange between bound peptide and peptide tumbling fast in aqueous solution, allowing the calculation of binding constants. Peptide-membrane interaction was also monitored by changes in peptide fluorescence intensity and emission wavelengths, as well as accessibility to a water soluble quencher. CD spectra showed that upon binding the peptides acquired secondary structure due to formation of intramolecular hydrogen bonds, favored by the decreased polarity at the lipid interface. While in most cases, bilayer binding was only observed when electrostatic interactions occurred between positively charged peptides and negatively charged phospholipids, electrostatic effects played a less important role in peptide-micelle interaction. These differences were ascribed to differences in molecular packing and curvature in both types of aggregates. The positive curvature of micelles is proposed to mimic the lipid organization of toroidal pores. Thus, the conformational behavior in the presence of micelles would correspond to that of peptides forming toroidal pores in bilayer membranes.

Supported by FAPESP, CNPq, CAPES.

1130-Plat

Cholesterol Effect on The Lipid Bilayer Perturbation Induced by Peptides Derived from the Membrane-Proximal External Region of HIV-1 gp41

Beatriz Apellaniz[1], Ana Garcia-Saez[2], Petra Schwille[2], **Jose L. Nieva**[1].
[1]Biophysics Unit, University of Basque Country, Bilbao, Spain,
[2]Biotechnologisches Zentrum der Techische UniversitÃ¤t Dresden, Dresden, Germany.

The conserved, membrane-proximal external region (MPER) of the human immunodeficiency virus type-1 envelope glycoprotein 41 subunit is required for fusogenic activity. It has been proposed that MPER functions by disrupting the cholesterol-enriched virion membrane. We have compared the effects of cholesterol on the membrane perturbations induced by N-preTM and PreTM-C, two peptides derived from MPER sequences showing tendency to associate with the bilayer interface or to transfer into the hydrocarbon-core, respectively. Capacities of N-preTM and PreTM-C for associating with lipid vesicles were comparable. However, supporting the existence of different membrane-bound structures, N-preTM established unstable pores that induced permeabilization following a graded mechanism, whereas PreTM-C pores were stable and permeabilized LUVs and GUVs following an all-or-none mechanism. Cholesterol did not alter these permeabilization mechanisms, but affected differently the lytic capacities of the peptides. N-preTM partitioning and induced leakage decreased as the bilayer area compressibility modulus (KA) increased. In contrast, cholesterol highly stimulated PreTM-C-induced leakage under conditions that did not affect partitioning. Finally, fluid phase co-existence stimulated leakage induced by both peptides, which were confined within liquid disordered domains. These results support specific roles for cholesterol in modulating MPER membrane-disrupting effects that are not dependent on raft formation.

1131-Plat

Dependence of Amyloid-β Oligomer (AβO) Interaction with Membranes on Preparation Method

Yuri Sokolov[1], Maria Lioudyno[1], Philip R. Dennison[2], James E. Hall[1], Suhail Rasool[3], Saskia C. Milton[3], Charlie G. Glabe[3], Prabhanshu Shekhar[4], Matteo Broccio[4], Frank Heinrich[5,4], Mathias Lösche[4,5].
[1]Dept Physiology and Biophysics, University of California, Irvine, Irvine, CA, USA, [2]Dept of Chemistry, University of California, Irvine, Irvine, CA, USA, [3]Dept Molec Biol and Biochmistry, University of California, Irvine, Irvine, CA, USA, [4]Physics Dept, Carnegie Mellon University, Pittsburgh, PA, USA, [5]NIST Center for Neutron Research, Gaithersburg, MD, USA.

AβOs reduce the resistance of lipid membranes to ion transfer in a dose-dependent fashion.[1] Combined conductance and structural studies suggest that AβOs at micromolar total peptide concentrations increase the dielectric constant in membrane cores by forming inhomogeneous patches within the membrane,[2] but some issues remain unresolved.[3] Here we compare the conductance increases induced by AβOs in membranes, both tethered and free-standing, for particles prepared by solubilization in hexafluoroisopropanol (HFIP) or NaOH. AβO aggregation and time course, and their association with membranes, are also characterized by their conformation-sensitive reaction with antibodies, dynamic light scattering, and neutron reflectometry. ^{19}F-NMR is used to quantify HFIP content in buffer and detect residual HFIP in AβO preparations. While prolonged evaporation from buffer reduced the HFIP concentration below the NMR detection limit we find that similarly treated AβO samples retain HFIP firmly bound to the peptide at a level of ~ 1HFIP per 5 amyloid peptides. While this amount is probably too low to account for the conductance effects of HFIP-prepared AβOs, we also observe that NaOH-prepared AβOs do indeed induce smaller conductance increases at the same concentrations. This study addresses the differences between HFIP-prepared and NaOH-prepared AβOs and how these may contribute to differences in their conductivity effects on membranes.

Supported by the NIH (1P01AG032131), the Hillblom Foundation and the AHAF (A2008-307).

[1]Sokolov, Y., *et al.* 2006. *J. Gen. Physiol.* 128:637-647.
[2]Valincius, G., *et al.* 2008. *Biophys. J.* 95:4845-4861.
[3]Capone R., *et al.* 2009. *Neurotox. Res.* 16:1-13.

1132-Plat

AFM Force Spectroscopy on TAT Membrane Penetration

Elizabeth A. Hager-Barnard, Benjamin D. Almquist, Nicholas A. Melosh.
Stanford University, Stanford, CA, USA.

We present a study of the interactions between cell-penetrating peptides (CPPs) and lipid stacks using Atomic Force Microscopy (AFM). Understanding how CPPs can pass through cell membranes is critical for designing optimal drug delivery agents. While CPPs like HIV-TAT, a positively charged 9-mer with six arginine groups, have been widely studied, their precise penetration mechanisms are still not well understood. New experimental methods are needed to characterize CPP behavior and determine whether TAT can penetrate bilayers directly. Direct measurement of TAT-lipid mechanics during the actual translocation event is an ideal method to elucidate the interaction forces, mechanisms and timescales of membrane penetration. We used AFM force

spectroscopy on lipid bilayer stacks with TAT 'δ-functionalized' probes to monitor both the TAT position within a single bilayer and the associated force with microsecond resolution. To our knowledge these results present the first direct quantification of the mechanics of TAT penetration and the first demonstration that the different regimes identified in dynamic force spectroscopy correspond to distinct mechanisms. The AFM results show that TAT by itself does indeed alter the membrane structure. Additional results from lysine oligomer probes indicate that TAT's arginine groups are key to these TAT-lipid interactions, since probes functionalized with a lysine oligomer did not induce bilayer thinning. Though TAT strongly interacts with the lipid bilayer, the energy barrier for TAT penetration is actually 38kT higher than for probes functionalized with 11-mercaptoundecanoic acid. These results corroborate many of the conclusions from molecular dynamics simulations on TAT-lipid systems, which indicate that TAT does not penetrate bilayers directly.

1133-Plat

Membrane Fusion is Induced by Antimicrobial and Cell Penetrating Peptides, to an Extent that Correlates with their Conformational Change

Parvesh Wadhwani, Johannes Reichert, Jochen Buerck, Anne S. Ulrich.
Karlsruhe Institute of Technology, Forschungszentrum Karlsruhe, Eggenstein-Leopoldshafen, Germany.

Antimicrobial peptides (AMPs) kill bacteria via membrane permeabilization, whereas cell penetrating peptides (CPPs) can cross cellular membranes without causing damage. Yet, many AMPs and CPPs resemble one another, being short cationic peptides, which tend to be unfolded in solution but assume some kind of amphiphilic structure in the membrane-bound state. Fusogenic peptides (FPs) represent a third functional class, responsible e.g. for viral infection, and they are described as short and hydrophobic sequences with a pronounced conformational plasticity.
Despite their distinctly different biological roles, we have tested the ability of all three classes of membrane-active peptides to trigger membrane fusion. The HIV1 fusion peptide FP23 is used as a reference to compare the fusion activities of several representative AMPs and CPPs with different conformational preferences and compositions. A fluorescence dequenching assay was used to monitor lipid mixing, and dynamic light scattering revealed the size-increase of the fused vesicles. Several AMPs and CPPs were thus found to be fusogenic to an even higher degree than FP23, which had not been expected. Some insight into the reason for this remarkable activity was obtained by monitoring the secondary structure of the peptides in aqueous buffer before, and in the membrane-bound state after fusion. We found a correlation between the extent of fusion and the extent of lipid-induced folding, suggesting that the energy released in the conformational change is responsible for perturbing the lipid packing in the bilayer and thereby triggering fusion.

1134-Plat

Lipid Clustering by Three Homologous Arginine-Rich Antimicrobial Peptides is Insensitive to Amino Acid Arrangement

Raquel F. Epand[1], Richard M. Epand[1], Christopher J. Arnusch[2], Brigitte Papahadjopoulos-Sternberg[3], Guangshun Wang[4], Yechiel Shai[2].
[1]McMaster University, Hamilton, ON, Canada, [2]Weizmann Institute, Rehovot, Israel, [3]NanoAnalytical Laboratory, San Francisco, CA, USA, [4]University of Nebraska, Omaha, NE, USA.

Membrane and antimicrobial properties of three short Arg-rich peptides containing the same amino acid composition but different sequences were determined in this study. These peptides, PFWRIRIRR-amide (PR-9), RRPFWIIRR-amide (RR-9) and PRFRWRIRI-amide (PI-9), all exhibit the ability to induce segregation of the anionic lipids from the zwitterionic lipids, as shown by changes in the phase transition properties of lipid mixtures detected by differential scanning calorimetry and also by freeze fracture electron microscopy. The Minimal Inhibitory Concentration (MIC) of these three peptides against several strains of Gram positive bacteria correlated well with the lipid composition of the bacterial membrane. The lower activity of these three peptides against Gram negative bacteria, particularly PI-9, could be explained by the interactions of these peptides with LPS as shown by isothermal titration calorimetry. The promotion of lipid domains by PR-9 as well as by a cathelicidin fragment, KR-12 that had previously been shown to induce lipid phase segregation, was directly visualized using freeze fracture electron microscopy. This work shows the insensitivity of phase segregation to the specific arrangement of the cationic charges in the sequence of these small cationic peptides as well as being independent of their tendency to form different secondary structures.

1135-Plat

N-Acylation of Antimicrobial Peptides Causes Different Mode of Cell Membrane Damage

Karl Lohner[1], Guenter Deutsch[1], Eva Sevcsik[1], Dagmar Zweytick[1], Jörg Andrä[2], Yechiel Shai[3], Sylvie E. Blondelle[4].
[1]Austrian Academy of Sciences, Graz, Austria, [2]Research Center Borstel, Borstel, Germany, [3]Weizmann Institute, Tel Aviv, Israel, [4]Burnham Institute, San Diego, CA, USA.

Lipopeptides such as polymyxins, octapeptins or daptomycin often show an increased activity against bacteria as compared to their non-acylated analogue. Thus, we have studied N-acylated synthetic peptides derived from a fragment of human lactoferrin (LF-11) to elucidate the interaction of these peptides with Gram-negative and Gram-positive bacteria and membrane mimetic systems using various biophysical and biological methods.
Calorimetric studies on liposomes composed of phosphatidylglycerol revealed that the parent peptide induced a phase separation into peptide-enriched and -poor domains, which however consist of a similar domain size as calculated by the cooperative units. In contrast, at the same lipid-to-peptide molar ratio (25:1) the N-acylated derivatives strongly broadened the phase transition range and lowered markedly the main transition temperature. This is indicative for rather small and inhomogeneous domains, which will result in large line defects increasing membrane permeability as observed in intact bacteria. Membrane destabilization of E. coli and S. aureus induced by the peptides was monitored by using the membrane-potential-sensitive dye DiIC1 and the extent of membrane damage caused by the peptides by the cationic dye SYTOX green, which cannot enter intact cells unless its membrane is disrupted by external compounds. In both assays the N-acylated peptides showed a dramatic increase of fluorescence indicating massive membrane damage. This is supported by electron micrographs, which clearly showed a loss of cytoplasmic content and membrane rupture in the presence of the N-acylated peptide. Nevertheless, the extent of cell membrane rupture does not necessarily strongly correlate with the MIC-value of the peptides emphasizing the different mode of interaction of (non)-acylated peptides, which in part may be related to different degree of interaction with cell membrane/wall components such as lipopolysaccharides and lipoteichoic acid.
Acknowledgement to EC-projects "ANEPID" and "BIOCONTROL"

1136-Plat

Protegrin-1 Orientation in Membrane Bilayers: Insights from Potential of Mean Force Calculations as A Function of Its Tilt and Rotation Angles

Huan Rui, Wonpil Im.
The University of Kansas, Lawrence, KS, USA.

Protegrin-1 (PG-1) belongs to the family of antimicrobial peptides. It interacts specifically with the membrane of a pathogen and kills the pathogen by releasing its cellular contents. To fully understand the energetics governing the orientation of PG-1 in different membrane environments and its effects on the physicochemical properties of the peptide, we have calculated the potentials of mean force (PMF) of PG-1 as a function of its tilt angle in explicit membrane bilayers composed of either DLPC (1,2-dilauroylphosphatidylcholine) or POPC (1-palmitoyl-2-oleoylphosphatidylcholine) lipid molecules. The resulting PMFs in explicit lipid bilayers were then used to search for the optimal hydrophobic thickness of the implicit membrane, in which a two-dimensional PMF in the tilt and rotation space was calculated. The calculated PMFs in explicit membrane systems clearly reveal that the energetically favorable tilt angle is affected by both the membrane hydrophobic thickness and the PG-1 rotation angle. Local thinning of the membrane around PG-1 is observed upon PG-1 tilting. The thinning effect is caused by different arginines in regard to the rotation orientation of the peptide. The two-dimensional PMF calculated in implicit membrane at specified rotation angles is in good accordance with those from the explicit membrane simulations. The ensemble-averaged Val16 ^{15}N and ^{13}CO chemical shifts calculated from the two-dimensional free energy distribution agree fairly well with the experimental values, suggesting the accuracy and reliability of the application of PMFs to understand important physicochemical properties of membrane peptides/proteins.

Platform V: Membrane Dynamics & Bilayer Probes

1137-Plat

Curvature Sorting of Lipids and Proteins in the Strong Segregation Limit: Curvature Mediated Domain Nucleation and Steady State Transport in Tubular Membranes with Phase Separation

Michael C. Heinrich, Aiwei Tian, Tom C. Lubensky, Tobias Baumgart.
University of Pennsylvania, Philadelphia, PA, USA.

Intracellular sorting centers, including the trans-Golgi network, the endoplasmic reticulum, and the endocytic recycling compartment, all contain membrane tube elements with cylindrical curvatures. The question of how curvature and sorting are coupled is central to the understanding of the function of organelle homeostasis, membrane trafficking, and intracellular sorting. Of particular interest, but underexplored, are non-equilibrium phenomena fundamentally linked to membrane transport.

Here we present a straightforward and well controlled model system that allows us to characterize lipid transport at steady state: ternary lipid mixture tubular membranes pulled from phase-separated giant unilamellar vesicles (GUVs) by means of optical tweezers. The tubule composition, when initially formed from the liquid-ordered (Lo) phase region of the vesicle, is dependent on the velocity at which it is pulled: fast extraction velocities create tethers of the Lo phase, while slow extraction velocities can generate tethers that are liquid-disordered (Ld) phase. Thus, the speed with which highly curved tubules are formed may possibly serve as a control variable in living cells to adjust tubule composition. Furthermore, in tubules which are initially Lo phase, we find curvature-induced nucleation of Ld domains at the neck between tubule and vesicle. These Ld domains display characteristic, curvature dependent parabolic growth behavior that can be understood via a straightforward analytical mass transfer model that we derived from linear irreversible thermodynamics. We have also developed numerical schemes that capture shape transitions of tubular membranes on the basis of measured biophysical parameters in support of our experimental findings.

1138-Plat

Dynamics of Bicelle Model Membrane Promote Domain Formation

Hyo Soon Cho, **Megan Spence.**
University of Pittsburgh, Pittsburgh, PA, USA.

We have created a magnetically-aligned bicelle model membrane system (containing POPC, DMPC, and cholesterol) that laterally separates to form lipid domains. Lipid domains have been observed in a number of ternary systems (cholesterol, saturated lipid, unsaturated lipid), but rarely in systems containing POPC and never in systems containing POPC and DMPC. Using pulsed-field gradient NMR techniques, we measured the lateral diffusion constant for the lipids as a function of diffusion time. The time dependence of the diffusion constant showed the presence of domains ~1um in size at 295K. The domains increase in size with temperature, until an isotropic membrane structure appears, indicating that the domains are liquid-disordered phase. Variable temperature 1H-MAS NMR of the domains supports this assignment. Bicelles are magnetically-aligned, highly perforated bilayers often used in solid state NMR for membrane protein structure determination. The formation of POPC/DMPC/cholesterol domains may result from the rapid (τc~10-6 s) undulations of the bicelle bilayer surface. The domain-forming bicelles are also suitable for NMR structure determination of raft-associated membrane proteins.

1139-Plat

Dynamics of 3D Axisymmetric Multicomponent Vesicles in A Viscous Fluid

Jin Sun Sohn[1], Shuwang Li[2], Xiaofan Li[2], John S. Lowengrub[1].
[1]University of California, Irvine, Irvine, CA, USA, [2]Illinois Institute of Technology, Chicago, IL, USA.

Multicomponent vesicles are hollow, closed biomembranes with a lipid bilayer membrane containing different types of lipids and cholesterol. Recent experiments on giant unilamellar vesicles demonstrate that there exists a variety of behavior of multicomponent vesicles. Under this understanding, we develop and investigate numerically a thermodynamically consistent model of three dimensional axisymmetric multicomponent vesicles in an incompressible viscous fluid. The model is derived using an energy variation approach that accounts for different lipid surface phases, the excess energy (line energy) associated with surface phase domain boundaries, bending energy, spontaneous curvature, Gaussian bending energy, local inextensibility and fluid flow via the Stokes equations. The equations are high-order (fourth order)nonlinear and nonlocal due to incompressibility of the fluid and the local inextensibility of the vesicle membrane. To solve the equations numerically, we develop a nonstiff, pseudo-spectral boundary integral method that relies on an analysis of the equations at small scales. We present simulations of multicomponent vesicles in a quiescent and an extensional flow and investigate the effect of varying the average surface concentration of an initially unstable mixture of lipid phases. The phases then redistribute and alter the morphology of the vesicle and its dynamics. A comparison of results with experimental vesicle morphologies yields good agreement.

1140-Plat

Lipid Phase Specific Organisation of the Transmembrane Anchor of Influenza Hemagglutinin

Joerg Nikolaus, Andreas Herrmann.
Humboldt University Berlin, Berlin, Germany.

Correct transport and localization of membrane proteins to distinct cellular organelles are crucial for cell growth but also for the infection cycle of enveloped viruses. Viral membrane proteins like hemagglutinin of influenza virus, anchored in the membrane via a single transmembrane domain (TMD), are transported to the plasma membrane and - together with other virus components - recruited to the budding site. Cholesterol and glycosphingolipid-enriched membrane microdomains are considered as assembly and budding sites for enveloped viruses such as influenza virus. Besides a most likely location of a sorting signal within the TMD sequence also the width of the bilayer is important, which is, amongst other factors, controlled by the cholesterol content of the membrane.

Using different fluorescent-based approaches we study the impact of membrane hydrophobic thickness and membrane packing properties on the sorting behavior of virus derived TMD peptides containing a Trp residue in its center. The emission λmax depending on the hydrophobicity of the surrounding of the Trp residue and parallax analysis of fluorescence quenching are used to determine the Trp location in the lipid bilayer revealing a transmembrane orientation. Membrane thickness is altered by the use of lipids having different acyl chain length and also by the addition of cholesterol or decane shifting λmax. Incorporation of Rhodamine labeled TMD into giant unilamellar vesicles prepared from lipids with varying length and also from ternary lipid mixtures forming distinct liquid phases allows us to study phase dependent TMD localization by fluorescence microscopy. Typically, in the model system the TMD sorts into the liquid disordered phase in contrary to the raft association of hemagglutinin in cells. To address the latter by a more appropriate system, we used viral lipids for vesicle preparation mimicking the natural environment of the TMD.

1141-Plat

Nanometric Phase Transitions on Phospholipid Membranes Using Plasmonic Heating of Single Gold Nanoparticles

Alexander S. Urban, Michael Fedoruk, Stefan Wimmer,
Fernando D. Stefani, Jochen Feldmann.
LMU Munich, Munich, Germany.

Lately impressive advances have been made revealing the structure and pathways of cellular and subcellular systems by optical techniques with nanometric resolution [1]. Full understanding of the function of these systems requires additional energetic information of the processes involved. In order to obtain such information locally, it is necessary to develop remotely controlled nanoscale heat sources.

We demonstrate the capability of single gold nanoparticles as optically controlled nanoscopic sources of heat. Gold nanoparticles attached to giant unilamellar vesicles in the gel-phase can induce reversible, local phase transitions to the fluid-phase when illuminated at their plasmon resonance [2]. The optically heated nanoparticles melt a nanoscale region of the membrane and exhibit an enhanced diffusion over the membrane. The diffusion is analyzed by single particle tracking for various phospholipids and laser power densities. As a result, we can control the nanoscale phase transition and obtain local information on the dynamics of the membrane.

The results illustrate the use of single gold nanoparticles for local nanoscale thermodynamic investigations on phospholipid membranes. The approach presented here can be easily extended by combining it with other microscopy methods and optical tweezers techniques. This may also open new possibilities to position nanoparticles on cell membranes and thermally manipulate biomolecules or membrane processes.

[1] R. Schmidt, C. A. Wurm, S. Jakobs, J. Engelhardt, A. Egner and S.W. Hell, Nat. Methods (2008) 5, 539
[2] A.S. Urban et al., Nanoletters (2009) 9, 2903-2908

1142-Plat

Dynamic and Static Measurements of A Single and Double Phospholipid Bilayer System

Justin D. Berry[1], Curt M. DeCaro[1], Daniel A. Bricarello[2], Yicong Ma[3], Mrinmay Mukhopadyay[3], Gang Chen[3], Zhang Jiang[4], Alec Sandy[4], Suresh Narayanan[4], Atul N. Parikh[2], Sunil K. Sinha[3], Laurence B. Lurio[1].
[1]Northern Illinois University, DeKalb, IL, USA, [2]University of California, Davis, Davis, CA, USA, [3]University of California, San Diego, La Jolla, CA, USA, [4]Argonne National Laboratory, Argonne, IL, USA.

We investigate the surface height fluctuations of single and double bilayers of DPPE supported on silicon using x-ray photon correlation spectroscopy (XPCS). In this techique, x-rays are incident on the membrane in a grazing incidence geometry and diffusely scattered x-rays are measured using an area detector. Time fluctuations of the scattering pattern can then be analyzed to yield the relaxation rate of surface height fluctuations. Bilayer and double bilayer systems were prepared utilizing combination of Langmuir-Blodgett and Langmuir-Schaeffer depositions. Static structural measurements were also made on these systems as well as on more complicated systems consisting of triple and five-fold bilayers of DPPE. Relationships between structure and dynamics of these systems will be discussed.

1143-Plat

Coexistence of Immiscible Mixtures of Palmitoylsphingomyelin and Palmitoylceramide In Monolayers and Bilayers

Jon V. Busto[1], Maria Laura Fanani[2], Luisina De Tullio[2], Jesus Sot[1], Bruno Maggio[2], **Felix M Goni**[1], Alicia Alonso[1].
[1]Unidad de Biofisica (CSIC-UPV/EHU), Leioa, Spain,
[2]Universidad Nacional de Cordoba, Cordoba, Argentina.

A combination of lipid monolayer- and bilayer-based model systems have been applied to explore the interaction and organization of palmitoylsphingomyelin (pSM) and palmitoylceramide (pCer). Langmuir balance measurements reveal favourable interactions between the lipid molecules. A thermodynamically stable point is observed in the range 30-40 mol % pCer. The pSM monolayer undergoes hyperpolarization and condensation with small pCer concentrations, narrowing the liquid-expanded (LE) to liquid-condensed (LC) pSM main phase transition by inducing intermolecular interactions and chain ordering. Beyond this point, the phase diagram no longer reveals the presence of the pSM-enriched phase. Differential scanning calorimetry (DSC) of multilamellar vesicles reveals a widening of the pSM gel-fluid phase transition (41°C) upon pCer incorporation, with formation of a further endotherm at higher temperatures that can be deconvoluted into two components. DSC data reflect the presence of pCer-enriched domains coexisting, at different proportions, with a pSM-enriched phase that is no longer detected in mixtures containing >30 mol% pCer. Epifluorescence microscopy of mixed monolayers at low pCer content shows concentration-dependent, morphologically different pCer-enriched LC domain formation over a pSM-enriched LE phase, in which pCer contents close to 5 and 30 mol% can be determined for the LE and LC phases respectively. Fluorescence confocal microscopy of giant vesicles further confirms formation of pCer-enriched lipid domains. Vesicles cannot form beyond 40 mol% pCer contents. Altogether, the presence of at least two immiscible phase-segregated pSM-pCer mixtures of different compositions is proposed at high pSM content. A condensed phase (with domains segregated from the liquid-expanded phase) showing enhanced thermodynamic stability occurs near a compositional ratio of 2:1 (pSM:pCer). These observations become significant on the basis of the ceramide-induced microdomain aggregation and platform formation upon sphingomyelinase activity on cellular membranes.

1144-Plat

Diffusion of Nano-Meter-Sized Domains on A Vesicle

Yuka Sakuma[1], **Masayuki Imai**[1], Naohito Urakami[2], Michihiro Nagao[3,4], Shigeyuki Komura[5], Toshihiro Kawakatsu[6].
[1]Ochanomizu University, Tokyo, Japan, [2]Yamaguchi University, Yamaguchi, Japan, [3]National Institute of Standards and Technology, Gaithersburg, MD, USA, [4]Indiana University, Bloomington, IN, USA, [5]Tokyo Metropolitan University, Tokyo, Japan, [6]Tohoku University, Sendai, Japan.

The lateral diffusion of nano-meter-sized constituents (proteins, lipid rafts and so on) in lipid bilayers is of biological interest because the biochemical functions may be diffusion controlled. Saffman and Delbrück (SD) dealt with this issue using a hydrodynamic theory and derived an expression of the diffusion coefficient D forsmall domain size limit as $D(r)=k_BT[\ln(\eta_m h/\eta_m r)-0.0773]/4\pi\eta_m h$, where η_m and η_w are the viscosities of the membrane and the aqueous phase, respectively, h is the membrane thickness, r is the radius of the diffusing object. In this study we addressed the SD model by direct measurement of the intermediate scattering function of the nano-meter-sized liquid ordered domains in the fluid membrane using a contrast matching technique of neutron spin echo. We prepared ternary small unilamellar vesicles (SUVs) composed of deuterated DPPC, hydrogenated DOPC, hydrogenated cholesterol. The obtained intermediate scattering functions for the phase separated SUVs were fitted by a double exponential function, $S(q,t)/S(q,0)=A\exp(-D_0q^2t)+(1-A)\exp(-(D_0+D_d)q^2t)$, where A is the numerical constant, $D_0$and D_d are the diffusion coefficients of whole SUV and nano-meter sized domain, respectively. The fitting of $S(q,t)/S(q,0)$ gave $D_d = 2.3 \times 10^{-12}$ m^2/s, where the domains have the mean radius of 7.5 nm. The obtained domain diffusion coefficient agrees well with the SD prediction of $D= 2.35 \times 10^{-12}$ m^2/s using Ns/m^2 and Ns/m^2. Furthermore, by combining present data with the diffusion coefficient of a DPPC single molecule in L_d phase of $D_{DPPC} \approx 3.5 \times 10^{-12}$ m^2/s, we clearly demonstrates that the SD model well describes the observed diffusion coefficients in nano-meter length scale.

Platform W: Protein-Nucleic Acid Interactions II

1145-Plat

Single Molecule Studies of the Recognition Sequence Finding Mechanism of Protelomerase Telk

Markita P. Landry[1], Wai Mun Huang[2], Toshio Yanagida[3], Yann Robert Chemla[1].
[1]University of Illinois at Urbana Champaign, Urbana, IL, USA,
[2]University of Utah Health Sciences Center, Salt Lake City, UT, USA,
[3]Osaka University, Osaka, Japan.

Protelomerase TelK is an enzyme responsible for forming DNA hairpins in linear prokaryotic DNA. The mechanism by which this protein recognizes its target sequence and both quickly and accurately catalyzes DNA hairpin formation is poorly understood. To investigate the target recognition process, we used TIRF microscopy to visualize quantum dot-labeled TelK interacting with both nonspecific DNA and DNA containing the TelK target sequence. While many sequence-specific DNA-binding proteins (SSDBP) have been shown to scan DNA in 1D as their primary method for locating their recognition sequence[1], we surprisingly find that TelK does not move laterally on either aforementioned DNA substrate and therefore does not search by 1D scanning. Measurements of a c-terminally truncated TelK mutant reveal the same behavior. Interestingly, this mutant forms DNA hairpins 50 times slower than wild type, and dissociates from nonspecific DNA at a comparably lower rate than full-length TelK. These results suggest that dissociation from nonspecific DNA is an essential step in the recognition sequence search. Complementary studies with high-resolution optical tweezers reveal that TelK binding to DNA is a highly tension dependent process and condenses the molecule by several nanometers, consistent with crystal structures of the protein-DNA complex[2]. Remarkably, this condensation is observed on nonspecific DNA as well, despite the fact that these DNA distortions are energetically expensive. These findings suggest that the TelK target sequence search may involve 3D hopping and intersegmental transfer in lieu of 1D scanning. This may represent a novel SSDBP recognition sequence search mechanism.

1. Halford, S. et al. Nucl. Ac. Res. 32 (2004)
2. Aihara, H. et al. Mol. Cell. 27, 901 (2007)

1146-Plat

Bacteriophage phi29 Translocates DNA Along A Left-Handed Helical Path During Packaging

Craig L. Hetherington[1], Aathavan Karunakaran[1], Paul Jardine[2], Shelley Grimes[2], Dwight Anderson[2], Carlos Bustamante[1].
[1]UC Berkeley, Berkeley, CA, USA, [2]University of Minnesota, Minneapolis, MN, USA.

Bacteriophage phi29 employs a homomeric ring of RecA-like ATPases in order to package its dsDNA genome into the capsid at near-crystalline density. Previous single-molecule measurements of packaging have revealed the coordination of motor subunits, the step size of the motor, and the sensitivity of the motor to substrate modifications, thereby suggesting structural and kinetic models for the mechanism of translocation. However, traditional single-molecule experiments measure only the projection of the motor's motion onto the DNA longitudinal axis.

We directly observe that phi29 translocates DNA along a left-handed helical path by monitoring rotation of a bead attached to the side of the substrate DNA in a laser tweezers. Simultaneously, the response to applied torque is measured. This novel experiment probes the details of force and torque generation by the packaging motor. Combining these measurements with angstrom-scale laser tweezers observations of motor stepping suggests specific geometric models for the interaction of the motor and DNA during translocation.

The rotor bead technique introduced here allows tracking of the complete three-dimensional trajectory of a dsDNA translocase in action. It also permits the application of torque in a laser tweezers apparatus using commercially-available microspheres.

1147-Plat
Reeling in DNA One Base at A Time: pcrA Translocation Coupled to DNA Looping Dismantles RecA Filaments
Jeehae Park[1], Sua Myong[1], Anita Niedziela-Majka[2], Jin Yu[3], Timothy M Lohman[4], Taekjip Ha[1,5].
[1]Univeristy of Illinois at Urbana Champaign, Urbana, IL, USA, [2]Washington University School of Medicine, St. Louis, IL, USA, [3]University of California at Berkeley, Berkeley, CA, USA, [4]Washington University School of Medicine, St. Louis, MO, USA, [5]5Howard Hughes Medical Institute, Urbana, IL, USA.
The mechanism of helicase translocation on DNA remains controversial and the translocase activity driving their non-canonical functions such as protein displacement is poorly understood. Here, we used single molecule fluorescence assays to study a prototypical superfamily 1 helicase, *Bacillus stearothermophilus* PcrA, and discovered a progressive looping of ssDNA that is tightly coupled to PcrA translocation on DNA. Variance analysis of hundreds of looping events by a single protein demonstrated that PcrA translocates on ssDNA in uniform steps of 1 nt, reconciling discrepancies in previous structural and biochemical studies. On the forked DNA, rather than acting on the leading strand to unwind the duplex, PcrA anchored itself to the duplex junction and reeled in the lagging strand using its 3'-5' translocation activity. PcrA maintained the open conformation, not the closed conformation observed in crystallographic analysis, during looping-coupled translcation. This activity could rapidly dismantle a preformed RecA filament even at 1nM PcrA, suggesting that the translocation activity and structure-specific DNA binding are responsible for removal of potentially deleterious recombination intermediates.

1148-Plat
Protein-Mediated DNA Loops are Resistant to Competitive Binding
Joel D. Revalee, Jens-Christian Meiners.
University of Michigan - Ann Arbor, Ann Arbor, MI, USA.
The lac Repressor protein (LacI) is a canonical genetic regulatory protein. It represses transcription of the lac operon in E. Coli by simultaneously binding to two distant operator sites on the bacterial DNA and bending the intervening DNA into a loop. A set of substrate DNA constructs with intrinsic A-tract bends have been engineered by Mehta and Kahn, which were optimized to form hyperstable loops. We present single-molecule measurements of LacI-mediated loop formation and breakdown rates on these optimized DNA constructs and demonstrate that repeated formation and breakdown of the loops does not cease in the presence of 100 nM of free competitor DNA. While this observation dovetails with bulk competition assays in which the presence of competitor DNA disrupts the looped complexes only very slowly, our measured loop lifetimes of minutes disagree with an inferred lifetime of days from the bulk assays. We conclude that the LacI-DNA complex can exist in some non-looped conformation, which can re-loop, but is unexpectedly resistant to competition. We discuss possible scenarios for such a conformation in light of the data.

1149-Plat
Single Molecule Analysis of Substeps in the Mechanochemical Cycle of DNA Gyrase
Aakash Basu[1], Lena Koslover[1], Allyn Schoeffler[2], Elsa Tretter[2], James M. Berger[2], Andrew J. Spakowitz[1], Zev D. Bryant[1].
[1]Stanford University, Stanford, CA, USA, [2]University of California Berkeley, Berkeley, CA, USA.
DNA gyrase is a molecular motor that harnesses the free energy of ATP hydrolysis to introduce negative supercoils into DNA. We have characterized the structural dynamics of processive supercoiling using a real-time single molecule assay in which DNA gyrase activity drives the directional, stepwise rotation of a submicron rotor bead attached to the side of a stretched DNA molecule. We are able to directly observe rotational pauses corresponding to rate-limiting kinetic steps under varying [ATP], and have used simultaneous measurements of DNA twist and extension in order to characterize transient supercoil trapping and DNA compaction during the reaction cycle. We have mapped out structural intermediates of the DNA:gyrase complex on a twist-extension plane, and have characterized transitions between these states driven by chemical events such as the cooperative binding of ATP. These measurements motivate several revisions to previous models based on lower resolution assays [1], and we will present our results in the context of a new branched kinetic model for the mechanochemical cycle. We are now using theoretical calculations together with measurements of force-dependent changes in extension in order to test specific geometric models for structural intermediates, and we have begun to analyze structure-function relationships using single-molecule analysis of gyrase fragments.
[1] Jeff Gore, Zev Bryant, Michael D. Stone, Marcelo Nollmann, Nicholas R. Cozzarelli, Carlos Bustamante, "Mechanochemical analysis of DNA gyrase using rotor bead tracking", Nature, 439 (2006)

1150-Plat
Two Structurally Different Families of DNA Base Excision Repair (BER) Proteins Diffuse Along DNA to Find Intrahelical Lesions
Andrew R. Dunn[1], Jeffrey P. Bond[1], David M. Warshaw[1], Susan S. Wallace[1], Neil M. Kad[2].
[1]The University of Vermont, Burlington, VT, USA, [2]The University of Essex, Colchester, United Kingdom.
Base excision repair (BER) proteins, endonuclease III (Nth) and VIII (Nei) from E. *coli* represent two distinct glycosylase families, which recognize and remove damaged DNA bases. One mechanism by which these glycosylases scan for DNA lesions is through a simple, one-dimensional diffusive search. To characterize this search mechanism, we have developed a single molecule assay in near TIRF to image Qdot-labeled, His-tagged Nth and Nei proteins interacting with YOYO-1 stained λ-DNA molecules elongated by hydrodynamic flow between 5μm silica beads. With an *in vitro* glycosylase activity assay, we confirmed that neither YOYO-1 stained DNA nor Qdot labeling significantly affects glycosylase activity. By imaging individual DNA "tightropes", we observed Qdot-labeled glycosylases interacting with DNA by either binding to or diffusing on DNA. With increasing ionic strength (50-500mM Kglutamate), although fewer glycosylases interacted per unit length of DNA, a greater fraction diffused along the DNA. At physiological ionic strength, (150mM KGlu) both Nth and Nei scan DNA for as much as 10 sec with a diffusion constant of ~1.5×10^5 bp^2 sec^{-1}, approaching the theoretical limit of rotational diffusion about the DNA helix. At these rates, the activation barrier for rotational diffusion of 0.7 K_bT is slightly below the maximum of ~2 K_bT for efficient target location. We observe no significant difference between Nth and Nei in the rate or mode of their DNA lesion search mechanism. Interestingly, at elevated ionic strengths, both families of glycosylases scan above the theoretical limit for free rotational diffusion (>5×10^5 bp^2 sec^{-1}). Therefore, the DNA/glycosylase interface may be optimized for physiological ionic strength, above which the glycosylase search mechanism shifts from rotational diffusion to a one-dimensional diffusion without rotation.

1151-Plat
Target-Site Search of DNA-Binding Proteins
Mario A. Diaz de la Rosa, Elena F. Koslover, Peter J. Mulligan, Andrew J. Spakowitz.
Stanford University, Stanford, CA, USA.
Gene regulatory proteins find their target sites on DNA remarkably fast; the experimental binding constant for *lac* repressor is three orders of magnitude higher than predicted by free diffusion alone. It has been proposed that nonspecific binding aids the search by allowing proteins to slide and hop along DNA. We develop a reaction-diffusion theory of protein translocation that accounts for transport both on and off the strand and incorporates the physical conformation of DNA. For linear DNA modeled as a wormlike chain, the distribution of hops available to a protein exhibits long, power-law tails. As a result, the long-time displacement along the strand is superdiffusive. Our analysis predicts effective superdiffusion coefficients for given nonspecific binding and unbinding rate parameters. Translocation rates experience a maximum with salt concentration (i.e., binding rate constant), which has been verified experimentally. Simulated protein trajectories on DNA (see figure) agree with our theoretical predictions of superdiffusive transport. Our analytical theory allows us to predict the binding and unbinding rate parameters that optimize the protein translocation rate and the efficiency of the search. Finally, we use our theory to predict rates of target site localization under various experimental conditions.

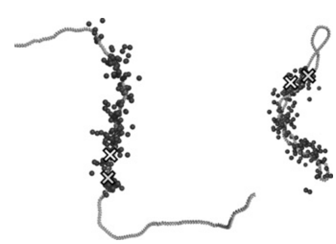

1152-Plat
Illuminating the DNA Binding Behavior of Mitochondrial Transcription Factor A
Géraldine Farge[1], **Onno D. Broekmans**[1], Niels Laurens[1], Linda Dekker[1], Maria Falkenberg[2], Erwin J.G. Peterman[1], Gijs J.L. Wuite[1].
[1]VU University Amsterdam, Amsterdam, Netherlands, [2]University of Gothenburg, Gothenburg, Sweden.

Mitochondria are the energy producing organelles of eukaryotic cells. Owing to their endosymbiotic evolutionary history, they contain their own genome (mtDNA) that encodes for thirteen proteins essential for ATP production.
In mammalian cells, multiple mtDNAs are compacted into protein-DNA complexes called "nucleoids". A major component of these nucleoids is the mitochondrial transcription factor A (TFAM), a member of the high mobility group (HMG) family of proteins. This abundant protein binds DNA with little sequence specificity, and is able to coat the entire mtDNA molecule. It not only serves a role in mtDNA packaging, but is also required for mitochondrial transcription. At this point, dynamics of the TFAM-DNA interaction remain unclear.
Experiments on single DNA molecules offer a very direct way to study TFAM dynamics. Tethered Particle Motion (TPM) experiments show that the system quickly equilibrates with the buffer, and that the end-to-end distance of the DNA decreases upon TFAM binding. Manipulations of single DNA molecules with two optical traps offer an explanation: TFAM decreases the DNA's stiffness (persistence length). A possible molecular mechanism for this decrease is that TFAM introduces bends in the DNA.
Adding single-molecule fluorescence to the dual optical trap illuminates TFAM's binding behavior. Literally seeing TFAM on the DNA, we can derive on- and off-rates, and determine that TFAM does not bind cooperatively. Interestingly and seemingly unrelated to its role in DNA organization, we also observe that TFAM can rapidly bind single-stranded DNA (ssDNA), but not when the ssDNA is under tension. The physiological function of TFAM binding to ssDNA could be related to its regulation of transcription.

Symposium 9: Biophysics of the Failing Heart

1153-Symp
What is the Effect of A Familial Hypertrophic Cardiomyopathy Mutation on Cardiac Myosin Function?
Susan Lowey.
University of Vermont, Burlington, VT, USA.
Familial hypertrophic cardiomyopathy (FHC) is a clinically and genetically heterogeneous disease which is a major cause of heart failure. The landmark discovery that a point mutation at residue 403 (R403Q) in the β-myosin heavy chain (MHC) can cause a lethal form of FHC was made in 1990, but the effect of this mutation on the functional properties of human cardiac myosin remains poorly understood. One problem has been that the prevalent mouse model for FHC expresses predominantly α-MHC. The β-MHC, however, is the predominant isoform in the ventricles of all larger mammals. Even though the α- and β-MHC share > 90 % sequence identity, they differ ~ 2-fold in enzymatic and mechanical properties, raising the possibility that the effect of a disease mutation may depend on the isoform backbone. To address this question we used a transgenic mouse model in which the endogenous α-MHC was replaced with transgenically encoded β-MHC. A His-tag was cloned at the N-terminus of α- and β-MHC, along with the R403Q mutation, to facilitate isolation of myosin or its head subfragment-1 (S1).We find that the steady-state ATPase activity and *in vitro* motility of mouse α-MHC is enhanced by the R403Q mutation, as reported previously, but the R403Q mutation in a β-MHC background shows a slight reduction in activity. A more in-depth analysis of the R403Q phenotype is being undertaken by stopped-flow kinetics to measure the nucleotide turnover in these mutant S1 isoforms. In order to determine the extent of species-dependent differences, we are comparing the functional properties of β-cardiac myosin in the mouse with those in the rabbit, a model system which more closely resembles humans in protein composition and disease phenotypes.

1154-Symp
Reduced Responsiveness to β-Adrenergic Agonists in Murine cMyBP-C Cardiomyopathy
Richard L. Moss, Carl Tong.
Univ Wisconsin Sch Med, Madison, WI, USA.
Myosin binding protein C (MyBP-C) is a thick filament accessory protein that has both structural and regulatory roles in striated muscle contraction. We are studying the roles of the cardiac isoform of MyBP-C in mouse models in which the cMyBP-C gene has been disrupted, resulting in ablation of the protein, and in mice expressing mutant protein in which residues that are phosphorylated *in vivo* by PKA have been replaced with ala or asp. Ablation of cMyBP-C results in a cardiac phenotype similar to many inherited cardiomyopathies in humans, i.e., septal hypertrophy, increased arrhythmic activity, and systolic and diastolic dysfunction. Studies of isolated myocytes from wild-type and null mice suggest that cMyBP-C regulates the kinetics of cross-bridge interaction with actin, a mechanism that is lost in the null mouse. Studies of myocytes from mouse lines expressing phosphorylation mutants of cMyBP-C indicate that PKA stimulation of contraction kinetics in myocardium is in large part due to phosphorylation of cMyBP-C, which appears to relieve a structural constraint on myosin and increases the likelihood of myosin binding to actin. Living myocardium expressing non-phosphorylatable cMyBP-C was found to exhibit depressed twitch force-frequency relationships and reductions in both frequency-dependent and β-agonist- induced acceleration of relaxation. These results can be explained by a model in which cMyBP-C phosphorylation accelerates cross-bridge interaction kinetics in wild-type myocardium, a regulatory mechanism that is lost in myocardium expressing the non-phosphorylatable mutant cMyBP-C. Supported by NIH R01 HL082900 and P01 HL094291.

1155-Symp
The Giant Elastic Protein Titin Role in Muscle Function and Disease
Henk Granzier.
University of Arizona, Tucson, AZ, USA.
No Abstract.

1156-Symp
Rescue of Familial Cardiomyopathies by Modifications at the Sarcomere Level and Ca^{2+} Fluxes
Beata M. Wolska.
University of Illinois, Chicago, Chicago, IL, USA.
Familial cardiomyopathies are commonly linked to missense mutations, deletions or truncations in sarcomeric, cytoskeletal, or intermediate filament proteins and give rise to hypertrophic cardiomyopathy (HCM), dilated cardiomyopathy (DCM) or restrictive cardiomyopathy. Although in the last two decades much information about the pathophysiology of genetically linked HCM and DCM has been provided by studies using transgenic animal models, there is still no therapy to prevent the development of the disease and increase survival in patients with HCM or DCM. Our emphasis here is on development of new therapies for treatment of HCM and DCM linked to mutations in thin filament proteins that are associated with increased and decreased myofilament sensitivity to Ca^{2+} respectively. We hypothesize that direct modifications of myofilament Ca^{2+} sensitivity and/or alteration in Ca^{2+} fluxes can serve as new therapeutic targets. Therefore if 1) HCM is associated with increased myofilament sensitivity to Ca^{2+}, interventions that desensitize the myofilament to Ca^{2+} may serve as potential new therapeutic targets and 2) DCM is associated with decreased myofilament sensitivity to Ca^{2+}, interventions that sensitize the myofilament to Ca^{2+} may serve as potential new therapeutic targets. There are several possible targets within myofilament proteins for altering myofilament Ca^{2+} sensitivity, in particular troponin I. Alterations in Ca^{2+} regulation by modification of sarcoplasmic reticulum Ca-ATPase (Serca2) or phospholamban levels are additional potential targets for HCM and DCM.

Minisymposium 2: Nanomedicine: Biophysical Approaches to Clinical Problems at the Nanoscale

1157-MiniSymp
4.0 Å Cryo-EM Structure of the Mammalian Chaperonin: TRiC/CCT
Yao Cong[1], Matthew Baker[1], Joanita Jakana[1], David Woolford[1], Stefanie Reissmann[2], Steven J. Ludtke[1], Judith Frydman[2], Wah Chiu[1].
[1]Baylor College of Medicine, Houston, TX, USA, [2]Stanford University, Stanford, CA, USA.
TRiC is a eukaryotic chaperonin essential for *de novo* folding of ~10% newly synthesized cytosolic proteins, many of which cannot be folded by other cellular chaperones. Unlike prokaryotic and archael chaperonins, each of its two rings consists of eight unique, but similar subunits. Using single particle cryo-EM, we determined the mammalian TRiC structure without any symmetry imposition at 4.7 Å resolution, which is the highest resolution asymmetric cryo-EM reconstruction to date. An analysis of this map allowed us to elucidate the relative orientation of the two rings and the two-fold symmetry axis location between them. A subsequent two-fold symmetrized map yielded a 4.0 Å structure, in which a large fraction of side chains and structural elements including loops and insertions appear as visible densities. These features permitted unambiguous identification of all eight individual subunits, despite their similarity. A Cα backbone model of the entire TRiC complex was subsequently refined from initial homology models against the cryo-EM density based on our subunit identification. A refined all-atom model for a single subunit

showed ~95% of the dihedral angles in the allowable regions of the Ramachandran plot. Our model reveals that the cavity walls of TRiC exhibit an overall positively charged surface property, the opposite of GroEL. The interior surface chemical properties likely play an important role for TRiC's unique substrate specificity.

1158-MiniSymp
Counting Hydrolyzed ATP On Single Tric Nanomachines in Solution
Yan Jiang, Nick Douglas, Nick Conley, Judith Frydman, W.E. Moerner.
Stanford University, Stanford, CA, USA.
Single biomolecules can be localized in aqueous solution using an Anti-Brownian Electrokinetic (ABEL) trap, which uses fluorescence imaging combined with actively applied electrokinetic forces in a microfluidic geometry. With this device, we have explored the ATP-induced cooperative transitions in the important multi-subunit eukaryotic chaperonin TRiC, a model for other multisubunit enzymes. ATP is labeled with Cy3 and incubated with Atto647 labeled TRiC in the presence of AlFx. The ATPs bind to up to 16 subunits in TRiC and are locked in their binding sites by AlFx after hydrolysis. A rotating 532nm confocal excitation beam is used for both trapping and measuring, and each TRiC complex is trapped until complete photobleaching of the Cy3 occurs. The number of photobleaching steps in the fluorescent intensity trace yields the number of hydrolyzed ATPs. In a separate measurement the total number of TRiCs and the number of TRiCs with one or more ATPs are determined. From these measurements, we obtain the distribution of the number of ATPs on each TRiC at different incubation ATP concentrations. As the ATP concentration increases from 25uM, the position of the major peak remains at 7-8 ATP/chaperonin while the height of the peak increases. For ATP concentrations above 200uM, all the TRiCs are found to have 7-8 ATP bound with a smaller probability of 6 or 9 ATP bound, and no other peak appears up to an ATP concentration of 1.5mM, suggesting each ring hydrolyzes at most 4 ATP. Only when the ATP concentration is lower than 25uM does the peak position move to smaller numbers. While the averages of our distributions can be fit with MWC model, the distributions themselves depart from the model. This new method may be applied to study the cooperativity behavior of other multi-subunit enzymes.

1159-MiniSymp
Reconstituting EphA2-Ephrin Signaling with Supported Membranes
Jay T. Groves, **Rebecca Petit**.
UC Berkeley, Berkeley, CA, USA.
The Eph family of receptor tyrosine kinases mediates cell patterning and tissue organization via their ability to govern intercellular interactions. Eph activation occurs when cell surface Eph receptors encounter their ligands, the ephrins, presented on the membrane of an adjacent cell. The resultant intracellular signaling strongly influences whether the eventual outcome of the cell-cell contact event will be adhesion or repulsion. Here, we examine the complex interplay between spatial, mechanical and biochemical regulation mechanisms in EphA2 signaling.
We recapitulate the native intercellular signaling geometry using a hybrid junction between live human breast cancer cells expressing EphA2 and a supported membrane functionalized with ephrin-A1. After cells contact the membrane for 1 hour, we observe spatial reorganization of EphA2-ephrin-A1 complexes on multiple lengthscales as well as pronounced changes in cell shape and signaling activity.
To further probe the reorganization phenomenon, we have investigated a panel of membrane-associated effector proteins with functions associated with motility and cytoskeletal remodeling to determine how they are affected by EphA2 reorganization. These observations provide new insight regarding the cellular transduction of spatio-mechanical feedback into biochemical signaling.

1160-MiniSymp
Engineering Vesicle Membranes for Cellular Reconstitutions
David L. Richmond, Eva M. Schmid, Sascha Martens,
Jeanne C. Stachowiak, Nicole Liska, Daniel A. Fletcher.
UC Berkeley, Berkeley, CA, USA.
Cells routinely sample their local environment, process this information through internal signaling, and respond accordingly. However, the sheer complexity that underlies cellular behavior makes cells notoriously difficult to understand and control. To address these issues, traditional cell biological approaches are often complemented with in vitro reconstitutions aimed at building 'cell-like' systems from individual components. Such reconstitutions can provide functional insights into biological processes and have great potential for improving drug delivery. However, these studies are still limited by the technical challenge of assembling giant lipid vesicles with embedded transmembrane (TM) proteins and complex cytosolic components.
Here we present a method for incorporating TM proteins into giant unilamellar vesicles (GUVs) with simultaneous control over the encapsulated components. This method is an extension of a previously developed microfluidic jetting technique for creating GUVs from planar bilayers, analogous to blowing bubbles from a soap film. The technique can now be used to incorporate TM proteins with controlled orientation and create an asymmetric lipid bilayer composition in order to assemble increasingly sophisticated 'cell-like' systems.
With this approach, we demonstrate encapsulation of small unilamellar vesicles (SUVs) carrying the vesicular fusion machinery (vSNAREs) into GUVs carrying the target fusion machinery (tSNAREs), closely mimicking the organization of synaptic vesicles in cells. Using fluorescence microscopy we track the location of SUVs in the lumen of GUVs and study the role of vesicle docking in the process of SNARE-mediated membrane fusion.

1161-MiniSymp
A Light-Gated, Potassium-Selective Glutamate Receptor for the Optical Inhibition of Neuronal Firing
Harald Janovjak[1], Dirk Trauner[2], Ehud Y. Isacoff[1].
[1]UC Berkeley, Berkeley, CA, USA, [2]University of Munich, Munich, Germany.
Genetically-targeted, light-activated ion channels and pumps have recently made it possible to manipulate activity in specific neurons and thereby probe their role in neuronal circuits, information processing and behavior. Here, we describe the development of a K+-selective ionotropic glutamate receptor that inhibits nerve activity in response to light. The receptor is a chimera of the pore region of a K+-selective bacterial glutamate receptor and the ligand binding domain of the light-gated mammalian kainate receptor LiGluR (iGluR6/GluK2). This new hyperpolarizing light-gated channel is turned ON and OFF by brief light pulses even at moderate light intensities. After optical activation the silencing of neuronal activity persist in the dark for extended periods, a feature that will prove advantageous for the dissection of neural circuitry in behaving animals.

1162-MiniSymp
Computational Nanomedicine: Simulating Protein Misfolding Disease
Vijay Pande.
Stanford Univ, Stanford, CA, USA.
Protein misfolding diseases such as Alzheimer's Disease (AD) and Huntington's Disease (HD) are challenging to study experimentally. Thus, computational methods, if they are able to be sufficiently accurate and reach sufficiently long timescales, can naturall contribute in this challenging area. I will discuss our recent results using novel methods within the Folding@home distributed computing project on progress towards a molecular understanding of protein aggregation involved in AD and HD. Specifically, I will detail our extensions to simulation Markov State Model methodology as well as specific predictions that arose from these simulations and experimental validation of these predictions. These results lead to a novel hypothesis for the structural basis of Abeta aggregation as well as the ability to explain existing experimental data.

Platform X: Membrane Protein Functions

1163-Plat
Using Giant Uni-Lamellar Vesicles to Study Ion Channel Activity and Interactions
Sophie Aimon, **Gilman ES Toombes**, Patricia Bassereau.
Institut Curie, Paris, France.
Unraveling the complicated dynamics of ion channel activity and interactions requires experimental systems in which ion channel activity and distribution can be measured while controlling ion channel concentration and membrane composition, tension and voltage. Many of the constraints imposed by existing techniques, such as planar Black Lipid Membranes (BLM), could potentially be circumvented by using Giant Uni-Lamellar Vesicles (GUVs). To explore this possibility, a method was developed to produce GUVs containing KvAP, a bacterial voltage-gated potassium channel [1]. Protein was first purified, fluorescently labeled and reconstituted into Small Unilamellar Vesicles (SUVs) which were then used to grow GUVs via an electro-formation procedure [2]. Incorporation of the fluorescently-labeled channels was confirmed via confocal microscopy while channel activity was studied with the patch-clamp technique. In parallel, attempts were made to adapt the "whole-cell" patch-clamp geometry for GUVs. While the absence of a cytoskeleton made the "whole-GUV" configuration quite difficult, this geometry is possible and its further development is important since it permits simultaneous control of the voltage inside the GUV and measurement of the entire membrane current. These results confirm the potential of GUVs for ion channel studies, and experiments measuring the effect

of membrane tension, composition and curvature on KvAP activity and distribution are currently underway.

[1] Ruta et. al., Nature, Volume 422, p180-185 (2003)
[2] Montes et. al., Biophysical Journal, Volume 93, p3548-3554 (2007).

1164-Plat
Lipid Membrane Composition has A Dramatic Effect on the Dynamics of the GlpG Rhomboid Protease from Escherichia Coli

Ana Nicoleta Bondar, Stephen H. White.
University of California at Irvine, Irvine, CA, USA.

Intramembrane proteases cleave transmembrane substrates to liberate physiologically important molecules. The proteolytic activity of these enzymes can be significantly influenced by the composition of the lipid membrane. Here, we find that the composition of the lipid membrane has a dramatic effect on the motions of the GlpG rhomboid serine protease from Escherichia coli.

In a 1-palmytoyl-2-oleoyl-sn-glycero-3-phosphatidylcholine (POPC) lipid bilayer, conformational changes of two critical structural elements of the protease, the cap loop close to the active site and the regulatory loop L1, occur within 40ns of unconstrained molecular dynamics simulations. In contrast, in a 1-palmytoyl-2-oleoyl-sn-glycero-3-phosphatidylethanolamine (POPE) lipid bilayer, a conformational transition of the cap loop is observed only after ~80ns, ~20ns after that of loop L1. This sensitivity of the enzyme motions on the lipid membrane composition is explained by differences in how POPC and POPE lipid headgroups hydrogen bond among themselves, and with protein amino acids. Tight interactions between a lipid headgroup and the active site restrict the dynamics of the cap loop.

An atomistic description of the structure and dynamics of the protease:substrate complex is a critical first step towards understanding how the protease works. Molecular dynamics simulations of GlpG together with the Spitz model substrate reveal that docking of the substrate to the enzyme involves a complex interplay of changes in the structure and dynamics of the substrate, the protease, and the surrounding lipid molecules.

This research was supported in part by the National Institute of General Medical Sciences (GM-74637 to S.H.W) and an allocation of computer time from the National Science Foundation through the TeraGrid resources at TACC (Ranger).

1165-Plat
Energetics of Glycophorin A Dimerization in Mammalian Plasma Membranes

Lirong Chen, Lawrence J. Novicky, Mikhail Merzlyakov, **Kalina Hristova**.
Johns Hopkins University, Baltimore, MD, USA.

Quantitative measurements of protein interaction strengths are crucial for describing signaling networks and predicting cellular responses to environmental stimuli. Of all interactions between biological macromolecules, interactions between membrane proteins are the least characterized, and their strength is often measured in model detergent and lipid systems that poorly mimic the complex biological membrane. Measurements in models systems, however, are not likely to yield accurate predictions, because interactions in the native cellular environment occur within the context of a crowded system.

Here we explore the utility of plasma membrane-derived vesicles as a model crowded environment for quantitative characterization of membrane protein interactions in mammalian membranes. In particular, we study the dimerization energetics of Glycophorin A (GpA), the primary sialoglycoprotein of human erythrocyte membranes, using the "quantitative imaging Föster resonance energy transfer (QI-FRET)" method. We determine the FRET efficiency, and the donor and the acceptor concentrations in single plasma membrane-derived vesicles loaded with GpA. These measurements yield, for the first time, the free energy of GpA dimerization in mammalian membranes. Supported by NSF MCB-0718841.

Li E, Placone J, Merzlyakov M, Hristova K (2008) Quantitative measurements of protein interactions in a crowded cellular environment. *Anal Chem* 80: 5976-5985

1166-Plat
Monitoring Proton Flux Quantitatively; Influenza Proton Channel A/M2

Thom Leiding[1], Alexei Polishchuk[2], William DeGrado[2], Cecilia Hägerhäll[1], Sergei Vinogradov[2], **Sindra Peterson Årsköld**[1].
[1]Center for Chemistry and Chemical Engineering, Lund, Sweden,
[2]University of Pennsylvania, Philadelphia, PA, USA.

An improved methodology for monitoring proton translocation across membranes is presented, along with results from the Influenza A virus proton channel A/M2.

We have constructed a liposome-production instrument which creates proteoliposomes from a lipid/detergent/protein mixture by gradually adding hydrophobic beads while continuously monitoring sample turbidity. The method is fast and reproducible, and facilitates enhanced control of key protein reconstitution parameters. It also enables synchronous measurements of protein-mediated ion flow and passive permeability across the bilayer. Two novel pH-sensors are presented: Glu3 and TCHP. These porphyrin-based probes are membrane-impermeable, do not interact with biological complexes, have physiologically appropriate pK, and display high extinction coefficients. Glu3 is also ratiometric in emission.

H^+, K^+ and Na^+ permeabilities were determined in liposomes of different lipid and cholesterol composition. The effect of detergent/lipid and lipid/protein ratios on ion permeability was systematically investigated. The proton channel A/M2, key to Influenza A virus propagation and an antiviral drug target, was successfully reconstituted. The proton translocation rate was determined to 8.3 protons per second and A/M2 tetramer. We also found that the presence of protein in the bilayer enhanced the passive ion permeability. Lowering the protein/lipid ratio minimized this effect, and prolonged the measurement window of proton movements to several minutes, and thus resulted in the most reliable data.

Preliminary data from membrane-spanning subunits of respiratory Complex I are also presented.

1167-Plat
The Role of the Protein-Conducting Channel in the Membrane Insertion of Transmembrane Segments

James C. Gumbart[1], Christophe Chipot[2], Klaus Schulten[1].
[1]University of Illinois, Urbana-Champaign, Urbana, IL, USA,
[2]Nancy Université, Nancy, France.

In all domains of life, the majority of membrane proteins are inserted into the membrane via a protein-conducting channel, also known as the SecY or Sec61 complex. In addition to a translocation pathway across the membrane, this channel features a unique lateral gate, which can open toward the membrane, permitting the sequential insertion of transmembrane segments (TMs). How this insertion occurs is still unclear, although a thermodynamic partioning between channel and membrane environments has been proposed. However, experiment- and simulation-based scales for the free-energy insertion cost of various amino acids differ, sometimes significantly as in the case of arginine (2-3 kcal/mol in experiment compared to 17 kcal/mol in simulation). Using free energy perturbation (FEP) simulations, we have calculated the insertion cost for an arginine located on a background poly-leucine helix, both in the center of a pure bilayer and in the center of a model of SecY featuring an open lateral gate. We find that the presence of SecY greatly reduces the membrane insertion cost for arginine, in agreement with prior simulations. We also consider the free energy cost for the insertion of the background helix from SecY to the membrane, which had been neglected previously.

1168-Plat
Nature as A Scaffold: The Rational Redesign of a Protein Pore

Khalil R. Howard, Mohammad M. Mohammad, Liviu Movileanu.
Syracuse University, Syracuse, NY, USA.

Our major goal is to engineer a transmembrane protein pore that acts as a single-molecule nanopore probe for sensing double-stranded DNA (dsDNA), folded proteins and their complexes with interacting agents. The protein of choice is Ferric hydroxamate uptake protein component A (FhuA), a multifunctional outer membrane protein found in E. coli., which facilitates the uptake of Fe^{3+}, along with phage binding and the translocation of small peptides. Using standard protein engineering, we modified the FhuA protein by removing the N-terminal 160 residue-long cork and by deleting several large extracellular loops to form an open protein pore with an elliptical cross section of ~ 49 x 36 Å. This engineered protein nanopore exhibits a stable open-channel activity for long periods of time, with a unitary conductance of ~5 nS. We show evidence that this engineered FhuA-based nanopore acts as a stochastic sensing element for detecting small folded proteins at single-molecule resolution.

Acknowledgements. This research was supported by grants from the National Science Foundation (DMR-0706517 and HRD-0703452) and the National Institutes of Health (R01 GM088403) as well as by Syracuse Biomaterials Institute (SBI).

1169-Plat
Modulation of the Lateral Mobility of Transmembrane Peptides with Hydrophobic Mismatch

Yann Gambin[1], Myriam Reffay[1], Emma Sierecki[2], François Homblé[3], Marc Genest[4], Robert S. Hodges[4], Nir Gov[5], **Nicolas Taulier**[6], Wladimir Urbach[7].
[1]Laboratoire de Physique Statistique de l'Ecole Normale Supérieure, Paris, France, [2]CNRS-Université Paris5, Paris, France, [3]Université Libre de Bruxelles, Bruxelles, Belgium, [4]University of Colorado, Denver, CO, USA, [5]The Weizmann Institute of Science, Rehovot, Israel, [6]CNRS - UMPC Paris,

Paris, France, [7]Laboratoire de Physique Statistique de l'Ecole Normale Supérieure, Paris, France.
An hydrophobic mismatch between protein length and membrane thickness can lead to a modification of protein conformation, function, and oligomerization. To study the role of hydrophobic mismatch, we have studied the change in mobility of transmembrane peptides in model bilayers. The studied peptides possess an hydrophobic helix of various length $d\pi$, and the hydrophobic thickness, h, of the bilayers can be tuned at will. For each mismatch value, using Fluorescence Recovery After Pattern Photobleaching (FRAPP), we precisely measured the diffusion coefficient D of the embedded objects and gained access to their apparent size. This enables us to observe the orientation or oligomerization state of the peptides versus their concentration, and discover that the effects of positive and negative mismatches on diffusion are highly asymmetric. For bilayers thinner than $d\pi$, the diffusion coefficient decreases and the derived characteristic sizes are larger than the peptide radii. As suggested by previous studies, the peptides should accommodate by tilting, and this scenario was confirmed by ATR-FTIR spectroscopy. As the membrane thickness increases, the value of the diffusion coefficient increases: the peptides raise (i.e. their tilt is reduced) and reach an upright position and a maximal mobility for $h \approx d\pi$. Using accessibility measurements, we show that when the membrane becomes too thick, the peptide polar heads sink into the interfacial region. Surprisingly, this "pinching" behavior does not hinder the lateral diffusion of the transmembrane peptides. But it creates interactions between the embedded peptides, and collective behaviors emerge. For low peptide concentration, the transmembrane anchorage of the peptide is broken as the bilayer is swollen. For intermediate concentrations, we observed the arrangement of small monodisperse clusters, while polydisperse macro-domains are formed at higher peptide density, leading to spontaneous and reversible formation of "vesicles".

1170-Plat

The Gating Mechanism of Yeast Aquaporin Studied by Molecular Dynamics Simulations

Gerhard Fischer[1], Urszula Kosinska-Eriksson[1],
Camilo Aponte-Santamaria[2], Madelene Palmgren[3], Cecilia Geijer[3], Kristina Hedfalk[1], Stefan Hohmann[3], Bert L. de Groot[2], Richard Neutze[1], Karin Lindkvist-Petersson[3].
[1]Department of Chemistry, Biochemistry and Biophysics, University of Gothenburg, Gothenburg, Sweden, [2]Computational Biomolecular Dynamics Group, Max Planck Institute for Biophysical Chemistry, Goettingen, Germany, [3]Department of Cell and Molecular Biology, University of Gothenburg, Gothenburg, Sweden.
Aquaporins are membrane proteins responsible for the permeation of water and other solutes through the cell membrane. They arrange in a tetrameric conformation, where each monomer acts as a highly efficient single-file water channel. The x-ray structure of the yeast aquaporin (Aqy1), recently found at a very high resolution (1.15 Angstrom), revealed the conformation of the extended N-terminus - an unusual feature within the family of aquaporins - occluding the water pore. In contrast, functional assays with spheroplast of P. pastoris showed a substantial increase in the water transport activity when Aqy1 was present compared to an assay where Aqy1 was deleted, indicating that Aqy1 is a gated water channel. Here we address the question of a putative gating mechanism of Aqy1 by using molecular dynamics simulations. Our findings suggest that Aqy1 may be regulated by both phosphorylation of a serine residue (Ser107) or membrane-mediated mechanical stress. Both possibilities lead to similar opening transitions after a local rearrangement of the residues Tyr31, Leu189, Ala190 and Val191, located in the gate of the pore. We observed that there is a principal collective motion causally involved in these gating transitions, and that is possible to attain reproducible opening events along this collective coordinate. The simulation results are therefore consistent with a mechanism in which both phosphorylation and mechanosensitive gating can trigger the channel opening. Aqy1 regulation may help yeast to survive rapid freezing and thawing, and sudden osmotic changes.

Platform Y: Protein Dynamics I

1171-Plat

Protein Similarity Derived Solely from Molecular Dynamics

Philip C. Biggin, Rune Lyngsø, Jotun Hein, Márton Münz.
Oxford University, Oxford, United Kingdom.
The dynamic motions of many proteins are central to their function. It therefore follows that the dynamic requirements of a protein are evolutionary constrained. In order to assess and quantify this, one needs to compare the dynamic motions of different proteins. Comparing the dynamics of distinct proteins may also provide insight into how protein motions are modified by variations in sequence and, consequently, by structure. The optimal way of comparing complex molecular motions is, however, far from trivial. The majority of comparative molecular dynamics studies performed to date relied upon prior sequence or structural alignment to define which residues were equivalent in 3-dimensional space. Here we discuss an alternative methodology for comparative molecular dynamics that does not require any prior alignment information. We show it is possible to align proteins based solely on their dynamics and that we can use these dynamics-based alignments to quantify the dynamic similarity of proteins. Our method was tested on 10 representative members of the PDZ domain family. As a result of creating pairwise dynamics-based alignments of PDZ domains, we have found evolutionarily conserved patterns in their backbone dynamics. We compare the results to other recently developed methods.

1172-Plat

Structure Fluctuations in Proteins and their Relationship to Amino Acid Propensities

Anatoly M. Ruvinsky[1], Ilya A. Vakser[2].
[1]Center for Bioinformatics, The University of Kansas, Lawrence, KS, USA, [2]Center for Bioinformatics and Department of Molecular Biosciences, The University of Kansas, Lawrence, KS, USA.
The spectrum and scale of fluctuations in protein structures affect the range of cell phenomena, including stability of protein structures or their fragments, allosteric transitions and energy transfer. The study presents a statistical-thermodynamic analysis of relationship between the sequence composition and the distribution of residue fluctuations in protein-protein complexes [1]. A one-node-per-residue elastic network model accounting for the nonhomogeneous protein mass distribution and the inter-atomic interactions through the renormalized inter-residue potential is developed. Two factors, a protein mass distribution and a residue environment, were found to determine the scale of residue fluctuations. Surface residues undergo larger fluctuations than core residues, showing agreement with experimental observations. Ranking residues over the normalized scale of fluctuations yields a distinct classification of amino acids into three groups: (i) highly fluctuating - Gly, Ala, Ser, Pro and Asp, (ii) moderately fluctuating - Thr, Asn, Gln, Lys, Glu, Arg, Val and Cys (iii) weakly fluctuating - Ile, Leu, Met, Phe, Tyr, Trp and His. The structural instability in proteins possibly relates to the high content of the highly fluctuating residues and a deficiency of the weakly fluctuating residues in irregular secondary structure elements (loops), chameleon sequences and disordered proteins. Strong correlation between residue fluctuations and the sequence composition of protein loops supports this hypothesis. Comparing fluctuations of binding site residues (interface residues) with other surface residues shows that, on average, the interface is more rigid than the rest of the protein surface and Gly, Ala, Ser, Cys, Leu and Trp have a propensity to form more stable docking patches on the interface. The findings have broad implications for understanding mechanisms of protein association and stability of protein structures.

1. A.M. Ruvinsky and I.A. Vakser. arXiv:0907.5021v1

1173-Plat

Direct Observation of Ligand Dynamics in Cytochrome *C* Using Time-Resolved FTIR Spectroscopy

Joerg Zimmermann, Megan C. Thielges, Floyd E. Romesberg.
The Scripps Research Institute, La Jolla, CA, USA.
Horse heart cytochrome *c* (cyt c) has emerged as a paradigm for the study of protein folding. The folding of reduced cyt *c* induced by photodissociation of CO from the CO-bound unfolded protein has been studied extensively. Following a nanosecond light pulse, four transitions have been resolved with time constants of approximately 1-5, 50-100, 200-500, and 1000-10,000 μs. While originally thought to be associated with CO rebinding to two different partially folded states of cyt *c*, the two slower process are now understood to reflect the bimolecular reassociation of CO followed by religation of the His18, which by the base elimination mechanism is induced to dissociate after CO photolysis. Thus, the two slower time constants turn out not to report on protein folding, but instead reflect the complexity of heme ligation. The two faster time constants have been attributed to ligation at the heme center by protein side chains. Here, to unambiguously determine the post-photodissociation steps involving CO, we monitored the CO vibration following photodissociation with step-scan FT IR spectroscopy. We find that like the slower timescale processes, the 50-100 μs timescale process is associated not with protein dynamics, but with CO ligand dynamics. The data clearly demonstrate that whatever the origins of the spectral changes, they clearly involve CO rebinding or changes in the environment of an already bound CO ligand. In addition to these fast dynamics, we also find multi-phasic CO rebinding on timescales of 1-100 s. The dependence of the associated amplitudes on denaturant concentration suggests that a unique species exists at intermediate denaturant concentrations, consistent with a folding-unfolding process of the protein driven by CO dissociation. This may

represent the first evidence for the long sought-after protein folding process triggered by photo-induced CO dissociation.

1174-Plat
Phosphorescence from Single Tryptophan in Amorphous Solid Human Serum Albumin Exhibits Solvent-Protein Dynamics Slaving

Andrew Draganski, **Richard D. Ludescher**.
Rutgers University, New Brunswick, NJ, USA.

The physical properties of amorphous biomolecules are important to the texture and stability of low-moisture foods, the stability of pharmaceuticals, the permeability of edible films, and the viability of organisms during anhydrobiosis. Protein stability is often improved via the inclusion of small-molecule excipients during freeze-drying and organisms overproduce sugars such as sucrose or trehalose during anhydrobiosis. The effect on internal protein dynamics caused by substitution of a protein's surface water molecules with small sugar molecules is unclear. To explore this question, we have analyzed tryptophan phosphorescence decays of human serum albumin (HSA) in the dry amorphous solid state. Phosphorescence is an ideal approach, as the long-lived triplet state of tryptophan is sensitive to the long time-scale molecular motions of proteins in the dry state. Human serum albumin (HSA) was chosen because it contains a single, buried tryptophan residue and thus can provide information on the local dynamics of a specific site in the interior of the protein. Amorphous protein films were prepared by spreading concentrated solutions of HSA with and without sugar onto quartz slides, followed by rapid drying and extensive desiccation. Phosphorescence intensity decays were collected and fit with multiple exponential functions. From the average lifetime of these fits the rates of nonradiative decay (kNR) of the triplet state were calculated; kNR is dependent on the microviscosity of the site and is thus a measure of molecular mobility of the HSA tryptophan site. At all temperatures this measure of molecular mobility was lower in the films containing sucrose. Break-point analysis of a kNR Arrhenius plot revealed two temperature regimes with a transition occurring at the glass transition temperature of sucrose. Research supported in part by the National Research Initiative of USDA-CSREES.

1175-Plat
Structural Dynamics of Light-Driven Proton Pumps

Magnus Andersson[1], Erik Malmerberg[2], Sebastian Westenhoff[2], Gergely Katona[2], Marco Cammarata[3], Annemarie B. Wohri[2], Linda C. Johansson[2], Friederike Ewald[4], Mattias Eklund[5], Michael Wulff[4], Jan Davidsson[5], Richard Neutze[2].
[1]University of California at Irvine, Irvine, CA, USA, [2]Gothenburg University, Gothenburg, Sweden, [3]European Synchrotron Radiation Facility, Grenoble, France, [4]European Synchrotron Radiation Facility, Grenoble, Sweden, [5]Uppsala University, Uppsala, Sweden.

In a recent publication (Andersson et al. (2009) *Structure*. 17(9):1265-75), we applied the emerging technique of time-resolved wide-angle X-ray scattering (TR-WAXS) to visualize the structural dynamics of two light-driven proton pumps, namely bacteriorhodopsin and proteorhodopsin, in real-time. Direct structural information was obtained over a time course of 360 ns to 100 ms. Our results establish that three conformational states are required to describe the respective photocycles of both proteins. Significant motions of the cytoplasmic half of helix F and the extracellular half of helix C are observed prior to the primary proton transfer event, which increase in amplitude following proton transfer. These results both simplify the structural description that have emerged from a range of biophysical techniques and reveal shared dynamical principals for proton pumping. Moreover, the measured magnitudes of the helical movements associated with the bacteriorhodopsin photocycle are larger than those anticipated by intermediate trapping studies. This demonstrates the effect of a crystal lattice on protein dynamics and shows the advantage of direct measurements in solution at room temperature.

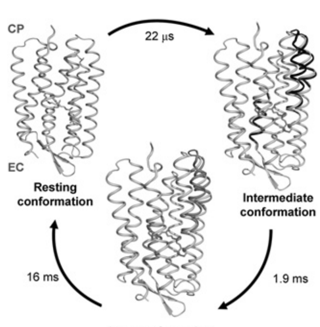

Figure 1. Schematic showing the observed helical rearrangements during the photocycle of bacteriorhodopsin.

1176-Plat
Mechanoenzymatics and Protective Mechanisms of Titins' Catalytic and IG Domains

Ulf Hensen[1], Lars Schaefer[1], Frauke Graeter[1], Joao M. Nunes[2], Daniel J. Mueller[2], **Helmut Grubmueller**[1].
[1]Max-Planck-Institute for Biophysical Chemistry, Goettingen, Germany, [2]Biotechnology Center, University of Technology, Dresden, Germany.

The giant titin filament controls many structural and functional properties of the sarcomere. Titin filaments connect M-line and Z-disc of the sarcomere and consist of four regions: the M-line, A-band, I-band, and Z-line. The different domains of titin (mainly immunoglobulin Ig and fibronectin-3 domains, and the catalytic domain titin kinase (TK)) exhibit dramatically different mechanical properties. We used atomistic molecular dynamics simulations to explore the coupling of mechanical stability with the enzymatic activity of titin kinase and the protective properties of Ig-domains. We showed that a unique autoinhibitory mechanism allows TK to act as a molecular force sensor, as relatively low forces already remove the autoinhibitory tail and prime the molecule for ATP binding. At much higher forces, the mechanical stability of Ig27 becomes important: In our studies, extensive dynamic force spectroscopy (DFS), Brownian dynamics, and molecular dynamics simulations worked together to examine mechanical stability of Ig27 under different loading rates. Our results suggest that Ig27 is perfectly suited to act as a molecular force buffer over a wide range of loading rates.

1177-Plat
Dynamics of apoB100-Containing Lipoproteins Determined by Incoherent Elastic Neutron Scattering

Christian Mikl[1], Judith Peters[2,3], Markus Trapp[2], Giuseppe Zaccai[4], **Ruth Prassl**[1].
[1]Institute of Biophysics and Nanosystems Research, Graz, Austria, [2]Institut de Biologie Structurale, Grenoble, France, [3]Université Joseph Fourier, Grenoble, France, [4]Institut Laue Langevin, Grenoble, France.

Apolipoprotein B100 (apoB100)-containing lipoproteins (very low density lipoprotein (VLDL) and low density lipoprotein (LDL)) are the principal fat and cholesterol carriers in blood. During metabolic conversion from VLDL to LDL, the particle size decreases (from ~ 80 nm to 20 nm) and lipid composition is changed, however, the amphiphilic apoB100 molecule remains bound to its lipoprotein particle and most likely compensates for structural changes due to its inherent conformational flexibility and dynamics .

Here, we report on motions in the time range of 100 ps to 1 ns in human-LDL, human VLDL and yolk-VLDL, which were recorded by elastic neutron-scattering temperature scans from 20K to 310 K using hydrated lipoprotein powders. The mean square displacement values $\langle u^2 \rangle$ were calculated from the scattering vector dependence of the elastic intensity *I(Q)*. The effective force constants $\langle k \rangle$, which are a measure for the resilience of the particle, were derived from the slopes in the $\langle u^2 \rangle$ vs. T scans. In the low-temperature harmonic regime we found no substantial differences between lipoprotein fractions ($\langle k \rangle$ ~1 N/m). Nevertheless, lipoproteins are softer compared to hydrated myoglobin powder (2 N/m) or purple membranes (1.7 N/m) [1]. Significant differences were observed with increasing temperatures. Both, human and yolk VLDL show two breaks in the scan with a steep increase in $\langle u^2 \rangle$ above 270K, whereas LDL shows a smooth behavior above a dynamic transition around 220K. Accordingly, at physiological temperatures VLDL-fractions are highly soft and mobile ($\langle k'' \rangle$ ~0.08 N/m) as compared to LDL ($\langle k' \rangle$ ~ 0.2 N/m). Sucrose, added as cryoprotectant, significantly modified the dynamics of VLDL, as it confers extreme stability to VLDL over the whole temperature range and substantially suppresses dynamic transitions.

[1] G. Zaccai, Science 288 (2000), 1604-1607

1178-Plat
Valine-Induced Packing Deficiencies of Transmembrane Domains Promote Helix Flexibility and Membrane Fusion

Christina Scharnagl, Stefan Quint, Simon Widmaier, Dieter Langosch.
Technical University Munich, Freising, Germany.

The helical transmembrane domains of fusion proteins are known to be functionally important and display an overabundance of helix-destabilizing Ile and Val residues. In an effort to systematically study the relationship of helix flexibility and fusogenicity, synthetic LV-peptides were designed whose hydrophobic core consists of Leu and Val residues at different ratios and at different positions (Hofmann et al., 2004; Poschner et al., 2009). The ability of the LV-peptides to fuse membranes increases with the content of helix-destabilizing residues. Molecular dynamics simulations were performed in order to characterize the backbone dynamics of these peptides in membrane-mimicking 80% TFE solvent and to relate the hydrogen-bond dynamics to experimental deuterium/hydrogen exchange kinetics. The analysis revealed that (i) the backbone dynamics of the helices increases systematically with Val content, (ii) that the impact of Val is due to stereochemical constraints within the helical structure and (iii) that side-chain packing mainly determines exchange kinetics. As a consequence, VxxV and VVxVV motifs promote helix destabilization whose relevance for membrane fusogenicity will be discussed.

Hofmann, M.W., K. Weise, J. Ollesch, A. Agrawal, H. Stalz, W. Stelzer, F. Hulsbergen, H. deGroot, K. Gerwert, J. Reed, and D. Langosch. 2004. De novo design of conformationally flexible transmembrane peptides driving membrane fusion. Proc. Natl. Acad. Sci. U S A 101:14776-14781.
Poschner, B.C., S. Quint, M. Hofmann, and D. Langosch. 2009. Sequence-specific conformational dynamics of model transmembrane domains determines their membrane fusogenic function. J. Mol. Biol. 386:733-741.

Platform Z: Mechanosensitive & TRP Channels

1179-Plat

Outer Pore Domain of TRPV1 Ion Channel is Required for Temperature-Independent Step During Temperature-Activation

Jorg Grandl[1], Sung Eun Kim[1], Valerie Uzzell[1], Badry Bursulaya[2], Matt Petrus[2], Michael Bandell[2], Ardem Patapoutian[1].
[1]The Scripps Research Institute, La Jolla, CA, USA, [2]Genomics Institute of the Novartis Research Foundation, La Jolla, CA, USA.

TRPV1 is the founding and best-studied member of the family of temperature-activated transient receptor potential ion channels (thermoTRPs). Voltage, chemicals, and heat allosterically gate TRPV1. Molecular determinants for TRPV1 activation by capsaicin, allicin, acid, ammonia, and voltage have been identified. However, many years after the discovery of TRPV1, the structures and mechanisms mediating temperature-sensitivity remain unclear. Recent studies of the related channel TRPV3 identified residues within the pore region required for heat activation. Here we describe both random and targeted mutagenesis screens of TRPV1 to identify single point-mutations that specifically affect temperature-activation. The mutations found are all located in the outer pore region, in close proximity to but distinct from residues previously implicated in acid-activation. Electrophysiological analysis shows that mutations affect a temperature-independent step that is part of the temperature-gating pathway. These results suggest that the outer pore plays a general role in heat-sensitivity of thermoTRPs.

1180-Plat

Temperature-Driven Activation of Thermotrps: A Distinct Pathway Involved

Fan Yang[1], Yuanyuan Cui[1,2], Kewei Wang[2], Jie Zheng[1].
[1]University of California, Davis, Davis, CA, USA, [2]Peking University Health Science Center, Beijing, China.

A group of thermosensitive transient receptor potential (ThermoTRP) channels, with high temperature sensitivity of channel gating, are the cellular temperature sensors. ThermoTRPs are polymodal receptors. Besides temperature they are gated by voltage, ligand, extracellular pH and other stimuli. How temperature changes drive activation conformational rearrangement remains unknown. Here we combine functional, mutational, and site-directed fluorescence studies to demonstrate that temperature-dependent activation uses a pathway distinct from those for ligand- and voltage-dependent activation.

We observed that neither strong depolarization nor application of capsaicin could significantly alter thermodynamics of temperature-driven TRPV1 activation. In addition, voltage and ligand exhibited additive gating effects over temperature gating. Indeed, a TRPV1 mutant in which part of the outer pore region was replaced by an artificial sequence showed virtually no temperature sensitivity but maintained near normal capsaicin sensitivity. Furthermore, site-directed FRET measurements showed that conformational changes in outer pore can only be induced by heating, but not by voltage or ligand. Together these observations suggest that a distinct pathway for temperature to gate TRPV1 involves the outer pore region.

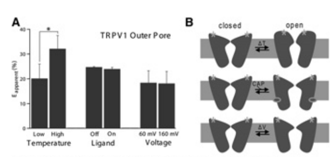

(A) FRET measurements. Fluorophores were attached to outer pore region of TRPV1. "Low" means temperature lower than 25°C, "High" means temperature above 40°C. 10 μM capsaicin is "Off" or "On". * indicates $P < 0.05$ (B) A schematic representation of the proposed gating conformational changes in TRPV1 induced by heat and capsaicin. The green stars represent fluorophores attached to the outer pore.

1181-Plat

Role Of Pip2 On Ca^{2+}-Dependent Desensitization of Trpv2

Jose Mercado, William N. Zagotta, Sharona E. Gordon.
University of Washington, Seattle, WA, USA.

TRPV2 is a member of the transient receptor potential superfamily of ion channels involved in chemical and thermal pain transduction. Unlike the related TRPV1 channel, TRPV2 does not appear to bind either calmodulin or ATP in its N-terminal ankyrin repeat domain. In addition, it does not contain a calmodulin-binding site in the distal C-terminal region, as has been proposed for TRPV1. Importantly, though, we have found that TRPV2 undergoes Ca^{2+}-dependent desensitization similar to TRPV1, suggesting that the mechanism of desensitization may be conserved in the two channels. To elucidate the molecular mechanism underlying Ca^{2+}-dependent desensitization in TRPV2 we used whole-cell recordings of F-11 cells transiently transfected with TRPV2. We found that prolonged applications of the TRPV2 agonist 2-APB led to nearly complete desensitization of the channel in the presence of extracellular Ca^{2+}. In contrast, no desensitization was observed in the absence of Ca^{2+}. TRPV2 desensitization was not altered in whole-cell recordings in the presence of calmodulin inhibitors or upon co-expression of mutant calmodulin, suggesting that CaM does not play a major role in Ca^{2+}-dependent desensitization of TRPV2. Interestingly, simultaneous confocal imaging and electrophysiological recording of whole cells expressing TRPV2 and a fluorescent PI(4,5)P2 binding probe showed a high degree of temporal correlation between the Ca^{2+} induced desensitization and depletion of PI(4,5)P2. Thus, Ca^{2+} influx through TRPV2 is sufficient to trigger a dramatic decrease in PI(4,5)P2 levels, presumably by activating PLC. We propose that the decrease in PI(4,5)P2 levels upon channel activation underlies at least a major component of Ca^{2+}-dependent desensitization of TRPV2.

1182-Plat

TRPM8 Cation Channel. Effects of Voltage, Cold and Menthol on Single-Channel Gating

Jose A. Fernandez, C. Norman Scholfield, J. Graham McGeown, Alexander V. Zholos.
Queen's University of Belfast, Belfast, United Kingdom.

Single-channel patch-clamp recording allows mechanistic insights into fundamental ion channel properties. Thus, a single kinetic model can formally describe the complex interactions during poly-modal activation of the channels. For TRPM8, activation depends on temperature, voltage and chemical signaling [1, 2], and such modeling provides the most comprehensive approach to the study of the channel. In this study, we examined the influence of voltage, cold and menthol on TRPM8 gating using patch-clamp recording techniques. In HEK293 cells stably expressing TRPM8, single-channel currents were measured (filtered at 2 kHz and sampled at 10 kHz) in cell-attached patches at different voltages (-100 to 140 mV), temperatures (20 or 30°C) and menthol concentrations (10 or 100 μM) ($n = 7$-11). As has been reported for whole-cell TRPM8 currents [3], shifts in the voltage-dependent single-channel open probability curve toward less positive potentials were induced by cold or menthol. Thus, the potential for half-maximal activation was reduced from 162.4 to 116.1 mV during cooling from 30 to 20°C, with a further shift to 52.8 mV with 100 μM menthol. To investigate the relationship between these modulators, we used different techniques - HJCFIT [4], QuB [5] and 2D fitting [6] - to develop a single-channel kinetic model aiming to identify the most likely potential-, menthol- and cold-regulated transitions. A model with 5 closed and 2 open states showing correlation between brief openings and long closings and between brief closings and long openings, was able to describe our macroscopic and single-channel data. Interestingly, temperature and menthol mimicked voltage-dependent activation of the channel at the model level by increasing the probability of transitions from long closed states to brief ones. This is the first complete kinetic model based on single-channel data for any of the TRP channels.

1183-Plat

Phosphoinositide Regulation of TRPM8 Channels in Planar Lipid Bilayers

Eleonora Zakharian, Tibor Rohacs.
UMDNJ New Jersey Medical School, Newark, NJ, USA.

The cold and menthol receptor TRPM8 is regulated by membrane phosphoinositides. To study the effects of lipids directly on the channel, we have reconstituted the purified TRPM8 in planar lipid bilayers. This system allows full control of the lipid composition in our experiments. The reconstituted channel was activated by menthol or cold, and its activity depended on the presence of specific phosphoinositides. In the presence of menthol, TRPM8 exhibited the highest probability of opening in the presence of phosphatidylinositol 4,5-bisphosphate [PI(4,5)P_2] with Po ~ 0.89 at $+100$ mV and Po ~ 0.4 at -100 mV. Less channel activity was induced by phosphatidylinositol 3,4-bisphosphate [PI(3,4)P_2] with Po ~ 0.53 at $+100$ mV and Po ~ 0.2 at -100 mV. Phosphatidylinositol 3,4,5-bisphosphate [PI(3,4,5) P_2] resulted in irregular TRPM8 channel currents and lower open probability with Po ~ 0.21 at $+100$ mV and Po ~ 0.087 at -100 mV. Among the tested lipids the lowest TRPM8 channel activity was induced by phosphatidylinositol 4-phosphate [PI(4)P] with Po ~ 0.12 at $+100$ mV and Po ~ 0.019 at -100 mV. The lipid specificity profile in lipid bilayers is very similar to that observed in excised patches. We have also studied the activation of TRPM8 channels in lipid bilayer with cold. Cooling the system with reconstituted TRPM8 channels also required the presence of PI(4,5)P_2. The main shift in the channel behavior was observed in the temperature range from 21°C to 18°C where the channel showed drastic changes in the open probability from 0.05 to 0.85 at $+100$ mV.

These results demonstrate that the TRPM8 protein is directly activated by cold, menthol and phosphoinositides.

1184-Plat

Activation of TRPML Channels in the Lysosome

Haoxing Xu, Xian-ping Dong, Dongbiao Shen, Xiang Wang.
Univ Michigan, Ann Arbor, MI, USA.

The mucolipin family of Transient Receptor Potential (TRPML) proteins is predicted to encode ion channels of intracellular endosomes and lysosomes. The physiological importance of TRPMLs has been established genetically. Mutations of human *TRPML1* cause type IV mucolipidosis (ML4), a devastating neurodegenerative disease; mutations in the mouse *TRPML3* result in the *varitint-waddler* (*Va*) phenotype with hearing and pigmentation defects. The broad-spectrum phenotypes of both ML4 and *Va* appear to result from certain aspects of endosomal/lysosomal dysfunction. Lysosomes, traditionally believed to be the terminal "recycle center" for biological "garbage", are now known to play indispensable roles in membrane traffic and multiple intracellular signaling pathways. The putative lysosomal function(s) of TRPML proteins, however, has been unclear until recently. Studies on animal models and cell lines in which TRPML genes have been disrupted or genetically depleted have discovered roles of TRPMLs in a variety of cellular functions including membrane traffic, signal transduction, and organellar homeostasis. Physiological assays on cells in which TRPMLs are heterologously over-expressed revealed the channel properties of TRPMLs, suggesting that TRPMLs mediate cation (Ca^{2+}/Fe^{2+}) efflux from endosomes and lysosomes in response to unidentified cellular cues. Using our recently developed lysosome patch-clamp technique, we screened a variety of cytosolic and luminal factors that are known to affect endolysosomal functions and have identified an endogenous agonist for TRPML channels. We are currently investigating the activation mechanism in detail.

1185-Plat

Structural Models of Two-Pore-Domain Potassium Channels Focus on TREK

Adina L. Milac[1], Andriy Anishkin[2], Sarosh N. Fatakia[3], Carson C. Chow[3], Sergei Sukharev[2], Robert H. Guy[1].
[1]National Cancer Institute, National Institutes of Health, Bethesda, MD, USA, [2]Department of Biology, University of Maryland, College Park, MD, USA, [3]National Institute of Diabetes and Digestive and Kidney Diseases, National Institutes of Health, Bethesda, MD, USA.

Two-pore-domain background potassium (K2P) channels comprise a distinct gene family of widely distributed, well modulated channels. K2P channels have two similar or identical subunits, each of which has four transmembrane (TM) and two pore-forming (P) segments. Here we focus on mechanosensitive TREK channels. Unfortunately, the only structures available to be used as templates belong to the 2TM channels superfamily. These are distantly related at sequence level with different structural features: four symmetrically arranged subunits, each having two TM segments flanking a P segment. Our model building strategy used two subunits of the template (KcsA) to build one subunit of the target (TREK-1). Our models of the closed channel differ substantially from those of the template, primarily because TM2 of the 2nd repeat is near the axis of the pore whereas TM2 of the 1st repeat is far from the axis. Segments linking the two subunits and immediately following the last TM segment were modeled *ab initio* as α-helices based on helical periodicities of hydrophobic and hydrophilic residues, highly conserved and poorly conserved residues, and correlated mutations in multiple sequence alignments. The N-terminus segment preceding residue 35, the long loop between first and second TM segments (residues 76-125), and C-terminus past residue 333 were not included in the model due to lack of template. Experimental analysis of the similarly-truncated channel with these loop and C-terminus residues deleted revealed near native-like behavior. The models were further refined by two-fold symmetry-constrained molecular dynamics simulations using a protocol we previously developed. We also built models of the open state and suggest a possible tension-activated gating mechanism in which the inner portion of the TM2 helix of the 2nd repeat swings radially outward. This mechanism will be tested experimentally.

1186-Plat

Electrostatic Interactions Between the Transmembrane and Cytoplasmic Domains Critically Stabilize Tension-Sensitive States in MSCS

Kenjiro Yoshimura, Kishore Kamaraju, Vladislav Belyy, Naili Liu, Andriy Anishkin, Sergei Sukharev.
University of Maryland, College park, MD, USA.

The small mechanosensitive channel MscS is a bacterial osmolyte release valve with homologs found in all walled organisms. E. coli MscS readily responds to abrupt steps of tension in the cytoplasmic membrane, but under sustained stimulation it enters the tension-insensitive inactivated state. Upon tension release, MscS recovers within 2 s. In the crystal structure of WT MscS, the gate region (end of TM3a) is the only connecting element between the transmembrane (TM) and the cytoplasmic (cage) domains. It has been predicted that the two domains can make additional contacts through salt bridges between D62 on the TM1-TM2 loop and the R128-R131 cluster on the cage. Our experiments show that disrupting this salt bridge with D62R(N) substitutions does not affect desensitization, but instead, it drastically speeds up the process of inactivation and decreases the rate of recovery. The mutations also open a path for silent inactivation at sub-threshold tensions bypassing channel opening. Swapping the charges (D62R/R131D) restores the normal inactivation phenotype. Our new models suggest that the D62-R128/131 bridge critically stabilizes the positions of the lipid-facing TM1-TM2 helices along central TM3s and their association through the F68-L111-L115 hydrophobic cluster which transmits force from the membrane to the gate, in both closed and open states. Simulations suggested that not only the G113 flexible region on TM3 is necessary for inactivation, but the G76 hinge on TM2 might be needed, too. Experiments confirmed that G76A substitution abolishes inactivation. Analyzing combined mutations with opposing effects on inactivation (D62N/G113A, D62N/G76A) reveals a strong contribution of the loop-cage interactions to the stability of tension-sensitive states. The predicted hinge action of G76 suggests that twisting of TM1-TM2 may be the inactivation mechanism that disrupts the bridges while disengaging these helices from the gate.

Platform AA: Unconventional Myosins

1187-Plat

News from the Myosin Tree: 1000 New Sequences, 100 New Species, 1 New Class

Martin Kollmar.
MPI for Biophysical Chemistry, Goettingen, Germany.

The myosins constitute one of the largest and most divergent protein families in eukaryotes. They are characterized by a motor domain that binds to actin in an ATP-dependent manner, a neck domain consisting of varying numbers of IQ motifs, and amino-terminal and carboxy-terminal domains of various length and function. Myosins are involved in many cellular tasks like organelle trafficking, cytokinesis, maintenance of cell shape, and muscle contraction. They are typically classified based on the phylogenetic analysis of the motor domain. In 2007, we have published the analysis of over 2200 myosins from more than 320 species that resulted in 35 myosin classes of which 16 had not been proposed before. Here, we present an update on the myosin tree that is now based on 3246 myosins from 422 species. All sequences were manually annotated and verified. Most of the newly sequenced species belong to taxa that have already been covered in the earlier analysis. However, 1 new class has been determined that is specific to metazoans. These class-36 myosins do not contain an N-terminal SH3-like domain and their tail consists of more than 10 transmembrane domains and a chitin synthase domain. In addition, the genome sequences of the amoeba Acanthamoeba castellanii and the coccolithophore Emiliana huxleyi revealed many new orphan myosins. All sequence related data is available via CyMoBase at www.cymobase.org.

1188-Plat

Processive Non-Muscle Myosin IIB Takes Load-Independent Backward Steps

Melanie Norstrom, Ronald S. Rock.
University of Chicago, Chicago, IL, USA.

Non-muscle myosin IIB (NMIIB) is a molecular motor involved in the regulation of cell polarity during cellular migration. NMIIB forms thick filaments like other members of the myosin II family. Recent studies have shown that a NMIIB dimer can bind both heads to actin simultaneously with different ADP release rates from leading and trailing heads. Gating of ADP release suggests that the two heads communicate with each other and may be capable of processive stepping. We performed single molecule optical trapping assays to examine the stepsize and dwelltime of NMIIB on actin filaments. Our results show that NMIIB is an unconventional myosin that walks processively by taking 5.5 nm backward and forward steps along the long-pitch helix of actin filaments. Forward steps and detachment are weakly force dependent, suggesting ADP release is the rate-limiting step in these transitions. Backward steps are independent of force, suggesting that backward steps occur before ADP release in the lead head. Nucleotide independent backstepping could be a common mechanism for back steps in myosin.

1189-Plat
Calcium Regulation of myo1b Tension Sensing
John H. Lewis, Joe Laakso, Tianming Lin, Henry Shuman, E. Michael Ostap.
University of Pennsylvania, Philadelphia, PA, USA.
We recently demonstrated that the widely expressed myosin-I isoform, myo1b, is exquisitely sensitive to tension (Laakso et al. 2008. Science. 321:133-6), where it transitions from a low duty-ratio to a high duty-ratio motor at very low opposing forces (< 1 pN). These forces are transmitted to the motor through the IQ-motif-containing light-chain-binding-domain (LCBD), which is structurally stabilized by calmodulin molecules. Calcium binding to these calmodulins affects the ATPase and motile properties of myo1b (Coluccio & Geeves. 1999. J. Biol. Chem. 274:21575-80). Using stopped-flow fluorescence, we confirmed that calcium accelerates the biochemical rates of phosphate and ADP release by 2 - 5 fold. We performed single molecule optical-trap experiments in the presence of 25 μM ATP and 0, 1 or 9 μM free calcium. At low forces in the presence of calcium, we found an acceleration of the actin detachment kinetics, which is consistent with stopped-flow measurements. We also found that the average displacement of the myo1b step decreases to ~ 0 nm. The decoupling of the LCBD displacement from the motor-domain kinetics prompted us to test how calcium impacts the force sensitivity of actin detachment kinetics. Using an isometric clamp, the addition of 9 μM calcium resulted in a 5-fold decrease in the distance parameter that describes force sensitivity. Finally, we measured the kinetics of calcium binding to myo1b and determined that it occurs in two steps. The first step is very fast and calcium dependent, while the second step is significantly slower and independent of calcium concentration. These results show clearly that calcium regulates the ability of myo1b to sense and sustain tension.

1190-Plat
Myosin 5A Walking Mechanism: The Structural Basis of Slow ADP Dissociatin from the Lead Head
Olusola Oke[1], Takeshi Sakamoto[2], Eva Forgacs[3], Peter Knight[1], Burgess Stan[1], James Sellers[4], **Howard D. White**[3], John Trinick[1].
[1]Leeds University, Leeds, United Kingdom, [2]Wayne State University, Detroit, MI, USA, [3]Eastern Virginia Medical School, Norfolk, VA, USA, [4]NHLBI, Bethesda, MD, USA.
Using electron microscopy and image averaging, we have observed myosin 5a walking along actin filaments in the presence of low concentrations of ATP. Most molecules are attached with 13 actin subunits between heads but ~10% are bound with 11 or 15 subunit spacings. Most lead heads are in the pre-powerstroke conformation, but some post-powerstroke lead heads are observed, especially at smaller separations where there is less strain in the myosin. Post-powerstroke lead heads have the converter at the front of the motor domain with its lever bent strongly backwards. Lead heads attached at the 13 subunit spacing are 98 % in pre-powerstroke state, tethered there by the trail head. However, heads spaced by 11 subunits are more evenly distributed (60:40) pre- to post-powerstroke. No post-powerstroke lead heads are seen in heads spaced by 15 actin subunits. These results are consistent with an energy difference of 10 kJ/mole between the pre- and post-power stroke conformations at 11 and 13 actin subunit separation. The post-powerstoke lead head is a new attached state of myosin: the motor domain has completed its powerstroke at the expense of severe lever distortion, but with little cargo movement. The rate of ADP dissociation from lead heads measured by stopped-flow fluorescence is >30 fold slower than from trail heads. The slower rate can be explained by a mechanism in which ADP only dissociates from the post-powerstroke state. ADP dissociation from the lead head is therefore inhibited by an unfavorable equilibrium between the pre-and post-powerstroke conformations. Supported by NIH EB00209.

1191-Plat
Processive Runs of Full Length Myosin VA Are Interrupted by Pauses and Dwells
Jessica M. Armstrong, Elena Krementsova, Shane R. Nelson, Kathleen M. Trybus, David M. Warshaw.
University of Vermont, Burlington, VT, USA.
Full length myosin Va (FL-MyoVa) forms an inhibited, folded conformation at low salt, stabilized by interactions between the globular tails and the heads. High ionic strength disrupts this interaction, resulting in an extended, active processive motor. In vivo, it has been postulated that cargo binding disrupts the folded conformation and activates the motor. It is possible that splice variations in the tail (-B+D+F, melanocyte; +B-D-F, brain) could modify the ability of myosin Va to form the inhibited state. Two FL-MyoVa splice variants and an HMM-MyoVa, with biotin tags for Qdot labeling, were expressed in Sf9 cells. Sedimentation velocity experiments showed similar transitions from the folded-to-extended conformation for the two splice variants as a function of salt. TIRF microscopy was then used to observe processive runs on actin. The velocities of both FL-MyoVa splice variants were similar, and increased 270% (171-460nm/sec) with increasing KCl concentration (25-200mM). In contrast, the velocity of HMM-MyoVa increased by a more modest 50% (381-586nm/sec). The trajectories of the FL-MyoVa and HMM-MyoVa were also strikingly different. Both FL-MyoVa splice variants underwent processive runs that were interrupted by periods during which the motor dwelled at fixed points on the actin filament, presumably in the folded, inhibited state. At lower KCl concentration, FL-MyoVa dwelled approximately half of the total trajectory duration. Increasing ionic strength decreased duration of the dwells. HMM-MyoVa was fully active and maintained continuous processive movement at all KCl concentrations. The slower overall velocities for the FL-MyoVa splice variants, compared to HMM-MyoVa, results from inclusion of the dwell periods. We propose that during a processive run, a single FL-MyoVa can switch between an active and inhibited state without dissociating from actin, and that this phenomenon is independent of splice variations in the tail domain.

1192-Plat
Simultaneous Observation of Tail and Head Movements of Myosin V During Processive Motion Provides Insight into Its Stepping Dynamics
Hailong Lu, Guy G. Kennedy, David M. Warshaw, Kathleen M. Trybus.
University of vermont, Burlington, VT, USA.
Processive stepping of myosin V (myoV) on actin has been studied either by tracking the position of the tail, which follows the motion of the molecule as a whole, or by tracking the position of one or both heads. Here we combine these two approaches, and attach a quantum dot (Qdot) to one of the motor domains, and a bead to the tail. Using optical trapping and total internal reflection microscopy, the position of one head and the tail are simultaneously observed as myoV moves processively on an actin filament against increasing load. Our results show that the head (Qdot) moves continually with 72.9 ± 10.3 nm step size, while the tail (bead) moves with a step size of 34.7 ± 8.6 nm. For every two tail steps, the head moves only one step. One of the tail steps takes place concurrently with the head step. Back steps were occasionally observed. Analysis shows that before taking a back step, the head moves 68 ± 11nm while the tail moves 31.9 ± 9.7nm, which suggests that the leading head lands on the 11th actin subunit instead of its normal 13th actin subunit. Interestingly, during a backstep the tail moves -28.6 ± 13.7nm, while the step size distribution for the head shows multiple peaks. This suggests that the head has multiple binding positions along the actin filaments, while the tail has a more defined conformation. Our observation supports a hand-over-hand model for processive movement of myoV, and reveals the cause of the back stepping behavior of myosin V under physiologically relevant loading forces (<2pN).

1193-Plat
Contribution of the Myosin VI Tail Domain to Processive Stepping and Intramolecular Tension Sensing
Alexander R. Dunn, Peiying Chuan, Zev Bryant, James A. Spudich.
Stanford University, Stanford, CA, USA.
Myosin VI is proposed to act as both a molecular transporter and as a cytoskeletal anchor in vivo. The structural traits and kinetic mechanisms by which myosin VI takes processive, ~36 nm steps along actin are controversial. In particular, the portion of the molecule C-terminal to the canonical lever arm, termed the medial tail (MT), has been hypothesized to act as either a lever arm extension or as a dimerization motif. We created constructs in which the MT is interrupted by glycine-rich molecular swivels in order to test competing models of the MT's contribution to processive stepping. Disruption of the MT results in decreased processive run lengths measured using single-molecule fluorescence microscopy and a decreased step size under applied load as measured in an optical trap (see Figure). We used single-molecule gold nanoparticle tracking and optical trapping to examine the mechanism of coordination between the heads of dimeric myosin VI. We conclude that intramolecular tension prevents ADP release from the lead head. This mechanism likely increases both the motor's processivity and its ability to act as an anchor under physiological conditions.

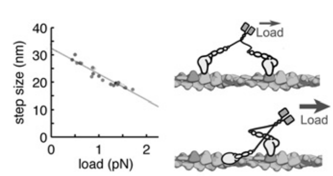

1194-Plat
Engineering A Controllable Bidirectional Molecular Motor
Lu Chen, Muneaki Nakamura, Tony Schindler, Zev D. Bryant.
Stanford University, Stanford, CA, USA.
Myosin superfamily motors play crucial roles in cellular functions such as motility, cell division and organelle trafficking. Different myosin classes are

specialized for motion toward either the (+) or (-) end of actin filaments. Previous work has shown that directionality of recombinant myosins may be altered via the genetic insertion [1] or removal [2,3,4] of structural motifs that redirect the lever arm. We have challenged our understanding of myosin structure and function by constructing novel myosin motors that can reversibly switch their direction of motion in response to an external signal. Our general strategy relies on controlling the effective length of lever arms by triggering helix-coil transitions. In one successful design using [Ca++] as the control signal, we have built myosin VI variants with chimeric lever arms composed of an alpha-actinin fragment [5] fused to two or more calmodulin-binding IQ repeats. In vitro motility assays show that the engineered motors reverse directionality in response to physiological levels of [Ca++], as expected.

[1] Tsiavaliaris, G., Fujita-Becker, S. and Manstein, D. J. (2004). *Nature*, **427**, 558-561.
[2] Bryant, Z., Altman, D. and Spudich, J. A. (2007). *Prot. Natl Acad. Sci. USA,***104**, 772-777.
[3] Park, H., Li, A., Chen, L., Houdusse, A., Selvin, P. R. and Sweeney, H. L. (2007). *Proc. Natl Acad. Sci. USA*, **104**, 778-783.
[4] Liao, J., Elting, M. W., Delp, S. L., Spudich, J. A. and Bryant, Z. (2009). *J. Mol. Biol*, **392**, 862-867.
[5] Anson, M., Greeves, M. A., Kurzawa, S. E. and Manstein, D. J. (1996). *EMBO J.***15**, 6069-6074.

Platform AB: Membrane Physical Chemistry I

1195-Plat

Quantification of the Nanomechanical Stablility of Multicomponent Lipid Bilayers

Shan Zou.
National Research Council Canada, Ottawa, ON, Canada.

Quantification of the mechanical stability of lipid bilayers is important in establishing the composition-structure-property relations, and shed light on understanding functions of biological membranes. We report a direct correlation of the self-organized structures exhibited in phase-segregated supported lipid bilayers consisting of dioleoylphosphatidylcholine/egg sphingomyelin/cholesterol (DEC) in the absence and presence of ceramide (DEC-Ceramide) with their nanomechanical properties using AFM imaging and high-resolution force mapping. Direct incorporation of ceramide into phase-segregated supported lipid bilayers formed ceramide-enriched domains, where the height topography was found to be imaging setpoint dependent. In contrast, liquid ordered domains in both DEC and DEC-Ceramide presented similar heights regardless of AFM imaging settings. Owing to its capability for simultaneous determination of the topology and interaction forces, AFM-based force mapping was used in our study to directly correlate the structures and mechanical responses of different coexisting phases. We also designed an experiment to directly probe and quantify the nanomechanical stability and rigidity of the ceramide-enriched platforms that play a distinctive role in a variety of cellular processes. Our force mapping results have demonstrated that the ceramide-enriched domains require both methyl β-cyclodextrin (MbCD) and chloroform treatments to weaken their highly ordered organization, suggesting a lipid packing different from typical gel states. Our results also show the expulsion of cholesterol from the sphingolipid/cholesterol- enriched domains as a result of ceramide incorporation. This work provides quantitative information on the nanomechanical stability and rigidity of coexisting phase-segregated lipid bilayers with the presence of ceramide-enriched platforms, indicating that generation of ceramide in cells drastically alters the structural organization and the mechanical property of biological membranes.

1196-Plat

Simulations of Lipid Bilayer Domain Formation: Effects of Steroid Structure and Asymmetry

Jason D. Perlmutter, Jonathan N. Sachs.
University of Minnesota - Twin Cities, Minneapolis, MN, USA.

There is a growing amount of evidence that laterally segregated domains of lipids are an integral part of biological membrane structure and function. Using Coarse Grain and Atomistic Molecular Dynamics Simulations we investigate the role of steroid structure and asymmetry in domain formation. Cholesterol, an essential component of animal membranes, appears to be well suited for ordering neighboring lipid chains and promoting domain formation. We demonstrate that alterations to the steroid headgroup hydrophobicity trigger a conversion from domain promoting to domain inhibiting. Those steroids which inhibit domain formation are observed to be less stable in the typical, upright orientation, and instead insert into the bilayer hydrophobic core and reside in an orientation perpendicular to the bilayer normal axis. A second set of simulations are used to address the role of bilayer asymmetry in domain formation. Cellular membranes are thought to be asymmetric, containing different lipid compositions on opposing leaflets, with the outer leaflet capable of domain formation and the inner leaflet uniformly disordered. These simulations suggest how domain formation is affected by an opposing uniformly disordered leaflet.

1197-Plat

Probing Structure and Dynamics of Lipid Microdomains with Tagged Proteins and Lipids: A Hybrid Particle-Continuum Simulation Approach

Jun Fan[1], Maria Sammalkorpi[1], Mikko P. Haataja[1,2].
[1]Department of Mechanical and Aerospace Engineering, Pinrceton University, Princeton, NJ, USA, [2]Princeton Institute for the Science and Technology of Materials, Program in Applied and Computational Mathematics, Princeton University, Princeton, NJ, USA.

Lipid rafts are functional microdomains in the cell membrane. They have been implicated in many important cellular processes such as signal transduction, protein sorting and viral entry. At th is point, our understanding of the collective dynamics of lipids and lipid clusters in vivo is rather limited. To this end, by employing a hybrid particle-continuum approach, we simulate the coupled dynamics of diffusing probe particles (both proteins and lipids) and the evolving membrane composition. Importantly, we demonstrate that the structure and dynamics of lipid microdomains can be extracted from the fluctuating dynamics of the probe particles. These results suggest novel experimental ways of exploring raft dynamics.

1198-Plat

Cholesterol-Rich Fluid Membranes Solubilize Ceramide Gel Domains. Implications for the Organization of Mammalian Membranes

Bruno M. Castro[1], Liana C. Silva[1,2], Rodrigo F.M. de Almeida[3], Manuel Prieto[1].
[1]CQFM and IN, Lisboa, Portugal, [2]Department of Biological Chemistry, Weizmann Institute of Science, Rehovot, Israel, [3]CQB, FCUL, Lisboa, Portugal.

A uniquely sensitive method for ceramide-domain detection allowed us to study in detail cholesterol-ceramide interactions in lipid bilayers with low (physiological) ceramide (Cer) concentrations, and ranging from low or no cholesterol (Chol) (a situation similar to intracellular membranes, such as endoplasmic reticulum) to high Chol, (similar to mammalian plasma membrane). Fluorescence spectroscopy and microscopy experiments were conducted showing that for low Chol amounts Cer segregates into gel domains that disappear upon increasing Chol levels. This was observed in raft (sphingomyelin/Chol-containing) and non-raft (sphingomyelin-absent) membranes, *i.e.* mimicking different types of cell membranes. Chol-Cer interactions have been described mainly as raft sphingomyelin-dependent. In this work, sphingomyelin independence is demonstrated. Moreover, we show that Cer-rich domains re-appear when either Chol is converted by cholesterol oxidase to cholestenone, or temperature is decreased. The inability of cholestenone-rich membranes to dissolve Cer-gel domains shows that the cholesterol ordering and packing properties are fundamental to the mixing process. Cer solubility is dependent on the average gel-fluid transition temperature of the remaining membrane lipids, and is higher in Chol-rich fluid membranes than in Chol-poor ones. We also show that the solubility of Chol in Cer domains is low. The results are rationalized by a ternary phospholipid/ ceramide/ cholesterol phase diagram, providing the framework for a better understanding of biochemical phenomena modulated by Chol-Cer interactions such as cholesterol oxidase activity, lipoprotein metabolism and lipid targeting in cancer therapy. It also suggests that the lipid compositions of different organelles are such that ceramide gel domains are not formed, unless a stress or pathological situation occurs.
Further details in Castro, BM, Silva, LC, Fedorov, A, de Almeida, RFM, and Prieto, M (2009). *J. Biol. Chem.***284** (5), 22978-22987.
FCT (Portugal) is acknowledged for research grants and scholarships.

1199-Plat

Texture of Membrane Gel Domains

Uffe Bernchou, Jonathan Brewer, Henrik Midtiby, John H. Ipsen, Luis A. Bagatolli, **Adam C. Simonsen**.
MEMPHYS, University of Southern Denmark, Odense M, Denmark.

In this work[1] we investigate the texture of gel (g) domains in supported binary lipid membranes. Lateral organization of lipid bilayer membranes is a topic of fundamental and biological importance. Whereas questions related to the size and composition of fluid domains are well studied, the possibility of texture in condensed solid/gel domains has received limited attention. Gel domains are expected to be prominent in skin membranes and in ceramide domains

during apoptosis. When using polarized light for two-photon excitation of the lipid probe Laurdan, the emission intensity is highly sensitive to the angle between the polarization and the tilt orientation of lipid acyl chains. By imaging the intensity variations as a function of the polarization angle, we map the lateral variations of the lipid tilt within domains. Results reveal that gel domains are composed of distinct subdomains with different lipid tilt directions. Vortex structures centered at the domain core can be observed. Texture patterns of the same type have historically been associated with the presence of hexatic order in monolayers. The hexatic phase is an intermediate phase between the crystal and fluid states, having short range positional order and long range orientation order. The present results provide some support for the notion that hexatic order may persist in bilayers. Using the generalized polarization (GP) function of Laurdan, we demonstrate that although gel domains have heterogeneous texture, the membrane phase state is uniform within domains.

[1] U. Bernchou et. al. 'Texture of Lipid Bilayer Domains'. J. Am. Chem. Soc., 2009. DOI: 10.1021/ja903375m

1200-Plat

Understanding the Behavior of Nanometer-Size Lipid Domains in Model Membranes: A Small Angle Neutron Scattering Study

Sumit Garg[1], Lionel Porcar[2], Paul Butler[3], Ursula Perez-Salas[4].
[1]Argonne National Lab, Argonne, IL, USA, [2]Institut Laue-Langevin, Grenoble, France, [3]National Institute of Standards and Technology, Gaithersburg, MD, USA, [4]University of Illinois at Chicago, Chicago, IL, USA.

Lipid-lipid phase separation is important in understanding the behavior of the biological membrane. Such phenomenon has been studied extensively in model lipid membranes using microscopy techniques where domains are found to be microns in size. In actual biological membranes, however, domains are smaller, and microscopy techniques are unable to detect them. A hypothesis to explain these small domains is that the cytoskeleton generates boundaries to compartmentalize the membrane into small sub-membrane regions with access to only small amounts of lipids in the lifespan of lipid domains. Therefore, to be able to correlate studies of model membranes to the actual plasma membrane, there is a need to characterize lipid domains in a system where they cannot grow more than few nanometers in size. To achieve such a goal, we use small Unilemellar Vesicles (ULVs) made of 1:1 and 3:7 ratios of DPPC (deuterated-DPPC) and DLPC respectively for which phase separation in large vesicles has been observed. Using small vesicles with varying sizes (diameters from 30nm to 400nm) not only provides a means to control curvature, but also limits the amount of available lipids for domain growth. Small Angle Neutron Scattering was used to characterize the size, density and average composition of the domains, which appeared as the temperature was lowered below Tm, the melting temperature of the system. The scattering curves were fitted using a pair-correlation method in order to extract the "local structure" of the vesicles. The results interestingly suggest that the nanometer domains in these systems do not coalesce to form a single stable domain as observed in giant vesicles. Overall, thiswork provides insight into the behavior of nano-meter size lipid-lipid phase separation as a function of composition, temperature, vesicle-size and curvature.

1201-Plat

Direct Imaging of the Structure of Lipid Rafts by Atomic Force Microscopy

Khizar H. Sheikh.
University College Dublin, Dublin, Ireland.

According to the fluid mosaic model, lipid bilayers have been thought of as two-dimensional homogenous mixtures of lipids, embedded with membrane proteins[1]. This model has recently been extended by the lipid raft model in which biologically functional structural lipid domains, rich in sphingolipids and cholesterol.[2]

Previously, a low-noise AFM system[3] was developed within the our group, capable of imaging the surface structure of lipid bilayers in aqueous buffer with Angstrom resolution.[4,5] We now extend this work to the structure of the these lipid raft components at Angstrom resolution and discover a subtle organisation of the lipids headgroups of the molecules in these structures, stabilised by a combination of salt bridges and hydrogen bonds.

References

1. S.J. Singer, G.L. Nicolson, *The fluid mosaic model of the structure of cell membranes*. *Science,* **175**, 720-31 (1972).
2. K. Simons, E. Ikonen, *Functional rafts in cell membranes*, Nature,**387,** 569-72 (2007)
3. T. Fukuma and S.P. Jarvis, *Development of liquid-environment frequency modulation atomic force microscope with low noise deflection sensor for cantilevers of various dimensions*, Review of Scientific Instruments, **77**, 043701 (2006).
4. T. Fukuma, M. J. Higgins and S. P. Jarvis, *Direct imaging of individual intrinsic hydration layers on lipid bilayers at Ångstrom resolution*, Biophysical Journal, **92**, 3603-3609 (2007).
5. T. Fukuma, M. J. Higgins and S. P. Jarvis, *Direct imaging of lipid-ion network formation under physiological conditions by frequency modulation atomic force microscopy*, Physical Review Letters, **98**, 106101 (2007).

1202-Plat

High Pressure Static and Time-Resolved X-Ray Studies of Inverse Phases in Cholesterol / Lipid Mixtures

Arwen I.I. Tyler, Gemma C. Shearman, Nicholas J. Brooks, Richard H. Templer, Oscar Ces, Robert V. Law, John M. Seddon.
Department of Chemistry and Chemical Biology Centre, Imperial College London, London, United Kingdom.

Non-bilayer phases are thought to be of considerable biological relevance. Whenever there is a topological change in the membrane, corresponding to events such as membrane fusion, non-bilayer structures are assumed to be adopted locally. Several complex three-dimensional lyotropic liquid crystal phases are already known, such as the bicontinuous cubic phases, but for many years only a single example was found - a cubic phase of spacegroup Fd3m - of a structure based upon a complex close packing of inverse micelles. We have recently reported the discovery (1) of a novel lyotropic liquid crystal phase, of spacegroup, $P6_3/mmc$, whose structure is based upon a hexagonal close packing of identical quasi-spherical inverse micelles.

Although a plethora of equilibrium phase diagrams have been published, there is a scarcity of knowledge regarding the kinetics and mechanisms of lyotropic phase transitions. If we are to further our knowledge of events such as membrane fusion then a comprehensive understanding of the processes governing phase transitions, the type of intermediates formed and the mechanism by which a transition occurs are vital.

A superb technique for monitoring and initiating the structural evolution of such systems, in the millisecond regime, is time resolved X-ray diffraction, using pressure as the trigger mechanism. We have employed this technique to investigate lamellar - non-lamellar ($P6_3/mmc$ phase) transition kinetics in cholesterol/ phospholipid/ diacylglycerol model membrane systems. Equilibrium pressure - temperature composition diagrams have been constructed, allowing us to choose appropriate pressure-jump parameters (temperature, initial and final pressures) for the kinetic studies.

(1) G. C. Shearman, A. I. I. Tyler, N. J. Brooks, R. H. Templer, O. Ces, R. V. Law, J. M. Seddon, *J. Am. Chem. Soc.* **131**, 1678 (2009)

Posters

Protein Conformation II

1203-Pos
Molecular Dynamics Simulations Predict A pH-Dependent Conformational Change in the C-Helix of Cell Cycle Checkpoint Kinase Wee1
Michael S. Chimenti[1], Mark J.S. Kelly[1], Diane L. Barber[2], Matthew P. Jacobson[1].
[1]Department of Pharmaceutical Chemistry, University of California, San Francisco, San Francisco, CA, USA, [2]Department of Cell and Tissue Biology, University of California, San Francisco, San Francisco, CA, USA.
Wee1 is the cell cycle checkpoint kinase that phosphorylates Tyr15 of Cdk1, maintaining it in an inactive state. Cdk1 regulates the transition from S to G2/M phases in eukaryotic cells and is activated upon dephosphorylation of residues Thr14 and Tyr15 and cyclin B1 binding. We previously reported that increased intracellular pH (pHi) (> 7.2) promotes G2/M transition. Moreover, we found that in cells having low pHi (< 7.2) the abundance of phosphorylated Cdk1 (pTyr15) is aberrantly sustained. We are testing the hypothesis that Wee1 kinase activity might be pH sensitive, with higher activity at lower pH. The C-helix in Wee1 contains four contiguous residues unique to the Wee1 family centered around His350, which faces the ATP binding site. Based on this observation, we hypothesized that changes in pHi could affect the C-helix conformation and hence catalytic activity (C-helix conformation modulates activity in many other kinases). Molecular dynamics simulations of Wee1 were performed while allowing His350 to be either neutral or charged, capturing the hypothetical protonation state of His350 at high and low pHi, respectively. Most portions of the kinase domain showed only small changes at the end of the two 10 ns simulations. However, when His350 was neutral, the C-helix adopted a conformation that closely mimics the inactive state of other kinases. In contrast, when His350 was charged, the C-helix adopted a conformation similar to the active state of other kinases wherein the C-helix was rotated towards the active site. These data suggest that pH-sensitivity in Wee1 may be mediated by the influence of the protonation state of His350 on the C-helix conformation. We are currently testing these predictions using NMR and biochemical approaches.

1204-Pos
The L49F Mutation in Erythroid Alpha Spectrin Induces Local Disorder in the Tetramer Association Region: Fluorescence And Molecular Dynamics Studies of Free and Bound Alpha Spectrin
Yuanli Song[1], Nina H. Pipalia[2], Leslie W.-M. Fung[1,2].
[1]University of Illinois at Chicago, Chicago, IL, USA, [2]Loyola University of Chicago, Chicago, IL, USA.
The bundling of the N-terminal, partial domain helix (Helix C') of human erythroid α-spectrin (αI) with the C-terminal, partial domain helices (Helices A' and B') of erythroid β-spectrin (βI) to give a pseudo spectrin structural domain (triple helical bundle A'B'C') has long been recognized as a crucial step in forming functional spectrin tetramers in erythrocytes. We have used fluorescence studies to obtain apparent polarity and Stern-Volmer quenching constants of Helix C' of αI bound to Helices A' and B' of βI. These properties were used to guide us in homology modeling with a previous NMR structure as the template. The homology models then became input structures for molecular dynamics simulations for both wild type (WT) and an αI clinical mutant Spectrin Lyon (L49F). The simulation output structures show a stable helical bundle for WT, but not for L49F. In WT A'B'C', four critical interactions were identified: two hydrophobic clusters and two salt bridges. However, in L49F, the C-terminal region of Helix C' was unable to assume a helical conformation and one critical hydrophobic cluster was disrupted. Other molecular interactions critical to the WT helical bundle were also weakened in L49F. We suggest that these conformational changes lead to a lower tetramer levels observed in Spectrin Lyon patients.

1205-Pos
Characterization of Conformational Transitions in Src Kinase using the String Method with Swarms-of-Trajectories and Markovian Milestoning
Wenxun Gan, Benoit Roux.
University of Chicago, Chicago, IL, USA.
Src tyrosine kinases are a family of signaling proteins playing key roles in intracellular signaling pathways. Dysregulation of Src activity has been implicated in several types of cancer. An important conformational change in Src involves the highly conserved DFG motif (Asp404, Phe405, Gly406) adjacent to kinase ATP-binding site. In the majority of available crystal structures, the DFG points into the ATP-binding site where it coordinates a magnesium ion (DFG-in conformation). A recent X-ray structure shows that c-Src is also able to adopt a DFG-out conformation, in which the DFG motif is flipped by approximately 180°. Understanding the factors controlling the flipping of the DFG motif is important for designing highly selective kinase inhibitors. We first determine atomistic pathway of DFG in-to-out transition using the string method with swarms-of-trajectories with all-atom molecular dynamics (MD) simulations. Images along the pathway are then used as centroids to construct a complete Voronoy tessellation in the collective variables space, which then serve as a ''basis set'' to define the discrete micro-states and to build a reduced stochastic model. MD trajectories with ''soft-wall'' restraining hyper-plane potentials are launched to keep a system inside each Voronoy cell. By monitoring the wall-to-wall transitions among the walls separating the Voronoy cells, we estimate the free energy and mean first passage time (MFPT) of DFG flipping. An improved understanding of the interplay of the structure, dynamics and activity of Src kinase will help the development of new inhibitors for targeted cancer therapy. [Supported by NIH grant CA093577]

1206-Pos
Probing the Structure of Membrane Proteins Using Pulsed EPR ESEEM Spectroscopy
You Zhou, Daniel J. Mayo, Robert M. McCarrick, Gary A. Lorigan.
Miami University, Oxford, OH, USA.
Current methods used for determining the secondary structure of membrane proteins require large sample sizes and have long data acquisition times. Therefore using pulsed EPR spectroscopic technique of Electron Spin Echo Envelope Modulation (ESEEM) is advantageous due to the requirement of less sample, short data acquisition, and high sensitivity. Using this technique, we can determine short to medium range distances (up to 8 Å) between a site-specific nitroxide spin label (MTSL) and a nearby NMR-active isotopic labeled residue for a variety of peptides and proteins which ultimately determine the difference between an α-helical and β-sheet secondary structure. The information can be obtained using a three-pulse ESEEM sequence which allows for the detection of the fundamental nuclear spin transitions. It is possible to calculate the radial distance between a paramagnetic electron and a weakly coupled nucleus because the modulation depth produced by a weakly dipolar-coupled nucleus is inversely proportional to the radial distance. This new method is applied to two different membrane peptides, M2δ AChR, and KIGAKI, which have α-helical and β-sheet structural components respectively. A nitroxide spin probe is attached to a specific Cys residue at a given position *I,* and a ^{2}H isotopic labeled residue is attached to a nearby residue ($i + 3$). The corresponding data shows that an α-helical structure will yield a very large ^{2}H peak, whereas a β-sheet will yield a much smaller ^{2}H peak, thus a difference can be observed between the two secondary structures. The ESEEM technique requires less protein sample (about 75 μg) and data acquisition only takes about 1 hour which makes it a simple, powerful, and effective technique in the determination of the secondary structure of a membrane protein.

1207-Pos
SDSL-EPR Study of a C-terminal Segment of Myelin Basic Protein in a Myelin Mimetic Environment
Lopamudra Homchaudhuri[1], Miguel De Avila[2], Stina B. Nilsson[2], Vladimir V. Bamm[2], Abdiwahab A. Musse[2], Graham S.T. Smith[2], George Harauz[2], Joan M. Boggs[1].
[1]The Hospital for Sick Children, Toronto, ON, Canada, [2]University of Guelph, Guelph, ON, Canada.
Myelin basic protein (MBP) is a peripheral membrane protein and a major component of human central nervous system myelin. It is a multifunctional, highly positively charged, intrinsically disordered protein that undergoes extensive post-translational modifications. Its multifunctionality includes among others, binding of cytoskeletal proteins to a membrane surface and polymerization and bundling of cytoskeletal proteins. These interactions are modulated by interaction of MBP with Ca^{2+}-calmodulin. We report here the use of site-directed spin labeling and continuous wave power saturation electron paramagnetic resonance spectroscopy (SDSL-EPR) to examine the conformation of segment A141-L154 of a recombinant 18.5 kDa murine isoform of MBP in a reconstituted membrane environment. This segment overlaps the primary calmodulin binding region (T147-D158) of MBP and is predicted, on the basis of helical wheel constructs, to form an amphipathic alpha helix. Solution NMR investigations also showed this region to exist as a transient alpha helix in 30% TFE. Our measurements using SDSL-EPR reveal that this region forms an extended helix with a period of ~3.8 residues per turn and with a tilt angle of ~4.3 degrees with respect to the plane of the lipid bilayer. The N-terminal end of the helix appears to be buried more deeply in the membrane bilayer than the C-terminal end. The C-terminal region of the segment bears two Lys residues whose side chains interact with the lipid head groups causing this end to be more exposed. The accessibility of the C-terminal region of A141-L154, which forms a part of the primary calmodulin binding segment, could facilitate interaction of this region

with cytosolic proteins viz., calmodulin and modulate cytoskeletal binding to the oligodendrocyte plasma membrane.
(Supported by CIHR, NSERC and MS Society of Canada)

1208-Pos
A Study of the Conformation of HIV Nef Bound to Lipid Membranes by Neutron Reflectivity
Michael S. Kent[1], Jaclyn K. Murton[1], Sushil Satija[2], Bulent Akgun[2], Hirsh Nanda[2], Joseph Curtis[2], Jaroslaw Majewski[3], Christopher Morgan[4], John R. Engen[4].
[1]Sandia National Labs, Albuquerque, NM, USA, [2]NIST, Gaithersburg, MD, USA, [3]Los Alamos National Labs, Los Alamos, NM, USA, [4]Northeastern University, Boston, MA, USA.
Nef is one of six HIV-1 accessory proteins and directly contributes to AIDS progression. Nef associates with membranes and may require a transition from a solution conformation to a membrane-associated conformation. It has been hypothesized that a transition from a ''closed'' conformational form to an ''open'' form enables interaction of Nef with cellular proteins. Despite its obvious disease importance, there is little or no direct information about the conformation of membrane-bound Nef. In this work we used neutron reflection to reveal details of the conformation of membrane-bound Nef. Nef was bound through an N-terminal His tag to Langmuir monolayers of DPPC mixed with a synthetic metal-chelating lipid. Several methods were found to achieve a dense monomolecular layer of membrane-bound Nef, despite its tendency to form oligomers at high concentration. At the conditions of this initial study (65% DSIDA 35 mol% DPPC, 20 mM Tris, 20 C, pH 8.2), for the large majority of the bound population the core domain of membrane-bound Nef lies within a few Å of the lipid headgroups. The N-terminal arm is directly against the lipid headgroups with a small portion inserted. The results also indicate that the disordered loop extends from the core domain into the solution. The data also suggest that for a very small fraction of the bound population the N-terminal arm extends normal to the membrane and the core domain is displaced ~50 Å from the membrane. Some ramifications of these results for the activity of Nef are discussed.

1209-Pos
Site-Directed Spin Labeling Electron Paramagnetic Resonance Studies of Flap Conformations and Flexibility in Multiple HIV-1 Protease Variants
Jamie L. Kear, Mandy E. Blackburn, Gail E. Fanucci.
University of Florida, Gainesville, FL, USA.
Human immunodeficiency virus type 1 protease (HIV-1PR) is a 99 amino acid homodimeric aspartic protease that plays an essential role in the maturation and life cycle of the retrovirus HIV-1, as it functions in regulating post-translational processing of viral polyproteins gag and gag-pol. Accessibility of substrate to the active site is mediated by the conformational changes within two β-hairpins, or flaps. Site-directed spin labeling (SDSL) in conjunction with continuous wave and pulsed electron paramagnetic resonance spectroscopy was used to monitor the conformations of the flaps in HIV-1PR. Six inactive (D25N) HIV-1PR constructs were purified and spin labels were incorporated into the flaps at the aqueous exposed sites K55 and K55'. Constructs included Subtypes B, C, F, circulating recombinant form CRF01_A/E, and patient isolates V6 and MDR 769. For all constructs, two naturally occurring cysteine residues (C67 and C95) were substituted to alanine residues to allow for site-specific labeling as well as to avoid intramolecular disulfide cross-linking. B, F, C, and CRF01_A/E constructs contained three stabilizing mutations that provide protection from autocatalytic cleavage: Q7K, L33I, and L63I. Pulsed EPR results have shown that sequence variations within the subtypes of HIV-1 protease alter the average flap conformations within the apo-enzymes. With detailed data and error analysis, these altered distance profiles can be understood as shifts in the conformational sampling of four distinct HIV-1PR conformations, with some states having enhanced flexibility or structural instability, which may play an important role in viral fitness and drug-resistance. Additionally, DEER data was collected on each construct in the presence of nine different FDA-approved protease inhibitors and a non-hydrolysable substrate mimic called Ca-P2. Continuous wave EPR was used to monitor the autoproteolysis of active (D25) Subtype F and CRF01_A/E constructs.

1210-Pos
Correlated Force-Optical Spectroscopy of Single Human Nucleolar Phosphoprotein-140 Immobilized on Nano-Array Patterns
Joon Lee[1], Won-Kyu Lee[2], Yeon Gyu Yu[2], Doo Wan Boo[1].
[1]Yonsei University, Seoul, Korea, Republic of, [2]Kookmin University, Seoul, Korea, Republic of.
Human nucleolar phosphoprotein-140 (hNopp140), an intrinsically unstructured protein (IUP), is known for its regulatory behavior of uncontrollable cell growth like in cancer and its unusual structural characteristics of a high percentage of flexible regions or extended loops. It is also one of the most highly phosphorylated mammalian proteins, of which interactions with ligands and other proteins depend strongly on the degree of phosphorylation. In this work, we employed a correlated force-fluorescence imaging and spectroscopic technique in conjunction with a nano-array patterning technique, to investigate the intrinsic shape of hNopp140 and its structural changes by phosphorylation, ligand binding and interactions with other proteins. For this, we prepared nano-array patterned surfaces containing hexagonally well-separated spots (~300 nm in diameter, ~ 2 um in distance), functionalized the spots with specific covalent linkers for targeting the cys residue of hNopp140, and immobilized single hNopp140 covalently on each spots. The presence of single hNopp140 on each spot was confirmed by single molecule fluorescence behavior of fluorescently labeled hNopp140 in TIRF mode and by subsequent high resolution AFM imaging. We finally performed single molecule force-fluorescence spectroscopy of hNopp140 itself and its complexes with ligands such as doxorubicin, mitoxantrone, and proteins such as CK2 under the precisely controlled nano-environments, and attempted to reveal the structural nature of hNopp140 and its intra- and inter-molecular interactions at single molecular level.

1211-Pos
Allosteric Inhibition of Thermus Thermophilus Phosphofructokinase
Maria Shubina-McGresham, Gregory D. Reinhart.
Texas A&M Univ, College Station, TX, USA.
Thermus thermophilus phosphofructokinase (TtPFK) comes from an extreme thermophile and exhibits entropically-driven inhibition by phosphoenolpyruvate (PEP). Interestingly, a PFK from the moderate thermophile Bacillus stearothermophilus also exhibits entropically-driven inhibition, while enthalphically-driven inhibition is observed for PFK from mesophilic E. coli. Although the thermodynamics of inhibition are similar for TtPFK and BsPFK, TtPFK exhibits a much weaker coupling between the inhibitor and substrate ($\Delta Gay = 1.60 \pm 0.04$ kcal/mol) when compared to that of BsPFK ($\Delta Gay = 5.0 \pm 0.9$ kcal/mol). Sequence alignment and crystal structures of BsPFK suggest that there is a network of interacting residues leading from the allosteric binding site to the active site. In the apo form, H215 forms a hydrogen bond with T158 and T156 interacts with D12 across the interface. In the inhibitor-bound form, T158 forms a hydrogen bond with D12. In TtPFK these interactions are missing due to substitutions at positions 215 (Ser) and 158 (Ala). Changing the amino acid residues at these positions to the corresponding amino acids in BsPFK resulted in an increase in coupling free energy to $\Delta Gay = 2.47 \pm 0.02$ kcal/mol for S215H and $\Delta Gay = 2.45 \pm 0.04$ kcal/mol for A158T. Currently the double mutant A158T/S215H is being investigated to see if the coupling can be augmented to the level of BsPFK coupling. Supported by NIH grant GM33216 and Welch Foundation grant A1548.

1212-Pos
Nucleotide Binding Induces Conformational Changes in Full-Length ClC-5
Leigh Wellhauser[1,2], Christine E. Bear[1,2].
[1]University of Toronto, Toronto, ON, Canada, [2]Hospital for Sick Children, Toronto, ON, Canada.
Mutations within the Cl^-/H^+ transporter ClC-5 lead to Dent's disease, a kidney condition characterized by proteinuria. Numerous disease-causing mutations in ClC-5 translate into truncations of the carboxy terminus (Ct), a region binding adenine nucleotides and mediating ATP-dependent regulation of ClC-5 activity [Meyer, S. *et al.,* 2007; Zifarelli, G. & Pusch, M., 2009]. As the mechanism underlying allosteric regulation of ClC-5 activity is unknown the major goal of this work was to capture dynamic nucleotide-dependent conformational changes in ClC-5 Ct. Sedimentation velocity on purified Ct revealed a more compact peptide with ATP bound evident by an increase in its sedimentation coefficient (1.18 to 1.23 $s_{20,\omega}$) and a decrease in its frictional coefficient ratio (1.55 to 1.46) with ATP present. Photo-affinity labelling of ClC-5 in crude membranes with the analog γ^{32}P-ATP-γbenzophenone ensured full-length protein directly bound ATP. As the intracellular Ct is tethered to the membrane domain through the R helix, conformational changes in response to ATP binding could evoke global structural changes in ClC-5. In support of this hypothesis, ATP binding mediated global conformational changes in membrane bound ClC-5 as revealed by ATP-dependent increases in the accessibility of endogenous cysteine residues (2.04 ± 0.34 times the control). Importantly, changes in accessibility were not observed in D727A ClC-5, the mutant unable to specifically bind ATP in photo-labelling experiments. Future work will focus on uncovering the physiological significance of nucleotide-dependent regulation of ClC-5 activity in endocytic uptake and acidification in the kidney. This work was funded by a Kidney Foundation of Canada operating grant to CB and a studentship from NSERC to LW.

Protein Dynamics I

1213-Pos
Dynamics and Co-Localization of the Electron Transport Chain of Escherichia Coli: Investigations Through Fluorescence Microscopy
Alex Robson, Mark Leake.
Oxford University, Oxford, United Kingdom.
Total Internal Reflection Fluorescence Microscopy (TIRFM) is a key tool in probing the dynamics and distribution of fluorescently tagged fusion proteins. This non-invasive *in vivo* technique is suited to the investigation of membrane-bound proteins due to the low cytoplasmic response, sometimes allowing for ~millisecond trajectory sampling of membrane bound fusion proteins. In addition, multi-wavelength TIRFM set-ups allow for investigations into co-localization of multiple fluorescently labeled protein species.
Presented here are simultaneous dual-color TIRFM investigations of key proteins involved in the branched Electron Transport Chain (ETC) in *Escherichia coli,* using a series of single and dual-labeled mutant strains. Of interest was the comparative degree to which these proteins reflected a 'free-diffusion-collision' model of protein interactions, to that of a 'solid state' model in which reacting proteins are confined and co-localized.This builds upon previous work that identified a key protein in the ETC as having a highly non-random heterogeneous distribution, being located into functional mobile membrane patches. We investigated the spatial distribution and the degree of co-localization of these protein pairs at the cellular level. We quantified the diffusion behavior of the observed trajectories comparing the relative populations which displayed freely diffusing characteristics (through standard Brownian motion), with the populations that exhibited confined or anomalous modes. We discuss the implications of the observed dynamics at the systems level, and how this relates to the overall functioning of the branched ETC.

1214-Pos
Spectroscopic Properties of Truncated GFP and Synthetic Strand Reassembly
Kevin P. Kent.
Stanford University, Stanford, CA, USA.
Semi-synthetic green fluorescent proteins (GFPs) can be prepared by producing truncated GFPs recombinantly and assembling them with synthetic β-strands of GFP. The yield from expressing the truncated GFPs is low, and the chromophore is either partially formed or not formed. An alternative method is presented in which full-length proteins are produced recombinantly with a protease site inserted between the structural element to be removed and the rest of the protein. The native peptide can then be replaced by cutting the protease site with trypsin, denaturing in guanidine hydrochloride to disrupt the complex, separating the native peptide from the rest of the protein by size exclusion, refolding the truncated protein, and mixing the truncated protein with a synthetic strand. We report the unusual spectroscopic properties of refolded GFP with strand 11 missing, which is surprisingly fluorescent considering the free chromophore in aqueous solution is very weakly fluorescent. We also report the slow reassembly kinetics of strand 11 with the truncated GFP.

1215-Pos
Measurement of Protein Binding Rates in Live Cells with FCS
Ariel Michelman-Ribeiro[1], Davide Mazza[2], Tilman Rosales[2], Timothy J. Stasevich[2], Hacene Boukari[2], Vikas Rishi[2], Charles Vinson[2], Jay R. Knutson[2], James G. McNally[2].
[1]NIST, Gaithersburg, MD, USA, [2]NIH, Bethesda, MD, USA.
In-vivo binding rates of transcription factors are of great biological interest, yet are difficult to measure or verify independently. The commonly used technique of FRAP has certain limitations, such as capturing fast dynamics, and measured association and dissociation constants have not been verified by other techniques (Sprague, B.L. et al., Biophys J 86, 3473 (2004)). The sister fluorescence technique, FCS, is sensitive to fast dynamics, and should be able to provide independent verification of binding parameters, if the appropriate model is applied. We have developed a new procedure for analyzing FCS autocorrelation functions in the presence of diffusion and binding. We present analysis of 2-photon FCS data collected from transcription factor fragments in live cells. We compare the diffusion and binding parameters with those obtained from quantitative FRAP and find consistency. (see Michelman-Ribeiro, A. et al., Biophys. J. 97, 337 (2009))

1216-Pos
Probing the Changes in Antibody Flexibility During Affinity-Maturation Using Single Molecule Spectroscopy
Elias Aba-Milki, Patricia B. O'Hara.
Amherst College, Amherst, MA, USA.
Affinity maturation of an immune response is characterized by the expression of antibody proteins with increasing specificity and selectivity over the course of an organism's response to a pathogen. Immature germ line antibodies contain sites that can bind to a host of related small molecules or small regions of larger molecules with low affinity. Over time, new antibodies with increasing affinity and selectivity are expressed. My experiments will test the hypothesis that affinity maturation is a direct result of the loss of flexibility characteristic of the immature germ line antibody binding site. Binding sites from more mature antibodies are pre-conformed to the small molecule epitopes on the pathogen and therefore not flexible, thus reducing the entropic cost of binding, leading to higher affinity.
Both intact and Fab fragments of antibodies at various stages of the immune response will be analyzed using fluorescence lifetime imaging microscopy (FLIM) at the single molecule level. This new technique is made possible through the construction of a single molecule fluorescence microscope. Lifetimes and lifetime distributions of donor and acceptor fluorescent labeling dyes tagged to the antibody will be measured for antibodies raised against two classes of small molecule haptens: diketone haptens and PLP-lysine derived haptens. Monoclonal antibodies producing cells have been derived from various points in the affinity maturation process. Lifetime images will be collected with and without hapten.

1217-Pos
Kinetics of Light-Induced Conformational Change in Phot1 LOV2-Jalpha Probed By Transient Tryptophan Fluorescence
Daniel Hoersch[1], Farzin Bolourchian[2], Harald Otto[1], **Maarten P. Heyn**[1], Roberto A. Bogomolni[2].
[1]Freie Universität, Berlin, Germany, [2]University of California, Santa Cruz, CA, USA.
We investigated the kinetics of the light-induced conformational changes of the LOV2-Jalpha domain of oat phototropin1 by transient tryptophan fluorescence spectroscopy from μs to seconds. The figure shows a typical time trace of the transient fluorescence change normalized by the initial fluorescence. Two new transitions were detected in the tryptophan fluorescence signal which are not observed in the UV-VIS absorption photocycle of LOV2. The corresponding time constants at 20 °C are 500 μs for the major component accounting for 88% of the overall amplitude and 4.3 ms for the minor component. The quantum yield of the tryptophan fluorescence is sensitive to the environment and is therefore a good marker for changes in the secondary and tertiary structure of the protein. The fluorescence transitions are presumably coupled to conformational changes of the protein that are not sensed in the chromophore binding pocket. From the temperature dependence of the transient fluorescence signal an activation energy of 18.2 kcal/mol was obtained for the conformational change.

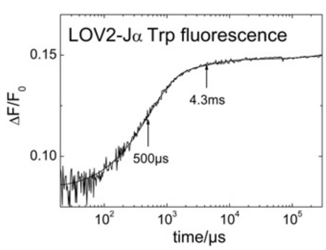

1218-Pos
The Contribution of Fast Protein Dynamics to Cytochrome P450 Molecular Recognition Characterized by Two-Dimensional Infrared Spectroscopy
Megan C. Thielges, Jean K. Chung, Michael D. Fayer.
Stanford University, Stanford, CA, USA.
While there is much interest in the potential contribution of fast protein dynamics to biological function, it remains a hotly debated topic in large part due to the challenges associated with experimentally characterizing fast protein motions. However, recent advances in the technique of two-dimensional infrared (2D-IR) spectroscopy now enable the study of fast protein fluctuations. One biological function where fast dynamics may play a particularly important role is molecular recognition. Molecular recognition of cytochrome (cyt) P450s is recognized as being particularly important to human health. Cyt P450s are a large family of enzymes that catalyze the hydroxylation of a wide variety of substrates and show varying degrees of substrate specificity. While dynamics have been implicated in the substrate specificity of cyt P450s, previous experimental studies have lacked sufficient time resolution. Thus, to overcome this limitation we are applying 2D-IR spectroscopic techniques toward the characterizing the role of dynamics in the substrate specificity of cyt P450 enzymes. Initial studies have focused on how the binding of different substrates affects the active site dynamics of the paradigmatic, relatively substrate-specific cyt P450cam. These and further studies of more substrate-promiscuous members of the cyt P450 family will assess the contribution of dynamics to molecular recognition, and provide a model for the contribution of fast protein motions to other biological systems.

1219-Pos
Discrete and Continuous Three Dimensional Simulations for Fluorescence Recovery In Bacteria
Gabriel Rosser, Mark C. Leake.
University of Oxford, Oxford, United Kingdom.
Recent evidence indicates that components of functional molecular complexes in living cells may turnover relatively rapidly over timescales of seconds. Experimental methods such as fluorescence recovery after photobleaching (FRAP) may be used to probe the kinetics of the dynamic turnover process. Several models exist to model the FRAP process within a cell, however the majority of these require assumptions specific to the size and topology of eukaryotic cells. In the present work we present a robust discrete stochastic simulation of the FRAP process in three dimensional space for application to turnover processes in the bacterial cytoplasm. This is compared with a complementary continuous numerical simulation based on the finite element method (FEM). The effect of the dimensions and shape of the bacterial cell are analysed to elucidate the rôle of boundary effects, and low copy number régimes are simulated to study the effect of intrinsic noise in such systems. We show how these simulations may be used to optimise kinetic parameters based on experimental data.

1220-Pos
pH Induced Dynamics Enables the Peptide Exchange of MHCII Molecules
Haruo Kozono[1], Naoki Ogawa[2], Osami Kanagawa[2], Yuji Sasaki[3].
[1]Tokyo University of Science, Noda, Chiba, Japan, [2]RIKEN, RCAI, Yokohama, Kanagawa, Japan, [3]The University of Tokyo, Kashiwa, Chiba, Japan.
MHC II acquires antigenic peptide at acidic endosomes, which contain proteases and DM for peptide generation and peptide exchange reactions. The mechanism of peptide exchange reaction catalyzed by DM is still an enigma. We noticed that peptide exchange can be completed by just lowering pH for most MHC II isotypes. Thermal denaturation studies by differential scanning colorimeter have shown that the MHC II are more stable at pH5 than pH7, and the effect was entropy driven which imply that molecular flexibility at low pH has some role for the reaction. Thus, we carried out the diffracted X-ray tracking (DXT) analysis of peptide/MHC II, which should detect even a slight movement of the peptide/MHC II complex at the single molecule level. The molecular movement of peptide/MHC II complexes appeared to be larger at pH5 than pH7 when low affinity peptide was bound. This sustains results of the thermodynamic studies. In order to test the effect of the increased flexibility, we artificially restrained the movement of MHC molecule. When MHC II was produced as leucine-zipper rigidified form at the C-terminus, the movement was heavily restricted on DXT measurement. Furthermore, the rigidified MHC II molecule show reduced peptide exchange capability. These results entail that the flexibility at lower pH has a role for the peptide exchange reaction of MHC II molecules.

1221-Pos
Molecular Mechanisms for Phosphorylation Driven Dissociation of Rb-E2F Complexes
Jason R. Burke[1], Jeffrey G. Pelton[2], Seth M. Rubin[1].
[1]University of California, Santa Cruz, CA, USA, [2]California Institute for Quantitative Biosciences, Berkeley, CA, USA.
The Retinoblastoma Protein (Rb) functions as a negative regulator of cell growth in part by physically sequestering and repressing the transactivation activity of E2F. It is well established that phosphorylation of Rb by Cyclin Dependent Kinases disrupts binding between Rb and E2F, however it is unknown which of the 15 CDK consensus phosphorylation sites on Rb are required to disrupt the interaction between the pocket domain of Rb and the transactivation domain of E2F (E2FTD). In this work, we use calorimetric assays to reveal that phosphorylation at S608/S612 and T356/T373 are together sufficient to reduce the affinity of E2FTD for Rb pocket 250-fold, the same as fully-phosphorylated Rb. Nuclear Magnetic Resonance is used to identify the phosphorylation-dependent conformational changes that directly inhibit E2FTD binding. Specifically, we have found that phosphorylation of S608/S612 promotes intramolecular binding between the flexible pocket linker and the pocket domain of Rb, while phosphorylation at T356/T373 enhances binding between the N-terminal domain and pocket domain of Rb. Taken together, our results reveal two novel mechanisms for how phosphorylation of Rb modulates binding between E2FTD and Rb pocket, and we describe for the first time a function for the N-terminal domain in the inactivation of Rb.

1222-Pos
Expanding the Range of Redox Potentials of the 2Fe-2S Clusters of the Outer Mitochondrial Membrane Protein MitoNEET
John A. Zuris[1], Mark L. Paddock[2], Andrea R. Conlan[1], Edward C. Abresch[2], Rachel Nechushtai[3], Patricia A. Jennings[1].
[1]Department of Chemistry and Biochemistry, University of California San Diego, La Jolla, CA, USA, [2]Department of Physics, University of California San Diego, La Jolla, CA, USA, [3]The Hebrew University of Jerusalem, Jerusalem, Israel.
MitoNEET is a recently discovered outer mitochondrial membrane protein that harbors a 2Fe-2S cluster bound to a unique 3Cys-1His coordination (1). We measured a pH-dependent redox potential with a value near 0 mV at pH 7.0 ($E_{m,7}$). This value lies intermediate between most low potential 4Cys-coordinated ferredoxin-like (Fd) centers (~-300 mV) and most high potential 2Cys-2His-coordinated Rieske centers (~+300 mV) (2). Upon replacing the single His87 ligand with Cys, we obtained an $E_{m,7}$ near -300 mV closer to that of Fd clusters (Figure). Upon replacing Lys55 located near His87 with Met, $E_{m,7}$ increases to near $+250$ mV, closer to that of high potential Rieske clusters (Figure). This shows that there is a large interaction between Lys55 and His87 and that mitoNEET is robust to large changes in the $E_{m,7}$ of its 2Fe-2S clusters. Thus, we have engineered stable mutant mitoNEET with $E_{m,7}$ values over a range of almost 600 mV.

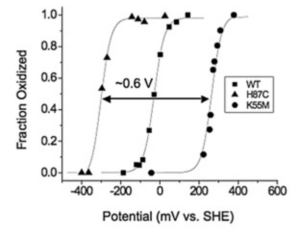

Figure. Spectroelectrochemical titrations of WT MitoNEET (squares) with H87C (triangles) and K55M (circles) mutants. The fraction oxidized versus solution potential was fit to a Nernst equation to obtain the redox potential. Measurements were done in 50 mM Tris 100 mM NaCl pH 8.0. All potential values were corrected to Standard Hydrogen Electrode (SHE).

(1) Paddock et al. (2007) Proc Natl. Acad. Sci USA 104, 14342-14347
(2) Meyer (2008) J Biol Inorg Chem 13, 157-170
Supported by NIH (GM41637, GM54038 and DK54441).

1223-Pos
"A Comparative Thermal Kinetic Investigation of the Fresh and Stale-Expired Protein Denaturing Transition"
Dipti Sharma.
UML, Lowell, MA, USA.
Protein, in eggs, has a biological quality greater than any other natural food. The quality of the protein in eggs means that all egg protein can be used for synthesis and limits the amount burned as fuel or stored as fat. Hence, the quality of egg protein can be an important factor in weight loss and essential to understand more facts about egg proteins. In this study, a comparative thermal kinetic investigation of the fresh and stale-expired proteins was made using calorimetric technique. Three different scans as temperature scans, heating rate scans and time scans were performed using differential scanning calorimetry varying temperature range from 0 °C to 200 °C and heating ramp rates from 1 °C/min to 20 °C/min. Two protein samples were used; one obtained from a fresh egg and other from the stale-expired egg from the same batch. The denaturing transition for the stale egg protein occurred at the higher temperature with smaller enthalpy and needed a larger activation than the fresh protein. This indicates that stale-expired egg provides less energy and need more energy to be activated or burnt than the fresh egg protein. Hence, the stale protein would increase more fat and need more energy to burn if eaten in the food.
Keywords: Calorimetry, fresh and stale Protein, Kinetics, Activation Energy, Denaturing transition, thermodynamics

1224-Pos
High-Order Correlations in Internal Protein Motions and Energetics
Arvind Ramanathan[1], Andrej Savol[2], Chris Langmead[1], Pratul Agarwal[3], **S. Chakra Chennubhotla**[2].
[1]Carnegie Mellon University, Pittsburgh, PA, USA, [2]University of Pittsburgh, Pittsburgh, PA, USA, [3]Oak Ridge National Laboratory, Oak Ridge, TN, USA.
Background: Despite originating as a linear sequence of amino acids, folded proteins display a remarkable diversity and specificity of motions, or dynamics, which constitute the building blocks of cellular metabolism. A growing body of evidence also suggests that these motions are hierarchical, involving a multitude of spatial and temporal scales. A key task in biology is thus to elucidate the relationship between hierarchical nature of protein dynamics and function. Characterizing these spatial/ temporal fluctuations in molecular dynamics (MD) simulations is critical to understanding enzyme catalysis, ligand binding, and allosteric signaling - all therapeutically exploitable processes.
Results: Using 0.5us simulation for ubiquitin, a 76 residue protein that labels other proteins for degradation, we show that positional deviations exhibit non-Gaussian behavior (kurtosis >> 3), at functionally important regions of the protein. To analyze the spatial deviations we propose a general and statistically rigorous method Quasi Anharmonic Analysis (QAA) that meaningfully captures non-Gaussian behaviors overlooked with established methods. QAA,

which is an extension of independent component analysis (ICA) techniques, is a more realistic encoding of protein fluctuations and atomic coupling since its basis vectors capture, in addition to variance, higher-order spatial statistics. QAA benefits from relaxing the constraint of orthogonality in basis vectors (e.g., PCA) or assumptions of Gaussian deviations. This coupling between the basis vectors from QAA allows one to elucidate how 'fast' and 'slow' motions in ubiquitin allow it to bind to different substrates with high specificity.
Conclusions: QAA is a novel approach to organize and visualize conformational landscape spanned by a protein. QAA naturally characterizes long-tailed distributions and separates conformational clusters with exceptional clarity when projected onto the novel representation space. The transitions we observe in ubiquitin signal biologically important structural shifts and highlight meaningful energetic barriers in the underlying energy landscape.

1225-Pos

An Electrohydrodynamic Model and Extensive MD Simulations Agree on the Positional and Intra-Residual Relaxations Up to Sub-Microsecond Dynamics

Rana A. Atilgan, Canan Atilgan.
Sabanci University, Istanbul, Turkey.

Our recent simulations have indicated that the number of water molecules within a cutoff distance of each residue scales linearly with protein depth. At physiological temperatures, while the translational memory of water molecules around a residue is proportional to its depth, the orientational memory is independent of the residues position[1]. These corroborate the recently reported result that water density fluctuations around hydrophobic surfaces are considerably larger than those near hydrophilic surfaces[2].
We develop an efficient, simple model that characterizes protein dynamics both at picosecond and sub-microsecond timescales[3], which are coupled through conformational motions and catalysis[4]. Our approach is based on our earlier two-degree-of-freedom model, coupling the protein's fluctuations to the vicinal layer[5]. It proves to be efficient in estimating dynamic transitions in different solvents. The model emanates from geometric Brownian motion, similar in spirit to those including hydrodynamic interactions[6]. In our formulation, however, the traditional intra-molecular interactions are coupled to an electrostatic field that increases the flexibility of the regions in contact with hydrophobic residues, and almost exhibits a decoupled dynamics from hydrophilic regions where the solvent friction term dominates. We derive analytically the decay of the positional fluctuations and the relaxation of the distances between the residues which are not in direct contact.
We have performed 200ns MD simulations both above and below the dynamic transitions of lysozyme and myoglobin to validate our analytical results. We obtain a remarkable agreement between simulations and our model for the decay time of both positional fluctuations and intra-residual distances.

1.J.Servantie, C.Atilgan, A.R.Atilgan, ArXiv:0905-4893.
2.A.J.Patel and D.Chandler, ArXiv:0909-4097.
3.O.B.Okan, A.R.Atilgan, C.Atilgan, BiophysJ, Oct2009.
4.W. Min, X.S. Xie, B. Bagchi, JPhysChemB, 112,454(2008).
5.C. Atilgan, A.O. Aykut, A.R. Atilgan, BiophysJ, 94,79(2008).
6.E. Caballero-Manrique etal, BiophysJ, 93,4128(2007).

1226-Pos

Trade-Off Between Localization and Expression Levels in Flagellar Pole Development of the Bacterium Caulobacter Crescentus

Carolina Tropini[1], Steve Sciochetti[2], Austin Newton[2], Kerwyn Casey Huang[1].
[1]Stanford University, Stanford, CA, USA, [2]Princeton University, Princeton, NJ, USA.

The bacterium Caulobacter crescentus is a model organism for cell cycle regulation and development. Upon division Caulobacter differentiates into two phenotypically distinct cells, a sessile stalked cell and a motile swarmer cell. Throughout the Caulobacter cell cycle, the localization of several key proteins is highly regulated. In this study, we address the importance of spatial localization in signal transduction and development using synthetic redesign of protein localization coupled with mathematical modeling. Development at the flagellar pole is controlled by the response regulator DivK, whose phosphorylation state is controlled by the histidine kinase DivJ and the phosphatase PleC. PleC localizes to the swarmer cell pole, while DivJ localizes at the stalked pole. To address the importance of localization, To address this question, we have constructed strains with a variety of PleC and DivJ localization patterns, including delocalization and mislocalization to the opposite pole. To determine whether phenotypic changes can be explained purely on the basis of altered localization, we have developed a mathematical model that suggests that flagellar pole development does not rely critically on precise localization of DivJ and PleC, and that developmental defects due to complete mislocalization of PleC can be compensated for by overexpression. Our results indicate that localization is not absolutely necessary for some cellular functions, but that localized proteins enhance the robustness of the system to fluctuations.

1227-Pos

Free Energy Profiles of Large Scale Protein Conformational Changes

Andrew J. Rader.
Indiana University-Purdue University Indianapolis, Indianapolis, IN, USA.

The function of many enzymes requires a transformation between widely different conformational states. Often simulations of all-atom models are not capable of determining the transformation between experimentally known end states because of the large system size and wide range of these conformational changes. However, the characterization of such transition pathways using coarse-grained models can identify significant features such as free energy barriers. In this study we employed a Monte Carlo simulation framework where bond lengths and bond angles are preserved in order to generate an initial pathway along the change in RMSD connecting these end point conformations. Within this framework, rotatable dihedral bonds along the main chain and side chain serve as the effective degrees of freedom. We then sampled conformations for each of the intermediates along this pathway without bias. The resulting conformations were combined in order to calculate the free energy profiles for these conformational changes in different proteins. These profiles yield realistic free energy barriers and indicate the degree to which conformational change is coupled to ligand binding in these enzymes.

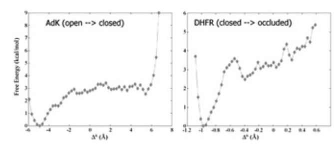

1228-Pos

A20 Negative Feedback Regulates Period of NF-KB Oscillations

Benedicte Mengel, Mogens Jensen, Sandeep Krishna, Ala Trusina.
Niels Bohr Institute, Copenhagen, Denmark.

The nuclear-cytoplasmic shuttling of NF-κB is characterized by damped oscillations of the nuclear concentration with a time period of around 1.5 hours. The NF-κB network contains several feedback loops modulating the overall response of NF-κB activity. While IκBα is known to drive and IκBϵ is know to dampen the oscillations the precise role of A20 negative feedback remains to be elucidated. Here we propose a reduced model of the NF-κB system focusing on three negative feedback loops (IκBα, IκBϵ and A20) which capture the experimentally observed responses in wild-type and knockout cells. We find that A20, like IκBϵ, efficiently dampens the oscillations although through a distinct mechanism. In addition however we have discovered a new functional role of A20 by which it controls the oscillation period of nuclear NF-κB. The design based on three nested feedback loops allows an exploration of different oscillatory responses where both period and amplitude decay can be modified. Based on these results we predict that adjusting the expression level of A20, by e.g. siRNA, the period can be changed from 1h to 3h.

1229-Pos

Systematically Defining Coarse-Grained Representations of Large Biomolecular Complexes

Zhiyong Zhang, Gregory A. Voth.
University of Utah, Salt Lake City, UT, USA.

Various biomolecular complexes are involved in many important biological processes. For example, the ribosome is a very large RNA-protein assembly that plays a central role in protein biosynthesis. Microtubules serve as a structural component of the cytoskeleton. It would be difficult to use large-scale atomistic molecular dynamics (MD) simulations to study the functional motions of these systems because of computational expense, and furthermore, high resolution atomic structures for such complexes may not even be available. Therefore various coarse-grained (CG) approaches have attracted rapidly growing interest, which enable simulations of large biomolecular complexes over longer effective timescales than MD simulations. We have developed a novel and systematic method for constructing CG representations of arbitrarily complex biomolecules, in order to preserve the large-scale and functionally relevant essential dynamics (ED) at the CG level. In the ED-CG scheme, the essential dynamics can be captured from principal component analysis (PCA) of a MD trajectory, elastic network model (ENM) of a single atomic structure, or a low-resolution cryo-electron microscopy density map. The method has been applied to the E. coli. ribosome and a microtubule to characterize CG models with different resolutions. The results illustrate that functionally important essential dynamics can still be captured even with aggressive coarse-graining.

1230-Pos
Integration of Computer Simulation and Neutron Scattering in the Characterization of Protein Dynamics
Nikolay Smolin, Benjamin Lindner, Hao-Bo Guo, Jeremy C. Smith.
Center for Molecular Biophysics, Oak Ridge National Laboratory, Oak Ridge, TN, USA.
Protein function often requires large-scale motion of functionally-important domains. Few techniques are available that can directly probe protein motions. Among the most direct is molecular dynamics simulation in which, using an empirical potential energy function, the equations of motion of a system of atoms are solved numerically. In this way detailed descriptions of protein dynamics can be built up for timescales up to about 100 ns. Integration of molecular dynamics simulations and neutron scattering provide insights of process in the proteins in the atomic details. An exciting new development in the experimental detection of functionally-important domain motions in proteins is the application of neutron spin-echo spectroscopy (NSE). Spin echo directly probes coherent (i.e., pair correlated) scattering on the 10-100 ns timescale. Recent work has demonstrated that domain motions in the tetrameric protein Alcohol Dehydrogenase (yADH) can be positively identified and characterized with this technique. Inspired by these results, we conducted theoretical calculations of the coherent time correlated neutron scattering from all-atomic molecular dynamics simulations data of the same protein. NSE allows the direct measurement of the intermediate scattering function and this way allows the direct comparison between simulation and experiment. The global translational and rotational diffusional components were decomposed and the internal dynamics of these functional domains characterized. The translational, rotational, and the internal effective diffusion constants were determined from the intermediate scattering function and the results compared with the NSE data.

1231-Pos
Pisqrd: A Novel Variational Scheme to Identify Dinamical Domains in Proteins
Raffaello Potestio, Francesco Pontiggia, Tyanko Aleksiev, Stefano Cozzini, Cristian Micheletti.
SISSA, Trieste, Italy.
A key biophysical problem is how to describe accurately the internal dynamics of proteins in terms of movements of few approximately-rigid subparts. This issue has important implications ranging from the analysis and interpretation of data from experiments or numerical simulations to the design of optimal coarse-graining schemes for multiscale description of the kinetics of interacting biomolecules.
We report on a novel variational clustering scheme that can be used to decompose proteins into rigid moduli (dynamical domains) by using internal dynamics data from atomistic molecular dynamics simulations or coarse-grained elastic network models. The method not only has a physically appealing and transparent formulation, but is also apt for efficient computational implementation.
By applying the decomposition scheme to several biomolecules of high biological interest, such as Adenylate Kinase or HIV-1 protease and other members of the hydrolase superfamily, we demonstrate that the identification of dynamical domains can provide valuable insight into the functionality of proteins and especially enzymes.
The decomposition algorithm is made freely available to the academic community in the form of a web server at the address http://pisqrd.escience-lab.org/.

1232-Pos
Enzyme Millisecond Conformational Dynamics Do Not Catalyze the Chemical Step
Andrei V. Pisliakov[1], Jie Cao[2], **Shina C. L.Kamerlin [2]**, Arieh Warshel[2].
[1]RIKEN Advanced Science Institute, Wako, Saitama, Japan, [2]University of Southern California, Los Angeles, CA, USA.
In recent years, the idea that dynamical coupling between the conformational motions and the chemical coordinate in an enzymatic reaction can be a key to understanding enzyme catalysis has attracted major experimental and theoretical interest. However, experimental studies have not to date been able to directly and conclusively establish that the conformational motions do in fact transfer energy to the chemical coordinate, and simulating enzyme catalysis on the relevant timescales has been impractical. Here, we have introduced a renormalization approach, which transfers the energetics and dynamics of the enzyme to an equivalent low-dimensional system, allowing us to simulate the dynamical coupling on a millisecond timescale. The resulting simulations establish (by means of several independent approaches) that the conformational dynamics is not remembered during the chemical step, and thus does not make a significant contribution to catalysis. Nevertheless, understanding the precise nature of this coupling is a question of great importance.

1233-Pos
Jamming Proteins with Slipknots and Their Free Energy Landscape
Joanna I. Sulkowska[1], Piotr Sulkowski[2], Jose N. Onuchic[1].
[1]The Center for Theoretical Biological Physics, San Diego, CA, USA,
[2]Caltech, Pasadena, CA, USA.
Theoretical studies of stretching proteins with slipknots reveal a surprising growth of their lifetimes when a stretching force is increased to an intermediate range.
We explain this behavior as arising from different unfolding routes at small and large forces.
Responsible for longer lifetimes at higher forces is the existence of an intermediate, metastable configuration with the slipknot jammed. Our studies are based on simulations performed within a coarsed grained model and quantified using a refined description of the geometry of the slipknots.
This allows us to determine the free energy landscape (FEL) of the protein, which supports recent analytical predictions.

1234-Pos
A Study Of Unfolding and the Beta Sheet-To-Alpha Helix Conformational Switch in Beta-Lactoglobulin
Tania Marin[1], **Laura J. Juszczak[1,2]**.
[1]Brooklyn College, Brooklyn, NY, USA, [2]The Graduate Center/CUNY, New York, NY, USA.
The enigma of protein folding stems from the seeming deficit of guidance for the folding process. Of tandem interest is the process of conformational switching from beta sheet to alpha helical structure. Consideration of these two processes brings to mind several questions such as, ''Are the local domains involved in events like hydrophobic collapse also involved in conformational switching? Is the protein largely unfolded during the conformational switch, or is unfolding limited to localized domains? Is the conformational refolding concerted or do domains refold in parallel? Indeed the answers to these questions may be protein-specific. One tried-and-true technique for studying the protein un/re/folding processes is Fourier transform infrared (FTIR) spectroscopy because the amide I band frequency (ca.1600 - 1700 cm^{-1}) tracks secondary structure changes. This study applies FTIR spectroscopy to the unfolding and beta sheet-to-alpha helix refolding of beta-lactoglobulin with analytical focus on the sequence of transitional domains leading to each final state. The appearance of transitional domains is indicated by transient absorption bands. We will examine the transitional bands for each process with the goal of identifying correlated domain changes.

1235-Pos
The Relative Significance of External and Internal Friction in Protein Conformational Changes
Imre Derenyi, Anna Rauscher, Gergely J. Szollosi, Zoltan Simon, Laszlo Graf, Andras Malnasi-Csizmadia.
Eotvos University, Budapest, Hungary.
One of the fundamental questions in enzyme reaction mechanisms is how the dynamical properties of the protein and the solvent affect the rate constant of an enzymatic reaction step. This intricate relationship between protein dynamics and enzyme kinetics is most clearly manifested by the temperature and viscosity dependence of the kinetic rate constants. It is, however, not at all obvious how to separate the effect of the internal friction of a protein (resulting from intrachain interactions) from that of external friction (due to the displacement of the solvent molecules) on the rates of conformational changes. By studying the activation of two trypsin mutants at different temperatures and different viscogenic cosolvent concentrations, we demonstrate that the introduction of small changes in the amino acid sequence of a protein (with little effect on the pre- and post-transition structures but allowing the conformational transition to advance along different pathways) can be a valuable tool in determining the magnitude and relevance of internal friction.
In particular, we show that a power law dependence of the rate constants of enzymatic reactions on the solvent viscosity provides the best and physically most sensible description of these processes. The fact that the exponent is strongly affected both by the substitution of a single amino acid and also by a change in the temperature indicates that (i) a considerable and pathway dependent fraction of the energy dissipation takes place internally in the protein; and (ii) the pathway of the reaction can be altered by changing either the amino acid sequence of the protein or the ambient temperature. The exponent can thus be used as a sensitive sensor for detecting pathway changes of conformational transitions.

1236-Pos
Solution Structure and Backbone Dynamics of Human Liver Fatty Acid Binding Protein
Jun Cai[1], Christian Lücke[2], Ye Qiao[1], Elena Klimtchuk[1], James A. Hamilton[1].
[1]Boston University School of Medicine, Boston, MA, USA, [2]Max Planck Research Unit for Enzymology of Protein Folding, Halle, Germany.
Liver Fatty Acid Binding Protein (L-FABP), a small (14 kDa) cytosolic protein most abundant in liver, performs several putative functions, including intracellular transport of fatty acids, nuclear signaling, and regulation of intracellular lipolysis. Among the various members of the intracellular lipid binding protein (iLBP) family, L-FABP is of particular interest, as it can bind more than one FA molecule at the same time and furthermore binds a large variety of other bulkier physiological ligands such as bilirubin and acyl CoA. To better understand these promiscuous binding and transport properties of L-FABP, we have applied multi-dimensional NMR spectroscopy for studies of its structure and backbone dynamics with and without the presence of ligands. The overall conformation of human L-FABP, as determined from NOE-derived distance restraints, shows a very typical b-clam motif comprised of 10 anti-parallel b-strands that are covered by 2 short nearly parallel a-helices. However, backbone dynamics of human L-FABP probed by hydrogen/deuterium exchange and ^{15}N relaxation measurements exhibit a conformational flexibility and backbone mobility that is remarkably different to that of other iLBPs. We hypothesize that the higher conformational flexibility of L-FABP helps to accommodate bulky ligands inside the binding cavity. Moreover, this structure and dynamic information of human L-FABP broadens our current understanding of the iLBP family and helps to explain its diversity and functional differences.

1237-Pos
Dynamic Predispositions of Protein-Protein Docking Orientation Revealed by Intrinsic Dynamic Domains
Lee Wei Yang[1], Shun Sakuraba[2].
[1]La Jolla Bioengineering Institute, La Jolla, CA, USA, [2]University of Tokyo, Tokyo, Japan.
Current study suggests that there exists an entropic restraint on protein-protein docking orientations. A physics-based, parameter-free approach has been developed to define intrinsic dynamic domains (IDDs) of proteins. Equilibrium dynamics of unbound protein pairs in 8 'difficult cases' are sampled by Gaussian Network Model (GNM) and dimension-reduced Elastic Network Model (dr-ENM). IDDs are defined for proteins in accord with the slowest motions projected onto reduced dimensions. Domain planes and axes are thereby determined using Linear Discriminant Analysis (LDA) and principal components (PCs) of the position covariance of the unbound partners. The unbound partners are then best-fitted onto themselves in the complexes and the relative orientations of domain axes/planes of the paired proteins are examined. Our results show that proteins dock into each other with clear dynamic preferences in their orientations such that the binding planes of proteins cut through their docking partners, and also the bending axes of the docking pairs tend to be perpendicular to each other, implying proteins in the complexes are dynamically silent in the direction of their docking pairs' vibrant movement. The dynamics-imposed restraints on protein docking orientations/locations shed light on entropic demands for proteins forming into complexes.

1238-Pos
Multiscale Modeling of Intra- and Inter-Molecular Communications Through Protein Structures
Jhih-Wei Chu.
University of California, Berkeley, Berkeley, CA, USA.
Intra- and inter-molecular communications through protein structures often manifest as changes in the structure or flexibility of protein conformation due to ligand binding and solvent composition. They are also ubiquitous mechanisms by which the biological functions are regulated in the cell. As an attempt to elucidate how the architecture and molecular interactions encoded in protein structures facilitate the functional responses of intra- and inter-molecular communications, we analyze how the binding of a calcium ion affects the structure and flexibility of a serine protease subtilisin in solved and crowded environments. Calcium binding has been shown to play a determining role in the enzyme activity of subtilisin, even though the binding site is distant from the active site. A fluctuation matching method is applied to parameterize the force constants of a coarse-grained elastic network model from long trajectories of all-atom molecular dynamics simulations. This multiscale method allows the quantification of how intra-molecular and inter-molecular interactions in protein structures respond to different configurations of calcium binding and solvation environments. First, we will present the distribution of mechanical interactions throughout the structures of subtilisin. Loop motions that are sensitive to calcium binding and protein-protein interactions in a crowded environment will be described. We will also present the analysis of inter-residue interactions and how they drive the observed changes in protein conformation. Finally, the implications in connecting protein flexibility and enzyme activity will be addressed.

1239-Pos
Multiscale Modeling of Structural Dynamics in Actomyosin Complex
Wenjun Zheng.
SUNY Buffalo, Buffalo, NY, USA.
To decrypt the mechanistic basis of myosin motor function, it is essential to probe the conformational changes in actomyosin with high spatial and temporal resolutions. In a computational effort to meet this challenge, we have performed a multiscale modeling of the allosteric couplings and transition pathway of actomyosin complex by combining coarse-grained modeling of the entire complex with all-atom molecular dynamics simulations of the active site. Our modeling of allosteric couplings at the pre-powerstroke state has pinpointed key actin-activated couplings to distant myosin parts which are critical to force generation and the sequential release of phosphate and ADP. At the post-powerstroke state, we have identified isoform-dependent couplings which underlie the reciprocal coupling between actin binding and nucleotide binding in fast myosin II, and load-dependent ADP release in myosin V. Our modeling of transition pathway during powerstroke has outlined a clear sequence of structural events triggered by actin binding, which lead to subsequent force generation, twisting of central β-sheet and the sequential release of phosphate and ADP. Finally we have performed atomistic simulations of active-site dynamics based on an on-path 'transition-state' myosin conformation, which have revealed significantly weakened coordination of phosphate by switch II, and a disrupted key salt bridge between switch I and switch II. Meanwhile the coordination of MgADP by switch I and P loop is less perturbed. As a result, the phosphate can be released prior to MgADP. This study has shed new lights on the controversy over the structural mechanism of actin-activated phosphate release and force generation in myosin motor.

1240-Pos
Diffusion and Alignment of Domain Repeats in Modular Proteins - A NMR Study
Joseph D. Walsh, Katlyn Meier, Rieko Ishima, Angela M. Gronenborn.
University of Pittsburgh, Pittsburgh, PA, USA.
Translational and rotational diffusion influences protein behavior in signaling cascades as well as other activities that involve protein-protein interactions. For modular proteins it is of interest to evaluate how the domains orient relative to each other within the single polypeptide chain. Often, the disposition of binding sites or motional properties are intimately linked to function and the relative orientation of and flexibility between domains are pivotal properties in that respect.
The present study concerned repeating domains that differ very little in sequence, and therefore allowed us to ask basic questions about the dependence of rotational diffusion and alignment with the magnetic field on linker lengths between the domains. Measuring residual dipolar couplings and relaxation properties by NMR as well as hydrodynamics provided insight into the diffusional behavior of such multi-domain proteins.

1241-Pos
Functional Motions of Immunoglobin Hypervariable Loops
Michael T. Zimmermann.
Iowa State University, Ames, IA, USA.
It is well known that the antibody structure IgG contains a Complimentary Determining Region (CDR) comprised of six hypervariable loops on each antigen binding fragment (Fab). Despite the great success of monoclonals in producing antibodies for a wide range of antigens we still do not fully understand the structure-function relationship between the entire IgG structure and the CDR. Here, we analyze flexibility and mobility in the hypervariable loops and build computational models supporting the hypothesis that the IgG structure has evolved to specifically facilitate coordinated movement of the CDR both in large-scale movements to bring the CDR to the antigen and in rearranging the atomic loop positions to intimately interact with its target. We find that low frequency normal modes predominantly act to move sequence variable regions of Fab domains and that such movements result in changes in mean squared internal distances within those regions; loops within a given variable domain move with respect to each other in the dominant modes. In the case of IgG, B-factors are heavily influenced by molecular interactions with other IgGs in the unit cell resulting in a thick lattice of tightly interconnected molecules. Some effects on functional motions of sequence deletions, insertions, and mutations are investigated.

1242-Pos

Interface Dynamics In Hub Proteins

Arianna Fornili[1], Alessandro Pandini[2], Franca Fraternali[1].
[1]King's College, London, United Kingdom, [2]National Institute for Medical Research, London, United Kingdom.

Dynamical properties of proteins may have a significant role in regulating protein-protein interactions. In particular, intrinsic disorder and disorder-order transitions have been claimed to be especially involved in the binding of proteins known as ''hubs'' [1], which are characterized by a high level of connectivity in protein-protein interaction (PPI) networks. We therefore started to investigate the dynamical properties of hubs through molecular simulations, to assess the role of conformational flexibility in promoting ''promiscuity'' of interactions.

For this study, a dataset of proteins with known structure and interaction partners was first prepared. To cope with the incompleteness of the interaction data contained in the Protein Data Bank (PDB), we mapped the PPI database IntAct [2], which collects interactions from a wide range of experimental techniques, onto the structure-based database PiSite [3]. The proteins were then partitioned into 'classes' with increasing number of interactions.

A preliminary survey of the dynamical properties of each class was done using two independent approaches, namely tCONCOORD [4] and the Gaussian Network Model [5]. For each complex, the interfaces were extracted using the POPSComp method [6,7]. The availability of information on both the dynamics and the interaction properties will allow to determine possible correlations between flexibility and binding diversity.

[1] Dosztnyi et al., J. Proteome Res., 5, 2985-2995 (2006).
[2] Kerrien et al., Nucleic Acids Res., 35, D561-D565 (2006).
[3] Higurashi et al., Nucleic Acids Res., 37, D360-D364 (2009).
[4] Seeliger et al., Structure, 15, 1482-1492 (2007).
[5] Bahar et al., Folding & Design, 2, 173-181 (1997).
[6] Fraternali et al., Nucleic Acids Res., 30, 2950-2960 (2002).
[7] Kleinjung et al., Nucleic Acids Res., 33, W342-W346 (2005).

Protein Folding & Stability: Interactions with Membranes & Lipids

1243-Pos

Resolving the Native Structure of *Escherichia Coli* OmpA

Rosetta N. Reusch, Alexander Negoda, Elena Negoda.
Michigan State University, East Lansing, MI, USA.

Modification of the sorting signal (residues 163-169) of outer membrane protein A (OmpA) of *Escherichia coli* by amphiphilic, water-insoluble oligo-(R)-3-hydroxybutyrates (cOHB) enables it to form narrow pores of ~ 80 pS in planar lipid bilayers at room temperature. Here we show that additional modifications of the C-terminal domain of OmpA in the periplasm enable it to refold into large pores in the outer membranes. Both narrow and large pore conformers migrate as 30 kDa proteins on SDS-PAGE gels. OmpA isolated from outer membranes (M-OmpA) refolds into large pores of ~ 450 pS after incubation in micelles or planar bilayers at elevated temperatures (E_a = 33.2 kcal/mol), whereas OmpA isolated from cytoplasmic inclusion bodies (I-OmpA) treated in the same manner continues to form only narrow pores. Western blot immunoassay using anti-OHB IgG and ^{1}H-NMR indicate that chymotrypsin-generated C-terminal segment 264-325 of M-OmpA contains cOHB, whereas the same segment of I-OmpA does not. Importantly, the narrow to large pore transition also fails to occur when M-OmpA is exposed to disulfide bond reducing agents. The results indicate that cOHB-modification of the sorting signal in the cytoplasm and of the C-terminal segment 264-325 in the periplasm as well as C_{290} -C_{302} disulfide bond formation in the periplasm are all necessary steps in folding OmpA to its native large pore structure. They further suggest that cOHB modification may be an important factor in protein targeting and protein folding.

1244-Pos

Spectroscopic Study of Anchoring Aromatic Residues in Membrane Proteins and Peptides: Applications to Protein Folding and Vesicle Disruption

Judy E. Kim, Katheryn M. Sanchez, Diana E. Schlamadinger,
Jonathan E. Gable, Beijing Wu.
UC San Diego, La Jolla, CA, USA.

Aromatic amino acids play critical roles in the stability and function of membrane-associated proteins and peptides. Here, we apply the site-selective vibrational tool, UV resonance Raman spectroscopy, to probe changes in the structure and microenvironment of tryptophan residues in integral membrane proteins and membrane-associated antimicrobial peptides. Alterations in molecular interactions, such as hydrogen-bonding states, cation-pi interactions, and local polarity, of tryptophan residues accompany the association and folding of these membrane-bound proteins to synthetic lipid bilayers. These results reveal the diversity of molecular interactions that help guide the in vitro assembly of membrane proteins and peptides in vesicles, and provide molecular clues to the mechanisms of membrane protein folding and vesicle disruption.

1245-Pos

Combining Genomic Information with Molecular Dynamics Simulation to Model Two-Component Signal-Transduction Systems

Alexander Schug.
UCSD, Center for Theoretical Biological Physics, San Diego, CA, USA.

Bacteria, archaea and some Eukaryotes employ so-called two-component signal transduction systems (TCS) as a means of adaptation to cellular and environmental stimuli. Typically, these systems feature a membrane bound sensor histidine kinase (SK), which modulates its autokinase activity in response to the stimulus and a transcription factor/response regulator (RR), which accepts a phosphoryl group from the SK and in turn mediates a cellular response. The phosphoryl-transfer requires the formation of a SK/RR complex ruled by transient interaction. This and other transient protein complexes involved in signal transduction are difficult to resolve by experimental means, such as X-ray crystallography or NMR, as evidenced by a lack of structural representatives for many such systems in the protein database PDB. The presented work demonstrates how theoretical methods can close this gap. A genomic direct coupling analysis extracts protein-protein interaction contacts from protein sequence databases. This information is integrated with experimentally determined structures of the unbound proteins in molecular dynamical simulation to understand protein docking and predict the structure of the protein complex. The reliability of this approach is demonstrated by achieving crystal resolution accuracy when reconstituting the known sporulation phosphotransferase complex between Spo0B and Spo0F, which is related to the TCS phsphotransfer complex. We introduce a structural model for the complex of TCS proteins TM0853 with TM0468, consistent with all available experimental data.

1246-Pos

Computer Simulations of Alzheimer's Beta Amyloid Interactions with Multicomponent Lipid Bilayers

Creighton Buie, Liming Qiu, Mark Vaughn, **Kwan H. Cheng**.
Texas Tech University, Lubbock, TX, USA.

Amyloidogenic protein unfolding and subsequent aggregation on cell surfaces are linked to many protein misfolding diseases, e.g., Alzheimer's (AD) and Parkinson's. Beta-amyloid (betaA), a 39 to 43 residue peptide, is released from neuronal membranes upon sequential proteolytic cleavages of a large transmembrane amyloid precursor protein by two secretases. An understanding of the conformational transitions and stability mediated by the lipid surface interactions is important for developing new strategies for the prevention and treatment of protein misfolding diseases. Using all-atom MD simulation techniques, we explore the initial folding and lipid insertion kinetics of betaA of both 40 and 42 residue long on the surfaces of well-defined lipid nanodomains with different cholesterol contents that mimic the neuronal lipid membranes. Several molecular clusters consisting of different initial conformations, alpha-barrel, beta-sheet and globular-coil, of betaA and stable mixed lipid bilayer in explicit solvent have successfully been constructed. The conformational transitions and stability of betaA on the lipid surface and in a partially inserted state on lipid nanodomains of different lipid compositions were systematically studied. The protein-induced membrane disruptions were examined by calculating the lipid order parameter, water permeability and bilayer thickness profiles of the lipid bilayers. The time-dependent secondary structure of betaA was used to gauge the unfolding events of the protein and its dependence on the lipid composition of the interacting bilayers. Our results revealed that the cholesterol content in the lipid bilayer strongly affects the initial lipid surface-induced unfolding and bilayer-insertion and stability behavior of betaA in our model bilayer systems. Our computer simulation data may provide useful computational insights on the controversial sensitization and protective roles of lipid membranes on the protein aggregation events in AD.

1247-Pos

Lipid-Membrane Mediated Tau Misfolding and Aggregation

Philip Camp[1], Jacek Biernat[2], Eckhard Mandelkow[2], Jaroslaw Majewski[3], **Eva Y. Chi**[1].
[1]University of New Mexico, Albuquerque, NM, USA, [2]Max-Planck-Unit for Struct. Mol. Biol., Hamburg, Germany, [3]Los Alamos Neutron Science Center, Los Alamos, NM, USA.

Neurofibrillary tangles comprise of aggregated tau protein are a pathological hallmark of Alzheimer's disease (AD). However, the molecular basis of the early tau aggregation events, such as the nature of the structural fluctuations that trigger the cascade of misfolding and aggregation events, are unknown.

Several studies suggest that tau in AD brains may exhibit abnormal interactions with the neuronal cell membrane. We hypothesize that the lipid membrane can mediate tau pathology by templating tau to misfold into an assembly-competent conformation and subsequently nucleating tau to aggregate into fibrils. We used lipid monolayers at the air/water interface as a model membrane to probe tau-membrane interactions. We found that although tau (hTau40) is highly soluble and charged, it is also highly surface active. hTau40 exhibits strong association with negative DMPG lipids, while exhibiting weaker interactions with the positive DMTAP and neutral DMPC lipids. Thus, tau-membrane interactions are strongly mediated by electrostatic interactions. To identify the hTau40 domain that is responsible for its interaction with membranes, we measured the interaction between different tau constructs (K18 and K32) and lipid membranes. Additionally, X-ray scattering experiments were carried out to elucidate the structural details of tau associated with lipid membranes. Our data show that tau's C-terminal, microtubule binding domain, is responsible for its association with the lipid membrane and that these binding events disrupts the ordering and structure of the membrane. Our study suggests that the ''soft'' nature of tau can give rise to rich dynamic behaviors at interfaces, such as the physiological lipid membrane interface. Our data implicate that the inner leaflet of the cell membrane, enriched in negatively charged lipids, can potentially recruit tau in the cytoplasm, which may be critical in initiating the cascade of pathogenic misfolding and aggregation events in AD.

1248-Pos

Global Bilayer Properties can Modulate Membrane Protein Oligomerization

Anbazhagan Veerappan, Dirk Schneider.
Institut für Biochemie und Molekularbiologie, ZBMZ, Albert-Ludwigs-Universität, Freiburg, Germany.

While sequence dependent oligomerization of individual transmembrane α-helices has been studied to some extent in the recent years, the influence of the lipid bilayer properties on defined helix-helix interactions remains largely uncharacterized. To study the potential impact of changing bilayer properties on a defined transmembrane helix-helix interaction we have followed association of fluorescently labeled glycophorin A transmembrane peptides in model membranes by fluorescence spectroscopy. Changes in Förster resonance energy transfer strongly suggest that the lipid bilayer thickness does significantly influence the monomer-dimer equilibrium of the transmembrane domain. Furthermore, the presence of cholesterol in model membranes promotes self-association of transmembrane helices by modulating the bilayer thickness and -more importantly- by affecting lipid acyl chain ordering. In addition, changes in the lipid composition, which modulate lipid bilayer curvature elasticity and the lateral pressure profile, affect GpA dimerization. In conclusion, the findings show that the physical state of a membrane can be critically involved in controlling specific and promiscuous interactions of α-helical transmembrane domains, as *e. g.* involved in membrane protein folding and assembly as well as in transmembrane signaling.

1249-Pos

Effects of Post-Translational Modifications on the Structure and Stability of Human LDL

Shobini Jayaraman.
Boston University School of Medicine, Boston, MA, USA.

LDL remodeling in vivo (by hydrolysis, oxidation, glycosylation, lipid transfer, drugs, etc.) may affect LDL entrapment in the arterial wall, which causes inflammation and promotes atherosclerosis. The molecular basis underlying the pro- or anti-atherogenic effects of modified LDL is unclear. To test whether LDL modifications lead to changes in LDL structure and stability, we used (i) myeloperoxidase and Cu2+ to produce LDL oxidized to various stages, (ii) phospholipase A2 (PLA2) to hydrolyze LDL phospholipids, (iii) beta-glucose to glycosylate apoB in LDL. Earlier we showed that heat denaturation of LDL is a kinetically controlled reaction that involves partial unfolding of the beta-sheet structure in apoB, protein dissociation, and changes in LDL morphology such as fusion and rupture. Here we test the effects of LDL modifications on these structural transitions.
Our results show that LDL oxidation leads to a gradual unfolding of the secondary structure in apoB (observed by far-UV circular dichroism, CD) and inhibits heat-induced LDL fusion (observed by turbidity, near-UV CD and electron microscopy). We propose that fusion inhibition results from modifications that increase surface-to-core ratio (e.g., transfer of polar lipids to LDL or lipolysis of apolar lipids), and/or from protein cross-linking upon advanced oxidation.
To assess the effect of PC hydrolysis, we hydrolyzed LDL phospholipids by PLA2, removed free fatty acids by albumin, and analyzed the structure and stability of modified LDL. CD spectroscopy showed no significant changes in the apoB secondary structure. Turbidity and electron microscopy showed that PC hydrolysis promotes LDL fusion, an effect that is reversed by albumin treatment. Consequently, free fatty acids promote lipoprotein fusion. Interestingly, glycosylation of apoB and LDL treatment with niacin also promote lipoprotein fusion. These results help understand molecular basis for LDL fusion in vivo and in vitro.

1250-Pos

Thermodynamics of Gndhcl Induced Unfolding of A Helical Membrane Protein in Mixed Micelles

Ernesto A. Roman[1], José M. Argüello[2], **F. Luis González-Flecha[1]**.
[1]University of Buenos Aires, Buenos Aires, Argentina, [2]Worcester Polytechnic Institute, Worcester, MA, USA.

Mechanisms of folding and stability of membrane proteins are poorly understood. This is linked to the known difficulties to establish reversible denaturation conditions for these proteins. In this work, we describe the equilibrium unfolding of CopA, an 804 residues Cu^{+}-transporting ATPase from *Archaeoglobus fulgidus*. Guanidinium hydrochloride induced a reversible decrease in fluorescence quantum yield, far UV ellipticity, and the loss of ATPase and phosphatase activities. Refolding of CopA from this unfolded state led to recovery of full biological activity and all the structural features characteristic of the native enzyme. The unfolding process showed typical characteristics of a two state process with $\Delta G_{ow} = 13$ kJ·mol^{-1} and $m = 4$ kJ·mol^{-1}·M^{-1}. These seemly atypical values suggest the existence of non-detectable unfolding intermediates. Moreover, the C_m was 3 M and the $\Delta Cp_w°$ 0.93 kJ·mol^{-1}·K^{-1}, giving account of the thermophilic character of this protein. Circular dichroism spectroscopic analysis of the unfolded state shows that most of the secondary and tertiary structure was disrupted. The fraction of Trp fluorescence accessible to soluble quenchers shifted from 0.48 in the native state to 0.96 in the unfolded state with a significant red shift of fluorescence Trp spectra. Also, hydrophobic patches in CopA, mainly located in the transmembrane region, were disrupted as indicated by the lack of fluorescence from the 1-aniline-8-naphtalenesulfonate probe at high concentration of denaturant. Nevertheless, the unfolded state had a small but detectable amount of residual structure, which might play a key role in both CopA folding and adaptation for working at high temperatures.

Protein-Ligand Interactions II

1251-Pos

Thermodynamics of Binding Silver Ion to Jack Bean Urease

Ali Akbar Saboury[1], Elaheh Poorakbar[2], Ghoamreza Rezaei-Behbehani[3].
[1]Institute of Biochemistry and Biophysics, University of Tehran, Tehran, Iran, Islamic Republic of, [2]Biology Department, Payam Noor University, Tehran, Iran, Islamic Republic of, [3]Chemistry Department, Imam Khomeini International University, Qazvin, Iran, Islamic Republic of.

Jack bean urease (JBU; E.C. 3.5.1.5) has six identical subunits, which each subunit consists of a single kind of polypeptide chain containing 840 amino acid residues with relative molecular mass of 90770, excluding the two nickel ions per subunit. Inhibition of urease by heavy metal ions is important special in view of heavy metal ion pollution. Silver ion nearly is always listed as one of the strongest inhibitors. Silver ions coordinate to nitrogen- (histidine) and possibly oxygen- (aspartic and glutamic acids) containing functional groups in urease. Here, a thermodynamic study of silver ions by JBU was carried out at two temperatures of 27 and 37°C in Tris buffer (30 mM; pH=7.0) using an isothermal titration calorimetry. There is a set of twelve identical and non-interacting binding sites for silver ions. The intrinsic dissociation equilibrium constant and the molar enthalpy of binding are 185 μM and −16.7 kJ/mol at 27°C and 229 μM and −16.3 kJ/mol at 37°C, respectively. The molar entropy of binding is +15.7 J K^{-1} mol^{-1}at 27°C and +17.1 J K^{-1} mol^{-1} at 37°C. Hence, the binding process of silver ion to HBU is not only enthalpy driven but also it is entropy driven, which the role of entropy driven should be more effective by increasing the temperature.

1252-Pos

A New ITC Assay for Measuring Ultratight and Low-Affinity Protein-Ligand Interactions

Georg Krainer[1], **Sandro Keller[2]**.
[1]Leibniz Institute of Molecular Pharmacology (FMP), Berlin, Germany,
[2]Technical University Kaiserslautern, Kaiserslautern, Germany.

Isothermal titration calorimetry (ITC) is the gold standard for the quantitative characterisation of protein-ligand and protein-protein interactions.[1] However, reliable determination of the dissociation constant (K_D) is typically limited to the range 100 μM > K_D > 1 nM. Nevertheless, interactions characterised by a higher or lower K_D can be assessed indirectly, provided that a suitable competitive ligand is available whose K_D falls within the directly accessible window.[2] Unfortunately, the established competitive ITC assay requires that the high-affinity ligand be soluble at high concentrations in aqueous buffer containing only minimal amounts of organic solvent. This poses serious problems

when studying protein binding of small-molecule ligands taken from compound libraries dissolved in organic solvents, as is usually the case during screening or drug development.
Here we introduce a new ITC competition assay that overcomes this limitation, thus allowing for a precise thermodynamic description of high- and low-affinity protein-ligand interactions involving poorly water-soluble compounds. We discuss the theoretical background of the approach and demonstrate some practical applications using examples of both high-affinity ($K_D < 1$ nM) and low-affinity ($K_D > 100$ μM) protein-ligand interactions.
[1] Velázquez Campoy and Freire, *Biophys. Chem.***2005**, *115*, 115.
[2] Sigurskjold, *Anal. Biochem.***2000**, *277*, 260.

1253-Pos
Binding of A Natural Sterol to the Osh4 Protein of Yeast and Membrane Attachment
Brent Rogaski, Jeffery B. Klauda.
University of Maryland, College Park, MD, USA.
Osh4 is an oxysterol binding protein homologue found in yeast that is essential for the intracellular transport of sterols and for cell life. It has been proposed that Osh4 acts as a lipid transport protein, capable of carrying sterols from the endoplasmic reticulum to the plasma membrane (PM).
Molecular dynamics (MD) simulations were used to analyze the binding of ergosterol to the Osh4 protein on an atomic level. During the course of 25-ns simulations, the sterol molecule remained tightly bound to the binding pocket of Osh4. These simulations revealed ergosterol binding was aided by both water-mediated interactions between the 3-hydroxyl (3-OH) group of ergosterol and surrounding polar residues as well as direct hydrogen binding between ergosterol and the Trp^{46} and Gln^{96} residues. Analysis of the interaction energy between ergosterol and Gln^{96} shows distinctly different states (−9.3 kcal/mol, −7.3 kcal/mol, and −4 kcal/mol), where the highest energy state was encountered 77% of the time.
In order to study how the Osh4 protein attaches to the PM, possible lipid binding sites were investigated through the use of a docking program as well as MD simulations. A model compound consisting of a phosphocholine lipid head group truncated at the C2 carbon solvated the Osh4 protein in conjunction with water. Protein/lipid interactions were observed and used to determine the proper orientation and placement of the protein with respect to a model membrane. We also developed a model yeast membrane containing ergosterol using CHARMM-GUI, and key membrane properties were investigated using data collected from a 60-ns MD simulation (areas per lipid, density profiles, and lipid dynamics). Ultimately, understanding how Osh4 attaches to the PM will lead to a clear understanding on how this protein transports sterols *in vivo*.

1254-Pos
Splitting of the Allosteric Function in Human Hemoglobin with an Altered Alpha1Beta1 Interface
Antonio Tsuneshige, Katsumi Takahashi, Takuro Ohara.
Hosei University, Tokyo, Japan.
Previously, it was shown that human semihemoglobins, i.e., hemoglobin dimers of the form (alpha)(beta) in which only one subunit, either alpha or beta, contained a functional heme group while the complementary apo subunit lacked heme, were sensitive to allosteric effectors, which caused modulation of their affinity for oxygen (Tsuneshige, A. et al. (2004) J. Biol. Chem. 279, 48959-48967). The presented evidences contradicted the classic tenet of the ‘‘two-state’’ model of allostery in which modulation of the affinity for oxygen could only be achieved by a tetrameric hemoglobin adopting the high-affinity ‘‘R’’ or the low-affinity ‘‘T’’ conformations in a reversible fashion.
For the present study, we have prepared a hemoglobin molecule in which the residues alpha104Cys and beta112Cys were chemically modified following a reaction of the sulhydryl groups with a thiopyridyl reagent. These two residues are present in the alpha1beta1 interface, thus we expected that their chemical modifications would impair drastically the intradimeric communication. Surprisingly, oxygenation curves at different pH values, or in the presence of the allosteric efector inositol hexakisphosphate (IHP) showed striking common characteristics: symmetric shape, presence of cooperative binding of oxygen, and a corresponding decrease in overall oxygen affinity in response to acidic conditions or the presence of IHP. Moreover, affinities for oxygen at low and high saturation levels were both affected in similar fashion under any solution condition. These results strongly suggest that the modified hemoglobin behave like dimers exhibiting allosteric properties.

1255-Pos
Contrasting Effects of Halides on the Structure and Function of A Multimeric Allosteric Protein
Takuro Ohara, Antonio Tsuneshige.
Hosei University, Tokyo, Japan.
We have used two halide salts, namely, sodium chloride and sodium iodide, and studied their impact on the oxygenation characteristics of adult human hemoglobin (Hb). Previous studies in our group showed that both the halide salts exerted similar effects on the Hb function at concentrations below 0.1 M, i.e., an overall decrease in the affinity for oxygen, as a result of a decrease in the affinity at low oxygenation levels. However, as the halide concentrations increased, while chloride continued producing a progressive but rather diminished effect, iodide reverted its effects on Hb: the overall affinity for oxygen rather increased. Careful analysis of the oxygenation curves revealed that while the affinity for oxygen decreased at high oxygen saturation levels, the affinity at low oxygen concentration increased markedly. These effects reached a plateau at a concentration of 2 M, but even more surprisingly, cooperativity was never canceled. The results hinted at the possibility that iodide ions were splitting the tetrameric Hb molecules into asymmetric dimers. Dimers have been and still are considered non-cooperative, high oxygen-affinity systems. Yet, our present data clearly contrast with the previous tenet since cooperativity index showed values as high as 1.6 in the presence of 2 M NaI. Determination of molecular weight by size exclusion chromatography, and the study of oxygenation characteristics of symmetric nickel-iron Hb hybrids in the presence of sodium iodide showed that in fact the tetrameric Hb splits into two dimers that, strikingly, remain allosterically functional.

1256-Pos
Exploring the Conformational Space for the Interactions of Aromatic Residue Analogs with Biologically Important Saccharides
Manju Kumari, Raghavan B. Sunoj, Petety V. Balaji.
Indian Institute of Technology Bombay, Mumbai, India.
Proteins interacting with carbohydrate ligands are getting a great deal of attention because of its important role in various biological processes. The crystal structures of several lectin-saccharide complexes have shown the presence of an aromatic residue in the binding site. The C-H hydrophobic patch of saccharide ‘‘stacks’’ against pi-cloud of aromatic residues forming CH-pi interactions, which are governed by dispersive and charge transfer interactions. The energetics of saccharide - aromatic residue interactions are dictated by their mutual position-orientations. It is conceivable that there exist low-energy position-orientations other than those found in the limited number of crystal structures of protein-carbohydrate complexes known to date. Hence, we have explored the conformational space for the interactions of 3-methylindole (3-MeIn), *p*-hydroxytoluene (p-OHTol) and toluene (Tol) (analogs of tryptophan, tyrosine and phenylalanine, respectively) with six saccharides. A Monte Carlo conformational search method was used to explore the features of the molecular potential energy surfaces. We found that the saccharides are densely populated above and below the pi-cloud of the aromatic ring of the amino acid residue but not along the edges. Clustering of conformers indicate the aromatic residues are spread out when interacting with C-H atoms as compared to that with -OH groups. The saccharides were capable of sliding on the surface of the aromatic residue. Four C-H groups can simultaneously participate in CH-pi interaction in 3-MeIn systems owing to its larger surface area. The β-D-Galactose and β-L-Fucose have been found to interact only through their b- and a-faces, respectively. Our ability to understand molecular flexibility through conformational search will further lead to advances in the design of drugs and to understand the advantages of selective choice of aromatic residues viz., tryptophan, tyrosine or phenylalanine in different carbohydrate binding proteins.

1257-Pos
From SPRI (Surface Plasmon Resonance Imaging) Affinity Capture Analysis Up to On-Chip MALDI-MS/MS Analyte Identification
Karen E. Steege Gall[1], Sophie Bellon[2].
[1]Horiba Jobin Yvon Inc., Edison, NJ, USA, [2]Horiba Jobin Yvon S.A.S., Orsay Cedex, France.
Multiplex format SPRi analysis allows direct visualization and thermodynamic analysis of biomolecular interactions, and is advantageously used for ligand-fishing of captured bio-molecules on multiple immobilized receptors. Mass spectrometry is a powerful tool for structural characterization and identification. Therefore, the combination of SPRi and MS into one concerted procedure is of a great interest for functional and structural analysis in the fields of proteomics, drug-discovery or diagnostic. We have implemented an on-chip MALDI analysis in which affinity captured bio-molecules are directly detected from the SPR-sensor surface.
The model presented was based on antigens-antibodies interactions. Antibodies, Anti-Beta-lactoglobulin, Anti-ovalbumin and a reference, were arrayed on biochip functionalized with a patented SAM-NHS surface chemistry and the SPR experiments were performed using a MS buffer. A mixture of label free antigens, Beta-lactoglobulin and ovalbumin, was injected and analyte capture was followed in real time. Following the collection of kinetic constants (Kon and Koff) information, the biochip was removed and each spot was submitted

to in situ digestion treatment and MALDI matrix deposition. The SPRi sensor surface was inserted directly in an appropriate MALDI plate holder and MALDI-MS and MS/MS complete identification of the retained antigens was performed directly from each individual spots on the biochip. Using this process, the transfer of the biochip into the MALDI apparatus consecutive to a SPR imaging experiment was straightforward without intermediate treatment that could lead to sample loss and/or contaminations.
A same surface array is dedicated to SPRi for affinity separation and subsequent MALDI-MS and MS/MS identification of the retained ligands from complex solution.

1258-Pos
Thermodynamic Principles of Metal Binding to Biological Systems
Purushottam D. Dixit, Dilip Asthagiri.
Johns Hopkins University, Baltimore, MD, USA.
We study the selective binding of the softer K+ ion over the harder Na+ and Mg++ ions to the 58 nucleotide ribosomal RNA fragment and the S2 site of the KcsA K+ channel using all atom MD simulations. The ribosomal RNA is interesting in that it binds the K+ over the harder Mg++ ion. We calculate the free energy of exchanging K+ with Mg++ in the binding site relative to the change in the aqueous solution. In order to explain the selectivity, we find that it is necessary to consider the change in the internal energy of the ion binding site. Interestingly, similar physics is observed in the KcsA S2 site. There we elucidate the role of coordination number fluctuations, ion-site binding energetics, and site-site interaction energetics in determining the selectivity of the S2 site for K+: once again, the reduced strain in the site in the presence of K+ (relative to Na+) explains selectivity. Thus, despite the uncommon origin and completely different chemical composition of the binding site, in both the cases the binding site is constricted in the presence of the harder ion and causes an increase in the unfavorable electrostatic strain. This strain is what leads to the observed selectivity for the softer K+ ion.

1259-Pos
Effect of Variants at the 78th Residue on Neocarzinostatin Chromophore Release
Hung-Wen Chi, Zhi-Ming Lu, Yu-Hua Luo, **Der-Hang Chin**.
National Chung Hsing University, Taichung, Taiwan.
Neocarzinostatin is a potent antitumor antibiotics chromoprotein complex. It consists of a labile enediyne chromophore and a protective carrier protein. Release of the bioactive chromophore is the initial key step in its cytotoxic mode of action. We showed that F78 of the carrier protein plays an important role in gating the release. To further study the structural role of 78th side chain in the release mechanism, we made variants at the 78th residue using a PCR-based *in vitro* mutagenesis method. The identity and purity of the expressed protein variants were confirmed by SDS-PAGE, UV, HPLC, and MS spectroscopy. Oxygenation was applied to promote formation of disulfide bonds when necessary, and the integrity of disulfide linkages was verified by a designed iodoacetamide-based test. Thermal denaturation study and CD spectroscopic analysis showed that stability and backbone conformation of these variants were conserved as compared to the wild-type protein. Two-dimensional ^{15}N-^{1}H HSQC NMR study suggested that the majority of residues around the binding cleft were not disturbed. Reconstitution of the enediyne chromophore into these protein variants showed efficient binding and the binding structure appeared to be similar to that of the native neocarzinostatin. Once the backbone structural effect was excluded, side chain structural effect on kinetic release was studied by monitoring fluorescence changes on samples containing glutathione and the reconstituted variants. The results showed that, except aromatic side chains, the basic variants increased the release rate more significantly than the acidic ones. Depended upon the length, steric hindrance, or hydrophobicity, the variants with aliphatic side chain also increased the release rate at different extent.

1260-Pos
Mechanical Regulation of a Cell Binding Site: Bacterial Adhesins can Distinguish Different Physical States of Fibronectin
Samuel Hertig.
ETH Zurich, Zurich, Switzerland.
Using extracellular matrix (ECM) fibers, we provide an experimental proof that mechanical forces can disrupt a bacterial binding site. Several bacterial species (gram positive and spirochetes, e.g. S. Aureus and B. Burgdorferi) express membrane-anchored fibronectin (Fn) binding proteins composed of multiple Fn-binding repeats (FnBRs), each of which bridges several Fn type I modules (FnI). As demonstrated here, the repetitive design of bacterial adhesins enables them to recognize the physical state of a multimodular protein: stretching fibrillar fibronectin causes a structural mismatch switching this multivalent binding site to low affinity as revealed at atomic resolution by steered molecular dynamics and confirmed utilizing a FRET-based Fn fiber stretching assay. The application of external mechanical force on the termini of Fn leads to an increase of the intermodular distance between the adjacent FnI modules, and the peptide can no longer bind via multivalent interactions. Even phylogenetically distinct bacteria use similar motifs to bind fibronectin, but have different numbers of FnBRs.

1261-Pos
Quantifying Water-Mediated Protein-Ligand Interactions in a Glutamate Receptor
Michelle A. Sahai.
University of Oxford, Oxford, United Kingdom.
It is becoming increasingly clear that careful treatment of water molecules in ligand-protein interactions is required in many cases if the correct binding pose is to be identified in molecular docking. Water can form complex bridging networks and can play a critical role in dictating the binding mode of ligands. A particularly striking example of this can be found in the ionotropic glutamate receptors. Despite possessing similar chemical moieties, crystal structures of glutamate and alpha-amino-3-hydroxy-5-methyl-4-isoxazole-propionic acid (AMPA) in complex with the ligand-binding core of the GluA2 ionotropic glutamate receptor revealed, contrary to all expectation, two distinct modes of binding. The difference appears to be related to the position of water molecules within the binding pocket. However, it is unclear exactly what governs the preference for water molecules to occupy a particular site in any one binding mode. In this work we use density functional theory (DFT) calculations to investigate the interaction energies and polarization effects of the various components of the binding pocket. Our results show i) that the ligand and its binding mode dictate the interaction energy of a key water molecule which can be thought of as part of the ligand rather than part of the protein ii) that polarization effects can be large and iii) that the interaction energy of a neighbouring water is particularly large (compared to the other waters in the binding pocket) and may offer a route to compounds with improved affinity if it can be displaced. We discuss the results within the broader context of drug-design.

1262-Pos
Epitope Mapping of Anti-DCP Antibody Using Fluorescence Correlation Spectroscopy
Qiaoqiao Ruan, Gangamani Beligere, Sergey Y. Tetin.
Abbott Lab, Abbott Park, IL, USA.
Des-gamma-carboxy prothrombin (DCP), also known as protein induced by vitamin K antagonist (PIVKA-II), is a recognized clinical marker for hepatocellular carcinoma. Prothrombin contains 10 gluamic acid (Glu) residues within its N-terminus (GLA domain) which are post modified to gamma-carboxyglutamic acid (GLA). DCP is an abnormal form of prothrombin in which some of the 10 glutamic acid residues remain unmodified. A monoclonal antibody was developed to specifically recognize DCP, but not prothrombin. In this study we identified the epitope of the anti-DCP antibody using a series of short peptides representing the GLA domain. For each peptide, a single Glu residue was replaced with a GLA residue. The critical Glu residues recognized by the antibody were identified in a competitive format using fluorescence correlation spectroscopy (FCS). We also evaluated the DCP specificity of the antibody using homologues peptide from various GLA domain proteins present in various blood coagulation factors. The dissociation constant of the antibody was determined using FRET based method.

1263-Pos
The Effect of Alpha-Helix Linker Length on Volatile General Anesthetic Binding to the Four-Alpha-Helix Bundle (Aα2-L38M)2
Lucia M. Morstadt, Jonas S. Johansson.
University of Pennsylvania, Philadelphia, PA, USA.
In order to investigate the effects of the length of the linker connecting the alpha-helices in the di-alpha-helical protein $A\alpha_2$-L38M on the overall structure and on the affinity of anesthetic binding to four-alpha-helix bundle ($A\alpha_2$-L38M)$_2$, we designed constructs containing six and four glycine residue linkers instead of the original eight, respectively. We used site-directed mutagenesis with primers designed to remove two and four glycine residues, respectively, out of eight residues of the original glycine linker present in the four-alpha-helix bundle ($A\alpha_2$-L38M)$_2$. Variant proteins were expressed in bacteria and purified to homogeneity using reverse-phase HPLC. Protein identities were verified using mass spectrometry. Our initial studies reveal that the variant four-alpha-helix bundle with a four glycine linker binds halothane with a dissociation constant of 1.00 ± 0.05 mM, as assessed using fluorescence spectroscopy. This represents a 10-fold decreased affinity for the volatile general anesthetic compared to the original ($A\alpha_2$-L38M)$_2$ design, which featured an eight glycine linker. The results indicate that the length of the glycine linker, and the resulting dynamic behavior of the four-alpha-helix bundle protein, dramatically influence volatile general anesthetic binding affinity.

1264-Pos

Escherichia Coli Redox Enzyme Maturation Proteins, TorD and DmsD Interact with GTP as Shown by Native Page Assays

Vy A. Tran, Raymond J. Turner.
University of Calgary, Calgary, AB, Canada.

The twin-arginine translocation (Tat) system can transport fully folded proteins across the cytoplasmic membrane. Transport is dependent on a twin-arginine motif within a cleavable signal peptide. Substrates for the Tat system include redox proteins, necessary for growth during anaerobic respiration. The transport of the catalytic subunits responsible for N- and S-oxide respiration, DmsAB and TorA are dependent on DmsD and TorD respectively. Both are system specific chaperones termed redox enzyme maturation proteins (REMP) and are predicted to play multiple roles in the maturation and export of redox enzymes, including the known role for binding to the twin-arginine motif. Upon successful translocation and signal peptide cleavage, the REMPs remain in the cytoplasm. The question arises as to what governs binding and release of the signal peptide in order for translocation to occur. Here, we propose that REMPs may function like general chaperones like DnaK/DnaJ which exhibit nucleotide binding and hydrolysis for substrate release. It is speculated that TorD binds GTP or the molybdopterin dinucleotide with low affinity. Furthermore, GTP binding sites have been predicted for Shewanella typhimurium TorD (1N1C.pdb) and Salmonella typhimurium DmsD (1S9U.pdb) structures. We have developed a native PAGE assay, showing both DmsD and TorD exhibiting different banding patterns in the presence of GTP, while being unaffected by ATP. Preliminary results indicate that the presence of the NTP counter ion Mg2+ in addition to GTP does not change the banding patterns. DmsD and TorD share the same highly alpha-helical structure. Therefore we have done structural alignments to the E. coli DmsD (3EFP.pdb) structure and mapped the residues predicted to bind GTP to identify targets for mutagenesis. Our work aims to definitively answer the question if these chaperones indeed bind GTP.

1265-Pos

Role of Dimerization in Poly-Ubiquitin Chain Formation

Benjamin W. Cook.
University of Western Ontario, London, ON, Canada.

The ubiquitin proteolysis pathway is responsible for protein degradation utilizing three enzymes, the ubiquitin-activating enzyme (E1), an ubiquitin-conjugating enzyme (E2), and a ligating enzyme (E3), that respectively activate, transfer and ligate ubiquitin (Ub) onto a target protein. Repeated cycles of this process results in a poly-ubiquitinated target protein that is degraded by the 26S proteasome. How the poly-Ub chains are formed remains unknown. One suggested model involves the dimerization of an E2 enzyme allowing Ub passage and ligation between adjacent E2 enzymes. We are examining this mechanism for the E2 enzymes Ubc1 and HIP2, which contain C-terminal UBA domains that allows for non-covalent Ub binding in addition to a thioester-bound Ub. The dimerization of these E2 enzymes was tested using sedimentation equilibrium and small angle x-ray scattering and showed that both are monomeric. Disulphide-bound E2-Ub complexes were used to mimic the thiolester, and these complexes had a weak propensity to dimerize. This was supported in ubiquitination assays that showed a thioester-bound Ub on an E2 could be transferred to a non-hydrolyzable, disulphide-bound Ub molecule on a second E2 enzyme. This suggests weak dimerization is likely sufficient to allow the first step of poly-Ub chain formation. We tested whether the length of the poly-Ub chains on HIP2 stimulates dimerization by creating HIP2-Ub_2 and HIP2-Ub_4 complexes. The ability of these species to dimerize was assessed via sedimentation equilibrium and NMR spectroscopy. The isolated UBA domain from HIP2 was used in competition experiments to determine how it might influence poly-Ub chain formation. This work provides the first structural evidence for poly-Ub chain formation as assembled on the E2 enzyme.

1266-Pos

How Insulin-Like Growth Factor Hormones, IGF1 And IGF2, Engage their Cognate Receptor

Harish Vashisth, Cameron F. Abrams.
Drexel University, Philadelphia, PA, USA.

The type 1 insulin-like growth factor receptor (IGF1R), a trans-membrane glycoprotein, is activated by binding of its cognate growth hormones, IGF1 and IGF2. The IGF family was suggested to play a key role in cancer development and progression, thereby making it a potential target for anti-cancer therapeutic efforts. However, the molecular mechanisms underlying hormone-receptor interactions are unclear, as are the molecular bases for differing affinity of each hormone, due in part to the fact that there have been so far no detailed structural models of IGFs-bound-IGF1R to test. Constructed using a homology model of the IGF1R ectodomain, and the NMR structures of IGF1/2, with the help of an MD-assisted Monte-Carlo approach, we present the first experimentally consistent all-atom structural models of IGF1/IGF1R and IGF2/IGF1R complexes. Our models are notable because each hormone remains stably bound in independent 36-ns long explicit-solvent molecular dynamics (MD) simulations. The asymmetric structural relaxation of the apo-IGF1R homology model in a 30-ns MD equilibration facilitated the computational docking of each hormone. Our predicted complexes are significant because we observe simultaneous contacts of each hormone with the site 1 (formed by L1 and CR), and site 2 (formed by L2, and the fibronectin domains), of the receptor, suggesting cross-linking of receptor subunits. Interestingly, we observe differences in recognition of each hormone by IGF1R, because IGF1 interacts relatively strongly with L1 and CR (IGF1R), whereas IGF2 has stronger interactions with L2 and the fibronectin domains. Our simulations also provide direct evidence in favor of previously suggested electrostatic complementarity between the C-domains of IGF1/2 and the CR-domain of the receptor. Additionally, we provide detailed hormone-receptor contacts that are consistent with earlier mutagenesis studies.

1267-Pos

Investigation of the Cu(II)-Binding Properties of Alpha-Synuclein

Christopher Dudzik.
U.C. Santa Cruz, Santa Cruz, CA, USA.

Parkinson's disease is a chronic, progressive, and often fatal neurodegenerative disorder that affects 1 in 100 individuals over the age of 60. The hallmark of Parkinson's disease is modified dopaminergic neurons termed Lewy Bodies, of which the protein Alpha synuclein is the primary fibular component. Epidemiological studies correlated long-term metal exposure (such as in an industrial setting) with an increased incidence of fatal Parkinson's disease. Fibril assays indicated that certain metals, notably Cu(II), Fe(III) and Al(III) increase the rate of in vitro alpha synuclein fibril formation. Our work seeks to elucidate the stoichiometry, affinities, chelating residues and binding motifs of Cu(II) to alpha synuclein. Using EPR spectroscopy to analyze recombinant alpha synuclein, mutants and synthetic peptides we have determined a heretofore unknown Cu(II) binding motif. This motif may provide insight into a possible explanation for the increase in the rate of alpha synuclein fibril formation.

1268-Pos

Thermodynamic and Hydrodynamic Characterization of the Interaction Between DmsD and the DmsA Twin-Arginine Leader Peptide

Tara M.L. Winstone, Raymond J. Turner.
University of Calgary, Calgary, AB, Canada.

The system specific chaperone DmsD plays a role in the maturation of the DMSO reductase enzyme through its interaction with the twin-arginine leader peptide of the catalytic subunit DmsA, prior to its assembly into the holo-enzyme. A pocket of residues, clustered together within the structure of DmsD, has previously been shown to be important for binding a fusion protein composed of 43 of the 45 amino acid residues of the DmsA leader peptide however the region of the DmsA leader peptide that interacts with DmsD has not been identified. Various portions of the DmsA leader peptide were synthesized and assayed for binding to DmsD using isothermal titration calorimetry. A peptide composed of 27 amino acid residues near the C-terminus of the DmsA leader sequence was found to bind to DmsD and subsequently used to characterize the thermodynamics of binding of each of the DmsD variant proteins previously shown to be important for binding to the DmsA leader peptide. Size exclusion chromatography and native-PAGE were used to determine the effect of peptide binding on multimeric state and electrophoretic mobility for each of the variant proteins. In the presence of the peptide, wild type DmsD migrates faster on native-PAGE but remains monomeric while some DmsD variant proteins undergo oligomerization while still changing to a the same faster migrating form on native-PAGE. The electrophoretic mobility, multimeric forms and thermodynamics of peptide binding of mutations in the chaperone leader-binding site are compared.

1269-Pos

Binding of Antibodies to Continuous Antigenic Epitopes

Sergey Y. Tetin, Qiaoqiao Ruan, Sylvia C. Saldana.
Abbott, Abbott Park, IL, USA.

Continuous, or linear, antigenic epitopes are common to proteins and peptides. The accessibility of continuous epitopes often depends on protein/peptide conformation and its proximity to disulfide bridges. Temperature dependence of the equilibrium binding constants and the kinetic rates were studied for anti-BNP mAb 3-631 by means of fluorescence spectroscopy. This antibody recognizes a relatively short amino acid sequence in the loop between cysteines 10 and 26 of human B-type natriuretic peptide.

Thermodynamic parameters including changes in the free energy, enthalpy and entropy measured at equilibrium are in a good agreement with the parameters

calculated from kinetic data. The differences in thermodynamic parameters measured for the cyclic and reduced peptide explain epitope mapping data obtained by NMR.

1270-Pos
Creating Steroidal Ligand-Receptor Pairs for Behavioral Studies of Androgen Receptor
Leslie A. Cruz[1], Marc B. Cox[2], Robert J. Fletterick[1].
[1]University of California San Francisco, San Francisco, CA, USA,
[2]University of Texas at El Paso, El Paso, TX, USA.
Heterologous agonist-receptor pairs designed after high resolution structural studies have yielded insights into specificity of signaling by protein kinases and G-protein coupled receptors. We are extending this concept to the realm of steroid nuclear receptors with a goal to learning the behavioral effects of steroid activation of the androgen receptor in the brain. We are designing a steroidal ligand-hormone receptor pair such that the novel ligand does not bind to endogenous androgen receptors (AR), and the designer receptor does not bind to endogenous androgens. We have synthesized novel steroids that do not bind endogenous AR. Since steroid binding affects the folding of the receptor, prediction of amino acid mutations in the androgen receptor that are needed to accommodate the steroidal ligand is difficult. To combat this issue, we are using a genetic selection in S. cerevisiae to reveal gain of function activity from a library of about $10 \perp 9$ randomly mutated AR ligand binding domains. In this experiment, yeast strains containing a hormone-inducible HIS3 gene select for full length AR mutants that are active in the presence of our novel steroids.

1271-Pos
Molecular Dynamics Study of 2-Arachidonoyl-Sn-Glycero-3-Phosphoinositol (2-AGPI) and Lysophosphatidylinositol (LPI) in a POPC Bilayer and their GPR55 Docking Sites
Evangelia Kotsikorou[1], Karla E. Madrigal[1], Diane L. Lynch[1],
Dow P. Hurst[1], Mary E. Abood[2], Patricia H. Reggio[1].
[1]University of North Carolina at Greensboro, Greensboro, NC, USA,
[2]Temple University, Philadelphia, PA, USA.
GPR55 is a Class A G protein-coupled receptor that has been shown to be activated by cannabinoids (Henstridge et al. FASEB J, 2008). The receptor is expressed in several mammalian tissues including several brain regions. It has been reported that GPR55 is also activated by LPI found in rat brain (Oka et al. BBRC, 2007), with 2-AGPI having the highest activity (Oka et al. J Biochem, 2009). Since 2-AGPI and LPI are lipids and are shown to interact with the membrane-embedded GPR55 receptor, we undertook a study of the location and conformations they can adopt in a phospholipid bilayer, as well as, of their interaction modes with GPR55. To this end, 2-AGPI and LPI were added to a fully hydrated, pre-equilibrated POPC bilayer (28 waters/lipid; 72 lipid molecules with 36 in each leaflet) and their behavior in POPC was studied using the NAMD2 molecular dynamics software package (NPAT ensemble; P = 1atm, T=310K) with the CHARMM27 parameter set including data for polyunsaturated lipids, and the TIP3P water model. The MD studies place the 2-AGPI and LPI headgroups in the water-lipid interface with the inositol moiety either upright and solvated in water or bent and buried in the POPC headgroups. Extensive ligand inter- and intramolecular hydrogen bonding contributes to the inositol location and conformation. 2-AGPI's acyl tail is extremely flexible and prefers compact to moderately extended conformations, whereas LPI's tail prefers more extended ones. Following these MD studies, the ligands were docked in a GPR55 model in the TMHs 1,2,3, 6 and7 region using K2.60 as the primary interaction site. [Support: NIH RO1 DA023204 (MEA) and KO5 DA021358 (PHR)]

1272-Pos
Diminished Cooperativity: Comparing Linker Lengths in Synaptotagmin I C2A Domain
Jesse R. Murphy[1], Kristofer J. Knutson[1], Jacob W. Gauer[1], R. Bryan Sutton[2],
Anne Hinderliter[1].
[1]University of Minnesota Duluth, Duluth, MN, USA, [2]Texas Tech University
Health Sciences Center, Lubbock, TX, USA.
Exocytosis of neurotransmitters is triggered by the initial influx of Ca2+. Synaptotagmin I is known to bind Ca2+ and the phospholipid membrane to modulate this process. The exact mechanism for this information transduction, however, is not well known. Synaptotagmin I contains two binding domains, C2A and C2B, that are tethered to a neurotransmitter containing, lipid vesicle with a flexible linker region. The wild type C2A domain acts as a Ca2+ dependent trigger by binding the calcium ions in a cooperative manner. We seek to understand the role that the linker region has on the binding properties of the protein. To do this, a shortened construct (amino acids 141-267 verses amino acids 97-265 of the previously studied long construct) has been utilized as a probe to examine the effects of the truncated linker region. Ca2+ and phospholipid binding assays have been carried out and monitored via steady state fluorescence to make a thermodynamic comparison between the two constructs. Binding partition functions have been derived for this purpose and clearly show the diminished linkage relationship between the binding sites of the shortened construct. This material is based in part upon work supported by the National Science Foundation under CAREER-MCB 0747339

1273-Pos
Selectin Mechanokinetics and Two-Dimensional Bond Formation Determine and are Reported by Nano-Motion Dynamic Patterns
Brian J. Schmidt, Jason A. Papin, Michael B. Lawrence.
University of Virginia, Charlottesville, VA, USA.
Binding between surface-tethered proteins at cellular interfaces has been considered two-dimensional because of the restricted motion of the two binding partners. Two-dimensional protein interactions between cells are critical for many biological processes, such as leukocyte vascular adhesion via selectins. Experimental measurements have yielded data on the kinetics of selectin bond formation and dissociation. Additionally, computational methods have been employed to integrate molecular and cellular properties to elucidate the factors that influence the dynamics of selectin-mediated rolling. Simulation methods focused on biomolecular properties promise to yield additional novel insights into the molecular component of adhesion with the assistance of measurements from improved assays. We performed an in silico investigation on the effects of the kinetic force dependence, molecular deformation, grouping adhesion receptors into clusters, two-dimensional bond formation, and nanoscale vertical transport on outputs that directly map to observable motions. Statistics describing the motion patterns tied simulated motions to experimentally reported quantities. Distributing adhesive forces among P-selectin/PSGL-1 molecules closely grouped in clusters was necessary to achieve pause times observed in microbead assays. Notably, rebinding events were enhanced by the reduced separation distance following initial sphere capture. The result demonstrates vertical transport can contribute to an enhancement in the apparent bond formation rate. The result also suggests a new mechanism that may be important for the rebinding events characteristic of stable leukocyte rolling. When selectin receptor and ligand are restricted to small, two-dimensional interaction zones during rolling, the resultant wobble was found to be dependent on the confinement model used. Insight into two-dimensional bond formation gained from flow cell assays might also therefore be important to understand processes involving extended cellular interactions, such as immunological synapse formation.

1274-Pos
Single-Molecule Force Spectroscopy of the Interactions Between Platelet Integrin αIIbβ3 and Monomeric Fibrin
Rustem I. Litvinov[1], Henry Shuman[1], David H. Farrell[2], Joel S. Bennett[1],
John W. Weisel[1].
[1]University of Pennsylvania, Philadelphia, PA, USA, [2]Oregon Health &
Science University, Portland, OR, USA.
Platelet-fibrin interactions under hydrodynamic blood shear are mediated by the integrin αIIbβ3, but the mechanism of αIIbβ3 binding to fibrin is largely unknown, although interactions with fibrinogen have been extensively studied. We used the optical trap to measure forces required to separate a laser-trapped-bead coated with monomeric fibrin from a pedestal coatedwith purified αIIbβ3. Experiments were performed with recombinant fibrin obtained from thrombin-treated fibrinogen, either wild-type or variants lacking putative integrin-binding sites. Integrin-fibrin interactions manifested as a bimodal force histogram with rupture forces from 20 pN to 140 pN, similar to αIIbβ3-fibrinogen but with somewhat higher binding probability. To test a role of the γ-chain C-terminal 400-411 dodecapeptide, the major αIIbβ3-binding site in fibrinogen, the most abundant fibrin (γA/γA) was replaced with a splicing variant (γ'/γ'), in which the γC-terminus has new amino acids from 408 to 427. Unexpectedly, the lack of the γC400-411 motif did not affect the ability of fibrin to interact with αIIbβ3, suggesting that this structure may not be a major integrin-binding site in fibrin. At the same time, fibrin-integrin interactions were partially inhibited by the γC-dodecapeptide, indicating that the γC400-411 motif still may be involved, perhaps indirectly. Two RGD motifs, one located in the αC region and the other in the coiled-coil connector, were tested as the potential binding sites by using fibrin(ogen) variants αD574E and αD97E. Both of them had a reduced integrin-binding strength and displayed the cumulative binding probability about 2/3 of that of the wild-type fibrin, suggesting that the RGD motifs play a role in the αIIbβ3-fibrin interactions. Free γC-dodecapeptide did not affect the reactivity of the D574E and D97E mutants. The results suggest that the αIIbβ3-fibrin interactions involve the RGD sites rather than the γC400-411 motif.

1275-Pos
Characterization of Selectin-Mediated Cell Binding in Shear Flow Using Micropatterning Technology and Modeling
Konstantinos Konstantopolous, ZiQiu Tong, Luthur Siu-Lun Cheung.
Johns Hopkins University, Baltimore, MD, USA.
Cellular interactions play an essential role in diverse (patho)physiological processes such as leukocytes extravasation and cancer metastasis. Selectins initiate the tethering and rolling of free-flowing cells on activated endothelium before the integrin-dependent firm adhesion under flow. Utilizing microfluidics devices and protein micropatterning technology, the adhesion kinetics of the HL-60 leukocyte-like cells to immobilized P-/L-selectin was investigated. Multiple selectin patches of varying lengths (6-160μm; in the direction of flow) and constant width (10μm) were patterned on a glass substrate to provide specific adhesion. A PDMS layer, which had been cured and peeled off from a 25μm height microchannel mold, was bonded on the patterned glass substrate to form the microfluidics device. Cell suspensions were perfused through the device under prescribed shear stresses varying from 0.25-2dyn/cm^2. Our data reveal the existence of a critical patch length, L_c, which represents the cell rolling distance to form an initial binding and is a function of the wall shear stress and the selectin density on the substrate. At $L<L_c$ no cell binding is detected on the patch. At $L\geq L_c$, the number of tethered cells increased with the patch length. A theoretical model was developed to analyze our data, and accounted for the selectin-mediated reversible binding kinetics, the shear-controlled association rate and two-pathway dissociation rate. Our model successfully fits to the experimental results and, in particular, the transition of the ''shear threshold phenomenon'' was correctly captured. Our model also shows that the ''shear threshold phenomenon'' is not observed if the selectin site density is $>$3000sites/μm^2. In summary, our analysis has identified the minimum cell rolling distance required for selectin-dependent binding to occur in a shear flow. Moreover, we have developed the first analytical equation to model cell binding with the shear threshold phenomenon.

1276-Pos
Distinguishing Binding from Allosteric Action in Escherichia Coli Phosphofructokinase
Bobby W. Laird, Gregory D. Reinhart.
Texas A&M Univ, College Station, TX, USA.
Thermodynamic linkage analysis involves the determination of binding parameters for substrate and allosteric ligand individually to free enzyme plus a coupling parameter that quantifies the nature and magnitude of allosteric interaction. Thus allosteric action can be differentiated from allosteric ligand and substrate binding affinities. Previously thermodynamic linkage analysis of the allosteric inhibition of E. coli PFK (EcPFK) by either phosphoenolpyruvate (PEP) or its analogs implied that different functional groups within the allosteric molecules play different roles in each of these two attributes. The data suggested in particular that the oxygen that bridges the phosphate group to the rest of the molecule in PEP plays a larger role in ligand binding than in allosteric signal propagation. In an effort to continue to elucidate the role of the PEP bridging oxygen the crystal structure of wild type EcPFK bound to PEP was determined for the first time. S58 was found to be in position for possible interactions with this bridging oxygen of PEP. EcPFK with the mutation S58A was constructed and characterized. The modified enzyme exhibits no variation in Km or Vmax compared to the wild type enzyme. However, the Kd for PEP is more than 85 times that of wild type while the allosteric coupling is diminished by 27%. The analysis of the S58A mutant provides additional evidence that the bridging oxygen in PEP primarily contributes to the binding free energy of PEP and makes a relatively minor contribution to the allosteric effect per se. Supported by NIH Grant GM33216 and Welch Foundation Grant A1548.

1277-Pos
Superheating of Ice in the Presence of Ice Binding Proteins
Yeliz Celik[1], Laurie A. Graham[2], Yee-Foong Mok[2], Maya Bar[3], Peter L. Davies[2], **Ido Braslavsky[1]**.
[1]Ohio University, Athens, OH, USA, [2]Queen's University, Kingston, ON, Canada, [3]Weizmann Institute of Science, Rehovot, Israel.
Antifreeze proteins (AFPs) are a class of ice binding proteins that are found in many cold-adapted organisms, where they serve as inhibitors of ice crystal growth and recrystalization. Adsorption-inhibition theory suggests that AFPs adsorb to ice surface and surface-adsorbed AFPs should prevent ice from melting as well as from freezing and evidence for such activity was shown experimentally (Knight and Devries, Science 1989). However, so far there has been no measurement of the melting inhibition of ice in AFP solutions. We examined a series of hyperactive and moderate AFPs and measured the melting hysteresis activity, which is defined as the elevation of the actual melting temperature above the equilibrium melting point. We observed that superheated ice crystals can be held stable for hours in AFP solutions. The measured superheating values were much more appreciable for hyperactive AFPs in comparison to moderate ones. The amount of this elevation was only a fraction of depression the freezing. Still, in these temperatures, we measured remarkably fast melting velocities of the superheated ice crystals which were proportional to the superheating values. Furthermore, we visualized fluorescently labeled AFPs on superheated ice crystals. The observation of superheating of by AFPs strongly suggest that AFPs adhere to ice surface as a part of their mechanism of action and the binding to ice surface is irreversible.

Membrane Protein Function II

1278-Pos
Bacterial Porin Disrupts Mitochondrial Membrane Potential and Sensitizes Host Cells to Apoptosis
Anke Harsman[1], Michael Meinecke[2], Thomas Rudel[3], Joachim Rassow[4], Richard Wagner[1].
[1]University of Osnabrueck, Osnabrueck, Germany, [2]MRC Laboratory of Molecular Biology, Cambridge, United Kingdom, [3]University of Wuerzburg, Wuerzburg, Germany, [4]Ruhr-Universität Bochum, Bochum, Germany.
The bacterial outer membrane porin PorB of Neisseria gonorrhoeae is an essential virulence factor of these pathogenic gram-negative bacteria which finally lead to the apoptotic degradation of host cells. In course of the infection process PorB is known to be transferred to the mitochondrial membranes of infected cells where it induces the dissipation of mitochondrial membrane potential by a so far unknown mechanism. Using single channel electrophysiology and spectroscopic techniques we were able to reveal the molecular mechanisms underlying this regulated process.
Based on a detailed study of the single channel characteristics of wildtype PorB and the mutant PorBK98Q lacking the putative ATP-binding site, we could identify the prerequisites for the formation of open pores in the mitochondrial inner membrane at physiological membrane potentials. Spontaneous incorporation of the β-barrel protein into membranes was followed by using CD-spectroscopy revealing large structural rearrangements during membrane insertion. We are now able to explain the molecular mechanisms by which targeting of bacterial toxin PorB to mitochondria of infected cells is setting up host cells to apoptosis.

1279-Pos
Functional Reconstitution of Membrane Proteins Monitored by Isothermal Titration Calorimetry
Nadin Jahnke[1], Oxana O. Krylova[1], Sandro Keller[2].
[1]Leibniz Institute of Molecular Pharmacology (FMP), Berlin, Germany, [2]Technical University Kaiserslautern, Kaiserslautern, Germany.
Membrane protein reconstitution denotes the transfer of a purified (but usually inactive) membrane protein from detergent micelles into lipid bilayers. The aim is to restore the native protein fold and function in a well-defined membrane environment. The reconstitution yield critically depends on a wide range of parameters, including temperature, pH, ionic strength, as well as the type and concentration of detergent, lipid, protein, and additives. Moreover, it is of paramount importance to initiate the reconstitution process from a suitable lipid-to-detergent ratio. Unfortunately, however, assessing the success of a reconstitution experiment has thus far been limited to a trial-and-error approach, which has substantially slowed progress in the field.
To address this problem, we have established high-sensitivity isothermal titration calorimetry (ITC) as a powerful tool for monitoring the reconstitution of membrane proteins into lipid vesicles. Using ITC, the complex changes in the physical state of a protein/lipid/detergent mixture during reconstitution can be followed in a non-invasive and fully automated manner. Here we exemplify this approach for the prokaryotic potassium channel KcsA, which we first purified in detergent micelles and then reconstituted into stable proteoliposomes at very high protein densities. Electrophysiological experiments performed in planar lipid membranes confirmed that KcsA regained its functional activity upon reconstitution.

1280-Pos
Quantitative Measurements of Receptor Interactions in Mammalian Cells: Implications for Human Pathologies
Sarvenaz Sarabipour, Kalina Hristova.
The Johns Hopkins University, Baltimore, MD, USA.
Receptor Tyrosine kinases (RTKs) are family of single-pass cell membrane receptors with extracellular ligand-binding domains and intracellular kinase domains, which conduct biochemical signals via lateral dimerization in the plasma membrane. Mutations in the transmembrane (TM) domains of these receptors are known to promote unregulated signaling. An example is the Ala391Glu mutation in the TM domain of FGFR3, which leads to pathologies

such as Crouzon syndrome and bladder cancer. This mutation has been shown to stabilize the isolated TM domain dimers in lipid membranes, but it is not known if it stabilizes the full length FGFR3 receptor dimers in the plasma membrane of mammalian cells.
To address the effect of the mutation in mammalian cells, we have determined free energies of dimerization for the wild type and mutant FGFR3 in mammalian (HEK293T and CHO) plasma membranes using the QI Förster resonance energy transfer (FRET) technique [Li et al.,2008]. The measured change in the dimerization free energy due to the Ala391Glu mutation is −1.2 kcal/mol, consistent with previous reports of hydrogen bond strength in proteins, as well as results for the isolated FGFR3 TM domains. Thus, we have shown that the mutation stabilizes the full length FGFR3 dimers in mammalian cells. We propose that this dimer stabilization is the major cause for FGFR3 overactivation and human pathologies.
Li E,Placone J,Merzlyakov M, Hristova K (2008) Quantitative measurements of protein interactions in a crowded cellular environment.Anal Chem 80:5976-5985.

1281-Pos
The Physical Basis Behind Achondroplasia, the Most Common Form of Human Dwarfism
Lijuan He, Kalina Hristova.
Johns Hopkins University, Baltimore, MD, USA.
Fibroblast growth factor receptor 3 (FGFR3) is a receptor tyrosine kinase which plays an important role in long bone development. The Gly380Arg mutation in FGFR3 transmembrane domain has been linked to achondroplasia, the most common form of human dwarfism. However, the exact mechanism underlying the pathology is under debate. One hypothesis is that the mutation stabilizes the active FGFR3 dimer in the plasma membrane. To test this hypothesis, here we measure the activation of wild type and mutant FGFR3 in mammalian cells, and analyze the activation using a physical-chemical model accounting for dimerization, ligand binding and phosphorylation probabilities. Our results demonstrate that the achondroplasia mutation does not increase the dimerization propensity of FGFR3. Instead, the data suggest that the mutation induces a structural change in the unliganded dimer. We propose that this structural change is a cause for pathogenesis in achondroplasia.

1282-Pos
Spectroscopic Design of Phospholamban Mutants to Treat Heart Failure
Simon J. Gruber[1], Suzanne Haydon[1], Kim N. Ha[1], Roger J. Hajjar[2], Gianluigi Veglia[1], David D. Thomas[1].
[1]University of Minnesota, Minneapolis, MN, USA, [2]Mt. Sinai Medical School, New York, NY, USA.
Ca^{2+} cycling through the SR in muscle cells is largely controlled by the Ca-pump (SERCA). SERCA transports Ca^{2+} into the SR and is inhibited by phospholamban (PLB) at submicromolar [Ca^{2+}], and this inhibition can be relieved by adrenergic stimulation. Contraction takes place when the Ca-release channel opens and the intracellular [Ca^{2+}] is high. One of the most common symptoms of heart failure (HF) is impaired calcium handling, frequently resulting from decreased SERCA activity. We are using EPR and NMR to study the relationships among structure, dynamics, and function of PLB, with the goal of designing LOF-PLB mutants (PLB_M) that can compete with WT-PLB and thus relieve SERCA inhibition. Several studies have shown that a pseudophosphorylated PLB (S16E-PLB) is effective for gene therapy in rodents and sheep, and we are using spectroscopic methods to refine this approach. We have developed a system for examining the function and interactions of SERCA and PLB in HEK cells. Active SERCA is expressed at a level high above basal ATPase activity, and cells are co-transfected with WT-PLB and/or PLB_M to measure SERCA inhibition in living cells. Unlike S16E-PLB, these mutants are able to respond to adrenergic stimulation. In addition to quantifying SERCA activity in the presence of PLB_M, we measure the ability of each mutant to compete with WT-PLB for binding to SERCA. This is done by measuring fluorescence resonance energy transfer (FRET) between labeled SERCA and WT-PLB. If PLB_M displaces WT-PLB, less energy is transferred between fluorophores and a decrease in FRET is observed. Based on these results, rAAV is used to test PLB_M in rodent and porcine models of HF for efficacy *in vivo* and ability to respond to adrenergic stimulation, with the goal of developing a novel, gene therapy based treatment for HF.

1283-Pos
The Activity of a Low-Affinity L-Arginine Transporter Quenches Peroxynitrite-Induced Fluorescence in Ventricular Cardiomyocytes
Jayalakshmi Ramachandran, **R. Daniel Peluffo**.
UMDNJ-New Jersey Medical School, Newark, NJ, USA.
We discovered a low-affinity, high-capacity L-arginine (L-Arg) transport process in rat cardiomyocytes consistent with the activity of the CAT-2A member of the y(+) family of cationic amino acid transporters (Peluffo, *J Physiol*, **580:**925-936, 2007), set to function in parallel with the previously described high-affinity, low-capacity CAT-1 (Lu et al., *Biosci Rep*, **29:**271-281, 2009). In assessing the role of a low-affinity transporter in this setting, we propose that CAT-2A protects cardiac muscle cells by ensuring the availability of proper L-Arg levels for the synthesis of nitric oxide (NO) *via* NO synthase (NOS). To test this hypothesis, acutely-isolated cardiomyocytes were loaded with the dye coelenterazine that greatly increases its fluorescence quantum yield in the presence of peroxynitrite ($ONOO^-$) and superoxide radicals. Cells were then exposed to 20 or 100 μM $ONOO^-$ and changes in fluorescence were followed with a spectrofluorometer. Addition of extracellular L-Arg reduced ONOO-induced fluorescence in a concentration-dependent manner, an effect that was not mimicked by D-arginine or L-lysine and was fully blocked by the NOS inhibitor L-NAME. L-Arg reduced fluorescence with K_i values of 0.84 ± 0.12 and 1.26 ± 0.16 mM at 20 and 100 μM $ONOO^-$, respectively. L-Arg ''zero effect'' on ONOO-induced fluorescence was also dependent on $ONOO^-$ concentration, with values of 145 and 363 μM for 20 and 100 μM $ONOO^-$, respectively. Below these values, decreasing concentrations of L-Arg progressively increased ONOO-induced fluorescence, an effect that was also blocked by L-NAME. All these effects can be explained by NOS-mediated NO synthesis, which may turn to $ONOO^-$ production at limiting L-Arg. Since $ONOO^-$ has detrimental effects on cardiac contractility, these results suggest a cardioprotective role for the low-affinity L-Arg transporter, ensuring proper supply of NOS substrate under a variety of physiological and pathological conditions.

1284-Pos
Studies on the Structure and Function of the Intracellular Region of the Plexin-B1 Transmembrane Receptor
Prasanta K. Hota[1], Yufeng Tong[2], Junia Y. Penachioni[3], Luca Tamagnone[3], Hee-Won Park[2], Matthias Buck[1].
[1]School of Medicine, Physiology and Biophysics, Case Western Reserve University, Cleveland, OH, USA, [2]Structural Genomics Consortium, Department of Pharmacology, University of Toronto, Toronto, ON, Canada, [3]Institute for Cancer Research and Treatment, University of Torino, Candiolo, Italy.
Plexin family are unique transmembrane receptors protein known to regulate several cellular processes including axonal guidance in the developing nervous system. Upon activation, plexin initiates signaling processes, which involve several small GTPases of the Ras and Rho families (R-Ras, Rac1, Rnd1, and RhoD) that regulates cytoskeletal dynamics and cell adhesion. Plexins are unique amongst transmembrane receptors because its several cytoplasmic regions interact directly with small GTPases. Specifically, plexins possess a domain with homology to GTPase activating proteins (GAPs). As part of their activation, plexin family shows GAP activity toward R-Ras. However, the mechanism of activation is not known till date because of lack of information about the structure and function of these receptor proteins. In this context, we have studied the structure, function of intracellular region of PlexinB1 and their binding interaction with small GTPase. The structure is monomeric and binds to Rac1, Rnd1 as well as Rras, but not H-Ras. These findings suggest that the monomeric form of the intracellular region is primed for GAP activity and extend a model for plexin activation.
[1] Tong, Y., et al. (2008) Structure 16, 246-258.[2] Bouguet-Bonnet, S. & Buck, M (2008) J.Mol.Biol. 377,1474-87.[3] Tong, Y, et al. (2007) J.Biol. Chem. 282, 37215-37224.[4] Hota, P. & Buck, M. (2009) Protein Science, 18(5):1060-71.[5] Tong, Y., et al. (2009) J. Biol. Chem. Submitted.

Protein Structure I

1285-Pos
Structural and Functional Studies of Bacterial Toxin-Antitoxin Systems
Gregory Verdon[1], Lauren DeStefano[2], Chi Wang[3], Gregory Boel[3], Guy Montelione[4], Nancy Woychik[5], John F. Hunt[3].
[1]Weill Medical College of Cornell University, New York, NY, USA, [2]UMDNJ-RWJMS Department of Molecular Genetics and Microbiology & Immunology, Piscataway, NJ, USA, [3]Columbia University, Dept. of Biological Sciences, New York, NY, USA, [4]Rutgers - State University of New Jersey, New Brunswick, NY, USA, [5]UMDNJ-RWJMS Department of Molecular Genetics and Microbiology & Immunology, PIscataway, NJ, USA.
TA systems have recently been linked to medically important processes such as biofilm formation, bacterial persistence after exposure to antibiotics, and bacterial pathogenesis. Toxin-Antitoxin (TA) systems are stable protein complexes consisting of a toxin, whose action is mechanistically distinct from exotoxins (e.g. botulinum, anthrax or cholera toxins), in complex with an antitoxin, its specific inhibitor. The release of TA toxin occurs under specific

conditions (e.g. stress). TA toxins have a bacteriostatic effect that can lead to cell death if sustained. Although the mechanisms of action for a few TA toxins have been uncovered, the intracellular targets of many others have not been identified. Our latest structural and functional data on such complexes will be presented.

1286-Pos
Overproduction, Purification and Structure Determination of Human Dual Specificity Phosphatase 14
George Lountos, Joseph Tropea, Scott Cherry, David Waugh.
National Cancer Institute-Frederick, Frederick, MD, USA.
Dual-specificity phosphatases (DUSPs) are enzymes that participate in the regulation of biological processes such as cell growth, differentiation, transcription and metabolism. A number of DUSPs are able to dephosphorylate phosphorylated serine, threonine and tyrosine residues on mitogen-activated protein kinases (MAPKs) and thus are also classified as MAPK phosphatases (MKPs). As an increasing number of DUSPs are being identified and characterized, there is a growing need to understand their biological activities at the molecular level. There is also significant interest in identifying DUSPs that could be potential targets for drugs that modulate MAPK-dependent signaling and immune responses, which have been implicated in a variety of maladies including cancer, infectious diseases and inflammatory disorders. Here, the overproduction, purification and crystal structure at 1.88 Angstroms resolution of human dual-specificity phosphatase 14, DUSP14 (MKP6), are reported. DUSP14 has been reported in the literature to play potentially important roles in T cell regulation and may also be involved in gastric cancer. The determination of the three-dimensional structure of DUSP14 should aide the study of DUSP14 at the molecular level and may also accelerate the discovery and development of novel therapeutic agents.

1287-Pos
Structural Studies on Mutants of HMG CoA Reductase from Pseudomonas Mevalonii
Moumita Sen, Nicklaus C. Steussy, Chandra Duncan, Victor W. Rodwell, Cynthia V. Stauffacher.
Purdue University, West Lafayette, IN, USA.
HMG-CoA reductase catalyzes the four-electron reduction of HMG-CoA to free CoA and mevalonate. This is one of the few double oxidation/reduction reactions in intermediary metabolism that take place in a single active site. In addition to the unusual enzymology, this reaction is of interest because it is the committed step of the fundamental mevalonate isoprenoid pathway. In animals this pathway produces cholesterol, the steroid hormones and a variety of signaling molecules based on the isoprenoid building block (1). In bacteria the pathway is equally important, and has been shown to be essential to the virulence of *Staphylococcal* and *Streptococcal* bacteria (2). To better understand the nature of this reaction, our laboratory has undertaken a comprehensive structural study of the mechanism of HMG-CoA reductase in bacteria utilizing the enzyme from *Pseudomonas mevalonii*.
HMG-CoA reductase is an obligate dimer, with each monomer consisting of a large domain, a small domain, and a flap domain (2, 3) that is disordered in the apoenzyme structure. The flap domain is ordered in the crystal structure only in the presence of ligand and co-factors, where it closes over the active site, positioned by a network of hydrogen bonds that include the ligand and co-factor. Two residues proposed to be important in flap domain movement have been mutated. Mutant proteins have been crystallized, soaked with various combinations of ligands and co-factors, and their structures have been solved at 1.95-2.40Å. These structures, reinforced with kinetic analysis of the mutants, demonstrate the essentiality of this closure in the reaction and reveal how these residues are involved in flap domain movement.

1288-Pos
Structure of the E. Coli Gyrase DNA Binding and Cleavage Core Reveals A Unique Domain
Allyn Schoeffler, James Berger.
University of California, Berkeley, Berkeley, CA, USA.
DNA topoisomerases are essential enzymes that sustain chromosome supercoiling homeostasis in all forms of life. DNA gyrase, a heterotetrameric type IIA topoisomerase, has the unique ability to introduce negative supercoils into DNA, helping maintain bacterial genomes in a compact, underwound state. Though all gyrase orthologs use a set of homologous domains and a central ‘‘two-gate’’ mechanism for passing one DNA segment through another, they also exhibit critical family-specific differences. For example, the metal- and DNA-binding TOPRIM domain of gyrases found in many gamma- and beta-proteobacteria contains a 170-amino acid insertion of unknown function. We have solved the crystal structure of the *E.coli* gyrase DNA binding and cleavage core, visualizing this insertion for the first time. Biochemical analyses of a structure-guided deletion mutant lacking this region reveal that it may help coordinate the activities of gyrase’s distal ATPase and DNA binding gates.

1289-Pos
Structure of Crohn'S Disease-Related Proteins and their Binding to Class II MHC
Lihui Liu, Guo Yi, Hongmin Li.
Wadsworth Center, Albany, NY, USA.
T cell response to enteric bacteria is important in inflammatory bowel disease. pfiT is a T-cell superantigen associated with human Crohn’s disease. The bacterial superantigens are a class of protein toxins that share the capacity to induce massive activation of the human immune system. These molecules simultaneously bind to major histocompatibility complex class II molecules on the surface of antigen-presenting cells and T-cell receptors (TCRs) on T cells to stimulate large numbers of T cells. The aim of this study is to analyze the molecular mechanism of superantigen recognition by host receptors. Here, we report the crystal structure of pfiT. This protein was overexpressed in *Escherichia coli* and purified though GST-affinity and size exclusion chromatography. The protein is selenomethionine labeled and single wavelength anomalous dispersion method was used for determination of the crystal structure. The superantigen crystallizes in the monoclinic space group $P2_1$, with two molecules in asymmetric unit cell. The structure was determined to 2.5Å resolution. In addition, we performed radiolabeled competitive binding assays between three superantigens: pfiT, *Mycoplasma arthritidis*-derived mitogen (MAM), PA2885, a novel open reading frame (ORF) in the *Pseudomonas aeruginosa* genome. Analyses showed that both the microbial homologuepfit and PA2885, just as potent superantigen MAM, are capable of binding to target mammalian cells. Moreover, we labeled these superantigens with FITC and analyzed them by FACS in PBMC. The statistic results show that antibody against HLA-DR has strong effect to block these SAg’ binding ability with PBMC, and antibodies against HLA-DQ and DP can also compete binding site in a much weaker manner. These findings support the concept that pfiT, PA2885, MAM are superantigens and can bind to class II MHC molecule .
Research is funded by the Crohn’ & Colitis Foundation of America.

1290-Pos
Structural and Metal-Binding Characterization of the C-terminal Metallochaperone Domain of the Membrane Fusion Protein SilB from *Cupriavidus Metallidurans* CH34
Beate Bersch[1], Kheiro-Mouna Derfoufi[2], Fabien De Angelis[2], Elisabeth Ngonlong Ekendé[2], Max Mergeay[3], Jean-Marie Ruysschaert[2], **Guy Vandenbussche[2]**.
[1]Institut de Biologie Structurale, Grenoble, France, [2]Université Libre de Bruxelles, Brussels, Belgium, [3]Belgian Nuclear Research Centre, Mol, Belgium.
The β-proteobacterium *Cupriavidus metallidurans* CH34 has an outstanding ability to grow on harsh environments such as heavy-metal contaminated sites. The regulated transport of heavy metal ions out of the cell via tripartite efflux systems is one of the mechanisms used by the bacteria for detoxification. These protein complexes span the entire bacterial cell envelope, and are composed of an inner membrane transporter belonging to the resistance nodulation cell division (RND) family, an outer membrane protein member of the Outer Membrane Factor (OMF) family, and a periplasmic adaptor protein, member of the Membrane Fusion Protein (MFP) family. SilABC is one of the 12 putative efflux systems detected in *C. metallidurans* CH34 genome and is most probably involved in silver and copper trafficking. We report here on the characterization of the C-terminal domain of the periplasmic adaptor protein SilB. This C-terminal extension exists only in SilB homologs and is not present in other MFPs. A potential Ag(I)/Cu(I) coordination site was detected on the basis of the amino acid sequence and the metal-binding specificity was confirmed by mass spectrometry. NMR solution structure of the apo-form showed that SilB C-terminal domain adopts a β-barrel structure. Comparison of chemical shift data between the apo-and metallated-form demonstrated the implication of two methionine, one histidine and one tryptophan residues in the metal coordination site. Fluorescence quenching and UV-visible data are consistent with a cation-tryptophan π-interaction. With respect to its three-dimensional structure and metal-binding specificity, the SilB C-terminal domain closely resembles CusF, a small periplasmic protein belonging to the CusCFBA efflux system involved in silver and copper resistance in *E. coli*. Our study suggests

that SilB C-terminal domain could function as a metallochaperone to the SilABC system.

1291-Pos

Crystal Structure and Metal-Binding Specificity of ZneB, the Periplasmic Adaptor Protein of A Heavy Metal Resistance System from Cupriavidus Metallidurans CH34

Fabien De Angelis[1], John K. Lee[2], Joseph D. O'Connell III,[2], Larry J.W. Miercke[2], Koen H. Verschueren[3], Vasundara Srinivasan[3], Rebecca A. Robbins[2], Cédric Govaerts[1], Jean-Marie Ruysschaert[1], Robert M. Stroud[2], Guy Vandenbussche[1].
[1]Université Libre de Bruxelles, Brussels, Belgium, [2]University of California in San Francisco, San Francisco, CA, USA, [3]Vrije Universiteit Brussel, VIB, Brussels, Belgium.

In Gram-negative bacteria, tripartite efflux systems are involved in the transport of a broad range of toxic compounds such as drugs or heavy metals out of the cell. These protein complexes span the entire bacterial cell envelope, and are composed of an inner membrane transporter belonging to the resistance nodulation cell division (RND) family, an outer membrane protein member of the Outer Membrane Factor (OMF) family, and a periplasmic adaptor protein, member of the Membrane Fusion Protein (MFP) family. The periplasmic adaptor plays an important role in the recruitment of the two integral membrane partners and for the assembly of a functional transport complex. It has been proposed that this component could also contribute to the binding of the substrate. We report here on the characterization of ZneB, the MFP of a Heavy Metal Efflux-RND system from Cupriavidus metallidurans CH34. Using mass spectrometry, we have demonstrated that ZneB has a high specificity for zinc binding with a metal stoichiometry of 1:1 to the protein. The protein was crystallized in the presence of zinc and the apo- and metallated-forms were detected in the same asymmetric unit. The involvement of two histidine and a glutamate residues in the metal ion coordination site was confirmed by site-directed mutagenesis. The comparison of apo- and Zn-bound conformations based on the crystal structures and on data obtained in solution reveals important conformational changes upon zinc binding, suggesting an active role of the MFP in the efflux mechanism. The characterization at the molecular level of the efflux system proteins and the comparison with their counterparts in homologous RND-type transport systems involved in multidrug resistance will allow a better understanding of the resistance mechanisms.

1292-Pos

Crystal Structure of the N-terminal Region of Brain Spectrin Reveals A Helical Junction Region and A Stable Structural Domain

Marta A. Witek[1], Shahila Mehboob[2], Yuanli Song[1], Fei Long[1], Bernard D. Santarsiero[2], M.E. Johnson[2], L.W.-M. Fung[1].
[1]University of Illinois at Chicago, Chicago, IL, USA, [2]Center for Pharmaceutical Biotechnology, Chicago, IL, USA.

The crystal structure of a recombinant protein consisting of the first 147 residues of brain α spectrin was solved to 2.3 Å. The N-terminal region consists of the partial domain (Helix C') and the anti-parallel, triple helical coiled-coil first structural domain (helices A1, B1, and C1). The data revealed that each asymmetric unit contained two crystallographically independent structures (1 and 2). The crystal structure of the first structural domain resembled that of the first structural domain of erythroid α-spectrin, determined before by solution NMR studies, with some specific differences, especially at the N-terminal region, including Helix C' and the region connecting Helix C' with the first structural domain (the junction region). The first ten residues are in a disordered conformation, followed by Helix C' with an apparent, flexible bend. The junction region exhibits a helical conformation in contrast with an unstructured junction region in erythroid α spectrin. A special feature that has not been reported in other spectrin domains is the long and flexible A1B1 loop of 13 residues. This loop is likely the recognition site for interaction with other proteins. Hydrogen bonds and hydrogen bond networks were identified in the first structural domain and compared with those in erythroid α-spectrin. We suggest that these hydrogen bonds might contribute toward the stability of brain and erythroid spectrin.

1293-Pos

An Overlapping Kinase and Phosphatase Docking Site Regulates Activity of the Retinoblastoma Protein

Alexander Hirschi[1], Matthew Cecchini[2], Rachel Steinhardt[1], Frederick A. Dick[2], Seth M. Rubin[1].
[1]UC Santa Cruz, Santa Cruz, CA, USA, [2]University of Western Ontario, London, ON, Canada.

Insights into the molecular mechanisms that regulate the phosphorylation state and corresponding activity of the retinoblastoma tumor suppressor protein (Rb) are fundamental to understanding the control of cell proliferation. While much focus has been placed upon regulation of Cyclin-dependent kinase (Cdk) activity towards Rb, less is known about Rb dephosphorylation catalyzed by the major Rb phosphatase, protein phosphatase-1 (PP1). Using x-ray crystallography, we have determined the crystal structure of a PP1:Rb peptide complex to 3.2Å that reveals an overlapping kinase and phosphatase docking site. Kinetic assays show that Cdk and PP1 docking to Rb are mutually exclusive and that this docking site is required for efficient dephosphorylation, as well as phosphorylation of Rb. Cell cycle arrest assays demonstrate that the ability of PP1 to compete with Cdks is sufficient to retain Rb activity and block cell cycle advancement. These results establish a novel mechanism for the regulation of Rb phosphorylation state in which kinase and phosphatase compete for substrate docking.

1294-Pos

Crystal Structures Of Yeast Mitochondrial ATPase with Uncoupling Mutations

Diana Arsenieva, Yamin Wang, Jindrich Symersky, Luke Vistain, David M. Mueller.
Rosalind Franklin University, North Chicago, IL, USA.

Yeast mitochondrial ATP synthase is a transmembrane protein responsible for synthesis of more than 90% of ATP under aerobic conditions. The water soluble portion of ATP synthase, F1, is composed of five subunits with stoichiometry $\alpha_3\beta_3\gamma\delta\epsilon$ and has a combined molecular weight of 360 kDa. The three active sites of ATPase are formed at the interfaces between alternating α- and β-subunits. ATPase is capable of efficient ATP hydrolysis, accompanied by rotation of central stalk subunits, $\gamma\delta\epsilon$, within the $\alpha_3\beta_3$ core and is capable of ATP synthesis if central subunits are forced to rotate in the opposite direction. A number of mutations in ATP synthase have been identified that result in the uncoupling of catalytic function and proton flow across the mitochondrial membrane. These uncoupling mutations cluster at the interface between γ-subunit and $\alpha_3\beta_3$ catalytic core of ATPase. In this work, four X-ray crystal structures of ATPase with single amino acid substitutions αN67I, αF405S, βV279F, and γI270T were solved at resolutions ranging from 3.2 Å to 2.74 Å. This study will present a structural comparison of the mutant structures with the wild type structures to understand the mechanism of coupling. However, the crystal structures likely represent the ground state of catalytic reaction cycle while the mutations may result in notable distortions of enzyme structure during other stages of catalytic cycle. Additionally, the uncoupling of the ATPase may be caused by changes in the energy of interaction between the portions that are rotating in the molecular machine thereby altering transition to the higher energy states. Structural based hypotheses are presented to explain the role of these residues in the coupling of the enzyme. Supported by NIH R01GM0662223

1295-Pos

Molecular Mechanism of the Peptidoglycan Hydrolysis by FlgJ, A Putative Flagellar Rod Cap Protein From Salmonella

Yuki Kikuchi[1,2], Hideyuki Matsunami[2,3], Midori Yamane[1], Katsumi Imada[1,2], Keiichi Namba[1,2].
[1]Graduate School of Frontier Biosciences, Osaka University, Suita, Osaka, Japan, [2]Dynamic NanoMachine Project, ICORP, JST, Suita, Osaka, Japan, [3]Okinawa Institute of Science and Technology, Urume, Okinawa, Japan.

The axial structure of the bacterial flagellum consists of three parts: the filament as a helical propeller; the hook as a universal joint; and the rod as a drive shaft connecting the hook and the rotor. The assembly of the axial structure, which occurs at its distal end, requires cap complexes attached to the growing end. FlgD and FliD are cap proteins necessary for hook and filament growth, respectively. For efficient penetration of the growing rod through the peptidoglycan (PG) layer, it is likely that the rod cap locally degrades PG. FlgJ is a putative rod cap protein with a PG-hydrolyzing activity (muramidase). Previous studies have shown that the N-terminal region of FlgJ interacts with the rod proteins and that the C-terminal region shows a sequence similarity to muramidase family, such as autolysin and AcmA. To understand the mechanisms of rod formation, we determined the atomic structure of a C-terminal fragment of FlgJ at 1.7 Å.

The crystal structure revealed the entire muramidase domain of FlgJ. In spite of no significant sequence similarity, the putative active site of FlgJ closely resembles that of hen egg white lysozyme (HEWL), which is a well-studied muramidase. A glutamic acid residue at position 184 in FlgJ is invariant among FlgJ family and the E184Q mutant of FlgJ shows no muramidase activity, indicating

that Glu184 is essential for its catalytic activity. We have also determined the residues involved in substrate recognition by single amino-acid substitution experiments based on the structure. These results indicate that a large conformational change of sub-domain is required to exert the muramidase activity. We will discuss a possible PG-hydrolyzing mechanism of FlgJ in flagellar assembly.

1296-Pos
Structure of the Newcastle Disease Virus F Protein in the Post-Fusion Conformation

Xiaolin Wen[1], Kurt Swanson[2,3], Robert A. Lamb[2,3], Theodore S. Jardetzky[1].
[1]Stanford University, Stanford, CA, USA, [2]Northwestern University, Evanston, IL, USA, [3]Howard Hughes Medical Institute, Evanston, IL, USA.

Newcastle disease virus (NDV) is a member of the Paramyxoviridae family. The NDV fusion (F) glycoprotein, which is responsible for merging the viral and cellular bilayers during entry. The X-ray crystal structures have been solved of F proteins in the post-fusion and the pre-fusion conformations, providing atomic level information regarding the conformational transitions accompanying fusion. However, our understanding of the similarities between different F glycoproteins in these two conformational states remains incomplete.

Here, we present the crystal structure of the secreted, uncleaved ectodomain of the NDV F protein. Previous structural analysis of a related NDV F protein was missing key elements of the functional regions of the protein, including two helical segments (HRA and HRB) that assemble into a stable six helix bundle (6HB) in the post-fusion form. We have produced the NDV F protein in pre- and post-fusion conformations, using analogous constructs that produced a pre-fusion PIV5 F structure and a post-fusion HPIV3 F structure. We demonstrate that the two NDV F proteins exhibit the pre-and post-fusion forms through EM analysis and we have solved the crystal structure of the post-fusion form of the NDV F protein. In contrast to the previously determined NDV F structure, our new crystal structure contains the 6HB at the base of the stalk region, consistent with the EM observations and the previously determined HPIV3 F structure. Global superposition of the NDV and HPIV3 structures demonstrates maximum correspondence between distal portions of the structures, with orientation or adjustments in linking domains and the extended HRA stalk. Electrostatic profiles of the NDV, HPIV3, and PIV5 F structures show elements of conserved charge distributions despite significant sequence differences in these glycoproteins, which may be important for their common functionality.

1297-Pos
Structure of DNA Binding Domain of Plant Telomere Binding Proteins Represents Unique Features of Telomere Binding Protein Family

Weontae Lee[1], Sunggeon Ko[1], Hyun-Soo Cho[1], Chaejoon Cheong[2].
[1]Yonsei University, Seoul, Republic of Korea, [2]KBSI, Ochang, Republic of Korea.

Telomeres, the ends of linear eukaryotic chromosomes, are composed of short repeats of G-rich sequences and play essential roles in genome stability with various telomere binding proteins. To characterize the binding mode of plant telomere DNA and telomere binding protein, we determined the structures of DNA binding domain and telomere complex of NgTRF1, atTRF and RTBP1, double strand telomere binding proteins of plants, by multidimensional NMR spectroscopy and X-ray crystallography. We have identified the DNA binding interface of the DNA binding domain of TBPs, which is composed of 4 α-helices by means of chemical shift perturbation analysis. The complex crystal structure of $NgTRF1^{561-681}$ and plant telomere DNA $(TTTAGGG)_2$ have shown the molecular details of the interaction between them and we confirmed the interaction biochemically through site-directed mutagenesis. From the comparison with the structure of human telomere binding protein, we tried to show the unique features of plant telomere binding protein in the mode of telomere DNA binding as well as the similarity with the telomere binding proteins in other organisms. To our knowledge, this is the first report of the complex structure of telomere binding protein and telomere DNA in plant.

1298-Pos
Structural and Functional Characterization of an Unusual SH3 Domain from the Fungal Adaptor Protein Bem1

Maryna Gorelik, Ranjith Muhandiram, Alan Davidson.
University of Toronto, Toronto, ON, Canada.

Protein interactions form the basis of most biological processes and in eukaryotes are often mediated by conserved modular domains that recognize linear motifs. Among the most common protein interaction domains is the SH3 domain that generally recognizes PxxP containing peptides. SH3 domains are approximately 60 amino acids long and are composed of five beta strands. We are studying the SH3 domain from the fungal adaptor protein Bem1p that plays an important role during polarized growth and activation of MAPK signaling pathways. This SH3 domain is unusual, even though its sequence conforms to the SH3 domain consensus, it requires an extra 40 amino acids at its C-terminus for folding. Furthermore, in addition to binding PxxP containing peptides, it also binds the Cdc42p GTPase in a PxxP-independent manner. We are using in vitro binding assays and NMR spectroscopy to structurally and functionally characterize this unusual SH3 domain. Contrary to a previous report, we find that the Bem1 SH3 domain can simultaneously bind the Cdc42p GTpase and PxxP-containing peptides and that the binding of one does not affect the affinity for the other. Structural characterization by NMR shows that the extra sequence contains two alpha helices that pack tightly against the SH3 domain and thus form an integral part of the fold. Our findings provide with an example of how a common protein interaction domain can evolve to have additional atypical structural features and associated functions.

1299-Pos
Structural Investigation of a Fibronectin Type III Domain Tandem from the A-band of the Titin

Andras Czajlik, Gary Thompson, Ghulam N. Khan, Arnout Kalverde, Steve W. Homans, John Trinick.
University of Leeds, Leeeds, United Kingdom.

Single molecules of the giant muscle protein titin span half muscle sarcomeres, from the Z-disk to the M-band, and have key roles in sarcomere assembly and elasticity. In the A-band titin is attached to thick filaments and here the sequence shows fibronectin type III and immunoglobulin-like domains. These are mostly arranged in regular patterns of eleven domains called the large super-repeats. The large super-repeat occurs eleven times and this entire region thus forms nearly half of the titin molecule. Through interactions with myosin and C-protein, it is involved in thick filament assembly. We are determining the atomic structure, dynamical properties and the inter-domain arrangement of overlapping double and triple domain fragments of the large super-repeat by NMR spectroscopy. Ultimately, we hope to combine the data to reconstruct the overall conformation of the super-repeat. Here we investigated the A59-A60 domain tandem, which was expressed in bacteria from cDNA. The assignment of the backbone atoms was obtained using triple resonance NMR experiments. An initial structure was determined by backbone chemical shifts and homology modeling using the CS23D and Rosetta software packages. It was refined using RDC data to give realistic models for both domains. As we expected, these are both double-β-sheet sandwich structures characteristic of fibronectin type III domains. We are also carrying out relaxation measurements to probe the dynamics of the domains and their linker region.

1300-Pos
Localization of the Fission Yeast U5.U2/U6 Spliceosome Subunits

Yoshimasa Takizawa, Melanie D. Ohi.
Vanderbilt University Medical School, Nashville, TN, USA.

The spliceosome is a dynamic macromolecular machine that catalyzes the excision of introns from pre-mRNA to generate protein-coding transcripts. The megadalton-sized spliceosome is composed of four small nuclear RNPs (U1, U2, U5, and U4/U6) and numerous pre-mRNA splicing factors. The formation of an active spliceosome is hypothesized to occur in a stepwise manner requiring the assembly and disassembly of large multiprotein/RNA complexes. A promising structural approach to obtain information about spliceosome complexes is single-particle cryo-electron microscopy (cryo-EM), a powerful technique that is ideal for determining the structures of large dynamic complexes at protein concentrations too low for crystallization. Formerly, our group determined structure of the fission yeast U5.U2/U6 spliceosome complex by cryo-EM. This U5.U2/U6 spliceosome complex contains the U2, U5, and U6 snRNAs, pre-mRNA splicing intermediates, U2 and U5 snRNP proteins, the Nineteen Complex (NTC), and second-step splicing factors. However, the location of these subunits in the complex was not determined. Using antibody labeling and single particle EM we are now localizing these individual subunits within the density map of the U5.U2/U6 spliceosome complex. This work now enables us to propose a structural model for U5.U2/U6 organization.

1301-Pos
3D Solution Structure of the C-terminal Chromodomain of the Chloroplast Signal Recognition Particle

Ananthamurthy Koteshwara, Kathir M. Karuppanan, Robyn Goforth, Ralph Henry, Suresh Kumar, K. Thallapuranam.
University of Arkansas, Fayetteville, AR, USA.

Chloroplasts use chloroplast signal recognition particle (cpSRP) pathway to import important cargo like light harvesting chlorophyll protein (LHCP).

cpSRP is unique among SRPs in being devoid of RNA. cpSRP consists of an evolutionarily conserved 54-kDa subunit (cpSRP54) and an unique 43-kDa subunit (cpSRP43). cpSRP43 subunit has four-ankyrin repeat domain at the N terminus and a C-terminal chromo domain (CD). The C-terminal CD of cpSRP43 has been shown to provide interaction sites for the cpSRP54 subunit. In addition, the chromodomain in the cpSRP43 subunit is also believed to be important for the formation of the transit complex with LHCP. In this context, we embarked on the structural characterization of the C-terminal CD using a variety of biophysical techniques including multidimensional NMR spectroscopy. Far UV circular dichroism spectrum of CD shows that the backbone of the protein is predominantly in the helical conformation. 1H-15N HSQC spectrum of CD is well- dispersed suggesting that the protein is structured. Complete resonance assignments (1H, 15N and 13C) in CD have been accomplished using a variety of triple resonance experiments. Chemical shift index plots show that CD is an $\alpha + \beta$ protein. A detailed analysis of the three-dimensional solution structure of CD will be presented. The three-dimensional solution structure of CD provides valuable insights into the molecular mechanism underlying the post-translational transport and integration of LHCP on the thylakoid membrane.

1302-Pos
The PSI SGKB Technology Portal - An Online Database of Structural Genomics Technologies

Lester Carter[1], Maggie Gabanyi[2], Helen M. Berman[2], Paul Adams[1].
[1]LBL, Berkeley, CA, USA, [2]Rutgers, New Brunswick, NJ, USA.

The Protein Structure Initiative (PSI) Structural Genomics KnowledgeBase (SGKB) technology portal is an online database of PSI-derived technologies. Information within the portal will be of use to scientists involved in all branches of molecular biology. Advances are described in all stages of the protein production pipeline, from initial target selection to cloning, expression, structure solution and structure analysis. Information is provided on robotics, high-throughput protocols, and software development.
The url for the website is: http//:technology.lbl.gov/portal/

1303-Pos
Protein Structure Initiative Material Repository (PSI-MR): A Resource of Structural Genomics Plasmids for the Biological Community

Catherine Cormier[1], Jean Chin[2], Joshua LaBaer[1].
[1]Arizona State University, Tempe, AZ, USA, [2]NIH/NIGMS, Bethesda, MD, USA.

The Protein Structure Initiative Material Repository (PSI-MR; http://psimr.asu.edu) provides centralized storage and distribution for the growing collection of more than 80,000 protein expression plasmids created by PSI researchers. These plasmids are an invaluable resource that allows the research community to dissect the biological function of proteins whose structures have been identified by the PSI. The plasmid annotation, which includes the full length sequence, vector information, and associated publications, is stored in a freely available, searchable database called DNASU (http://dnasu.asu.edu). Each PSI plasmid is also linked to a variety of additional resources, including the PSI Structural Genomics Knowledgebase (PSI-SGKB: http://kb.psi-structuralgenomics.org), which facilitates cross-referencing of a particular plasmid to protein annotations and experimental data. Nearly 16,000 PSI plasmid samples are currently available and can be requested directly though the website. The PSI-MR has also developed a novel strategy to avoid the most common concern encountered when distributing plasmids, namely the complexity of material transfer agreement (MTA) processing and the resulting delays this causes. It is in this context that we developed and successfully implemented the Expedited Process MTA, in which we created a network of institutions that agree to the terms of transfer in advance of a material request, thus eliminating the delay researchers would typically encounter while their institution is processing the MTA. Our hope is that by creating a repository of expression-ready plasmids and expediting the process for receiving these plasmids, we will help accelerate the accessibility and pace of scientific discovery.

1304-Pos
How to use the PSI Structural Genomics Knowledgebase to Enable Research

Andrei Kouranov[1], John Westbrook[1], Margaret Gabanyi[1], Yi-Ping Tao[1], Raship Shah[1], Torsten Schwede[2], Konstantin Arnold[2], Florian Kiefer[2], Lorenza Bordoli[2], Paul Adams[3], Lester Carter[3], Wladek Minor[4], Rajesh Nair[5], Joshua LaBaer[6], Helen M. Berman[1].
[1]Rutgers University, Piscataway, NJ, USA, [2]University of Basel, Basel, Switzerland, [3]Lawrence Berkeley National Laboratory, Berkeley, CA, USA, [4]University of Virginia, Charlottesville, VA, USA, [5]Columbia University, New York, NY, USA, [6]Arizona State University, Tempe, AZ, USA.

The Protein Structure Initiative Structural Genomics Knowledgebase (PSI SGKB, URL: http://kb.psi-structuralgenomics.org) is a web resource designed to turn the products of the structural genomics and structural biology efforts into knowledge that can be used by the biological community to understand living systems and disease. We will present examples and demonstrate how to use the PSI SGKB to enable biological research. For example, a protein sequence or PDB ID search will provide a list of protein structures from the Protein Data Bank, associated biological descriptions (annotations), homology models, structural genomics protein target information, experimental protocols, and the ability to order available DNA clones. A text search will find technology reports and publications that were created by the PSI's high-throughput research efforts. Web tools that aid in bench top research, such as protein construct design, are also available. Created in collaboration with the Nature Publishing Group, the Structural Genomics Knowledgebase Gateway provides a research library, editorials about new research advances, news, and an events calendar also present a broader view of structural genomics and structural biology. The PSI SGKB is funded by the NIGMS.

1305-Pos
NIGMS PSI:Biology Initiative – High-Throughput-Enabled Structural Biology

Peter C. Preusch, Ravi Basavappa, Jean Chin, Charles Edmonds, Ward Smith, Catherine Lewis.
Nat Inst Gen Med Sciences, Bethesda, MD, USA.

The primary goal of the Protein Structure Initiative:Biology (PSI:Biology) to be funded by the National Institute of General Medical Sciences (NIGMS) is to apply high-throughput structural biology to important biological problems (http://www.nigms.nih.gov/Initiatives/PSI/psi_biology/). This will be accomplished by establishing partnerships between centers for structure determination and biologists with interests in particular proteins or collections of proteins. The PSI:Biology network centers will include: 1) Centers for High-Throughput Structure Determination, 2) Centers for Membrane Protein Structure Determination, 3) the PSI:Materials Repository, and 4) the PSI:Biology Knowledgebase. The partnerships, established through Consortia for High-Throughput-Enabled Structural Biology Partnerships, will define targets for structure determination and provide funds for functional studies in the applicants' laboratories and for a portion of the cost for structure determination in the center. In addition to protein structures and models, the PSI:Biology network will generate and make available reagents and plasmids for expressed proteins to support functional studies in the research community. NIGMS encourages Partnership applications from biologists or groups of biologists with biological questions that will benefit from the determination of relevant protein structures. The PSI:Biology high-throughput approach will enable examination of families of proteins related to the target proteins, an approach that has proven highly successful in generating the first structure of a family member and then allowing many other family members to be modeled. Examples of current partnerships include using structural genomics, modeling and systems biology to generate a three-dimensional reconstruction of the central metabolic network of the bacterium, *Thermotoga maritima*, and the discovery of novel enzymatic mechanisms for the enoylase and amido hydrolase classes of enzymes. Additional opportunities for researchers to join the PSI:Biology network will be provided through ongoing and future program announcements. Researchers may also suggest proteins for structure determination through the PSI Community Nomination site at: http://cnt.psi-structuralgenomics.org/CNT/targetlogin.jsp.

1306-Pos
Technology Development Highlights Generated from the Center for Eukaryotic Structural Genomics

George N. Phillips Jr.,, John Primm, David Aceti, Craig A. Bingman, Ronnie Frederick, Shin-ichi Makino, Francis Peterson, Frank Vojtik, Russel Wrobel, Zsolt Zolnai, Brian Volkman, Brian G. Fox, John L. Markley.
UW Madison, Madison, WI, USA.

The Center for Eukaryotic Structural Genomics (CESG) aims to be the leading center for developing and disseminating tested technologies to efficiently solve structures of eukaryotic proteins. We create, evaluate, and optimize innovative protocols for producing eukaryotic proteins in active forms. We seek to improve the efficiency of all stages from target selection-design to three-dimensional structure determination by X-ray crystallography or NMR spectroscopy, including development of bioinformatic techniques and LIMS tools. Using our protein production platform, we refine methods for improving the yield of structures from high-value targets, in particular proteins from humans and other vertebrates. CESG has a substantial outreach component; more than 400 targets from outside requestors have been accepted for study with a structure success rate of 5%, which compares favorably with the eukaryotic success rates for the

total PSI effort. These eukaryotic targets frequently present unique challenges. All CESG protein production protocols and Technology Dissemination Reports are accessible through the PSI Knowledgebase: http://kb-psi-structuralgenomics.org/KB/ and CESG's website. Selected technology developments are presented here. These include advances in expression vector design, enhanced methodology for cell based and wheat germ cell-free expression systems, new software to improve the quality and reduce time for structure determination by X-ray crystallography and NMR, and optimized techniques for the production of TEV protease for use in our protein production platform. We actively share our advances with the biotechnology, pharmaceutical, and academic communities through collaborations, oral presentations, peer-reviewed articles, submissions to public databases and material distribution channels, including PepcDB, PDB, BMRB, PSI Materials Repository, and technology transfer workshops.

Supported by NIH/NIGMS Protein Structure Initiative grants GM074901 and GM064598. We acknowledge ALL members of the CESG team for their dedicated work.

1307-Pos

Effective Protein Crystallization Screening with Synthetic Zeolite Molecular Sieves as Hetero-Epitaxic Nucleant

Michihiro Sugahara, Yuko Kageyama-Morikawa, Naoki Kunishima.
RIKEN, Sayo-cho, Japan.

Protein crystallization is still a major bottleneck in structural biology. As the current methodology of protein crystallization is a type of screening, it is usually difficult to crystallize important target proteins. The hetero-epitaxial growth from the surface of mineral crystal as a nucleant had been thought to be effective to enhance the chance of protein crystallization. However, generally applicable hetero-epitaxial nucleants for protein crystallization have never been found. Recently, we have reported a protein crystallization method using synthetic zeolite molecular sieves as a hetero-epitaxic nucleant. This method is based on the packing space expansion of protein crystals by a directed nucleation on the material surface, thereby providing new crystal forms with a substantial improvement of diffraction quality in some cases. In this work, a sparse matrix crystallization screening experiment of xylanase from *Trichoderma longibrachiatum* was performed with and without molecular sieves, using a commercially available sparse matrix screening kit. A result of crystallization screening of xylanase showed that molecular sieves promotes the crystallization of xylanase, suggesting that the hetero-epitaxic nucleate approach allows us to improve the effectiveness of the sparse matrix screening of protein crystallization. Interestingly, molecular sieves 5A and 13X provided a new crystal form under the crystallization condition containing zinc, in which a zinc-mediated protein sheet looked favorable for the hetero-epitaxic 3D crystal growth.

1308-Pos

Structural Biology Reveals A New Protein Family from *S.Cerevisiae* with A Novel Fold and Implicated in the Metabolism Control And Drug Resistance

Tatiana Domitrovic[1], Guennadi Kozlov[2], João G. Freire[1], Claudio A. Masuda[3], Marcius S. Almeida[3], Monica Montero-Lomeli[3], Edna Matta-Camacho[2], Kalle Gehring[2], Eleonora Kurtenbach[1].
[1]Instituto de Biofisica Carlos Chagas Filho, UFRJ, Rio de Janeiro, Brazil, [2]Department of Biochemistry, McGill University, Montréal, QC, Canada, [3]Instituto de Bioquimica, UFRJ, Rio de Janeiro, Brazil.

We have undertaken a small-scale structural genome project focusing on *S. cerevisiae* ORFs without characterized functional motifs or known primary sequence homologs. The cloning, expression and purification screening of 9 targets sequences, led to the determination of the crystal structure of Yer067w by Multiple Anomalous Diffraction at 1.7 Å resolution. This 20 KDa protein present an alpha-beta fold where the 7-stranded beta-sheet is backed by 4 alpha-helices on one side. Interestingly, a structure-based search using the servers SSM or DALI retrieved only proteins with insignificant superposition scores, indicating that Yer067w represents a novel fold superfamily. The phylogenetic analysis of Yer067w primary sequence homologs showed that this protein belongs to a well-conserved family exclusive to Ascomycetes. To further understand Yer067w role we have searched for functional hints using yeast strains deleted for this gene and its paralog *YIL057C*. Microarray analysis of Δyer067w revealed important modifications in expression of genes related to oxidative phosphorylation, amino acids and lipid metabolism. In a screening for phenotypes, we verified that all mutants presented growth deficiencies in non fermentative carbon sources and Western bolt analysis showed that the presence of both proteins are tightly linked to growth on respiratory substrates or low nutrient conditions, suggesting that both proteins are important to the metabolism in glucose free media. Furthermore, Yer067w mutants revealed an antifungal drug resistance phenotype, presenting an increment of 2 times in the MIC for Nystatin and anphotericin B. This work highlights the importance of functional characterization of unknown ORFs for the comprehension of yeast cells metabolism and for uncover new regulatory elements. Support: FAPERJ, CNPq, CIHR

Protein Aggregates I

1309-Pos

Thermodynamic Instability of A Self-Assembled 16-Residue Alanine-Based Oligopeptide in Aqueous Media: Hydrogel, Fibril, and Beaded Filament Formation

Thomas J. Measey[1], Konstantin Kornev[2], Reinhard Schweitzer-Stenner[1].
[1]Drexel University, Philadelphia, PA, USA, [2]Clemson University, Clemson, SC, USA.

Oligoalanines with greater than ca. 14 residues, which have been doped with charged residues (e.g. lysine), usually adopt α-helical conformations in aqueous media.[1] In contrast, Ac-$(AAKA)_4$-NH_2 aggregates instantaneously when dissolved in aqueous media at concentrations ranging from 70 μM to 7 mM. Evidence from UV circular dichroism (UV-CD) and FTIR spectroscopies suggest a mostly β-sheet like conformation. Kinetics studies of the initially formed conformations suggest a transition from a mostly β-like to a mostly PPII-like conformation, in contrast to typical fibril formation/growth studies. AFM images of freshly prepared samples indicate a porous, tissue-like architecture. Addition of salts (e.g. NaCl) stabilizes this architecture, resulting in the formation of a macroscopic hydrogel. β-sheet and hydrogel formation by such an amino acid sequence is quite unusual, as it does not obey typical rules required for peptide hydrogel formation. In particular, there are no alternating complimentary charges, nor alternating hydrophilic and hydrophobic residues. Without the added stabilization provided by the addition of salts, however, the peptide transitions from a mostly β-sheet-like structure to a PPII-like conformation, possibly via triple helix formation, as evidenced by both electronic and vibrational CD. AFM images suggest the formation of a heterogeneous mixture of assemblies, including bead-like filaments as well as networks of well-defined, intertwined fibrils. Potential applications for peptide hydrogels include drug delivery devices and tissue engineering scaffolds. In this regard, release studies of model peptides which have been trapped within the peptide hydrogel will be presented, as well as rheological characterization of the hydrogel as a function of salt and peptide concentration.

[1] Scholtz, J. M.; Marqusee, S.; Baldwin, R. L.; York, E. J.; Stewart, J. M.; Santoro, M.; Bolen. D. W. *Natl. Acad. Sci. U.S.A.* **1991**, *88*, 2854-2860.

1310-Pos

The Self-Aggregation of A Polyalanine Octamer Promoted by its C-terminal Tyrosine and Probed by A Strongly Enhanced VCD Signal

Thomas J. Measey[1], Kathryn B. Smith[2], Sean M. Decatur[3], Liming Zhao[1], Guoliang Yang[1], Reinhard Schweitzer-Stenner[1].
[1]Drexel University, Philadelphia, PA, USA, [2]Mount Holyoke College, South Hadley, MA, USA, [3]Oberlin College, Oberlin, OH, USA.

The 8-residue alanine oligopeptide, Ac-A_4KA_2Y-NH_2(AKY8), was found to form amyloid-like fibrils upon incubation at room temperature in acidified aqueous solution, at peptide concentrations $>$ 10 mM. The fibril solution exhibits an enhanced VCD couplet in the amide I' band region, which is nearly 2 orders of magnitude larger than typical polypeptide/protein signals in this region. Such intensity enhancements have recently been observed for insulin and lysozyme fibrils.[1] We performed simulations of the VCD and IR amide I' band profile using a simplified excitonic coupling model. Preliminary results suggest that inter-sheet coupling is responsible for the VCD intensity enhancement. The UV-CD spectrum of the fibril solution shows circular dichroism in the region associated with the tyrosine side chain absorption. A similar peptide, Ac-A_4KA_2-NH_2 (AK7), lacking in a terminal tyrosine residue, does not aggregate. These results suggest a pivotal role for the C-terminal tyrosine residue in stabilizing the aggregation state of this peptide. It is speculated that interactions between the lysine and tyrosine side chains of consecutive strands in an antiparallel arrangement, e.g. via cation-π interactions, are responsible for the stabilization of the resulting fibrils. These results offer considerations and insight for the de novo design of self-assembling oligopeptides for biomedical and biotechnological applications, and highlight the usefulness of VCD as a tool to probe amyloid fibril formation.

[1] Ma, S.; Cao, X.; Mak, M.; Sadik, A.; Walkner, C.; Freedman, T.B.; Lednev, I.K.; Dukor, R.K.; Nafie, L.A. *J. Am. Chem. Soc.***2007**, 129, 12364-12365.

1311-Pos

Molecular Basis for the Catalysis of B-Sheet Formation by Water-Nonpolar Interfaces

Ana Nikolic[1], Stéphanie Baud[2,1], Sarah Rauscher[1], Régis Pomès[1].
[1]Hospital for Sick Children, Toronto, ON, Canada, [2]Université Champagne-Ardennes, Reims, France.

Recent studies suggest that the toxicity of several neurodegenerative pathologies such as Alzheimer's and Parkinson's diseases involves the interaction of oligomeric aggregates of amyloidogenic proteins with the neuronal membrane. We examine the physical and structural basis of peptide adsorption and aggregation in a model membrane using molecular dynamics simulations. Blocked amphipathic octapeptides with simple, repetitive sequences, $(Gly\text{-}Ala)_4$ and $(Gly\text{-}Val)_4$, are used as models of β-sheet-forming polypeptide chains found in the core of amyloid fibrils. Placed in aqueous solution in the presence of an n-octane phase mimicking the nonpolar core of lipid membranes, the peptides spontaneously partition at the octane-water interface. The adsorption of nonpolar sidechains displaces the conformational equilibrium of the peptides from a heterogeneous ensemble characterized by a high degree of structural disorder towards a more ordered ensemble favoring β-hairpins and elongated β-strands. Once adsorbed at the interface, peptides spontaneously aggregate and rapidly evolve β-sheet structure on a 10-to100-ns time scale, while aggregates of the same peptides in water remain amorphous. The catalysis of β-sheet formation at the water-membrane interface results from the combination of the hydrophobic effect and of reduced conformational entropy of the polypeptide chain. While the former drives interfacial partition and displaces the conformational equilibrium of monomeric peptides, the planar interface further facilitates β-sheet organization by increasing peptide concentration and reducing the dimensionality of self-assembly from three to two dimensions. These findings have general implications to the formation of β-sheets on the surface of globular proteins and to amyloid self-organization on the surface of biological membranes.

1312-Pos

Oligomerisation, Fibrillation and Activity of Hen Lysozyme in Alkaline Medium: A Concentration Dependent Investigation

Vijay K. Ravi, Nividh Chandra, Rajaram Swaminathan.
Indian Institute of Technology Guwahati, Guwahati, India.

Oligomerisation and fibrillation are hallmarks of protein misfolding diseases like Alzheimer's, Prion, Parkinson's, systemic amyloidosis and so on. Hen egg-white lysozyme (HEWL) which spontaneously aggregates at pH 12.2 under room temperature as shown by us previously is an excellent model protein for aggregation studies. The present work was focussed on investigating the role of protein monomer concentration on the size and morphology of aggregates. For this purpose we employed HEWL concentrations ranging from 120 μM to 300 nM. Our findings reveal that A) FRET efficiency between dansyl labelled HEWL and dabcyl labelled HEWL in the aggregate, monitored over 12 hours was inversely proportional to HEWL monomer concentration B) Size exclusion chromatography after 12 hours showed that while all aggregates of 50 & 120 uM HEWL eluted much later, a small population of aggregates from 10 uM HEWL eluted early through the void volume C) Binding of ANS revealed fluorescence spectra that were gradually blue shifted and more intense, over 12h, in the following order with aggregates of $120 > 50 > 3$ uM, while for 300 nM, these spectra were fairly invariant in emission wavelength and intensity over 12 hours. D) HEWL enzymatic activity decreased almost uniformly with time in alkaline pH for all concentrations suggesting a concentration independent early unfolding step E) AFM images showed extensive fibrils in 3 & 0.3 μM HEWL within 12 hours but predominantly large globular aggregates with 120 μM and 50 μM HEWL samples in the same time period. The above results clearly suggest that size and morphology of HEWL aggregates at alkaline pH are critically dependent on the initial monomer concentration.

1313-Pos

The Addition of an Osmolyte, Trimethylamine N-Oxide Promotes Secondary Structure Heterogeneity Among Amyloid Fibrils

Melissa J. Paulite, Nikhil Gunari, Gilbert C. Walker.
University of Toronto, Toronto, ON, Canada.

We demonstrated that secondary structure heterogeneity was observed among mature amyloid fibrils synthesized by the addition of an osmolyte, called trimethylamine N-oxide (TMAO) by promoting the formation of anti-parallel β-sheet structure along with parallel β-sheet structure. In regards to amyloid fibrils formed in the absence of TMAO, only parallel β-sheet secondary structure was observed. This structural effect was observed regardless of pH. The amyloid fibrils were investigated via Fourier-transform infrared spectroscopy and near-field microscopy, and the characterized by circular dichroism and UV-Vis spectroscopy. Using FTIR spectroscopy, the peak observed at 1630 cm^{-1} indicates the presence of parallel and/or anti-parallel β-sheet structure and a peak at 1692 cm^{-1} denotes the presence of anti-parallel β-sheet structure. This latter peak, which appears only in the TMAO-containing fibril solutions, indicates that TMAO promotes anti-parallel β-sheet fibrils in solution.

1314-Pos

Structural and Functional Analysis of Amyloid Fibril Formation by Two Closely Related Light Chains

Douglas Martin, Marina Ramirez-Alvarado.
College of Medicine, Mayo Clinic, Rochester, MN, USA.

Light chain amyloidosis (AL) is a hematological disorder in which a clonal population of B cells expands and secretes enormous amounts of immunoglobulin light chain protein. These light chains misfold and aggregate into amyloid fibrils, leading to organ dysfunction and death. In AL the sequence of the light chain is unique for each individual, giving rise to a highly variable course of disease. We are studying two proteins, designated AL09 and AL103, derived from the κI O18:O8 germline that are highly similar in sequence, yet had significant differences in the disease phenotype. We have studied the *in vitro* kinetics of fibril formation and the structure of the resulting fibrils in order to explain this phenomenon.

We have begun by undertaking a systematic study of different solution properties and co-solutes that may affect fibril formation in these two proteins. We find that even though the proteins have similar thermodynamic properties, their fibril formation behavior is very different. AL09 readily forms fibrils under virtually every condition studied, while AL103 forms fibrils both more slowly and under fewer conditions. We have also explored the potential role of different glycosaminoglycans (GAGs) in the fibril formation process, specifically looking at the role of the size and charge of the GAG molecules. Furthermore, we have analyzed fibrils formed by these two disease proteins using limited proteolysis and mass spectrometry and have determined that in spite of their different phenotype the fibrils share a significant portion of their amyloid-forming core residues. Further structural studies are ongoing to determine how proteins with such different fibril formation kinetics can share a common amyloid structure.

Funding by AHA SDG 06 3007N, NIH GM071514, and NIH F30DK082169

1315-Pos

Instantaneous Fibril Formation of α-Synuclein by Lateral Association of the Preformed Oligomeric Granules

Daekyun Lee, Jung-Ho Lee, Ghibom Bhak, Sang-Gil Lee, **Seung R. Paik**.
Seoul National University, Seoul, Republic of Korea.

Elucidation of underlying mechanism of amyloidogenesis is a central issue not only for developing prophylactic and therapeutic means against amyloid-related diseases including Parkinson's and Alzheimer's diseases, but also for utilizing protein fibrils as nanomaterials for future nanobiotechnology. While the nucleation-dependent fibrillation is the prevailing notion to illustrate the amyloid fibril formation, we demonstrate an alternative mechanism of amyloidogenesis with α-synuclein, a pathological component of Parkinson's disease, in which the amyloid fibrils are formed via lateral association of the preformed oligomeric species of α-synuclein by acting as an assembling unit. Homogeneous oligomeric granules of α-synuclein were isolated in the middle of the lag period during the fibrillation kinetics. In the presence of an organic solvent of hexane, the granules instantaneously turned into the fibrillar structures which are indistinguishable from the amyloid fibrils obtained without the hexane treatment. Moreover, accelerated fibril formation of α-synuclein was also observed by imposing shear force on the granular structures by either centrifugal filtration or rheometer. Both organic solvent and physical influence might cause granules to experience structural rearrangement, resulting in the granular assembly into amyloid fibrils. As consequence, we propose a double-concerted fibrillation model to explain the *in vitro* fibrillation of α-synuclein, in which two consecutive associations of monomers and subsequent oligomeric granules are responsible for the eventual amyloid fibril formation.

1316-Pos

New Fluorescent Probe for Continuous Monitoring of Alpha-Synuclein Aggregation

Dmytro A. Yushchenko[1], Jonathan A. Fauerbach[2], Alexander P. Demchenko[3], Elizabeth Jares-Erijman[2], Thomas M. Jovin[1].
[1]MPI for Biophysical Chemistry, Goettingen, Germany, [2]Departamento de Química Orgánica, Universidad de Buenos Aires, Buenos Aires, Argentina, [3]Palladin Institute of Biochemistry, Kiev, Ukraine.

The aggregation of the presynaptic protein alpha-synuclein (AS), associated with Parkinson's disease, results in fibrils with a cross-beta-amyloid structure. Thioflavin T (ThT) is widely used for the identification and quantification of

such amyloid fibrils *in vitro*. However, it exhibits poor sensitivity and reproducibility, requires sampling, and is insensitive to the early stages of aggregation. We introduced a new sensor molecule for the *continuous* monitoring of AS aggregation, denoted AS-140HC, consisting of the AS mutant (A140C, C-terminus) labeled with the 3-hydroxychromone dye MFC[1]. MFC exhibits two fluorescence bands (N* and T*) arising from Excited State Intramolecular Proton Transfer (ESIPT)[2]. The intensity ratio of (I_{T*}/I_{N*}) reflects the microenvironment of the probe. Addition of AS-140HC in the range of 0.5-5% to wild type AS allows the monitoring of aggregation via the strong increase of I_{T*}/I_{N*} (panel A), which occurs at a much earlier stage of aggregation than the ThT response (panel B). See also refs [3-6].

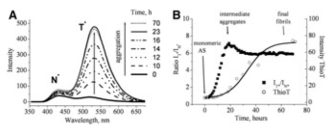

[1] manuscript in preparation; [2] Demchenko et al., Biophys J., 2009, 3461; [3] poster Fauerbach et al.; [4] poster Shvadchak et al.; [5] Caarls et al., J. Fluor, 2009, DOI 10.1007/s10895-009-0536-1; [6] Celej et al., Biochemistry 2009, 7465.

1317-Pos
Characterization of Alpha-Synuclein Early Aggregates by Atomic Force Microscopy

Jonathan Fauerbach[1], Dmytro Yushchenko[2], Alexander Demchenko[3], Thomas M. Jovin[2], Elizabeth A. Jares-Erijman[1].
[1]Departamento de Química Orgánica, Facultad de Ciencias Exactas y Naturales (FCEyN), Universidad de Buenos Aires (UBA), Buenos Aires, Argentina, [2]Laboratory of Cellular Dynamics, Max Planck Institute for Biophysical Chemistry, Göttingen, Germany, [3]A. V. Palladin Institute of Biochemistry, 9 Leontovicha Street, Kiev, Ukraine.

αlpha-synuclein (AS) is a key player in the development of Parkinson's disease. Neither the mechanism of its aggregation nor its role in neurotoxicity have been established as yet. However, it has been proposed that early oligomeric species may be the most cytotoxic [1].

Through the use of a covalently attached dual fluorescent emission ESIPT dye [2], we are able to monitor continuously the entire aggregation process *in vitro* [3]. Examination of samples by AFM has revealed a new pantheon of supramolecular species varying greatly in size and form. We identify a progression of structures starting from the unstructured monomer and proceeding through (i) spherical microaggregates (''fuzzy balls''); (ii) concatenated linear beaded fibrils (''fuzzy fibrils''); (iii) ring-like assemblies; (iv) circular ''platforms'' supporting nascent fibers [''acunas'' = amyloid cunas (Spanish for cradle)]; and (v) terminal amyloid fibers.

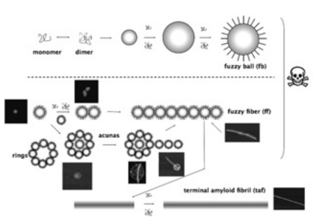

[1] A.L.Fink, **Acc. Chem. Res.**, 2006, **39**, 628-634; V.N.Uversky, **Curr. Prot. Peptide Sci.**, 2008, **9**, 507-540.
[2] V.V.Shynkar et al., **J. Phys. Chem. A.**, 2004, **108**, 8151-8159.
[3] Manuscripts in preparation; poster Yushchenko et al.

1318-Pos
Sickle Hemoglobin Fiber Kinetics Revealed by Optical Pattern Generation

Zenghui Liu, Alexey Aprelev, Mikhail Zakharov, Frank A. Ferrone.
Drexel University, Philadelphia, PA, USA.

Sickle hemoglobin (HbS), a mutant of normal adult hemoglobin (HbA), will polymerize at concentrations above a well-defined solubility. HbS polymerization occurs by a double nucleation mechanism. A fundamental element of the mechanism is the growth of individual fibers, whose diameter (20 nm) precludes direct optical visualization. We have developed a photolytic method to measure the HbS fiber growth speed in HbS carbon monoxide derivative (COHbS) solutions. The idea of this method is that a single fiber entering a region of concentrated deoxyHbS will generate large numbers of additional fibers by heterogeneous nucleation, allowing the presence of the first fiber to be inferred even if it is not directly observed optically. We implement this method by projecting an optical pattern consisting of three parts: a large incubation circle, a small detection area, and a thin channel connecting the two. The connecting channel is turned on for just a short time; only if fiber growth is fast enough will the detection circle polymerize. Our fiber growth rates obtained from pure HbS, HbS/HbA mixtures, and partial photolysis of HbS validate a simple growth rate equation including any non-polymerizing species in the activity coefficient calculation. The monomer on-rate is determined to be 82 ± 2 /mM/Sec. The monomer off-rate is 751 ± 79 molecules/sec in agreement with earlier DIC observations of 850 ± 170 molecules/sec. The method predicts a solubility of 16.0 ± 1.1 g/dl in good agreement with 17.2 g/dl from sedimentation methods. The preceding values are for 25°C. Our measurements also rationalize the observed growth rate of the dense mass of fibers that grows more slowly along the channel and which can be visualized directly. Future uses of this method include HbS fiber bending and HbS solution fluctuations.

1319-Pos
Do Different Ligands Produce Different Effects in Sickle Hemoglobin Polymer Growth?

Donna Yosmanovich, Alexey Aprelev, Maria Rotter, Frank A. Ferrone.
Drexel University, Philadelphia, PA, USA.

Sickle Hemoglobin (HbS) is a variant of human hemoglobin with a point mutation on two subunits. This mutation causes HbS molecules to grow into polymers when the ligands it transports are released it and changes conformation from an R (relaxed) state to a T (tense) state. The polymer mass that grows inside a red blood cell can cause it to become too rigid to deform to pass through tight capillaries. This causes vaso occlusion and is one of many side effects of sickle cell disease. Polymer growth can be measured by fully photolyzing an HbS sample with a laser, thereby causing the solution molecules to release all their ligands and switch into a T-state. However, in vivo, the partial pressure of oxygen rarely falls below 50% which makes the Hb a combination of fully, partially and un-liganded species. Equilibrium and kinetic measurements were done previously on fractional O2, CO and NO species, although a complete systematic comparison has never been conducted to quantify all of the differing data. A comparison of previous data along with new kinetic results will be presented. Partially ligated crystal protein structures will also be employed to rationalize the results.

1320-Pos
Light Scattering Measurements of Hemoglobin Critical Fluctuation and the Energy Landscape For Polymerization

Yihua Wang[1], Alexey Aprelev[1], Suzanna Kwong[2], Robin W. Briehl[2], Antonio Emanuele[3], Frank A. Ferrone[1].
[1]Drexel University, Philadelphia, PA, USA, [2]Albert Einstein College of Medicine, Bronx, NY, USA, [3]University of Palermo, Palermo, Italy.

We have developed a novel method for measuring light scattering to observe critical fluctuations in hemoglobin (Hb) solutions. A small rectangular cell (0.2 x 4.0 x 30 mm) is filled with 24 μL of Hb solution. An optical fiber with outer diameter of 125 μm (62.5 μm core) is sealed into the cell in contact with the solution, and light scattering is measured at 90°. The flat faces of the cell permit measuring absorbance spectra to ensure sample integrity. The scattering source is a 785 nm laser diode that delivers 1.5 mW to the sample. Scattered light is detected by a Hamamatsu GaAs(Cs) PMT via a LWD microscope objective. Measured scattered light intensity agrees ($\pm 10\%$) with scattered intensity expected from Hb fluctuations. Sample temperature is controlled by a thermoelectric stage and raised in a series of user-controlled steps. Temperature may be conveniently returned to prior values to insure reversibility. Assuming that the divergence in scattering that is observed signifies a spinodal, all our measured experiments agree with published spinodals for deoxyHbS, and deoxyHbA. In addition we have obtained data for COHbA, and cross-linked deoxyHbA. Spinodal lines for COHbA and deoxyHbA are essentially indistinguishable, despite differences in quaternary structure. Spinodal lines for cross-linked deoxyHbA and regular deoxyHbA coincide at high c values, but differ significantly at lower ones. In conclusion, changes of quaternary structure cause alterations to spinodal lines when polymerization is possible. This kind of data can be used to explore free energy landscapes having features inaccessible to techniques based on equilibrium thermodynamic properties.

1321-Pos
Sickle Cell Occlusion in Microchannels

Alexey Aprelev, William Stephenson, Hongseok (Moses) Noh, Frank A. Ferrone.
Drexel University, Philadelphia, PA, USA.

Sickle Cell disease is the result of a genetic mutation on the surface of the hemoglobin molecule that makes it capable of polymerization upon deoxygenation. Such polymerization leads to impaired circulation and tissue damage due to the rigidity of the polymer mass. A powerful method for studying the reaction is to replace the physiological ligand (oxygen) by CO, which can be readily and reversibly photolyzed by a strong light source such as a laser. This provides a means of initiating and sustaining the reaction for as long as desired, followed by full reversal once the light is turned off. This method has been used with both solutions and cells. Here we have coupled the method to a microfluidic system to observe directly how photolytically sickled cells occlude small channels, of width ranging from 2 to 10 μm. Because the thickness of the channels is 2 to 5 μm, it is completely spanned by the red cell. This fixed path length permits microspectrophotometry of the cell to determine the internal

Hb concentration. The same cell is oscillated back and forth along the channel by changing pressure, and tracking of the cell determines its frictional coefficient. Light from an Argon ion laser is imaged on the cell, causing it to lose CO and subsequently rigidify. The functional effect of the rigidity is seen as the cell's ability to oscillate becomes impaired. This can be compared with the mass of polymer that forms within the cell. Such information is critical for understanding the details of how polymer formation results in vaso-occlusion.

1322-Pos

Miccrorheology of Sickle Hemoglobin Gels

Mikhail Zakharov[1], Alexey Aprelev[1], Matthew S. Turner[2], Frank A. Ferrone[1].

[1]Drexel University, Philadelphia, PA, USA, [2]University of Warwick, Coventry, United Kingdom.

Sickle cell disease is a rheological disease, yet no quantitative rheological data exists on microscopic samples. We have developed a novel method for probing the microrheology of sickle hemoglobin gels, based on magnetically driven compression of 5-8 μm thick emulsions containing hemoglobin droplets of ~100 μm diameter. By observing the expansion of the droplet area as the emulsion is compressed, our method can resolve changes in thickness of a few nm with temporal resolution of ms. Carbon monoxide bound to sickle hemoglobin was dissociated by laser illumination allowing the resulting deoxyhemoglobin to form gels in target droplets. The amount of polymer formed was determined by observing, in the target droplet, the residual concentration in a small region that was unilluminated by the laser. Thickness was monitored by observing a non-photolyzed reporter droplet adjacent to the target droplet.

Gels were formed at different initial concentrations, temperatures and fractional saturation with CO. In addition, some gels were formed in small spatial regions which then were allowed to grow to the full extent of the target droplet, to contrast with the same sample gelled completely in the target droplet ab initio, thereby creating a different domain structure in the gel. We find that all the gels behave as Hookean springs with linear and repeatable dependence of thickness on force. This allowed us to determine Young's modulus, which ranged from 300 to 1500 kPa for the gels which varied in polymerized hemoglobin concentration from 6 g/dl to 12 g/dl. A highly simplified model for the gel, treating it as a simple lattice with fixed junctions, describes the observed quadratic concentration dependence of Young's modulus data. These measurements provide a quantitative rationale for pathophysiology in the disease.

1323-Pos

Unraveling the Pressure Effect on Nucleation Processes of Amyloidogenic Proteins

Roland Winter.

TU Dortmund University, Dortmund, Germany.

Fully or partially unfolded proteins may undergo non-native self-assembly as a competing pathway to native functional folding, and are the first steps in the nucleation and fibrillation process of proteins, which can lead to a series of diseases including Alzheimer's and type II Diabetes Mellitus. Up to date, still little is known about the nucleation event initiating fibril formation of proteins and how it is influenced by thermodynamic variables, such as temperature, pressure and the activity of cosolutes, although such factors are often responsible for the polymorphic nature of the fibrils formed. Pressure tuning in combination with calorimetric, spectroscopic and structural techniques revealed new insights into the pre-aggregated regime as well as mechanistic details about concurrent aggregation pathways and the differential stability of insulin aggregates [1-4]. Here we focus now on a simple model within the framework of classical nucleation theory that is able to shed light on the effect of pressure on the nucleation process of amyloidogenic proteins. With the input parameters determined and the pV-corrected free energy term of the classical nucleation theory, the experimental data follow the theoretical predictions remarkably close. The negative activation volume observed suggests that the transition state for nucleation and subsequent growth is less hydrated and more densely packed than the partially unfolded insulin monomers entering the nucleation pathway. The insights provided by the model presented will be very helpful to quantify the influence of pressure on protein aggregation/fibrillation reactions in general.

1. N. Javid, R. Winter, et al., Phys. Rev. Lett. 99 (2007) 028101
2. S. Grudzielanek, V. Smirnovas, R. Winter, J. Mol. Biol. 356 (2006)
3. V. Smirnovas, R. Winter, Biophys. J. 94 (2008) 3241-32462
4. R. Mishra, R. Winter, Angew. Chem. Int. Ed. 47 (2008) 6518-6521

1324-Pos

Point Substitution in Albebetin Sequence Accelerates the Amyloid Structure Formation

Vitaly A. Balobanov[1], Yakov S. Anisimov[1], Rita V. Chertkova[2], Nelly B. Ilyina[1], Victor D. Vasilyev[1], **Valentina E. Bychkova**[1].

[1]Institute of Protein Research RAS, Pushchino, Moscow Region, Russian Federation, [2]Shemyakin-Ovchinnikov Institute of Bioorganic Chemistry RAS RAS, Moscow, Russian Federation.

It is suggested that partially folded states play a key role in amyloid formation. So, it was of special interest to investigate a protein the "wild" type of which is initially in this state. Albebetin, a de novo protein, is an example of such proteins and can form amyloid structures during long incubation at high temperature. On the other hand, it was predicted theoretically that single point substitution His65 by Phe may strengthen amyloid formation by this protein. Properties of the obtained mutant protein were investigated by far UV CD. The amyloid formation was monitored by ThT fluorescence and electronic microscopy under various conditions. Interaction with phospholipids vesicles was also studied. It was shown that the His65Phe mutant was able to form amyloid structures even at more moderate conditions than the "wild" type did. Additionally, the amyloid growth rate for the mutant protein was substantially higher of that for the "wild" type. Temperature decrease led to reduced rate of amyloid structure growth, while enhancing of ionic strength accelerated amyloid formation and increased its yield. EM images showed fibrillar morphology of formed aggregates. Investigation on amyloid formation by the de novo protein may shed light on common features of amyloid structures. This work was supported by RFBR 09-04-01348, partly by the Howard Hughes Medical Institute Award 55005607 to A.V. Finkelstein, by the RAS Program on "Molecular and Cellular Biology", by Federal Agency for Science and Innovations 02.740.11.0295, and Program of Scientific Schools 2791.2008.4.

1325-Pos

Amino Acid Modifications in the N terminal Sequence of htt Exon-1 Modulate In Vitro Aggregation

Rakesh Mishra, Ravindra Kodali, Ronald Wetzel.

University of Pittsburgh, Pittsburgh, PA, USA.

Huntington's disease (HD) is one of ten neurodegenerative diseases caused by expanded CAG repeats. A characteristic feature of postmortem HD brains is the presence of intra-nuclear inclusions comprising N terminal mutant Huntingtin (htt) fragments. Based on these and other results, it was posited that protein aggregation might play a crucial role in mediating disease pathologies. Using exon-1 peptide models, we have been able to delineate a clear link between polyglutamine expansion and aggregation propensities as modulated by the first 17 residues adjacent to polyglutamine in the N terminus (httNT). Here we investigate the effect of httNT amino acid modifications - in particular mutations designed to block or mimic putative post-translational modification (PMTs) - on the aggregation of these exon-1 peptides. A particularly striking result was that exon-1 peptides in which both httNT serine residues are mutated to the phospho-Ser mimic aspartate aggregate more slowly and form irregular/immature aggregates, compared to peptides with WT httNT sequence. These results nicely correlate with results in a tg mouse model of HD, in which the Ser->Asp double mutant produces no aggregates and does not develop HD symptoms (X. W. Yang, personal communication). Analysis of single Ser to Asp mutants suggests that these mutations act in concert to produce these effects. Over the PMT mutations studied, we observed a correlation between net hydrophobicity and aggregation propensity. This observation was further corroborated in two multiple mutants containing mutations not associated with PMTs that are designed to either increase or suppress net hydrophobicity. We believe our data to date support our hypothesis that one to a few mutations or PMTs in the N terminal segment can have significant effects on the development of HD pathology, possibly mediated largely by biophysical effects.

1326-Pos

Prefibrillar Formation Conditions of *f*À-Lactoglobulin by Titration and Chaotropes Urea and KSCN Under Thermal Load

Rolando Valdez, Lorenzo Brancaleon, Jerimah Bapcock.

University of Texas at San Antonio, San Antonio, TX, USA.

The harmful growth of toxic oligomers in the formation of protein amyloid fibrils have been connected to degenerative diseases like Alzheimer's and Huntington's diseases. Understanding the fundamental mechanisms behind protein unfolding and subsequent fibrillogenesis may provide a way to stop the process from occurring. The purpose of this study was to identify favorable fibril growth conditions for a globular model protein β-lactoglobulin using the chaotropes urea and KSCN, along with titration of a pH 7.04 phosphate buffer solution at 40°C over five days. Time-resolved and steady-state fluorescence was used to examine the shift in emission of the tryptophan amino acids over the applied denaturation ranges. BLG, a dimer in native form, monomerized and partially unfolded at 5 M Urea, 2 M KSCN and at pH 2 in phosphate buffer in vitro. Exposure of the solutions to continuous heat over time caused a increase in the lifetimes and red shift in the emission spectra , indicating the

possible beginning of nucleation. The study has provided a base for continuation of the study of oligomerization and subsequent fibrillation of BLG, which may provide a fundamental mechanism of formation transferable to other proteins in vivo.

1327-Pos
Amyloid Gels: Formation of an Insulin Fibrillar Network

Mauro Manno[1], Daniela Giacomazza[1], **Jay Newman[2]**, Vincenzo Martorana[1], Pier Luigi San Biagio[1].
[1]Italian National Research Council, Institute of Biophysics, Palermo, Italy, [2]Union College, Schenectady, NY, USA.

The formation of insulin amyloid fibrils is important not only for the development of reliable drugs and drug delivery systems, but also for modeling the basic properties of protein self-assembly. Fibrillation kinetics are typically characterized by an initial apparent lag-phase, related to the formation of oligomer, protofibrils and aggregation nuclei. Afterwards, aggregation proceeds over a wide range of length scales via fibril elongation, thickening and/or flocculation, and eventual gelation. Here, we focus on the formation of such a gel, made of insulin amyloid fibrils, upon incubation at high temperature and low pH. By light scattering and rheological techniques, we monitor the development of the structural, dynamical and mechanical properties of fibrillar aggregates, up to the dynamic arrest of the sample and the appearance of a non-ergodic behavior, which marks the occurrence of gelation. Atomic force microscopy imaging on incubated samples highlight the existence of a fibrillar network , as well as a complex hierarchy of different morphologies. Also, small and large angle dynamic light scattering experiments clearly show a non-diffusional dynamic behavior. Our experiments were able to reveal the structural details hidden in the apparent lag-phase, displaying the slow fibril nucleation and elongation. We confirm that this initial stage is followed by an exponential growth of structures of different sizes. These two kinetic stages of structural growth are mirrored by the kinetics of the viscoelastic properties and, in particular, by the growth of the elastic modulus. Our results show that the appearance of a noteworthy elastic network is associated with the initial fibril nucleation and elongation rather than with the formation of larger structures which cause the eventual gelation.

1328-Pos
Hybrid Amyloid Fibril Genesis with Components of Sporadic and Familial Alzheimer's Disease

Julian Ollesch, Marcus Fändrich.
Max-Planck Research Unit for Enzymology of Protein Folding, Halle(Saale), Germany.

Generally, Alzheimer's Disease (AD) develops spontaneously. Nevertheless, many families with an inheritable occurrence were identified. Of these, a considerable number shows mutations in the Alzheimer Precursor Protein (APP) gene concerning regions of the Aß1-40 peptide, as e. g. the ''Flemish'' A21G [APP A692G] or the ''Iowa'' mutant D23N[APP D694N]. All except two of today's known Aß1-40 mutations in familial AD were reported heterozygously dominant. Therefore, an interaction of wild type (WT) and mutated (MUT) Aß peptide is likely to occur in the brain of affected patients.
Here we report on the extended co-fibrillation analysis of WT and MUT Aß1-40 peptide. Thioflavin-T fluorescence data of cofibrillation kinetics indicated a collateral aggregation process, correlated with the MUT:WT ratio.
Coherently, the fibril morphologies of cofibrillates as observed in negative contrast transmission electron micrographs also appear to correlate with the MUT:WT peptide ratio.
We interpret these results that MUT peptide with a preferred fibril conformation can template the fibril formation of the morphologically pluripotent WT dose-dependently. This may explain the strain-like symptomatic of different familial AD cases.

1329-Pos
Iapp Preamyloid Oligomers Accumulate in the Heart and Contribute to Cardiac Dysfunction in Type-2 Diabetes

Sanda Despa[1], Flavia Andronic[1], Phung Thai[1], Jeffrey H. Walton[1], Kenneth B. Margulies[2], Donald M. Bers[1], **Florin Despa[1]**.
[1]University of California, Davis, CA, USA, [2]University of Pennsylvania, Philadelphia, PA, USA.

Islet amyloid polypeptide (IAPP), a hormone co-secreted with insulin by pancreatic β-cells, forms amyloids when overexpressed. IAPP amyloids accumulate in pancreatic islets and are a hallmark of type-2 diabetes mellitus (T2DM). Recently, IAPP amyloids were found in kidneys of T2DM patients, suggesting that IAPP can deposit in organs other than pancreas. Apparently, the toxic effects to cells are mediated by the preamyloid oligomers. Here, we investigated whether IAPP preamyloid oligomers are present in the heart in T2DM. Using immunochemistry, we found significantly increased levels of IAPP oligomers (by $18 \pm 3\%$) in failing hearts from T2DM humans vs. non-diabetics and in hearts from T2DM rats transgenic for human IAPP (by $88 \pm 15\%$) vs. T2DM rats expressing only rat non-amyloidogenic IAPP. Most likely, IAPP accumulation in the heart occurs in the pre-diabetic state, **when** IAPP is oversecreted in the blood. To investigate the acute effect of IAPP oligomers on cardiac function, we incubated isolated rat cardiac myocytes with exogenous IAPP (5 and 50 μM) for 1-2 h. 50 μM IAPP significantly increased Ca transient amplitude (by $73 \pm 19\%$) in myocytes contracting at 2 Hz. For rapid screening and analysis of sites susceptible for IAPP accumulation we designed a noninvasive water proton NMR protocol. We deciphered the magnetic signal of water surrounding preamyloid oligomers. The variation of this signal was correlated with population distributions of oligomers and fibrils by using immunochemistry and electron microscopy. We found that embryonic amyloids generate hyper-intense magnetic signals, which are distinct from hypo-intense magnetic signals induced by amyloid plaques. These results suggest that IAPP preamyloid oligomers contribute to cardiac dysfunction in T2DM. Water proton NMR may prove a useful non-invasive method for detecting these molecular entities in the heart.

1330-Pos
Small Molecule Inhibitors of Islet Amyloid Polypeptide Fibrillogenesis and Cytotoxicity

Mazin Magzoub, James A. Hebda, Andrew Miranker.
Yale University, New Haven, CT, USA.

Protein fiber formation is associated with diseases ranging from Alzheimer's to type II diabetes. The fiber formation is a complex reaction, which includes a number of conformational and oligomeric intermediate states. In recent years, it has become clear that it is these states, and not the end product (i.e. fibers) of amyloid formation that are the toxic agents associated with disease. These insights indicate that small molecule screens must to be directed at assembly mechanism in order to maximize the prospects for success. Islet amyloid polypeptide (IAPP) is a 37 residue peptide hormone co-secreted with insulin by the ß-cells of the pancreas. In patients with type II diabetes, this protein aggregates as amyloid in a process that is correlated with ß-cell dysfunction and the loss of ß-cell mass. In in vitro studies, the addition of soluble IAPP has been shown to be toxic to many ß- and non-ß-cell lines. IAPP fibrillogenesis, as is the case for many other amylodiogenic proteins, can be catalyzed by lipid bilayers. Paradoxically, while amyloid fibers are ß-sheet rich, membrane-stabilized states are α-helical. We have identified a small molecule alpha helix mimetic, IS5, which inhibits bilayer catalysis of fibrillogenesis, and rescues IAPP-induced toxicity in cell culture. Importantly, IAPP:IS5 interactions localize to the putative α-helical region of IAPP, revealing that α-helical states are on pathway to fiber formation. Normally, IAPP is not amyloidogenic as its cosecreted partner, insulin, prevents self-assembly. Here, we show that IS5 inhibition is synergistic with insulin. IS5 therefore represents a new approach to amyloid inhibition as the target is an assembly intermediate that may additionally restore functional IAPP expression.

1331-Pos
Zinc Inhibits Human Islet Amyloid Polypeptide (IAPP) Amyloidogenesis

Kevin Hartman, Jeffrey R. Brender, Vivekanandan Subramanian, Daniel W. Youngstrom, Ayyalusamy Ramamoorthy.
University of Michigan, Ann Arbor, MI, USA.

Human Islet Amyloid Polypeptide (hIAPP) is a highly amyloidogenic protein found in islet cells of patients with type II diabetes. Because hIAPP is highly toxic to beta-cells under certain conditions, it has been proposed that hIAPP is linked to the loss of beta-cells and insulin secretion in type II diabetics. One of the interesting questions surrounding this peptide is how the toxic and aggregation prone hIAPP peptide can be maintained in a safe state at the high concentrations found in the secretory granule where is stored. We show here through a combination of NMR, ITC, CD, and Thioflavin T fluorescence that zinc, which is found at millimolar concentrations in the secretory granule, binds to hIAPP with a Kd of approximately 100 nM and inhibits hIAPP amyloid fibrillogenesis in the micromolar range. NMR spectroscopy shows that zinc interacts with hIAPP through coordination to His18 and a probable cation - pi stacking interaction with Phe15. ITC binding experiments with the rat variant of IAPP, which lacks His18, indicated an additional binding site with approximately 1 mM affinity. The lower affinity binding site was localized to Arg11 by NMR. The binding of zinc also alters the structure of hIAPP, rigidifying the N-terminal region of the protein in a near-helical conformation stabilizing the non-amyloid form of the peptide. The inhibition of the aggregated and toxic forms of hIAPP by zinc provides a possible mechanism between the recent discovery of linkage between deleterious mutations in the SLC30A8 zinc transporter, which transports zinc into the secretory granule, and type II diabetes.

Intrinsically Disordered Proteins I

1332-Pos
Effects of pH on Conformational Equilibria of Intrinsically Disordered Proteins
Albert H. Mao, Scott L. Crick, Caitlin L. Chicoine, Rohit V. Pappu.
Washington University in St. Louis, St. Louis, MO, USA.
Intrinsically disordered proteins (IDPs) adopt an ensemble of conformations under native physiological conditions. Despite their lack of folded structure, they perform important physiological functions and are predicted to constitute around 30% of the eukaryotic proteome. The success of disorder prediction using a protein's primary structure suggests that the propensity for disorder is encoded in the amino acid sequence. Recently, we found that net charge per residue segregates IDP sequences along a globule-to-coil transition, enabling construction of a sequence-space phase diagram that subdivides IDPs based on the polymeric character of their conformational ensembles. Here, we explore the effects of two perturbations that leave sequence composition unchanged: sequence permutation and pH titration. Using atomistic Monte Carlo simulations in ABSINTH implicit solvent, we find that permutants of an arginine-rich IDP sequence exhibit nearly identical polymeric attributes, yet differ in the details of their conformational ensembles. In contrast, fluorescence correlation spectroscopy shows a decrease in translational diffusion times with increasing pH, suggesting that electrostatic and conformational modulation of protonation equilibria is significant even for solvent-exposed titratable groups on flexible protein backbones. The effect is sufficient to induce a collapse transition in a polyarginine polypeptide at a pH well below the pKa of the arginine sidechain. We conclude that the polymeric character of an IDP is largely determined by its sequence composition, but emphasize the importance of accurate constant pH simulation technology in investigating details of its conformational equilibria.
Supported by grants 5T32GM008802 from the NIH National Institute of General Medical Sciences and MCB 0718924 from the National Science Foundation.

1333-Pos
Development of New Predictors of Intrinsically Disordered Proteins and Residues
Bin Xue[1,2], Christopher J. Oldfield[1], Weilun Hsu[1], Vladimir Uversky[1,2], A. Keith Dunker[1].
[1]Center for Computational Biology and Bioinformatics, Department of Biochemistry and Molecular Biology, Indiana University School of Medicine, Indianapolis, IN, USA, [2]Institute for Intrinsically Disordered Protein Research, Indiana University School of Medicine, Indianapolis, IN, USA.
The concepts of intrinsic disorder (ID) and intrinsically disordered proteins (IDP) are being increasingly accepted by the scientific community. Although without unique 3D structures under physiological conditions, IDPs play important roles in many crucial biological processes, such as signaling, recognition, and regulation. However, identification of ID residues and IDPs is still challenging. Experimental methods are both time consuming and expensive. Computational methods are frustrated by the modest accuracy, especially on boundary regions and on short disordered segments. In attempts to improve the prediction accuracy, we developed four new predictors: CDF-all, PONDR-FIT, SPA, and Chopper. All these predictors showed some improvements over previous methods. CDF-all and PONDR-FIT employed artificial neural networks to refine the prediction results of six individual predictors (PONDR-VLXT, PONDR-VL3, PONDR-VSL2, IUpred, FoldIndex, and Top-IDP). CDF-all predicts the disordered status of the entire sequence, while PONDR-FIT gives the disorder tendency of each residue. SPA was specifically designed for short peptides by creating sequence ensembles and taking the average of PONDR-VLXT predictions over the ensemble. Chopper cuts the query sequence into short segments and applies SPA on each short segment. The final prediction of Chopper is a refined average of SPA. Since the development of the first disorder predictor in 1997, there are currently more than 50 predictors. Although new predictors are continuously coming, the prediction accuracy seems to be approaching a ceiling. Our approach as demonstrated by these four methods is to develop new prediction strategies. CDF-all and PONDR-FIT integrate several individual predictors. SPA and Chopper enable focus on regions giving lower accuracies. These new approaches each provide additional improvement over previous predictors, but none of these new approaches significantly surpasses the ceiling, which is estimated to be near 85% accuracy for two state, structure/disorder, predictions.

1334-Pos
Structural Disorder Within Henipavirus Nucleoprotein and Phosphoprotein
Sonia Longhi, Johnny Habchi, Laurent Mamelli, Hervé Darbon.
AFMB, UMR 6098, CNRS and Universities Aix-Marseille I and II, Marseille, France.
Henipaviruses are newly emerged viruses within the Paramyxoviridae family. Their negative-strand RNA genome is packaged by the nucleoprotein (N) within a helical nucleocapsid that recruits the polymerase complex made of the L protein and the phosphoprotein (P). Using both computational and experimental approaches we herein show that Henipaviruses N and P proteins possess large intrinsically disordered regions. By combining several disorder prediction methods, we show that the N-terminal domain of P (PNT) and the C-terminal domain of N (NTAIL) are both mostly disordered, although they contain short order-prone segments. We then report the cloning, the bacterial expression, purification and characterization of Henipavirus PNT and NTAIL domains. By combining gel filtration, circular dichroism and nuclear magnetic resonance, we show that both NTAIL and PNT belong to the premolten globule sub-family within the class of intrinsically disordered proteins.

1335-Pos
Searching for the Native Molten Globules
Vladimir N. Uversky, A. Keith Dunker, Bin Xue, Christopher J. Oldfield.
Indiana University School of Medicine, Indianapolis, IN, USA.
Many biologically active proteins are either completely disordered or contain disordered regions of substantial size. These proteins are known as intrinsically disordered proteins, IDPs, among different names. The flexibility of these proteins and regions serves as the basis for their biological functions, where they are often involved in protein-protein interaction, regulation, recognition and signal transduction. These proteins are common in nature and are frequently associated with the pathogenesis of various human diseases Furthermore, intrinsic disorder-based protein-protein interactions, which are commonly accompanied by the disorder-to-order transitions, represent very attractive targets for novel drug development aiming at the specific inhibition of disease-associated protein-protein interactions. Therefore, it not surprising that IDPs have recently gained considerable attention. It is recognized now that ID comes in several flavors and that IDPs show an extremely wide diversity of their structural properties. The major pitfall of the current studies on IDPs in general and on the inhibition of the IDP-based protein-protein interactions in particular is that they are mostly focused on the extended IDPs almost completely ignoring a very substantial subset of IDPs, native molten globules. The goal now is to fill this gap and to identify and structurally and functionally characterize a set of native molten globules. The hypotheses that will be tested are the following: (i) native molten globules are very common in nature; (ii) native molten globules possess recognizable structural and functional properties and therefore can be found computationally and experimentally; (iii) native molten globules are frequently associated with human diseases.

1336-Pos
Exploring the Binding Diversity of Intrinsically Disordered Proteins
Wei-Lun Hsu.
Indiana University School of Medicine, Indianapolis, IN, USA.
Intrinsically disorder proteins often perform their functions through the binding of a short, loosely structured region from one protein onto the binding site of a protein partner. These short binding regions go by various names including eukaryotic linear motifs (ELMs), short linear motifs (SLiMs) and molecular recognition features (MoRFs). All of these represent a class of disordered protein that executes molecular recognition and binding functions typically via a disorder-to-order structural transition. Previous studies from our group showed 2 distinct examples of hub proteins, a disordered hub example (p53) and an ordered hub example (14-3-3), performing one-to-many signaling and many-to-one signaling, respectively. In the former, a single disordered region binds to multiple structured partners. In the latter, many distinct disordered regions bind to a single structured partner. Both alternatives use the MoRF mechanism described above. In this study, we tried to expand our previous work to find more examples and to determine whether the prevalence of the MoRF mechanism is common or rare through analyzing protein complexes deposited in PDB that consist of short nonglobular fragments bound to large globular partners. After examining and clustering the various MoRFs, we found 298 disordered hub examples and 246 ordered hub examples. Further experiments are providing detailed information about how intrinsic disorder facilitates binding to diverse partners. Exploring these examples is yielding a much clearer picture of the conformational changes that occur upon binding and showing that, in general, flexibility allows both subtle and complex structural variation thereby enabling different sequences to fit into the same binding site and the same

sequence to morph into differently shaped binding sites. These results indicate that the observations made previously on the single examples of many-to-one and one-to-many signaling generalize to many hundreds of other well characterized protein-protein interactions.

1337-Pos

Energy Landscape Analysis Reveals Residual Order in Histone Tail Dynamics

Davit Potoyan, Garegin Papoian.
University of North Carolina at Chapel Hill, Chapel Hill, NC, USA.

Histone tails are highly flexible N terminal protrusions of histone proteins which help to fold DNA into dense superstructures known as chromatin. On a molecular scale histone tails are polyelectrolites with high degree of conformational disorder, allowing them to function as bio-molecular ''switches", regulating various genetic regulatory processes. Because of being intrinsically disordered, the structural and dynamical aspects of histone tails are still poorly understood. In this work we have carried out 3 microsecond all atom replica exchange molecular dynamics (REMD) simulations of four histone tails, H4, H3, H2B and H2A, to probe for their intrinsic conformational preferences. Our subsequent energy landscape analysis demonstrated that some tails are not fully disordered, but contain residual secondary structure elements. In particular, H4 formed beta hairpins, H3 and H2B adopted alpha helical elements while H2A was fully disordered. We also carried out polymer physics based analysis of the histone tails' conformational ensembles. We found an intriguing re-entrant contraction-expansion of the tails upon heating, which is caused by the way mobile counterions associate with the protein chains at various temperatures.

1338-Pos

Connecting Unfolded Protein Dynamics and Aggregation

Lisa J. Lapidus[1], Yujie Chen[1], Vijay R. Singh[1], Steven A. Waldauer[1], Eric Buscarino[1], Vince A. Voelz[2], Vijay S. Pande[2].
[1]Michigan State University, East Lansing, MI, USA, [2]Stanford University, Stanford, CA, USA.

Solving the ''protein folding problem'' will require a better understanding of the allowed conformations and dynamics of the unfolded state. Fundamentally, unfolded protein dynamics should be determined by the hydrophobic pattern of each sequence. As proof of this hypothesis, we have constructed a random wormlike chain model that is re-weighted to favor random conformations that have residues of similar hydrophobicity in close proximity. This model gives remarkable quantitative agreement with measurements of intramolecular contact formation for various sequences. Furthermore we have found that the intramolecular diffusion coefficient of various sequences in folding conditions vary by ~ 3 orders of magnitude. We find such dynamics qualitatively agree with those predicted by molecular dynamics in implicit solvent. The fastest sequences are intrinsically disordered proteins and peptides and the slowest sequences are well-behaved proteins with folding times of at least 1 ms. In between these two regimes are sequences prone to aggregation in which intramolecular diffusion is just fast enough to expose hydrophobes to solvent long enough to form bimolecular interactions.

1339-Pos

Investigation of the Intrinsically Disordered Protein IA3 by Multiple SDSL-EPR Techniques

Natasha L. Pirman, Gail E. Fanucci.
University of Florida, Gainesville, FL, USA.

Intrinsically disordered proteins (IDPs) are proteins that contain little to no secondary or tertiary structure and are often functional proteins that are essential in biological systems. Many IDPs undergo a conformational change where the lack of intrinsic structure is relieved upon binding to its target protein. Due to the very nature of unstructured proteins, characterization of the conformational propensities and function of these proteins present a major challenge. Site-directed spin labeling (SDSL) coupled with electron paramagnetic resonance (EPR) spectroscopy is a valuable tool in characterizing the mobility and conformational changes of proteins. This combined technique, however, is not often used to investigate intrinsically disordered proteins (IDPs). IA3 is a 68 residue IDP that has been extensively characterized by various biophysical techniques and was used in this study as a model system to show SDSL-EPR may be employed to characterize conformational changes in IDPs. The TFE-induced disordered-to-α-helical transition of IA3 was monitored by various SDSL-EPR techniques. CW-EPR experiments were performed at X-, Q-, and W-band resonant frequencies and reveal conformational changes can be observed at all three frequencies, with the W-band spectra revealing the most striking changes in dynamics upon inducing α -helical secondary structure by TFE. Low temperature CW-EPR and DEER distance measurements were also performed to evaluate the ability of these methods in characterizing the induced α-helical conformation.

1340-Pos

Coupled Folding and Binding of pKID with KIX Domain Investigated by Multicanonical Molecular Dynamics Simulation in Explicit Solvent

Koji Umezawa, Jinzen Ikebe, Haruki Nakamura, Junichi Higo.
Osaka University, Suita, Osaka, Japan.

Intrinsically disordered proteins (IDPs) do not form any rigid tertiary structures alone. Most of them bind corresponding proteins and fold into an ordered structure to play important roles in biological functions such as signal transduction cascades. The phosphorylated kinase induced domain (pKID) is one of IDPs. The pKID adapts an ordered helical structure while binds to the KIX domain. This structural property of pKID is called ''coupled folding and binding''. From nuclear magnetic resonance (NMR) studies a kinetics model of the coupled folding and binding has been proposed: there are four states of pKID (disordered, encounter complex, intermediate, and ordered helical structure). However, the details of these states at atomic level were still unclear.

In order to obtain the free energy landscapes and the stable complex structures at various temperatures for the system, where pKID, the KIX domain, water and ions are included and they can interact with each other, multicanonical molecular dynamics (McMD) simulation was performed with the all-atom model in explicit solvent. McMD simulation is one of generalized ensemble methods, which can search conformational space much wider than a conventional molecular dynamics simulation, as well as the replica-exchange molecular dynamics (REMD). In this study, starting from completely disordered and unbound states of pKID, the helices of pKID were reproduced as approaching to the KIX domain at adequate low temperature. Additionally, we found a different binding mode from the NMR model. Interestingly, this binding mode is similar to that of the activation domain of the mixed lineage leukemia (MLL) transcription factor upon binding to the KIX domain.

1341-Pos

On the Origins of Intrinsically Disordered Proteins

Jintao Liu, Faeder R. James, **Carlos J. Camacho**.
University of Pittsburgh, Pittsburgh, PA, USA.

A large number of proteins are sufficiently unstable that their full three dimensional structure cannot be resolved. The origins of this intrinsic disorder are not well understood, but its ubiquitous presence undercuts the principle that a protein's structure determines its function. Here, we present a quantitative theory that makes novel predictions regarding the role of intrinsic disorder in protein structure and function. In particular, we discuss the implications of analytical solutions of a series of fundamental thermodynamic models of protein interactions in which disordered proteins are characterized by positive folding free energies. We validate our predictions by assigning protein function using the Gene Ontology classification, in which Protein Binding, Catalytic Activity and Transcription Regulator Activity are the three largest functional categories, and performing genome-wide surveys of both the amount of disorder in these functional classes and binding affinities for both prokaryotic and eukaryotic genomes. Specifically, without assuming any a priori structure-function relationship, the theory predicts that both Catalytic and low-affinity Binding ($K_d > 10^{-7}$ M) proteins prefer ordered structures, while only high-affinity Binding proteins (found mostly in eukaryotes) can tolerate disorder. Relevant to both Transcription and signal transduction, the theory also explains how increasing disorder can tune the binding affinity to maximize the specificity of promiscuous interactions. Collectively, these studies provide insight into how natural selection acts on folding stability to optimize protein function.

1342-Pos

Concerted Involvement of Long-Range Electrostatic Interactions and Fly-Catsing in Recognition of Intrinsically Disordered Proteins

Debabani Ganguly, Jianhan Chen.
Kansas State University, Manhattan, KS, USA.

Intrinsically disordered proteins (IDPs) are the functional proteins that exist as dynamical ensemble under physiological conditions. IDPs play crucial roles in cellular signaling and regulation, and often fold upon binding to specific targets. In particular, the ability to interact with multiple targets appears to be a hallmark of IDPs. Two ideal mechanisms, namely fly-casting/induced folding and conformational selection, are possible for coupled folding and binding to the specific targets. Evidence recently accumulated to suggest that induced folding might be prevalent in IDP recognition. Our recent analysis reveals that both IDPs and the vicinity of their binding sites on the substrate surface are enriched with charges. Our hypothesis is the long-range electrostatic interactions between these charged residues triggers the promotion of the unfolding of residual structure in unbound IDPs and enhance the binding efficiency via the fly-casting effects. Go-like coarse-grained protein model has been used to investigate the interaction mechanisms of IDP complex pKID:KIX. Initial results appear to support the concerted involvement of long-range electrostatic interactions and fly-casting.

1343-Pos

Reverse Regulation: Controlling Intrinsically Disordered Domains with Structured Elements

Ying Liu, Annie Huang, Jordan McIntyre, **Sarah E. Bondos**.
Texas A&M Health Science Center, College Station, TX, USA.

Intrinsic disorder in proteins correlates with alternatively spliced motifs, protein interaction domains, and post-translational modification sites. Consequently, there are many examples of intrinsically disordered regions sensing multiple cellular signals and responding by modulating the activity of a structured functional domain. Conversely, we have discovered two examples of the reverse process - regulation of an intrinsically disordered domain by a structured protein element - using the *Drosophila* Hox transcription factor Ultrabithorax (Ubx) as a model system. Both *in silico* and *in vitro* approaches identified a large (~150 a.a.) intrinsically disordered domain within the Ubx transcription activation domain, which is bounded on its C-terminus by an alpha helix. In cell culture promoter-reporter assays, point mutations that enhance helix stability increase transcription activation, whereas mutations that destroy helix structure abrogate transcription activation, leaving repression and DNA binding intact. Indeed, two amino acid changes are sufficient to disable a 150 a.a. intrinsically disordered domain. These mutations alter Ubx function in a tissue-dependent manner in *Drosophila*, emphasizing the fact that *in silico* prediction and *in vitro* characterization of intrinsically disordered domains is relevant to the function of the protein in a live animal. In the second example, we monitored DNA binding as a function of osmotic stress to discover DNA binding triggers a conformational change that exposes significant additional surface area in N-terminal half of Ubx, including the intrinsically disordered domain. This conformational change provides an opportunity for DNA, via the structured DNA-binding homeodomain, to impact both transcription regulation and protein interactions by the intrinsically disordered domain. This regulatory mode could potentially select the mode (activation vs. repression) of transcription regulation by Ubx in response to DNA sequence.

1344-Pos

Single-Molecule FRET Reveals Altered Binding-Induced Folding Landscape of PD-Related Mutant Protein Alpha-Synuclein

Crystal R. Moran, Allan Chris M. Ferreon, Yann Gambin, Ashok A. Deniz.
The Scripps Research Institute, La Jolla, CA, USA.

The abundantly-expressed and intrinsically disordered protein (IDP) α-synuclein represents an interesting target for biophysical studies of both protein folding and the molecular mechanism(s) of neurodegenerative diseases in humans. Filamentous intracellular inclusion bodies, composed primarily of this protein, are the defining hallmark of Parkinson's disease (PD, the second most common neurodegenerative disorder after Alzheimer's disease) and other related synucleinopathies. Furthermore, three single-amino acid substitutions in α-synuclein have been linked to dominantly inherited familial forms of the disease. Despite much effort and growing interest, much remains to be understood about its normal physiological and disease-related function and the structures associated with them. Like many other IDPs, α-synuclein lacks a well-defined *in vitro* structure, and appears to rely on molecular binding partners to modulate its structure and induce potentially functional folds. Due to the protein's characteristic structural plasticity, structural features that do exist are difficult to observe by conventional techniques that rely on ensemble conformation averaging. To overcome this limitation and begin to understand the complicated folding behavior of this and similar proteins, we employed single-molecule Förster resonance energy transfer (smFRET), which avoids conformation averaging, to probe conformation distributions of a PD-related mutant of α-synuclein as a function of binding-induced folding. These experiments resulted in a detailed binding-induced folding landscape for this α-synuclein mutant. A comparison of this folding landscape with that of the wild-type protein revealed clear conformational consequences of the disease-related mutation and may represent not only a potential clue to the molecular mechanism(s) of PD, but also to the fundamental protein-folding phenomenon of aggregation and amyloid formation.

1345-Pos

α-Synuclein N-Terminus Elicits Vesicle Binding and Folding Nucleation

Tim Bartels[1], Logan S. Ahlstrom[2], Avigdor Leftin[2], Christian Haas[3], Michael F. Brown[2], Klaus Beyer[2].
[1]Harvard University, Boston, MA, USA, [2]University of Arizona, Tucson, AZ, USA, [3]Ludwig-Maximilians-University, Munich, Germany.

α-Synuclein (αS) is a natively unfolded protein predominantly found in pre-synaptic terminals of the central nervous system and implicated in several neurodegenerative disorders, such as Parkinson's disease. The αS monomer may undergo a transition from its disordered solution state into an amphipathic helical conformation upon membrane interaction. Its folding may regulate the fusion of synaptic vesicles with the pre-synaptic nerve terminal. Moreover, the structured monomer may be a necessary intermediate to forming high molecular weight species characteristic of the disease state (1). Here we show the affinity of the αS N-terminus to bind to and fold on highly curved lipid bilayers. Using CD spectroscopy and isothermal titration calorimetry, we investigated lipid-protein interactions of αS N-terminal synthetic peptides and truncated mutants with small unilamellar vesicles having a phase transition near physiological temperature. Moreover, lipid mixtures that undergo phase separation were studied (2). We found the membrane-induced binding and helical folding of the first 25 residues to be highly cooperative. Folding occurs electrostatically or as a result of a change in lipid ordering across the lipid phase transition. Stepwise removal of the first five amino acids of αS by site-specific truncation resulted in a substantial decrease in mean residue ellipiticity. This specifically indicates which N-terminal residues are critical for lipid binding and folding nucleation in the full-length protein. A chemically truncated mutant lacking portions of the N- as well as the C-terminus yielded only a small decrease in binding affinity in comparison to wild-type αS, but led to significant helical destabilization. Our findings highlight the importance of the αS N-terminus in folding nucleation and provide a framework for elucidating lipid-induced conformational transitions in the full-length protein. [1] K. Beyer (2007) Cell Biochem. Biophys. 47, 285-299. [2] T. Bartels et al. (2008) JACS 130, 14521-14532.

1346-Pos

Effects of Vesicle Diameter and Lipid Composition on α-Synuclein Binding

Elizabeth Middleton, Elizabeth Rhoades.
Yale University, New Haven, CT, USA.

Parkinson's Disease is characterized by the presence of fibrillar deposits of alpha-Synuclein (αS) in the *substantia nigra*. αS is an intrinsically unstructured protein that becomes α-helical upon binding lipid membranes. Many studies indicate that the toxic form of αS may be pre-fibrillar oligomers formed in solution or upon binding to cell membranes or synaptic vesicles. The effects of curvature and lipid composition on αS binding were studied by using Fluorescence Correlation Spectroscopy (FCS) to quantitatively measure the binding affinity of αS for synthetic lipid vesicles. Vesicles were prepared with different diameters, and lipid compositions included several anionic lipids, fluid phase, and gel phase vesicles. Binding of the wild-type protein was compared to the three pathological mutants: A30P, A53T, and E46K. Our findings indicate that bilayer curvature does affect the affinity of αS for net negatively charged vesicles, while affinity is mostly invariant to the anionic lipid used.

1347-Pos

Vesicle-Bound Alpha-Synuclein: Are the Helices Anti-Parallel or Extended?

Malte Drescher[1], Bart D. van Rooijen[2], Gertjan Veldhuis[2], Frans Godschalk[1], Sergey Milikisyants[1], Vinod Subramaniam[2], **Martina Huber**[1].
[1]Leiden University, Leiden, Netherlands, [2]University of Twente, Twente, Netherlands.

The Parkinson's disease-related protein α-Synuclein (αS) is a 140 residue protein that is natively unfolded in solution. The membrane-binding properties of αS are implied in its physiological or pathologic activity. The protein was investigated by spin-label EPR using the electron-electron-double resonance (DEER) method to measure the distance between pairs of spin labels. For four double mutants of αS, distances were determined in the vesicle-bound and free form. An antiparallel arrangement of the helices 1 and 2 was found, revealing a horseshoe conformation (Drescher et al., JACS 2008). Applying the same method to single mutants, aggregates with an antiparallel arrangement of helix 2 of the partners are found. Mobility analysis of five singly spin-labeled mutants showed that the membrane affinity of helix 2, comprising residues 45 - 90, decreases with decreasing negative charge of the membrane surface, suggesting differential binding of αS to membranes (Drescher et al., CBC 2008). Recently, there is substantial debate about the actual conformation of αS on different membranes (Jao et al., PNAS 2008; Georgieva et al., JACS 2008; Bortuolus et al., JACS 2008). We will discuss this and show further aspects of the interaction of αS with small unilamellar POPG vesicles, highlighting the structure of the bound form of αS under these conditions.

1348-Pos

A Single Molecule Fluorescence Study on the Consequences of Alpha-Synuclein Oxidation

Eva Sevcsik, Elizabeth Rhoades.
Yale University, New Haven, CT, USA.

Parkinson's Disease (PD) is a neurodegenerative disorder characterized by the deposition of fibrillar amyloid inclusions in the substantia nigra region of the brain. Aggregation of alpha-synuclein (aS), an abundant presynaptic protein, is thought to play an essential role in the pathogenesis of PD. Oligomeric intermediates of the aggregation process have been implicated in neuronal cell death, possibly by compromising cell membrane integrity. Oxidative stress appears to

be directly involved in the pathogenesis of PD; indeed, extensive accumulation of nitrated aS has been detected in amyloid aggregates in PD post-mortem brain tissue. In vitro, oxidative modifications to aS can inhibit fibrillation and lead to the build-up of stable oligomers, which may cause increased toxicity. Here, we use single molecule fluorescence techniques (fluorescence correlation spectroscopy and single molecule Förster energy transfer) to investigate the influence of oxidative modifications on the molecular mechanisms of aS aggregation and membrane interaction. aS is unstructured in solution but residues 1-90 form an alpha-helix upon binding lipid bilayers. Tyrosine nitration leads to decreased binding of aS to lipid vesicles, which might entail a loss of aS native function. Interestingly, we find that nitration of tyrosines located at the C-terminus of the protein, which stays unstructured upon membrane binding, can modulate the affinity of the N-terminus. Another consequence of nitrative insult to the protein is the formation of di- and oligomeric aS species by di-tyrosine cross-linking. We find that protein cross-linking does not perturb the protein's ability to form an alpha-helix upon membrane binding, although the binding affinity is altered. Nitrative stress has been implicated to be involved in PD pathology and the characterization of its effects on aS conformation and membrane interaction will help to refine our understanding of the toxic form(s) of aS.

1349-Pos
Nature of the Low pH Alpha Synuclein Conformational State Revealed with Single Molecule Fluorescence
Adam Trexler, Elizabeth Rhoades.
Yale University, New Haven, CT, USA.
Alpha-Synuclein (αS) is a natively unstructured protein that is strongly implicated in Parkinson's disease (PD) pathogenesis. Aggregated αS is the main component of Lewy body plaques, a hallmark of PD, but smaller αS oligomers are thought to be the cytotoxic agent responsible for neuronal death in the disease. Thus, understanding how this monomeric, unstructured protein becomes a toxic oligomeric state is a vital question in understanding the role of αS in PD. Low pH has been shown to induce the formation of a partially folded structure in αS, which is likely the first step in αS aggregation pathways. We use single molecule Förster resonance energy transfer (smFRET) and fluorescence correlation spectroscopy (FCS) to study a low pH αS conformational state. smFRET measurements have shown that C-terminal residue 130 makes close contact with the central, hydrophobic region of αS at low pH. The N-terminal helix-forming region of αS undergoes little change from neutral to low pH. We have also used guanidine denaturation experiments monitored by smFRET to study the stability of the low pH state. Characterizing the nature of the low pH αS state is critical for understanding this transition, as therapeutic targeting of this state could stop the aggregation process before it even begins.

1350-Pos
Monitoring the Lipid- Binding Properties of Beta- and Gamma- Synuclein using Fluorescence Correlation Spectroscopy (FCS)
Vanessa C. Ducas, Elizabeth Rhoades.
Yale University, New Haven, CT, USA.
The synucleins are a family of natively unstructured proteins consisting of α-, β-, and γ-synuclein, which are primarily expressed in neurons. The synucleins have been linked to the pathogenesis of various neurological disorders, such as Parkinson's disease (α-synuclein) and Dementia with Lewy bodies (α- and β-synuclein). Interestingly, β-synuclein might also have a protective role in neurodegenerative diseases that are associated with formation of α-synuclein aggregates. γ-synuclein was first identified in breast cancer cells, and was later found to be overexpressed in other types of cancer, such as ovarian cancer and retinoblastoma. Recent studies indicated that overexpression of γ-synuclein promotes cancer cell survival and metastasis. Still, the biological relevance of the synucleins is yet to be elucidated. All the synucleins share a 6-residue motif, KTKEGV, in their N-terminal region that is commonly found in lipid-binding proteins (apolipoproteins), and it is thought that their native function likely entails binding to biomembranes. In this study, we use fluorescence correlation spectroscopy (FCS) to monitor the lipid- binding properties of β- synuclein and γ-synuclein. Our findings will help determine the underlying factors governing the synuclein- membrane interactions, as well as the strength of these interactions, which would not only reflect the native functions of these proteins, but would also help understand their involvement in disease states.

1351-Pos
Determining the the Effects of Disorder on Binding Affinity
Wai Kit Ma, Rebecca Sacora, Matthew Gage.
Northern Arizona University, Flagstaff, AZ, USA.
It has long been believed that proteins require a defined three-dimensional structure to perform their specific functions. However, a class of proteins called intrinsically disordered proteins has been identified that do not require a stable structure to perform their functions. These proteins play important roles in many diverse biological processes including signal transduction, transcription, and cell division. Therefore, understanding how these proteins recognize and bind to other proteins to perform their functions is an important question. FlgM is an 88-residue intrinsically disordered protein from bacteria that regulates flagella synthesis by binding the RNA transcription factor Sigma 28. When FlgM is bound to Sigma 28, it inhibits transcription of the genes encoding the late flagella proteins. The FlgM protein is an interesting IDP since FlgM genes from different bacteria exhibit different degree of disorder region. Specifically, our lab has shown that the FlgM gene from A. aeolicus is significantly more ordered than the S. typhimurium FlgM. It is predicted that the more ordered the protein, the higher the affinity of the FlgM for Sigma 28. We are using a combination of Isothermal Titration Calorimetry (ITC) and fluorescence to determine the equilibrium binding constant and the binding kinetics for FlgM binding to Sigma 28 using proteins from a series of different bacteria, including A. aeolicus, S. typhimurium, E. coli, P. aeruginosa, and B. subtilis.

1352-Pos
Mechanism of Small-Molecule Binding by Intrinsically Disordered Proteins
Steven J. Metallo[1], Ariele Viacava Follis[1], Dalia I. Hammoudeh[1], Edward V. Prochownik[2].
[1]Georgetown University, Washington, DC, USA, [2]Children's Hospital of Pittsburgh, Pittsburgh, PA, USA.
We have demonstrated multiple examples of small molecules that are capable of specific binding to relatively short segments of intrinsically disordered (ID) proteins. Molecules that bind to the ID monomer of the cMyc bHLHZip protein are capable of disrupting the extensive protein-protein interface normally formed between cMyc and its heterodimerzation partner Max. The kinetics of the disruption is dependent on the location of the small-molecule binding site along the bHLHZip structure. One site allows rapid disruption with the small molecule acting as a wedge while two other sites are inaccessible to inhibitors when cMyc is dimerized and function only by trapping cMyc when it is in the dissociated, monomeric state. High-affinity, bivalent inhibitors retain the fast disruption profile of one of the constituent parts.

Ribosomes & Translation

1353-Pos
Simulations of the Ribosome Suggest Reversible Transitions and Parallel Pathways are Involved in the Large-Scale Functional Motions of tRNA During Translation
Paul C. Whitford[1], Peter Geggier[2], Roger Altman[2], Scott C. Blanchard[2], Jose' N. Onuchic[3], Kevin Y. Sanbonmatsu[1].
[1]Los Alamos National Laboratory, Los Alamos, NM, USA, [2]Weill Cornell Medical College, New York, NY, USA, [3]Center for Theoretical Biological Physics, UCSD, La Jolla, CA, USA.
Through model building and large-scale computer simulations, we present a structural framework for understanding the molecular mechanisms of transfer RNA (tRNA) motion through the ribosome. In the context of tRNA accommodation (the process by which tRNA enters the ribosomal complex), these models predict that highly-specific functional motions are determined by the atomic details of the ribosome. Significant findings include 1) large-scale reversible fluctuations in tRNA position precede complete tRNA accommodation, 2) the accommodation process possesses multiple kinetic intermediates that may be related to ribosomal ''proofreading'' and 3) parallel pathways of accommodation may allow incoming tRNA molecules to be re-routed in response to changes in cellular conditions. In addition to illuminating the role of the ribosome's structure, this work also predicts that large changes in entropy in the individual tRNA molecules lead to energetically favorable accommodation pathways. The dynamics predicted in these models are validated through comparison with crystallographic data, explicit-solvent simulations and smFRET experiments.

1354-Pos
Fast Biosynthesis of GFP Molecules - A Single Molecule Fluorescence Study
Georg Büldt[1], Alexandros Katranidis[1], Ramona Schlesinger[1], Knud H. Nierhaus[2], Ingo Gregor[3], Michael Gerrits[4], Jörg Fitter[1].
[1]Research Centre Jülich, D-52425 Juelich, Germany, [2]Max-Planck Institut für molekulare Genetik, D-14195 Berlin, Germany, [3]University of Göttingen, III Institute of Physics, D-37077 Göttingen, Germany, [4]RiNA GmbH, D-14195 Berlin, Germany.
Numerous studies showed that protein folding and maturation can differ substantially between *de novo* synthesized proteins and *in vitro* refolded proteins.

In classical folding studies folded proteins are initially denatured into an unfolded state before the (re-) folding process can be studied. It has been demonstrated that protein folding takes place already during the elongation of the nascent chain (co-translational folding).
Here we present an approach employing a two color single molecule sensitive fluorescence wide-field microscope in order to visualize surface tethered fluorescently labeled ribosomes and *de novo* synthesized GFP molecules in real time [1]. Suppression of protein release after synthesis keeps the synthesized GFP bound to the ribosome and allows to image GFP fluorescence for extended observation times.
We demonstrate that the characteristic time for the production of the mature GFP mutant Emerald (GFPem) is five minutes, which is one of the fastest maturation times for a GFP mutant observed so far. Early GFPem molecules appear even faster, within one minute. Processes precedent to chromophore formation, such as polypeptide synthesis and protein folding, are fast and last less than one minute. Thus cellular processes within a time range of a few minutes can be followed by GFPem.
[1] A. Katranidis et al. (2009)Angewandte Chemie Int. Edit., **48**, 1758-1761

1355-Pos
Fluctuating tRNA Guided by Induced Fit as a Basis of High Fidelity Translation by the Ribosome
Padmaja P. Mishra, Wenhui Ren, Mohd Tanvir Qureshi, Tae-Hee Lee.
Pennsylvania State University, University park, PA, USA.
Positional fluctuations and structural flexibility of molecules play important roles in various cellular processes. We implemented a single molecule method that can simultaneously measure fluorescence resonance energy transfer (FRET) and the anisotropy of FRET acceptor emission. Based on the method, we monitored the process of aa-tRNA selection by the ribosome and evaluated the positional fluctuations of a cognate and a near-cognate tRNA at the GTPase activated state. The FRET measurements revealed that a cognate tRNA at the GTPase activated state samples the ''A'' site of the ribosome more frequently than a near-cognate. A cognate tRNA is found fluctuating more slowly within a more restricted space as compared to a near-cognate. These results suggest that induced fit steers a fluctuating cognate tRNA more accurately toward the ''A'' site of the ribosome. Based on our findings, we propose that fluctuating tRNA guided by induced fit may be the basis of high efficiency tRNA selection by the ribosome.

1356-Pos
Simulations of the Bacterial Ribosomal Decoding Switch
Andrea C. Vaiana[1], Helmut Grubmueller[1], Kevin Y. Sanbonmatsu[2].
[1]Max Planck Institute for Biophysical Chemistry, Göttingen, Germany,
[2]Los Alamos National Laboratory, Los Alamos, NM, USA.
Gentamicin is a potent antibiotic often used in therapy for methicillin-resistant Staphylococcusaureus. Gentamicin works by flipping a conformational switch on the ribosome, disrupting the reading head (i.e., 16S ribosomal decoding bases A1492-A1493 used for decoding messenger RNA. We use explicit solvent all-atom molecular simulation to study the thermodynamics of the ribosomal decoding site and its interaction with gentamicin. The replica exchange molecular dynamics simulations allow enhanced sampling of the unbinding free-energy landscape, including a rigorous treatment of enthalpic and entropic effects. The decoding bases flip on a timescale faster than that of gentamicin binding, supporting a stochastic gating mechanism for antibiotic binding, rather than an induced-fit model where the bases only flip in the presence of a ligand. The study also allows us to explore the nonspecific binding landscape near the binding site and reveals that, rather than a two-state bound/unbound scenario, drug dissociation entails shuttling between many metastable local minima in the free-energy landscape. Additional simulations address the effect of mutation/modification of the A-site on the free energy landscapes. In particular, mutations of base A1408 known to confer high-level resistance in ''superbug'' bacteria to common antibiotic therapies are investigated. Special care is dedicated to validation of the obtained results, both by direct comparison to experiment and by estimation of simulation convergence.

1357-Pos
Single-Molecule Study of Programmed Ribosomal Frameshifting
Jin-Der Wen[1], Laura Lancaster[2], Harry Noller[2], Carlos Bustamante[3], Ignacio Tinoco[3].
[1]National Taiwan University, Taipei, Taiwan, [2]University of California, Santa Cruz, Santa Cruz, CA, USA, [3]University of California, Berkeley, Berkeley, CA, USA.
Programmed ribosomal frameshifting is involved in regulation of gene expression at the translation level in bacteria, and the frameshifting efficiency has to be well controlled. For example, the dnaX gene of *E. coli* encodes two subunits (gamma and tau) of the DNA polymerase III, and the ratio of these two subunits is determined by the frameshifting efficiency. Factors that affect frameshifting have been extensively studied in vitro and in vivo, but the dynamic features of this process are still not well understood. Here we use optical tweezers to follow stepwise translation in real time at the single ribosome level to understand how frameshifting is controlled. Our preliminary data show that the ribosome pauses for various times at, or even one to two codons prior to, the slippery sequence where frameshifting occurs. The pause may be caused, at least in part, by an internal Shine-Dalgarno sequence, which is located upstream to the slippery sequence and is known to induce frameshifting. Correlation between pause duration and occurrence of frameshifting is under investigation.

1358-Pos
Single-Molecule Optical-Tweezers Studies of Ribosome Translation and Unwinding of Messenger RNA
Xiaohui Qu[1], Jin-Der Wen[1], Steven B. Smith[1], Laura Lancaster[2], Harry F. Noller[2], Carlos Bustamante[1], Ignacio Tinoco Jr.[1].
[1]University of California, Berkeley, CA, USA, [2]University of California, Santa Cruz, CA, USA.
Ribosomes translate the genetic code in an mRNA into a protein; three nucleotides-one codon-code for one amino acid. Because natural mRNAs contain base-paired regions, the ribosome needs to unwind these structures into single-strands before the structured regions can be translated. Furthermore, mRNA secondary and tertiary structures are involved in translation regulation mechanisms, such as frame-shifting. Bulk studies have shown that mRNA structures slow down the translation rate and that the unwinding is inherent to the ribosome. But the unwinding mechanism is not well understood. We used optical tweezers to apply force to the ends of an mRNA hairpin being translated by a single ribosome. At constant force, the mRNA end-to-end distance increases as the ribosome translates the message and converts double-stranded RNA into single strand. This technique allows observation of codon-by-codon translation. The translation rate dependence on force provides information on the ribosome unwinding mechanism. We found that the translation rate increases quickly as force is increased within a narrow force range, but the rate plateaus below and above this force range. We also found that the translation rate on duplex mRNA (low force plateau) is ~50% of the rate on single-stranded mRNA (high force plateau). The observed force dependence is inconsistent with a passive unwinding model, or the active unwinding models that have been applied to T7 and NS3 helicases. Instead, the data call for a different type of active unwinding mechanism. This result suggests that there might be fundamental differences in the unwinding mechanism of ribosomes and of other nucleic acid helicases. Our results show a tight coupling of the ribosome translation and unwinding activities, and should facilitate understanding of translation regulation mechanisms, such as frame-shifting.

1359-Pos
Insights into Translational Termination from Crystal Structures of the 70S Ribosome Bound to Release Factor
Hong Jin, Albert Weixlbaumer, Cajetan Neubauer, Rebecca Voorhees, Sabine Petry, David Loakes, Ann Kelley, Venki Ramakrishnan.
MRC-Laboratory of Molecular Biology, Cambridge, United Kingdom.
Here we report high-resolution crystal structures of release factor 2 (RF2) bound to 70S ribosome. These structures emulate the translational states directly before and after hydrolysis of the ester bond in peptidyl-tRNA on the ribosome during translational termination. Our structures show detailed molecular interactions between the ribosome decoding center and RF2 upon stop-codon recognition. After a stop-codon is recognized, the universally conserved GGQ motif extends directly into the peptidyl transferase center forming a tightly packed catalytic core. Nucleotide A2602 in the 23S rRNA forms a favourable stack with the GGQ motif in RF2. The ribose of the A76 in the peptidyl-tRNA adopts C2'-endo conformation. Our structures help to rationalize a decade of biochemical and computational data on translational termination. Based on the structures, a mechanistic model on how the ester bond in the peptidyl tRNA is hydrolyzed is proposed.

1360-Pos
Realtime Observation of tRNA Dynamics at High Concentrations in Single Molecule Translation
Sotaro Uemura[1,2], Jonas Korlach[3], Benjamin Flusberg[3], Stephen Turner[3], Joseph D. Puglisi[1].
[1]Stanford University, Stanford, CA, USA, [2]Japan Science and Technology Agency, Tokyo, Japan, [3]Pacific Biosciences, Menlo Park, CA, USA.
Conventional TIRF methods can probe the dynamics of complex biological systems, but only at concentrations of fluorescent components that are less

than ~50 nM due to high background signals. The zero-mode waveguide (ZMW) is a nanophotonic structure consisting of a hole in a metal film on a transparent substrate. In conjunction with laser-excited fluorescence, they provide observation volumes on the order of zeptoliters, three to four orders of magnitude smaller than far-field excitation volumes, allowing fluorescence detection in the μM range. Here, we apply ZMWs and novel detection instrumentation developed by Pacific Biosciences and demonstrate direct observation of multiple rounds of binding and release of tRNAs at high concentrations on various mRNA templates during protein synthesis.
The applicability of ZMWs to translation was confirmed by recapitulation of prior single molecule experiments. We delivered ternary complex of EF-Tu(GTP) with Phe-Cy5-tRNA^{Phe} into the A site of ribosomal initiation complexes with fMet-tRNA^{fMet} with Cy3 in P site immobilized on ZMW surface. FRET observation and tRNA arrival time measured in ZMW at any states was consistent with the prior results obtained by TIRF. Next we monitored the elongation cycle through multiple arrival events of dye-labeled tRNAs onto mRNA-programmed ribosomes. Using a fMet-Phe-Phe-Phe mRNA template, we observed multiple arrivals (up to 3) of Cy5-labeled phe-tRNA^{Phe} in the presence of EF-G; event number and duration depend as expected on EF-G concentration. We demonstrated multicolor observation of three tRNAs using Cy2-labeled Lys-tRNA^{Lys} with Cy2 enables to observe three color elongation cycles for fMet-Phe-Lys-Phe or fMet-(Phe-Lys)x6 mRNA template with green, red and blue excitations. These experiments show that we can observe translation in real time from the perspective of tRNA ligands, and will reveal aspects of translation such as time-dependent tRNA occupancy of the ribosome.

1361-Pos
Following Movement of the L1 Stalk between Three Functional States in Single Ribosomes
Dmitri N. Ermolenko[1], Peter V. Cornish[2], David W. Staple[1], Lee Hoang[1], Robyn P. Hickerson[1], Taekjip Ha[2], Harry F. Noller[1].
[1]Department of Molecular, Cell and Developmental Biology and Center for Molecular Biology of RNA, University of California, Santa Cruz, CA, USA, [2]Department of Physics, University of Illinois, Urbana-Champaign, IL, USA.
The L1 stalk is a mobile domain of the large ribosomal subunit E site that interacts with the elbow of deacylated tRNA during protein synthesis. Using single-molecule FRET, we follow the real-time dynamics of the L1 stalk and observe its movement relative to the body of the large subunit between at least three distinct conformational states: open, half-closed and fully-closed. Pre-translocation ribosomes undergo spontaneous fluctuations between the open and fully closed states. In contrast, post-translocation ribosomes containing peptidyl-tRNA and deacylated tRNA in the classical P/P and E/E states, respectively, are fixed in the half-closed conformation. In vacant ribosomes, the L1 stalk is observed either in the fully closed or fully open conformation. Several lines of evidence show that the L1 stalk can move independently of intersubunit rotation. Our findings support a model in which the mobility of the L1 stalk facilitates binding, movement and release of deacylated tRNA by remodeling the structure of the 50S subunit E site between three distinct conformations, corresponding to the E/E classical, P/E hybrid and vacant states.

1362-Pos
Side-Chain Reactivity of a Nascent Peptide in the Ribosomal Exit Tunnel
Jianli Lu[1], Zhengmao Hua[2], William R. Kobertz[2], **Carol Deutsch**[1].
[1]Department of Physiology, University of Pennsylvania, Philadelphia, PA, USA, [2]Department of Biochemistry and Molecular Pharmacology, UMASS Medical School, Worcester, MA, USA.
Nascent peptides begin to fold in the ribosomal exit tunnel. This is not a unilateral act by the peptide. The tunnel, ~100Å in length and 10-20 Å in width, collaborates and is an active participant in translation. The precise mechanisms for this teamwork are unknown. To probe these peptide-tunnel interactions, we have engineered different side-chains adjacent to a cysteine in a molecular tape measure positioned at various locations inside the tunnel. In each case, we measured the kinetics of cysteine modification with a series of reagents of increasing size: trimethyl-, triethyl-, tripropyl-, and tributyl-ammonium maleimides. Three conclusions may be drawn. First, for a given side-chain and a given reagent, the modification rates decrease in going deeper into the tunnel from the exit port to the peptidyltransferase center (PTC). Second, the ratio of modification rate constants for trimethyl to tributyl reagent for an identical reporter cysteine increases monotonically with increasing distance into the tunnel from the exit port. Third, the tunnel near the exit port is relatively insensitive to the choice of adjacent side-chain, whereas a site deeper in the tunnel exhibits side-chain dependent reactivities. As a given amino acid moves along the tunnel during peptide elongation, its interactions with the tunnel are both site-specific and tuned to the unique primary sequence of each nascent peptide. [Supported by NIH grant GM 52302].

1363-Pos
A Universal Zone in the Ribosomal Exit Tunnel for Helix Formation in Kv1.3
LiWei Tu, **Carol Deutsch**.
Department of Physiology, University of Pennsylvania, Philadelphia, PA, USA.
Crystal structures of Kv channels have given us a reasonably complete view of the structure of a mature Kv channel. However, details of its structure acquisition are missing. We now report on the biogenesis of secondary structure of the transmembrane segments and intervening linkers of Kv1.3. Using a combination of accessibility assays, both cysteine pegylation (Tu et al., 2007; Lu and Deutsch, 2005) and N-linked glycosylation (Mingarro et al., 2000), we derive the following principles of folding for nascent sequences within their native contexts. First, native helical transmembrane sequences initially form helices only within the distal 20Å of the ribosomal tunnel near the exit port. We refer to this region as the α-zone. Helix formation in transmembrane segments thus occurs vectorially from N- to C-terminus as each segment moves sequentially into the α-zone. Second, linker sequences also form compact structures inside the α-zone even in the absence of helix formation of their C-terminal flanking transmembrane segments. Third, helical structures, whether transmembrane or linker segments, formed in the tunnel retain their helicity in the translocon. These principles emerge from a diversity of native transmembrane and linker sequences that comprise Kv1.3 and may therefore be applicable to protein biogenesis in general.
[Supported by NIH grant GM 52302].
References: Tu et al., Biochemistry 46: 8075, 2007; Lu and Deutsch, Biochemistry 44: 8230, 2005; Mingarro et al., BMC Cell Biol. 1: 3, 2000.

1364-Pos
Single- Molecule Force Measurement for 30S- mRNA Interaction in Translation Initiation
Tomoaki Masuda[1], Ryo Iizuka[1], Takashi Funatsu[1], Sotaro Uemura[2].
[1]The University of Tokyo, Tokyo, Japan, [2]Stanford University, Stanford, CA, USA.
Bacterial ribosome is a molecular machine composed of 30S and 50S subunits that translates the genetic code in mRNA into an amino acid sequence through repetitive cycles of tRNA selection, peptide bond formation and translocation. Translation initiation is one of the essential processes in protein synthesis that involves the assembly of initiator fMet-tRNA^{fMet} and three initiation factors (IF1, IF2 and IF3) to 30S subunit with GTP hydrolysis by IF2 to form 70S-mRNA-fMet-tRNA^{fMet} complex efficiently and correctly. These processes are occurred with dynamic intersubunit rotation and repositioning of IF2 and initiator tRNA. We expect that GTP hydrolysis by IF2 plays a key role in 30S-mRNA interactions as well. To understand the dynamics of 30S-mRNA interactions, we performed rupture force measurement between 30S subunit and mRNA by optical tweezer assay.
The rupture force for 30S-mRNA complex in the absence of tRNAs and any IFs showed a single distribution with a peak at 5.7 pN. The addition of tRNA^{fMet} to the complex increased the rupture force to 15.2 pN, while the rupture force for 70S-mRNA-tRNA^{fMet} complex showed 16.5 pN. These results show that the binding of tRNA^{fMet} to the 30S-mRNA complex contributes to the initiation stability, which is greater than 50S binding.
Intriguing results were obtained in the presence of IF2. The rupture force for 30S-mRNA-fMet-tRNA^{fMet}-IF2(GTP) showed 16.1 pN, which is not significantly different from 15.2 pN for 30S-mRNA- tRNA^{fMet}. However, the binding of 50S subunit to this complex led to significant changes, the rupture force for 70S-mRNA-fMet-tRNA^{fMet}-IF2(GDPNP) and 70S-mRNA-fMet-tRNA^{fMet}-IF2(GDP) showing 22.1 pN and 20.5 pN, respectively. These results indicate that IF2 with GTP hydrolysis contributes the initiation stability in 30S-mRNA interactions, which enables efficient initiation of protein synthesis.

1365-Pos
Structural Analysis of Bound Molecules to Ribosome by EM-Fitting
Atsushi Matsumoto.
Japan Atomic Energy Agency, Kizugawa, Japan.
In the previous study, we systematically analyzed many three-dimensional electron microscopy (EM) density maps of 70S ribosome at various functional states available in the EM DataBank to reveal the global conformational differences between the 70S ribosome structures by our new flexible-fitting approach, in which the best-fitting atomic model for each EM map was built by deforming the PDB structure of the 70S ribosome using normal mode analysis of the elastic network model.

In this study, we analyze the structures of smaller molecules bound to ribosome, such as tRNA and elongation factors, which are included in the EM density maps of the 70S ribosome, by building atomic models of these molecules in the bound state. The structures of these bound molecules may be different from those in the isolated state or the X-ray crystal structures. In this analysis, we need to spot these molecules in the EM density map, which is occupied mostly by the 70S ribosome. By fitting the atomic model of the 70S ribosome into the EM density map and eliminating the density of the regions overlapped with the atomic model, we are able to extract the regions for the bound molecules. Our results show that the best-fitting atomic model of the 70S ribosome built in our previous sturdy can extract the regions for the bound molecules more clearly than the original PDB structure.

1366-Pos
Spontaneous Vs. Allosteric Dissociation of E-Site tRNA During Polypeptide Elongation

Chunlai Chen[1], Benjamin Stevens[1,2], Jaskiran Kaur[3], Diana Cabral[3], Zeev Smilansky[2], Barry S. Cooperman[3], Yale E. Goldman[1].
[1]Pennsylvania Muscle Institute, University of Pennsylvania, Philadelphia, PA, USA, [2]Anima Cell Metrology, Inc., Bernardsville, NJ, USA, [3]Department of Chemistry, University of Pennsylvania, Philadelphia, PA, USA.

During ribosome-catalyzed polypeptide chain elongation, dissociation of the deacylated tRNA from the E-site has been proposed to be either spontaneous or triggered allosterically by binding of the next cognate ternary complex to the A-site. Using fluorescent labeled tRNAs, we have measured single molecule fluorescence intensities and single molecule FRET between adjacent tRNAs in the ribosome. From these measurements we have been able to determine tRNA occupancy in the ribosome, and thus whether E-site tRNA dissociates before or after A-site occupancy. In the former case there are a maximum of 2 simultaneously bound tRNAs, while the latter case results in transient binding of 3 tRNAs simultaneously. In a total internal reflection florescence microscope, ribosomes were attached to glass microscopes slides via a biotinylated mRNA coding for MRFFRFY.... (single letter amino acid sequence). When synthesis was initiated with $tRNA^{fMet}$ fully charged with formylated-Met, 60-70% of the ribosomes lost their E-site tRNA prior to ternary complex binding (2-tRNA pathway) at the 2^{nd} and 3^{rd} elongation cycles (R and F respectively). In contrast, for synthesis initiated with uncharged initiator $tRNA^{fMet}$, >90% of the ribosomes followed the 2-tRNA pathway in the 2^{nd} cycle, but only ~15% in the 3^{rd} cycle (~75% following the 3-tRNA route, 10% not categorized). In cycles 4 and 5, almost all ribosomes followed the 2-tRNA pathway. Thus, the length of the peptide chain and/or the specific amino acids bound to the P-site tRNA strongly influence the allostery of E-site tRNA dissociation. Such allostery is also sensitive to the presence or absence of polyamines, Mg^{2+} concentration, and the specific codons in positions 2 and 3. Supported by NIH R01grant GM080376 and NIST ATP grant 70NANB7H7011 through Anima Cell Metrology, Inc.

1367-Pos
Enhancement of Single Molecule Fluorescence Signals by Colloidal Silver Nanoparticles in Studies of Ribosome Dynamics

Shashank Bharill[1], Chunlai Chen[2], Ben Stevens[2,3], Jaskiran Kaur[4], Wlodek Mandecki[5], Ignacy Gryczynski[1], Zygmunt Gryczynski[1], Barry S. Cooperman[4], Yale E. Goldman[2].
[1]UNTHSC, Fort Worth, TX, USA, [2]PMI, University of Pennsylvania, Philadelphia, PA, USA, [3]Anima Cell Metrology, Inc., Bernardsville, NJ, USA, [4]Department of Chemistry, University of Pennsylvania, Philadelphia, PA, USA, [5]Department of Microbiology and Molecular Genetics, UMDNJ, Newark, NJ, USA.

Metal enhanced fluorescence (MEF), in which a surface plasmon near a noble metal alters the spectral properties of an organic fluorophore, increases fluorescence intensity without a concomitant increase in photobleaching rate. To improve recordings of single molecule fluorescence signals from individual ribosomes, we studied the emission of Cy3- and Cy5-labeled ribosomes and tRNAs attached near 50-80 nm silver colloidal particles on a glass microscope coverslip. The fluorescence of Cy3 and Cy5 labeled initiation complexes (ICs) near 50 nm silver particles was increased 4- and 5-fold, respectively, compared to labeled ICs in the absence of silver colloids. Photobleaching lifetime was not significantly accelerated, resulting in 4-5 fold enhancement of total photon emission before photobleaching. Fluorophores showing enhanced fluorescence were colocalized with the colloidal particles, as detected by light scattering. Other ribosomes or tRNAs that were farther away had intensities similar to those on plain glass. Aggregates of silver colloidal particles themselves produced wavelength-shifted luminescence similar to fluorescence, presumably due to resonance between nearby metal particles. With ribosomes bound to the glass substrate near the silver particles via a short mRNA, interaction between $tRNA^{Arg}$-Cy3 in the ribosomal P-site and fMet-Arg-Phe-$tRNA^{Phe}$-Cy5 in the A-site had FRET efficiency and dynamics similar to ribosomes farther away and on plain glass. Binding of Cy5-Arg-$tRNA^{Arg}$ to ICs labeled with Cy3 on the large subunit protein L11, in the absence of the translocase EF-G, produced FRET efficiency and dynamics characteristic of specific codon-dependent A-site binding. Addition of EF-G reduced FRET efficiency, as expected. These tests demonstrate that the colloidal silver nanoparticles increase fluorescence and total photon emission without compromising the biophysical activity of ribosomes.
Supported by NIH grants GM080376 and HG004364.

1368-Pos
Establishing a Fluorescence-Based Helicase Assay for Monitoring Eukaryotic Protein Synthesis Initiation

Ali Ozes, **Christopher S. Fraser**.
University of California, Davis, Davis, CA, USA.

Efficient mRNA recruitment to the human ribosome requires a region of single stranded RNA close to the cap structure. The eukaryotic initiation factor 4A (eIF4A) is a DEAD box helicase that is essential for unwinding any stable secondary structure that would inhibit this step. Although studied for many years, the majority of helicase assays involving eIF4A and its associated proteins have failed to rigorously analyze the kinetic events that occur during mRNA unwinding. To provide this kinetic understanding we have developed a continuous fluorescence-based assay to measure RNA duplex unwinding events. This assay utilizes an RNA oligonucleotide modified with cyanine 3 (Cy3) annealed to a complimentary strand modified with black hole quencher (BHQ). Separation of the RNA duplex region significantly enhances the Cy3 fluorescence, enabling us to measure RNA helicase activity in real time by fluorescence spectroscopy. Data will be presented to show how we are using this assay to determine the kinetic role of accessory factors on the helicase activity by eIF4A. Moreover, we show how this data combined with a continuous coupled ATPase assay is enabling us to determine the relationship of ATP hydrolysis to the unwinding of duplex RNA by this DEAD box helicase.
We will also present data employing RNA duplexes of different lengths, allowing us to understand how the processivity of eIF4A is influenced by other initiation components.
This study will provide us with the foundation to begin understanding the kinetic framework of mRNA recruitment to the human ribosome.

DNA, RNA Structure & Conformation I

1369-Pos
Structure and Mechanism of the glmS Ribozyme

Julie Soukup, Danielle Renner.
Creighton University, Omaha, NE, USA.

The self-cleaving glmS ribozyme is a mechanistically unique functional RNA among both riboswitches and RNA catalysts as its catalytic activity provides the basis of genetic regulation and depends upon glucosamine-6-phosphate (GlcN6P) as a coenzyme. A substantial body of biochemical and biophysical data relating the structure and function of the glmS ribozyme has been amassed, in our laboratory and others, in a relatively short period of time since its discovery. However, a precise and comprehensive mechanistic understanding of coenzyme function in glmS ribozyme self-cleavage has not been elaborated. Careful consideration of the available biochemical and biophysical data relating the structure and function of the glmS ribozyme necessitates that general acid and general base catalysis in a coenzyme-dependent active site mechanism of RNA cleavage are inherently interdependent. We propose a comprehensive mechanistic model wherein the coenzyme, GlcN6P, functions both as the initial general base catalyst and consequent general acid catalyst within a proton-relay thus fulfilling the apparent biochemical requirements for activity. This analysis in combination with other considerations regarding the effects of coenzyme binding on riboswitch structure and function suggests that the development of glmS ribozyme agonists as prospective antibiotic compounds must satisfy strict chemical requirements for binding and activity.

1370-Pos
Antibiotic Development by Investigation of the glmS Riboswitch

Danielle Renner, Julie Soukup.
Creighton University, Omaha, NE, USA.

Although bacterial infections have always been of significant interest to researchers and physicians, the drug-resistant bacterial strains that have recently developed are causing new concerns and are much more difficult to combat. Our current methods for treating bacterial infections include broad-spectrum

antibiotics which target only a small number of bacterial processes. However, with the discovery of riboswitches, we are developing new ways to fight bacterial infections which make use of their own natural metabolic pathways, essentially causing bacteria to destroy themselves. Riboswitches are found in non-coding regions of messenger RNAs and these RNA elements bind to ligands to control the expression of nearby genes. The glucosamine-6-phosphate (glmS) riboswitch is unique in that upon binding its ligand, glucosamine-6-phosphate (GlcN6P), it undergoes self-cleavage and is therefore also a catalytic RNA. The cleavage event targets the RNA for subsequent degradation, thereby repressing further gene expression. To study the glmS riboswitch, initial experiments were performed to determine the mechanism followed upon binding of the natural ligand. Since then, analogs of the natural ligand have been obtained and are being tested for their catalytic capabilities through kinetic analyses and rate constant calculations. Once successful candidates have been determined, these non-natural ligands will be introduced into live bacterial cultures, hopefully disrupting normal cell metabolism and reproduction. If successful, these analogs could be used as novel antibiotics, offering a more specific mode of targeting a wide variety of bacterial species.

1371-Pos

Folding of the Thiamine Pyrophosphate (TPP) Riboswitch

Peter C. Anthony, Christian F. Perez, Cuauhtémoc García-García, Steven M. Block.
Stanford University, Stanford, CA, USA.

TPP riboswitches regulate the expression of thiamine-synthesis (*thi*) genes through a variety of mechanisms, all of which involve binding of TPP to a structured aptamer formed in the untranslated region (UTR) of a *thi* mRNA. We used a high-resolution, single-molecule optical trapping assay to characterize mechanically the folding of the TPP riboswitch aptamer located in the 3'UTR of the *thiC* gene of *Arabidopsis thaliana*. Each RNA molecule, containing either the complete aptamer sequence or a portion thereof, was transcribed *in vitro,* annealed to DNA handles via single-stranded overhangs, and placed in a "dumbbell" experimental geometry[1]. By applying tension to the ends of the RNA molecule under equilibrium conditions and measuring the corresponding extensions, we observed transitions among several well-defined folding states, which we discuss in the context of secondary and tertiary structures formed by the aptamer[2]. One low-force state of the full aptamer, corresponding to the formation of structural elements located near the three-helix junction, was abolished by mutating a single nucleotide believed to participate in specific tertiary contacts within the junction[2,3]. We observed that the mutant aptamer does not bind TPP or other substrates (thiamine, thiamine monophosphate), and that the wild-type aptamer only binds substrates concomitant with entry into the fully-folded state. We also studied the energetics of substrate binding under non-equilibrium conditions by rapidly increasing or decreasing the extension of the aptamer and measuring the hysteresis in force. The number of phosphates on the substrate modulated the amount of work required to induce substrate unbinding, the height and location of the energy barrier to substrate unbinding, and the amount of RNA released.

1. Greenleaf WJ, et al (2005). PRL 95, 208102.
2. Thore S, et al (2006). Science 312, 1208-1211.
3. Sudarsan N, et al (2005). Chemistry & Biology 12, 1325-1335.

1372-Pos

Structure and Function of a Potential Mammalian Riboswitch

Kelley Wanzeck, Natalie Erbs, Katie Del Vecchio, Julie Soukup.
Creighton University, Omaha, NE, USA.

Riboswitches, found in untranslated regions of mRNAs, bind to specific cellular metabolites and undergo a conformational change which modifies expression of a nearby coding region of the mRNA. This coding region is involved in the synthesis of the same metabolite, thereby providing an efficient feedback mechanism of genetic control. To date, various riboswitches have been described to effectively control genetic expression in bacterial cells, but none have been discovered in mammals. We are investigating the structure and function of a potential mammalian riboswitch, thought to control polyamine biosynthesis. Polyamines surround cellular DNA to stabilize the DNA negative charge. To validate this small RNA as a new riboswitch, we are using in-line probing to verify specific metabolite binding and subsequent conformational change. Additionally, to verify the ability of the potential riboswitch to control gene expression, in vivo studies are being performed using a reporter gene system. Successful results from both of these investigations will determine whether this small RNA is a true riboswitch. Further investigations will include determination of its tertiary structure. It is known that cancer cells require a higher concentration of polyamine due to their increased replication rate. Thus, a combination of structural and functional studies of this RNA may prove useful in the development of novel cancer therapies.

1373-Pos

Dynamics of the Catalytic Pocket of a Diels-Alder Ribozyme

Tomasz Berezniak[1,2], Petra Imhof[1], Andres Jäschke[2], Jeremy C. Smith[3].
[1]Computational Molecular Biophysics, Interdisciplinary Center for Scientific Computing, University of Heidelberg, Heidelberg, Germany, [2]Institute of Pharmacy and Molecular Biotechnology, University of Heidelberg, Heidelberg, Germany, [3]Center for Molecular Biophysics, Oak Ridge National Laboratory, Oak Ridge, TN, USA.

The Diels-Alder ribozyme, an in vitro-evolved highly abundant ribonucleic acid enzyme, accelerates the formation of carbon-carbon bonds between a diene and a dienophile in a [4+2] cycloaddition reaction, a reaction with broad application in biochemistry and organic chemistry.

We have examined the ribozyme in the unbound form in solid and liquid phase by means of Molecular Dynamics simulations of 1 microsecond total simulation time. Our simulations confirm highly dynamic state of the catalytic pocket as observed by recent NMR spectroscopy studies.

However, the preformed catalytic pocket architecture, suggested previously based on X-ray investigations, exists only under certain conditions. Simulations of the crystal state show that at the temperature of 100K the catalytic pocket remains in its starting conformation. Yet, at the transitional temperature of 250K a collapse of the catalytic pocket occurs, and the ribozyme adopts an ezymatically inactive closed conformation of the pocket.

Simulations in solution performed at 300K at different magnesium ions concentration reveal that the stabilization of the catalytic pocket depends on high amounts of Mg-ions. At higher Mg^{2+} concentrations the cations are more likely to bind to the backbone of those residues that bridge the opposite strands of the pocket, which leads to stabilization of the enzymatically active open conformation. Simulations with artificial constraints confirm and quantify the effect of backbone stabilization on a catalytically active state. At too low Mg-ion concentrations, catalytically inactive states with a collapsed catalytic pocket dominate. In these conformations the ribozyme is not able to host any reactant. The catalytically active state with an open pocket is a metastable state that can only be accessed and is only sufficiently stabilized at a high enough magnesium concentration, explaining the experimentally found full catalytic activity dependence on the Mg-ions concentration.

1374-Pos

Structural Probing of the T Box Antiterminator-tRNA Complex

Jennifer Hines, John A. Means, Abigael Muchenditsi, Akwasi Agyeman.
Ohio University, Athens, OH, USA.

Structural changes in a unique RNA-RNA binding interaction were probed using 2-aminopurine. The 5′-untranslated leader region (5′-UTR) of the T box family of genes folds into a structure that selectively recognizes a specific tRNA through two unique base-pairing events. The first involves base pairing between the anticodon of cognate tRNA and a tri-nucleotide sequence (specifier sequence) in the specifier loop of stem 1 in the 5′-UTR. The second base pairing event involves the non-aminoacylated tRNA acceptor end base pairing with the first four nucleotides at the 5′-end of a bulge in a highly conserved antiterminator element. In the absence of the stabilization of the uncharged tRNA acceptor end base pairing to the antiterminator element, the more thermodynamically stable terminator element forms and transcription terminates. In this manner, the leader region specifically recognizes cognate tRNA and responds structurally to the charging ratio of the tRNA to regulate transcription, thus making the T box mechanism an example of a riboswitch. Interestingly, the predicted thermodynamic stabilization provided by the four base pairs between the tRNA acceptor end and the antiterminator is not sufficient to overcome the predicted stability difference between the antiterminator and the terminator elements. Consequently, additional structural factors likely play a role in stabilizing the resulting complex. The structural changes induced in both the antiterminator element and the tRNA were investigated using a model system to determine what additional factors, beyond base pairing, contribute to stabilization of the resulting tRNA-antiterminator complex. Fluorescence monitoring of the base analog 2-aminopurine at select positions throughout a model complex indicated that binding results in an induced-fit and a highly stacked environment at the binding interface. These structural features contribute to the overall stabilization of the complex beyond the four base pairs.

1375-Pos

Nanosecond Motions of the Substrate-Recognition Duplex in a Group I Intron Assessed by Site-Directed Spin Labeling

Gian Paola G. Grant[1], Phuong Nguyen[1], Nathan Boyd[2], Daniel Herschlag[2], **Peter Qin[1]**.
[1]Department of Chemistry, University of Southern California, Los Angeles, CA, USA, [2]Department of Biochemistry, Stanford University, Stanford, CA, USA.

The *Tetrahymena* group I intron recognizes its oligonucleotide substrate in a two-step process. First, a substrate recognition duplex, called the P1 duplex,

is formed. The P1 duplex then docks into the pre-folded ribozyme core by forming tertiary contacts. P1 docking controls both the rate and the fidelity of substrate cleavage and has been extensively studied as a model for the formation of RNA tertiary structure. However, previous work has been limited to studying millisecond or slower motions. Here we investigated nanosecond P1 motions in the context of the ribozyme using site-directed spin labeling (SDSL) and electron paramagnetic resonance (EPR) spectroscopy. A nitroxide spin label was covalently attached to a specific site of the substrate oligonucleotide, the labeled substrate was bound to a pre-folded ribozyme to form the P1 duplex, and X-band EPR spectroscopy was used to monitor nitroxide motions in the 0.1 to 50 ns regime. Using substrates that favor the docked or the undocked states, it was established that the nitroxide was capable of reporting P1 duplex motions. Using these nitroxide labeled substrates, it was found that the J1/2 junction connecting P1 to the ribozyme core controls nanosecond P1 mobility in the undocked state (Grant et.al., 2009, JACS, 131, 3136-7). This may account for previous observations that J1/2 mutations weaken substrate binding and give rise to cryptic cleavage. This study establishes the use of SDSL to probe nanosecond dynamic behaviors of individual helices within large RNA and RNA/protein complexes. Work is underway to investigate P1 motions in various mutant ribozymes in order to establish detailed correlations between nanosecond dynamics of P1 with ribozyme tertiary folding and catalytic activity. This may help in understanding the relationship between RNA structure, dynamics, and function.

1376-Pos

Mapping the Global Conformation of the Phi29 Packaging RNA Dimer Using Deer Distance Constraints

Xiaojun Zhang[1], Mamoon Hatmal[2], Ian Haworth[2], Peter Z. Qin[1].
[1]University of Southern California, Department of Chemistry, Los Angeles, CA, USA, [2]University of Southern California, School of Pharmacy, Los Angeles, CA, USA.

The insertion of bacteriophage phi29 genomic DNA into its preformed procapsid requires the DNA packaging motor, which is the strongest known biological motor. The packaging motor is an intricate ring-shape protein/RNA complex. The RNA component, called the packaging RNA (pRNA), is indispensable for motor function, and may play an essential role in motor ATPase activity. Current structural information on pRNA is limited, which hinders our effort on understanding motor function. Here, we use site-directed spin labeling and pulse EPR spectroscopy to map the global structure of a pRNA dimer that has been shown to be a functional intermediate in assembling the ring-shaped pRNA complex in the packaging motor. In our studies, nitroxide pairs were attached to specific sites of a truncated monomeric pRNA construct, the labeled monomers were then assembled into dimers in the presence of Mg2+, and inter-nitroxide distances were measured using DEER (Double Electron-Electron Resonance) spectroscopy. In parallel, an unbiased pool of models that contains variable pRNA conformations was generated, which treats pRNA as a 3-way junction construct, and a set of corresponding inter-nitroxide distances was predicted for each model. Intra-molecular DEER distances were used to obtain the monomeric structures of pRNA in dimer, which are then used to build the structural pool for pRNA dimers. A very small number of models were selected. We expect that this work will provide much-needed structural information regarding pRNA, as well as establishing a new methodology for analyzing global conformations in complex RNAs.

1377-Pos

Accurate Distance Constraints for RNA Structures Using Deer Spectroscopy

Victoria J. DeRose[1], Nak-Kyoon Kim[2], Michael K. Bowman[3], Brandon Green[1], Adam Unger[1], Stefan Stoll[4], R. David Britt[4].
[1]University of Oregon, Eugene, OR, USA, [2]University of California, Los Angeles, CA, USA, [3]University of Alabama, Tuscaloosa, AL, USA, [4]University of California, Davis, CA, USA.

Understanding structure-function relationships in RNA and RNA-protein complexes requires robust methods for obtaining structural information on a variety of length scales. DEER (double electron-electron resonance) is emerging as a powerful method for very accurate ($\pm$ 2 Å over 15-80 Å) distance measurements between pairs of nitroxide labels that can be placed using several available conjugation sites in RNA nucleobases or phosphodiester linkages. Here, we show the potential for DEER spectroscopy in monitoring global RNA folding and also small changes in RNA structure within a model system that is based on the Hammerhead ribozyme. This catalytically active RNA, a three-helix junction motif with a buried active site, undergoes cation-dependent folding transitions that are linked to activity. Nitroxide labels placed at strategic positions allow helix-docking and active-site core rearrangements to be monitored by measuring the dipolar coupling between paramagnetic sites. This poster will present the results of DEER measurements obtained at both X-band and Q-band, where the higher-frequency Q-band spectroscopy significantly enhances the sensitivity of this technique. Mg^{2+}-dependent global folding, and evidence for a smaller local structural change with higher added metal concentrations, are both observed in this RNA. Since labels can be placed at targeted sites within both nucleic acids and proteins, and there is no inherent limitation on macromolecular size, DEER spectroscopy has potential for obtaining high-resolution structural information in complex RNAs and in large RNA or DNA-protein complexes.

1378-Pos

Filtering RNA Decoys with Small Angle X-Ray Scattering and Clustering Analysis

Adelene Y.L. Sim, Michael Levitt.
Stanford University, Stanford, CA, USA.

RNA molecules have previously been regarded as ''boring'' molecules which merely relay genetic information from DNA to proteins. However, they are now known to also exhibit a wide range of gene regulation functions. For instance, the RNA riboswitch binds to ligands, and then undergoes structural changes that regulates either transcription or translation. Like proteins, the function of an RNA depends on its three dimensional structure. Here, we discuss how we can incorporate low-resolution experimental data (namely, small angle x-ray scattering) to score the RNA models (also known as decoys). We have also studied the similarities of clusters from multiple k-means clustering runs on the decoys to help us distinguish well-sampled predicted structures from noise. Use of this clustering analysis allows us to effectively reduce the effects of outliers, which commonly plague low-resolution experimental scoring functions.

1379-Pos

Molecular Dynamics and Distribution of Ions in Kissing Loop

Abhishek Singh, Latsavongsakda Sethaphong, Yaroslava G. Yingling.
North Carolina State University, Raleigh, NC, USA.

RNAs have hierarchical folding of structure which is endowed with abilities to catalyze biochemical reactions, support ligand binding, and proteins recognition. Ionic environment assist RNA to form stable higher order structures. In this study, molecular dynamics simulations were used to analyze the monovalent cationic distributions within RNA loop-loop complexes taken from separate viral species. We demonstrate that cations in show strong preferential distribution around kissing loop region however, ion dynamics do not indicate concrete evidence of specific binding. Cationic spatial localization was observed in a variety of kissing loops. Simulations results reveal the presence of electronegative channels that formed through the major groove of all RNA loop-loop helices and attract and retain the cations. Significant drop of diffusion coefficients was observed for ions inside ionic channels. Effect of sequence on the ion distribution was observed by carrying out mutational studies on the bacterial and viral kissing loops. Molecular dynamics results show strong correlation of ionic propensity regulated by sequence.

1380-Pos

Portability of a Common Nucleic Acid Hairpin Loop Motif Between RNA and DNA

Joshua M. Blose[1], Kenneth P. Lloyd[2], Philip C. Bevilacqua[3].
[1]Cornell University, Ithaca, NY, USA, [2]University of Massachusetts, Worcester, MA, USA, [3]The Pennsylvania State University, University Park, PA, USA.

Hairpins are common nucleic acid secondary structures that perform both structural and functional roles. Recently, we reported that r(UNCG) and r(GNRA) hairpin families use molecular mimicry and electrostatic factors to attain exceptional thermodynamic stability with a CG closing base pair (cbp) (*J. Amer. Soc.* **2009** 131, 8474-8484). Although these loop families fold with different global structures, the tetraloops are stabilized by displaying the same functional groups and partial charges to the major groove edge of the CG cbp. Herein, we compare the r(GNRA) tetraloop family to the DNA triloop family d(GNA), which is also exceptionally stable with a CG cbp and possesses same sheared GA base pair between the first and last positions of the loop (*Biochemistry* **2009** 48, 8787-8794). Interactions of d(GNA) loops with the cbp were probed with nucleobase and functional group modifications and the resulting effects on stability were compared to those from similar substitutions in r(GNRA) hairpins. Interruption or deletion of loop-cbp interactions in d(GNA) was consistent with electrostatic interactions identified through nonlinear Poisson-Boltzmann (NLPB) calculations. Moreover, loop stability changed in a manner consistent with similar loop-cbp interactions for d(GNA) and r(GNRA) loops. We also compared the relationship of ΔG°_{37} and log[Na^{+}] for d(GNA) and r(GNRA) loops and found a decreased salt dependence for both loop families with a CG cbp. Similarity of loop-cbp interactions shows portability of the loop-cbp motif across polymer type and loop size and indicates RNA and DNA converged on a similar molecular solution for stability.

1381-Pos
Single Molecule FRET Characterization of DNA G-Quadruplexes Formed In The Promoter of Human MEF2D and TNNI3 Genes
Wenhua Zhou, **Liming Ying**.
Imperial College London, London, United Kingdom.
DNA G-quadruplexes are enriched near the transcription start site (TSS) of the human genes and have been suggested to be involved in gene transcription and translation. Informations about G-quadruplex conformation and dynamics is crucial to our understanding of the roles of quadruplex in gene regulation as well as to the development of novel therapeutic agents that interact with the quadruplex therefore modulate gene expression. Single molecule fluorescence resonance energy transfer (smFRET) can resolve conformational heterogeneity and dynamic fluctuations in nucleic acids, providing unique insights into the biophysics of quadruplex. We have recently elucidated the conformational heterogeneity and dynamics of the quadruplexes formed in the promoter of human c-myc and c-kit genes by smFRET. Here we present single molecule analysis of DNA quadruplex elements found in the TSS of the promoter of the MEF2D, a member of MEF2 (myocyte enhancer factor-2) family of transcription factors which regulate the response of heart to cardiac stress signals, and also in the chromosome 19 specific minisatellite sequences in the promoter of human cardiac troponin I (TNNI3), a gene encodes constituent protein of the troponin complex on the thin filament of cardiac muscle.

1382-Pos
Structural Diversity of G-Quadruplexes: Potassium Concentration Effect
Chang-Ting Lin[1,2], Ting-Yuan Tseng[1,2], Ta-Chau Chang*[1,2].
[1]National Yang-Ming University, Taipei, Taiwan, [2]Institute of Atomic and Molecular Sciences, Academia Sinica, Taipei, Taiwan.
G-quadruplex (G4) structure, folded from Guanine-rich sequences, is a well known unique DNA secondary structure through Hoogsteen base pairing in the presence of monovalent cation. The importance of G4 structure is not only in human telomeres for protecting the ends of chromosomes, but also in several gene promoters for regulating gene expression.
Here we have combined gel electrophoresis, circular dichroism, and thermal melting to study the possible coexistence of the intramolecular and intermolecular G-quadruplexes in the presence of various concentrations of potassium cation (K^+). Our results showed that an appreciable amount of intermolecular G-quadruplex structures are detected in c-myc even at 1mM K^+, and increases at high K^+ concentration. Together with the quantification system, the amounts of intramolecular G-quadruplex structures of c-myc and bcl2 decrease as a function of K^+ concentration. However, no discernible intermolecular structures of human telomeric sequences up to 150 mM K^+ solution. In addition, upon late change of K^+ concentration at room temperature, no appreciable exchange between intra- and intermolecular structures of blc2 is observed. Moreover, the change in melting temperature upon altering K^+ concentration indicate that K^+-quadruplex association is faster than the K^+-quadruplex dissociation. Further thermodynamic studies based on differential scanning calorimetry and isothermal titration calorimetry measurements will be discussed.

1383-Pos
Does the Unfolding State of the Human Telomere Exist Upon Ion Exchange?
Jen-Fei Chu[1,2], Zi-Fu Wang[3], Hung-Wen Li[3], Ta-Chau Chang*[2,3].
[1]Department of Chemistry, National Taiwan Normal University, Taipei, Taiwan, [2]Institute of Atomic and Molecular Sciences, Academia Sinica, Taipei, Taiwan, [3]Department of Chemistry, National Taiwan University, Taipei, Taiwan.
The guanine-rich (G-rich) repeats of human telomere, $d(TTAGGG)_n$, can form different G-quadruplex (G4) structures in the presence of sodium and potassium cations. Folding of telomeric DNA into G4 structure could inhibit telomerase activity for cancer cell growth. Understanding the formation of G-quadruplexes and the conformational flexibility is essential not only for revealing their biological role, but also for developing anticancer drugs. Recently, Phan *et al.* found that the anti-parallel G4 structure of $d[(GGGTTA)_3GGGT]$ (NF3) with two G-quartet layers is quite different from the undetermined G4 structure of $d[AGGG(TTAGGG)_3]$ (HT22) with three G-quartet layers in K^+ solution. We found similar spectral conversion of circular dichroism for both sequences in Na^+ solution upon K^+ titration, even in the molecular crowding environment, which is more physiological condition. We further use the FRET efficiency from Cy3-DNA-Cy5 to monitor the time trace upon Na-K exchange. Our results show that the FRET efficiency in K^+ solution is similar to that in Na^+ solution for both HT22 and NF3. However, the time trace shows more different in normal condition than in crowding condition. The conversion rate is slower under molecular crowding environment. In addition, the stopped-flow FRET study shows a fast arising with ~300 ms for HT22 and ~200 ms for NF3 followed by decay without observing significant FRET efficiency drop, implies that within the time resolution of ~10 ms the unfolding intermediate state is unlikely the mechanism for the spectral conversion upon K^+ titration. Moreover, we have applied ITC to measure the formation heat of G4 structure and further confirmed that there are different conformations between H22 and NF3 under potassium stabilized G4 solution. Our results suggest that the spectral conversion of G4 under potassium titration is more likely due to loop rearrangement.

1384-Pos
Metadynamics Study of the Free Energy Surface of a G-Quadruplex DNA Structure
Juan-Antonio Mondragón-Sánchez[1], Edmundo Mendieta-Fernández[1], Ramon Garduño-Juárez[2], Gilberto Sánchez-González[3].
[1]Universidad del Papaloapan, Loma Bonita, Mexico, [2]Instituto de Ciencias Físicas, Universidad Nacional Autonoma de México, Cuernavaca, Morelos, Mexico, [3]Facultad de Ciencias, Universidad Autónoma del Estado de Morelos, Cuernavaca, Morelos, Mexico.
Molecular Dynamics Simulations of Biomolecules present some limitations as the current accessible time scales which are significantly shorter that the time scale of a majority of biologically interesting conformational changes, and the evaluation of free energy fails due to the problem of trapping in free energy minima. In this work, we studied the conformational transitions of a four stranded nucleic acid structure (G-quadruplex) formed by a guanine-rich strands by means of Metadynamics method which is a technique to enhance sampling of conformational space systems as to built free energy surface in a modest quantity of time. We present one and two dimensional free energy surfaces of G-quadruplex in terms of properly selected collective variables. Our results show that free energy surfaces present two well defined local minima. We associate two different structural conformations to these minima by comparing with experimental data.

1385-Pos
Local Dynamic Studies of Guanine Residues within the Human Telomeric DNA G-Quadruplexed Conformation
Xiuyi Liu[1,2], Yasemin Kopkalli[1], Aleksandr V. Smirnov[3], Tilman Rosales[3], Mary E. Hawkins[4], Jay R. Knutson[3], Lesley Davenport[1,2].
[1]Brooklyn College, Brooklyn, NY, USA, [2]The Graduate Center, New York, NY, USA, [3]Heart, Lung and Blood Institute, NIH, Bethesda, MD, USA, [4]National Cancer Institute, NIH, Bethesda, MD, USA.
Formation and stabilization of guanine-rich G-quadruplexed DNA conformations can inhibit the abnormal activity of the enzyme telomerase in tumor cells, making it a target for potential cancer therapeutics. To study the effect individual guanine residues have on the folding process and stabilization of the G-quadruplex conformations, the fluorescence of HT_4 oligonucleotides incorporating the fluorescent guanine analog 6-methyl-8-(2-deoxy-D-ribofuranosyl) isoxanthopterin (6MI) into different tetrads of the quadruplex (G1,G4,G5,G9 and G11) were investigated. This guanine probe exhibits changes in fluorescence intensity sensitive to base-stacking and hydrogen-bonding. Fluorescence intensities quench for G4, G5, G9 and G11, and de-quench for G1 when each 6MI-labelled oligonucleotide folds to the G-quadruplex conformation with addition of K^+-ion. This suggests stronger base-stacking interactions with neighboring bases for G4, G5, G9 and G11, compared with G1 located on the 5'-end. Fluorescence intensity peaks observed for G1 and G11 also show significant red wavelength shifts with folding. This suggests these guanine positions may be more exposed to a polar environment within the folded state. Fluorescence lifetime studies of the labeled quadruplex sequences reveal that the observed intensity quenching arises predominantly from fast (sub-nanosecond) quasi-static self-quenching. This self-static quenching apparently arises from the proximity of 6MI to neighboring bases. The ''dark'' component (A_{dark}) dominates the decay behavior for both the folded and unfolded conformations of each 6MI-labeled sequence. With folding, the contribution of A_{dark} increases for all labeled oligonucleotide sequences as the conformation is now more compact. This effect is greatest for those 6MI replacements located in the loop regions. Overall these studies suggest individual guanines play different roles in the stabilization of G-quadruplex structures. This work was supported by NIH SCORE Grant S06 GM 060654.

1386-Pos
Benzo[b]Fluorenone as a Quadruplex Interactive Agent (Qia): Binding Studies and Quadruplex Formation with the Human Telomeric HT4 Sequence
Yasemin Kopkalli[1], Meylyn Chery[1], Brian W. Williams[2], Lesley Davenport[1].
[1]Brooklyn College of the City University of New York, Brooklyn, NY, USA, [2]Bucknell University, Lewisburg, PA, USA.
Many previously investigated agents capable of binding to and stabilizing G-quadruplex DNA conformations possess aromatic, planar chemical structures.

Here, initial investigations on the interaction of benzo[b]fluorenone (BF) with the human telomeric forming oligonucleotide HT4 using circular dichroism (CD), thermal melting and steady-state fluorescence are reported. CD studies suggest that BF exhibits binding selectivity for G-quadruplex over model double-stranded DNA structures. BF binds to hybrid-mixed type quadruplex structures in the presence of physiological concentrations of K^+ ions (100mM). However, even in the absence of salt, BF can induce an anti-parallel type quadruplex conformation. Thermal melting studies on quadruplex HT4 in the presence and absence of salt show BF has little effect on the melting temperature, suggesting that BF may associate with the G-quadruplex structure through a non-intercalating mode. As BF is known to be a solvatochromic fluorophore, steady state fluorescence emission spectra were taken for BF titrated with the HT4 quadruplex formed at 100mM K^+, to explore the ability of BF to act as a potential probe of the environment of its binding site. Based on the red shift of BF emission, BF/quadruplex association appears to involve a relatively polar and hydrogen-bonded environment. This work was supported by NIH SCORE Grant S06 GM 060654.

1387-Pos
Which Comes First, The Deformation or the Binding?
Sungchul Hohng, Sangsu Bae.
Seoul National University, Seoul, Republic of Korea.
Which comes first, the deformation or the binding?
High specificity of protein-DNA interaction is often related with specific deformation of the binding site. B-Z transition is the most dramatic structural change induced by protein-DNA interaction, where some segment of DNA abruptly changes from the right-handed B-DNA to the left-handed Z-DNA by the help of specific proteins.
Here, we report single-molecule FRET studies on protein-induced Z-DNA formation. DNA duplexes with six CG-repeats were prepared. To monitor the conformational dynamics of the CG-repeat, we labeled Cy3 and Cy5 at each end of the CG-repeat. Surface-immobilized DNA molecules did not show any structural dynamics in normal physiological conditions. When a Z-DNA inducing protein, Zα, was added to the buffer solution, however, fluorescence intensity increased abruptly without any accompanying FRET change. Abrupt FRET change occurred with time delay (~10 minute at 25°C on average). When the proteins were washed out, molecules didn't recover the original FRET value for more than 3 hours, but molecules without the FRET change readily recovered their original fluorescence intensity. From these result, we conclude that Zα protein weakly interact with B-DNA, but the interaction becomes extremely strong once Z-DNA is formed.
Next, we prepared a DNA duplex with methylated cytosine in the CG repeat. With millimolar Ni^{2+} in the buffer solution, we observed the intrinsic B-Z transition dynamics, and Z-DNA stabilization by Zα proteins. The transition time from B-DNA to Z-DNA, however, was not affected by the presence of Zα proteins, which strongly support that Zα protein induces Z-DNA by passively trapping Z-DNA structure transiently formed by the intrinsic B-Z transition dynamics. Even though we cannot directly observe Z-DNA, Z-DNA's are actually waiting there inside the cell to play their biological roles on time.

1388-Pos
Monitoring Structural Transitions of a DNA Holliday Junction Using an Acoustic Wave Sensor
Achilleas Tsortos.
FORTH, Heraklion-Crete, Greece.
Structural DNA nanotechnology deals with building DNA molecules with particular geometrical features; creating nanoscale shapes and patterns using long DNA scaffolds, as in DNA origami, or changing DNA shape in a controlled way and in response to an external stimulus, as in molecular switches. Such nanomachines can perform computation, actuation and diagnostic tasks.
We took advantage of a biomolecular structure comprising a four-way DNA (Holliday) junction which belongs to a molecular machines group capable of moving between distinct states. This particular molecular switch exists in either an open (extended) or closed (coaxially stacked) conformation and it is proposed to be used as a principle for sequence-specific nucleic acid recognition. In this study we used the quartz crystal microbalance with energy dissipation (QCM-D) to study the applicability of this structure to detect DNA hybridization on a device surface and test its potential to act as a controllable switch.
We present a novel way of monitoring in real time both oligonucleotide binding and the transition from the closed to the open state of the junction. This transition can be reversed and repeated indefinitely in a fully controllable way.

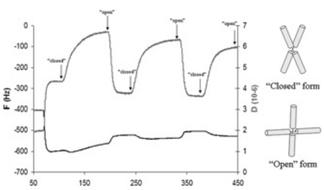

1389-Pos
Single Molecule FRET Measures Structure and Fast Dynamics of DNA and RNA Four-Way Junctions
Claus A.M. Seidel, Stanislav Kalinin, Suren Felekyan, Alessandro Valeri, Simon Sindbert.
Heinrich-Heine University Duesseldorf, Duesseldorf, Germany.
Using a confocal fluorescence microscope multiparameter fluorescence detection (MFD) enables us to simultaneously collect all fluorescence information such as intensity, lifetime, anisotropy in several spectral ranges) from picoseconds to seconds. MFD and fluorescence correlation spectroscopy is applied to perform single-molecule FRET studies with an ultimate level of precision in determining separations with FRET of 1% of the Förster radius [J.Phys.Chem.B 110, 6970 (2006), J.Phys.Chem.B 112, 8361 (2008)]. In addition we can unambiguously distinguish between stochastic processes and broadening due to static or dynamic heterogeneity. In this way we measured bends and kinks in dsDNA. The high accuracy allowed us the detection of sequence-dependent DNA bending by 16° [PNAS 105, 18773 (2008)]. Moreover we studied the Mg-dependent structural dynamics of a four-way DNA (Holliday-) junction in order to find out whether the postulated extended square structure accumulates indeed as an intermediate or whether it should be considered more as a very short lived transition state. We found a complex Mg dependent kinetics, which must be described by a four species model with only two distinct FRET and two kinetic levels. The species with the same FRET value differ in their conformational flexibility: one is quasi-static, the other is dynamic. Our FRET data are clearly inconsistent with an accumulation of a single extended square junction structure at very low Mg concentrations. Finally we compare the structure and dynamics of DNA- and RNA four-way junctions. Thereby the structure of RNA four-way junction was characterized by 24 FRET distances, which allowed us to prove the existence of 3 of the 4 possible stacking conformers. These studies show that sm FRET studies are valuable tool to complement the structural and dynamic information obtained by X-ray crystallography or NMR spectroscopy.

Protein-Nucleic Acid Interactions II

1390-Pos
Kinetic Enhancement of NF-kB/DNA Dissociation by IkBα
Vera Alverdi, Byron Hetrick, Simpson Joseph, Elizabeth A. Komives.
UCSD, La Jolla, CA, USA.
The nuclear factor kappa B (NF-kB) family of transcription factors is involved in inter- and intracellular signaling, cellular stress response, growth, survival, and apoptosis. Specific inhibitors of NF-κB transcription including IκBα, IκBβ, and IκBε, block the transcriptional activity of p65 and c-Rel-containing NF-κB dimers. DNA binding by NF-kB is inhibited by the ankyrin repeat protein kappa B (IkBα), which sequesters NF-kB to the cytosol. The mechanism and kinetics of DNA binding inhibition by IkBα are still unknown, but we recently demonstrated that NF-kB can be ''stripped'' off DNA by IkBα. We are investigating the effect of IkBα on the association and dissociation rates of NF-kB/DNA complex formation using titration measurements, stop flow fluorescence and ITC. We are using pyrene labeled DNA or IkBα or NF-κB to study the fluorescence changes occurring during the NF-kB ''stripping''. Our results show that IkBα increases the dissociation rate of the DNA from the NF-kB complex in a concentration-dependent manner and with high efficiency. We are studying also IkBβ which appears to stabilize the NF-kB/DNA interaction. This could suggest the formation of a ternary complex DNA/NF-κB/IkBβ.

1391-Pos
Prion Aptamer, Free and Bound States
Abigail Miller, Lori Goldner.
NIST, Gaithersburg, MD, USA.
Aptamers are short single strands of DNA or RNA that bind to proteins, peptides, and small molecules. They are likely to fold into different structures when free in solution than when they are bound to a molecular target. The free structures are difficult to determine experimentally, though they can be modeled by calculating the minimum thermodynamic states. We test the validity of the thermodynamic models of a prion aptamer using single molecule pair Forster resonance energy transfer (spFRET) as a structural reporter. The FRET states of the unbound aptamers, the hybridized aptamers and the aptamers bound to PrP peptides are characterized. The DNA aptamers to PrP has a pair of thermodynamic states of roughly the same energy at 25 oC. Their presence in solution is characterized by comparing the single stranded aptamers to its hybridized configuration, thereby removing any internal structure of the aptamers. We demonstrate the existence of both unbound thermodynamic states as well as different interactions between the aptamer and each PrP peptide from static data measuring spFRET in solution.

1392-Pos
Salt Concentration and Force Affect HU-DNA Interaction
Botao Xiao[1], Reid C. Johnson[2], John F. Marko[1].
[1]Northwestern University, Evanston, IL, USA, [2]University of California, Los Angeles, Los Angeles, CA, USA.
HU is one of the most abundant proteins in bacterial nucleoid and participates in nucleoid compaction and regulation. We used magnetic tweezers to study the dependence of DNA condensation by HU on force, salt and HU concentration. DNA bending exhibited only flexible hinge behavior at 150 mM and 200 mM NaCl, which may be considered physiological levels. No binding was observed at 300 mM NaCl. We tracked the disassociation of HU-DNA complexes in real time and found HU binding to be fully reversible in salt concentration above 100 mM NaCl. The 90% disassociation lifetime, $t_{0.9}$, extended when the initial HU concentration in which the complexes formed was increased. If the salt concentration was raised while keeping the initial HU concentration and pulling force fixed, however, the $t_{0.9}$ decreased. Taking 150 nM HU and 0.08 pN force for example, the average $t_{0.9}$ was 233.0 minutes for 100 mM NaCl, 41.6 minutes for 150 mM, and 6.1 minutes for 200 mM. In addition, if the pulling force was increased from 0.08 pN to 0.28 pN, the $t_{0.9}$ decreased by an amount dependent on the initial HU concentration. Our results suggested that HU-DNA association and disassociation can be regulated by a combination of mechanical tension, salt and HU concentration.

1393-Pos
Molecular Properties of Telomeric TRF1/TRF2 - DNA Systems
Bartlomiej Tomiczek[1], Joanna Bidzinska[1], Karina Dzedzej[1], Jacek Czub[1,2], Andrzej Skladanowski[1], **Maciej Baginski**[1].
[1]Gdansk University of Technology, Gdansk, Poland, [2]Max Planck Institute for Biophysical Chemistry, Gottingen, Germany.
Telomeres are nucleoprotein complexes that protect the ends of linear eukaryotic chromosomes from degradation and fusion. Human telomeric DNA contains tandem arrays of double stranded TTAGGG repeats. Telomeric DNA forms specific complexes with many different proteins (shelterins), among which TRF1 and TRF2 are the most essential for the maintenance of telomere structure and function. TRF1 is a negative regulator of telomere length whereas TRF2 is involved in formation of telomeric higher order structures (t-loops), and functions more related to capping the DNA end. Both proteins bind to DNA as pre-formed homodimers. Although cellular functions of both these proteins are different, their structures are very similar. Both TRF1 and TRF2 contain two conserved sequence motives which form specific domains, namely homodimerisation and Myb-DNA binding domains.
In order to reveal the molecular properties of both proteins and also differences between binding modes of TRF1 and TRF2 to telomeric DNA, detailed studies of both binding domains have been performed. We carried out molecular dynamic simulations of TRF1 and TRF2 binding domains and their complexes with DNA. Starting models of studied systems were based on X-ray structures of TRF1 and TRF2 Myb-DNA binding domains [1]. The results have revealed structural differences between bound proteins and structural differences of their binding patterns with DNA. Additionally, we provide experimental evidence that interaction of both shelterins and DNA can be specifically perturbed by small molecular weight ligands. These results support the idea that TRF1/TRF2 - DNA systems are potential new targets for anticancer therapy.
1. R. Court, L. Chapman, L. Fairall, D. Rhodes, EMBO Reports 6 (2005) 39-45.

1394-Pos
Nucleic Acid Chaperone Activity of the Yeast Ty3 Retrotransposon Nucleocapsid Protein
Kathy R. Chaurasiya[1], Hylkje Geertsema[1], Fei Wang[1], Gael Cristofari[2], Jean-Luc Darlix[2], Mark Williams[1].
[1]Northeastern University, Boston, MA, USA, [2]LaboRetro INSERM #758, Lyon, France.
Reverse transcription in retroviruses and retrotransposons requires nucleic acid chaperones, which facilitate the rearrangement of nucleic acid secondary structure. The nucleic acid chaperone properties of the human immunodeficiency virus type-1 (HIV-1) nucleocapsid protein (NC) have been extensively studied, and nucleic acid aggregation, duplex destabilization, and rapid protein binding kinetics have been identified as major components of its activity. However, the properties of other nucleic acid chaperone proteins, such as retrotransposon Ty3 NC, a likely ancestor of HIV-1 NC, are not well understood. We used single molecule DNA stretching as a method for detailed characterization of Ty3 NC chaperone activity. Wild type Ty3 NC strongly aggregates both double-stranded DNA (dsDNA) and single-stranded DNA (ssDNA), and melted DNA exhibits rapid reannealing in its presence. We also studied several Ty3 NC mutants to identify the roles of functional regions of the protein. We found that the N-terminal basic residues contribute to duplex stabilization, while the zinc finger at the C-terminus counteracts this effect. The mutants examined lack the rapid kinetics of wild type Ty3 NC, indicating that both the basic residues and the zinc finger are required for optimum chaperone activity, which is consistent with previous biochemical experiments. Ty3 NC therefore has a chaperone mechanism similar to that of HIV-1 NC. Although Ty3 NC does not exhibit the strong duplex destabilization of HIV-1 NC, this is consistent with the weaker secondary structure of the Ty3 long-terminal repeat region, which suggests that strong duplex destabilization is not needed for NC to facilitate minus-strand transfer during reverse transcription. This research was supported in part by funding from INSERM and ANRS (France).

1395-Pos
5′-Single Stranded DNA Duplex Junctions Provide Specific Loading Sites for the *E. coli* UvrD Single Stranded DNA Translocase
Eric J. Tomko[1], Nasib K. Maluf[2], Timothy M. Lohman[1].
[1]Washington University School of Medicine, St. Louis, MO, USA, [2]School of Pharmacy, University of Colorado, Denver, CO, USA.
E. coli UvrD is a 3’ to 5’ SF1 helicase/ translocase involved in a variety of DNA metabolic processes. UvrD can function either as a helicase to unwind duplex DNA or simply as a single stranded (ss) DNA translocase. The switch between helicase and ss translocase activities *in vitro* is controlled by the UvrD oligomeric state, such that a UvrD monomer has only ssDNA translocase activity, whereas at least a dimeric form of UvrD is required to activate its helicase activity *in vitro*. A 3’-ssDNA partial duplex provides a high affinity site for UvrD monomer binding, however, the monomer is inhibited from initiating DNA unwinding. Here we show that a UvrD monomer also binds with specificity to duplex DNA junctions with a 5’-ssDNA flanking region, with nearly a 20-fold higher specificity than for ssDNA. Furthermore, the UvrD monomer can initiate 3’ to 5’ ssDNA translocation from this site. The higher specificity for the junction results in time courses that reflect the ssDNA translocation of two populations of UvrD monomers: I.) UvrD initially bound a the 5’-ss/dsDNA junction and II.) UvrD initially bound to random sites along the 5’-ssDNA tail. Our results suggest that the population of UvrD initially bound at the junction translocates with different translocation kinetic parameters. We hypothesize that a 5’-ss-duplex DNA junction may serve as a high affinity loading site for the monomeric UvrD translocase, and that this may facilitate its role as an anti-recombinase to disassemble RecA nucleoprotein filaments formed within a ssDNA gap or at arrested replication forks.

1396-Pos
Mechanisms of Nucleotide Cofactor Interactions with the RepA Protein of Plasmid RSF1010
Maria J. Jezewska, Iraida E. Andreeva, Michal R. Szymanski, Wlodek Bujalowski.
Univ Texas Medical Branch, Galveston, TX, USA.
The dynamics of the nucleotide binding to a single, noninteracting nucleotide-binding site of the hexameric helicase RepA protein of plasmid RSF1010 has been examined, using the fluorescence stopped-flow method. The experiments have been performed with fluorescent analogs of ATP and ADP, TNP-ATP, and TNP-ADP. In the presence of Mg2+, the association of the cofactors proceeds as a sequential three-step process.
The sequential nature of the mechanism indicates the lack of significant conformational equilibria of the helicase prior to nucleotide binding. The major conformational change of the RepA helicase - nucleotide complex occurs in the formation of (H-N)2., which is characterized by a very high value of the partial equilibrium constant and large positive changes of the apparent enthalpy and entropy. Strong stabilizing interactions between subunits of the RepA hexamer contribute to the observed dynamics and energetics of the internal transitions of the formed complexes. Magnesium mediate the efficient and fast conformational transitions of the protein, independent of the structure of the cofactor phosphate group. The ssDNA bound to the enzyme preferentially selects a single intermediate of the RepA - ATP analog complex, (H-N)2, while the DNA has no effect on the intermediates of the RepA - ADP complex. Allosteric interactions between the nucleotide- and the DNA-binding site are established in the initial stages of the complex formation. In the presence of the ssDNA, all transitions in nucleotide binding become sensitive to the structure of the cofactor phosphate group.

1397-Pos
Dynamics of the ssDNA Recognition by the RepA Hexameric Helicase of Plasmid RSF1010. Analyses Using Fluorescence Stopped-Flow Intensity and Anisotropy Methods
Wlodek Bujalowski, Maria J. Jezewska, Iraida E. Andreeva, Michal R. Szymanski, Roberto Galletto.
Univ Texas Med Br, Galveston, TX, USA.
Kinetic mechanism of the ssDNA recognition by the RepA hexameric replicative helicase of the plasmid RSF1010 and the nature of formed intermediates, in the presence of the ATP nonhydrolyzable analog, AMP-PNP, have been examined, using the fluorescence intensity and anisotropy stopped-flow, and analytical ultracentrifugation methods. Association of the RepA hexamer with the ssDNA

oligomers, which engage the total DNA-binding site and exclusively the strong DNA-binding subsite, is a minimum four-step sequential mechanism. Extreme stability of the RepA hexamer precludes any disintegration of its structure and the sequential character of the mechanism indicates that the enzyme exists in a predominantly single conformation prior to the association with the nucleic acid. Moreover, the hexameric helicase possesses a DNA-binding site located outside its cross channel. The reaction steps have dramatically different dynamics, with rate constants differing by two - three orders of magnitude. Such behavior indicates a very diverse nature of the observed transitions, which comprises binding steps and large conformational transitions of the helicase, including local opening of the hexameric structure. Steady-state fluorescence anisotropies of intermediates indicate that the entry of the DNA into the cross channel is initiated from the 5' end of the bound nucleic acid. The global structure of the tertiary, RepA - ssDNA - AMP-PNP complex is very different from the structure of the binary, RepA - AMP-PNP complex, indicating that, in equilibrium, the RepA hexamer - ssDNA - AMP-PNP complex exists as a mixture of partially open states.

1398-Pos

Energetics of the E. Coli Pria Helicase Interactions with the Double Stranded DNA

Michal R. Szymanski, Maria J. Jezewska, Wlodzimierz Bujalowski.
University of Texas Medical Branch, Galveston, TX, USA.

Quantitative analyses of the interaction of the Escherichia coli monomeric PriA helicase with the double-stranded DNA (dsDNA) have been studied with fluorescent dsDNA oligomers, using quantitative fluorescence titrations, analytical ultracentrifugation, and fluorescence resonance energy transfer methods. The experiments have been performed with different dsDNA oligomers, long enough, to encompass the total DNA-binding site, as well as the DNA-binding site proper of the enzyme. Interactions with the dsDNA oligomers were examined as a function of different temperature, salts, and nucleotide cofactors. The stoichimetry of the PriA helicase - dsDNA is different from the stoichiometry of the analogous complexes with the ss conformation of the nucleic acid, indicating a very different orientation of the helicase on the dsDNA. Surprisingly, the intrinsic dsDNA-affinity of the enzyme is dramatically higher than the ssDNA affinity, indicating strong selectivity of the helicase for the dsDNA conformation of the nucleic acid. The intrinsic affinities are salt-dependent and the formation of the PriA helicase - dsDNA complex is accompanied by a net ion change. Moreover, the presence of nucleotide cofactors has a profound effect on the dsDNA interactions of the enzyme with the DNA. The interactions of the PriA helicase with the dsDNA are characterized by very weak, if any, cooperative interactions. The significance of these results on activities of the PriA helicase in the cell metabolism is discussed.

1399-Pos

Mechanistic Studies at the Single Molecule Level Reveal the Dynamics of HCV Polymerase Protein in Complex with RNA

Pierre Karam, Colins Vasquez, Wayne Mah, Megan Powdrill,
Matthias Götte, Gonzalo Cosa.
McGill University, Montreal, QC, Canada.

Viral RNA-dependent RNA polymerases (RdRp) that belong to the Flaviviridae family, including hepatitis C virus (HCV), are capable of initiating de novo RNA synthesis. The non-structural protein 5B (NS5B) in HCV shows RdRp activity that is required for viral replication. Due to its critical role in life cycle, understanding the mechanism of mRNA synthesis in HCV is fundamental for current drug discovery efforts.

We will present our results on studies on the enzymatic activity of the Hepatitis C Virus (HCV) RNA polymerase protein. Our studies, conducted with state-of-the-art fluorescence single molecule methodologies, aim to elucidate the dynamics of key protein/nucleic acid complexes.

Our work was conducted on DNA:RNA templates labeled with Cy5/Cy3 (Acceptor/Donor) fluorophores capable of undergoing Forster Resonance Energy Transfer (FRET). Binding of NS5B caused a significant increase in FRET. The SM-FRET studies on RNA-protein complexes revealed protein dynamics occurring with time scales of a few seconds. These dynamics change with the RNA template length, and with the presence of complementary DNA strands. Taken together, our single molecule studies provide for the first time direct evidence on the polymerase-substrate binding process and the effect of template length on protein dynamics.

1400-Pos

Single-Molecule Visualization of the Oligomeric form of *Escherichia Coli* UvrD Helicase *In Vitro*

Yuko Ayabe Chujo[1], Yoshie Harada[2], **Hiroaki Yokota[2,3]**.
[1]The University of Tokyo, Kashiwa, Japan, [2]Kyoto University, Kyoto, Japan, [3]PRESTO, JST, Tokyo, Japan.

Escherichia coli UvrD protein is a superfamily 1 DNA helicase which plays a crucial role in nucleotide excision repair and methyl-directed mismatch repair. There is a general consensus that the enzyme unwinds a duplex DNA from a 3′ end single-stranded DNA (ssDNA) tail, a gap or a nick. However, conflicting models for the unwinding mechanism have been proposed. Concerning its stoichiometry, some biochemical studies have suggested that the enzyme has optimal activity as an oligomeric form. However, a structural study has indicated that the enzyme functions as a monomer deduced from structural analysis of UvrD-DNA complexes. To address this issue, we attempted to unravel the number of UvrD molecules bound to DNA in the presence and absence of nucleotide by single-molecule fluorescence microscopy. We performed single-molecule visualization of a Cy5-labeled Cys-Ala mutant (Cy5-UvrDC640A), in which Cys52 was labeled with high specificity, bound to 18-bp duplex DNA having a 12, 20 or 40-nt ssDNA tail under several Cy5-UvrDC640A concentrations (0.5, 1.0 and 2.0 nM). We analyzed the number of Cy5 photobleaching steps to quantify the number of UvrD molecules bound to the DNA in the absence and presence of an ATP analog, ATPγS. All the distributions of the number agreed well with the predicted distributions which support the model that UvrD protein is bound to the DNA as an oligomeric form. In the presence of ATP, inefficient DNA unwinding in the absence of free Cy5-UvrDC640A in solution and higher fluorescence intensity of Cy5-UvrDC640A compared to that non-specifically attached on the surface were observed. These results indicate that an oligomer of UvrD is the active form of the helicase.

1401-Pos

Mechanism of DNA-Dependent Enzymatic Activation of E. Coli RecQ Helicase

Kata Sarlos, Mate Gyimesi, Mihaly Kovacs.
Eotvos University, Budapest, Hungary.

RecQ family helicases, which are widespread from humans to bacteria, play essential roles in homologous recombination mediated DNA double strand break repair. Escherichia coli RecQ helicase suppresses illegitimate recombination, initiates homologous recombination, and stabilizes stalled replication forks as part of the recF pathway. Many aspects of RecQ function have been investigated in detail. However, a detailed understanding of the mechanoenzymatic mechanism of RecQ (or other superfamily-2 helicases) is still missing. Here we present a detailed quantitative model of the DNA-dependent ATPase mechanism of Escherichia coli RecQ helicase, based on steady-state, rapid transient kinetic and fluorescence spectroscopic data. We show that the binding of DNA to RecQ does not influence the rapid and reversible process of nucleotide (ATP, ADP) binding. The interaction of RecQ with DNA, however, is important for ATP hydrolysis, which is unfavorable in the absence of DNA. The high DNA-binding affinity of the post-hydrolysis state of RecQ indicates that this step may be coupled to translocation on DNA. Our data suggest that the rate-limiting step of the cycle is the hydrolysis step in the absence of DNA, whereas in DNA bound state the reversible hydrolysis and the irreversible phosphate release together determine the rate of the reaction. Translocation along single-stranded DNA enhances the ATPase activity of RecQ. Our data show that, once bound to ssDNA oligonucleotides, RecQ performs processive translocation until it reaches the 5' end, from which it rapidly dissociates to avoid futile cycling. These mechanistic findings will lead to a deeper understanding of superfamily-2 helicase function.

1402-Pos

E. Coli RecBC Helicase Actively Translocates on Both Strands during DNA Unwinding

Colin G. Wu, Timothy M. Lohman.
Washington University School of Medicine, Saint Louis, MO, USA.

E. coli RecBCD is a bipolar DNA helicase consisting of two superfamily-1 motor subunits: RecB (3' to 5' directionality) and RecD (5' to 3' directionality). Although these subunits have opposite translocation polarities, they function in unison and unwind duplex DNA in the same net direction by acting on opposite ends of the nucleic acid. We have investigated previously the mechanism of initiation of DNA unwinding by the single motor RecBC helicase, which lacks the RecD motor subunit. In order to understand the relationship between single stranded (ss) DNA translocation and DNA unwinding, we compared the ssDNA translocation mechanisms of the RecB monomer and the RecBC heterodimer using stopped-flow fluorescence approaches. The RecB monomer translocates 3' to 5' along the linear ssDNA lattice with a macroscopic rate of 803 $\pm$ 13 nt/sec. This is about two times faster than the rate determined previously for RecBC unwinding ($mk_{obs} = 348 \pm 5$ bp/sec). RecBC can also translocate on ssDNA in the 3' to 5' direction with a similar rate ($mk_t = 920 \pm 6$ nt/sec). Remarkably, we also find that RecBC is able to translocate along ssDNA with the opposite directionality (5' to 3'). These results suggest an allosteric communication between the RecB motor domain and another region of the RecBC enzyme that allows RecBC to actively translocate along both DNA strands during DNA unwinding, without the aid of the RecD subunit. (supported by NIH GM045948).

1403-Pos
Probing Protein Diffusion and Dissociation Mechanisms on DNA Using Fluorescence-Force Spectroscopy
Ruobo Zhou[1], Rahul Roy[1], Alexander G. Kozlov[2], Timothy M. Lohman[2], Taekjip Ha[1].
[1]University of Illinois at Urbana-Champaign, Urbana, IL, USA, [2]Washington University School of Medicine, St. Louis, MO, USA.
Single-stranded (ss)DNA binding (SSB) proteins tightly bind to ssDNA and protect it from degradation during DNA replication, recombination and repair. For subsequent DNA processing, SSB proteins need to be displaced from ssDNA and replaced by other proteins. The recently discovered activity that E. coli SSB can diffuse on ssDNA [1] may facilitate these processes, but little is known about the diffusion mechanism. Here we use single-molecule fluorescence-force spectroscopy [2] to study DNA-protein interactions and show that ssDNA can be progressively unraveled from the surface of a single E. coli SSB tetramer with increasing force between 1-6 pN, followed by SSB dissociation at about 9 pN. Our data also indicate that SSB diffuses on ssDNA primarily via a reptation rather than a rolling mechanism. These approaches provide unique insights into the mechanical regulation of DNA-SSB interactions and are generally applicable to many other protein-nucleic acid systems.
[1] R. Roy, Kozlov, A. G., Lohman, T. M. and T. Ha. SSB protein diffusion on single-stranded DNA stimulates RecA filament formation. Nature (2009, in press)
[2] S. Hohng, R. Zhou, M. K. Nahas, J. Yu, K. Schulten, D. M. J. Lilley and T. Ha. Fluorescence-force spectroscopy maps two-dimensional reaction landscape of the Holliday junction. Science 318, 279-283 (2007).

1404-Pos
Understanding DNA Condensation: From Simple Ions to Complex Proteins
Jason DeRouchey, Don C. Rau, Adrian Parsegian.
NIH, Bethesda, MD, USA.
We have used osmotic stress coupled with X-ray scattering to probe the thermodynamic forces between DNA helices in the presence of various cations. First, lysine, arginine, & alkylamines were investigated as a function of length. For all three systems, intermolecular forces are repulsive for mono- and divalent cations. Longer polyvalent cations mediate attractive forces and DNA spontaneously condenses into a hexagonal array. Repulsions were found to be unique for a given chemistry and independent of length, DNA-DNA attractions vary monotonically with length or charge. The magnitude of attractions increases with increasing polycation length, reaching a limiting value at 6-10 repeats. Interestingly, this limit seems to be known in naturally occurring peptides that interact with nucleic acids and utilize similarly sized repeat motifs such as the hexaarginine repeat commonly found in protamines used for DNA packaging in spermatids. To better understand the nature of complex proteins on DNA, the effect of uncharged amino acids were studied using model hexaarginine peptides. Amino acid chemistry, position and length are examined. Better understanding the cation mediated attractions and repulsions helps us to elucidate the interplay between ion entropy and the correlations that are common to nearly all theories for counter-ion induced attractions.

1405-Pos
DNA Interaction Kinetics of HIV-1 Nucleocapsid and Gag Proteins
Jialin Li[1], Christopher Jones[2], Siddhartha A. Datta[3], Alan Rein[3], Robert J. Gorelick[4], Ioulia Rouzina[5], Karin Musier-Forsyth[2], Mark C. Williams[1].
[1]Northeastern University, Boston, MA, USA, [2]The Ohio State University, Columbus, OH, USA, [3]HIV Drug Resistance Program, Frederick, MD, USA, [4]AIDS and Cancer Virus Program, Frederick, MD, USA, [5]University of Minnesota, Minneapolis, MN, USA.
The human immunodeficiency virus type 1 (HIV-1) Gag protein is essential for retroviral assembly. During viral maturation, Gag is processed to form matrix, capsid, and nucleocapsid (NC). NC is initially cleaved into the larger NCp15, then to NCp9, and finally to NCp7. NCp7 functions as a nucleic acid chaperone during retroviral replication, in which it rearranges nucleic acids to facilitate reverse transcription and recombination. The role of Gag and intermediate forms of NC in facilitating nucleic acid remodeling is not well understood, although it is likely that they also function as chaperones during viral assembly and early steps of reverse transcription. To investigate the capability of Gag and precursor forms of NC to act as nucleic acid chaperones, we use single DNA molecule stretching to probe how these proteins alter DNA aggregation, duplex destabilization, and DNA interaction kinetics. These characteristics are critical for efficient nucleic acid chaperone activity. Duplex annealing in the presence of NCp7 indicates that this protein dissociates rapidly from single-stranded DNA. In contrast, Gag inhibits DNA annealing, as indicated by strong hysteresis observed when stretching and relaxing DNA in the presence of Gag. We use a new method to measure the rate at which DNA that has been melted by force is able to reanneal in the presence of Gag and NC proteins. The results show that DNA annealing in the presence of Gag occurs on the time scale of minutes, compared to ~1 second for annealing in the presence of NCp7. Further studies of reannealing kinetics in the presence of NCp9, NCp15, and Gag deletion constructs will elucidate the role of specific protein domains in determining Gag- and NC-DNA interaction kinetics.

1406-Pos
Replacement of a Single Aromatic Residue in HIV-1 Nucleocapsid Protein Strongly Alters its Nucleic Acid Chaperone Activity
Hao Wu[1], Micah J. McCauley[1], Robert J. Gorelick[2], Ioulia Rouzina[3], Karin Musier-Forsyth[4], Mark C. Williams[1].
[1]Northeastern University, Boston, MA, USA, [2]AIDS and Cancer Virus Program, SAIC-Frederick, Inc, Frederick, MD, USA, [3]University of Minnesota, Minneapolis, MN, USA, [4]Ohio State University, Columbus, OH, USA.
The human immunodeficiency virus type 1 (HIV-1) nucleocapsid (NC) protein plays an essential role in several stages of HIV-1 replication. One important function of HIV-1 NC is to act as a nucleic acid chaperone, in which the protein facilitates nucleic acid rearrangements important for reverse transcription and recombination. NC contains only 55 amino acids, with 15 basic residues and two zinc fingers, each having a single aromatic residue (F16 and W37). Despite its simple structure, HIV-1 NC appears to have optimal chaperone activity, including the ability to strongly aggregate nucleic acids, destabilize nucleic acid secondary structure, and facilitate rapid protein-nucleic acid interaction kinetics. Here we use single molecule DNA stretching experiments to measure the characteristics of wild type and mutant HIV-1 NC that are important for nucleic acid chaperone activity. This work allows us to directly relate HIV-1 NC structure with its function as a nucleic acid chaperone. By stretching single DNA molecules in the presence of these proteins, we measure the ability of the proteins to destabilize dsDNA, and when the protein is relaxed we determine the capability of the protein to facilitate nucleic acid annealing. We show that the single amino acid substitution W37A significantly slows down NC's DNA interaction kinetics, while retaining NC's helix-destabilization capabilities. In contrast, the substitution F16W results in a protein that strongly resembles wild type NC. Thus, elimination of a single aromatic residue strongly reduces NC's chaperone activity. The results of these studies are consistent with in vivo HIV-1 replication measurements, which show that the aromatic W37 residue is required for efficient retroviral replication.

1407-Pos
Correlation Between DNA Binding Thermodynamics and Functional Behavior of Pol I DNA Polymerases
Hiromi S. Brown, Vince J. LiCata.
Louisiana State University, Baton Rouge, LA, USA.
Primer-template DNA (pt-DNA) binding by DNA polymerases is the first step of the polymerization cycle. We have previously characterized the thermodynamics of pt-DNA binding with respect to temperature for the ''large fragments'' of DNA polymerase I, Klentaq and Klenow, from *Thermus aquaticus* and *Escherichia coli*, respectively. Results with both polymerases showed that DNA binding is enthalpy-driven near their respective physiological temperatures. Here, nucleotide incorporation activity was measured with respect to temperature to examine how the thermodynamics of initial pt-DNA binding relates to the enzymatic activities of Klentaq and Klenow. For both polymerases it is observed that a negative enthalpy of initial binding (ΔH) is required for nucleotide incorporation activity, and that a negative entropy of binding ($T\Delta S$) inhibits the catalytic activity. Nucleotide incorporation activity was also examined with respect to KCl concentration. As reported previously, thermodynamic linkage plots for pt-DNA binding with respect to KCl concentration ($\partial \ln 1/Kd$ versus$\partial \ln[\mathrm{KCl}]$) exhibit negative slopes for both polymerases and indicate net ion releases of ~3 and ~5 ions upon pt-DNA binding by Klentaq and Klenow, respectively. Interestingly, linkage plots for the steady-state rate of incorporation activity with respect to KCl concentration ($\partial \ln 1/ssRate$-versus$\partial \ln[\mathrm{KCl}]$) exhibit the same slopes as the linkage plots of pt-DNA binding. This result suggests that salt dependence of initial pt-DNA binding dictates the salt dependence of the overall incorporation activity. It is striking that for both salt and temperature dependences, the detailed thermodynamics of DNA binding so directly correlate with overall functional behavior.
This work is supported by National Science Foundation.

1408-Pos
Dna Binding and Translocation by S. Cerevisiae RSC
Allen Eastlund, Shuja Malik, Christopher Fischer.
University of Kansas, Lawrence, KS, USA.
We have studied the mechanisms of double-stranded DNA binding and double-stranded DNA translocation by a truncated construct of the RSC chromatin

remodeling complex from S. cerevisiae. We monitored the double-stranded DNA translocation activity of RSC through its ability to actively displace streptavidin from biotin labeled double-stranded DNA. This displacement activity is ATP-dependent and is correlated with the translocation of the complex along the double-stranded DNA. We have also characterized the double-stranded DNA translocation of RSC through the use of a fluorescence-based stopped-flow assay in which the translocation of the complex is monitored through the interactions of the complex with fluorophores attached to the ends of the DNA. The kinetics of double-stranded DNA binding were also monitored using a fluorescence-based stopped-flow assay. The results indicate that double-stranded DNA binding occurs through a two-step mechanism, similar to what has been reported for other chromatin remodeling complexes and genetically related helicases.

1409-Pos
***E.coli* SSB Under Tension**
Rustem G. Khafizov[1], Alexander G. Kozlov[2], Timothy M. Lohman[2], Yann R. Chemla[1].
[1]University of Illinois, Urbana, IL, USA, [2]Washington University School of Medicine, St Louis, MO, USA.
E. coli SSBs (single-stranded DNA binding proteins) are essential accessory proteins in replication, recombination and during DNA repair. They not only protect ssDNA from chemical and nucleolytic attack, but also associate with many genome maintenance proteins. *E. coli* SSBs are tetrameric and have at least two binding modes: SSB_{35} and SSB_{65}, which bind 35 and 65 nucleotides, respectively. Proteins in the SSB_{35} mode bind cooperatively, interacting with each other and creating long nucleoprotein filaments. In this study, we present mechanical studies of SSB bound to ssDNA using dual trap, high-resolution optical tweezers. This assay allows us to probe the interaction of SSBs to ssDNA constructs of various lengths, in real time, with nanometer resolution. By directly detecting wrapping of ssDNA by a single protein, we are able to characterize the thermodynamics and kinetics of nucleoprotein complex formation. Mechanical pulling of our constructs in the presence of SSBs reveals that the protein condenses ssDNA in the force range 0-8pN and that tension can be used to modulate the binding mode of SSBs. Binding kinetics further indicate that SSBs bind to ssDNA in two successive processes consisting of a loose binding step in which the protein associates weakly with its substrate, followed by a wrapping step in which ssDNA is condensed.

1410-Pos
Analysis of Nucleic Acid Conformations and Amino Acid Propensities in Single-Stranded Binding Proteins
Phillip Steindel, Douglas Theobald.
Brandeis University, Waltham, MA, USA.
Single stranded DNA- or RNA-protein complexes appear in a number of biological pathways, particularly those relating to DNA replication, gene regulation, and chromosome stability. Protein-nucleic acid binding in these complexes has been studied for some time, and a number of structures of these complexes exist; however, few consistent rules for binding have been determined. In particular, DNA and RNA conformation appears to vary widely, even when bound to homologous proteins (e.g., telomere end-binding proteins). No systematic study of nucleic acid conformational has been done, so it is unknown how different these conformations actually are from each other or from double-stranded DNA and RNA. In addition, no comparison of amino acid propensity for single stranded versus double stranded nucleic acids has been done. To those ends, we have built a non-redundant database of single stranded binding proteins. We have calculated various base step conformational and find wide statistical distributions for these parameters, but with some significant differences from double stranded nucleic acids.

1411-Pos
Binding and Bending Parameters of Integration Host Factor to Four-Way Holliday Junction
Olga Buzovetsky.
Wesleyan University, Middletown, CT, USA.
Binding and Bending Parameters of Integration Host Factor to Four-Way Holliday Junction
Integration host factor (IHF) is a small heterodimeric protein that sequence specifically binds the minor groove of DNA and facilitates a bend of nearly 180 degrees. This bending is crucial for cellular processes such as recombination, replication and transcription. Previous work in the Mukerji lab characterized the binding properties of the structurally similar but sequence non-specific DNA-binding protein HU, to duplex and Holliday junction DNA. This research demonstrated that HU binds to the central region of the junction with nanomolar affinity and prefers the stacked form of the Holliday junction. Given the similarities in structure and function of HU and IHF, we elected to study the binding capability of IHF to the Holliday junction. We have compared the binding affinity of IHF for Holliday junction DNA with its binding affinity to duplex DNA with and without a consensus sequence. Binding measurements were performed using florescence intensity and anisotropy methods and confirmed with the gel mobility shift assay. All binding assays established that IHF binds to the Holliday junction lacking a consensus sequence with high affinity (~3 nanomolar Kd) similar to HU, suggesting that both proteins might recognize and bind similar structural aspects of the Holliday junction. Moreover, anisotropy affinity measurements demonstrated that IHF binds the Holliday junction with similar affinity as it does to duplex DNA containing its consensus sequence. The span of binding capabilities exhibited by IHF indicate that it can function both as a specific and non-sequence specific DNA binding protein.

1412-Pos
Inhibition of Eukaryotic RNase P
Michael C. Marvin, Scott C. Walker, David R. Engelke.
University of Michigan, Ann Arbor, MI, USA.
Ribonuclease P (RNase P) is an essential RNA enzyme found in all phylogenetic domains that is best known for catalyzing the 5' endonucleolytic cleavage of precursor transfer RNAs (pre-tRNAs). In bacteria, the enzyme consists of a single, catalytic RNA subunit and one small protein, while the archaeal and eukaryotic enzymes have 4-10 proteins in addition to a similar RNA subunit. The RNA has been shown to act as a ribozyme at high salt *in vitro*; however the added protein optimizes kinetics and makes specific contacts with the pre-tRNA substrate. The bacterial protein subunit also appears to be required for the processing of non-tRNA substrates by broadening substrate recognition tolerance. In addition, the immense increase in protein content in the eukaryotic enzyme suggests substantially enlarged capacity for recognition of additional substrates. Recently, intron-encoded box C/D snoRNAs and HRA1 RNA were shown to be likely substrates for yeast RNase P. In addition, yeast RNase P seems to be inhibited by single stranded RNA. This inhibition was shown to be specific to *S.cerevisiae* RNase P but not bacterial RNase P with poly-ribonucleic acid homopolymers having varying levels of inhibition (polyG>polyU>>poly A>>>polyC). This inhibition is also size dependent with larger RNA being inhibitory. In addition, the sequence specificity seen with the small homoribopolymers is lost, as larger RNA of various sequences show relatively high levels of inhibition. To further characterize the extent of RNase P inhibition by these various inhibitors, the location of the inhibitor contact is being mapped by crosslinking. Individually 6xHis tagged strains are being used to enable isolation of crosslinks induced by UV light. The characterization of the eukaryotic specific inhibitor interaction with yeast RNase P will provide further information about the evolution of the essential activity of tRNA processing.

1413-Pos
Finding the Right 'Mis'Match: Millisecond Conformational Dynamics of MutS-DNA Complex During DNA Damage Recognition
Velmurugu Yogambigai, Ranjani Narayanan, Serguei V. Kuznetsov, Manju Hingorani, Anjum Ansari.
UIC, Chicago, IL, USA.
Errors in replication and recombination cause base-pair mismatches and insertion-deletion loops (IDLs) in DNA, which, if unchecked, lead to mutations implicated in cancer and heart disease. Thus, repair pathways that detect such errors and initiate their repair are vital to preserving DNA integrity. This study focuses on prokaryotic *T. aquaticus* (*Taq*) MutS and its eukaryotic homolog *S. cerevisiae* $MutS_\alpha$, both proteins that recognize mispairs and IDLs in DNA and recruit downstream proteins to rectify the damage. Structural studies have shown that MutS-bound DNA is bent at the mispair/IDL site. However, the underlying mechanism of recognition of these target sites is not well understood. In particular, the role of DNA flexibility at the target site in the recognition mechanism remains unclear. We employ nanosecond laser temperature jump (T-jump) to perturb the MutS-DNA complex, and monitor the conformational relaxation dynamics on microsecond-to-milliseconds time-scales relevant to the formation of the initial recognition complex that triggers DNA repair. We have carried out equilibrium and kinetic measurements on DNA labeled with 2-aminopurine (2AP) adjoining a T-bulge, in complex with *Taq* MutS and$MutS_\alpha$. Equilibrium fluorescence measurements as a function of increasing temperature reveal a sharp increase in 2AP fluorescence at ~40°C for $MutS_\alpha$, and at ~70°C for *Taq* MutS, indicating a significant conformational change in the MutS-DNA complex near their optimal physiological temperatures. Relaxation kinetics monitored with 2AP fluorescence in response to a rapid T-jump show relaxation kinetics in *Taq* MutS near 70°C, occurring with a time constant of a ~10 milliseconds. This rapid phase has not been observed in previous dynamics studies, and we propose that it may correspond to the transition from a non-specific MutS-DNA complex to a specific complex that signals initiation of repair.

Membrane Physical Chemistry II

1414-Pos
Spatially-Resolved Fluorescence Spectra of Patterned Lipid Bilayers
Teiwei Luo, **Alfred Kwok**.
Pomona College, Claremont, CA, USA.
Planar supported lipid bilayers can be micropatterned such that the lipid composition of localized regions differ from that of the surrounding region. These micropatterned bilayers can serve as model systems to study the dynamics of microdomains in lipid bilayers. We have obtained spatially-resolved fluorescence spectra of bilayers patterned with alternating rows of 1% Rhodamine-DMPE/POPC and lipid voids with epifluorescence and TIRF (total internal reflection fluorescence) excitation. A 60X water immersion objective is used to image a 100-micron slice of the bilayer onto the entrance slit of an imaging spectrograph. A CCD camera at the exit port of the spectrograph records the fluorescence spectra from the bilayer. In conventional fluorescence spectroscopy, the signal from all the pixels of each column of the CCD camera, which corresponds to signal from a specific wavelength, is integrated to produce a single spectrum. In our experiment, such integration is not performed. Since the fluorescence spectra from the alternating rows of Rhodamine-DMPE/POPC and voids are imaged onto different rows of the CCD camera, their spectra can be spatially resolved.

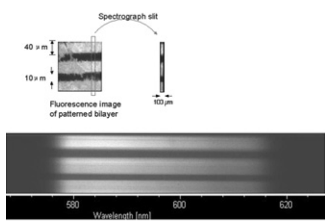

Spatially resolved fluorescence spectrum

1415-Pos
Tethered Lipid Bilayers that Mimic the Composition of Neuronal Membranes
Matteo Broccio[1], Rima Budvytyte[2], Gintaras Valincius[2], Mathias Loesche[1].
[1]Physics Dept, Carnegie Mellon University, Pittsburgh, PA, USA,
[2]Institute of Biochemistry, Vilnius, Lithuania.
For the study of biomolecular interactions with membranes, biomimetic lipid membrane models are a trade-off between robustness and amenability to various characterization techniques on the one hand and limitations in the compositional variety characteristic of biological membranes on the other. We have developed tethered bilayer lipid membranes (tBLMs) as a long-term stable and versatile experimental model in which thiolated lipopolymers span a hydrated layer that separates the membrane from its solid support[1]. Such tBLMs may be prepared either by ''rapid solvent exchange''[2], which leads to highly insulating bilayer but provides limited control over membane composition, or by vesicle fusion, which provides better control over membrane composition but leads to membranes with lower resistance. Here we report on tBLMs that mimic mammalian neuronal membrane lipid compositions by containing various phospholipids, cholesterol, sphingomyelin and cerebrosides. Electrochemical parameters of these neuronal membrane mimics as a function of composition were studied with electrochemical impedance spectroscopy. In tBLMs prepared by rapid solvent exchange, membrane capacitance has a sigmoidal dependence on cholesterol content. These results are compared with those from tBLMs prepared by the fusion of vesicles, whose cholesterol content can be determined with routine biochemical assays. This work aims at establishing complex membrane mimics for studies of Aβ oligomer interactions with bilayers to assess their influence on the lipid component of neuronal membranes in Alzheimer's disease.
Supported by the NIH (1P01AG032131) and the AHAF (A2008-307).
[1]Valincius, G., et al., 2008. Biophys. J. 95:4845-4861.
[2]Cornell, B.A, et al., 1997. Nature 387:580-583.

1416-Pos
Fabrication of a Membrane Interferometer Containing Electrodes
Laura D. Hughes, Prasad V. Ganesan, Steven G. Boxer.
Stanford University, Stanford, CA, USA.
Despite the advantages of supported lipid membranes, one remaining problem has been the incorporation of membrane proteins, as membrane proteins tend to lose their functionality near a surface. To address this limitation but retain the advantages of a nearby surface, we have developed a system where a lipid bilayer is separated a few hundred nanometers from an atomically flat mirror (Ganesan and Boxer, PNAS, 2009, vol. 106, p. 5627). This mirror allows the use of Fluorescence Interference Contrast Microscopy (FLIC) and Variable Incidence Angle-FLIC (VIA-FLIC), two surface characterization techniques that precisely locate the height of fluorescent objects relative to the silicon surface with nanometer resolution. Both FLIC and VIA-FLIC have been used to measure changes in curvature of the bilayer in response to osmotic perturbations of the solution above the bilayer. Current work focuses on changing the architecture of the substrate to allow access to the volume both above and below the bilayer. These changes to the substrate will enable concurrent electrical and optical measurements of voltage-gated membrane proteins, as well as increased control over osmotic balance. Progress towards this goal will be described.

1417-Pos
Conformational Flexibility in Membrane Binding Proteins: Synaptotagmin I C2A
Jacob W. Gauer[1], Jesse Murphy[1], Kristofer Knutson[1], R. Bryan Sutton[2], Greg Gillispie[3], Anne Hinderliter[1].
[1]University of Minnesota Duluth, Duluth, MN, USA, [2]Texas Tech University Health Sciences Center, Lubbock, TX, USA, [3]Fluorescence Innovations, Bozeman, MT, USA.
Thermodynamic parameters capture the averaged contribution to a system's energetics. In the case of binding proteins, such as Synaptotagmin I, the first step toward addressing how and where the energy is distributed within that protein is to ascertain the magnitude of the interactions within that protein. Our aim is to understand how binding information is conveyed throughout this protein during the role it plays in regulated exocytosis. While many detailed molecular approaches have identified putative regions where interactions occur, it is their energetics that dictates their response. Here, denaturation studies of the C2A domain of Synaptotagmin I were carried out in conditions that are physiologically relevant to regulated exocytosis where calcium ions and phospholipids were either present or absent. Denaturation data was collected using two techniques: differential scanning calorimetry (DSC) and lifetime fluorescence. A global analysis approach combining these data sets was used where the data was simultaneously fit to models derived from thermodynamic principles. The enthalpy associated with the denaturation of the C2A domain of Synaptotagmin I in the absence of all ligands was found to be quite low when compared to other proteins of the similar molecular weight. This suggests some conformational flexibility in the interactions which hold the protein together. In addition, the denaturation behavior is shown to be different upon binding ligand, suggesting that conformational flexibility is impacted by ligand binding. This material is based in part upon work supported by the National Science Foundation under CAREER - MCB 0747339.

1418-Pos
Protrusive Growth and Periodic Contractile Motion in Surface-Adhered Vesicles Induced by Ca^{2+}-Gradients
Tatsiana Lobovkina[1], **Irep Gözen**[1], Yavuz Erkan[1], Jessica Olofsson[1], Stephen G. Weber[2], Owe Orwar[1].
[1]Chalmers University of Technology, Göteborg, Sweden, [2]University of Pittsburgh, Pittsburgh, PA, USA.
Local signaling, cell polarization, and protrusive growth are key steps in directed migration of biological cells guided by chemical gradients. Here we present a minimal system which captures several key features of cellular migration from signaling-to-motion. The model system consists of flat, negatively charged phospholipid vesicles, a negatively charged surface, and a local, and controllable point-source supply of calcium ions. In the presence of a Ca^{2+} gradient, the surface-adhered vesicles form protrusions in the direction of the gradient. We also observe membrane shape oscillations between expanded (flattened), and spherical states as a function of the Ca^{2+}-concentration. The observed phenomena can be of importance in explaining motile action in prebiotic, primitive, and biomimetic systems, as well as in development of novel soft-matter nano- and microscale mechanical devices.

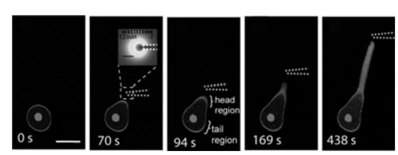

1419-Pos
Deposition of Model Biomimetic Membranes on a Soft Support
Agnieszka Gorska[1,2], Malgorzata Hermanowska[2], Aleksander Balter[1], Beate Klösgen[2].
[1]Institute of Physics, Nicolaus Copernicus University, Torun, Poland,
[2]Institute of Physics and Chemistry, University of Southern Denmark, Odense, Denmark.
The lipid bilayer is the first site of all cellular interactions with the extracellular environment. The interactions between the membrane and its local surroundings are influenced by the presence of charges, within the membrane itself and as well in the near environment. The investigation of a biomimetic system requires an environment which will not modify the basic properties of the membrane to be probed. In this study a polyelectrolyte multilayer (PEM) consisting of alternating layers of chitosan and heparin (CHIT/HEP) as a soft and highly

hydrated supporting cushion for membrane deposition was chosen for investigation. Polyelectrolyte multilayered films were prepared using layer-by-layer physi-sorption with either terminating positively (CHIT) or negatively (HEP) charged PE layers. Thereafter the vesicle fusion technique was applied to deposit model membranes onto the support. In this study giant unilamellar vesicles (GUV) and small unilamellar vesicles (SUV) composed of a mixture of zwitterionic POPC and its cationic derivative E-POPC were used, the latter providing a positive surface charge density in the lipid bilayer. The topology and integrity of the lipid layer on its PEM-support were investigated by a combination of confocal fluorescence microscopy and atomic force microscopy.

1420-Pos

Mechanics of POPC Bilayers in Presence of Alkali Salts

Hélène Bouvrais[1,2], Olav S. Garvik[1], Tanja Pott[2], Philippe Méléard[2], John H. Ipsen[1].
[1]MEMPHYS - Center for Biomembrane Physics, Odense, Denmark,
[2]UMR-CNRS 6226, ENSCR, Rennes, France.

Membranes mechanical properties are affected by solvent properties, i.e. the salt content. In this study, we use POPC GUVs (Giant Unilamellar Vesicles) as model membranes and we measure the membrane mechanical moduli by flickering analysis and micropipette technique for a series of alkali salt solutions. Salt concentration effects and ion specificity are investigated in these measurements. Membrane mechanical moduli are shown to display a complex dependence on the salt solution composition.

1421-Pos

Reproduction of Fatty Acid Vesicles

Nicole Pfleger[1], Albert J. Markvoort[2], Rutger Staffhorst[1], Rutger A. van Santen[2], Ben de Kruijff[1], Antoinette J.A. Killian[1].
[1]Utrecht University, Utrecht, Netherlands, [2]TU Eindhoven, Eindhoven, Netherlands.

Compartmentalization is an essential step for the origin of life to allow for the formation of more complex biotic building blocks. Possibly in early life preliminary compartments were formed out of prebiotic molecules, such as fatty acids. These molecules organize in bilayers at neutral pH and they show intriguing behavior with respect to self-reproduction of vesicles [1], in that fast addition of fatty acid at high pH to preexisting seed vesicles at neutral pH results in a fast formation of new vesicles with a size distribution that is closely related to that of the seed vesicles. The mechanism behind this so-called matrix effect is still a puzzle. One possibility would be that the fatty acids insert in the outer monolayer of the vesicle and that an excess of material in the outer leaflet with respect to the inner leaflet is then the driving force for budding and subsequent fission. In order to test this possible mechanism, we varied the rate of addition (insertion) of the new material. Slow addition would give the system time for movement of fatty acids from the outer leaflet to the inner leaflet and thus to remove this imbalance. Our results show that such a decrease of the addition rate indeed leads to growth of the vesicles instead of division, supporting our hypothesis. We also found, by including a fluorescent dye which is self-quenching at high concentrations, that during the fission process the content of the vesicles does not leak to the exterior. These observations agree well with results and predictions from coarse-grained molecular dynamics [2] and provide a plausible mechanism for the matrix effect [1].

[1] Luisi et al. J. Phys. Chem. B 2008, 112, 14655-14664 [2] Markvoort et al., in preparation

1422-Pos

Effect of Solubilization on Rhodopsin Thermal Denaturation in Rod Outer Segment Disk Membranes

Scott Corley, Arlene Albert.
University of Connecticut, Storrs, CT, USA.

The photoreceptor, rhodopsin is a GPCR in rod outer segment disk membranes. Activation by light converts the dark-adapted form, rhodopsin to the bleached form, opsin. Differential scanning calorimetry (DSC) studies showed that rhodopsin and opsin each exhibit an irreversible scan rate dependent endothermic transition (Tm) at approximately 72°C and 55°C respectively as well as a scan rate dependent exothermic transition. Solubilization was used to examine the contribution of the bilayer. Disk membranes were subjected to sub-solubilizing and solubilizing concentrations of octylglucoside (OG) until rhodopsin was completely delipidated. DSC experiments were performed using a MicroCal VP-DSC microcalorimeter. Samples were scanned at 15, 30, 60 and 90°/hr. Because the protein transitions are irreversible, a second scan was used to determine the baseline. As the OG partitioned into the bilayer the endothermic Tm and EACT (activation energy of denaturation) rapidly decreased. Both then remained constant following rhodopsin solubilization. At low detergent concentration the exothermic Tm increased rapidly then remained constant after solubilization. Unlike the endothermic EACT, the degree of solubilization had little effect on the exothermic transition EACT. Digitonin was also used to examine the effect of solubilization. Unlike OG, this detergent binds to cholesterol which is constitutes approximately 10% of the disk lipids (average). The endothermic transition was less affected by digitonin than by OG. The EACT was also determined by thermal bleaching and was in agreement with the DSC data. These results indicate an endothermic transition is observed due to a weakening of the tertiary structure interactions as rhodopsin is heated. This may be accompanied by changes in the packing of the trans-membrane helices as well as changes in protein-lipid interactions. It is likely the exothermic transition results from aggregation.

1423-Pos

A Coarse Grained Molecular Dynamics Study of Self-Reproduction of Fatty Acid Vesicles

Albert J. Markvoort[1], **Bram van Hoof**[1], Nicole A. Pfleger[1,2], Rutger A. van Santen[1], Peter A.J. Hilbers[1].
[1]Technische Universiteit Eindhoven, Eindhoven, Netherlands,
[2]Universiteit Utrecht, Utrecht, Netherlands.

The formation of self-reproducing fatty acid vesicles is believed to be a quintessential building block required for (the origin of) life. In literature a number of vesicle reproduction experiments have been reported [1]. Of particular interest is the so called matrix effect where the final size distribution of vesicles formed upon addition of new surfactants is strongly biased toward the size distribution of pre-existing vesicles. However, the mechanism behind this is poorly understood. Here, we regard this mechanism using coarse grained molecular dynamics simulations with a parameter set based on a previously published force field [2]. These simulations show fission of a vesicle on continuous addition of new fatty acid molecules to the vesicle exterior. The new molecules are incorporated in the outer leaflet of the vesicle's membrane. As the rate of fatty acid redistribution among the leaflets by means of flip-flop is lower than the rate of fatty acid uptake in the outer leaflet, an excess of molecules in the outer leaflet compared to the inner leaflet is formed. This results in spontaneous membrane curvature, causing the vesicle to deform into twin-vesicles. Eventually, the built-up spontaneous curvature induces the formation of a narrow neck, that finally breaks, resulting in full fission. Importantly, no leakage from the interior of the vesicles was observed. The reproduction pathway shown in these simulations agrees with published experimental data, as well as with new data from our group (see abstract Nicole Pfleger). Our coarse grained molecular dynamics simulations offer further insight at the molecular level of the self-reproduction pathway of fatty acid vesicles.

[1] Luisi et al. (2008) J. Phys. Chem. B 112, 14655-14664.
[2] Markvoort et al. (2005) J. Phys. Chem. B 109, 22649-22654.

1424-Pos

On the Miscibility of Cardiolipin with the Major Lipid Components of the Bacterial Inner Membrane

Maria Frias[1], Matthew G.K. Benesch[2], Ruthven N.A.H. Lewis[2], **Ronald N. McElhaney**[2].
[1]University of Buenos Aires, Buenos Aires, Argentina, [2]University of Alberta, Edmonton, AB, Canada.

The thermotropic phase behavior and organization of model membranes derived from binary mixtures of tetramyristoylcardiolipin (TMCL) with dimyristoyl phosphatidylethanolamine (DMPE) and dimyristoyl phosphatidylglycerol (DMPG) were studied by differential scanning calorimetry (DSC) and fourier transform infrared (FTIR) spectroscopy. Cardiolipin-containing DMPE and DMPG model membranes all exhibit complex multi-component hydrocarbon chain-melting (L_β/L_α) phase transitions upon heating and cooling. This suggests that TMCL is poorly miscible with both DMPE and DMPG and that the domains formed prior to the onset of the L_β/L_α phase transitions are probably retained in the liquid-crystalline state. For all mixtures, the temperatures of the L_β/L_α phase transitions are generally higher than those predicted by an ideal mixing of the components, and the enthalpies of these phase transitions seem to be better correlated with the component mol fraction of hydrocarbon chains than with the molar composition of the mixture *per se*. Finally, when cooled to low temperatures, cardiolipin-rich (i.e., > 30 mol % TMCL) membranes tend to form lamellar-crystalline phases which exhibit spectroscopic characteristics comparable to those exhibited by the lamellar crystalline phases of pure cardiolipin. Together, our experimental observations indicate that cardiolipin is poorly miscible with major lipid components of one of the biological membrane systems (Escherichia coli) in which it occurs naturally. The possibility that it may also be poorly miscible in the biologically relevant liquid-crystalline phase also has interesting structural and functional implications.

Supported by the Canadian Institutes for Health Research, the Alberta Heritage Foundation for Medical Research and by the Consejo Nacional de Investigaciones Científicas y Técnicas (Argentina).

1425-Pos

Measurement of the Duration and Critical Exponent of Concentration Fluctuations in Lipid Bilayers Near the Critical Point

Aurelia R. Honerkamp-Smith, Sarah L. Keller.
University of Washington, Seattle, WA, USA.

Membranes containing a wide variety of ternary mixtures of high chain-melting temperature lipids, low chain-melting temperature lipids, and cholesterol undergo lateral phase separation into coexisting liquid phases at a miscibility transition. Large composition fluctuations appear in lipid membranes prepared near miscibility critical points. We have measured the effective dynamic critical exponent relating the decay time τ_0 of membrane composition fluctuations to the wavenumber k through= $\tau \sim k^{-z_{eff}}(\xi)$, where the correlation length ξ characterizes the size of the largest fluctuations. We find that z_{eff} increases from roughly 2 at $\xi \rightarrow 0$ to $z_{eff} = 2.31 \pm 0.03$ at $\xi = 16\mu m$. Changes in lipid composition are known to affect membrane protein activity. We find that submicron membrane fluctuations corresponding to a wavenumber of $(50nm)^{-1}$ persist for at least 0.8 ± 0.3 ms, on the order of times required for changes in protein configuration (e.g. 1ms). Therefore, similar and longer-lived fluctuations in cell membranes can potentially alter protein function.'' To our knowledge, we present the first measurement of in a 2-dimensional system of conserved order parameter, whether with or without conserved momentum.

1426-Pos

Interaction of a Novel Iron Chelator with Model Membranes

Andreia Leite[1], Paula Gameiro[1], Baltazar de Castro[1], Maria Rangel[2].
[1]Requimte, Faculdade de Ciências, Universidade do Porto, Porto, Portugal,
[2]Requimte, Instituto de Ciências Biomédicas Abel Salazar, Universidade do Porto, Porto, Portugal.

A novel fluorescent hexadentate iron chelator developed in our laboratory has been shown to inhibit the growth of *Mycobacterium avium* inside macrophages. Apart from its high affinity to iron, the compound seems to possess a key molecular structure to cross biological membranes, thus reaching the targets to deprive bacteria from iron.

To get insight on the partition and location of this new compound, fluorescence spectroscopic studies are being performed in large unilamellar liposomes.

To be able to separate liposome surface effects from lipophilicity, we measured the fluorescence anisotropy of two fluidity probes (DPH and TMA-DPH) in DMPC and DMPG liposomes prepared with the iron chelator. The results indicate that the primary interaction is near the lipid headgroup, with a partial molecular immersion in the outer leaflet, favouring negatively charged lipids. Our results suggest the importance of the first membrane penetration through the outer headgroups in the effectiveness of bacteriostatic agents with intracellular activity.

Acknowledgements Partial financial support for this work was provided by ''Fundação para a Ciência e Tecnologia'' (FCT, Lisboa) through Project (PTDC/QUI/67915/2006); A.L thanks FCT for a PhD grant (SFRH/BD/30083/2006).

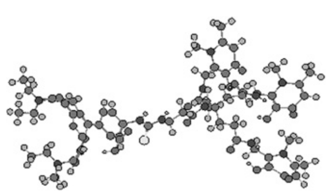

1427-Pos

Unraveling the Mechanism of Membrane Binding by Annexin 5

Kristofer J. Knutson, Jacob Gauer, Jesse Murphy, Anne Hinderliter.
University of Minnesota-Duluth, Duluth, MN, USA.

Protein-membrane interactions are a vital mechanism of propagating signals both across the membrane and between cells. To control the magnitude and specificity of this type of cell signaling at the membrane, clustering of similar lipids and proteins has been observed in the cell via the formation of lipid microdomains. To address the thermodynamic basis of this type of signal propagation, we investigated how lipid microdomains form in response to annexin a5 binding to model membranes using Isothermal Titration Calorimetry (ITC). Annexins are known to bind to negatively charged (e.g., phosphatidylserine [PS]) membranes in a Ca2+ dependent manner that lead to the formation of PS-enriched microdomains. Based on Differential Scanning Calorimetry (DSC) results, we suggest that that annexin functions to order lipid acyl chains upon binding and that the ordering of phospholipids can lead to the formation of these microdomains. Using ITC, we have analyzed the membrane binding affinity of annexin for both gel and fluid state mixtures. Binding analysis of these isotherms show that annexin binds fluid state mixtures with a significantly lower Kd than gel state lipids, which would be consistent with the hypothesis that the ordered nature of gel state lipids reduces the binding affinity of annexin for that lipid. In addition, because the binding is entropically dominated but exhibits greater affinity for fluid compared to gel state lipids, we suggest that annexin binding is driven by the release of water molecules as fluid lipids have more water of hydration. Interestingly, the enthalpy associated with the binding process for both gel and fluid state lipid mixtures is weak, which is indicative of a similar binding mechanism for the mixtures, albeit that binding of lipid is exothermic for fluid state and endothermic for gel state.

1428-Pos

Drug Release from Liposomes can be Modulated by the Extent of Cholesterol Superlattice in the Lipid Membrane

Berenice Venegas, **Parkson L.-G. Chong**.
Temple University School of Medicine, Philadelphia, PA, USA.

Liposomes have been used as drug carriers for targeted delivery. Much attention has been paid to the stealth properties of the liposome in order to avoid the immune system and have a prolonged circulation time. An aspect in the liposome design as a drug delivery system that has been relegated is the passive drug leakage from liposomes. In this work we investigated how lateral distribution of lipids in membranes can affect the overall leakage of an entrapped drug. For this study we used the antivascular drug Combretastatin A4 disodium-phosphate (CA4P) that has entered clinical trials for the treatment of a variety of cancers and is naturally fluorescent. CA4P was encapsulated in liposomes composed of 1-palmitoyl-2-oleoyl-sn-glycero-3-phosphocholine (POPC)/cholesterol at a quenching concentration (30 mM). Cholesterol content was varied in steps of 0.4 mol% in a range of concentrations covering the theoretically predicted critical mole fractions (Cr, e.g., 20.0, 22.2, 25.0, 33.3, 40.0 and 50.0 mol%) for maximal sterol superlattice formation. The non-encapsulated CA4P was removed by size exclusion column chromatography. The leakage was followed in real time by exciting CA4P at 328nm and reading fluorescence at 400nm. The results obtained show that at Cr the leakage of CA4P is faster than at non-critical mole fractions. Although cholesterol superlattice domains have tighter lipid packing, the defects that are produced in the interfaces between regular and irregular domains enhance the overall membrane permeability. Therefore the extent of cholesterol superlattice can be used to modulate the release of encapsulated drugs. Ongoing work is aimed to observe how this modulation will affect CA4P treatment using endothelial and mammary cancer cell lines. (supported by DOD breast cancer program)

1429-Pos

Measuring Passive Transport Using Confocal Microscopy of Giant Lipid Vesicles

Su Li, Noah Malmstadt.
University of Southern California, Los Angeles, CA, USA.

The ability of a molecule to pass through the plasma membrane without the aid of any active cellular mechanisms is central to that molecule's pharmaceutical characteristics. Existing techniques for measuring this passive transport capacity are hampered by the presence of an unstirred layer (USL) which dominates transport considerations across the bilayer. We are developing assays based on confocal microscopy of giant unilamellar vesicles (GUVs) that allow for the detailed investigation of passive transport processes and mechanisms. At the size of GUVs (generally less than 100 μm), the effect of the USL on membrane transport processes is minimized, giving more accurate values of membrane permeability.

We have constructed several series of drug-like fluorescent molecules by covalently modifying the dye 4-nitrobenzo-2-oxa-1, 3-diazole (NBD). A series of molecules of increasing hydrophilicity was constructed from polyethylene glycol (PEG) having 4, 8, and 12 repeating units. Alkane chains with 3, 5, and 7 carbons were used as the hydrophobic representatives. Transport of both series of modified NBD molecules was observed by tracking NBD fluorescence as the molecules passed through the GUV membrane. Weak acyclic acid with 2, 4, and 6 carbons were also examined, using a pH-sensitive dye to track their transport.

An analytical theoretic passive transport model was devised, original data was regressed to the model, and permeability was calculated for each dataset. Finite element modeling (FEM) was used to simulate the experiments. The simulation supported the experimental results well.

1430-Pos

Buffer Properties Revealed with Model Lipid Membranes

Megan M. Koerner, Matthew J. Justice, Bruce D. Ray, Horia I. Petrache.
Indiana University Purdue University Indianapolis, Indianapolis, IN, USA.

Numerous kinds of buffers including MOPS, MES and HEPES are used to control the pH of biological samples. We have investigated how these particular buffers alter the charge state of lipid membranes. As measured by x-ray scattering, polar but neutral lipids such as phoshatidylcholine (PC) form multilamellar vesicles (MLVs) in buffer solutions. Previous work has shown that the highly uniform equilibrium spacing between lipid membranes is easily influenced by the presence of weakly binding charges such as bromide ions in monovalent salt solutions [1]. In general, the MLVs shrink or expand (swell)

depending on how the balance of attractive and repulsive force is shifted by the nature of the aqueous solution. We performed small angle x-ray scattering measurements to reveal how the buffers modify lipid interactions. Buffers loosely associate with the lipid membrane and alter their surface charge causing the MLVs to swell. Interestingly, as opposed to monovalent salts which charge up the PC membranes negatively, MOPS charges PC membranes positively. We have used small angle x-ray scattering to measure the modification of membrane forces and we have measured the diffusion of lipid aggregates in electric fields to determine the charging effect of the buffers on PC membranes. By measuring how buffers modify the electrical state of lipid membranes we can better understand how buffers behave at the interface of biological membranes.

[1] H. I. Petrache, T. Zemb, L. Belloni, and V. A. Parsegian. *Proc. Natl. Acad. Sci.*, 2006, 103:7982-7987.

1431-Pos

Molecules Pushing Molecules: Dynamic Consequences of Crowding

Philip A. Gurnev[1], Rudolf Podgornik[2], Joel A. Cohen[3], Sergey M. Bezrukov[1], V. Adrian Parsegian[4].
[1]National Institute of Child Health and Human Development, Bethesda, MD, USA, [2]Department of Physics, Faculty of Mathematics and Physics, University of Ljubljana, and Theoretical Physics Department, J. Stefan Institute, Ljubljana, Slovenia, [3]Department of Physiology, A. A. Dugoni School of Dentistry, University of the Pacific, San Francisco, CA, USA, [4]Department of Physics, University of Massachusetts, Amherst, MA, USA.

Membrane pores, such as alpha-hemolysin, sieve molecules to provide passage. Large polymers are excluded while monomers and small polymers can pass. At high concentrations, flexible polymers lose their size that exists under dilute conditions. Rather, flexible polymers look more like strings with regions of limited coherence. This transition is clear from the shift in osmotic pressure vs. polymer concentration: van't Hoff regime in the dilute limit but des Cloizeaux regime at higher concentrations. Under crowded conditions, a polymer previously unable to enter the alpha-hemolysin pore suddenly enters when the apparent limiting size is in the region of limited coherence. Mixtures of small and large polyethylene glycols show exclusion in this range where the larger species exert stress that drives the smaller polymers into and across pores at concentrations far larger than those in the bathing solution. This coupling of polymer activities and consequent conferred mobility creates a new form of crowding-driven transport.

1432-Pos

Effect pf PAH Concentration on Sops Liposomes

Ricardo L. Esparza[1], María Leticia Valenzuela Sánchez[1], Araceli Arteaga Jiménez[2], César Márquez Beltrán[3], Amir Maldonado Arce[1].
[1]Universidad de Sonora, Hermosillo, Mexico, [2]Universidad Autónoma de Puebla, Puebla, Mexico, [3]Universidad de Sonora URN, Caborca, Mexico.

We have prepared SOPS liposomes using the hydration technique. Optical microscopy experiments show that the size and shape of the liposomes do not change when they are swell with a glucose/sucrose solution. To the SOPS liposome system we add the polyelectrolyte PAH (Poly-Allylamine Hydrochloride), producing a drastic change in the liposome structure. We have studied the influence of PAH on the liposome shape and size distribution by means of Differential interference contrast microscopy (DIC). The results show that PAH interacts with the SOPS liposomes forming PAH-SOPS complexes.

1433-Pos

Localized Photothermal Heating of Temperature Sensitive Liposomes

Natalie A. Forbes, Joseph A. Zasadzinski.
University of California, Santa Barbara, Santa Barbara, CA, USA.

A drug delivery system consisting of a temperature sensitive liposome coupled to hollow gold nanoshells allows precise spatial and temporal control of drug release. A small fraction of lysolipid in a primarily dipalmitoylphosphatidylcholine (DPPC) liposome lowers the membrane transition temperature to that obtainable by mild hyperthermia, while simultaneously enhancing the membrane permeability at the transition temperature. Hollow gold nanoshells coupled to the liposomes heat the membrane when irradiated by a continuous wave near-infrared laser. The heat generated by the nanoshells can be tuned to control local membrane temperature, and hence the membrane permeability and rate of drug release. This system could be used to deliver anticancer drugs directly to a tumor site. Additionally, the ability to correlate drug release with membrane temperature allows us to empirically determine the local heat generated by the hollow gold nanoshells upon laser irradiation.

1434-Pos

Phase Diagram of a 3-Component Lipid Mixture Containing a Polyunsaturated Phosphatidylcholine

Tatyana Konyakhina, Gerald W. Feigenson.
Cornell University, Ithaca, NY, USA.

Polyunsaturated acyl chains have special influences on the mixing and phase behaviors of lipid mixtures. Their high degree of unsaturation affects the physical properties of biomembranes in ways that are still not fully understood, and their high concentration in some membranes makes them key players in membrane structure. We are investigating the 3-component phase diagram for the biologically relevant mixture of brain-SM/ 18:0-22:6 PC/ cholesterol. Fluorescence microscopy imaging of giant unilamellar vesicles (GUVs) was employed for phase boundary visualization and phase identification of the 3-component mixture. Fluorescent lipid probes having complementary partitioning behavior are used in FRET measurements to enable more quantitative analysis. Of particular interest is the region of Lo + Lα phase coexistence, which shows macroscopic phase separation.

1435-Pos

Investing Early Signaling Events in IgE-FcεRI Activation Using SEM

Ethan N. Chiang, Sarah L. Veatch, David Holowka, Christopher Ober, Barbara A. Baird.
Cornell University, Ithaca, NY, USA.

Antigen-mediated cross-linking of immunoglobulin E (IgE) bound to its high affinity receptor FcεRI on mast cells initiates a transmembrane signaling cascade that results in cell activation and exocytotic release of chemical mediators involved in allergic response. Plasma membrane lipids and proteins redistribute as part of this transmembrane signaling process. To understand the functional role of these redistributions, resolution of their size, composition and structure on the nanometer scale is required. We utilize high resolution scanning electron microscopy (SEM) to directly visualize sub-micron membrane domains in intact cell membranes. In our experiments, the distribution of gold-labeled proteins and lipids is analyzed at the surface of intact fixed cells using backscattered electron detection. In parallel, we also observe membrane topography using secondary electron detection. We use a pair-correlation function analysis to quantify protein distributions and parameterized domain size. We have mapped the distribution of a variety of proteins, both related and non-related to the IgE signaling pathway. Using this experimental and quantitative method, we observe dramatic changes in the nano-scale membrane distribution of IgE due to stimulation with multivalent ligands. In resting cells, IgE receptors are clustered into small domains less than 30nm. After stimulation, receptors redistribute into large domains that are correlated at long length-scales and subsequently reduce in size at long stimulation times. We also observe cross-linking-dependent rearrangement of several inner leaflet-associated proteins implicated in early signaling events. In contrast, outer leaflet GPI-anchored proteins are not affected. We have also quantified the co-redistribution of IgE with other membrane proteins after stimulation using cross-correlation functions. These findings provide valuable insights into the mechanisms that drive the selective nanoscopic reorganization of plasma membrane proteins during immune cell signaling.

1436-Pos

Fluorescence Measurements in Fruit Fly (Drosophila Melanogaster)

Lin Shin Teo.
National University of Singapore, Singapore, Singapore.

Drosophila melanogaster is a widely used animal model in developmental biology. In *Drosophila*, the wealth of genetic tools allows expression of any given marker or construct in specific cells or tissues within the organism. This is especially advantageous since particular cells can be studied in their natural 3D organization, avoiding possible artefacts and deviations from the physiologically relevant situation that may be introduced in cell cultures. For the study of molecular dynamics within cells and cell membranes on a single molecule level, we performed fluorescence correlation spectroscopy (FCS) within the *Drosophila* embryonic nervous system. Using a GAL4 driver expressed in a small subset of neurons, we expressed fluorescently tagged fusion membrane proteins, CD8 and flotillins-2, in two identified motor neurons per hemisegment of the embryonic central nervous system (CNS). We obtained autocorrelation curves for membrane and cytoplasmic probes which show diffusion times that correspond to their respective subcellular locations. By additionally expressing (non-tagged) proteins which influence lipid metabolism, example ceramidase, we are able to follow changes in the molecular dynamics of membrane proteins. With this approach, we are studying the biophysical properties of the cellular membrane *in vivo* and *in situ* and will extend this in the future to different genetic backgrounds. The study shows that *in vivo* analyses provide us greater insights into the role of membrane dynamics in the context of development, differentiation and pathogenesis of diverse diseases.

1437-Pos

The Influences of Electric Fields on Lipid Membranes

Andreas Blicher, Thomas Rainer Heimburg.
Niels Bohr Institute, Copenhagen, Denmark.

When phospholipid membranes are exposed to electric fields a variety of phenomena can be observed, such as phase separation, domain movement, electroporation, -deformation, -fusion, and -striction to name but a few. Understanding such responses is of both fundamental interest as well as of practical application.
Various thermodynamic susceptibilities of lipid membranes increase strongly in the melting transition, leading to large changes in, for instance, membrane conductivity, compressibility, bending elasticity, relaxation time, and geometry. Another such property (susceptibility) of the membrane is its electrical capacitance. In the phase transition both area and thickness change significantly, but also the dielectric coefficient can increase due changes in membrane composition. This coupling of the membrane's capacitance to its phase state implies that transient currents will appear if the membrane is pushed into the phase transition by changes in e.g. pH, membrane potential, pressure or temperature. On this poster we will show some of these phenomena, and discuss them in the context of the recently proposed soliton model of nerve signal propagation by Heimburg and Jackson, where the coupling between the electrical aspects and the phase state of the system is of central importance.

1438-Pos
Fret Reveals Coexisting Nanoscopic Fluid Phases in POPC/DSPC/Cholesterol
Frederick A. Heberle, Gerald W. Feigenson.
Cornell University, Ithaca, NY, USA.
Ternary lipid bilayer systems containing dioleoylphosphatidylcholine (DOPC) or diphytanoylphosphatidylcholine (DiPhyPC) as the low melting temperature lipid yield remarkably consistent phase diagrams when probed by methods with a wide range of spatial and temporal sensitivity. The resulting phase diagrams invariably show a large region of fluid/fluid phase coexistence at biologically relevant compositions, and have generated considerable interest as a potential explanation for lipid raft phenomena observed in plasma membrane. However, the unusual lipids DOPC and DiPhyPC are rare in mammalian plasma membranes. In contrast, phase diagrams with the biologically abundant palmitoyloleoylphosphatidylcholine (POPC) as the low melting lipid have mixed interpretations: studies using methods like fluorescence anisotropy and quantum yield (which have nanometer spatial resolution) report fluid/fluid coexistence that microscopy studies fail to detect. An explanation of these results in terms of first-order phase coexistence with nanometer-sized phase domains has proven controversial in the absence of a known mechanism for limiting lipid domain size. We show that the compositional dependence of FRET in the ternary systems DOPC/DSPC/chol and POPC/DSPC/chol is remarkably similar, and can be interpreted as arising from probe partitioning between phase domains. In addition, we present a quantitative model for the dependence of FRET efficiency on domain size and demonstrate its applicability to these systems.

1439-Pos
Quantitative IR Spectroscopy Studies of Changes in Lipid Dynamics and Organization in Isolated Stratum Corneum Exposed to Basic pH
Peter Saad[1], Daniel Moore[2], David J. Moore[2], Evan Flach[1], **Carol R. Flach[1]**, Richard Mendelsohn[1].
[1]Rutgers University, Newark, NJ, USA, [2]International Specialty Products, Inc., Wayne, NJ, USA.
The outer layers of the epidermis, the stratum corneum (SC), provide the barrier function that is essential to life, primarily through the extracellular lamellar lipid matrix. Previous IR spectroscopy studies of isolated SC have shown the presence of ordered lipid bilayers, packed in orthorhombic and hexagonal domains. This lipid organization is essential to the barrier function of SC. In the current work we have investigated the effect of basic pH on lipid organization in SC. The outer surface of skin is routinely subjected to pH 10 solutions when exposed to soaps during cleansing. This exposure to basic pH has been shown to result in reduced barrier function and can lead to clinical irritation of the skin. Using IR spectroscopy methods previously developed in our laboratories to study isolated SC, we have examined the effect of pH 10 exposure on lipid organization in SC, monitoring both the intra- and inter-molecular lipid organization. The results of these studies show the T_m of SC lipids is significantly increased after pH 10 exposure. Furthermore, the change in bilayer T_m is not reversible. To explore changes in lipid packing underlying the pH-induced change in T_m, we are developing quantitative approaches evaluating changes in the amount of orthorhombic and hexagonal chain packing in normal and challenged SC. The results of these quantitative approaches to chain packing are being correlated to the changes in conformational order and increasing T_m after SC is exposed to pH 10. We will present our IR spectroscopic data showing irreversible increases in lipid T_m and the accompanying quantitative analysis of lipid packing changes.

1440-Pos
Phase Diagram of a 3-Component Lipid Mixture of PS/PE/CHOL to Model the Inner Leaflet of a Plasma Membrane
Nelson F. Morales-Penningston, Shih Lin Goh, Gerald W. Feigenson.
Cornell University, Ithaca, NY, USA.
The two leaflets of an animal cell plasma membrane are compositionally asymmetric: the outer leaflet has a relatively high concentration of phosphatidylcholine (PC) and sphingomyelin (SM), and the inner leaflet has most of this membrane's phosphatidylethanolamine (PE) and almost all of its phosphatidylserine (PS). The overall cholesterol mole fraction is high, with its distribution between the two leaflets uncertain. Whereas model membrane studies using lipids mimicking the outer leaflet composition have revealed complex mixing behavior including solid/liquid and liquid/liquid phase separations, the mixing behavior of the inner leaflet is still poorly understood. We have constructed a phase diagram for a model mixture of the inner leaflet using a high melting temperature PS, a low melting temperature PE, and cholesterol. Dipalmitoyl PS (DPPS) and palmitoyloleoyl PE (POPE) are in the solid (L_β) and liquid disordered (L_α) phases, respectively, at the experimental temperature of 30°C. A combination of fluorescence microscopy and fluorescence resonance energy transfer (FRET) between fluorescent lipid probes was used to map all regions of the phase diagram. An L_β/L_α coexistence region was observed up to at least 15% cholesterol.

1441-Pos
Lipid Monolayer Line Tension Measurements and Model Convolution
Andrew H. Nguyen[1], Erkan Tuzel[2], Benjamin L. Stottrup[1].
[1]Augsburg College, Minneapolis, MN, USA, [2]Worcester Polytechnic Institute, Worcester, MA, USA.
Research into the phase separation of coexisting liquid phases in mixed phospholipid/sterol monolayer systems is an important experimental approach to understand the lateral inhomogeneities or ''lipid rafts'' within lipid membranes. We present measurements of line tensions between immiscible phases in mixed monolayer systems of phospholipids and the cholesterol analog 25-hydroxycholesterol. This hydroxycholesterol is an interesting modulation of the cholesterol structure for both its implicated pathological effect on the plasma cell membrane as well as its unique phase diagram. In addition to these experimental studies we will also discuss ongoing work to improve our line tension measuring tools. Model-convolution microscopy is a technique that can be used to assess the effectiveness of image processing routines by testing them against experimenter determined parameters. Here a theoretical model is used to generate the underlying structure of an image and this is convolved with the point spread function of light. We will also present results obtained using this technique to study the importance and necessity of the incompressibility constraint in the Fourier analysis of lipid domains.

1442-Pos
The Complex and Unexpected Ionization Behavior of Phosphoinositides
Edgar E. Kooijman, Katrice E. King, Mahinda Gangoda, Arne Gericke.
Kent State University, Kent, OH, USA.
The phosphorylated forms of phosphatidylinositol, among all minor membrane lipid species, are arguably the most important in the regulation of intracellular signaling processes. Specificity is achieved by the selective phosphorylation of the inositol headgroup, which can carry a total of three phosphomonoester groups. Many proteins have developed special binding domains that facilitate specific binding to particular phosphoinositide species, while other proteins interact with phosphoinositides via nonspecific electrostatic interactions. Here we describe the ionization properties of all three naturally occurring bisphosphates as well as phosphatidylinositol 3,4,5-trisphosphate in model lipid membranes composed of phosphatidylcholine. We find substantial differences in ionization behavior between the three bisphosphates, and the ionization behavior of the trisphosphate is extraordinarily complex, indicating the crucial role of phosphate substitution pattern. The results are explained by intramolecular hydrogen bonds in the headgroups of the individual phosphatidylinositol polyphosphates. Surprisingly however, we also find evidence for intermolecular hydrogen bond interactions, suggesting that e.g. $PI(4,5)P_2$ can cluster in model membranes. Additionally, we investigated the effect of other major membrane lipid species on the ionization properties of $PI(4,5)P_2$, specifically cholesterol and phosphatidylethanolamine. Preliminary results are discussed in terms of possible intermolecular interactions.

1443-Pos
Effect of Polymer on the Elastic Properties of Membranes
Ramon Iniguez, Heriberto Acuna, **Amir Maldonado**.
Universidad de Sonora, Hermosillo, Mexico.
Macromolecules interacting with membranes can modify physical properties of the latter such as the bending rigidity or their local topology. The addition of a

water-soluble polymer, PEG, to the lamellar phase of DMPC or of several surfactants, induces a topological transformation to a vesicular phase. Such transition can be understood in terms of a modification of the elastic properties of the membranes. In this work we perform a dynamic light scattering (DLS) study of the effect of PEG on phospholipid and surfactant bilayers. The experimental results show that the addition of the polymer slows down the dynamics of the membranes. From fits to an available theory for the scattering of dilute membrane systems, we have calculated the bending elastic modulus of the bilayers. This modulus increases with increasing polymer concentration, thus confirming that the macromolecule modifies the elastic properties of the membranes.

Membrane Active Peptides II

1444-Pos
Effects of a Membrane-Active Amphibian Antimicrobial Peptide on the Bacterial Proteome

Ludovica Marcellini[1], Marina Borro[1], Giovanna Gentile[1], Lorenzo Stella[2], Donatella Barra[1], **Maria Luisa Mangoni[1]**.
[1]University of La Sapienza, Rome, Italy, [2]University of Tor Vergata, Rome, Italy.

Ribosomally synthesized antimicrobial peptides (AMPs) are conserved components of the innate immunity of all life forms and represent the most ancient and efficient weapon against microbial pathogens.
The emergence of multidrug-resistant microbes has urgently required the discovery of new antibiotics with a new mode of action, and AMPs represent promising candidates. Intense research focusing on AMPs is currently directed to the elucidation of their mode(s) of action.
Nevertheless, very little is known about their effects on intact bacteria.
Here we report on Esculentin 1-18 [Esc(1-18)], a linear peptide covering the first 18 N-terminal residues of the full length amphibian peptide esculentin-1b. Esc(1-18) retains the antimicrobial activity of esculentin-1b against a wide range of microorganims, with negligible effects on mammalian erythrocytes. To expand our knowledge on the molecular mechanism underlying the antimicrobial activity on Gram-negative bacteria, we investigated the effects of this peptide on *Escherichia coli*, by studying its: i) structure in membrane mimicking environment; ii) killing kinetic; iii) bactericidal activity in different media; iv) ability to permeate both artificial and bacterial membranes; v) capacity to synergize with conventional antibiotics; vi) effect on cell morphology and proteome by means of electron microscopy and proteomic techniques, respectively.
These studies have indicated that Esc(1-18) (i) kills *E. coli* via membrane-perturbation; (ii) elicits identical changes in the bacterium's protein expression pattern, at both lethal and sub-lethal concentrations; and (iii) preserves antibacterial activity under conditions closer to those encountered *in vivo*. This is in contrast with many host defence peptides that kill microorganisms by altering intracellular processes and lose activity in physiological solutions. Importantly, to the best of our knowledge, this is the first case showing the effects of an amphibian AMP on the protein expression profile of its bacterial target.

1445-Pos
A New Look at an Old Friend: Novel Insights Into Pore Formation by Alamethicin

Aram J. Krauson, William C. Wimley.
Tulane University, New Orleans, LA, USA.

Alamethicin is a 20-amino acid long antibiotic peptide produced by the fungus *Trichoderma viride.* In the literature, alamethicin is the most commonly cited example of a barrel-stave model pore-forming peptide. In this model, amphipathic peptides form a long-lived transmembrane pore by aligning hydrophobic and hydrophilic residues with the lipid bilayer and aqueous pore respectively. It has been reported that voltage-independence of alamethicin pores relies on salt and peptide concentrations. We have developed a set of fluorescence-based assays for leakage, stable pore formation and lipid flip-flop using large unilamellar vesicles (LUVs) to help define the mechanism and potency of pore forming peptides. An additional pre-incubation assay differentiates dynamic pores from long-lived pores. When applied to alamethicin, our suite of assays show that, at 2.0 μM peptide, alamethicin forms voltage-independent pores in anionic or zwitterionic vesicles at peptide-to-lipid ratios as low as 1:2000. Less than 20 peptides per vesicle is sufficient to allow for complete vesicle permeabilization. Even after overnight incubation with vesicles, alamethicin promotes continuous lipid flip-flop, and is able to permeabilize multiple additions of new vesicles. Other pore forming peptides tested at this P:L ratio do not promote continuous flip-flop and do not exchange into new vesicles. We postulate that, unlike other pore-forming peptides, which mostly behave like classical barrel-stave pores, alamethicin is in a continuous dynamic equilibrium between transmembrane, interfacially bound and aqueous forms.

1446-Pos
Effect of L- to D-Peptide Isomerisation on the Activity of Antimicrobial Peptide Anoplin

Amy Won, Mourin Khan, Sorin Gustin, Akuvi Akpawu, Stahs Pripotnev, Anatoli Ianoul.
Carleton University, Ottawa, ON, Canada.

Isolated from the venom sac of solitary spider wasp, Anoplius samariensis, Anoplin is the smallest linear α-helical antimicrobial peptide found naturally up to date. It has broad spectrum activity against both Gram-positive and Gram-negative bacteria, and little hemolytic activity toward human erythrocytes (1,2). Previous studies showed that substitution of all amino acids in the peptide with D-isomers can increase the bioavailability and reduce peptide degradation without affecting the antimicrobial properties since the net charge and the hydrophobicity are retained (3). In the present work, two stereoisomers of Anoplin were studied using UV resonance Raman spectroscopy, Langmuir Blodgett, atomic force microscopy, calcein leakage assay and antimicrobial assay. UV resonance Raman data indicate that the two forms of the peptide adopt similar conformations in aqueous buffer and in membrane mimicking solutions. Monolayer isotherms show that D-Anoplin has a lightly greater area per molecule than L-Anoplin. Finally, membrane rupturing ability of both stereoisomers was found to depend strongly on membrane composition.

(1) Konno, K., Hisada, M., Fontana, R., Lorenzi, C.C.B., Naoki, H., Itagaki, Y., Miwa, A., Kawai, N., Nakata, Y., Yasuhara, T., Neto, J.R., de Azevedo Jr., W.F., Palma, M.S. and Nakajima, T. (2001) Biochim. Biophys. Acta 1550: 70-80.
(2) Ifrah, D., Doisy, X., Ryge, R.S. and Hansen, P.R. (2005) J. Pept. Sci. 11: 113-121.
(3) Wade, D., Boman, A., Wahlin, B., Drain, C.M., Andreu, D., Boman, H.G. and Merrifield, R.B. (1990) Proc. Nat. Acad. Sci. 87: 4761-4765.

1447-Pos
Biophysical Studies of Cecropin-Mellitin Antimicrobial Peptides with Improved Selectivity

Heather Kaminski, **Jimmy B. Feix**.
Medical Coll of Wisconsin, Milwaukee, WI, USA.

Antimicrobial peptides (AMPs) have received much attention as models for the development of antibiotics capable of meeting the challenge of drug-resistant infections. Our research has focused on a linear, 15-residue cecropin-mellitin (CM) hybrid peptide designated CM15. In these studies we compare the biological activities and membrane interactions of CM15 and lysine substituted derivates designed to have optimized amphipathicity upon membrane binding. Previous studies have shown that these lysine enriched peptides maintain the high antimicrobial activity of the parent peptide but have substantially decreased hemolytic effects (Sato and Feix, Antimicrob. Agents Chemother. 52, 4463, 2008). Using model membranes to understand the differences that govern peptide-membrane interaction, we have performed a series of biophysical experiments including circular dichroism (CD), fluorescence, and site-directed spin labeling (SDSL) electron paramagnetic resonance (EPR) spectroscopy. These experiments establish the structures of the membrane-bound peptides, determine the extent of membrane lysis, and allow determination of partition coefficients and depth of penetration. Our results show that differences in red cell hemolysis can be reconstructed using model membranes, and provide insights into the mechanism of membrane disruption. This work was supported by award number R01GM068829 from the National Institute Of General Medical Sciences.

1448-Pos
Structural Modifications to Convert Melittin from a Cytolytic Peptide to a Stable Cargo Linker

Hua Pan, Olena Ivashyna, Joshua L. Hood, Eric Christenson, Gregory M. Lanza, Paul H. Schlesinger, Samuel A. Wickline.
Washington Univ. School of Medicine, St Louis, MO, USA.

Melittin is a 26 amino acid peptide that comprises more than half of the dry weight of the venom of the honeybee Apis Mellifera. In previous studies, we demonstrated that melittin stably bound to the lipid membrane of perfluorocarbon (PFC) nanoparticles and served as an active anti-cancer therapeutic agent *in vivo (Soman et al. J Clin Invest. 2009)*. Here, we report the structure modification that converts the mellittin to a cargo linker for **post-formulation** liposome customization. We introduced point mutations and truncations to define the lytic and membrane binding activities of melittin. For each of the mutations, lytic activity of the peptides was tested by the carboxyfluorescein fluorescence dequenching assay on carboxyfluorescein encapsulated liposomes. Among all six melittin mutations, the mutation, D1-7, with the first 7 amino acids removed (VLTTGLPALISWIKRKRQQ) dramatically reduces the melittin lytic activity. Using immobilized Giant Unilamellar Vesicles (GUV), we illustrated that at peptide:lipid ratio of 40:1, D1-7 bound to the GUV without pore forming, while at peptide:lipid ratio of 1:83, melittin already formed pores on the GUV

membrane. These results suggest that D1-7 eliminates the lytic activity but retains the strong lipid membrane binding. For further confirmation, we measured liposome sizes and zeta potentials with and without D1-7 loading. Consistently, D1-7 did not affect the size of the liposome, but shifted the zeta potential (or surface charge) of the liposome towards the positive voltage range, because D1-7 is a positively charged peptide. Among numerous existing nanosystems for drug delivery, liposomes are approved by FDA for anti-cancer and gene therapy. Accordingly, this linker and/or its refinements could enhance the therapeutic potential of approved liposomal drugs by enabling flexible incorporation and cargo multiplexing through post-formulation surface editing.

1449-Pos
Cationic, Helical Antimicrobial Peptoids with Biomimetic Antimicrobial Activity
Rinki Kapoor.
Stanford University, Stanford, CA, USA.
Increasingly prevalent resistance of pathogenic bacteria to conventional small-molecule antibiotic drugs is creating an urgent need for the discovery of new classes of antibiotics that are active against biofilms. Bacteria that are multidrug resistant (MDR) are of increasing concern for infectious disease. Current treatment of these infections that involve resistant organisms may require 6-12 months of antibiotic treatment, creating difficulties with compliance.
We are continuing to develop oligo-N-substituted glycine (peptoid) mimics of cationic, helical antimicrobial peptides (AMPs), and some of our recently acquired data indicate that peptoids could address the problem of growing resistance. Peptoids have been shown to have extremely broad-spectrum activity, and certain peptoids function well in the presence of serum proteins. Their biophysical mechanism of action makes it difficult for bacteria to evolve resistance to them. We have tested our most promising peptoids, peptides and commercial antibiotics in vitro against bacterial biofilms of a variety of important bacterial organisms. We show that certain peptoids can be as active as the preferred conventional antibiotics against bacterial infections, even at low micromolar doses. Small, structured biomimetic oligomers such as our antimicrobial peptoids may offer a new class of drugs that are useful in treating persistent bacterial infections.

1450-Pos
Investigation of a Sequence-Modified Antimicrobial Peptide
Luba Arotsky, Michael Urban, Gregory A. Caputo.
Rowan University, Glassboro, NJ, USA.
Antimicrobial peptides serve as one of the first lines of defense in the immune systems of higher organisms. These peptides specifically target and neutralize infecting bacteria in the host organism while exhibiting little or no toxic effect on host cells. The peptide C18G is a highly cationic, amphiphilic peptide derived from the C-terminal sequence of the human protein platelet factor 4 (involved in blood coagulation and wound repair) exhibited antibacterial activity against both gram positive and gram negative bacteria. Using a modified C18G sequence that did not significantly affect antimicrobial efficacy (Tyr3 changed to Trp and all Lys changed to Arg (C18G Y3W K R)). The binding affinity was measured with fluorescence spectroscopy using the W in the peptide sequence as a probe of peptide environment. Small unilamellar lipid vesicles were used to investigate the binding affinity of the peptide to bilayers composed of variable amounts of DOPC, POPG, and POPE. DOPC and POPE have a zwitterionic head group, whereas POPG has an anionic charged head group. These studies showed binding affinity had a dramatic dependence on lipid composition. The effect of pH on peptide binding and behavior was also examined and, as expected, also impacted binding affinity. Quenching of the Trp fluorescence by acrylamide was performed to confirm that the Trp was located in the membrane. Likewise circular dichroism (CD) spectroscopy was used to determine the structure of the peptide upon interaction with the lipid vesicles. Additionally, in an assay monitoring membrane permeabilization of *E. coli* the C18G Y3W K R peptide was shown to permealize bacterial membranes in a concentration dependent manner.

1451-Pos
Structural Aspects of the Interaction of Nk-2 Derived Peptides with Cancer Cells
Yasemin Manavbasi[1], Yana Gofman[2], Nir Ben-Tal[2], Regine Willumeit[3], Dagmar Zweytick[1], Karl Lohner[1].
[1]Austrian Academy of Sciences, Graz, Austria, [2]Department of Biochemistry, Tel Aviv University, Tel Aviv, Israel, [3]GKSS - Research Center, Geesthacht, Germany.
Antimicrobial peptides have gained interest as potential anti-cancer agents, e.g. inhibition of tumour growth in human prostate xenografts was shown by host defense like lytic peptides (1). We showed by Annexin V binding that, in prostate tumour cells, negatively charged phosphatidylserine (PS) accumulates in the outer plasma membrane leaflet, which normally resides in the inner leaflet. Thus, surface exposure of PS may make these cells susceptible to killing by these cationic peptides.
The aim of this study is to develop short peptide sequences derived from NK-2, which was shown to have anti-tumour activity (2). NKCS (Cys of NK-2 exchanged by Ser) is composed of two α-helices connected with a hinge region. Initially we studied the interaction of the parent peptide and its N- and C-terminal part with membrane mimetic systems. Vesicle leakage experiments revealed that the N-terminal fragment exhibits similar affinity towards PS as NKCS. Thermodynamic experiments indicate that the N-terminal helix resembles the properties of NKCS. Furthermore, calorimetric studies revealed that NKCS and its fragments have no significant effect on the thermotropic behaviour of PC liposomes mimicking healthy mammalian cell membranes. Both circular dichroism and Monte-Carlo simulation using the bilayer parameters derived from our structural characterization of the lipid model systems showed that the selectivity for PS correlated with the alpha-helical content of the peptides. The C-terminal part was less structured showing lower affinity to PS containing membranes. Thus, the shorter N-terminal peptide can be used as a template for further optimization, as in vitro tests on a human prostate carcinoma cell line showed significant cell damage.
(1) Papo N. et al., Cancer Res. 66 (2006) 5371-8.
(2) Schröder-Borm H. et al., FEBS Lett. 579 (2005) 6128-61.
Acknowledgement: EC - Marie-Curie Action: BIOCONTROL (MCRTN - 33439)

1452-Pos
Antimicrobial Peptide Mimics as Potential Anticancer Agents:Interactions of Acyl-Lysine Oligomer C12K-7Alpha8 with Ganglioside/DPPC Mixtures
Anastasia Antipova[1], Andrey Ivankin[1], Inna Radzishevsky[2], Amram Mor[2], **David Gidalevitz**[1].
[1]Illinois Institute of Technology, Chicago, IL, USA, [2]Technion-Israel Institute of Technology, Haifa, Israel.
Recently, antimicrobial peptides (AMPs) have emerged as a promising anticancer remedy. Negative charge of the bacterial membranes gives some measure for selectivity of cationic AMPs, since mammalian cell membranes are largely zwitterionic. Accumulating evidence indicates that lipid composition of the cancer cell membranes is different from a healthy cell, displaying net membrane surface negative charge. Understanding the nature of the negatively charged membrane domains could provide a new basis for anticancer therapy drug design using antimicrobial peptides or their synthetic mimics. Here, we examine the effect of membrane glycosylation, which is shown to be increased in cancer cells, on activity of AMP analogs. In this work we probe interactions of antimicrobial peptide mimic, based on acyl-lysine architecture (OAK), C_{12} K-7α_8, with Langmuir monolayers containing monosialoganglioside GM_3 and disialoganglioside GD_3. Langmuir isotherms and fluorescence microscopy imaging results of pure GM_3 and GD_3 monolayers indicate a single liquid-extended (LE) phase. Constant pressure insertion assays show significant insertion of C_{12} K-7α_8 in both GM_3 and GD_3 monolayers at 30mN/m. AMP analogue insertion was also observed for GM_3: DPPC (30:70) and GD_3: DPPC (30:70) mixed monolayers, however at smaller extent as expected. Synchrotron grazing Incidence X-Ray diffraction (GIXD) data show a disordered phase for GD_3 and a weak ordering for GM_3, which disappears immediately after introduction of the AMP. X-ray Reflectivity data indicate the thinning of the lipid layer upon peptide insertion.

1453-Pos
Cancer Cell Proliferation is Inhibited by Phlip Mediated Delivery of Membrane Impermeable Toxin Phalloidin
Ming An[1], Dayanjali Wijesinghe[2], Oleg A. Andreev[2], Yana K. Reshetnyak[2], Donald M. Engelman[1].
[1]Yale University, New Haven, CT, USA, [2]University of Rhode Island, Kingston, RI, USA.
We wish to use the pH-(Low)-Insertion-Peptide (pHLIP) to transport therapeutic agents to acidic tumors, with the ultimate goal of improving the treatment of cancer. pHLIP inserts into a lipid bilayer under slightly acidic conditions (pH 6-6.5), forming a transmembrane helix. We demonstrate here that pHLIP-mediated translocation of a cell-impermeable, polar toxin phalloidin can inhibit the proliferation of cancer cells. The delivery constructs, pHLIP-K(rho)C(aph) and pHLIP-C(aph), both carry the phalloidin toxin at the inserting C-terminus, via a disulfide linkage that could be cleaved in cells. The constructs differ in that a lipophilic rhodamine moiety is also attached to the inserting end, near the phalloidin cargo, in pHLIP-K(rho)C(aph). After a brief incubation with 2-4 μM of pHLIP-K(rho)C(aph) at pH 6.1-6.2 (for 1-3 h), proliferation of HeLa, JC, and M4A4 cancer cells were severely disrupted ($>$ 90% inhibitions). Cells

treated with pHLIP-K(rho)C(aph) also showed signs of cytoskeletal immobilization, consistent with the knowledge that phalloidin binds to F-actin and stabilizes the filament against depolymerization. However, the antiproliferative effect was not observed with pHLIP-C(aph). The insertion behavior of both constructs were studied in POPC liposomes using Trp fluorescence: pHLIP-K(rho)C(aph) and pHLIP-C(aph) insert with the same apparent pK of 6.1-6.2, similar to that of pHLIP (without any cargo). However, kinetic experiments suggest that pHLIP-C(aph) inserts much slower than pHLIP-K(rho)C(aph), possibly accounting for its lack of antiproliferative effects in cell assays. In short, our results obtained with pHLIP-K(rho)C(aph) lay the foundation for the development of a new class of anti-tumor agents that would selectively enter and destroy cancer cells while not affecting normal cells. Such pHLIP-mediated delivery of otherwise cell-impermeable agents may enhance the efficacy of treatment, as well as significantly reducing the side effect.

1454-Pos
Membrane Superficial Charge Modification Affects Miotochondrial Permeabilization by Derivatives of the Polycationic Peptide Btm-P1
Victor V. Lemeshko.
Universidad Nacional de Colombia, Medellin, Colombia.
Polycationic peptides demonstrate antimicrobial and anticancer properties. Earlier we designed, on the basis of the protoxin Cry11Bb, a 26-aa polycationic peptide BTM-P1, which demonstrated ionophoric and antimicrobial activities. It could be modified in the future to enhance anticancer action. In this work we found that the reverse peptide, BTM-RP1, has one order of magnitude lower capacity than BTM-P1 to permeabilize rat liver mitochondria. The activity of BTM-RP1 was increased by its modifications with tryptophane attached to its N-terminal (BTM-WRP1) or C-terminal (BTM-RP1W). The similar modifications of BTM-P1 peptide did not increase, or even decreased (BTM-P1W) the peptide activity. All these peptides, designed by us, were synthesized by Gen Script Company (USA) (>90% purity). When 10 μM cationic fluorescent probe safranin O, but not endogenous NAD(P)H fluorescence, was used as indicator of mitochondrial energization, the inner membrane potential markedly recovered after a decrease caused by each of 3 serial additions of 1 μM BTM-RP1. We also found that safranin O significantly decreased the rate of mitochondrial swelling induced by BTM-RP1 or by its tryptophane derivates. These data suggest that the superficial electrical charge of biomembranes, in addition to the trans-membrane potential, significantly affects the membrane permeabilization and selectivity in cell killing by polycationic peptides. We conclude that agents modifying superficial electrical charge of biological membranes could be used to influence the peptide cytotoxicity and selectivity. (Colciencias grant #111840820380 and the National University of Colombia grant #20101007930).

1455-Pos
Structure-Function Investigation of A Novel Dendrimeric and Lipidated Antimicrobial Peptide
Mariano A. Scorciapino[1,2], Andrea Ardu[1], Jochen Buerck[3], Carla Cannas[1], Mariano Casu[1], Andrea Giuliani[4], Giovanna Pirri[4], Andrea C. Rinaldi[5], Anne S. Ulrich[3,6].
[1]Dep. of Chemical Sciences - University of Cagliari, Monserrato, Italy, [2]CNR/INFM SLACS (Sardinian LAboratory for Computational materials Science), Monserrato (CA), Italy, [3]Institute for Biological Interfaces – Karlsruhe Institute of Technology, Karlsruhe, Germany, [4]Research and Development Unit - Spider Biotech S.r.l, Colleretto Giacosa (TO), Italy, [5]Dep. of Biomedical Sciences and Technologies – University of Cagliari, Monserrato, Italy, [6]Institute of Organic Chemistry – Karlsruhe Institute of Technology, Karlsruhe, Germany.
Antimicrobial peptides are usually polycationic with high affinity for bacterial membranes. Upon approaching the lipid bilayer, they tend to fold into an amphiphilic structure and bind to the membrane. In order to understand the detailed mode of action of such antimicrobial peptide inside the membrane, and to understand which properties of the peptide and/or lipids are important for selectivity, it is fundamental to examine the peptide structure and its association with lipid bilayers. In this work, first experiments were carried out to assess the thermodynamic and kinetic parameters of a promising novel antibiotic dendrimeric peptide interacting with lipid bilayers. With the goal of enhancing the antimicrobial activity of a particular sequence with the polyvalent framework of a dendrimer, two identical deca-peptides were assembled via a lysine-linker, carrying at the same time an octanoyl-lipid anchor. A highly active compound was obtained, but its structure and mode-of-action remain unexplored. The dendrimer and the linear deca-peptide were studied in parallel, to highlight the relevant properties and differences between dendrimeric structure and simple amino-acid sequence. Experiments were performed with different zwitterionic/negatively-charged lipids mixtures in order to assess the role of lipid surface charge. In particular, monolayer intercalation was investigated with microtensiometry. Fluorescence spectroscopy was applied to study thermodynamics and kinetics of the binding process. Circular dichroism, multidimensional liquid-state NMR, and solid-state NMR of oriented samples allowed to obtain first information on the 3D structure of the peptide both in the free and membrane-bound state. Transmission electron microscopy images showed the formation of highly intriguing aggregates with, to our knowledge, a previously unreported kind of branched three-dimensional morphology.

1456-Pos
Effects of Bacillus Lipopeptides on Lipid Membrane Structure and Dynamics
Mozhgan Nazari, Mustafa Kurdi, Hiren Patel, Heiko Heerklotz.
UofT, Toronto, ON, Canada.
Bacillus subtilis strain QST713 produces a unique combination of lipopeptides from the surfactin (SF), fengycin (FE) and iturin (IT) families. The fungicidal activity of this peptide mix is used by a biopesticide for crop protection and believed to be based on the permeabilization of target membranes by the peptides. To shed light on the activity, selectivity and synergisms of the peptides, we have studied their membrane binding and the subsequent effects on the structure and dynamics of the membrane. We measured the time-resolved fluorescence and fluorescence anisotropy of intrinsic tyrosine and hydrophobic dyes (e.g., DPH), time-resolved dipolar relaxation of Laurdan, interaction thermodynamics by ITC, and size and zeta potential of vesicles by DLS. The results are compared with the effects of synthetic surfactants and provide valuable information about the molecular background of the very unusual leakage and lysis behaviour of the lipopeptides.

1457-Pos
Rapid Binding and Transmembrane Diffusion of Pepducins in Phospholipid Bilayers
Kellen B. Fontanini[1], Jay Janz[2], Richard Looby[2], James A. Hamilton[1].
[1]Boston University School of Medicine, Boston, MA, USA, [2]Ascent Therapeutics, Cambridge, MA, USA.
Pepducins are GPCR-targeted lipopeptides designed to anchor in the cell membrane lipid bilayer and modulate the receptor/G protein signal transduction pathway via an allosteric mechanism. It is thus presumed that pepducins cross the plasma membrane by some mechanism, possibly passive diffusion. The goal of this research is to study the biophysical transport properties of pepducins in model membranes. We utilized fluorescent probes that measure the binding (fluorescein phosphatidylethanolamine - FPE) and diffusion (pH probe - pyranine) of charged ligands across the lipid bilayer of large unilamellar vesicles (LUV) comprised of egg-phosphatidylcholine. We tested pepducins with a palmitate or myristate linked to the N-terminal of the peptide sequence (KKSRALF). The GPCR target for these pepducins is the protease activator receptor 1 (PAR1). Addition of pepducins (0.16-5.0 mol%) to LUVs labeled in the outer leaflet with FPE or containing entrapped pyranine produced a fast (<2s) and dose-dependent increase in the fluorescence of both probes. The fast response of FPE, resulting from the insertion of positive charges (lysine and arginines residues) into the outer leaflet, demonstrated rapid partitioning into the membrane. The increase in pyranine fluorescence indicated alkalinization of the intravesicular compartment, probably due to protonation of the lysine residues. In order for this to be detected, the pepducin must cross the membrane. The peptide alone (not acylated) did not cause any change in the fluorescence of either FPE or pyranine. These data are consistent with favorable partitioning of pepducins into the membrane and rapid passive diffusion to the sites of their action at the cytosolic leaflet of the plasma membrane.

1458-Pos
Nanostructure Determines Antifungal Activity of De Novo Designed pH Dependent Histidine Containing Ultra-Short Lipopeptides
Christopher J. Arnusch[1], H. Bauke Albada[2], Rob M.J. Liskamp[2], Yechiel Shai[1].
[1]Weizmann Institute of Science, Rehovot, Israel, [2]University of Utrecht, Utrecht, Netherlands.
Antimicrobial peptides are an essential part of the innate immune system of most living things and the understanding of the biophysical properties and the different mechanisms of action are crucial for the de-novo development of simple and effective analogs. More specifically, antimicrobial lipopeptides have been gaining increased attention because of the pressure for new antimicrobial agents against resistant pathogens. The addition of a lipophilic fatty acid has proven to be an effective method to increase the association of a peptide with the membrane, thus increasing the biological activity of certain peptide sequences. Previously, we reported that linear ultrashort cationic lipopeptides even as short as 4 amino acids have potent antimicrobial and antifungal properties. We described the minimum peptide length, and fatty acid length

necessary for activity. Also, innate-immunity-like peptides were described that contained multiple histidine residues. Although these peptides consisted of 12 to 15 amino acids, these were less toxic to the host, and were lytic to numerous pathogens and cancer cells at slightly acidic environments. Here we report the design of an ultrashort histidine containing peptide whose antifungal activity could be significantly increased in a covalent trimeric form. Low micromolar activity was observed for Aspergillus fumigatus and Cryptococcus neoformans but not Candida albecans. Using transmission electron microscopy, we observed that this trimeric ultrashort histidine containing peptide formed distinct and differing nanostructures at pH 5 and 7, which could explain the activity differences. Since various organs or areas of the human body have a slightly acidic pH environment such as tumors, gastric lumen and lung-lining fluids in cystic fibrosis and asthma, understanding the importance of nanostructure-activity relationships of these pH dependent ultrashort peptides could lead to improvements in the delivery and administration of the peptides.

1459-Pos
Spectroscopic Studies of the Interaction of Native and TOAC-Labeled Peptide Hormones with Model Membranes: Angiotensin II

Nélida Marín[1], Erick Poletti[2], Clóvis Ryuichi Nakaie[2], Shirley Schreier[1].
[1]University of São Paulo, São Paulo, Brazil, [2]Federal University of São Paulo, São Paulo, Brazil.

The peptide hormone angiotensin II (DRVYIHPF, AII) plays an important role in the renin-angiotensin-aldosterone system. AII derivatives containing the paramagnetic amino acid 2,2,6,6-tetramethylpiperidine-1-oxyl-4-amino-4-carboxylic acid (TOAC) replacing residues 1 ($TOAC^1$-AII) and 3 ($TOAC^3$-AII) were synthesized and their conformational properties, as well as those of the native peptide, were examined in the presence of model membranes - micelles of 1-palmitoyl-2-hydroxy-phosphatidylcholine (LPC) and 1:1 mol:mol LPC: 1-palmitoyl-2-hydroxy-phosphatidylglycerol (LPG) and large unilamellar vesicles (LUV) of 1-palmitoyl-2-oleoyl phosphatidylcholine (POPC) and 1:1 mol:mol POPC:1-palmitoyl-2-oleoyl phosphatidylglycerol (POPG). Experiments were conducted at pH 4.0, 7.0, and 10.0 to evaluate the effect of peptide charge on peptide-membrane interaction. Fluorescence spectra showed that the peptides bound to negatively charged micelles to a much larger extent than to zwitterionic micelles. CD spectra of AII and $TOAC^1$-AII showed acquisition of secondary structure upon binding to LPC:LPG micelles at pH 4.0; the changes occurred to a lesser extent at the higher pHs. In the case of $TOAC^3$-AII, binding had a small effect on peptide conformation since the TOAC ring imposes a more constrained conformation already in solution. In the case of bilayers, the peptides interacted only with POPC:POPG LUV, especially at pH 4.0. Line broadening of EPR spectra of the labeled peptides also provided evidence for interaction of the labeled peptides with negatively charged micelles and bilayers. In several cases, two-component spectra were obtained, one due to the peptides in solution and the other to the bilayer-bound population, allowing for the calculation of partition coefficients. The rigidity of the TOAC-labeled analogue is very likely responsible for its inability to acquire the correct receptor-bound conformation, leading to loss of biological activity. These data show that spectroscopic studies can provide relevant information regarding peptide-membrane interaction.

1460-Pos
Unraveling the Molecular Basis of the Selectivity of the HIV-1 Fusion Inhibitor Sifuvirtide Towards Phosphatidylcholine-Rich Rigid Membranes

Henri G. Franquelim, A. Salomé Veiga, Nuno C. Santos,
Miguel A.R.B. Castanho.
Instituto de Medicina Molecular, Lisbon, Portugal.

Sifuvirtide, a 36 amino acid anionic peptide, is a novel HIV-1 fusion inhibitor with improved antiretroviral activity. The selective ability of this peptide to interact with lipid bilayers has already been identified (Franquelim et al, *J Am Chem Soc* 2008, **130**, 6215-23) and the aim of this work is to evaluate the interaction of sifuvirtide with several biomembrane model systems, retrieving details of its mode of action at the membrane level. Since this peptide has aromatic residues, fluorescence spectroscopy techniques were mostly used. The interaction was assessed by partition and fluorescence quenching experiments. Results showed no significant interaction with large unilamellar vesicles composed by sphingomyelin and ceramide. In contrast, sifuvirtide presented selectivity towards vesicles composed by phosphatidylcholines (PC) in the gel phase, in opposition to fluid phase PC vesicles. The interaction of this peptide with gel phase PC (zwitterionic) membranes ($K_p = 1.2\times10^2$) is dependent on the ionic strength, which indicates the mediation of electrostatic interactions at an interfacial level. The effects of sifuvirtide on the lipid membranes' structural properties were further evaluated using dipole potential membrane probes, zeta-potential, dynamic light scattering and atomic force microscopy measurements. The results show that sifuvirtide does not cause a noticeable effect on lipid bilayer structure. Altogether, one can conclude that sifuvirtide presents a specific affinity towards rigid PC membranes (in agreement with the adsorption model previously proposed), and the interaction is mediated by electrostatic factors, not affecting the membrane architecture. Because saturated PC lipids are found in high concentration in lipid rafts, but mainly in the viral envelope, the efficacy of sifuvirtide may be related to its screening ability towards those regions, allowing an increased concentration of this peptide drug near the fusion site.

1461-Pos
Fusion Peptide of Gp41 Self Associates in the Model Membrane and then Interacts with its Trans-Membrane Domain

Hirak Chakraborty[1], David G. Klapper[2], Barry R. Lentz[1].
[1]Biochemistry and Biophysics Department & Molecular and Cellular Biophysics Program, University of North Carolina at Chapel Hill, Chapel Hill, NC, USA, [2]Microbiology & Immunology Department, University of North Carolina at Chapel Hill, Chapel Hill, NC, USA.

We have examined the peptide structure and membrane packing when the fusion peptide (FP) of gp41 was added either in the membrane alone or in the membrane containing gp41 the trans-membrane domain (TMD). Circular Dichroism (CD) measurements showed that FP is mostly in a beta sheet conformation independent of FP concentration. TMD has ~ 30% helical, ~25% beta sheet and the complex of TMD and FP has less alpha helix than the TMD itself, which indicates the TMD looses its alpha helical structure upon interacting with FP. DPH and TMA-DPH fluorescence anisotropy revealed that FP alone increased the interior packing of the membrane, but FP in the presence of TMD increased the interior packing at lower concentrations of FP and then decreased it at higher concentrations. FP alone increased membrane surface packing at lower concentrations but increased it at higher concentrations. In the presence of TMD, FP addition decreased surface packing cooperatively. From the lifetime of TMA-DPH in H2O and D2O we documented water penetration into the membrane. FP alone increases water penetration slightly whereas FP in presence of TMD significantly increased water penetration into the interface region of the membrane in a cooperative fashion. The fluorescence lifetime of C6NBDPC revealed that FP alone fills more space than the FP in the presence of TMD. In summary, our results clearly demonstrate that gp41 FP forms a complex with the gp41 TMD to alter both TMD structure and membrane structure. It remains to be seen whether this complex promotes membrane fusion. Supported by NIGMS grant 32707 to BRL.

1462-Pos
HIV Fusion Peptides Significantly Soften Lipid Bilayers

Pavlo Shchelokovskyy[1], Stephanie Tristram-Nagle[2], Reinhard Lipowsky[1], Rumiana Dimova[1].
[1]Max Plank Institute of Colloids and Interfaces, Potsdam, Germany,
[2]Carnegie Mellon University, Pittsburgh, PA, USA.

The fusion peptide (FP) of the human immunodeficiency virus (HIV) is found on N-terminus of the viral envelope glycoprotein gp41 and is believed to play an important role in the virus entry process. In order to understand the immediate effect of this peptide on the cell membrane we have studied the influence of the synthetic fusion peptide residue FP-23 on the mechanical properties of model lipid bilayers. For this purpose, giant unilamellar vesicles (GUV) were prepared by electroformation from the unsaturated lipid dioleoylphosphatidylcholine mixed in various ratios with the fusion peptide. The bending stiffness of the vesicles was measured with two different methods: fluctuation analysis and aspiration with micropipettes. The data obtained from both of these approaches show that the bending stiffness of the membrane decreases gradually with increasing the concentration of the fusion peptide in the bilayer. Even low concentrations of only a few mol % FP-23 are sufficient to decrease the bending stiffness of the lipid bilayer by more than a factor of two. This observation is in agreement with previous results obtained with X-ray scattering on stacked lipid layers; see Tristram-Nagle and Nagle, Biophys. J. 93: 2048 (2007). Ongoing research is carried out to investigate the effect of FP-23 on the spontaneous fusion of GUVs.

1463-Pos
Augmentation of Single Channel Water Permeability by Modification of Membrane Anchoring

Florian Zocher[1], Tanya Polupanowa[2], Danila Boytsov[1], Guillem Portella[3], Bert de Groot[4], Ulf Diederichsen[2], Peter Pohl[1].
[1]Universitaet Linz, Linz, Austria, [2]Universitaet Göttingen, Göttingen, Germany, [3]Institute for Research in Biomedicine, Barcelona, Spain,
[4]Max Planck Institute for Biophysical Chemistry, Göttingen, Germany.

Water transport through very narrow channels occurs according to the single file mechanism. While entering the channel, every water molecule loses most of its neighbouring water molecules. The energetic costs are thought to be

compensated, at least in part, by interactions with the channel wall and by interactions with the lipid headgroups at the channel mouth. Consequently, differences in single channel permeability (pf) measured for gramicidin A channels embedded into different lipids were interpreted in terms of differences in water dehydration costs. However, recent atomistic molecular dynamics simulations identified lipid headgroup interactions with the channel entrance leading to transient blocking of the channel. This observation suggests that the lipid environment affects the channel not only by changing the water energetics but also by mechanically blocking the entrance. To test this hypothesis we measured ion and water fluxes through acylated gramicidin-A derivatives, which were reconstituted into solvent free diphytanoyl-phosphatidyl-choline membranes. Ion conductance of channels with C9 and C10 acyl-chain anchors differed only by about 20 % from wild type gramicidin-A conductance. Similarly, the anchor had only a minor effect on dimer stability as indicated by a decrease in channel lifetime from 2.3 s to 2 s or 1.6 s for the C9 and C10 derivatives, respectively. As the gramicidin channels most of the time do not contain ions, the acyl-chain anchor affects water transport more efficiently. Two C9 anchors increased pf by a factor 2 or 3 depending on their position. In contrast, derivates with only one C9 or C10 acyl anchor showed no increase in pf. Taken together with data about the lipid dependency of pf, these results indicate that the lipid headgroups affect single file transport by both changing the solvation energy and by blocking the channel entrance.

1464-Pos
Amyloid Oligomers Increase the Lifetime and Single Channel Conductance of Gramicidin Channels
Yuri Sokolov, Saskia C. Milton, Charles G. Glabe, James E. Hall.
UCI, Irvine, CA, USA.

Our previous data suggest that Aβ does not itself contribute a new intrinsic conductance to the membrane but instead alters physical properties of the membrane specifically increasing the apparent dielectric constant of hydrocarbon region. This change could in turn affect the properties of membrane ion channels.

In order to test this notion we compared the effects of amyloid oligomers on the single channel conductance and mean open time of gramicidin in 2 M NaCl and CsCl using DOPC and a series brominated lipids that change the dielectric properties of lipid bilayer at different depths into the membrane (11,12-bromo-16:0, 10,9- bromo-16:0 and 7,6- bromo-16:0, PC). Amyloid oligomers always increase the single channel conductance and mean open time both in 2 M NaCl and CsCl regardless of the nature of lipid used. The single channel conductance of gramicidin in brominated lipid membranes is always lower than that in DOPC membranes.

In terms of a simple three-barrier two- site model such as that used by Barnett et al., 1986, this suggests that amyloid oligomers lower the energies of both Cs and Na ions in the gramicidin channel but at different critical locations relative to the barrier profile. For Na^+, amyloid oligomers lower the principal central barrier and thus increase the translocation rate of Na^+ at a given voltage. For Cs^+, amyloid oligomers act as if they lower the energy of the Cs ion in the channel, but in such a way as to increase the depth of one or both of the two wells in the barrier profile. Brominated lipids apparently increase the depth of the wells at the ends of the channel consistent with their X-ray locations.

Supported by the Hillblom Foundation and NIH 1P01AG032131.

1465-Pos
Observation of Beta-Amyloid Formation Via Membrane Binding
Yen Sun, Tzu-Hsuan Chen, Chang-Chun Lee, Huey W. Huang.
Rice University, Houston, TX, USA.

Alzheimer's Aβ-40 and penetratin exhibited the same conformation changes upon binding to membranes. Recently we have studied the thermodynamics of membrane-mediated β-aggregate formation in equilibrium experiments using penetratin-lipid mixtures. The results showed that penetratin bound to the membrane interface in the α-helical conformation at low peptide-to-lipid (P/L) ratios. As P/L exceeds a lipid dependent critical value P/L*, small β-aggregates were formed, which served as the nuclei for large β-aggregates. We tested this free energy description in a kinetic experiment using GUVs. A GUV made of 7:3 DOPC/DOPG and 0.2% lipid dye was aspirated by a micropipette and transferred to a solution of containing penetratin in various concentrations. As the peptides began to bind to the GUV, the membrane area initially expanded till it reached a maximum (this corresponds to P/L->P/L*). Then the area began to decrease from the maximum expanded value (corresponding to P/L exceeding P/L* where the membrane thinning decreases with increasing P/L). Concomitant with the area decrease, lipid aggregates began to appear on the surface of GUV and some of them came off the GUV surface.

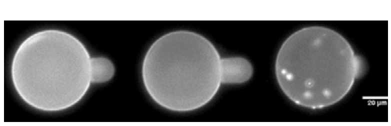

1466-Pos
Membrane Mediated Peptide Conformation Change from Alpha-Monomers to Beta-Aggregates
Chang-Chun Lee, Yen Sun, Huey W. Huang.
Rice University, Houston, TX, USA.

The major component of Alzheimer's disease amyloid plague, β-amyloid protein 1-40 and the peptide penetratin exhibited the same membrane mediated conformation changes. Both peptides are random coils in solution but change to α-helical or β-like conformations in the presence of negatively charged lipid membranes. Both peptides change from α to β conformations as the lipid charge increases or as the peptide concentration increases. Since the principle behind these phenomena might clarify the molecular mechanism of β-amyloid formation, we investigated the correlation between the peptide conformation of penetratin and its effect on the membrane thickness in four different lipids with varying degrees of chain unsaturation. The results revealed a new effect of membranes on penetratin , i.e., as the degree of chain saturation increased, the peptide changed from α-helical to β-like conformation. We found that penetratin in the helical conformation was bound to the interface and thinned the membrane. In contrast, penetratin in the β-conformation had little effect on the bilayer thickness, therefore it was most likely bound on the surface of lipid headgroups. From the systematic results we were able to deduce the molecular mechanism in terms of free energies that explains the effect of membrane binding on the secondary structure of penetratin. The mechanism could be the prototype for the membrane-mediated version of nucleation-dependent amyloid formation proposed by Jarrett and Lansbury. It might explain why membrane binding has been suspected as the catalyst for polymerization leading to amyloid formation.

1467-Pos
The Hydrophobic Surfactant Proteins Induce Cubic Phases Without Altering Spontaneous Curvature
Mariya Chavarha[1], Hamed Khoojinian[1], Leonard C. Schulwitz[1], Samares C. Biswas[1], Shankar B. Rananavare[2], Stephen B. Hall[1].
[1]Oregon Health & Science University, Portland, OR, USA, [2]Portland State University, Portland, OR, USA.

Prior evidence suggests that the hydrophobic surfactant proteins, SP-B and SP-C, promote adsorption of the surfactant lipids to the alveolar air/water interface by facilitating formation of a rate-limiting negatively curved stalk between the vesicular bilayer and the interface. In support of the proposed model, the physiological mixture of the surfactant proteins (SP), in amounts as low as 0.03% (w:w), induce 1-palmitoyl-2-oleoyl phosphatidylethanolamine (POPE) to form inverse bicontinuous cubic (Q_{II}) phases, in which each leaflet has the saddle-shaped net-negative curvature predicted for the hypothetical stalk. One mechanism by which the proteins might promote formation of the Q_{II} phases is by altering the spontaneous curvature of the lipid leaflets. If the lipid-protein mixtures form the inverse hexagonal (H_{II}) phase, then a shift in spontaneous curvature would change the dimensions of the unit cell. POPE forms H_{II} structures only above 71°C, and only for 0-0.03% SP. To obtain H_{II} structures with a wider range of protein contents, we substituted lipids that form H_{II} structures at lower temperatures. X-ray diffraction showed that 1,2-dioleoyl phosphatidylethanolamine and its stereoisomer 1,2-dielaidoyl phosphatidylethanolamine form Q_{II} phases with SP at or above 0.03%. During heating from 10 to 95°C, both lipids form H_{II} structures over the full range of protein concentrations from 0-3% SP. The dimensions of the H_{II} unit cell were unaffected by the content of protein. The lack of any effect of the surfactant proteins on the size of the H_{II} phase indicates that the proteins facilitate formation of the Q_{II} phases, and suggests that they promote adsorption, by a mechanism other than changing spontaneous curvature. (Studies conducted at the Stanford Synchrotron Radiation Lightsource).

1468-Pos
Modifications to Surfactant Protein B Structure and Lipid Interactions Under Ards Conditions: Consequences of Tryptophan Oxidation
Muzaddid Sarker, Jarratt Rose, John Bartlett, Mitchell Browne, **Valerie Booth**.
Memorial University of Newfoundland, St. John's, NL, Canada.

Oxidation of Surfactant Protein B (SP-B) is one of several mechanisms proposed to lead to inactivation of lung surfactant in patients with Acute Respiratory Distress Syndrome (ARDS). We have used solution NMR, circular dichroism and molecular dynamics simulation to explore the consequences of oxidation of the tryptophan residue in fragments of SP-B. These fragments include the N-terminal helix of SP-B, as well as Mini-B, a fragment that includes both the N-and C-terminal helices. The fragments were studied in a number of conditions including aqueous solution, organic solvent, zwitterionic and anionic micelles, as well as monolayers. Tryptophan oxidation was found to

result in both the partial loss of α-helical structure, as well as differences in peptide positioning with respect to the lipids.

1469-Pos
Antimicrobial Peptides in Toroidal and Cylindrical Pores
Maja Mihajlovic, Themis Lazaridis.
The City College of New York, New York, NY, USA.
Antimicrobial peptides (AMPs) are small, usually cationic peptides, which permeabilize biological membranes. Understanding their mechanism of action might help design better antibiotics. Using molecular dynamics (MD) simulations, we investigate the preference of alamethicin and melittin for pores of different shapes. In the simulations, an alamethicin hexamer initially embedded in a pre-formed cylindrical pore preserves the pore shape or closes the pore if glutamines in the N-terminus are not located within the pore. On the other hand, when a melittin tetramer is embedded in a toroidal pore or in a cylindrical pore, at the end of the simulations the pore is lined both with peptides and lipid headgroups, and, thus, can be classified as a toroidal pore. These observations agree with the prevailing views that alamethicin forms barrel-stave pores whereas melittin forms toroidal pores. The melittin tetramer interacts more strongly with lipids in the toroidal pore than in the cylindrical one, due to more favorable electrostatic interactions. Using an implicit membrane model, modified to include pores of different shapes, we show that melittin is better solvated in toroidal pores than in cylindrical ones.

Membrane Structure I

1470-Pos
Hybrid Lipids as a Biological Line-Active Component
Robert Brewster[1], Sam A. Safran[2].
[1]Caltech, Pasadena, CA, USA, [2]Weizmann Institute of Science, Rehovot, Israel.
The lipid raft hypothesis posits that certain cellular functions are mediated by small (nanometric to tens of nanometers) domains rich in sphingolipids and cholesterol. These sphingolipids have two completely saturated hydrocarbon tails that show good orientational order in the membrane. The surrounding phase consists mostly of lipids with at least one unsaturated bond in the hydrocarbon tails which forces a ''kink'' in the chain and inhibits ordering. In vitro, this phase separation can be replicated; however, the finite domains coarsen into macroscopic domains with time. We have extended a model for the interactions of lipids in the membrane, motivated by the work in (Elliott et al., PRL 2006 and Garbes Putzel and Schick, Biophys. J. 2008), which depends entirely on the local ordering of hydrocarbon tails. We generalize this model to INCLUDE an additional species THAT IS LINE ACTIVE and identify a biologically relevant component, a hybrid lipid with one fully saturated hydrocarbon chain and one chain with at least one unsaturated bond, that may serve as a line-active component. we show that in some cases, the hybrid is capable of reducing the line tension between the saturated and unsaturated domains to zero, thus stabilizing finite sized domains in equilibrium. We then present simple packing arguments that predict the expected size of such domains as a function of the molecular volume and area per headgroup of the composing lipids which is dictated by parameters such as cholesterol concentration, chain length and degree of unsaturation.

1471-Pos
Characterization of Horizontal Lipid Bilayers as a Model System to Study Lipid Phase Separation
Richard Wagner, Frank Erdmann, Alf Honigmann.
University Osnabrueck, Osnabrueck, Germany.
Black lipid membranes are widely used as a model system to study ion channel activity with electrophysiological techniques. In this study we characterize the properties of the bilayer system with respect to its dynamics of lipid phase separation using single molecule fluorescence fluctuation and electrophysiological techniques. On the nanosecond time scale we determined the rotational motions of fluorescently labeled lipids using confocal time resolved anisotropy to probe the microscopic viscosity of the membrane. Simultaneously long range mobility was investigated by the lateral diffusion of the lipids through the laser focus with fluorescence correlation spectroscopy. Depending on the solvent used for membrane preparation, lateral diffusion coefficients between $D_{lat} = 10$ - 25 $\mu m^2/s$ and rotational diffusion coefficients of $D_{rot} = 2.8\ 10^7\ s^{-1}$ - $1.4\ 10^7\ s^{-1}$ were measured in pure liquid disordered (Ld) membranes. In ternary mixtures containing saturated, unsaturated phospholipids and cholesterol, liquid ordered (Lo) domains segregated from the Ld phase at 23°C. The lateral mobility of lipids in Lo domains was ~8-fold lower compared to the Ld phase while the rotational mobility decreased by a factor of 1.5. Burst integrated steady state anisotropy histograms as well as anisotropy imaging were used to visualize the rotational mobility of lipid probes in phase separated bilayers. The electrical conductance of pure Ld and ternary bilayers was linearly dependent on the temperature. No discrete current fluctuations were found near the phase transition between coexisting Ld and Lo domains. Our results demonstrate that horizontal bilayers can be used as an alternative model system for lipid phase separation (taking solvent partitioning into account) favorably when electrical properties of the membrane want to be studied in parallel

1472-Pos
Phase-Field Modeling and Simulations of Lipid Membranes Coupling Composition with Membrane Mechanical Properties
Chloe M. Funkhouser[1], Francisco J. Solis[2], Katsuyo Thornton[1].
[1]University of Michigan, Ann Arbor, MI, USA, [2]Arizona State University, Glendale, AZ, USA.
The plasma membrane, a lipid bilayer membrane surrounding all mammalian cells, is not homogeneous, but rather contains domains termed 'rafts,' defined as regions enriched with cholesterol and saturated lipids. Understanding how and why these rafts form is of great importance to cell biologists and immunologists, since they are involved in many important cell functions and processes including endocytosis, cell adhesion, signaling, protein organization, lipid regulation, and infection by pathogens. These raft structures also show great potential for technological applications, especially in connection with biosensors and drug delivery systems. We examine the formation and evolution of lipid raft-like domains in multicomponent lipid membrane vesicles using a continuum-level simulation method. Our objective is to investigate how various physical parameters input into the model, such as spontaneous curvature, bending rigidity, and phase fraction, affect the dynamics and equilibrium morphological phases formed in two-phase lipid membrane systems. This model is applied to membranes with spherical background geometries, simulating the compositional and shape evolution of lipid vesicles, coupled using a modified Helfrich free energy. The compositional evolution is modeled using a phase-field method and is described by a Cahn-Hilliard-type equation, while the shape changes are described by relaxation dynamics in which the vesicle surface area is conserved. We find that the compositional and morphological evolution are significantly altered when the mechanical coupling is present by comparing the results with those of systems where this coupling is absent. More specifically, we find that the evolution is significantly slowed when the phases have equal and opposite spontaneous curvatures and are present in roughly equal amounts. We also investigate equilibrium shapes formed by completely phase-separated vesicles as a function of spontaneous curvature, bending rigidity, and phase fraction.

1473-Pos
Computation of Lipid Headgroup Interactions
Andrew M. Smith[1], Adriana L. Rogozea[2], Carina M. Poltera[2], Gonzalo Ordonez[1], Shubho Banerjee[3], Horia I. Petrache[2].
[1]Butler University, Indianapolis, IN, USA, [2]Indiana University Purdue University Indianapolis, Indianapolis, IN, USA, [3]Rhodes College, Memphis, TN, USA.
The equilibrium structure of lipid aggregates is determined by the balance of numerous forces between hydrophobic acyl chains, hydrophilic lipid headgroups, and the lipid's environment. Among these forces, lipid headgroup interactions are both important to the stability of lipid structures and responsible for many of the interactions between biological membranes and aqueous solutes including ions and soluble peptides. In order to model these headgroup interactions, we consider the electrical properties of the headgroup molecules via the multipole expansion. While common lipid headgroups such as phosphatidylcholine are electrically neutral, they are characterized by non-zero higher order terms in the multipole expansion. Making a dipole approximation, we employ a two dimensional lattice of classical dipoles to model the headgroup networks of lipid aggregates. Restrictions to each dipole's position and orientation are imposed to account for the effect of hydrocarbon chains which are not included in the model. A Monte Carlo algorithm is used to calculate headgroup-headgroup interactions and network energies in both dipole and point-charge approximations.

1474-Pos
X-Ray Scattering from Gold Labeled Supported Membranes
Curt M. DeCaro[1], Laurence B. Lurio[1], Justin Berry[1], Sunil K. Sinha[2], Gang Chen[2], Atul Parikh[3], Adrian Brozell[3].
[1]Northern Illinois University, DeKalb, IL, USA, [2]University of California at San Diego, San Diego, CA, USA, [3]University of California in Davis, Davis, CA, USA.

X-ray scattering is a promising tool with which to characterize systems of solid-supported membranes. There are many different scattering techniques used in the characterization, but all suffer from a necessarily low electron density contrast between the membrane and the water medium in which it must exist. Labeling membranes with a high-contrast scatterer such as gold is a promising avenue to solve this problem. In this work, silicon-supported membranes of 1,2-dipalmitoyl-sn-glycero-3-phosphocholine (DPPC) were prepared by both standard Langmuir-Blodgett deposition and fusion of vesicles onto the substrate surface. Membranes are characterized using specular x-ray reflectometry, and modeled to fit physical systems. One percent by count 1,2-dipalmitoyl-sn-glycero-phosphoethanolamine (DPPE) with a gold tag attached was then added to both systems. Gold labeled membranes were then characterized and modeled. The effect of gold labeling is shown to characteristically change the membrane density profile in addition to enhancing density contrast between the membrane and the water medium.

1475-Pos

Analysis of the Structure and Interaction in Two-Dimensional Assemblies of Tobacco Mosaic Viruses on Model Lipid Membranes

Lin Yang, Suntao Wang, Masafumi Fukuto.
Brookhaven National Laboratory, Upton, NY, USA.

We created two-dimensional (2D) assemblies of tobacco mosaic viruses (TMVs) and characterized their structures using Atomic Force Microscopy (AFM) and X-ray scattering. The TMVs were adsorbed on an oppositely charged, fluid lipid monolayer supported by a solid substrate and submerged in a buffer solution. The lipid monolayer confined the viral particles within a plane, while providing them with lateral mobility so that overall the TMV assembly behaved like a 2D liquid. The inter-particle interaction is controlled by the chemical condition in the buffer. The degree of structural orders observed varied, depending on both the inter-particle interaction and the lateral mobility of the particles. Quantitative analysis of the X-ray scattering data provides information on the nature of the interaction between TMVs as well as possible membrane deformation due to the contact with TMVs. This study provides the proof-of-concept that X-ray scattering may be used to study the structure of membrane associated proteins in substrate-supported single bilayer under near-native conditions.

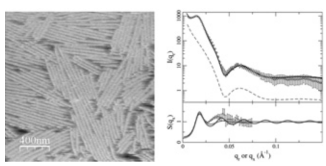

1476-Pos

Structure and Water Permeability of Fully Hydrated Diphytanoylpc

Stephanie Tristram-Nagle[1], Dong Joo Kim[1], Nadia Akhunzada[2], Norbert Kučerka[3], John C. Mathai[4], Mark Zeidel[4], John Katsaras[3], John F. Nagle[1].
[1]Carnegie Mellon University, Pittsburgh, PA, USA, [2]Douglass College, Rutgers University, New Brunswick, NJ, USA, [3]Canadian Neutron Beam Centre-NRC, Chalk River, ON, Canada, [4]Beth Israel Deaconess Medical Center and Harvard Medical School, Boston, MA, USA.

Diphytanoylphosphatidylcholine (DPhPC) is a branched chain lipid often used for model membrane studies, including peptide/lipid interactions, model ion channels and lipid raft studies. This work reports results of volume measurements, water permeability measurements P_f, X-ray scattering from oriented samples, and x-ray and neutron scattering from unilamellar vesicles at T=30 °C. The volume/lipid was $V_L = 1427 \pm 1$ Å^3. The area/lipid was found to be 83 $\pm$ 1 Å^2 when only x-ray data were used in the H2 model analysis (Klauda et al., Biophys. J. 2006) and A = 80.3 $\pm$ 1 Å^2 when both x-ray and neutron data were combined with the SDP model analysis (Kucerka et al., Biophys. J. 2008). P_f was measured to be 7.04 $\pm$ 0.97 x10^{-3} cm/sec, which is considerably smaller than predicted by the recently proposed 3-slab model (Nagle et al., J. Gen. Physiol. 2008). This suggests that water flow through the branched chain region becomes the rate limiting step instead of the entry of water through the interfacial region when the chains are not branched. The DPhPC head-head thickness (D_{HH}= 36.1 Å), the bending modulus (K_C=6.4 $\pm$ 1.5 x10^{-21}J) and the Hamaker parameter (H=4.5 x10^{-21}J) were similar to the linear chain lipid DOPC. Even though DPhPC does not occur in mammalian cell membranes, these similarities are consistent with DPhPC bilayers being an appropriate model for many cell membrane studies. This work was supported by grants from National Institutes of Health (GM44976, JFN,STN,) and (DK43944,JCM,MZ).

1477-Pos

Osmotic Membrane Deformation Revealed by Solid-State ^{2}H NMR and Small-Angle X-Ray Scattering

K.J. Mallikarjunaiah[1], Avigdor Leftin[1], Jacob J. Kinnun[1], Matthew J. Justice[2], Adriana L. Rogozea[2], Horia I. Petrache[2], Michael F. Brown[1].
[1]University of Arizona, Tucson, AZ, USA, [2]Indiana University-Purdue University, Indianapolis, IN, USA.

Phospholipid membranes are implicated in cellular homeostasis together with a multitude of key biological functions. Many regulatory functions are known to be mediated through protein-lipid interactions. An important feature of pressure-sensitive membrane proteins (mechanosensitive channels, rhodopsin) is that their activation is coupled to membrane tension and curvature elastic stress [1,2]. Solid-state ^{2}H NMR and small-angle X-ray scattering (SAXS) studies of bilayer ensembles of phospholipids under osmotic stress enable membrane structural deformation to be determined. Here we highlight the results from a combined NMR and SAXS approach utilizing pressure-based force techniques that control membrane structure [3] and tension [1].Our ^{2}H NMR results using both osmotic pressure (PEG osmolyte) and gravimetric pressure (low water concentration) techniques show that the segmental order parameters (S_{CD}) of liquid-crystalline DMPC approach very large values $\approx$0.35 at $\approx$30 °C. These correspond to $\approx$20% change in bilayer structural properties (cross-sectional area per lipid and acyl chain thickness) versusthefully hydrated membrane. The two stresses are thermodynamically equivalent because the change in chemical potential when transferring water from the interlamellar space to the bulk water phase corresponds to the induced pressure. A simple theoretical framework based on a unified thermodynamic description is developed. It is shown that the gating threshold for mechanosensitive channels may be shifted to higher or lower values due to lipid-mediated control of channel properties. These findings demonstrate the applicability of solid-state ^{2}H NMR spectroscopy and SAXS together with membrane stress techniques for investigating the mechanism of pressure sensitivity of membrane proteins. [1] S.I. Sukharev *et al*. (2001) *Biophys. J.***81**, 917-936. [2] A.V. Botelho *et al*. (2006) *Biophys. J.***91**, 4464-4477. [3] H.I. Petrache, M.F. Brown. (2007) *Methods in Membrane Lipids*, Humana Press, 339-351.

1478-Pos

A Modified Lipid Force Field for Charmm: Development and Application to Single-Celled Organism Membranes

Jeffery B. Klauda[1], Richard M. Venable[2], Richard W. Pastor[2].
[1]Universtiy of Maryland, College Park, MD, USA, [2]National Institutes of Health, Bethesda, MD, USA.

Biological membranes form a barrier to protect the cell from its environment and selectively control the entrance/exit of small molecules. Molecular simulations of these biological membranes require an accurate lipid force field (a major component of the membrane). Previously, extensive *ab initio* quantum mechanical (QM) calculations have been used to improve the aliphatic portion of the CHARMM27 lipid force field. Although this was a significant improvement, the lipid head group required additional modifications to agree with experimental lipid bilayer deuterium order parameters (S_{CD}) and solvation free energies. Therefore, we modified the atomic charges in the carbonyl-glycerol region and fit dihedral energy terms to high-level QM calculations and/or experiment. Molecular dynamics (MD) simulations with this new force field, referred to as CHARMM36 (C36), resulted in a significant improvement to the S_{CD}'s and water hydration for DPPC lipid bilayers. The calculated electrostatic profile and lipid bilayer surface tension decreased significantly. Consequently, the C36 force field resulted in excellent surface areas per lipid (and other properties) with NPT simulations, which is a significant improvement from the C27r force field that required constant area simulations (NPAT) to prevent some bilayers from laterally condensing. MD simulations of other pure lipid bilayers and monolayers also agreed favorably with experimental densities, monolayer surface tensions, and S_{CD}'s. The success of the C36 force field allowed for the study of complex lipid membranes in single-celled organisms. Model membranes were developed and simulated for yeast (six phospholipids, cholesterol, and 25-hydroxysterol) and Chlamydia (five unbranched lipids, a branced lipid, and cholesterol). These membranes are currently being used to study intracellular sterol transport and a porin protein that induces an immune response.

1479-Pos

Calculation of Partition Coefficients of Chain Anchors in Liquid-Ordered and Liquid-Disordered Phases in Model Lipid Bilayers

Mark Uline[1], Gabriel Longo[2], Michael Schick[3], Igal Szleifer[1].
[1]Northwestern University, Evanston, IL, USA, [2]International School for Advanced Studies, Trieste, Italy, [3]University of Washington, Seattle, WA, USA.

We calculate partition coefficients of various chain anchors in liquid-ordered and liquid-disordered phases utilizing a theoretical model of a bilayer membrane containing cholesterol, dipalmitoylphophatidylcholine (DPPC), and dioleoylphosphatidylcholine (DOPC). The model qualitatively reproduces experimentally observed phase diagrams of this ternary system [R. Elliott,

I. Szleifer, M. Schick, Phys. Rev. Letters, 96, 098101,2006]. The partition coefficients are calculated as a function of chain length, degree of saturation, and temperature. Perhaps our most important, model-independent, observation is that the partition coefficients must depend upon the relative compositions of the two liquid phases which coexist. For given phases in coexistence, we find that saturated anchors prefer the denser liquid-ordered phase and that their partition coefficients generally increase with the length of the anchor. Unsaturated chains and other bulky anchors prefer the less dense liquid-disordered phase. The fraction of anchors in the liquid-ordered phase decreases with decreasing degree of saturation of the anchors. For a given number of double bonds, the partition coefficient depends upon their location, with those near the chain ends causing a smaller decrease in the fraction of anchors in the liquid-ordered phase than double bonds closer to the middle of the anchor. The effect of doubling the number of chains in an anchor is to increase the partitioning into the liquid-ordered phase when the tails are nearly as long or longer than those comprising the bilayer, but is minimal when they are relatively short. A reduction of temperature also increases the partition coefficient of long chains, but again has little effect on shorter ones.

1480-Pos

Xerogel-Supported Lipid Bilayers: Effect of Surface Curvature and Surface Chemistry on Bilayer Properties

Emel I. Goksu[1], Barbara A. Nellis[1,2], Joe H. Satcher Jr.[2],
Subhash H. Risbud[1], Marjorie L. Longo[1].
[1]UC Davis, Davis, CA, USA, [2]Lawrence Livermore National Laboratory, Livermore, CA, USA.

Aerogels are a special class of interconnected nanoscale colloidal-like particles or polymeric chains derived from highly cross-linked inorganic or organic gels that are dried under specific conditions to preserve the tenuous solid network. Aerogels have been used or considered for use in various technical applications such as laser experiments, sensors, thermal insulation, optics, electronic devices, catalysts, cosmic dust collection and X-ray laser research. Xerogels are similar to aerogels but are dried by solvent evaporation at ambient conditions which results in a decreased porosity. Here, we demonstrate a different use of xerogels, as a scaffolding material to support lipid bilayers. We prepared various xerogel structures including silica, titania, alumina, iron oxide, phloroglucinol-formaldehyde (PF), resorcinol-formaldehyde (RF) and cellulose acetate, characterized the surfaces and confirmed lipid mobility by fluorescence recovery after photobleaching (FRAP). Subsequently, we studied DOPC/DSPC phase-separated lipid bilayers supported on silica xerogels vs. smooth mica. It was concluded, using atomic force microscopy and FRAP, that the bilayers on silica xerogel follow the surface curvature rather than being smoothly suspended on the silica interconnected colloidal particles. We used the nanometer-scale corrugations induced in the bilayer to observe the effect of curvature on the phase-separation of ternary mixtures (DOPC/DSPC/Cholesterol). It was observed that the cholesterol concentration of miscibility was significantly greater for silica xerogel-supported ternary bilayers (> 60 mol% chol) compared to smooth mica-supported ternary bilayers (~40 mol% as expected for free bilayers). This is explained as curvature-induced movement of cholesterol from the bilayer to the fusion vesicles in the medium. In summary, this study illustrates the use of xerogel structures as supports for lipid bilayers and is promising in terms of enlightening the details of curvature and surface chemistry on the behavior of the biomembranes.

1481-Pos

What is the Difference Between a Supported and a Free Lipid Bilayer?

Chenyue Xing, **Roland Faller**.
UC Davis, Davis, CA, USA.

Supported Lipid Bilayers are an abundant research platform for understanding the behavior of real cell membranes as they allow for additional mechanical stability and enable characterization techniques not reachable otherwise. However, in computer simulations these systems have been studied only rarely up to now. Here we present a systematic study of the changes that a support inflicts on a phospholipid bilayer using coarse-grained molecular modeling.

We characterize the density and pressure profiles as well as the density imbalance induced by the support. It turns out that the changes in pressure profile are strong enough that protein function should be impacted leading to a previously neglected mechanism of transmembrane protein malfunction in supported bilayers. We also determine the diffusion coefficients and characterize the influence of different corrugations of the support. We then determine the free energy of transfer of phospholipids between the proximal (close to the surface) and distal leaflet of a supported membrane using the coarse-grained Martini model. It turns out that there is at equilibrium about a 2-3% higher density in the proximal leaflet. These results are in favorable agreement with recent data obtained by very large scale modeling using a water free model where flip-flop can be observed directly. We compare results of the free energy of transfer obtained by pulling the lipid across the membrane in different ways. There are small quantitative differences but the overall picture is consistent. We are additionally characterizing the intermediate states which determine the barrier height and therefore the rate of translocation. Simulations in atomistic detail are performed for selected systems in order to confirm the findings.

1482-Pos

Microscopy with Nanoapertures to Reveal Membrane Organization with 1 Microsecond and 100 Nanometer Resolution

Christopher V. Kelly, David A. Holowka, Barbara A. Baird,
Harold G. Craighead.
Cornell University, Ithaca, NY, USA.

Current hypotheses for plasma membrane organization depend critically on a variety of length and time scales that are outside the resolution of conventional experimental techniques. Our novel approach utilizes nanoapertures to examine membrane organization and dynamics with near-field optical fluorescence microscopy without incorporating a scanning probe or perturbing the membrane. Conventional microscopy excitation sources and fluorescent probes are used to enable fluorescence correlation spectroscopy (FCS) on living cell membranes with super-resolution. The nanoapertures confine the excitation light to a sub-diffraction limit length scale, providing a 25-fold decrease in the illuminated area of the membrane as compared to diffraction-limited illumination.

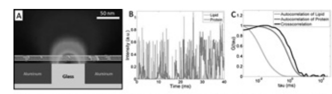

Nanoscale apertures have been fabricated to create illumination areas 25 times smaller than diffraction-limited illumination spots. (A) Thin aluminum films with <100 nm diameter apertures filled with glass allow for near-field illumination of membranes without inducing membrane curvature or requiring a scanning probe. Intensity vs. time of randomly diffusing lipids and slowly diffusing proteins can be analyzed with FCS, as simulated in (B) and (C), to reveal diffusion rates individual components (autocorrelation) that may diffuse as a complex (crosscorrelation). These rates may depend on local membrane structure and state of cell activation.

1483-Pos

Budding and Vesiculation Induced by Conical Membrane Proteins

Thorsten Auth, Gerhard Gompper.
Forschungszentrum Jülich, Jülich, Germany.

Conical inclusions in a lipid bilayer generate an overall spontaneous curvature of the membrane that depends on concentration and geometry of the inclusions. Examples are integral and attached membrane proteins, viruses, and lipid domains. We propose an analytical model to study budding and vesiculation of the lipid bilayer membrane, which is based on the membrane bending energy and the translational entropy of the inclusions. If the inclusions are placed on a membrane with similar curvature radius, their repulsive membrane-mediated interaction is screened. Therefore, for high inclusion density the inclusions aggregate, induce bud formation, and finally vesiculation.

1484-Pos

A Comparison of the Membrane Properties of the Lipid Modifications of Proteins

Daniel Huster.
University of Leipzig, Leipzig, Germany.

Though ubiquitous in nature and relevant for ~10% of all cellular proteins, posttranslational lipid modifications of proteins show an astonishing variety. Common motifs include myristoylations, palmitoylations, prenylations, and cholesterol modifications. All these structures show characteristic membrane properties. In recent years, we have studied a number of systems and elucidated the structure and dynamics of membrane embedded lipid modifications of proteins using solid-state NMR methods. In the presentation, a comparison of the membrane properties of several systems will be given: Farnesylated/hexadecylated Ras, myristoylated GCAP, myristoylated Src, and a transmembrane model peptide featuring lipid modifications of varying lengths between 2 and 16 carbons. Membrane embedded lipid chains show a remarkable structural and dynamical variety. For instance, the 16:0 Ras lipid chain can vary its length between 8.7 and 15.5 Å to perfectly match the hydrophobic thickness of the host membrane. Also, the myristoylation of GCAP perfectly adapts to the thickness of the host membrane. In contrast, the myristoyl chain of Src exceeds the length of the host membrane lipids because of Born repulsion of the positively charged amino acids in the direct vicinity of the N-terminal myristoylation. The projected length of a lipid modification in the membrane is adjusted by the introduction of *gauche* defects, which can be precisely determined from the ^{2}H NMR data. The compression or elongation of a protein lipid chain with respect to the chains of the phospholipid host membrane is accompanied by characteristic changes of the segmental mobility, which is manifested in a distinctive correlation of ^{2}H NMR nuclear relaxation times and order parameters. Thus, in spite of fulfilling the same biological function of membrane anchoring, the structural and dynamical features of protein lipid chains are distinctly different suggesting an additional role in biology.

1485-Pos

Structure Analysis of Synaptic Vesicles by Solution Small-Angle Scattering of X-Rays

Simon Castorph[1], Matthew Holt[2], Dietmar Riedel[2], Lise Arleth[3], Michael Sztucki[4], Reinhard Jahn[2], Tim Salditt[1].
[1]Universität Göttingen, Göttingen, Germany, [2]Max Plack Institut für Biophysikalische Chemie, Göttingen, Germany, [3]University of Copenhagen, Frederiksberg, Denmark, [4]European Synchrotron Radiation Facility, Grenoble, France.

The release of neurotransmitters from neurons, in response to stimulation, forms the basis of communication in the nervous system. Neurotransmitters are stored in small membraneous organelles, synaptic vesicles (SVs), within the presynaptic terminal. These vesicles undergo an elaborate cycle of fusion with the plasma membrane (releasing neurotransmitter), followed by retrieval and reformation and transport back to the plasma membrane for further rounds of fusion [1].

In recent years there has been enormous progress in our knowledge of the molecular composition and structure of synaptic vesicles [2]. However, we still lack a detailed view of the physical properties of this trafficking organelle as it proceeds through its life-cycle.

Here we use small-angle x-ray scattering (SAXS) to determine the average radial density profile rho(r) and the size polydispersity of SVs [3]. We show that SAXS can be used to study the supra-molecular structure of an entire functional organelle under physiological conditions. The profile rho(r) of SVs including structural parameters of the protein layers, as well as the polydispersity function p(R), are derived with no free prefactors on an absolute scale. The measured SV structure on length scales between the constituent biomolecules and the SV size confirms the main aspects of recent numerical modeling [2], which was based on the crystal structures of the constituent proteins and stoichiometric knowledge from biochemical studies. In addition, we present first evidence of a laterally anisotropic structure, indicative of larger protein clusters.

[1] T. Südhof, Annu. Rev. Neurosci. **27** (2004) 509.
[2] S. Takamori *et al,* Cell **127** (2006) 831.
[3] S. Castorph *et al,* in preparation.

1486-Pos

Implications of Criticality in Membrane Bound Processes

Benjamin B. Machta, Sarah Veatch, Stefanos Papanikolaou, James Sethna.
Cornell, Ithaca, NY, USA.

Recent work in giant plasma membrane vesicles (GPMVs) isolated from living cells demonstrates that these GPMVs can be tuned with a single parameter (temperature) to criticality, not far from in vivo temperatures [1,2]. Criticality requires the fine-tuning of two parameters suggesting important biological function, and its presence resolves many of the paradoxes associated with putative lipid rafts. Here we present a minimal model of membrane inhomogeneities. We incorporate criticality using a conserved order parameter Ising model coupled to a simple actin cytoskeleton interacting through fields which act as point-like pinning sites. Using this model we make a host of experimentally testable predictions that are in line with recent published findings. At low temperatures our 'actin' fields prevent macroscopic phase separation from developing. At physiological temperatures we find inhomogeneities in the form of critical fluctuations with a length scale of roughly 20nm. Individual constituents making up these liquid domains are mobile, but the correlated regions themselves can last as long as the cytoskeleton persists. We predict anomalous diffusion of components which strongly segregate into either phase, with a length-scale given by the size of actin compartments. In addition we predict that the instantaneous shapes of the correlated regions will be fractal on short distances and can conform to and feel the effects of the cytoskeleton at larger distances without positing any further superstructures. This is explained by an effective long ranged interaction mediated by the Ising order parameter. In general we find Ising criticality organizes and spatially segregates membrane components by providing a channel for interaction over large distances.

[1] Veatch et al., ACS Chem Biol. 2008 3(5):287-93
[2] Honerkamp-Smith, Veatch, and Keller, Biochim Biophys Acta. 2008 (in press)

1487-Pos

Structure and Dynamics of Lipid-Modified Antimicrobial Peptides in Anionic and Zwitterionic Membranes Investigated by Solid-State NMR

Holger Scheidt[1,2], **Alexander Vogel**[1].
[1]Martin Luther University Halle-Wittenberg, Halle, Germany, [2]University of Leipzig, Leipzig, Germany.

The increasing prevalence of antibiotic resistant strains of bacteria necessitates the development of new antibiotic drugs, preferably operating via novel pathways to avoid cross-resistance with drugs already in use. The group of Shai and coworkers has recently proposed a new set of very short lipid-modified antimicrobial peptides showing promising properties for possible application. We investigated two of these peptides, C16-KGGK and C16-KAAK in two different lipid environments, one more resembling mammalian membranes (POPC) and the other closer to bacterial membranes (POPE/POPG 2:1). Investigations were conducted on powder-type samples at a lipid/peptide ratio of 9:1 and a temperature of 303K. First, the host membranes were investigated using ^{31}P solid-state NMR clearly showing no influence of the peptides on the lamellar membrane phase state. Information about the chain dynamics and membrane packing properties was obtained using ^{2}H solid-state NMR. Order parameters of the lipids were slightly reduced upon addition of the peptide. However, the lipid modifications generally exhibit higher order parameters than the surrounding lipids meaning that the length of the peptide lipid modifications is larger than that of the lipid acyl chains. This is in agreement with ^{1}H NMR NOESY data exhibiting interactions between amino acid side chains and phospholipids suggesting a peptide backbone location in the headgroup region of the membrane. The dynamics of the lipid modifications were investigated by means of ^{2}H R_{1Z} relaxation rates. While other lipid-modified peptides exhibit square law plots that are bent the ones obtained for the antimicrobial peptides are linear and resemble that of saturated lipids. Therefore the lipid modifications of the antimicrobial peptides are less flexible and longer than that of other lipid-modified peptides allowing the peptide backbone to be located in the lipid headgroup region.

1488-Pos

Curvature Sensing by the Epsin N-terminal Homology (ENTH) Domain Measured on Cylindrical Lipid Membrane Tethers

Benjamin R. Capraro[1], Michael C. Heinrich[1], Youngdae Yoon[2], Wonwha Cho[2], Tobias Baumgart[1].
[1]Department of Chemistry, University of Pennsylvania, Philadelphia, PA, USA, [2]Department of Chemistry, University of Illinois at Chicago, Chicago, IL, USA.

The protein epsin is believed to be involved in generating the high membrane curvature necessary for vesicle formation in clathrin-mediated endocytosis. To assess the hypothesis that membrane curvature-dependent binding underlies this function, we quantify the curvature dependence of the area density of the epsin ENTH domain bound to cylindrical membranes of adjustable curvature. By fluorescence microscopy, we observe curvature-induced repartitioning of membrane-bound ENTH between flat and highly curved membranes, in cylindrical tethers pulled from micropipette-aspirated giant unilamellar vesicles. We analyze our measurements using a thermodynamic theory and determine the first Leibler curvature-composition coupling coefficient to be reported for an endocytic accessory protein. Thus our results clearly demonstrate and quantify the curvature sensing of epsin.

We believe our method will prove useful generally in relating molecular interactions to macroscopic cell membrane remodeling.

1489-Pos

Correlation Function Analysis Corrects Artifactual Self-Clustering and Reveals Significant Co-Localization of Fceri and Lyn in Resting RBL-2H3 Mast Cells

Sarah Veatch, Ethan Chiang, David Holowka, Barbara Baird.
Cornell University, Ithaca, NY, USA.

We use pair auto- and cross-correlation functions to quantify lateral heterogeneity within the plasma membranes of intact RBL-2H3 mast cells. 5nm and 10nm gold-antibody conjugates are used to specifically label plasma membrane proteins and lipids, and these are visualized using scanning electron microscopy with backscatter detection. An automated image-processing algorithm identifies positions of gold particle centers, enabling the processing of large datasets with high particle densities. Consistent with previous studies, we find that gold particles labeling a variety of plasma membrane lipids and proteins are highly self-clustered in resting cells. In contrast to previous studies, we find that this apparent self-clustering can be accounted for by multiple gold particles binding to single target proteins with Gaussian-shaped binding surfaces. This is demonstrated by imaging antibodies covalently conjugated to a silicon surface, by comparing correlation functions for a wide range of cell surface labels with varying surface densities, and by measuring cross-correlations between identical but distinguishable pools of either IgE-FcεRI or GM1 labeled with cholera toxin B on the cell surface. After correcting for artifactual clustering, we find that all (>5) proteins and lipids examined are not auto-correlated in resting cells at physiological temperatures, within experimental error bounds. In contrast, we find significant cross-correlation between IgE-FcεRI and the inner leaflet signaling protein Lyn in these unstimulated cells, and this co-clustering is only moderately modulated when membrane cholesterol levels are altered with

MβCD. Significant large-scale self-clustering of IgE-FcεRI occurs upon cross-linking with multivalent antigen, and we describe analytical methods to correct for multiple gold binding and quantify clustering in these stimulated cells. Our correlation function particle distribution approach is likely to have wide applicability in nanoscale image analysis.

1490-Pos
Design of a Biologically Relevant Supported Bilayer Platform for the Study of Membrane Active Peptides

Janice Lin, John Szymanski, Peter C. Searson, Kalina Hristova.
The Johns Hopkins University, Baltimore, MD, USA.

Membrane active peptides represent a class of soluble proteins that interact and disrupt the plasma membrane. Examples of these include antimicrobial peptides, cancer therapeutics, and cell-penetrating peptides. These peptides are amphipathic and, in a concentration dependent manner, can self assemble to destabilize the lipid bilayer. These peptides are rich in positively charged lysine and arginine residues and thus have a strong preference for negatively charged bilayers. In order to study the insertion mechanism and kinetics of these peptides, we have designed a negatively charged, supported bilayer platform on silicon. The negative charge serves to electrostatically drive peptides to bind to the lipid bilayer interface. Furthermore, this platform is electrically addressable through electrochemical impedance spectroscopy, which yields bilayer resistance, thickness, and structural heterogeneity data. This platform consists of an asymmetrical bilayer with 10 mol% negatively charged POPS, cholesterol, and POPC in the upper leaflet and DPhPC lipids in the lower leaflet, all supported by a PEG cushion on a silicon wafer. Resistances up to $2*10^4$ Oηµ cm^2 and capacitances of 0.8 υF cm^{-2} have been measured for the platform. The high resistance allows for high accuracy in the detection of the activity of membrane active peptides of interest.

1491-Pos
***Staphylococcus aureus* Enriched in Ordered Lipids Present Resistance Towards the Antibacterial Agent sPLA$_2$-IIA: An Unusual Mechanism to Survive**

Hector Jackson Ocampo Ariza, Johanna Paola, Chavez Escobar,
Jorge L. Romero Becerra, Martha J. Vives, Chad Leidy.
Universidad de los Andes, Bogota, Colombia.

Bacterial membranes present solid-ordered/liquid-disordered (*so/ld*) cooperative melting event close to physiological temperature. The cellular advantage of this thermotropic melting event is yet to be determined. We show that this thermal behavior provides resistance towards a membrane active antibacterial agent.

Phospholipase A_2 type IIA (sPLA$_2$-IIA) is a hydrolytic enzyme which presents antibacterial properties towards Gram positive bacteria. The enzyme has higher activity in *ld* phase compared to *so* phase in anionic membranes. We show that the lipid phase behavior of Staphylococcus aureus (*S.aureus*) membranes as measured by FTIR modulates sPLA$_2$-IIA by inducing a sharp drop in activity below the melting temperature of the membrane (centered at 15.3°C).

The effects of sPLA$_2$-IIA treatment on cell viability are also investigated. While above the main melting event viability drops to 20% of the initial CFU after treatment, below the main melting event cell viability only drops to 60% under the same treatment. This strongly suggests that cells in the solid-ordered phase are better adapted to survive the enzymatic insult.

These results led us to explore if a subpopulation of *S.aureus* enriched in ordered lipids can be selected after repeated treatment with sPLA$_2$-IIA at 37°C. After selecting for resistance at 37°C we measured growth curves, membrane order, and cell viability as a function of treatment temperature. The results suggest that at 37°C there is a bacterial subpopulation with increased membrane rigidity that insures survival of the colony to an insult by sPLA$_2$-IIA. This subpopulation also presents a longer latency period which can be explained by the increased presence in ordered lipids, which are known to inhibit cell division. Even if the growth conditions are not optimal, the presence of this subpopulation ensures survival from the antibacterial insult.

1492-Pos
Lifetime of Hyaluronan Containing Tethers Obeys a Generalized Bell Model

Marius C. Staiculescu[1], Phillip Stein[1], Mingzhai Sun[2], Imre Derenyi[3],
Gabor Forgacs[1].
[1]University of Missouri Columbia, Columbia, MO, USA, [2]Lewis-Sigler Institute for Integrative Genomics, Princeton, Princeton, NJ, USA,
[3]Department of Biological Physics, Eotvos Roland University, Budapest, Hungary.

Hyaluronan (HA), an unbranched non-sulfated glycosaminoglycan, is an important component of the extracellular and pericellular matrix of various cell types. It has key roles in many biological processes such as wound healing, angiogenesis, embryonic development, tumor progression and invasion. HA is especially abundant around tumor cells in malignant gliomas where it is associated with high invasivity and a poor prognosis. However it is unknown how malignancy is correlated with the biomechanical properties of the cellular glycocalyx and the lifetime of the chemical bonds formed by HA with its ligands. Here we introduce a method applicable to the study of biophysical properties of cellular glycocalyx through tether extraction. Specifically, we reveal the extent of the cellular ECM of a glioma cell line (HB), we demonstrate that tethers formed through non specific binding can be pulled from the cellular glycocalyx and by using a magnetic tweezers we determine the lifetime of these tethers. To calculate lifetime we simultaneously extract multiple tethers under constant force using paramagnetic beads as force transducer. We demonstrate that the stochastic lifetimes of these tethers and thus the bonds they are associated with are exponentially distributed and can be parametrized by a generalized Bell model. We determine the maximum likelihood estimates of the relevant parameters, such as force-free dissociation constant and reactive compliance. We test the consistency of our approach using computer simulations. This method could be employed in the development of therapies which interfere with HA organization and HA-receptor binding.

1493-Pos
Analytical Derivation of Thermodynamic Properties of Bolalipid Membrabe

Sergei I. Mukhin, Boris B. Kheyfets.
Moscow Institute for Steel and Alloys, Moscow, Russian Federation.

A model of bilayer lipid membrane with bola-lipids is studied. The bola-lipid is modeled by linking tails of the hydrophobic chains in the opposite monolayers within bilayer. We use for analytical derivations a flexible string model of hydrocarbon chain (Mukhin, Baoukina 2005) with modified condition at the linked chains ends. Calculated lateral pressure profiles are asymmetrical due to different concentrations of the U-shaped bolalipids in the opposite monolayers, Fig. 1, and orientational order parameters for linked and regular chains differ significantly at the monolayers interface, Fig. 2.

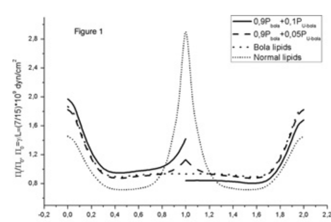

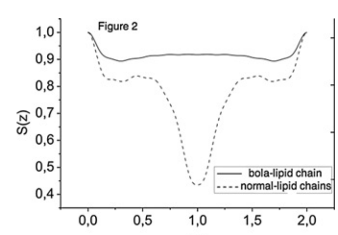

1494-Pos
Highly Stable Poly(Lipid) Bilayers for Long-Term Ion Channel Recordings

Benjamin A. Heitz, Robert P. Cordero, S. Scott Saavedra,
Craig A. Aspinwall.
University of Arizona, Tucson, AZ, USA.

Long-term ion channel (IC) screening using cell-based assays is currently limited by throughput and cell to cell variability. ICs isolated and reconstituted into suspended lipid membranes offer an isolated view into IC structure and function, but IC recordings are limited by the short lifetime of the bilayer. Polymerizable lipids (poly(lipids)) offers one potential strategy for long-term

investigation and screening of ICs and has been investigated with several model ion channels.
The electrical properties and stability of lipid bilayers suspended across glass micropipettes compared natural and polymerized lipids. Breakdown voltage, capacitance, and conductance of the several pure and mixed polymerizable/non-polymerizable lipid bilayers were determined using a patch clamp apparatus.
Using, polymerizable phospholipids, we have synthesized membranes with markedly enhanced lifetimes from ca. 3 hours to upwards of 3 weeks. These poly(lipid) bilayers have been used to monitor IC activity of alpha-hemolysin for ca. 1week before loss of alpha-hemolysin. However, poly(lipid) bilayers are rigid and do not support the function of ICs that require membrane fluidity, To address this limitation, binary bilayers composed of poly(lipids) and non-polymerizable lipids were investigated. The resulting mixed bilayers demonstrate markedly enhanced long term stability compared to non-polymerized bilayers and facility IC studies. Alamethicin, a model for voltage-gated ion channels, was shown to be non-functional when reconstituted into homogeneous poly(lipid) bilayers, whereas reconstitution in to mixed bilayers revealed alamethicin activity that and enhanced membrane stability.
A functional, truncated form of the K_{ATP} channel complex, 6xHis-EGFP-Kir6.2d26, was chosen as a model ligand-gated IC, expressed and purified from yeast. Long-term goals are to reconstitute the truncated version of K_{ATP} channels into polymerizable and non-polymerizable bilayers using varying strategies into biomimetric sensing platforms screening ligands and drug candidates for activity.

1495-Pos
Solid-Supported Bilayer Lipid Membranes from Lipid Mixtures: Structure and Composition
Prabhanshu Shekhar[1], Frank Heinrich[1,2], Hirsh Nanda[2], Mathias Loesche[1,2].
[1]Physics Dept, Carnegie Mellon University, Pittsburgh, PA, USA, [2]NIST Center for Neutron Research, Gaithersburg, MD, USA.
Biological membranes are of overarching importance for all aspects of cell structure and function in living organisms. Planar tethered bilayer lipid membranes (tBLMs) are synthetic membrane models stabilized by the proximity of a solid substrate that enhances its long-time stability by orders of magnitude.[1,2] A nanometer-thin hydration layer between the bilayer and the substrate ensures that the biomimetic lipid membrane remains fluid with in-plane lipid dynamics similar to that in vesicles.[3] In this work we establish tBLMs composed of binary and ternary lipid mixtures as more complex, and hence more realistic, membrane models. Such membranes may be used for studies of protein-membrane interactions.[4] Biophysical properties of mixed tBLMs vary significantly with bilayer composition. We report a structural and compositional characterization by neutron reflectometry of tBLMs that comprise various lipid compositions including cholesterol. With specific deuteration of selected bilayer components, such studies enable the determination of volume fractions of individual lipid species in the asymmetric tBLM. A new composition-space model was developed to interpret neutron reflectivity data of such systems. This model enables for the first time to extract more detailed information about the bilayer leaflet proximal to the substrate and lets us explore in more detail the distribution of lipid components across the bilayer. Such a detailed structural and compositional assessment is the prerequisite for more detailed studies of the association of amyloid-beta oligomer particles with membranes in studies on the origin of Alzheimer's disease.[4]
Supported by the NIH (1P01AG032131) and the AHAF (A2008-307).
[1]D.J. McGillivray, et al.2007. Biointerphases 2:21-33.
[2]F. Heinrich, et al. 2009. Langmuir 25:4219-4229.
[3]S. Shenoy, et al. 2009. Soft Matter, submitted.
[4]G. Valincius, et al., 2008. Biophys. J. 95:4845-4861.

1496-Pos
Condensing and Fluidizing Effects of Gangliosides on Various Phospholipid Films
Matthew T. Davidson, **Shelli L. Frey**.
Department of Chemistry, Gettysburg College, Gettysburg, PA, USA.
In model membrane mixtures that mimic lipid raft compositions, the more ordered domains are enriched in the ganglioside, G_{M1}, which contains four neutral sugars and a negatively charged sialic acid. To understand the organization and partitioning of G_{M1} in cell membranes, the outer leaflet of the cell membrane was modeled using Langmuir monolayers of DPPC and varying concentrations of G_{M1}. At low biologically relevant concentrations, G_{M1} condenses the DPPC monolayer while at higher concentrations, it fluidizes, with a switch-over point between the two behaviors at a ratio of 3:1 DPPC:G_{M1}. Atomic force microscopy performed on deposited monolayers indicated that G_{M1} is located in nanoscale clusters within the condensed DPPC domains. The total surface area of these nanosize domains is larger than that attributable to G_{M1} molecules alone, suggesting the regions are due to G_{M1} and DPPC packing preferentially in condensed complexes due to variations in molecular geometry.
To further study this effect, geometry of the phospholipid was varied. The zwitterionic lipid, 1,2-dimyristoyl-*sn*-glycero-3-phosphoethanolamine (DMPE), with its smaller headgroup cross-sectional area compared to DPPC, was combined with various ratios of G_{M1}. Additivity plots constructed for the mixtures to show deviations from ideal mixing indicated a 3:2 DMPE:G_{M1} ratio was most condensed compared to the individual components. Molecular geometry of the phospholipid headgroup plays a role in the condensation effect of G_{M1} on neighboring phospholipids. Additional experiments on certain monolayer mixtures of 1,2-dilauroyl-*sn*-glycero-3-phosphoethanolamine (DLPE) and G_{M1}, components that are each fluid in pure monolayers, showed formation of condensed domains. This indicates the condensation effect of G_{M1} is strong enough to induce biologically relevant ordering phase transitions. Results will also be shown from experiments combining phospholipids containing negatively charged phosphatidylglycerol headgroups with G_{M1} to show the effect of electrostatic repulsion on the induced condensation.

1497-Pos
Determining the Water Content of Lipid Membranes by Neutron Diffraction
Ella Mihailescu[1], David Worcester[2], Francisco Castro-Roman[3], Monica Fernandez-Vidal[1], Stephen H. White[1].
[1]University of California, IRVINE, CA, USA, [2]University of Missouri, Columbia, MO, USA, [3]CINVESTAV-IPN, Departamento de Física, Mexico DF, Mexico.
Knowledge of the structure of fluid lipid bilayers is essential for understanding complex biological phenomena in cellular membranes. Water, in particular, is an important component of the membrane since membrane proteins anchor and function in cellular membranes through interactions with water and lipid polar headgroups. Here we present an experimental method to determine directly the content of water in a membrane, at thermodynamic equilibrium with its environment, which does not require knowledge of the density of water. Neutron diffraction and specific lipid deuteration is employed to determine the number of waters in a unit cell (lipid alone or lipid/peptide and lipid/cholesterol mixtures) of oriented lipid multilayers hydrated from water vapor phase, under various humidity conditions. Having determined the number of deuterium atoms per lipid by Mass Spectroscopy, the number of water molecules per lipid can be determined with high precision by neutron diffraction, using the content of deuterium in the sample as a calibration measure. The number of water molecules per unit cell will be presented for a few lipid types (phosphocholines or charged-headgroup lipids), and compared with results obtained by other methods. The extent to which the water held in a membrane is altered by the presence of cholesterol or a voltage-sensing trans-membrane peptide will be demonstrated.

1498-Pos
Observation of Intermediates in Lamellar to Cubic Phase Transformations of Lipid Nanoparticles
Xavier Mulet[1], Xiaojuan Gong[2,3], Lynne J. Waddington[4], Calum J. Drummond[1,5].
[1]CSIRO Molecular and Health Technologies, Clayton , VIC, Australia, [2]CSIRO Molecular and Health Technologies, North Ryde, NSW, Australia, [3]School of Chemistry, F11, The University of Sydney, Sydney University, Australia, [4]CSIRO Molecular and Health Technologies, Parkville, VIC, Australia, [5]CSIRO Materials Science and Engineering, Clayton, VIC, Australia.
Self-assembled lipid systems have recently come to prominence in medical applications as potential carriers for a range of bioactive agents (1); these include medical imaging, therapeutic compounds. One of their primary advantages is versatility as they can be adapted to different agents and target sites. During the preparation of cubic phase lipid nanoparticulate dispersions, we observed the presence of new intermediates during the transition from the fluid lamellar lyotropic phase to the cubic phase. This phase transition is regarded as a model for membrane-fusion processes(2). Many organelles demonstrate highly ordered cubic membrane structures. Determining the mechanistic origins of such lipid organelle complexity has been elusive.
We increased the lifetime of very short-lived non-equilibrium intermediate structures by the use of steric stabilizer in the dispersions. These structures were characterized using synchrotron small-angle X-ray scattering and

cryo-transmission electron microscopy. We visualised the intermediate initial bilayer contacts and stalk formation, followed by pore development, pore evolution into 2D hexagonally packed lattices, and finally creation of 3D bicontinuous cubic structures (3).
In a biological context, the experimental corroboration of transitional lipid self-assembly structures furthers the understanding of organelle morphogenesis and maturation.
The ability to manipulate intermediate structures in nanoparticulate dispersions of self-assembled structures may provide a unique system for encapsulation and controlled release of bioactives. The capability to control intermediate transformations may also permit the development of flexible growth media for applications such as in-cubo integral membrane protein crystallization or liquid crystal templating of nanostructured materials.
1.Drummond, C.J.; et al., Current Opinion in Colloid & Interface Science 1999, 4, (6), 449-456.
2. Conn, C.E.; et al., Physical Review Letters, 2006, 96, (10), 108102
3. Mulet X., et al., ACS Nano, 2009, 3 (9), 2789-2797

1499-Pos
Native Pulmonary Surfactant Membranes in Mice Show Coexistence of Two Different Phases in Bilayers and Monolayers: When the Lipid Composition can Predict the Structural Phase Segregations
Jorge Bernardino de la Serna, Søren Hansen, Hans K. Hannibal-Bach, Uffe Holmskov, Adam C. Simonsen, Jens Knudsen, Luis A. Bagatolli.
University of Southern Denmark, Odense, Denmark.
Pulmonary surfactant is a surface active material composed both of lipids (aprox. 90% by weight) and proteins (aprox. 10%) produced by type II pneumocyte cells in the alveoli. This tension-active material forms a unique air-liquid interface at the alveolar cell surface that reduces surface tension close to 0 mN/m and maintains lung volumes and alveolar homeostasis at the end of the expiration. There are four pulmonary surfactant proteins (SP-A, -B, -C and -D). SP-A and -D have an important role in the immunological response against pathogens. The particular lipid composition of the lung surfactant suggests that surfactant mono- and bi-layer-based structures could exhibit lateral phase segregation at physiological temperatures. This work shows that in native pulmonary surfactant membranes a close lipid compositional study is crucial to understand the structure and biophysical function of these complex mixtures. Observing Giant Unilamellar Vesicles under conventional and two-photon excitation microscopy allow us to characterize and quantify the coexistence of two fluid-like phases in the wild-type (wt) native pulmonary surfactant membranes and a gel/fluid-like segregation pattern in the Knocked-out protein D (KOD) membranes. The atomic force microscopy studies of supported Langmuir-Blodgett bilayers and monolayers at different surface pressure show the same phase pattern before the collapse surface pressure of native pulmonary surfactant (~40mN/m). Above this surface pressure different protruded structures can be observed arising from the more fluid phases. A closer look at the lipid composition reveals a higher content of saturated phospholipid species in the KOD native pulmonary surfactant membranes. This last finding explain the coexistence phenomena observed and allow us to conclude that the pulmonary surfactant segregation pattern could be predicted by an accurate lipid compositional study.

Membrane Receptors & Signal Transduction I

1500-Pos

WITHDRAWN.

1501-Pos
Quantitative GPCR Assay Using Time-Resolved Fret
Adam M. Knepp, Thomas P. Sakmar, Thomas Huber.
www.sakmarlab.org, Rockefeller University, New York, NY, USA.
Quantitative study of membrane proteins presents considerable technical challenges. Here, we report a time-resolved fluorescence resonance energy transfer (TR-FRET) assay to quantify functional Chemokine (C-C motif) Receptor 5 (CCR5). CCR5 is a seven-transmembrane helical G protein-coupled receptor (GPCR) expressed primarily on immune cells. It is of significant interest due to its role as the co-receptor of R5-tropic HIV-1. The TR-FRET assay exploits energy transfer between a long-lived europium cryptate donor fluorophore and an appropriate acceptor. We have developed a homogeneous sandwich-type immunoassay with labeled antibodies against a conformationally-sensitive epitope on the extracellular domain of CCR5 and an engineered C-terminal 1D4-mAb epitope. The assay yields a quantitative FRET signal corresponding to the total amount receptor. To quantitate ‘‘functional’’ receptor, a labeled anti-HA (hemagglutinin) antibody against an engineered N-terminal HA epitope is used in conjunction with labeled MIP-1a, a chemokine ligand for CCR5. We are also interested in quantifying the degree of chemical labeling of unnatural amino acids incorporated into expressed GPCRs by amber codon suppression technology. The Staudinger-Bertozzi ligation links a commercially-available FLAG-phosphine reagent to p-L-azidophenylalanine. A europium-labeled anti-FLAG antibody can then be used in another version of the sandwich assay. The resulting FRET signals are directly proportional to amount of total, functional, and labeled receptor, but must be calibrated precisely to extract an absolute concentration. Calibration is accomplished by measuring binding of a fluorescent derivative of a small-molecule CCR5 antagonist. The assay is highly specific due to the long lifetime of the europium donor, and nanomolar concentrations of receptor are detectable. This GPCR assay technology can be used to optimize CCR5 reconstitution conditions and can be readily extended to other members of the chemokine receptor family.

1502-Pos
Effects of Sensory Rhodopsin II Complexation with its Cognate Transducer HtrII on the Local Environment of Internal Water Molecules
Mikkel Jensen[1], **Erica C. Saint Clair[1]**, Alan Gabel[1], Vladislav B. Bergo[1], Elena N. Spudich[2], John L. Spudich[2], Kenneth J. Rothschild[1].
[1]Boston University, Boston, MA, USA, [2]University of Texas Medical School, Houston, TX, USA.
Recent studies indicate that internal water molecules play a critical role in membrane protein function. Here we report evidence that the local environment of one or more internal water molecules in sensory rhodopsin II (SRII) is altered by interaction with its cognate transducer HtrII. The SRII-HtrII complex mediates blue-light repellent phototaxis in halophilic archaea, using a signaling pathway similar to that in bacterial chemotaxis. We studied the photocycle of SRII and a SRII-HtrII fusion complex from *Natronobacterium pharaonis* using low-temperature static and room temperature time-resolved Fourier transform infrared (FTIR) difference spectroscopy. When cooled to 80 K, and illuminated the protein is trapped in its K state. A shift of 2 cm^{-1} between SRII (3626 cm^{-1}) and SRII-HtrII (3628 cm^{-1}) is found for a negative OH stretching band assigned to an internal water molecule, most likely located near the active Schiff base. In contrast, the OH stretching band for this water in the K state appears at the same frequency (3619 cm^{-1}) for both the free and complexed receptor. Similar shifts are observed upon hydration with H_2O^{18} shifted to a lower frequency confirming these bands arise from the OH stretching mode of water. Data are also presented on the effects of lipid environment on structural changes of internal water molecules and the receptor-transducer interactions. This work was supported by National Institutes of Health Grants
R01GM069969 (to K.J.R.) and R37GM27750 (to J.L.S.), U.S. Department of Energy Grant DE-FG02-07ER15867, and the Robert A. Welch Foundation (to J.L.S.).

1503-Pos
Exploring the Mechanics and Energetics of Epidermal Growth Factor Receptor Activation
Marco Cavalli, Marco Ceruso.
The City College of New York, New York, NY, USA.
The activation of epidermal growth factor receptor (EGFR) is a complex molecular process. To date, because of technical limitations in dealing with a full-length receptor construct, our understanding of this process comes from structural and biochemical studies of isolated fragments of the receptor. Here we seek detailed molecular insight into the activation process of EGFR in the context a full-length receptor construct. To be able to handle computationally such a large protein (~1000 amino acids) we have developed ELNEDIN: a coarse-grained modeling approach that can describe reliably the dynamics and interactions of proteins. We have built full-length models of human EGFR in the active (extended) and inactive (tethered) states. The models include explicit representations of the lipid membrane and aqueous environments. The conformational space of the tethered and extended state at equilibrium was sampled extensively in the microsecond time scale using a combination of classical molecular dynamics and enhanced sampling techniques. Using these enhanced sampling techniques we have also generated paths that describe the transition from the tethered to the extended state, i.e. the activation of the receptor. These paths have yielded a clear molecular picture of the sequence of conformational changes that lead to activation of EGFR. This picture is remarkably consistent with that derived from experimental approaches, but it also provides new insights into the activation process. Notably, it shows how the conformational changes that occur on the extracellular side of the membrane affect the structure dynamics of the intracellular components of the receptor. Finally, the free-energy surface associated the activation was obtained

and a putative model for the transition state is proposed. This information can now be used to rationalize the energetic and conformational effects of oncogenic mutations and the binding of antibodies.

1504-Pos
Oligomerization of Membrane Receptors: FRET Analysis Using Coiled-Coil Tag-Probe Labeling and Spectral Imaging

Yoshiaki Yano, Kaoru Omae, Katsumi Matsuzaki.
Kyoto University, Kyoto, Japan.

Oligomerization of membrane receptors in living cell membranes plays an important role in regulation of receptor activity and trafficking. Förster resonance energy transfer (FRET) techniques are often employed to detect receptor oligomerization using receptors fused with fluorescent/luminescent proteins. However, the large size of fluorescent proteins often interferes localization and function of target receptors. Furthermore, controlling the labeling ratio (donor/acceptor), which is important for analysis of FRET, is usually difficult when two fusion receptors with different colors are co-expressed. Posttranslational labeling methods using a short tag peptide and a fluorescent probe that specifically binds to the tag enable a smaller size of label and easy control of labeling ratio in multicolor labeling [1,2]. We recently developed a quick (< 1 min) and surface-specific tag-probe method using a high-affinity heterodimeric coiled-coil formation between the E3 tag (EIAALEK)3 attached to the target receptor and the Kn probes (KIAALKE)n (n = 3 or 4) labeled with a fluorophore [3]. Here we examine oligomerization of the metabotropic glutamate receptor (mGluR) using this novel technique. The receptors were labeled with Rhodamine Green (donor) or Tetramethylrhodamine (acceptor) fluorophores. A constant FRET signal was observed for mGluRs transiently expressed in CHO cells, indicating constitutive oligomer formation. Spectral imaging and demixing of emission spectra abolish crosstalk between channels that is inevitable in conventional filter detection therefore simplify quantification of FRET efficiency from sensitized acceptor emission, allowing analysis of stoichiometry of the oligomerization.

[1] Murel et al. Nat. Mathods (2008) 5, 561-567.
[2] Meyer et al. PNAS (2006) 103, 2138-2143.
[3] Yano et al. ACS Chem. Biol. (2008) 3, 341-345

1505-Pos
How does the State of Aggregation of Rhodopsin in Retinal Discs Influence the Variability of its Activated Life Time?

Samuel A. Ramirez, Chad Leidy.
Universidad de los Andes, Bogota, Colombia.

Single photon responses (SPRs) in the retinal rod are less variable than expected assuming that deactivation of the receptor rhodopsin (R*) occurs in a single memoryless step. It has been suggested that SPRs reproducibility can be explained by a sequential increase of affinity of R* to the protein involved in its deactivation arrestin (Arr) which leads to a reduction in the life-time variability of R*. This increase in affinity is promoted by a serial phosphorylation of rhodopsin catalyzed by rhodopsin- kinase (RK).
This deactivation mechanism has been tested successfully by means of stochastic simulation assuming rapid diffusion of all signaling molecules. However, evidence suggests that, in native rod discs, rhodopsin is found forming dimers organized in paracrystalline arrays covering about half of the membrane surface.
In this work, we test the hypothesis that packing induced crowding effects, in conjunction with the competitive interactions between R* an the other proteins involved in the signaling cascade (G protein (G), RK, and Arr) will influence the variability of the half-time of R*. In particular, we explore whether the local decrease of inactivated G around R* (as it becomes activated by R*) facilitates interactions of the receptor with Arr and RK, increasing the probability of R* deactivation. This would then lead to a reduction in its trial to trial variation.
In order to explore these issues, we implement a mesoscopic Monte Carlo simulation in a two-dimensional grid representing the membrane, and follow the stochastic encounters and reactions between the species involved in the signal cascade. We perform the simulations and present data on the variability of the half life of R* under two scenarios: rapid diffusion of all proteins, and immobile paracrystalline arrays of rhodopsin.

1506-Pos
Comparative Interaction of Tricyclic Antidepressants and Mecamlyamine with the Human $\alpha4\beta2$ Nicotinic Acetylcholine Receptor

Joringel F. Kaiser[1], Katarzyna M. Targowska-Duda[2], Dominik Feuerbach[3], Krzysztof Jozwiak[2], Hugo R. Arias[1].
[1]Midwestern University, Glendale, AZ, USA, [2]Medical University of Lublin, Lublin, Poland, [3]Novartis Institutes for Biomedical Research, Basel, Switzerland.

We compared the interaction of tricyclic antidepressants (TCAs) with that for the noncompetitive antagonist mecamylamine with the human (h) $\alpha4\beta2$ nicotinic acetylcholine receptor (AChR) in different conformational states, by using functional and structural methods. The results established that: **(a)** TCAsinhibit ($\pm$)-epibatidine-induced Ca^{2+} influx in HEK293-h$\alpha4\beta2$ cells with potencies that are in the same concentration range (IC_{50} = 2.2-6.8 μM) as that for mecamylamine (IC_{50} = 3.0 $\pm$ 0.7 μM), **(b)** [^{3}H]imipramine binds to a single binding site located in the h$\alpha4\beta2$ AChR ion channel with relatively high affinity (K_d = 0.83 $\pm$ 0.08 μM), **(c)** TCAsinhibit [^{3}H]imipramine binding to h$\alpha4\beta2$ AChRs with affinities (K_i = 1.0-2.1 μM) higher than that for mecamylamine (K_i = 143 $\pm$ 31 μM), **(d)** imipramine and mecamylamine do not differentiate between desensitized and resting AChRs, **(e)** imipramine interacts with the desensitized AChR mainly by an entropy-driven process, whereas the interactions with the resting AChR are mediated by a combination of enthalpic and entropic components, and **(f)** neutral imipramine and mecamylamine interact with a domain formed between the leucine (position 9') and valine (position 13') rings by van der Waals contacts, whereas protonated mecamylamine interacts electrostatically with the outer ring (position 20'). Our data indicate that although TCAs interact with a binding domain located between the leucine and valine rings, and mecamylamine predominantly acts at the outer ring and by intercalating between two M2 segments, both drugs may efficiently inhibit the ion channel.

1507-Pos
Common Dynamic Behavior of Inactive G-Protein Coupled Receptor Structures for Diffusible Ligands

Juan Carlos Mobarec, Marta Filizola.
Mount Sinai School of Medicine, New York, NY, USA.

The crystal structures of three different family A G-protein coupled receptors (GPCRs) for diffusible ligands, i.e., engineered forms of human β2-adrenergic (B2AR) and adenosine A2A receptors (A2AR), as well as a turkey β1-adrenergic receptor (B1AR) mutant, have recently become available in the literature. Although the overall helical-bundle topology is conserved among these three inactive GPCR structures, several differences emerge from their comparison, particularly at TM1, the extracellular region, the cytoplasmic side of helices TM5-TM7, the ligand-binding pocket, and the long loop regions. Although one cannot exclude the possibility that crystallographic artifacts may be causing some of these structural differences, it remains to be addressed whether these different GPCR structures would share a common dynamic behavior during molecular dynamics simulations in an explicit lipid-cholesterol-water environment. The results of nanosecond-scale simulations of ligand-free inactive crystallographic forms of B2AR, B1AR, and A2AR were analyzed in terms of inter-residue contact variability over time. Contacts that remained in place during most of the simulations were recognized as stable contacts. Among them, the most stable contacts were found to be common among the three GPCR structures, and to involve residues that are conserved among family A GPCRs. We propose that these stable contacts define a common dynamic behavior of inactive GPCR structures for diffusible ligands, and are therefore important for keeping the receptors in an inactive state.

1508-Pos
Protonation Switches in GPCR Activation: Physiologically Significant Rhodopsin Photointermediates

James W. Lewis[1], Karina Martinez-Mayorga[2], Istvan Szundi[1], David S. Kliger[1], Michael F. Brown[3].
[1]University of California, Santa Cruz, Santa Cruz, CA, USA, [2]Torrey Pines Institute for Molecular Studies, Port Saint Lucie, FL, USA, [3]University of Arizona, Tucson, AZ, USA.

Rhodopsin is a paradigm for GPCRs, yet unlike other class A members, its bound chromophore's UV/vis absorbance provides excellent time-resolved information about GPCR activation steps. At least three species equilibrate on the millisecond time scale after rhodopsin photoexcitation in a membrane lipid environment. The first equilibrium is pH-independent and involves Meta I_{480}, the visible absorbing, protonated Schiff base (PSB) species, and Meta IIa, the UV absorbing, deprotonated SB species. The second equilibrium, involving spectrally silent proton uptake by Meta IIa to produce Meta IIb, accounts for the fact that low pH causes anomalous disappearance of the protonated SB species, Meta I_{480}. The equilibria affect production of the G protein-activating species R* and are of great interest. However they must be studied promptly because inactivation steps follow, and long illumination increases secondary photolysis of photoproducts. We used time-resolved absorbance measurements of bovine rhodopsin on the microsecond-to-hundred millisecond

time scale to study kinetics of lumirhodopsin decay and the effect of membrane environment on the first equilibrium constant, K_1, and on the pK_a of the second equilibrium. Reconstituted membranes of rhodopsin with POPC, DOPC, or a mixture of DOPC and DOPE were studied at 30°C. We also extended previous 20°C studies of the pH dependence of the equilibria in the native disk membranes, to determine how increased temperature affects lumirhodopsin decay through the purely transient 380 nm absorbing species, Meta I_{380}, into the final equilibrium mixture. Meta I_{380} has recently attracted substantial interest, since time-resolved circular dichroism measurements on the microsecond timescale suggest the chromophore has a different conformation than in later 380-nm photointermediates. Our results suggest SB deprotonation precedes other activating changes in the protein. Significant details are now emerging that give new insights into rhodopsin activation and complement FTIR and spin-label approaches.

1509-Pos
Multi-Scale Dynamics of Rhodopsin Activation as a Paradigm for GPCR Function

Blake Mertz, Andrey V. Struts, Michael F. Brown.
University of Arizona, Tucson, AZ, USA.

G-protein coupled receptors (GPCRs) are membrane proteins that act as signaling cascade initiators responsible for a myriad of cellular processes. Ligand binding causes GPCR conformational changes that allow the receptor to interact with its cognate G-protein. Several techniques have structurally characterized rhodopsin photointermediates, but none have directly revealed the protein dynamics.Here we report a model whereby ps-ns ligand dynamics are coupled to the μs-ms protein motions during activation. These protein motions represent activated conformational substates on a hierarchy of time scales. Previous models propose that rhodopsin activation is a simple switch whereby retinal isomerizes from an 11-*cis* to an *all-trans* conformer, transforming from an inverse agonist to an agonist. In contrast, our model is motivated by FTIR and UV-visible results showing thermodynamic coupling to several substates in rhodopsin activation (metaI, metaII$_a$, and metaII$_b$) [1]. Furthermore, new ^{2}H NMR data from selectively labeled retinal ligands bound to rhodopsin are able to show that each retinylidene methyl group, especially the C9-methyl, acts as a dynamical hotspot in the activation pathway [2]. Relaxation times are fitted to three-fold jump and continuous diffusion models and correlated to methyl rotation rates in the different rhodopsin activation states, revealing distinct site-specific characteristics for each photointermediate. Recent solid-state NMR [3] and EPR [4] studies showed appreciable protein movements in the photointermediate pathway, further supporting our data. An activation mechanism emerges whereby conformational substates depend on a multivariate energy landscape encompassing retinal and protein dynamics as well as lipid bilayer interactions. [1] M. Mahlingam *et al*. (2008) *PNAS*105, 17795-17800. [2] M.F. Brown *et al.* (2009) *BBA*, in press. [3] S. Ahuja *et al*. (2009) *J. Biol. Chem.*284, 10190-10201. [4] C. Altenbach *et al*. (2008) *PNAS*105, 7439-7444.

1510-Pos
Consequences of Fast, Stochastic Rhodopsin Shutoff for a Model of Phototransduction in Rods

Owen P. Gross, Edward N. Pugh, Marie E. Burns.
Univ. of California, Davis, Davis, CA, USA.

Rod photoreceptors signal the number and timing of photon absorption, a property that requires that each single photon response be of similar amplitude from trial to trial. How such reproducibility is achieved has been the subject of much experimental and theoretical work, which has demonstrated the importance of multiple steps in rhodopsin deactivation and diffusion of second messengers (Mendez et al., 2000; Bisegna et al., 2008). So far, all previous models have assumed that rhodopsin lifetime is significantly longer than recent measurements indicate (Krispel et al., 2006; Burns and Pugh, 2009). Additionally, recent biochemical studies have provided new details about the dependence of rhodopsin deactivation on phosphorylation level (Vishnivetskiy et al., 2007) that should inform a complete model of light response kinetics and reproducibility. We have implemented a spatio-temporal model of phototransduction in which the rhodopsin deactivation scheme is a stochastic multi-step process lasting no more than 50 ms. The parameters of this model were constrained using an extensive data set obtained from a variety of transgenic mouse lines, each developed to perturb rhodopsin activity, PDE deactivation, or Ca^{2+} feedback. Our simulations demonstrate the relative contributions of stochastic rhodopsin deactivation, Ca^{2+} feedback to guanylate cyclase, and second messenger diffusion to single photon response variability under biologically relevant constraints.

1511-Pos
Functional Structures of Photo-Activated Rhodopsin Disk Membranes Using Single Particle Tracking

Sebastian Haase, Tai-Yang Kim, **Ulrike Alexiev**.
Freie Universitaet Berlin, Berlin, Germany.

Heterotrimeric G-proteins interact with their G-protein coupled receptors (GPCRs) via key binding elements comprising the receptor-specific C-terminal segment of the alpha-subunit and the lipid anchors at the alpha-subunit N-terminus and the gamma-subunit C-terminus. Direct information about diffusion and interaction of GPCRs and their G-proteins is mandatory for an understanding of the signal transduction mechanism. By using fluorescence microscopy and single particle tracking we showed that the encounters of the alpha-subunit C-terminus with the GPCR rhodopsin change after receptor activation revealing inhomogeneous and restricted diffusion of the receptor (1). To obtain further information about the underlying membrane structure in the signaling state of rhodopsin we now constructed high-resolution transducin visits maps on rhodopsin disk membranes using the inherent information from the single molecule traces.

(1) Kim, T.Y., Uji-i, H., Moeller, M., Muls, B., Hofkens, J. and Alexiev, U. *Biochemistry* 48, 3801-3803(2009)

1512-Pos
Molecular Dynamics Simulations of Active Receptor-G Protein Complex in a Lipid Bilayer

Thomas Huber, Parag Mukhopadhyay, Thomas P. Sakmar.
www.sakmarlab.org, Rockefeller University, New York, NY, USA.

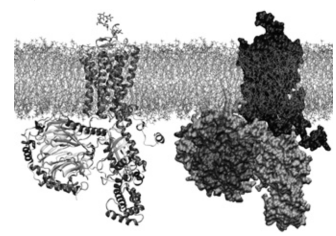

The crystal structure of opsin in its putative active state, the G-protein interacting conformation (Ops*-$G_t\alpha CT_{K341L}$), is arguably the most important breakthrough since the reports of structures for ground-state rhodopsin and the β_2-adrenergic receptor. We use this structure as a template and propose a structural model of the complex with full-length transducin (Ops*-$G_t\alpha\beta\gamma$) based on additional experimental structures including dark-state rhodopsin and holotransducin (Gt, $G_t\alpha\beta\gamma$•GDP). We dock Gt with a reconstructed model of C-terminal α5 helix of $G_t\alpha$ to the open binding site in Ops*. Our model differs from others that propose a requirement for a 40°-tilt of $G_t\alpha\beta\gamma$ relative to the α5 helix in order to avoid steric clashes between $G_t\beta\gamma$ and the membrane. We further report a new method based on grid potentials to embed the complex into a POPC bilayer membrane. Compared with our previous molecular dynamics (MD) studies of the inactive states of rhodopsin[1] and β_2-adrenergic receptor,[2] these new simulations shed light on the role of the protonation state of the opsin residues K296(7.43) and E134(3.49) in stabilizing the receptor-G-protein complex. 1) T.Huber, et al. (2004) Biophys.J. 86:2078-2100. 2) T.Huber, et al. (2008) Biochemistry 47:11013-11023.

1513-Pos
Studying the Diffusion Characteristics of Different Activity States of the Human Adenosine-A3 Receptor Using Fluorescence Correlation Spectroscopy

Ross Corriden, Leigh Stoddart, Stephen Briddon, Stephen J. Hill.
University of Nottingham, Nottingham, United Kingdom.

The adenosine-A_3 receptor is one of four known G-protein coupled receptors activated by the nucleoside adenosine. Here we use fluorescence correlation spectroscopy (FCS) in conjunction with pharmacological and molecular biology approaches to investigate the diffusion characteristics of different activity states of the human A_3-receptor. Initial FCS experiments using Chinese hamster ovary (CHO) cells expressing the wild type human A_3-receptor and the fluorescent adenosine receptor antagonist XAC-X-BY630 revealed both fast and slow moving complexes at the cell membrane, with average diffusion co-efficients of 1.58 ± 0.16 μm^2/s (τ_{D2}) and 0.081 ± 0.007 μm^2/s (τ_{D3}), respectively. At concentrations of XAC-BY630 ranging from 1-10 nM the amount of τ_{D3}, but not τ_{D2}, increased in a concentration-dependent manner. Pre-incubation of cells with the A_3-receptor specific antagonist MRS1220 at concentrations ranging from 0.3-300 nM significantly reduced the amount of slow moving (τ_{D3}) complexes in a concentration-dependent manner, indicating that they represent receptor bound ligand. Parallel experiments in which CHO cells were transfected with GFP tagged wild-type A_3-receptor (wt), a G-protein uncoupled mutant (W243A, W243F), or a constitutively active

mutant (R108A) were performed to investigate the diffusion characteristics of these ‘inactive’ and ‘active’ states of the A_3-receptor. One slow moving complex was identified at the cell membrane of wild-type A_3-GFP transfected cells, with a diffusion co-efficent (0.087 $\mu m^2/s$) similar to that of τ_{D3} for the XAC-X-BY630; similar complexes were identified in the mutant A_3-receptor cell lines.We have subsequently used FCS in conjunction with fluorescent agonist and antagonist A_3-receptor ligands to compare the ligand binding and diffusion properties of these different activity states of the receptor at the subcellular level.

1514-Pos

Computational Insight into the Ligand-Induced Conformational Specificity of G-Protein Coupled Receptors

Davide Provasi, Juan Carlos Mobarec, Marta Camacho Artacho, Marta Filizola.

Mount Sinai School of Medicine, New York, NY, USA.

Several observations in the G-protein coupled receptor (GPCR) literature support the existence of ligand-specific intermediate conformational states that are likely to be involved in differential activation of signaling pathways. Fluorescence spectroscopy studies provide direct evidence for ligand-specific receptor conformations of the β2-adrenergic receptor, making this system an attractive target to test the ability of computational methodologies to predict different activated states of GPCRs. To this end, we designed a computational strategy that combines adiabatic biased molecular dynamics (ABMD) and metadynamics simulations. Firstly, ABMD is used to generate transition paths between the experimental inactive crystal structure of the β2-adrenergic receptor and a conformation containing established features of activated states of GPCRs (modeled using the opsin crystal structures). Secondly, metadynamics is applied to study how ligands with different efficacies affect the free-energy of different metastable states identified along these putative activation pathways. The calculated free-energy profiles of the different ligand-β2 adrenoceptor complexes help rationalize the published experimental results, including the different kinetics of catecholaminergic agonists such as epinephrine, norepinephrine, dopamine, and isoproterenol. Representative structures of the identified energy basins suggest specific residues and contacts that may help stabilize different activated states of the receptor. This information holds promise for the crystallization of different GPCR conformations.

1515-Pos

Structural and Kinetic Modeling of an Activating Helix Switch in the Rhodopsin-Transducin Interface

Peter W. Hildebrand.

Uni Berlin Charite, Berlin, Germany.

Extracellular signals prompt G protein-coupled receptors (GPCRs) to adopt an active conformation (R*) and to catalyze GDP/GTP exchange in the α-subunit of intracellular G proteins (Gαβγ). Kinetic analysis of transducin ($G_t\alpha\beta\gamma$) activation shows that an intermediary $R^*G_t\alpha\beta\gamma$GDP complex is formed which precedes GDP release and formation of the nucleotide-free R*G protein complex. Based on this reaction sequence we explore the dynamic interface between the proteins during formation of these complexes. We start from the R* conformation stabilized by a $G_t\alpha$ C-terminal peptide (GαCT) obtained from crystal structures of the GPCR opsin. Molecular modeling allows reconstruction of the fully elongated C-terminal α-helix of $G_t\alpha$ (α5) and shows how α5 can be docked to the open binding site of R*. Two modes of interaction are found. One of them - termed stable or S-interaction - matches the position of the GαCT peptide in the crystal structure and reproduces the hydrogen bridge networks between the C-terminal reverse turn of GαCT and conserved E(D)RY and $NPxxY(x)_{5,6}F$ regions of the GPCR. The alternative fit - termed intermediary or I-interaction - is distinguished by a tilt (42°) and rotation (90°) of α5 relative to the S-interaction. It shows different α5 contacts with the $NPxxY(x)_{5,6}F$ region and the second cytoplasmic loop of R*. From the two α5 interactions, we derive a ‘helix switch’ mechanism for the transition of $R^*G_t\alpha\beta\gamma$GDP to the nucleotide-free R*G protein complex. It illustrates how α5 might act as a transmission rod to propagate the conformational change from the receptor-G protein interface to the nucleotide binding site.

1516-Pos

Agonist-Specific Effects of TM V Serine Mutations on Dopamine D2S Receptor Voltage-Sensitivity

Kristoffer Sahlholm, Daniel Marcellino, Johanna Nilsson, Kjell Fuxe, Peter Århem.

Karolinska Institutet, Stockholm, Sweden.

Voltage-sensitivity has recently been demonstrated for agonist potency and affinity at certain G protein-coupled receptors. Using an electrophysiology assay in Xenopus oocytes, we have previously shown that the potency of dopamine in activating G protein-coupled potassium channels (GIRK) via the dopamine D2S receptor is reduced by depolarization from −80 to 0 mV. We recently investigated the voltage-sensitivities of a range of structurally related dopaminergic agonists at the D2S receptor.

The findings of this study led us to propose that a conformationally constrained interaction of the agonist with transmembrane segment (TM) VI of D2 is required for voltage-sensitivity. The hypothesis assumes that for the flexible phenethylamines, two hydroxyls (such as in dopamine) interacting with the conserved serines in TM V are necessary for voltage-sensitivity. Conversely, N,N-dipropyl-2-aminotetralin (DPAT) agonists do not require hydroxyls for voltage-sensitivity due to their inherently more rigid structure. To test this hypothesis, we mutated three conserved serines in TM V (S193A, S194A, and S197A) which have been shown to mediate binding to agonist hydroxyls. The voltage-sensitivity of non-hydroxylated DPAT was similar to that observed with the wild-type receptor at all of the three mutants, suggesting that the mutations did not allosterically alter the voltage-sensing properties of the receptor.

The S193A mutation drastically diminished voltage-sensitivity of dopamine, concomitantly with a marked reduction in potency. However, the S194A mutation which slightly decreased potency, did not appreciably affect the voltage-sensitivity of dopamine. At the S197A mutant, dopamine efficacy was decreased to such a degree that voltage-sensitivity could not be assessed.

In the literature, S193 has consistently been assigned a major role in dopamine binding. Our results suggest that this residue might also be important for voltage-sensitive interactions between dopamine and the D2S receptor.

1517-Pos

Influence of Membrane Composition on Function of Human Peripheral Cannabinoid Receptor CB2

Tomohiro Kimura, Alexei A. Yeliseev, Krishna Vukoti, Klaus Gawrisch.

NIH/NIAAA, Bethesda, MD, USA.

The human peripheral cannabinoid receptor CB2 is abundant in tissues of immune and hematopoietic systems. CB2 belongs to the class of heptahelical G-protein coupled receptors and regulates a wide range of physiological functions through binding of endogenous and exogenous cannabinoid ligands. We studied the influence of electrical surface potential of membranes and of hydrocarbon-chain order on rates of G-protein activation by CB2. The membrane surface potential was determined by a measurement of the electrophoretic mobility of proteoliposomes, while lipid hydrocarbon-chain order was quantified by a measurement of the order parameters using ^{2}H NMR. The receptor, expressed in *E. coli*, was purified and functionally reconstituted into lipid bilayers composed of phosphatidylcholine (PC), phosphatidylserine (PS), and cholesteryl hemisuccinate (CHS). CB2 was fully activated with the synthetic agonist CP-55,940. The rate of G-protein activation by the receptor increased about two-fold with increasing CHS content in the lipid matrix from 25 to 41 mol%. Similar effect was observed with increasing PS content. The increased activation rate correlated with a larger negative ζ-potential caused by the negatively charged headgroups. The increased order of lipid acyl chains due to interactions with the cholesteryl backbone of CHS had no significant effect on G-protein activation rates, as confirmed by addition of cholesterol instead of CHS. The results indicate the importance of anionic lipids for efficient coupling between the CB2 receptor and G-proteins.

1518-Pos

A Polybasic Region in the C-terminus of M3 Muscarinic Acetylcholine Receptors Mediates an Interaction with Gq Heterotrimers

Kou Qin, Sudha Kuravi, Nevin Lambert.

Medical College of Georgia, Augusta, GA, USA.

G protein-coupled receptors (GPCRs) form stable complexes with heterotrimeric G proteins when the former are activated and when the latter are not bound to guanine nucleotides. In addition to these active-state ternary (ligand-receptor-G protein) complexes some GPCRs have been suggested to form preassembled or precoupled complexes with G proteins prior to activation. We have previously reported that immobile M3 muscarinic receptors (M3Rs) decrease the mobility of heterotrimers that contain Gαq, consistent with an M3R-Gq complex. This interaction is unaffected by receptor ligands in intact cells, and is specific for M3Rs and Gq, as immobile M4Rs do not decrease the mobility of Gq heterotrimers, and immobile M3Rs do not decrease the mobility of GoA heterotrimers. In order to determine the structural basis of this interaction, we constructed a series of CFP-labeled M3R/M4R chimeras and tested their ability to decrease the mobility of venus-labeled Gq (Gq-V) using fluorescence recovery after photobleaching (FRAP). A chimera consisting of the M3R with the c-terminus of the M4R (M3M4ct) did not decrease Gq-V mobility. A polybasic region

(565KKKRRK570) immediately following helix 8 in the c-terminus of M3R was found to be necessary for the decrease in Gq-V mobility. We tested the hypothesis that an electrostatic interaction was involved in the interaction between M3Rs and Gq by repeating our FRAP experiments in permeabilized cells exposed to buffer solutions with high and low ionic strength. High ionic strength solutions inhibited the decrease in Gq mobility, whereas low ionic strength solutions enhanced this effect. These results suggest that an electrostatic interaction mediates an interaction between the c-terminus of M3Rs and Gq heterotrimers. The functional significance of this interaction is currently under study.
Supported by grant GM078319 from the National Institutes of Health.

1519-Pos
The Human Muscarinic Receptor Couples to GαI3 Via Catalytic Collision
Shai Berlin, Daniel Yakubovich, Tal Keren-Raifman, Nathan Dascal.
Tel Aviv University, Ramat Aviv, Tel Aviv, Israel.
Hundreds of G-protein coupled receptors (GPCR) are encoded in the human genome. All GPCRs react to a vast variety of ligands and initiate the G-protein activation cycle, by catalyzing the exchange of GDP by GTP on the Gα subunit. Classically, this mode of activation has been proposed to be of catalytic collision coupling nature, where a single receptor sequentially activates several G-proteins. However, recent biophysical and imaging studies challenged this concept and suggested that some GPCR and G-proteins form stable non-dissociating complexes prior to and after activation. We were interested in determining the mode of coupling between the human muscarinic 2 receptor (m2R) and Gαi3βγ. We used the G-protein activated K+ channel (GIRK) as a reporter for receptor activation and systematically quantified receptor's and channel's plasma membrane concentrations using fluorescent methods and radioligand assays. We found a decrease in activation time at high receptor density, with no change in channel concentration. However, maximal amplitude was attained at lower receptor density, suggesting an amplification process. No change in Gβγ concentration was observed, as judged by the unchanged Gβγ-dependent basal activity of GIRK. Additionally, increasing amounts of m2R did not increase Gαi concentration. Together, these results suggest a catalytic collision coupling mechanism. We constructed a model describing m2R's activation scheme and predicted that excessive Gα subunits should slow the activation process by occupying the activated receptor in "dead-end" interactions, not leading to channel activation. Increasing amounts of two fluorescent Gαi3 subunits were used to test the prediction. Indeed, both subunits slowed the evoked-current, without change in current amplitude. These results, together with our previous observations, suggest that the m2R activates Gαi3 via a catalytic collision coupling mechanism, where one receptor diffuses and activates several Gαβγ subunits, leading to the activation of GIRK.

1520-Pos
Structural Characterization of the N-terminal Region of the Saccharomyces Cerevisiae G-Protein Coupled Receptor, Ste2P
Stephanie Kendall[1], Chunhua Shi[2], Shelley Forgeron[3], Michele C. Loewen[1].
[1]University of Saskatchewan, Saskatoon, SK, Canada, [2]Carleton University, Ottawa, ON, Canada, [3]National Research Council of Canada, Saskatoon, SK, Canada.
Binding of α-factor pheromone to the G-protein coupled receptor, Ste2p, initiates signal transduction events that lead to mating of the yeast *Saccharomyces cerevisiae*. Recent indirect evidence also implicates the N-terminal region of Ste2p in modulating cell wall degradation and membrane fusion during later steps of mating. Toward deciphering mechanisms, structural studies have been initiated on the N-terminus of Ste2p. Initially, residues 1-71 of Ste2p were expressed as a fusion protein with HIS and KSI tags and affinity purified from *E.coli* in mg quantities. Subsequent cyanogens bromide cleavage at methionines yielded a hydrophobic peptide (Ste2p 2-54) that consistently disappeared upon HPLC enrichment. Similarly, a chemically synthesized fragment corresponding to Ste2p residues 14-43 could not be purified by HPLC. However, the addition of three lysines to both termini was found to decrease hydrophobicity sufficiently to enable HPLC purification. Circular dichroism studies of a chemically synthesized K^3-Ste2p-14-43-K^3 peptide indicated mostly random structure, with ~45% β-strand and a small percentage of α-helix in buffered water. The structure was found to be stable at temperatures up to 40°C. These results correlate with predicted 2o structure for the Ste2p N-terminal domain including: random chain with a β-strand-loop-β-strand fold followed by a C-terminal α-helix (Shi et al., J. Cell. Biochem. 107:630-38) and recent NMR evidence suggesting α-helix in a C-terminal overlapping region (residues 39-47; Neumoin *et al.,* 2009 Biophysical Journal 96: 3187-96). Preliminary ^1H-^1H NOESY and TOCSY NMR data for the K^3-Ste2p 14-43-K^3 peptide have been collected. As well, a recombinant version of K^3-Ste2p-2-43-K^3 is being produced to extend the N-terminal region to be analyzed and facilitate isotopic labeling for complete structural elucidation.

1521-Pos
Arrestin can Bind to a Single G-Protein Coupled Receptor
Hisao Tsukamoto, Abhinav Sinha, Mark DeWitt, **David L. Farrens**.
Oregon Health and Science University, Portland, OR, USA.
Termination of G protein-coupled receptor (GPCR) signaling typically involves phosphorylation of the receptor, followed by binding of a protein called arrestin. Here we tested the minimal stoichiometry required for this interaction, by determining if a single rhodopsin molecule can bind arrestin. To do this, we prepared nanoscale phospholipids particles, so-called nanodiscs, which contain only monomeric rhodopsin and measured their ability to bind visual arrestin. Our data clearly show that visual arrestin can bind to monomeric phosphorylated rhodopsin to stabilize its active form, called metarhodopsin II. Interestingly, we find beta-arrestin can also bind to monomeric rhodopsin in nanodiscs and stabilize metarhodopsin II. Together, these results suggest that in general, the minimal unit for arrestin binding is a monomeric GPCR.

1522-Pos
Solid-State NMR Demonstrates that Active Signaling Complexes of Bacterial Chemoreceptors Do Not Adopt the Proposed Trimer-Of-Dimers Structure
Daniel J. Fowler, Robert M. Weis, Lynmarie K. Thompson.
University of Massachusetts, Amherst, MA, USA.
The receptor dimers that mediate bacterial chemotaxis form signaling complexes with CheW and the kinase CheA. Based on the packing arrangement observed in two different crystal structures of two different receptor cytoplasmic fragments, two different models have been proposed for receptor signaling arrays: the trimers-of-dimers and hedgerow models. We have identified an inter-dimer distance predicted to be substantially different by the two models, labeled the atoms defining this distance through isotopic enrichment, and measured it with ^{19}F-^{13}C REDOR. This was done in two types of receptor samples: isolated bacterial membranes containing overexpressed, intact receptor, and soluble receptor fragments reconstituted into kinase-active signaling complexes. In both cases, the distance found was incompatible with *both* the trimers-of-dimers and the hedgerow models. Comparisons of simulated and observed REDOR dephasing were used to deduce a closest-approach distance at this interface, which provides a constraint for the possible arrangements of receptor assemblies in the kinase-active signaling state.

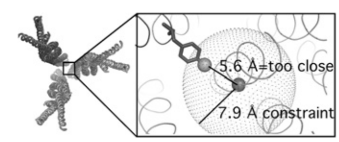

This research was supported by U.S. Public Health Service Grant GM47601; DJF was partially supported by National Research Service Award T32 GM08515.

1523-Pos
Site-Specific Fluorescent Labeling of Purified G-Protein-Coupled Receptors Using Genetically-Encoded Unnatural Amino Acids
Shixin Ye, Manija A. Kazmi, Terence Duarte, Saranga Naganathan, Thomas P. Sakmar, Thomas Huber.
www.sakmarlab.org, Rockefeller University, New York, NY, USA.
The introduction of unique chemical groups into proteins by means of site-directed mutagenesis with unnatural amino acids has numerous applications in protein engineering and functional studies. We first introduced *p*-acetyl-L-phenylalanine (Acp) or *p*-azido-L-phenylalanine (Azp) into the prototypical G protein-coupled receptor (GPCR) rhodopsin at specific sites. We employed an amber codon suppression system where the mutant opsin gene was co-expressed with the appropriate orthogonal pair of engineered tRNA and amino-acyl tRNA synthetase. We then used hydrazone (hydrazide) or Staudinger-Bertozzi (phosphine) ligation chemistry for the keto group (in Acp) or azido group (in Azp), respectively, to link a fluorophore at various solvent accessible sites in rhodopsin. In side-by-side comparisons of the two chemical ligation chemistries, which were carried out

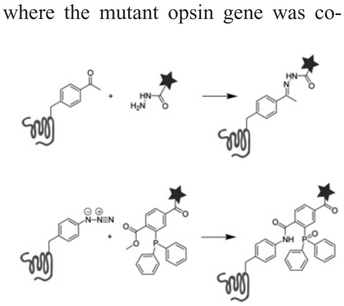

under physiological conditions where receptor function is maintained, we conclude that the azido group serves as a more satisfactory chemical handle than the keto moiety. The fully-functional fluorescently-labeled receptor should prove useful for kinetic studies of ligand-receptor interaction.

1524-Pos
Probing the Binding Sites and Transmembrane Prolines of GPCRs Using Unnatural Amino Acids

Ethan B. Van Arnam, Kristina N. McCleary, Michael M. Torrice, Kiowa S. Bower, Elizabeth H. Jensen, Henry A. Lester, Dennis A. Dougherty.
California Institute of Technology, Pasadena, CA, USA.

We describe a general application of the nonsense suppression methodology for unnatural amino acid incorporation in functional G protein-coupled receptors (GPCRs). We have evaluated key aromatic residues in the binding sites of the M2 muscarinic acetylcholine receptor and the D2 and D4 dopamine receptors. In addition, highly conserved transmembrane proline residues of the D2 dopamine receptor have been probed with proline analogues and α-hydroxy acids. Receptors were expressed in *Xenopus* oocytes, and activation of a G protein-coupled, inward-rectifying K^+ channel (GIRK) provided, after optimization of conditions, a quantitative readout of receptor function. Incorporation of a series of fluorinated tryptophan derivatives at W6.48 of the D2 receptor establishes a cation-π interaction between the agonist dopamine and W6.48, suggesting a reorientation of W6.48 on agonist binding, consistent with proposed ''rotamer switch'' models. Interestingly, no comparable cation-π interaction was found at the aligning residue in the M2 receptor. Incorporation of α-hydroxy acids at transmembrane proline sites 4.59, 5.50, 6.50, and 7.50 yielded D2 receptors with EC_{50} values similar to wild-type, whereas natural amino acids other than proline proved detrimental to receptor function. We propose that lack of hydrogen bond donor ability, common to both proline and α-hydroxy acids, is key to the functional role of proline within GPCR transmembrane helices.

1525-Pos
Anodic Aluminum Oxide Nanopores as Substrate for Functional and Structural Studies on G Protein-Coupled Membrane Receptors

Olivier Soubias[1], Tomohiro Kimura[1], Holly C. Gaede[2], Alexei A. Yeliseev[1], **Klaus Gawrisch[1]**.
[1]SNMR, LMBB, NIAAA, NIH, Bethesda, MD, USA, [2]Dept. Chem. Texas A&M Univ., College Station, TX, USA.

Functional and structural studies on GPCR are ideally conducted on single, protein-carrying bilayers with unrestricted access for ligands and G-proteins. It is desirable to have a large accessible surface area and protection from a solid support. Reconstitution of GPCR into bilayers supported by porous anodic aluminum oxide (AAO) nanopores meets those requirements. Extrusion of proteoliposomes through the nanopores resulted in formation of tubules of a single lipid bilayer that covers the inner surface of pores. We successfully reconstituted the GPCRs rhodopsin and recombinant peripheral cannabinoid receptor CB2 at functional conditions and high concentration into the cylindrical AAO nanopores with a diameter of 200 nm and a length of 60 μm. One square centimeter of AAO filter yielded 500 cm^2 of membrane surface. The lipid tubules are open at both ends such that buffer passes easily through the pores. Detergents used for protein reconstitution are flushed out within minutes. By ^2H NMR we demonstrated that neither lipid headgroups nor hydrocarbon chains of fluid bilayers are perturbed by the solid support. Photoactivation of rhodopsin in the pores, monitored by UV-vis spectrophotometry, was indistinguishable from rhodopsin in unsupported liposomes. Metarhodopsin-II in the tubules activated G-protein that was delivered through the pore openings. By NMR diffusion experiments we determined that tubular bilayers are assembled as short pieces with a length of a micrometer or less that adhere to the surface by their edges. The tubules possess undulation with a radius of curvature of 100-400 nm. We have evidence for a layer of water with an average thickness of 3 nm between the bilayers and the pore surface. It explains why neither protein function nor fluid bilayer properties are perturbed by the solid support.

1526-Pos
Novel Technology to Study Chemokine Receptor Signaling Complexes

Amy Grunbeck, Thomas Huber, Shixin Ye, Sourabh Banerjee, Thomas P. Sakmar.
Rockefeller University, New York, NY, USA.

C-C chemokine receptor 5 (CCR5) is a G protein-coupled receptor (GPCR) involved in immune responses and it is the primary co-receptor required for HIV-1 cellular entry. To obtain functional heterologous over-expression of engineered GPCRs is one of the major hurdles in GPCR research aimed at elucidating structure-activity relationships. It can be especially difficult to obtain structural information about GPCRs in signaling complexes with other cellular proteins that form a so-called ''signalosome.'' We have developed two new technologies for investigating the structure and function of GPCRs, which we have now applied to CCR5. First, we have established a membrane nanoparticle system called NABBs (nanoscale apolipoprotein bound bilayers), which are self-assembling discs that maintain receptors in a native-like membrane environment outside of the cell. We have incorporated functional CCR5 into NABBs and plan to use this platform to reconstitute the ternary complex with chemokine ligand and G protein from purified components. In addition, we have adapted unnatural amino acid mutagenesis for use with GPCRs. This is a method to incorporate amino acids with unique side chains at specific sites in the receptor. We introduced p-benzoyl-L-phenylalanine, into CCR5 at various positions on both the extracellular and intracellular surface of the protein using the amber suppression technology. Since the benzoyl moiety is a photo-activatable crosslinker, these mutants can now be used to map the specific sites of interaction between ligand, receptor, and G protein as predicted from molecular modeling and molecular dynamics simulations. Our methods will form the basis of a new experimental paradigm in the structural biology of signaling complexes on a mesoscopic level. Ultimately, these methods will be useful for developing a chemically-precise model for how an extracellular ligand stimulates a GPCR to activate a cytosolic G protein.

1527-Pos
Single-Cell Biochemical Assays for the Molecular Targets of Disease

Christopher Sims, Nancy Allbritton, Dechen Jiang, Shan Yang, Angie Proctor, Ryan Phillips.
University of North Carolina, Chapel Hill, NC, USA.

Molecularly targeted therapies are at the forefront of clinical science, and are expected to lead to personalization of medical treatments for each patient. Most such therapies are directed at inhibiting specific signal transduction enzymes or pathways, thus creating a critical need for assays capable of measuring the activities of these proteins in disease models and in patient samples. The ability to measure relevant enzyme activity in primary cell samples at baseline and/or after treatment would provide the ability to tailor patient therapy based on aberrant signal transduction, validate mechanisms of resistance in patients, and would offer an invaluable pharmacodynamic tool to assess whether resistance is associated with inadequate target inhibition. Here we report our current efforts to create the analytical and chemical tools needed to directly measure the enzymatic activities of therapeutic targets including protein kinases, lipid modifying enzymes and the proteasome. Fluorescent reagents are under development that report the activity of these various enzymes in model cells lines and primary cells. The basic design incorporates enzyme substrates that are modified to create compounds which can be loaded into cells where they are modified by the enzyme of interest. Work has included modification of peptides to confer membrane permeability and to achieve long intracellular lifetimes. Microelectrophoretic separations combined with low-level fluorescence detection enable the quantitative analysis of these compounds from single mammalian cells. This capability addresses three major issues currently faced in the biochemical analysis of clinical samples: the need for direct measurement of the enzymatic activity of target proteins; sample size requirements that are feasible for clinical implementation; and sample heterogeneity that can mask pertinent aspects related to therapeutic response.

Calcium Fluxes, Sparks & Waves II

1528-Pos

Polyhistidine Peptide Inhibitor of the Aβ Calcium Channel Potently Blocks the Aβ-Induced Calcium Response in Cells

Nelson Arispe[1], Stewart R. Durell[2], Yinon Shafrir[2], **H. R. Guy[2]**.
[1]Uniformed Services University School of Medicine, USUHS, Bethesda, MD, USA, [2]NCI, NIH, Bethesda, MD, USA.

Based on the consistent demonstrations that the Aβ peptide of Alzheimer's disease forms calcium permeant channels in artificial membranes, we have proposed that the intracellular calcium increase observed in cells exposed to Aβ is initiated by calcium fluxes through Aβ channels. We have found that a small four histidine peptide, NAHis04, potently inhibits the Aβ-induced calcium channel currents in artificial lipids membrane. Here we report that NaHis04 also potently blocks the intracellular calcium increase which is observed in cells exposed to Aβ. PC12 cells loaded with Fura 2AM show a rapid increase in fluorescence with rapidly return to base line after Aβ is added to the medium. This fluorescence change occurs even when the medium contains nitrendipine, a voltage-gated calcium channel blocker, but fails to occur when application of Aβ is preceded by addition of NAHis04. Steep dose response curves of percentage of responding cells and cell viability show that NAHis04 inhibits in the μm range in an apparently cooperative manner. We have developed numerous models of Aβ pores in which the first part of the Aβ sequence forms a large beta barrel ending at His13. We have modeled how up to four NAHis04 peptides may block these types of pores by binding to side chains of Aβ residues Glu 11, His 13, and His 14.

1529-Pos

Elucidation of Ca^{2+} Influx through Alzheimer's Aβ Channels in the Aβ-Induced Cellular Ca^{2+} Response

Nelson J. Arispe.
Uniformed Services University of the Health Sciences, Bethesda, MD, USA.

The Alzheimer's disease Aβ peptide interaction with the plasma membrane of cells results in a response characterized by the elevation of the intracellular (cytoplasmic) Ca^{2+} concentration which may critically perturb Ca^{2+} homeostasis. Calcium influx into the cytosol can occur across the plasma membrane via receptor-mediated, voltage-gated, store-operated calcium channels, or from internal stores. Based on the ion channel formation by Aβ peptides on artificial membranes *w*e have proposed that perturbation in Ca2+ homeostasis induced by Aβ could be caused by external calcium entering through ion channels formed by Aβ in the plasma membrane. The activity of these channels would permit the entrance of extracellular calcium ions into the cell, subsequently triggering the release of calcium from internal stores. To elucidate the contribution of calcium influx through the Aβ ion channels to the Aβ-induced calcium response we used specific blockers of plasma membrane channels and specific inhibitors of the mechanisms that permit the release of calcium from the ER, the largest intracellular store. With all those mechanisms blocked and inhibited, we visualized a fast raising, short-lasting calcium entry immediately after PC12 cells were exposed to Aβ. This calcium signal was identified as calcium flowing through the Aβ channels by using specific Aβ channel blockers. The Aβ channel blockers did not affect other mechanisms that contribute to the cytosolic calcium increase, and their use prevented the calcium entry through the Aβ channels and consequent development of the whole cellular Aβ-induced calcium response.

1530-Pos

Functional Analysis of GPCR and Calcium Channel Targets Using Quest Fluo-8

Jinfang Liao, Chunmei Wei, Haitao Guo, Xing Han, **Zhenjun Diwu**.
ABD Bioquest, Inc., Sunnyvale, CA, USA.

Calcium flux assays are preferred methods in drug discovery for screening G protein coupled receptors (GPCRs) and calcium channels. Quest Fluo-8 AM, Fluo-3 AM and Fluo-4 AM are evaluated for several GPCR and ion channel targets. They share the same assay principle. All the three fluorogenic calcium indicators are in the form of non-fluorescent AM esters. Once inside cells, the lipophilic AM blocking groups are cleaved by non-specific cellular esterases, resulting in negatively charged fluorescent dyes that stay inside cells, and their fluorescence intensities are greatly enhanced upon binding to calcium. When cells stimulated with bioactive compounds, the receptor signals release of intracellular calcium, which greatly increase their fluorescence signals. In conclusion, Fluo-3 AM, Fluo-4 AM and Quest Fluo-8 AM are robust tools for evaluating GPCR and calcium channel targets and screening their agonists and antagonists with fluorescence microplate readers, fluorescence microscopes or flow cytometers.

1531-Pos

Persistent Calcium Sparklet Activity of L-Type Calcium Channels: Link Between PKC and c-Src

Jyoti Gulia[1], Manuel F. Navedo[2], Peichun Gui[1], Jun-Tzu Chao[1], Luis F. Santana[2], Michael J. Davis[1].
[1]University of Missouri, Columbia, MO, USA, [2]University of Washington, Seattle, WA, USA.

Ca^{2+} sparklets are a fluorescence signal associated with Ca^{2+} entry through L-type calcium ($Ca_v1.2$) channels, which are primary Ca^{2+} entry pathway in many excitable cells. Ca^{2+} sparklets are quantal in nature (q = 34 nM $\Delta[Ca^{2+}]_i$) and their activity is categorized as low ($0<nP_s<0.2$) or persistent ($nP_s>0.2$), where n = no. of quantal levels and P_s = active sparklet probability. Both types of Ca^{2+} sparklets are present in vascular smooth muscle cells (VSMCs) but only low activity Ca^{2+} sparklets are present in heterologously expressed $Ca_v1.2$ channels unless PKCα is activated. The latter effect presumably requires $Ca_v1.2$ phosphorylation, perhaps at the canonical PKA phosphorylation site, S^{1901}, yet the exact phosphorylation site remains unclear. Using TIRF microscopy in conjunction with whole cell voltage clamp, we detected persistent Ca^{2+} sparklet activity in HEK 293 cells co-expressing $S^{1901}A$ $Ca_v1.2c$ and PKCα, indicating that PKCα does not phosphorylate S^{1901}. Also, persistent Ca^{2+} sparklets were detectable in cells expressing WT $Ca_v1.2c$ in the absence of PKCα if c-Src was co-expressed. Furthermore, Ca^{2+} sparklet activity was reduced in cells expressing WT $Ca_v1.2c$ and kinase dead c-Src (7/9 cells). To test if phosphorylation of a previously identified $Ca_v1.2c$ tyrosine phosphorylation site (Y^{2122}) by c-Src mediated persistent Ca^{2+} sparklet activity, we co-expressed $Y^{2122}F$ $Ca_v1.2c$ and c-Src in HEK cells. Persistent Ca^{2+} sparklet activity was present under these conditions; however, Ca^{2+} sparklet activity was reduced in cells co-expressing $Y^{2139}FCa_v1.2c$ and c-Src. These data suggest that c-Src may phosphorylate $Ca_v1.2c$ at Y^{2139} under basal conditions to produce persistent Ca^{2+} sparklet activity. Future experiments on HEK cells expressing $Y^{2139}FCa_v1.2c$ and PKCα will allow us to determine if persistent Ca^{2+} sparklet activity in VSMCs is evoked by a common mechanism involving PKCα and c-Src.

1532-Pos

Optical Stimulation of Ca^{2+} Transients in Smooth Muscle Cells

John Harris, Gail McConnell, John G. McCarron.
University Of Strathclyde, Glasgow, United Kingdom.

The modulation of intracellular Ca^{2+} plays a huge role in controlling important cell functions such as cell division, signaling, contraction and cell death. To date, intracellular Ca^{2+} dynamics have mainly been investigated using electrophysiological measurement techniques such as patch clamp experiments often used in combination with fluorescence imaging techniques. To activate intracellular channels, drugs are often used. However, because of diffusion and mixing constraints there is little precision in the time course of channel activation and deactivation. In addition, the invasive nature of conventional whole cell patch clamp techniques disturbs the intracellular environment and may so alter channel behaviour.

We report a non-invasive technique that induces controlled Ca^{2+} responses in isolated smooth muscle cells using a holosteric incoherent light source as a stimulus. Using a conventional epi-fluorescence microscope configuration, cells labeled with a Ca^{2+} fluorescent indicator (Fluo-3AM) were stimulated using the low intensity light (<1.5mW ≅ λ=488nm) and the resultant Ca^{2+} transients were visualized using a highly sensitive CCD camera. We will describe the cell stimulation protocol used and present data demonstrating the efficacy of this low cost and minimally invasive technique. We will also describe the investigation into the origin of the light induced Ca^{2+} responses.

1533-Pos

Agonist-Evoked Calcium Wave Progression Requires Calcium and Ip_3 in Smooth Muscle

John G. McCarron, Susan Chalmers, Debbi MacMillan, Marnie L. Olson.
University of Strathclyde, Glasgow, United Kingdom.

Smooth muscle responds to IP_3-generating agonists by producing Ca^{2+} waves to spread information within and between cells. The mechanism of wave progression has been investigated in voltage-clamped single smooth muscle cells. Agonist-evoked waves initiated as a uniform rise in $[Ca^{2+}]_c$ over a substantial length (~30 μm) of the cell. During regenerative propagation, the wave-front was approximately 1/3 the length (~9 μm) of the $[Ca^{2+}]_c$ change at the initiation site. The wave-front progressed at a constant velocity though amplitude varied through the cell. Differences in sensitivity to IP_3 may explain the variation in amplitude; local release of IP_3 evoked $[Ca^{2+}]_c$ increases of varying amplitude in different regions of the cell. The wave-front does not progress by Ca^{2+}-dependent positive feedback alone. In support, colliding $[Ca^{2+}]_c$

increases evoked in response to IP_3, released locally in two parts of the cell, did not annihilate but approximately doubledin amplitude. This result suggests that the $[Ca^{2+}]_c$ increase, generated by local release of IP_3, had not regeneratively propagated but diffused passively from the release site. Notwithstanding, Ca^{2+} was required for IP_3-mediated wave progression to occur. Increasing the Ca^{2+} buffer capacity in a small (2 μm) restricted region of the cell immediately in front of a carbachol-evoked Ca^{2+} wave, by photolyzing the caged Ca^{2+} buffer diazo-2, halted progression at the site of photolysis. Failure of local increases in IP_3 to evoke waves appears to arise from the restricted nature of the IP_3 increase to small areas within the cell. When IP_3 was elevated throughout a localized increase in Ca^{2+} propagated as a wave. Together, these results suggest that waves initiate over a relatively large length of the cell and both IP_3 and Ca^{2+} are required for active propagation of the wave-front to occur.

1534-Pos
Increased Calcium Response to Depolarization in Voltage Clamped Skeletal Muscle Cells of a Transgenic Model of Amyotrophic Lateral Sclerosis

Jingsong Zhou, Jianxun Yi, Eduardo Rios.
Rush University, Chicago, IL, USA.

Mitochondrial Ca uptake is believed to help regulate mitochondrial metabolism and synthesis of ATP to meet the demands of muscle contraction. Whether mitochondrial Ca uptake modifies Ca signaling during EC-coupling remains an open question. While studies show that mitochondria in skeletal muscle may take up Ca during contraction, it is not known whether altered mitochondrial Ca uptake can play a role in pathophysiological conditions. Our study on ALS mouse model G93A shows that ALS muscle fibers display defective mitochondria with loss of their inner membrane potential in fiber segments. The finding of localized mitochondrial defects in ALS fibers presents a unique opportunity to test whether changes in mitochondrial function can affect intracellular Ca signaling, as Ca release activity can be compared in regions with or without depolarized mitochondria in the same muscle fiber. By loading muscle fibers with TMRE (a probe of mitochondrial membrane potential) and fluo-4 (a Ca indicator) we characterized simultaneously mitochondrial function and Ca release activity in living muscle fibers. The fiber segment with depolarized mitochondria shows greater osmotic stress-induced Ca release activity. Abolishing mitochondrial inner membrane potential by FCCP or blocking mitochondrial uniporter by Ru360 exacerbates the osmotic stress-induced hyperactive Ca release. Furthermore, we evaluated the voltage-induced Ca transient by patch-clamping ALS fibers and found that fiber segments with depolarized mitochondria displayed 5~25% greater Ca transients. Our study constitutes a direct demonstration of the importance of mitochondria in shaping cytosolic Ca signaling in skeletal muscle. Malfunction of mitochondrial Ca uptake may play an important role in muscle degeneration of ALS. Supported by MDA/NIH.

1535-Pos
CICR and Calcium-Dependent Inactivation, Quantified Through the Response to Artificial Ca Sparks in Single Muscle Cells

Lourdes Figueroa[1], **Vyacheslav Shkryl[1]**, Jingsong Zhou[1],
Atsuya Momotake[2], Graham Ellis-Davies[3], Lothar A. Blatter[1],
Eduardo Rios[1], Gustavo Brum[4].
[1]Rush University, Chicago, IL, USA, [2]Tsukuba University, Ibaraki, Japan,
[3]Drexel University, Boston, PA, USA, [4]Universidad de la República,
Montevideo, Uruguay.

Local calcium stimuli (artificial sparks) generated by 2-photon breakdown of the cage NDBF-EGTA were applied to evoke Ca release from the SR in single skeletal or cardiac muscle cells undergoing fast Ca imaging with the low affinity dye fluo 4FF. The figure shows selected sequential images of the Ca transient generated by a frog skeletal muscle fiber with permeabilized plasmalemma, in response to a spark (elicited *outside* the fiber to avoid photodamage). Two types of responses were observed: (i) an all-or-none wave -shown- that propagates over the entire cell and (ii) graded responses, which fail to propagate. Release analysis (Ríos, JGP 1999; Figueroa, this meeting) separates SR release from simple diffusion of photo-released Ca into cells. The technique yields a sensitive measure of threshold $[Ca^{2+}]$ for release activation, which in the example (0.3 mM $[Mg^{2+}]_{cyto}$) was 1 μM, and can monitor inactivation by combining multiple stimuli. Modeling of these responses aims at describing quantitatively the properties of activation, as well as the roles of inactivation and depletion in the control of Ca release. Other details and acknowledgments are presented elsewhere (Figueroa, this meeting.)

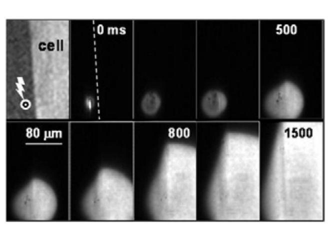

1536-Pos
Flux in Artificial Ca Sparks Generated by 2-Photon Release from a Novel Cage Confocally Imaged at Microsecond Resolution

Lourdes Figueroa[1], Jingsong Zhou[1], Vyacheslav Shkryl[1], Lothar A. Blatter[1],
Atsuya Momotake[2], Graham Ellis-Davies[3], Eduardo Rios[1], Gustavo Brum[4].
[1]Rush University, Chicago, IL, USA, [2]Tsukuba University, Ibaraki, Japan,
[3]Drexel University, Philadelphia, PA, USA, [4]Universidad de la República,
Montevideo, Uruguay.

Control of calcium signaling in striated muscle relies on concurrent actions of calcium ions to promote and inhibit release channel opening. To understand these actions we developed artificial Ca sparks generated by 2-photon (2P) release from NDBF-EGTA (Momotake, Nature Methods 2006) as quantifiable local stimuli. A ''Dual Scanner'' (Zeiss) delivers IR laser flashes through a LSM 510 scanner, while rapidly imaging fluorescence of a $[Ca^{2+}]$ monitor via a slit scanner (5-LIVE; *ca* 100 μs/line). Ca sparks of 0.1 to 10 μM (A, B) are elicited in a droplet after microseconds of 2P irradiation at 720 nm and imaged with the low affinity dye fluo 4FF. Reaction-diffusion analysis (Ríos, JGP 1999) yields the flux of Ca photorelease (C). This flux, which initially reaches several hundred mM/s, decays with τ of 2-3 ms. The technique is used to measure physico-chemical properties of calcium ligands, including bio-sensors. Applied inside muscle fibers (Figueroa, this meeting) it serves to quantitatively characterize calcium control in cells.

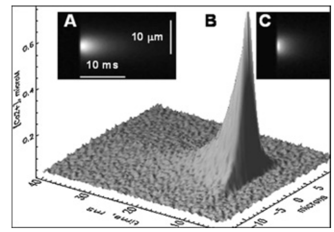

Instrument purchased with a S10 NCRR award and Hasterlik Family matching funds. Supported by NIAMS, NHLBI/NIH and MDA.

1537-Pos
Effects of High [BAPTA] Inside Mouse Muscle Fibers Reveal a Role of Calcium in the Termination of Voltage-Operated Calcium Release from the SR

Carlo Manno, Monika Sztretye, Eduardo Rios.
Rush University, Chicago, IL, USA.

Striated muscles have a termination mechanism that causes the flux of Ca release from the SR, whether activated by an action potential or a voltage pulse, to rapidly cease after an early peak. This mechanism is viewed as a fundamental property that insures stability and ''gradedness'' in the control of Ca signals. To probe this termination, the evolution of Ca release flux was derived from cytosolic Ca transients elicited by SR-depleting depolarizations of long duration, in voltage-clamped cells of mouse FDB muscle. In the presence of 5 mM of the Ca buffer BAPTA, the release flux underwent major changes compared with a 10 mM [EGTA] ''reference'' situation (studied by Royer, J Physiol 2008). Ca release reached an early peak and then decayed to a sustained phase that was higher and briefer than in reference, often including a second rise or ''hump''. In BAPTA, measurable release only lasted 100 ms or less. Its time integral -which measures the SR Ca content releasable by depolarization_was on average 1.4 mM (n=12 cells), compared with 2.1 mM for 18 cells in reference.

An increase in flux with conserved releasable content indicates that BAPTA promotes flux and hastens emptying of the SR without greatly changing its storage properties (including lumenal $[Ca^{2+}]$). A greater Ca flux driven by a similar $[Ca^{2+}]$ gradient requires greater and/or more sustained channel openness. These observations suggest the presence of a release channel-inhibiting mechanism (CDI) mediated by binding of cytosolic Ca^{2+} to open or closed channels, a mechanism more susceptible to interference by BAPTA than the slower-reacting EGTA. Work funded by NIAMS/NIH and an MDA grant to Dr. Jingsong Zhou, who we thank for continued support.

1538-Pos
D4cpv-Casq1. A Novel Approach for Targeting Biosensors Yields Detailed Dynamic Imaging of Calcium Concentration Inside the Sarcoplasmic Reticulum of Living Cells

Monika Sztretye[1], Jianxun Yi[1], Leandro Royer[2], Jingsong Zhou[1],
Björn Knollmann[3], Paul D. Allen[4], Feliciano Protasi[5], Eduardo Ríos[1].
[1]Rush University, Chicago, IL, USA, [2]Université Bordeaux 2, Bordeaux,
France, [3]Vanderbilt University, Nashville, TN, USA, [4]Brigham and
Women's Hospital, Boston, MA, USA, [5]CeSI-Univ. G. d'Annunzio, Chieti,
Italy.

Dynamic imaging of $[Ca^{2+}]$ inside the SR of skeletal muscle is hampered by the limited sensitivity of available ratiometric biosensors (Rudolf, JCB 2006) and faces difficulties of calibration when using non-ratiometric dyes (Kabbara and Allen, J Physiol 2001). Impressed by the apparently perfect targeting of

calsequestrin 1 (Casq1) and its fusion constructs to terminal cisternae of the SR, we deviced an alternative approach: the fusion of murine Casq1 and D4cpv -a cameleon of high dynamic range and affinity adequate for the SR (Palmer, Chem & Bio 2006) - was expressed in the FDB of live adult mice. The fusion protein expressed well, localizing largely to terminal cisternae. Calibrations in situ revealed a good dynamic range of its Ca^{2+}-dependent ratio signal ($R_{max}/R_{min} = 4$). Sensor affinity is being measured using untargeted sensor, expressed in the cytosol, or purified sensor in solution. Assuming a $K_d = 240$ μM, the resting $[Ca^{2+}]_{SR}$ was 0.6-1 mM in 20 cells. Consistent with the kinetics of the related sensor D1 in solution ($k$on = 256 s^{-1}, Palmer, PNAS 2004), D4cpv signals rapidly followed the decrease in $[Ca^{2+}]_{SR}$ that results from Ca^{2+} release upon voltage-clamp depolarization. Potential interference by the presence of Casq in the fused sensor was minimized by using a deletion mutant of Casq1 as targeting sequence. A first conclusion is that long-lasting depolarization may reduce $[Ca^{2+}]_{SR}$ below 10% of resting value. From the Casq1-D4cpv-monitored $[Ca^{2+}]_{SR}$ we derived the SR Ca buffering power -ratio of total/free $[Ca^{2+}]_{SR}$- and found that it decreases upon depletion of SR Ca. As shown elsewhere (Sztretye et al, this meeting), this anomalous buffering feature depends on the presence of calsequestrin inside the SR. Funded by NIAMS/NIH and MDA.

1539-Pos
Ca Depletion and Ablation of Calsequestrin Similarly Increase the Evacuability of the Ca Store of Skeletal Muscle
Monika Sztretye[1], Leandro Royer[2], Carlo Manno[1], Jingsong Zhou[1], Björn Knollmann[3], Paul D. Allen[4], Feliciano Protasi[5], **Eduardo Rios[1]**.
[1]Rush University, Chicago, IL, USA, [2]Université Bordeaux 2, Bordeaux, France, [3]Vanderbilt University, Nashville, TN, USA, [4]Brigham and Women's Hospital, Boston, MA, USA, [5]CeSI-Univ. G. d'Annunzio, Chieti, Italy.
At ~200 ms during a voltage pulse the flux of Ca release induced by membrane depolarization of mouse muscle exhibits a characteristic acceleration of decay, or shoulder, associated with SR depletion. The shoulder reflects an increase in evacuability E, an index calculated from the flux, equal to the ratio of release permeability, P, and SR Ca buffering power, B (Royer, J Physiol 2008). To tell whether this rise in E reflects an increase in P or a decrease in B we recorded flux and calculated E in FDB cells from mice lacking either calsequestrin 1 (Paolini, J Physiol 2007) or both isoforms of calsequestrin, the main Ca buffer in the SR. In both null mice the flux waveform lacked the shoulder, and E was elevated, adopting from the start the high value reached upon depletion in the wild-type. Hence, low E requires the presence of calsequestrin inside the store. In aqueous solutions the Ca-binding capacity of calsequestrin decreases at low $[Ca^{2+}]$ (Park, JBC 2005). Therefore we hypothesized that the increase in E during a pulse is due to an analogous effect of decaying $[Ca^{2+}]_{SR}$ on the Ca-buffering capacity of calsequestrin *in situ*. Confirming the hypothesis, when the SR was depleted in cells voltage-clamped in zero Ca external solutions, the kinetics of release became similar to that of calsequestrin-null cells, featuring no shoulder and a high initial E.
Low evacuability simply implies that the SR may release Ca with minimal decrease in $[Ca^{2+}]_{SR}$, therefore conserving the driving force for subsequent release. A functional correlate is the ability to sustain Ca release and Ca transients during the high frequency activation of physiological contractions and exercise. Funded by NIAMS/NIH and MDA.

1540-Pos
Compromised Ca^{2+} Sparks Signaling in the Skeletal Muscle of Diabetic Type 2 Mice
Andoria Tjondrokoesoemo, Noah Weisleder, Jianjie Ma.
UMDNJ, Piscataway, NJ, USA.
Type 2 diabetes mellitus (DM) is a prevailing epidemic metabolic disease that is mainly characterized as insulin resistant and β-cell dysfunction that leads to aberrant glucose metabolism in skeletal muscle. Altered homeostatic capacity for effective $[(Ca^{2+})_i]$ signaling may underlie the reduced contractile dysfunction associated with DM. Measurement of osmotic stress induced Ca^{2+} sparks on the young control wild-type (WT)C57Bl/6J and db/db type 2 DM mice models show that Ca^{2+} sparks frequency is significantly attenuated in the db/db fibers (36 ± 6 events/min) when compared to control (107 ± 7 events/min). These findings suggest that Ca^{2+} sparks can be used as a readout of the Ca^{2+} handing characteristic of skeletal muscle fibers, as we have previously shown in muscular dystrophy and aging muscle. This idea is supported with additional studies that show therapeutic agents for diabetes can modulate Ca^{2+} spark signaling. Treatment of 10 nM glucagon like peptide 1 (GLP1), an incretin hormone associated with increased insulin secretion, significantly increases the Ca^{2+} sparks frequency in the db/db muscle (120 ± 10 events /min), similar to the level of untreated WT. The plot of Ca^{2+} sparks localization shows that treatment of GLP1 in either db/db or WT does not alter the peripheral subsarcolemmal distribution of Ca^{2+} sparks, implying that the factor responsible for maintaining Ca^{2+} sparks localization near the membrane remains intact. Studies in β-cell suggests that increased specific intracellular signaling cascade can be regulated by GLP-1. We find that these signaling cascades can also contribute to the activation of Ca^{2+} sparks in skeletal muscle.

Local Calcium Signaling

1541-Pos
A Technique to Accelerate Stochastic Markov Chain Monte Carlo Simulations of Calcium-Induced Calcium Release in Cardiac Myocytes
George Williams[1], Aristide Chikando[2], Gregory Smith[3], Mohsin Saleet Jafri[1].
[1]George Mason University, Fairfax, VA, USA, [2]University of Maryland Biotechnology Institute, Baltimore, MD, USA, [3]College of William and Mary, Williamsburg, VA, USA.
Considerable insight into intracellular calcium (Ca) responses has been obtained through the development of whole cell models that are based on molecular mechanisms, e.g., the kinetics of intracellular Ca channels and the feedback of Ca upon these channels. However, a limitation of most deterministic whole cell models to date is the assumption that channels are globally coupled by a "common pool" of [Ca], when in fact channels experience localized "domain" [Ca]. More realistic stochastic Monte Carlo simulations are capable of capturing the influence of local [Ca] on channel gating. Unfortunately, such local control models of calcium-induced calcium release (CICR) are computationally expensive due to the explicit representation of 10,000 to 20,000 release sites, each containing 50 to 300 stochastically gating Ca channels. Here, we present a novel technique called vectorized gating that optimizes the solution time of Markov chain Monte Carlo (MCMC) simulations. Additionally, as this technique leverages vector and matrix algebra it can benefit from the use of the advanced NVIDIA TESLA graphics processing unit (GPU) to further accelerate MCMC models. NVIDIA TESLA cards utilize the parallel nature of the NVIDIA CUDA architecture and are powered by up to 960 parallel processing cores. Benchmark simulations indicate that the GPU-enhanced vectorized gating technique is significantly faster than CPU-only driven calculations. The vectorized gating technique also lends itself to the direct calculation of an adaptive time step which optimizes speed while maintaining numerical stability. These computational enhancements are utilized to facilitate study of sarcoplasmic reticulum (SR) leak from clusters of ryanodine receptor (RyR) Ca channels in cardiac myocytes.

1542-Pos
In Situ Calibration of Cytoplasmic and Nucleoplasmic Calcium Concentration in Adult Rat and Mouse Cardiac Myocytes
Senka V. Ljubojevic, Stefanie Walther, Burkert M. Pieske, Jens Kockskämper.
Medical Unevrsity of Graz, Graz, Austria.
Quantifying subcellularly resolved Ca^{2+} signals in cardiac myocytes is essential for understanding Ca^{2+} fluxes in excitation-contraction and excitation-transcription coupling. Translation of changes in Ca^{2+}-dependent fluorescence into changes in $[Ca^{2+}]$ relies on the indicator's behavior *in situ,* but properties of fluorescent indicators in different intracellular compartments may differ. Thus, we determined the *in situ* calibration of a frequently used Ca^{2+} indicator, Fluo-4, and evaluated its use in reporting cytoplasmic and nucleoplasmic Ca^{2+} signals in isolated cardiac myocytes.
Calibration solutions were made by mixing known quantities of EGTA and CaEGTA solutions and the free $[Ca^{2+}]$ was confirmed with a Ca^{2+}-sensitive electrode. Solutions contained metabolic inhibitors and cyclopiazonic-acid (5μM) to block active Ca^{2+} transport and the Ca^{2+} ionophore A-23187 (10μM) to allow equilibration of $[Ca^{2+}]$ between bath solution and cell interior. Ventricular rat and mouse myocytes were loaded with Fluo-4/AM (8μM, 20min). Fluo-4 fluorescence (excitation/emission: 488/>505nm) was recorded using a Nipkow dual disc-based confocal microscope.
Concentration-response curves were obtained and a significant difference in the apparent Ca^{2+} binding affinities (K_d) of Fluo-4 between cytoplasmic (993 ± 56nM; 1026 ± 65nM) and nucleoplasmic (1211 ± 73nM; 1251 ± 71nM) compartments was observed for both mouse and rat cells, respectively (both n=15, P<0.01). The established curves were used to transform raw Fluo-4 fluorescence signals during electrically stimulated $[Ca^{2+}]$ transients

(1Hz, room temperature) into nucleoplasmic and cytoplasmic [Ca^{2+}]. There was a significant difference in diastolic (121 ± 24nM *vs* 149 ± 35nM; 99 ± 17nM *vs* 121 ± 26nM) and systolic (420 ± 148nM *vs* 364 ± 102nM; 787 ± 172nM *vs* 491 ± 157nM) [Ca^{2+}] between cytoplasmic and nucleoplasmic compartments in mouse and rat cells, respectively (both n=15; P<0.01).
The results reveal that, in cardiac myocytes, the Ca^{2+}-dependent fluorescent properties of Fluo-4 differ between cytoplasm and nucleoplasm and that significant differences between cytoplasmic and nucleoplasmic [Ca^{2+}] exist during diastole as well as systole.

1543-Pos
Control of Ca Release Synchrony by Action Potential Configuration in Murine Cardiomyocytes

Johan Hake[1], Guro F. Jølle[2,3], Halvor K. Mørk[2,3], Ivar Sjaastad[2,3], Ole M. Sejersted[2,3], William E. Louch[2,3], Glenn T. Lines[1].
[1]Simula Research Laboratory, Lysaker, Norway, [2]Institute for Experimental Medical Research, Oslo University Hospital - Ullevål, Oslo, Norway.
[3]Centre for Heart Failure Research, Faculty of Medicine, University of Oslo, Oslo, Norway.

Spatially non-uniform or ''dyssynchronous'' sarcoplasmic reticulum (SR) Ca release has been reported in cardiomyocytes from failing hearts. Using a murine model of congestive heart failure (CHF) following myocardial infarction, we investigated whether altered action potential (AP) configuration promotes release dyssynchrony. We observed that APs (1 Hz) were prolonged in cardiomyocytes isolated from the viable septum of CHF hearts, compared to and sham-operated controls (SHAM). Representative AP recordings were included in a detailed computational model of the Ca dynamics in the dyad. The model predicted reduced driving force for L-type Ca current and more dyssynchronous opening of ryanodine receptors during stimulation with the CHF AP than the SHAM AP. These predictions were confirmed in isolated cardiomyocyte experiments, when cells were alternately stimulated by SHAM and CHF AP voltage-clamp waveforms. However, when a train of like APs was used as the voltage stimulus, the SHAM and CHF AP produced a similar Ca release pattern. In this steady-state condition, both modeling and cell experiments showed that greater integrated Ca entry during the CHF AP lead to increased SR Ca content. We modeled the effect of increased SR Ca content by increasing the Ca sensitivity of the ryanodine receptor, which we observed increased the synchrony of ryanodine receptor activation. Thus, at steady-state, Ca release synchrony was maintained during the CHF AP as greater ryanodine sensitivity offset the de-synchronizing effects of reduced driving force for Ca entry. Our results suggest that dyssynchronous Ca release in failing mouse myocytes results from alterations such as T-tubule re-organization, and not electrical remodeling.

1544-Pos
Imaging of the Ryanodine Receptor Distribution in Rat Cardiac Myocytes with Optical Single Channel Resolution

David Baddeley[1], Isuru D. Jayasinghe[1], Leo Lam[1], Sabrina Rossberger[1,2], Mark B. Cannell[1], **Christian Soeller**[1].
[1]University of Auckland, Auckland, New Zealand, [2]University of Heidelberg, Heidelberg, Germany.

We have applied a new optical super-resolution technique based on single molecule localisation to examine the peripheral distribution of a cardiac signalling protein, the ryanodine receptor (RyR), in rat ventricular myocytes. Using high-resolution antibody labeling data we show that the new imaging approach, termed localization microscopy, can give novel insight into the distribution of large proteins, with optical single channel resolution. We present, to our knowledge, the first direct data showing evidence for a two-dimensional array-like arrangement of RyRs in cardiac muscle. Morphological analysis of peripheral RyR clusters in the surface membrane revealed a mean size of ~14 RyRs per cluster, almost an order of magnitude smaller than previously estimated. Clusters were typically not circular (as previously assumed) but elongated with an average aspect ratio of 1.9. Edge-to-edge distances between adjacent RyR clusters were often less than 50 nm suggesting that peripheral RyR clusters may exhibit strong inter-cluster signalling. The cluster size varied widely and followed a near-exponential distribution. We show that this distribution is compatible with a stochastic cluster assembly process and construct simple cluster growth models that generate size distributions very similar to our experimental observations. Based on the placement and morphology of RyR clusters we suggest that calcium sparks may be the result of the concerted activation of several clusters forming a functional 'supercluster' whose gating is controlled by both cytosolic and sarcoplasmic reticulum luminal calcium levels. The new imaging approach can be extended to other cardiac proteins and should yield novel insight into excitation-contraction coupling and the control of cardiac contractility.

1545-Pos
Synchronization of Spontaneous Stochastic RyR Activation in Ventricular Myocytes (VM) by Camp or Disengagement of Phospholambam (PLB) From SERCA2

Syevda Sirenko[1,2], Tatiana M. Vinogradova[1], Larry R. Jones[3], Victor Maltsev[1], Edward G. Lakatta[1].
[1]Laboratory of Cardiovascular Science, National Institute on Aging, NIH, Baltimore, MD, USA, [2]MedStar Research Institute, Baltimore, MD, USA, [3]Krannert Institute of Cardiology, Indianapolis, Indianapolis, IN, USA.

Stochastic RyR activation underlies Ca^{2+} sparks in VM. Here we show that in saponin ''skinned'' VM, bathed in 100 nM Ca^{2+} at 35°C, cAMP converts this stochastic spontaneous RyR activation (Ca^{2+} sparks-confocal linescan imaging) into synchronized, rhythmic RyR activation (Fig. A) about an average dominant frequency 2.2 ± 0.13 Hz (n=3). Of note, cAMP does not alter the SR Ca^{2+} load assessed by the rapid application of caffeine (107 ± 17.3 nM Ca^{2+} n=9 prior and 121 ± 19.3 nM Ca^{2+} n=3 during cAMP exposure). When Ca^{2+} pumping into SR is selectively accelerated by a PLB antibody (2D12, 0.013 mg/ml) that disengages PLB from SERCA2, stochastic RyR Ca^{2+} release becomes rhythmic (Fig. B) about an average dominant frequency of 2.6 + 0.21 Hz (n=5). The amplitude of the integrated spontaneous Ca^{2+} release signal during any given epoch increases when stochastic RyR activation becomes synchronized, i.e. converted to rhythmic activation (Fig. C). This cAMP-generated rhythmicity of spontaneous RyR activation of VM mimics rhythmic spontaneous diastolic Ca^{2+} releases in sinoatrial nodal pacemaker cells which have a basal high level of intrinsic cAMP-dependent signaling.

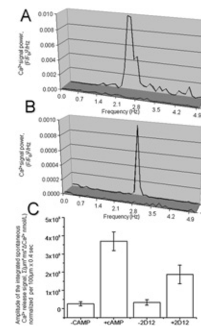

1546-Pos
Subcellular Mechanisms of Early Impaired Calcium Homeostasis with Chronic Beta$_1$-Adrenergic Stimulation in Mice

Frank R. Heinzel[1], Shelina Khan[2], Patrick Freidl[1], Simon Sedej[1], Felix Hohendanner[1], Paulina Wakula[1], Brigitte Korff[2], Stefan Engelhardt[3], Burkert Pieske[1].
[1]Medical University of Graz, Graz, Austria, [2]University of Göttingen, Göttingen, Germany, [3]Institute of Pharmacology and Toxicology, TU Munich, Munich, Germany.

Chronic beta-adrenergic stimulation leads to heart failure (HF). In mice overexpressing beta1-adrenoceptors (TG), increased diastolic Ca load in cardiomyocytes at early age is pivotal for the development of HF. The mechanisms underlying intracellular Ca dysregulation are unclear. We examined cytosolic Ca transients (Fluo4-AM, field stimulation), Na-Ca-exchanger (NCX) function and protein expression, cytosolic Na (SBFI) and T-tubular structures (Di8-ANEPPS) in cardiomyocytes from young (8-16 wks) TG mice and wildtype (WT) littermates.
Results: Systolic [Ca] amplitude was unchanged, time to peak [Ca] (140 ± 5 vs. 127 ± 3 ms) and [Ca] decay (time constant, tau, 223 ± 16 vs. 182 ± 9 ms) were significantly prolonged in TG vs. WT. Diastolic Ca leak from the SR (quantified as tetracaine-sensitive change in diastolic [Ca] or diastolic Ca spark frequency) was unchanged. However, cytosolic Ca removal by NCX during coffein application was significantly slower (tau, 3683 ± 337 in TG vs. 2304 ± 272 ms in WT), indicating reduced forward mode NCX activity. NCX protein expression was unchanged. Preliminary results indicate increased cytosolic [Na] in young TG. Furthermore, confocal line scans revealed delayed (> 15 ms until half-maximal) systolic Ca release in 24.7 ± 2.6 (TG) vs. 4.6 ± 1.4% (WT) of the intracellular regions (n=32 and 31 cells, resp., p<0.01). The extent of dyssynchronous Ca release correlated with time to peak systolic [Ca] (R=0.51, P<0.001) and was associated with a lower density and increased irregularity of T-tubules in TG (22.8 ± 1.6% of cell volume in TG vs. 26.1 ± 2.5% in WT). In summary, in early HF remodeling with chronic beta1-adrenergic stimulation, slowed cytosolic Ca clearance isnot related to increased diastolic SR Ca leak but associated with decreased NCX forward mode activity, which may be related to increased cytosolic [Na]. Reduced T-tubule density with dyssynchronous, slowed systolic Ca release additionally contribute to increased cytosolic Ca load.

1547-Pos
Rational Design and Structrual Analysis of Ca^{2+} Biosensor and Application in Skeletal Muscle Cells

Shen Tang, Hing-Cheung Wong, Jin Zou, Yun Huang, Jenny J. Yang.
Georgia State University, Atlanta, GA, USA.

Quantitative and real-time detection of Ca^{2+} signaling in internal Ca^{2+} store sarcoplasmic reticulum (SR) of skeletal muscle cells is essential to explore

the mechanism of various diseases such as malignant hyperthermia, central core diseases, brody diseases and so on highly related with SR calcium abnormal handling. To overcome the limitation of reported genetically encoded Ca^{2+} sensors based on natural Ca^{2+} binding proteins of perturbing Ca^{2+} signaling, we report a novel design of calcium biosensor for the first time by rational de novo engineering a non-natural Ca^{2+} binding site into a single enhanced green fluorescent protein (EGFP), which can successfully quantitatively reveal the subcellular calcium signaling by fluorescence change. These developed Ca^{2+} sensors exhibit K_d values measured inside the mammalian cells in situ optimal for the measurement of Ca^{2+} in the SR. Metal selectivity of the sensors for Ca^{2+} in competition to excessive biological metal ions such as Mg^{2+}, K^{+}, Na^{+} has been examined. In addition, these developed sensors can be targeted to the SR of muscle cells, and detected the Ca^{2+} signaling induced by various agonists and antagonists interacting with SR membrane Ca^{2+} pumps or receptors. Moreover, they exhibit fast response to Ca^{2+}. Further, their optical and conformational properties have been investigated using various spectroscopic methods, including high resonance resolution NMR. Moreover, more than 70% of the amino acids of the EGFP-based designed sensor have been successfully assigned using heteronuclear-labeled proteins. Our studies further reveal the key factors that contribute to the molecular mechanisms of the fluorescence change upon calcium binding and dynamic properties of our designed Ca^{2+} sensors.

1548-Pos

Orai1 Mediates Store-Operated Ca2+ Entry in Normal Skeletal Muscle and Exacerbated Ca2+ Entry in Dystrophic Muscle

Xiaoli Zhao, Noah Weisleder.
Robert Wood Johnson Medical School, Piscataway, NJ, USA.

Duchenne muscular dystrophy (DMD) is the most common form of muscular dystrophy, in which loss of dystrophin expression results in compromised sarcolemmal integrity. Although evidence shows that defects in Ca2+ homeostasis is a causal factor for the progressive cell death observed in DMD, the mechanism of Ca2+ deregulation is still under debate. Several laboratories showed that enhanced Ca2+ entry might serve as a pathological factor in dystrophic muscles. In this study, we explored the role of store operated Ca2+ entry (SOCE) in Ca2+ deregulation of dystrophic muscles. We used real-time PCR and Western blotting to detect known isoforms of Orai and STIM1 and determined that Orai1 was the most abundant in skeletal muscle and was significantly upregulated in muscles from mdx mice, while STIM1 levels remained largely unchanged. Furthermore, Mn2+ quenching of fura-2 fluorescence was applied to measure SOCE activity in flexor digitorum brevis (FDB) fibers and a significant increase in SOCE activity was detected in mdx fibers. Similar levels of resting [Ca]i was identified in wt and mdx groups, while peak response to C/R was significantly higher in mdx fibers than wt. Furthermore, we electroporated shRNA probe against mouse Orai1 into FDB muscle of living mice to produce effective knockdown (KD) of Orai1 expression. Two weeks after Orai1 KD, SOCE activity was eliminated in both wt and mdx muscle fibers and peak response to caffeine and ryanodine in mdx fiber sreturned to a level comparable to wt muscle fiber. Therefore, our study established that Orai1 is an essential component of SOCE machinery in adult skeletal muscle and indicates that Orai1-mediated SOCE could be the major pathway for additional Ca2+ entry into mdx muscle fibers, which would eventually lead to progression of DMD.

1549-Pos

Orai1 and STIM1 Mediate Capacitative Ca^{2+} Entry in Mouse Pulmonary Arterial Smooth Muscle Cells

Lih Chyuan Ng[1], Deepa Ramduny[1], Judith A. Airey[1], Cherie A. Singer[1], Phillip S. Keller[1], Xiao-Ming Shen[1], Honglin Tian[1], Maria L. Valencik[2], Joseph R. Hume[1].
[1]Department of Pharmacology, University of Nevada School of Medicine, Reno, NV, USA, [2]Department of Biochemistry, University of Nevada School of Medicine, Reno, NV, USA.

Previous studies in mouse pulmonary arterial smooth muscle cells (PASMCs) showed that TRPC1 and STIM1 mediates the sustained component of capacitative Ca^{2+} entry (CCE) but the molecular candidate(s) that mediate the transient component of CCE remains unknown. The aim of the present study was to further examine if Orai1 mediates the transient component of CCE through activation of STIM1 protein in mouse PASMCs.In primary cultured mouse PASMCs loaded with fura-2, cyclopiazonic acid (CPA) caused a transient followed by a sustained rise in intracellular Ca^{2+} concentration ($[Ca^{2+}]_i$).The transient but not the sustained rise in $[Ca^{2+}]_i$ was partially inhibited by nifedipine. The nifedipine-insensitive transient rise in $[Ca^{2+}]_i$ and the increase in Mn^{2+} quench of fura-2 fluorescence caused by CPA were both reduced in cells treated with Orai1 siRNA. These responses to CPA were further reduced in cells treated with Orai1 and STIM1 siRNA. Moreover, over-expression of STIM1 enhanced the rise in $[Ca^{2+}]_i$ and the increase in Mn^{2+} quench of fura-2 fluorescence caused by CPA and these responses were reduced in cells treated with Orai1 siRNA. RT-PCR revealed Orai1 and STIM1 mRNAs, and Western blot analysis identified Orai1 and STIM1 proteins in mouse PASMCs. Furthermore, Orai1 was found to co-immunoprecipitate with STIM1 and immunostaining showed co-localization of Orai1 and STIM1 proteins. These data provide direct evidence that the transient component of CCE is mediated by Orai1 channel through activation of STIM1 in mouse PASMCs. [Supported by HL49254, NCRR P20RR15581 (JR Hume) and AHA Scientist Development Grant (LC Ng)]

1550-Pos

In Smooth Muscle, Mitochondrial Movement is Restricted in Native Cells and Unrestricted and Trafficked When Cells are in Culture

Susan Chalmers[1], Chris D. Saunter[2], John M. Girkin[2], Gordon D. Love[2], John G. McCarron[1].
[1]University of Strathclyde, Glasgow, United Kingdom, [2]Durham University, Durham, United Kingdom.

Positioning of mitochondria in the cell is important for the local provision of ATP and for regulation of $[Ca^{2+}]_c$ signals, lipid and reactive oxygen species production, redox control and initiation of cell death signals. In smooth muscle, mitochondrial Ca^{2+} uptake promotes Ca^{2+} release from the sarcoplasmic reticulum via by IP_3R, suggesting a localised removal of the ion from the IP_3R cytosolic face that maintains channel activity$_1$. The close physical interaction that this relationship implies is not compatible, however, with the reported free movement of mitochondria throughout the cytosol. Here, image correlation based single particle tracking of mitochondria in freshly-isolated single smooth muscle cells from guinea-pig colon, shows that mitochondria displayed very limited movement. Brownian motion of mitochondria was detected but did not generate any significant displacement of the organelle over time. Neither the actin depolymerising agent latrunculin B (10 μM), nor the microtubule disrupter nocodazole (10 μM) increased mitochondrial movement. In contrast, when freshly-isolated smooth muscle cells were maintained in cell culture conditions for 14 days mitochondrial motility was substantially increased. Mitochondria displayed rapid, directed motion and Brownian movement resulted in displacement of the mitochondria over time. These results suggest that in freshly-isolated smooth muscle cells, mitochondria are either confined or tethered to limit movement; whereas when the same cells divide and proliferate in culture these restraints are lost, mitochondria display random-walk diffusive motion and are accessible to the intracellular trafficking machinery.

1. Chalmers S & McCarron JG (2008) J Cell Sci. 121:75-85.
2. Saunter CD *et al.* (2009) FEBS Lett. 583:1267-73.

*These authors contributed equally to this work. The Wellcome Trust (070854/Z/05/Z), British Heart Foundation (PG/08/066) and Science & Technology Facilities Council (ST/F003722) funded this work.

1551-Pos

Synchronization of Waveform Analysis with Monitoring of Localized [Ca2+] in the Beating Flagellum of Single Sperm

Donner F. Babcock.
University of Washington, Seattle, WA, USA.

Much past work indicates that in mammalian sperm Ca^{2+} is the messenger that controls waveform flagellar symmetry, and that the cAMP messenger controls beat frequency. We have now constructed an imaging system that uses dual pulsed-LED sources and records interleaved stop-motion brightfield and fluorescence images of individual loosely-tethered mouse sperm loaded with the Ca^{2+} probe fluo-4. The brightfield images report flagellar beat frequencies of 2-4 hertz for resting sperm, and the fluo-4 images report similar $[Ca^{2+}]$ (~150 nM) in the head, the midpiece, and the cytoplasmic droplet located at the flagellar midpiece/principal-piece junction. Stimulation (10-20s) by local perfusion with alkaline-depolarizing medium K8.6 raises $[Ca^{2+}]$ ~4-fold in each region. The $[Ca^{2+}]$ rises first in the droplet, then the midpiece, and finally in the head. Recovery towards baseline is slow ($t_{1/2}$>30s). Analysis of the waveform shows that increases in flagellar beat asymmetry accompany the increased $[Ca^{2+}]$ but that beat frequency remains unchanged before, during, and after stimulus. The delayed Ca^{2+} responses in midpiece and head are consistent with evoked localized entry through CatSper ion channels in the principal piece with subsequent diffusional redistribution. The accompanying increases in beat asymmetry without increases in frequency suggests that evoked Ca^{2+} entry does not engage cAMP-mediated signaling in sperm.

Support by HD12629-27 from the Eunice Kennedy Shriver NIH/NICHD by cooperative agreement U54 of the Specialized Cooperative Centers Program in Reproduction and Infertility Research

1552-Pos
Deriving Cellular Ca(2+) Dynamics from Puff Characteristics - A New Approach in Mathematical Modeling
Kevin Thurley, Falcke Martin.
Max-Delbrück-Center, Berlin, Germany.
It has recently been shown that Ca(2+) spikes are stochastic and that the Ca(2+) concentration is subject to huge intracellular gradients. These findings underline the need for stochastic models taking single molecule state transitions into account (Master Equations are impossible due to the high number of states). We developed such a modeling concept based on the fact that for cellular concentration dynamics, it is only relevant whether channels are open or closed, but not in which open or closed state they are. That requires a non-Markovian formulation of the theory which we will present. This formulation permits direct integration of measurable quantities into the model, whereas detailed knowledge of physiologic parameters is not necessary. Therefore, input and output can be directly compared with experiments, if we consider observables like the probability that no spike happens or the average spike length. The model covers experimentally observed modes of system behavior like bursting, spiking or local events. Statistic properties of interspike intervals are in good accordance with experimental data. Since we have developed an analytic description as well as an efficient simulation algorithm, we are in a position to analyze a broad range of possible system configurations based on a solid theoretical background. In particular, we find that the spiking pattern can be predicted merely from two parameters, the cluster coupling and the average channel open time. The latter is probably constant and the former can be regulated by second messengers or by the number of active clusters, e. g. This implies that local dynamics emerges to a single control parameter determining global dynamics. Since we expect similar mechanisms to work in various fields of biology (e.g. cAMP dynamics and DNA replication), our theory should be widely applicable.

1553-Pos
Simulations of Calcium Oscillations in Pancreatic Acinar Cells
Peng Wang[1], Andrew Quong[2], Amy Y. Liu[1].
[1]Georgetown University, Washington DC, DC, USA, [2]Thomas Jefferson University, Philadelphia, PA, USA.
Pancreatic acinar cells have developed sophisticated Ca^{2+} signaling mechanisms, which have important physiological roles on enzyme and fluid secretion. In response to stimulation, Ca^{2+}signals in pancreatic acinar cells are modulated in a precise spatiotemporal manner necessary for normal secretory function and are generally confined to the apical pole. Meanwhile, abnormal, prolonged global elevation of cytosolic Ca^{2+} concentration has been proposed to be the crucial trigger for pancreatitis. In this study, we have constructed and validated a computational model to gain insights into the generation of different Ca^{2+} signaling patterns in pancreatic acinar cell. Specifically this model allows us to examine the roles of and interactions between inhomogeneous distributed IP_3 and rynodine receptors, the passive and active roles of the mitochondrial barrier that separates the apical and basal regions, and dimensionality. Preliminary results indicate that both the topology of the mitochondrial barrier and mitochondrial Ca^{2+} uptake have significant impact in both confining and maintaining the apical oscillations, supporting the idea that mitochondria are active and crucial elements of Ca^{2+} signaling in pancreatic acinar cells. In addition, when using the same parameters for the kinetics, changing from a two-dimensional to three-dimensional model of the cell yields qualitatively different results for the apical Ca^{2+} oscillation.

1554-Pos
Calcium Dynamics in Cardiac Mitochondria
Moradeke A. Bamgboye, W.J. Lederer.
UMB - UMBI, Baltimore, MD, USA.
Mitochondria play a significant role in the metabolic control of cardiac ventricular myocytes. They not only are the dominant intracellular organelle (~35% of the intracellular volume) but they have been reported to influence: intracellular Ca^{2+} concentration ($[Ca^{2+}]_i$)locally and dynamically, cellular apoptosis and cellular function. Many of the specific findings, however, are in dispute. We have used the high affinity calcium indicator Rhod2 to measure mitochondrial Ca^{2+} in permeabilized cells. (Fig 1). We do observe changes in mitochondrial Ca^{2+} ($[Ca^{2+}]_{mito}$) when $[Ca^{2+}]_i$ changes but these changes are modest.

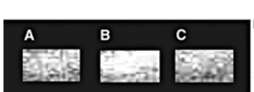

Fig. 1. Mitochondrial Calcium increase. A. Rhod2-loaded single mitochondria under "control" conditions ; **B.** Same mitochondrion 13 s later when $[Ca^{2+}]_i$ is elevated; **C.** Same mitochondrion 17 s after B when $[Ca^{2+}]_i$ has returned to control level.

Ryanodine Receptors I

1555-Pos
Biophysical and Cellular Characterisation of Alternatively Spliced Isoforms of the Human Cardiac Ryanodine Receptor (RyR2)
Wai Yin Yeung, N Lowri Thomas, Saptarshi Mukherjee, Matthew V. Davies, F Anthony Lai, Alan J. Williams, Christopher H. George.
Cardiff University, Cardiff, United Kingdom.
Developmentally regulated and tissue-specific alternative splicing of the human cardiac ryanodine receptor (RyR2) may represent an innate mechanism for tuning intracellular Ca^{2+} handling. The precise molecular basis of channel modulation by alternative splicing (30bp and 24bp inserts encoding FAIDSLCGFG and VTGSQRSK, respectively) remains unknown. To further explore the mechanistic basis of altered RyR2 function by alternative splicing we expressed and characterised recombinant human RyR2 channels. We measured the Ca^{2+} activation of detergent-free homotetrameric channels using an *in vitro* ryanodine binding assay and showed that $RyR2^{24+}$ exhibited Ca^{2+}-sensitive ryanodine binding (EC_{50} $0.65 \pm 0.01 \mu M$; B_{max} at ambient $[Ca^{2+}] > 5 \mu M$, 380 ± 48 fmol/mg) that was entirely comparable to channels formed from 'unspliced' RyR2 subunits (EC_{50} $0.52 \pm 0.17 \mu M$; B_{max} 350 ± 33 fmol/mg). In marked contrast, $RyR2^{30+}$, the predominant isoform in human embryonic hearts, did not exhibit Ca^{2+}-sensitive ryanodine interaction at equilibrium and binding was greatly reduced even at $[Ca^{2+}]$ up to 0.5mM (B_{max} 56 ± 5 fmol/mg). RyR2 mutations in the putative Ca^{2+} pore-lining helix abolish RyR2 interaction with ryanodine in 'steady state' assays (Wang et al., JBC 278 2003). Our finding that insertion of the FAIDSCLCGFG sequence distal to amino acid 1477 in $RyR2^{30+}$ ablates Ca^{2+}-sensitive ryanodine binding suggests that long range conformational interactions within the polypeptide may regulate the interaction with ryanodine and/or the Ca^{2+} sensitivity of the channel. The precise kinetics of ryanodine interaction with channels purified using sucrose density gradients were determined in single channel lipid bilayer experiments using K^+ as the permeant ion. The effects of synthetic peptides corresponding to the 30bp and 24bp splice epitopes on channel functionality *in vitro* and in living cardiac cell-based assays were also studied. Our data provides novel insights into the mode of RyR2 channel regulation by alternative splicing.

1556-Pos
Stabilisation of Ryanodine Binding to RyR2 - How Many Monomers are Involved?
Nia Lowri Thomas[1], Matthew V. Davies[1], S.R. Wayne Chen[2], Alan J. Williams[1].
[1]Wales Heart Research Institute, Cardiff University School of Medicine, Cardiff, United Kingdom, [2]Dpetartment of Physiology and Biophysics, University of Calgary, Calgary, AB, Canada.
An important contribution to our ability to study structure and function of the Ryanodine Receptor (RyR) Ca^{2+} release channel was the discovery of the plant alkaloid ryanodine, which binds to the channel only in the open state. Indeed the $[^3H]$-ryanodine binding assay is a widely utilised experimental technique and provides quantifiable information regarding the density and functional properties of a population of RyRs. Despite this, the precise molecular basis of the ryanodine-RyR interaction remains largely undefined. The inner helix of the pore of the cardiac mouse RyR (mRyR2) has been proposed as crucial for this interaction, and the mutation Q4863A has been shown to abolish ryanodine binding (at equilibrium) but is still functional in all other respects i.e. Ca^{2+} release in cells and at the single channel level (J Biol Chem 2003, 278, 51557-51565). The Q4863A mutation destabilises ryanodine once it is bound at the high affinity site (Mol Membr Biol 2007, 24, 185-93). Our aim is to use this mutant to establish the number of wild-type (WT) mRyR2 monomers necessary to stabilise bound ryanodine in the tetramer.
Assuming that WT and Q4863A monomers associate equally, the probable occurrence of each homo/heterotetramer type can be calculated using binomial theory, and subsequently the $[^3H]$-ryanodine binding level of each predicted if 1,2,3 or all 4 WT monomers are required to stabilise the interaction. In practice, ryanodine stabilisation has been determined by measuring $[^3H]$-ryanodine binding to mixed heterotetramer populations of mRyR2 under maximally activated conditions following co-expression of WT and Q4863A monomers in differnt ratios in HEK293 cells. Initial results show that 2 WT monomers are required for high affinity binding. The mechanisms governing binding will be investigated at the single channel level. Supported by the British Heart Foundation and HSFA.

1557-Pos

Association of Triadin to the Junctional Sarcoplasmic Reticulum of Skeletal Muscle Cells

Daniela Rossi, Cristina Bencini, Francesca Benini, Stefania Lorenzini, Marina Maritati, Vincenzo Sorrentino.
University, Siena, Italy.

The junctional sarcoplasmic reticulum (jSR) of skeletal muscle cells contains several proteins that participate to the mechanisms of Ca2+ release in the process of excitation-contraction coupling. Among these proteins, ryanodine receptor, triadin, junctin and calsequestrin have been found to associate into a stable complex. We recently reported that assembly of jSR domains is accompanied by a strong decrease in the mobility fraction of jSR proteins (Cusimano et al., PNAS 2009). In particular, we found that the mobility of triadin appeared to be mediated by its intraluminal region (aa 232-729). In order to identify the minimal regions required for association of triadin to the jSR, deletion mutants of the luminal domain (triadin Δ232-440 and triadin Δ441-729) were generated and expressed in primary muscle myotubes. Analysis of the mobility fraction of these mutants showed that they do not differ from wild type triadin, indicating that either one of the two regions is sufficient to provide a strong association of the protein to the jSR. Interestingly, we found that the luminal region of triadin contains several defined domains, including a coiled coil region and short amino acids repeats, that are present in the region between aa 232-440 and aa 441-729, where they may mediate protein-protein interactions. Results on the role of these amino acid repeats in mediating triadin association with the jSR will be reported.

1558-Pos

Time-Resolved FRET Detection of Structural Distributions Involving FKBP12.6 and Calmodulin Bound Within Macromolecular RyR Channels

Razvan L. Cornea, Florentin R. Nitu, David D. Thomas, Bradley R. Fruen.
UNIVERSITY OF MINNESOTA, Minneapolis, MN, USA.

We used multi-exponential analysis of time-resolved (TR) fluorescence decays to investigate the array of distances underlying fluorescence resonance energy transfer (FRET) between donors and acceptors bound within functional RyR channels in sarcoplasmic reticulum membranes. Previously, we have used steady-state (SS) FRET to demonstrate that CaM is oriented with the N-lobe proximal to the FKBP12.6 subunit on each lateral face of the RyR tetrameric complex (Cornea et al. 2009). Here, we used cysteine mutagenesis and sulfhydryl-specific fluorescent labeling to attach Alexa Fluor (AF) donor probes to single-cysteines at FKBP12.6 sites 49 or 85 (denoted D49 and D85), and acceptor probes to calmodulin (CaM) N-lobe sites 26 or 34 (denoted A26 and A34). The fluorescence of RyR-bound donor-labeled FKBP12.6 was decreased in the presence of saturating acceptor-labeled CaM, indicating FRET. Förster analysis of TR- and SS-FRET data of donor/acceptor pairs AF350/AF488 and AF488/AF568 (with different ranges of sensitivity) yielded similarly-ranked energy transfer efficiencies: D85/A26 $\geq$ D49/A26 $>$ D49/D34 $>$ D85/34. Distances calculated from these FRET efficiencies are remarkably similar for the two different donor/acceptor probe pairs. However, this kind of analysis can extract only averaged distances from an RyR sample in which distinct biophysical states are known to co-exist. Further multi-exponential analysis of the donor-only (AF350-FKBP12.6) and donor+acceptor (AF350-FKBP12.6/AF488-CaM) TR-FRET data sets resolved at least two simultaneous distance populations for each pair of labeled sites. These distances and their distribution responded to changes in [Ca^{2+}]. We conclude that TR-FRET provides a powerful approach for resolving dynamic transitions between structural states within functional, multimeric RyR channels. Further studies will aim to determine whether these findings reflect transitions between different conformations of CaM itself, or of the underlying RyR channel.

1559-Pos

FKBP12.6 Inhibits Resting Ryanodine Receptor Activity but PKA-Dependent Phosphorylation Does Not Alter FKBP12.6-RyR2 Binding in Rat Permeabilized Myocytes

Tao Guo[1], Razvan Cornea[2], Sabine Huke[3], Emmanuel Camors[4], Yi Yang[4], Eckard Picht[4], Bradley Fruen[4], Donald Bers[4].
[1]Rush University Medical Center, Chicago, IL, USA, [2]University of Minnesota, Minneapolis, MN, USA, [3]Vanderbilt University School of Medicine, Nashville, TN, USA, [4]University of California, Davis, CA, USA.

FK506-binding proteins FKBP12.6 and FKBP12 are associated with the cardiac ryanodine receptor (RyR2), and PKA dependent hyperphosphorylation of RyR2 has been proposed to interrupt the FKBP12.6-RyR2 interaction and activate RyR2 opening. However, the physiological function of FKBP12.6/12.0 in cardiac myocytes and the role of PKA-dependent RyR2 phosphorylation are controversial. We used permeabilized rat ventricular myocytes, and fluorescently-labeled FKBP12.6/12.0 to directly measure in situ binding of FKBP12.6/12.0 to RyR2, with simultaneous Ca sparks measurements as an RyR2 functional index. We found that both FKBP12.6 and FKBP12 concentrate at the Z-line, consistent with RyR2 binding. However, only FKBP12.6 inhibits resting RyR2 activity. Assessment of fluorescent FKBP binding at the Z-line of permeabilized myocytes revealed a high affinity of FKBP12.6-RyR2 (Kd = 0.97 $\pm$ 0.1 nM) and much lower affinity of FKBP12-RyR2 (Kd = 206 $\pm$ 70 nM). Fluorescence recovery after photobleach of FKBP in myocytes confirmed these different affinities and showed that the main difference was in koff. Activation of RyR2 phosphorylation by PKA had no significant affect on either binding kinetics or affinity of FKBP12.6/12-RyR2. Using quantitative immunoblots, we determined the concentration of endogenous FKBP12 in intact myocytes was ~1 μM, while FKBP12.6 is at most ~150 nM. Taken together, our data suggest that FKBP12.6 binds to and stabilizes the resting RyR2 but cAMP-dependent RyR2 phosphorylation does not dissociate FKBP12.6 (or FKBP12) from RyR2 in the myocyte environment. More important, this study highlights the importance of in situ binding properties measurement and clarifies some aspects of controversy.

1560-Pos

FKBP12 and FKBP12.6 Exert Opposing Actions on the Single-Channel Behaviour of Both RyR1 and RyR2

Elisa Venturi[1], Elena Galfrè[1], Mano Sitsapesan[1], Samantha Pitt[1], Yan Dai[1], Stephen O'Neill[2], Rebecca Sitsapesan[1].
[1]University of Bristol, Bristol, United Kingdom, [2]University of Manchester, Manchester, United Kingdom.

It is widely believed, that in striated muscle, FKBP12.6 selectively binds to RyR2 but that FKBP12 is the binding partner for RyR1. Few studies have addressed whether FKBP12 can modulate RyR2 function or whether FKBP12.6 can affect RyR1. Our recent single-channel studies show that FKBP12 activates RyR2 with nanomolar affinity but because binding is rapidly reversible, this interaction is unlikely to be detected by Western blot analysis. We have therefore compared how FKBP12 and FKBP12.6 affect the single-channel properties of RyR1 and RyR2 reconstituted into bilayers. Using Ca^{2+} as the permeant ion, cytosolic addition of 500 nM FKBP12 significantly decreased the open probability (Po) of RyR1 from 0.021 $\pm$ 0.005 (SEM; n = 4) in controls to 0.001 $\pm$ 0.001 (SEM; n = 4; $P<0.05$). This effect was irreversible after perfusing away the FKBP12. In contrast, 200 nM and 1 μM FKBP12.6 increased RyR1 Po. This effect was also irreversible after washout of FKBP12.6 but could be antagonised by addition of FKBP12. In comparison, FKBP12 is a reversible activator of RyR2 whereas FKBP12.6 has little intrinsic action itself but can antagonise FKBP12-induced activation. The presence or absence of FKBP12/12.6 did not lead to the appearance of sub-conductance gating states in RyR2 but, after FK-506 treatment or addition of FKBP12.6 to RyR1, sub-conductance states were frequently observed. Since FKBP12 activates RyR2 but is antagonised by FKBP12.6, and FKBP12.6 activates RyR1 but is antagonised by FKBP12, the ratio of FKBP12/FKBP12.6 levels in the cytoplasm will be critical in determining RyR activity *in situ*. Changes in the cytoplasmic FKBP12/FKBP12.6 ratio may be important in heart failure, where it has been suggested that less FKBP12.6 binds to RyR2.

Supported by the British Heart Foundation

1561-Pos

Use of Rapamycin Reveals Evidence of the Physiological Roles of FKBP12 and FKBP12.6 In Cardiac Excitation-Contraction Coupling

Elena Galfrè[1], Elisa Venturi[1], Samatha J. Pitt[1], Mano Sitsapesan[1], Rebecca Sitsapesan[1], Stephen O'Neill[2].
[1]University of Bristol, Bristol, United Kingdom, [2]University of Manchester, Manchester, United Kingdom.

A huge body of evidence suggests that FKBP12.6, which binds tightly to RyR2, is an important physiological regulator of cardiac excitation-contraction (EC) coupling yet its mechanism of action remains elusive. Our recent single-channel studies now reveal that RyR2 activity may be controlled by the opposing actions of FKBP12.6 and FKBP12. To investigate how these proteins regulate RyR2 function in cardiac cells we have used rapamycin to dissociate FKBP12 and FKBP12.6 from RyR2 in isolated rat permeabilised ventricular myocytes. In control myocytes perfused with Fluo-5F, spontaneous waves of Ca^{2+}-induced Ca^{2+}-release were induced by 234 nM Ca^{2+} in the mock cytoplasmic solution. Treatment for 4-6 min with 20 μM rapamycin, reduced the frequency of the Ca^{2+}-waves from 0.57 ± 0.07 Hz to 0.18 ± 0.05 Hz (SEM; n=5; $P<0.002$) and led to the appearance of 'mini-waves' that did not propagate throughout the cell. Rapamycin treatment also increased baseline Fluo-5F fluorescence intensities by 204 ± 47% (SEM; n=8; $P<0.05$), an effect that was completely reversed by perfusion with a physiological level of FKBP12 (3 μM; n=4; $P<0.001$) but not with 200 nM FKBP12.6 (n=4). In rapamycin-treated cells, FKBP12 (from 0.15 ± 0.06 Hz to 0.27 ± 0.07 Hz (SEM; n=6; $P<0.025$) was

able to increase wave frequency. On the other hand, FKBP12.6 was not (from 0.12±0.04 Hz to 0.16±0.04 Hz (SEM; n=4; $P>0.35$). Our results indicate that FKBP12 may have an important role as an activator of RyR2 in cardiac cells. Further work is required to determine the individual and combined roles of FKBP12 and FKBP12.6 in cardiac EC-coupling.
Supported by the British Heart Foundation.

1562-Pos
FKBP12 is a High Affinity, Reversible Activator of RyR2, and FKBP12.6 Antagonises Its Actions

Rebecca Sitsapesan[1], Samantha J. Pitt[1], Elisa Venturi[1], Elena Galfre[1], Stephen O'Neill[2], Mano Sitsapesan[1].
[1]University of Bristol, Bristol, United Kingdom, [2]University of Manchester, Manchester, United Kingdom.

FKBP12.6 binds tightly to RyR2 and evidence suggests that it plays a vital physiological role in regulating channel activity. Moreover, changes in FKBP12.6/RyR2 interactions have been implicated in heart failure. Controversy exists, however, as to how FKBP12.6 affects the single-channel behaviour of RyR2. Furthermore, although higher levels of FKBP12 than FKBP12.6 are present in cardiac cells, the effects of FKBP12 on RyR2 are virtually unresearched. We have therefore compared the effects of FKBP12 and FKBP12.6 on the single-channel function of sheep RyR2 incorporated into bilayers under voltage-clamp conditions. We find that FKBP12 increases RyR2 open probability (Po) in a dose-dependant, reversible manner with an EC_{50} of 51 nM. In the presence of 10 μM cytosolic Ca^{2+}, physiological levels of FKBP12 (3 μM) increased Po from 0.187±0.051 in controls to 0.657±0.111 (SEM; n=14; $P<0.001$). In contrast, under identical experimental conditions, FKBP12.6 did not significantly increase or decrease RyR2 Po, however, it was able to antagonise the actions of FKBP12, shifting the EC_{50} value for FKBP12 to 4 μM. Our experiments demonstrate that FKBP12 has high affinity for RyR2 and that at physiological concentrations (1-3 μM) is an effective activator of the channel thereby suggesting that FKBP12 may have a more important role in cardiac excitation-contraction coupling than previously thought. We hypothesise that FKBP12.6 is a very low efficacy (but high affinity) partial agonist of RyR2 and that the balance between the effects of FKBP12 and FKBP12.6 is crucial for normal EC-coupling in cardiac cells.
Supported by the British Heart Foundation

1563-Pos
Imperatoxin Induces a Biphasic Response in Ca^{2+} Sparks

Erin M. Capes, Hector H. Valdivia.
University of Wisconsin-Madison, Madison, WI, USA.

Imperatoxin induces a biphasic response in Ca^{2+} sparks
Imperatoxin A (IpTxa), isolated from the venom of the African scorpion *Pandinus imperator,* has been shown to specifically activate ryanodine receptors (RyR) and to be capable of translocating across cell membranes. IpTxa enhances [^{3}H]ryanodine binding to sarcoplasmic reticulum (SR) and stabilizes subconducting states in single channels. We previously demonstrated that IpTxa alters the amplitude of calcium transients in intact field-stimulated cells, causing a rapid increase in transient amplitude. This is followed by a gradual decrement in amplitude to a new steady state at lower amplitude than in control. The current study seeks to clarify how IpTxa acts on RyRs to perturb Ca^{2+} handling in cardiomyocytes. We employed visualization of IpTxa-modified Ca^{2+} sparks in saponin-permeabilized cells to facilitate direct titration of RyRs with known concentrations of IpTxa, ranging from 500pM to 50nM. In addition, we modified our sparks protocol to enable a comparison of the caffeine-releasable SR Ca^{2+} load before and after treatment with the toxin. Our results demonstrate that IpTxa induces a biphasic RyR response, typified by a transient increase in spark frequency, amplitude, FWHM, and FDHM, which is rapidly followed by a sharp decrease in the same parameters. Comparison of pre- and post-toxin caffeine-releasable SR Ca^{2+} consistently reveals that SR content has been reduced as a result of IpTxa perfusion to approximately 75% of control. These results are consistent with the biphasic response observed in Ca^{2+} transient experiments. We believe that IpTxa sensitizes RyR to luminal Ca^{2+}, leading to increased Ca^{2+} release and subsequent depletion of Ca^{2+} from the SR. Our findings have exciting implications for translational research into cardiac diseases such as catecholaminergic polymorphic ventricular tachycardia, in which acute RyR hyperactivity is hypothesized to trigger arrhythmias leading to sudden cardiac death.

1564-Pos
Role of Hydrophobic Interactions in the Block of the Ryanodine Receptor by *Shaker* B Inactivation Peptides

Cedric Viero[1], **Sammy Mason**[1], Mark Bannister[2], Matthew Davies[1], Alan J. Williams[1].
[1]Wales Heart Research Institute, Cardiff, United Kingdom, [2]Imperial College, London, United Kingdom.

Shaker B K^+ channel NH_2-inactivation peptides (*Sh*BP) block both sheep and mouse cardiac ryanodine receptor Ca^{2+} release channels (RyR2). We provide new evidence for the presence of hydrophobic residues in the conduction pathway of RyR2 and their role in the block by wild-type (WT) and mutant *Sh*BP. RyR2 proteins were expressed in HEK cells, purified and their single channel activity recorded in lipid bilayers. Four peptides were synthesised and tested: i) WT *Sh*BP MAAVAGLYGLGEDRQHRKKQ, ii) a ''less hydrophobic'' peptide (LHBP) MAQVQGLYGLGEDRQHRKKQ, and 2 ''more hydrophobic'' peptides (MHBP), iii) MHBPI MAVVAGLYGLGEDRQHRKKQ and iv) MHBPII MAAVVGLYGLGEDRQHRKKQ. All peptides blocked the ryanodine-modified RyR2 channel from the cytosolic face in a concentration- and voltage-dependent manner. At a holding potential of +50 mV in symmetrical 210 mM KCl, we found an affinity constant K_D of 39.54 ± 3.90 μM for WT *Sh*BP, 65.90 ± 12.99 μM for LHBP, 27.79 ± 4.29 μM for MHBPI and 44.56 ± 9.38 for MHBPII. The association rates K_{on} of the peptides varied with concentration (2.92 ± 0.08 $s^{-1}.\mu M^{-1}$ for WT *Sh*BP, 3.85 ± 0.32 $s^{-1}.\mu M^{-1}$ for LHBP, 2.96 ± 0.22 $s^{-1}.\mu M^{-1}$ for MHBPI and 2.31 ± 0.25 $s^{-1}.\mu M^{-1}$ for MHBPII). Dissociation rates K_{off} were independent of concentration (115.30 ± 7.90 s^{-1} for WT *Sh*BP, 253.52 ± 24.49 s^{-1} for LHBP, 82.14 ± 5.48 s^{-1} for MHBPI and 102.97 ± 8.30 s^{-1} for MHBPII). Furthermore the block induced by the peptides could be reduced by an increase of the salt concentration at the luminal side of the channel. These findings indicate that hydrophobic interactions between RyR2 and inactivation peptides are necessary for the block, and that the binding sites of the peptides are within the pore. This research was supported by the BHF.

1565-Pos
Crystallographic Insights into the Cardiac Ryanodine Receptor N-terminal Domain and its Disease Mutants

Paolo A. Lobo, **Filip Van Petegem**.
University of British Columbia, Vancouver, BC, Canada.

Ryanodine receptors (RyRs) are large channels governing the release of Ca^{2+} from the sarcoplasmic or endoplasmic reticulum. They are required for the contraction of both skeletal (RyR1) and cardiac muscles (RyR2). Mutations in RyR genes have been associated with severe genetic disorders, but high-resolution data describing the disease variants in detail has been lacking. We have solved the crystal structures of the N-terminal domains of both RyR2 (2.55Å) and RyR1 (3.0Å), along with structures of various RyR2 disease mutants. The N-terminal domain in both RyR1 and RyR2 consists of a core beta trefoil domain flanked by an alpha helix. Two cysteine pairs display a highly increased flexibility, making them ideal candidates to receive redox modifications. Crystal structures of several RyR2 disease mutants (1.7Å - 2.2Å) show that most of the mutations cause distinct local changes to the surface of the protein, highlighting at least two putative binding interfaces required for normal RyR function. One RyR2 disease mutant causes significant changes in the thermal stability of the N-terminal domain, accompanied by large conformational changes in the structure.

1566-Pos
Structural Mapping of the Ryanodine Receptor Type 1 Using A Fret-Based Method

James D. Fessenden.
Boston Biomedical Research Institute, Watertown, MA, USA.

The type 1 ryanodine receptor (RyR1) mediates excitation contraction coupling in skeletal muscle by releasing stored intracellular calcium in response to cellular depolarization. This 2.2 MDa homotetrameric protein is associated with numerous regulatory proteins that modulate its activity in vivo. Understanding the structure and conformational dynamics of this immense macromolecular complex is an enormous challenge in skeletal muscle biology. In this report, structural determinations of RyR1 were performed using Förster resonance energy transfer (FRET) measurements. In this system, the FRET donor was green fluorescent protein (GFP) fused to RyR1, which could then transfer energy to Cy3NTA, a site-specific FRET acceptor targeted to poly-histidine segments inserted into RyR1. Energy transfer was monitored as a decrease in GFP fluorescence occurring when Cy3NTA was bound to a His tag in close proximity to the GFP donor fused either to position 1 or position 618 of RyR1. Cy3NTA was targeted to each of three ''divergent regions'' (DR) poorly conserved among the three RyR isoforms (DR1; position 4430, DR2; position 1323, DR3; position 1861). While minimal FRET was detected between N-terminally fused GFP and Cy3NTA targeted to these divergent regions, significant energy transfer was detected from GFP at position 618 to Cy3NTA targeted to DR2 or DR3. These experiments indicate that these donor and acceptor sites are in close proximity to each other and also demonstrate the utility of this FRET-based technique for further structural mapping of RyR1. (Supported by NIH grant R21ARO56406).

1567-Pos
FRET Detection of Calmodulin Binding and Structural Rearrangements Within the Cardiac RyR2 Calcium Release Channel

Bradley R. Fruen, Mallory Turner, Florentin R. Nitu, David D. Thomas, Razvan L. Cornea.
University of Minnesota, Minneapolis, MN, USA.

Calmodulin (CaM) binds to a conserved domain of the ryanodine receptor isoforms expressed in skeletal muscle (RyR1) and cardiac muscle (RyR2) to evoke isoform-specific changes in channel gating. To better understand CaM's interactions with the RyR2 isoform, we are using fluorescence resonance energy transfer (FRET) to define the orientation and kinetics of CaM binding, and to resolve structural rearrangements linked to channel regulation. A FRET donor was targeted to the RyR2 cytoplasmic assembly by preincubating cardiac sarcoplasmic reticulum membranes with a fluorescent-labeled FKBP12.6 (F-FKBP). An acceptor fluorophore was attached within the N-lobe of CaM (F-CaM). A decrease in F-FKBP fluorescence upon addition of F-CaM provided a specific, real-time readout of CaM binding to the RyR2, despite the presence of additional non-RyR CaM targets in the cardiac membranes. FRET demonstrated that the affinity of F-CaM binding to RyR2 was greater in 100 μM than in 30 nM Ca^{2+}. The maximal FRET observed in the presence of saturating [F-CaM] increased as a function of [Ca^{2+}] (30 nM to 1 mM). The Ca^{2+} dependence of this increase in FRET was similar to the Ca^{2+} dependence of [^{3}H]ryanodine binding to RyR2 assayed in equivalent media (K_{Ca} ~5 μM). A marked decrease in FRET between FKBP12.6 and CaM was observed when the acceptor was shifted from CaM's N-lobe to CaM's C-lobe. We conclude that CaM binds to the RyR2 in an extended conformation, with its N-lobe oriented nearest to the FKBP12.6 subunit. CaM's conformation and orientation when bound to the RyR2 are therefore similar to what has been demonstrated previously for the RyR1 isoform (Cornea *et al.*, 2009). Ca^{2+} dependent changes in FRET between FKBP12.6 and CaM may reflect structural changes within the RyR2 linked to channel activation by Ca^{2+}.

1568-Pos
Localization of Potential Calmodulin Binding Sequences onto the Three Dimensional Structure of the Cardiac Ryanodine Receptor Reveals A Binding Pocket for Calmodulin

Xiaojun Huang[1], Ruiwu Wang[2], Andrea Koop[2], S.R. Wayne Chen[2], Terence Wagenknecht[1], **Zheng Liu[1]**.
[1]Wadsworth Center, Albany, NY, USA, [2]University of Calgary, Calgary, AB, Canada.

Calmodulin (CaM), a 16 kDa ubiquitous calcium-sensing protein, is known to bind tightly to the cardiac calcium release channel/ryanodine receptor (RyR2) at low and high Ca2+ concentrations, and modulate the function of the channel. CaM binding studies using RyR fragments or synthetic peptides have revealed that multiple regions in the RyR's primary sequence may be involved in CaM binding. However, the locations of these potential CaM binding regions in the three dimensional structure of RyRs have yet to be determined. In the present study, we inserted GFP or GST into these proposed CaM binding sequences and mapped some of them onto the three-dimensional structure of intact RyR2 by cryo-electron microscopy and single particle image analysis. Surprisingly, we found that some of these potential CaM binding regions, e.g. Arg-3595 and Lys-4269, are located in close proximity and are adjacent to the CaM binding sites that were mapped previously by 3D cryo-EM. These observations suggest that multiple regions in the RyR2 sequence may form a binding pocket for CaM. (Supported by NIH and CIHR).

1569-Pos
Ryanodine Receptor Channels are Regulated by Specific Binding of A Membrane Phospholipid Metabolite

Akira Uehara.
Fukuoka Univ, Fukuoka, Japan.

Sphingosylphosphatidylcholine (SPC) is metabolized from sphingomyelin (SM) of a minor cell membrane phospholipid during the apoptosis and the hyperlipidemia. Lysophosphatidylcholine (LPC) is produced from phosphatidylcholine (PC) of a major membrane phospholipid during the ischemia. These lipid metabolites are known to modify a variety of ion channels. In the present study, we examined in detail with the planar lipid bilayer method how the cardiac RyR channels are modified by SPC and LPC. The cis-side addition of SPC blocked the channels at the μM level, while the trans-side addition of SPC did not affect. SPC hardly change the membrane capacitance. A kinetic model held in the SPC effect. SPC could thus exert a specific effect via its binding to the cytoplasmic domain of the RyR molecule. On the other hand, both cis-side and trans-side additions of LPC activated the RyR channels at the μM level. LPC significantly increased the membrane capacitance. No kinetic model held in the LPC effect. Unlike SPC, LPC could thus exert a nonspecific indirect effect on the RyR channel via a fusion of LPC into the membrane lipids.

1570-Pos
Molecular Determinants of Ca^{2+} Release Termination in the Cardiac Ryanodine Receptor

Xixi Tian, Yijun Tang, Ruiwu Wang, Wenqian Chen, S.R. Wayne Chen.
University of Calgary, Calgary, AB, Canada.

A longstanding question in the field of excitation-contraction coupling in cardiac muscle is how Ca^{2+} release from the sarcoplasmic reticulum (SR) is terminated. Recent studies have suggested that SR Ca^{2+} release terminates as a result of luminal Ca^{2+} dependent inactivation of the Ca^{2+} release channel/ryanodine receptor (RyR2). However, the molecular basis of luminal Ca^{2+} dependent inactivation of RyR2 is unknown. We have previously shown that the pore region of RyR2 is critical for the initiation of spontaneous Ca^{2+} release or store overload induced Ca^{2+} release (SOICR). In the present study, we determined whether the pore region of RyR2 is also important for Ca^{2+} release termination. To this end, we mutated each residue within the inner helix and the helix bundle crossing, and generated stable, inducible HEK293 cell lines expressing theses mutants. Using the fluorescence resonance energy transfer (FRET)-based luminal Ca^{2+} sensing protein, D1ER, we monitored the luminal Ca^{2+} dynamics in HEK293 cells expressing RyR2 wt and mutants during Ca^{2+} overload. Interestingly, we found that the G4871R mutation significantly lowered the critical luminal Ca^{2+} level at which Ca^{2+} release is terminated (the termination threshold), but it had no effect on the critical luminal Ca^{2+} level at which spontaneous Ca^{2+} release or SOICR occurs (the SOICR threshold), as compared with wt. In contrast, the I4862A mutation markedly lowered the SOICR threshold with little impact on the termination threshold. On the other hand, the Q4876A mutation lowered both the SOICR and termination thresholds, whereas the E4872A mutation raised both thresholds. Taken together, our data demonstrate that the pore region of RyR2 is an important determinant of both activation and termination of Ca^{2+} release, and suggest that the pathways for Ca^{2+} release activation and termination are distinct but overlap.

1571-Pos
Modulation of Synchronous Gating in Skeletal Muscle Ryanodine Receptor Channels (RyR1) by Nucleotides or Phosphorylation

Jake T. Neumann, Julio A. Copello.
Southern Illinois University School of Medicine, Springfield, IL, USA.

In skeletal muscle fibers, local Ca^{2+} sparks and global Ca^{2+} transients arise from the synchronous activation of arrays of calcium release channels (RyR1) in the sarcoplasmic reticulum. Marx et al. (1998) first described that synchronous Ca^{2+} signaling in cells could be explained by the coordinated gating of neighboring RyR1 channels; i.e. ‘‘coupled gating’’. We have previously reported that coupled gating of multiple RyR1 channels requires luminal Ca^{2+} as current carrier and ATP/Mg^{2+} in the cytosolic solution. Here, we have reconstituted into planar lipid bilayers multiple RyR1 channels from skeletal muscle SR microsomes and determined their modulation by different nucleotides. As found for ATP, we determined that ADP and AMP can activate RyR1 and favor coupled gating. Contrarily, ITP, GTP and TTP did not affect channel behavior. A priori, the ATP action seems more robust than that of ADP/AMP (remains after addition of Mg^{2+}). Consequently, we tested the possibility of a phosphorylation-mediated mechanism to explain ATP efficacy. However, we found that addition of PKA, CaMK or phosphatases did not significantly affect channel activity. The lack of effects of kinases/phosphatases was confirmed with macroscopic assays of SR Ca^{2+} release. Thus, our results suggest that nucleotide modulation of RyR1 seems to be specific for adenine nucleotides (especially ATP) and that RyR1 behavior in skeletal muscle does not appear to be significantly modulated by phosphorylation. (Supported by NIH R01 GM078665)

1572-Pos
Modification of Cardiac Ryanodine Receptors by Reactive Carbonyl Species Alter Conductance and Gating

Shouqiang Ouyang[1], Chengju Tian[1], Chun-Hong Shao[1], Wayne Chen[2], Keshore Bidasee[1].
[1]University of Nebraska Med Ctr, Omaha, NE, USA, [2]University of Calgary, Calgary, AB, Canada.

Previously, we and others found that ventricular myocytes isolated from streptozotocin (STZ)-induced diabetic rats exhibited enhanced spontaneous Ca^{2+} releases. To date, molecular mechanisms underlying this phenomenon remains incompletely understood. This study was designed to determine whether carbonyl adducts previously found on RyR2 during diabetes contribute to its dysregulation. Male Sprague-Dawley rats were injected with STZ. Six weeks later, diabetic rats were divided into two groups: one group was treated with insulin for two weeks while the other group received no treatment. Non-diabetic controls were run alongside. After eight weeks, RyR2 was isolated and proteoliposomes prepared. Following incorporation into the lipid bilayer, diabetic RyR2, which contained elevated levels of carbonyl adducts, activated to a greater

extent with 1.0 μM Ca^{2+} than control RyR2 (P_o was 5X greater in diabetic RyR2). Two weeks of insulin treatment blunted the enhanced Ca^{2+} responsiveness. When added to the *cis* chamber the potent reactive carbonyl species (RCS), 80 μM methylglyoxal increased the open probability (P_o) of RyR2 3-fold (0.05 to 0.16) within 10 min and this increase was independent of holding potential. Increasing [MGO] further to 160 μM, reduced the conductance of RyR2 by 25% without changing P_o. Incubating RyR2 with MGO (5-500 μM with 200 μM free Ca^{2+} in buffer) dose-dependently reduced its ability to binding [3H]ryanodine. Singly mutating R1611, R2190 and K2888 to W or Y, to mimic adducts previously found on them during diabetes, resulted in gain-of-function of RyR2 (P_o increased >2-fold at 3.3 μM Ca^{2+}). Mutating c-terminal R4462, and R4683 to W or Y resulted in loss-of function of RyR2. We conclude that modification of RyR2 by RCS during diabetes is responsible in part for its dysregulation. (This work was funded by NIH and Nebraska Redox Biology Center)

1573-Pos
Gating of the Purified Human Cardiac Ryanodine Receptor (hRyR2) in the Absence of Regulatory Accessory Proteins

Saptarshi Mukherjee, Nia Lowri Thomas, Laila Guzadhur,
Chloe E. Maxwell, Alan J. Williams.
Cardiff University, Cardiff, United Kingdom.

The cardiac ryanodine receptor (RyR2) mediates Ca^{2+} efflux from intracellular stores to effect myocyte contraction during excitation-contraction coupling. Mutations in this channel perturb Ca^{2+} release function, leading to triggered arrhythmias that may cause sudden cardiac death (SCD). The exact molecular mechanisms by which SCD-linked RyR2 dysfunction occurs constitutes a burgeoning area of cardiac research. Most studies so far have concentrated on the secondary effects of mutation on channel function by virtue of affecting channel modification by phosphorylation and accessory protein binding, with no great emphasis on elucidating the gating mechanisms of the channel itself. Our aim is to elucidate the mechanistic basis of wild-type (WT) hRyR2 activation by its primary activating ligand, Ca^{2+}, under precisely controlled conditions in the absence of any accessory proteins with a view to determining the effect of mutation on hRyR2 gating in the same way. hRyR2 channels, recombinantly expressed in HEK293 cells, were purified and studied at the single channel level in symmetrical 210mM KCl under reducing conditions. *Trans* (luminal) Ca^{2+} was buffered at 50nM using EGTA, while *cis* (cytosolic) Ca^{2+} buffering was stringently controlled using EGTA, HEDTA and NTA to achieve free Ca^{2+} concentrations in the range of 0-500 μM. Preliminary data obtained from sigmoidal dose-response curves of P_o vs pCa for 10 WT hRyR2 channels yields an EC_{50} of 3.25 ± 1.04 μM, resulting in a maximum P_o greater than 0.8 (in 5 out of 10 channels). This increase in P_o resulted from an increase in the frequency of channel openings, until P_o of 0.8 - above which any increases in P_o resulted from an increase in open times. Likely gating mechanisms will be discussed with a view to mutant channel analysis.
Supported by the British Heart Foundation

1574-Pos
S-Adenosyl-L-Methionine Activation of Cardiac Ryanodinr Receptors is Associated with an Increased Frequency of Subconductance Sates

Angela J. Kampfer, Edward M. Balog.
Georgia Institute of Technology, Atlanta, GA, USA.

The biological methyl group donor, S-adenosyl-L-methionine (SAM) activates the cardiac ryanodine receptor (RyR2). Previously we investigated the mechanism underlying SAM regulation of RyR2 with [^{3}H]ryanodine binding to cardiac SR vesicles. SAM enhances Ca^{2+} -activation of RyR2 and increases the apparent affinity of ryanodine for the channel. Notably, methyltransferase inhibitors have no effect on SAM-activation, and SAM-mediated methylation of RyR2 is not detected. Furthermore, the concentration dependence for SAM and ATP-induced increase in [^{3}H]ryanodine binding overlap. Presently, we investigated the affect of SAM on native RyR2 channels incorporated into planar lipid bilayers. Channel were grouped according to initial P_o values under control conditions (10 μM cytosolic Ca^{2+}), those with $P_o < 0.2$ (n=7), and $P_o > 0.2$ (n=5). For channels with an initial $P_o < 0.2$, SAM caused a rapid (within seconds) increase in P_o ($p < 0.05$). The SAM-induced increase in P_o was due primarily to an increase in mean open time ($p<0.05$; n=3). Interestingly, SAM activation was associated with an increased frequency of subconducatance states. In contrast, the increase in channel P_o caused by 2mM ATP was not associated with the appearance of subconductance states. Thus, the effect on subconductance states appears specific to SAM. This work highlights the complexity underlying SAM regulation of RyR2. The data suggest ligand binding is among the multiple mechanisms responsible for SAM-activation of RyR2.

1575-Pos
Molecular Interplay between the Heart Lim Protein (HLP) and RyR2 in Murine Heart

Dong Woo Song, So Yeon Park, Do Han Kim.
Gwangju Institute Science and Technology, Gwangju, Korea, Republic of.

HLP is a heart-specific LIM-only protein having two LIM domains each consisting of two zinc fingers. Through the bacterial 2 hybrid screening and a following LC-MS/MS study, we have found that HLP interacts with the cytosolic divergent region of mouse heart RyR2. The direct interaction between RyR2 and HLP was confirmed by GST pull-down and co-immunoprecipitation assays. HLP was partially co-localized with RyR2 in HL-1 cells and rat adult cardiomyocytes. siRNA or Adenovirus-mediated knock-down of HLP in HL-1 cells and neonatal cardiomyocytes led to more than 70% decrease in the expression of HLP, without a concomitant change of other Ca^{2+} handling proteins (e.g. SERCA, RyR2, calsequestrin and DHPR). Ca^{2+} transient measurement of fura2-loaded cardiomyocytes by 1Hz field stimulation demonstrated that silencing of HLP decreased the peak amplitude of Ca^{2+} transient (~ 15%) in HL-1 cells and in neonatal cardiomyocytes. Currently, various deletion-mutants of LIM protein are being used to characterize the RyR2 binding sites in HLP. (This work was supported by the Korean Ministry of Science and Technology grant, Systems Biology Research Grant, M1050301001-6N0301-0110, and the 2009 GIST Systems Biology Infrastructure Establishment Grant).

1576-Pos
Mitsugumin-29 Regulates RyR1 Activity In Mouse Skeletal Myotubes

Ji-Hye Hwang, Jin Seok Woo, Eun Hui Lee.
The Catholic Univ. of Korea, Seoul, Republic of Korea.

Canonical-type transient receptor potential cation channel type 3 (TRPC3) in plasma membrane allows the entry of Ca^{2+} ions into various cells. In skeletal myotubes, functional interaction between TRPC3 and RyR1 (ryanodine receptor1, a Ca^{2+} channel in sarcoplasmic reticulum (SR) membrane) regulates the gain of skeletal excitation-contraction coupling (*J. Biol. Chem.*, 2006). Mitsugumin-29 (MG29) is a four membrane-spanning protein and is found in both plasma and SR membrane. MG29 has been known as a TRPC3-interacting protein in skeletal myotubes (*Biochem. J.*, 2008).
To identify critical region(s) of MG29 that participate in binding to TRPC3 or the role of MG29 in skeletal muscle, N-terminus, three intervenient loops among four transmembrane regions, and C-terminus of MG29 were expressed in E. coil as N-terminal GST-fused forms, and subjected to co-immunoprecipitation assay with intact TRPC3 from rabbit skeletal muscle. Cytoplasmic N-terminus and a loop between first and second transmembrane domains of MG29 effectively bound to TRPC3. Two deletion mutants of MG29 (missing the TRPC3-binding sites: deleting the N-terminus only or longer N-terminus covering the loop region) was expressed in mouse skeletal myotubes, and the myotubes was subjected to the measurement of Ca^{2+} transients with Fura-2 or Fluo-4. The later mutant showed significantly decreased responsiveness of RyR1 to caffeine, suggesting that MG29 may be a mediator between the functional interaction between TRPC3 and RyR1.

1577-Pos
Phosphorylation of Excitation-Contraction Coupling Components in a Guinea-Pig Model of Heart Failure

Mark L. Bannister[1], Mark Scoote[2], Martyn P. Kingsbury[1], Mark A. Turner[1], Jolanda van der Velden[3], Desmond J. Sheridan[1], Alan J. Williams[4], Sian E. Harding[1].
[1]Imperial College, London, United Kingdom, [2]Colchester Hospital University, Colchester, United Kingdom, [3]VU University Medical Centre, Amsterdam, Netherlands, [4]Wales Heart Research Institute, Cardiff, United Kingdom.

Phosphorylation status appears to be a key determinant of excitation-contraction coupling ion channel and pump function. Dysfunction of the ryanodine receptor (RyR) secondary to catecholaminergic drive and phosphorylation has been proposed as a factor in contractile dysfunction and arrhythmia patho-physiology in the failing heart. The phosphorylation states of RyR, along with those of phospholamban and troponin I have been investigated by immunoblotting, and quantitated by comparing levels in failing hearts with basal levels, minimum levels after beta-blocker treatment and maximal levels achieved by ex vivo treatment with isoprenaline. We found that RyR residue Ser2809 was phosphorylated to 124 $\pm$ 11 % (n = 5, $P > 0.05$) of control (sham-operated, basal) in heart failure under basal conditions and 143 $\pm$ 12 % (n = 6, $P < 0.05$) with isoprenaline treatment, and residue Ser2030 was 94 $\pm$ 10 % (n = 8, $P > 0.05$) for heart failure and 199 $\pm$ 9 % (n=6, $P < 0.05$) for isoprenaline treatment. Phosphorylation levels at Ser16 of phospholamban were higher: 159 $\pm$ 17 % (heart failure, n = 7, $P < 0.05$) and 366 $\pm$ 95 % (isoprenaline treatment, n = 5, $P < 0.05$). At Ser23/24 of troponin I there is no significant

change in heart failure (n = 5, P < 0.05) but a 230 ± 92 % increase with isoprenaline treatment (n = 6, P < 0.05). Basal levels of phosphorylation are thus relatively low at RyR Ser2030, phospholamban Ser16, and troponin I Ser23/24, and are not significantly increased in heart failure, but are substantially increased by isoprenaline treatment. In contrast, the phosphorylation level at Ser 2809 is already high and can be increased only moderately by isoprenaline.

1578-Pos
Inhibition of RyR2-S2814 Phosphorylation Prevents Heart Failure by Reducing SR Ca Leak
Ralph J. van Oort, Na Li, Jonathan L. Respress, Angela DeAlmeida, **Xander H. Wehrens**.
Baylor College of Medicine, Houston, TX, USA.
Abnormal regulation of RyR2 by Ca2+/calmodulin-dependent protein kinase 2 (CaMKII) has been suggested as a cause of sarcoplasmic reticulum (SR) Ca2+ leakage and contractile dysfunction in heart failure. We hypothesized that CaMKII phosphorylation of RyR2 is crucial for heart failure development. We generated RyR2 knockin mice in which CaMKII phosphorylation site S2814 was mutated to alanine (S2814A) to prevent phosphorylation. Cardiac function and dimensions monitored by echocardiography were similar in S2814A and WT mice up to 12 months of age. WT (n=13) and S2814A mice (n=9) were subjected to transverse aortic constriction (TAC) to induce pressure overload. At 8 weeks after TAC, S2814A mice displayed a similar hypertrophic response and decrease in ejection fraction (EF) as WT mice. At 16 weeks after TAC, however, EF was significantly lower in WT (32.5 +/- 3.4%) compared to S2814A mice (43.0 +/- 2.9%) suggesting inhibition of heart failure development in the latter. This rescue effect was further verified by a lower lung-weight-to-tibia-length ratio and a decrease in expression levels of the cardiac stress genes ANF and BNP in S2814A mice compared to WT mice at 16 weeks after TAC. Ca2+ imaging in cardiomyocytes, isolated from S2814A and WT mice at 16 weeks after sham or TAC surgery, demonstrated an decreased incidence of spontaneous SR Ca2+ release (SCR) events in S2814A (29.7% of myocytes) compared to WT (61.3% of myocytes; P<0.01). Whereas CaMKII inhibitor KN93 reduced the incidence of SCR events in WT to 36.1% (P<0.01 vs. WT TAC), KN93 did not have an effect of SCR in S2814A myocytes (30.0%; P=NS vs. S2814A TAC). Together, our results demonstrate that blocking CaMKII phosphorylation of RyR2 prevents SR Ca2+ leak, and inhibits or delays the progression to congestive heart failure in S2814A mice.

1579-Pos
Luminal Regulation of Single RyR2 Channels by Cardiac Calsequestrin
Marcia Cortes-Gutierrez[1], Heather R. Orrell[1], Simon Williams[2], Patricio Velez[1], **Ariel L. Escobar[1]**.
[1]UC Merced, Merced, CA, USA, [2]TTUHSC, Lubbock, TX, USA.
We examined the hypothesis that calsequestrin (CSQ2) can regulate the RyR2 activity using a combination of single channel electrophysiology and lanthanide resonance energy transfer (LRET). Under steady-state, open probability (Po) of RyR2 of cardiac SR fractions from dog is modulated by luminal [Ca2+]. Po increased when luminal [Ca2+] was increased from 6 μM to 2 mM at a fixed cytosolic [Ca2+] of 2 μM. This effect on RyR2 appears to be mediated by luminal sites. Interestingly, RyR2 Po also increases when 2 mM Mg2+ was added to the luminal side. To gain mechanistic insights on the Casq2-mediated luminal regulation, we used the binding of Casq2 to Tb+3 as a functional assay. Luminescence produced by LRET between the tryptophan's of purified dog Casq2 and the lanthanide increased as function of the [Tb+3]. This fluorescence was reduced as [Ca2+] increased suggesting that Ca2+ binds to purified Casq2 by displacing tightly bound Tb+3 from a common binding site. To further explore the specificity of this regulation, we expressed recombinant dog Casq2 in E coli. The specificity of this interaction was assessed by LRET lifetime measurements. Interestingly, we found that the displacement of Tb3+ by Ca2+ was not significantly different than the displacement of Tb3+ by Mg2+ (~ 2.5 mM) suggesting that Ca2+ and Mg2+ share a common binding site. Finally, we explore the hypothesis that Tb3+ bound to Casq2 was able to modulate the RR2 activity. At fixed cytosolic [Ca2+] of 2 μM, Po of single RyR2 increased as a function of luminal [Tb+3 (KD ~ 500 nM, Hill coeff. ~4). These results are consistent with the idea that a multimeric form of Casq2 acts as luminal divalent cation sensor and translates it into changes in RyR2 gating. Supported by NIH R01-HL-084487 to AE.

1580-Pos
Ca SR Leak is Modulated by CaMKII Phosphorylation on RyR2-S2814
Yi Yang[1], **Laetitia Pereira[1]**, Ralph J. van Oort[2], Xander H.T. Wehrens[2], Donald M. Bers[1].
[1]UC Davis, Davis, CA, USA, [2]Baylor College of Medicine, Houston, TX, USA.
CaMKII has been shown to increase cardiac SR Ca leak through RyRs. RyR2-S2814 has been suggested as the phosphorylation site responsible for SR Ca leak triggering cardiac arrhythmias in heart failure. Here we test the requirement of S2814 for these effects, in knock-in mice expressing only RyR2-S2814A or -S2814D. Ca spark frequency (CaSpF) and SR load were studied in intact and permeabilized cardiomyocytes using confocal microscopy. At baseline CaSpF is higher in S2814D vs. WT (8.7±0.4 (n=9) vs 6.44±0.3, n=8, p<0.01) without altered SR Ca load. Activation of endogenous CaMKII (1.2 μM Ca-calmodulin) in WT increases CaSpF as described by Guo et al (Circ. Res, 2006), but only to the level seen in S2814D at baseline. Moreover, CaMKII did not further increase CaSpF in S2814D myocytes. In RyR2-S2814A CaMKII activation produces a very small CaSpF increase vs WT (19 vs 60%), and that response in S2814A is secondary to increased SR Ca load (by 15%, n=10, p<0.01). In intact myocytes (as above), basal CaSpF was highest in S2814D vs. WT and S2814A (which were similar). Baseline Ca transients were not different among the groups. The cAMP activated GTP exchange factor Epac may activate CaMKII to induce SR Ca leak (Pereira et al, J Physiol, 2007). In WT mice the Epac activator 8-CPT enhanced CaSpF and decreased both SR Ca load and Ca transient amplitude (consistent with a primary effect on SR Ca leak). However, 8-CPT had no effect on any of these parameters in either S2814A or S2814D myocytes. These data indicate that RyR2-S2814 is the critical RyR2 site responsible for CaMKII-dependent enhancement of SR Ca leak and potential arrhythmogenesis in heart failure, and confirm that Epac signaling can work through this same pathway.

1581-Pos
RyR2 NH2-terminal Mutations Associated with Cardiomyopathies Reduce the Threshold for Ca2+ Release Termination
Yijun Tang.
Department of Physiology and Pharmacology, University of Calgary, CALGARY, AB, Canada.
Naturally occurring mutations in the cardiac Ca2+ release channel/ryanodine receptor (RyR2) have been linked not only to cardiac arrhythmias and sudden death, but also to cardiomyopathies. The causal mechanisms underlying RyR2-associated cardiomyopathies are unknown. We have previously shown that RyR2 mutations linked to catecholaminergic polymorphic ventricular tachycardia (CPVT) reduce the threshold for store overload induced Ca2+ release (SOICR), also known as spontaneous Ca2+ release during Ca2+ overload. To determine the impact of RyR2 mutations associated with cardiomyopathies, we generated stable, inducible HEK293 cells expressing the RyR2 wt and the exon-3 deletion, R420W, and L433P mutants, and monitored the luminal Ca2+ dynamics in these wt and mutant cells using the fluorescence resonance energy transfer (FRET)-based luminal Ca2+ sensing protein, D1ER. Consistent with other CPVT mutations, the exon-3 deletion, R420W, and L433P mutations reduce the SOICR threshold. Interestingly, we found that these mutations also lower the critical luminal Ca2+ level at which Ca2+ release is terminated (the termination threshold). To further assess the role of the NH2-terminal region of RyR2 in Ca2+ release termination, we deleted the first NH2-terminal 305 amino acid residues and found that this NH2-terminal deletion also lowers the termination threshold for Ca2+ release. Our data demonstrate that the NH2-terminal region of RyR2 plays an important role in Ca2+ release termination, and suggest that alterations in the termination of Ca2+ release via RyR2 may cause cardiomyopathies (Supported by NIH and CIHR).

1582-Pos
Modulation of Neuroscretory Granule Mobilization and Neuropeptide Release by Ryanodine Receptors in Neurohypophysial Terminals
Jose R. Lemos, Edward Custer, James McNally, **Sonia Ortiz-Miranda**.
Univ. of Massachusetts Medical School, Worcester, MA, USA.
The neuropeptides oxytocin (OT) and vasopressin (AVP) are contained in large dense core vesicles (LDCV) and are released at the neurohypophysis (NH). The mobilization and translocation of vesicles to exocytotic release sites is modulated by cytosolic Ca^{2+}. Intracellular structures and organelles able to store and release Ca^{2+} are significant contributors of cytosolic Ca^{2+}. The presence of ryanodine receptors (RyR) in LDCV of NH terminals, coupled with the demonstration that pharmacological activation of these receptors can induce spontaneous focal Ca^{2+} transients, make them ideal modulators of cytosolic levels of Ca^{2+}, and therefore, vesicle mobilization and subsequent neuropeptide (NP) release.
To test this hypothesis, the association of LDCV in an area within 0.45 μm of the plasma membrane was assessed using immunolabeling of Neurophysin I (OT) and II (AVP) along with high stringency deconvolution techniques in isolated NH terminals. We found that the total amount of membrane associated NP-immunoreactivity varies significantly between terminal type; significantly higher in OT than in AVP terminals. This membrane associated distribution

pattern can be enhanced by exposure to agonist concentrations (1-5 μM) of ryanodine in OT terminals only. RyR antagonists, 8-Br-cADPR or higher concentrations (>10 μM) of ryanodine had the opposite effect; significantly reducing the amount of OT associated with the membrane area.
Additionally, Ca^{2+}-evoked NP release from permeabilized terminals was increased by agonist concentrations of ryanodine and conversely, decreased by antagonist concentrations of this drug. Agonist concentrations of ryanodine were also able to increase the asynchronous phase of low frequency electrically stimulated capacitance increases from isolated NH terminals. Thus, the ryanodine-sensitive mobilization of secretory granules seems to have a functional role in modulating secretion of neuropeptides from NH terminals. [Supported by UMass Grant P60037094900000 (SOM) and NIH Grant NS29470 (JRL)]

1583-Pos
Reactive Cysteines of Ryanodine Receptor Type 1 Influence Function and Response to Oxidative Stress

Diptiman D. Bose[1], Genaro C. Barrientos[1], Benjamin T. Yuen[1], Stevie Maxwell[1], Claudio F. Perez[2], Paul D. Allen[2], Isaac N. Pessah[1].
[1]University of California, Davis, Davis, CA, USA, [2]Brigham and Women's Hospital, Boston, MA, USA.

Redox modulation of the skeletal muscle ryanodine receptor1 (RyR1) plays a key role in determining the responsiveness of the Ca^{2+} release channel to physiological modulation. The sensitivity of RyR1 to redox stress may be conferred by seven previously identified hyper-reactive cysteines (1040, 1303, 2426, 2606, 2611, 2625 and 3635). Wild type RyR1 ($_{wt}$RyR1), and seven hyper-reactive cysteine mutations of RyR1 were stably expressed in HEK-293 cells and their contribution to RyR1 function evaluated. Addition of RyR1 activator 4-chloro-*m*-cresol (4-CMC) elicited an increase in $[Ca^{2+}]_i$ in the $_{wt}$RyR1cells but failed to produce a Ca^{2+} response in the C1303S, C2606S, C2436S and C7S (expressing all seven cysteine mutations) expressing cells, while the C1040S and C2611S mutations significantly attenuated 4-CMC mediated Ca^{2+} response. Microsomal fractions isolated from C1040S, C2611S, C2436S and C3635S bound to ^{3}[H]Ry while C7S and C1303S showed significantly lower, levels of RyR-binding, although significantly above preparations from RyR-null HEK 293. The sensitivity of RyR1 to 1, 4-napthoquinone (NQ) appears to depend on the expression of RyR1 and the presence of reactive cysteines. Sensitivity to NQ-induced cytotoxicity was determined by the multi-Tox fluorescence assay. NQ decreased cell viability in a dose-dependent manner, but the $_{wt}$RyR1 cells were less sensitive than C2606, C1040S, C2611S and the C7S mutants. These data indicate the role of hyper-reactive cysteines in regulating RyR1 function and its response to oxidative stress. Supported by NIH AR43140.

1584-Pos
Triclosan Uncouples Excitation-Contraction Coupling in Skeletal Myotubes Without Blocking RyR1

Gennady Cherednichenko[1], Roger A. Bannister[2], Kurt G. Beam[2], Isaac N. Pessah[1].
[1]Department of Molecular Biosciences, University of California, Davis, CA, USA, [2]Department of Physiology and Biophysics, University of Colorado, Denver, CO, USA.

The chlorinated diphenylethers are a class of broad-spectrum antimicrobial agents. One of the most potent and widely used member of this group is triclosan (TCS; 2,4,4′-trichloro-2′-hydroxydiphenylether). We studied the effects of TCS in primary myotube cultures using Ca2+ imaging with Fluo 4 and whole-cell voltage clamp. Acute perfusion with 10 mM TCS resulted in a significant but transient elevation in cytosolic Ca2+ in unstimulated (resting) myotubes, an effect not seen in RyR null (dyspedic) cells. TCS caused a rapid decline in the amplitude of electrically evoked Ca2+ transients culminating in complete loss of Ca2+ transients. Upon failure of excitation-contraction (EC) coupling, RyR1 remained responsive to application of caffeine (20mM). Caffeine-induced release of SR Ca2+ in the presence of TCS was comparable to, or greater than, that measured in the control period indicating that the release channels remained functional and the SR stores were replete with prolonged TCS exposure. Acute submicromolar TCS (0.5 μM) enhanced Ca2+ transient amplitude at 0.1 Hz stimulus, whereas pre-incubation of myotubes with TCS for 24 hr was sufficient to alter the relationship between stimulus frequency and Ca2+ transient amplitude across the entire stimulation frequency range. TCS (10 μM) also completely inhibited depolarization-triggered extracellular Ca2+ entry and suppressed DHPR mediated Ca2+ current to that observed in dyspedic cells. These ucoupling effects were observed without any influence on the magnitude of store-operated Ca2+ entry (SOCE) in myotubes. These results are the first to identify that TCS (and possibly related structures) impairs EC coupling by uncoupling orthograde and retrograde signaling between RyR1 and DHPR in skeletal muscle. Supported by NIH AR055104 (K.G.B.), AR43140 and ES011269 (I.N.P.), and MDA4319 (K.G.B.) and MDA4155 to (R.A.B.).

Motions of the Cell Surface Molecules

1585-Pos
Method for In-Vitro Studies of Cellular Interactions at the Interface of Two Tissues

Ara Arutunyan, Zaruhi Karabekian, Nikki Gillum-Posnack, **Narine Sarvazyan**.
The George Washington University, Washington, DC, USA.

We describe a simple and reliable experimental technique that enables one to create a high fidelity linear interface between two opposing cell layers. The method employs a custom designed lid that fits a standard 3cm cell culture dish. During cell plating, the dish is divided by a 200 micron thick separator that is part of the lid. The separator is covered in a thin layer of parafilm that forms a hermetic seal with the underlying coverslip and creates a temporary gap between the two cell plating environments. After cells attach, the custom lid is replaced with a standard lid and cells are allowed to grow under standard cell culture conditions. When expanding cell layers fill the gap, a linear interface is formed between the two opposing fields. Paracrinal factors released from an approaching cell front as well as direct physical and molecular interactions between two cell types affect intercellular orientation, individual cell morphology, and the degree of cells invasion into the opposing layer. The local interface appearance thus depends on a specific cell pair and may vary dramatically. We describe several types of such interfaces for different cell pairs, including cardiomyocytes, fibroblasts, melanocytes, endothelial cells and colon carcinoma cell lines. The method serves as a practical in vitro tool to study cell growth and invasion that occur on the interface of two neighboring tissues.

1586-Pos
A Zoo of Dynamic Pattern Formation by Bacterial Cell Division Proteins

Vassili Ivanov, Kiyoshi Mizuuchi.
NIDDK.NIH, Bethesda, MD, USA.

Min proteins of the *Escherichia coli* cell division system oscillate between the cell poles *in vivo. In vitro* on a solid-surface supported lipid bi-layer these proteins exhibit a number of interconverting modes of collective ATP-driven dynamic pattern formation including not only the previously described propagating waves, but also near uniform in space surface concentration oscillation, propagating filament like structures with a leading head and decaying tail, and moving and dividing amoeba-like structures with sharp edges. We demonstrate that the last behavior most closely resembles *in vivo* system behavior. The simple reaction-diffusion models previously proposed for the Min system fail to explain the results of *in vitro* self-organization experiments. We propose hypotheses that initiation of MinD binding to the surface is controlled by counteraction of initiation and dissociation complexes; the binding of MinD is stimulated by MinE and involves polymerization-depolymerization dynamics; polymerization of MinE over MinD oligomers triggers dynamic instability leading to detachment from membrane.

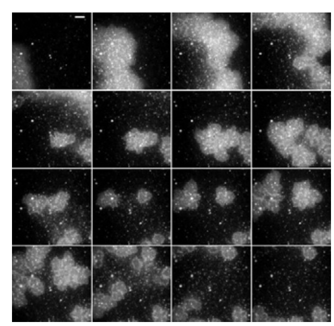

Fig. 1. MinD (green) and MinE (red) wave transforms into running and dividing amoebas. Frames were taken every 40 s, the scale bar is 5 μm.

1587-Pos
Active Re-Modelling of Cortical Actin Regulates Spatiotemporal Organization of Molecules on a Living Cell Surface

Kripa Gowrishankar.
Raman Research Institute, Bangalore, India.

Cell surface proteins such as lipid-tethered GPI-anchored proteins, Ras-proteins and several glycoproteins, are distributed as monomers and nanoclusters on the surface of living cells. The spatial distribution and dynamics of formation and breakup of these nanoclusters is unusual and controlled by the active remodeling dynamics of the underlying cortical actin (CA). To explain these results, we propose a novel mechanism of nanoclustering, based on the active hydrodynamics of the CA and its coupling to local membrane composition. In addition, our theory makes a falsifiable prediction – GPI-APs must exhibit anomalous concentration fluctuations resembling those at criticality; we confirm this using a fluorescence-based assay. Our work addresses a central issue

in cell biology, namely the nature of molecular organization and its spatiotemporal regulation on the plasma membrane.

1588-Pos
Membrane Anchor Dependent Colocalization in Cellular Membranes Observed by Fluorescence Cross-Correlation Spectroscopy
Sara B. Triffo, Hector H. Huang, Adam W. Smith, Jay T. Groves.
University of California, Berkeley, Berkeley, CA, USA.
Membrane anchors exist on many proteins in a variety of combinations of enzymatically attached fatty acids and glypiations. These anchors play a part in protein trafficking within cells and in associating proteins with cell membranes. They are also frequently found on well-known signaling proteins. Given the variety of anchor composition, we question whether these anchors play a more significant role in the lateral sorting or dynamic colocalization of proteins within cell membranes. To observe this *in vivo*, we create fusion proteins of red and green fluorescent proteins with the consensus protein lipidation motif of various signaling proteins and express both red and green constructs in HEK293T cells. The dynamic colocalization of red and green fluorescent proteins, and therefore the dynamic colocalization of membrane anchors, can be directly observed using Fluorescence Cross-Correlation Spectroscopy (FCCS). FCCS allows us to observe dynamic colocalization on the nanometer length scale. Unlike FRET, FCCS can detect positive colocalization regardless of orientation and at lengths larger than 10nm. Recent results will be discussed.

1589-Pos
Growth of the E. Coli Outer Membrane
Eliane H. Trepagnier, Julie A. Theriot.
Stanford University, Stanford, CA, USA.
The outer membrane (OM) of E. coli is composed of four elements: lipopolysaccharide (LPS), phospholipids, OM proteins, and lipoproteins. Together these elements form a continuous protective layer, defending the bacterium against harsh environments and toxic chemicals. Maintenance of an intact OM requires that synthesis and insertion of new OM components keep pace with bacterial growth. At present, little is known about where new OM is incorporated, or how its growth is regulated. We use video microscopy to examine the behavior of fluorescently labeled LPS and specific OM proteins on the surfaces of growing bacteria. Initially, labeled LPS and OM proteins in an individual cell exhibit a uniform peripheral distribution. As the bacterium elongates, fluorescent spots emerge, subsequently drift apart from one another, and occasionally bifurcate. Arresting bacterial growth with Rifampin halts the motion of the fluorescent spots, resulting in a fluorescence pattern which remains stable over a period of hours. We hypothesize that the appearance and divergence of these fluorescent spots of labeled OM is due to insertion of newly synthesized, unlabeled OM components. We track the motion of these spots on the surfaces of E. coli, and measure the convergence and divergence of adjacent tracks on the periphery of the cell. Our data suggest that new OM is incorporated in patches and distributed non-uniformly, with the bulk of the new material inserted along the lateral walls of the cell and lower rates of insertion in the polar regions of the cell.

1590-Pos
Single-Molecule Study of the Dynamics of Lipid-Like Molecules in the E. Coli Outer Membrane
Alyssa J.C. Garrelts, Kenneth P. Ritchie, Onkar Sharma,
William A. Cramer, Yi-Ju Hsieh, Barry L. Wanner.
Purdue University, West Lafayette, IN, USA.
While there have been many studies on the diffusion of membrane lipids in eukaryotic cells, which have given insight into the structure and organization of these membranes, little is known to date of their mobility in bacterial membranes, specifically the Gram negative bacteria, *Escherichia coli*. The *E. coli* outer envelope consists of inner and outer lipid membranes that are separated by a periplasmic space containing the cell wall. The outer membrane is unique in that it is thinner than mammalian plasma membranes and consists of a phospholipid inner leaflet with a predominantly lipopolysaccharide (LPS) outer leaflet. Here we look at the diffusion of the fluorescent lipid analog 3,3′-dioctadecylindocyanine iodide (DiI(C_{18})) and Alexa488-LPS in the outer membrane of live E. coli cells using single molecule imaging/tracking techniques. The diffusion coefficient of DiI(C18) was found to be $(5.2 \pm 0.2) \times 10^{-11}$ cm^2/sat time scales of 0.33 *s*. By contrast, the diffusion coefficient of DiI(C18) in human epithelial cancer cells of the nasopharanyx (KB) is found to be $(1.94 \pm 0.2) \times 10^{-8}$ cm^2/s, in good agreement with previously measured diffusion coefficients of DiI(C18) in other mammalian cells. The mobility of LPS in the outer membrane and the implications of the slow diffusion of DiI(C_{18}) on the structure of the outer membrane of *E. coli* will be discussed.

1591-Pos
Investigation of the Confining Potential of Toxin Receptors in Membrane Microdomains by Single Molecule Tracking with Lanthanide-Doped Nanoparticles
Silvan C. Türkcan[1], Jean Baptiste Masson[2], Didier Casanova[1],
Guillaume Voisinne[2], Genevieve Mialon[3], Thierry Gacoin[3], Jean Pierre Boilot[3],
Michel Popoff[4], Massimo Vergassola[2], Antigoni Alexandrou[1].
[1]Ecole Polytechnique, Laboratoire d'optique et bioscience, Palaiseau, France,
[2]Unité de Génétique in Silico, Institut Pasteur, Paris, France, [3]Ecole
Polytechnique, Laboratoire de Physique de la Matière Condensée, Palaiseau,
France, [4]Unité Bactéries Anaérobies et Toxines, Institut Pasteur, Paris,
France.
We coupled photostable and non-blinking $Y_{0.6}Eu_{0.4}VO_4$ nanoparticles to epsilon toxins produced by *Clostridium perfringens* type B and D, which bind to a specific receptor on MDCK cells. Single-molecule tracking using these labels shows that the toxin receptor exhibits confined motion within microdomains.

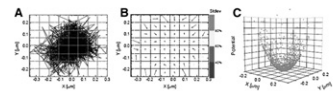

To analyze the receptor trajectories, we introduced a novel approach based on an inference method [1]. Our only assumption is that the receptor moves according to the Langevin equation of motion. This method fully exploits the information of the ensemble of the trajectory (Fig. A), in contrast to the usual mean square displacement analysis, which focuses only on a single observable, the second-order moment. Applying both techniques to collected trajectories, we can highlight the difference in extracted parameters.
From the shape of the confining potential (Fig. C), which is obtained by mapping the forces (Fig. B) inside domains, we can deduce information about the mechanism of confinement. In combination with experiments on cholesterol depletion and cytoskeleton depolymerization, this technique will shed light into the nature of the membrane micropatterning.
[1] J.-B. Masson et al, *Phys. Rev. Lett.*102, 048103 (2009).

1592-Pos
Mechanisms Regulating the Diffusion of the Lipid Raft Marker Cholera Toxin B Subunit
Charles A. Day, Kimberly R. Drake, Minchul Kang, **Anne K. Kenworthy**.
Vanderbilt University, Nashville, TN, USA.
The B subunit of cholera toxin (CTXB) is generally accepted as a marker of lipid rafts. Compared to other raft markers or lipid-anchored proteins, CTXB exhibits relatively slow diffusion. A variety of mechanisms could potentially account for this slow diffusion of CTXB, including crosslinking of small raft domains, confinement by the actin cytoskeleton, association with caveolae, incorporation into actively maintained domains, or molecular crowding effects in response to elevated membrane protein density. We evaluated the role of each of these mechanisms in controlling the lateral diffusion of CTXB in the current study by employing fluorescence recovery after photobleaching (FRAP) of fluorescently labeled CTXB following actin depolymerization, ATP depletion, cholesterol depletion, labeling across a range of CTXB concentrations, or in caveolin-1 knockout MEFs. Of these conditions, only cholesterol depletion significantly altered the diffusional mobility of CTXB. Furthermore, we tested whether the slow diffusion of CTXB is an intrinsic property of its receptor by examining the effects of CTXB on the diffusion of a fluorescent GM1 analog. The results of this experiment showed that CTXB slows the diffusion of its receptor. However, binding of CTXB to cells did not affect the diffusion of another raft marker (YFP-GL-GPI), a non-raft marker (YFP-GT46), or a fluorescent lipid analog (DiIC16). Taken together, these data suggest that CTXB diffusion is not limited by actin corrals, caveolae, molecular crowding effects, or the intrinsically slow diffusion of GM1. In addition, they suggest that crosslinking of small rafts induced by CTXB binding does not substantially alter the dynamics of membrane domains enriched in other types of raft or non-raft proteins or lipids.

1593-Pos
Direct Observation of Hop Diffusion of Lipid and Protein Molecules in the Plasma Membrane by High-Speed Single Fluorescent-Molecule Imaging
Takahiro K. Fujiwara[1], Shinji Takeuchi[2], Yosuke Nagai[2],
Kazuhide Hanaka[2], Kokoro Iwasawa[1], Kenichi G.N. Suzuki[1,3],
Akihiro Kusumi[1].
[1]ICORP-JST, Institute for Integrated Cell-Material Sciences (iCeMS) and
Institute for Frontier Medical Sciences, Kyoto University, Kyoto, Japan,
[2]Photron Limited, Tokyo, Japan, [3]PRESTO-JST, Kyoto, Japan.

Previously, using single-particle tracking at a temporal resolution of 0.025 ms, employing a 40-nmΦ colloidal gold probe, we have shown that virtually all of the lipid and protein molecules incorporated in the plasma membrane undergo hop diffusion. Based on this and many other observations, we proposed a model in which the entire plasma membrane is parcelled up into apposed domains due to the presence of the actin-based membrane skeleton (fence) and its associated transmembrane proteins (pickets), and membrane molecules undergo short-term confined diffusion within a domain (compartment), and long-term hop diffusion between the compartments. However, due to technological limitations, the observation of hop diffusion was only possible with a 40-nmΦ-colloidal gold probe, which might artifactually induce hop diffusion. To circumvent this problem, here, we developed a new high-speed, high-sensitivity CMOS camera system, which allowed us to track single fluorescently (0.5-nmΦ)-labeled molecules at a temporal resolution of 0.1 ms, the fastest single fluorescent-molecule imaging ever made. This camera system gave the position determination accuracy for single fluorescent molecules of $\approx$35 nm at a 0.1-ms time resolution. Virtually, all molecules of a phospholipid (DOPE) and a transmembrane protein, transferrin receptor, were found to undergo hop diffusion over the 110-nm compartments with median residency times of 9 ms and 33 ms, respectively, in the plasma membrane of a human epithelial T24 cell line. Meanwhile, in the actin-depleted, blebbed membrane, all of the DOPE and transferrin receptor molecules exhibited simple-Brownian diffusion. These results are in an excellent agreement with the previous high-speed gold-particle tracking data, and clearly indicate the necessity for the paradigm shift for the plasma membrane structure and dynamics, from the single continuous fluid model to the partitioned fluid model.

1594-Pos

Cluster Size Formation and its Effect on Protein Sorting in the Immunological Synapse

Niña C. Hartman[1], Jeffrey A. Nye[1], Cheng-Han Yu[1], Wan-Chen Lin[1], Jay T. Groves[1,2].
[1]UC-Berkeley, Berkeley, CA, USA, [2]Howard Hughes Medical Institute, Berkeley, CA, USA.

Micron-scale assemblies of molecules is thematic in biology, although oftentimes their exact function and mechanism of formation are unknown. A hallmark example is the immunological synapse (IS). T cell detection of pathogenic invasion on an antigen-presenting cell leads to the arrangement of receptor-ligand pairs into well-defined concentric zones. Specifically, T cell receptors (TCR) bound to peptide-presenting major histocompatibility complex (MHC), occupy the central zone surrounded by a ring of leukocyte function associated antigen-1 (LFA-1) bound to intercellular adhesion molecule-1 (ICAM-1). We postulate that the differences in cluster sizes between large TCR:pMHC micro-clusters and small LFA-1:ICAM-1 complexes prior to centripetal actin transport determine their differential sorting. To study this, we increase the LFA-1 cluster size two additional degrees beyond its native state by crosslinking LFA-1 or ICAM-1 on the supported membrane with a bivalent or tetravalent crosslinker. Progressively more central localization of LFA-1 proportional to the degree of crosslinking results until LFA-1 occupies the central zone with TCR. The different clustering states are identified using fluorescence correlation spectroscopy (FCS). Furthermore, the addition of a costimulatory interaction also increases radial transport. Thus, we demonstrate that the well-regulated event of clustering is a critical parameter in determining spatial patterning in the IS. We propose a sorting mechanism based on frictional protein coupling to actin, which is consistent with our observations and may be generalized to all membrane proteins in the IS.

1595-Pos

Flow Induced Protein Reorganization on Cell Surfaces

Eric Stellamanns[1], Sravanti Uppaluri[1], Niko Heddergott[2], Markus Engstler[2], Thomas Pfohl[3,1].
[1]Max Planck Institute for Dynamics and Self-Organization, Göttingen, Germany, [2]Department of Zoology, University of Würzburg, Würzburg, Germany, [3]Department of Chemistry, University of Basel, Basel, Switzerland.

Living in an environment of continuous flow the unicellular human bloodstream parasite Trypanosoma brucei utilizes shear forces to remove hostile antibodies from its surface. African trypanosomes are spread via the bite of the Tsetse fly and cause the so called sleeping sickness in human and various diseases in animals as well. Their motility is driven by a single flagellum attached along the whole length of the cell and is essential for survival within the hostile immune system.
We emulate the bloodstream environment with PDMS microfluidic devices by means of flow velocity, shear gradients and confinement to examine the effect on trypanosome surface protein sorting and motility. Using highly fluorescent quantum dots (Qdots) to mimic antibodies and optical tweezers to control the cells, we are able to observe protein sorting in real time in order to quantify hydrodynamic drag driven protein reorganization in living cell membranes.

1596-Pos

Different Types of Lateral Diffusion Measurements Reveal that Unlike HA, Dc-SIGN is Immobilized in Microdomains

Michelle S. Itano[1], Aaron K. Neumann[1], Feng Zhang[2], Wolfgang J. Parak[2], Nancy L. Thompson[1], Ken Jacobson[1].
[1]University of North Carolina, Chapel Hill, NC, USA, [2]Philipps Universitat Marburg, Marburg, Germany.

Hemagglutinin (HA), from influenza virus, and DC-SIGN, a dendritic cell C-type lectin that binds many pathogens including viruses, bacteria, and fungi, form microdomains on the plasma membrane. We investigated the dynamics of these proteins using Scanning FCS (S-FCS), defined valency quantum dot-based Single Particle Tracking (SPT) and Fluorescence Recovery After Photobleaching (FRAP). Using FRAP we verified that HA has a large mobile fraction (~80%) that is characterized by a diffusion coefficient of ~0.09 um^2/sec and that it exchanges with the surround (Ellens et al. (1990) *Biochemistry,* **29**(41): 9697-9707). By contrast, neither DC-SIGN or Δ35-DC-SIGN, a DC-SIGN mutant missing the cytoplasmic tail, recovered after photobleaching, even after many minutes, indicating that these molecules do not exchange significantly with the surround. In order to determine the dynamics of molecules within the domains, we utilized a confocal line S-FCS method that permits the autocorrelation function between the same pixel in successive linescans (acquired in the form of a carpet or kymograph) to be calculated on the ms timescale. HA lateral motion within its microdomain is characterized by a diffusion coefficient of ~0.10 um^2/sec, similar to that measured outside the domain by FRAP. On the other hand, DC-SIGN and Δ35-DC-SIGN do not diffuse within the domain. We are currently using quantum dots that have been conjugated to a *single* streptavidin in order to examine lateral dynamics within these domains. Such nanoparticles will obviate a consistent interpretative limitation for gold and quantum dot SPT; namely, that particle valency cannot be specified with absolute certainty for the particle whose motion is tracked. Further characterization of these surprisingly stable DC-SIGN domains that are important for pathogen entry into dendritic cells is in progress.
Supported by NIH GM 41402 (KJ &NLT)

1597-Pos

Psychostimulants Affect Dopamine Transporter Lateral Mobility and Membrane Microdomain Distribution

Jeffrey S. Goodwin[1], Tina Patel[1], Anne K. Kenworthy[2], Habibeh Khoshbouei[1].
[1]Meharry Medical College, Nashville, TN, USA, [2]Vanderbilt University, Nashville, TN, USA.

Neurotransmitter reuptake by transporters is a major mechanism for terminating synaptic transmission. The human dopamine transporter (hDAT) is one of the main targets for psychostimulants, and is critical to DA homeostasis. Lipid rafts are specialized membrane microdomains that serve as organizing centers to regulate different cellular processes such as neurotransmission and trafficking. To begin to understand how psychostimulants, methamphetamine (METH) and amphetamine (AMPH), affect hDAT microdomain association, we utilized fluorescence recovery after photobleaching (FRAP) and density-gradient centrifugation. Our FRAP studies revealed significant changes in the rate (D) and extent (Mf) of the fluorescence recovery into the bleached region of the plasma membrane in cells expressing YFP-hDAT in the presence of METH but not AMPH. Substitution of five N-terminal Ser with Ala, (cannot be phosphorylated) or Asp (pseudo-phosphorylated), and removal of the 22 N-terminal amino acids restored the diffusion rate of the transporter to control levels. Using density-gradient centrifugation, we found that YFP-hDAT is distributed into both, classically defined, membrane raft and non-raft fractions. Incubating with METH and AMPH shifted YFP-hDAT from non-raft to raft fractions. We have previously shown that METH uniquely modulates the biophysical properties of DAT. Our present findings suggest that METH and AMPH cause hDAT to partition into lipid raft membrane microdomains, and the decrease in the hDAT diffusion rate evoked by METH- vs. AMPH-occupied DAT could suggest that the N-terminal domain of the transporter is associated with a distinct group of proteins when exposed to these psychostimulants, and may thus describe an underlying mechanism behind the addictive biological differences between these psychostimulants.

Nucleocytoplasmic Transport

1598-Pos
Choreography of Importin α/CAS Complex Assembly and Disassembly at the Nuclear Pore Complex

Changxia Sun[1], Murray Stewart[2], **Siegfried M. Musser[1]**.
[1]Texas A&M Health Science Center, College Station, TX, USA, [2]MRC Laboratoy of Molecular Biology, Cambridge, United Kingdom.

Nuclear pore complexes (NPCs) mediate the exchange of proteins and RNAs between the cytoplasm and the nucleoplasm of eukaryotic cells. Signal-dependent transport cargos must assemble with soluble nuclear transport receptors to form transport complexes, which must then be disassembled after transport. The assembly and disassembly of transport complexes is promoted by proteins near the cytoplasmic and nucleoplasmic exit sides of the NPC. Here we report the use of single molecule fluorescence resonance energy transfer (smFRET) and particle tracking to investigate the choreography of importin alpha/CAS complex assembly and disassembly in permeabilized cells. Importin alpha acts with importin beta to transport cargos into the nucleus. We directly show that importin alpha/CAS complexes form in the nuclear basket region of the NPC, at the termination of the nuclear import process. These newly formed importin alpha/CAS complexes are preferentially released into the nucleus rather than immediately exported to the cytoplasm. The rapid dissociation of some importin alpha/CAS complexes at the NPC is consistent with the formation of a transient (2-4 ms lifetime) cargo/importin alpha/CAS complex, which disassembles either by losing a CAS or a cargo molecule. These data indicate that assembly and disassembly reactions occur concomitantly and stochastically. Importin alpha mutants confirm that the nucleoporin Nup50 promotes importin alpha/CAS complex assembly and that the smFRET signals observed at the NPC result from specific interactions rather than chance encounters. The disassembly of importin alpha/CAS complexes occurs after export in the cytoplasmic filament region of the NPC. This disassembly reaction is promoted by RanGTPase activating factors, indicating that GTP hydrolysis catalyzes the dissociation process. Thus, we clearly demonstrate the power of single particle tracking and smFRET for monitoring molecular interactions with high time resolution (2 ms) in a complex system.

1599-Pos
New Insights Into Intranuclear mRNP Dynamics

Roman Veith[1], Johannes Anzt[1], Thomas Sorkalla[2], Eugen Baumgart[1], Hanns Häberlein[2], Jan Peter Siebrasse[1], Ulrich Kubitscheck[1].
[1]Institute of physical and theoretical Chemistry, Bonn, Germany, [2]Institute of Biochemistry and Molecular Biology, Bonn, Germany.

Messenger ribonucleoprotein particles (mRNPs) move randomly within the nucleoplasm on their way to the nuclear pore [1]. In interphase the decondensed chromatin of mammalian cells largely governs the structure of the intranuclear environment and therefore has a strong impact on mRNP mobility. The salivary gland cell nuclei of *Chironomus tentans* harbor giant polytene chromosomes, where chromatin is compact and surrounded by extended regions of nucleoplasm void of chromatin. This allows studying mRNP mobility under conditions, which presumably correspond to that of interchromatin channels in mammalian cell nuclei. In this domain we examined the intranuclear movement of a specific endogenous mRNP, the BR2 mRNP, by high-speed single molecule fluorescence microscopy [2]. mRNP dynamics could be characterized by four diffusion coefficients, $0.015\mu m^2/s$, $0.23\mu m^2/s$, $0.7\mu m^2/s$ and $3.7\mu m^2/s$, respectively.

We now used 2'-O-Me-RNA oligonucleotides and molecular beacons to label the mRNPs *in vivo,* and studied the mobility of the BR2 mRNPs by complementary state-of-the-art fluorescence microscopy techniques: single molecule tracking, FCS, line scanning FCS and raster image correlation spectroscopy. These quantitative methods revealed that mobility components $>3\mu m^2/s$ were likely due to unbound oligonucleotides. The remaining components were shown to be typical for BR2 mRNP movement with all techniques and labelling approaches used.

The BR2 mRNPs moved in a discontinuous manner in the chromatin-free nucleoplasm. That reflects transient interactions between diffusing BR2 mRNPs and submicroscopic intranuclear structures not containing chromatin. To reveal the nature of the transient mRNP immobilization we examined the impact of the nuclear actin-binding protein hrp65-2, as well as hrp65-1 on mRNP mobility. Altogether, our experiments provided a comprehensive view on the intranuclear trafficking of native mRNPs.

[1] Gorski SA, Dundr M, T. Misteli. CurrOpinCellBiol. 2006 Jun; 18(3): 284-90.
[2] Siebrasse JP, Veith R, Dobay A, Leonhardt H, Daneholt B, U. Kubitscheck. PNAS. 2008 Dec 23; 105(51):20291-6.

1600-Pos
Observation of Single Nuclear Export Receptors at the Nuclear Pore Complex

Ulrike Schmitz-Ziffels, Andreas Veenendaal, Jan Peter Siebrasse, Ulrich Kubitscheck.
University of Bonn, Bonn, Germany.

Nucleocytoplasmic transport across the nuclear pore complex (NPC) permanently occurs in mammalian cells via a multitude of pathways. The NPC is the only entrance to and exit from the nucleus for macromolecules. Therefore detailed study of the transport process is of great importance for both an understanding of the mechanism as well as development of specific manipulation techniques relevant e.g. for drug delivery.

Single molecule fluorescence microscopy allows observing particles and molecules during the transit across the nuclear envelope revealing dwell times, which reflect the time needed for translocation. We were able to determine dwell times of several import receptors in vitro [1] and in live cells [2].

Here, we focus on nuclear export, which is difficult to explore, because the nuclear interior and its functional factors are experimentally less accessible than the cytoplasm. We examined the NPC translocation of soluble export receptors: CRM1, which among others exports NES bearing cargos, CAS, which exports Importin alpha, Tap and NXT1, which function as mRNA export factors. Dwell times are observed both in an in vitro system based on digitonin-permeabilized cells and in vivo microinjecting receptors into the nucleus. To maintain their functionality the mentioned proteins can only be labelled with a low dye to protein ratio and are therefore prone to photobleaching and rather dim. Hence HILO illumination [3] has been applied to perform experiments. Selective illumination of only a thin sheet within the cells next to the coverslip allows working with relatively low laser power and yields a signal-to-noise ratio superior to that obtained with epi-illumination.

[1] U. Kubitscheck et al, JCB 2005, 168, 233-243.
[2] T. Dange et al, JCB 2008, 183, 77-86.
[3] M. Tokunaga et al, Nat. Methods 2008, 5, 159 - 161.

1601-Pos
Oligomerization and Nucleocytoplasmic Transport of NTF2 Revealed by Brightness Analysis and Two-Photon Photoactivation

Patrick J. Macdonald, Yan Chen, Jinhui Li, Joachim D. Mueller.
University of Minnesota, Minneapolis, MN, USA.

Small molecules - less than 40 kD - diffuse freely through nuclear pores between the cytoplasm and nucleus. Large proteins and macromolecular complexes require active transport across the nuclear envelope via soluble transport factors or carrier molecules. Some carrier molecules themselves form complexes as they cycle between the nucleus and cytoplasm. One such transport factor is NTF2, which is known to play a primary role in the maintenance of the Ran gradient, but the oligomeric state of NTF2 and its function in transport are not well established. We observe that NTF2 exists as a monomer-dimer equilibrium in the cell, and we characterize several NTF2 mutants to investigate the influence of NTF2 dimerization on nucleocytoplasmic transport. We apply two-photon activation in vivo to examine the transport of photoactivable GFP-tagged carrier proteins. We also use fluorescence fluctuation spectroscopy and brightness analysis in the cell to investigate the oligomerization of the NTF2 mutants. We establish the efficacy of brightness analysis in a cell free expression system and use it to check oligomerization of NTF2 and its mutants in vitro. This work is supported by NIH grant R01GM064589.

1602-Pos
A Functional Map of the Nuclear Pore Complex Via High Precision Tracking of Single Molecules

Alan R. Lowe, Jake Siegel, Petr Kalab, Merek Siu, Karsten Weis, Jan T. Liphardt.
University of California, Berkeley, CA, USA.

All materials entering or exiting the eukaryotic cell nucleus pass through Nuclear Pore Complexes (NPCs), large transport channels embedded in the nuclear envelope. NPCs allow passive diffusion of small molecules, while larger cargos require transport receptors to facilitate passage. How NPCs achieve this exquisite selectivity remains unclear. We have developed a single molecule imaging assay, based on small (18nm diameter) custom protein-coupled Quantum Dots (QDs), to study the motion of cargos as they approach, translocate and exit the NPC. Optical tracking of the QD cargos with a mean spatial precision of 6nm and a temporal resolution of 25ms, allowed us to characterize individual steps involved in the import reaction and characterize NPC selectivity. Single cargo trajectories reveal a size-selective cargo barrier positioned in the cytoplasmic moiety of the central channel and the majority of the QDs are rejected early rather than spending long periods of time partitioned in the channel.

Within the channel, cargos move in a non-directional manner, consistent with anomalous subdiffusion in a crowded volume, with dimensions of ~55 nm in width and ~68 nm in length. By varying the number of import receptors on the surface of the cargo, we find that the translocation is not governed by simple receptor-NPC binding interactions and that the central channel behaves in accordance with the 'selective phase' model. Finally, in the absence of Ran, cargos still explore the entire volume of the NPC, but have a dramatically reduced probability of exit into the nucleus from the pore, suggesting that NPC entry and exit steps are not equivalent and that the pore is functionally asymmetric to importing cargos.

1603-Pos
Single Molecule Imaging of the Calcium Ion Regulation of Nuclear Pore Passive Permeability
Ashapurna Sarma, Weidong Yang.
Bowling Green State University, Bowling Green, OH, USA.
Nuclear pore complex (NPC) is the sole pathway for direct communication between the cytoplasm and the nucleoplasm of eukaryotic cell. Based on the criteria of the molecular size exclusion, the NPC allows unregulated passive diffusion of small molecules (< 40 kDa) and facilitated translocation of larger molecules (up to 50 MDa). While recent evidence suggests a third transport mode: Ca^{2+} regulated transport. In details, the nuclear pore permeability can be regulated by Ca^{2+} stored in the lumen of nuclear envelope and endoplasmic reticulum. However, the mechanism of Ca^{2+} regulated transport remains poorly understood. Here we applied a speedy single molecule fluorescence microscopy to characterize the dependence of the nuclear pore passive permeability on the Ca^{2+} store concentration by snapshots of real-time transient movements of 3 - 40 kDa dextran molecules through the NPCs. We observed novel features under real-time trafficking conditions that escape detection by ensemble measurements: decreased amount of Ca^{2+} in the store induced restricted passive diffusion of dextran molecules with longer diffusion times and lower transport efficiencies through the NPCs. Dextran molecules cannot penetrate deeply into the nuclear pore and the majority were rejected or trapped by likely barriers formed on both sides of NPCs when the stored calcium was significantly depleted. Our results suggest that a filamentous structure that occludes the NPC may be altered by the depletion of calcium in the store.

1604-Pos
Single-Molecule Snapshots of Three-Dimensional Distribution of Transient Interactions in the Nuclear Pore Complex
Jiong MA, Weidong Yang.
Bowling Green State University, Bowling Green, OH, USA.
Translocation of macromolecules through the nuclear pore complex (NPC) is hindered by the phenylalanine-glycine (FG) repeats barrier unless they are chaperoned by transport receptors in eukaryotic cells. However, challenged by measuring a series of transient interactions between the transport receptor and the FG repeats, the precise mechanism of the facilitated translocation remains unclear. We applied single-point edge-excitation sub-diffraction (SPEED) microscopy to obtain a three-dimensional density map of the transient interactions with a spatiotemporal resolution of 9 nm and 400 µs. We observed novel features under real-time trafficking conditions that escape detection by conventional electron microscopy: the actual pathway of facilitated translocation through the NPC is not completely restricted by the NPC architecture; the primary interaction sites between Importin β1 (Imp β1, a major transport receptor) and the FG repeats locate symmetrically on the cytoplasmic and nucleoplasmic sides of the nuclear pore; Imp β1 only rarely occupies a central channel of approximate 10-20 nm diameter along the NPC axis, but the Imp β1-assisted cargo molecules expand their pathways into the central channel.

1605-Pos
Squeezing through the Pore - Conformational Plasticity in Nuclear Import
Nicole Dölker, Helmut Grubmüller.
MPI for Biophysical Chemistry, Goettingen, Germany.
In eukaryotic cells, exchange of macromolecules between the cytoplasm and the nucleus is mediated by specialized transport factors. By binding to these transporters, cargo molecules which are otherwise excluded from entering the nucleus can traverse the nuclear pore efficiently. Most of the proteins mediating nuclear import and export belong to the importin beta family. The transport cycle of importin beta starts with recognition of the cargo in the cytoplasm. The importin-cargo complex then crosses the permeability barrier of the nuclear pore and enters the nucleus, where the complex dissociates upon binding of RanGTP to importin beta.
Importin beta has a superhelical structure and exhibits a great intrinsic flexibility, which is needed for recognition of a wide variety of ligands [1]. Although small angle scattering data, as well as previous molecular dynamics studies, indicate that in solution importin beta adopts a rather open conformation, most crystal structures exhibit a compact conformation of the superhelix [2, 3].
We carried out all-atom molecular dynamics simulations of importin beta in aqueous solution and in hydrophobic media and found a large influence of the hydrophobicity of the environment on conformation and dynamical properties of importin beta. Our results indicate that the structural plasticity of importin beta is not only important for cargo recognition, but that its dependence on the environment plays an important role in the transport process. We propose a mechanism by which opening and closing of importin beta during nuclear import facilitate cargo binding, transport and release.
[1] Conti, E.; Müller, C. W. & Stewart, M. Curr Opin Struct Biol 2006, 16, 237-244.
[2] Fukuhara, N.; Fernandez, E.; Ebert, J.; Conti, E. & Svergun, D. J Biol Chem 2004, 279, 2176-2181.
[3] Zachariae, U. & Grubmüller, H. Structure 2008, 16, 906-915.

1606-Pos
Polymer Brushes and the Nuclear Pore Complex
Ajay Gopinathan[1], Yong Woon Kim[2], Roya Zandi[3], Michael Colvin[1], Michael Rexach[4].
[1]University of California, Merced, CA, USA, [2]Korea Institute for Advanced Study, Seoul, Republic of Korea, [3]University of California, Riverside, CA, USA, [4]University of California, Santa Cruz, CA, USA.
The nuclear pore complex (NPC) is an important macromolecular structure that gates the aqueous pores between the cytoplasm and nucleoplasm of cells and controls all nucleo-cytoplasmic transport and communication such as the import of proteins from the cytoplasm and the export of RNA from the nucleus. The NPC forms a barrier that maintains a tight seal against cytoplasmic particles larger than 4 nm while simultaneously allowing the facilitated transport of specially ''tagged'' particles up to 40 nm diameter, at speeds comparable to free diffusion! The key to the selectivity is hypothesized to be due to a large number of NPC proteins that fill the pore and potentially interact with each other and the cargo. However, despite numerous studies on the structure and properties of individual NPC proteins, the actual structure of the complex within the nuclear pore and its mechanism of operation are virtually unknown with leading models of nuclear pore transport assuming vastly different morphologies for the NPC protein complex filling the nuclear pore. Here, we use a bottom-up approach, applying the physics of polymer brushes to understand the three dimensional architecture of the complex based on experimental understanding of the properties of individual NPC proteins. Our results indicate that there exist transitions between distinct brush morphologies (open and closed states of the gate), which can be triggered by the presence of cargo with specific surface properties. This has led to development of the Discrete Gate Model - an experimental data driven theoretical model. The resulting transport mechanism, that we propose, is fundamentally different from existing models and points to a novel form of gated transport in operation within the nuclear pore complex. Our results can also be extended to designing and optimizing novel forms of biomimetic transport based on this mechanism.

1607-Pos
Formation of the Bicoid Gradient in D. Melanogaster in Unfertilized Versus Fertilized Eggs
Jeffrey A. Drocco, Eric F. Wieschaus, David W. Tank.
Princeton University, Princeton, NJ, USA.
The concentration profile of Bicoid protein in *D. melanogaster* is an example of a morphogen gradient that has been well studied by quantitative methods. Various models have been proposed which suggest that the layer of syncitial nuclei which forms in the embryo prior to gastrulation plays a significant role in the formation of this gradient. In particular, given the small cytoplasmic diffusion constant of 0.3 microns^2/s reported by Gregor *et al.*, it has been proposed that the nuclear motion coincident with mitotic divisions serves to extend the length scale of the gradient. In this work we present time series measurements of the Bicoid gradient in unfertilized eggs, which lack nuclei other than a single female pronucleus. We find that the unfertilized gradient takes a form similar to the fertilized gradient modulated by a uniform positive offset across the egg, consistent with the claim that syncitial nuclei do not extend the length of the gradient. In addition, we present results of simulation to argue that nuclear trapping combined with observed nuclear motion is insufficient to resolve the paradox of a small diffusion constant and an embryo-length gradient.

1608-Pos
Endothelin and Phenylephrine Both Trigger Nuclear IP_3 Elevation, but Differ in Ability to Activate Nuclear HDAC5 Export
Chia-Wei J. Chang[1,2], Kathryn Helmstadter[1], Gregory Mignery[2], Julie Bossuyt[1], Donald Bers[1].
[1]University of California - Davis, Davis, CA, USA, [2]Loyola University Chicago, Maywood, IL, USA.

We previously found that both ET-1 and phenylephrine (PE) induced similar HDAC5 phosphorylation and nuclear export in adult cardiac myocytes (which contributes to hypertrophic signaling). However, ET-1 requires IP_3 receptor (IP_3R) activation (at the nucleus) and CaM-CaMKII activation to mediate this full effect, while PE does not. That is, IP_3R inhibition or CaMKII block do not prevent PE-induced HDAC5 nuclear export, despite the fact that both agonists can activate IP_3 production. Here we test whether the apparent IP_3-independence of PE signaling is due to a failure of IP_3 elevation in the nucleus (i.e. IP_3 produced at the plasma membrane may be degraded before reaching the nucleus). Using a nuclear targeted FRET-based IP_3 sensor (Fire-1-Nuc) we assessed changes in nuclear [IP_3] upon ET-1 and PE application in adult rabbit ventricular myocytes. Both ET-1 and PE induce rapid and robust elevation of nuclear [IP_3] reaching an early peak in <1 min. While the ET-1-induced a slightly larger peak nuclear [IP_3], the PE-induced rise is more sustained (lasting more than 10 min). These results demonstrate that a PE induces a strong rise in nuclear [IP_3], and does not support the hypothesis that PE fails to induce a nuclear IP_3 signal (compared to ET-1). We cannot rule out the possibility that the kinetic differences in nuclear [IP_3] between these agonists contribute to different downstream signaling. Another explanation is that PE-induced nuclear IP_3 is less effective than ET-1-induced IP_3 in driving activation of nuclear CaM and CaMKII to phosphorylate HDAC5. That is, an IP_3-independent effect of one of these agonists could prevent or promote the ability of IP_3 to signal in the nucleus.

1609-Pos
Phosphorylation Dependent Nuclear Transport of Human Dutpase

Gergely Rona[1], Eniko Takacs[1], Zoltan Bozoky[1], Zsuzsa Kornyei[2], Mate Neubrandt[2], Judit Toth[1], Ildiko Scheer[1], Emilia Madarasz[2], Beata G. Vertessy[1].
[1]Institute of Enzymology, BRC, HAS, Budapest, Hungary, [2]Institute of Experimental Medicine of the Hungarian Academy of Sciences, Budapest, Hungary.

The nuclear isoform of human dUTPase plays an important role in maintaining genomic integrity. Its expression is strictly cell cycle regulated and is known to be a phosphoprotein in vivo. However, the role of this phosphorylation remained unknown.

Here we show regulation of the nuclear transport of human dUTPase via phosphorylation of a serine residue on its nuclear localisation signal. We found that hyperphosphorylation mimicking mutants (glutamic acid) are localized solely in the cytoplasm while hypophosphorylation mimicking mutants (glutamine) localize in the nucleus as the endogenously regulated protein. Our video microscopy studies have also shed light on the nuclear import dynamics of the wild type dUTPase and that of the mutants. These results showed that the phosphorylated wild type form may re-enter the nucleus (after cell division) only after a considerable delay of several hours while mutants that cannot be phosphorylated re-accumulate within the nucleus much faster. The delay observed with the wild type enzyme may indicate that either dephosphorylation or de novo protein synthesis is required. To reveal the mechanism by which cells accumulate sufficient amount of dUTPase in their nucleus after cell division, we are currently conducting protein transfection based experiments.

We are also trying to characterize the interaction of the human dUTPase with its possible partner in nuclear trafficking, importin-alpha. Based on Native-PAGE and ThermoFluor experiments, we detected a relatively high affinity complex of dUTPase with importin-alpha. Complex formation was also observed in the case of the hypophosphorylation mimicking mutant (S11Q), but not with the hyperphosporylation mimicking mutant (S11E). We also conduct crystallographic studies of the complex using various dUTPase NLS peptides.

Voltage-gated Na Channels II

1610-Pos
Stable Expression of Brain Sodium Channels in Human Cells by Multiplexed Transposon-Mediated Gene Transfer

Kris M. Kahlig[1], Sai Saridey[2], Aparna Kaja[2], Melissa A. Daniels[1], Alfred L. George Jr.[1], Matthew H. Wilson[2].
[1]Vanderbilt University, Nashville, TN, USA, [2]Baylor College of Medicine, Houston, TX, USA.

Generation of cultured human cells stably expressing one or more recombinant gene sequences is a widely used approach in biomedical research, biotechnology and drug development. Conventional methods are not efficient and have severe limitations especially when engineering cells to co-express multiple transgenes or multi-protein complexes. We harnessed the highly efficient, non-viral and plasmid-based *piggyBac* transposon system to enable concurrent genomic integration of multiple independent transposons harboring distinct protein-coding DNA sequences. Flow cytometry of cell clones derived from a single multiplexed transfection demonstrated ~60% (three transposons) or ~30% (four transposons) co-expression of all delivered transgenes despite selection of a single marker transposon. We validated multiplexed *piggyBac* transposon delivery by co-expressing large transgenes encoding a multi-subunit neuronal voltage-gated sodium channel (SCN1A) containing a pore-forming subunit and two accessory subunits while using two additional genes for selection. Previously unobtainable robust sodium current was demonstrated through 38 passages, suitable for use on an automated high-throughput electrophysiology platform. Co-transfection of three large (up to 10.8 kb) *piggyBac* transposons generated a heterozygous SCN1A stable cell line expressing two separate alleles of the pore-forming subunit and two accessory subunits (total of four sodium channel subunits) with robust functional expression. We concluded that the *piggyBac* transposon system can be used to perform multiplexed stable gene transfer in cultured human cells and this technology may be valuable for applications requiring concurrent expression of multi-protein complexes.

1611-Pos
The Functional Effect of R1648H, a Sodium Channel Mutation that Causes Generalized Epilepsy with Febrile Seizures Plus in Splice Variants of SCN1A

EMILY V. FLETCHER[1], Holger Lerche[2], Dimitri M. Kullmann[1], Stephanie Schorge[1].
[1]INSTITUTE OF NEUROLOGY, LONDON, United Kingdom, [2]UNIVERSITÄTSKLINIKUM ULM, ULM, Germany.

SCN1A, the gene that encodes the alpha subunit of the voltage-gated sodium channel Nav1.1, is alternatively spliced at exon 5. SCN1A contains two copies of exon 5, denoted 5N and 5A (for 'Neonatal' and 'Adult' according to their developmental expression). There are 3 amino acid substitutions between the splice variants, all within the D1:S3/S4 extracellular linker. It is unknown how exons 5N and 5A alter channel function. Because patients with Generalized Epilepsy with Febrile Seizures plus (GEFS+) frequently exhibit age-dependent changes in seizure frequency and severity, we have asked whether the GEFS+-associated SCN1A mutation R1648H differentially affects Nav1.1-5N and Nav1.1-5A.

We examined brain tissue obtained from patients undergoing epilepsy surgery to examine the relative proportion of SCN1A transcripts containing exons 5A and 5N. A significantly greater proportion of Nav1.1 mRNA in epilepsy tissue contain exon 5N than in control brain tissue. We expressed either splice variant of SCN1A in HEK293 cells, and recorded whole-cell currents with a CsCl-based pipette solution. Nav1.1-5N demonstrated a leftward shift of both activation (Nav1.1-5N: V50= $-18.3\pm$-0.6 mV ; Nav1.1-5A: $-15.3\pm$-0.5 mV; $P<0.05$) and inactivation (Nav1.1-5N: V50= $-60.0\pm$-1.0 mV; Nav1.1-5A: $-54.0\pm$-1.1 mV). The GEFS+ mutation R1648H, did not affect activation or current density for either variant. The mutation also failed to increase the size of the persistent current evoked by prolonged depolarising steps. Instead, a hyperpolarizing shift in inactivation was observed when the mutation was expressed in Nav1.1-5A but not Nav1.1-5N channels (mutant: V50 inactivation = $-60.9\pm$-1.0 mV; wild-type: $-54\pm$-1.1 mV). This suggests that R1648H leads to a net loss of function in adult neurons. This effect may lead to an impairment of recruitment of GABAergic interneurons that preferentially express Nav1.1.

1612-Pos
Traumatic Brain Injury and Axonal Sodium Loading: Modeling the Impact of Left-Shifted Nav Channel Operation at Blebbed Nodes of Ranvier

Pierre-Alexandre Boucher[1], Béla Joós[1], Catherine E. Morris[2].
[1]Université d'Ottawa, Ottawa, ON, Canada, [2]OHRI, Ottawa, ON, Canada.

Traumatic brain injury like stretch immediately (<2 min) and irreversibly causes a TTX-sensitive axonal [Ca2+] increase that, in situ, underlies an untreatable pathology, diffuse axonal injury. Nav1.6-expressing mammalian cells, we showed, immediately (<2 min) exhibit TTX-sensitive Na+-leak following traumatic stretch (Wang et al 2009 Am J Physiol 297: in press). In situ, even mild axonal stretch injury can trigger adverse positive feedback so that leaks progress irreversibly to lethality. Though clinical trials are underway using Nav channel blockers that might reduce the severity of this outcome, molecular understanding of Nav channel damage has been lacking. Recently, however, we showed that activation and steady-state inactivation of recombinant Nav1.6 channels both irreversibly left-shift (up to -20 mV) in traumatized membrane (Wang et al 2009) as if their voltage sensors are responding to the increased bilayer disorder of traumatized (blebbed) membrane. In axonal membrane traumatized to various extents, this should smear out the window current range leftward between the normal range toward the resting potential range,

effectively degrading a well-confined window conductance into a TTX-sensitive ''Na+-leak''.
To assess whether minor membrane trauma could lead to Na+ (and hence Ca2+) loading of axons, we model partially left-shifted Nav operation in a free-running human node of Ranvier. Included are Kv and Nav conductances (linear and electrodiffusion driving forces, respectively) and a Na/K pump, with [ion]s (and associated ENa and EK) in realistic-sized intra- and extracellular compartments changing due to net ion fluxes. Left-shifting a fraction of the Navs immediately triggers a damped action potential burst then a voltage plateau dominated by window current. If resting conductances are large enough, pumping restores the system for several minutes, then more bursting starts and more ENa rundown occurs.

1613-Pos
Modulation of Nav 1.5 Variants by Src Tyrosine Kinase
Bagavananthem Andavan, **Gowri Shankar**, Rosa Lemmens-Gruber.
University of Vienna, Wien, Austria.
Cardiac sodium channel (Na_v 1.5) splice variant Q1077 deleted (hH1c1) and Q1077 present (hH1c3) mutants are present in 45% and 25 % of human population. In previous studies, Src tyrosine kinase (Fyn) showed opposite effects on cardiac and neuronal sodium channel inactivation. Half maximum inactivation of cardiac sodium channels was shifted to more positive potentials, whereas in neuronal channels it was shifted into the hyperpolarizing direction, despite having conserved Y1495, which is the site of phosphorylation in both channels. Activation was not affected.
In our study we found that Fynhas a different action on the cardiac sodium channel variants hH1c1 and hH1c3. Experiments were performed by means of the patch clamp technique in the whole cell mode. Fyn was transiently expressed with CD8 in stably expressed HEK293 cells embodying hH1c1 and hH1c3 clones. In hH1c1, Fyn shifted the activation (V_{mid} -51.6 $\pm$ 1.5 to -63.9 ± 1.0) and inactivation curves (V_{mid} -64.4 $\pm$ 0.7 to -72.5 ± 0.4) to more negative potentials, which could be reversed by the kinase inhibitor PP2 (activation: V_{mid} -63.9 ± 1.0 to -52.0 ± 1.9, and inactivation: V_{mid} -72.5 ± 0.4 to -63.7 ± 0.7). In contrast, in hH1c3 Fyn shifted both activation (V_{mid} -86.2 $\pm$ 2.3 to -65.8 ± 0.5) and inactivation (V_{mid} -85.1 ± 0.7 to -63.4 ± 0.3) curves to more positive potentials. PP2 reversed the shift of both, activation (V_{mid} -63.4 ± 0.3 to -88.2 ± 1.0)and inactivation (V_{mid} -63.4 ± 0.3 to -87.2 ± 1.7).
Above result proclaims that hH1c1 and hH1c3 encoding for Nav 1.5 are differently regulated by Fyn. These data will be pertinent in understanding the role of Q1077, which is present in the transport associated region that plays a pivotal role in regulating Fyn function.

1614-Pos
Calmodulin Regulation of the Neuronal Voltage-Dependent Sodium Channel
Michael D. Feldkamp, Liping Yu, Madeline A. Shea.
Univeristy of Iowa, Iowa City, IA, USA.
Calmodulin (CaM) is an essential eukaryotic calcium sensor comprised of two homologous domains (N, C). Ca^{2+} binding to CaM changes its conformation and determines how CaM recognizes and regulates target proteins such as the neuronal voltage-dependent sodium channel ($Na_v1.2$) which is essential for the generation and propagation of action potentials. $Na_v1.2$ is a multimer with one pore-forming α-subunit and one or more β-subunits. CaM binds to an IQ-motif (IQxxxBGxxxB, B=K,R) of $Na_v1.2$ that is near the C-terminus of the α-subunit. Prior thermodynamic studies showed that this IQ peptide ($Na_v1.2_{IQp}$, KRKQEEVSAIVIQRAYRRYLLKQKVKK) selectively lowers the Ca^{2+}-binding affinity sites in the C-domain of CaM, without affecting the N-domain (Theoharis et al, *Biochemistry* 2008). This selective decrease correlates with $Na_v1.2_{IQp}$ having a higher affinity for apo CaM than for calcium-saturated CaM. Structural studies of complexes of CaM bound to target peptides or proteins demonstrated that the 4-helix bundle of the CaM C-domain adopts an ''open'' conformation when Ca^{2+}-saturated. There is only one high-resolution structure (2IX7) of apo CaM bound to an IQ motif; it shows the C-domain having a ''semi-open'' conformation. To understand the Ca^{2+}-dependent conformational switching CaM when regulating $Na_v1.2$, we applied heteronuclear NMR methods. Amide exchange, hnNOE, and chemical shift perturbation experiments revealed residue-specific changes consistent with a ''semi-open'' conformation of the apo C-domain of CaM when bound to $Na_v1.2_{IQp}$. NMR experiments are complete and analysis is underway to determine the solution structure of the apo C-domain of CaM bound to $Nav1.2_{IQp}$. Understanding the interface between CaM and the IQ-motif of the channel will result in a more complete model of how CaM regulates $Na_v1.2$ function at low physiological [Ca^{2+}] in neuronal tissues. NIH GM57001

1615-Pos
Electrophysiological Characteristics of Neonatal Nav1.5 Expressed in a Highly Invasive Human Breast Cancer Cell Line: Sensitivity to pH and Divalent Cations
Mustafa B. Djamgoz, Rustem Onkal.
Imperial College London, London, United Kingdom.
Electrophysiological recordings from human carcinoma cell lines have shown consistently that strongly metastatic cells express functional voltage-gated sodium channels (VGSCs). The predominant VGSC in metastatic breast cancer, in vitro and in vivo, is the 'neonatal' splice form of Nav1.5. In this developmentally regulated D1:S3 splice variant of Nav1.5, there are 31 nucleotide differences between the 5'-exon ('neonatal') and the 3'-exon ('adult') forms, resulting in 7 amino acid differences in D1:S3-S3/S4 linker. In particular, a conserved negative aspartate residue in the 'adult' is replaced with a positive lysine. 'Neonatal' and 'adult' Nav1.5 α-subunit splice variants were stably transfected into EBNA-293 cells and their electrophysiological properties were investigated by whole-cell patch-clamp recording. Compared with the 'adult' isoform, the 'neonatal' channel exhibited (1) depolarized threshold of activation and voltage at which current peaked; (2) much slower kinetics of activation and inactivation; (3) ~50% greater transient charge (Na^+) influx; (4) a slower recovery from inactivation; and (5) larger persistent Na^+ currents. Mutating the lysine in the 'neonatal' channel back to aspartate resulted in the electrophysiological parameters studied reverting strongly back towards the 'adult', i.e. the lysine residue was primarily responsible for the electrophysiological differences. The charge difference between the two Nav1.5 isoforms was 'challenged' by H^+ and Cd^{2+}. The main differential effect occurred at pH 5.25-5.75 in which the activation parameters of 'neonatal' Nav1.5 were affected significantly less. The biophysical characteristics of 'neonatal' Nav1.5 observed could have significant developmental and pathophysiological consequences. In particular, the prolonged Na^+ influx can alter intracellular Ca^{2+} and/or pH homeostasis, at least in microdomains, and channel activation remains relatively efficient under extreme acidosis.

1616-Pos
Sodium Channel Variants Associated with Atrial Fibrillation Exhibit Abnormal Fast and Slow Inactivation
Dao W. Wang, Nila Gillani, Dan M. Roden, Dawood Darbar,
Alfred L. George.
Vanderbilt University Medical Center, Nashville, TN, USA.
Mutations and rare genetic variants in *SCN5A*, the gene encoding the cardiac voltage-gated sodium channel $Na_V1.5$, have been associated with inherited predisposition to ventricular arrhythmia. More recently, *SCN5A* variants have been identified in families segregating atrial fibrillation. We evaluated the biophysical properties of seven novel *SCN5A* variants associated with atrial fibrillation identified by our previous genetic study to elucidate potential molecular mechanisms underlying this common arrhythmia. Functional properties of E428K, H445D, N470K, E655K, T1131I, R1826C and V1951M were assessed by whole-cell patch clamp recording of recombinant mutant channels heterologously expressed with the human β1 subunit in tsA201 cells. One variant (R1826C) did not exhibit substantial differences in biophysical properties of activation or fast inactivation, and another variant (E655K) only exhibited minor differences in recovery from inactivation as compared with wildtype (WT) channels. However, two mutants (H445D, T1131I) exhibited significant shifts in the voltage-dependence of activation toward more negative potentials ($p < 0.005$), and four other mutant channels (E428K, H445D, N470K, V1951M) exhibited significant shifts in the voltage-dependence of steady-state inactivation toward more positive potentials as compared with WT channels. Further, H445D and V1951M exhibited more rapid onset, impaired recovery and enhancement of slow inactivation evoked by 1000 ms depolarizing prepulses as compared with WT channels. For the five variants with either hyperpolarized activation voltage-dependence or depolarized steady-state inactivation, we predict increased window current as defined by the overlap of these two curves. Increased window current and enhanced slow inactivation of some variants is further predicted to alter excitability and/or conduction in myocardial tissue and is a plausible mechanism by which *SCN5A* variants may increase vulnerability to atrial fibrillation.

1617-Pos

Mutation of Cardiac Nav1.5 in an Hisian-Type Arrhythmia, Associated with Dilated Cardiomayopathy

Mohamed-Yassine Amarouch[1], Samuel Saal[2], Géraldine Bertaux[3], Laurence Faivre[2], Isabelle Baró[1], jean-Jacques Schott[1], Florence Kyndt[1], Gildas Loussouarn[1], Gabriel Laurent[3].
[1]Inserm UMR915, l'institut du thorax, Nantes, France, [2]Centre de Génétique, hôpital d'Enfant, CHU Dijon, Dijon, France, [3]Service de Cardiologie, hôpital le Bocage, CHU Dijon, Dijon, France.

Cardiac sodium channels are complexes including alpha and beta1 subunits allowing sodium influx during the depolarization phase of the ventricular action potential. The pore-forming alpha subunit, Nav1.5, is encoded by *SCN5A.* Using a candidate-gene approach, we detected a variant of *SCN5A*, leading to the R222Q substitution by screening one family with cardiac arrhythmia resulting in frequent premature ventricular contractions, non sustained ventricular tachycardia and dilated cardiomyopathy. Arrhythmia mechanisms involved ectopic foci originating from the proximal part of the His-Purkinje system. To evaluate the incidence of this substitution on Nav1.5 function, whole-cell patch-clamp experiments were performed on COS-7 cells transfected with the human alpha and beta1 subunits. The presence of the mutation at the heterozygous or homozygous state did not modify the sodium current density. In contrast, the activation curve was shifted toward more negative potentials (V1/2act, WT: -30.6 ± 2.1 mV, n=11; R222Q: -42.3 ± 1 mV, n=11, $p<0.001$; heterozygous: -37.2 ± 1.6 mV, n=9; $p<0.05$) and the slope was changed in the heterozygous condition only (WT: 5.7 ± 0.3 mV, R222Q: 6.5 ± 0.4 mV, heterozygous: 7.1 ± 0.3 mV; $p<0.01$). Activation kinetics were also accelerated in mutant homozygous condition only ($p<0.001$, versus WT). Inactivation voltage sensitivity was also changed (V1/2inact, WT: -79.6 ± 0.7 mV, n=10; R222Q: -84.6 ± 0.7 mV, n=8, $p<0.001$; heterozygous: -82.2 ± 1 mV, n=9; $p<0.05$), its kinetics accelerated ($p<0.001$ versus WT for both mutant and heterozygous conditions) and the slope was changed in the mutant homozygous condition only (WT: 5.6 ± 0.2 mV; R222Q: 4.8 ± 0.2 mV; $p<0.01$; heterozygous: 5.3 ± 0.1 mV). Finally, recovery from inactivation was not modified by the R222Q mutation. We studied the impact of the current biophysical changes in cellular models of the Purkinje and ventricular action potentials. The premature ventricular contractions are explained by the appearance of electrical abnormalities rather in Purkinje fibers than in ventricular cardiomyocytes.

1618-Pos

Block and Permeation of the Hypokalemic Periodic Paralysis Gating Pore In Nav1.4 Channels

Stanislav Sokolov, Todd Scheuer, William A. Catterall.
University of Washington, Seattle, WA, USA.

We reported previously that naturally occurring hypokalemic periodic paralysis (HypoPP) mutations of voltage sensing arginines in domain II of the skeletal muscle sodium channel $Na_v1.4$ produce gating pore currents at hyperpolarized membrane potentials. These small but persistent currents produce a gain-of-function that would contribute to the pathophysiology of HypoPP. Here we investigate biophysical properties of the gating pore with mutations in R2 in more detail. We confirm that Na^+ currents through the gating pore can be blocked by Ba^{2+} and Zn^{2+} at mM concentrations. Block is voltage-dependent and is substantially increased by strongly negative holding potentials. Voltage-dependent block develops with kinetics consistent with preferential binding of divalent cations to the resting conformation of the voltage sensor. Trivalent cations such as Gd^{3+}, La^{3+}, Yb^{3+} block Na^+ gating pore currents with higher affinity than divalents (hundreds of nM), but with much less voltage dependence. We also probed permeation through the gating pore. Currents through the $Na_v1.4$/R2G gating pore carried by guanidinium (Gu^+) are ~25 fold larger than Na^+ currents. Smaller derivatives like ethyl-guanidine also permeate through the gating pore better than sodium. Bulkier guanidine derivatives block both Na^+ and Gu^+ gating pore conductances at mM concentrations. Interestingly, HypoPP mutant $Na_v1.4$/R2H, which is proton-selective in physiological saline, is also permeable to Gu^+ despite its lack of permeability to monovalent alkali metal cations. The high Gu^+ permeation through these gating pores is consistent with the expected favorable environment for the guanidinium side chains of the native arginine gating charges. Our studies reveal conformation-dependent divalent cation block of these HypoPP mutant gating pores, as well as block by guanidine derivatives, which may provide potential targets for therapeutically active compounds.

1619-Pos

Mutation in Nav1.5 Associated with Brugada Syndrome - a Mutational Hotspot?

Nicole Schmitt[1], Kirstine Calloe[1], Christian Veltmann[2], Ryan Pfeiffer[3], Martin Borggrefe[2], Christian Wolpert[2], Rainer Schimpf[2], Jonathan M. Cordeiro[3], Charles Antzelevitch[3].
[1]University of Copenhagen, Copenhagen N, Denmark, [2]University of Mannheim, Mannheim, Germany, [3]Masonic Medical Research Laboratory, Utica, NY, USA.

Several studies have demonstrated an association between Brugada syndrome (BrS) and mutations in genes encoding ion channel subunits including SCN5A, CACNA1C, CACNB2b, SCN1B, and KCNE3. Mutations in SCN5A, encoding the voltage-gated sodium channel Nav1.5, represent the majority with greater than 293 mutations in SCN5A linked to the syndrome (Kapplinger et al, Heart Rhythm, In press 2009). We identified a missense mutation (G1408R) in SCN5A in a large BrS family. Intriguingly, this mutation had been reported earlier in two independent studies and has also shown to be associated with Sick Sinus Syndrome (SSS) and Cardiac Conduction Defect (CCD) (Kyndt et al, 2001; Benson et al, 2003). Nav1.5-G1408R channels heterologously expressed in CHO cells and studied using patch-clamp techniques failed to generate any sodium channel current (INa). Co-expression of the mutated channels with wild-type (WT) channels resulted in a 50% reduction of current amplitudes with no changes in kinetic properties when compared with WT channels. The residue resides in the DIII pore region and is conserved among species. We addressed the importance of this amino acid at position 1408 by replacing it with another small neutral amino acid (G1408A) and by substituting a negatively charged aspartic acid (G1408D). Our results show that substituting glycine with alanine retains WT behavior while exchange to the positively charged arginine (G1408R) or negatively charged aspartic acid leads to a complete loss-of-function. In conclusion, we describe a SCN5A mutation associated with BrS which results in a loss of function of INa important for action potential generation. Further, we show that the presence of a neutral hydrophobic amino acid at this position is crucial for normal channel function.

1620-Pos

Do Sodium Channel α - α Interactions Contribute to Loss-of-Function Observed in Brugada Syndrome?

Krekwit Shinlapawittayatorn, Xi Du, Haiyan Liu, Eckhard Ficker, Isabelle Deschenes.
Case Western Reserve University, Cleveland, OH, USA.

The pathogenesis of Brugada Syndrome (BrS) has been associated with mutations in the cardiac sodium channel gene SCN5A, resulting in loss-of-function. Recently, the L325R mutation has been proposed to cause BrS through a dominant-negative effect. Dominant-negative effects are usually the consequence of mutant subunits assembling with wild-type (WT) into non-functional channel multimers. In contrast, sodium channel α-subunits are not believed to oligomerize. However, there is increasing evidence suggesting the existence of α-α interactions between sodium channels. Therefore, we tested whether the dominant-negative effect seen in some BrS mutations is due to interactions between sodium channel α-subunits. We co-expressed a dominant-negative BrS mutation, L325R, with WT channels at different molar ratios. Channels containing the mutation alone did not elicit current. When WT and L325R channels were co-transfected in a 1:1 and 4:1 WT:L325R ratios, the normalized peak INa densities were reduced respectively to $29.8 \pm 6.2\%$ and $57.3 \pm 5.8\%$ of the control WT confirming the dominant-negative effect of this mutation. When using a binomial distribution, our results were fitted best by a configuration suggesting the interaction of two channel monomers. We also investigated the existence of channel-channel interactions using the BrS mutation L567Q. This mutation displays biophysical alterations possibly too small to explain the clinical phenotype. Interestingly, co-expression of L567Q with WT channels produced a significant reduction in INa density which could possibly also be caused by channel-channel interactions and therefore explain the clinical manifestation of the disease. In conclusion, our experiments using BrS mutations, now suggest the idea of a dimerization of sodium channel α-subunits.

1621-Pos

An Intronic Mutation of SCN4A Associated with Myotonia Raises an Aberrantly Spliced Isoform with Disrupted Fast Inactivation

Tomoya Kubota[1], Masanori P. Takahashi[1], Takashi Kimura[2], Saburo Sakoda[1].
[1]Osaka University, Osaka, Japan, [2]Hyogo College of Medicine, Hyogo, Japan.

Genetic defects of voltage-gated ion channel genes are responsible for several inheritable skeletal muscle diseases. Mutations of skeletal muscle sodium channel, SCN4A, have been shown to associate with myotonia and periodic paralysis. So far, most of the disease mutations of SCN4A are located in coding regions and the mutated channels show disruption of fast inactivation or enhancement of activation. We found a patient with myotonia caused by aberrantly spliced channel due to a mutation located at an intron of SCN4A. Moreover, this mutant channel showed gain of function defect, disruption of fast inactivation.
A case was 35 year-old male who showed well-developed Herculean musculature and generalized muscle stiffness aggravated with cold exposure. We performed sequence analysis of SCN4A and CLCN1 using genomic DNA extracted from patient's lymphocytes. Moreover the mRNAs of SCN4A expressed in patient's muscle were analyzed by RT-PCR and nucleotide sequence. We constructed an expression vector of the channel isoform expressed in patient's muscle and measured Na current with whole cell configuration using HEK293t cells on which channels are expressed transiently.
No mutations were identified in all exons of either SCN4A or CLCN1. Replacement of 5 nucleotides to a single nucleotide was detected in intron 21 of SCN4A. The mutation is located at downstream of exon 21 which could serve as splicing donor site. RT-PCR and nucleotide sequence analysis of cDNA showed three aberrantly spliced isoforms. The only in-frame isoform should result in insertion of 35 amino acids between domain III and IV. This isoform expressed in HEK cells showed marked defect in fast inactivation.
Disease mutations located at non-coding region of voltage-gated ion channel genes usually show loss-of function, and this is the first example which shows gain-of function defect.

1622-Pos
Properties of the Domain-II Voltage Sensor Determining the Function of $Na_v1.8$ (SCN10A) Channels
Jana Schirmeyer, Enrico Leipold, Stefan H. Heinemann.
Friedrich Schiller University Jena, Jena, Germany.
$Na_V1.8$ voltage-gated sodium channels are primarily expressed in dorsal root ganglia neurons and are implicated in pain perception. One of their remarkable features is their activation at relatively depolarized membrane voltages ($V_a = -5.3 \pm 1.5$ mV compared to -40.2 ± 2.2 mV for skeletal muscle $Na_V1.4$). Searching for the underlying molecular determinants, we constructed domain chimeras between rat $Na_V1.4$ and $Na_V1.8$ channels and assayed them with the whole-cell patch-clamp method after expression in Neuro-2A cells. While we could not obtain any current response with 8444, i.e. a construct with domain-I from $Na_V1.8$ and the remaining domains from $Na_V1.4$, analysis of chimeras 4844 ($V_a = -12.8 \pm 2.2$ mV), 4484 (-40.4 ± 1.5 mV) and 4448 (-25.7 ± 2.0 mV) suggests that the depolarized activation voltage mainly results from domain-II. The voltage sensor in domain-II of $Na_V1.8$ harbors a double KK motif in the S3/S4 linker (KK726 and KK747), a feature unique for $Na_V1.8$ channels. Mutating the KK motifs to the corresponding residues of $Na_V1.4$ results in a left-shift in activation for KK747NV ($V_a = -15.6 \pm 1.3$ mV). The reverse mutations in $Na_V1.4$, QG634KK and NV655KK, have a qualitatively opposite effect. Furthermore, the KK motifs seem to interfere with the μO-conotoxin MrVIA, which is known to interact with the voltage-sensor of domain II via a sensor-trapping mechanism. Mutants KK747NV and KK726QG-KK747NV are blocked by 400 nM MrVIA by $91 \pm 1\%$ and $86 \pm 8\%$ respectively, compared to $64 \pm 4\%$ for $Na_V1.8$ wild-type channels. In addition, toxin dissociation at +40 mV is about 1.5 times faster for KK726QG-KK747NV than for wild-type channels. Thus, the KK motifs in the S3/S4 linker of $Na_V1.8$ domain-II voltage-sensor take part in channel gating compatible with the ''paddle model'' and provide a molecular explanation for the gating mechanism unique to $Na_V1.8$ channels.

1623-Pos
A Conserved Double-Tyrosine Motif in the Cardiac Sodium Channel Domain III-IV Linker Underlies Calcium Dependent Ca2+/Calmodulin Binding and Regulation of Inactivation Gating
Maen Sarhan, Filip Van Petegem, Christopher Ahern.
University of British Columbia, Vancouver, BC, Canada.
Voltage-gated sodium channels maintain the electrical cadence and stability of neurons and muscle cells by selectively controlling the transmembrane passage of their namesake ion. The degree to which these channels contribute to cellular excitability can be managed therapeutically or fine-tuned by endogenous ligands.
Intracellular calcium, for instance, heavily modulates sodium channel inactivation, the process by which sodium conductance is negatively regulated. We explore the molecular basis for this effect by investigating the interaction between the ubiquitous calcium binding protein calmodulin (CaM) and the putative sodium channel inactivation gate comprised of the cytosolic linker between homologous channel domains III-IV (DIII-IV). Experiments using isothermal titration calorimetry (ITC) show that CaM binds in a calcium-dependent manner to a novel motif in the center of the DIII-IV linker, N-terminal to a region previously reported to be a CaM binding site. An alanine scan of aromatic residues in recombinant DIII-DIV linker peptides reveals that while multiple side-chains contribute to CaM binding, two tyrosines (Y1494 and Y1495) play a crucial role in binding the CaM C-lobe. The functional relevance of these observations is then ascertained through electrophysiological measurement of sodium channel inactivation gating in the presence and absence of calcium. Experiments on patch-clamped transfected tsA201 cells show that only the Y1494A mutation of the five sites tested renders sodium channel steady-state inactivation insensitive to cytosolic calcium.
The results demonstrate that calcium dependent CaM binding to the DIII-IV linker double tyrosine motif is required for calcium regulation of the cardiac sodium channel.

1624-Pos
Extracting Thermodynamic Parameters from Site-Specific Observables: Chi-Value Analysis
Sandipan Chowdhury, Baron Chanda.
University of Wisconsin, Madison, WI, USA.
Interactions between different structural domains are important determinants of the function and regulation of allosteric proteins. Prevalent theories to understand the thermodynamic basis of cooperativity have frequently constrained the interactions between the different domains to come up with a mathematical model which can reproduce the complex behavior of a global thermodynamic observable such as ligand binding or enzyme activity. Such simple phenomenological models, in general, are not amenable to molecular description of cooperative interactions. Here, we provide the theoretical framework of a method, the chi-value analysis, which can elucidate the thermodynamic effect of molecular level perturbations. The chi value analysis involves extracting a site-specific parameter (chi value) associated with a structural domain and observing how the chi value is altered by a mutation. Through this formalism, based on classical statistical mechanics, we show that the chi value analysis can be used to deconstruct and quantify the energetic effects of mutations even in a complex macromolecular system consisting of a large number of structural units interacting via a complex network of interactions. Using models of the multi-domain voltage-dependent sodium and large-conductance calcium activated potassium channels, we have performed extensive numerical simulations to probe the validity of the chi value analysis. Our theory may provide a general approach to understand the detailed energetics underlying cooperative behavior of multi-domain proteins.

1625-Pos
Modeling the Outer Pore of Sodium and Calcium Channels
Denis B. Tikhonov, Boris S. Zhorov.
McMaster University, Hamilton, ON, Canada.
In the absence of x-ray structures of sodium and calcium channels, their homology models based on x-ray structures of potassium channels are used to design and rationalize experiments. A challenge is to model the outer-pore region that folds differently from potassium channels. Here we report a model of the outer-pore region of NaV1.4, which is based on a large body of experimental data, including specific contacts of toxins with individual channel residues. The model inherits from our previous model the general disposition of the P-helices, the selectivity-filter residues, and the outer carboxylates, but provides a novel view on the role of other highly conserved residues in the outer pore. In the absence of secondary-structure elements, structural stability of the outer pore should be supported by specific contacts. We propose a network of such contacts including intra- and inter-domain H-bonds, knob-into-the-hole contacts, and hydrophobic interactions. Glycine residues downstream the selectivity filter are proposed to participate in knob-into-hole contacts with P-helices and S6s. These contacts explain known tetrodotoxin resistance of snakes adapted to toxic prey due to NaV1.4 mutation Ile/Val in the P-helix of repeat 4. Polar residues in P-helices, which are five positions upstream from the selectivity-filter residues, form H-bonds with the ascending-limb backbones. The exceptionally conserved tryptophans are engaged in inter-repeat H-bonds to form a ring whose π-electrons would facilitate the passage of ions from the outer carboxylates to the selectivity filter. The outer-pore model of CaV1.2 derived from the NaV1.4 model is also stabilized by the ring of exceptionally conservative tryptophans and H-bonds between P-helices and ascending limbs. In this model a highly conserved aspartate downstream the selectivity-filter glutamate in repeat II facilitates passage of calcium ions moving to the selectivity-filter ring through the tryptophan ring.
Supported by CIHR.

Voltage-gated K Channels-Gating II

1626-Pos
Does the Linker in Ci-VSP Function as a PI(4,5)P2 Binding Domain?
Susy C. Kohout[1], Sarah C. Bell[1], Qiang Xu[2], Daniel L. Minor[2], Ehud Y. Isacoff[1].
[1]University of California, Berkeley, Berkeley, CA, USA, [2]University of California, San Francisco, San Francisco, CA, USA.
Proteins are often composed of multiple domains which confer specialized functions to the full length protein. The voltage sensing domain (VSD) from voltage-gated ion channels is one such domain. Originally thought to be restricted to ion channels, we now know that it can also confer voltage control to enzymes. The Ciona intestinalis voltage sensor-containing phosphatase (Ci-VSP) is composed of the unique combination of a VSD coupled to a lipid phosphatase. The coupling between these two domains is intriguing since it means that a modular VSD can control two very different effectors, a pore or an enzyme. The original characterization of Ci-VSP suggested that the inter-domain linker played a role in activating the protein while more recent work has shown evidence supporting the hypothesis that the inter-domain linker functions as a phosphatidylinositol 4,5-bisphosphate (PI(4,5)P2) binding domain (PBM) (1,2). This function is similar to that of the N-terminus of PTEN, a well-known lipid phosphatase that shares a high degree of homology to Ci-VSP. We chose disease-causing mutations from PTEN, introduced them into Ci-VSP and probed Ci-VSP's voltage-dependent movements and phosphatase activity using voltage clamp fluorometry, two electrode voltage clamp, and biochemical methods. We find that the linker composition is critical for activity where single amino acid mutations either decrease or eliminate activity. We also found that upon PI(4,5)P2 depletion, the voltage dependent motions of the VSD were altered when the linker was intact, but not when the linker was mutated. Our data suggests that the linker both couples to the two domains and also serves as a PBM, regulating via its interaction with PI(4,5)P2.
1. Murata, Y., et al, (2005) Nature 435, 1239-1243
2. Villalba-Galea, C. A., et al, (2009) J Gen Physiol 134, 5-14

1627-Pos
Sensing Charges of Ci-VSP
Carlos A. Villalba-Galea[1,2], Ludivine Frezza[2], Ernesto Vargas[2], Francisco Bezanilla[2].
[1]Virginia Commonwealth University, Richmond, VA, USA, [2]The University of Chicago, Chicago, IL, USA.
The *Ciona intestinalis* Voltage Sensor-containing Phosphatase (Ci-VSP) is a member of the Voltage Sensitive Phosphatase family that exhibits membrane potential-controlled enzymatic activity. Alignments of the amino acid sequence of Ci-VSP against Voltage Gated Channels (VGC) indicate that its Voltage Sensing Domain (VSD) is formed by four transmembrane segments. The putative fourth segment (S4) of Ci-VSP extends between the arginine (R) in position 217 and the glutamine (Q) in position 239, containing five arginines, which might be the voltage sensing charges. Although it has been shown that R229 and R232 are critical for voltage sensing in Ci-VSP (Murata *et al.*, 2005), the role of the remaining charges is still unclear. To address this issue, we have performed a partial Histidine Scanning of the S4 of Ci-VSP, following the paradigm established for the VGC *Shaker* (Starace and Bezanilla, 2004). The voltage dependence of the sensing current of the R217H mutant was modulated by pH. Decreasing the external pH shifted the Q-V curve towards positive potentials, while a pH increase had the converse effect, consistent with the finding that neutralizing R217 (R217Q) produces a negative shift of the voltage dependence of Ci-VSP (Kohout *et al.*, 2008). However, the total net charge of R217H did not change with pH, indicating that R217 does not participate in sensing the membrane potential. When the second arginine is replaced by histidine, the resultant mutant (R223H) exhibits a voltage dependent proton current which closes at positive potentials, resembling the current recorded from *Shaker*-W434F with its first gating charge replaced by histidine (R362H). This result strongly suggests that R223 has access to both the intra- and the extracellular media depending on voltage. Taken together, our results indicate that R223 is the most extracellularly located sensing charge of the Ci-VSP S4 segment. (Support: NIHGM030376)

1628-Pos
Modular Nature of the Main Domains in Voltage Sensitive Phosphatases
Jérôme Lacroix[1], Christian R. Halaszovich[2], Daniela N. Schreiber[2], Francisco Bezanilla[1], Dominik Oliver[2], **Carlos A. Villalba-Galea**[1,3].
[1]The University of Chicago, Chicago, IL, USA, [2]Philipps-Universität Marburg, Marburg, Germany, [3]Virginia Commonwealth University, Richmond, VA, USA.
Voltage Sensitive Phosphatases (VSPs) constitute a family of enzymes controlled by membrane potential. Its members have a Voltage Sensing Domain (VSD) in the N-terminus and a Phosphatase Domain (PD) in their C-terminus, both connected by a Phospholipid Binding Motif (PBM). Remarkably, N- and C-terminal domains display high homology to two different types of proteins. The VSD of VSPs resembles the VSD of voltage gated channels; while their PD shares a striking homology to the tumor suppressor phosphoinositide phosphatase PTEN. This feature of VSPs makes them look like natural chimeras. Recently, it has been shown that the catalytic activity of Ci-VSP, a member of the VSP family, depends on the binding of the PBM onto the membrane, which is, in turn, controlled by the membrane potential-driven movement of the VSD. For PTEN, it is known that the binding of PTEN onto the plasma membrane mediated by its N-terminus is *sine qua non* for enzymatic activity.Based on this similarity, we built a chimera by replacing the PD of Ci-VSP by PTEN. This chimera, Ci-VSPTEN, was successfully expressed in *Xenopus* oocytes and displayed sensing currents resembling those observed in Ci-VSP. As for its enzymatic characteristics, Ci-VSPTEN was expressed in CHO cells and its activity tested by measuring membrane association of GFP-tagged phosphoinositide sensors by TIRF microscopy. Depolarization-induced decline in membrane fluorescence indicated that Ci-VSPTEN has voltage dependent $PI(3,4,5)P_3$ 3'-phosphatase activity. Because the binding of the PBM induces an allosteric activation of PTEN, these observations strongly support the idea that the binding of the PBM onto the membrane is a key step in the activation of Ci-VSP. In a broader view, these results show that the VSD and the PD of Ci-VSP, and presumably other VSPs, are naturally modular. (Support: GM030376, DFG OL240/2)

1629-Pos
Two Structurally Distinct Pathways for the Voltage-Sensing S4 Helices
Jerome J. Lacroix[1], Fabiana V. Campos[2], Ludivine Frezza[1], Walter Sandtner[3], Francisco Bezanilla[1].
[1]Department of Biochemistry and Molecular Biology, University of Chicago, Chicago, IL, USA, [2]Department of Biological and Environmental Sciences, University of Jyvaskyla, Jyvaskyla, Finland, [3]Medical University of Vienna, Vienna, Austria.
In voltage-dependent ion channels, the movement of the voltage-sensing S4 helices produces gating currents. The charge displaced as a function of the membrane potential (Q-V) is well described by a sequential two-state Boltzmann relation, indicating that there are at least two steps of gating charge movement from their Resting state to the Active state. In addition, it has been shown that at a maintained positive potential, the S4 helices of voltage-gated Na, Ca and K channels and the voltage sensitive phosphatase Ci-VSP, undergo a slower secondary conformational transition stabilizing the sensor in a Relaxed (inactivated) state. From the Relaxed state, the Q-V relation exhibits a strong shift towards negative potentials when compared to the Q-V relation measured from the resting state. We engineered gating perturbations in the Shaker potassium channel, by substituting specific aromatic residues in positions spatially close to the S4. One of these mutants, in position I241 of S1, part of the hydrophobic plug of the voltage sensor, when mutated to tryptophan (I241W), produces a strong split in the Q-V when measured from the resting state. By labeling M356C with TMRM we also find the same split in the fluorescence-voltage curve. We propose that the presence of the tryptophan in the 241 position favors an interaction with one of the positively-charged arginines along the S4, thus stabilizing a fleeting intermediate state in the gating pathway. However, in the I241W mutant, the split in the Q-V almost disappears when the gating currents are measured from the relaxed state and the same result is seen with the fluorescence-voltage curve. This result and the effect of other tryptophan perturbations near the S4 segment strongly support the existence of two structurally distinct gating pathways for the movement of the S4 helices. Supported: NIHGM030376.

1630-Pos
Zinc Inhibition of Monomeric and Dimeric Proton Channels Suggests Cooperative Gating
Boris Musset[1], Susan M.E. Smith[2], Vladimir V. Cherny[1], Deri Morgan[1], Sindhu Rajan[3], Thomas E. DeCoursey[1].
[1]Rush University Medical Center, Chicago, IL, USA, [2]Emory University, Atlanta, GA, USA, [3]University of Chicago, Chicago, IL, USA.
Voltage gated proton channels are strongly inhibited by Zn^{2+}, which binds to His residues. However, in a molecular model based on similarity between proton channels and the voltage sensing domain of K^+ channels, the two externally accessible His are too far apart to coordinate Zn^{2+}. In view of the proton channel existing as a dimer, we hypothesize that a high affinity Zn^{2+} binding site is created at the dimer interface by His residues from both monomers. Consistent with this idea, Zn^{2+} effects are weaker on monomeric channels. In addition, monomeric channels opened exponentially, and dimeric channels opened sigmoidally, suggesting a Hodgkin-Huxley type process in which multiple

subunits undergo a conformational change that precedes opening. This is surprising, because each monomer is thought to contain a separate conduction pathway. Monomeric channel gating had twice weaker temperature dependence than dimeric channels, consistent with a more complex gating mechanism in the dimer. Finally, monomeric channels opened 6.6 times faster than dimeric channels. Combined, these observations suggest that the native proton channel is a dimer in which the two monomers are closely apposed and interact during a cooperative gating process.

1631-Pos
Strong Negative Cooperativity Between Subunits in Voltage-Gated Proton Channels

Carlos Gonzalez, Hans P. Koch, Ben M. Drum, Hans Peter Larsson.
University of Miami, Miami, FL, USA.

Voltage-activated proton (H_V) channels are essential components in the innate immune response. Hv channels are dimeric channels with one proton permeation pathway per subunit. It is not known how Hv channels are activated by voltage and whether there is any cooperativity between subunits during voltage activation. Using cysteine accessibility measurements and voltage clamp fluorometry, we show that the fourth transmembrane segment S4 functions as the voltage sensor in H_V channels from *Ciona Intestinalis*. Surprisingly, in a dimeric H_V channel, the S4s in both subunits have to move to activate the two proton permeation pathways. In contrast, if H_V subunits are prevented from dimerizing, then the movement of a single S4 is sufficient to activate the proton permeation pathway in a subunit. These results suggest a strong negative cooperativity between subunits in dimeric H_V channels.

1632-Pos
High-Resolution Crystallographic Analysis of the Kcsa Gating Cycle from Cysteine-Trapped Open Channels

Luis G. Cuello[1], D. Marien Cortes[1], Eduardo Perozo[2].
[1]Texas Tech University Health Science Center, Department of Cell Physiology and Molecular Biophysics, Lubbock, TX, USA, [2]The University of Chicago, Department of Biochemistry and Molecular Biology, Chicago, IL, USA.

The K+ channel pore domain contains all the elements necessary to catalyze the selective permeation of K+ ions, in addition to regulate events underlying activation and inactivation gating. In KcsA, an inactivation process related to C-type inactivation in eukaryotic channels has been attributed to putative conformational changes at the selectivity filter (SF)[1]. Previously, we have provided crystallographic evidence for the conformational changes associated to C-type inactivation, albeit at relatively low-resolution [2]. Here, we have taken advantage of a cysteine-bridged locked open KcsA-mutant to study the structural changes at the selectivity filter when the activation gate (AG) is open and the filter transitions between its conductive and non-conductive conformations. We report the structures of KcsA for the non-inactivating mutant E71A at 2.1 Å; the fully inactivated mutant Y82A at 2.32 Å; and the non-inactivating mutant F103A at 2.64 Å, where the allosteric coupling between the two gates (AG and SF) has been impaired. This set of high-resolution structures for different KcsA kinetic states represent a sharp improvement over the resolution of non-cysteine trapped mutants and will be interpreted in relation to their complementary functional characterization.

1. Cordero-Morales, J.F., et al., Molecular determinants of gating at the potassium-channel selectivity filter. Nat Struct Mol Biol, 2006. 13(4): p. 311-8.
2. Cuello, L.G., et al. (2008). Structural basis of K+ channel C-type inactivation: Crystal structure of KcsA in the Open/C-type inactivated conformation. 52nd Annual meeting of the Biophysical Society. Mini-symposium

1633-Pos
Gating-Related Conformational Changes in the Outer Vestibule of KcsA: a Fluorescence and Pulsed-Epr Analysis

H. Raghuraman, Eduardo Perozo.
Institute for Biophysical Dynamics, The University of Chicago, Chicago, IL, USA.

In K^+ channels, the selectivity filter and surrounding structures play a crucial role in inactivation gating and flicker. KcsA is a pH-gated K^+ channel and its gating is modulated by transmembrane voltage. In this work, we monitored the gating-related structural dynamics in the outer vestibule of KcsA using site-directed NBD fluorescence and pulsed-EPR analysis. Fluorescence polarization results show that in KcsA, the dynamics of the outer vestibule is substantially different when comparing inactivating (wild type) and non-inactivating (E71A) forms of the channel. In addition, the rate of solvent relaxation (dynamics of hydration) is found to be faster in non-inactivating form of KcsA upon gating as determined by red edge excitation shift (REES) analysis. This increased rate of solvent relaxation correlates well with the increased rotational mobility of the outer vestibule residues in the open, non-inactivating state (E71A at pH 4). To gain further insight on the dynamic properties of these conformational fluctuations in the outer vestibule of KcsA during gating, four pulse Double-Electron-Electron Resonance (DEER) EPR spectroscopy is being currently used. This approach allows for the determination of inter-subunit distances between 20-60 Å, directly informing on the overall distance distribution. We have used tandem dimer constructs of spin-labeled KcsA for the residues corresponding to the outer vestibule of KcsA to determine average distances and distance distributions at low pH, under conditions that stabilize the inactivated (wild-type filter) and the non-inactivating (E71A) states. The results will be discussed in terms of the conformational transitions in the outer vestibule during activation and inactivation gating.

1634-Pos
An Engineered Cysteine-Bridge Locks KcsA Inner Bundle Gate in Its Open Conformation

Luis G. Cuello[1], D. Marien Cortes[1], Eduardo Perozo[2].
[1]Texas Tech University Health Science Center, Department of Cell Physiology and Molecular Biophysics, Lubbock, TX, USA, [2]The University of Chicago, Department of Biochemistry and Molecular Biology, Chicago, IL, USA.

Ion channels undergo conformational changes that allow them to transition along defined kinetic states. Previously, we have carried out an extensive crystallographic characterization of the key kinetic states that form the K+ channel gating cycle. Key among them is the structure of KcsA with the inner bundle gate in its open conformation and the selectivity filter in its inactivated (non conductive) form. Aiming to obtain high-resolution structural information of these trapped states, we have engineered a series of cysteine-bridges in the activation gate of a constitutively open KcsA mutant based on the structural properties of the open gate. We reasoned that restricting the conformational freedom of the activation gate, by locking it in the open conformation, would lead to a significant improvement in the resolution of the crystallographic data. This was carried out through a series of cysteine mutants in both TM1 and TM2 which generated covalently concatenated channels, even in the absence of an external oxidative agent. Biochemical and functional analyses suggested that channels were covalently locked open and that the crosslinked channel was stable under a variety of conditions, highly thermally resistant and was monodisperse under gel filtration chromatography. This new approach should help obtain high-resolution structural information of KcsA mutants trapped in different kinetic states and provide additional correlation to the functional characterization of each kinetic state.

1635-Pos
pH-Dependent Gating of KcsA Potassium Channel

Matsuki Yuka, Masayuki Iwamoto, Hirofumi Shimizu, Shigetoshi Oiki.
University of Fukui, Fukui, Japan.

KcsA potassium channel is a pH-dependent channel and is activated when cytoplasmic side becomes acidic. In KcsA channel there are two gates in series along the permeation pathway: the filter gate and the helix gate. Recently crystal structure of the full-length KcsA channel was revealed and the pH-sensitive domain was identified. It is crucial to elucidate functional properties of the helix gate in relation to the pH sensing. However, complicated behavior of the filter gate makes the single-channel analysis difficult for the wild-type KcsA channel. Here we examined pH-dependence of the helix gate and its gating kinetics using an inactivation-free mutant, E71A. The E71A channel was reconstituted into the planar lipid bilayer membrane and the gating behavior was recorded during stepwise changes in cytoplasmic pH. In contrast to the wild-type KcsA, the open probability was almost 100% at pH 3.0. Flickery gating was observed in the negative potentials. As the pH approached to neutral the channel became closed and recovered when pH was returned to acidic. We found that the pH dependency of E71 channel was shifted towards neutral compared to that of the wild-type channel. Frequent transitions between open and closed states were observed around the pKa, from which kinetic properties of the helix gate were analyzed. The mechanism underlying the shift of the pH-sensitivity will be discussed.

1636-Pos
Electron Spin Echo Envelope Modulation (ESEEM) Reveals the Footprint of the Voltage Sensor on the KvAP Pore Domain

John A. Cieslak, Adrian Gross.
Northwestern University Feinberg School of Medicine, Chicago, IL, USA.

In voltage gated potassium channels, two interfaces between the central pore domain (PD) and the peripheral voltage sensor domain (VSD) must exist for the efficient transduction of membrane potential changes into mechanical opening of the gate. The first interface, located between the S4-S5 linker (VSD) and the S6 helix (PD), couples VSD motion to PD motion. Additionally, a strong secondary interface is mechanistically required to act as an anchor point between the domains so that force can be efficiently transduced to the PD. However, no such interface is apparent in any current crystal structure. As multiple studies have identified the S1 helix as the likely point of anchoring of the VSD,

we set out to determine the interaction footprint of the VSD on the PD using ESEEM spectroscopy. We have previously demonstrated that deuterium ESEEM is well suited to investigate the interaction of membrane proteins with their surrounding environment. In the present study, we determine the water accessibility profile of the KvAP PD in the presence and absence of the VSD. We show that a region of the PD near the monomer interface demonstrates decreased deuterium coupling in the presence of the VSD compared to what would be expected based on residue immersion depth. Furthermore, the observed deuterium coupling at this region increases to expected levels upon removal of the VSD. We conclude that the protected region of the PD represents the interaction footprint of the VSD on the surface of the pore.

1637-Pos
Down-State Model of the KvAP Full Channel
Eric V. Schow, Alexandr Nizkorodov, J. Alfredo Freites, Stephen H. White, Douglas J. Tobias.
University of California at Irvine, Irvine, CA, USA.
Voltage-gated potassium (Kv) channels have at least two distinct conformations, an ''up'' state, corresponding to the open/activated state of the channel, and a ''down'' state, corresponding to the resting state of the channel. Kv channels are tetramers that consist of a central pore domain (PD) and four peripheral voltage-sensing domains (VSDs) that respond to changes in the transmembrane (TM) potential. The PD opens and closes via mechanical coupling to the VSDs, which undergo large conformational changes as the TM potential changes. The molecular mechanism of these changes is poorly understood, because the Kv crystal structures reported to date are exclusively in the up state. We have recently reported a down-state model of the isolated VSD of KvAP that is consistent with existing experimental data. Based on this down-state model, we have now generated a down-state model for the KvAP full channel using targeted molecular dynamics. We used the end point of an equilibrated simulation of the KvAP full channel in the up state as a starting point and four symmetrically arranged down-state VSDs as targets. The PD was unconstrained during the simulation. Preliminary results suggest that, as expected, steric interactions between the S4-S5 linker and the intracellular half of S6 result in a measurable narrowing of the pore. We compare our model to the closed-state structure of the KcSA channel (2001, Science 280: 69), which consists of a Kv-homologous PD but no VSD, and to the Kv1.2 mammalian channel down-state model of Pathak et al (2007, Neuron 56: 124). This work is supported by NIH grants GM74637 and GM86685 and NSF grant CHE-0750175, and we are grateful for the allocation of computer time on the NSF-supported Teragrid resources provided by the Texas Advanced Computing Center.

1638-Pos
Interactions Between Lipids and Voltage Sensor Paddles Detected with Tarantula Toxins
Mirela Milescu, Frank Bosmans, Kenton J. Swartz.
NIH/NINDS, Bethesda, MD, USA.
Studies on voltage-activated potassium (Kv) channels show that modification of the surrounding lipids can alter channel function, raising the possibility that lipids interact directly with specific regions of Kv channels. We explored the interaction of lipids with S1-S4 voltage-sensing domains from different voltage-activated ion channels and voltage-sensing proteins, and used tarantula toxins that bind to S3b-S4 paddle motifs within the membrane to detect lipid-paddle interactions. We found that the conversion of sphingomyelin to ceramide-1-phosphate alters the gating and pharmacology of voltage-activated channels, and that the paddle motif determines the effects of lipid modification. We also found that mutations in two defined regions of the paddle motif weaken toxin binding to the paddle by disrupting lipid-paddle interactions. Our results show that lipids bind to voltage sensors and demonstrate that the pharmacological sensitivities of voltage-activated ion channels are influenced by the surrounding lipid membrane.

1639-Pos
Conformational Changes in Potassium Channel Voltage-Sensing Domains Reconstituted into Different Lipids
Dmitriy Krepkiy, Kenton J. Swartz.
NIH, Bethesda, MD, USA.
In the voltage-activated potassium channels, S1-S4 voltage-sensing domains control opening and closing of an associated pore domain. The S3b-S4 paddle motif within these domains moves at the protein-lipid interface to drive channel activation in response to changes in voltage. Electrophysiology experiments show that changes in the lipid composition significantly alters the energetics of voltage activation (Ramu, Y., 2006; Schmidt, D., 2006, 2009; Milescu, M., 2009). In particular, interactions between S4 Arginines and lipid phosphodiester groups have been proposed to be crucial for activation of voltage sensors; in the absence of the phosphodiesters, voltage sensors appear to be confined to the resting state. In order to define the structural basis of these interactions we purified the S1-S4 domain from KvAP and homogeneously reconstituted it in either a POPC:POPG (1:1) lipid mixture or DOTAP, a lipid without a phosphate group. Although the α-helical secondary structure is identical in these lipids as observed by circular dichroism spectroscopy, the fluorescence properties of single Trp70 in the middle of S2 helix is quenched when the S1-S4 domain is reconstituted into DOTAP. We investigated the chemical environment of the S3b-S4 paddle in different lipids by labeling a residue in the tip of the S3b-S4 paddle (Ala111Cys) with the fluorophore Bimane. The fluorescent properties of Bimane are significantly different upon reconstitution in DOTAP as compared to POPC:POPG lipid mixture. The relative fluorescence intensity of Bimane is two-fold higher in DOTAP compared to POPC:POPG, and in DOTAP, Bimane exhibits significant (~80 nm) Red Edge Excitation shift. These data suggest that there are changes in structure of S1-S4 reconstituted in different lipids, which might correspond to the conformational changes between resting and activated states. The work is in progress to characterize these changes by structural biology techniques.

1640-Pos
Divalent Cations are Antagonists of the Sodium-Dependent Potassium Channel Slo2.2
Gonzalo Budelli, Celia Santi, Alice Butler, Lawrence Salkoff.
Washington University in St. Louis, St Louis, MO, USA.
We studied the effect of different divalent cations on the Na^+-dependent potassium channel Slo2.2 (Slack) using inside-out patches from *Xenopus* oocytes and a Slack-HEK cell line heterologously expressing Slack channels. In the presence of intracellular sodium, the addition of divalent cations reduces significantly Slack currents recorded in macropatches. Among the divalent cations studied, the most effective in reducing channel activity was Cd^{++} followed by Ni^{++}, Ca^{++} and Mg^{++}. Several results suggest that this effect is not caused by blocking the pore of the channel. First, the decrease in currents is not voltage dependent as expected for a cation blocking the channel pore. Second, single channel recordings show a decrease in open probability but not a significant reduction in single channel conductance. Third, some of these cations activate rather than block the Ca^{++}-dependent channel Slo1, which is likely to have a pore structure similar to Slo2.2. Outside-out patches have been used to show that divalent cations do not have an inhibitory effect when applied to the extracellular side of the channel. We propose that the divalent cations may be competing with Na^+ for the Na^+ binding site. To test this hypothesis, we will examine the effect of divalent cations on several channel mutants and chimeras. These experiments also may help to reveal the structure and localization of the Na^+ binding site.

1641-Pos
Four and a Half Lim Domains (FHL) Genes Reduce Conductivity of the KCNA5 Channel
Ivana Poparic[1], Astrid Gorischek[2], Valerie Wagner[2], Klaus Wagner[1], Christian Windpassinger[1], Wolfgang Schreibmayer[2].
[1]Institute of Human Genetics, Medical University of Graz, Graz, Austria,
[2]Department of Biophysics, Medical University of Graz, Graz, Austria.
Myopathies are inherited muscle disorders characterized by weakness and atrophy of voluntary skeletal muscles, sometimes including the cardiac muscle. A phenotypically distinct, X-linked myopathy with postural muscle atrophy, termed XMPMA, has been recently described and linked to mutations in the *FHL1* gene. FHL1, a member of LIM-only proteins, is expressed in skeletal and cardiac muscle and suggested to play a role in sarcomere synthesis and assembly. Three splice variants (A, B and C) exist, which differ in expression pattern, binding partners and subcellular localization. A mutation found in a large XMPMA family (C224W) affects only isoforms A and B.
Aim of our study is to functionally characterize mutated FHL1 isoforms and their interaction with the voltage-gated potassium channel (KCNA5 or Kv1.5), which is involved in cardiac excitability. These interactions may partly explain the cardiac involvement within the clinical spectrum of XMPMA patients.
K^+ currents were recorded in Xenopus leavis oocytes injected with KCNA5 mRNA with or without coexpression of $FHL1A^{WT}$, $FHL1A^{C224W}$ or FHL1C. Upon coexpression of all three FHL1 proteins, K^+ current density was differently decreased, when compared to oocytes expressing KCNA5 alone. Kinetics of the channel was not affected. These results support the role of FHL1 as a key molecular component in regulation of expression of KCNA5. Future experiments will concentrate on colocalization and molecular interaction of FHL1 and KCNA5 in mammalian *in vitro* systems (HL1 cells).
Support by Graz Medical University ***Ph.D. programme*** and ***County of Styria*** (GZ: A3-16.R-10/2009-112).

1642-Pos

Identification of Regulatory Phosphorylation Sites in Slack and Slick Sodium Activated Potassium (K_{Na}) Channels

Matthew R. Fleming, Jack Kronengold, Yangyang Yan, Tukiet T. Lam, Erol E. Gulcicek, Fred J. Sigworth, Angus C. Nairn, Leonard K. Kaczmarek.
Yale University, New Haven, CT, USA.

Na^+-activated potassium channels (K_{Na} channels), which are encoded by the *Slack* and *Slick* genes contribute to neuronal adaptation during sustained stimulation, and, in auditory brainstem neurons, may regulate the accuracy of timing of action potentials. These channels have been found to be modulated very potently by activation of protein kinase C (PKC) and by receptors linked to activation of this kinase. Activators of PKC increase the amplitude of Slack-B currents and slow their rate of activation, and in contrast, activation of PKC decreases the amplitude of Slick currents. Heteromeric Slack/Slick channels are regulated by PKC to a greater extent than either Slack-B or Slick heteromers (90% decrease in amplitude). Previous experiments using Liquid Chromatography tandem Mass Spectrometry (LC-MS/MS) have identified three serine residues in Slack-B that are phosphorylated under basal conditions, but are not within consensus sites for PKC. In order to study the mechanisms of regulation of Slack and Slick channels by phosphorylation, we have begun to identify the specific residues that undergo phosphorylation by protein kinase C. Consensus sequence analysis predicts that there are 13 potential sites of possible PKC phosphorylation in the Slack-B sequence. We have constructed individual site mutants for each of these sites in which the serine/threonines have been mutated to alanines to prevent phosphorylation at these residues. These mutants were expressed in *Xenopus* oocytes and their response to a PKC-activating phorbol ester (TPA) was characterized by two-electrode whole cell clamp electrophysiology. Of the 13 consensus site mutants, only one generated currents that matched wild-type Slack-B currents in their amplitude and kinetic behavior, but completely failed to respond to application of TPA, suggesting that the phosphorylation state of a single residue regulates Slack-B current amplitude and rate of activation.

1643-Pos

Voltage Sensor Activation Facilitates Magnesium-Gated Channel Opening in BK Channels

Ren-Shiang Chen, Yanyan Geng, Karl L. Magleby.
University of Miami Miller School of Medicine, Miami, FL, USA.

Under physiological conditions, Mg^{2+} is an intracellular activator of Ca^{2+}- and voltage-activated potassium (BK) channels. To investigate gating by Mg^{2+} acting through its low affinity site located under each S4 voltage sensor (Yang et al. 2007, 2008; Horrigan & Ma 2008), we studied a BK channel in which the high affinity Ca^{2+} sites in both the RCK1 domain and the calcium bowl were disabled by mutation. Using single-channel recording from inside-out patches to measure channel activation after voltage steps from -100 mV to $+100$ mV, we found that 10 mM Mg^{2+} reduces the latency to first opening after the voltage step and increases channel activation through an increase in the number of openings per burst and mean open duration. This suggests that Mg^{2+} can bind to both closed and open states of the channel, but it is not clear whether the closed-state binding occurs at the negative or positive potential. Therefore we recorded single-channel activity in macro-patches held at a constant -50 or -100 mV. At -50 mV, when the voltage sensors are occasionally activated, 10 mM Mg^{2+} decreases the duration of the closed intervals between bursts of activity and increases burst duration through an increase in the number of openings per burst and mean open duration. At -100 mV, when the voltages sensors are mainly deactivated, 10 mM Mg^{2+} has little effect on the closed intervals between bursts or mean open duration, and most of the bursts are unitary, consisting of a single brief opening. The above data are consistent with a model in which Mg^{2+} can bind to the BK channel in the closed conformation when the voltage sensors are activated. The bound Mg^{2+} then facilitates opening. Supported by NIH grant AR32805.

1644-Pos

Zn2+ Activates Human Large-Conductance Ca2+-Activated K+ Channel

Shangwei Hou[1], Leif E. Vigeland[1], Guangping Zhang[2], Rong Xu[1], Min Li[3], Stefan H. Heinemann[4], Toshinori Hoshi[1].
[1]University of Pennsylvania, Philadelphia, PA, USA, [2]The University of Chicago, Chicago, IL, USA, [3]Johns Hopkins University, Baltimore, MD, USA, [4]Friedrich Schiller University Jena, Jena, Germany.

Zinc plays a crucial role as an integral structural and catalytic factor in many transcription factors and enzymes and this metal ion (Zn2+) is also increasingly recognized as a potential intracellular signaling molecule. However, the direct Zn2+ sensors especially those membrane localized are not fully established. Using inside-out patch clamp recording, we observed that heterologously expressed human large-conductance and voltage-and Ca2+-activated K+ (BKCa, Slo1 BK, or KCa1.1) channels were quickly and reversibly activated by intracellular Zn2+. Zn2+ did not affect the unitary conductance but significantly increased the channel open probability. Macroscopic current measurements showed that Zn2+-mediated activation of the channel was accompanied by a leftward shift of the conductance-voltage (G-V) curve by up to 75 mV. The effect of Zn2+ was antagonized by high concentrations of intracellular H+ or Ca2+, indicating the three factors activate BK channels via a common mechanism. Mutagenesis experiments showed that mutation of H365 to arginine, a critical residue for the channel activation by H+ and Ca2+, fully abolished the effect of Zn2+. In addition, mutation of two other nearby acidic residues D367 or E399 to alanine also partially impaired the effect of Zn2+. Collectively, our results suggest that a novel multifunctional structure located in the regulator of conductnace for K+ (RCK)1 domain is involved in Zn2+ coordination and activation of the Slo1 BK channel and indicate a potential role of Slo1 BK channel in Zn2+ signaling in both physiological condition and hypoxic/ischemic diseases in which [Zn2+]i is significantly increased. (Supported in part by NIH)

1645-Pos

Molecular Determinants For hSlo1 Bk Channel Activation by Dihydroabietic Acid Derivatives

Guido Gessner[1], Yong-Mei Cui[2], Yuko Otani[2], Tomohiko Ohwada[2], Toshinori Hoshi[3], Stefan H. Heinemann[1].
[1]Center for Molecular Biomedicine, Dept. Biophysics, FSU Jena, Jena, Germany, [2]Graduate School of Pharmaceutical Sciences, University of Tokyo, Tokyo, Japan, [3]Department of Physiology, University of Pennsylvania, Philadelphia, PA, USA.

Large-conductance calcium- and voltage-activated potassium (BK) channels are key players in vasoregulation and in the control of neurotransmitter release. Use of an alternative exon9 results in a neuronal variant of BK channels (e9alt) with altered amino acid sequence extending from the middle of S6 to a cytosolic linker connecting to the RCK gating ring (C-linker of 14 residues). hSlo1 wild-type (e9), splice variant and mutant channels were heterologously expressed in HEK 293 cells and analyzed in inside-out patches. Channels were characterized with respect to activation by transmembrane voltage, intracellular calcium and dihydroabietic acid derivatives (DHAAs). diCl-DHAA, triCl-DHAA and Cym04 (10 μM, Cui et al. (2008) Bioorg Med Chem Lett 18:6386-6389) were found to activate e9 channels via shifting their voltage dependence by up to ~40 mV to hyperpolarized potentials in the virtual absence of calcium. In contrast, e9alt channels did not exhibit a left-shift in activation. The most active compound, Cym04, was used to identify the molecular determinants for BK activation by DHAAs by mutagenesis. Differences between e9 and e9alt in calcium- and voltage-dependent gating are brought about by residues within S6 and in the C-linker. In contrast, molecular determinants for activation by Cym04 reside in the C-linker: of the 10 residues differing between e9 and e9alt, amino-acid exchanges G327L, K330N, S337N and S340G had a high impact on channel activation by Cym04. Mutation S340G almost completely abolished BK activation by Cym04 without markedly changing calcium- and voltage-dependent gating. The linker connecting the RCK gating ring and the pore of BK channels therefore represents a candidate region for binding DHAA-type, isoform-specific BK channel activators.

1646-Pos

An Epilepsy-Associated Mutation Enhances BK Channel Activity by Altering the Coupling of Calcium Sensing to Gate Activation

Junqiu (Alex) Yang[1], Gayathri Krishnamoorthy[1,2], Akansha Saxena[1], Guohui Zhang[1], Jingyi Shi[1], Huanghe Yang[1], Kelli Delaloye[1], David Sept[3], Jianmin Cui[1].
[1]Washington University in St. Louis, Saint Louis, MO, USA, [2]Case Western Reserve University, Cleveland, OH, USA, [3]University of Michigan, Ann Arbor, MI, USA.

Voltage and Ca^{2+} activated BK channels modulate neuronal activities. Previous studies found that Ca^{2+} binding sites and the activation gate are spatially separated, but how Ca^{2+} binding couples to gate opening is not clear. We address this question by studying how a mutation in BK channels, which is associated with generalized epilepsy and paroxysmal dyskinesia (D434G in hSlo, the epilepsy mutation), enhances Ca^{2+} sensitivity. The epilepsy mutation is located in a structural domain (the AC region) that connects the S6 transmembrane segment with the cytoplasmic domain and close to a putative Ca^{2+} binding site. Mutagenesis studies show that the AC region is important in the coupling between Ca^{2+} binding and gate opening. We found that discrete locations in the AC region that are distant from the epilepsy mutation alter the functional effects of the mutation. Thus, the epilepsy mutation enhances Ca^{2+} sensitivity by an allosteric mechanism affecting the coupling between Ca^{2+} binding and gate opening. Interestingly, mutating the Asp residue to

amino acids other than Gly does not result in the same phenotype as the epilepsy mutation, suggesting that a change in protein flexibility is involved in the effects of the mutation. Consistent with this result, altering the flexibility of the channel protein by changing viscosity of the intracellular solution also modulates Ca^{2+} sensitivity; and the epilepsy mutation reduces such modulation, possibly because it has already altered the flexibility. These results are consistent with a model that the peptide loop where the putative Ca^{2+} binding site and the epilepsy mutation are located acts as a spring-hinge for the conformational change of the AC region during channel opening; Ca^{2+} binding and the epilepsy mutation affect channel gating by altering the function of this spring-hinge.

1647-Pos
Regulation of Drk1 Channels by Carbon Monoxide and Carbon Monoxide-Releasing Molecule-2

Andres Jara-Oseguera, Gisela E. Rangel-Yescas, Leon D. Islas.
National Autonomous University of Mexico, Mexico City, Mexico.

Carbon monoxide is a poisonous gas that is also syntethized in several tissues in the body, where it acts as a signaling molecule. CO has been shown to regulate ion channels such as voltage-dependent calcium channels (VDCC) and large-conductance calcium-activated potassium (BK) channels, a mechanism which is important for oxygen sensing in the carotid body. The Kv2.1 channel has been implicated with oxygen sensing in the pulmonary arteries and the ductus arteriosus, a process which may be regulated by carbon monoxide. We therefore investigated the effects of carbon monoxide and tricarbonyl dichlororuthenium dimmer (CORM-2), a widely used carbon monoxide releasing molecule, on the Kv2.1 channel. We found that, unlike with VDCC and BK channels, CORM-2 does not have the same effect as carbon monoxide: CO does not have an effect on the channel, while CORM-2 acts as an intracellular allosteric inhibitor of channel function. CORM-2 slows channel activation and deactivation kinetics by reducing the voltage-dependence of the rate constants. It also reduces overall open probability without affecting steady-state voltage-dependence. Manganese-decacarbonyl, another carbon-releasing molecule also does not have an effect on the Kv2.1, while ruthenium red seems to have biphasic effects, one mimicking the action of CORM-2 on the channel and the other representing voltage-dependent pore block, which suggests that CORM-2's actions on the Kv2.1 are independent from its CO-releasing properties.

1648-Pos
Mechanism of Kv1 Channel Redox Modulation by Kvβ

Yaping Pan, Jun Weng, Ming Zhou.
College of Physicians and Surgeons, Columbia University, New York City, NY, USA.

The *Shaker* type voltage-dependent K^+ channels (Kv1) are expressed in a wide variety of cells and essential to regulating membrane potential and cellular excitability. All Kv1 channels assemble with cytoplasmic β subunits (Kvβ) to form a stable complex. Kvβ is an aldo-keto reductase that utilizes NADPH as a cofactor, and certain Kvβs have an N-terminal segment that blocks the channel by the N-type inactivation mechanism. The enzymatic activity and channel inactivation are functionally coupled: when the Kvβ1-bound NADPH is oxidized, the N-type inactivation is inhibited and, as a result, current increases. To understand the molecular basis of the coupling, we first focused on the N-terminal segment of Kvβ1 that induces channel inactivation. We have identified a stretch of amino acid residues from the N-terminus that are required for redox modulation, which we define as the Redox Regulation Sequence (RRS). Based on our studies, we found that it is likely that the RRS binds directly to the aldo-keto reductase core of Kvβ. To test this hypothesis, and to eventually construct a mechanism for redox modulation, we have started to identify regions on the AKR core that may serve as the ''receptor site'' for the RRS. Initial mutational studies have identified a candidate receptor site, and structural and biochemical studies will further examine how the physical interaction is achieved, and how the interaction is dependent on the redox state.

1649-Pos
Quantifying the Absolute Number of Voltage Gated EGFP Tagged Ion Channels by Fluorescence Intensity Measurements

Claudia Lehmann, Hansjakob Heldstab, Tamer M. Gamal El-Din, Nikolaus G. Greeff.
University of Zurich, Zurich, Switzerland.

In the past, much work has been done to evaluate the gating charge, q, of single voltage gated K+ or Na+ channels. A figure of about 13 e is generally accepted for K+ channels. For Na+ channels, the figure of q estimated by various methods, is less well established and ranges from 5 to 15 e. Recently, we determined the gating charge of single Na+ channels indirectly to be about 6 e by applying our newly determined ratio of q K+ /q Na+ $= 2.5 \pm 0.4$ (Gamal El-Din et al. 2008) and assuming 13 e for q K+. Hereby we used the total fluorescence intensity of EGFP tagged channels expressed in X. laevis oocytes as a measure for the relative number of ion channels and correlated it to the total gating charge, Q.
Currently, we develop a more direct method to estimate the total number of ion channels per oocyte. Analysis of microscopic images of oocytes has been done according to Gamal El-Din et al. (2008). In addition, calibration of EGFP fluorescence intensity with EGFP solutions was done in a hemocytometer. Additional refinements for several correction factors have been tested to obtain reliable absolute numbers of ion channels: Especially the attenuation of the fluorescence from fluorophores at circumferential areas of the oocyte compared to those from frontal areas was taken into account. To obtain a measure of the attenuation factor we used oocytes homogeneously labeled with an extrinsically fluorescent dye and compared the total fluorescence intensity, extrapolated from cirumferential areas, with those extrapolated from frontal areas. Transfer of the attenuation factor of extrinsically labeled oocytes to the instrinsically EGFP labeled oocytes is being discussed and labeling profiles are shown.

1650-Pos
Voltage Clamping a Supported Bilayer

Homer C. Hyde, **Minh D. Nguyen**, Francisco Bezanilla.
The University of Chicago, Chicago, IL, USA.

Supported bilayer has many advantages over conventional black lipid bilayer. A supported bilayer is highly stable and can be made with a large surface area. Membrane proteins can be incorporated in very large numbers without disruption of the bilayer, thereby allowing robust macroscopic recordings. A very important advantage is that incorporated proteins are immobile. This lack of mobility is essential for the study of conformational changes with single molecule fluorescence. We are interested in studying gating charge movement and conformational changes in voltage dependent membrane proteins such as a voltage dependent K+ channel. For this purpose, we have developed an essentially electrostatic voltage clamp system for a supported bilayer that allows measurement of intramembrane transient currents but not DC currents. The supported bilayer is formed by liposome fusion on top of a semiconductor substrate that serves as the reference electrode. Electrolyte solution is present above the bilayer where an Ag/AgCl electrode serves as the active electrode. The electrode pair is connected to conventional voltage clamp electronics that imposes the voltage and measures the current. We verified supported bilayer formation by the decrease of the total capacitance. Furthermore, we have verified that a voltage is imposed across the bilayer by using voltage dependent fluorescent membrane probes. The electrolyte/supported bilayer/electrode system is essentially linear across a voltage range of −300 to +300 mV. We have seen that direct incorporation of the voltage dependent protein KvAP into the supported bilayer modifies the kinetics of the transient currents as well as the voltage dependence of charge movement. This method opens the possibility for studies of simultaneous gating charge movement electrically and voltage dependent conformational change spectroscopically in purified membrane proteins.
Support: NIH GM030376.

1651-Pos
Validation of Automated Patch-Clamp Instrumentation Competency for Herg Channel Liability Detection in Lead Optimization Programs

Arturo Picones, Kendra Kim.
Exelixis, Inc., South San Francisco, CA, USA.

Avoidance of HERG Channel liability is an established regulatory requirement given its capabilities in predicting acquired Long-QT Syndrome, a cardiopathology which may lead to life threatening arrhythmias (Torsade de Points). The sensitivity and precision of patch-clamp electrophysiology, the gold standard in HERG safety pharmacology, have been expanded into the high throughput necessities of the drug discovery industry. This report presents results obtained in the early detection of possible HERG liabilities within

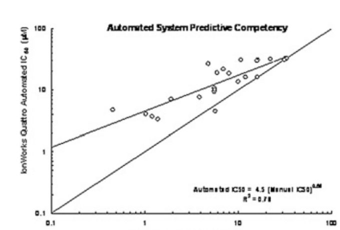

lead optimization programs at Exelixis. Whole-cell recordings from an in-house developed cryopreserved CHO cell line heterologously expressing HERG channels were obtained with IonWorksQuattro™. Ion channel expression was unaltered for >10 months (>400 pA/well). Only population patch-clamp wells with seal test >25 MΩ and peak tail currents >100 pA were selected for analysis. Success rates consistently obtained were >90%. Pharmacological analysis, characterized by automated IC50 determinations, were compared with equivalent studies performed with a Giga-Ω seal manual patch-clamp system to evaluate the predictive competency of the automated instrumentation and then validate its effective impact on quantitative SAR analysis for the selection and prioritization of lead compounds, avoiding potential QT prolongation liabilities at early stages.

1652-Pos
Electrostatic Tuning of Cellular Excitability
Sara I. Börjesson[1], Teija Parkkari[2], Sven Hammarström[1], Fredrik Elinder[1].
[1]Linköping University, Linköping, Sweden, [2]Kuopio University, Kuopio, Finland.
Voltage-gated ion channels regulate the electric activity of excitable tissues like the heart and the brain. Therefore, treatment for conditions of disturbed excitability is often based on drugs that target ion channels. Traditional ion-channel drugs aim at plugging the ion-conducting pore. We instead propose a novel pharmacological mechanism for how to regulate channel activity by targeting the voltage sensor of voltage-gated K channels. By studying the effect of different free fatty acids and fatty acid derivatives we show that charged lipophilic substances can tune channel opening and consequently excitability by an electrostatic interaction with the channel. Polyunsaturated fatty acids shift the voltage dependence of activation of the Shaker K channel in hyperpolarizing direction. The negative carboxyl charge is crucial for the effect. A positively charged arachidonic acid derivative (arachidonyl amine) was synthesized and shown to instead shift the voltage dependence in depolarizing direction. Thus, the direction of the effect on the channel's voltage dependence is determined by the charge of the substance. Uncharged methyl esters of polyunsaturated fatty acids do not affect the voltage dependence. Computer simulations of membrane excitability demonstrate that small changes in the voltage dependence of Na and K channels have prominent impact on excitability and the tendency for repetitive firing. For instance, a shift in the voltage dependence of a K channel with −5 or +5 mV corresponds to a three-fold increase or decrease in K channel density, respectively. We suggest that electrostatic tuning of ion channel activity can be a new and powerful pharmacological approach to affect cellular excitability.

1653-Pos
Arming Antibodies for Subtype-Selective Photo-Inhibition of Voltage Gated Potassium Channels
Jon T. Sack[1,2], Nick Stephanopoulos[3], James S. Trimmer[1].
[1]University of California, Davis, CA, USA, [2]Institute for Design of Intelligent Drugs, Protean Research, Palo Alto, CA, USA, [3]University of California, Berkeley, CA, USA.
Establishing the molecular identity of native voltage-gated potassium (Kv) channels has been a particularly challenging problem. Mammalian Kv channels arise from a family of more than 40 genes and few inhibitors are selective for any one Kv subunit type. The identification of channel types underlying native ionic currents has been greatly aided by the availability of subtype specific inhibitors, but drugs of great selectivity have not yet been discovered for most Kv subunits. There exist, however, extensively characterized monoclonal antibodies against extracellular S1-S2 linker epitopes that exhibit clear specificity for Kv4.2, Kv2.1 or Kv1.1. Unfortunately, none of these antibodies have been found to inhibit channel currents.
A proven strategy for targeted inhibition of proteins is to label antibodies with chromophore ''warheads'' that induce oxidative damage to the target protein upon illumination. Photo-stimulation of certain chromophores leads to the generation of singlet oxygen, which has a 40 Å half-maximal radius of oxidative damage, suitable to oxidize the protein target when conjugated to an antibody. Porphyrins are amongst the most efficient photo-induced generators of singlet oxygen known, having greater extinction coefficients, lower sensitivity to photobleaching, and higher quantum yields for singlet oxygen than compounds, such as fluorescein, classically used for targeted photo-inhibition of proteins. We have synthesized a series of porphyrin derivatives that irreversibly inhibit Kv4.2 or Kv2.1 currents upon illumination. Covalent attachment of porphyrin to an anti-Kv4.2 antibody has resulted in selective inhibition of Kv4.2 at a 10 nM concentration. By attaching warheads to subtype-selective antibodies, we aim to find a serial solution to the problematic dearth of subunit-specific Kv inhibitors.

Anion Channels

1654-Pos
Cholesterol Depletion Facilitates Recovery from Hypotonic Cell Swelling of CHO
Gregory Kowalsky[1], Derek Beam[2], Frederick Sachs[3], Susan Hua[4], **Irena Levitan**[1].
[1]University of Illinois at Chicago, Chicago, IL, USA, [2]Analytical Instruments, Reichert, Bufallo, NY, USA, [3]University of Bufallo, Bufallo, NY, USA, [4]University of Bufallo, Bufallo, NY, USA.
The maintenance of cell volume homeostasis prevents pathological cell swelling that can lead to severe cellular dysfunction or death. A key step in maintaining cell volume in many cell types is activation of volume-regulated anion channels (VRAC). Our earlier studies showed that activity of VRAC is facilitated by a decrease in cellular cholesterol (Levitan et al 2000). These observations suggest that lowered cholesterol should also facilitate regulatory volume decrease (RVD), a process used by cells to recover from hypotonic swelling. The main constraint in testing this prediction, however, has been the lack of adequate methods to rapidly and reproducibly measure changes in cell volume of substrate-attached cells. In this study, we address this question using a novel microfluidic methodology from Reichert Inc. (CVC-7000), to measure cell volume response to hypotonic challenges (30% osmotic gradient) in real time. Cholesterol depletion facilitated the recovery from swelling via a more rapid onset of RVD (~130 s vs. 215 s in control and cholesterol depleted cells, respectively) and a higher degree of volume recovery after 10 min (41% ± 6% vs. 65% ± 6% in control and cholesterol depleted cells, respectively). In contrast, enriching the cells with cholesterol had no effect on RVD. These observations are consistent with our previous studies showing that while cholesterol depletion increases cell stiffness, cholesterol enrichment has no effect (Byfield et al 2004). These observations suggest that cholesterol depletion, and the consequent increase in cell stiffness, facilitates RVD by enhancing the activity of VRAC.

1655-Pos
Expression and Novel Function of Bestrophin-2 in Goblet Cells in Mammalian Colon
Kuai Yu.
Emory University, Atlanta, GA, USA.
Anion channels and transporters in the gastrointestinal epithelium play essential roles in fluid secretion and absorption and participate in regulating the pH and ionic composition of the gut luminal contents. Diarrheas produced by bacterial enterotoxins such as cholera and rotavirus are associated, respectively, with activation of two kinds of Cl- channels, the cystic fibrosis transmembrane conductance regulator (CFTR) and Ca2+-activated Cl- channels (CaCCs). Although the roles and mechanisms of CFTR are relatively well understood, CaCCs have remained enigmatic partly because their molecular identity has remained in question. Here we have investigated the role of bestrophin-2, a candidate CaCC protein, in colon using a mouse knockout model. Best2-/- knockout mice exhibit a greatly reduced amplitude of cholinergic (Ca2+)-stimulated anion secretion, consistent with Best2's potential role as a CaCC. However, unexpectedly, Best2 is expressed in the basolateral membrane of mucin-secreting colonic goblet cells and not in the apical membrane of colonocytes as predicted if it was a CaCC. Analysis of the cholinergically-stimulated anion secretion revealed that a large fraction of the current was carried by HCO3-, was unaffected by CFTR blockers, and was carried by Best2 channels. Whole cell patch clamp analysis of isolated colonocytes revealed two kinds of Ca2+-activated Cl- channels, currents with linear I-V relationships carried by Best2 and reduced in the knockout and outwardly-rectifying currents that resemble currents carried by TMEM16A, another candidate CaCC protein that is expressed on the apical membrane of surface colonocytes and is probably involved in Cl- absorption. These results provide a new perspective on cholinergic regulation of colonic secretion and may have relevance to colitis and inflammatory bowel disease, two diseases that exhibit defective anion transport. Further, they provide new insights into the functions of the enigmatic bestrophin family of anion channels.

1656-Pos
TMEM16A is Expressed in Vascular Tissues that Display Robust Calcium-Activated Chloride Currents
Alison J. Davies[1], **Abigail S. Forrest**[2], Thomas A. Jepps[1], William Sones[1], Rajesh Raghunathan[2], Iain A. Greenwood[1], Normand Leblanc[2].
[1]St Georges University of London, London, United Kingdom, [2]University of Nevada Reno, Reno, NV, USA.
Calcium activated chloride (Cl_{Ca}) channels are an important contractile mechanism in smooth muscle cells. Activation of these channels by calcium (Ca^{2+}) ions leads to Cl^- efflux and membrane depolarization. This depolarization then favors the activation of voltage-gated Ca^{2+} channels (e.g. L-type), providing a positive feed-back loop that allows for sustained contraction.

The molecular candidate encoding for this channel has remained elusive, although a number of suggestions have been investigated. The latest contender to emerge is TMEM16A (Anoctamin). Evidence so far confirms that over-expression of TMEM16A generates Cl^- currents with the same time-dependent kinetics and Ca^{2+} sensitivity as recorded through Cl_{Ca} channels in smooth muscle cells.
This study investigated expression profiles of TMEM16A in a number of vascular tissues across a number of species. The aim of this study was to confirm the role of TMEM16A as a potential candidate encoding for Cl_{Ca} currents (I_{ClCa}) in native vascular myocytes.
Smooth muscle cells were enzymatically isolated from the mouse portal vein (PV), aorta and carotid artery (CA), rat pulmonary artery (PA), and the rabbit PA. Robust I_{ClCa}, exhibiting distinctive voltage-dependent kinetics, were recorded from all of the tissue preparations mentioned.
RT-PCR was performed, using species-specific primers designed against the available sequences for TMEM16A. Mouse aorta, PA, CA and PV, rat aorta, PA and PV, and rabbit PA tissues were studies. All samples showed clear expression of TMEM16A.
Immunocytochemistry revealed specific expression of TMEM16A in rat PA, and mouse PV, CA and aorta isolated myocytes. This was apparent throughout the cytoplasm, with punctuate ''hotspots''. Western blot analysis showed bands of the expected molecular weight in mouse aorta, PV and CA.
In summary, we have demonstrated that TMEM16A is a viable candidate for the encoding of Cl_{Ca} channels in vascular smooth muscle.

1657-Pos
TMEM16A is a Calcium-Activated Chloride Channel in Pulmonary Artery Smooth Muscle Cells
Tammaro Paolo, Boris Manoury.
University of Manchester, Manchester, United Kingdom.
Calcium-activated chloride channels (CaCCs) play pivotal roles in many physiological processes. In vascular smooth muscle, activation of these ion channels by agonist-induced Ca^{2+} release provokes membrane depolarisation, increased Ca^{2+} entry through L-type Ca^{2+} channels and ultimately vasoconstriction. The molecular identity of vascular CaCCs is not fully understood. Here we present evidence that TMEM16A (or Anoctamin1), a member of the transmembrane 16 (TMEM16) protein family forms CaCCs in pulmonary artery smooth muscle cells (PASMCs). Patch-clamp analysis in acutely isolated PASMCs revealed strongly outward rectifying Ca^{2+}-activated Cl^- currents which activated slowly at positive potentials and showed large deactivating tail currents upon repolarisation, very similar to heterologous TMEM16A currents (Caputo *et al*. (2008) *Science* 322, 590-594; Yang *et al.* (2008) *Nature* 455, 1210-1215; Schroeder *et al.* (2008) *Cell* 134, 1019-1029). High levels of TMEM16A mRNA were identified in rat pulmonary arteries and various other vascular smooth muscle cell types. Downregulation of TMEM16A gene expression in primary cultured PASMCs, with small interfering RNA, was accompanied by almost total loss of whole-cell CaCC currents. Our data suggest that TMEM16A forms calcium-activated chloride channels in rat pulmonary artery smooth muscle.

1658-Pos
Regulation and Gating of mAno1 by Voltage and Calcium
Qinghuan Xiao, Kuai Yu, Yuanyuan Cui, H Criss Hartzell.
Emory University, Atlanta, GA, USA.
Ca-activated chloride channels play important roles in epithelial secretion, regulation of vascular tone, control of membrane excitability, olfactory transduction, and photoreception. Recently, Ano1 (TMEM16a) has been identified as a Ca2+-activated chloride channel. Activation of Ano1 exhibits both Ca2+- and voltage- dependence. However, the structures and mechanisms responsible for Ca2+- and voltage-dependent activation remain unknown. mAno1 exhibits a strong outward rectification at <0.5 μM Ca2+ concentration with little inward current. As Ca2+ concentration is increased, inward current increases. We hypothesized that Ano1 has two Ca2+ binding sites, a high affinity site that controls the outward current and a low affinity site that controls inward current. We further hypothesized that a region in the first intracellular loop characterized by five contiguous glutamates (444EEEEE448) was the potential high-affinity Ca2+ sensor. To test this, HEK-293 cells were transfected with wild type mAno1 and mutants in the region surrounding the five glutamates and studied by whole cell and inside-out excised patch recording. In the absence of intracellular Ca2+, wild type mAno1 could be activated by very strong depolarizations ($> +100$ mV). In the presence of Ca2+, the G-V relations were well fit with the Boltzmann equation. V1/2 was 73 mV at 10 μM intracellular free Ca2+. Increasing Ca2+ shifted the G-V relation to the left. We mutated the putative Ca2+ binding site by deleting the last glutamate of the cluster plus the 3 trailing amino acids (del448EAVK451), substituting the first four glutamates with alanines (444EEEE/AAAA447), and substituting of each negatively charged amino acid with alanine. These mutations altered both voltage-dependent and Ca2+-dependent gating of the channel in complex ways that are consistent with this region being an integral component of Ca2+ dependent gating of the channel.

1659-Pos

WITHDRAWN.

1660-Pos
The Preference of the CLC-0 Pore for Charged Methanethiosulfonate Reagents
Xiao-Dong Zhang, Wei-Ping Yu, Tsung-Yu Chen.
University of California, Davis, CA, USA.
Previous experiments from our laboratory showed that the negatively-charged methanethiosulfonate (MTS) reagent, 2-sulfonatoethyl MTS (MTSES) modified a cysteine residue at the Y512 position of CLC-0 faster than the positively-charged 2-(trimethylammonium)ethyl MTS (MTSET). This observation suggested a hypothesis that the pore of CLC-0 may be built with a positive intrinsic pore potential. The hypothesis, however, is challenged by our most recent finding that the preference for the negatively charged MTS reagent is significantly reduced when the cysteine is placed at a deeper pore position, E166. In this study, we examine the discrepancy in the preference for charged MTS reagents between the Y512C and E166C mutants. We find that the inhibition of E166C by intracellularly-applied MTS reagents is contaminated by the modification of an endogenous cysteine because MTS modification rates of the E166A and E166C mutants are similar to each other. We identify that C229, which is located at the dimer interface of the channel, is the endogenous cysteine responsible for this contamination. After C229 is mutated, CLC-0 resumes a preference for selecting the negatively-charged over the positively-charged MTS reagents in modifying E166C, re-confirming the idea of a positive intrinsic potential in the pore. Our study also suggests a communication between the pore region near E166 and the dimer interface near C229 because the inhibition of the channel due to the modification of C229 is dependent upon the amino acid placed at position 166.

1661-Pos
Regulation of the Chloride/Proton Exchanger CLC-5 By Internal pH
Matthias Grieschat, Christoph Fahlke, **Alexi K. Alekov**.
Med. Hochschule Hannover, Hannover, Germany.
ClC-5 transports anions and protons across intracellular membranes and is necessary for endosomal/lysosomal acification. Similar to other ClC transporters, ClC-5 can switch between two different transport modes and operate either as anion-proton exchanger or as anion channel, depending on the type of external anion. So far, only some regulatory mechanisms that affect the functional mode of these transporters have been described. We here use combined whole-cell patch clamp and fluorescent intracellular pH recordings in transfected tsA201 cells to characterize ClC-5 mediated transport under various ionic conditions. Asymmetric lowering of intracellular pH results in small increases of both total and proton current amplitudes that might be well explained by changes in the electrochemical gradient imposed by such a maneuver. With internal Cl^--based solution (pH 7.4) exchange of external Cl^- with SCN^- results in ~5-fold increase in total ClC-5 currents at positive voltages. At higher internal proton concentration (pH 6) the same change of external anion composition results in a 70-fold increase in total currents. The voltage dependence of channel opening is not significantly altered, excluding shifts of the activation curve as a mechanistic explanation. For mutant ClC-5 lacking the ''proton glutamate'', E268H ClC-5, the simultaneous effect of internal protons and external SCN is significantly less pronounced. These findings imply that acidic internal pHs change the protonation state of the proton glutamate and promote the action of external uncoupling anions. In addition, they imply that ClC-5 might even mediate uncoupled anion transport at physiological anion compositions. ClC exchangers may utilize part of the proton electrochemical driving force between the intra/extravesicular sites of intracellular compartments to establish anion concentration gradients. The described effects of intracellular pH might be an important part in this pathway and contribute to regulation of endosomal/lysosomal physiological function.

1662-Pos
Alteration of Extracellular pH Dependence of CLC-5 By Modifications of Two Conserved Charged Residues
Giovanni Zifarelli, **Michael Pusch**.
Istituto di Biofisica, Genoa, Italy.
The endosomal Cl(-) / H(+) antiporter, ClC-5, is inhibited by low extracellular pH. This could be caused by the saturation of a titratable residue which is directly involved in proton translocation towards the extracellular solution; alternatively, the reduction of currents at low pH could reflect an unspecific electrostatic effect of some titratable residue on proton and / or chloride movement within the external vestibule. To gain insight into the mechanism of the pH dependence we investigated the possible involvement of two highly conserved charged residues (D76 and K210) which are located in the extracellular vestibule. Mutants D76G and D76H drastically altered pH dependence. Preliminary experiments indicated that also K210C slightly altered the pH dependence. Interestingly, the K210C mutant could be modified by pCMBS (p-chloromercuriphenylsulfonic acid): application of 100 μM pCMBS led to a partial and irreversible inhibition of K210C mediated currents (but not WT ClC-5 currents). Our results favor the idea that neither D76 nor K210 are directly involved in proton translocation. However, further experiments, exploiting the possibility to modify K210C with various cysteine modifying reagents, are necessary to draw such a firm conclusion.

1663-Pos
Role of the Q-R Linker in H^+/Cl^- Coupling in a CLC Exchanger
Christopher Hills, **Sophie Bruce**, Alessio Accardi.
University of Iowa, Iowa City, IA, USA.
Members of the CLC family function as Cl^- channels or as H^+/Cl^- exchangers. Despite this mechanistic divide the two CLC sub-classes share many functional and structural traits. CLC-ec1, a transporter, can be transformed into a Cl^--selective pore by simultaneously removing the intra- and extra-cellular gates. This entailed mutating two residues, E148 and Y445, which are conserved in both CLC channels and transporters. While the extracellular gate regulates channel gating, the intracellular one does not. We hypothesized that in the channels the intracellular gate's position is shifted so that it does not regulate ion passage anymore.
The linker connecting helices R and Q is 1-2 amino-acids shorter in the channels than in the transporters. We investigated whether shortening this linker disrupts the intracellular gate of CLC-ec1 while preserving Y445. To this end we deleted two residues, G441 and K442, in the Q-R linker. This deletion, ΔGK, functionally mirrors the gate-removed Y445A mutant: H^+ transport is nearly abolished with slight effects on Cl^- transport. We then tested the effects of single-residue deletions. The ΔG mutant is similar to the WT while the ΔK deletion impairs H^+ transport like the ΔGK deletion. K442 however is not involved in H^+ transport: Alanine or Methionine substitutions have no significant effects.
Lastly, we incorporated in CLC-ec1 increasing portions of the CLC-0 channel. Introduction of the CLC-0 Q-R linker into CLC-ec1 recapitulates the functional effects of the ΔGK and ΔK mutations. Introduction into CLC-ec1 of up to the full helix R from CLC-0 led to no further effects on H^+ transport.
In conclusion we found that the length of the Q-R linker is critical for H^+/Cl^- coupling in CLC-ec1 while the chemical properties of the residues in the linker do not seem to matter.

1664-Pos
Proton Block of Human CLC-5 Cl^-/H^+ Exchanger
Alessandra Picollo, Mattia Malvezzi, Alessio Accardi.
University of Iowa, Iowa City, IA, USA.
CLC-5 is a human Cl^-/H^+ exchanger of the CLC family. It is expressed in intracellular compartments such as endosomes, where it regulates their acidification and is indirectly involved in the re-uptake of small molecular weight proteins in renal proximal tubule. Mutations in the CLC-5 gene lead to Dent's disease, a human disorder characterized by low molecular-mass proteinuria, kidney stones and renal failure. CLC-5 currents are strongly outwardly rectifying suggesting that the rates in the transport cycle are highly asymmetrical so that Cl^- influx and H^+ efflux is permitted while the converse is not. Additionally CLC-5 currents are strongly inhibited by low external pH. It has been proposed that the rectification arises from the voltage dependence of a H^+ transport step and that the pH dependence is a result of a reduction in the total driving force for turnover. We studied the extracellular pH dependence of CLC-5 currents between pH 9 and 4.5. We found that the pH dependence is not solely due to changes in the driving force. Rather, we found that the degree of current inhibition is voltage dependent: at less positive potentials H^+ inhibition becomes stronger. This is consistent with a direct modulation of CLC-5 activity by H^+ at a single site located ~70% deep into the electric field. We propose that this site is E211, the extracellular gating glutamate. In the presence of extracellular SCN^- H^+ transport is abolished but both rectification and H^+ inhibition remain largely unaltered. This suggests that H+ transport determines neither the pH dependence nor rectification. We propose that the extracellular pH inhibition of CLC-5 currents arises from H^+ trying to drive the transport cycle in the non-permissive direction. In other words, inhibition of the CLC-5 currents by extracellular H+ is a consequence of its rectification.

1665-Pos
A Monomeric Variant of the CLC-ec1 Transporter
Janice L. Robertson, Ludmila Kolmakova-Partensky, Christopher Miller.
HHMI/Brandeis University, Waltham, MA, USA.
CLC-ec1, a prototypical Cl-/H+ exchanger of the CLC family, is a homodimer in which each subunit is thought to act as a fully functional transporter. Why then is this protein a dimer and what are the factors driving dimer formation? In this study, we address these questions by destabilizing the CLC-ec1 subunit-subunit interface. We substituted tryptophan residues to create steric mismatches at the interface that would also favor lipid interactions. A single mutation, I422W, was sufficient to destabilize the CLC-ec1 complex resulting in a shift from dimer to monomer position on gel-filtration chromatography. Glutaraldehyde cross-linking of I422W in both detergent and phosphatidyl-choline/phosphatidyl-glycerol liposomes showed that the mutant remained a monomer compared to the wild-type protein; however dimer formation was observable at high concentrations. The I422W mutant was functional as measured by 36Cl- uptake, passive Cl- efflux and Cl- driven H+ pumping in E. coli phospholipids. A Poisson-counting method demonstrated that I422W re-dimerizes in these phosphatidyl-ethanolamine-rich liposomes, even at very low protein/lipid ratio. Altogether, these findings suggest that we have purified an isolated monomeric variant of CLC-ec1 that demonstrates shifted dimerization energetics depending on the lipid environment. We continue to search for mutations that will more severely destabilize the dimer, in attempts to obtain a transport-competent, monomeric CLC exchanger.

1666-Pos
Analysis of the CLC-1 ATP Binding Site by Structure-Guided Mutagenesis
Pang-Yen Tseng, Tsung-Yu Chen.
Center for Neuroscience, University of California, Davis, Davis, CA, USA.
The CLC-1 chloride channel is abundantly expressed on the cell membrane of skeletal muscles, and thus plays an important role in controlling the muscle excitability. We previously showed that ATP can modulate the common gating of CLC-1, presumably by binding to a potential binding site at the C-terminal cytoplasmic region of the channel. The X-ray crystallographic study by others revealed the structure of the ATP-binding site, and two residues, Y617 and D727, were identified to be important for the ATP binding. Based on the CLC-5 C-terminal structure, we identify that besides V634 and E865 of CLC-1 (corresponding to Y617 and D727 of CLC-5), V613 and E860 are also important for the ATP modulation of the CLC-1 common gating. Mutating V634 to either alanine or aspartate abolishes the ATP modulation effect. Surprisingly, mutations of V634 to aromatic amino acids increase the ATP affinity: V634F and V634Y mutations decrease the apparent K1/2 by ~30- and ~13-fold, respectively. Mutations of E865 to alanine and serine abolish the ATP modulation, while a charge-conserved mutation, E865D, greatly decreases the efficacy of the ATP effect_the maximal shift of the V1/2 of the common gate P-V curve is ~10-20 % of that in the WT channel. Mutations of V860 and V613 to various amino acids also greatly reduce the efficacy of the ATP modulation. Double mutant cycle analyses show that V634 and V613 are strongly energetically coupled, with a coupling coefficient (Ω) of ~25, while V634 and E865 may be only weakly coupled with a Ω value of ~1.6. These results support the idea that ATP likely binds directly to the C-terminus of CLC-1 to modulate the common gating of the channel.

1667-Pos
Substrate-Driven Conformational Changes in CLC-ec1 Observed by Fluorine NMR
Shelley Elvington, Corey Liu, Merritt Maduke.
Stanford University, Stanford, CA, USA.
The CLC "Cl^- channel" family consists of both Cl^-/H^+ antiporters and Cl^- channels. This scenario presents a unique opportunity to investigate the molecular similarities and differences underlying these mechanisms. Although gating in CLC channels is known to involve large, cooperative conformational changes between protein subunits, it has been hypothesized that conformational changes in the antiporters may be confined to small movements localized near the Cl^- permeation pathway. However, to date few studies have directly addressed this issue, and therefore little is known about the molecular movements that underlie CLC-mediated antiport. The crystal structure of the *E. coli* antiporter ClC-ec1 provides an invaluable molecular framework for such studies,

but this static picture alone cannot depict the protein movements that must occur during ion transport. To address this issue, we have utilized fluorine NMR to monitor substrate-induced conformational changes in ClC-ec1. We show that substrate-driven conformational change is not constrained to the Cl^- permeation pathway alone, and that the ClC-ec1 subunit interface participates in protein movement. Furthermore, removal of the protein's H^+ transport ability does not eliminate the H^+-dependent protein movement observed in the intact antiporter. Finally, we observe that a ClC-ec1 ''channel-like'' mutant is not subject to the same substrate-dependent conformational changes that occur in the ClC-ec1 transporters. Together, these results provide new insight into conformational change in ClC-ec1 and lay an essential foundation for future studies on ClC-ec1 protein dynamics.

1668-Pos

Cardioprotective Role For the CLC-3 Chloride Channel in the *mdx* Mouse Model of Duchenne Muscular Dystrophy

Nathanael Heyman, Ryan Wuebbles, Linda Ye, Dayue Duan, Joe Hume, Dean Burkin.
University of Nevada, Reno, NV, USA.

Duchenne Muscular Dystrophy (DMD) is the most common human X-linked disease affecting 1/3,500 male births. DMD patients suffer from severe, progressive muscle wasting with clinical symptoms first detected between 2 to 5 years of age. As the disease progresses patients are confined to a wheelchair in their early teens and die in their early twenties from cardiopulmonary failure. There is currently no effective treatment or cure for DMD. DMD patients and *mdx* mice (the mouse model for DMD) have mutations in the dystrophin gene that result in an absence of the dystrophin protein. Dystrophin is a 427 kDa protein located under the sarcolemma on the inner cytoplasmic membrane of skeletal and cardiac muscle cells and provides structural and functional integrity to muscle. Although therapies have been developed that target skeletal muscle disease, increasing evidence suggests correcting the cardiomyopathy is critical to the survival of DMD patients. As the cardiomyopathy progresses, the hearts of DMD patients and *mdx* mice exhibit arrhythmias, conduction abnormalities and left ventricular dilation. Recent studies have shown that the chloride ion channel ClC-3, a candidate protein responsible for volume-regulated chloride channels in heart, plays a critical cardioprotective role against the development of hypertrophy and failure (*J Mol. Cell. Cardiol.* 2009 Jul 15. [Epub ahead of print]).Using transgenic mice including heart specific ClC-3 knockout *mdx* mice, echocardiography and electrophysiology, we analyzed the role of ClC-3 in modulating cardiac disease progression in dystrophic mice. Our preliminary results indicate ClC-3 may be a major modifier of cardiac disease progression in *mdx* mice and targeting ClC-3 expression or function may provide a novel therapeutic approach for the treatment of dilated cardiomyopathy in DMD (supported by 3P20RR015581 from the National Center for Research Resources).

1669-Pos

Blocking Kinetics of CFTR Channel by Aromatic Carboxylic Acid Positional Isomers Characterised using a Novel Amplitude Distribution Analysis Method

Ying-Chun Yu[1], **Yoshiro Sohma[1,2]**, Yumi Nakamura[1], Tomoka Furukawa[1,3], Yohei Matsuzaki[1,4], Seiko Kawano[5], Tzyh-Chang Hwang[2], Masato Yasui[1].
[1]Dept. of Pharmacology, Keio University School of Medicine, Tokyo, Japan, [2]Dalton Cardiovascular Research Center, University of Missouri-Columbia, Columbia, MO, USA, [3]Dept. of Biomolecular Engineering, Tokyo Institute of Technology, Tokyo, Japan, [4]Dept. of Pediatrics, Keio University School of Medicine, Tokyo, Japan, [5]Dept. of Health and Nutrition Sciences, Komazawa Women's University Faculty of Human Health, Tokyo, Japan.

To investigate the pore structure of the cystic fibrosis transmembrane conductance regulator (CFTR) channel, we performed a systematic pore probing on CFTR channel pore with a series of small aromatic carboxylic acids, including their positional isomers, e.g., 9-anthracene carboxylic acid (9-AC) and 1-anthracene carboxylic acid (1-AC).

Small compounds presumably interacting the channel protein with a few points are sensitive to structural changes of the binding site. However such low affinity blockers show fast - intermediate blocking kinetics which give us the overall affinity, but not on- and off- rates separately. To overcome this problem, we developed an iterative simulation method to estimate the on- and off- rate constants in the 9-AC or 1-AC block from the single channel amplitude distribution.

The newly developed Amplitude Distribution Analysis (ADA) program first generated a single-channel current according to the given kinetic scheme and added a Gaussian noise to the currents for mimicking the background noise. The simulated currents were low-pass filtered and digitized at the same frequencies as those in the experiments and binned into an amplitude histogram. Then the program repeats a direct likelihood comparison between the simulated and experimental current amplitude distributions to find the best fitted values for the blocking kinetic parameters.

The ADA program showed that the off-rate of 1-AC block is 3-fold slower than that of 9-AC and the on-rate of 1-AC is ~3-fold faster than that of 9-AC. The voltage-dependences of on- and off- rates of 1-AC are similar to those of 9-AC, respectively. These suggest that 1-AC and 9-AC block CFTR channel by binding to a common binding site which should be modeled by a combination of a positive charge tightly surrounded by hydrophobic residues.

1670-Pos

Effects of Aromatic Carboxylic Acids on Genistein- and Curcumin- Potentiated G551D-CFTR

Yumi Nakamura[1], Akiko Hanyuda[1], Ying-Chun Yu[1], Tomoka Furukawa[1,2], Yohei Matsuzaki[1,3], Yoichiro Abe[1], Silvia Bompadore[4], Tzyh-Chang Hwang[4], Masato Yasui[1], Yoshiro Sohma[1,4].
[1]Dept. of Pharmacology, Keio University School of Medicine, Tokyo, Japan, [2]Department of Biomolecular Engineering, Tokyo Institute of Technology, Tokyo, Japan, [3]Dept. of Pediatrics, Keio University School of Medicine, Tokyo, Japan, [4]Dalton Cardiovascular Research Center, University of Missouri-Columbia, Columbia, MO, USA.

The Cystic fibrosis transmembrane conductance regulator (CFTR) chloride channel plays an important role in salt and water transport across epithelia and defective function due to mutations in the CFTR gene cause cystic fibrosis (CF). The glycine-to-aspartate missense mutation at position 551 (G551D) is the third most common CF-associated mutation and G551D-CFTR is characterized by a very low open probability despite of its normal trafficking to the plasma membrane.

Numerous small molecules have been shown to increase the activity of G551D-CFTR presumably by binding to the CFTR protein. Among the many G551D-CFTR potentiators, a bioflavonoid found in legumes, genistein is perhaps the most extensively studied. More recently it was reported that a component of the spice turmeric, curcumin strongly activated G551D-CFTR. However, The mechanism through which these compounds increase G551D-CFTR activity is still unclear. On the other hand, we have previously reported that anthracene-9-carboxylate (9-AC) showed an inhibitory effect and an potentiation effect on CFTR channels by binding to two chemically distinct sites for each effect (Ai *et al,* 2004).

In this study, we made a functional probing on genistein-potentiated G551D-CFTR and curcumin-potentiated G551D-CFTR using 9-AC and its positional isomer, anthracene-1-carboxylate (1-AC). In wild type- (WT-) CFTR, 9-AC induced a large voltage-independent enhancement and a voltage-dependent inhibition in the whole-cell (WC) current. 1-AC induced a smaller enhancement and a larger voltage-dependent block in WT-CFTR WC currents in compared with 9-AC. In the other hand, both 9-AC and 1-AC induced only a weak voltage-dependent inhibitions in genistein-potentiated G551D-CFTR WC currents whereas, in curcumin-potentiated G551D-CFTR WC currents, 9-AC and 1-AC induced similar effects to those in WT-CFTR. These suggest that curcumin and genistein potentiated G551D-CFTR via different mechanisms. We speculate that genistein-potentiated and curcumin-potentiated G551D-CFTRs might have different protein conformations.

1671-Pos

Optimization of the NBD1 Site Improves the Function of G551D-CFTR Channels

Ming-Feng Tsai, Kangyang Jih, Min Li, Tzyh-Chang Hwang.
Missouri University, Columbia, MO, USA.

CFTR chloride channels comprise two nucleotide binding domains (NBD1 and NBD2). Mutations (for example, G551D) that impair CFTR function result in the lethal genetic disease cystic fibrosis (CF). It's established that the opening and closing of CFTR are mainly controlled by ATP binding and hydrolysis respectively in NBD2 while ATP binding at NBD1 can modulate the stability of the open state. Using a non-hydrolytic ligand MgPPi, we locked open CFTR channels with mutations at NBD1. We found that two W401 mutations significantly increased the lock-open time (W401F: 72 ± 3s; W401Y: 51 ± 6s; WT: 27 ± 2s). These gain-of-function mutations are unexpected since the W401-equivalent residue Y1219 in NBD2 can be effectively replaced by tryptophan but not phenylalanine. As the ATP molecule bound in NBD1 may interact with NBD2's signature sequence (LSHGH), we extended our study to this region. We found that reverting the histidine residue 1348 to the canonical glycine (H1348G) similarly stabilized the lock-open state ($\tau = 67 \pm 8$s). Once W401F, H1348G, or W401F/H1348G mutations were incorporated into G551D channels which no longer respond to ATP, the mutant channels become ATP-responsive with basal activity increased by ~10-fold for W401F/G551D-, ~4-fold for H1348G/5G551D-, and ~25-fold for W401F/H1348G/G551D-channels. The increased

channel activity is mainly due to an increased open-time. The results shown here suggest that NBD1 and NBD2 may employee different chemical mechanisms in binding ATP and that NBD1 can be a potential molecular target for developing CFTR potentiators for CF-related mutants. The effects of different nucleotides (for example, GTP and UTP) on NBD1 and NBD2 will be studied to gain a better understanding of the chemical mechanism underlying nucleotide-NBD interaction.

1672-Pos

The Inhibition Mechanisms of the Regulatory Domain of Cyctic Fibrosis Transmembrane Conductance Regulator

Guangyu Wang.
Gregory Fleming James Cystic Fibrosis Research Center, and Department of Physiology and Biophysics, University of Alabama at Birmingham, Birmingham, AL, USA.

The cyctic fibrosis transmembrane conductance regulator (CFTR) is a member of the human C subfamily of ATP-binding cassette (ABC) transporters but functions as a chloride channel. Activity of CFTR is tightly controlled not only by ATP binding-induced NBD1-NBD2 dimerization but also by phosphorylation of the unique regulatory (R) domain by protein kinase A (PKA). The R domain has multiple phosphorylation sites for which only Ser737 and Ser768 are inhibitory. The underlying mechanisms are unclear because neither the structure of the R domain nor its interactions with other parts of CFTR have been fully illuminated. Here I applied the crystal structure of bacterial transporter Sav1866 and sulfhydryl-specific crosslinking strategy to determine which part of CFTR interacts with the R domain regulating channel activity. The results show that diamide-induced disulfide bond crosslinking of S768C to H950C, K951C, H954C or S955C from cytoplasmic loop 3 (CL3) inhibited the channel activity and inhibition was reversed by DTT. Similarly, disulfide crosslinking of S737C to H954C, S955C or Q958C also suppressed the channel activity. Furthermore, mutation of these residues to alanines weakened the curcumin-induced relative PKA-dependence which was completely removed by deletion of the R domain. Finally, activation of a double mutant H950R/S768R CFTR did not need any PKA while either H950R or S768R construct needed it. These results suggest that S768 and S737 may form putative H-bonds with hydrophilic residues of CL3 and thus inhibit the channel activity in the unphosphorylated state. In the phosphorylated state, a putative ferrous bridge involving H950, H954, C832, D836, H775 and H667 at the CL3-R interface may inhibit the channel activity. All these observations are consistent with the recent electron cryomicroscopy-based structural model on which the R domain is closed to cytoplasmic loops regulating channel gating.

1673-Pos

CFTR Cytosolic Loop Mutations Allosterically Promote ATP Independent Channel Gating

Wei Wang, Jianping Wu, Karen Bernard, Ge Li, Guangyu Wang, Mark Bevensee, Kevin L. Kirk.
UAB, Birmingham, AL, USA.

CFTR channel gating normally depends on ATP binding and NBD dimerization. Optimal CFTR channel activation further requires phosphorylation of the R domain. How ATP binding at the NBDs and phosphorylation of the R domain regulate CFTR channel gating are not fully understood. In the present study, we demonstrate that mutations in the CFTR Cytosolic Loops (CL) markedly promote channel opening in the absence of ATP and NBD2, presumably by an allosteric mechanism. In excised inside-out patches, we observed that single or double mutations of K978 and K190 in CL 3 and 1 induced large ATP independent currents (5-70% of current before removing ATP). These mutant channels deactivated with a slow time constant (49.11 ± 4.58 sec) when ATP was removed by Hexokinase/glucose and subsequent bath perfusion. A K978 point mutation greatly increased the ATP sensitivity of channel activation by decreasing the EC_{50} (by 8-fold) for ATP activation, which is consistent with the slow deactivation following ATP removal. K978 mutations markedly enhanced G551D channel activity, a disease mutant that fails to respond to ATP, and Δ1198-CFTR, a mutant that lacks NBD2, indicating that the K978 mutations affect channel gating downstream of NBD dimerization. Interestedly, R domain phosphorylation further stimulated K978/G551D and K978/Δ1198 combined mutants, indicating that the R domain regulates channel activity independently of NBD dimerization. Similarly, K978 mutations also increased the activation rate at low dose (3 U/ml) of PKA, indicating that K978 mutations also enhance the PKA sensitivity of channel activation. Our results support an allosteric gating mechanism in which loops 1 and 3 functionally link ATP binding and NBD dimerization to CFTR channel opening.

1674-Pos

Accessibility of Cysteines Within the NBD Interface in a CFTR Channel

Luiz A.P. Chaves.
Rockefeller University, New York, NY, USA.

Opening and closing of a CFTR channel is accompanied by ATP-driven formation and hydrolysis-triggered disruption of a head-to-tail NBD1-NBD2 heterodimer where composite interfacial sites, between the Walker motifs of one NBD and the LSGGQ-like (ABC signature) sequence of the other, each enclose an ATP molecule. Only the ''NBD2'' composite site (containing NBD2 Walker motifs) is catalytically competent. The ATP-bound tight NBD1-NBD2 heterodimer is linked to the open-channel state, but the disposition of the NBDs in the closed-channel state of CFTR, in the absence of ATP or after its hydrolysis, remains unknown. To address this, we assess accessibility to various size MTS reagents of single interfacial target cysteines introduced into the ABC signature sequence of the competent site (at NDB1 position S549), or of the dead site (at NBD2 position S1347), or at mid-interface positions S605 of NBD1 or A1374 of NBD2, in full-length cys-depleted CFTR-C(832-1458)S,expressed in *Xenopus* oocytes and examined in excised patches. Cysteines at all four positions were readily accessible to MTSET in closed channels in the absence of ATP. For channels opening and closing in 3 mM ATP, the reaction rate depended on MTSET concentration and was $\sim 10^5\ M^{-1}s^{-1}$ at 5 μM at position 549, and was similarly rapid at corresponding position 1347. In closed channels without ATP, cysteines at 549, 605, 1347, and 1374 were all also readily accessible to MTS reagents of increasing size, e.g., MTS-biotin, MTS-THAE (trihexylammonium-ethyl) and MTS-verapamil, up to ~11Åx16Åx10Å, suggesting substantial separation between NBD1 and NBD2, throughout the NBD interface, in closed CFTR channels. (Supported by NIH DK51767).

1675-Pos

Strict Coupling Between CFTR's Catalytic Cycle and Gating of its Channel Pore Revealed by Distributions of Open Burst Durations

László Csanády[1], Paola Vergani[2], David C. Gadsby[3].
[1]Semmelweis University, Budapest, Hungary, [2]University College London, London, United Kingdom, [3]The Rockefeller University, New York, NY, USA.

CFTR, the ABC protein defective in cystic fibrosis, functions as an anion channel. Once phosphorylated by protein kinase A, a CFTR channel is opened and closed by events at its two cytosolic nucleotide binding domains (NBDs). Formation of a head-to-tail NBD1/NBD2 heterodimer, by ATP binding in two interfacial composite sites between conserved Walker A and B motifs of one NBD and the ABC-specific signature sequence of the other, has been proposed to trigger channel opening. ATP hydrolysis at the only catalytically competent interfacial site is suggested to then destabilize the NBD dimer and prompt channel closure. But this gating mechanism, and how tightly CFTR channel opening and closing are coupled to its catalytic cycle, remain controversial. Here we determine the distributions of open burst durations of individual CFTR channels, and use maximum likelihood to evaluate fits to equilibrium and non-equilibrium mechanisms and estimate the rate constants that govern channel closure. We examine partially- and fully-phosphorylated, wild-type CFTR channels, and two mutant CFTR channels each bearing a deleterious mutation in one or other composite ATP binding site. We show that the wild-type CFTR channel gating cycle is essentially irreversible and tightly coupled to the ATPase cycle, and that this coupling is completely destroyed by the NBD2 Walker-B mutation D1370N but only partially disrupted by the NBD1 Walker-A mutation K464A. [NIH R01-DK051767, NIH FIC R03-TW007829, Wellcome Trust 081298/Z/06/Z]

1676-Pos

ΔF508 CFTR Expressed In *Xenopus* Oocytes Exhibits Unique Thermal Sensitivity

Xuehong Liu, Allison Landstrom, Nicolette O'Donnell, David C. Dawson.
Oregon Health & Science University, Portland, OR, USA.

The deletion of a phenylalanine at position 508 is the most common, disease-related mutation in the CFTR protein. ΔF508 CFTR channels are assembled in mammalian cells, but exhibit two deficiencies thought to underlie the disease phenotype: impaired trafficking and defective gating. The CFTR trafficking defect is partially mitigated at low temperature so that *Xenopus* oocytes are ideal for studying the physical properties of ΔF508 channels under physiological conditions. In order to investigate possible effects of the Phe deletion on the intrinsic stability of CFTR channel function in the plasma membrane, we monitored channel activity at room temperature (~23°C) and during a brief (10-12 minute) period of elevated temperature (28°C to 37°C). In oocytes expressing wild type CFTR, a temperature challenge resulted in a reversible increase in the conductance; a result of a simultaneous increase in single-channel conductance and open probability. Both parameters, however, returned to baseline values

when the temperature was returned to 23°C. In marked contrast, conductance due to ΔF508 CFTR channels exhibited a transient increase within a minute after the temperature challenge, followed by a quasi-exponential decline of about 80-90% of the initial conductance ($t_{1/2} = 4$ minutes at 37°C). The temperature induced decrease in ΔF508 CFTR conductance was not reversed by returning the temperature to 23°C. The second-site reverent construct, R553M/ ΔF508 CFTR, previously shown to rescue CFTR function in mammalian cells (Teem et al. 1993. *Cell*. 73:335-346), exhibited a thermal response that was indistinguishable from wild type. Preliminary data suggests that this ''thermal instability'' that is readily detectable when ΔF508 CFTR is expressed in *Xenopus* oocytes, reflects an intrinsic structural defect in the channel protein that results in a temperature-sensitive alteration in gating and could potentially trigger the retrieval of surface protein documented in mammalian cells.

1677-Pos

Riding the Conformational Wave to the Open Channel State in the CFTR Chloride Channel

Guiying Cui, Cody Freeman, **Nael A. McCarty**.
Emory University School of Medicine, Atlanta, GA, USA.

The pore structure of the CFTR chloride channel is unknown. We showed previously that R352 in TM6 forms a salt bridge with D993 in TM9; charge-destroying mutations at either site destabilized the open state, affecting conductance, selectivity, and pore blockade. Other pairs of interacting residues also contribute to stabilizing the open state. We continued these experiments to determine how steps leading to the dimerization of the NBDs upon binding of nucleotide relate to the steps leading to pore opening, using single-channel recordings of WT-CFTR and channels bearing a cysteine or alanine at 352, 993, or both. In R352C-CFTR, but not R352A-CFTR, modification of the cysteine by positively-charged $MTSET^{+}$ and $MTSEA^{+}$ recovered the stability of the open state. In D993C-CFTR, but not D993A-CFTR, negatively-charged $MTSES^{-}$ recovered the stability of the open state. In contrast, D993C-CFTR modified by $MTSET^{+}$ retained the instability of the open state. The R352C/D993C-CFTR double mutant exhibited instability of the open state in both the absence and presence of DTT, suggesting that R352C did not form a disulfide with D993C. In WT-CFTR, exposure to AMP-PNP led to greatly prolonged channel openings, as expected. However, this response was not found for R352A-CFTR. Surprisingly, R352C/D993C-CFTR could be latched open by the bifunctional crosslinker, MTS-2-MTS, such that channels could not close upon washout of ATP. MD simulations based on CFTR homology models (see Dawson Lab abstract) predict conformational states in which R352 and D993 approach each other to within van der Waals distances. These results suggest that the binding of ATP at CFTR's NBDs initiates a conformational wave, which leads to a change in pore structure from the closed to the open state, the latter being stabilized by inter-TM interactions including the R352-D993 salt bridge. (Support: NIH-2R56DK056481-07)

1678-Pos

Homology Modeling and Molecular Dynamics Simulation Predict Side-Chain Orientations and Conformational Changes in the Pore of the CFTR Chloride Channel

Christopher Alexander[1], Anthony Ivetac[2], Yohei Norimatsu[1],
Mark Sansom[3], David C. Dawson[1].
[1]Oregon Health and Science University, Portland, OR, USA, [2]University of California San Diego, La Jolla, CA, USA, [3]University of Oxford, Oxford, United Kingdom.

We recently presented two homology models of the CFTR chloride channel, one based on homology to the prokaryotic ABC transporter, Sav1866, and a second based on a 5 ns molecular dynamics (MD) simulation of the first (Alexander et al, *Biochemistry* in press, 2009). Predictions for side-chain orientations were in excellent agreement with the results of a cysteine scan of transmembrane segment six (TM6) using both channel-permeant and channel-impermeant, thiol directed probes. Here we present the results of an extended MD simulation, along with the results of a cysteine scan of TM12. Scanning results confirm the model predictions for ''pore-lining'' and ''not pore-lining'' residues in TM12 and support the notion that pore narrowing prevents the reaction of deeper-lying cysteines in TM12 toward larger, thiol-directed probes like $MTSET^{+}$ and $MTSES^{-}$ when these compounds enter the channel from the outside. The extended MD simulation predicts movements of pore elements that are in agreement with previously reported results of state-dependent reactivity of a cysteine at position 337 (Norimatsu et al, *Biophysical Journal* 96(3):468a-469a, 2009), and the postulated formation of a salt-bridge between R352 (TM6) and D993 (TM9) (Cui et al, *Biophysical Journal* 91(5):1737-48, 2008, and poster from the McCarty Lab). Supported by NIH, the Cystic Fibrosis Foundation, the American Lung Association, the Wellcome Trust, and the BBSRC.

1679-Pos

Identification of Possible Binding Sites for the CFTR Pore Blocker, GlyH-101

Yohei Norimatsu[1], Anthony Ivetac[2], John Kirkham[1], Leah Frye[3],
Mark Brewer[3], Mark Sansom[4], David C. Dawson[1].
[1]Oregon Health & Science University, Portland, OR, USA, [2]University of California San Diego, La Jolla, CA, USA, [3]Schrodinger Inc., Portland, OR, USA, [4]University of Oxford, Oxford, United Kingdom.

The last decade has seen the discovery by means of high throughput screening of a wide range of small-molecule modulators of the CFTR chloride channel. These compounds act by altering anion conduction, channel gating and/or trafficking of the CFTR protein. However, binding sites for these molecules on CFTR or other cellular constituents have yet to be identified. GlyH-101 is a CFTR modulator that blocks the channel by entering from the extracellular side and binding to a site within the pore. In an effort to identify possible GlyH-101 binding sites within the pore of the CFTR channel, we applied the small-molecule docking program, ''Glide'' (Schrodinger, Inc.), to a series of molecular models of CFTR, derived by means of molecular dynamics simulation from a homology model based on the prokaryotic ABC transporter, Sav1866 (Dawson and Locher, Nature 443: 180-185, 2006; Alexander et al., Biochemistry in press, 2009). One of the potential GlyH-101 binding sites identified by Glide lies in close proximity to two residues in the sixth transmembrane segment (TM6), F337 and T338, where substituted cysteines are ''protected'' by GlyH-101 from reaction with thiol-directed probes (Norimatsu et al., Biophys. Journal 96: 468a-469a, 2009). These results suggest an approach to identifying the binding site(s) for GlyH-101 and other small molecules within the CFTR protein. Supported by NIH, Cystic Fibrosis Foundation, American Lung Association, the Wellcome Trust, and the BBSRC.

Mechanosensitive Channels

1680-Pos

Mechanosensitivity of a Voltage-Gated Ion Channel, Na_v1.5

Arthur Beyder, James L. Rae, Cheryl Bernard, Gianrico Farrugia.
Mayo Clinic, Rochester, MN, USA.

Voltage-gated ion channels are often found in tissues where electrical and mechanical stimuli coexist. The mechanosensitive, voltage-gated sodium channel Na_v1.5 (encoded by SCN5A) is expressed in two such electromechanical organs, the heart and the gastrointestinal tract. Mutations in SCN5A are frequently pathogenic and may affect mechanoelectrical coupling. The aim of this study was to assess mechanical sensitivity of Na_v1.5 at the molecular level. SCN5A was expressed in HEK cells and studied using a pipette pulled and fire polished to ensure that a small number (2-50) of channels were reliably present in cell-attached micropatches. This allowed resolution of both single channel events and averaged behavior. Both positive and negative pressures (up to 50mmHg) produced visible patch distention, an increase in patch current at all voltages and large hyperpolarizing shifts in steady-state voltage-sensitivity of activation and inactivation. From voltage dependence of activation at rest ($V_{1/2} = -30$mV at 0mmHg), pressure resulted in graded shifts of $V_{1/2}$ for activation and inactivation of -0.71mV/mmHg and -0.72mV/mmHg, respectively. Channel kinetics were predictably affected by the voltage shifts, but channel opening and fast inactivation were otherwise unaffected by pressure. Single channel traces showed that unitary conductance was unaffected, rather peak currents appeared to increase due to an increase in the number of active channels in the patch. These effects were minimally reversible for as long as 30 minutes after a single stretch stimulus. Patch excision resulted in an immediate shift of activation $V_{1/2}$=-75mV and loss of stretch sensitivity. Application of the inhibitor of actin polymerization, cytochalasin D, diminished sensitivity to stretch (-0.42mV/mmHg). Our work demonstrates that mechanical stress at physiologically relevant levels affects voltage sensing of Na_v1.5 channels, without affecting the pore, channel gate and fast inactivation. Supported by NIH DK52766.

1681-Pos

Integrin-Dependent and -Independent Potentiation of L-type Calcium Current (Cav1.2) by Cell Stretch

Peichun Gui[1], Gerald W. Zamponi[2], George E. Davis[1], Michael J. Davis[1].
[1]Department of Medical Pharmacology & Physiology, University of Missouri-Columbia School of Medicine, Columbia, MO, USA, [2]Molecular Neuroscience Research Group, University of Calgary, Calgary, AB, Canada.

Stretch-induced (myogenic) contraction of vascular smooth muscle (VSM) requires calcium influx through L-type calcium channels (Cav1.2). Integrins play a role in this process because alpha5 beta1 and alphaVbeta3 integrin blocking antibodies prevent myogenic constriction. Recent studies in our lab indicate that Cav1.2 current is potentiated by alpha5beta1 integrin activation and requires phosphorylation by PKA and c-Src of Cav1.2 C-terminal residues. To test

whether Cav1.2 channels are mechanosensitive and the possible role of integrins in this process, patch clamp methods were used to investigate the properties of either native or heterologously expressed Cav1.2 cannels by stretch of single cells plated onto a flexible substrate. Thin silicone membranes were coated with either fibronectin (FN) or poly-l-lysine (PLL) to assess integrin-dependent and -independent responses, respectively, and stretched using two blunt micropipettes driven in equal and opposite directions by piezoelectric translators. Graded stretch to 130% of resting cell length induced graded increases in Cav1.2 current (up to 63%) in HEK 293 cells expressing the neuronal channel isoform (Cav1.2c). The increase in current was ~2-fold greater for cells adhering to FN than for cells on PLL. On FN, 130% longitudinal stretch of primary VSM cells induced ~50% increases in Cav1.2 current. However, the magnitude of stretch-activated Cav1.2 current was the same on FN or PLL for cells expressing a Cav1.2 construct containing two C-terminal mutations (Y2122F/S1901A) to prevent phosphorylation by PKA and c-Src, or for cells expressing a Cav1.2 construct with the C-terminus truncated. Our results suggest that the Cav1.2 channel can be potentiated by membrane stretch, with one component due to intrinsic mechanosensitivity of the channel and a second component due to signaling through an integrin-dependent process.

1682-Pos
Dissecting the Molecular Mechanism of How Force Activates Yeast TRP Channel TRPY1

Zhenwei Su, Ching Kung, Yoshiro Saimi.
UW-Madison, Madison, WI, USA.

Though clear for the prokaryotic mechanosensitive (MS) MscL and MscS, how mechanical force activates eukaryotic MS channels remains poorly understood. Several members of transient receptor potential (TRP) channel family are apparently involved in animal mechanosensations and are therefore promising MS-channel candidates. The yeast homolog, TRPY1, expressed in the yeast vacuolar membrane, can clearly be gated by hyper-osmotic shock *in vivo* and by directly stretching excised vacuolar membrane patches under patch clamp. Here, we investigated the structure-function relationship of TRPY1 by mutagenesis, aiming at dissecting how force is sensed by TRPY1 and how force opens the channel gate. TRP channels share general organization with well-studied voltage-gated potassium channels, being tetramers with each subunit consisting of six transmembrane helices (S1-S6) and N- and C-terminal cytoplamic domains. We found that the C-terminal cytoplasmic domains of TRPY1 harbor Ca^{2+} binding motifs, which confer TRPY1 Ca^{2+} activation. We demonstrated that the Ca^{2+} activation and the force activation are synergistic and the two gating mechanisms act in parallel. We proposed that force is perceived by the transmembrane domains. Our further in-depth analyses showed that strategic insertions of long peptide linkers before S4-S5 linker and after S6 can surprisingly yield functional channels with largely intact mechanosensitivity, highlighting the crucial roles of the pore module in TRPY1 mechanosensitivity. Together with our detailed scanning mutagenesis, we will discuss possible molecular mechanisms on how force activates TRPY1.

1683-Pos
Inactivation of the Bacterial Mechanosensitive Channel MscL Involves Flexible Transmembrane Helices and a 'Dry' Gate

Kishore Kamaraju, Andriy Anishkin, Naili Liu, Sergei Sukharev.
University of Maryland, College Park, MD, USA.

MscL, a mechanosensitive channel of large conductance, is an emergency release valve residing in the cytoplasmic membrane of E. coli. Under osmotic shock, when membrane tension approaches the lytic limit of ~10 mN/m, MscL opens a 3 nm pore relieving osmotic stress. The conformational transition in the pentameric complex was previously envisioned as a tilting iris-like motion of tightly coupled pairs of the centrally located TM1 and peripheral TM2 helices. Wetting the hydrophobic constriction formed by the rings of L19 and V23 was identified as is the rate-limiting step over a barrier of more than 50 kT. While adaptation of MscL was reported, the channel was generally considered non-inactivating. Special pressure protocols involving prolonged conditioning steps and short saturating test pulses revealed that after a 30 s exposure to half-saturating pressure (p0.5) in spheroplast patches, about 20% of MscL population reversibly inactivates. The channels return to the resting state within 1 s upon pressure release. Introduction of a flexible double glycine motif (A91G/I92G) in TM2 dramatically increased the rate of inactivation resulting in a 90% silent channel population after a 10 s step to p0.5. Single-channel traces revealed a split of concerted 70 pA opening transitions into a staircase of irregular ~7 pA substates in the double glycine mutant. The additional hydrophilic substitution in the constriction (V23T/A91G/I92G) pre-hydrates the pore, reduces p0.5 by ~55% and, while generating multiple substates, completely abolishes inactivation. In extrapolated-motion simulations TM2 kinks at A91G/I92G and its C-terminal end separates from TM1. We propose that in WT MscL TM1s and TM2s are tightly coupled, whereas in the double glycine mutant the unsupported TM1s may reform the tight hydrophobic seal independent of the positions of TM2s thus creating a tension-insensitive non-conductive state.

1684-Pos
Caveolin and Cholesterol Control of Mechanosensitive Channels in Muscle

Thomas M. Suchyna[1], Hiaxia Huang[2].
[1]SUNY at Buffalo, Buffalo, NY, USA, [2]Dept. of Physiology, Capitol Medical University, Beijing, China.

In Duchene muscular dystrophy the loss of the cytoskeletal element dystrophin modifies the localization of sarcolemma components and the stress distribution to those components. There is a change in the distribution of caveolae and dysregulation of mechanosensitive ion channels (MSCs) both of which may contribute to the elevated Ca2+ levels present in dystrophic myotubes. Caveolae are curved cholesterol rich membrane structures associated with dystrophin that contain many signaling molecules. We have shown that overexpression of Caveolin-3 in mouse myotubes increases the incidence of MSCs in patches and average MSC current. However, it has no effect on their kinetics of activation. Cholesterol depletion by MβCD produces an even larger increase in MSC incidence and average patch current, and also significantly decreases the relaxation rate of the membrane as observed by membrane capacitance changes. We have used miRNA against TRP channels (TRPC1, TRPC4, TRPC6, TRPV2) that have been reported to mechanosensitive in various systems to try and determine the identity of the channel revealed by cholesterol depletion. Average patch current and immunofluorescence staining has been used to determine the level of knockdown of the individual TRP channel subunits.

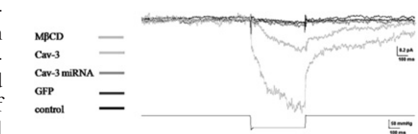

1685-Pos
Clustering and Functional Interaction of MscL Channels

Asbed M. Keleshian[1], Stephan L. Grage[2], Tamta Turdzeladze[2], Andrew R. Battle[1], Wee C. Tay[1], Stephen A. Holt[3], Sonia Antoranz Contera[4], Michael Haertlein[5], Martine Moulin[5], Prithwish Pal[6], Paul R. Rohde[6], Kerwyn C. Huang[7], Anthony Watts[4], Anne S. Ulrich[2], **Boris Martinac**[6].
[1]University of Queensland, Brisbane, Queensland, Australia, [2]Karlsruhe Institute of Technology, Karlsruhe, Germany, [3]Rutherford Appleton Laboratory, Didcot, United Kingdom, [4]University of Oxford, Oxford, United Kingdom, [5]Institut Laue-Langevin, Grenoble, France, [6]Victor Chang Cardiac Research Institute, Darlinghurst (Sydney), NSW, Australia, [7]Stanford Universit, Stanford, CA, USA.

Mechanosensitive channels allow bacteria to respond to osmotic stress by opening a nanometer size pore in the cellular membrane. While the underlying mechanism has been studied intensively on the basis of individual channels, the work described here sheds light on the behavior of an ensemble of mechanosensitive channels of large conductance (MscL) in the membrane. Evaluating the spatial distribution of MscL channels in the bilayer using patch clamp, fluorescence, neutron scattering and reflection techniques, as well as atomic force microscopy and mathematical modeling, MscL was found to form clusters under a wide range of conditions. Within the cluster, MscL is closely packed, but still active and mechanosensitive. The channel activity, however, is modulated by the presence of neighbouring proteins, indicating functional protein-protein interactions. Collectively, the results demonstrate a potential functional role for self-assembly of MscL in the membrane.

Supported by the grants from the Australian Research Council and the National Health and Medical Research Council of Australia, DFG Centre for Functional Nanostructures (project E3.4), Engineering and Physical Sciences Research Council (EPSRC) and European Union.

1686-Pos
A Kinetic Characterization of the Human Erythrocyte Mechano-Activated K^+ Channel Inactivation Process

Jesus G. Romero, Zambrano Angeles.
Universidad Central de Venezuela, Facultad de Ciencias, Instituto de Biología Experimental, Laboratorio de Fisiología Molecular y Biofísica. Escuela de Biología, Caracas, Venezuela, Bolivarian Republic of.

Human erythrocyte (hRBC) shows a live span of 120 days, as these cells lack nucleus and organelles a question arises: which is the subjacent molecular process to this tightly controlled programme cell death (the biological clock)? It has been proposed that the increased Ca^{2+} concentration characteristic of the senescent cells is due to a mechanical stress at the microcirculation level. Using the Patch Clamp Technique, we had characterized a mechano-activated K^+

channel which shows a sigmoid dependence of *Po* on applied pressure, a mean conductance of 17pS, and is Ca^{2+} modulated (*140mM*KCl, *10mM*NaCl, *1mM*$CaCl_2$, *pH*7.0)(HEMKCA)(1,2), and had proposed a new hypothesis for the senescent process of hRBC with this channel as the responsible for the molecular clock. This channel presented an inactivation process producing an exponential decay of *Po* (τ=4.55 $\pm$ 1.95min). Here we present a complete kinetically characterization of this inactivation process: intriguingly, this process seemed to begin just when a voltage step is applied and ionic current started, suggesting that the activation process is necessary but not sufficient to allow the inactivation development. We had characterized the burst mode activity of this channel (17.43 $\pm$ 17.15 events/burst, 264.27 $\pm$ 291.3ms burst duration and 15.67 $\pm$ 7.1ms intraburst interval). The decay in *Po* produced by the inactivation seemed to be the effect of decay in the number of events per burst, probably related to burst duration decay, with no effect in intraburssts variables like intraburst intervals and intraburst mean duration. We present a complete kinetic model for this channel with two independent kinetic branches: one for the non-inactivated mode and the other for the inactivation pathway. This inactivation mechanism is presented as a molecular damper (security system) in our new hypothesis for the hRBC senescence.

(1)(2005) Biophys. J.88(1):593
(2)(2008) Biophys. J.91(1):1101
CDCH PI 03-00-6135-2008

1687-Pos
Deletion Analysis of the Mechanosensitive TREK-1 Channel
Grigori Maksaev[1], Naili Liu[1], H. Robert Guy[2], Sergei Sukharev[1].
[1]University of Maryland, College Park, MD, USA, [2]National Cancer Institute, National Institutes of Health, Bethesda, MD, USA.
TREK-1, the first functionally characterized mechanosensitive K channel from the two-pore family (K2P) is involved in protective regulation of resting potential in CNS neurons and many other tissues. The structural basis of TREK-1 sensitivity to stretch and other factors such as arachidonic acid (AA) and anesthetics remains unknown. Attempts to use existing K channel structures as templates for TREK-1 modeling have identified several motifs that are not present in canonical K channels, which include divergent cytoplasmic N- and C-termini, and a characteristic 50-residue extracellular loop in the first homologous repeat. To characterize functional roles of these domains, we analyzed TREK-1 deletion and cysteine mutants in patch-clamp experiments. In response to steps of suction, the control TREK-1-EGFP fusion protein expressed in HEK-293 cells produced transient currents in cell-attached patches and non-inactivating sustained currents upon patch excision. Responses in both configurations were augmented by AA. Deletion of the extracellular loop (Δ76-124) reduced functional surface expression of channels and increased background activity, but the activation by tension augmented by AA was fully retained. Further deletion of the C-terminal end (Δ76-124, Δ334-411) produced no additional effect. In an attempt to generate cysteine-free version of the channel, we additionally mutated two cysteines in the transmembrane domain. C219A did not compromise channel activity, whereas C159A/S was essentially inactive. Experiments in the presence of mercaptoethanol suggested that none of these cysteines form functionally-important disulfides. The functional deletion mutant without C219 is now topologically closer to other K channels and makes an amenable system for homology modeling and testing by disulfide cross-linking.

1688-Pos
Hot Or Hot? Differentiating the Effects of Heat and Capsaicin on the TRPV1 Channel
Claudia S. Haarmann, Alison K. Haythornthwaite, Michael George, Juergen Steindl, Christian Grad, Matthias Beckler, Sonja Stoelzle, Cecilia Farre, Andrea Brueggemann, David Guinot, Niels Fertig.
Nanion Technologies, Munich, Germany.
The temperature-sensitive ion channel family is receiving increasing attention as a potential contributor to pain states. In particular, ion channels activated by noxious heat, for example the TRPV1 channel, could provide a novel target for the treatment of chronic pain.
Using an automated patch clamp system, TRPV1 receptors expressed in CHO cells were activated using either noxious heat or the ligand capsaicin. Antagonists can be used to block either the heat- or capsaicin-activated TRPV1 response. Since blocking the heat response of TRPV1 can have undesirable effects on core body temperature in animals and

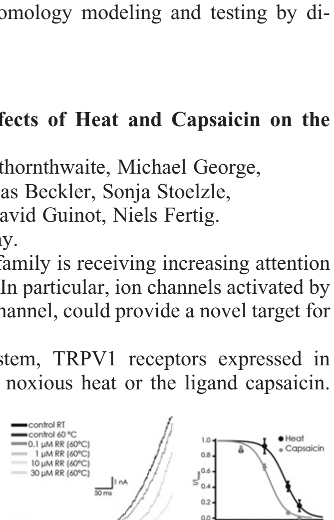

humans, being able to discriminate between antagonising the ligand-activated vs. the heat-activated response of TRPV1 channels may be important for discovering novel compounds with a reduced side-effect profile. Data will be shown of TRPV1 currents activated by increasing temperature and block of the heat-activated response by ruthenium red. Data will also be presented showing different antagonist profiles for ligand- and heat-activation of TRPV1.

1689-Pos
Heat and Capsaicin Activate TRPV1 Channels to Different Open States:
Yuanyuan Cui[1,2], Fan Yang[1], Kewei Wang[2], Jie Zheng[1].
[1]Physiology and Membrane Biology UC Davis, Davis, CA, USA,
[2]Neuroscience Research Institute Peking University, Beijing, China.
Both heat and capsaicin can strongly activate TRPV1 channels. However, the underlying mechanism by which the activation gate responds to these two distinct stimuli is unknown.
We use single-channel recordings of the wildtype and mutant TRPV1 channels with large unitary conductance to compare channel activation driven by each of the gating modalities. As shown in the figure, the heat-induced openings (top trace) exhibit much shorter open times than those of ligand-induced channel openings (bottom trace). In addition, we observe that at saturating concentrations capsaicin can only partially open TRPV1 channels. Raising temperature in the presence of capsaicin leads to an increase in open probability.
These results demonstrate that heat and capsaicin gate the channel to different open states, suggesting that they do not share the same activation pathway.

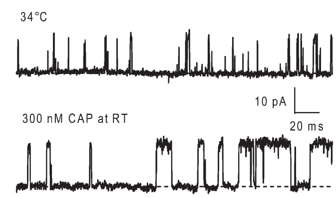

1690-Pos
Study Heat-Induced TRP Channel Activation Using Near-Infrared Laser As a Heat Source
Fan Yang[1], Wei Cheng[2], Changsen Sun[2], Jie Zheng[1].
[1]UC Davis, Davis, CA, USA, [2]Dalian University of Technology, Dalian, China.
Rapid and reliable temperature change is required for the study of temperature-dependent channel gating mechanisms. We use continuous near-infrared (CNI) laser as a heat source to rapidly increase the local temperature at a cell or a cell-free patch membrane containing temperature-sensitive TRP channels. The photothermal effects of laser irradiation can be characterized by transient changes in fluorophore emission, liquid junction potential, and function of membrane proteins. The CNI laser-based method is advantageous over perfusion-based heating methods mainly in speed but also in its reproducible temperature raising profile and minimal interference with perfused solutions containing channel agonists/antagonists.

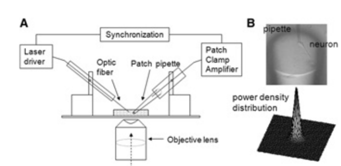

1691-Pos
The Proximal C-Terminal Region of TRPV1 Controls Phosphoinositide Selectivity
Carmen A. Ufret-Vincenty, Rebecca M. Klein, Sharona E. Gordon.
University of Washington, Seattle, WA, USA.
The lipid messenger PIP2 is a critical modulator of multiple membrane proteins, including TRPV1 ion channels. We have previously reported that PIP2 is an important cofactor for activation of TRPV1. A critical question to elucidate the molecular mechanism of activation is where in the channel is the binding site for PIP2. Here we report that a single amino-acid mutation, located in a region of the C-terminus proximal to the transmembrane domains of TRPV1, inverts selectivity of these channels for phosphoinositides by making PI(4)P a stronger activator than PIP2. An *in vitro* FRET-based binding assay shows this proximal site is capable of binding PIP2. In addition, the distal C-terminal region, previously proposed as a candidate site for PIP2 binding, is not required for PIP2 regulation. We also addressed a recent report suggesting that an integral membrane protein called Pirt acts as the PIP2 sensor for regulation of TRPV1. Pirt expression did not appear to alter TRPV1 apparent affinity for PIP2. In summary, these results implicate the C-terminus proximal site as a PIP2 interacting domain. More importantly, PIP2 binding to this proximal site is central to TRPV1 activation.

1692-Pos
TRP'Ing on QPatch in Multi-Hole Mode
Rasmus B. Jacobsen, Hervør L. Olsen, Søren Friis, Rikke Schrøder, M.K. Jensen, Morten Sunesen.
Sophion Bioscience A/S, Ballerup, Denmark.
Transient receptor potential (TRP) channels are non-selective cationic channels that are widely distributed in mammalian tissues. Their specific physiological functions are largely unknown. Proposed functions include responses to pain, temperature, touch, osmolarity, pheromones, and taste. But due to the lack of specific blockers and the full understanding of their mechanisms of activation studies of TRP channels have been difficult and unexpectedly slow.
The emergence of automated patch clamp (APC) systems has increased the number of new targets available for ion channel drug development and has augmented throughput.
In order to facilitate tests of large compounds libraries on e.g. TRP targets, we have recently developed two multi-hole APC systems: QPatch HTX and QPatch 16X. The multi-hole technology allows the simultaneous recording of 10 cells in parallel per recording site thereby increasing the signal to noise ratio and the success rate.
In this study, we have validated several TRP channels for their activation by their appropriate agonist e.g. Menthol, Capsaicin and temperature. We have found that using the QPatch in multi-hole mode significantly increased the volume of electrophysiology data that can be generated. Our results demonstrate that the QPatch multi-hole systems are capable of generating high quality data from a wide range of the channels belonging to the TRP family of receptors.
We believe that the combination of high throughput and high quality data in a single system has more than a ''transient potential'' to advance the understanding of the complex mechanisms of action exhibited by difficult targets such as the TRP channels.

1693-Pos
TRPV1 Modulates Acetylcholine Release From Motor Nerve Terminals
Baskaran Thyagarajan, Joseph G. Potian, Vishwendra Patel, Carmen C. Garcia, Joseph J. McArdle.
UMDNJ - New Jersey Medical School, Newark, NJ, USA.
Transient receptor potential (TRP) proteins are expressed ubiquitously throughout the body. Previous studies demonstrated expression of TRPV1, the capsaicin receptor, in sensory neurons. Recently, we reported TRPV1 expression in mouse motor nerve endings (MNEs; J. Pharmacol. Exp. Ther. Aug 04. 2009) where we observed that capsaicin protected MNEs from botulinum neurotoxin A (BoNT/A). We hypothesized that capsaicin reduced clathrin coated pit (CCP) dependent endocytosis of BoNT/A and demonstrate the regulatory influence of TRPV1 in exo-endocytic processes of MNEs. Phrenic nerve diaphragm muscle preparations isolated from isoflurane anesthetized adult mice were analyzed for the nerve-evoked twitch and transmitter release (TR). Capsaicin produced a concentration-dependent decline of twitch tension (TT), an effect attributed to suppression of stimulus-evoked acetylcholine release (SEAR) since these capsaisin concentrations reduced the amplitude of endplate currents. These effects of capsaicin were antagonized by capsazepine, the TRPV1 antagonist. To understand the mechanism whereby capsaicin reduced TR, we studied cholinergic Neuro 2a cells. Acute exposure to capsaicin altered the subcellular distribution of clathrin heavy chain (CHc) and AP2, two proteins essential to CCP formation. Wortmannin, (non selective PI3K/PI5K inhibitor), inhibited the TT and SEAR of the isolated nerve-muscle preparations and delocalized CHc and AP2 in Neuro 2a cells. Chlorpromazine, an inhibitor of CCP dependent endocytic pathway [Cell Mol. Biol. Lett. 2004; 9 (3): 475-81], mimicked the effects of capsaicin on AP2 delocalization. These data suggest that endogenous TRPV1 proteins are coupled to the exo-endocytic mechanisms that regulate neuromuscular transmission and that activation of TRPV1 with high capsaicin concentrations reduces exocytosis of acetylcholine by down regulating the compensatory CCP dependent endocytic pathways.

1694-Pos
Direct and Indirect Effectors of the TRPM2 Cation Channel
Balázs Tóth, László Csanády.
Semmelweis University, Budapest, Hungary.
TRPM2 is a Ca^{2+} permeable cation channel which plays a role in physiological and pathophysiological processes linked to oxidative stress. TRPM2 channels are co-activated by intracellular Ca^{2+} and ADP ribose (ADPR). In addition, in intact cells, a large number of compounds appear to modulate TRPM2 activity. Superfusion of TRPM2-expressing cells with hydrogen-peroxide (H_2O_2) activates TRPM2 currents, just as intracellular dialysis of cyclic ADPR (cADPR) or nicotinic acid adenine dinucleotide phosphate (NAADP). Importantly, H_2O_2, cADPR, and NAADP enhance ADPR-induced TRPM2 whole-cell currents. Finally, in intact cells AMP acts as a TRPM2 inhibitor. Because in whole-cell recordings the entire cellular machinary involved in nucleotide- and Ca^{2+}-homeostasis is in place, compounds might affect TRPM2 activity either directly, by binding to the TRPM2 protein, or indirectly, by altering the local concentrations of the primary ligands ADPR and Ca^{2+}. To identify direct modulators of TRPM2 activity, we have studied the effects of H_2O_2, AMP, cADPR, NAADP, and nicotinic acid adenine dinucleotide (NAAD) in inside-out patches excised from *Xenopus* oocytes expressing human TRPM2, by directly exposing the cytosolic faces of the patches to these compounds. H_2O_2 (1 mM) and enzymatically purified cADPR (10 μM) failed to activate, while AMP (200 μM) failed to inhibit TRPM2 currents. NAADP acted as a partial agonist (maximal efficacy ~50%) while NAAD was a full agonist, but both with low affinities ($K_{0.5}$=104 and 35 μM). Neither of H_2O_2, cADPR, and NAADP enhanced activation by ADPR. Thus, in a physiological context the above compounds do not directly affect the TRPM2 channel protein. [OTKA grant F68143]

1695-Pos
Trpc3-Mediated Electrical Remodeling of Cardiac Myocytes
Zora Saad, **Klaus Groschner**.
University of Graz, Graz, Austria.
Recent evidence suggests a key role of transient receptor potential (TRP) channels in cardiac pathophysiology with TRPC3 as one potential key player in cardiac remodeling. TRPC3 is typically up-regulated by hypertrophic stimuli and may be involved in distorted Ca2+ signaling that drives pathological remodeling. As TRPC proteins generate non-selective cation conductances, we hypothesized that these channels may not only govern Ca2+-mediated gene expression but exert in addition a severe impact on basic electrical properties and excitability of the myocardium. Utilizing the patch clamp technique we characterized membrane currents and electrical properties of cardiomyocytes in response to enhanced TRPC3 expression in the murine HL-1 model. Stimulation of TRPC3-overexpressing HL-1 cells with endothelin-1 [100 nM] (ET-1) as a Gqi-PLC-activator gave rise to a conductance with features distinctly different from the properties described for TRPC3 conductance in expression systems. In HL-1 cells, the TRPC3 over-expression-induced conductance in physiological solutions reversed at about −50 mV, displayed profound outward rectification and was suppressed by the TRPC3-inhibitor Pyr3 [10 μM] (ethyl-1-(4-(2,3,3-trichloroacrylamide)phenyl)-5-(trifluoromethyl)-1H-pyrazole-4-carboxylate). As a result of this conductance, action potential duration was effectively shortened by ET-1 in HL-1 myocytes over-expressing the TRPC3, while this effect was minute in wild-type myocytes. Moreover, TRPC3 over-expression enabled significant depolarizing effects of ET-1 along with action potential shortening and reduction of refractory period. Our results suggests that increased expression of TRPC3 in cardiomyocytes may significantly contribute to electrical remodeling in hypertrophic hearts, generating changes in action potential morphology that are likely to promote arrhythmias.

1696-Pos
Critical Role of Pertussis Toxin Sensitive G Proteins in the Activation of TRPC4 and TRPC5 Channels
Rui Xiao[1], Jinbin Tian[1], Jisen Tang[1], Alexander V. Zholos[2], **Michael X. Zhu[1]**.
[1]The Ohio State University, Columbus, OH, USA, [2]Queen's University Belfast, Belfast, United Kingdom.
Canonical transient receptor potential 4 and 5 (TRPC 4 and TRPC5) are non-selective cation channels. Their activation causes membrane depolarization and intracellular Ca^{2+} increases. TRPC4 has been implicated in neurotransmitter release, endothelial-dependent regulation of vascular tone, endothelial permeability, and excitation-contraction coupling of intestinal smooth muscles while TRPC5 has been shown to be important for neurite extension and growth cone morphology and behavior responses to fear conditioning. The activation mechanisms of TRPC4/C5 remain unresolved. Most studies have indicated that stimulation of phospholipase C activates TRPC4/C5 channels. Using whole-cell patch clamp recording and fluorescence membrane potential measurements, we show here that $G_{q/11}$ signaling pathway alone is insufficient for the full activation of TRPC4/C5. Channel activities are greatly enhanced with co-stimulation of $G_{i/o}$-coupled receptors, including μ opioid, 5-HT_{1A} serotonin, M2 muscarinic, and D2 dopamine receptors. Stimulation of the $G_{i/o}$-coupled receptors alone also activates TRPC4/C5 in a pertussis toxin-sensitive manner. We further show that the effect of $G_{i/o}$ proteins cannot be attributed to the stimulation of phospholipase C-β through Gβγ subunits as activation of the $G_{i/o}$-coupled receptors induced no detectable intracellular Ca^{2+} signal unless TRPC4/C5 are co-expressed. In addition, the activated form of $G\alpha_{i/o}$ rather than Gβγ appears to be involved in the TRPC4/C5 activation. A

more direct role of $G_{i/o}$ proteins in TRPC4/C5 activation is supported by the demonstration that $G\alpha_i$ and $G\alpha_o$ subunits physically bind to the C-terminus of TRPC4. We suggest that a concerted action of $G_{q/11}$- and $G_{i/o}$-mediated signaling pathways is required for the full activation of TRPC4/C5, making these channels coincident detectors of multiple environmental cues. We have tested the co-dependence of native TRPC4/C5-like currents in smooth muscle cells, endothelial cells and neurons. (Supported by AHA Grant-in-Aid 0755277B and NIH grant RO1 DK081654)

1697-Pos
Function of Ion Channels in Cell Migration
Albrecht Schwab, **Albrecht Schwab**.
Universität Münster, Münster, Germany.
The prognosis of tumor disease is greatly influenced by the formation of metastases. A critical step of the socalled metastatic cascade is the ability of tumor cells to migrate away from the primary tumor. Ion channels and transporters are an an integral part of the cellular migration machinery that complement and regulate other components of the cellular motor. KCa3.1 channels for example are upregulated in many tumor cells. Their inhibition slows down migration and prevents its chemokinetic acceleration. KCa3.1 channel activity supports migration among others by inducing localized changes of cell volume at the rear part of crawling cells. TRPC1 channels are involved in coordinating the movement of the protruding front withe retracting rear part of migrating cells. Thus, genetic ablation of channels leads to a marked impairment of persistent migration. In addition, TRPC1 channels are also part of the cellular compass during directed migration in a chemotactic gradient. Silencing of TRPC1 activity by means of RNA interference or pharmacologically with GsMTx-4 impairs chemotaxis towards FGF-2. Reducing TRPC1 channel activity blocks directed cell migration as efficiently as does inhibition of particular steps of growth factor-induced signaling like phospholipase C or phosphatidylinositol-3-OH kinase. Taken together, ion channels are crucial for multiple aspects of tumor cell motility.

1698-Pos
A Combined Spectroscopic and Biochemical Approach to Counting MscL Subunits
Chris S. Gandhi[1], Troy A. Walton[1,2], Douglas C. Rees[1,2].
[1]California Institute of Technology, Pasadena, CA, USA, [2]Howard Hughes Medical Institute, Pasadena, CA, USA.
The mechanosensitive channel of large conductance (MscL) is a homooligomeric, stretch activated membrane protein responsible for regulating osmotic pressure in bacteria and archaea. Increasing membrane tension activates the protein resulting in a ~2.9 nS non-selective pore. Two MscL crystal structures have been solved in distinct conformations and oligomeric states. M. tuberculosis MscL is a non-conducting pentamer while S. aureus MscL is a partially expanded tetramer. The primary sequences of these proteins are 38% identical and 57% similar. Given their high relatedness, the structures raise interesting questions regarding the assembly and activation of MscL homologs. We have been interested in understanding the molecular determinants responsible for the differences between the two structures, specifically the switch between tetrameric and pentameric species. Using a combination of multi-angle light scattering and mass tagging followed by Blue Native PAGE, we have characterized the oligomeric states of several MscL homologs and chimeras. We find that the two methods are in good agreement with each other and single molecule measurements. Potential reasons for the differences in oligomeric states will be discussed.

1699-Pos
TREK Channel Pore Probed by Cysteine Scanning Mutagenesis and Structural Modelling
Paula L. Piechotta[1], Phill J. Stansfeld[2], Murali K. Bollepalli[1], Markus Rapedius[1], Isabelle Andres-Enguix[3], Lijun Shang[3], Hariolf Fritzenschaft[1], Mark S.P. Sansom[2], Stephen Tucker[3], Thomas Baukrowitz[1].
[1]Institut für Physiologie II, Friedrich-Schiller-Universität Jena, Jena, Germany, [2]Structural Bioinformatics and Computational Biochemistry Unit, Department of Biochemistry, University of Oxford, Oxford, United Kingdom, [3]Clarendon Laboratory, Department of Physics, University of Oxford, Oxford, United Kingdom.
The TREK channel belongs to the superfamily of two-pore-domain potassium channels (K2P-channels) that are made up of four transmembrane segments (TM1 - TM4) and two pore-forming domains that are arranged in tandem. The activity of these channels is directly regulated by the intracellular pH, heat, polyunsaturated fatty acids, phospholipids and mechanical stretch. Currently little is known about the pore structure and how these different stimuli gate the pore in structural terms. To this end we employed systematic cysteine scanning mutagenesis on the four TM domains and functionally characterised these mutants in several respects: I) using chemical cysteine modification we identified pore lining residues, II) by measuring detailed pH dose response curve we identified residues involved in the pH gating mechanism and III) by studying different pore blocking compounds we identified potential blocker interacting residues. These sets of functional data will be evaluated in the context of structural models of the TREK channel pore in the closed and open state.

1700-Pos
Coupling of Water Permeation with Mechano-Gating In the E-Coli Mechanosensitive Channel MscL
Yasuyuki Sawada[1], Masahiro Sokabe[1,2].
[1]Nagoya University Graduate School of Medicine, Nagoya, Japan.
[2]ICORP/SORST Cell Mechanosensing, JST, Nagoya, Japan.
The bacterial mechanosensitive channel of large conductance MscL is constituted of homopentamer of a subunit with transmembrane inner and outer α-helices, and its 3D structure of the closed state has been resolved. Understanding the gating process driven by tension in the membrane is one of the major subjects in MscL study. Although several models for its opening process have been proposed based on molecular dynamics (MD) simulations, as they do not include MscL-lipid interactions, it remains unclear which amino acids sense membrane tension and how the sensed force induces channel opening. We performed MD simulations for the mechano-gating of MscL embedded in the lipid bilayer. Upon tension generation in the bilayer, Phe78 in the outer helix was dragged by lipids, leading to a tilting of the helices. Among amino acids in the outer helix, Phe78 at the water-lipid interface showed the strongest interaction with lipids, thus may work as a major tension sensor. Neighboring inner helices cross each other in the inner leaflet, forming the most constricted part of the pore. In the closed state of MscL, Leu19 and Val23 in the constricted part form stable hydrophobic environment. As tension increased, the crossings moved toward the cytoplasm associated with an expansion of the constricted part and the hydrophobic environment was broken followed by water penetration and permeation. It seemed that water penetration and permeation accelerated the pore opening probably by decreasing the hydrophobic interaction between Leu19 and Val23. We performed MD simulations of the GOF mutant G22N with almost the same pore size of the wild type, and found that G22N mutant permeated water molecules without tension increase in the bilayer. This spontaneous water permeation seemed to be mediated by hydrogen bonds between Asn22 and water molecules.

1701-Pos
Significance of the *Corynebacterium Glutamicum* YggB Protein in Fine-Tuning of Compatible Solute Accumulation
Kirsten Börngen[1], Andrew R. Battle[2], Nina Möker[3], Susanne Morbach[3], Kay Marin[3], Boris Martinac[4], **Reinhard Krämer**[3].
[1]University of Cologne, Köln , Germany, [2]University of Queensland, Brisbane, Queensland, Australia, [3]University of Cologne, Köln, Germany, [4]Victor Chang Cardiac Research Institute, Sydney, New South Wales, Australia.
Based on structural similarity, the *yggB* gene product of *Corynebacterium glutamicum* belongs to the family of MscS-type mechanosensitive channels. In order to clarify its physiological significance in response to osmotic shifts in detail, we studied the properties of YggB using both patch-clamp techniques and betaine efflux kinetics. After heterologous expression in an *E. coli* strain devoid of mechanosensitive channels, in patch-clamp analysis of giant *E. coli* spheroplasts YggB showed the typical pressure dependent gating behavior of a stretch-activated channel with a current/voltage dependence indicating a strongly rectifying behavior. Apart from that, YggB is characterized by significant functional differences with respect to conductance, ion selectivity and desensitation behavior as compared to MscS from *E. coli*. Deletion and complementation studies in *C. glutamicum* showed a significant contribution of the YggB protein to betaine efflux in response to hypoosmotic conditions. As a novel finding, detailed analysis of concomitant betaine uptake (by the betaine transporter BetP) and efflux (by YggB) under hyperosmotic conditions revealed that YggB acts as a key player in osmoregulation in *C. glutamicum* by fine-tuning the steady state concentration of compatible solutes in the cytoplasm which are accumulated in response to hyperosmotic stress.

1702-Pos
Measuring the Release of Fluorescein from MscL-Loaded Liposomes with Stressed Lipid Bilayers
Alexander Foo[1], Andrew R. Battle[1], Brad J. Marsh[1], Ben Hankamer[1], Boris Martinac[2].
[1]The University of Queensland, Brisbane, Queensland, Australia, [2]Victor Chang Cardiac Research Institute, Sydney, New South Wales, Australia.
The bacterial mechanosensitive ion channel of large conductance (MscL) acts as an emergency release valve to protect against osmotic stress[1,2]; its pore diameter is estimated to increase by >25Å on opening[3,4]. To investigate mechanisms for controlling the gating of this channel for use in targeted drug delivery systems, we have encapsulated the fluorescent dye 5,6-carboxyfluorescein (CF) into liposomes (diam. 100 nm) via sonication and extrusion using the Liposo-Fast system, followed by incorporation of MscL protein. Functional assays of MscL by patch-clamping confirmed that the dye did not affect the protein incorporation, and unencapsulated dye was removed by column purification. Liposomes were incubated with different concentrations of the amphipath L-α-Lysophosphatidylcholine (LPC) dissolved in ~3% MeOH for 30 min to induce stress on liposomal membranes[5]. Dye release from the liposomes via MscL was monitored as increased fluorescence in the external medium. The percentage fluorescence change quantified using a BMG Omega Polarstar Reader (excitation at 485nm and emission at 535nm). Based on these results, we demonstrate cargo release by MscL by means of manipulating the curvature of liposome membranes[4].
1. Martinac, B., *J. Cell Sci.*, **117**, 2449-2460 (2004).
2. Perozo, E., *Nat. Rev. Mol. Biol.* , **7**, 109-119 (2006).
3. Cruickshank, C.C., Minchin, R., Le Dain, A., and Martinac, B. Biophys J **73,** 1925-1931 (1997)
4. Perozo, E., Cortes, D.M., Sompornpisut, P. Kloda, A. and Martinac, B. Nature 418: 942-948 (2002)
5 Perozo, E., Kloda, A., Cortes, D.M., Martinac, B., *Nat. Str. Biol.* 9, 696-703(2002)
Supported by grants from the Australian Research Council (ARC) and National Health and Medical Research Council (NHMRC). A.Foo is a UQ Scholarship recipient.

1703-Pos
Osmotically Challenging Single Escherichia Coli Cells: 1,2,3,Ready,Burst!
Elvis Pandzic, Stephanie Deboeuf, Paul Wiseman, Maria Kilfoil.
McGill University, Montreal, QC, Canada.
We use high spatial and temporal resolution spinning-disk confocal microscopy, fluorescent-labeling strategies, and automated image analysis to investigate the response of the mechanosensitive channel MscL to osmotic stress in living E. coli bacteria. We establish the viability of individual cells using a red-fluorescent nucleic acid stain, propidium iodide, and correlate it with cellular levels of EGFP-tagged MscL. We demonstrate that MscL promotes integrity of the cell membrane in the face of environmental osmotic pressure. For these experiments, a micro-fluidic device with temperature control and multi-generational capability was developed to determine which cells are viable and dividing following exposure to osmotic stress, and to study the ability of cells to recover from temporally varying stress stimuli.

1704-Pos
The Role of MscS Cytoplasmic Domain As An Osmolyte Filter
Ramya Gamini[1], Marcos Sotomayor[2], Christophe Chipot[3], Klaus Schulten[1].
[1]University of Illinois at Urbana Champaign, Urbana, IL, USA, [2]Harvard Medical School, Boston, MA, USA, [3]Nancy Universite, Nancy, France.
Mechanosensitive (MS) channels, inner membrane proteins of bacteria, open and close in response to mechanical stimuli such as changes in membrane tension during osmotic stress. In bacteria, these channels act as safety valves thus preventing cell rupture upon hypoosmotic shock.The MS channels of small conductance, MscS, are homoheptameric and consist of a large cytoplasmic (CP) domain that features a balloon-like, water filled chamber opening to the cytoplasm through seven side pores and a small distal pore. This CP domain is considered to be a molecular sieve, which prevents a loss of essential osmolytes and metabolites at the cytoplasmic side. In bacteria, glutamate is a predominant anion that helps to maintain potassium pools at an optimum level and also is a prevalent osmoprotectant maintaining the cell turgor. We have explored, using molecular simulations, the free energy landscape characterizing the translocation and exit of a glutamate ion through one of the side pores, to illustrate the role of the CP domain in selective filtering of glutamate. The adaptive biasing force (ABF) method is applied to the glutamate molecule to determine the free energy barrier along the chosen translocation pathway. The transport kinetics of glutamate based on the measured free energy profile, suggests the presence of an entropic barrier that slows down the passage of glutamate through the pore but lets water pass quickly. A low enthalpic barrier of ~4 k_BT is sufficiently low to prevent glutamate from clogging the pore. Analysis of the electrostatic potential of the CP domain indicates that the CP interior presents an environment relatively unfavorable for anions.

Biophysics of Ion Permeation

1705-Pos
Cholesterol Deficiency, Statins and Rhabdomyolysis
Thomas H. Haines.
Rockefeller University, New York, NY, USA.
Cholesterol's (CH) function cannot be to stiffen membranes because: 1) We synthesize CH but cannot burn it for energy; 2) Mankind has over 100 genes devoted to CH management, regulation, trucking, biosynthesis, degradation, etc. 3) Unlike CH plant sterols have branches on their sidechains. 4) Most cultured animal cells die without CH. 5) We have >2 ABC intestinal transporters that selectively block phytosterol uptake. 6) The lipid mole fraction of CH rises and falls with the $[Na^+]$ that faces the membrane. Literature evidence is here gathered that shows cells in vivo leak Na^+ due to the $\Delta\Psi$ and the blood $[Na^+]$ which is 0.1M. Although the Na^+ leakage is slow (10^{-12} cm/sec) compared to H^+ leakage (10^{-5} cm/sec), the high $[Na^+]$ makes them equivalent. Furthermore the presence of 1/3 mole% CH, as typically found in membranes facing blood, reduces the Na^+ leakage to 1/3 that found in bilayers lacking CH. FDA data suggest excess statins taken by ~200 patients in the last 8 years resulted in lethal rhabdomyolysis (RH). If cholesterol's function is to limit Na^+ leakage (Prog. Lipid Res. 40 (2001) 299), then 3 times as much ATP is needed to compensate for leaked Na^+. Muscle cells, lacking a pentose shunt cannot make much NADPH, which is essential for CH synthesis. Such a CH deficiency in muscle would provoke Na^+ leakage into cells that may burst because of osmotic swelling. A common feature of RH in autopsies is that salt is found in the muscle cells. Due to the branches on their side chains, plant sterols appear to be designed to inhibit H^+ leakage (op cit.). They are only found where the plasma membrane has a H^+ gradient. CH is only found in cells where the plasma membranes facing Na^+.

1706-Pos
Ion Channel Activity of Pentameric Phospholamban
Serena Smeazzetto[1], Michael Henkel[2], Tommaso Ferri[3], Gerhard Thiel[2], Maria Rosa Moncelli[1].
[1]University of Florence, Sesto Fiorentino, Firenze, Italy, [2]Technische Universität Darmstadt, Darmstadt, Germany, [3]University of Rome ''La Sapienza'', Roma, Italy.
Phosholamban (PLN) is an integral membrane protein, which is involved in the contractility of cardiac muscles by regulating the sarco/endoplasmic CaATPase (SERCA). PLN exists in equilibrium between monomer and pentamer. Monomeric, unphosphorylated PLN inhibits SERCA, whereas PLN phosphorylation releases the inhibition and allows calcium translocation into sarcoplasmic reticulum. The pentameric PLN structure (1,2) and its possible activity as ion channel (3,4) are still a matter of debate. In order to understand if PLN pentamer can have ion channel activity, we have performed experiments by using two different biomimetic systems, namely supported nanoBLMs and traditional BLMs.
Conductivity measurements on nanoBLMs show that PLN pentamer can form a pore, which is permeable to small ions such as Na^+, Cl^- and ClO_4^-, but not to the bigger choline (Cho^+) ion (radius 3,3Å). These data are in agreement with the hypothesis of Oxenoid and Chou (1), according to which the narrowest part of the wt-PLN pentamer is about 3,6Å in diameter. Moreover, single channel recordings on BLMs reveal independent current fluctuations between a closed and a defined opening state at two distinctly different conductances. Also in previous experiments small unitary channel fluctuations with two different conductances were observed (5).
In conclusion the present results and previous works (1,5), support the view that PLN works as an ion channel.
We thank G. Veglia for providing phosphplamban and Ente Cassa di Risparmio di Firenze for financial support.
1.K.Oxenoid and J. Chou Proc Natl Acad Sci U S A. (2005) 102, 10870-5.
2.N. J. Traaseth et al. Proc. Natl. Acad. Sci. U S A. (2007) 104, 14676-14681.
3.T. Kim et al. Proteins. (2009) 76, 86-98.
4.L. Becucci et al. Biophys. J. (2009) 96, L60-L62.
5.R. Kovacs et al. J. Biol. Chem. (1988) 263, 18364-18368.

1707-Pos
Molecular Dynamics of Trace Amine Transport through Neuronal Membranes
Bruno L. Tomberli[1], Jarrod Nickel[1], Mithila Shitut[2], Mark D. Berry[1,2].
[1]Brandon University, Brandon, MB, Canada, [2]University of Saskatchewan, Saskatoon, SK, Canada.
The trace amines are a family of endogenous compounds, synthesized in neurons, for whom a family of receptor proteins has been identified. Unlike neurotransmitter receptors, trace amine receptors do not appear to be expressed at the plasma membrane of cells, rather remaining in the cytosol. This requires trace amines readily cross the lipid bilayer in order to interact with the receptor and effect signal tranduction. It has previously been assumed that this occurs via passive diffusion. However, the unknown rate of passive diffusion in allowing trace amines to cross the synaptic cleft has hindered the progress of recent studies attempting to determine their physiological role (M.D. Berry, *J. Neurochem*, **90**, 257-271, (2004), A. G. Ianculescu *et al*, Endocrinology, **150**, 1991 (2009)). Molecular dynamics (MD) simulations have been carried out to determine the position dependent diffusion constant, $D(z)$,and the Potential of Mean Force (PMF) of several trace amines both inside and outside the membrane. From this data, the trace amine flux through the membrane can be calculated. Using specialized free energy simulation techniques, MD trajectories have been generated and analyzed to determine the mean force exerted on the trace amines, 2-phenylethylamine (2PE), its protonated form, 2PE+ and on 3-iodothyronomine, at distances ranging from 20 angstrom right to the middle of a symmetric sphingomyelin membrane. Preliminary results indicate a potential barrier ~13 Kcal/mol for 2PE+ and ~20Kcal/mol for 2PE. These relatively high potential barriers are consistent with a very low transmembrane flux due to passive diffusion. The contribution this information makes to the question of yet-undiscovered transporters for trace amines is discussed in the conclusions.

1708-Pos
Induction of Liposome Leakage by Photodynamic Action: Dependence on the Kind of Fluorescent Probe
Yuri Antonenko, Aleksey Kuzevanov, Alina Pashkovskaya, Elena Kotova.
Belozersky Institute, Moscow State University, Moscow, Russian Federation.
Photosensitized damage to liposome membranes was studied by using different dye-leakage assays based on fluorescence dequenching of a series of dyes upon their release from liposomes. Irradiation of liposomes with red light in the presence of a photosensitizer, trisulfonated aluminum phthalocyanine ($AlPcS_3$), resulted in the pronounced leakage of carboxyfluorescein, but rather weak leakage of sulforhodamin B and almost negligible leakage of calcein from the corresponding dye-loaded liposomes. The photosensitized liposome permeabilization was apparently associated with oxidation of lipid double bonds by singlet oxygen as evidenced by the requirement of unsaturated lipids in the membrane composition for the photosensitized liposome leakage to occur and the sensitivity of the latter to sodium azide. The fluorescence correlation spectroscopy measurements revealed marked permeability of photodynamically induced pores in liposome membranes for such photosensitizers as $AlPcS_3$ and $AlPcS_4$. It was proposed that the difference in permeability of these pores to carboxyfluorescein and calcein was associated with size restriction. Verification of this hypothesis by studying the effect of PEGs of different molecular weights is under way.

1709-Pos
Intrinsic Versus Extrinsic Voltage Sensitivity of Blocker Interaction with an Ion Channel Pore
Juan R. Martinez-Francois, Zhe Lu.
Howard Hughes Medical Institute, Department of Physiology, University of Pennsylvania, Philadelphia, PA, USA.
Many physiological and pharmacological agents act by occluding the conduction pore of ion channels. A hallmark of charged blockers is that their apparent affinity for the pore usually varies significantly with membrane voltage. Two models have been proposed to explain voltage dependence of channel block. One model - prevalent during the past three decades - assumes that the charged blocker itself directly senses the transmembrane electric field, i.e., that blocker binding is intrinsically voltage dependent. In the alternative model, the blocker does not directly interact with the electric field; instead, blocker binding acquires apparent voltage dependence solely through the concurrent movement of permeant ions across the field. Although less frequently invoked, this latter model may better explain voltage dependence of channel block by large organic compounds that are too bulky to fit into the narrow part of the pore where the electric field is steep. To date no systematic investigation has been carried out to distinguish between these voltage-dependent mechanisms of channel block. When the voltage dependence of block by organic compounds is believed to be extrinsic, it has never been demonstrated that the block can be rendered voltage independent - the most fundamental characteristic of the extrinsic mechanism. In the present study we find that a retinal cyclic nucleotide-gated (CNG) channel can be blocked via either mechanism, depending on the nature of the blocker. With this channel as a model, we systematically examine both intrinsic and extrinsic types of voltage dependence of channel block, and illustrate their electrophysiological hallmarks and analytical characteristics.

1710-Pos
Self-Consistent Calculations of the Current and Access Resistance in Open Ion Channels
Rodrigue Tindjong.
Lancaster University, Lancaster, United Kingdom.
The problem of calculating the current and access resistance in open ion channels is considered. A self-consistent analytic solution is introduced for an arbitrary number of species within the Poisson-Nernst-Planck (PNP) equations formalism. The model considered is a cylindrical channel of radius a in the protein which allows ions to cross a membrane that is bathed by two solutions of different concentration on its left and right-hand sides. Electro-diffusion in this system is described by the Poisson equation combined with the continuity equations for the mobile ions. The PNP equations are solved in the bulk in the Boltzmann approximation in 3D, assuming spherical symmetry, and in the pore in a 1D approximation. The boundary conditions (BCs) for the potential and concentration are set at infinity. The internal BCs for the current and the gradient of the potential are set at the surfaces of two hemispheres of radius a. The two solutions are matched together at the internal BCs using an iterative procedure in a self-consistent way. The method allows for calculation of the currents for an arbitrary number of ions species that have different diffusion constants in the channel and in the bulk. The sizes of the ions are taken into account by introducing a ''filling factor'' as an additional fitting parameter. The method is applied to model experimental I-V characteristics of the Gramicidin A channel for various concentrations, yielding qualitative good agreement.

1711-Pos
Effect of Charge Fluctuations on Conduction in Biological Ion Channels
Rodrigue Tindjong.
Lancaster University, Lancaster, United Kingdom.
How open ion channels are able to conduct ions with a throughput comparable to free diffusion, and yet remain highly selective, is an unresolved scientific conundrum of long standing. To shed new light on this problem, the effect of charge fluctuations on the conduction of open ion channels is investigated theoretically. The model considered is a cylindrical channel across the membrane bathed by two solutions of different concentration. The charge fluctuations at the channel mouth are analyzed using Brownian Dynamics simulations and shown to have the form of trichotomous noise on the timescale of nanoseconds. The channel potential with a local minimum at the selectivity site due to the fixed wall charge is calculated by solution of the 3D Poisson equation for two configurations, with one ion moving along the channel axis in the presence or absence of the fluctuating charge at the channel mouth. It is shown that narrow channels act as electrostatic amplifiers of the modulation of the potential barriers at the selectivity site, due to charge fluctuations at the channel mouths. This modulation at the selectivity site was largely neglected in earlier research. It results in a leading order contribution to the transition rates of open ion channels. The proposed model of ion permeation takes into account the dynamical effect of the charge fluctuations through the resultant shot noise, which flips the electrostatic potential at the selectivity site, causing it to fluctuate between three values at a rate corresponding to the random arrivals of ions at the channel mouth. The model is applied to calculation of the current-voltage characteristics of Gramicidin A channel for different concentrations and is shown to be in good agreement with experimental results, including the effect of current saturation at high concentrations.

1712-Pos
Free Energy Calculations along Complex Proton Transport Pathways
Yong Zhang, Gregory A. Voth.
University of Utah, Salt Lake City, UT, USA.
Ion transport processes through protein channels is an essential component of cellular function. One especially interesting example is the ClC-ec1 antiporter, which transports proton (H^+) and chloride ions (Cl^-) in opposite directions with a stoichiometric ratio of 1:2. In this work, the multistate empirical valence bond (MS-EVB) molecular dynamics method has been applied to simulate the explicit translocation of a Grotthuss shuttling excess proton from the intracellular residue Glu203 to the extracellular residue Glu148 through a transient water chain inside the channel. The minimum energy proton transport pathway was first identified using the string method and the free energy profile, i.e., the

potential of mean force (PMF), was calculated along the path. The electrostatic coupling between the excess proton and chloride ion was also explored. These studies therefore provide a more detailed picture of the proton transport process in the ClC-ecl antiporter.

1713-Pos
Ion Selectivity in the Aspartate Transporter Glt_{PH}
Michael Thomas, Dylan Jayatilaka, Ben Corry.
University of Western Australia, Perth, Australia.
The aspartate transporter Glt_{PH} is an integral membrane protein that catalyses the movement of aspartate across lipid bilayers. Glt_{PH} utilises established ion gradients, transporting two sodium ions with each aspartate molecule. Previous studies have shown that the ion binding sites demonstrate selectivity for Na^+ over both Li^+ and K^+ ($Na^+ > Li^+ > K^+$) [1]. The sodium binding motif is similar to that of another sodium dependent leucine transporter, LeuT. Computational studies have attributed different mechanisms to ion selectivity in each of the two sodium binding sites in LeuT [2]. Selectivity in the first site results from the binding of the negatively charged carboxylate group of the substrate resulting in strong electrostatic interactions while selectivity in the second site is enforced by an almost rigid cavity of coordinating ligands held in place hydrogen bonding networks.
Using various computational techniques, we describe the thermodynamic contributions to the free energy of binding that give rise to the experimentally observed selectivity sequence $Na^+ > Li^+ > K^+$ in Glt_{PH} and compare and contrast them to those in LeuT.
[1] Boudker, O. et al. Nature 2007, 445, 387-393
[2] Noskov, S.; Roux, B. J. Mol. Biol. 2008, 377, 804-818

1714-Pos
Microscopic Mechanism of Ion Selectivity in the Nak Pump
Haibo Yu[1], Pablo Artigas[2], Benoit Roux[1].
[1]Department of Biochemistry and Molecular Biology, University of Chicago, Chicago, IL, USA, [2]Department of Cell Physiology and Molecular Biophysics, Texas Tech University Health Science Center, Lubbock, TX, USA.
The sodium/potassium pump establishes the Na+ and K+ concentration gradients across the plasma membrane of animal cells and therefore plays an essential role in maintaining cell volume and secondary active transport of other solutes. The crystal structures of the Na+/K+ pump provide atomic insight into the binding of K+ ions and conformational transitions during the functional cycle. However, important details about the ion-selectivity remain to be addressed. In particular, 2 out of the 3 binding sites are shared between Na+ and K+ and it is not clear how this pump selects K+ over Na+ when in the outwardly facing conformation (E2P) or Na+ over K+ when in the inwardly facing conformation (E1). We have undertaken free energy calculations to understand the physical principles that govern the ion selectivity in Na+/K+ pump and dissected various factors that may contribute to the selectivity. We found that the pump elegantly modulates the electrostatic environment of the binding sites to achieve the corresponding selectivity. Our results are consistent with available experimental data and provide new hypothesis to test experimentally. [Supported by NIH grant GM062342].

1715-Pos
The Role of Architectural and Structural Forces in Ion Selectivity
Haibo Yu[1], Sergei Y. Noskov[2], **Benoit Roux**[1].
[1]University of Chicago, Chicago, IL, USA, [2]University of Calgary, Calgary, AB, Canada.
A novel theoretical framework is presented to clarify the role of architectural and structural forces in ion selectivity by expressing the relative free energy of bound ions in terms of a reduced local system coupled to a potential of mean force (PMF) representing the influence of the surrounding environment. The PMF is separated into two contributions. The first includes all the harsh forces keeping the ion and the coordinating ligands confined to a small microscopic region, but do not prevent the ligands from adapting to ions of different radii. The second regroups all the remaining forces that serve to dictate a precise geometry of the coordinating ligands best adapted to a given ion. In the limit where the precise geometric forces are dominant, the binding site is almost rigid and ion selectivity is controlled by the ion-ligand interactions according to the classic ''snug-fit'' mechanism of host-guest chemistry. In the limit where the precise geometric forces are negligible, the ion and ligands behave as a self-organized ''confined droplet'' that is free to fluctuate and adapt to a smaller ion. But selectivity can also occur under such conditions. In the small and crowded volume, ion selectivity is determined by the ion-ligand and ligand-ligand interactions and is controlled by the number and the chemical type of ion-coordinating ligands. The theoretical framework is used to analyze K+ binding sites in the KcsA channel and Na+ binding sites in the LeuT transporter.

1716-Pos
Mechanisms of Ion Permeation through Gramicidin a Channels
Yuhui Li[1], Olaf S. Andersen[2], Benoit Roux[1].
[1]Department of Biochemistry and Molecular Biology, The University of Chicago, Chicago, IL, USA, [2]Department of Physiology and Biophysics, Weill Medical College of Cornell University, New York, NY, USA.
Gramicidin A (gA) channels make an ideal system to test all-atom molecular dynamics (MD) of membrane proteins and mechanisms of ion permeation. In addition to being the most studied membrane ''protein'', gA channels are tiny, allowing for long MD runs and calculations of potential of mean force (PMF) in tractable time. The binding sites at either end of the gA channel can both hold a single cation. At low concentration, permeation occurs as a series of independent events in which one cation at a time moves across the pore. Ion permeation usually is described using the ion position z in the direction of the pore axis as a ''reaction coordinate''. But it is not known whether z is a good reaction coordinate to describe the process. A powerful tool to characterize the mechanism of ion permeation in the gA channel is the ''committor'' probability: the fraction of trajectories initiated from a given position that first commit to the left or right binding site of the channel. We evaluate the committor probability distribution function to identify the physical reaction coordinates of a K+ in gA using extensive MD calculations. At high concentration, permeation is dominated by 2-ion processes where cations are bound at either ends of the small pore. To understand the impact of double ion occupancy on the mechanism of ion permeation, we calculate the 2-ion PMF. The results show that if the first ion resides in the inner binding sites at one end of the channel, then the outer and inner binding sites for the second ion at the other end of the channel become shallow. The energetics of double occupancy is explained by considering the dipole moment fluctuation of the single-file water molecules inside channel. [Supported by NIH grant GM070971].

1717-Pos
Thermodynamically Dominant Hydration Structures of Ions and their Role in Ion-Specificity
Safir Merchant, **Dilip Asthagiri**.
Johns Hopkins University, Baltimore, MD, USA.
To understand the basis of ion-specific effects in biology, it is necessary to first understand the hydration structure and thermodynamics of ions. Based on a multi-state organization of the potential distribution theorem, we present new insights on the role of ion-water interactions and water density fluctuations at the size-scale of the ion in determining the ion-hydration structure and thermodynamics. We find that the hydration free energy of the ion depends on three quantities: 1) the hydration free energy of the ion in a specified n-coordinate state, where in the n-coordinate state n water molecules are present within the coordination volume of the ion; 2) the probability, xn, of observing that n-coordinate state around the ion; and 3) the probability, pn, of observing n water molecules in the coordination volume in the absence of the ion. Based on this development we find that only a small subset of water molecules in the first hydration shell of the ion sense the chemical type of the ion. Further, these core-water molecules tend to attenuate the interaction of the ion with the rest of the medium, and thus the higher coordination states of the ion more sensitively reflect density fluctuations of the solvent medium at the size scale of the observation volume. The relevance of this development in understanding ion-pairing and the selective binding of ions to biological molecules is discussed.

1718-Pos
On the Domain of Applicability of Currently used Force Fields for the Calculation of the Activity of Alkali Ions at Physiological Ionic Strength
Chao Zhang[1], Simone Raugei[1], Bob Eisenberg[2], Paolo Carloni[1].
[1]SISSA, Trieste, Italy, [2]Rush Medical Center, Chicago, IL, USA.
Alkali ions are present in virtually all biological processes. Their energetic properties have been so far predicted mostly by MD or MC calculations based on effective potentials derived for infinite diluted conditions (i.e. a single ion surrounding solely by water molecules) [1]. However, in physiological conditions, the concentration of K+ is sub-molar in the cytoplasm [2], and it may be by one, or even two, orders of magnitude larger near globular proteins or nucleic acids and in the active sites of of enzymes or channels [3-5]. The presence of a large ionic strength I is likely to limit the accuracy of the currently used potentials.
Here we will discuss recent calculations of the activity coefficients for K+,Na+ ions at increasing I. Such coefficients have been obtained by calculating the excess chemical potentials from thermodynamics integration [6], with several commonly used biomolecular force fields. Preliminary results show that classical force fields generally overestimate the activity coefficients of ions.
[1] M. Patra and M. Karttunen. J. Comput. Chem., 25:678-689, 2004.

[2] F.M. Ashcroft. Ion Channels and Disease. Academic Press, 1999.
[3] D. A. Doyle, J. M. Cabral, R. A. Pfuetzner, A. Kuo, J. M. Gulbis, S. L. Cohen, B. T. Chait, and R. MacKinnon. Science, 280:69-77, 1998
[4] C. Domene, S. Vemparala, S. Furini, K. Sharp, and M. L. Klein. J. Am. Chem. Soc, 130:11, 2008.
[5] P. Auffinger and Y. Hashem. Curr. Opin. Stru. Biol, 17:325-333, 2007.
[6] M. Ferrrario, G. Ciccoti, E. Spohr, T. Cartailler, and P. Turq. J. Chem. Phys., 117:4947-4953, 2002

1719-Pos
Voltage Profile along the Permeation Pathway of an Open Channel
Jin Chen[1], Jorge E. Contreras[1], Albert Y. Lau[2], Vishwanath Jogini[2], Benoît Roux[2], Miguel Holmgren[1].
[1]NINDS, Bethesda, MD, USA, [2]Department of Biochemistry and Molecular Biology, The University of Chicago, Chicago, IL, USA.
In ion channels, the transmembrane potential plays a critical role in ion conduction by acting as a driving force for permeant ions. At the microscopic level, the transmembrane potential is thought to decay non linearly across the ion permeation pathway because of the irregular three-dimensional shape of the channel pore. To experimentally explore the voltage profile of an open channel, we studied the voltage dependence of chemical modification of cysteines substituted along the permeation pathway of cyclic nucleotide-gated (CNG) channels. Because ion conduction through these channels is not sensitive to voltage at maximal open probabilities, nor they desensitize or inactivate when exposed to ligand, CNG channels are an ideal model to these studies. Our functional observations indicate that most of the voltage drop across the permeation pathway occurs along the selectivity filter region of CNG channels. The experimental data are in good agreement with continuum electrostatic calculations using a homology model of an open CNG channel. The focusing of the transmembrane potential across the selectivity filter indicates that the electromotive driving force is coupled with the movement of the permeant ions in the filter, maximizing the efficiency of this process.

1720-Pos
Microscopic Mechanism of Ion Permeation through K^+ Channel
Takashi Sumikama[1], Iwao Ohmine[2], Shigetoshi Oiki[3].
[1]Institute for Molecular Science, Okazaki, Aichi, Japan, [2]Kyoto University, Kyoto, Kyoto, Japan, [3]Fukui University, Yoshida, Fukui, Japan.
One of the most basic roles of ion channel is the passive transport of ions through the hydrophilic pore enabling the dehydration of ions. Since the determination of the x-ray crystallographic structure of the K^+ channel, many theoretical studies on the ion permeation have been performed. However, the microscopic mechanism of ion permeation, the essence of ion channel, has not been clarified yet.
We study the passive transport of ions through the K^+ channel, Kv1.2, by the molecular dynamics simulation in which the electric field is applied. A number of ion permeation is successfully observed. The number of permeated ion, i.e., the channel conductance is mostly proportional to the ion concentration of the bulk. The number of ions in the central cavity also depends on the ion concentration. Although the ions and water molecules are transported alternately, surprisingly, the other manner of ion permeation is also observed. That is, ions can permeate without intervening water molecule at high concentration, on the other hand, a permeating ion is accompanied by two water molecules at low concentration. Therefore, the microscopic mechanism of ion permeation depends on the ion concentration, and the physiological fact that an ion permeates per a water molecule is considered to be the average of these two cases. We also discuss the role of the central cavity by comparing the ion permeation in the channel with that in the model channel.

1721-Pos
Multi-Ion Mechanism of Potassium Channel Rejection of Na and Li Ions
Ilsoo Kim, Toby W. Allen.
University of California, Davis, CA, USA.
Ion channels catalyze rapid and selective ion movement across cell membranes to control electrical and chemical activity in the body. Potassium channels have the remarkable ability to pass K ions at near diffusion-limited rates, while exquisitely blocking Na ions. The mechanisms of channel selectivity, based on simulation and experimental studies of KcsA blocking by Na and Li ions, will be discussed. Through free energy perturbation and potential of mean force calculations, we find that Na and Li can bind deep into the S4 site of the selectivity filter, coordinated by a plane of four carbonyl oxygen atoms, rather than the usual eight-ligand cage of K. However, we demonstrate that a different multiple-ion mechanism is required for Li or Na ion entry into the filter from the aqueous cavity, involving large energetic barriers that are not encountered by K. We also revisit calculations of the thermodynamic stability of these ions in other sites of the filter, within the framework of a multiple-ion free energy calculation, with some surprising results. We conclude that, under physiological conditions, the rejection of intracellular Na or Li from KcsA occurs upon entry to the filter and is not due to reduced thermodynamic stability at any site inside the filter.

1722-Pos
Exploring the Permeation Mechanism of Valinomycin Across Lipid Membranes
Borislava Bekker, Toby W. Allen.
University of California, Davis, CA, USA.
Valinomycin is a potassium specific ionophore used to transport ions down an electrochemical gradient across lipid membranes. Its small size, high selectivity, and strong antibiotic activity make it an interesting target for molecular dynamics simulations. At the same time its conformational flexibility, which strongly depends on the polarity of its environment, poses a challenge. This work was undertaken in order to elucidate the mechanism of valinomycin mediated potassium transport across a lipid bilayer. We have explored several advanced sampling techniques, but chose to perform multi-dimensional free energy calculations that explore conformational space while computing the potential of mean force for membrane translocation. By computing free energy surfaces with and without a bound K^+ ion and calculating the free energetics of the ion binding process, we can describe a cycle that reveals the overall permeation mechanism. Our results using implicit and explicit solvent and membrane models will be discussed.

1723-Pos
Investigating Ion Channels using Chemical Synthesis
Francis Valiyaveetil.
Oregon Health And Science University, Portland, OR, USA.
Chemical synthesis is a powerful method for precise modification of the structural and electronic properties of proteins. The difficulties in the synthesis and purification of peptides containing transmembrane segments have presented obstacles to the chemical synthesis of integral membrane proteins. We will present a modular strategy for the semi-synthesis of integral membrane proteins in which solid phase peptide synthesis is limited to the region of interest, while the rest of the protein is obtained by recombinant means. This modular strategy considerably simplifies the synthesis and purification steps that have previously hindered the chemical synthesis of integral membrane proteins. We will discuss a sandwich-intein fusion strategy and a sumo-fusion and proteolysis approach for obtaining the membrane spanning peptides required for the semi-synthesis. We will demonstrate the feasibility of the modular approach by the semi-synthesis of the K^+ channel, KcsA and the non-selective cation channel NaK. The use of chemical synthesis in functional investigations of the KcsA and the NaK channels will also be presented.

1724-Pos
$[K^+]$ Induced Conformational Dynamics of the Selectivity Filter of KcsA Monitored by Solid-State NMR
Manasi Bhate, Benjamin Wylie, Lin Tian, Ann McDermott.
Columbia University, New York, NY, USA.
A solid-state NMR study of the selectivity filter of the prokaryotic potassium channel KcsA in a lipid bilayer is presented. The selectivity filter is highly conserved in both bacterial and mammalian channels and chelates K^+ very specifically. The selectivity filter is known to exist in many different conformations depending on the identity and local concentration of the permeant ion. Transitions between these different conformations have not been quantitatively characterized in a native bilayer environment. We have used 2D and 3D heteronuclear correlation spectra to site-specifically assign residues in full-length KcsA reconstituted into a lipid bilayer. We report two distinct conformations of the selectivity filter of KcsA in the presence of K^+ and Na^+. We report significant changes in the chemical shifts of key residues in the filter as the permeant ion is changed from K^+ to Na^+. Chemical shift analyses using the SPARTA database indicate that the observed conformations are consistent with a K^+-bound and a Na^+-bound state. Solid-state NMR characterization of both the K^+ and the Na^+ bound state is important for ensuing studies of channel dynamics, for which, these conformations can be considered limiting structures. Simultaneous detection of both conformers at low ambient K^+ suggests that the K^+ and the Na^+ bound states are in slow exchange on the NMR timescale ($<500\ s^{-1}$).

1725-Pos

The E71A Mutation Alters Selective Ion Permeability in KcsA

Wayland W.L. Cheng, Colin G. Nichols.
Washington University School of Medicine, Saint Louis, MO, USA.

The mechanism of selectivity in potassium channels has been extensively studied using the prokaryotic potassium channel, KcsA. Computational studies suggest that a glutamate-aspartate H-bond behind the selectivity filter in KcsA may play a role in determining the permeation properties of the channel. However, the mutant E71A , which disrupts this H-bond interaction and abolishes pH-dependent inactivation is reported to have either no effect on K+ selectivity (1) or to increase K+ selectivity (2) as measured by reversal potentials. Using an 86Rb+ flux assay, WT KcsA exhibits strong K+ selectivity, such that there are no measurable 86Rb+ fluxes supported by Na+ and Li+. In contrast, both Na+ and Li+ support significant 86Rb+ fluxes in the E71A mutant, indicating an enhanced Na+ and Li+ permeability.

In eukaryotic inward rectifying potassium channels (Kir), the E71 equivalent residue is part of a glutamate-arginine salt bridge that, when disrupted dramatically reduces K+ selectivity. KirBac1.1 is a prokaryotic channel that serves as a structural model of eukaryotic Kirs, but contains an H-bond in the equivalent position, similar to KcsA. By patch-clamping giant liposomes, we show that KirBac1.1 is K+-selective (PNa/PK < 0.08) as measured by reversal potentials shifts, but, like KcsA E71A, shows significant Na+ and Li+-driven 86Rb+ fluxes. We also find that the KcsA E71A mutant, similar to WT KirBac1.1. This loss of stability in these channels may suggest that the differences observed in permeation result from a weakened interaction with ions at the selectivity filter. Studies to examine ion permeation in eukaryotic Kir channels by 86Rb+ flux are ongoing.

1. H. Choi, L. Heginbotham, Biophys.J. 86, 2137 (2004).
2. J. F. Cordero-Morales et al., Nature Structural & Molecular Biology 13, 311 (2006).

1726-Pos

Characteristic Frequency Analysis of Inward Rectifier Kir 2.1

John Rigby, Steven Poelzing.
University of Utah, Salt Lake City, UT, USA.

INTRODUCTION: Impedance spectroscopy cannot distinguish between ion channel subtypes. We hypothesized that amplitudes of specific characteristic frequencies will correlate with the current amplitude passed by a specific ion channel subtype (characteristic frequency). We chose to test this hypothesis using the human inward rectifying potassium channel, Kir 2.1.

METHODS: IV-relationships were generated using a standard voltage step protocol (−140 to 0mV, 7mV steps) performed in whole-cell voltage clamp mode on HEK293 cells stably transfected with KCNJ2, which encodes Kir 2.1. Noise functions containing equal magnitudes of 1-15 kHz frequencies (amplitudes: 25, 50, 75 or 100mV) were inserted into each voltage step. The real component of the Fast Fourier transform (FFT) of the output signal was calculated with and without noise for each step potential. The magnitude of each frequency as a function of voltage step was correlated with the IV-relationship.

RESULTS: In the absence of noise (control), magnitudes of all frequencies correlated poorly ($|R|<0.15$) with the IV relationship. With noise, magnitudes of frequencies between 0.2-1 and 2-4 kHz demonstrated high negative ($R < -0.9$) and positive correlation ($R > 0.9$) respectively, with the IV-relationship. Two nodes of zero correlation were also found (1.39 +/- 0.10 kHz and 8.49 +/- 0.74 kHz). Increasing noise amplitude increased the absolute value of the correlation for the aforementioned frequencies without significantly changing the nodes of zero correlation.

CONCLUSIONS: These data suggest that the observed frequency response reflects current passing through Kir 2.1 channels. However it remains unknown whether any of these characteristic frequencies are unique to Kir2.1. Identifying characteristic frequencies of other ion channel subtypes could allow simultaneous measurement of multiple ionic currents.

1727-Pos

Calcium Channels Exhibit Electric Field Dependent Valve-Like Behavior

James P. Barger, Patrick F. Dillon.
Michigan State University, East Lansing, MI, USA.

We propose a new model characterizing the valve nature of ion channels. There are four fundamental elements that any physiological valve must possess: a tube, a one-way gating mechanism, a gate-sensitive force, and a conducted substance. Macroscopic valves (heart or veins) have the gating mechanism attached to the tube. In our model of ion channels, the gating mechanism is the hydration state of the ion. A sufficient membrane electric field at the surface of an ion channel will strip water molecules from the ion, allowing the ion to enter the channel. The electric field decays exponentially away from the membrane within several nanometers. If the ion channel extended too far from the membrane, negligible hydration stripping would occur, the hydration shell would remain around the ion, and the ion could not enter the channel. Our measurements of ion mobility in an electric field show that hydration stripping occurs at 400 V/cm, corresponding to 7 nm from the membrane. Calcium ion channels extend 4 nm externally from the membrane, and will have the ion hydration shells stripped from the ion at the channel entrance. Internally, the calcium ion channel extends 12 nm from the membrane. A stripped calcium ion will enter on the external side of the channel, but upon exiting on the internal side, will rehydrate and be unable to re-enter the channel, creating one-way flow. Thus, the calcium channels exhibit valve behavior, with the channel being the tube, the hydration shell the gating mechanism, the electric field the gate-sensitive force, and the stripped ion the conducted substance. This model can be extended to other ion channels. The macroscopic valves are thyroporetic (tube-attached gate), while the ion channel valves are thyrofluidic (conductor-attached gate).

1728-Pos

Selecting Ions by Size in a Calcium Channel: the Ryanodine Receptor Case Study

Dirk Gillespie[1], Le Xu[2], Gerhard Meissner[2].
[1]Rush University Medical Center, Chicago, IL, USA, [2]University of North Carolina, Chapel Hill, NC, USA.

Calcium channels not only distinguish between ions of different charge (e.g., Ca2+ vs. Na+), but also between of the same charge but of different size (e.g., Na+ vs. K+). Size selectivity in calcium channels is analyzed in the ryanodine receptor (RyR) using a recent permeation model of RyR. This model describes ion permeation as electrodiffusion and ions as charged, hard spheres. RyR is modeled as five conserved negatively charged amino acids whose terminal carboxyl groups are very flexible. The model correctly reproduces experiments where three different monovalent cations compete for the pore at many different concentrations. Size selectivity occurs both because smaller ions fit into the crowded selectivity filter better and because they can screen the protein's negative side chains more effectively.

1729-Pos

Insights from a Toy Model of Calcium Channels on Sieving Experiments and Eisenman Sequences

Daniel M. Krauss[1], Dirk Gillespie[2].
[1]Grinnell College, Grinnell, IA, USA, [2]Rush University Medical Center, Chicago, IL, USA.

A simplified model of a calcium channel is used to re-evaluate interpretations of both sieving experiments and Eisenman selectivity sequences in calcium channels. In the model channel, the carboxyl groups of the calcium channel selectivity filter are approximated as a homogeneous liquid of half-charged oxygens (two for each carboxyl group) separated from the bath by a semipermeable membrane that allows permeating ions into the selectivity filter, but does not allow the oxygens to leave the filter. Sieving experiments are usually interpreted with the logic that the physical diameter of a channel is equivalent to the largest particle that will go through that channel. However, our model has no radial geometric constraints, but still produces results that show net flux of ions quickly dropping to zero as the ions increase in diameter. These results indicate that forces like crowding of ions in the pore act on large ions that keep them from entering the channel. These forces are related to the pore diameter, but the results of the experiments should not be interpreted as indicating the pore diameter directly. We also used this simplified model to attempt to discern why the 11 Eisenman selectivity sequences are the only ones that have been observed. By altering the dielectric constant of the selectivity filter (and thereby the penalties for shedding waters of hydration), as well as oxygen concentration within the channel, we observed the circumstances under which each Eisenman sequence appears. We also observed a small number of non-Eisenman sequences.

1730-Pos

Molecular Simulation of Ompf Channel in Salts of Divalent Cations: Molecular Insight on Charge Inversion

Marcel Aguilella-Arzo[1], Carles Calero[2], Jordi Faraudo[2].
[1]Universitat Jaume I, Castelló de la Plana, Spain, [2]Institut de Ciència de Materials de Barcelona-CSIC, Bellaterra, Spain.

Extensive recent experimental and theoretical work has shown that the interaction of biologically relevant divalent cations (such as Mg2+, Ca2+) has surprising properties. One of the most fascinating and unexpected effect is the so-called charge inversion or charge reversal phenomenon: cations accumulate at the interface in excess of its own bare charge, thus inverting the effective

charge of the interface. Recently, charge inversion has been reported in the bacterial channel OmpF, in the presence of salts of divalent cations [Alcaraz et al. Biophys. J. 96 (2009) 56]. Aiming to get an insight on the atomistic mechanism of the cation interaction with the protein, we have performed extensive MD simulations of a realistic model of the OmpF WT protein in a POPC membrane in MgCl2 and explicit water. The simulations were computationally highly demanding, with half million atoms in a simulation box and production runs around 25 nsec.
The simulations were performed employing the NAMD simulation package running in 128 processor at the CESGA Supercomputing Center. Our main result is that we have observed charge inversion of certain important acidic groups. The observed charge inversion is accompanied by a change in the transport mechanism of ions inside the channel and a reversal in the selectivity of the channel. Overall, our simulations give an accurate microscopic image of this unexpected effect with potentially important biological and nanotechnological implications.

1731-Pos
Increased Salt Concentration Promotes Negative Cooperativity in OmpF Channel

Antonio Alcaraz[1], Elena García-Giménez[1], Vicente M. Aguilella[1],
Ekaterina M. Nestorovich[2], Sergey M. Bezrukov[2].
[1]University Jaume I, Castellon, Spain, [2]PPB, NICHD, National Institutes of Health, Bethesda, MD, USA.
The concept of positive cooperativity appeared in the study of oxygen uptake by hemoglobin to explain that when a molecule of oxygen binds makes it easier for a second molecule to bind. Quite the reverse, negative cooperativity refers to the situation where the presence of the first molecule makes it more difficult for the second molecule to bind. We study here the effect of salt on the pH titration of the OmpF channel, paying attention to the current noise, conductance and ion selectivity that are analyzed in terms of the Hill formalism. In all cases, values lower than 1 are found, suggesting a negative cooperativity. Although OmpF porin is a trimer, it was shown by a number of different methods that each monomer is identical and functionally independent. Thus, the slowed-down channel titration is a property of each monomer. Surprisingly, we find that increasing salt concentration promotes negative cooperativity, which is seen as a salt-induced decrease of the Hill coefficient. This observation seems to exclude direct electrostatic interactions between protonation sites as the source of the phenomenon, suggesting another, more subtle mechanism(s). The binding of cations to certain acidic residues has a crucial effect at low pH because results in an inhibition of channel conductance that additionally provides an anionic selectivity to the channel. This suggests that the binding site could play a certain role in the protection of the bacteria against acidic media

1732-Pos
Anions from the Hofmeister Series: Single Molecule Detection with a Solitary Protein Nanopore

Dijanah C. Machado, Claudio G. Rodrigues, Annielle M.B. da Silva,
Janilson J.S. Júnior, **Oleg Krasilnikov**.
Federal University of Pernambuco, Recife, Brazil.
Nanopores have emerged in recent years as versatile single molecule detectors. The sensing principle is based on transient interruptions in the ion-current of an electrolyte, induced by the entry, transport, and exit of a particular analyte from the pore. The improving the detection capability of the nanopore is essential. Recently (Rodrigues et al., 2008) we have shown that the ‘‘salting out’’ are responsible for the KCl-induced enhancement in identification of individual molecules of poly(ethylene glycol) using solitary α-hemolysin nanoscale pores. The result suggested that specific ion effects may take place. Hofmeister effects are almost ubiquitous (Lo Nostro et al., 2006). Despite the huge number of studies devoted to this issue that date back more than a century, their origin is still debated. There are only isolated studies of the phenomenon at the confined spaces. For this reason, we focused on the effect of monovalent anions on a simple bimolecular complexation reaction between poly(ethylene glycol) and α-hemolysin nanoscale pore at the single-molecule level.
We find that the type of anions used here has dramatic influence on the ‘‘on-rate’’ constant of the reaction (the difference reaches several hundred times). As a consequence of this, the transition rate and the detection limit of the nanopore based sensor is correspondingly changed. The all probed anions follow the Hofmeister ranking according to their influence on the on-rate constant ($F^- > Cl^- > Br^- > I^-$) and the solubility of the analyte ($F^- < Cl^- < Br^- < I^-$). Therefore, salting-out phenomenon is responsible for the anion-induced effect on single molecule detection with a solitary protein nanopore. These results will advance the development of devices with sensor elements based on single nanopores.
Supported by CNPq, RENAMI and InstINAMI, Brazil.

1733-Pos
Extension of Poisson-Nernst Planck Theory of Ion Conductivity with Soft-Repulsion Potential between Ions and Protein. Sensitivity of I-V Properties of α-Hemolysin Channel on its Penetration Depth into Membrane

Nikolay A. Simakov, Maria G. Kurnikova.
Carnegie Mellon University, Pittsburgh, PA, USA.
A soft repulsion (SR) potential between mobile ions and protein atoms is introduced to Poisson-Nernst-Plank (PNP) theory of ion transport as an alternative to commonly used hard sphere repulsion (HR). Two sets of SR were tested: one is parameterized for all atoms of 20 essential amino-acid residues using full atomic molecular dynamic simulation (SR-MD); and another is a truncated Lennard-Jones potential (SR-LJ). The effect of different models of short-range interaction between protein atoms and mobile ions (HR, SR-MD and SR-LJ) were studied using α-hemolysin channel protein. In addition, four different methods of setting the diffusion coefficients were analyzed in order to evaluate the effect of diffusion distribution on predicted currents. Our calculations show that the diffusion distribution has a strong influence on the size of total currents whereas has significantly less effect on rectifications, reverse potentials and selectivity. Therefore, for proper modeling of these properties, the potential of mean force (PMF) may play a more important role than the diffusion distribution. SR-MD has a better approximation of PMF near the protein surface than HR and significantly improves selectivity predictions.
Additionally, we have studied the dependency of α-hemolysin I-V properties on the penetration depth of the channel into the membrane. The results show that rectification and reverse potentials are very sensitive to the penetration depth. The depth, predicted by matching calculated rectification with the experimentally determined one, is in a very good agreement with the neutron reflection experimental result. Our free energy estimation also indicates that there is a minima near the predicted depth.

1734-Pos
Monitoring Ion Channel Charge Displacements using Radio Frequencies

Sameera Dharia, Gregory Dittami, Richard Rabbitt.
University of Utah, Salt Lake City, UT, USA.
Here we introduce a new technique to examine voltage-dependent ion-channel biophysics using radio frequency (RF) interrogating electric fields. The approach exposes the cell membrane to an RF electric field and measures vibrational electric current evoked by the RF field. *Xenopus* Oocytes transfected to express Shaker-B IR ion channels were used as the experimental model. A 500 kHz RF signal was applied to the membrane using extracellular bipolar metal electrodes, and RF charge displacement measurements were made during traditional two-electrode whole-cell voltage clamp. Voltage clamp was used to depolarize the oocytes and measure whole-cell K^+ current at several transmembrane potentials. The RF interrogation signal was superimposed on top of the comparatively slow (DC) voltage clamp command signal. Results show that the measured RF membrane current was a function of DC membrane potential. The RF current was separated into conduction and displacement components to examine the voltage-dependent RF conductance, G_{RF}, and capacitance, C_{RF}. Remarkably, the RF capacitance, C_{RF}, had a voltage sensitivity and half-activation voltage that correlated with the Shaker-B IR channel DC conductance measured using whole-cell voltage clamp. These data are consistent with the hypothesis that electrostatic interactions between the channel protein and K+ in the pore constrain the mobility of K+ and lead to changes in RF capacitance with membrane depolarization. The approach might offer a means to examine electrostatic interactions associated with ion channel function or to estimate voltage dependence of channel activation using extracellular RF signals. [supported by NIH R01DC04928, NSF IGERT DGE-9987616]

Cardiac Electrophysiology I

1735-Pos
Action Potential Duration Adaptation and Reverse-Rate Dependency in Human Ventricular Myocytes: Insights from a Computer Model
Eleonora Grandi, Donald M. Bers.
University of California Davis, Davis, CA, USA.
We recently developed and validated a novel mathematical model for Ca handling and ionic currents in human ventricular myocytes that is more robust than previous models in recapitulating relative contributions of various repolarizing K currents, and in describing Ca cycling processes (Biophys J. 2009;96(3) S1:664a-665a). Here, we present intriguing results on some emergent properties of this model. With increasing pacing frequency, AP shortening and parallel increases in intracellular [Ca] and [Na] are predicted. Remarkably, accumulation of $[Na]_i$ at fast rates predominates in the AP shortening (e.g. vs. K current changes), due to outward shifts in Na-pump (I_{NaK}) and Na-Ca exchange (I_{NaCa}) currents. Indeed, when clamping $[Na]_i$ to prevent Na accumulation, APD does not change with heart rate. No APD adaptation occurs when we prevent only I_{NaK} and I_{NaCa} from sensing the $[Na]_i$ rise (i.e. neither fast nor background Na currents contribute), and simulations indicate that I_{NaK} is dominant over I_{NaCa} in this effect. Moreover, acute Na-pump blockade is expected to causes gradual AP shortening as seen experimentally, that is secondary to gradual Na accumulation (after instantaneous APD prolongation due to block of outward I_{NaK}). We speculate that the increased $[Na]_i$ seen in heart failure may limit the AP prolongation that is caused by reduced K currents and increased late Na current. Our model (uniquely among human AP models) recapitulates reverse-rate dependence of APD upon I_{Kr} block, e.g. drug-induced AP prolongation is larger at slow stimulation rates. Simulation indicates that this is not due to frequency dependent properties of repolarizing currents (e.g. I_{Ks}), but is ''intrinsic'' to the system. That is, when AP repolarization is slower (at lower frequency with smaller net repolarizing current) any given current change (I_{Kr} block) causes a larger APD change.

1736-Pos
Effects of Stochastic Channel Gating and Stochastic Channel Distribution on the Cardiac Action Potential
Jan P. Kucera, Enno de Lange.
University of Bern, Bern, Switzerland.
Cardiac ion channels exhibit stochastic conformational changes that determine their open-close gating behavior, leading ultimately to the action potential (AP). However, in computational models of conduction, ion currents are usually represented deterministically. Moreover, the natural intercellular variability of the number of membrane and gap junctional channels is never considered. Our aim was to quantify the effects of stochastic current fluctuations and channel distributions on AP duration (APD) and intercellular conduction delays (ICDs) using a ventricular cell model (Rudy et al.) with Markovian formulations of the principal ion currents (I_{Na}, $I_{Ca,L}$, I_{Kr}, I_{Ks} and I_{K1}). Stochastic channel transitions were simulated explicitly and channel counts were drawn randomly from Poisson distributions.
In single cells paced at 1 Hz, stochastic channel gating generated APD variability (APD $= 143 \pm 1.8$ ms) with a coefficient of variation (CVar) of 1.3%. APD variability decreased at higher pacing frequencies. I_{Ks} fluctuations contributed most (85%) to APD variance, followed by those of $I_{Ca,L}$ and I_{Kr} (12% and 2%, respectively). Poissonian channel distribution induced APD variability with a CVar of 0.65%. In cell strands, the CVar of APD was strongly decreased by intercellular coupling. During conduction, stochastic channel gating generated ICD variability with a CVar of 0.25%. Reduction of I_{Na} or gap junctional coupling slowed conduction, but did not increase the CVar of ICDs above 1%. Poisson distribution of membrane channels exerted a similar small effect. However, during strong gap junctional uncoupling (60-200 channels/junction, conduction velocity <1 cm/s), Poisson distribution of gap junction channels resulted in a large ICD variability (>20%), highly heterogeneous conduction patterns and conduction blocks.
Therefore, the variability of the number of channels in different gap junctions contributes to the heterogeneity of conduction patterns observed previously in experiments in cardiac tissue with altered intercellular coupling.

1737-Pos
Comparison of the Effects of the Transient Outward Potassium Channel Activator NS5806 on Canine Atrial and Ventricular Cardiomyocytes
Kirstine Calloe[1], Natalie Chlus[2], Eyal Nof[3], Thomas Jespersen[1], Søren-Peter Olesen[1], Charles Antzelevitch[2], Jonathan Cordeiro[2].
[1]University of Copenhagen, Copenhagen, Denmark, [2]Masonic Medical Research Laboratory, Utica, NY, USA, [3]Sheba Medical Center Tel Hashomer, Ramat Gan, Israel.
Objective: NS5806 activates the transient outward potassium current (Ito) in canine ventricular cells. We compared the effects of NS5806 on canine ventricular versus atrial tissues and myocytes. Methods: NS5806 (10 μM) was evaluated in arterially-perfused canine right atrial and left ventricular wedges. Atrial and ventricular epi- and endocardial cells were isolated by enzymatic dissociation. Current and voltage-clamp recordings were made in the absence and presence of NS5806. Results: In ventricular wedges NS5806 increased phase 1 repolarization in epi- and midmyocardial cells. A minor effect on conduction and upstroke velocity also was observed. In contrast, application of NS5806 to atrial preparations slowed upstroke velocity and reduced excitability, consistent with sodium channel block. In ventricular myocytes, NS5806 increased the magnitude of Ito by 80% and 16% in epi and endo, respectively (at +40 mV). In atrial myocytes, NS5806 increased peak Ito by 25% and had no effect on the sustained pedestal current, IKur. INa density in atrial myocytes was nearly 100% greater than in endocardial myocytes. NS5806 caused a negative shift in steady-state mid-inactivation (V1/2) for both cell types (73.9 ± 0.27 to -77.3 ± 0.21mV for endocardial and -82.6 ± 0.12 to -85.1 ± 0.11mV for atrial cells). The shift in V1/2 resulted in a reduction of INa in both cell types. However, the more negative V1/2 in atrial cells suggests that atrial cells lose excitability at more depolarized voltages than endocardial cells which may explain the greater reduction of excitability in atrial vs ventricular wedges by NS5806. Conclusion: NS5806 produces a prominent augmentation of Ito with little effect on INa in the ventricles, but a potent inhibition of INa with little augmentation of Ito in atria.

1738-Pos
Intracellular Zn^{2+} Release Modulates Cardiac Ryanodine Receptor Function and Cellular Activity
Esma N. Zeydanli[1], Erkan Tuncay[1], Aytac A. Seymen[1], Ayca Bilginoglu[1], Nazli Sozen[1], Mehmet ugur[1], Guy Vassort[2], **Belma Turan**[1].
[1]Ankara University School of Medicine, Ankara, Turkey, [2]INSERM U-637 Physiopathologie Cardiovasculaire, Montpellier, France.
Several Ca^{2+}-binding proteins bind also Zn^{2+}, suggesting that Zn^{2+} can modulate the structure and function of many proteins involved in heart function. We first investigated intracellular Zn^{2+} homeostasis and its possible role in cardiac excitation-contraction (EC)-coupling by using confocal microscopy in adult rat cardiomyocytes loaded with either Zn^{2+}- or Ca^{2+}-specific dye, FluoZin-3 or Fluo-3, respectively. The local ionic releases (sparks) recorded in FluoZin-3 loaded cells were significantly smaller, shorter and less frequent than those of the Fluo-3 loaded cells under control resting conditions. Following 1-μM zinc-pyrithione exposure, the amplitude of the FluoZin-3 sparks increased by 35% leaving Ca^{2+}-sparks unaffected, and a 10-mV leftward shift was observed in the L-type Ca^{2+}-current (I_{Ca})-voltage relation without significant effect on maximal I_{Ca} density. Applications of either caffeine or ryanodine, and either a mitochondrial (MT) protonophore or a MT complex I inhibitor suggested that both sarcoplasmic reticulum and mitochondria are intracellular Zn^{2+} pools. Our western-blot data further showed that there are correlations between the intracellular Zn^{2+} level and the hyperphosphorylation levels of RyR2 and CAMKII as well as with total PKC activity. Additionally, hyperphosphorylation levels of both ERK-1 and NF-κB also showed a strong dependency on internal Zn^{2+}-level. In conclusion, intracellular Zn^{2+} might have an important role in the regulation of heart function including transcription and gene expression, implying that intracellular Zn^{2+} not only has a role in EC-coupling but it is also a major intracellular second messenger in cardiomyocytes.
(*Supported by TUBITAK SBAG-107S427&SBAG-107S304)*

1739-Pos
Uneven Expression Patterns of KCNQ1 and KCNE Subunits in the Heart Impact on the Function of Slow Delayed Rectifier (I_{Ks}) Channels
Dimitar P. Zankov[1], Min Jiang[1], Mei Zhang[1], Yu-Hong Wang[1], M. Horie[2], F. Toyoda[2], H. Matsuura[2], Gea-Ny Tseng[1].
[1]Virginia Commonwealth University, Richmond, VA, USA,
[2]Shiga University of Medical Science, Otsu, Japan.
Background: I_{Ks} has 2 major components: pore-forming (KCN)Q1 channel & regulatory (KCN)E1 subunits. Human heart expresses other members of the KCNE family (E2 - E5) that can all associate with Q1 & confer distinctly different channel phenotypes. The expression patterns of Q1 & different KCNE subunits in the heart, and their relation to the I_{Ks} channel function, is not clear. **Methods:** We use immunoblotting to quantify the protein levels of Q1 & E1 - E3 in different regions of the heart, and use patch clamp to quantify I_{Ks} current density and gating kinetics in left atrial (LA) and ventricular (LV) myocytes. We use the guinea pig model because of the robust cardiac I_{Ks}. **Results**: Immunoblot data: (1) Q1 protein is more abundant in atria (A) than in ventricles (V) (immunoblot densitometry ratio of A:V ~ 1:0.4), (2) E1 & E2 proteins are more

abundant in V than in A (E1 ratio ~ 1:2 - 3; E2 ratio ~ 1:2), (3) the E3 Ab recognizes a specific 20 kDa band in A but not in V. Patch clamp data: (1) I_{Ks} current density is much higher in LA than in LV myocytes, (2) I_{Ks} half-maximal activation voltage is more negative in LA than in LV myocytes, (3) I_{Ks} activates faster in LA than in LV myocytes. **Conclusion**: Q1 and E3 are more abundant in A than in V, while E1 & E2 have the opposite expression pattern. The uneven protein expression patterns can enhance I_{Ks} contribution to atrial action potential repolarization by generating a higher I_{Ks} density, that can reach a higher degree of activation in the action potential plateau range, than its counterpart in the ventricles.

1740-Pos
CaMKII Regulation of the Dynamic L-Type Ca^{2+} Current and Na^{+}/Ca^{2+} Exchange Current During Action Potential in Cardiac Myocytes

Tamas Banyasz[1,2], Leighton T. Izu[1], **Ye Chen-Izu[1]**.
[1]UC Davis, Davis, CA, USA, [2]Univ. of Debrecen, Debrecen, Hungary.

The L-type Ca^{2+} current ($I_{Ca,L}$) and the Na^{+}/Ca^{2+} exchange current (I_{NCX}) are the main inward currents that contribute to the depolarization during cardiac action potential (AP) plateau and later phases. Pathological changes of $I_{Ca,L}$ or I_{NCX} can cause early or delayed afterdepolarization (EAD, DAD). The steady-state kinetics of $I_{Ca,L}$ and I_{NCX} have been characterized in previous studies. However, the non steady-state dynamics of $I_{Ca,L}$ and I_{NCX} during the AP cycle still remain unclear. Here we report the new data on the dynamic $I_{Ca,L}$ and I_{NCX} during the cell's AP recorded using the *self AP-clamp* method. **Results:** (***1***) The I_{NCX} was isolated using its specific inhibitor SEA0400 at 3 μM. The data show that I_{NCX} is an inward current during most of the AP cycle. Importantly, I_{NCX} is the dominant contributor to a pronounced inward *foot current* at AP phases-3&4. This foot current is important because it depolarizes the cell at the late phases of AP and directly links to EAD or DAD. (***2***) Furthermore, the foot current is abolished by Ca^{2+}-calmodulin dependent kinase II (CaMKII) inhibition. (***3***) The $I_{Ca,L}$ was isolated using 10 μM nifedipine. The dynamic $I_{Ca,L}$ takes the form of a spike at AP phase-1 and a dome at phase-2. (***4***) Both $I_{Ca,L}$ and I_{NCX} during the AP are affected by using EGTA to buffer the SR Ca^{2+} release and prevent the CaMKII activation. **Conclusion**: Here we show for the first time the dynamic $I_{Ca,L}$ and I_{NCX} currents during the cell's AP in physiological milieu. CaMKII modulation of the foot current might explain, in part, the effect of elevated CaMKII activity on promoting arrhythmias in the hypertrophied and failing hearts.

1741-Pos
KCNQ1/KCNE1 K+ Channels Associated with Long QT Syndrome are Expressed in Early Stage Human Embryonic Stem Cell-Derived Cardiomyocytes

Cecile Terrenoire[1], George K. Wang[1], Eric Adler[2], Aaron D. Kaplan[3], Kevin J. Sampson[1], Jonathan Lu[1], Robert S. Kass[1].
[1]Columbia University, New York, NY, USA, [2]OHSU, Portland, OR, USA, [3]Mount Sinai School of Medicine, New York, NY, USA.

Human embryonic stem cell-derived cardiomyocytes (hESC-CMs) are not only a potential source of functional cardiac tissue that can be utilized as a drug screening platform or agents for cell-based therapy but also offer great potential in studies of heritable cardiac arrhythmias known as channelopathies. Many major cardiac ion channels have been reported to be expressed in hESC-CMs. However, the presence of KCNQ1/KCNE1 (I_{Ks}) K^{+} channels critical to cardiac repolarization particularly during sympathetic nerve stimulation and associated with the most common variant of congenital Long QT syndrome (LQT1), to date has not been reported. Here we report investigation of the cellular electrophysiological properties of hESC-CMs during the first 34 days of cytokine directed differentiation with a focus on I_{Ks} channels. All beating hESC-CMs studied had action potentials with cardiac phenotypes and expressed L-type calcium channels (n=26) and pacemaker channels (n=27) while 68% of cells (n=11 out of 16) expressed I_{Kr}, the potassium current associated with LQT2, defined as E4031-sensitive outward current measured during prolonged depolarization. I_{Ks}, the potassium current associated with LQT1, was identified by its biophysical and pharmacological properties: recorded in 29% of cells (n=5 out of 17), I_{Ks} was defined as an outward current slowly activating during prolonged depolarization, insensitive to E4031 (5 μM) and blocked by Chromanol 293B (30 μM). qPCR experiments confirmed the presence of I_{Ks} channels α- (KCNQ1) and β- (KCNE1) subunits in these hESC-CMs. This is the first report of I_{Ks} channel expression in hESC-CMs providing strong evidence in support of their use in mechanistic and pharmacological investigations of LQT1 and other heritable arrhythmia syndromes linked to mutations in the genes coding for I_{Ks} channel subunits and/or accessory proteins.

1742-Pos
LQT1 Genotype in Tachypaced Cardiomyopathy Causes Discordance of Baseline and VF Refractoriness

Ohad Ziv[1], Emily Lau[1], Lorraine Schofield[1], Lenny Chaves[1], Xuwen Peng[2], Bum-Rak Choi[1], Gideon Koren[1].
[1]Rhode Island Hospital, Providence, RI, USA, [2]Pennsylvania State University, Hershey, PA, USA.

Reduction of the slow outward rectifier (I_{ks}) and calcium disregulation accompany tachypacing induced cardiomyopathy (TICM). While TICM I_{ks} downregulation prolongs APD, its effect on refractoriness during VF is less clear. We used a transgenic rabbit model of Long QT 1 (LQT1) to investigate the effect of loss of I_{ks} on VF refractoriness in TICM.

Five LQT1 and littermate control rabbits underwent rapid RV pacing followed by *in vivo* electrophysiological studies and VF inductions. Dual voltage-calcium epicardial optical mapping was performed on whole hearts at baseline and in VF. *In vivo,* a strong correlation for ventricular effective refractoriness and VF interval was seen in LMC-TICM, but not in LQT1-TICM (r = 0.83 vs r = 0.36; p<0.05). Optical mapping demonstrated APD prolongation in LQT1-TICM compared to LMC-TICM (224 ± 18ms vs. 191 ± 15ms), but surprisingly higher VF frequencies in LQT1-TICM (15.7 ± 0.8 vs 12.6 ± 0.7Hz; p<0.05). In spatial VF frequency maps, LMC-TICM showed a negative VF frequency-APD map correlation (−0.43 ± 0.24), while LQT1-TICM demonstrated a paradoxical positive correlation (0.22 ± 0.14; p<0.05). Calcium-voltage discordance was increased in LQT1-TICM compared to controls (see fig). LQT1-TICM leads to dissociation between baseline and VF refractoriness demonstrating high frequency VF associated with calcium-voltage discordance.

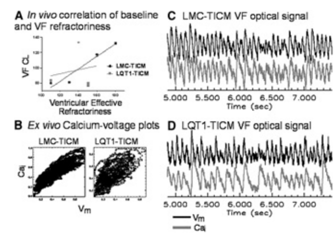

1743-Pos
Unique Molecular Profile of Transient Outward Potassium Current (I_{to}) Subunits in Cardiac Purkinje Fibers

Ling Xiao, Balazs Ordog, Maya Marmabachi, Ange Maguy, Stanley Nattel.
Montreal Heart Institute, Montreal, QC, Canada.

Background and objective: Cardiac Purkinje-fiber (PF) tissue plays a key role in conduction and arrhythmogenesis. The transient outward K^{+}-current (I_{to}), an important cardiac repolarizing conductance, has unusual kinetic and pharmacological properties in PF cells (PCs), suggesting a distinct and presently-unknown molecular basis. The present study addressed the differential expression of putative I_{to}-subunits in PF versus left-ventricular (LV) myocardium.

Methods: I_{to} was recorded with whole-cell voltage-clamp at 36°C from isolated PCs or LV cardiomyocytes before and after the K^{+}-channel blocker TEA. The regional mRNA expression-levels of I_{to} α-subunit (Kv4.3, Kv3.4) and β-subunit (KChIP2, NCS-1, Kvβ1, KChAP, KCNE1-5, and DPPX_S/_L) candidates were determined by real-time PCR.

Results: I_{to} from PCs was more sensitive to TEA than LV: 10 mM TEA reduced I_{to} by 53 ± 10% (N = 5) in PCs versus −4 ± 8% (N = 5) in LV cells, P<0.01. The mRNA levels of I_{to} α-subunits Kv4.3 and Kv3.4 were significantly higher (by about 2.7 and 159-fold respectively: e.g., epicardium versus PF 1.67 ± 0.38 vs 3.58 ± 1.14 ΔΔ-Ct units, P<0.05 for Kv4.3, 0.0001 ± 0.0001 vs 0.044 ± 0.020, P<0.05 for Kv3.4; N = 9/group) in PF-tissue than in LV. KChIP2 was much richer in LV epicardium (2.91 ± 0.73) and midmyocardium (0.92 ± 0.26) than in LV endocardium (0.09 ± 0.02, P<0.01) and PF (0.07 ± 0.03, P<0.01). NCS-1 was abundantly expressed in PF-tissue (1.95 ± 0.68), at about 400×LV values (epicardium 0.10 ± 0.03, midmyocardium 0.16 ± 0.07, endocardium 0.15 ± 0.04). KCNE1 and KCNE3-5 mRNA levels were significantly higher (eg, by 2.8, 2.9, 3.4and 6.0-fold vs epicardium) in PF than in all LV zones, whereas Kvβ1, KCNE2, KChAP and DPPX_S/_L subunits were similarly expressed among these four regions.

Conclusion: Cardiac PF-tissue has a unique expression profile of I_{to}-subunits that may account for its unusual properties. Expression studies are under way to determine the precise biophysical mechanisms.

1744-Pos
Decreased Phosphorylation of the Gap Junction Protein Connexin43 and Increased Anisotropy of Conduction as a Consequence of Myofilament Ca2+ Sensitization

Raghav Venkataraman[1], Sung In Kim[1], Veniamin Y. Sidorov[1], James D. Potter[2], Bjorn C. Knollmann[1], Franz Baudenbacher[1], **Sabine Huke[1]**.
[1]Vanderbilt University, Nashville, TN, USA, [2]University of Miami, Miami, FL, USA.

Increased myofilament Ca^{2+} sensitivity is associated with an increased susceptibility for arrhythmias, as previously demonstrated in mice expressing Ca^{2+} sensitizing troponin T (TnT-I79N) mutations and after acute application of the Ca^{2+} sensitizer EMD57033. We hypothesized that the arrhythmia risk is increased due to altered regulation of connexin43 (Cx43), subsequently leading to a slowing of cardiac conduction.
Methods: Fast (longitudinal) and slow (lateral) conduction velocity (CV) was calculated using epi-fluorescence maps from isolated hearts by plotting local CVs against orientation. Phosphorylated Cx43 (P1, P2) from these hearts migrated slower in SDS PAGE and at least three distinct bands could be separated (P0,P1,P2).
Results: The lateral CV, but not the longitudinal CV, was significantly reduced in TnT-I79N mice compared to control (16.9 ± 0.8 cm/s ($n = 11$) vs. 21.5 ± 1.4 cm/s ($n = 11$) respectively, $p<0.05$). As a direct consequence the anisotropy of conduction (fast/slow) was increased in TnT-I79N hearts (to 3.2 ± 0.2 vs 2.3 ± 0.1 in control). This change in CV was associated with decreased Cx43 phosphorylation (un-phosphorylated P0-Cx43 increased to $146 \pm 20\%$ of control, $p<0.05$). Blebbistatin, a Ca^{2+} desensitizer and contractile uncoupler, prevented ventricular arrhythmias in TnT-I79N hearts. Strikingly, blebbistatin also prevented the increase in anisotropy and the decrease in Cx43 phosphorylation, while it had no effect in control hearts. Conversely, acutely increasing Ca^{2+} sensitivity with EMD decreased Cx43 phosphorylation (P0-Cx43 $491 \pm 147\%$, $n = 4$, $p< 0.05$) and rapidly slowed lateral conduction velocity (to 18.2 ± 1.3 vs 22.9 ± 1.1 cm/s in control, $p<0.05$) thereby increasing anisotropy (to 2.64 ± 0.1 vs 2.17 ± 0.07 in control) and rendered control hearts susceptible to arrhythmia induction.
Conclusion: These data suggest that decreased Cx43 phosphorylation and increased conduction anisotropy is at least in part responsible for the increased arrhythmia susceptibility associated with myofilament Ca^{2+} sensitization.

1745-Pos
Electron-Conformational Model of SR-Based Ca^{2+} Clock Mode
Alexander M. Ryvkin[1,2], Alexander S. Moskvin[1], Olga E. Solovyova[1,2], Vladimir S. Markhasin[2].
[1]the Ural State University, Ekaterinburg, Russian Federation, [2]Instiute Immunology & Physiology RAS, Ekaterinburg, Russian Federation.
Most of the calcium that activates cardiac contraction comes from the sarcoplasmic reticulum (SR) from where it is released through the Ryanodine Receptors (RyRs). It is well known that the SR overload results in the release of Ca from the SR in the form of waves driving some cardiac arrhythmias. Recently it has been experimentally documented that the isolated SR is capable to spontaneously and rhythmically release Ca^{2+} (SR-based Ca^{2+} clock). This self-sustained intracellular Ca^{2+} oscillator contributes substantially to the late phase of the diastolic depolarization of cardiac pacemaker cells under normal physiological conditions. Interaction of ''a surface membrane oscillator'' and ''an internal oscillator'' with ''cycles of Ca^{2+} uptake and release by the SR'' can drive normal cardiac automaticity. To describe the SR-based Ca^{2+} clock mode we propose a simple, physically-reasonable electron-conformational (EC) model for the RyR and present a theory to describe the RyR lattice dynamics. Each RyR is modelled with a single open and closed electronic state. In addition to the fast electronic degree of freedom, RyR channels are characterized by a slow classical conformational coordinate, which specifies the RyR channel conductance. The RyR gating implies a conformational Langevin dynamics, Ca^{2+}-induced electronic transitions, quantum tunneling and thermal transitions. The cooperativity in the RyR lattice is assumed to be determined by the inter-channel conformational coupling. Model simulations of the of 11x11 RyR cluster revealed different regimes depending on the cis- and trans-Ca concentrations and parameters of EC-model. The SR overload is shown to result in RyR lattice auto-oscillations with spontaneous RyR channel openings and closures. We have studied this Ca^{2+} clock mode, in particular, its stability, under different model suggestions as regards the RyR conformational potential (diabatic and adiabatic regimes), EC-model parameters.
Supported by the RFBR 07-04-96126

1746-Pos
Design of a Fluorescence-Based System for Measurement of Transmembrane Potential Variations of Electrically and Mechanically Stimulated Cardiomyocytes
James Elber Duverger, Philippe Comtois.
Montreal Heart Institute, Montreal, QC, Canada.
Cardiomyocytes are electrically-active heart cells whose electrical properties vary with the local electrical and mechanical environment. Variations in myocytes electrical properties are known to play a role on abnormal rhythms.
The purpose of the project is to design a fluorescence-based photodetection system for measurement of transmembrane potential variations by combined electrical and mechanical stimulations in post-culture cardiomyocytes.
The isolated cardiomyocytes are seeded on a 10mm x 10mm x 0.127mm silicon sheet held by a pair of pliers, coupled to a stretcher apparatus made of two linear guide systems and two computer controlled linear stepper motors. The cells are kept in bubbled Tyrode solution and are electrically stimulated during the 10 minutes staining by the voltage-sensitive dye di-8-Anepps (Invitrogen) at 5 μmol/L concentration. Field electrical stimulation is done by a pair of parallel carbon electrodes with grounded anode. The cathode voltage is supplied by a bipolar isolation amplifier circuit whose input is a set of pulses from the digital-to-analog converter of a National Instruments card (NI USB-6221). The light source is a green LED array (wavelength = 523nm, NTE Electronics Inc.), with intensity controlled by a Darlington array receiving TTL signals. The emitted fluorescence is filtered ($\lambda > 610$nm), converted to voltage with a fast photodiode (S1226-5BK, Hamamatsu), and amplified by an instrumentation amplifier (AD524ADZ, Analog Digital Inc). The voltage is then digitized with a National Instruments card, filtered and saved for post-experiment analysis.
Each sub-system has been successfully validated. Testing the whole system with cardiac-derived HL1 cells allowed final improvement on the signal-to-noise ratio and optimization of excitation intensity. This ready to use bioinstrument will play a key role in further studies on cultured cardiomyocytes.

1747-Pos
In Vitro Cardiac Safety Profiling of a Novel Benzyl-Ethylamine Compound
Xiaoqin Liu, James T. Limberis, Sheila Thomas, Zhi Su, Gary A. Gintant, Bryan F. Cox, Vincent L. Giranda, Ruth L. Martin.
abbott, Abbott park, IL, USA.
When developing novel compounds for any clinical indication, the possibility of untoward cardiovascular effects must be addressed. To evaluate the cardiac electrophysiologic effects of A-674563 ((S)-1-benzyl-2-[5-(3-methyl-1H-indazol-5-yl)-pyridin-3-yloxy]-ethylamine), a novel benzyl-ethylamine, we profiled the compound in a series of cellular and tissue assays. In canine Purkinje fibers (30 min exposure; 2 sec BCL), A-674563 elicited concentration dependent depolarization with shouldering of the terminal repolarization phase (20 μM) and increased abnormal automaticity (60 μM). In papillary muscles, concentration dependent depolarization was also seen, but the effect was much less potent; 60 μM induced shouldering of the terminal phase of repolarization. Contractility was assessed using percent changes in fractional shortening of sarcomere length (FS) in rabbit left ventricular myocytes. A-674563 reduced FS in a concentration dependent manner; 10% at 2 μM and 47% at 20 μM. Effects on ionic currents were further evaluated using heterologously expressed cardiac ion channel cell lines. A-674563 inhibited Cav1.2, expressed in HEK cells, with an IC_{50} of 20 μM, suggesting that the decreased contractility seen in native cells is due to L-type calcium channel block. The compound reduced Nav1.5 (HEK cells) by 50% at 20 μM and inhibited Kir2.1 (tSA201 cells) with an IC_{50} of 35 μM. Block of these channels would be expected to reduce the upstroke velocity, depolarize the cellular membrane and lead to abnormal automaticity as was seen in the tissue assays. Although A-674563 caused minimal prolongation of action potential duration in tissues up to 60 μM, it inhibited hERG (HEK cells) with an IC_{50} of 0.7 μM. This potent block was most likely offset by the concomitant block of multiple cardiac ion channels. In conclusion, A-674563 affects multiple cardiac ion channels to elicit depolarization and increased automaticity in native cardiac tissues.

1748-Pos
Stretch-Sensitivity of Stretch-Activated BK_{Ca} Channels in Post-Hatch Chick Ventricular Myocytes
Gentaro Iribe, Keiji Naruse.
Okayama University, Okayama, Japan.
We have previously reported the electrophysiological properties of stretch-activated BK_{Ca} (SAKCA) channels cloned from cultured chick embryonic ventricular myocytes. However, the physiological role of SAKCA channels in the post-hatch heart *in situ* is not clear. We have investigated the effects on the SAKCA current of cell length changes, applied axially using a pair of carbon fibers attached to opposite ends of an isolated ventricular myocyte of a 2 week-old chick. Whole-cell currents were recorded using the patch-clamp technique, while the cells were either held at resting length, or stretched to cause a 10% increase in sarcomere length. Stretch did not affect whole-cell currents immediately after the stretch was applied. However, sustained stretch for 3 minutes significantly increased outward currents. This stretch-induced change was reversed by applying 10 nM Iberiotoxin, a specific BK_{Ca} channel blocker, or a Na^{+}/Ca^{2+} free environment. These results were reproduced in a computer simulation study, suggesting that stretch does not activate SAKCA channels directly, but does so in a secondary manner via a stretch-induced increase in the cytosolic Na^{+} concentration followed by an increased Ca^{2+} influx.

1749-Pos
Multiple Mechanisms Contribute to Cardiotoxicity Observed with the Antidepressant Desipramine

Dierk Thomas[1], Lu Wang[2], Xiaoping Wan[2], Ingo Staudacher[1], Sabrina Obers[1], Ramona Bloehs[1], Jana Kisselbach[1], Ioana Baldea[1], Patrick A. Schweizer[1], Hugo A. Katus[1], **Eckhard Ficker[2]**.
[1]Medical University Hospital Heidelberg, Heidelberg, Germany, [2]Case Western Reserve University, Cleveland, OH, USA.

The cardiotoxicity of antidepressants is well recognized. Common electrocardiographic changes precipitated in particular by an overdose include QRS widening as well as prolongation of the QT interval and torsade de pointes tachycardia. QT prolongation by antidepressants has usually been associated with acute block of hERG/I_{Kr} currents. This study has been designed to provide a more complete picture of the molecular mechanisms underlying cardiac side effects induced by the antidepressant desipramine. We have studied acute block in HEK/hERG WT cells using patch-clamp recordings and found that desipramine reduced hERG currents with an IC_{50} value of 11.9μM. In HEK/hERG F656V, a mutation that reduces drug binding, hERG currents were blocked half-maximally with 48.3μM. We used Western blots to monitor the effects of desipramine on hERG trafficking. In these experiments we found that the fully-glycosylated cell surface form of hERG was reduced with an IC_{50} of 5.1μM on overnight incubation. When long-term effects were studied using electrophysiological current recordings, hERG tail currents were decreased with an IC_{50} of 7.5μM. Accordingly, hERG surface expression was reduced by desipramine when monitored directly using a cell-based assay (IC_{50}, 17.3μM) or confocal imaging. Importantly, the reduction in surface expression was not attenuated by mutation of residue F656 in the drug binding site of hERG. In guinea pig ventricular myocytes action potential duration was prolonged in a dose-dependent manner as expected on acute desipramine exposure. However, long-term exposure increased action potential duration only marginally. Finally, desipramine triggered apoptosis in cells expressing hERG channels. Taken together, desipramine exerts adverse cardiac effects by at least three different mechanisms: (1) direct hERG channel block, (2) disruption of hERG trafficking, and (3) induction of apoptosis.

1750-Pos
Arrhythmogenic Activity and Channel Remodeling in Ventricles of Dilated Cardiomyopathy (DCM) Model Mice

Takeshi Suzuki[1], Masami Sugihara[1], Hiroto Nishizawa[1], Akihito Chugun[1], Takashi Murayama[1], Takashi Sakurai[1], Hiroyuki Daida[1], Sachio Morimoto[2], Yuji Nakazato[1], Nagomi Kurebayashi[1].
[1]Juntendo University School of Medicine, Tokyo, Japan, [2]Kyushu University Graduate School of Medicine, Fukuoka, Japan.

Introduction: Dilated cardiomyopathy (DCM) is a disease characterized by weakened and dilated heart which often leads to lethal arrhythmia and sudden death. Recently a knock-in mouse model of DCM was created by mutation of cardiac troponin T (ΔK210) based on human familial DCM. Because they died suddenly at a high probability during 8-12 weeks old but rarely died before 6 weeks, we compared the properties of cardiac muscles of mutant mice between 4 and 8 weeks to explore the cause of sudden death. **Methods and Results**: Left ventricular (LV) muscles were isolated from wild type (WT) and homo mutant hearts and were loaded with di-4-ANEPPS. Membrane potential signals were determined using a laser scanning confocal microscope. Gene expression levels were quantified by real-time RT-PCR. In mutant hearts at 8 weeks, spontaneous action potentials were frequently seen and action potential duration was prolonged compared to those from WT. These features were not obvious at 4weeks. Real-time PCR analysis of mutant LV showed age dependent changes in gene expression levels of some K^+ channels including Kv4.2. **Conclusion**: These results suggest that the age-dependent alteration in various ion channels may contribute to both APD prolongation and abnormal automaticity, then enhance susceptibility to lethal arrhythmias in the DCM model mice.

1751-Pos
New Insights into Sexual Dimorphism During Progression of Heart Failure and Rhythm Disorders

Jerome Thireau[1], Franck Aimond[1], Denise Poisson[2], Bei Li Zhang[2], Patrick Bruneval[3], Véronique Eder[4], Sylvain Richard[1], Dominique Babuty[5].
[1]Inserm U637, Physiopathologie cardiovasculaire, Montpellier, France, [2]FRE Université–CNRS-3092, Physiologie des Cellules Cardiaques et Vasculaires, Université François-Rabelais, Tours, France, [3]Service d'anatomo-pathologie, Université Paris V, Paris, France, [4]Département de Médecine Nucléaire et Ultrasons, Hôpital Trousseau, Tours, France, [5]FRE Université–CNRS-3092, Physiologie des Cellules Cardiaques et Vasculaires, Université François-Rabelais, Tours, France.

Mice overexpressing the human beta2-adrenergic receptors (TG4 mice) develop heart failure (HF) leading to higher mortality than WT mice. HF appears earlier in TG4 males and those animals have a more severe phenotype than TG4 females, with earlier appearance of sudden cardiac death, corroborating observations in human before menopause. We assessed the electrophysiological status of TG4 male and female mice through heart rate variability analysis (HRV), intracardiac electrophysiological exploration (IEE) and patch-clamp study in order to understand female protection. The role of gonadal hormones in HF progression was studied through gonadectomy procedure. HRV was decreased in TG4 comparing with WT, with a higher decrease in males (−48%) than in females (−35%). IEE revealed a lengthening of infrahisian conduction time (+29%) associated to a larger QRS duration (+27%) only in TG4 males. A high prevalence of spontaneous and electro-inducible premature ventricular contractions was observed only in old-TG4 males. No difference was observed in females with regards to arrhythmias. Gonadectomy improved cardiac phenotype in TG4 males whereas ovariectomy worsened it in females. TG4 left ventricular cardiomyocytes were hypertrophied only in males (169 ± 7 vs. 204 ± 11 pF, n = 20) but male and female TG4 presented an increase in action potential repolarisation with no gender-related difference as compared with WT (+200%). Longer action potentials reflected a significant decrease in outward voltage-gated K+ current densities in male and female TG4 cells. Assessment of histological alterations confirmed that high mortality in TG4 males is associated with severe cardiac fibrosis while in female no difference was found between WT and TG4 mice.
In summary, the progression and severity of HF in TG4 mice are linked to sex-hormones. A link between fibrosis, conduction time, and mortality was established in relation with sex hormones.

1752-Pos
Efficient Biolistic Transfection of Fresh Adult Cardiac Myocytes with a Tagged Kv1.5 Channel

Tiantian Wang, Alireza D. Zadeh, Ying Dou, Charitha L. Goonasekara, David F. Steele, David Fedida.
University of British Columbia, Vancouver, BC, Canada.

Modulation of ion channel trafficking is a potent means by which a cardiomyocyte can regulate its excitability. Much has been learned about the roles of motifs within K+ channels that affect their trafficking to the cell surface. However, by necessity, previous studies have relied on model expression systems, because the transfection of adult cardiomyocytes has, to date, proved intractable. Rat neonatal myocytes can be transfected but the currents expressed in these cells are quite different from those of adult cardiomyocytes. Viral transduction systems are effective in adult cells but require sophisticated containment facilities and prolonged culture of the myocytes, during which time substantial dedifferentiation generally occurs.
We have developed a new method that, for the first time, allows the ready and convenient transfection of acutely isolated adult rat cardiac myocytes. Using a low pressure adaptation of a Bio-Rad Helios gene gun procedure, we have achieved efficient transfection of rat ventricular myocytes bombarded within two hours of myocyte isolation with gold particles coated with pcDNA3 constructs encoding tagged Kv1.5 constructs. Expression is rapid, robust, and detectable less than 24 hours post-transfection in myocytes retaining both current profiles and gross morphology comparable to freshly isolated cells. Using this system, we unequivocally demonstrate that tagged Kv1.5 is efficiently localized to the intercalated disk in ventricular myocytes and that it is expressed at the surface of that structure. We further demonstrate that Kv1.5 deletion mutations known to reduce the surface expression of the channel in heterologous cells similarly reduce the surface expression in transfected ventricular myocytes, although targeting to the intercalated disk per se, was generally unaffected. Thus, this new transfection method is an effective tool for the study of cardiac ion channel expression and targeting in a physiologically relevant system.

1753-Pos
Generation of Sodium-Permeable Cav1.3 Channel: Insights into the Molecular Basis for the Sustained Inward Current in Cardiac Pacemaker Cells

Futoshi Toyoda, Wei-Guang Ding, Hiroshi Matsuura.
Shiga University of Medical Science, Otsu, Japan.

The sustained inward current (I_{st}) is a novel pacemaker current identified in spontaneously active sinoatrial and atrioventricular node cells of rabbits, guinea-pigs, rats and mice. Because I_{st} is activated and produces an inward current over the entire range of the slow diastolic depolarization, its contribution to the pacemaker activity has been suggested. However, due to the absence of specific blockers and unidentified molecular determinants, it is still difficult to directly investigate the significance of I_{st} in cardiac automaticity. Although I_{st} is a Na^+ current, its pharmacological properties are qualitatively identical with those of L-type Ca^{2+} current ($I_{Ca,L}$). In the present study, we generated a Na^+-permeable $Ca_V1.3$ channel by a substitution of key glutamate residue

in the Ca^{2+}-selective filter of the pore with lysine (E1160K). The $Ca_V1.3$-E1160K channel expressed in HEK cells evoked an inward current carried by Na^+ even in the presence of extracellular Ca^{2+} (1.8 mM). The Na^+ current was characterized by a slow inactivation kinetics, a low activation threshold (~−60 mV) and sensitivity to $I_{Ca,L}$ blockers such as nifedipine, diltiazem and Cd^{2+}. These properties of the $Ca_V1.3$-E1160K current were very similar to those of I_{st}, suggesting that an $I_{Ca,L}$ channel variant with altered ion selectivity may mediate I_{st}. Besides, application of the $Ca_V1.3$-E1160K channel to the biological pacemaker would be an intriguing approach to understand the impact of I_{st} on cardiac pacemaking.

1754-Pos

Evidence of a Pro-Arrhythmic Substrate in the Failing Right Ventricle of Pulmonary Hypertensive Rats

David Benoist, Rachel Stones, Olivier Bernus, Mark Drinkhill, Ed White.
University of Leeds, Leeds, United Kingdom.

Arrhythmic risk is increased in patients with heart failure. We have investigated the arrhythmic state of the failing right ventricle in a model of pulmonary hypertension (PAH).

Wistar rats were injected intraperitoneally with monocrotaline (MCT, 60 mg/kg) to induce PAH and right ventricular failure within 3-4 weeks and compared to age-matched saline-injected animals (CON).

In vivo measurement of ECG parameters using radiotelemetry indicated modification of T wave-parameters in MCT treated animals e.g. a prolonged QT interval (CON 49.7 ± 2.0 *vs.* MCT 76.2 ± 2.5 ms, $P<0.001$) and time from the peak to the end of the T-wave (Tpe, CON 25 ± 1.8 *vs.* MCT 33.1 ± 1.7 ms, $P = 0.007$) (CON $n = 6$, MCT $n = 7$).

Animals were humanely killed upon showing clinical symptoms of HF. Monophasic action potentials (MAPs) were recorded at the right ventricular epicardial surface of isolated hearts and a S1-S2 protocol used to construct standard APD restitution curves. MAP duration was significantly prolonged in failing hearts (MAP90, 39.9 ± 1.9 ms in CON *vs.* 80.7 ± 3.5 ms in MCT, $P<0.001$) and standard restitution slopes were steeper (mean maximum slope was 0.18 ± 0.02 CON *vs.* 0.73 ± 0.28 MCT, $P<0.001$).

Optical action potentials were recorded at stimulation frequencies between 5-12 Hz using the voltage-sensitive dye di-4-ANEPPS and dynamic APD and conduction velocity restitution curves measured. The failing right ventricle exhibited steeper restitution and conduction velocity restitution curves (mean maximum slope for conduction velocity was 0.013 ± 0.004 MCT *vs.* 0.002 ± 0.001 CON, $P<0.001$). At high pacing frequencies, arrhythmias were induced in failing but not in control hearts.

T-wave modification, APD prolongation, steeper APD and conduction velocity restitution curves are typically associated with a pro-arrhythmic state. We conclude that the failing right ventricle of pulmonary hypertensive rats have an elevated risk of developing arrhythmias. The underlying mechanisms are under investigation.

1755-Pos

Pregnant Mice Exhibit an Increase in the Automaticity and the Pacemaker Current I_F in Sinoatrial Node Cells

Laurine Marger[1,2], Céline Fiset[1,2].
[1]Institut de Cardiologie de Montreal, Montreal, QC, Canada, [2]Université de Montreal, Montreal, QC, Canada.

The incidence of some types of arrhythmias is increased during pregnancy. Changes in hormonal levels, autonomic tone and hemodynamic parameters associated with pregnancy can be involved in these arrhythmias. Moreover, our preliminary findings show that resting heart rate is elevated in pregnant mice. Since increased resting heart rate is a risk factor for the development of cardiac arrhythmias it is important to understand specifically how pregnancy alters pacemaker function. Thus the purpose of the present study was to examine the effects of pregnancy on automaticity in sinoatrial cells (SANC) as well as the ion currents that underlie cardiac pacemaker function. Spontaneously beating cells were isolated from the sinoatrial node (SAN) from pregnant mice (PM) and non-pregnant mice (NPM). Current-clamp recordings revealed that the beating rate of PM-SANC (319 ± 10 bpm; $n = 17$) was elevated in comparison to SANC from NPM (282 ± 16 bpm, $n = 10$). Moreover, SANC action potential threshold (E_{th}) was more depolarized in PM (PM -38 ± 2, $n = 16$; NPM -43 ± 2 mV, $n = 10$; $p<0.05$) and the upstroke velocity of diastolic depolarization also was faster (PM 0.39 ± 0.05 mV/ms, $n = 14$; NPM 0.21 ± 0.05 mV/ms, $n = 10$ $p<0.05$). Next voltage-clamp experiments were used to investigate pacemaker current (I_f), the predominant ionic mechanism underlying cardiac automaticity. Results showed that peak I_f density at −100 mV was higher in PM-SANC (-26 ± 4 pA/pF, $n = 13$) compared to NPM-SANC (-15 ± 2 pA/pF, $n = 8$; $p<0.05$). Overall, the results show that I_f is increased during pregnancy and this likely contributes to the increase in beating rate in SANC. These alterations in pacemaker activity could contribute to the higher heart rate observed in pregnancy.

1756-Pos

Regulation of Volume-Sensitive Chloride Current in Cardiac HL-1 Myocytes

Wu Deng, Frank J. Raucci Jr., Lia Baki, **Clive M. Baumgarten**.
Medical College of Virginia, Virginia Commonwealth University,
Richmond, VA, USA.

HL-1 cells derived from mouse atrial myocytes retain many features of differentiated adult cardiomyocytes, continuously divide, and are emerging as a useful experimental tool. Features of several HL-1 cation channels have been described, but the characteristics of its Cl^- channels are unknown. We studied regulation of volume-sensitive Cl^- current, $I_{Cl,swell}$, under conditions that isolate anion currents. Modest osmotic swelling (0.85T; T, times-isosmotic) elicited robust outwardly-rectifying Cl^- currents in virtually every HL-1 cell (typically, 15 - 30 pA/pF at +60 mV; $E_{Cl} = -40$ mV). As expected for $I_{Cl,swell}$, Cl^- current in 0.85T was fully inhibited by DCPIB (10 μM) and was outwardly rectifying in both physiological and symmetrical Cl^- gradients. Regulation of HL-1 $I_{Cl,swell}$ matched that in enzymatically dissociated adult cardiomyocytes. In 0.85T, HL-1 $I_{Cl,swell}$ was fully blocked by both the NADPH oxidase inhibitor gp91ds-tat (500 nM) and the mitochondrial ETC inhibitor rotenone (10 μM), and in isosmotic bath solution (1T), DCPIB fully suppressed H_2O_2-induced (100 μM) $I_{Cl,swell}$. Furthermore, as in adult cardiomyocytes, endothelin-1 (ET-1; 10 nM) activated a DCPIB-sensitive current in 1T that was outwardly-rectifying in HL-1 cells with physiological and symmetrical Cl^- gradients. ET-1-induced HL-1 $I_{Cl,swell}$ was suppressed by the ET_A receptor blocker BQ123 (1 μM) and by blocking ROS production with gp91ds-tat. HL-1 $I_{Cl,swell}$ also was activated by bacterial sphingomyelinase (0.03 U/mL) that produces ceramide. These findings in HL-1 cells recapitulated the biophysical and pharmacological features of $I_{Cl,swell}$ and its regulation by ROS, endothelin, and ceramides in adult myocytes. Our data indicate that HL-1 cells are a useful tool for dissecting the regulation and role of $I_{Cl,swell}$ in cardiac myocytes.

1757-Pos

The LQT1 Phenotype of the KCNQ1 H258R Mutant is Unmasked by Faster Stimulation Rates

Alain J. Labro, Inge R. Boulet, Evy Mayeur, Jean-Pierre Timmermans,
Dirk J. Snyders.
University of Antwerp, Antwerp, Belgium.

The long QT syndrome is a cardiac disorder caused by a delayed ventricular repolarization. LQT1 is linked to mutations in the KCNQ1 gene that codes for the six transmembrane spanning α-subunit of the channel complex that underlies I_{Ks} *in vivo*. The LQT1 mutation H258R, located in the S4-S5 linker, resulted in subunits that failed to generate current in a homotetrameric condition. However, association with hKCNE1 'rescued' the mutant subunit and generated I_{Ks}-like currents. Compared to WT hKCNQ1/hKCNE1, H258R/hKCNE1 displayed accelerated activation kinetics, slowed channel closure and a hyperpolarizing shift of the voltage-dependence of activation, thus predicting an increased K^+ current. However, current density analysis combined with subcellular localization indicated that the H258R subunit exerted a dominant negative effect on channel trafficking. The co-expression hKCNQ1/H258R/hKCNE1, mimicking the heterozygous state of a patient, displayed similar properties. During repetitive stimulation the mutant yielded more current compared to WT at 1 Hz but this effect was counteracted by the trafficking defect at faster frequencies. Thus at faster stimulation rates there would be less repolarizing K^+ current compared to WT, explaining the disease causing effect of the mutation. In terms of H258R being 'rescued' by hKCNE1, it seems less likely that this occurs through a pure chaperone-type mechanism and based on the altered gating kinetics we suggest that hKCNE1 rescues H258R by restoring the gating machinery. It has been proposed that hKCNE1 modulates hKCNQ1 kinetics by stabilizing the interaction between the S4-S5 linker and bottom part of S6. Therefore, we speculate that the H258R mutation disrupts the contact with S6 resulting in distorted subunit folding. The association with hKCNE1 then stabilizes the electromechanic coupling and in this way compensates for the destabilization caused by the H258R mutant.

1758-Pos

In Vitro Cardiac Repolarization Assays: Guinea Pig Papillary Muscles *Vs.* Canine Purkinje Fibers

Pamela Franklin, Jonathon Green, James Limberis, Xiaoqin Liu,
Ruth Martin, Bryan Cox, Gary Gintant, Zhi Su.
Abbott, Abbott Park, IL, USA.

Compounds	APD_{90}		APD_{30-90}
	CPF†	GPPM†	GPPM†
DMSO 0.1%	2 ± 1	1 ± 2	3 ± 3
Tolterodine 700 nM	55 ± 3	15 ± 5*	39 ± 10#
Moxifloxacin 450 µM	178 ± 15	81 ± 12#	140 ± 26#
E-4031 0.2 µM	146 ± 11	36 ± 5*	53 ± 6*
Cisapride 10 µM	34 ± 4	22 ± 4*	63 ± 11#
Haloperidol 2.66 µM	3 ± 4	12 ± 3*	32 ± 5*
A-935142.0 60 µM	-24 ± 2	-18 ± 2*	-13 ± 5*

†Values are expressed as a mean percent change from baseline ± SEM. n = 4-6
*p<0.05 vs. vehicle (unpaired t-test); # p<0.05 vs. vehicle (Mann-Whitney)

Delayed or accelerated cardiac repolarization is potentially proarrhythmic. In this study, we compared a guinea pig papillary muscle APD (GPPM-APD) assay to a canine Purkinje fiber APD (CPF-APD) assay in assessing drug effects on cardiac repolarization. Papillary muscles (right ventricle) and Purkinje fibers were stimulated at 0.5 Hz, action potentials were recorded using microelectrode techniques, repolarization assessed using $APD_{30,\ 50,\ 90}$ values, and the calculated triangulation parameter, $APD_{30\text{-}90}$. Eight compounds (6 positives, 2 negatives) were tested in both preparations. Percent changes in APD_{90} values obtained with the GPPM-APD assay were less than those obtained in the CPF-APD assay (table). Repolarization parameters in the GPPM-APD assay exhibited a rank sensitivity order of $APD_{30} < APD_{50} \approx APD_{90} < APD_{30\text{-}90}$ in detecting effects of the five hERG blockers on repolarization. APD_{90} was the most sensitive parameter in detecting effects of the hERG activator (A-935142.0). These results suggest the GPPM-APD assay and the CPF-APD assay are valuable in assessing drug effects on cardiac repolarization with comparable effects in both assays.

1759-Pos

Increased Cardiac Risk in Concomitant Methadone and Diazepam Treatment: Pharmacodynamic Interactions in Cardiac Ion Channels

Yuri A. Kuryshev, Glenn E. Kirsch, Arthur M. Brown.
ChanTest Corporation, Cleveland, OH, USA.

Methadone, a synthetic opioid used in the treatment of chronic pain and in maintenance of withdrawal from opioid dependence, has been linked to QT prolongation, potentially fatal torsades de pointes, and sudden cardiac death. Concomitant use of benzodiazepines, such as diazepam, in methadone maintenance treatment appears to increase the risk of sudden death. Our objective was to determine the effects of methadone and diazepam singly and in combination on the major cardiac ion channels, responsible for the cardiac repolarization, stably expressed in mammalian cells. Using automated patch-clamp technique (PatchXpress®) for ion channel current recording, we found that methadone produced concentration-dependent block of hERG ($IC_{50} = 1.7$ µM), $hNa_v1.5$ (11.2 µM tonic block; 5.5 µM phasic block), $hCa_v1.2$ (26.7 µM tonic; 7.7 µM phasic) and hK_vLQT1/hminK (53.3 µM). Diazepam demonstrated much less potent block to block of these ion channels: the IC_{50} values were 53.1, >100 tonic and 47.7 phasic, 89.0 tonic and 82.1 phasic, and 86.4 µM for hERG, $hNa_v1.5$, $hCa_v1.2$ and hK_vLQT1/hminK, respectively. Co-administration of 1µM diazepam with methadone had no significant effects on methadone-induced block of hERG, $hCa_v1.2$ and hK_vLQT1/hminK channels, but caused a 4-fold attenuation of $hNa_v1.5$ block (44.2 µM tonic and 26.6 µM phasic). Thus, although diazepam alone does not prolong the QT interval, the relief of the methadone-induced Na^+ channel block may leave hERG K^+ channel block uncompensated, thereby creating a potentially greater cardiac risk.

1760-Pos

Optimization of a Cav1.2 Cell Line for Use on QPatch and PatchXpress

Ruth L. Martin, James T. Limberis, Xiaoqin Liu, Kathryn Houseman, Zhi Su, Wende Niforatos, Bryan F. Cox, Gary A. Gintant.
Abbott Laboratories, Abbott Park, IL, USA.

Ion channel currents comprise the cardiac action potential and are important in cardiac safety liability assessment of potential drug candidates. The gold standard for assessing ion channel activity is the voltage clamp technique, but this technique is a very low throughput process. Planar patch technology (QPatch and PatchXpress) allows for moderate throughput by providing automated, simultaneous whole cell voltage clamp recordings from cells heterologously expressing the channel of interest. Ion channels routinely screened for cardiovascular safety are hERG (Kv11.1), Nav1.5, Kir2.1 and KvLQT/minK using either PatchXpress or QPatch instruments. In this study, we highlight the validation of Cav1.2 (L-type calcium channel) on our automated electrophysiology systems for cardiovascular safety screening. The L-type calcium channel is expressed in the cardiovascular system both in smooth and cardiac muscle. Potent L-type calcium channel antagonists can lower blood pressure, reduce cardiac contractility, and potentially increase the P-R interval on the electrocardiogram (ECG). Cav1.2 was expressed in CHO cells using a tetracycline inducible vector. Because of this we needed to optimize expression level by varying the induction variables. Addition of an L-type antagonist (verapamil) also provided benefit by keeping well-expressing cells viable after induction. In order to optimize flexibility in performing experiments, we also prepared the cells as a cryo-preserved subtrate. Cav1.2 channel kinetics for both activation and inactivation were investigated, and potencies of 8 reference compounds (weak and strong antagonists) were assessed on both platforms. In conclusion, we have optimized tissue culture conditions, cell preparation and voltage clamp protocols on two automated electrophysiology platforms to provide cardiac safety evaluation of drug candidates using an inducible Cav1.2 cell line.

1761-Pos

Pacemaker Cells of the Atrioventricular Node are $Ca_V1.3$ Dependent Oscillators

Pietro Mesirca[1], Laurine Marger[1], Angelo Torrente[1], Jorg Striessnig[2], Joel Nargeot[1], Matteo E. Mangoni[1].
[1]IGF CNRS, Montpellier, France, [2]University of Innsbruck, Innsbruck, Austria.

The atrioventricular node (AVN) can generate pacemaker activity in case of failure of the sino-atrial node (SAN). However, the mechanisms underlying pacemaking in AVN cells (AVNCs) are poorly understood. Voltage-dependent ion channels such as hyperpolarization-activated HCN channels, L-type $Ca_v1.3$ and T-type $Ca_v3.1$ channels are known to play a role in pacemaking of sino-atrial node cells (SANCs). Here, we investigate the role of these channels in AVNCs pacemaker activity using genetically modified mouse strains and show that they differentially impact pacemaking of AVNCs than of SANCs. Indeed, contrary to SANCs, $Ca_v1.3$ channels are necessary for pacemaking of AVNCs and accounted for the predominant fraction of $I_{Ca,L}$. Inactivation of $Ca_v3.1$ channels impaired automaticity in AVNCs by promoting sporadic block of automaticity and spontaneous cellular arrhythmia.
Abolition of the cAMP sensitivity of HCN channels shifted the I_f activation to voltages negative to that spanning the diastolic depolarization and prevented AVNCs automaticity in basal conditions. However pacemaker activity could be restored to control levels by adrenergic receptor stimulation.
Inactivation of both $Ca_v1.3$ and $Ca_v3.1$ results in abolishment of pacemaking. Inhibition of TTX-resistant (I_{Nar}) Na+ current showed that this is a key contributor of the action potential (AP) threshold and upstroke velocity.
Conclusion: 1. Spontaneous firing rate in AVNCs is strongly dependent from $Ca_v1.3$-mediated L type calcium current and from TTX resistant sodium current ($I_{Na,r}$). 2. In AVNCs the $Ca_v1.3$ isoform seems to be predominant compared to $Ca_v1.2$ isoform. 3. The fact that hyperpolarization of $Ca_v1.3^{-/-}$AVNCs pacemaking can be observed suggests that the absence of pacemaker activity is not due to the impossibility to generate the upstroke phase of the AP but probably due to an imbalance between outward and inward currents during the diastolic depolarization.

1762-Pos

Development of Novel System for the Functional Analysis of the Cardiomyocytes Network Model Using *On-Chip* Cellomics Technology

Fumimasa Nomura[1], Tetsuo Kitamura[2], Tomoyuki Kaneko[1], Kenji Yasuda[1].
[1]Tokyo Medical & Dental Univ., Tokyo, Japan, [2]Mitsubishi Chemical Medience Co., Kamisu, Japan.

Spatial and temporal regulation of cellular orientation is one of the key to resolve the mechanism of organs and tissues that are complexly intertwined with epigenetic factors, such as cellular network size and orientation of cellular-type. To study the dynamics of synchronous beating rhythm in the cardiac myocytes, we tried to develop the agarose micro-chamber (AMC) system on the multi-electrode array (MEA) chip, and extra-cellular signals of cardiomyocytes in geometrically patterning chambers were recorded with *On-Chip* MEA system. The chip set consists with the type of MEA chip, pattern of AMC and cellular-type, for example, primary *mouse* embryonic, ES and iPS derived cardiomyocyts. By using the cell handling by micropipette and additional fabrication to the AMC during the cultivation, we are able to construct the normal and disordered model. For example, we made the loop structure as reentry model having length of the circuit above the millimeter. Under this system, it is possible to obtain a multiple of information about individual cell (as constitutional unit) and entire network (as organ model) by field potential recordings (FPs) and optical imaging. Pseudo-ECG, which sum the FPs obtained from each electrode, means whole network signal and duration time of pseudo-ECG corresponds to QT interval. From analysis of individual FPs, direction of the excitement propagation and conduction velocity is resolved. Waveform analysis of FPs give us the relative intensity of Na^+, Ca^{2+} and K^+ currents and field potential duration (FPD) corresponding to action potential duration (APD). *On-Chip* geometric re-constitutive approaches are powerful tools for stepwise cell network construction and long-term measurement of it, and also will make possible the development of the novel system for the toxicity studies of drugs.

1763-Pos

Comparison of Computationally and Experimentally Determined Single I_{Kr} Channel Activity During Pacemaking in Sinoatrial Node Cells

Marieke W. Veldkamp, Ronald Wilders, Lennart N. Bouman,
Tobias Opthof, Antoni C.G. van Ginneken.
Academic Medical Center, Amsterdam, Netherlands.

Background: The contribution of the rapidly activating delayed rectifier current (I_{Kr}) to sinoatrial (SA) node pacemaking, is mainly derived from computational models. The mathematical representation of I_{Kr} therein, is based on voltage-clamp data in SA-node cells, but to what extent computational I_{Kr} activity accurately describes true dynamic behavior of I_{Kr} during the SA-node action potential (AP), remains to be established.

Methods: With the dual electrode patch clamp technique, we simultaneously recorded spontaneous APs (whole-cell) and single I_{Kr} channel activity (cell-attached-patch) from isolated rabbit SA-node cells. To allow comparison between measured I_{Kr} channel activity and computational I_{Kr} activity, a model rabbit SA-node cell (Zhang et al. Am J Physiol Heart Circ Physiol. 2000; 279: H397-H421) was action potential clamped by our experimentally recorded APs.

Results: In experiments, I_{Kr} channel openings were detected during AP repolarization and diastolic depolarization. The open probability (P_o) was very low (<0.15) early during repolarization, but rapidly increased towards final repolarization, reaching a maximum of 0.27 ± 0.03 (mean $\pm$ SEM, n = 4) shortly before the maximum diastolic potential (MDP). During the subsequent diastolic depolarization, P_o gradually declined to a value of 0.08 ± 0.02 (mean $\pm$ SEM, n = 4) just before take-off of the next AP. P_o obtained from the computational model followed a qualitatively similar course during SA-node automaticity, but values were doubled. That is: P_o rapidly increased from zero to a maximal value of 0.63 shortly before MDP, and then declined to 0.18 towards the end of diastolic depolarization.

*Conclusions***:** The computational model well-described the time- and voltage dependent changes in P_o of I_{Kr} channels during SA-nodal pacemaking, however, P_o was over-estimated by a factor of 2 in all phases of the pacemaker cycle.

TRP Channels

1764-Pos

Modelling the Membrane Potential Dependence on Non-Specific Cation Channels in Canine Articular Chondrocytes

Rebecca Lewis, Gregor Purves, Julia Crossley, Richard Barrett-Jolley.
University of Liverpool, Liverpool, United Kingdom.

In a previous report, we showed that the predominant ion channel in potassium-free solutions was a gadolinium III (Gd^{3+}) sensitive non-specific cation channel, with functional characteristics similar to that expected for transient receptor potential (TRP) type channels.

In this study reverse transcription-PCR (RT-PCR) was used to investigate the expression of TRP channels in canine articular chondrocytes. Both a mathematical model based on the Goldman-Hodgkin-Katz voltage equation and current clamp whole-cell electrophysiology were then used to investigate the effect of these channels on membrane potential (*Vm*).

Chondrocytes isolated from canine articular cartilage were cultured for 5 days in Dulbeccos Modified Eagles Medium with 10% Foetal Calf Serum. For RT-PCR analysis, total RNA was extracted from first passage cells. Electrophysiological recording was carried out on first to third passage cells.

RT-PCR analysis of chondrocyte mRNA, and subsequent sequencing of products, showed a member of the TRP vanilloid group of channels (TRPV4) to be present; sequence homology to the human TRPV4 was 94%. We have so far failed to find mRNA for the functionally similar TRPC3 and TRPC6 channels. Using whole-cell and single-channel data from our own experiments and the literature, our model predicts the membrane to be heavily dependent on the activity of TRPV4. Simulated block of all non-specific cation channels in the chondrocyte membrane leads to a predicted −27mV change in *Vm*. This prediction closely matches our current clamp experiments with 100μM Gd^{3+} inducing a -32 ± 1mV (n = 6) change of *Vm*.

Previously, large-conductance chloride and voltage-sensitive potassium channels have been reported to be important in the maintenance of chondrocyte *Vm.* The data presented here showsthat the TRPV4 channel also has a significant contribution to maintenance of the chondrocyte *Vm*.

1765-Pos

Regulation by Calcium of Polycystin-2 (TRPP2) and Hetero-Complexes with TRPC1

María del Rocío Cantero[1], Horacio F. Cantiello[2,3].
[1]Instituto de Investigaciones Cardiológicas, Capital Federal, Argentina,
[2]Massachusetts General Hospital, Charlestown, MA, USA, [3]Instituto de Investigaciones Cardiológicas, Buenos Aires, Argentina.

Polycystin-2 (PC2, TRPP2) and the canonical TRPC1 are TRP superfamily members that act as non-selective cation channels, with multiple subconductance states and permeability to calcium. Recent studies from our laboratory (Zhang et al., *Hum Mol Genet*, 2009) indicated that both channels, form homo and hetero-tetramers with distinct functional properties. Both TRP channels are implicated in calcium transport and signaling events, therefore, their regulation by calcium is relevant to their role in cell function. Here we studied the effect of cytoplasmic and external calcium on the regulation of PC2, TRPC1 and PC2/TRPC1, channel function. Lowering cytoplasmic calcium (0.3 nM) with either BAPTA or EGTA inhibited PC2 channel function. This inhibition was extrinsic to the channel complex, and was dependent of external calcium concentrations. Titration of cytoplasmic calcium recovered PC2 channel activity, with a Hill coefficient of 5 and an apparent affinity constant of 1-5 nM. The addition of either BAPTA (2 mM) or EGTA (1 mM) to TRPC1 to lower cytoplasmic calcium concentrations did not inhibit the current (single channel conductance) mediated by the TRPC1 homo-tetrameric channel. In contrast, low calcium decreased TRPC1's mean open probability by 50%. In addition, low cytoplasmic calcium did not inhibit PC2 channel function when hetero-complexed with TRPC1. These data suggest that the formation of structural hetero-complexes between PC2 and TRPC1 confers important regulatory changes to either channel's function, such as the sensory response to cytoplasmic calcium concentrations, thus providing functional diversity to their channel properties in endogenous environments such as the primary cilium or the plasma membrane, where they locate.

1766-Pos

Evaluation of the QPatch HT and HTX Systems As Methods for Ion Channel Screening

Mark McPate[1], Sarah Lilley[1], Martin Gosling[1], Søren Friis[2],
Rasmus B. Jacobsen[2], Pamela Tranter[1].
[1]Novartis Institutes for Biomedical Research, Horsham, United Kingdom,
[2]Sophion Biosciences, Ballerup, Denmark.

The introduction of high throughput planar automated electrophysiology systems has brought the potential of ion channels as targets for pharmacological modulation to the forefront. Sophion Biosciences QPatch systems are fully automated electrophysiology platforms generating high resistance seals with resultant ion channel biophysical and pharmacological properties similar to conventional patch clamp recordings. In this study, using a CHO cell line stably expressing the TRPM2 channel, the performance of the QPatch HTX, which records from a population of 10 cells per recording site, was evaluated against the QPatch HT which records from a single cell per recording site.

TRPM2 can be challenging to measure, particularly when determining inhibitor potencies, due to poor recording stability characterised by current rundown. A compound set was screened against TRPM2 on the QPatch HT and HTX to assess their relative performances. There was a good correlation between the IC_{50} values generated on the two systems ($r^2 = 0.91$). The current rundown on the QPatch HTX was considerably reduced compared to the QPatch HT (19.5 $\pm$ 1.5% and 37.5 $\pm$ 3.0% respectively, mean $\pm$ SEM, n = 4 experiments, 767 cells profiled). This resulted in an increase in the number of successful recordings obtained from 51.6 $\pm$ 7.1% for HT to 83.1 $\pm$ 4.5% for HTX (Mean $\pm$ SEM, n = 4 experiments, 912 cells profiled) for a 5 point IC_{50} assay and from 67.2 $\pm$ 8.9% for HT to 98.6 $\pm$ 1.4% for HTX (Mean $\pm$ SEM, n = 3-4 experiments, 480 cells profiled) for a single concentration assay.

The QPatch HT has made a significant impact on the volume of high quality electrophysiology data that can be generated. This preliminary study suggests that the QPatch HTX system can further enhance throughput, particularly with channels where current stability is problematic.

1767-Pos

Activating Mutations Reveal a Role of TRPML1 in Lysosomal Exocytosis

Xiang Wang, Xian-ping Dong, Dongbiao Shen, Haoxing Xu.
University of Michigan, Ann Arbor, MI, USA.

The contents of lysosomes undergo exocytosis (lysosomal exocytosis) in response to an increase of intracellular Ca^{2+}. Emerging evidence suggests that lysosomal exocytosis plays important roles in a variety of cell biological functions including neurotransmitter release, neurite outgrowth, and plasma membrane repair. The putative Ca^{2+} channel in the lysosome that mediates intralysosomal Ca^{2+} release, however, has not been identified. The mucolipin TRP (TRPML) proteins are a family of endolysosomal cation channels with genetically established importance in man and rodent. Mutations of human *TRPML1* cause type IV mucolipidosis, a devastating pediatric neurodegenerative disease. In this study, we found that although TRPML1-mediated currents can only be recorded in late endosome and lysosome (LEL) using the lysosome patch clamp technique, several proline substitutions in TRPML1 (such as $TRPML1^{V432P}$) display gain-of-function (GOF) constitutive activities at both

the plasma membrane (PM) and endolysosomal membranes. Although wild-type TRPML1 localized exclusively in LEL and were barely detectable in the PM, the GOF mutants were not restricted to LEL compartments, and most significantly, exhibited significant surface expression. As a Ca^{2+}-permeable channel, the constitutive Ca^{2+} permeability due to Pro substitutions may allow TRPML1 proteins traffic to the PM via Ca^{2+}-dependent lysosomal exocytosis, resulting in the surface expression and whole cell currents of TRPML1. Consistent with the hypothesis, surface staining of lysosome-associated membrane protein-1 (Lamp-1) was dramatically increased in cells expressing GOF TRPML1 channels. Interestingly, the extent of the lysosomal exocytosis appeared to be correlated with the degree of channel gain-of-function of TRPML1 mutants. Our results suggest that upon unidentified cellular stimulations, TRPML1 mediates intralysosomal Ca^{2+} release to trigger lysosomal exocytosis. Currently we are investigating whether inhibiting exocytosis could reduce surface expression of GOF TRPML1 mutants, and whether stimulating exocytosis could enhance surface expression of TRPML1.

1768-Pos
TRPM8 Near-Membrane Dynamics and Channel Stabilization after Stimulation
Luis Veliz, Carlos Toro, Luis Arias, Jenifer Villegas, **Sebastian E. Brauchi**.
Universidad Austral de Chile, Valdivia, Chile.
TRPM8 is a non-selective cation channel expressed on a subset of peripheral neurones, and is the molecular machine that allow us to detect cold signals from our surroundings. Some members of the TRP channel family changes their cellular distribution in response to agonist stimulation. Here, we will describe membrane/near-membrane dynamics of TRPM8-GFP containing particles in both, HEK-293T and F-11 transfected cells. 2D and 3D trajectories together with the velocity of individual protein containing vesicles were obtained by Total Internal Reflexion of Fluorescence Microscopy (TIRFM) and single particle tracking (SPT), and analyzed by plotting of the mean-square displacement against time. Four characteristic types of motion were observed: (a) stationary; (b) simple Brownian diffusion; (c) directed diffusion; and (d) confined diffusion, in which particles undergoing Brownian diffusion are confined within a limited area. Our data suggests that TRPM8, when inserted into the plasma membrane, is confined into small domains of about 3 um in diameter, in which receptor molecules resides in the time scale of 2-8 s. In the absence of stimuli TRPM8 vesicles constantly move along a network that cover the plasma membrane, periodically stopping, most often just briefly. Stimulation halted this hop-diffusion probably by stabilizing TRPM8 channels, as a result, release from plasma membrane became significantly slower. This slow release of TRPM8 determined the overall increase of available receptors.
Support from: Fondecyt 11070190; Pew Program in Biomedical Sciences; SeedingLabs.

1769-Pos
Ligand Stoichiometry of TRPM8
Thomas Voets, Annelies Janssens.
KU Leuven, Leuven, Belgium.
Temperature-sensitive TRP channels (thermoTRPs) play a key role in somatosensory thermosensation. Several thermoTRPs, including the heat-activated TRPV1 and the cold-activated TRPM8, are not only sensitive to changes in temperature but also to ligands that evoke a thermal sensation, such as the ‘hot pepper’ compound capsaicin (TRPV1) and the cooling agent menthol (TRPM8). Recent data indicate that the binding site of these lipophilic compounds is located in the so-called ‘sensor domain’ made up of transmembrane domains S1-S4. For example, mutating S4 arginine at position 842 in TRPM8 to histidine (mutant R842H) produces a channel with unaltered cold and voltage sensitivity, but with a ~100-fold reduction in menthol affinity. Given that TRP channels are tetramers and that the sensor domains are spatially apart, a functional TRPM8 channel can potentially bind four menthol molecules. However, the contribution of each individual menthol binding event to channel gating is unknown. To address this question, we made vectors encoding tandem tetramers with all possible combinations of WT and R842H subunits. Expression of these vectors in HEK293 cells exclusively produced protein of the expected tetrameric molecular weight, and whole-cell recordings further confirmed that the tandem linkage of subunits did not significantly affect channel gating. This approach will further be used to determine the exact stoichiometry of menthol-induced TRPM8 gating.

1770-Pos
Exploring Structural Relationships between TRP and Kv Channels
Jeet Kalia, Kenton J. Swartz.
NINDS, NIH, Bethesda, MD, USA.
Transient Receptor Potential (TRP) ion channels are homotetrameric, non-selective cation channels that are expressed in diverse cell types in eukaryotes, ranging from yeast to humans. TRP channels have been implicated in many physiological roles such as thermosensation, mechanosensation, chemesthesis, hearing, and sensing pain. Indeed, TRP channels are gated by a plethora of stimuli. For example, TRPV1 is activated by heat, voltage, and small molecules such as capsaicin, and TRPM8 is activated by cold, voltage and cooling agents such as menthol. The molecular mechanisms underlying this polymodal gating of TRP channels are poorly understood. In contrast, the mechanism of voltage-activation of the voltage-gated potassium (Kv) channels is well understood. The architectural similarity of TRP channels and Kv channels, in addition to several mutagenesis-based reports published on TRP channels, raise the possibility that the mechanisms of voltage gating of these two families of ion channels may have common features. To address this hypothesis, we have created a series of chimeras between the Kv channel, Kv2.1, and two TRP channels, TRPV1 and TRPM8, and studied them using electrophysiological techniques. Replacing the critical S3b-S4 paddle motif of Kv2.1 with analogous regions of TRPV1 or TRPM8, results in channels that activate in response to membrane depolarization. In both instances, the slopes of voltage-activation relations were decreased in the chimeras as compared to wild-type Kv2.1.These results are consistent with the hypothesis that TRP channels contain a structural motif related to the paddle motifs in Kv channels, and that this motif can sense voltage in the context of a Kv channel. We are currently testing whether this motif can sense voltage in TRP channels and exploring structural relationships between these two families of channels.

1771-Pos
TRPM3 Expression and Function in Vascular Smooth Muscle
Jacqueline Naylor, Jing Li, Fanning Zeng, Piruthivi Sukumar,
Yasser Majeed, Carol J. Milligan, Bhaskar Kumar, Karen E. Porter,
David J. Beech.
University of Leeds, Leeds, United Kingdom.
The Transient Receptor Potential (TRP) channels form a diverse superfamily of cation channels. Currently there are few well characterised, selective, physiological regulators of TRP channels, which can impede the discovery of native channel functions. TRPM3, a member of the melastatin subfamily of TRP channels, is reported to form constitutively active Ca^{2+}-permeable cation channels activated by sphingolipids, hypotonic shock, and the neurosteroid pregnenolone sulphate. Expression is predominantly in brain and kidney, although expression has recently been reported in pancreatic β-cells. Here we report TRPM3 expression and function in vascular smooth muscle cells. Anti-TRPM3 blocking antibody and short-interfering RNA targeted to TRPM3 were used to confirm the involvement of TRPM3 in the pregnenolone sulphate elicited Ca^{2+} influx in cultured human vascular smooth muscle cells. Although pregnenolone sulphate is a useful pharmacological and potentially therapeutic agent, the physiological significance in the vasculature is unknown. We therefore screened for novel modulators, and found that cholesterol inhibited both pregnenolone sulphate-induced and constitutive TRPM3 activity. The data suggest TRPM3 is a novel calcium-entry channel of vascular smooth muscle cells.
The research was supported by a BBSRC Industrial Co-operative Award in Science and Engineering, the Wellcome Trust and the British Heart Foundation.

1772-Pos
Clotrimazole Potentiates TRPM3 Responses to Pregnenolone Sulfate
Joris Vriens, Bernd Nilius, Thomas Voets.
K.U.Leuven, Leuven, Belgium.
Clotrimazole (CLT) is an antifungal compound commonly used in over-the-counter medications for the topical treatment of fungal infections of the skin, vagina, and mouth. CLT exerts its antifungal actions by inhibiting P450-dependent enzymes. TRPM3a2 (1), a splice variant of TRPM3, is rapidly and reversibly activated by pregnenolone sulfate (PS) and nifedipine (1). Here, we demonstrate that CLT strongly potentiates the response of TRPM3a2 to pregnenolone sulfate (PS) stimulation. Direct application of CLT to TRPM3a2 has no effect, however preapplication of CLT followed by PS stimulation strongly potentiates the TRPM3a2 response. The potentiation by CLT is reversible, repetitive and independent of external calcium. At CLT concentrations above 1 mM, the intensity of potentiation does not dependent CLT dose but rather on PS concentration. The response to PS after priming with CLT was relatively slow, suggesting a modulation in the signaling cascade rather than a direct effect. We conclude that CLT potentiates the TRPM3a2 response in an indirect manner, possibly by preventing further metabolization of pregnenolone sulfate by inhibiting P450-dependent enzymes.
(1) kindly provided by J. Oberwinkler, S. Phillip, V. Flockerzi, Homburg (Saar), Germany
(2) Wagner TF, Loch S, Lambert S, Straub I, Mannebach S, Mathar I, Düfer M, Lis A, Flockerzi V, Philipp SE, Oberwinkler J, Transient receptor potential M3 channels are ionotropic steroid receptors in pancreatic beta cells, Nat Cell Biol. 2008;10(12):1383-4

1773-Pos
Complex Regulation of TRPV1 by Phosphoinositides

Viktor Lukacs, Baskaran Thyagarajan, **Tibor Rohacs**.
UMDNJ - New Jersey Medical School, Newark, NJ, USA.

TRPV1 is a nonselective highly calcium permeable cation channel present in the peripheral nervous system exclusively in polymodal nociceptors. A sensory integrator of several noxious stimuli, TRPV1 plays a crucial role in the development of inflammatory pain and hypersensitivity. Plasmamembrane phosphoinositides are recognized as important regulators of TRPV1 function; the precise nature of their effect is, however, controversial.

Phosphatidylinositol-4,5-bisphosphate (PIP_2) has initially been proposed to tonally inhibit TRPV1 via a C-terminal inhibitory domain. Furthermore, receptor-mediated depletion of PIP_2 was proposed to be involved in sensitization of TRPV1 in response to pro-inflammatory agents. However, in subsequent studies including our own, direct intracellular application of PIP_2 reproducibly potentiated TRPV1 currents rather than inhibiting them. In addition, PIP_2 depletion concurrent with robust TRPV1 activation is an important contributing factor to channel desensitization consistent with the activating effect of $PIP_{2.}$

We attempt to address this controversy utilizing multiple independent approaches to selectively regulate plasmamembrane PIP_2 levels in heterologous expression systems. Our results show that TRPV1 currents in intact cells elicited by low to moderate, but not high agonist concentrations are potentiated in response to PIP_2 depletion. Conversely, increasing PIP_2 levels inhibits low but not high agonist-induced TRPV1 currents. These effects are reduced or absent in the mutant channel lacking the putative C-terminal inhibitory domain. The inhibitory effect of PIP_2 however was never observed in excised patches even at low agonist concentrations. Our results are consistent with an agonist concentration-dependent dual regulatory effect of PIP_2. The inhibitory effect furthermore appears to be indirect. Such dual effects of PIP_2 have previously been described for voltage-gated calcium channels as well as other TRP channels and raise important questions as to the identity of interacting molecules conferring the inhibitory effect and the physiological relevance of such complex regulation.

1774-Pos
TRPV1 Activation by Allyl Isothiocyanate

Maarten Gees, Wouter Everaerts, Yuji Karashima, Aurelia Apetrei, Bernd Nilius, Thomas Voets, Karel Talavera.
Ku Leuven, Leuven, Belgium.

Allyl isothiocyanate (mustard oil, MO) is a highly reactive electrophilic compound known to cause irritation, pain and inflammation. These effects are thus far thought to be mediated by activation of TRPA1, a Transient Receptor Potential (TRP) cation channel expressed in nociceptive neurons. Recent research has shown that TRPV1, the heat and capsaicin receptor, can be also activated by reactive compounds such as allicin and leek and onion extracts. Here, we show that both human and mouse TRPV1 are activated by MO, at concentrations at which TRPA1 undergoes fast desensitization and block. In Ca2+ imaging experiments of intact HEK293 cells, MO induces an increase of the intracellular Ca2+, which was not present when Ca2+ was omitted in the bath solution. Activation of TRPV1 by MO is dose-dependent and is caused by a shift of the voltage dependence of channel activation to more negative potentials, similar to the activation of TRPV1 by capsaicin. Stimulation of TRPV1 by MO can be observed in inside-out patches, indicating a membrane-delimited mechanism of activation. Furthermore, the heat-induced activation of TRPV1 could be sensitized with sub-activating MO concentrations.

Notably, MO was able to stimulate a large population of sensory neurons isolated from Trpa1 KO mice. This population was significantly reduced in Trpa1/Trpv1 double KO mice, indicating the physiological importance of TRPV1 activation by MO. WT, Trpa1 and Trpv1 KO mice displayed significantly stronger aversion to MO than double KO mice in forced drinking and open field exploration assays. The identification of TRPV1 as a novel target of MO is essential for the full understanding of the mechanisms of action of this compound in vivo and prompts to re-evaluate the results of previous research, in which MO was used as specific activator of TRPA1.

1775-Pos
Molecular Determinants of the Activation Gate of the TRPV1 Channel

Hector Salazar[1], Andrés Jara-Oseguera[2], Andrés Nieto-Posadas[1], Itzel Llorente[1], León D. Islas[2], Tamara Rosenbaum[1].
[1]Instituto De Fisiologia Celular, U. Nacional Autonoma De Mexico, D.F. Mexico City, Mexico, [2]Facultad de Medicina, U. Nacional Autonoma De Mexico, D.F. Mexico City, Mexico.

The ability of ion channels to transit among different conformations allows them to regulate different types of cellular functions. Transient Receptor Potential Vanilloid 1 (TRPV1)channels participate in several types of physiological responses such as pain detection and inflammation, little is known about how their structural components convert different types of stimuli into channel activity. To localize the activation gate of these channels, we used the substituted cysteine accessibility method (SCAM) and inserted cysteines along the S6 segment of the TRPV1 channel and assessed their accessibility to thiol-modifying agents and silver. Our results show that access to the pore of the TRPV1 is gated by the S6 both in response to capsaicin binding and to increases in temperature, that the pore-forming S6 segments are helical structures and that there are two constrictions in the pore. One located at residue L681 which hampers the access to large molecules and one located at residue Y671 which impedes the entrance of smaller ions a and constitutes the activation gate of these channels. These data have also allowed us to produce a model of this region in the structure of TRPV1 based on functional findings.

1776-Pos
Interactions between Quaternary Ammoniums and the Gate of the TRPV1 Channel

Andrés Nieto-Posadas[1], Héctor Salazar[1], Itzel Llorente[1], León D. Islas[2], Tamara Rosenbaum[1].
[1]División de Neurociencias, Instituto de Fisiología Celular, Universidad Nacional Autonóma de México, Mexico, Mexico, [2]Departamento de Fisiología, Facultad de Medicina, Universidad Nacional Autonóma de México, Mexico, Mexico.

TRP channels play a fundamental role in neuronal signalling and in the detection of painful stimuli and inflammatory processes. The TRPV1 (vanilloid 1) channel functions as an integrator of noxious chemical and physical signals known to cause pain. Structural and functional information of the pore domain shows that access to the pore is gated by the S6 in response to capsaicin and temperature. Our group recently found the presence of two intracellular constrictions: L681 which obstructs the ion conduction pathway for large molecules and Y671 which obstructs the ion conduction pathway for small permeating molecules and constitutes de activation gate of TRPV1 channels. Quaternary ammoniums (QA) are a family of pore blockers that have been successfully used in structure-function studies. Previous results using QA on TRPV1 show that these compounds block the channel in a state-dependent fashion. Since it has been shown that aromatic residues interact with quaternary ammoniums by direct hydrophobic interactions we decided to test if the actions of tetrabutylammonium (TBA) are mediated by the interaction with the aromatic residue Y671 . Our preliminary results indicate that this residue is not involved in the binding of TBA to TRPV1.

1777-Pos
Sensitization of Vanilloid Receptors TRPV3

Beiying Liu[1], Jing Yao[1], Michael X. Zhu[2], **Feng Qin**[1].
[1]SUNY-Buffalo, Buffalo, NY, USA, [2]Ohio State University, Columbus, OH, USA.

Vanilloid receptors of the transient receptor potential family have functions in thermal sensation and nociception. Among them, TRPV3 is expressed in skin keratinnocytes and has also been implicated in flavor sensation in oral and nasal cavities as well as being a molecular target of some allergens and skin sensitizers. The channel displays a unique property that repeated stimulation results in gradual increases of its activity, a process that is known as sensitization and is observed in both native cells and cell lines. Transient calcium release from internal stores has been thought to underlie the sensitization process through a mechanism involving relief of Ca2+-dependent inhibition of the channel due to calmodulin binding at the distal N-terminal. In support of the hypothesis is the differential effect of the calcium chelators BAPTA and EGTA, where BAPTA, which has a fast buffering kinetics, is able to modulate the sensitization, while EGTA is ineffective. Here we suggest an alternative mechanism for the sensitization process. We distinguish two types of sensitizations; one is reversible and the other irreversible. The irreversible sensitization is intrinsic to the gating of the channel, while the reversible one such as that mediated by BAPTA is attributable to a modulation effect. We show that analogs of BAPTA that apparently lack Ca2+ buffering capability similarly sensitize the channel. We conclude that the sensitization of the channel, including the effects of BAPTA, also involves a membrane-delimited mechanism.

1778-Pos
Ca2+ Inhibition of Cation Conductance through TRPV1 Receptors

Damien S.K. Samways, Terrance M. Egan.
Saint Louis University, St. Louis, MO, USA.

TRPV1 receptors are polymodal cation channels that show a marked permeability to Ca2+. In the present study, we used single channel electrophysiology and whole cell patch clamp photometry to further study the interaction of extracellular Ca2+ ([Ca2+]o) with the recombinant TRPV1 receptor expressed in HEK293 cells. In the presence of and 140 mM [NaCl]o, we observed that

[Ca2+]o attenuates the amplitude of capsaicin (0.5 microM)-evoked single channel currents through TRPV1 receptors within a physiologically relevant concentration range (Kd = 2 mM, Hill slope = 1.1). The inhibition was observed at a range of positive and negative membrane potentials, being more pronounced at negative potentials. Use of patch clamp photometry revealed that at −60 mV in the presence of 10 mM [Ca2+]o, which is almost maximally effective for inhibiting single channel current amplitudes (56%), the fractional of the current carried by Ca2+ current was only 40%. Thus, Na+ still carries most of the cation current through the TRPV1 receptor even when Ca2+ is likely occupying the site responsible for its inhibiting cation conductance. Finally, we observed that neutralizing the charge on single amino acids located in the mouth of the putative pore and known to contribute to Ca2+ selection by TRPV1 receptors, Asp646, Glu648 and Glu651, did not alter the inhibitory effect of 2 mM [Ca2+]o. To summarize, although Ca2+ has been reported to increase the open probability of TRPV1 receptors, this divalent cation also attenuates conductance through the channel pore via an unknown mechanism seemingly discreet from that contributing to the high Ca2+ permeability of these receptors.

1779-Pos

Distinct Modulations of Human Capsaicin Receptor by Proton and Magnesium Through Different Domains

Shu Wang, **Huai-hu Chuang**.
Cornell University, ITHACA, NY, USA.

The capsaicin receptor (TRPV1) is a nonselective cation channel that integrates multiple painful stimuli, including capsaicin, protons and heat. Protons facilitate the capsaicin- and heat -induced currents by decreasing thermal threshold or increasing agonist potency for TRPV1 activation. In the presence of saturating capsaicin, rat TRPV1 (rTRPV1) reaches full activation, with no further stimulation by protons. Human TRPV1 (hTRPV1), a species ortholog with high homology to rTPRV1, is potentiated by extracellular protons and magnesium, even at saturating capsaicin. We investigated the structural basis for protons and magnesium modulation of fully capsaicin-bound human receptors. By analysis of chimeric channels between hTRPV1 and rTRPV1,We mapped the required domain and a single amino acid residue responsible for further potentiation of capsaicin efficacy by protons. We also showed that magnesium ions could also exert similar effects for capsaicin activation of human TRPV1, but through a different functional domain. Our results demonstrate that capsaicin efficacy of hTRPV1 correlates with the extracellular ion milieu, and unravel the relevant structural basis of modulation by protons and magnesium.

1780-Pos

Interactions between DAG, IP_3 and PIP_2 Govern Activation of Heterotetrameric TRPC6/C7 Channel Activity in Rabbit Portal Vein Myocytes

Min Ju, Sohag N. Saleh, Anthony P. Albert, William A. Large.
St George's University of London, London, United Kingdom.

Previously we have shown that synergism between inositol-1,4,5-trisphoshate (IP_3) and diacylglycerol (DAG) mediates activation of TRPC6-like channel activity by noradrenaline (NA, Albert & Large, 2003) in rabbit portal vein myocytes. Moreover, a recent study showed that endogenous phosphatidylinositol-4,5-bisphosphate (PIP_2) produced a marked inhibitory action on TRPC6 activity in mesenteric artery myocytes (Albert et al, 2008). In the present work we investigated interactions between DAG, IP_3 and PIP_2 in regulating TRPC6-like activity in portal vein myocytes using patch clamp and immunoprecipitation methods.

In inside-out and cell-attached patches, bath application of respectively 10 μM IP_3 and the cell-permeable IP_3 analogue, 10 μM 6-IP_3, both potentiated OAG-induced TRPC6-like channel activity by 3-fold but had no effect when applied on their own. In inside-out patches, pre-treatment with 20 μM wortmannin, to deplete endogenous PIP_2 levels, increased OAG-evoked channel activity by 75-fold compared to control patches. Moreover, anti-PIP_2 antibodies activated TRPC6-like activity in quiescent inside-out patches. In wortmannin-treated inside-out patches, 10 μM diC8-PIP_2 inhibited OAG evoked channel activity (IC_{50} = 0.74 μM) which was rescued by over 50 % by co-application of 10 μM IP_3. Anti-TRPC6 and anti-TRPC7 antibodies inhibited TRPC6-like activity induced by NA by over 80%, but channel activity was unaffected by other TRPC antibodies. Co-immunoprecipitation studies showed association between TRPC6 and TRPC7 proteins and that both these channel proteins interacted with PIP_2. Pretreated with 6-IP_3, reduced association between PIP_2 and TRPC7 but not TRPC6, whereas OAG reduced PIP_2 interactions with TRPC6 but not TRPC7.

These results indicate that endogenous PIP_2 has a pronounced inhibitory action on TRPC6/TRPC7 heteromeric channels in portal vein myocytes. Moreover channel activation by DAG requires both this triglyceride and IP_3 to remove associations between PIP_2 and these channel proteins.

1781-Pos

Isoform-Selective Physical Coupling of TRPC3 Channels to IP3 Receptors in Smooth Muscle Cells Regulates Arterial Contractility

Adebowale Adebiyi, Guiling Zhao, Damodaran Narayanan,
Candice M. Thomas, John P. Bannister, Jonathan H. Jaggar.
University of Tennessee Health Science Center, Memphis, TN, USA.

Many vasoconstrictors bind to phospholipase C (PLC)-coupled receptors on arterial smooth muscle cells, leading to an intracellular inositol 1,4,5-trisphophate (IP_3) elevation and vasoconstriction. IP_3-induced vasoconstriction can occur independently of intracellular Ca^{2+} release and via IP_3 receptor (IP_3R) and canonical transient receptor potential (TRPC) channel activation, but signaling mechanisms mediating this effect are unknown. Here, we studied the mechanisms by which IP_3Rs stimulate TRPC channels in smooth muscle cells of resistance-size cerebral arteries. Immunofluorescence resonance energy transfer (immuno-FRET) microscopy in smooth muscle cells indicated that endogenous type 1 IP_3Rs (IP_3R1) are in close spatial proximity to TRPC3, but distant from TRPC6 or TRPM4 channels. Endothelin-1 (ET-1), a PLC-coupled receptor agonist, elevated the immuno-FRET signal between IP_3R1 and TRPC3, but not between IP_3R1 and TRPC6 or TRPM4. IP_3R1 co-immunoprecipitated with TRPC3, but not with TRPC6. An antibody targeting TRPC3 channels and TRPC3 channel knockdown with short hairpin RNA inhibited IP_3-induced nonselective cation current (I_{Cat}) activation, whereas an antibody to TRPC6 and TRPC6 channel knockdown had no effect. Biotinylation indicated that ET-1 did not alter total or plasma membrane-localized TRPC3. RT-PCR demonstrated that a calmodulin and IP_3R binding (CIRB) domain is present on the C-terminus of both TRPC3 and TRPC6 channels. A CIRB domain peptide attenuated IP_3- and ET-1-induced I_{Cat} activation. A peptide corresponding to the IP_3R region that can interact with TRPC channels activated I_{Cat}. A HIV-1 TAT-conjugated CIRB domain peptide reduced IP_3- and ET-1-induced vasoconstriction in pressurized arteries. These data indicate that IP_3 stimulates direct coupling between IP_3R1 and membrane-resident TRPC3 channels in arterial smooth muscle cells, leading to I_{Cat} activation and vasoconstriction. Data also indicate that close spatial proximity between IP_3R1 and TRPC3 establishes this isoform-selective functional interaction.

1782-Pos

Molecular and Structural Basis of Dual Regulation of a Canonical TRP Channel by Calmodulin

Ming-Hui Li, Lin-ling He, Zafir Buraei, Yong Yu, Liang Tong, Jian Yang.
Columbia University, New York, NY, USA.

The canonical transient receptor potential (TRPC) channels are widely distributed and have diverse biological functions. They are activated by stimulation of phospholipase C-coupled receptors, resulting in membrane depolarization and Ca^{2+} influx, which in turn feedback to regulate the channel activity through the Ca^{2+}-binding protein calmodulin (CaM) and other signaling pathways. Previous biochemical studies indicate that TRPC subunits contain one to four putative CaM-binding sites. One of these sites is named the "CaM-IP_3receptor binding" or CIRB site (because it also interacts with an IP_3 receptor fragment *in vitro*). The CIRB site is conserved in all seven TRPC subunits. CaM exerts either stimulatory or inhibitory effects on different TRPC channels. However, the molecular mechanism of CaM modulation of TRPC channels is unclear. We have solved the crystal structure of the complex of CaM and the CIRB site of TRPC5 channels, which regulate growth cone morphology and neurite growth, and require CaM for agonist-induced activation. The structure shows that the two lobes of a single Ca^{2+}-bound CaM (Ca^{2+}/CaM) bind two CIRB peptides arranged in parallel. This peptide dimerizes only in the presence of Ca^{2+}/CaM, suggesting that Ca^{2+}/CaM binding to the CIRB site may induce major conformational changes in intact channels. Structure-based mutagenesis studies show that Ca^{2+}/CaM binding to the CIRB site is not required for agonist-induced channel activation, but it safeguards the channel against inhibition produced by CaM binding to another site on the channel. We have identified this inhibitory site and found it to be a novel CaM-binding motif that can interact with not only Ca^{2+}/CaM but also $CaM_{1234,}$ a mutant CaM deficient in binding Ca^{2+}. Our results provide new insights into the intricate feedback regulation of a canonical TRP channel.

1783-Pos

TRPC3 is Essential for Maintenance of Skeletal Muscle Cells

Jin Seok Woo, Eun Hui Lee.
The Catholic Univ. of Korea, Seoul, Republic of Korea.

During membrane depolarization associated with skeletal excitation-contraction (EC) coupling, L-type Ca^{2+} channels (dihydropyridine receptor (DHPR) in the transverse (t)-tubule membrane) undergo conformational changes that are transmitted to Ca^{2+}-release channel (ryanodine receptor

type 1) in the sarcoplasmic reticulum (SR) causing Ca^{2+} release from the SR. Canonical-type transient receptor potential cation channel 3 (TRPC3), an extracellular Ca^{2+} entry channel in the t-tubule and plasma membrane, is required for full-gain of skeletal EC coupling. The present study examined additional role(s) for TRPC3 in skeletal muscle other than mediation of EC coupling. We created a stable myoblast line (MDG/TRPC3 KD myoblast) with reduced TRPC3 expression by knock-down of TRPC3 using retrovirus-delivered small interference RNAs in $\alpha 1_S$DHPR-null muscular dysgenic myoblasts to eliminate any DHPR-mediated EC coupling-related events. Unlike $\alpha 1_S$DHPR-null muscular dysgenic myoblasts, MDG/TRPC3 KD myoblasts exhibited dramatic changes in cellular morphology (e.g., unusual expansion of both cell volume and the plasma membrane, and multi-nuclei) and increased Ca^{2+} content in both the endoplasmic reticulum and cytoplasm of resting myoblasts. Moreover, these myoblasts failed to differentiate into myotubes. Therefore, TRPC3 in skeletal myoblasts is essential for maintenance of skeletal muscle.

1784-Pos

Effects of Cardiac Specific Inhibition of TRPC Channels on Cardiac Hypertrophy and Ca2+ Handling

Petra Eder, Xu Wu, Jeffery D. Molkentin.
Cincinnati Children's Hospital Medical Center, Cincinnati, OH, USA.

TRPC channels have been identified as components of Ca2+ signaling pathways that promote maladaptive growth of the myocardium. Transgenic mice over-expressing TRPC3 or 6 exhibited an increased propensity towards hypertrophic progression in response to pressure overload, in part through a Ca2+-dependent calcineurin-NFAT signaling pathway. Moreover, different TRPC subunits are known to be up-regulated in heart failure and in hypertrophic hearts after pressure overload. In this study we inhibited TRPC channel function with dominant negative (dn) TRPC mutants and examined the ensuing effect on cardiac hypertrophy and Ca2+ influx dynamics. One of these mutants comprises an N-terminal TRPC4 fragment that we used to generate cardiac restricted transgenic mice. Intracellular Ca2+ signals were measured in adult cardiac myocytes of wildtype (WT) and dn-TRPC4 mice that underwent TAC (transverse aortic banding) or a sham procedure. Isolated myocytes maintained in Ca2+-free buffer were store-depleted with CPA while being treated with Ang II, followed by perfusion with Ca2+ containing buffer to analyze Ca2+ influx with Fura-2 fluorescence. WT myocytes showed essentially no Ca2+ entry, however, hypertrophic myocytes that underwent TAC showed abundant Ca2+ influx. SKF96365 inhibited this Ca2+ influx, suggesting a role for TRPC channels. Indeed, isolated myocytes from dnTRPC4 transgenic mice subjected to TAC lacked this Ca2+ influx, confirming that TRPC channels mediate this previously unrecognized influx activity associated with hypertrophy in cardiac myocytes. Interestingly, Ca2+ transients from myocytes of dn-TRPC4 mice showed increased peak amplitudes, which might indicate an increased cardiac contractility and cardiac performance when dn-TRPC4 is expressed. More importantly, dnTRPC4 mice showed significant attenuation of cardiac hypertrophy following TAC stimulation. These data show that inhibition of TRPC channels exerts ameliorative effects on the development of cardiac hypertrophy by decreasing Ca2+ signals that likely regulate pro-hypertrophic pathways.

1785-Pos

Analysis of the Role of TRPC3 in Ca^{2+} Signaling of RBL-2H3 Mast Cells

Hannes Schleifer[1], Michael Poteser[1], Isabella Derler[2],
Christian Oliver Kappe[1], Christoph Romanin[2], Klaus Groschner[1].
[1]University of Graz, Graz, Austria, [2]Johannes Kepler University Linz,
Linz, Austria.

Direct or indirect involvement of TRPC channels in store-operated Ca^{2+} entry (SOCE) has repeatedly been proposed. In this study, we explored the role of TRPC3 in SOCE-associated Ca^{2+} signaling of RBL-2H3 mast cells by employing both genetic and pharmacological strategies. Mast cells overexpressing a fluorescence-tagged, functional TRPC3 fusion protein displayed enhanced Ca^{2+} entry in a classical thapsigargin-induced store depletion/calcium re-entry protocol. A well-characterized dominant-negative, n-terminal fragment of TRPC3 (aa 1-302) reduced SOCE significantly down to basal entry. A similar extent of inhibition was observed with a dominant negative mutant of Orai1 (E106Q). Two pore mutants of TRPC3 (E616K and E630Q), which represent a non-functional, dominant negative protein and a protein with distinctly altered cation permeability, respectively, failed to affect SOCE in RBL-2H3 cells. The pyrazol compound Pyr3 (ethyl-1-(4-(2,3,3-trichloroacrylamide)-phenyl)-5-(trifluoromethyl)-1H-pyrazole-4-carboxylate), which was recently proposed as a selective inhibitor of TRPC3 channels, effectively suppressed SOCE in wild-type controls as well as TRPC3 over-expressing cells. Our results argue against a role of TRPC3 as part of the store-operated Ca^{2+} permeation pathway in RBL-2H3 cells and point towards an indirect link between TRPC3 and SOCE.

Supported by the FWF project P18475 and P19820

1786-Pos

Role of TRPC1 in Myoblasts Differentiation and Muscle Development

Philippe Gailly.
University of Louvain, Brussels, Belgium.

Myoblasts migration is a key step in myogenesis. It allows myoblasts alignment and their fusion into myotubes. The process has been shown to involve m- or μ-calpains, two calcium-dependent cysteine proteases. Fluorometric measurements of calpain activity in cultured cells showed a peak at the beginning of the differentiation process. We also observed a concomitant and transient increase of the influx of Ca^{2+} and of the expression of TRPC1 protein. After repression of TRPC1 in myoblasts by siRNA and shRNA, this transient influx of calcium was significantly reduced and the concomitant peak of calpain activity was abolished. Interestingly, myoblasts fusion into myotubes was significantly slowed down, due to a reduced speed of cell migration. Accordingly, migration of control myoblasts was inhibited by 2 to 5 μM GsMT×4 toxin, an inhibitor of TRP channels or by 50 μM Z-Leu-Leu, an inhibitor of calpain. These effects were not observed in TRPC1 knocked down cells. Moreover, TRPC1 knocked down myoblasts also accumulated of myristoylated alanine-rich C-kinase substrate (MARCKS), an actin-binding protein, substrate of calpain. We therefore suggest that an entry of calcium through TRPC1 channels induces a transient activation of calpain, a subsequent proteolysis of MARCKS, allowing in its turn, myoblasts migration and fusion. The role of TRPC1 in muscle regeneration, a process involving myoblasts migration and differentiation, is under study.To further characterize the role of TRPC1 in muscle development, we compared morphological and mechanical parameters of muscles from $TRPC1^{+/+}$ and $TRPC1^{-/-}$ mice. We observed that muscles from $TRPC1^{-/-}$ mice display a smaller fibre cross-sectional area and generate less force per cross section area. They do not present other major signs of myopathy but were more sensitive to muscle fatigue.

1787-Pos

Structural and Molecular Basis of the Assembly of the TRPP2/PKD1 Complex

Yong Yu[1], Maximilian H. Ulbrich[2], Ming-hui Li[1], Zafir Buraei[1],
Xing-Zhen Chen[3], Albert C.M. Ong[4], Liang Tong[1], Ehud Y. Isacoff[2],
Jian Yang[1].
[1]Columbia University, New York, NY, USA, [2]University of California, Berkeley, Berkeley, CA, USA, [3]University of Alberta, Edmonton, AB, Canada, [4]University of Sheffield, Sheffield, United Kingdom.

Autosomal dominant polycystic kidney disease (ADPKD) is one of the most common genetic diseases in human and is caused by mutations in PKD1 and TRPP2 proteins. PKD1 (also known as polycystin-1 or PC1) is a large integral membrane protein with 11 putative transmembrane regions, a large extracellular N terminus and a short intracellular C terminus. PKD1 is generally thought to function as a cell surface receptor that couples extracellular stimuli to intracellular signaling. TRPP2 (also known as polycystin-2, PKD2 or PC2) is a member of the transient receptor potential (TRP) channel family. It has 6 putative transmembrane segments and a pore-forming loop and forms a Ca2+-permeable nonselective cation channel. How mutations in PKD1 and TRPP2 lead to ADPKD is unclear but these two proteins likely share some common functions since mutations in them produce similar pathological manifestations. These two proteins associate physically through their C-termini and form functional complexes. However, the subunit composition of this complex and the molecular mechanism of its assembly are unknown. By combining biochemistry, X-ray crystallography, and a single molecule imaging method to determine the subunit composition of proteins in the plasma membrane of live cells, we find that this complex contains 3 TRPP2 and 1 PKD1. A C-terminal coiled coil domain of TRPP2 is critical for the assembly of this complex. This coiled coil domain forms a homotrimer and binds to a single coiled coil domain in the C-terminus of PKD1. Mutations that disrupt this coiled coil trimer abolish the assembly of both full-length TRPP2 homotirmer and the TRPP2/PKD1 heteromeric complex, and diminish the surface expression of both proteins. These finding have significant implications for the assembly, regulation and function of the TRPP2/PKD1 complex, and for the pathogenic mechanism of some ADPKD-producing mutations.

1788-Pos

Immunodetection and Oligomerisation of TRPM1

Marcel Meissner, Natarajan Sivaraman, Frank Schmitz, Veit Flockerzi.
University of Saarland, Homburg, Germany.

To study expression and assembly of TRPM1 channels we cloned seven full lengths TRPM1 cDNAs from mouse eye which represent splice variants and encode proteins of 1462, 1506, 1512, 1578, 1584, 1622 and 1628 amino acid residues. These TRPM1 protein variants vary in their N terminus, in a putative extracellular loop and the predicted pore region. For expression analyses we prepared polyclonal and monoclonal antibodies directed against various antigenic epitopes of TRPM1. All antibodies detect proteins of the size expected for TRPM1 in the eye, in lung and skeletal muscle. They immunoprecipitate the TRPM1 protein from mouse retina and specifically label postsynaptic dendrites of bipolar cells adjacent to the ribbon synapse. All TRPM1 proteins contain a coiled-coil domain in their C termini and isolated fragments comprising this coiled-coil domain have been shown to form dimers (1). We show that after disruption of this coiled-coil domain by site directed mutagenesis the full-length TRPM1 proteins still assemble to dimers and higher molecular protein complexes and interact with each other, apparently by additional intermolecular interactions of TRPM1 sequences within the N-terminus. Similarily, a related TRPM protein, TRPM4, still forms dimers after destruction of a C-terminal coiled-coil domain, most probably via interactions of N-terminal protein sequences.

1 Tsuruda PR, Julius D, Minor DL Jr (2007) Neuron 51, 201-212.

1789-Pos

A Reduction of Glucose-Induced Bursting Frequency in Pancreatic Islets Correlates with Decreased Insulin Release and Impaired Glucose Tolerance in TRPM5-/- Mice

Barbara Colsoul[1], Anica Schraenen[1], Katleen Lemaire[1], Roel Quintens[1], Leentje Van Lommel[1], Andrei Segal[1], Robert Margolskee[2], Zaza Kokrashvili[2], Grzegorz Owsianick[1], Karel Talavera[1], Thomas Voets[1], Patrick Gilon[3], Bernd Nilius[1], Frans Schuit[1], Rudi Vennekens[1].
[1]K.U.Leuven, Leuven, Belgium, [2]Mount Sinai School of Medicine, New York, NY, USA, [3]Universite Catholique de Louvain, Bruxelles, Belgium.

Glucose homeostasis is critically dependent on insulin release from pancreatic beta cells, which is strictly regulated by glucose-induced simultaneously oscillations in membrane potential (V_m) and cytosolic calcium concentrations $[Ca^{2+}]_{cyt}$. We propose that TRPM5, a Ca^{2+}-activated monovalent cation channel, is a positive regulator of glucose-induced insulin release. Micro-array screening and immunostaining reveal high and selective expression of TRPM5 in pancreatic islets. Whole cell current measurements in WT pancreatic islet cells demonstrate a Ca^{2+}-activated non-selective cation current with properties comparable to TRPM5 measured in over-expression, including the bell-shaped dependency on intracellular Ca^{2+}, time constant of activation and permeation properties. This current is significantly reduced in *Trpm5*$^{-/-}$ cells. Ca^{2+}-imaging and electrophysiological analysis show that glucose-induced oscillations of V_m and $[Ca^{2+}]_{cyt}$ have a reduced frequency in *Trpm5*$^{-/-}$ islets. WT islets display either slow or fast oscillations, or mixed oscillations, consisting of fast oscillations superimposed on slow ones. In contrast, *Trpm5*$^{-/-}$ islets never show a fast oscillation pattern. Fast oscillations in V_m show a shorter burst interval, due to a higher slope of depolarization towards the threshold potential for burst initiation. Our results indicate that TRPM5 accelerates the depolarization during the interburst interval, initiating rapid oscillations and higher insulin release. As a consequence, glucose-induced insulin release from *Trpm5*$^{-/-}$ pancreatic isletsis significantly reduced, resulting in an impaired glucose tolerance in these mice. Pharmacological modulation of TRPM5 activity may represent a novel means to adjust insulin release in diabetic patients.

1790-Pos

Physiological Role of the Oxidative Stress-Sensitive TRPM2 Ca^{2+} Channel in Immunocytes

Shinichiro Yamamoto, Hiroshi Takeshima, Yasuo Mori.
Kyoto University, Kyoto, Japan.

It is known that a large amount of reactive oxygen species (ROS) exist at inflamed sites. ROS induce chemokines responsible for the recruitment of inflammatory cells at inflamed sites. Here, we demonstrate that the plasma membrane Ca^{2+}-permeable channel TRPM2 controls ROS-induced chemokine production in monocytes/macrophages. In monocytes from *Trpm2*-defecient mice, H_2O_2-induced Ca^{2+} influx and production of the macrophage inflammatory protein-2 (CXCL2), which exhibit potent neutrophil chemotactic activity, were impaired. In the inflammation model dextran sulfate sodium-induced colitis, CXCL2 expression was attenuated by *Trpm2* disruption. Interestingly, the number of recruited neutrophils was significantly reduced in DSS-treated *TRPM2* KO mice, whereas that of DSS-induced macrophages after infiltration into inflamed sites, was indistinguishable in WT and *TRPM2* KO mice. Importantly, TRPM2 deficiency failed to impair important aspects of CXCL2-evoked neutrophil chemotaxis, including Ca^{2+} response, *in vitro* migration, and *in vivo* infiltration after DSS administration. Thus, TRPM2-mediated Ca^{2+} influx induces chemokine production in monocytes that aggravates inflammatory neutrophil infiltration. We propose functional inhibition of TRPM2 channels as a new therapeutic strategy for treating inflammatory diseases.

1791-Pos

Multi-Dimensional Characterization of the Desensitization Behavior of Temperature- and H+-Activated Human TRPV1 Channels using Microfluidics

Maria Millingen, **Erik T. Jansson**, Per Lincoln, Aldo Jesorka, Owe Orwar.
Chemical and Biological Engineering, Göteborg, Sweden.

This work describes the pH- and temperature-dependence of acute desensitization and tachyphylaxis in human TRPV1 channels. We use an in-house developed microfluidic device and associated methods, which independently can control the temperature and the solution environment (e.g. the pH) around patch-clamped cells, as well as the time a cell is exposed to different solutions. Thus, cells can be stimulated and controlled in a multi-dimensional parameter space. Our results show that if TRPV1 channels are exposed repeatedly to low pH applications, the rate of desensitization becomes progressively slower, whereas the rate of channel activation remains unchanged. Also, both the rate of activation and the rate of acute desensitization increase at higher temperatures. The extent of tachyphylaxis is found to be dependent on pH, temperature, and exposure time. We also show that both the desensitization rate and the extent of tachyphylaxis are correlated to current density. This could be due to the fact that Ca^{2+} is an important factor for both acute desensitization and tachyphylaxis, and since TRPV1 is permeable to Ca^{2+}, the current density is proportional to Ca^{2+} influx.

1792-Pos

A Novel Tarantula Toxin Irreversibly Activates TRPV1

Christopher J. Bohlen[1], Avi Priel[1], Jan Siemens[1,2], David Julius[1].
[1]University of California, San Francisco, San Francisco, CA, USA,
[2]Max-Delbruck-Centrum fur Mlekulare Medizin, Berlin, Germany.

Spider venoms contain an evolutionarily honed pharmacopeia of natural toxins that target membrane receptors and ion channels to produce shock, paralysis, pain, or death. Toxins evolve to interact with functionally important protein domains, including agonist binding sites, ion permeation pores, and voltage-sensing domains, making them invaluable reagents with which to probe mechanisms underlying channel activation or modulation. We have identified a novel tarantula peptide toxin that serves as an irreversible agonist for the heat/capsaicin-activated channel, TRPV1. The toxin contains two independently functional Inhibitor Cysteine Knot (ICK) domains, endowing it with an antibody-like bivalency that results in extremely high avidity for its multimeric channel target. We are using this new toxin as a tool to help dissect the unique properties of TRPV1.

Muscle: Fiber & Molecular Mechanics & Structure II

1793-Pos

Passive Force Augmentation in Actively Stretched Myofibrils and Sarcomeres

Tim R. Leonard, Walter Herzog.
University of Calgary, Calgary, AB, Canada.

Single skeletal muscle myofibrils were stretched actively and passively ($pCa^{2+} = 3.5$ and 8 respectively) from optimal length to beyond myofilament overlap (4.0μm) and individual sarcomere lengths and the associated stretch forces were measured. Actively stretched myofibrils produced much more force than passively stretched myofibrils at all sarcomere lengths, including when all sarcomeres were beyond myofilament overlap (Figure 1). In order to confirm that cross bridge based acto-myosin forces were not present at sarcomere lengths beyond myofilament overlap, passively and actively stretched myofibrils were deactivated and activated, respectively at 5μm. In both cases,

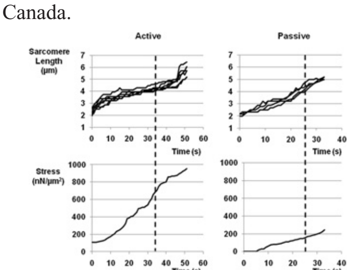

Figure 1. Individual sarcomere length and force traces for single active and passive myofibrils. Actively stretched myofibrils show much greater force than passively stretched myofibrils at sarcomere lengths beyond myofilament overlap where actin-myosin based cross-bridge forces are zero. Dashed vertical line denotes when all sarcomeres are beyond myofilament overlap.

no change in force was observed, indicating that active cross bridge forces were not present at long (5μm) length. Based on these results, we suggest that there is a dramatic passive force augmentation in passively stretched myofibrils and the individual sarcomeres.

1794-Pos

Role of Sarcomere Disruption in Stretch-Induced Force Loss of Myofibrils

Appaji Panchangam, Walter Herzog.
University of Calgary, Calgary, AB, Canada.

Stretching of activated skeletal muscle results in loss of force. In the absence of direct evidence, it is often assumed that sarcomere disruption is the cause of stretch-induced force loss. We stretched mechanically isolated rabbits psoas myofibrils on the descending limb of the length-tension relationship and asked the specific questions: does sarcomere disruption occur and does it affect the magnitude of stretch-induced force loss? Myofibrils were mounted on an inverted microscope with one end attached to a glass micro needle and the other to a silicon nitrate force lever. Myofibrils (n=11) were maximally activated at an average resting sarcomere length of 2.8 ± 0.2 μm. At peak isometric stress (234 ± 92 kN m^{-2}), myofibrils were stretched by 34.3 ± 5.2 % at a speed of 3.3 % s^{-1} and immediately returned to the reference lengths at the same speed. Myofibrils were subsequently relaxed and re-activated after 3-5 minutes of rest to reassess post-stretch stress. Post-stretch isometric stress was reduced by 34 ± 9.6 % compared with pre-stretch stress. Eight out of 11 myofibrils had no sarcomere disruption after stretching while the remaining 3 myofibrils had a small percentage of sarcomeres pulled beyond filament overlap suggesting sarcomere disruption. The average stress reduction in the disrupted and non-disrupted myofibrils was the same (27 ± 13 % vs 36 ± 8%; p = 0.83). We conclude from these results that stretch-induced loss of force in myofibrils can occur in the absence of sarcomere disruption, and that sarcomere disruption does not increase force loss following myofibril stretch.

1795-Pos

Active Force Augmentation for Physiologically Relevant Stretches in Myofibrils and Mechanically Isolated Sarcomeres

Azim Jinha, Tim R. Leonard, Walter Herzog.
University of Calgary, Calgary, AB, Canada.

We reported previously that forces in actively stretched myofibrils and sarcomeres were up to four times greater than forces in passively stretched myofibrils at sarcomere lengths >4μm. These increased forces were independent of actin-myosin based cross-bridge forces and were absent when titin was eliminated. Here, we demonstrate that such force augmentation also occurs for physiologically relevant sarcomere lengths (2.4-4.0μm). Actin-myosin based cross-bridge forces and non cross-bridge based forces were distinguished by assuming that sarcomeres reached a steady-state cross-bridge distribution in the first 0.4μm of stretch. The forces due to stretching could then be calculated and added to the passive forces measured during passive stretching (Figure 1) to obtain the expected forces during active stretching. Subtracting the expected from the experimentally measured forces during active stretching, the force augmentation was obtained. Mean force augmentation towards the end stretching reached values in excess of the mean maximal active isometric forces at optimal sarcomere length, suggesting that force augmentation not associated with actin-myosin based cross-bridge forces is highly relevant in actively stretched myofibrils and isolated sarcomeres.

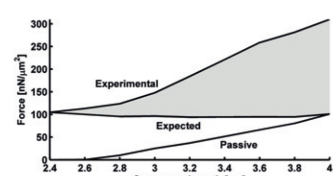

1796-Pos

The Contribution of Calcium and Stretch-Activated Tension to Power Generation by Drosophila Indirect Flight Muscle

Qian Wang, Cuiping Zhao, Douglas M. Swank.
Rensselaer Polytechnic Institute, Troy, NY, USA.

Recent studies suggest small insects might regulate muscle power output by operating their stretch activated indirect flight muscles (IFM) at less than saturating calcium levels during flight instead of varying the number of muscle fibers recruited. Calcium levels have also been found to correlate with wing beat frequency, suggesting calcium concentration might influence aerodynamic power. To test the effects of calcium concentration on muscle power generation, we used the work loop technique to measure *Drosophila* indirect flight muscle (IFM) oscillatory power generation under optimal length change parameters. Maximum power was 2.2 ± 0.4 nW/mm^3 at pCa = 4.7 ± 0.09. The threshold for muscle power generation occurs at ~ pCa 6.1, with pCa_{50} = 5.8 ± 0.05 and the Hill coefficient = 7.2 ± 3.7. Over the steepest portion of the curve, and above the estimated minimum power required for flight, about pCa 6.0 to 5.5, muscle power increases 2.5-fold. We compared the contributions to muscle power from calcium activated isometric tension to the contribution from the tension generated by stretch-activation during flight by imposing a 2.5% ML, 1.5 ms stretch. The pCa_{50} for calcium activated tension was 6.1 ± 0.05 and Hill coefficient was 4.6 ± 1.3. The pCa_{50} for stretch activated tension was 5.8 ± 0.07 and Hill coefficient was 3.8 ± 1.3. Following a stretch at pCa 4.5, total isometric tension increased from 2.5 ± 0.3 mN/mm^2 to 16.4 ± 1.2 mN/mm^2 of which 11.4 ± 1.1 mN/mm^2 was contributed by passive elastic elements. As calcium is increased from pCa 6.0 to 5.5, stretch-activated tension contributes 1.0 ± 0.3 mN/mm^2 of additional tension while calcium tension contributes 0.4 ± 0.2 mN/mm^2. We conclude that if calcium levels vary between pCa 6.0 to 5.5 during flight, then the contribution of stretch tension to additional power is about twice that of calcium tension.

1797-Pos

Dual Regulation Mechanisms for Ca^{2+}-Activated and Stretch-Activated Forces in Asynchronous Flight Muscle of Insect: Mechanical and X-Ray Evidence

Hiroyuki Iwamoto.
SPring-8, JASRI, Sayo-gun, Hyogo, Japan.

During flight of insects, their flight muscles (IFMs) are often endothermically maintained at an optimal temperature. In the case of bumblebee, this temperature is ~42°C At saturating [Ca^{2+}], glycerinated bumblebee IFM fibers develop large Ca^{2+}-activated (CA) force of ~50 kPa above 20°C, as well as stretch-activated (SA) force. Below the critical temperature of 15°C, the CA force is sharply suppressed. Surprisingly, the SA force is not suppressed even at 5°C. This suggests that the inhibition of CA force at low temperatures is not due to myosin inactivation, but it is an issue of regulation. The CA force-pCa curve remains sigmoidal at lower temperatures, and the pCa_{50} value is only slightly affected, indicating that myosin is unable to develop large CA force even if troponin is saturated with Ca^{2+}. The mechanism for temperature-dependent CA force regulation is further investigated by X-ray diffraction, by recording semi-static patterns in the stretch and release phases of a repeated stretch-release protocol. At 5°C, the 2nd actin layer line (ALL) is increased from 5% at rest (relative to 6th ALL) to 19% in the release phase, indicating that the myosin binding sites on actin are almost fully open even when the CA force is suppressed. In the stretch phase, the 2nd ALL is further enhanced to 26%. At 20°C, the 2nd ALL intensity is enhanced to 25 and 29% in the release and stretch phases, respectively. These results suggest that a pathway after thin-filament activation is blocked at low temperatures, and SA force could be regulated independently of this pathway. The critical temperature for CA force development is also found in other insects, such as a true bug *Nezara* (T=20-25°C), but not in a giant waterbug *Lethocerus*.

1798-Pos

Contractile Properties of Human Fetal Skeletal Muscle Proteins

Alice W. Ward, Galina Flint, Anita E. Beck, Michael J. Bamshad, Michael Regnier.
University of Washiington, Seattle, WA, USA.

Congenital contracture syndromes associated with myofilament proteins are present in 1 out of every 1000 live births. Because the myosin heavy chain protein family has several isoforms unique to the pre-natal development of muscle, it is important to know the contractile properties of this tissue to determine how mutations affect performance and development. However, information on human fetal muscle contractile properties is lacking. We are beginning to characterize the contractile properties of this tissue using in vitro motility assays, where we can deconstruct which proteins of developing muscle can be attributed to differences seen in patients with congenital contracture syndromes. Embryonic myosin was isolated from human fetal muscle samples at 15.4 weeks gestation. An in vitro motility assay was performed at 30 degrees C with an ionic strength of 0.17 to determine the predominant myosin's enzymatic properties. The max speed of filaments on human fetal skeletal myosin (1.9 um/s) was significantly lower than filaments on adult rat skeletal myosin (4.8 um/s) under the same conditions. The Km values were similar between the human fetal (0.02 mM) and adult rat (0.03mM) myosins. Ongoing work includes studying the effects of increased ADP, substitution of ATP with dATP, studying Ca2+ regulation of in vitro motility assays using actin and thin filament regulatory proteins purified from fetal muscle of approximately the same gestational period, and skinned muscle cell experiments. By utilizing these assays, we can develop a more mature understanding of muscle contraction during development and form better hypotheses about the mechanism of how specific mutations lead to these contracture syndromes. Establishing these contractile properties will lead to better hypotheses regarding the development of contractures in utero and how it is affected by mutations associated with congenital contracture syndromes. Supported by HL65497 (Regnier) and HD48895 (Bamshad).

1799-Pos

Phosphorylation of Myosin Binding Protein-C Alters the Proximity of Cross-Bridges to Actin and Accelerates Myocardial Twitch Kinetics

Brett A. Colson[1], Peter P. Schemmel[2], Peter P. Chen[1], Tanya Bekyarova[2], Daniel P. Fitzsimons[1], Thomas C. Irving[2], Richard L. Moss[1].
[1]University of Wisconsin Medical School, Madison, WI, USA, [2]Illinois Institute of Technology, Chicago, IL, USA.

The strength and kinetics of cardiac contraction vary on a beat-to-beat basis in efforts to match cardiac output in response to changing circulatory demands. In living myocardium, the beta-adrenoreceptor agonist dobutamine initiates protein kinase A (PKA)-mediated phosphorylations of Ca^{2+} handling proteins and contractile proteins including cardiac myosin binding protein-C (cMyBP-C) and cardiac troponin I (cTnI), which leads to potentiation of twitch force and faster kinetics of force development and relaxation. Our previous studies in skinned myocardium suggest that PKA phosphorylation of cMyBP-C disrupts its interaction with myosin subfragment 2 (S2), which relieves the tether-like constraint of myosin heads imposed by cMyBP-C, and thereby accelerates cross-bridge cycling kinetics. To examine the relative role of cMyBP-C phosphorylation in altering twitch kinetics, we recorded twitch force and low-angle x-ray diffraction patterns in between twitches and near maximum twitch force in intact trabeculae isolated from murine myocardium electrically stimulated at 0.5 Hz in the presence and absence of dobutamine. Our data suggest that phosphorylation of cMyBP-C caused a radial or azimuthal displacement of cross-bridges towards the thin filament *in vivo* prior to the twitch, which contributes to the accelerated contraction kinetics following twitch stimulation. These results suggest that interactions between cMyBP-C and the S2-domain of myosin heavy chain are dynamically regulated by phosphorylation of cMyBP-C and function to modulate the availability and cooperative binding of cross-bridges to actin during the myocardial twitch.

1800-Pos

Myosin Crosslinking and EPR Capture the Start of Force Generation in Muscle Fibers

Ryan N. Mello, Amanda Laden, Robert Harris, Leanne J. Anderson, David D. Thomas.
University of Minnesota, Minneapolis, MN, USA.

Crosslinking the two most reactive Cys (SH1 and SH2) of the myosin catalytic domain (CD) inhibits force production and ATP hydrolysis and locks myosin in a weak actin-binding conformation with the CD immobilized and orientationally disordered. These results suggest that crosslinking traps a state in which the myosin head is on the cusp of force generation. In the present study, we measured the structural dynamics of myosin's light chain domain (LCD) in skeletal muscle fibers during rigor, relaxation, and with SH1 and SH2 crosslinked. To measure LCD structural dynamics, we exchanged spin labeled RLC for native RLC in permeabilized muscle fibers, with retention of function, then used EPR spectroscopy to measure structural dynamics. EPR spectra indicate when SH1 and SH2 are crosslinked, the LCD is in an orientation intermediate between relaxation and rigor, indicative of a state beginning to generate force. The saturation transfer EPR (STEPR) spectrum from these fibers does not change with crosslinking, demonstrating that that the LCD undergoes very slow dynamics, as in rigor, and is less dynamic than relaxation. In order to relate LCD structural dynamics with those of the CD, we measured CD structural dynamics in fibers by directly crosslinking SH1 and SH2 with BSL. EPR spectra from these fibers reveal that the CD is highly disordered, with dynamics ten times slower than in relaxation. Thus when SH1 and SH2 are crosslinked, both domains exhibit structural dynamics intermediate between relaxation (pre-power stroke) and rigor (post-power stroke). This supports the conclusion that SH1-SH2 crosslinking traps a state analogous to an initial force-generating state. We propose that this state is the missing link needed to explain how myosin undergoes a transition from dynamic disorder to order as it converts chemical energy to mechanical work.

1801-Pos

Passive Properties of Single Skeletal Muscle Fibers are Altered in Heart Failure Patients

Mark S. Miller, Joan M. Braddock, David G. Moulton, Kimberly A. Ward, Peter VanBuren, Martin M. LeWinter, Philip A. Ades, David W. Maughan, Michael J. Toth.
University of Vermont, Burlington, VT, USA.

We previously demonstrated that myosin heavy chain (MHC) content is decreased in skeletal muscle fibers from heart failure patients, thereby altering Ca^{2+}-activated (pCa 4.5) contractile properties. In this study, we examined chemically-skinned, single human skeletal muscle fibers under relaxed conditions (low [Ca^{2+}], pCa 8) using small amplitude sinusoidal analysis to determine whether the loss of MHC content affects their viscoelastic properties. We obtained *vastus lateralis* (quadriceps) muscle from needle biopsies of 9 patients and 5 sedentary controls. Surprisingly, Type I (slow twitch) and Type IIA (fast twitch) fibers produced slight but significant positive oscillatory work under relaxed conditions at 25°C, indicating the presence of cross-bridge cycling. This positive oscillatory work persisted when [Ca^{2+}]levels were lowered even further (to pCa 9). Addition of 40 mM 2,3-butanedione monoxime (BDM) or 100 μM blebbistatin, inhibitors of skeletal muscle myosin ATPase, to a subset of Type I and IIA fibers eliminated their positive work output and reduced their high frequency elastic and viscous moduli. Type I fibers from heart failure patients had lower isometric tensions as well as lower elastic and viscous moduli compared to controls; whereas, Type IIA fibers from patients had tension values similar to controls, while the frequency of maximum work output (an indicator of myosin kinetics) was greater. Taken together, these results demonstrate that cross-bridges contribute to the viscoelastic properties of human skeletal muscle in the 'relaxed' state (low intracellular [Ca^{2+}]) and that cycling myosin heads may contribute to resting muscle tone. As under Ca^{2+}-activated conditions, heart failure affects relaxed muscle properties differentially depending upon fiber type. Decreased resting muscle tone in heart failure patients may decrease postural stability and contribute to a reduced ability to perform activities of daily living.

1802-Pos

Correction of Error in Fiber Length Due to Lever Arm Rotation During Mechanical Tests of Single Muscle Fibers

SeungJun Choi[1], Sangil Kim[2], Jeffrey J. Widrick[1], Jae-Young Lim[1,3].
[1]Krivickas Muscle Cell Laboratory, Spaulding Rehabilitation Hospital and Harvard Medical School, Boston, MA, USA, [2]Department of Oceanic and Atmospheric Sciences, Oregon State University, Corvallis, OR, USA, [3]Department of Rehabilitation Medicine, Seoul National University College of Medicine, Seongnam, Republic of Korea.

The single muscle fiber preparation is a popular technique to assess mechanical properties at the cellular level and how these properties change with aging, disease, exercise, etc. Fibers are usually attached to wires extending perpendicularly from the lever arm of a high speed motor and force transducer that are then mounted to the stage of a microscope. Because of lever arm rotation, the fiber does not move along the optical plane, introducing a length measurement error if length is measured along the optical plane. The purpose of this study was to 1) calculate the error of lever arm movement and 2) provide a correction equation. The error was calculated assuming 2 mm fiber length at up to 50% displacement, because this is a commonly used stretch or slack magnitude (~15% slacking with unloaded shortening velocity, ~30% lengthening response to eccentric contraction, ~50% stretch with passive tension). The range of error was hyperbolically enlarged as either lever arm length or optical plane stretch magnitude increased, and this error was exacerbated with the increase of both factors. For example, with a 5 mm connector attached to the lever arm, the relative error [100×(actual displacement-target displacement)/target displacement] was 0.59%, 1.36%, and 1.78% with 10, 30, and 50% of stretch or slacking, respectively. However, with a 10 mm connector, the relative error was 2.38%, 5.66%, and 7.64%, and in the case of a 15 mm connector, the relative error increased dramatically up to 5.36%, 12.69%, and 17.10%. We suggest the following correction equation to eliminate potential errors; $q=b+f-r|mT+1|/(m^2T^2+m^2+T^2+1)^{1/2}$, where q = observed fiber length, b=connector length, f=fiber length, h=lever arm length, $r=(b^2+h^2)^{1/2}$, $m=-h/(b+f)$, $T=[p^2-(d-r)^{1/2}/(d^2+r^2-p^2)]^{1/2}$, p=target fiber length, and $d=[(b+f)^2+h^2]^{1/2}$.

1803-Pos

Using White Noise to Probe Actomyosin Cycling Kinetics During Shortening and Lengthening in Drosophila Flight Muscle Fibers

Bertrand C.W. Tanner, David W. Maughan, Bradley M. Palmer.
University of Vermont, Burlington, VT, USA.

Our laboratory routinely measures demembranated muscle fiber mechanics using small amplitude sinusoidal length perturbation analysis and estimates kinetics of actomyosin cycling and myosin attachment time. We have developed a complementary measurement technique using small, random changes in muscle length (white-noise length stimuli) that simultaneously cover a broad frequency spectrum, comparable with the sinusoidal length perturbations. We find the white-noise technique provides a description of the viscoelastic properties that is consistent with sinusoidal analysis measurements, rapidly capturing much of the physiological behavior associated with contracting muscle fibers. The white-noise technique samples a vast range of system behavior in a fraction of the time required to complete sinusoidal analysis, and does not require the linear response underlying sinusoidal analysis methods. Thus, we combined the white-noise stimuli with a linear shortening and lengthening transients to probe cross-bridge cycling behavior during these periods of varied load. Preliminary measurements using demembranated dorsal longitudinal

flight muscle fibers from *Drosophila melanogaster* indicate faster cross-bridge cycling kinetics during lengthening and slower cycling during shortening, compared to isometric contraction. During isometric contraction we estimate a myosin attachment time of 5.0 ms, and 4.6 versus 5.5 ms during the lengthening and shortening transients, respectively. These initial applications of the white-noise system analysis technique show promise for future studies probing molecular processes that underlie complicated length transients associated with normal muscle contraction.

1804-Pos

The Isotonic Velocity Transient Following a Sudden Rise in Force Imposed on the Muscle Sarcomere During Unloaded Shortening Reveals a Rate Limiting Step in Detached Myosin Motors

Luca Fusi, Vincenzo Lombardi, Gabriella Piazzesi.
University of Florence, Sesto Fiorentino, Italy.

Energy balance studies indicate that ATP splitting by myosin motors during rapid shortening of skeletal muscle is not sufficient to account for the energy (mostly heat) output (Rall et al., *J Gen Physiol* 68(1), 13, 1976; Homsher et al., *J Physiol* 321, 423, 1981). We investigated the kinetic step of the myosin ATP-ase cycle related to this phenomenon in single muscle fibers from *Rana esculenta* (~2.15 μm sarcomere length, 4°C), by recording the isotonic velocity transient following a force step from zero to the isometric tetanic value (T_0). Once the isometric tetanus had developed, the force was first clamped to zero for a range of times from 10 ms to 18 ms (during which the fiber shortened at the maximum velocity by 30 nm hs^{-1} to 50 nm hs^{-1}) and then raised again to T_0 in a stepwise manner (~120 μs). The elastic lengthening induced by the force step was followed by a transient isotonic lengthening, the size of which ranged from 40 to 60 nm hs^{-1} depending on the size of the preceding shortening. The lengthening velocity was larger for larger shortening size and progressively decreased to approach the isometric condition with a half-time of 2-3 ms. Similarly, the half-sarcomere stiffness recovered the isometric value e_0 from the unloaded shortening value of 0.4 e_0 with an exponential time course with τ ~3 ms. We conclude that during rapid shortening a ~3 ms-transition between detached states of the myosin motor, likely related to the ATP hydrolysis, becomes rate limiting. Accumulation of motors in the state preceding the hydrolysis step can account for the unexplained energy during rapid shortening. Supported by MIUR (Italy).

1805-Pos

Effect of Inorganic Phosphate on the Rate of ADP Release During Ramp Shortening in Activated Permeabilized Fibers from Rabbit Psoas Muscle

Marco Caremani, Timothy G. West, **Michael A. Ferenczi**.
Imperial college London, London, United Kingdom.

A coumarin-labeled recombinant phosphorylated nucleoside diphosphate kinase (P~NDPK-IDCC; West et al., 2009; Biophys.J. 96:3281-3294), was used as a fluorescence probe for time-resolved measurement of changes in [MgADP] during steady shortening of single permeabilized rabbit psoas fibers at 12°C (pCa 4.5, pH 7.1, ATP 5.7mM). A fiber contracted from the relaxed state by immersion into a Ca^{2+} activation solution at 0°C. Temperature activation was then initiated by immersion of the fiber into silicone oil at 12°C. The activation solutions were prepared with either zero added P_i or with 10 mM added P_i at constant ionic strength (0.15 M). The decline in fluorescence intensity emission (470nm) associated with MgADP-dependent dephosphorylation of P~NDPK-IDCC (60 μM) was monitored during activation and during a period of isovelocity shortening. Fluorescence emission (580 nm) of a rhodamine dye was measured simultaneously to correct the P~NDPK-IDCC signal for the effects of fiber movements and volume changes. The rate of MgADP release in the absence of added P_i increased from 0.7 $\pm$ 0.07 $mM \cdot s^{-1}$ at 0.2 fiber-lengths$\cdot s^{-1}$ to approximately 3.4 $\pm$ 0.25 $mM \cdot s^{-1}$ for shortening velocities between 1 and 2 fiber-lengths$\cdot s^{-1}$. When 10 mM P_i was added, the rate of ADP release at 0.2 fiber-lengths$\cdot s^{-1}$ was 0.48 $\pm$ 0.05 $mM \cdot s^{-1}$ and 2.6 $\pm$ 0.4 $mM \cdot s^{-1}$ at 1-2 fiber-lengths$\cdot s^{-1}$. In the absence of added Pi, the rate of ATP hydrolysis calculated from the appearance of ADP is similar to that calculated previously from the appearance of P_i using MDCC-labeled phosphate binding protein, over the same range of fiber shortening speeds (He et al., 1999, J. Physiol. 517: 839-854). Thus P_i slows the ATPase rate by 25-30%, both in the isometric and isotonic state. The energetic consequences will be discussed.

1806-Pos

Cross-Bridges and Sarcomere Stiffness in Single Intact Frog Muscle Fibers

Giovanni Cecchi, Barbara Colombini, Marta Nocella, Giulia Benelli, Maria Angela Bagni.
University of Florence, Firenze, Italy.

The number of cross-bridges formed in activated skeletal muscles is a key information for both energetics and mechanics of muscle contraction. In this study we determined the cross-bridge number in single fibers by measuring the tension $P_c$which forcibly detached the cross-bridge by fast stretches (Bagni et al. 2005, *J. Physiol* 565). Fibers, isolated from the tibialis anterior muscle of *Rana esculenta*, were mounted between an electromagnetic motor and a fast force transducer. Sarcomere length was measured by means of a striation follower device. Measurements were made during tetanus rise in normal Ringer and in sub-maximal tetanic contractions in Ringer-BTS (*N*-benzyl-p-toluene sulphonamide, 1 μM) at 5°C at sarcomere length of 2.1 μm.

The results were compared with fiber stiffness, another indicator of cross-bridge number, measured with 4 kHz sinusoidal length oscillations (1 $nmhs^{-1}$ p-p amplitude). The stiffness-tension relation was the same both during the tetanus rise and Ringer-BTS and showed the non-linearity expected from the myofilament compliance. However, the data could not be fitted satisfactorily with a simple model made of cross-bridge and linear filament compliances in series. A good fit was obtained by assuming that a fraction (~14%) of attached bridges at tetanus plateau was generating no-force. Relative myofilament and cross-bridge compliance resulted 0.37 and 0.63 respectively. The stretch data showed a linear relation between $P_c$and tension with a slope consistent with the presence of the non-force generating bridges suggested by stiffness data. These results suggests the existence of a possible non-linearity between cross-bridge force and stiffness and show that the relation between fiber stiffness and cross-bridge number is not as simple as usually assumed.

1807-Pos

Ultrafine Striations in Skeletal Muscle Revealed by 3D Super-Resolution Fluorescence Microscopy

Amal Akel, Douglas D. Root.
University of North Texas, Denton, TX, USA.

Super-resolution three-dimensional imaging was achieved using newly synthesized photoactivatable quantum dot probes. Semiconductor quantum dots are nanoparticles with high photostability and brightness. They were modified with a novel quencher system to make them photoactivatable. The unique properties of these photoactivatable quantum dots enable single-fluorophore localization in three dimensions using a confocal microscopy optical sectioning method with a piezo scanner. To image skeletal muscle at resolutions exceeding that of the standard confocal microscope, the photoactivatable quantum dots were conjugated to secondary antibodies. Myofibrilar bundles were dual- labeled using both a primary antibody to myosin rod with the secondary antibody-conjugated photoactivatable 655 nm quantum dot and a primary antibody against tropomyosin with the secondary antibody-conjugated photoactivatable 525 nm quantum dot. During the 3D acquisition on a spinning disk confocal with piezo scanner, different individual quantum dots were photoactivated during each of hundreds of cycles. A sufficient number of single quantum dots were localized, reduced to their center of mass and then reconstructed to a super-resolution image. The resulting super-resolution image shows a sub-diffraction resolution in both lateral and axial directions. The broad absorbance band of quantum dots enables the excitation of both quantum dots with the same laser type. This technique enables the relative localization of two different myofibril proteins at nanometer scale resolutions in solution demonstrates ultrafine striations in the staining pattern with widths less than 70 nm in axial and lateral dimensions that are not evident by conventional confocal microscopy due to its resolution constraints. The bands appear to be related to the presentation of epitopes at the surface of thin and thick filaments and may be related to thick and thin filament binding proteins and/or structural variations in the actin and myosin filaments.

1808-Pos

Structural and Functional Gradients with Temperature in the Flight Muscle of Manduca Sexta

Nicole T. George[1], Jiangmin Liu[2], Lacy Simons[2], Thomas L. Daniel[1], **Thomas C. Irving**[2].
[1]University of Washington, Seattle, WA, USA, [2]Illinois Institute of Technology, Chicago, IL, USA.

The force/extension curve of the flight muscle of the Hawkmoth, *Manduca sexta* is remarkably similar to that of mammalian cardiac muscle suggesting that it may serve as a useful model system for certain aspects of cardiac muscle structure and function (J Exp Biol. 2004;207:2455). More recently, it was discovered that these animals maintain an astonishing thermal gradient of 8.8 C in the 5 mm distance dorsal to ventral in their dorso-longitudinal flight muscles (DLMs). Does the existence of this thermal gradient necessarily imply a functional gradient? Do these changes in function have, as their basis, changes in structure? Twitch dynamics of individual fibers within the DLM in intact animals are temperature dependent so that mechanical power output (and it's phase dependence) varies with depth in the tissue. A surprising observation was that all five sub-units in the DLM were simultaneously activated. Cooler

muscles subjected to 25 hz stimulation (flight frequency) are partially fused with (likely) little crossbridge turnover. To assess the structural correlates of temperature gradients, we performed small-angle x-ray fiber diffraction measurements as a function of position along the dorsal-ventral thermal gradient in intact moth thoraces. The equatorial intensity ratio (I_{20}/I_{10}) in unstimulated muscle increased by ~25% in the first 1 −1.5 mm traversing from dorsal to ventral, implying that increased temperature was associated with increased association of the myosin heads with the thin filaments presumably predisposing them towards more productive acto-myosin interaction. Interestingly, X-ray patterns from skinned muscle preparations improved with increasing temperature indicating better structural order. Together, these observations suggest that cooler, superficial muscles may act mainly as elastic energy storage, whereas warmer deeper muscles may do the bulk of the mechanical work.

1809-Pos
Positioning of Myosin-Binding Protein C in Skeletal Muscle
Hugh E. Huxley.
Brandeis univ., Waltham, MA, USA.
Frog striated muscle gives a pair of X-ray meridional reflections at spacings of ~419Å and ~442Å, which Offer (CSH Symp.37, 83-97, 1972) and Rome (ibid., 331-339) have shown are related to the disposition of C-protein in two sets of bands at ~430Å intervals on either side of the H-zone, giving rise to interference fringes that sample the underlying 430Å reflection. However, there are problems with this simple interpretation.
We have studied these reflections at high resolution on the BioCAT beam line at the Argonne National Lab., in both relaxed and contracting muscles, and during the onset of activation. In resting muscle, two main peaks can generally be seen in the relevant region, usually at ~419Å and ~442Å as previously described, but the latter peak is about 4 times more intense than the former, which would require an underlying sampled peak at ~437Å. It seems unlikely that the C-protein repeat is different from the helical repeat of the myosin filament to which it is attached (429.6Å), and more probable that some second component is involved, namely a ''forbidden'' first order myosin meridional reflection, as discussed by Malinchik and Lednev (JMRCM 13, 406-419, 1992), The interference fringes generated by this repeat would interact in a complex way with those from C-protein, since the reflections would in general have different phases. We find that the observed patterns, with very strong ~442Å reflections, can be modeled very satisfactorily even when both underlying repeats are kept at 429.6Å.
Passive stretch of semitendinosus muscles to sarcomere lengths up to the 3.2 - 3.5 μm range, where overlap between the C-protein bands and actin becomes zero, has little effect on the spacing of these reflections. However, that does not mean there is no interaction between C-protein and actin.

1810-Pos
Different Orientation of Two Heads of a Myosin Crossbridge in Full-Filament Overlapped and Overstretched Muscles Obtained by X-Ray Fiber Diffraction
Kanji Oshima[1], Yasunori Takezawa[2], Yasunobu Sugimoto[2], Katsuzo Wakabayashi[2].
[1]The Center for Advanced Medical Engineering and Informatics, Osaka University, Osaka, Japan, [2]Division of Biophysical Engineering, Graduate School of Engineering Science, Osaka University, Osaka, Japan.
A novel method using the cylindrically averaged difference Patterson function was applied to correct a sampling effect due to the hexagonal filament array on the thick filament-based layer-line intensities from frog skeletal muscles at the full-filament overlap length. Using the corrected intensity data and the mixed structural model of a thick filament with two different axial periodicities of the myosin crossbridges, we performed an optimum search of azimuthal orientation of two heads of a myosin crossbridge and compared the optimum orientation to that from muscles stretched beyond filament overlap reported previously. The result showed that the myosin crossbriges in the regular repeating region had a similar configuration in both muscles. Two heads of a myosin crossbridge formed a windmill-shape when seen from the top of the filament and one head of a myosin crossbridge seemed to be almost in contact with another head in a pair at an adjacent crown level along the filament axis. One head was toward the converter domain of the other head, similar to regulated myosin heads in Tarantula muscles in which the intramolecular head-head interaction occurs. In the perturbed region, however, myosin crossbridges had different configurations in these muscles. In top view, two heads of a myosin crossbridge showed a U-shape structure in the overstreched muscles while a cross-shape structure in muscles with the full-filament overlap. One myosin head seemed to be in contact with the other head at the same axial crown level. The models suggest that the disposition of two-headed myosin crossbridges is stabilized by the head-head interaction at same or different axial crown levels. Probably this would be related to the inhibition mechanism of actomyosin interaction in the relaxed muscles.

1811-Pos
Relative Contribution of Attached and Detached Myosin Heads to the X-Ray Pattern from Skeletal Muscle
Massimo Reconditi[1], Gabriella Piazzesi[1], Malcolm Irving[2], Vincenzo Lombardi[1].
[1]University of Florence, Florence, Italy, [2]King's College London, London, United Kingdom.
In the X-ray diffraction pattern from skeletal muscle the third order myosin-based meridional reflection, M3, originates from the axial repeat of myosin heads along the thick filament. Changes in the intensity (I_{M3}), spacing (S_{M3}), and fine structure (R_{M3}) of the M3 reflection in contracting skeletal muscle at full filament overlap (~2.1 μm sarcomere length) have been measured in many different protocols (Piazzesi *et al. Nature***415**:659,2002; Reconditi *et al. Nature***428**:578, 2004; Linari *et al. J. Physiol.***567**:459, 2005; Huxley *et al. J. Mol. Biol.***363**:743, 2006; Huxley *et al. J. Mol. Biol.***363**:762, 2006; Brunello *et al. PNAS***104**:20114, 2007; Piazzesi *et al. Cell***131**:784, 2007). These studies showed the presence of a fixed periodic mass that is insensitive to filament sliding and attributed to detached myosin heads, but estimates of the relative contribution of the detached heads to the M3 reflection ranged from 0.3 to 0.6. Here we show that this parameter can be constrained by the dependence of the M3 reflection on sarcomere length (*sl*). When *sl* is increased from 2.1 to 3.20 μm, decreasing the fraction of myosin heads that are overlapped by actin filaments from 1 to 0.3 (and thus, according to Piazzesi *et al.* 2007, the fraction of actin-attached myosin heads from 0.3 to 0.09), force and I_{M3} decrease in proportion to filament overlap, while S_{M3} and R_{M3} are approximately constant (Linari *et al*. *PNAS***97**:7226, 2000). These results suggest that in isometric contraction at full filament overlap the contribution to I_{M3} of detached myosin heads is no more than 35% of that of attached heads and that there is very little axial offset between the two head populations.

1812-Pos
Myosin ATP Turnover Rate: a Mechanism Involved in Thermogenesis in-Resting Skeletal Muscle Fibers
Melanie A. Stewart.
UCSF, San Francisco, CA, USA.
Thermogenesis by resting muscle varies with conditions and plays an active role in homeostasis of body weight. The low metabolic rate of living resting muscles requires that ATP turnover by myosin be inhibited relative to the purified protein in vivo. This inhibition has not been previously seen in in vitro systems. We used quantitative epifluorescence microscopy of fluorescent nucleotides to measure single molecule turnovers in relaxed permeable skeletal muscle fibers. We observed two lifetimes for nucleotide release by myosin: a fast component with a lifetime of 0.2-0.3 minutes, similar to that of purified myosin, and a slower component with a lifetime of 3.8+/− 0.4 minutes. We define the latter component to be the 'super relaxed state'. The fraction of myosins in the super relaxed state was decreased at lower temperatures, by substituting GTP for ATP or by increased levels of myosin phosphorylation. All of these conditions have also been shown to cause increased disorder in the structure of the thick filament. We propose a model in which the structure of the thick filament modulates the nucleotide turnover rates of myosin in relaxed fibers. Modulation of the relative populations of the super relaxed and conventional relaxed states would have a profound effect on muscle thermogenesis, with the capacity to significantly alter whole body metabolic rate. The mechanism proposed provides a new target for therapeutics with the potential to treat to obesity or help in controlling high blood sugar levels.

Muscle Regulation II

1813-Pos
A Disulfide Bond at Cys 190 of Tropomyosin Alters Tryptic Cleavage Pattern
John P. Sumida, David Yampolsky, Sherwin S. Lehrer.
Boston Biomedical Research Institute, Watertown, MA, USA.
Native tropomyosin (Tm), an α-helical coiled-coil, possesses a charged acidic amino acid (Asp 137) that occurs in a hydrophobic position which destabilizes the coiled-coil. This region is sensitive to tryptic cleavage and is important in the proper regulation of the myosin activate ATPase, (Sumida, John P., Wu, Eleanor, Lehrer, Sherwin S, JBC 283, 2008). Thermal stability measurements of Tm suggest a long-range interaction between the Asp 137 position and the Cys 190 position. In the current work, we present further evidence of long-range interactions along the length of tropomyosin.

Native frog Tm was cross-linked with DTNB at Cys 190. Tryptic cleavage patterns of this cross-linked species were compared to a control Tm in which the Cys 190 groups were maintained reduced state using DTT. The course of tryptic cleavage of the cross-linked molecule was altered compared to the fully reduced molecule. Proteolysis of the cross-linked molecule produced new tryptic fragments seen in a reduced SDS gel at 30kDa and 20kDa. Trypsin cleaves reduced tropomyosin at Arg 133 to produce two new tryptic fragments (17kDa and 15kDa). The observation that cross-linked Tm exhibits a change in the cleavage rate, and affects the cleavage pattern, demonstrates a long-range effect of the cross-link at Cys 190 on the site of trypsin cleavage, Arg 133. This finding adds evidence to the idea that ''flexibility'' is associated with a locally fluctuating region in the middle of the molecule which has implications on our understanding of how Tm moves on the actin surface, and provides insight into understanding how single point mutations in Tm may result in dysfunction and disease associated with various myopathies.

1814-Pos
Tropomyosin Pseudo-Phosphorylation and Muscle Kinetics

Brandon J. Biesiadecki[1], Marco Lofrano Alves[2], Ganapathy Jagatheesan[3], Bin Liu[1], Beatrice Scellini[4], Chiara Tesi[4], Jonathan P. Davis[1], Corrado Poggesi[4], David F. Wieczorek[3], Beata M. Wolska[2], R. John Solaro[2].
[1]The Ohio State University, Columbus, OH, USA, [2]The University of Illinois at Chicago, Chicago, IL, USA, [3]University of Cincinnati, Cincinnati, OH, USA, [4]Universita di Firenze, Firenze, Italy.

Tropomyosin contains a phosphorylation site at Ser-283 located within the head-to-tail overlap region that regulates muscle contraction. Previously we demonstrated that recombinant wild-type (Tm-WT) and pseudo-phosphorylated (Tm-S283D) alpha tropomyosin, expressed and purified from insect cells, exhibit regulated ATPase activity and troponin T binding similar to that reported for non-phosphorylated and phosphorylated tropomyosin (pTm) purified from muscle. We further demonstrated transgenic mice expressing the pseudo-phosphorylated tropomyosin (Tm-S283D Tg) exhibit increased mortality and decreased rate of relaxation in the work performing heart preparation. These changes occur in the absence of altered steady state maximal force or calcium-sensitive force development in skinned papillary bundles. In light of these findings, we sought to investigate the effect of pTm on the kinetics of cardiac muscle function. Using an extraction/replacement protocol, we measured force kinetics in a myofibril preparation. Results demonstrate no significant difference between myofibrils replaced with Tm-S283D or Tm-WT in maximal force, the rate of force activation, or the rate of force redevelopment, implying pTm does not play a role in altering muscle activation or cycling kinetics. To investigate if pTm affects the kinetics of thin filament inactivation we measured the rate of calcium disassociation from troponin C. Results demonstrate thin filaments reconstituted with Tm-S283D decreased the rate of calcium disassociation from troponin C consistent with the previously observed relaxation impairment. Finally, to determine the effects of pTm on systemic alterations in cardiovascular performance we measured heart function in Tm-S283D Tg mice by echocardiography. Results demonstrate Tm-S283D Tg mice exhibit trends towards impaired cardiac contractility compared to non-transgenic mice including decreased peak systolic velocity and ejection fraction. Overall, these findings demonstrate tropomyosin phosphorylation contributes to the regulation of cardiac dynamics; however, the precise role of pTm in the development of cardiac dysfunction remains elusive.

1815-Pos
Studies of the Mid Region of Tropomyosin Using an Incorporated Tryptophan Analogue

Julie J. Mouannes, Tomoyoshi Kobayashi, Daniel Leek, Larry Tobacman.
University of Illinois at Chicago, Chicago, IL, USA.

Striated muscle contraction is controlled by highly sensitive alterations in thin filament conformation that involve a Ca2+-dependent interaction between troponin I (TnI) and actin-tropomyosin (Tm). To study these interactions, 5-OH Tryptophan (OHW) was incorporated into striated muscle alpha-tropomyosin. A Single Trp tropomyosin mutant, Q135W, was generated and expressed in Trp auxotrophs. OHW incorporation was 76%. Thin filaments containing Q135W retained excellent function: 12-fold Ca2+ regulation in myosin S1-thin filament MgATPase assays. Fluorescence emission titrations with increasing amounts of Ca2+ were performed (emission max 338nm) in presence of thin filaments comprised of cardiac troponin, F-actin, and Q135W tropomyosin. Similar titrations using troponin, actin, and wt Trp-free tropomyosin produced low fluorescence (ex wavelength 312 nm). Ca2+ decreased the OHW fluorescence of Q135W-containing thin filaments by 7.0 +/− 0.4 %. This transition occurred with K = 1.8 +/− 0.3 uM −1, consistent with the affinity of the cardiac thin filament regulatory calcium site on TnC. OHW Q135W tropomyosin is a novel tool for monitoring thin filament behavior, in particular for detecting Ca2+ binding to troponin. Troponin has been viewed as binding to the C-terminus of tropomyosin, which does not include the mid-tropomyosin residue 135 that is found in the current study to be Ca2+-sensitive. However, the findings may be related to recent results, suggesting that the TnI C-terminus of troponin bridges from one actin strand to the other, and contacts tropomyosin near residue 146. Galinska-Rakoczy et al, JMB 2008. Mudalige et al, JMB2009. Finally, human cardiac troponins with defective inhibitory activity due to alterations in the TnI inhibitory region have been generated. They are currently under study using this tropomyosin.

1816-Pos
Loss of Function in β-Tropomyosin (TPM2) Mutants Causing Nemaline Myopathy or Cap Disease

Massimiliano Memo[1], Elina Nuutinen[2], O'Neal Copeland[1], Carina Wallgren-Pettersson[2], Steven Baxter Marston[1].
[1]Imperial College London, London, United Kingdom, [2]University of Helsinki, Helsinki, Finland.

Nemaline myopathy (NM) and cap disease (CD) are two congenital skeletal muscle myopathies characterized by general muscle weakness with early neonatal onset. They are both clinically and genetically heterogeneous, but at the histological level they present characteristic pathology: nemaline rod-like bodies within myofibers generating from the Z-discs for NM and cap-like structures at cell periphery underneath the sarcolemma for CD. Recently several different mutations on the TPM2 gene, coding for the -tropomyosin (-Tm) isoform expressed in skeletal muscles (especially slow-twitch type 1 fibers), have been reported to cause either NM or CD. In this study six -Tm mutants connected either to NM (K7, E117K, Q147P) or to CD (E41K, K49, E139) and the wild type form have been expressed in a baculovirus/sf9 system. This system, being based on eukaryotic cell cultures, permits the N-terminal acetylation of -Tm, which has been shown to be important for its linear head-to-tail polymerisation. Thin filaments reconstituted with these recombinant proteins have been tested with the *in vitro* motility assay finding a considerable loss of function for each of them. K7, Q147P, K49 and E139 showed, through indirect observations, a reduced affinity to actin, possibly explained by destabilising the Tm homodimer itself or important actin-Tm binding sites. With all mutants the Ca^{2+}-induced increase in sliding speed was greatly reduced, indicating an altered TroponinT-Tm interaction, but thin filaments Ca^{2+} switching was unaltered. The three NM mutants showed a reduced Ca^{2+}-sensitivity, whereas two of the CD mutants showed an increase. E41K had a different phenotype and seemed to strongly inhibit filament motility. A well-defined scenario is taking shape and further studies could directly correlate these findings with the etiology of the diseases.

1817-Pos
An Evolutionary Structural Bioinformatics Analysis of the Actin Binding Protein, Tropomyosin

Bipasha Barua, Sarah E. Hitchcock-DeGregori.
RWJMS-UMDNJ, Piscataway, NJ, USA.

Tropomyosin is a two-chained, α-helical coiled-coil protein that associates end-to-end to form a continuous strand along actin filaments and regulates the functions and stability of actin. Mutations in tropomyosin cause skeletal and cardiomyopathies. We have carried out a phylogenetic analysis of tropomyosin to identify its conserved residues and to elucidate their importance for binding actin. Actin is a highly conserved protein and our hypothesis is that the actin binding sites of tropomyosin have been conserved through evolution to retain its actin-binding function. Phylogenetic trees of 60 coding sequences were constructed from tropomyosin genes from 19 species within the phyla Chordata, Hemichordata and Echinoderm. The rates of substitution (ω) at amino acid sites (codons) in the protein sequence were calculated to identify the most conserved sites (lowest ω) using CODEML in PAML 4.1. A total of 103 out of 284 residues were identified as highly conserved ($\omega \leq 0.015$), of which 24 are in *a* and *d* positions of the heptad repeat involved in the hydrophobic coiled coil interface, 38 are in potential interhelical *e-g* position salt bridges important for folding of the coiled coil, and 41 are in *b*, *c*, or *f* surface positions available for binding to other proteins, such as actin. The conserved residues at the *b*, *c*, and *f* surface positions were selected for initial mutagenesis studies with mutations to alanine. Preliminary actin binding co-sedimentation assays carried out for three tropomyosin mutants showed a 2- to 3-fold decrease in actin-binding affinity compared to the wild-type protein. Further analysis of mutations at other conserved surface positions and their effect on actin-binding affinity and stability of the mutant proteins are in progress. *Supported by Muscle Dystrophy Association.*

1818-Pos

Mechanical Properties of Human Cardiac Tropomyosin in Familial Hypertrophic Cardiomyopathy (FHC) Probed by Atomic Force Microscopy

Campion Loong, P. Bryant Chase.
Florida State University, Tallahassee, FL, USA.

α-Tropomyosin (αTm) is a 66kDa alpha-helical coiled-coil protein in thin filaments of cardiac muscle. Together with the Troponin complex (Tn), it is responsible for Ca^{2+} regulation of striated muscle contraction. When Ca^{2+} is released from sarcoplasmic reticulum and bound to Tn, the complex undergoes a conformational change that moves Tm away from myosin binding sites on actin, sites that are blocked in the absence of Ca^{2+}. This allows actomyosin cross-bridge cycling, resulting in force generation and/or sarcomere shortening. A Tm mutation (E180G) found in some FHC patients results in altered thin filament function including enhanced Ca^{2+} sensitivity. This study seeks to investigate at the single molecule level our hypothesis that the E180G mutation alters mechanical properties of αTm. Recombinant, bacterially-expressed wild type (WT) and E180G mutant αTm's were deposited and dried on separate mica surfaces coated with poly-lysine. Topographical AFM images of the samples were taken in AC-mode (Asylum Research, Santa Barbara, CA) at a resolution of 0.5x0.5 nm^2/pixel. Images were analyzed in MATLAB to obtain estimates of single Tm end-to-end distances, which were normalized with the ratio between the measured and expected contour lengths. The normalized mean squared end-to-end distance ($<R^2>$) for the E180G mutant (N=309) was ~4% smaller ($P<10^{-3}$) than that for WT (N=307). $<R^2>$ of a linear molecule is related to its average flexural rigidity. Differences between WT and mutant may point to a mutation-induced alteration in local structure or flexibility of the molecule as a whole. This prompts for further study to investigate the nature of the observed change. Furthermore, a quantitative model relating end-to-end length distribution to the persistence length of αTm will be instrumental in understanding the molecular mechanics underlying FHC. Support: NIH and American Heart Association.

1819-Pos

EPR as a Tool to Study the Dynamic of Tropomyosin in the Muscle Fiber - Use of a Bifunctional Spin Label

Roni F. Rayes[1], Michael A. Geeves[2], Piotr G. Fajer[1].
[1]Institute of Molecular Biophysics, Florida State University, Tallahassee, FL, USA, [2]University of Kent, Department of Biosciences, Canterbury, United Kingdom.

Tropomyosin (Tm), an alpha-helical coiled-coil protein, is a key regulatory protein in muscle contraction. Little is known about the role of Tm dynamics in muscle regulation and more specifically dynamics in the three states of the thin filament. In this work, the flexibility of four different regions of Tm was determined with Saturation Transfer Electron Paramagnetic Resonance (ST-EPR). The use of bi-functional labels allowed us to immobilize the probe and prevent the motion of the label with respect to protein surface. The rotational correlation time of the bi-functional spin label on Tm was 40 ns compared to 25 ns for a conventional mono-dentate spin label. The spin label was attached to i, i+4 positions of the coiled-coil, obtained by cysteine mutagenesis. The bi-functionally labeled Tm di-mutants were reconstituted into ''ghost muscle fibers'' from which the myosin filaments and intrinsic regulatory proteins (tropomyosin, troponin) were removed. The filaments were reconsituted with Tn and decorated with myosin S1. We found that there is a gradient of flexibility of Tm along its length in the muscle fiber with the C-terminus mutant A268C/E272C being less mobile (two-fold), as compared to the rest of the mutants. Introduction of troponin decreases the flexibility of the four mutants, specifically the two mid-region mutants H153C/D157C and G188C/E192C by 25% and 30% respectively. The addition of calcium did show a decrease in the flexibility of the C terminus mutant A268C/E272C by 20%. The effect of calcium addition on the two other mutants and the effect of addition of S1 on the four mutants were not significant. Thus, although there is a gradient of flexibility in Tm, its dynamics does not change within different states of thin filament activation.

1820-Pos

Comparison of the Conformational Stabilities of Striated Alpha-Tropomyosins Adapted to Different Temperature Regimes

David H. Heeley, Michael Hayley, Tatiana Chevaldina.
Memorial Univeristy, St. John's, NL, Canada.

The conformational stabilities of alpha-striated tropomyosins from warm and cold blooded sources have been compared using circular dichroism (CD) and differential scanning calorimetry. Alpha-tropomyosins from rabbit and shark share 95% sequence identity. There are three replacements in the core: residues Thr179Ala, Ser190Cys and Ser211Ala. At low temperature (pH 7) the two tropomyosins are equivalent in molar ellipticity at 222nm, however, shark tropomyosin unfolds over a wider temperature range than the mammalian counterpart. The dependence of this ellipticity on temperature (0.1M salt, pH 7, 2mg/mL protein + dithiothreitol in the case of rabbit tropomyosin) is characterized by the following transitions: shark, ~33 (main, ~two-thirds of total change in signal) and ~54°C and rabbit, ~41 (main) and ~49°C. At ~10mg/mL, the ΔTm for shark tropomyosin becomes larger on account of an upward shift in the minor transition, otherwise the results of calorimetry are in agreement with those of CD. Analysis of fragments CN1A (residues 11-128, Tm ~59°C) and CN1B (residues 142 - 281, Tms ~20 and 35°C) by far-UV CD and intact protein by near-UV CD (Tm ~ 32°C), shows that the most stable section of shark tropomyosin is located in the amino-terminal half of the molecule, possibly the first ~100 amino acids. The enhanced flexibility (lower stability) of the remainder of the molecule coincides with the presence of a row of destabilising 'core' amino acids between residues 179 - 221. A final point is that conformational stability is insensitive to the presence of a covalently bound phosphate group, consistent with the structural disordering of the corresponding region of each tropomyosin.

1821-Pos

Tropomyosin and Troponin-T Isoform Differences in Jaw-Closing Muscles of Rodentia and Carnivora that Express Masticatory Myosin

Peter J. Reiser, Radhika Patel, Sabahattin Bicer.
Ohio State University, Columbus, OH, USA.

We recently reported that, contrary to prevailing dogma, masticatory (''super-fast'') myosin is expressed in jaw-closing muscles of some members of Rodentia (Reiser et al., J. Exp. Biol. 212:2511-2519, 2009). Whereas virtually all mammalian limb muscle fibers express tropomyosin-β (Tm-β), along with fast-type or slow-type Tm-α, jaw-closing muscle fibers that express masticatory myosin in members of Carnivora express a unique isoform of Tm-α and do not express Tm-β (Rowlerson et al., Biochem. Biophys. Res. Commun. 113:519-525, 1983; Hoh et al., Proc. Aust. Physiol. Pharmacol. Soc. 20:192P, 1989). The goal of this study was to examine thin filament protein isoform composition in jaw-closing muscles of rodents that express masticatory myosin and compare the results to those from members of Carnivora. Tm or troponin-T (TnT) specific antibodies and immunoblotting were used to probe homogenates of limb and jaw-closing muscles of six species of Rodentia and three species of Carnivora. The results verify the almost exclusive expression of Tm-α, presumably the unique isoform reported earlier, in the jaw-closing muscles of Carnivora and reveal that members of Rodentia express both Tm-α and Tm-β in jaw-closing muscles, similar to limb muscles in the same species. The results also indicate that the same complement of TnT isoforms are expressed in jaw-closing and limb muscles of Carnivora, but differ markedly between the two muscle groups in Rodentia. Fast-type TnC and TnI appear to be expressed in jaw-closing muscles of both orders. It is postulated that the differences in Tm and TnT isoform expression patterns between Carnivora and Rodentia may impart fundamental differences in calcium-sensitivity of force generation to accommodate markedly different feeding styles, with shared expression of masticatory myosin, between these two animal orders. Supported by the National Science Foundation.

1822-Pos

What Region of Tropomyosin Interacts with the N-terminal Half of Troponin T?

Amal W. Mudalige[1], Sherwin S. Lehrer[2].
[1]Boston Biomedical Research Institute, Watertown, MA, USA,
[2]Boston Biomedical research Institute, Watertown, MA, USA.

The thin filament of striated muscle is made up of troponin C, troponin I and troponin T (TnT) bound to actin- tropomyosin (actinTm). Previous photochemical cross-linking studies revealed that TnT interacts more closely with Tm near residue 174 than Tm near residue 146 (Mudalige et.al., JMB 2008).

To determine the cross-linking site of TnT with Tm174, photolysed thin filaments were subjected to limited chymotryptic digestion. SDS-PAGE showed the presence of a new band corresponding to a molecular weight close to the molecular weight of cross-linked Tm-TnT2 and Tm-TnT1 (where TnT2 and TnT1 are the two major chymotryptic peptides of TnT) suggesting that Tm174 cross-linked with either the TnT1 or TnT2 regions of TnT or both. From preliminary MALDI-TOF analysis of trypsin in-gel digestion of the Tm174-TnT band(s), two new tryptic peptides were observed corresponding to a Tm174 tryptic peptide linked to three possible TnT tryptic peptides: 1) 171-174; 2) 139-144; 3) 113-115. Further analysis will determine if Tm 174 in the C-terminal half of TnT is close to the TnT1 (1-159) or TnT2 (160-282) regions of TnT. However, a preliminary photolysis study with the cross-linker at Tm100 showed no cross-linked bands in contrast to Tm174, suggesting that the N-terminal half of Tm does not interact with TnT. Further studies are underway to confirm this proposal. Supported by NIH HL22461-29.

1823-Pos

Effects of Human Cardiac Troponin T Mutations Associated with Cardiomyopathy

Susan Nguyen, Jennifer Chen, Shannamar Dewey, Qian Xu,
Aldrin V. Gomes.
University of California, Davis, Davis, CA, USA.

Mutations in troponin, an important muscle protein complex, can result in cardiomyopathy by interfering with the normal muscle activity of the heart. Troponin T (TnT) is the largest subunit of troponin and is involved in binding the troponin complex to the thin filament. Investigation of two mutations associated with cardiomyopathy in TnT, I90M and R173Q, showed different physiological characteristics. The TnT I90M mutation was identified as the causative agent of familial hypertrophic cardiomyopathy (FHC) in a large multi-generational Chinese family and at least two family members with this mutation died of sudden cardiac death. Another mutation in TnT, R173Q, was identified as the underlying cause of dilated cardiomyopathy (DCM). Patients with the TnT R173Q mutation experienced prenatal onset DCM and supraventricular tachycardia at a young age. Functional troponin complexes containing wild-type or mutant TnT's demonstrated similar maximal actomyosin ATPase activity. The inhibitory ability of the troponin complexes containing the I90M mutation was significantly reduced relative to wild-type TnT. Most RCM mutations investigated to date showed a reduced ability to inhibit actomyosin ATPase activity but the RCM mutation, R173Q, did not affect the inhibitory ability of troponin. The mutations showed increased (I90M) and decreased (R173Q) calcium sensitivity of actomyosin ATPase activity consistent with what has been observed for most FHC and DCM mutations. The mutations reduced the rate of degradation of these proteins by calpain relative to wild-type TnT. Overall, these results suggest that although calcium sensitivity may be an indicator of the type of cardiomyopathy no clear trends in maximal or minimal ATPase activity exist that can be used to characterize DCM and FHC mutations.

1824-Pos

Functional Consequences of a Novel Cardiac Troponin T Mutation Linked to Infantile Restrictive Cardiomyopathy

Michelle S. Parvatiyar[1], Shi Wei Yang[2], José R. Pinto[1], Michelle A. Jones[1], Jingsheng Liang[1], Gregor U. Andelfinger[2], James D. Potter[1].
[1]Univ of Miami, Miller School of Medicine, Miami, FL, USA, [2]CHU Sainte-Justine Research Center, Montreal, QC, Canada.

A novel double deletion in cardiac troponin T (cTnT) of two highly conserved amino acids (N100 and E101) was identified in the cardiac cDNA of a pediatric transplant recipient. The patient previously presented with restrictive and hypertrophic cardiomyopathy. Family work-up was negative, and she was found to harbor a *de novo* mutation. Electron microscopy revealed the presence of myofibrillar disarray and fibrosis. To further define this cTnT mutation as a cause of the disease, functional studies were performed. Functional effects of the single and double cTnT mutants (ΔN100, ΔE101 and ΔN100/ΔE101) were analyzed in porcine skinned papillary muscle. Fibers were displaced with exogenous cTnT mutants or WT, Ca^{2+} unregulated force was measured and then reconstituted with binary cTnI.cTnC complex. The ΔN100 and ΔE101 mutations showed opposing changes in the Ca^{2+} sensitivity of force development compared to WT. The ΔN100 mutation increased this by 0.29 pCa units and the ΔE101 mutation, in contrast, decreased it by 0.28 pCa units. Interestingly, the ΔN100/ΔE101 mutation shifted the Ca^{2+} sensitivity to the left (+ 0.19 pCa units). This finding is compatible with the preserved systolic function in this patient. ΔE101 was the only mutation that decreased the maximal force recovery compared to WT. In contrast, ΔN100 and ΔN100/ΔE101 did not show significant changes in this parameter. Both ΔN100 and ΔN100/ΔE101 exhibited decreased cooperativity of force development, suggesting altered intra-filament protein-protein interactions. These data show that residue N100 has a predominant effect over E101 and its absence is much more deleterious for cTnT function. In addition, the strength of the functional data validates this novel cTnT deletion mutant as the cause of this cardiomyopathy. Supported by NIH HL-42325(JDP), AHA 0825368E (JRP), AHA 09POST2300030 (MSP) and CIHR GMHD 79045 (GA).

1825-Pos

Biophysical and Biochemical Studies of Human Slow Skeletal Troponin T Isoforms in Slow Skeletal Muscle

Michelle A. Jones[1], José R. Pinto[1], Qian Xu[2], Aldrin V. Gomes[2], Michelle S. Parvatiyar[1], Jingsheng Liang[1], James D. Potter[1].
[1]Univ of Miami, Miller School of Medicine, Miami, FL, USA, [2]University of California, Davis, Davis, CA, USA.

A paucity of information exists concerning the functional roles of the human slow skeletal troponin T isoforms (HSSTnT isoforms) in different muscle types. Three HSSTnT isoforms have been found in slow skeletal muscle: HSSTnT1 (+ Exons 5 and 12), HSSTnT2 (+5, −12), HSSTnT3 (−5, −12) and HSSTnT4 (−5, +12, only found at the mRNA level). Soleus rabbit skinned fibers were displaced with HSSTnT1, 2, 3 or 4 and reconstituted with human SSTnI-C/STnC complex. The extent of Tn displacement was analyzed by measuring the Ca^{2+} unregulated force (UF) at pCa 8.0 after SSTnT treatment. The UF ranged from 63 to 73%. The Ca^{2+} sensitivity increased between SSTnT isoforms: isoform 1 ($pCa_{50} = 5.73$) < isoform 2 ($pCa_{50} = 5.80$) < isoform 3 ($pCa_{50} = 5.84$). HSSTnT4 yielded a $pCa_{50} = 5.78$. Using a reconstituted fast skeletal muscle system, the actomyosin ATPase activity containing different HSSTnT isoforms was determined. The HSSTnT isoforms did not alter ATPase activation or inhibition in the presence or absence of Ca^{2+}. Potential interactions between human cardiac troponin C (HcTnC), rabbit skeletal tropomyosin (RsTm) and human cardiac troponin I (HcTnI) with SSTnT were mapped. Dot blot analysis using HRP conjugated proteins revealed new interactions between SSTnT peptides and HcTnC, RsTm and HcTnI. These results may help identify the functional differences that occur between SSTnT isoforms due to their alternative splicing. Supported by NIH HL-042325(JDP) and AR-050199 (JDP) and AHA 0825368E (JRP).

1826-Pos

Does the DCM Functional Phenotype Predominate over that of HCM and RCM?

José Renato Pinto, Erin Alexander, Michelle Jones, Jingsheng Liang, James D. Potter.
Univ of Miami Miller School of Medicine, Miami, FL, USA.

In vitro investigations into Hypertrophic Cardiomyopathy (HCM) and Restrictive Cardiomyopathy (RCM) show that mutations in cardiac Troponin T (cTnT) produce a pathogenic state via increase in myofilament Ca^{2+} sensitivity, whereas mutations in cTnT that cause Dilated Cardiomyopathy (DCM) decrease Ca^{2+} sensitivity and maximal force. Our aim was to determine whether combinatory mutations of an HCM, RCM and a DCM in cTnT yield an intermediate or dominant functional phenotype that could be correlated with the clinical condition seen in patients. Standard laboratory methods were used for cloning, expression and purification of the WT and mutants: ΔK210 (DCM), I79N (HCM), ΔE96 (RCM), ΔK210/I79N, ΔK210/ΔE96 and ΔE96/I79N. Porcine papillary skinned fibers were displaced with cTnT WT or mutant and reconstituted with HCTnI-TnC. The Ca^{2+} sensitivity of force development, maximal force and basal force were evaluated. The extent of TnT displacement was analyzed by measuring the unregulated tension at pCa 8.0 after cTnT treatment and none of the mutants showed an inability to displace the native cTn complex. Both double mutants (ΔK210/I79N and ΔK210/ΔE96) containing the DCM mutant showed a rightward shift in the Ca^{2+} sensitivity with a decrease in maximal force. In addition, the ΔK210 mutation rescued the impaired relaxation produced by the RCM mutation (ΔE96). From the skinned fiber data, ΔK210 has a dominant effect over I79N and DE96 mutations in cTnT. Circular dichroism measurements demonstrated that all three double mutants had lower alpha helical content than WT. In contrast, single mutants I79N (significantly) and DK210 (showed a tendency) to increase alpha helical content. These results suggest that cTnT can exist in multiple conformations that may be responsible for these distinct functional phenotypes. NIH HL-67415 and HL-42325 (JDP), AHA 0825368E (JRP).

1827-Pos

Cardiomyopathy-Causing Deletion K210 in Cardiac Troponin T Alters Phosphorylation Propensity of Sarcomeric Proteins

Liliana S. Duke[1], Mary L. Garcia-Cazarin[1], C. Amelia Sumandea[1], Gail A. Sievert[1], C. William Balke[1], Dong-Yun Zhan[2], Sachio Morimoto[2], **Marius P. Sumandea**[1].
[1]University of Kentucky, Lexington, KY, USA, [2]Kyushu University, Fukuoka, Japan.

Ca^{2+} desensitization of myofilaments is indicated as a primary mechanism for the pathogenesis of familial dilated cardiomyopathy (DCM) associated with the deletion of lysine 210 (ΔK210) in cardiac troponin T (cTnT). ΔK210 knock-in mice closely recapitulate the clinical phenotypes documented in patients with this mutation. Considerable evidence supports the proposition that phosphorylation of cardiac sarcomeric proteins is a key modulator of function and may exacerbate the effect of the deletion. In this study we investigate the impact of K^{210} deletion on phosphorylation propensity of sarcomeric proteins. Quantitative analysis of cardiac myofibrils isolated from ΔK210 hearts identified a decrease in basal phosphorylation of cTnI (46%), cTnT (29%) and MyBP-C (31%) compared with wild type controls. Interestingly, immunoblot analyses with phospho-specific antibodies show augmented phosphorylation of cTnT-Thr^{203} (28%) and decreased phosphorylation of cTnI-$Ser^{23/24}$ (41%) in mutant myocardium. *In vitro* kinase assays indicate that ΔK210 increases phosphorylation propensity of cTnT-Thr^{203} three fold without changing cTnI-$Ser^{23/24}$

phosphorylation. Molecular modeling of cTnT-ΔK210 structure reveals changes in the electrostatic environment of cTnT helix (residues 203-224) that lead to a more basic environment around Thr^{203}, which enhances PKC-dependent phosphorylation. In addition, yeast two-hybrid assays indicate that cTnT-ΔK210 has enhanced binding to cTnI compared with cTnT-wt, and may impair Ca^{2+} sensing/transmission leading to myofilament desensitization. Collectively, our observations suggest that cardiomyopathy-causing ΔK210 has far-reaching effects influencing posttranslational modifications of key sarcomeric proteins, and potentially cTnI-cTnT interaction.

1828-Pos

Em and Single Particle Analysis of Troponin at Low and High Ca^{2+}

Hyun Suk Jung[1], Duncan Sousa[2], Larry S Tobacman[3], Roger Craig[4], William Lehman[2].
[1]Korea Basic Science Institute, Daejeon, Republic of Korea, [2]Boston University School of Medicine, Boston, MA, USA, [3]University of Illinois-Chicago, Chicago, IL, USA, [4]University of Massachusetts Medical School, Worcester, MA, USA.

Crystal structures of the troponin ''core-domain'' formed in the presence and absence of Ca^{2+} display a bilobed TnC subunit mounted on a semi-rigid scaffold formed from major stretches of TnI and TnT. A central coiled-coil of TnI and TnT is flanked by single TnI and TnT helices to form the W-shaped supporting structure, which appears to be little changed by the binding of Ca^{2+} (Takeda et al., 2003; Vinogradova et al., 2005). In contrast, at low Ca^{2+}, the central helix joining C- and N-lobes of TnC melts, and the ''regulatory'' C-terminal domain of TnI dissociates from the N-lobe of TnC (Vinogradova et al., 2005). Consistent with biochemical studies, the C-terminal TnI sequences in the thin filament are thought to latch onto actin and constrain tropomyosin in the blocked state at low-Ca^{2+}. Their dissociation from actin at high-Ca^{2+} and association with the N-terminal lobe of Ca^{2+}-saturated TnC may relieve the constraint (Galinksa-Rakoczy et al., 2008). These conclusions remain uncertain, however, because troponin is only semi-rigid (so crystal packing forces may have influenced the structure) and the troponin complex used for crystallization contained truncated subunits. Here we have studied isolated, intact troponin molecules using negative stain electron microscopy and single-particle image processing. Averaged projection views and 3D reconstructions of the isolated molecules show many of the same features seen in the crystal structures. Comparison of reconstructions of low and high Ca^{2+} data suggests that the TnC N-lobe of cardiac troponin may be further from the core domain in the EM than in the crystal structure.
Funding: HSJ (KBSI-T29760); NIH: WL (HL36153), LST (HL38834, HL63774), RC (AR34711, RR08426).

1829-Pos

Nanobiology of the Cardiac Myofilament

Mathivanan Chinnaraj[1], Wen-Ji Dong[2], Herbert C. Cheung[3], **John M. Robinson**[4].
[1]International Center for Public Health, Newark, NJ, USA, [2]Washington State University, Pullman, WA, USA, [3]University of Alabama at Birmingham, Birmingham, AL, USA, [4]South Dakota State University, Brookings, SD, USA.

The cardiac myofilament is a protein assembly that provides Ca-regulated force development enabling the heart to undergo alternating periods of contraction and relaxation. Troponin (Tn), a three-member protein assembly within the myofilament, acts as a Ca-sensitive switch. Here, using single pair FRET in freely diffusing assemblies of Tn, we show that Tn incompletely activates after binding regulatory Ca. The reserved population of inactive Tn appears to function as a nanoscopic form of cardiac reserve that can be can be manipulated by cell signaling mechanisms to fine-tune cardiac contractility. The results are discussed in terms of an energetic model of the cardiac myofilament.

1830-Pos

Investigating the Effect of Cardiomyopathy-Causing Mutations in Cardiac Troponin-T on Calcium Buffering *In Situ*

Paul J. Robinson, Yin Hua Zhang, Barbara Casadei, Hugh Watkins, Charles Redwood.
University of Oxford, Oxford, United Kingdom.

In vitro investigation of the effects of cardiomyopathy-causing mutations in thin filament regulatory proteins has demonstrated that hypertrophic cardiomyopathy (HCM) and dilated cardiomyopathy (DCM) are caused by distinct primary alterations of cardiac contractility and myofilament calcium affinity. We hypothesise that chronically altered calcium-buffering by mutant thin filaments leads to altered calcium handling and, via calcium-dependent signalling pathways, contributes to disease pathogenesis. We aim to study the *in situ* effect on calcium flux of a HCM and a DCM causing mutation in human cardiac troponin T (cTnT) (R92Q, R131W respectively), by adenoviral mediated expression of mutant protein in adult guinea pig cardiomyocytes. The adenoviral vectors co-express GFP and western blot analysis of FACS-sorted, GFP-expressing cells showed that recombinant cTnT comprised 45-50% of the total cTnT in these cardiomyocytes, 48 hours after infection. Analysis of unloaded sarcomere shortening showed that at an excitation frequency of 2 Hertz, cardiomyocytes infected with R131W cTnT elongated the time to 50% relaxation and reduced the magnitude of contraction, whilst R92Q cTnT reduced the time to 50% relaxation and increased the contractile magnitude compared to wild type. Analysis of calcium transients of the same cells using fura-2 loading, indicates that the R92Q mutation reduces calcium transient amplitude, whilst the R131W mutation increases the time to complete calcium reuptake, with no change to the transient amplitude, despite the observed decrease in contraction. We are currently assessing the caffeine transients of these cells to investigate alterations to overall SR load and measuring alterations to components of calcium-dependent signalling cascades which may link the acute effects of cTnT mutations to macroscopic remodelling observed in the pathological disease states of HCM and DCM.

1831-Pos

The Small Molecule Smooth Muscle Myosin Inhibitor, CK-2018571, Selectively Inhibits ATP Hydrolysis and Relaxes Smooth Muscle *In Vitro*

Sheila Clancy, Zhiheng Jia, Malar Pannirselvam, Xiangping Qian, Bradley Morgan, Fady Malik, Jim Hartman.
Cytokinetics, Inc., South San Francisco, CA, USA.

Smooth muscle contraction is driven by cyclical, nucleotide-dependent changes in myosin conformation that alter its affinity for actin, produce force, and generate movement. We used a high throughput screen to identify compounds that inhibit the ATPase activity of smooth muscle myosin; optimization of the initial hit compounds has resulted in compounds with nanomolar affinity. A potent representative of this chemical series, CK-2018571, inhibits the steady-state ATPase activity of human smooth muscle myosin at low nanomolar concentrations, approximately 10-fold lower than are required to inhibit non-muscle myosin, the most closely related myosin II. Selectivity between smooth and striated myosin IIs are >100-fold. Transient kinetic studies demonstrate that CK-2018571 inhibits the myosin-catalyzed hydrolysis of the γ-phosphate group of ATP, with no effect on nucleotide binding or release from the enzyme. Actin co-sedimentation assays indicate that CK-2018571 stabilizes a weak actin-binding conformation of myosin in the presence of ATP. Consistent with this mechanism, CK-2018571 relaxes skinned rat tail artery muscle tissue at low micromolar concentrations. Importantly, this relaxation occurs regardless of whether the skinned muscle has been activated by calcium or by thiophosphorylation of the myosin regulatory light chain, supporting evidence that CK-2018571 relaxes smooth muscle tissue by direct inhibition of activated smooth muscle myosin. The ability of CK-2018571 to relax intact tracheal smooth muscle and aortic ring preparations at micromolar concentrations suggests this mechanism may prove useful in diseases of smooth muscle hypercontractility, such as hypertension and asthma.

1832-Pos

Direct Interaction between the C-terminus of the Myosin Light Chain Phosphatase Targeting Subunit and Myosin Phosphatase-Rho Interacting Protein

EunHee Lee[1], Daivd B. Hayes[1,2], Terence C. Tao[1], Walter F. Stafford[1].
[1]Boston Biomedical Research Institute, Watertown, MA, USA,
[2]MedImmune, Inc., Gaithersburg, MD, USA.

Both the Ca^{2+} signal and the alteration of the Ca^{2+} sensitivity of the contractile apparatus regulate smooth muscle contraction. Myosin light chain kinase (MLCK) phosphorylated the 20 kDa regulatory myosin light chain (MLC20) resulting in contraction. Myosin light chain phosphatase (MLCP) dephosphorylates MLC20 causing relaxation. Thus, the balance between the activities of MLCK and MLCP determines the level of MLC20 phosphorylation.
MLCP consists of a 38 kDa catalytic subunit (PP1cδ), a 110 kDa targeting subunit (MYPT1), and a 21 kDa small subunit (M21). MYPT1 provides the substrate specificity and the regulation of phosphatase activity. It was reported that myosin phosphatase-Rho interacting protein (M-RIP) bound MYPT1 and thus targeted MLCP to the actomyosin contractile filament based on yeast-two hybrid and cell biological assays.
To determine if MYPT1 binds to M-RIP directly, we performed analytical ultracentrifugation (AUC) study using purified peptides of MYPT1 and M-RIP.

Circular dichroism and AUC analysis illustrated that the M-RIP peptide spanning residues 724-878 of M-RIP is a coiled coil and forms a dimer. The AUC analysis demonstrated that the C-terminal coiled-coil region of MYPT1 spanning residues 924-991 did not bind the M-RIP peptide, whereas the C-terminal random coiled-coil region of MYPT1 (synthetic LZ) spanning residues 991-1030 did bind, forming a heterotrimer. In addition, three individual glutamic acid residues (amino acids 998-1000) of MYPT1 were critical for binding. We replaced the glutamic acids either all three at a time or one at a time with glutamine residues. In addition, we replaced all three glutamic acids with aspartic acids. However none of these mutants bound to synthetic LZ demonstrating that these three glutamic acid residues are essential for binding.

1833-Pos

A Dynamic Approach Reveals Nonmuscle Myosin Influences the Overall Smooth Muscle Cross-Bridge Cycling Rate

Bilge Guvenc[1], Cansel Ustunel[2], Necla Ozturk[1], Frank Brozovich[2].
[1]Department of Biophysics, Hacettepe Medical School, Ankara, Turkey,
[2]Department of Cardiovascular Diseases. Mayo Medical School, Rochester, MN, USA.

The mechanism of force maintenance in smooth muscle has yet to be elucidated, but recent evidence suggests that nonmuscle myosin IIB (NMIIB) contributes to the mechanical properties of smooth muscle. This study was designed to determine the affects of NMIIB on the overall cross-bridge cycling rate. Aortic smooth muscle strips from homozygous NMIIB KO ($B^{+/-}$) and WT littermates were stimulated to contract (80 mM KCl) and the force response to a sinusoidal change in length (~1% Lo) at frequencies between 0.25 and 125 Hz was recorded. The length perturbation and the corresponding force were expanded into Fourier series to calculate the stiffness and phase frequency responses and the data was illustrated in Bode diagrams. Steady state tension was significantly less for the $B^{+/-}$ than for the WT mice. Frequency analysis revealed two distinct regions in the Bode plots, and the individual regions were fit to find the asymptotes representing the low and high frequency regions. The intersection of the two asymptotes occurred at 12.86 ± 0.243 Hz for WT and 17.33 ± 0.261 Hz for $B^{+/-}$. Further, the slope of the relationship between tension/stiffness and frequency was significantly higher for the WT than $B^{+/-}$ mice. These data suggest in WT mice that the force per attached cross-bridge is higher and duty cycle longer. These data demonstrate a decrease in NMIIB produces a fall in the force per attached cross-bridge and an increase in the overall cross-bridge cycling rate. These data could suggest that a decrease in the relative expression of NMIIB would decrease steady state force more than stiffness to decrease both the force per attached cross-bridge and internal load to shortening and result in an increase in the overall cross-bridge cycling rate.

Key words: Nonmuscle Myosin, Stiffness, Frequency Response

1834-Pos

Structural Change of N-terminus in Smooth Muscle Myosin Regularly Light Chain using Accelerated Molecular Dynamics

Zhuan Qin[1], Lianqing Zheng[2], Wei Yang[2,3], Kenneth A. Taylor[1,2].
[1]Department of Biological Science, Florida State University, Tallahassee, FL, USA, [2]Insititute of Molecular Biophysics, Florida State University, Tallahassee, FL, USA, [3]Department of Chemistry and Biochemistry, Florida State University, Tallahassee, FL, USA.

A novel accelerated molecular dynamics method (the Orthogonal Space Random Walk algorithm, OSRW) is applied to study the effect of the regulatory light chain (RLC) phosphorylation on the structure of the light chain binding domain of smooth muscle myosin. Smooth muscle myosin is activated by phosphorylation on the S19 (and T18 subsequently) at the N-terminus of the RLC that causes a conformational change from the closed inhibited asymmetric structure (Wendt et al. PNAS 2001) to the open structure by an unknown mechanism. The N-terminus also plays an important role in stabilizing the folded 10S conformation that is soluble at physiological ionic strength. However, X-ray structures of the RLC do not show the 24-residue N-terminus, which holds the phosphoration site. Thus, we are performing MD simulations on the 21 residues of the N-terminus as well as the RLC with part of the heavy chain. The phosphorylated N-terminus shows a bent α-helical conformation, where the S19 interacts with the R16. The unphosphorylated N-terminus has showed a straight α-helical conformation. Those simulations are carried out in explicit water under near-physiological conditions. The OSRW has demonstrated hundreds of times sampling capacity in compared with regular MD, which will promote our understanding on the phophorylation activation mechanism. This work is supported by NIAMSD.

1835-Pos

Additional Sites are Involved in the Regulation of Caldesmon by PAK Phosphorylation

Svetlana S. Hamden[1], Mechthild M. Schroeter[2], Joseph M. Chalovich[1].
[1]East Carolina University, Greenville, NC, USA, [2]University of Cologne, Cologne, Germany.

Caldesmon is an actin- and myosin-binding protein that is rich in smooth muscle. Caldesmon inhibits the actin activation of myosin catalyzed ATPase activity and may have additional functions in smooth muscle. The activity of caldesmon is controlled by phosphorylation and by binding to other factors such as Ca^{++}-calmodulin. Caldesmon is a substrate for p^{21}-activated kinase, PAK, which is reported to phosphorylate chicken gizzard caldesmon at two sites, Ser672 and Ser702. We investigated PAK phosphorylation of caldesmon using a 22kDa C-terminal caldesmon fragment. We also substituted Ser672 and Ser702 with either alanine or aspartic acid residues to mimic non-phosphorylated and constitutively phosphorylated states of caldesmon, respectively. We found that the aspartic acid mutation of caldesmon weakened calmodulin binding but had no effect on the inhibitory activity of caldesmon. Phosphorylation of the aspartic acid double mutant with recombinant PAK resulted in additional phosphorylation at Thr627, Ser631, Ser635 and Ser642. Phosphorylation at these sites by PAK was slow, but produced further weakening of calmodulin binding and reduced the inhibitory activity of caldesmon in the absence of calmodulin. Phosphorylation at the additional sites was without effect on Ca^{++}-Calmodulin binding if Ser672 and Ser702 were not phosphorylated, but was sufficient to release inhibition of actomyosin ATPase activity. This work raises the possibility that phosphorylation in the region of residues 627-642 significantly alters the activity of caldesmon.

1836-Pos

Purinoceptor Signaling in Arterial Smooth Muscle is Regulated by G-Protein-Coupled Recptor Kinase-2

Gavin E. Morris, Diane E. Everitt, John Challiss, John M. Willets.
University of Leicester, Leicester, United Kingdom.

The regulation of arterial smooth muscle cell (SMC) contraction by adenine and uridine nucleotides, plays a key role in controlling systemic blood pressure. In SMCs, UTP activates P2Y receptors (subtypes 2/4/6), which couple via $G\alpha_{q/11}$-proteins to stimulate phospholipase C, increasing IP_3/Ca^{2+} concentrations and leading to SMC contraction. Continuous or repeated receptor stimulation reduces responsiveness to further stimulation, a process termed desensitization. Receptor desensitization is often regulated by G protein-coupled receptor kinases (GRKs), which phosphorylate receptors, enhancing their interaction with β-arrestins and uncoupling them from G-proteins.

We investigated the regulation of receptors responding to UTP, which mediates concentration-dependent contraction in rat mesenteric arteries. To characterize adaptations that occur on repeated UTP additions, changes in IP_3 and $[Ca^{2+}]_i$ were assessed using single-cell imaging. Receptor desensitization was assessed by challenging mesenteric SMCs with an EC_{50} concentration of UTP (10 μM) for 30 sec before (R1) and after (R2) the addition of a maximal UTP concentration (R_{max}, 100 μM, 30 sec) with 5 min washout periods. The change in R2 relative to R1 was used to characterize P2Y receptor desensitization. By extending the washout period after R_{max} a time-dependent recovery of IP_3/Ca^{2+} responses were observed. To evaluate the involvement of individual GRKs in this process, cells were transfected with catalytically-inactive, dominant-negative GRK mutants.

Using IP_3 generation to indicate receptor recovery (R2/R1%), over-expression of ^{D110A,K220R}GRK3 ($34 \pm 4\%$), ^{K215R}GRK5 ($38 \pm 7\%$), or ^{K215R}GRK6 ($29 \pm 8\%$) caused similar reductions in IP_3 levels to those in empty-vector-transfected cells ($23 \pm 5\%$). In contrast, expression of ^{D110A,K220R}GRK2 ($58 \pm 7\%$) markedly attenuated receptor desensitization (n=10-19 cells, >3 animals). Furthermore, siRNA-mediated knockdown (>75%) of GRK2 protein also attenuated agonist-induced receptor desensitization compared to control ($68 \pm 8\%$ versus $29 \pm 6\%$, respectively, n=8-12). In conclusion, this work implicates GRK2 as the pre-eminent GRK isoenzyme regulating UTP signaling in SMCs.

1837-Pos

TR-FRET Experiments and MD Simulations Resolve Structural States of Smooth Muscle Regulatory Light Chain

David J.E. Kast, L. Michel Espinoza-Fonseca, Christina Yi, David D. Thomas.
University of Minnesota, Minneapolis, MN, USA.

We have combined time-resolved fluorescence resonance energy transfer (TR-FRET) and molecular dynamics (MD) simulations to elucidate structural changes in the phosphorylation domain (PD) of chicken gizzard smooth muscle regulatory light chain (RLC) bound to smooth muscle myosin. The PD is absent in crystal structures, leaving uncertainty about the mechanism of regulation. Donor-acceptor pairs of probes were attached to three site-directed di-Cys mutants, each having one Cys at position 129 in the C-terminal lobe and the other at position 2, 3, or 7 in the N-terminal PD. Labeled RLCs, with and without phosphorylation at S19, were reconstituted into myosin S1. Time-resolved FRET identified two structural states of the RLC, closed and open, which are present in both unphosphorylated and phosphorylated biochemical states. Phosphorylation shifts the equilibrium toward the open state by 20-30%. Molecular dynamics simulations, guided by these and previous spectroscopic studies, confirm the existence of the open and closed structural states and produce atomic resolution models of these states. In the closed state, the PD interacts with the surface of the C-terminal lobe. In the open state, the PD is more helical and straight, resides farther from the C-terminal lobe, and is more mobile. Phosphorylation stabilizes the open state by forming a specific salt bridge between R16 and phosphorylated S19. This conformational shift is consistent with a mechanism of regulation that catalyzes large structural changes within myosin at a low energetic cost. This work was supported by grants from NIH (AR32961, AR07612) and the Minnesota Supercomputing Institute. We thank Igor Negrashov for excellent technical assistance.

1838-Pos
Stimulated Actin Polymerization Induces Force Potentiation in Swine Carotid Artery
Christopher M. Rembold, Ankit Tejani.
University of Virginia, Charlottesville, VA, USA.
The phenomenon of post-tetanic potentiation, in which a single submaximal contraction or series of submaximal contractions strengthens a subsequent contraction, has been observed in both skeletal and cardiac muscle.
In this study, we describe a similar phenomenon in swine carotid arterial smooth muscle. We find that a submaximal K^+ depolarization increases the force generation of a subsequent maximal K^+ depolarization - we term this ''force potentiation.''
Force potentiation was not associated with a significant increase in crossbridge phosphorylation or shortening velocity during the maximal K^+ depolarization, suggesting that the potentiated force was not caused by higher crossbridge cycling. We found that measures of stimulated actin polymerization (higher prior Y118 paxillin phosphorylation, higher prior F actin, and transition to a more solid rheology evidenced by lower noise temperature and phase angle) present prior to the maximal K^+ depolarization predicted the degree of force potentiation.
Increased prior contraction alone did not induce force potentiation since readdition of Ca^{2+} to Ca^{2+}-depleted tissues induced a partial contraction that was not associated with changes in noise temperature or with subsequent force potentiation.
These data suggest that stimulated actin polymerization may produce a substrate for increased crossbridge mediated force, a process we observe as force potentiation.

1839-Pos
Is Slower Myosin Cross-Bridge Kinetics in Tg-D166V Preparations Due to Decreased Myosin RLC Phosphorylation?
Priya Muthu[1,2], Katarzyna Kazmierczak[1], Jingsheng Liang[1], Anna I. Rojas[1], Michelle Jones[1], Julian Borejdo[2], Danuta Szczesna-Cordary[1].
[1]University of Miami Miller School of Medicine, Miami, FL, USA,
[2]University of North Texas Health Science Center, Fort Worth, TX, USA.
In this report we have investigated a particularly malignant phenotype of Familial Hypertrophic Cardiomyopathy (FHC) associated with the 166 Aspartic Acid to Valine (D166V) mutation in the ventricular myosin regulatory light chain (RLC). We show that the rates of myosin cross-bridge attachment and dissociation are significantly different in isometrically contracting cardiac myofibrils from transgenic (Tg)-D166V compared to Tg-WT mice. A single molecule approach was taken where the fluorescence anisotropy of rhodamine phalloidin labeled actin protomers was measured in cardiac myofibrils undergoing isometric contraction. Orientation of an actin molecule oscillated between two states, corresponding to the actin-bound and actin-free states of the myosin cross-bridge. The rates of cross-bridge attachment as well as cross-bridge dissociation were significantly decreased in isometrically contracting Tg-D166V myofibrils (binding, 1.4 s^{-1}; detachment, 1.2 s^{-1}) compared to Tg-WT myofibrils (binding, 3 s^{-1}; detachment, 1.3 s^{-1}). The duty ratio of the cross-bridge cycle, equal to the fraction of the total cycle time that cross-bridge remains attached to actin, was 47% inTg-D166V myofibrils and 30% in Tg-WT. Immunoblotting of cardiac myofibrils used for kinetics studies demonstrated a large reduction in RLC phosphorylation in Tg-D166V vs. Tg-WT myofibrils. These data are in accord with our previous findings in skinned and intact papillary muscles showing slower fiber kinetics and prolonged force transients in Tg-D166V fibers compared to Tg-WT preparations (Kerrick et al., FASEB J. 23: 855, 2009). Similarly, the level of RLC phosphorylation in muscle extracts from Tg-D166V ventricles was decreased. Our cellular and single molecule data suggest that a mutation-dependent decrease in RLC phosphorylationcould initiate the slower kinetics of the D166V cross-bridgesand ultimately lead to abnormal cardiac muscle contraction. Supported by NIH-HL071778 (DSC), NIH-AR048622 (JB) and NIH-HL090786 (to JB and DSC).

1840-Pos
Biochemical Phenotypes Associated with the Myosin Essential Light Chain Mutations
Alexander Raytman, Shaurya Joshi, Katarzyna Kazmierczak, Michelle Jones, Priya Muthu, Danuta Szczesna-Cordary.
University of Miami Miller School of Medicine, Miami, FL, USA.
To investigate the effects of familial hypertrophic cardiomyopathy (FHC) mutations in the ventricular myosin essential light chain (ELC) we have exchanged the human ventricular wild type (WT) and two FHC ELC mutants (A57G, E143K) for the endogenous porcine ELC in isolated and purified pig cardiac myosin.To elucidate the importance of the long N-terminus of cardiac myosin ELC for the actin-myosin interaction, we also exchanged the N-terminal truncation mutant ELC-Δ43 into native porcine myosin. The phenotype associated with the A57G mutation consists of a classic asymmetric hypertrophy with varying pathology and disease progression including sudden cardiac death (SCD) (Lee, *et al.* (2001) *Am Heart J***141**, 184-9). The E143K mutation is associated with a restrictive cardiomyopathy and SCD phenotype (Olson *et al.* (2002) *Circulation***105**, 2337-40). We hypothesized that FHC ELC mutants may bind to the myosin heavy chain with a lower affinity than ELC-WT, thus affecting the structural integrity of the thick filaments in muscle. SDS-PAGE demonstrated that indeed the A57G mutation yielded lower percent exchange in cardiac porcine myosin compared to WT. We further hypothesized that as a consequence the interaction of ELC-mutant myosin with actin will be affected. All ELC-mutant myosins were tested for their ability to bind actin using fluorescence spectroscopy and pyrene-labeled F-actin. We observed a significantly decreased binding affinity for both FHC mutants while the binding of the ELC-Δ43 mutant myosin to F-actin was stronger than WT. The latter supports the hypothesis that the N-terminus of ELC acts as a molecular constrain inhibiting the actin-myosin interaction. Lower binding affinity of myosin containing the A57G and E143K mutations might be responsible for the development of the pathologic cardiac phenotype observed in patients carrying these FHC mutations. Supported by NIH HL071778 and NIH HL090786.

Cardiac Muscle I

1841-Pos
Abnormal Thin Filament Calcium Binding Associated with Cardiac Muscle Diseases Can be Corrected Through TnC Mutagenesis
Bin Liu[1], Ryan S. Lee[1], Jack A. Rall[1], Svetlana B. Tikunova[2], Jonathan P. Davis[1].
[1]The Ohio State University, Columbus, OH, USA, [2]University of Houston, Houston, TX, USA.
The Ca^{2+} sensitivity of cardiac muscle force development can be adversely altered during disease. Since troponin C (TnC) is the Ca^{2+} sensor for muscle contraction, TnC's Ca^{2+} binding properties may be affected by the disease related protein modifications. To test this hypothesis, a fluorescent TnC was utilized to measure the Ca^{2+} binding sensitivity of TnC in the physiologically relevant biochemical model system of reconstituted thin filaments. Consistent with the pathophysiology, the inherited restrictive cardiomyopathy (RCM) mutation TnI R192H and ischemia induced truncation of TnI (residues 1-192) increased TnC's Ca^{2+} binding sensitivity ~3 fold and ~7 fold, respectively; while the dilated cardiomyopathy (DCM) mutation TnT deltaK210 decreased TnC's Ca^{2+} binding sensitivity ~ 3 fold. Since the symptoms of the diseases may be caused by the abnormal Ca^{2+} binding, correcting the Ca^{2+} binding might improve cardiac function. To achieve this goal, we have engineered TnC constructs with a wide, yet adjustable, range of Ca^{2+} binding sensitivities by modulating the negatively charged residues in the Ca^{2+} chelating loop and/or by replacing key hydrophobic amino acids in the regulatory domain of TnC with polar Gln. We were able to correct both the increased and decreased thin filament Ca^{2+} sensitivities caused by the disease associated proteins via replacing the wild type TnC with specifically engineered TnC constructs. Additionally, engineered TnC constructs can correct the disease related abnormal Ca^{2+} sensitivity of the acto-myosin ATPase assay and the force-pCa relationship in skinned trabeculae. This study can potentially lead to a novel therapeutic strategy for treating cardiac muscle diseases.

1842-Pos
Sarcomere Length Dependent Contractile Activation is Reduced in Rat Trabeculae Exchanged with cTn Containing the L48Q cTnC Variant Independently of Strong Binding Cross-Bridges
F. Steven Korte, **Erik R. Feest**, Maria V. Razumova, Michael Regnier.
University of Washington, Seattle, WA, USA.
Calcium sensitivity of the force-pCa relationship depends strongly on sarcomere length (SL) in cardiac muscle. It can also be influenced by maneuvers that alter the distribution of cross-bridges within the cross-bridge cycle. We have demonstrated that cardiac trabeculae have left-shifted and virtually eliminated SL dependence of force-pCa relationship following passive exchange with cTn containing a mutant (L48Q) cTnC (with enhanced TnC-TnI interaction). Here we designed experiments to investigate the importance of strongly bound crossbridges and lattice spacing in modulating the force-pCa relationship of WT and L48Q cTnC-cTn exchanged trabeculae. Using 3% dextran at SL = 2.0 μm to osmotically compress preparations to widths ~SL = 2.3 μm, we observed increased maximal force but not increased pCa_{50} in L48Q cTnC-cTn exchanged trabeculae. Conversely, crossbridge inhibition with of 2,3-butanedione monoxime (BDM, 7 mM) at SL 2.3 μm decreased maximal force and Ca^{2+} sensitivity in native and WT-cTn exchanged trabeculae to levels measured at ~SL = 2.0 μm. L48QcTnC-cTn exchanged preparations treated with BDM also decreased maximal force to that seen at SL = 2.0 μm, but demonstrated no shift in Ca^{2+} sensitivity. This result is similar to decrease in maximal force but no shift in Ca^{2+} sensitivity for L48Q cTnC-cTn exchanged preparations at SL 2.0 vs. 2.3 μm. The combined results further support the idea that L48Q cTnC confers crossbridge independence on thin filament activation. It may also imply that native thin filaments are dependent on strong crossbridge binding for full activation because of relatively weak cTnC-cTnI interaction. Finally, the relative strength of cTnC-cTnI interaction may be an important determinant in length dependent activation of cardiac muscle. Support provided by NIH HL65497 (MR) and T32 HL07828 (FSK).

1843-Pos
Engineering Troponin C to Improve Cardiomyocyte Contraction and Relaxation Following Myocardial Infarction
Kate O. Buckley.
University of Washington, Seattle, WA, USA.
Gene based therapies targeting cardiac myofilaments offer a novel way to halt or even reverse cardiac dysfunction following infarction by enhancing contractility of the heart. Experiments here were designed to test the ability of an engineered troponin C (L48Q), with increased Ca^{2+} binding affinity to abrogate contractile deficits of isolated adult rat cardiomyocytes from rat hearts infarcted by permanent ligation of the left descending coronary artery. After 4 weeks cardiomyocytes from these and sham-operated, non-infarcted hearts were cultured and incubated with adenoviral constructs containing cDNA for either GFP + WT cTnC or GFP + L48Q cTnC. After 48-72 hours, stimulated cardiomyocyte contraction and relaxation were measured using video microscopy (IonOptix). In a sub-set of cardiomyocytes intracellular Ca^{2+} transients were measured following incubation with Fura-2. Myocardial infarction resulted in decreased extent (8.6 +/- 1.0 %) and velocity of shortening (93.4 +/- 13.0 μm/s) and relaxation velocity (51.3 +/- 6.4 μm/s), compared to control myocytes (12.1 +/- 2.4 % and 147.3 +/- 16.7 μm/s and 118.8 +/- 16.3 μm/s, respectively). Expression of L48Q cTnC in cardiomyocytes from infarcted hearts increased fractional shortening, shortening velocity, and relaxation velocity to near control values of 10.9 +/- 1.3 % and 165.0 +/- 23.6 μm/s and 141.7 +/- 32.2 μm/s, respectively. Interestingly, the peak Ca^{2+} transient amplitude was increased in cardiomyocytes from infarcted hearts, from 9.9 +/- 0.5 % in control cells to 23.0 +/- 2.69 % in cells from infarcted hearts, which was also restored to near control values with L48Q cTnC transfection to 11.9 +/- 0.8 %. These results suggest that targeted expression of L48Q cTnC may improve myocardial function in infarcted hearts by reversing contractile dysfunction and improving sensitivity to intracellular Ca^{2+}. Funding provided by NIH_HL091368 (MR, CEM), AHA_T32 HL07828 (FSK).

1844-Pos
Calcium Sensitivity, Force Frequency Relation and Cardiac Troponin I: Critical Role of PKA and PKC Phosphorylation Sites
Genaro A. Ramirez-Correa, Sonia Cortassa, Brian Stanley, Wei Dong Gao, Anne M. Murphy.
Johns Hopkins School of Medicine, Baltimore, MD, USA.
Transgenic models with mutants of cardiac troponin I, cTnI-PKA S22,23D ($cTnIDD_{22,23}$) or cTnI-PKC S22A,S23D,S42,S44D (cTnI PKA/PKC) displayed differential force-frequency relationships (FFR) *in vivo*. We hypothesized that these cTnI phospho-mimics would impact cardiac muscle force development and Ca^{2+} sensitivity in opposite directions in a rate dependent fashion. Our study shows that $cTnIDD_{22,23}$ increases (while cTnI PKA/PKC decreases) its ability to generate normal force per unit of $[Ca^{2+}]i$ when stimulation frequency increases. Force-$[Ca^{2+}]_I$ hysteresis-loops revealed that $cTnIDD_{22,23}$ shows an increased calcium sensitivity in the activation phase of force-$[Ca^{2+}]_i$ loops at 1 to 4 Hz when compared to NTG (Figure1E). An integrated computational model that encompasses electrophysiology, Ca^{2+} dynamics, contractile and mitochondrial activity (ECME model) indicates that these cTnI mutants might change the association-dissociation constants for Ca^{2+} binding, both the low- and/or high-affinity binding sites, of troponin complex. Our data indicate that cTnI phosphorylation at PKA sites is a crucial mediator of the FFR by increasing the frequency-dependent myofilament sensitivity; which might be achieved by adaptive changes on association-dissociation constants for Ca^{2+} binding of the troponin complex.

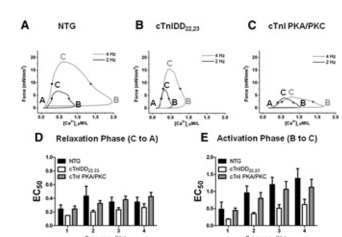

1845-Pos
Impact of Ischemia/Reperfusion Associated TnI Degradation on Cross-Bridge Dynamics in Skinned Rat Cardiac Trabeculae
Kittipong Tachampa[1,2], Helen Wang[1], Pieter P. de Tombe[1].
[1]Loyola University Chicago, Maywood, IL, USA, [2]Chulalongkorn University, Bangkok, Thailand.
Proteolytic degradation of Troponin I (cTnI) may be the cause for the depressed contractility that is seen in myocardial stunning. Here, we studied the impact of a proteolytic fragment $cTnI_{63-193}$ (identified by McDonough et al, 1999) on cross-bridge cycling dynamics in isolated myocardium. Murine $cTnI_{63-193}$ mutant, as well as wild type cTnC and cTnT, were expressed in *E.coli*. Next, FPLC purified Troponin (cTn) complex containing either wild type cTnI or $cTnI_{63-193}$ was exchanged for endogenous cTn in skinned rat cardiac trabeculae; Western blot analysis confirmed that >75% cTn was exchanged. Myofilament chemo-mechanical cross-bridge dynamics were determined as function of $[Ca^{2+}]$ at SL=2.2 μm using an enzyme-coupled UV absorbance technique (de Tombe & Stienen, 1995).Compared to wild-type exchange, $cTnI_{63-193}$ exchanged fibers displayed ~30% decrease in myofilament Ca^{2+} sensitivity (EC_{50}). In contrast, neither maximal tension development, nor maximal ATPase activity (and consequently tension-cost), were significant different between the groups, nor was cooperative thin filament activation (Hill coefficient). We conclude that

$cTnI_{63-193}$ found following severe ischemic/reperfusion affects cardiac function predominantly via decreased myofilament Ca^{2+}-sensitivity. Our results may benefit rational drug development aimed to prevent ischemic/reperfusion injury in patients.

1846-Pos
TnI Switch Peptide Position within Cardiac Troponin as Studied by cw-Epr and DEER

Jean Chamoun[1,2], James A. Cooke[2], Louise J. Brown[2], Peter G. Fajer[1].
[1]FSU, Tallahassee, FL, USA, [2]Macquarie University, Sydney, Australia.

Muscle contraction is regulated by the troponin complex which is a heterotrimer protein consisting of a Ca^{2+} binding subunit (TnC), an inhibitory subunit (TnI) and a Tropomyosin binding subunit (TnT). Calcium binding to TnC ('ON' state) initiates a series of structural changes in the thin filament proteins leading to muscle contraction. In the low Ca^{2+} 'OFF' state, the TnI subunit induces muscle inhibition through its two actin binding domains (residues 133-148 and 166-210). Another region of TnI termed the 'switch peptide' (residues 150-161) is essential for a complete relieve of muscle inhibition in the ON state. The position of the switch peptide is vital since it affects the whereabouts of both TnI actin binding domains. In the $+Ca^{2+}$ cardiac Tn core crystal structure, the switch peptide is depicted to be close to the N-lobe of TnC (Takeda et al., Nature, 2003) but no or limited knowledge is known about its position in the absence of Ca^{2+}. We studied the proximity of the switch peptide to two domains within Tn in both the 'ON' and 'OFF' states. Two intermolecular distances from each end of the switch peptide back to the N-lobe of TnC (TnI152/TnC35, TnI152/TnC84, TnI160/TnC55) and one intramolecular distance (TnI129/TnI160) within TnI were measured with Conventional Electron Paramagnetic Resonance (cw) and Double Electron Electron Resonance (DEER) methods. In the 'ON' state, both the intramolecular and intermolecular distances were less than 2.5nm with narrow distance distributions indicative of restricted movement. Upon removal of Ca^{2+}, distances increased considerably (TnI129/160 to 5nm and TnI151/TnC35 to 3.3nm) with an accompanying increase in the distance distributions suggesting a more flexible, non-bound, switch peptide.

1847-Pos
Molecular Function of the C-terminal Domain of Cardiac Troponin I

Danamarie Moonoo[1], Nancy L. Meyer[2], Vanessa Inchausti[1], Nicolas M. Brunet[3], Vincent LaBarbera[2], P. Bryant Chase[2], **Brenda Schoffstall**[1].
[1]Barry University, Miami Shores, FL, USA, [2]Florida State University, Tallahassee, FL, USA, [3]Donders Institute for Brain, Cognition and Behaviour, Radboud University, Nijmegen, Netherlands.

Ca^{2+} regulation of cardiac muscle contraction is dependent upon regulation by tropomyosin (Tm) and troponin (Tn); the extreme C-terminus of the inhibitory subunit of Troponin (cTnI) binds to actin at low $[Ca^{2+}]$ and is presumed to hold Tm in a closed position preventing actomyosin interaction. cTnI's C terminus (''mobile domain'' (MD)) is the site of several human mutations that lead to familial hypertrophic cardiomyopathy (FHC), therefore it is of interest to clarify the specific function and importance of this domain in cardiac muscle contraction. We have demonstrated that even in the absence of Tm, Tn is able to enhance thin filament sliding speed and heavy meromyosin ATPase activity. To explore the possibility that the MD plays a role in enhancement of myosin activity in cardiac muscle, we have utilized an all-cardiac protein (porcine cardiac actin and myosin, recombinant human cardiac Tm-Tn) *In Vitro* Motility assay to detect alterations in Ca^{2+} regulation of cardiac actomyosin interaction in the presence of two specific human recombinant cTn MD structural mutants. ''K164Δ'' is truncated after cTnI K164 and ''LINK 2c2'' has an inserted 8-amino acid linker before cTnI K164. At pCa5, K164Δ showed no significant difference from WT in filament sliding speed at most Tn-Tm concentrations tested, while sliding speed with LINK 2c2 was significantly slower than WT. Conversely, at pCa9, K164Δ was unable to stop actomyosin interaction, with sliding speeds significantly faster than WT; LINK 2c2 regulated the same as WT at pCa9 for most concentrations tested. Our *in vitro* cardiac muscle experimental data suggest that (1) the MD of TnI is a key player in Ca^{2+} regulation of cardiac muscle contraction, and (2) the C-terminal Mobile Domain of cTnI is not responsible for observed functional enhancement of myosin at saturating $[Ca^{2+}]$.

1848-Pos
Effect of Hypertrophic Cardiomyopathy Associated Troponin I Mutations on thin Filament Dynamics

Sameeh A. Al-Sarayreh, Mohammed El-Mezgueldi.
University of Leicester, Leicester, United Kingdom.

Troponin I plays an essential role in the regulation of cardiac muscle contraction. Together with troponin C and T, troponin I induces Ca^{2+} dependent co-operative transitions of thin filaments between a blocked, a closed and an open state. 29 mutations were found in cardiac troponin I in families with hypertrophic cardiomyopathy. Although unknown, the mechanism of molecular dysfunction is likely to involve an aberrant thin filament responsiveness to changes in intracellular level of Ca^{2+}. Our hypothesis is that these mutations modify important parameters in the cooperative-allosteric transitions of thin filaments. Here we aimed at using transient kinetics to assess the effect of hypertrophic cardiomyopathy TnI mutations (Q130R, R145G, and A157V) on the rate and equilibria of thin filament switching between the blocked, closed and open states. We found that TnIQ130R and TnIA157V did not affect the equilibrium constant between the blocked and the closed states (K_B). In contrast TnIR145G substantially increased K_B in the absence of Ca^{2+}. An increase in K_B is likely to lead to incomplete relaxation. We also investigated the effect of these mutations on the cooperative behaviour of thin filaments. TnIQ130R and A157V did not affect the size of the cooperative unit n while TnIR145G decrease n value to less than 7. Calcium binding to thin filaments was monitored by change in the fluorescence of IAANS-TnC^{C84S}. Thin filaments reconstituted with TnI mutations showed a change in calcium affinity and the rate of Ca^{2+} dissociation. These findings suggest that mutations in different regions of troponin I are likely to have different biochemical effect highlighting the unique molecular mechanism for each of these mutations.

1849-Pos
N-Terminal Truncated Cardiac TnI Extends Frank-Starling Response of the Heart

Hanzhong Feng[1], X.-P. Huang[2], J.-P. Jin[1].
[1]Physiology Department, Wayne State University, Detroit, MI, USA, [2]Department of Biomedical Sciences, Florida Atlantic University, Boca Raton, FL, USA.

Cardiac TnI (cTnI) has a unique N-terminal extension containing the PKA phosphorylation sites, and its removal by restricted proteolysis in cardiac adaptations to hemodynamic stress and β-adrenergic deficiency provides a functional compensation via improving myocardial relaxation (Barbato et al., JBC 2005; Feng et al., JBC 2008). By transgenic expression of N-terminal truncated cTnI (cTnI-ND) in the cardiac muscle of cTnI knockout mice, we examined the function of hearts containing purely cTnI-ND. Working hearts from the double transgenic mice showed no hypertrophy and normal baseline function as compared with the wild type controls, confirming the non-destructive nature of cTnI-ND. When preload was raised to examine the Frank-Starling response, left ventricular relaxation velocity was better maintained in cTnI-ND hearts than that in wild type controls. The effect of cTnI-ND on enhancing relaxation resulted in lower left ventricular end diastolic pressure and maintained left ventricular contractile velocity and end systolic pressure, especially at high preloads. The overall outcome was larger stroke volumes from cTnI-ND hearts at increased preloads than the responses of wild type hearts. The enhanced range and extent of positive response of cTnI-ND hearts to preload demonstrates that the removal of cTnI N-terminal extension by restricted proteolysis provides a novel mechanism to maximize the Frank-Starling effect in cardiac adaptation against hemodynamic and inotropic stresses.

1850-Pos
Functional Effects of Two Troponin I Mutations Linked to Restrictive Cardiomyopathy

Shannamar Dewey[1], Josephine Chen[1], Susan Nguyen[2], Qian Xu[1], Aldrin v. Gomes[1].
[1]University California, Davis, Davis, CA, USA, [2]University California, Davis, Davis, CA, USA.

Mutations in cardiac troponin, a protein complex that regulates muscle contraction, have been shown to be linked to cardiomyopathies, which commonly lead to chest pains, myocardial infarction, or sudden cardiac death. The troponin complex consists of three proteins: Troponin T, Troponin I (TnI), and Troponin C (TnC). In recent clinical studies, two novel mutations in cardiac TnI were discovered co-segregated with cardiomyopathy, but their specific functional effects remain unknown. These mutations are the first frameshift mutations in cTnI known to be linked to restrictive cardiomyopathy (RCM). The deletion of two adenines at codon 177 (Delbp529AA) in cardiac TnI, was discovered in a six year old female RCM patient. The second cTnI mutation included in this investigation was the result of a deleted guanine in codon 168 which caused a frame shift and premature stop codon at 176 (DelG502). cTnI DelG502 was associated with sudden cardiac death. It was found during column purification that the 34 residue truncation of cTnI removed or greatly decreased its binding affinity for TnC. However, the Delbp529AA mutant protein, containing 32 alternate C-terminal residues, was successfully purified and formed a functional troponin complex. Actomyosin ATPase assays demonstrated similar maximal ATPase activity for complexes containing TNNI3 Delbp529AA compared to wild type complexes. cTnI Delbp529AA showed increased calcium sensitivity of ATPase and less inhibitory function compared to wild-type cTnI. Calpain

digestion studies indicate that cTnI Delbp529AA is degraded at a faster rate than wild-type cTnI. These results suggest that the poor prognosis of patients carrying these RCM-linked mutants is due to protein dysfunction at multiple levels and suggest possible mechanisms of RCM pathology.

1851-Pos
Identification of Unknown Protein Kinase Cα Phosphorylation Sites on Both Human Cardiac Troponin I and T

Viola Kooij[1], Sander R. Piersma[2], Kay W. Tang[1], Conny R. Jiménez[2], Pingbo Zang[3], Jennifer E. van Eyk[3], Anne M. Murphy[3], Jolanda van der Velden[1], Ger J.M. Stienen[1].
[1]Institute of cardiovascular research, Vu Medical Center Amsterdam, Amsterdam, Netherlands, [2]Oncoproteomics laboratory, Vu Medical Center Amsterdam, Amsterdam, Netherlands, [3]Department of cardiology, John Hopkins University, Baltimore, MD, USA.

Protein kinase C (PKC) isoforms have been shown to play an important role in the development of heart failure. Most research performed on PKCα has been done in rodents and direct evidence in human heart failure is limited. Our previous study showed a decrease in Ca^{2+}-sensitivity in failing tissue upon PKCα treatment of cardiomyocytes via phosphorylation of cardiac troponin I (cTnI), cardiac troponin T (cTnT) and myosin binding protein C (cMyBP-C). This study aims to determine the targets of PKCα on cTnI and cTnT. Western immunoblotting revealed that PKCα is less abundant but more active in failing compared to donor tissue. PKCα treatment of donor and failing tissue was able to phosphorylate Thr-143, which is a known PKCα site on cTnI, but endogenous phosphorylation levels were very low. LC-MS analysis of purified human recombinant cTn complex incubated with PKCα identified two novel phosphorylation sites, Ser-199 located on cTnI and Ser-189 on cTnT. Both sites are located in conserved regions on cTnI and cTnT. The PKA sites Ser23/24 on cTnI are phosphorylated by PKCα in purified human recombinant cTn complex, but there is no cross phosphorylation in donor and failing tissue. In conclusion, endogenous Thr-143 phosphorylation is low, which makes its involvement in heart failure unlikely. Exogenous PKCα phosphorylation of Thr-143 and Ser-199 on cTnI and Ser-189 on cTnT could possibly explain the decrease in Ca^{2+}-sensitivity observed and further research on the site-specific effects is warranted.

1852-Pos
Rescuing Myopathic Phenotype of Abnormal Cardiac Troponin T with a Single Amino Acid Substitution in Cardiac Troponin I

Bin Wei[1], Xu-Pei Huang[2], J.-P. Jin[1].
[1]Wayne State University, Detroit, MI, USA, [2]Florida Atlantic University, Boca Raton, FL, USA.

Troponin T (TnT) and troponin I (TnI) are two subunits of the troponin complex. We previously found a single amino acid substitution in the TnT-binding helix of cardiac TnI (cTnI) in wild turkey hearts that expressed abnormally spliced myopathic cardiac TnT (cTnT) (Biesiadecki *et al., JBC* 279:13825-32, 2004). To test the potential role of this cTnI modification in rescuing a cTnT abnormality, we developed transgenic mice expressing the cTnI variant (K118C) with or without a deletion of endogenous cTnI gene to mimic homozygote and heterozygote wild turkeys. Double and triple transgenic mice were created to combine the cTnI-K118C allele with an allele encoding the abnormally spliced cTnT (exon 7 deletion). Functional analysis in *ex vivo* working hearts found that cTnI-K118C had no destructive effect on cardiac muscle and baseline heart function but was able to rescue the decreases in cardiac function caused by cTnT exon 7 deletion. Further characterizations showed that cTnI-K118C significantly blunted the inotropic response of cardiac muscle to β-adrenergic stimulation whereas the PKA-dependent phosphorylation of cTnI was unchanged. These data indicate that TnI-TnT interaction is a critical link in Ca^{2+} signaling and β-adrenergic regulation of myocardial contraction, providing a novel target for the treatment of heart failure.

1853-Pos
H2-Helical Region of Cardiac Troponin T Contributes to Length-Dependent Regulation of Cardiac Contractile Activation

Steven J. Ford, Ranganath Mamidi, Kenneth B. Campbell, Murali Chandra.
Washington State University, Pullman, WA, USA.

An alpha-helical region of cardiac troponin T, cH2(T), is centrally positioned in the core domain of the troponin complex (Takeda et al., Nature 2003 vol.424(6944):p35-41). cH2(T)-troponin I and cH2(T)-troponin C interactions have been illustrated through biochemical studies and visualized in the crystal structure of the core domain of human cardiac troponin, suggesting an important regulatory role for cH2(T). However, little is known about how the cardiac-specific structure of cH2(T) relates to cardiac-specific contractile function. To better understand the functional significance of cH2(T), we created a chimeric rat cardiac troponin T (TnT) in which cH2(T) was replaced by the corresponding helical region of rat slow skeletal TnT and studied how replacement of native TnT with chimeric TnT affected contractile function of rat cardiac muscle. We measured isometric force, ATPase activity, and length-dependent contractile dynamics in detergent skinned papillary muscle bundles reconstituted with either wild-type or chimeric TnT, held at either sarcomere length (SL) 2.0 μm or 2.2 μm. Preliminary studies suggest that the SL dependence of Ca^{2+}-activated maximal force production and tension cost was depressed in bundles containing chimeric TnT. For example, bundles containing the chimeric TnT showed an 8.4% decrease in force production when SL was decreased from 2.2 μm to 2.0 μm, whereas bundles containing the wild-type TnT showed a 43.9% decrease in force production. In addition, length-dependent contractile dynamics were significantly altered in bundles containing the chimeric TnT. For example, the length-dependent rate constant of crossbridge recruitment was slower, and the rate constant of crossbridge detachment was faster in bundles containing the chimeric TnT. Thus, our data suggest that cH2(T) plays a role in cardiac-specific length-mediated myofilament activation, an important mechanism underlying the Frank-Starling relationship.

1854-Pos
Structural and Functional Characterization of the TNT1 Domain of Cardiac Troponin T

Rachel K. Moore, Pia J. Guinto, John Wilson, Gary Gerfen, Jil C. Tardiff.
Albert Einstein College of Medicine, Bronx, NY, USA.

Familial Hypertrophic Cardiomyopathy (FHC) is a primary cardiac muscle disorder and a common cause of sudden cardiac death among young people in the field. The majority of disease-causing mutations in the thin filament protein hcTnT are found within the TNT1 domain. This domain has not been crystallized and its structural details are poorly defined, limiting our ability to understand the mechanism of disease for these mutations. A highly charged region is found at the C-terminal end of TNT1 (158-RREEEENRR-166) in which this highly alpha helical domain may unwind to create a flexible hinge that is necessary for normal function. We aim to determine the structural details and function of this region using SDSL-EPR and regulated in vitro motility (R-IVM) assays. The purpose of our R-IVM experiments is two-fold: to functionally analyze our spin labeled proteins and to gain insight into the function of TNT1 in the presence of cysteine substitutions. R-IVM data shows a progressive increase in the severity of the functional effects of cysteine substitution and spin labeling across the putative hinge region, suggesting that this region is dynamically important and may be making critical interactions with other components of the sarcomere. CW-EPR spectra of spin labeled hcTnT in Troponin ternary complexes show an increase in spin label mobility from residue 153 to 157 and 177, consistent with a decrease in alpha helical character across the putative hinge region. Preliminary doubly labeled CW-EPR experiments show that interspin distance between hcTnT residues 157 and 177 exceed 25A. Interspin distance measurements using doubly labeled hcTnT will further elucidate the secondary and tertiary structure of this region. Additional spin label pairs are currently being investigated using both CW-EPR and DEER techniques to determine the structural details of this important region.

1855-Pos
Tropomyosin-Kappa Alters Cardiac Dynamics in a Mouse Heart Model

Chehade Karam[1], Marko Alves[1], Beata M. Wolsa[1], Sudarsan Rajan[2], David F. Wieczorek[2], R. John Solaro[1].
[1]University of Illinois at Chicago College of Medicine, Chicago, IL, USA, [2]University of Cincinnati College of Medicine, Cincinnati, OH, USA.

Tropomyosin-kappa (TPM1κ), a novel TM isoform, is exclusively expressed in the human heart. Alternative splicing of the α-TM gene generates TPM1κ, in which the skeletal muscle exon 2b is replaced by the smooth muscle exon 2a. We previously reported that TPM1κ expression was increased in the hearts of patients with chronic dilated cardiomyopathy (DCM). To understand how the TPM1κ isoform affects cardiac dynamics, we generated transgenic (TG) mice expressing TPM1κ in the myocardium. Most of the native TM (90%) is replaced by TPM1κ. In situ cardiac dynamics were determined by echocardiographic analysis. Results demonstrated that the TG hearts exhibited a diastolic dysfunction associated with a dilation of the left ventricle compared with the non transgenic (NTG) controls. We also compared force-pCa relations in detergent extracted (skinned) fiber bundles isolated from NTG and TG-TPM1κ hearts at sarcomere lengths (SL) 1.9 μm and 2.3μm. Our data demonstrated a significant decrease in the Ca2+ sensitivity of the

myofilaments from TG hearts at both SL compared to NTG ones. There was an equal leftward shift of the force-pCa curves from both NTG and TG hearts when SL was increased to 2.3 μm. In addition, NEM-S1, a mimic of strongly bound, rigor cross-bridges, was not able to induce activation of TG myofilaments to the same extent as in the NTG controls. To determine whether isoform switching affects sarcomeric protein phosphorylation, we performed two-dimensional difference in gel electrophoresis (2D-DIGE) and Western blots using TM, TPM1κ, and Serine-283P specific antibodies. We observed an increase in the total phosphorylation of TPM1κ compared with that of α-TM. MLC2, TnI, and TnT phosphorylation was not significantly affected. Our results demonstrate that the increased cardiac expression of TPM1κ alters cardiac dynamics in a similar way to DCM-linked point mutations of TM.

1856-Pos

Distribution of Voltage Gated Sodium Channels in Rabbit Cardiomyocytes During Development

Cynthia Gershome[1,2], Eric Lin[1,2], Haruyo Kashihara[1,2], Glen F. Tibbits[1,2].
[1]Molecular Cardiac Physiology Group, Simon Fraser University, Burnaby, BC, Canada, [2]Cardiovascular Sciences, Child and Family Research Institute, Vancouver, BC, Canada.

We and others have postulated that in neonatal cardiomyocytes sodium currents may influence Ca^{2+} influx through reverse-mode NCX activity by inducing strong membrane depolarization and/or local sodium accumulation profoundly modify contractility. To study the role of voltage-gated sodium channels ($Na_V1.X$) and reverse mode NCX activity through development, the expression and distribution of $Na_V1.X$ was determined using Western blot analysis, immunocytochemistry, confocal microscopy and image analysis in cardiomyocytes isolated from 3 and 56 days old rabbits. Immunoblot analysis revealed a robust expression of the skeletal muscle isoform ($Na_v1.4$) in neonatal cardiomyocytes which decreased 6-fold by 56 days (p<0.01). The neuronal isotype $Na_v1.1$ was found to have comparatively low levels of expression throughout development and followed a similar pattern as that of Nav1.4. $Na_v1.1$ levels decreased by 9 fold in the 56 day cardiomyocyte (p<0.01). The cardiac isoform ($Na_v1.5$) expression was also robust in the neonatal and adult cardiomyocytes but the protein levels did not vary significantly throughout development by western blot analysis. The distribution of $Na_v1.4$ and $Na_v1.5$ was punctate in nature on the cell periphery in both 3 and 56 day cardiomyocytes. Both $Na_v1.4$ and $Na_v1.5$ co-localized with NCX in 3 and 56 day cardiomyocytes. In neonatal cardiomyocytes, $Na_v1.4$-NCX and $Na_v1.5$-NCX colocalization relationship remained the same, while in the adult, $Na_v1.5$-NCX colocalization decreased by 50% due to the increase in the separation distances between $Na_v1.5$ and NCX in the adult. Taken together, our results suggest that in the neonate heart, $Na_v1.4$ may dictate the role of NCX in regulating Ca^{2+} influx during contraction.

1857-Pos

Characterization of L-Type Ca Channel Currents ($I_{Ca,L}$) in Zebrafish Cardiomyocytes

Ping-Cheng Zhang[1], Xiao Ye Sheng[2], Leif Hove-Madsen[3], Glen F. Tibbits[1,2].
[1]Simon Fraser University, Burnaby, BC, Canada, [2]Child and Family Research Institute, Vancouver, BC, Canada, [3]Hospital de la Santa Creu i Sant Pau, Barcelona, Spain.

The zebrafish is an important model for the study of vertebrate cardiac development with a rich array of genetic mutations for functional interrogation. The similarity of the zebrafish cardiac action potential duration with that of humans further enhances the role of this model to study cardiac arrhythmias. Despite this, little is known about basic excitation-contraction coupling in the zebrafish heart. Single cardiomyocytes were isolated from the adult zebrafish heart by enzymatic perfusion of the cannulated ventricle. Using an amphotericin-perforated patch clamp in whole cell configuration, $I_{Ca,L}$ was characterized in the zebrafish cardiomyocytes at RT. Simultaneous recordings of the voltage dependence of $I_{Ca,L}$ amplitude and cell shortening showed a typical bell-shaped I-V relationship for $I_{Ca,L}$ with a maximum at 10 mV whereas cell shortening showed a monophasic increase with membrane depolarization, and reached a plateau at membrane potentials above 20 mV. $I_{Ca,L}$ was 53, 100, and 17% of maximum at −20, +10 and +40 mV while cell shortening was 62, 95, and 96% of maximum respectively, suggesting that $I_{Ca,L}$ is the major contributor to the activation of contraction at voltages below 10 mV whereas the contribution of reverse-mode NCX becomes increasingly more important at membrane potentials above 10 mV. The $T_{1/2}$ for the recovery of $I_{Ca,L}$ from inactivation was 96 ms and the $V_{1/2}$ for voltage-dependent inactivation was −27.6 mV. In conclusion, we demonstrate that: 1) healthy and viable myocytes can be obtained by enzymatic perfusion of the heart; 2) ventricular myocytes exhibited large $I_{Ca,L}$ density (>12 pA/pF) over a range of stimulation frequencies (0.5 to 3 Hz) and 3) a monophasically increasing contraction - voltage relationship which is in contrast to the bell-shaped relationship observed in human and other mammalian cardiomyocytes.

1858-Pos

Electrophysiological Determinants for Arrhythmogenesis Following Premature Stimulation In Murine Hearts

Rudolf M. Duehmke, **James D. Stefaniak**, Iman S. Gurung, Laila Guzadhur, Yanhui R. Zhang, Andrew A. Grace, Christopher L.H. Huang.
University of Cambridge, Cambridge, United Kingdom.

Background: Circus type re-entry is classically associated with reduced action potential (AP) conduction velocity through partially refractory tissue resulting in unidirectional conduction block. We assessed the extent to which premature extrasystolic APs under such conditions resulted in ventricular arrhythmogenesis in isolated Langendorff-perfused murine hearts.

Methods and Results: A novel programmed electrical stimulation (PES) protocol applied trains of 8 S1 stimuli at 100 ms intervals followed by extrasystolic S2 stimuli at successively decreasing S1S2 intervals. S2 stimulus strengths required to overcome refractoriness, reduce ventricular effective refractory period (VERP) and thereby elicit extrasystolic APs, increased with shortened S1S2 intervals, despite constant durations at 90% recovery (APD_{90}) of the preceding APs. Critical interval, CI, the difference APD_{90}-VERP, consequently increased with stimulus strength. The corresponding latencies and peak amplitudes of the extrasystolic APs consequently sharply increased and decreased respectively with CI thereby potentially replicating necessary conditions for re-entrant, circus-type, arrhythmia. The dependence of CI upon stimulus strength tended to consistent limiting values expected from approaches to absolute refractory periods. These values were greater in arrhythmogenic (mean CI 18.9 ± 0.55 ms, n=4) than in non-arrhythmogenic hearts (mean CI 15.1 ± 0.37, n=4; P=0.001, ANOVA), despite their statistically indistinguishable APD_{90} (arrhythmogenic hearts: 40.9 ± 2.23 ms, n=4 vs non-arrhythmogenic hearts: 36.5 ± 2.61ms, n=4; p>0.05, ANOVA) or VERP values (arrhythmogenic hearts: 22.5 ± 2.66 ms, n=4 vs non-arrhythmogenic hearts: 21.8 ± 2.53 ms, n=4; p>0.05, ANOVA).

Conclusions: These findings suggest existence of a specific CI (CI*) in turn corresponding to specific conditions of latency and action potential amplitude that would be sufficient to result in arrhythmogenesis.

1859-Pos

Effect of Sodium Homeostasis on Action Potential Duration Alternans in Cardiac Ventricular Cells

Leonid Livshitz, Yoram Rudy.
Washington University in St. Louis, St Louis, MO, USA.

Beat-to-beat alternation of action potential (AP) duration (alternans) is a precursor of fatal cardiac arrhythmias. The effect of the time course of intracellular Ca2+ transient on AP duration (APD) alternans was studied extensively, and the Na+/Ca2+ exchanger (INCX) was identified as a major coupling link between Ca2+ alternans and APD alternans. However, the role of Ca2+ -independent factors such as the Na+/K+ pump (INaK) in the coupling between the Ca2+ and AP subsystems has been overlooked.

We used computational models of AP and Ca2+ cycling in guinea-pig and canine myocytes to study effects of rate-dependent Na+ homeostasis on APD and the Ca2+ transient. We found that rate-dependent Na+ accumulation increases both the amplitude and frequency range of APD alternans in the guinea-pig, but decreases the amplitude of APD alternans in canine cells. The mechanism is as follows: in canine, Ca2+ and APD alternans are concordant (large Ca2+ is accompanied by long APD) and APD prolongation is due to inward INCX enhancement at a late phase of the AP. INaK enhancement by Na+ accumulation blunts the effect of INCX and decreases APD alternans amplitude. In the guinea pig, alternans are discordant (large Ca2+ transient with short APD) due to enhanced Ca2+ -dependent inactivation of L-type Ca2+ current and increased Ca2+-dependent slow delayed rectifier IKs at high Ca2+. Additional APD shortening by INaK increases the amplitude of the discordant alternans.

In conclusion, INaK enhancement due to Na+ accumulation decreases the amplitude of concordant APD-Ca2+ alternans and increases the amplitude of discordant APD-Ca2+ alternans. This mechanistic insight is relevant to arrhythmogenesis in heart failure where INCX is upregulated and INaK downregulated, amplifying APD alternans in larger mammals (canine) and possibly humans.

1860-Pos

Mechanisms of Abnormal Ca^{2+} Transients in Pathophysiological Ventricular Muscles Determined by Ca^{2+} and Membrane Potential Imaging

Nagomi Kurebayashi[1], Hiroto Nishizawa[1], Takeshi Suzuki[1], Takao Shioya[2], Yuji Nakazato[1].
[1]Juntendo University School of Medicine, Tokyo, Japan, [2]Saga University, Tokyo, Japan.

Abnormal Ca^{2+} signals, including delayed/desynchronized onset of Ca^{2+} transients, occasional missing Ca^{2+} transients and Ca^{2+} transient alternans, are often observed in cardiac muscles under pathophysiological conditions. To investigate how these abnormal Ca^{2+} responses can be generated, we monitored membrane potential and Ca^{2+} signals using a fluorescent membrane potential indicator and a Ca^{2+} indicator in the same preparation. Papillary muscles were dissected from guinea pig ventricles and loaded with di-4-ANEPPS and rhod-2 AM. Mono-wavelength Ca^{2+} signals and ratiometric action potential signals were sequentially obtained using the Nipkow-disc confocal microscope and W-view system. Control signals were obtained from cardiac muscles paced in a normal Krebs solution, whereas abnormal Ca^{2+} signals were induced by pacing them in a non-flowing Krebs solution. There were two types of causes for the failed and alternating Ca^{2+} transient generation, i.e., failed or alternating immature action potential generation and abnormal EC coupling with relatively constant action potentials. In cells showing delayed initiation of Ca^{2+} transients, action potential onset was also delayed and the rate of rise was slower than that in healthy cells. Effects of an inhibitor of gap junction channels and a Na^+ channel blocker suggest that the delayed onset of action potentials can be explained primarily by impaired gap junctions and partly by Na^+ channel inactivation.

1861-Pos

Competitive Regulation of Calcium and Zinc Ions in Cardiomyocyte Contraction-Relaxation Function

Ting Yi, Zengyi Chen, Rich Lachapelle, Bradley M. Palmer.
Unversity of Vermont, Burlington, VT, USA.

Zinc (Zn^{2+}) and calcium (Ca^{2+}) ions are divalent cations having common chemical properties leading to their competing for the same regulatory channels and pumps in the intact cardiomyocyte. Diastolic dysfunction may be due in part to elevated diastolic Ca^{2+} concentration ($[Ca^{2+}]$). We hypothesized that Zn^{2+} reduces systolic and enhances diastolic function due to its effects on Ca^{2+} regulation. We examined the effects of 32μM extracellular zinc ($[Zn^{2+}]_{ext}$) exposure and intracellular zinc ($[Zn^{2+}]_{int}$) accumulation on rat cardiomyocyte function. We measured sarcomere dynamics, $[Ca^{2+}]_{int}$ by Fura-2FF and $[Zn^{2+}]_{int}$ by FluoZin-3 under three $[Zn^{2+}]$ conditions: no $[Zn^{2+}]_{ext}$ and low $[Zn^{2+}]_{int}$; 32μM $[Zn^{2+}]_{ext}$ and low $[Zn^{2+}]_{int}$; 32μM $[Zn^{2+}]_{ext}$ and high $[Zn^{2+}]_{int}$. Cardiomyocytes were paced at 2Hz, exposed to 2mM $[Ca^{2+}]_{ext}$ at 37°C. After reaching $[Zn^{2+}]_{int}$ steady-state, 10mM caffeine was rapidly applied to measure sarcoplasmic reticulum (SR) Ca^{2+} content and Na^+-Ca^{2+} exchanger (NaCaX) efflux rate. Sarcomere shortening velocity and peak shortening were significantly ($P<0.05$) reduced with $[Zn^{2+}]_{ext}$ exposure in either low or high $[Zn^{2+}]_{int}$ conditions. Interestingly, peak shortening was significantly enhanced with high $[Zn^{2+}]_{int}$ compared to low $[Zn^{2+}]_{int}$. Diastolic sarcomere length was significantly increased with high $[Zn^{2+}]_{int}$. Peak $[Ca^{2+}]_{int}$ was significantly reduced under 32μM $[Zn^{2+}]_{ext}$ with high $[Zn^{2+}]_{int}$, which was consistent with lower SR Ca^{2+} content detected by caffeine experiment. SR Ca^{2+} uptake rate by SERCA and NaCaX efflux rate were not affected by $[Zn^{2+}]_{int}$. All the above changes due to Zn^{2+} were not observed in control cardiomyocytes without $[Zn^{2+}]_{ext}$ exposure. These findings suggest that Zn^{2+} competes with Ca^{2+} for calcium channels (L-type and SR release channels) and thereby reduces contractile function without affecting SERCA or NaCaX. Interestingly, high $[Zn^{2+}]_{int}$ causes a slightly increased contractile function despite the reduction in peak $[Ca^{2+}]_{int}$, suggesting that $[Zn^{2+}]_{int}$ enhances myofilament contraction by mechanisms yet to be explained.

1862-Pos

Cellular Mechanisms of Contractile Impairment in Human Chronic Atrial Fibrillation

Raffaele Coppini, Cecilia Ferrantini, Alessandra Rossi, Chiara Tesi, Alessandro Mugelli, Corrado Poggesi, Elisabetta Cerbai.
University of Florence, Florence, Italy.

Chronic Atrial Fibrillation (cAF) is associated with contractile impairment. Down regulation of L-Type Ca^{2+}current plays a major role in determining contractile dysfunction. However, additional EC-Coupling changes could be involved in human cAF. We dissected atrial trabeculae from left atrial appendages of cAF patients undergoing cardiac surgery and used them for simultaneous force and action potential recordings. Cells isolated from the same samples were used for Ca^{2+}current, Ca^{2+}transients, and reticular Ca^{2+}content(caffeine) measurements. Samples from sinus rhythm (SR) patients were used as controls. Despite 75%reduction in basal force, positive inotropic responses to isoproterenol, stimulation pauses, and high $[Ca^{2+}]_e$ were preserved in cAF. Basal Ca^{2+}current and Ca^{2+}transients were decreased (30%of SR) but showed a greater increase upon inotropic stimuli, reducing the difference with SR. No difference was found in time-course of mechanical restitution, suggesting no major impairment of Ryanodine Receptor function. The finding that sarcoplasmic reticulum Ca^{2+} content was not reduced in cAF suggests that Ca^{2+}release impairment could be due to a change from synchronous EC Coupling to *propagated* Ca^{2+}-induced Ca^{2+}-release (CICR), in which a fast subsarcolemmal Ca^{2+}rise is followed by Ca^{2+}diffusion-mediated signal propagation toward the cell core. The following observations in cAF preaparations supports this idea: 1)Ca^{2+}transients showed a fast monophasic rise(subsarcolemmal Ca^{2+}-release only) but exhibited a biphasic, dome-shaped aspect (peripheral rise followed by inward Ca^{2+}-wave spread) upon inotropic stimulations; 2)Ca^{2+}recirculation fraction decreased, suggesting an increased role of NCX*vs.*SERCA, consistent with a non-propagated peripheral Ca^{2+}rise; 3)twitch force transitorily increased after abrupt reduction of intracellular Ca^{2+} buffering by the SERCA blocker CPA. Reduction in T-tubules density and/or increased cytosolic Ca^{2+}buffering (e.g.increased myofilament Ca^{2+}sensitivity) could be crucial in cAF for transition to *propagated*-CICR and Ca^{2+}-wave spread impairment. Ca^{2+}trigger enhancement or Ca^{2+}diffusion improvement could promote recruitment of deeper myofibril layers and increase twitch force.

1863-Pos

Ionic Cellular Mechanisms for the Brugada Syndrome in Canine Myocytes

Paul Niklewski, Min Dong, Hong-Sheng Wang.
University of Cincinnati, Cincinnati, OH, USA.

Background: The Brugada syndrome is a right ventricular (RV) arrhythmia that is believed to be responsible for up to 20% of sudden cardiac deaths. The disease is related to mutations of cardiac Na, Ito, or Ca channel genes. In this study we used a combination of dynamic clamp and computational modeling to address two questions; the cellular mechanism of the electrical abnormality in Brugada syndrome and the potential basis of the RV wall contractile abnormality in the syndrome.

Results: Tetrodotoxin (TTX, 1 −3 μM) was used to reduce cardiac INa by ~50-75%, to mimic a Brugada syndrome-like setting in canine ventricular myocytes. Such INa reduction resulted in prolongation of action potential duration (APD) or all-or-none repolarization in RV epicardial myocytes, but not in RV endocardial or LV cells. These repolarization changes were associated with attenuation or blocking of myocyte contraction and peak Ca transient. Dynamic clamp and mathematical modeling were used to examine the interplay of INa and Ito and its influence on AP morphology. Both reduction of INa and increase of Ito have similar bi-phasic effects on APD. Reduction of INa shifts the APD-Ito density curve to the left. As a result, in the presence of a large Ito, INa reduction either prolongs APD or results in collapse of the AP, depending on the exact density of Ito.

Computational modeling showed that these repolarization changes alter myocyte Ca dynamics mainly by reducing Ca influx through the L-type conductance.

Conclusion: INa reduction alters repolarization by shifting the APD-Ito relationship and reducing the threshold for Ito-induced all-or-none repolarization. These cellular electrical changes suppress myocyte EC coupling and mechanics. As such, the contractile abnormality of the RV wall in Brugada syndrome may be secondary to the electrical abnormalities.

1864-Pos

Role of the Transient Outward Current In Regulating Mechanical Properties of Canine Ventricular Myocytes

Min Dong, Sujuan Yan, Paul Niklewski, Yamei Chen, **Hong-Sheng Wang**.
University of Cincinnati, Cincinnati, OH, USA.

Background: The transient outward current (Ito) is a major repolarizing current in the heart. Reduction of Ito density is consistently observed in human heart failure (HF) and animal HF models. It has been proposed that Ito, via its influence on phase 1 repolarization of the action potential, facilitates L-type $Ca2+$ current activation and sarcoplasmic reticulum $Ca2+$ release, and that its downregulation may contribute to the impaired contractility in failing heart.

Results: We used the dynamic clamp to examine the influence of Ito on the mechanical properties of canine left ventricular myocytes. In endocardial

myocytes, where the native Ito is small, simulation of an epicardial-level Ito accentuated the phase 1 repolarization and significantly suppressed cell shortening by 19%. The peak amplitude of Ca2+ transient was also reduced in the presence of simulated Ito, although the rate of rise of the Ca2+ transient was increased. Conversely, subtraction, or ''blockade'' of the native Ito using the dynamic clamp enhanced contractility in epicardial cells. These results agree with the inverse correlation between Ito levels and myocyte contractility and Ca2+ transient amplitude in epicardial and endocardial myocytes. Action potential clamp and computational modeling show that phase-1 notch depth vs peak L-type influx has an inverted-U shape; shallow phase-1 notch enhances Ica-L peak, while moderate to strong phase-1 repolarization reduces Ica-L influx.
Conclusion: Our results show that Ito acts as a negative, rather than positive regulator of myocyte mechanical properties in large animals.

1865-Pos
FRET Microscopy Reveals that Phospholamban Binds More Avidly to SERCA1a than SERCA2a
Zhanjia Hou, Zhihong Hu, **Seth L. Robia**.
Loyola University Chicago, Maywood, IL, USA.
SERCA1a and SERCA2a have been used interchangeably in mutagenic and structural analyses of the PLB-SERCA interaction, since in vitro studies have shown their functional inhibition by PLB is equivalent. To quantify the quaternary structure and binding energetics of PLB binding to SERCA isoforms, fluorescence resonance energy transfer (FRET) from Cer-SERCA1a or Cer-SERCA2a to YFP-PLB was measured in live AAV-293 cells. FRET efficiency increased with increasing protein expression level to a maximum of 28.8% for PLB-SERCA1a and 28.1% for PLB-SERCA2a, suggesting the complexes have the same quaternary conformation. Unexpectedly, the data also revealed that PLB has a 2.6 fold higher apparent affinity for SERCA1a relative to SERCA2a. To test whether the observed difference in affinity arises from differential distributions of SERCA E1/E2 enzymatic substates, cells were treated with 1mM EGTA and 0.5uL/mL calcium ionophore A23187. Under these conditions, PLB still showed greater affinity for SERCA1a over SERCA2a, suggesting that the differential affinities are intrinsic properties of the SERCA isoforms. The data suggest that PLB preferentially binds SERCA1a over SERCA2a, which may be an important strategic consideration for therapeutic overexpression of SERCA isoforms in cardiac muscle.

1866-Pos
Dislocations and Helicoids in Myofibrillar Z-Disks of Mammalian Ventricular Myocytes and Implications for Calcium Handling
Isuru D. Jayasinghe[1], Pan Li[2], Arun V. Holden[3], David J. Crossman[1], Mark B. Cannell[1], Christian Soeller[1].
[1]Department of Physiology, School of Medical Sciences, University of Auckland, Auckland, New Zealand, [2]Center for Biomedical Computing, Simula Research Laboratory, Martin Linges Vie 17, Fornebu, Norway, [3]Institute of Membrane and Systems Biology, Faculty of Biological Sciences, University of Leeds, Leeds LS2 9JT, United Kingdom.
The sarcomeric organization in rat ventricular myocytes has been examined using confocal microscopy to clarify the detailed 3D structure of myofibrillar z-disks. Dislocations across z-disks visualized by immuno-labeling of α-actinin were present in myocytes at slack (~1.8 μm) and long sarcomere lengths (~2.2 μm). The dislocations coincided with variations in myofibrillar direction and often myofibrils appeared to be twisted along the cell length. 3-D visualization and segmentation at high resolution revealed that z-disks in these regions often were in a helicoid arrangement that extended over ~15-20 sarcomeres. Similar z-disk topology was also observed in rabbit and human ventricular cells suggesting a common role in maintaining cell structure and sarcomere assembly. Dual color fluorescence imaging of α-actinin and ryanodine receptor (RyR) clusters demonstrated that their placement at z-lines also resulted in helicoid arrangements in regions of z-disk dislocations. As a result the effective axial spacing between RyR clusters was smaller than the sarcomere length. Rat, rabbit and human t-systems in areas of dislocations were studied by labeling with anti-caveolin-3 and wheat germ agglutinin. Most t-tubules closely followed the z-lines in these species, although a perfect helicoid architecture was not observed due to t-system elements that extended in axial or oblique directions.To investigate the consequences of the complex arrangement of z-lines a model of stochastic Ca^{2+} dynamics was constructed based on the distribution of Ca^{2+} release units (CRUs) that were experimentally determined from high resolution confocal RyR data. This demonstrated the importance of the non-planar CRU arrangement in sustaining Ca^{2+} waves that spread axially in conditions of simulated overload. We conclude that the complex organization of z-disks and CRUs must be captured in detailed mechanistic models.

1867-Pos
Caveolae Differentially Control Phosphorylation of Sarcoplasmic Reticular Proteins Following β_2 Adrenoceptor Stimulation in the Adult Cardiac Myocyte
David MacDougall, John Colyer, Sarah Calaghan.
University of Leeds, Leeds, United Kingdom.
Caveolae, small flask-like lipid rafts, play a key role in shaping the spatial characteristics of the β_2-adrenoceptor cAMP signal and confining this to the sarcolemmal compartment in the adult cardiac myocyte. Here we determine the consequences of disrupting caveolae for the ability of β_2 signalling to target sarcoplasmic reticular proteins phospholamban (PLB) and the ryanodine receptor (RyR). Experiments were performed with dissociated adult rat ventricular myocytes. Selective β_2 adrenoceptor stimulation was achieved with 10 μM zinterol in the presence of 300 nM CGP20712A (CGP). Disruption of caveolae (using the cholesterol depleting agent methyl-β-cyclodextrin, MBCD) resulted in inotropic and lusitropic responses to β_2 stimulation (70.2 ± 9.7% increase in shortening; 13.3 ± 1.3 % decrease in time to half relaxation) which were absent in control cells (n=12-20 myocytes, $P<0.001$). PLB contributes to inotropic and lusitropic responses via protein kinase A (PKA)-dependent phosphorylation at Ser^{16}. In agreement with functional data, MBCD-treated myocytes showed a marked 561 ± 144% increase in Ser^{16}-phosphorylated PLB in response to β_2 stimulation (relative to that in cells exposed to CGP alone) which was absent in control cells (93 ± 31% of that with CGP alone) (n=4, $P<0.05$). By contrast, we saw no significant increase ($P>0.05$) in phosphorylation of one of the PKA-targeted sites of RyR, Ser^{2809}, in either control (112 ± 11%) or MBCD-treated (116 ± 18%) myocytes in response to β_2 stimulation (n=5). These preliminary data suggest that caveolae selectively control cAMP signals even within the same broad (sarcoplasmic reticular) compartment of the adult cardiac myocyte. Disruption of caveolae allows β_2 cAMP-dependent signalling to access a sub-compartment of the sarcoplasmic reticulum which contains PLB, but not one which contains RyR.

1868-Pos
Solute Transport in the Transverse Tubules of Cardiac Ventricular Myocytes
Brian M. Hagen[1], Marcel A. Lauterbach[2], Eva Wagner[3], Stefan W. Hell[2], Stephan E. Lehnart[3], W. Jonathan Lederer[1].
[1]University of Maryland Biotechnology Institute, Baltimore, MD, USA,
[2]Max Planck Institute for Biophysical Chemistry, Goettingen, Germany,
[3]University Medical Center, Goettingen, Germany.
Electrical excitation in mammalian cardiac ventricular myocytes underlies the activation of cell-wide Ca^{2+} release and hence contraction. This process can occur rapidly in relatively large myocytes because transverse tubules (TTs) penetrate deep into the cells. The TT network also permits extracellular solute to be carried into the cell volume and thereby allows for improved inflow and egress of substrates. We have studied TT morphology in relaxed and contracted cells with the aim to characterize transport function and physical properties of the TT system.
Using living isolated rat ventricular myocytes, we examined the movement of substrate within the TTs under different conditions using sulforhodamine B and fluorescence imaging. In addition, we examined the TT network with respect to its size, shape and complexity using super-resolution STED (stimulated emission depletion) microscopy. The lipophilic indicator Di-8-ANEPPS was used to identify and characterize the TTs. A rapid bulk solution changer was used to measure the extracellular marker sulforhodamine B concentration changes within the T-tubule matrix at rest and during field stimulation. STED imaging of resting myocytes revealed tubules of about 250 nm in diameter (see related abstract: Wagner et al. 2010). We hypothesized that if TTs collapse and expand dynamically during contraction, solute within the TT network would exchange more rapidly during contractions than when the myocytes are quiescent. Testing this hypothesis by rapid solution change revealed that TT solute exchange was significantly faster during stimulated contraction in single heart cells. Consistent with this finding was the observation that inhibition of contraction by cytochalasin D treatment in paced myocytes reduced the rate of solute exchange. These results suggest that TT solute exchange is accelerated by the mechanical deformation of the TTs during contraction. Future work should enable us to test this hypothesis more directly.

1869-Pos

Effects of Dietary Lipids on Stress-Dependent Depolarization of Cardiac Mitochondrial Membrane

Aristide C. Chikando[1,2], Ramzi Khairallah[2], William Stanley[2], W. Jonathan Lederer[1,2].
[1]University of Maryland Biotechnology Institute, Baltimore, MD, USA, [2]University of Maryland School of Medicine, Baltimore, MD, USA.

Mitochondria play an important role in cardiac cellular physiology by generating ATP, contributing to the production and scavenging of reactive O_2 species (ROS) and by influencing intracellular Ca^{2+}. It has been hypothesized that dietary fatty acids (FA), specifically polyunsaturated FA, can affect mitochondrial function including those noted above. We have examined how FAs may influence mitochondrial membrane potential ($\Delta\Psi_{mito}$) measured with tetramethyl rhodamine methyl ester (TMRM) when the mitochondria are stressed by light at 543 nm. We examined the time-course of photon-stress on $\Delta\Psi_{mito}$ in single ventricular myocytes from rats on a lipid-restricted diet. The stress-illumination was limited to a square region of a single cell that covered about 20% of the cell cross-section. The illumination was repeated at 3 second intervals over the period of an hour. The repeated illumination led to gradual depolarization of mitochondria within the imaged region, the rate of which was distinct in each dietary group (see Fig. 1). The effects of photon-stress are altered by cyclosporin A and N-acetyl cysteine and these will be discussed. Measurement of the rate of oxygen consumption showed that depolarized mitochondria respired well but were uncoupled.

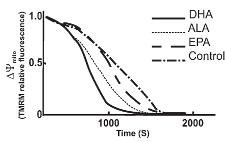

Fig. 1 - Time-course of mitochondrial depolarization in the region imaged. Each curve represents the mean of 4 time-courses examined in cells taken from the hearts of an animal (~4 animal per study group) fed a control diet (broken) or a diet enriched with DHA (solid), EPA (long dashes) and ALA (short dashes). Each curve is significantly different from the other curves (P<0.05).

Microtubules & Microtubule-associated Proteins

1870-Pos

Structural Changes of Microtubules During GTP Hydrolysis Revealed by X-Ray Fiber-Diffraction

Shinji Kamimura[1], Hiroyuki Iwamoto[2], Daisuke Miyashiro[3].
[1]Dept. Biol. Sci., Chuo Univ., Tokyo, Japan, [2]Research & Utilization Division, SPring-8, Sayo, Hyogo, Japan, [3]Dept. Life Sci., Univ. Tokyo, Komaba, Tokyo, Japan.

Microtubule (MT) is one of the most essential cytoskeletal elements in the eukaryote cells, which supports the mitosis, cell architecture and motility as well as the intracellular transportation. Tubulin dimers in a GTP-binding state (GTP-tubulin) are assembled onto MT-ends and make them stable. However, the following slow hydrolysis of GTP to GDP occurring in β-tubulin is assumed to weaken the lateral interactions among protofilaments and MTs in an uncapped state (MT-ends without GTP-tubulin) disassemble and shrink quickly. Such features of dynamic instability would be closely related to various MT functions. In the present study, we tested how the GTP-hydrolysis was related to the structural changes of MTs by X-ray fiber diffraction analysis (BL45XU, SPring-8, λ=0.09 nm). By comparing diffraction peaks between GMPCPP- and GTP-taxol-MT, we found that 8 nm meridional reflection intensity (arrow in the figure) appeared only in GTP-taxol-MTs, which are assumed to consist mostly of GDP-tubulin. It would reflect some structural differences between GDP- and GTP-tubulin in situ. The change of tubulin-pitch by GTP-hydrolysis was also found. This is the first demonstration to show structural changes of MTs under physiological conditions.

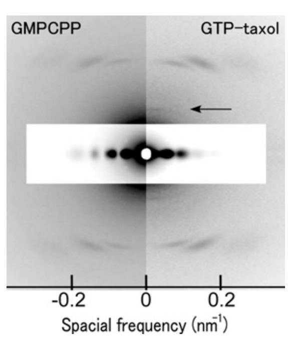

1871-Pos

Protein Friction Limits Diffusive and Directed Movements of Kinesin Motors on Microtubules

Volker Bormuth[1], Vladimir Varga[1], Jonathon Howard[1], Erik Schäffer[2].
[1]Max Planck Institute of Molecular Cell Biology and Genetics, Dresden, Germany, [2]TU-Dresden, Biotec, Dresden, Germany.

Friction limits the operation of macroscopic engines and is critical to the performance of micromechanical devices. We report measurements of friction in a biological nanomachine. Using optical tweezers, we characterized the frictional drag force of individual kinesin-8 motor proteins interacting with their microtubule tracks. At low speeds and with no energy source, the frictional drag was related to the diffusion coefficient by the Einstein relation. At higher speeds, the frictional drag force increased nonlinearly, consistent with the motor jumping 8 nanometers between adjacent tubulin dimers along the microtubule, and was asymmetric, reflecting the structural polarity of the microtubule. We argue that these frictional forces arise from breaking bonds between the motor domains and the microtubule, and they limit the speed and efficiency of kinesin.

1872-Pos

Structural Basis for Microtubule Binding by the Anti-Parallel Microtubule Crosslinker PRC1 (Protein Regulator of Cytokinesis-1)

Radhika Subramanian[1], Elizabeth M. Wilson-Kubalek[2], Elizabeth A. Campbell[1], Matthew J. Bick[1], Seth A. Drast[1], Ronald A. Milligan[2], Tarun M. Kapoor[1].
[1]Rockefeller University, New York, NY, USA, [2]The Scripps Research Institute, La Jolla, CA, USA.

Successful cytokinesis is essential for maintaining genome stability. The central spindle, an array of antiparallel microtubules formed prior to cytokinesis, is required for complete furrow ingression to form two daughter cells. Members of the conserved MAP65 family (Ase1, AtMAP-65, PRC1) play a key role in organizing microtubules in the central spindle. Invitro studies indicate that members of this protein family can crosslink microtubules with an anti-parallel orientation bias. We have combined structural methods and single molecule fluorescence to understand the structural basis for biased crosslinking by the human MAP65 protein PRC1.

We describe the crystal structure of the conserved domain of PRC1. This domain is capable of binding microtubules (Kd ~ 6 uM), but shows no sequence similarity to other known microtubule binding proteins. This domain has a spectrin fold, a motif ubiquitous in proteins interacting with the actin cytoskeleton, but not seen previously in microtubule binding proteins. Cryo-EM and helical image analysis yielded a 3D map of PRC1 bound to microtubules. Docking the crystal structure into the EM map gives us a structural view of PRC1-microtubule interactions.

PRC1 also has a proteolytically sensitive Lys/Arg rich domain that is thought to regulate microtubule binding. Single-molecule assays reveal that the presence of this domain allows the protein to undergo long diffusional sliding on microtubules. Constructs in which this domain is truncated show reduced interaction-lifetime and crosslinking efficiency.

These results suggests that the two domains act together to achieve biased anti-parallel crosslinking. We propose a model where oriented binding and polarity bias is achieved by the spectrin domain and the positively charged flexible domain enhances the probability of biased crosslinking by increasing the dwell time of PRC1 on microtubules via a diffusive binding mechanism.

1873-Pos

Trapping and Polymerization of Tubulin Within Phospholipid Vesicles

Joseph B. Pesavento, Hector H. Huang, Nitash P. Balsara, Kenneth H. Downing.
Lawrence Berkeley National Laboratory, Berkeley, CA, USA.

Microtubules are cylindrical aggregates (diameter ~25 nm) of the protein tubulin. They play important roles in cellular structure, protein trafficking, cell motility, intracellular transport, meiosis, and mitosis. They can switch stochastically between periods of tubulin polymerization and dissolution, termed dynamic instability, and can individually apply an extensive force at a significant distance on the cellular scale (Howard and Hyman 2003). Previous light microscopy has been used to characterize the forces that produce membrane distortions when microtubules assemble inside lipid vesicles (Fygenson et al. 1997; Emsellem et al. 1998).

We have examined this phenomenon by cryo-EM to gain insights on membrane deformation and to visualize the detailed structure of the microtubule ends as they are constrained near the inner membrane surface. Vesicles need to be of sufficient size, typically 1 μm diameter, to contain sufficient tubulin to form a microtubule long enough to span the vesicle. This has presented a challenge given limitations on the thickness of EM samples.

To date, we have visualized microtubule polymers in even small vesicles that often produce significant distortion, along with microtubules that form outside the vesicles. Quite unexpectedly, it appears that in certain cases the vesicles are deformed by the microtubule, sometimes with long protrusions, while in other cases in vesicles of similar size, the microtubules are deformed by the vesicles, with a number of sharp bends. This presents an opportunity to gain insights on the factors involved in both lipid bilayer and microtubule strength and flexibility. Ultimately we will image these samples using electron tomography to describe all of the effects in three dimensions. Determination of the nature of the dynamic instability and microtubule growth and vesicle tensile strength resulting from microtubule elongation will provide insight into the nature of cellular architecture, plasticity, and deformation.

1874-Pos

Highly Variable Microtubule Assembly Dynamics Reflect Near-Kilohertz Kinetics: Evidence Against Traditional Linear Growth Theory

Melissa K. Gardner[1], **Blake D. Charlebois[2]**, Imre M. Jánosi[3], Alan J. Hunt[2], David J. Odde[4].

[1]Max Planck Institute of Molecular Cell Biology and Genetics, Dresden, Germany, [2]University of Michigan, Ann Arbor, MI, USA, [3]Eötvös University, Budapest, Hungary, [4]University of Minnesota, Minneapolis, MN, USA.

Microtubules are intracellular polymers that dynamically grow and shorten at their ends via the stochastic addition and loss of alpha-beta-tubulin heterodimers. The kinetics of tubulin assembly are central to the regulation of microtubule dynamics by microtubule-associated proteins and therapeutic drugs. Previously, rates of tubulin subunit exchange at the ends of growing microtubules have been estimated using a linear growth theory that assumes tubulin dissociation occurs at a constant rate regardless of the free tubulin concentration. However, by measuring the variance of microtubule assembly at the nanometer scale, we find that stochastic tubulin dynamics are an order of magnitude faster than previously estimated. This discrepancy is explained by molecular-level simulations showing that the tubulin dissociation rate during microtubule growth is not constant, but rather should increase with increasing tubulin concentration. This indirect effect is due to a concentration-dependent bias in simulated microtubule tip structure, as has been experimentally observed. Our analyses indicate that the published tubulin subunit addition and loss rates at growing microtubule ends *in vitro* have been consistently underestimated in the literature: the variance in the assembly rate *in vitro* is too high to be consistent with the previous low kinetic rate estimates, and we conclude that both tubulin addition and tubulin loss events occur on the millisecond time scale, far faster than the previously believed 10-1000 millisecond scale. More generally, we demonstrate that the fixed off rate originally used in the linear growth theory of Oosawa and assumed in most subsequent models, fails to describe the behavior of self-assembled polymers having both lateral and longitudinal bonding interactions between subunits.

1875-Pos

Filament Localization with Nanometer Accuracy

Felix Ruhnow[1], David Zwicker[2], Stefan Diez[1].

[1]Max Planck Institute of Molecular Cell Biology and Genetics, Dresden, Germany, [2]Max Planck Institute for the Physics of Complex Systems, Dresden, Germany.

Recent developments in optical microscopy and nanometer tracking of single fluorescent molecules (or alternative subresolution particles) have greatly enhanced our understanding of biomolecular processes in vivo and in vitro. In particular, fitting the intensity profiles of nanometer-sized objects to 2D-Gaussian models allows their two-dimensional localization with an accuracy in the one-nanometer range, primarily only limited by the number of photons collected. Here, we present a novel algorithm which adapts 2D-Gaussian models to precisely determine the contour, as well as the end points, of curved filaments whose structures are characterized by subresolution diameters and micrometer lengths. Utilizing surface-immobilized microtubules (diameter of 25 nm, densely labeled with fluorophores) we demonstrate positional accuracies of ~2 nm and ~15 nm when localizing the center line and the end points of the filament, respectively. We report on the application of the algorithm to determine (i) the dynamics of microtubule polymerization/depolymerization and (ii) the speed of microtubules gliding over motor-coated surfaces. Combined with methods to measure nanometer heights above substrate surfaces (such as fluorescence interference contrast or parallax), our algorithm - which is also readily applicable to fluorescently labeled actin or DNA/RNA filaments - presents a promising tool for optical 3D-nanometry.

1876-Pos

The Effect of Human Microtubule-Associated-Protein Tau and Ionic Strength on the Assembly Structure of Microtubules: Synchrotron X-Ray Scattering and Binding Assay Study

M.C. Choi[1], U. Raviv[1], H.P. Miller[1], M.R. Gaylord[1], E. Kiris[1], D. Ventimiglia[1], D.J. Needleman[1], P.J. Chung[1], J. Deek[1], N. LaPointe[1], M.W. Kim[2], L. Wilson[1], S.C. Feinstein[1], C.R. Safinya[1].

[1]UCSB, Santa Barbara, CA, USA, [2]KAIST, Daejon, Republic of Korea.

Microtubules (MTs), a major component of the eukaryotic cytoskeleton, are 25 nm protein nanotubes with walls comprised of assembled protofilaments built from $\alpha\beta$ heterodimeric tubulin. In neural cells, different isoforms of the microtubule-associated-protein (MAP) tau regulate tubulin assembly and MT stability. Using synchrotron small angle x-ray scattering (SAXS) and binding assay, we examine the effects of human MAP tau on the assembly structure of taxol-stabilized MTs. We find that tau regulates the distribution of protofilament numbers in MTs as reflected in the observed increase in the average radius of MTs with increasing the tau/tubulin molar ratio. Further, we describe that tau-MT interactions are mediated to a large extent via electrostatic interactions: the binding affinity of tau to MTs is ionic strength dependent. Supported by DOE DE-FG02-06ER46314, NSF DMR-0803103, NIH NS35010, NIH NS13560. (Ref) M.C. Choi, S.C. Feinstein, and C.R. Safinya et al. *Biophys. J.* 97; 519 (2009).

1877-Pos

A Fluorescent GTP Analogue as a Single Molecule Fluorescence Label of Microtubules

Erik K. Anderson, Douglas S. Martin.

Lawrence University, Appleton, WI, USA.

Microtubules are cytoskeletal polymers which play a role in cell division, cell mechanics, and intracellular transport. Dynamic studies of microtubule function make use of fluorescent labels via antibodies, paclitaxel, and direct attachment to the tubulin protein. However, these labels suffer from drawbacks such as transient labeling, occlusion of functional sites on the microtubule surface, or structural non-specificity. Here we report a new, complementary fluorescent labeling technique that avoids these drawbacks. A fluorescently modified GTP analogue is used to polymerize microtubules from tubulin dimers. This GTP analogue binds selectively to the exchangeable GTP-binding site (E-site) on the tubulin dimer, which is available only during polymerization. The E-site affinity of this GTP analogue is about 100 fold weaker than that of GTP. Because this labeling technique places a bright fluorophore at a defined location within the microtubule lattice, it may facilitate observations of microtubule dynamics with increased precision.

1878-Pos

Kinesin-Calmodulin Fusion Protein as a Molecular Shuttle and Marker for Plus End of Microtubule

Takeshi Itaba[1], Hideki Shishido[1], Kiyoshi Nakazato[1], Eisaku Katayama[2], Shigeru Chaen[3], Shinsaku Maruta[1].

[1]Soka university, Hachioji, Japan, [2]The University of Tokyo, Minato-ku, Japan, [3]Nihon University, Setagaya-ku, Japan.

In the present study, we have demonstrated that the novel molecular shuttle with reversible cargo-loading system by using calmodulin (CaM) and M13 peptide. We designed a kinesin (K560) chimera protein with CaM fused at the C-terminal tail region of K560 (K560-CaM). K560-CaM was expressed using an Escherichia coli expression system and purified. We successfully observed that K560-CaM transported quantum dot-conjugated M13 peptide along the microtubule in the presence of Ca2+ by the total internal reflection fluorescence microscopy. Reversible Ca2+dependent cargo-loading system was achieved by changing the Ca2+ concentration in the flow cell. K560-CaM was adsorbed onto the fluorescently unlabeled microtubule adhered on the glass surface in flow cell using non-hydrolyzable ATP analogue, AMP-PNP which stabilize the microtubule binding state of kinesin. Subsequently, Qdot-M13 was added in the presence of Ca2+ to be loaded on K560-CaM adsorbed on the microtubule. The fluorescence of Qdot-M13 loaded onto K560-CaM along a microtubule was observed after washing excess unbound Qdot-M13. When the Ca2+ solution in the flow cell was replaced by the Ca2+ free solution, Qdot-M13 was unloaded. Even after the several times alternate exchange of the solution in the flow cell with Ca2+ and EGTA solutions, the K560-CaM adsorbed onto microtubule by AMP-PNP showed stable Ca2+ dependent cargo loading. When excess ATP was added into the flow cell, K560-CaM-Qdot started to move along the microtubule. Interestingly, 145 seconds later, K560-CaM-Qdot accumulated at plus end of microtubule and showed fluorescent clumps as marker for plus end of microtubule.

1879-Pos

High Resolution Structural Characterization of the Human Spastin Protein and its Complex With Tubulin

Jennifer L. Taylor, F. Jon Kull.

Dartmouth College, Hanover, NH, USA.

Hereditary spastic paraplegia (HSP) is a motor neuron disease caused by a progressive degeneration of the motor axons of the corticospinal tract. A number of different proteins have been implicated in the pathology of HSP, including mitochondrial proteins, a kinesin motor, spartin and spastin. Of the autosomal dominant cases of HSP, approximately 40% are caused by point mutations or exon deletions in spastin. Because of spastin's significant role in the development of HSP, there have been an increasing number of studies on this protein and its role in axonal degeneration. Recent studies have shown that spastin has a microtubule severing activity, and that this activity is linked to the manifestation of neurological disorders in Drosophila. Until recently very little structural information has been available for the spastin protein, and the mechanism by which it severs microtubules remains elusive. The goal of this study is to

determine the high resolution crystal structure of the human spastin protein both alone and in complex with a domain of tubulin. To this end, we have expressed and purified a construct of human spastin and a C-terminal tubulin construct, to which spastin binds. We have also crystallized spastin and collected a 3.3 angstrom data set and are now attempting to crystallize the spastin-tubulin complex. Visualization of such a complex will provide details as to how spastin binds to and severs microtubules, and will also help to explain how point mutations in the spastin gene lead to altered protein activity and a disease phenotype.

1880-Pos

Characterization of Tau Interactions with Lipid Vesicles

Jocelyn M. Traina, Shana Elbaum, Elizabeth Rhoades.
Yale University, New Haven, CT, USA.

A number of neurodegenerative diseases, including Alzheimer's disease, are associated with the deposition of aggregated tau protein in the form of neurofibrillary tangles (NFTs). Although a causal relationship between NFTs and disease has not been conclusively resolved, it is hypothesized that either the aggregates themselves or the process of aggregation is pathological. Tau is an intrinsically unstructured protein expressed in neurons, primarily functioning to stabilize and catalyze microtubule assembly. Studies indicate that tau binding of lipid vesicles may serve as a mimic of microtubule binding. We measured the affinity of the various constructs of tau encompassing the microtubule binding region to synthetic lipid vesicles using fluorescence correlation spectroscopy (FCS). Importantly, we observe that the binding behavior is dramatically affected by solution pH. At pH 7.4, the protein binds stably and we are able to extract a partition coefficient for both wild-type and the disease-associated point mutant, P301L. However, at low pH, binding to lipid bilayers triggers rapid aggregation of the tau fragments, which we were able to confirm as amyloid using Thioflavin T binding and electron microscopy.

1881-Pos

Tubulin is an Amphiphilic Protein Whose Interaction With Membranes is Regulated by its Charged Carboxy-Terminal Tails

Dan L. Sackett.
NICHD / NIH, Bethesda, MD, USA.

Tubulin is an acidic heterodimeric protein whose negative charges are significantly (~40% of total negative charge) located on the 10-15 residue long, glutamic acid-rich, unstructured, carboxy-terminal tails (CTT) found on both α- and β-subunits (though not on the monomeric γ-tubulin). Unsurprisingly, tubulin is a quite water-soluble protein. However, it has been consistently reported to be a component of highly purified membranes, including plasma membranes, intracellular membranes such as Golgi and mitochondrial outer membranes, and vesicle membranes as in clathrin-coated endocytic vesicles. In these preparations, tubulin is non-microtubular and is tightly associated with the membrane, often requiring detergent for solubilization. Tubulin has also been shown to associate tightly with liposomes make of purified lipid only, including neutral lipid. The exact mechanism of tubulin-membrane association has not been defined, nor has it been shown that there is only one mechanism. Tubulin could dock with lipid-embedded proteins, for example. We have shown that tubulin binds to VDAC in the mitochondrial outer membrane, with functional consequences for mitochondrial function, and this binding requires and is mediated by the CTT. Thus the CTT can enhance membrane binding of tubulin. This cannot be the mechanism for liposome interaction, since there is no protein present other than tubulin. We show by charge-shift electrophoresis and non-ionic detergent extraction that (a) tubulin behaves as an amphiphilic protein, and (b) the CTT can regulate interaction with amphipathic molecules.

Cell & Bacterial Mechanics & Motility II

1882-Pos

Mechanics of the Cell Nucleus as a Function of Lamin Expression in Granulocyte Differentiation

Amy C. Rowat[1], Diana E. Jaalouk[2], David A. Weitz[1], Jan Lammerding[2].
[1]Harvard University, Cambridge, MA, USA, [2]Brigham Women's Hospital/Harvard Medical School, Cambridge, MA, USA.

The ability of cells to deform through narrow spaces is critical for processes ranging from immune function to metastasis. Neutrophils are the most abundant white blood cell, which are required to transit through spaces less than 1/5 of the cell's diameter. As the nucleus is typically the stiffest organelle in the cell, the lobulated shape of the neutrophil nucleus is thought to facilitate its transit. However, neither the mechanical properties of the nuclei, nor the mechanism underlying the transition from ovoid to lobulated nuclear shape, are fully understood. We used HL60 cells as a differentiable model system to study nuclear shape transitions and the effects on cell mechanics. To elucidate the effects of the nuclear envelope protein, lamin A, we genetically modified the cells to generate subpopulations of cells with well-defined lamin A levels. Quantitative image analysis revealed that increased lamin A expression inhibits the nuclear shape transition to the typical lobulated morphology. To determine the effect on whole-cell mechanics, we measured cell deformability by flowing cells through channels of a microfluidic device, monitoring transit time and nuclear deformation. In addition, we performed functional assays to test if the impaired transition in nuclear morphology is also associated with defects in phagocytotic function, and thus reflect overall impairment of differentiation due to increased lamin levels. These results help to elucidate the molecular mechanism of granulocyte differentiation, and may have possible implications for understanding reduced immune function in aging, where lamin A has been reported to accumulate at the nuclear envelope.

1883-Pos

Model for Microtubule-Actin Interactions in Growth Cone Motility

Erin M. Craig[1], Andrew W. Schaefer[2], Paul Forscher[2], Alex Mogilner[1].
[1]University of California, Davis, Davis, CA, USA, [2]Yale University, New Haven, CT, USA.

A growth cone is a motile structure on the tips of axons that guides axon extension to synaptic targets during nervous system development. In order to translate chemotactic signals into a mechanical response, the microtubule and actin filaments in the growth cone self-organize into a motile lamellipodial structure. A meshwork of actin filaments in the lamellipodium are continually transported inward by myosin-driven forces, at a speed that matches actin polymerization at the leading edge. This creates a stationary actin treadmill when actin adhesion to the substrate is low, and allows leading edge protrusion when actin adhesion increases in response to guidance cues. A population of highly dynamic microtubules that explore the P domain in stochastic bursts of growth and shrinking have also been shown to play an essential role in growth cone steering. Cooperation between these two filament systems is known to be essential for directed motility. We present initial results from a theoretical model of the growth cone cytoskeleton in the lamellipodium, testing the hypothesis that dynamic microtubules and actin work cooperatively to guide growth cone motility. We simulate dynamically unstable microtubules that transiently attach to actin retrograde flow, actin-myosin-adhesion force balance, and test several scenarios for feedback between microtubules and actin. Our theoretical work is guided by direct visualization of actin and microtubule dynamics during growth cone advance with fluorescent speckle microscopy.

1884-Pos

Examining Mechanical Properties of Vertebrate Meiotic Spindles

Yuta Shimamoto[1], Yusuke Maeda[1], Shin'ichi Ishiwata[2], Albert J. Libchaber[1], Tarun M. Kapoor[1].
[1]The Rockefeller University, New York, NY, USA, [2]Waseda University, Tokyo, Japan.

Accurate chromosome segregation during cell division relies on the self-organization of a dynamic multi-component apparatus, the microtubule-based bipolar spindle. Through genetic, biochemical, and cell biological approaches, the complete 'parts list' of the components, including microtubule-based motor proteins, which are responsible for the assembly and maintenance of the meiotic spindle are now available. However, how spindle self-organization is controlled through integration of forces generated by multiple biomolecular processes remains mysterious. Here we report a calibrated microneedle-based system that allows application of sub-nanoNewton forces at specific sites within the metaphase spindle assembled in Xenopus egg extracts. Our set-up allows direct force measurements and can be combined with multi-mode high resolution microscopy along with chemical perturbations of specific spindle components. Using this system we applied sinusoidal strain to the metaphase spindle, keeping the range $<5\%$ to minimize nonlinearities of the response. The stress response was measured over the frequency ranged between 0.01 Hz and 2 Hz. Based on the resultant stress-strain relationship we determined the frequency-dependent mechanical properties of the spindle. The spindle response showed a typical characteristic time-scale of ~50 s, at which the mechanical property changed from solid-like to liquid-like. Additional experiments examining stress relaxation, which may reflect the dynamics of structural reorganization, revealed a similar time-scale. This transition disappeared when the spindles were treated with AMPPNP, a slow-hydrolyzing ATP analog, suggesting that the characteristic time-scale is determined by an ATP-dependent processes within the spindle. The contribution of key mitotic motors such as dynein and kinesin is being examined by pharmacological or immunological perturbations. Together, these analyses will allow us discuss models for how forces in the self-organizing meiotic spindle are integrated.

1885-Pos
A Mechanomolecular Model for Chromosome Movement During Mitosis
Blerta Shtylla, James P. Keener.
University of Utah, Salt Lake City, UT, USA.
During mitosis chromosomes attach to dynamic microtubules in order to move to the cell equator. Kinetochores facilitate chromosome movement by maintaining a floating grip on inserted polymerizing or depolymerizing microtubules. In many vertebrates, chromosomes experience striking oscillatory movement both close to a pole and around the equator. Several chemical species that affect microtubule dynamics as well as proteins that bind to the microtubule lattice have been localized at kinetochores. Yet, there is no clear understanding of the force producing mechanism at microtubule attachment sites, and of how movement is controlled and coordinated at kinetochores so that a chromosome pinpoints the cell equator. Here we develop a mathematical model of chromosome motility that addresses the above two questions. First, we consider force production at kinetochores by developing a molecular motor model that describes molecular scale interactions between several kinetochore binders and an inserted microtubule. We find that for weak binding and low activation energies, the motor produces velocities that are fairly insensitive to loads and depend on the inserted polymer growth/shortening rates, in agreement with chromosome movement data. Then, we incorporate the molecular motor into a chromosome movement model in which motility results due to feedback between mechanical loads that arise from spindle-chromosome interactions and kinetochore chemical reactions that involve a force sensing kinase and a microtubule depolymerase.
Numerical simulations show that kinetochore chemical control of movement is a robust mechanism for chromosome oscillations and centering at the equator. Further, we observe that proper transition between mitotic stages is strongly influenced by kinetochore reactions, which indicates that motility does not solely result from ‘‘tug of war’’ between opposing forces. We find that our proposed mechanism is sufficient to recreate chromosome movement from prometaphase to anaphase, in good agreement with experimental data.

1886-Pos
Probing the Force-Balancing Mechanism of the Meiotic Spindle in Xenopus Egg Extracts
Jun Takagi[1], Takeshi Itabashi[1], Yuta Shimamoto[2], Tarun M. Kapoor[2], Shin'ichi Ishiwata[1].
[1]Waseda University, Tokyo, Japan, [2]The Rockefeller University, New York, NY, USA.
During cell division, the meiotic spindle equally segregates replicated genomes into two daughter cells. Errors in this process cause birth defect and cancer.
Spindles are mainly composed of microtubules (MTs) and molecular motors. Various studies have revealed key regulators, such as Kinesin-5 (plus-end directed kinesin tetramer), depolymerizing kinesins and microtubule-associated proteins (MAPs). These exert forces for sliding MTs or regulating MT dynamics in the spindle, so that the spindle maintains a rugby ball-like structure at metaphase. These forces are also known to generate a poleward flux of spindle MTs. At metaphase, size and shape of the spindle are maintained constant in spite of the dynamic nature of spindle MTs. This indicates forces exerted by molecular motors and MTs are well balanced in the spindle.
In this study, we developed micromanipulation techniques for changing spindle shape to disrupt steady state force balance of the spindle without any changes in molecular components of the spindle. Spindles spontaneously assembled in Xenopus egg extracts were stretched along their pole-to-pole axis using two glass micro-needles. When the spindles were briefly stretched, they recovered their original size and shape after a while. In contrast, when spindles were kept stretched, they gradually recovered their original shape with the increase in the spindle width, resulting in the enlargement in size. This result indicates that the meiotic spindle has an ability to adjust its size and shape to the externally applied force. Our findings provide new insights into the force-balancing mechanism of the spindle.

1887-Pos
A Mechanical Model of Actin Stress Fiber Formation and Substrate Elasticity Sensing in Adherent Cells
Sam Walcott, Sean X. Sun.
Johns Hopkins University, Baltimore, MD, USA.
Tissue cells sense and respond to the stiffness of the surface on which they adhere. Precisely how cells sense surface stiffness remains an open question, though various biochemical pathways are critical for a proper stiffness response. Here, based on a simple mechanochemical model of biological friction, we propose a mechanical model for cell mechanosensation as opposed to previous more biochemically-based models. Our model of adhesion complexes predicts that these cell-surface interactions provide a viscous drag that increases with the elastic modulus of the surface. Using the force-velocity relation of myosin II, we show that myosin generates greater force the slower the adhesion complexes slide. Then, using a simple cytoskeleton model, we show that an external force applied to the cytoskeleton causes actin filaments to aggregate and orient parallel to the direction of force application. The greater the external force, the faster this aggregation occurs. As the steady-state probability of forming these bundles reflects a balance between the time scale of bundle formation and destruction (due to actin turnover), more bundles are formed when the cytoskeleton time-scale is small (i.e. on stiff surfaces), in agreement with experiment. As these bundles seem related to stress fibers, large bundles of actin that appear preferentially on stiff surfaces, our mechanical model provides a mechanism for stress fiber formation and stiffness sensing in cells adhered to a compliant surface.

1888-Pos
Dynamic Adaption of Actin Stress Fibers in Response to Stretch
Roland Kaunas.
Texas A&M University, College Station, TX, USA.
Actin stress fibers are mechanosensitive structural elements that respond to stretching to regulate cell morphology, stress fiber alignment, signal transduction and cell function. Adherent cells maintain a level of prestress largely dependent on myosin contractility, suggesting that stress fibers self-adjust to an equilibrium level of stress. Here a quantitative model is developed to describe a potential mechanism for fibers to re-establish stress equilibrum in response to changes in fiber length. The model involves dynamic changes in fiber reference length regulated by myosin-actin cross bridging, where the force-velocity relationship for individual sarcomeres is expressed as a hyperbolic Hill-type model. Under static conditions, the basal level of fiber tension and pre-extension are determined by the number of sarcomeres bundled together in the fiber and the stall force of the constituent myosin filaments. Following a step increase in fiber length, tension initially increases elastically, but then relaxes with a characteristic time constant dependent on the rate of myosin cross bridge dynamics. Returning the fiber to the original length results in a drop in tension below equilibrium, followed by a relatively rapid return to equilibrium.The model predicts that stress fibers respond to cyclic stretch in a manner dependent on frequency, ATP concentration, equilibrium sarcomere length, and sarcomere stiffness with relaxation times ranging from 0.02 to 0.8 sec based on model parameter values extracted from the literature. The modeling results are consistent with various experimental findings and provide molecular insight into how stress fibers determine and maintain mechanical equilibrium in response to changes in length.

1889-Pos
Spatially Dissecting the Viscoelastic Recoil and Cell Shape Contributions of Actomyosin Stress Fiber Bundles
Kandice Tanner[1], Mina J. Bissell[2], Sanjay Kumar[1].
[1]University of California, Berkeley, Berkeley, CA, USA, [2]Lawrence Berkeley National Laboratory, Berkeley, CA, USA.
The ability of a living cell to distribute contractile stresses against the extracellular matrix (ECM) in a spatially heterogeneous fashion underlies many fundamental behaviors, including motility, polarity, and assembly into multicellular tissues. Here we investigate the biophysical basis of this phenomenon at unprecedented spatial and mechanical resolution by using femtosecond laser ablation to sever contractile stress fibers located in specific cellular compartments and measure regional variations in fiber viscoelastic retraction and contribution to cell shape stability. Upon photodisruption, myosin light chain kinase-dependent stress fibers located along the cell periphery recoil much more slowly than rho-associated kinase-dependent stress fibers located in the cell center, with severing of peripheral fibers uniquely triggering a dramatic contraction of the entire cell. Remarkably, selective pharmacological dissipation of peripheral fibers significantly accelerates the retraction of central fibers, suggesting transference of tensile loads from one population of stress fibers to another in order to stabilize cell shape. These results suggest that stress fibers regulated by different myosin activators exhibit different mechanical properties and cell shape contributions. These data also illustrate the potential of femtosecond laser ablation to spatially map the microscale contractile mechanics of living cells.

1890-Pos

The Non-Equilibrium Thermodynamics and Kinetics of Focal Adhesion Dynamics

Krishnakumar Garikipati, Joseph E. Olberding, Michael Thouless, Ellen M. Arruda.
University of Michigan, Ann Arbor, MI, USA.

We consider a focal adhesion to be made up of molecular complexes, each consisting of a ligand such as fibronectin, an integrin molecule, and associated plaque proteins. Free energy changes drive the binding and unbinding of these complexes and thereby control the focal adhesion's dynamic modes of growth, treadmilling and resorption. The free energy changes include mechanical and chemical contributions. We have identified a competition among four thermodynamic driving forces for focal adhesion dynamics: (1) the work done during the addition of a single molecular complex of a certain size, (2) the chemical free energy change associated with the addition of a molecular complex, (3) the elastic free energy change associated with deformation of focal adhesions and the cell membrane, and (4) the work done on a molecular conformational change. We have developed a theoretical treatment of focal adhesion dynamics as a nonlinear rate process governed by a classical kinetic model, and demonstrate the limitations of the associated linear response theory. We also express the rates as being driven by out-of-equilibrium thermodynamic driving forces, and modulated by kinetics. In the resulting model, the mechanisms governed by the four effects described above allow focal adhesions to exhibit a rich variety of behavior without the need to introduce special constitutive assumptions for their response. The reaction-limited case is considered. Our central findings are that growth, treadmilling and resorption are all predicted by a very simple chemo-mechanical model. Treadmilling requires symmetry breaking between the ends of the focal adhesion, and is achieved by driving force (1) above. In contrast, depending on its numerical value (2) causes symmetric growth, resorption or is neutral, (3) causes symmetric resorption, and (4) causes symmetric growth.

1891-Pos

Effect of Emodin on Traction Force of Breast Cancer Cells

Shy Chyi Wuang, Chwee Teck Lim.
National University of Singapore, Singapore, Singapore.

Tumor cells sense, process and respond to biological, chemical and mechanical cues in their environment. Regardless of the type of stimuli, the biochemical output of the cells is well studied, from phenotypic changes to protein and gene expression. However, the mechanical output from cells (other than cell elasticity) has not been emphasized. In this study, we have demonstrated the effect of emodin (an anti-cancer drug) on human breast cancer cells in terms of their mechanical response, cytoskeleton changes and the expression of adhesion-related structures. Emodin causes the cell traction forces to increase due to cell rounding and the associated pulling of the ECM which are attributable to emodin's anti-adhesive effect. The traction forces may then decrease and these lower forces depict the compromised well-being of the apoptosizing cells. The variations in traction forces were correlated to morphological and cytoskeletal changes. Such mechano-chemical relationships also reveal cell-matrix interactions and the results have significant implications for understanding relationships which can reveal cell-matrix interactions and help in the quantitative assessment of drug efficacy.

1892-Pos

Substrate Contributions in Elastic Pillar Arrays: Correction of Cellular Force Measurements

Ingmar Schoen, Wei Hu, Viola Vogel.
ETH Zurich, Zurich, Switzerland.

The generation of tensile forces by cells is crucial for adhesion, migration, and cell to cell communication. The magnitude and direction of attachment forces are routinely measured by the deflection of elastic pillars on which the cells have been cultured. As the experimental calibration of the pillar spring constant is tedious, many studies use bulk material properties plus pillar dimensions for the force calculations and consider only bending and shear of the pillar. In this paper we show that all models that neglect the elastic substrate beneath the pillar systematically overestimate the applied forces, typically by more than 20%. Using finite element simulations we find that the elastic substrate accounts for 10-35% of the total deflection at the pillar top. The additional contribution arises from substrate warping at the pillar base and a consequent tilting of the pillar axis. The theoretical findings were verified by experiments with a macroscopic pillar model. We derive an analytical formula which can be used to correct the force calculations for given material properties and pillar aspect ratio. We further investigate the substrate-mediated crosstalk between pillars. We find that the force-loaded pillar acts as a force dipole and the coupling of a second pillar can be described in the framework of its dipole field. The crosstalk diminishes with the third power of the pillar-to-pillar distance and is under the detection limit for most practical cases. Our results highlight the importance of correcting for the systematic errors when comparing cellular forces that were derived from pillar arrays with different dimensions.

1893-Pos

High Resolution Force Distribution of Migrating and Spreading Cells

Saba Ghassemi[1], Matthew R. Stachowiak[2], Giovanni Meacci[2,3], Pere Roca-Cusachs[3], Michael P. Sheetz[3], Ben O'Shaughnessy[2], James Hone[1].
[1]Department of Mechanical Engineering, Columbia Universirty, New York, NY, USA, [2]Department of Chemical Engineering, Columbia University, New York, NY, USA, [3]Department of Biological Sciences, Columbia University, New York, NY, USA.

Cell motility is crucial for the immune system and its misregulation is associated with cancer and other diseases. Migration is a complex cellular activity with many proteins coordinating within a subcellular motility machine. The machine's parts conspire to propel the cell forward by exerting forces on the environment with spatial variations down to the nanoscale. In this work we measured and statistically characterized the force distributions with the aim of illuminating underlying mechanisms. We cultured mouse embryonic fibroblast cells expressing GFP-actin on dense arrays of flexible nanoengineered pillars. During cell spreading pillar deflections quantitatively revealed cell traction patterns on the substrate. Simultaneous actin imaging enabled the cellular force map to be visualized within the evolving cell contour. The greatest forces were exerted in a ~10-20 micron strip behind the leading edge and are directed inward. We analyzed time profiles of forces exerted on single pillars as the cell passed over the pillar location. Forces were relatively short lived and showed more fluctuation for pillars with smaller diameter than for larger ones. When the protruding cell edge reaches a pillar a period of large traction force begins, typically lasting several minutes, with maximum stress on the order of several nN/μm2. Stiffer substrates provoked larger tractions than more compliant substrates. Once the front of the cell has passed by, a drastic reduction in traction occurs. Spatial force distribution and its evolution were characterized by correlation functions relative to the leading edge. By varying the geometric parameters of the pillars, we probed a range of effective substrate rigidities. In summary, we combined high resolution measurements, statistical analysis and quantitative modeling to characterize and interpret signature features of migrating and spreading cell force maps.

1894-Pos

Oxldl-Induced Decrease in Lipid Order of Membrane Domains is Inversely Correlated with Endothelial Stiffness and Network Formation

Tzu-Pin Shentu[1], Igor Titushkin[1], Dev K. Singh[1], Keith J. Gooch[2], Papasani Subbaiah[1], Michael Cho[1], Irena Levitan[1].
[1]University of Illinois, Chicago, IL, USA, [2]Ohio State University, Columbus, OH, USA.

Oxidized Low Density Lipoprotein (OxLDL) is a major factor in development of atherosclerosis. Our earlier studies have shown that exposure of endothelial cells (EC) to oxLDL increases EC stiffness, facilitates the ability of the cells to generate force and facilitates EC networks formation in 3D collagen gels. In this study, we show that oxLDL induces a decrease in lipid order of membrane domains and that this effect is inversely correlated with endothelial stiffness, contractility and network formation. Local lipid packing of cell membrane domains is assessed by Laurdan two-photon imaging, endothelial stiffness was assessed by measuring cellular elastic modulus using Atomic Force Microscopy (AFM), cell contractility was estimated by measuring the ability of the cells to contract collagen gels and EC angiogenic potential was estimated by visualizing endothelial networks within the same gels. Furthermore, we also show that the impact of oxLDL on endothelial biomechanics and network formation is fully reversed by supplying the cells with a surplus of cholesterol suggesting that changes in membrane cholesterol underlie oxLDL-induced effects on endothelial biomechanics. In contrast, exposure to sphingomyelinase C (SMase C) has no effect on endothelial stiffness and network formation, indicating that hydrolysis of sphingomyelin cannot be responsible for these effects. Based on these observations, we suggest that disruption of lipid packing of cholesterol-rich membrane domains plays a key role in oxLDL-induced changes in endothelial biomechanics.

1895-Pos

Spatiotemporal Analysis of Traction Work Produced by Migrating Amoeboid Cells

Baldomero Alonso-Latorre, Juan C. del Álamo, Effie Bastounis,
Ruedi Meili, Richard A. Firtel, Juan C. Lasheras.
University of California, San Diego, La Jolla, CA, USA.

Amoeboid cell motility is a complicated process requiring the regulated activity and localization of many molecules and resulting in the cyclic repetition of a relatively small repertoire of shape changes. These changes are driven by the traction work produced by the cell, which can be estimated by measuring the forces and displacements exerted by the cells on their substrate during migration. We have developed and applied a novel implementation of Principal Component Analysis to identify and sort out the most important shape changes in terms of traction work produced by chemotaxing *Dictyostelium* cells. For this purpose, we acquired time-lapse recordings of cell shape and traction forces of *Dictyostelium* cells migrating on deformable substrates. Using wild-type cells as reference, we investigated the effect of altering myosin II activity by studying myosin II null cells and essential light chain null cells. Our results indicate that the spatio-temporal variation of the traction work produced by *Dictyostelium* cells can be described with a reduced number of modes. In fact, only four modes are needed to account for 65% of the traction work exerted by all cells lines studied. Furthermore, the first mode alone accounts for more than 40% of the traction work. Spatially, this mode consists of the attachment of the cell predominantly at two areas at front and back, contracting towards the center of the cell. The time evolution of this mode is approximately periodic and coincides with the time evolution of cell length. Each one of the remaining modes accounts for less that 10% of the traction work. Their temporal and spatial organization is less clear, suggesting that the cell performs a traction work cycle composed of a repetitive sequence of steps over which random fluctuations are imposed.

1896-Pos

Dynamic Force Generation within the Immune Synapse

Keyue Shen[1], Michael L. Dustin[2], **Lance C. Kam**[1].
[1]Columbia University, New York, NY, USA, [2]New York University School of Medicine, New York, NY, USA.

Increasing evidence suggests mechanical forces modulate T cell function. In this report, we investigate forces applied by mouse CD4+ T cells onto an underlying substrate as a model of the interface between T cells and antigen presenting cells. Traction force microscopy was carried out using microfabricated arrays of elastomer (polydimethylsiloxane, Sylgard 184, PDMS) pillars; cells induce deflections of the pillars which can be measured and used to estimate force applied to each structure. We chose a pillar geometry of 1 micrometer diameter and 5-9 micrometer height. These pillars were coated with a 1:1 mix of activating antibodies to CD3 and CD28, which ligate and activate the TCR complex and costimulatory CD28 signal. Traction force microscopy carried out on mouse naïve CD4+ T cells 1 hour after seeding revealed that naïve cells exert forces onto these pillar arrays with magnitude on the order of 50 pN per structure. Moreover, force application by a given cell is periodic, with a cycle on the order of minutes. To investigate the physiological implications of these forces, we measured IL-2 secretion by T cells seeded onto planar PDMS substrates of varying rigidity, which was controlled by varying the ratio of base : curing agent, yielding bulk moduli of 2 MPa to 25 kPa. Substrates were coated with activating antibodies to CD3 and CD28 prior to cell seeding, and the per area concentration of antibodies varied less than 10% across the different moduli. Activation of naïve T cells, measured as IL-2 secretion over six hours, was 50% greater on the stiffest vs. softest elastomers, and each condition was statistically different from all others (Kruskal-Wallis methods, alpha = 0.05). These results demonstrate a functional impact of mechanical forces on T cell activation, and reveal new dynamics of the immune synapse.

1897-Pos

Opposing Activities of Hydrostatic Pressure and Actomyosin Contraction Drive Mitotic Cell Rounding

Martin P. Stewart[1], Daniel J. Mueller[1], Jonne Helenius[1], A.A. Hyman[2].
[1]Biotechnologisches Zentrum, Dresden, Germany, [2]MPI-CBG, Dresden, Germany.

During mitosis adherent tissue culture cells undergo a dramatic shape change, from essentially flat to nearly spherical. The forces and mechanisms that drive this shape change remain unexplained. Here we investigate the nature of mechanical forces associated with mitotic cell rounding. We show that as cells round up they generate substantial outward directed forces, at times exceeding 100 nN in our assay. The force depended on both an intact actomyosin cortex and transmembrane ion gradients. A functional actomyosin cortex was required to establish a rounding force and disrupting it during mitosis triggered an increase in cell volume. Addition of pore forming toxins to disrupt cation gradients decreased the rounding force and allowed actomyosin dependent cell shrinkage. We postulate that mitotic cell rounding is governed by regulating both an outwardly directed hydrostatic pressure and an inwardly directed cortical tension. Together osmolaric pressure and actomyosin cortex dependent surface tension control cell volume and shape.

1898-Pos

Strain Distribution and Relaxation in the Stretched Axons of Sensory Neurons

Joshua Chetta, Sameer Shah.
University of maryland, College Park, MD, USA.

The mechanical environment of a neuron strongly influences its function. In response to an externally applied tensile load, a number of morphological responses have been demonstrated in the axons of cultured neurons. We have developed methods to understand cellular mechanisms governing these responses. Rat sensory neurons were seeded onto a flexible silicone substrate and were imaged during substrate stretch. This configuration resulted in uniform tensile loading along the length of the neuron. Stationary mitochondria, believed to be docked to the axonal cytoskeleton, were used as fiduciary markers for elements of the cytoskeleton. Their positions were determined before and after an applied substrate strain (percent change in length) of 10%, and used to calculate the resulting ''instantaneous'' strain of regions along the axon. There was dramatic heterogeneity in the measured strain along the length of the stretched axons. This variability was particularly evident in regions of the axon less than 35 microns long. Measured strain in regions longer than this was less variable and was closer to the expected 10% strain. These results suggest a length scale over which local structural elements may be altered to modulate the biomechanical response of the axon. Following the initial stretch, the substrate was held at 10% strain and the axons imaged for 20 minutes during ''relaxation.'' Compared to unstretched axons, mitochondrial pairs in stretched axons showed little coordinated movement with each other at all length scales. Additionally, mitochondria in stretched axons showed larger displacements during the initial phase of relaxation, but after 18 minutes, the displacements were much smaller than those seen in unstretched axons. Collectively, this work presents the axon as a dynamic and heterogeneous structure, which interacts mechanically with the extracellular environment in more complex ways than previously thought.

1899-Pos

On the Relationship of Tissue Surface Tension to Microscopic Parameters

Eva-Maria Schoetz, M. Lisa Manning.
Princeton University, Princeton, NJ, USA.

It has long been established that biological tissues are viscoelastic materials, and that embryonic tissues in particular have an ability to flow over large distances on long time scales. The mechanical properties of these tissues likely play an important role in cell movements and pattern formation during embryogenesis, cancer and regeneration, and they can be measured using rheology techniques such as tissue surface tensiometry (TST).

Over the past 40 years, two theories have been advanced to explain the microscopic origins of tissue surface tension: the differential adhesion hypothesis (DAH) and the differential interfacial tension hypothesis (DITH). While the DAH contributes surface tension to adhesive energies, the DITH contributes it purely to cortex tensions. The DAH has been able to successfully explain a vast range of data on embryonic and cancer cell aggregates and tissues over the last decades, however, recent studies on single cells appear to support the DITH.

Here we show that a simple mechanical model which accounts for cell-cell adhesion, cortical tension, and fluid incompressibility can explain the two types of experimental data within a single framework. We find that tissue surface tension is a careful balance between adhesive and tensile forces, which are interdependent and cannot be altered independently; the relative strength of adhesive and tensile forces determines the measured macroscopic surface tension. In addition, the model predicts that cells on the surface of an aggregate alter their morphology as the surface tension changes, and we will present experimental data from embryonic tissues that are consistent with these predictions.

1900-Pos
Cortical Oscillations as a Model for Studying Cytoskeleton Regulation During Cell Spreading

Nancy Costigliola, Maryna Kapustina, Gabriel Weinreb, Timothy Elston, Ken Jacobson.
UNC Chapel Hill, Chapel Hill, NC, USA.

Cell spreading and attachment are integral to multiple physiological processes including wound healing, immune cell-antigen recognition, and tumor cell metastasis. We have discovered that Swiss 3T3 fibroblasts and CHO cells undergo periodic oscillations of the cell body during cell spreading that last from .5 hours after attachment to 1.5 hours and longer. The amplitude and duration of the oscillating phenotype are increased when microtubules are depolymerized. Previously we developed a mechanochemical ODE model describing a possible negative feedback from actomyosin based contractility to stretch-activated calcium channels in propagating cell oscillations. Cortical oscillations provide an ideal model for studying cytoskeleton regulation because the oscillation mechanism is easily quantifiable through the relative phase, amplitude, and period of native oscillations vs. those that have experienced perturbations. Further, we examine the spatiotemporal distribution of $[Ca^{2+}{}_i]$ during cell oscillations. We propose that the interplay of the calcium and Rho A pathways both contribute to the propagation of cortical oscillations, with high levels of active Rho A replacing the need for highly dynamic calcium signaling.

1901-Pos
Foraging Strategies for Starving and Feeding Amoeba

Simon F. Norrelykke, Edward C. Cox.
Princeton University, Princeton, NJ, USA.

Do individual cells have a search strategy when their target is outside their range of detection? Does this strategy change when a high density of targets is encountered?
To answer these questions, we observed single, well-isolated cells of the social amoeba Dictyostelium as they forage for bacteria on a flat surface. Time-lapse movies of this predator-prey system were recorded and analyzed. By varying the concentration of the food source over several orders of magnitude the dynamics of the amoebae as they responded to their environment could be studied.
At low bacterial density the amoebae scooped up the bacteria as they passed over them without any detectable change in motion. At higher bacterial density the amoebae slowed down, picking up essentially all bacteria encountered, and were found to change their long-timescale behavior from an unbiased random walk to a self-avoiding random walk. This way the amoebae avoids searching for food in already depleted regions. A single amoeba typically ingested 250 bacteria before pausing for 15 min to divide.

1902-Pos
Cell Elastic Modulus Cytometry using Diode-Bar Optical Stretchers

Ihab Sraj[1], Justin Chichester[2], Erich Hoover[2], Ralph Jimenez[3], Jeff Squier[2], Charles D. Eggleton[1], David W.M. Marr[2].
[1]University of Maryland Baltimore County, Baltimore, MD, USA, [2]Colorado School of Mines, Golden, CO, USA, [3]University of Colorado, Boulder, CO, USA.

The mechanical deformation of biological cells using optical forces is an efficient experimental method to study cellular mechanical properties that may identify cell types and detect disease states. However, the low throughput has significantly limited its utility and application due to the need to sequentially isolate and probe individual cells. We have implemented a pseudo steady-state high-throughput optical stretcher in which anisotropic forces from an inexpensive laser diode stretch osmotically swollen bovine erythrocytes in a continuous microfluidic flow at a rate of ~ 1 cell/second. This measurement rate is a factor of 10-100 higher than previous demonstrations of optical stretching. We also simulate the deformation of elastic capsules induced by single diode-bar optical stretcher with and without flow. Finally, we demonstrate how theory can be applied to determine the elastic modulus of individual cells from experimental measurements of the equilibrium deformation. Analysis of the deformed cells results in a shear modulus in the range of reported values from $2.5x10^{-3}$ dyne/cm to $1.3x10^{-2}$ dyne/cm for swollen human erythrocytes. This new optical approach has the potential to be readily integrated with other cytometric technologies, and with the capability of measuring cell populations, thus enabling true mechanical-property based cytometry.

1903-Pos
Isoform-Specific Contributions of Alpha-Actinin to Glioma Cell Mechanobiology

Shamik Sen, Sanjay Kumar.
Univ. of California, Berkeley, Berkeley, CA, USA.

Glioblastoma Multiforme (GBM) is a malignant astrocytic tumor associated with low survival rates because of aggressive infiltration of tumor cells into the brain parenchyma. Expression of the actin binding protein alpha-actinin has been strongly correlated with the invasive phenotype of GBM in vivo. To probe the cellular basis of this correlation, we have suppressed expression of the nonmuscle isoforms alpha-actinin-1 and alpha-actinin-4 and examined the contribution of each isoform to the structure, mechanics, and motility of human glioma tumor cells in culture. While subcellular localization of each isoform is distinct, suppression of either isoform yields a phenotype that includes dramatically reduced motility, compensatory upregulation and redistribution of vinculin, reduced cortical elasticity, and reduced ability to adapt to changes in the elasticity of the extracellular matrix (ECM). Mechanistic studies reveal a reciprocal relationship between alpha-actinin and non-muscle myosin II in which depletion of either alpha-actinin isoform reduces myosin expression and maximal cell-ECM tractional forces, and inhibition of myosin-mediated contractility alters subcellular distribution of both isoforms of alpha-actinin. Our results demonstrate that both alpha-actinin-1 and alpha-actinin-4 make critical and distinct contributions to cytoskeletal organization, rigidity-sensing, and motility of glioma cells, thereby yielding mechanistic insight into the observed correlation between alpha-actinin expression and GBM invasiveness in vivo.

1904-Pos
The Optical Mouse Trap: in Vivo Probing of Capillary Viscoelasticity

Nadja Nijenhuis[1], **Marcel Bremerich**[2], Hans Vink[3], Jos A.E Spaan[1], Christoph Schmidt[2].
[1]Academic Medical Center, University of Amsterdam, Amsterdam, Netherlands, [2]Georg-August-Universität Göttingen, Göttingen, Germany, [3]Cardiovascular Research Institute, Maastricht University, Maastricht, Netherlands.

Optical traps have proven to be a versatile quantitative non-contact manipulation tool. We here demonstrate an optical trap in vivo. We used it to perform microrheology and measure viscoelasticity inside capillaries of a living mouse. We also studied particle interactions with the vascular endothelial boundary layer. It has been reported that the lumen of capillaries is covered with a very sensitive at least 0.5 µm thick polymer layer, the endothelial glycocalyx (EG) which is extruded by and attached to the endothelial cells that line the inside of blood vessels. The EG is crucial for the chemical and physical protection of the vessel wall and also serves as a mechanosensor for shear flow. We found no indication of elastic response, suggesting the EG is a primarily viscous polymer layer. We also observed the adhesive interaction of blood platelets with the vessel wall after introducing photo-chemical damage by fluorescence excitation of injected dye.

1905-Pos
Mapping Elasticity Down to the Molecular Scale: a Novel High-Resolution Approach to Study Cell Mechanics

Claudia Friedsam[1,2], Donald E. Ingber[3], David A. Weitz[2], Ozgur Sahin[1].
[1]Rowland Institute at Harvard, Cambridge, MA, USA, [2]Dept. of Physics, Harvard University, Cambridge, MA, USA, [3]Wyss Institute for Biologically Inspired Engineering at Harvard University, Children's Hospital, and Harvard Medical School, Boston, MA, USA; Harvard School of Engineering & Applied Sciences, Cambridge, MA, USA, Boston, MA, USA.

The mechanical properties of cells govern a variety of processes critical for the control of their behavior, and they are strongly determined by the cytoskeleton. These observations have inspired numerous studies on cells and reconstituted cytoskeletal networks. However, it remains a challenging task to relate structural and mechanical properties on the molecular scale within living materials.

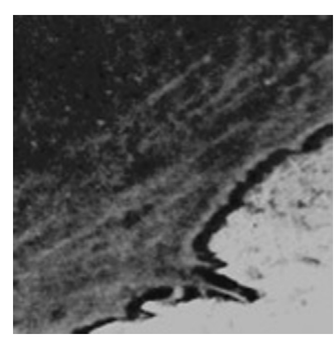

To analyze cell mechanical properties on the molecular scale, we used recently developed torsional harmonic cantilevers to obtain high-speed force-distance curves in parallel to high-resolution AFM tapping mode images in fluid. By applying this technique, we were able to acquire stiffness maps of

living cells at an unparalleled spatial and temporal resolution (50-100 nm, 4-8 min for a 30 μm scan). Furthermore, we were also able to map the elasticity of a reconstituted actin network, which has not been achieved before. In combination with optical techniques this opens up a unique simultaneous view of the mechanics of the living cell and the mechanical properties of its relevant molecular components.
Elasticity maps of a live HUVEC cell (30 μm scan)

1906-Pos
What is Measured By Passive Microbead Rheology?
Jay D. Schieber, **Ekaterina Pilyugina**.
Illinois Institute of Technology, Chicago, IL, USA.
It is often claimed that the dynamic modulus G* of a viscoelastic medium can be measured by following the trajectory of a small bead subject to Brownian motion. In the pioneering manuscript that introduced the idea [T. Mason and D. Weitz, Physical Review Letters 74, 1250 (1995)], this equivalence between the autocorrelation function and G* was assumed. Later work claimed that a correspondence could be proven, but to our knowledge, the proof has never been shown. We use here an analytic solution of the forces on a sphere undergoing arbitrary displacement in an arbitrary viscoelastic medium combined with the fluctuation-dissipation theorem to derive what is actually measured in the microbead rheology experiment. We find that a convolution of G* is indeed measured in the followed autocorrelation function. Under certain restrictions the autocorrelation function is a direct measurement of the dynamic modulus as is typically used. We examine experimental data published in the literature and are unable to find any data where the restrictions do not hold. Nonetheless, the results suggest that the technique could also be used at higher frequencies, if proper analysis is made of the data.

1907-Pos
Intracellular Diffusion in Fission Yeast Cells Depends on Cell Cycle Stage
Christine Selhuber-Unkel[1], Pernille Yde[1], Kirstine Berg-Sørensen[2], Lene Oddershede[1].
[1]Niels Bohr Institute, Copenhagen, Denmark, [2]Danish Technical University, Kgs. Lyngby, Denmark.
During the cell cycle, rearrangements of the cytoskeletal network play an essential role, in particular for the success of cell division. In order to quantify the influence of cytoskeletal rearrangements on the viscoelastic properties of the intracellular space, we studied the diffusion of endogenous lipid granules within single fission yeast cells in the different stages of the cell cycle. The position of the granules was tracked with optical tweezers at nanometer and sub-millisecond resolution and the data were analyzed with a power spectral analysis. We found that the majority of the lipid granules underwent subdiffusive motion during all stages of the cell cycle, i.e. the mean squared displacement of the granule is $2Dt^{\alpha}$ with $\alpha<1$. With our experiments we have shown that α is significantly smaller during interphase than during any stage of mitotic cell division and, surprisingly, we did not find significant differences of α in the different stages of cell division. These results indicate that the cytoplasm is more elastic during interphase than during cell division and that its elasticity is relatively constant during the stages of cell division.

1908-Pos
A Comparison of Single-Cell Elasticity of Osteogenic Cells Measured with the Optical Stretcher and Holographic Microscope
Michael G. Nichols, Anya K. Burkart, Joy L. Chaput, Robert P. Thomen, Kristina G. Ward, Semere M. Woldemariam.
Creighton University, Omaha, NE, USA.
While it has been known for some time that bone mass is remodeled in response to mechanical stress, the identity of the primary mechanosensor has yet to be clearly established. To determine if cellular elasticity may play a role in the cell's ability to detect a pressure variation, we have used the optical stretcher to measure the elasticity of individual osteogenic cells. To determine cell elasticity from measurements of cellular deformation, the optical pressure on the cell surface is computed using a ray optics model which assumes a value for the index of refraction of the cell. Previously we have estimated this value from measurements of other eukaryotic cells, but the optical pressure varies significantly with small changes in refractive index. Therefore, digital holographic microscopy is used to improve estimates of this critical parameter. We consider the overall impact that a spatial variation in the index of refraction can have on the determination of the optical stress, and compare single-cell elasticity measurements of red blood cells, 2T3 osteoblast and MLO-Y4 osteocyte cells.
* This work was supported by P20 RR016475 from the INBRE Program of the National Center for Research Resources.

Microtubule Motors-Kinesin-1

1909-Pos
An Atomic-Level Engine that Accounts for Kinesin Motility and Catalysis
Charles V. Sindelar[1], Kenneth H. Downing[2].
[1]Brandeis University, Waltham, MA, USA, [2]Lawrence Berkeley National Laboratory, Berkeley, CA, USA.
Kinesin motor proteins convert the energy of ATP hydrolysis into stepping movement along microtubules. In this process, the microtubule can be considered as kinesin's regulatory partner, responsible for activating the enzyme's functional behavior. In the absence of atomic resolution structures describing the kinesin-microtubule complex, the mechanism of this activation has remained unknown. We use cryo-electron microscopy to derive atomic models describing the complete, microtubule-attached, kinetic cycle of a kinesin motor. The resolution of our reconstructions (~8Å) enabled us to unambiguously build crystallographically-determined conformations of kinesin's key subcomponents into the density maps. The resulting models reveal novel arrangements of kinesin's nucleotide-sensing switch loops and of its microtubule binding element known as the switch II helix. Based on these models, we present a detailed molecular mechanism accounting for kinesin's force generation cycle. In this mechanism, the switch loops control a seesaw-like movement of the catalytic domain relative to the switch II helix, which remains fixed on the microtubule surface. Microtubules couple the seesaw movement to ATP binding by stabilizing the formation of extra coils at the N terminus of the switch II helix, which interact directly with the switch loops. Tilting of the seesaw to assume the ATP-bound orientation in turn elicits a power stroke by the motor domain's force-delivering element known as the neck linker. This sequence of events accounts for the essential mechanics of kinesin's force-delivery cycle, and also yields a new model for the catalytically active conformation of kinesin's ancestral relative, myosin.

1910-Pos
Free Energy Changes During Kinesin's Force-Generating Substep
Wonmuk Hwang[1], Matthew J. Lang[2], Martin Karplus[3].
[1]Texas A&M University, College Station, TX, USA, [2]MIT, Cambridge, MA, USA, [3]Harvard University, Cambridge, MA, USA.
We have previously suggested that Kinesin-1 generates force by transient folding between the N-terminal cover strand and the C-terminal neck linker domains into a beta-sheet, the so-called cover-neck bundle (CNB). Once formed, the CNB has a conformational bias sufficient to move the neck linker forward. Replica exchange molecular dynamics simulations have been performed to elucidate the energetics of CNB formation with and without load. Without load, the CNB state is weakly favorable compared to non-CNB states by 0.85 kcal/mol at 300 K, which is in agreement with a previous experimental value based on electron paramagnetic resonance, 0.72 kcal/mol (Rice et al, Biophys. J. 84:1844 (2003)), although the identity of the states involved is not certain. In non-CNB states the mobile neck linker points mostly forward in the ATP-like conformation of the motor head, so there is relatively little conformational difference with the CNB-state. By contrast, when a 10-pN rearward load is applied at the end of the beta9 part of the neck linker, a new local energy minimum appears for a rearward-pointing state. Compared to the CNB state, the free energy of the rearward-pointing state is higher by 2.96 kcal/mol at 300 K. This indicates that the CNB readily forms under applied load and thus is able to move the neck linker forward. The significance of these results for the mechanism by which kinesin-1 walks on microtubules will be discussed.

1911-Pos
Neck-Linker Length is a Critical Determinant of Kinesin Processivity
Shankar Shastry, William Hancock.
Pennsylvania State University, University Park, PA, USA.
The kinesin neck-linker domain is a key mechanical element underlying processive kinesin motility. Not only is neck-linker docking thought to be the dominant conformational change in the kinesin hydrolysis cycle, chemomechanical communication between the two head domains must necessarily be transmitted through the two neck-linker domains and their shared coil-coil. Hence, the length of the neck-linker is expected to have a strong influence on kinesin run length, a quantitative measure of processivity. Across different kinesin families, motors with longer neck-linker domains, such as Kinesin-2 are generally less processive than Kinesin-1, which has the shortest neck-linker domain among N-terminal kinesins. However, there is disagreement in the literature as to whether artificially extending the Kinesin-1 neck-linker alters the motor run length. Using single molecule TIRF analysis to visualize GFP-tagged motors in 80 mM PIPES buffer, we find that lengthening the Kinesin-1 neck-linker by three amino acids results in a five-fold reduction in run length. Consistent

with this, when the Kinesin-2 neck linker was matched to the effective length of Kinesin-1 by deleting three residues and substituting an alanine for a proline, the Kinesin-2 run length nearly matched that of Kinesin-1. These results demonstrate that run length scales with neck linker length for both Kinesin-1 and Kinesin-2 and is sufficient to account for differences in processivity. In addition, we find that adding positive charge to neck linker inserts enhances processivity, providing a possible explanation for the lack of dependence of run length on neck-linker length observed by others. Our data is consistent with the hypothesis that increasing neck linker compliance reduces processivity by disrupting front head gating and potentially provides a unifying principle across kinesin families - longer neck-linkers lead to less processive motors.

1912-Pos

Optimal Size of the Neck Linker is Important for the Coordinated Processive Movement of Kinesin-1

Hiroshi Isojima, Teppei Mori, Michio Tomishige.
Department of Applied Physics, The University of Tokyo, Tokyo, Japan.

Kinesin-1 is a dimeric motor protein that walks along microtubules by alternately moving two motor 'heads'. Several recently published papers including ours provided evidences that kinesin dimer takes one-head-bound state while waiting for ATP and ATP-binding triggers the tethered head to bind to the forward tubulin-binding site. However, it is still not clear why rebinding of the tethered head, which is freely diffusing, to microtubule is prohibited during the ATP-waiting state. To explain this mechanism, we proposed a model based on the crystal structural analysis (Makino et al, this meeting) that ADP release of the tethered head is prohibited because the neck linker would be stretched out if both heads become nucleotide-free due to a steric hindrance posed on the neck linker. This model predicts that if the neck linker is artificially extended, the tethered head can easily rebind to the microtubule. To test this prediction, we engineered neck linker extended mutants by inserting poly-Gly residues and observed their conformational states using single-molecule FRET technique. We found that 5 amino acid extension of the neck linker allows the tethered head to rapidly rebind to the microtubule even in the absence of ATP, and that in this state both neck linkers adopt backward-pointing conformation. The neck linker extended mutants showed processive motility with reduced velocities compare to the wild-type, although the microtubule-activated ATPase rate was not changed, which are consistent with our previous results using poly-Pro insertion (Yildiz et al 2008). There results suggest that optimal size of the neck linker is important to prevent rebinding of the tethered head while waiting for ATP and to efficiently couple ATP hydrolysis energy with forward step.

1913-Pos

The Neck Linker of Kinesin-1 Functions as a Regulator of ATP Hydrolysis Reaction

Xiao Ling[1], Masahide Kikkawa[2], Michio Tomishige[1].
[1]Department of Applied Physics, University of Tokyo, Tokyo, Japan,
[2]Department of Cell Biology & Anatomy, University of Tokyo, Tokyo, Japan.

Kinesin-1 is a highly processive motor that moves along microtubule in a hand-over-hand manner. The neck linker that connects two motor domains has pivotal role in the head-head coordination but its exact role is still controversial. It have been widely believed that the neck linker acts as a mechanical element to propel the tethered head forward, however, we recently proposed an alternative model (biased-capturing model) based on crystallographic and cryo-EM analyses, in which the neck linker docking is not required for the forward stepping. We hypothesized that the neck linker docking rather functions to activate rate-limiting ATP hydrolysis reaction.

To test this hypothesis, we engineered a series of monomeric kinesin mutants whose neck linker was truncated and carried out biochemical and structural analyses. As the neck linker was deleted further from the C-terminus, microtubule-activated ATPase rate of the mutant kinesin decreased and it becomes almost undetectable when whole neck linker was removed. Single molecule fluorescent imaging showed that the neck linker-less monomer stably bound to the microtubule even in the presence of 1 mM ATP. Cryo-EM observation of the neck linker-less mutant on the microtubule in the presence of saturating AMP-PNP displayed a structure similar to that of nucleotide-free wild-type kinesin.

These results indicate that kinesin without the neck linker can bind to the microtubule but is incapable of proceeding ATP hydrolysis reaction, which is consistent with the idea that the neck linker acts as an activator of ATP hydrolysis reaction. This mechanism can explain the front head gating mechanism for head-head coordination: the neck linker of the leading head is pulled backward and the head cannot proceed ATP hydrolysis so that the head cannot detach until the trailing head detaches from microtubule.

1914-Pos

Coupling of Kinesin-1 Neck Linker Docking to the Nucleotide Binding Site

David D. Hackney.
Carnegie Mellon Univ., Pittsburgh, PA, USA.

Coupling of nucleotide binding to docking of the neck linker of kinsin-1 is important for generation of directional motility. One approach towards determining the magnitude of this coupling is to use isotopic exchange reactions to evaluate the free energy differences between states. Kinesin-1 monomer head domains catalyze the slow MT-dependent synthesis of bound ATP from bound ADP and free Pi (MT•E•ADP + Pi → MT•E•ATP + HOH) that results in oxygen isotopic exchange of $^{18}O/^{16}O$ between water and Pi. The tethered head domain of a kinesin dimer bound to MTs, however, catalyzes ATP synthesis at a 20-fold faster rate (Proc.Natl.Acad.Sci.USA 102, 18228 (2005)). This more rapid rate of ATP synthesis with a dimer suggests that the tethered head can bind to the microtubule behind the strongly attached head, because this positions the neck linker of the tethered head toward the plus end of the microtubule and would facilitate its docking on synthesis of ATP.

Isotopic exchange analysis of other constructs with alterations in the neck linker is in progress. One approach is to delete part of the neck linker and therefore prevent reversible docking. DKH335 has lost the C-terminal part of the neck linker that makes extensive contacts with the core. During net ATP hydrolysis, the full length head domain DKH346 resynthesizes ATP on average once in 40 turnovers. In contrast, DKH335 is reported here to hydrolyze ATP with no detectable ATP resynthesis (ATP resynthesis occurs only once in >500 turnovers). This is consistent with more rapid Pi release in the absence of a requirement for coupled neck linker undocking or with destabilization of bound ATP in the absence of neck linker docking.

Supported by NSF grant MCB-0615549.

1915-Pos

Activity Scales and ATP Hydrolysis: Understanding the Thermodynamics of Molecular Motor Kinesin

Neha Awasthi, Volker Knecht, Reinhard Lipowsky.
MPI for Colloids and Interfaces, Golm, Germany.

Kinesin is a molecular motor that transports cargo along microtubule tracks and like most other molecular motors, is powered by ATP hydrolysis. The chemical energy derived from the ATP reaction cycle is converted into mechanical work. Understanding the thermodynamics of ATP hydrolysis coupled with the motor (an enzyme), can offer insights into the mechanism and energy landscape of the system [1]. Activity scales were introduced [1] as thermodynamic parameters with this motivation.

We present a scheme to estimate activity scales for ATP hydrolysis by relating them to the free energies of formations.

Extending the concept, we show that these activity scales are well-defined for chemical species in *any* equilibrium reaction. Hence, a complex equilibrium reaction can be *decomposed* in terms of the activity scales of the respective species. The equilibrium constant for the reaction can also be calculated if the activity scales are known. A quantum mechanical simulation scheme is used to calculate activity scales. Results are presented for some gas phase equilibrium reactions involving small molecules. The accuracy of the calculated activity scales is related to the level of theory used for the quantum mechanical simulations. We discuss the implications and challenges of such simulations in solvent environments for large molecules in biochemical reactions.

[1] R. Lipowsky and S. Liepelt, J. Stat. Phys. 130, 39, 2008.
[2] Neha Awasthi, V. Knecht, and R. Lipowsky, in preparation.

1916-Pos

Single Molecule Visualization of Self-Regulated Kinesin Motility

Tomonobu M. Watanabe, Toshio Yanagida, **Atsuko H. Iwane**.
Osaka Univ., Suita, Japan.

Kinesin-1 is an ATP-driven molecular motor that transports various cargoes in cells by binding its motor domain to microtubules. Its tail domain is thought to self regulate this binding. Here we inhibited kinesin ATPase activity and motility by interacting the heavy chain C-terminal tail region with the N-terminal motor domain. Ionic strength was found to heavily influence this self-regulation as both tail domain binding to the motor domain and ATPase activity were dependent on KCl concentration in in vitro experiments. Single molecule imaging experiments showed that the tail domain did not affect motility velocity but did lower the binding affinity of the motor domain to the microtubule. The decrease in binding was coupled to ATPase inhibition. Tail domain transfected into living cells failed to bind to microtubules, but did inhibit the interaction between the motor domain and microtubule, in agreement with the in vitro investigations. From these results, we propose a mechanism to describe this ion strength

dependent self-regulation, which allows kinesin to efficiently utilize ATP for cargo transport.

1917-Pos
Kinesin's Light Chains Inhibit the Head- and Microtubule-Binding Activity of its Tail
Yao Liang Wong, Sarah E. Rice.
Northwestern University, Chicago, IL, USA.
Kinesin-1 comprises two heavy chains (KHCs) and two light chains (KLCs). The KHC tail inhibits ATPase activity by interacting directly with the enzymatic KHC heads, and the inhibitory segment of the tail also binds to microtubules. We have discovered a novel role for the KLCs in regulating the head- and microtubule-binding activities of the kinesin-1 tail. We show that KLCs reduce the affinity of the head-tail interaction over ten-fold. Functional assays confirm that the KLCs attenuate tail-mediated inhibition of kinesin-1 activity. We also show that KLCs block tail-microtubule binding. Inhibition of head-tail binding requires both steric and electrostatic factors. Inhibition of tail-microtubule binding is largely electrostatic and is more pronounced at physiological pH (pH 7.4) than under acidic conditions (pH 6.6). Full inhibition requires a negatively-charged linker region in the KLCs, between its KHC-interacting and cargo-binding domains. Our data support a model wherein KLCs promote activation of kinesin-1 for cargo transport by suppressing both the head-tail and tail-microtubule interactions. Additionally, KLC-mediated inhibition of tail-microtubule binding may influence kinesin-1's emerging role in microtubule sliding and cross-linking.

1918-Pos
The Kinesin-1 Tail Binds to Microtubules in a Manner Similar to Tau
Mark Seeger, Sarah Rice.
Northwestern University, Chicago, IL, USA.
The kinesin-1 molecular motor contains two microtubule binding sites: an ATP-dependent site in the head domain and an ATP-independent site in the tail domain. In this work we show that the tail binds to microtubules with a sub-micromolar affinity, and that binding is mediated largely by electrostatic interactions. The tail binds to a site on microtubules that is distinct from the head domain binding-site but overlaps with the binding-site of the microtubule associated protein (MAP) tau. Tail binding also stimulates the assembly and promotes the stability of microtubule filaments in a manner similar but not identical to tau. The tail's microtubule binding-site is in close proximity to its regulatory and cargo-binding regions, which suggests that the tail-microtubule interaction described in this work may prove to play an important role in the activity and regulation of the kinesin-1 motor in the cell.

1919-Pos
To Block or not to Block: Isoform Specific Regulation of Kinesin Mediated Transport by the Microtuble Associated Protein Tau
Derrick P. McVicker, Andrew R. Thompson, Christopher L. Berger.
University of Vermont, Burlington, VT, USA.
The microtubule associated protein (MAP) tau is known for its role in modulating microtubule (MT) dynamics in the neuron and has also been implicated in the regulation of kinesin-mediated axonal transport. Previous work has demonstrated that tau has a large inhibitory effect on kinesin's processive run length and binding frequency on MTs that is both concentration and isoform dependent, with the 3 repeat form (3RS) having a much larger inhibitory effect than the four repeat isoform (4RL). In the current study we have used stopped-flow kinetics to elucidate the mechanism by which tau inhibits kinesin-mediated transport in an isoform specific manner. We demonstrate that, in the presence of 3RS-tau, MTs are segregated into two populations, one in which kinesin can bind normally and one in which kinesin can still bind, but with a reduction of its on-rate. The observed on-rates do not vary with increasing tau concentration, but the relative amplitudes of each population do, with the population of MTs with a lower affinity for kinesin increasing at the expense of the population of MTs that kinesin can bind normally. Thus, our data suggests inhibition of kinesin by 3RS- tau is primarily of a non-competitive nature, ruling out a strictly steric blocking mechanism. On the other hand, a single population of MTs is observed in the presence of 4RL-tau, in which kinesin's binding rate is reduced in a linear fashion with increasing tau concentration, suggesting this isoform competitively blocks kinesin binding through a steric blocking mechanism. Taken together, our findings demonstrate a fundamental difference in the manner by which different isoforms of tau inhibit kinesin motility and provide new insight into the potential role of these MAPs in regulating axonal transport.

1920-Pos
Key Residues on Microtubules Responsible for Activation of Kinesin ATPase
Seiichi Uchimura[1], Yusuke Oguchi[2], You Hachikubo[1], Shin'ichi Ishiwata[2], Etsuko Muto[1].
[1]RIKEN, Saitama, Japan, [2]Waseda University, Tokyo, Japan.
The enzymatic activity of molecular motors such as myosin, kinesin, and dynein is enhanced when they bind to cytoskeletal filaments. In the kinesin-microtubule (MT) system, MT binding accelerates ADP release from kinesin, thereby increasing the overall rate of ATP hydrolysis. This ADP release is coupled to kinesin transition from a weak-binding to a strong-binding state; therefore, it is essential for kinesin stepping.
We aimed to identify the critical residues on MTs involved in the weak- and strong-binding states by conducting a mutational analysis of tubulin using a yeast expression system. A comprehensive set of charged-to-alanine mutations in the area of MT spanning helix H11 to H12 in both α- and β-tubulin was expressed in yeast cells (36 mutations); the substitution of 8 residues resulted in a haploid lethal mutant, whereas the substitution of the other 4 residues led to slow cell growth. These findings indicated that the 12 residues probably play a vital role in the in vivo MT functions. Single molecule motility assay of kinesin with these mutant MTs revealed that 2 independent regions on the MT, the H11-12 loop/H12 of α-tubulin and H12 of β-tubulin, are essential for kinesin motility. Measurement of unbinding force showed that in the ADP state, kinesin-MT interaction is mediated via α-tubulin, whereas in the nucleotide-free and 5′-adenylylimidodiphosphate (AMP-PNP) states, this interaction is mediated via both α- and β-tubulin. Furthermore, mutations in the binding site in α-tubulin result in a reduction of the rate of ATP hydrolysis (k_{cat}), while mutations in the binding site in β-tubulin lower affinity for MTs (K_mMT). Thus, these findings suggest that kinesin releases ADP upon initial contact with α-tubulin, and is further locked on the MT via α- and β-tubulin.

1921-Pos
Open-Source Stochastic Simulation for Modeling Kinesin-1 Kinetics
Lawrence J. Herskowitz, Andy R. Maloney, Brigette D. Black, Brian P. Josey, Anthony L. Salvagno, Steven J. Koch.
University of New Mexico, Albuquerque, NM, USA.
Kinesin-1 (conventional kinesin) is a homodimeric motor protein important for axonal transport. It has been well studied through ensemble and single-molecule assays. However, the enzymatic stepping cycle is complex, with many rate constants that are modulated by interaction of the two motor domains. This makes it difficult to predict how changes in a given rate constant may affect observable properties such as processivity, velocity, or stall force. We have written a simulation of kinesin walking using a Stochastic Simulation Algorithm. The model allows for interactions between the heads, and includes states that are not considered part of the normal cycle. This adds to the complexity of the model but also allows for probing rare events, such as those that lead to a finite processivity. Also included are rate constant dependencies on force and concentrations of ATP, ADP, and Pi, which may provide insight into other processes under investigation, such as kinesin backstepping. We intend to use the simulation to aid in interpreting our own gliding motility assay results and to place upper and lower limits on values for rate constants. Our source and executable codes will be freely available.
Acknowledgements: This work was supported by the DTRA CB Basic Research Program under Grant No. HDTRA1-09-1-008.

1922-Pos
Structural Basis for the Mechanochemical Coupling of Kinesin-1 Revealed by Crystal Structural and Biochemical Analyses
Tsukasa Makino[1], Masaru Tanokura[2], Michio Tomishige[1].
[1]Department of Applied Physics, the University of Tokyo, Tokyo, Japan,
[2]Department of Applied Biological Chemistry, the University of Tokyo, Tokyo, Japan.
Kinesin-1 is a dimeric motor protein that moves along microtubules in a hand-over-hand manner. To move in such a coordinated manner, two motor domains have to coordinate their ATP hydrolysis reactions. Recent studies showed that ATP hydrolysis cycle of kinesin motor domain can be affected by either microtubule-binding or external strain posed to the neck linker, but the exact mechanisms are still unknown. At the last annual meeting, we reported the first crystal structure of nucleotide-free kinesin-1 and that the structure explains how kinesin's two motor domain coordinate to move processively. Here, to understand the mechanochemical coupling mechanism, we carried out detailed analysis of the kinesin crystal structure along with biochemical characterizations of alanine-mutant at key residues. First we modeled nucleotide-free kinesin-microtubule complex by docking to the 9Å cryo-EM density map by Sindelar et al (2007) and identified several possible salt bridge pairs between kinesin

and tubulin surface, two of which are involved in stabilizing the extra turns of switch II helix (α4) formed toward the nucleotide-binding pocket. In contrast, only few salt bridge formations are possible in ADP state, explaining why ADP release causes specific and tight binding to microtubule. The structural change of α4 promotes hydrogen bond and hydrophobic interactions of highly conserved residues in α4 with switch II loop, pulling switch II loop away and promoting ADP release from nucleotide pocket. ADP release and ATP binding cause rotational movements of α4 and also rotational movements of nucleotide-binding P-loop and its surrounding elements. These nucleotide-dependent domain motions alter the mobility of the neck linker, providing structural basis for how kinesin's two motor domains coordinate to move processively.

1923-Pos
Probing the Mechanism of Kinesin-1 Motion in Three Dimensions Using the Photonic Force Microscope

George M. Jeppesen, J.K. Heinrich Hoerber.
University of Bristol, Bristol, United Kingdom.

Kinesin-1 is a molecular motor essential for cellular function. It transports components around the cell by a processive movement along microtubules while hydrolysing ATP. Although extensively studied by a variety of techniques, the mechanism used by these single-molecule motors to produce this efficient motion on the nanometer scale is not fully understood.

In our investigations we use the Photonic Force Microscope (PFM) to trap and track a 500nm bead attached to a kinesin motor as it interacts with a microtubule *in vitro.* The PFM is an optical trap capable of recording a trapped dielectric particle's motion in three dimensions with nanometre spatial and microsecond temporal resolutions. Using the data recorded we can infer information about the molecular motor's position and its mechanical properties. By characterising different conformational states of the kinesin molecule from its changing mechanical properties as it processes, we expect to learn more about the cycle of events that make kinesin movement possible.

An understanding of how nature achieves this motion on the nanoscale will help combat diseases related to kinesin's malfunction and will allow production of similar artificial nanomachines in the future.

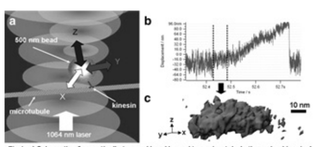

Fig.1: a) Schematic of an optically trapped bead bound to a microtubule through a kinesin-1 molecule. b) Position trace of a bead attached to a kinesin motor travelling along a microtubule orientated in the Y-axis. c) 3D iso-energy profile of bead centre positions in the bound state highlighted on graph.

1924-Pos
Multiple Interacting Kinesin-1 Motors Cooperate Negatively

Michael R. Diehl, D. Kenneth Jameson, Mathew Zimmerman,
Jonathan D. Driver, Arthur R. Rogers.
Rice University, Houston, TX, USA.

Many sub-cellular commodities are transported by more than one motor, and it is well-known that the combined function of motors can lead to unique transport behaviors. Yet, little is known about how grouping multiple motor proteins influences the motile properties of cargos, and in particular, relationships between the structural / compositional organization of motor complexes and key collective transport parameters (run lengths, detachment forces) have not been established.We have taken important steps towards solving this problem by synthesizing the first set of structurally-defined complexes of interacting kinesin-1 motors. Furthermore, we have developed 'single-molecule' assays that can examine new and important aspects of collective motor dynamics; namely, whether multiple motors cooperate in a positive or negative fashion and if these behaviors influence ensemble transport properties of multiple motor systems. Herein, we demonstrate that interactions among two elastically-coupled kinesin molecules lead to negative motor cooperativity, and that this behavior influences collective motor force production. We also describe how such effects can reconcile differences between measurements of cargo motions *in vitro* and in living cells.

1925-Pos
Kinesin-1's Behavior at Obstacles

Till Korten, Oliver Wüseke, Felix Ruhnow, Stefan Diez.
Max Planck Institute of Molecular Cell Biology and Genetics, Dresden, Germany.

Using single molecule stepping assays, we were able to show that kinesin-1 stops when it encounters an obstacle in its path on the microtubule lattice. Based on the stepping mechanism of kinesin-1, we propose the following model to explain why the molecule stops at obstacles:

Kinesin-1's processivity requires the rear head to stay bound until the leading head is firmly attached to the next tubulin dimer. The fact that kinesin-1 follows a single protofilament limits the choice of forward binding to the next tubulin dimer along the same protofilament. Therefore, if a large molecule is blocking the next tubulin dimer, the leading head cannot bind and the rear head cannot detach. This situation effectively stalls the kinesin-1 molecule until it detaches from the microtubule or a forward binding site becomes free.

Based on this model, we were able to calculate the dissociation rate of kinesin-1 in the stopped state. This calculated value agreed very well with a direct measurement, indicating that the model accurately describes kinesin-1's behavior at obstacles. A very similar dissociation rate has been measured previously for single-headed kinesin-1 mutants, suggesting that kinesin-1 waits at obstacles in a one-head bound state.

Interestingly, in about 50 % of the observed stopping events, kinesin-1 did not detach at the end of the stopping phase, but overcame the obstacle and continued to walk. The rate with which kinesin-1 exited the stopped phase by overcoming the obstacle was almost identical to the dissociation rate measured for stopping events. Therefore, it is likely that kinesin-1 overcomes a roadblock by detaching from the microtubule and then, instead of leaving into solution, reattaching next to, or behind the obstacle.

1926-Pos
In Vitro Analysis of the Effect of Microtubule Acetylation on Kinesin Motility

Neha Kaul, Kristen J. Verhey, Edgar Meyhöfer.
University of Michigan, Ann Arbor, MI, USA.

Plus end-directed intracellular transport by kinesins on microtubules in eukaryotic cells directs cargo to the cell's periphery, but to carry out polarized transport, additional signals from microtubules must be recognized by cargo-carrying kinesins. One emerging hypothesis, supported by *in vivo* observations of preferential kinesin-1 transport along acetylated microtubules, suggests that post-translational modifications (PTMs) of tubulin subunits in subsets of microtubules serve as markers for intracellular transport. Here we are examining if and how acetylation of microtubules directly regulates kinesin motility. As a source of acetylated and unacetylated microtubules, we have used *Tetrahymena* doublets extracted from a wild type strain and a mutant strain wherein the otherwise acetylated Lysine-40 is mutated to an Arginine. For obtaining fluorescently-labeled kinesin, lysates were extracted from COS cells transfected with Kinesin-1 genetically labeled with three-tandem monomeric citrines (3xmCit-KHC). To evaluate the effect of acetylation on Kinesin-1 motility, we used TIRF (Total Internal Reflection Fluorescence) microscopy to perform single molecule *in vitro* motility assays and measure the velocity and run length of 3xmCit-KHC on acetylated and unacetylated doublet microtubules. Our observations show that while the *in vitro* velocity remains unaltered, twice as many binding events can be observed for 3xmCit-KHC on wild-type doublets than on unacetylated doublets. We conclude that the motor domain of Kinesin-1 directly recognizes acetylation of microtubules and has a greater tendency to bind acetylated microtubules than unacetylated microtubules. We suggest that acetylation of microtubules enhances the binding affinity of Kinesin-1, which in turn allows preferential transport by Kinesin-1 along acetylated microtubules. To exclude differences between motility assays as source for the observed preferential binding of Kinesin-1 to acetylated microtubules, we are now comparing the binding and motility of Kinesin-1 for acetylated and unacetylated microtubules in the same motility assay.

1927-Pos
Surface Passivation for Molecular Motor Protein Assays

Andy Maloney, Brigette D. Black, Lawrence J. Herskowitz,
Anthony L. Salvagno, Linh N. Le, Brian P. Josey, Steven J. Koch.
The University of New Mexico, Albuquerque, NM, USA.

In kinesin motiliy assays, it has been shown that the surfaces with which kinesin interacts must be passivated in order to prevent kinesin from denaturing on them. The most popular surface blocker is the casein family of milk proteins. Casein is usually purified to various degrees from bovine milk and has many unknowns associated with it when reconstituted and used in motor protein assays. In order to obtain a clearer picture of how kinesin and microtubules interact, a cleaner surface passivation needs to be found. The interaction of kinesin with microtubules has been studied extensively, however, there are fewer studies that investigate how the interaction of kinesin and microtubules changes due to surface passivation. One recent study has shown that the differing components of casein (termed alpha, beta, and kappa) can significantly affect microtubules in gliding motility assays [1]. Gliding motility assays are assays where a glass cover slip is passivated and kinesin is prevented from interacting directly with the substrate. Microtubules are then propelled by the motor activity of a bed of immobilized kinesin molecules. Lipid molecules are fatty acids that can be purified to a much greater extent than casein can. Also, lipid molecules exhibit the same amphiphilic behavior as casein, they adhere to glass easily, and can be easily functionalized. Lipids are thus an attractive alternative

to casein proteins for surface passivation. We report preliminary results on the surface passivation performance of lipid molecules and other materials in gliding motility assays. [1] Vivek Verma, William O Hancock, Jeffrey M Catchmark, ''The role of casein in supporting the operation of surface bound kinesin,'' J. Biol. Eng. 2008; 2: 14. PMID: 18937863

1928-Pos
''Popoffs'' Under a Transverse Force Reveal the Number and Location of Active Kinesin Motors During Motility Assays
Todd Fallesen, George Holzwarth, Jed Macosko.
Wake Forest University, Winston-Salem, NC, USA.
Determination of the number of active motors pulling a single MT or bead during motility assays has proven difficult. Traditional protein concentration assays, such as Bradford, cannot distinguish between active and inactive motors. We attach a superparamagnetic bead to the (+) end of a microtubule. When placed in a magnet with uniform magnetic field gradient, the bead pulls on the MT with a controllable 0-10 pN force. If the force is perpendicular to the gliding direction of the MT, a short section of the MT ''pops off'' the surface every 2 to 5 s, as shown in the diagram. This detachment is characterized by rapid motion of the superparamagnetic bead in the direction of higher magnetic field gradient followed by normal microtubule gliding velocity when the MT is pulled taut. The length of the short section between ''popoffs'' is the distance between active kinesins along a microtubule.

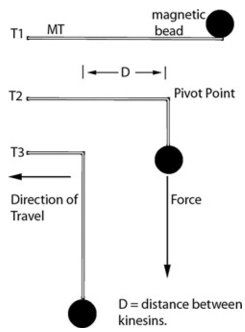

1929-Pos
Calcium Dependent Regulation of Kinesin Function using Binding System of CaM and M13 Peptide
Kiyoshi Nakazato, HIdeki Shishido, Shinsaku Maruta.
Soka Univ., Hachioji, Japan.
Kinesin is known as a dimeric motor protein, which carries cellular cargoes along microtubules by hydrolyzing ATP. Calmodulin (CaM) is a calcium binding protein that participates in cellular regulatory processes. CaM undergoes a conformational change upon binding to calcium, which enables it to bind to specific proteins for a specific response. We have previously demonstrated that kinesin fused with CaM at the C-terminal binds reversibly to M13-Qdots in a calcium dependent manner. In this study, we have tried to make the calcium dependent reversible dimerization of kinesin utilizing CaM- target peptide M13 binding system in order to control motility of kinesin. First we have designed and prepared the cDNA of the truncated kinesin (355 amino acids) that does not form dimer. Subsequently we prepared the cDNA encoding two kinesin chimeric proteins in which C-terminal of kinesin355 was fused with calmodulin (kinesin355-CaM) and fused with M13-GFP (Kinesin355-M13-GFP). The cDNAs of the kinesin chimeras were cloned into expression vector pET21a and transformed into E.coli BL21. The kinesin chimeras were successfully expressed and purified by Co-Chelate column. These kinesin chimeras showed normal ATPase activities. Furthermore, K355-CaM bound to M13-YFP in a calcium dependent manner. And the calcium dependent interaction between kinesin355-CaM and kinesin355-M13-GFP was examined.

Membrane Transport

1930-Pos
The Sodium-Glucose Co-Transporter SGLT1 - Could Light Help Prevent Type II Diabetes?
Christine Keipert[1], Inga Bick[2], Catrin Brosch[2], Petr Obrdlik[2], Klaus Fendler[1].
[1]Max Planck Institute of Biophysics, Frankfurt am Main, Germany, [2]IonGate Bioscienes GmbH, Frankfurt am Main, Germany.
The sodium-glucose co-transporter SGLT1 is responsible for the active transport of glucose in small intestine and kidney. Consuming food with high degrees of carbohydrates and glucose leads to a temporary, rapid increase of blood glucose levels via the absorption of glucose and galactose through SGLT1. This influences the glucose homeostasis and increases the insulin resistance of peripheral tissue. The subsequent ''glucose-toxicity'' leads to degeneration of beta-cells and, in last consequence, to the generation of type II diabetes. The reduction of oral glucose availability by inhibition of SGLT1 with flavonoids or other ''nutraceuticals'' might be one possibility to prevent type II diabetes.
The transport of glucose via SGLT1 is electrogenic and coupled to the co-transport of sodium ions. Its features are examined using cell-free, solid-supported-membrane-based electrophysiology, namely the SURFE^{2}R technology platform (IonGate Biosciences), where transporter-containing membrane fragments or vesicles are mechanically and electrically coupled to a gold-coated biochip. For SGLT1, it is important to establish a membrane potential prior to substrate application, to enhance the sensitivity of the assay. This potential can be built up via a SO_4/Cl^- gradient across the membrane. The following detectable transport activity is in the range of 300-1000 pA.
To avoid unspecific side effects and to speed up screening, the electrochemical SO_4/Cl^- gradient can be replaced by a light-driven gradient. Therefore, we generated cell lines with light polarizable membranes, where the application of light generates a membrane potential. With this technique it is possible to achieve higher throughput and a better signal-to-noise ratio in drug screening.

1931-Pos
Adaptation of Animals to Different Types of Oxidative Stress: The Role of Mitochondrial Potassium Transport Systems
Galina D. Mironova.
Institute Theiretical and Experimental Biophysics, RAS, Pushchino, Russian Federation.
We studied parameters of the ATP-dependent influx of potassium into mitochondria, which were isolated from rats varying in their resistance to ischemia and from hypoxia-adapted animals. It has been found that in the heart and liver mitochondria, the rates of the ATP-dependent potassium influx and H_2O_2 production (in case of ATP-inhibited transport) are higher in the hypoxia-resistant rats, as compared to those in the hypoxia-sensitive animals. When adapted to low oxygen, the hypoxia-sensitive rats demonstrated rates of the both processes increasing to the levels observed in the hypoxia-resistant animals. However, the concentration of potassium in the mitochondria of hypoxia-resistant and adapted animals decreased. This indicates that adaptation to hypoxia stimulates not only the influx of potassium into mitochondria, but also K^+/H^+ exchange. The activation of such a potassium cycle can lower the production of ROS, which plays a crucial role in the lethal cell injury associated with cardiac ischemia and reperfusion. It has been further found that uridine and UMP (precursors of UDP, a metabolic activator of mitoK_{ATP}) greatly decreased the index of ischemic alteration upon 60-min acute ischemia, as well as the size of infarction zone under ischemia-reperfusion conditions. The inhibitors of K_{ATP} channels (glibenclamide and 5-HD) reversed the anti-ischemic effect of uridine and UMP. These agents also exerted an anti-arrhythmic effect, which was completely abolished by glibenclamide but not 5-HD. It should be noted that uridine and UMP recovered the levels of ATP, phosphocreatin and glycogen, which were decreased during ischemia, while glibenclamide and 5-HD eliminated these effects. Also demonstrated was the effectiveness of uridine in the reduction of lipopolysaccharide-induced inflammation (another model of oxidative stress).

1932-Pos
Investigation of Proton-Potassium Exchange During Fermentation of Glycerol by Bacteria *escherichia Coli* at Alkaline and Acidic pH
Anna Poladyan, Arev Avagyan, Armen Trchounian.
Yerevan State University, Yerevan, Armenia.
Production of molecular hydrogen (H_2) by bacteria from a variety of renewable, cheap and abundant carbon sources is a developing new area of technology. Recently it has been shown that bacteria *Escherichia coli* is able to ferment glycerol and produce H_2 via formate hydrogen lyase (FHL) system probably (1). It was demonstrated that in *E. coli* during fermentation of glucose depending of medium pH H_2 produces via two forms of FHL-1 and FHL-2, constituted by formate dehydrogenase H and hydrogenase 3 (H3) or hydrogenase 4 (H4): at alkaline pH FHL-2 was shown to relate with the proton translocating F_0F_1-ATPase and potassium uptake TrkA system (2).
In this study it's shown that at acidic (pH 5.5) and alkaline (pH 7.5) medium in *E. coli* wild typefermenting glycerol protons expelled via F_0F_1-ATPase with low rate compared with the glucose fermentation. The potassium uptake was very low. During fermentation of glycerol at alkaline pH H^+ extrusion was stimulated in *ΔhyfG or ΔfhlA* (with defective H4 or activator of FHL, respectively)and not markedly changed in *ΔhyaB orΔhybC* mutants (with defective H1 or H2). The H^+ extrusion was almost the same in all these mutants at acidic pH. The results indicate that at alkaline pH when F_0F_1-ATPase activity is low H3 or H4 but not other hydrogenases may participate in the H^+ extrusion or have proton translocating ability.

1. *Dharmadi,Y., Murarka, A. and Gonzalez, R.* (2006) Biotechnol. Bioeng. 94, 821-828.
2. *Poladyan, A. and Trchounian, A.* (2009) In Bacterial Membranes. Ed. A. Trchounian, Research Signpost, Kerala (India), pp.197-231.

1933-Pos
Molecular Dynamics Simulations Reveal TolC Flexibility in the AcrB Interface Region
Martin Raunest, Fischer Nadine, Christian Kandt.
University of Bonn, Bonn, Germany.
Over-production of multi-drug efflux pumps is a prominent example of how bacteria gain resistance against antibiotics. In Escherichia coli the AcrA/B-TolC efflux pump is capable to expel a broad range of drugs, using the energy of proton-motive force. The detailed functional mechanism of this efflux system is not fully understood yet. While AcrB is the engine in this system, the outer membrane protein TolC acts as an efflux duct that also interacts with a numerous other inner membrane translocases. TolC occurs in at least two states, one that is impermeable for drugs and one where drug passage is possible. To gain insight into TolC ground state dynamics, we performed a series of 5 independent, unbiased 150ns MD simulations of closed state wild type TolC (PDB ID 1EK9) in a phospholipid/water environment at 0.15M NaCl concentration. Simulations were performed using GROMACS 4.0.3 and G53a6-GROMOS96 force field. While TolC remains closed between a ''bottleneck region'' outlined by Asp-374 &371 and above, we observe opening and closing motions in the AcrB interface region near Gly-365. This local flexibility could be of functional relevance in the AcrB-TolC complex formation. In all simulations the Asp-371&374 aspartate ring region was stable, displaying no fluctuations in the cross-sectional area of the TolC channel. Whereas previous studies found potassium ions to bind frequently, stabilizing a closed TolC conformation in the AcrB interface region, we observe frequent and unhindered passage of sodium ions. However, in one simulation a consecutive binding event of two sodium ions occurs between Gly-365 and Asp-374, stabilizing a similarly closed conformation for more than 15 ns. We introduce a new tool to analyze protein-internal cavities and record pore profiles based on time-averaged water & protein residence probabilities.

1934-Pos
Plant Aquaporins Co-Expression Senses Differentially the Intracelluar pH
Karina Alleva[1], Jorge Bellati[1], Mercedes Marquez[1], Victoria Vitali[1], Cintia Jozefkowicz[1], Gabriela Soto[2], Gabriela Amodeo[1].
[1]Laboratorio de Biomembranas, Departamento de Fisiología, Facultad de Medicina, Universidad de Buenos Aires, Buenos aires, Argentina, [2]Instituto de Ingeniería Genética y Biología Molecular (INGEBI-CONICET), Buenos aires, Argentina.
The plant plasma membrane (PM) expresses two types of aquaporins: PIP1 and PIP2. These PIP are characterized by: i- the faculty to reduce water permeation through the pore after cytosolic acidification as a consequence of gating process, ii- the ability to modulate membrane water permeability by co-expression of both types.
We investigated if these functional characteristics of PIP can act together to give a new and relevant modulation response to acidification. To test our hypothesis we used PIP1 and PIP2 from different plant sources (Beta vulgaris roots and Fragaria x ananassa fruits). The experimental approach used was to perform a functional study of PIP by means of the heterologous expression system Xenopus oocytes and analyzed the oocyte PM water permeability coefficient (Pf) when PIP are injected.
Briefly, the Pf was increased ten-fold by PIP2, but it remained low for both control oocytes and PIP1 injected ones. Moreover, when oocytes expressed PIP2, a partial (70%) pH inhibitory response under cytosolic acidification (pH 6) was detected.
When PIP1-PIP2 co-expression was assayed, Pf was enhanced seven-fold in comparison with Pf obtained by PIP2 expression alone. Furthermore, the pH dependent behavior showed that PIP1-PIP2 co-expression accounts for different pH sensitivity by shifting the EC50 of the inhibitory response from pH 6.1 to pH 6.9, compared to PIP2.
Our results show that: i- PIP co-expression impacts on the membrane water permeability not only by modulating the water transport capacity but also the pH regulatory response, improving in this way membrane plasticity, ii- this PIP behavior is not a tissue specific and/or species-dependent response but a more general one.
In conclusion, aquaporin co-expression widens and enhances regulatory properties that control adjustment of water movements which might be of great importance to react to variable osmotic and pH stress.

1935-Pos
Membrane Transport of Hydrogen Sulfide: No Facilitator Required
John C. Mathai[1], Andreas Missner[2], Philipp Kügler[2], Sapar M. Saparov[2], Mark L. Zeidel[1], John K. Lee[3], **Peter Pohl**[2].
[1]Beth Israel Deaconess Medical Center and Harvard Medical School, Boston, MA, USA, [2]Johannes Kepler University, Linz, Austria, [3]University of California, San Francisco, CA, USA.
Hydrogen sulfide (H_2S) has emerged as a new and important member in the group of gaseous signalling molecules. However, the molecular transport mechanism has not yet been identified. Prediction of its actual membrane permeability, P_M, according to Overton's rule (1) is hampered by the fact that the partition coefficient into the organic phase is not known. Because of structural similarities with H_2O, it was hypothesized that aquaporins may facilitate H_2S transport across cell membranes. We tested this hypothesis by reconstituting the archeal aquaporin AfAQP from sulfide reducing bacteria *Archaeoglobus fulgidus* into planar membranes and by monitoring the resulting facilitation of osmotic water flow and H_2S flux. To measure H_2O and H_2S fluxes, respectively, sodium ion dilution and buffer acidification by proton release were recorded in the immediate membrane vicinity. Both $[Na^+]$ and pH were measured by scanning ion selective microelectrodes. A lower limit of $P_{M,H2S} > 0.5 \pm 0.4$ cm/s was calculated by numerically solving the complete system of differential reaction diffusion equations and fitting the theoretical pH distribution to experimental pH profiles. Even though reconstitution of AfAQP significantly increased water permeability through planar lipid bilayers, $P_{M,H2S}$ remained unchanged. The fact that cholesterol and sphingomyelin reconstitution did not turn these membranes into a H_2S barrier indicates that H_2S transport through epithelial barriers, endothelial barriers and membrane rafts also occurs by simple diffusion and does not require facilitation by membrane channels (2).
1. Missner, A & Pohl, P (2009) 110 years of the Meyer-Overton rule: Predicting membrane permeability of gases and other small compounds ChemPhysChem 10:1405-1414.
2.Mathai, JC, Missner, A, Kügler, P, Saparov, SM, Zeidel, ML, Lee, JK, Pohl, P (2009) No facilitator required for membrane transport of hydrogen sulfide Proc.Natl. Acad. Sci. USA 106:16633-16638.

1936-Pos
Protein Transport Through the Anthrax Toxin Channel: Molecular Mechanisms
Daniel Basilio, Alan Finkelstein.
Albert Einstein College of Medicine, Bronx, NY, USA.
Bacillus anthracis, the causative agent of anthrax, produced a toxin composed of a translocase heptameric channel, $(PA_{63})_7$, which allows its two substrate proteins, lethal and edema factor (LF and EF), to translocate across a host cell's endosomal membrane, disrupting the cell's normal function. Protein translocation through the channel, reconstituted in lipid bilayers, is driven (N-terminal end first) by a proton electrochemical potential gradient. The $(PA_{63})_7$ channel strongly disfavors the entry of negatively charged residues on proteins, and hence the acidic side chains on LF_N (the N-terminal 263 residues of LF) enter protonated; these protons are released into the *trans* solution upon exiting the channel, thereby making this a proton-protein symporter. Consistent with this idea, a single SO_3^-, which is essentially not titrateable, introduced at most positions in LF_N, drastically inhibited voltage-driven LF_N translocation. The lumen of the $(PA_{63})_7$ 14-strand β barrel is ~15 Å wide and can barely accommodate an alpha-helix with its side chains. Translocation through the lumen thus requires the substrates to unfold. Here we present an approach using biotin-streptavidin chemistry to determine the length of the translocating polypeptide chain within the channel as it is traversing the $(PA_{63})_7$ channel lumen, with the goal of shedding light on the structure of the polypeptide chain as it crosses the channel. We created a stopper at the LF_N C terminus and attached a biotin at the N terminus. Translocation proceeds until the C terminus reaches the channel's *cis* entrance, and binding of the N-terminal biotin with streptavidin added to the *trans* side of the membrane, locks the polypeptide chain within the channel. By reducing the distance between the N-terminal biotin and the C-terminal stopper by deletion constructs, we can determine the minimum length that allows streptavidin to grab the N-terminal biotin.

1937-Pos
Transport of Cephalosporin Antibiotics Across the Outer Membrane
Marcos Lovelle[1], Mahendran Kozhinjampara R.[2], Tivadar Mach[1], Mathias Winterhalter[2], Paula Gameiro[1].
[1]REQUIMTE Facultade de Ciências do Porto, Porto, Portugal, [2]Jacobs University, Bremen, Germany.
Antibiotic resistance is emerging in Gram-negative bacteria worldwide. The outer membrane of Gram-negative bacteria is a formidable selective barrier, and a major factor in broad-spectrum antibiotic resistance. Influx of antibiotics into the Periplasm of bacteria is facilitated by proteins that form channels in the outer membrane. We studied the influx of several cephalosporin antibiotics through the major Escherichia coli porins OmpF and OmpC.
Conductance measurements through purified single porins reconstituted in artificial lipid bilayers allowed us to count the passage of single antibiotic molecules. Statistical analysis of transport events yields the kinetic parameters at the single molecular level. Fluorescence steady-state measurements were used to quantify the interaction between the antibiotics and the porin channels and verify the calculation of translocation kinetics. For the first time, we have been able to characterize facilitated translocation of several β-lactams through OmpC (most expressed porin in vivo) and quantified the distinguishable permeation properties of ceftriaxone, ceftazidime and cefpirome through both outer membrane porins OmpF and OmpC - concluding a stronger interaction with OmpF than OmpC for all three cephalosporins -especially ceftazidime-.
Our approach may be of great benefit to the understanding of porin-drug interaction at the molecular scale and may contribute to the rational design of more efficient antibiotics.

1938-Pos
Molecular Basis of Enrofloxacin Affinity to a Membrane Channel of E. Coli - When Binding Does Not Imply Translocation
Tivadar Mach[1], Kozhinjampara R. Mahendran[2], Eric Hajjar[3], Isabel Sousa[1], Marcos Lovelle[1], Amit Kumar[3], Paula Gameiro[1], Mathias Winterhalter[2], Matteo Ceccarelli[3].
[1]REQUIMTE, Faculdade de Ciências, Porto, Portugal, [2]Jacobs University Bremen, Bremen, Germany, [3]University of Cagliari, Monserrato (CA), Italy.
The molecular pathway of enrofloxacin, a fluoroquinolone antibiotic, across the main outer membrane channel OmpF of E. coli is investigated. Through high-resolution ion current fluctuation analysis we count single enrofloxacin channel penetrations, showing a binding to OmpF comparable to the affinity-enhanced translocation through substrate specific channels. A single point mutation D113N increases the dissociation rate 30 times, making the interaction comparable to other antibiotics, corresponding to their weaker binding in a non-specific channel. Molecular dynamics simulations elucidate translocation barriers: WT OmpF has two symmetric binding sites for enrofloxacin located at each channel entry separated by a large barrier in the centre, inhibiting antibiotic translocation. Removal of the negative charge on 113 removes the central barrier shifting both peripheral binding sites to one central site enabling translocation. Fluorescence steady-state measurements confirm simulations. Our results demonstrate that a single mutation of the porin results in a substantial modification of translocation. This example demonstrates how translocation through a channel depends not only on the strength of the substrate-channel interaction, but on a local affinity site counteracting the conformational entropy change at the smallest constriction.

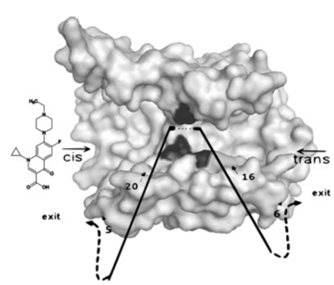

1939-Pos
Permeation of Antibiotics through Bacterial Porins: Screening for Influx on a Single Molecular Level
Mahendran R. Kozhinjampara[1], Mohamed Kreir[2], Niels Fertig[2], Jean-Marie Pages[3], Eric Hajjar[4], Matteo Ceccarelli[4], Mathias Winterhalter[1].
[1]Jacobs university, Bremen, Bremen, Germany, [2]Nanion Technologies GmbH, Munich, Germany, [3]Université de la Méditerranée, Marseille, France, [4]University of Cagliari, Cagliari, Italy.
Chip based automated patch clamp technique provides an attractive biophysical tool to quantify solute permeation through membrane channels. Proteo-Giant Unilamellar Vesicles (GUVs) were used to form stable lipid bilayer across the micrometer sized hole and single channel recordings were achieved with very low background noise. Influx of antibiotics into the periplasm of gram-negative bacteria is facilitated by porins that form channel in the outer membrane. Influx of two major class of antibiotics- cephalosporin and fluroquinolones through major *E.coli* porins OmpF and OmpC was investigated. Ion current fluctuations through porins in the presence of penetrating antibiotics revealed thermodynamic and kinetic parameters of substrate binding from which we calculated flux. We have been able to show rapid and efficient screening of antibiotics through bacterial porins at a single-molecule scale. In vitro activity of antibiotics was determined by microbiological assays which correlates with the results obtained from lipid bilayer measurements. In addition, molecular modelling provided details on the interaction of the molecules with the channel surface, revealed the preferred orientation of the antibiotic along its pathway and the position of affinity sites. Our approach may contribute to the rational design of new antibiotics against clinical bacterial strains for the most efficient delivery to target sites.

1940-Pos
Probing the Molecular Mechanism of Passive Transport
Noah Malmstadt, Su Li, Peichi Hu.
University of Southern California, Los Angeles, CA, USA.
The passive transport of small molecules across the plasma membrane is the major pathway by which orally delivered drugs enter circulation and a major route of delivery into target cells. While molecular dynamics simulations suggest that molecules diffusing through lipid bilayers are subject to a complex, dynamic environment, the analytical framework for describing passive transport continues to treat the membrane as a uniform material. The study of passive transport is complicated by the shortcomings of current experimental techniques, in which transport tends to be dominated by diffusion through a stagnant layer adjacent to the membrane.
We have developed an approach to probing passive transport that eliminates these artifacts and allows for a study of relationships between molecular structure and transport properties. This approach consists of confocal microscopy of the diffusion of small molecules into giant unilamellar lipid vesicles (GUVs). Experiments and finite element models show that due to small size of GUVs relative to the characteristic diffusive length scale of transported molecules, no significant stagnant layer is established. In addition, confocal imaging allows for observation of the steady-state association of diffusing molecules with the membrane itself, while other technologies only allow for detection of transported molecules.
We have concurrently developed a fabrication technology that yields GUVs in which each leaflet of the bilayer has a different lipid composition. This allows a novel investigation of the relevance of the asymmetry of the plasma membrane to passive transport.
A series of fluorescent molecules of varying hydrophobicity was synthesized. Time-series images of these molecules crossing GUV membranes were captured, and these images were fit to both an analytical model of membrane permeation and a finite element model of permeation with diffusion. Lipid composition was varied to reproduce the range of compositions observed in human plasma membranes.

1941-Pos
Supported Bilayers with Excess Membrane Reservoir (SUPER): Novel Templates for Vesicular and Non-Vesicular Transport Studies
Thomas J. Pucadyil, Sandra L. Schmid.
The Scripps Research Institute, La Jolla, CA, USA.
Our understanding of membrane-localized processes has largely been gained from the use of liposome-based systems. However reactions involving budding and fission of membranes are difficult to analyze using liposome-based systems since their buoyancy imposes a fundamental limitation on separating end-products of such reactions. Supported bilayers formed by liposome fusion on glass represent an attractive solution. Conventional supported bilayers are however deficient in membrane reservoir necessary for membrane budding and fission reactions. We report a novel system of supported bilayers with excess membrane reservoir (SUPER) and have analyzed factors that contribute to their formation. The excess reservoir in this system originates from higher binding affinity of liposomes to glass and depends on the presence of anionic lipids in the membrane and high salt content in the buffer. This template formed on silica beads allows the seamless application of microscopy-based assays to analyze membrane-localized processes as well as sedimentation-based assays to isolate vesicular and non-vesicular products released from the membrane. We demonstrate the utility of SUPER templates by the direct visualization of amphiphile-induced membrane tubulation prior to solubilization and

dynamin-catalyzed membrane fission prior to vesiculation. Our results highlight the general applicability of SUPER templates in analyzing several forms of vesicular and non-vesicular transport processes.

1942-Pos

Nanopore Formation in Cells Exposed to Nanosecond Electric Pulses

Andrei G. Pakhomov[1], Angela M. Bowman[1], Bennett L. Ibey[2], Olga N. Pakhomova[1].
[1]Old Dominion Univ., Norfolk, VA, USA, [2]Air Force Research Laboratory, Brooks City Base, San Antonio, TX, USA.

Chemical and physical insults such as electroporation may compromise the membrane integrity and allow leak ion currents through *de-novo* formed lipid pores. These pores are thought to short-circuit the membrane and hinder ion channels' physiological function rather than to complement it. However, here we report that brief electric stimuli can trigger formation of membrane pores with specific behaviors that are traditionally considered to be unique for protein ion channels; still other behaviors of these pores distinguish them from both ''conventional'' electropores and any known ion channels. We found that a single electric shock (600-ns duration, 1 to 5 kV/cm) causes minutes-long increase of membrane electrical conductance due to formation of long-lived, voltage- and current-sensitive, rectifying, cation-selective, asymmetrical pores of nanometer diameter (''nanopores''). Once induced, nanopores oscillate between open and quasi-open (electrically silent) states, followed by either gradual resealing or abrupt breakdown into larger pores, with immediate loss of nanopore-specific behaviors. The formation and extended lifetime of nanopores were verified by non-electrophysiological methods, namely by fluorescent detection of Tl^+ uptake and of phosphatidylserine externalization. Apparently, nanopores are not unique to cell stimulation with nanosecond electric pulses, but may form under various physiological and pathological conditions. Nanopores appear adequately equipped for certain functions that are traditionally ascribed to ion channels. Clear distinction between nanopores- and ion channels-mediated currents may be critical for understanding how these currents are controlled.

Supported by NIH (NCI) R01CA125482.

1943-Pos

Inhibition of Membrane Stretching Prevents Lipid Pore Enlargement in Cells Porated by Nanosecond Electric Pulses (NSEP)

Mikhail A. Rassokhin, Andrei G. Pakhomov.
Old Dominion University, Norfolk, VA, USA.

Recent studies established that nsEP cause formation of stable pores in plasma membrane of mammalian cells. Pores formed by a single nsEP of moderate intensity (e.g., one 600-ns pulse at 3-5 kV/cm) were permeable to alkali cations, but not to a larger propidium cation (van der Waals dimensions 1.6 x 1.4 x 0.8 nm), suggesting that the pore diameter does not exceed 1.4 nm. However, higher nsEP amplitudes and/or exposures to multiple pulses could cause minor propidium uptake. Meanwhile, the mechanism of transformation of initial ''nanopores'' into larger, propidium-permeable pores remains unclear.

One mechanism potentially responsible for nanopore enlargement could be membrane stretching caused by osmotic cell swelling following nsEP exposure. In isoosmotic and even hyperosmotic bath media, membrane permeabilization to small inorganic ions leads to equalization of their concentrations inside and outside of cells. However, larger molecules cannot escape the porated cell interior, creating additional osmotic pressure. To prevent nsEP-induced swelling, the bath buffer can be supplemented with a membrane-impermeable compound, which would prevent the increase of intracellular osmolarity.

We demonstrated that addition of sucrose (8-40 mM) to the bath buffer decreases or eliminates propidium uptake by nsEP-exposed cells (60-ns, 30 pulses at 30 kV/cm). However, addition of isosmotic amount of NaCl caused little or no protective effect. These data are indicative of the fact that membrane stretching by osmotic cell swelling could indeed be the cause of nanopores enlargement. This hypothesis is being additionally tested to exclude a potentially biasing effect of sucrose and NaCl addition on the efficiency of initial nanopore opening.

The work was supported by R01CA125482 from the National Cancer Institute.

1944-Pos

Lipid Raft and Arf6-GTPase Dependent Endocytosis of the hERG Potassium Channel

Rucha Karnik, Andrew J. Smith, David J. Elliott, Tarvinder K. Taneja, Kathyrin Aviss, Asipu Sivaprasadarao.
Multi-disciplinary Cardiovascular Research Centre, Institute of Membrane and Systems Biology, Faculty of Biological Sciences, University of Leeds, Leeds, United Kingdom.

The voltage-gated hERG potassium channel is critical for the repolarisation phase of the cardiac action potential. Genetic mutations leading to a decrease in the number of hERG channels at the cell surface lead to potentially fatal Long QT syndrome which is reflected by an elongated QT interval in the ECG. It is therefore important to understand the trafficking mechanisms that regulate the surface density of hERG. Here we have investigated the endocytic pathway of an epitope (hemagglutinin A) tagged hERG, expressed in HeLa cells, using techniques in molecular cell biology, electrophysiology and biochemistry. Our results demonstrate that the majority of the hERG channel is rapidly internalized from the plasma membrane in a dynamin and clathrin independent manner. Endocytosis of hERG is dependent on cholesterol rich lipid rafts and ADP-ribosylation factor 6 (Arf6). Depletion of cholesterol from cell membrane by treatment with methyl-β-cyclodextrin and disruption of Arf6 activity by over-expression of inactive Arf6 mutants or aluminum fluoride resulted in an inhibition of hERG endocytosis, leading to an increase in hERG currents. Majority of the internalized hERG channel was found in lipid rafts isolated by density gradient centrifugation, identified by the presence of raft marker proteins including flotillin and the co-expressed GFP-tagged GPI anchor protein. Raft associated caveolin, Rac-1 and RhoA-GTPase do not appear to be required for hERG endocytosis. A small fraction of hERG, however, appears to undergo endocytosis via clathrin mediated endocytosis. Following internalization the channel enters Rme1 positive recycling endosomes and also Lamp1-positive late endosome/lysosomal compartments. The significance of lipid-raft and Arf6 dependent endocytosis of hERG in cardiac physiology has yet to be understood. This work was funded by the British Heart Foundation.

1945-Pos

High-Resolution Frap of the Cilium-Localized Somatostatin Receptor 3 Reveals the Presence of a Lateral Diffusion Barrier at the Cilium Base

Ivayla I. Geneva[1], Peter D. Calvert[2].
[1]SUNY Upstate Medical U, Syracuse, NY, USA, [2]SUNY Upstate Medical University, Syracuse, NY, USA.

It is well known that certain proteins localize to the cilia of cells where they perform various specialized functions, such as sensing the physical environment of the cell. Protein localization to subcellular compartments is important for normal cell function and mutations preventing protein localization to cilia are implicated in devastating human pathologies including blindness, deafness, infertility, obesity and many others.

While the mechanisms for transport of proteins to cilia are well-studied, the mechanisms for maintaining their localization to cilia are not understood. One proposed mechanism for the latter predicts the existence of a selective barrier at the base of the cilium that regulates the free movement of both water-soluble and membrane-bound proteins into and out of the ciliary compartment. We directly tested this hypothesis by examining the mobility of the murine somatostatin receptor 3 protein (SSTR3), a G-protein-coupled receptor that naturally localizes to the ciliary membrane of inner-medullary collecting duct (IMCD3) cells.

Using multiphoton fluorescence recovery after photobleaching (MPFRAP) we estimated the diffusion coefficient and measured the equilibration time of SSTR3-EGFP or SSTR3-PAGFP fusion proteins in IMCD3 cell cilia. We found that SSTR3 fusion proteins rapidly, equilibrate along the length of cilia without change in the total mass, indicating that the membrane-bound protein is highly mobile but remains confined inside the cilium. This finding is consistent with the hypothesis that lateral membrane diffusion at the base of the cilium is constrained.

Mitochondria in Cell Life & Death

1946-Pos
Mechanisms Underlying Fructose-Induced Oxidative Stress in the Cytosol and Mitochondria

Lawrence D. Gaspers, Andrew P. Thomas, Veronique Douard, Ron P. Ferraris.
New Jersey Medical School, Newark, NJ, USA.

High levels of dietary fructose are increasingly recognized as an important nutritional factor in the development of nonalcoholic fatty liver disease and intestinal inflammation in both humans and animal models. The signals linking excessive fructose intake on one hand and the onset of these pathologies are not known. We have employed genetically encoded biosensors sensitive to changes in superoxide anion (O_2^-) or hydrogen peroxide (H_2O_2) concentrations to test the hypothesis that fructose metabolism increases the production of reactive oxygen species (ROS) in hepatocytes or intestinal cells. The data indicate that acute treatment with physiological concentrations of fructose (1 - 10 mM) significantly increased the formation of mitochondrial O_2^- as well as mitochondrial and cytosolic H_2O_2. The xanthine oxidase inhibitor, allopurinol, inhibited fructose-induced increases in cytosolic H_2O_2, but was unaffected by apocynin, a NADPH oxidase inhibitor. These data are consistent with the well known effects of acute fructose treatment to reduce ATP levels and stimulate the breakdown of purines. Fructose-induced ROS production in the mitochondria was not altered by allopurinol treatment, whereas apocynin strongly suppressed mitochondrial derived ROS. Fructose administration transiently increased ROS formation in all mitochondria regardless of the subcellular localization and this was paralleled by a sustained rise in mitochondrial membrane potential and an increase in pyridine nucleotide fluorescence. The activation of mitochondrial metabolism was followed by large amplitude O_2^- bursts in a subset of mitochondria. The addition of mitochondrial respiration inhibitors blocked the effects of fructose on mitochondrial, but not cytosolic ROS production. Taken together, these data indicate that fructose treatment stimulates mitochondrial metabolism leading to an increase in ROS production through an apocynin sensitive pathway. Finally, we show that chronic consumption of fructose results in markedly higher baseline levels of mitochondrial ROS in hepatocytes.

1947-Pos
Uncoupling of Mitochondrial Inner Membrane Potential has Opposite Effects on ROS balance in Heart Mitochondria in Situ Versus in Vitro

Miguel A. Aon, **Sonia Cortassa**, Brian O'Rourke.
Johns Hopkins University, Baltimore, MD, USA.

The balance between reactive oxygen species (ROS) production and scavenging is determinant of cell survival and electrical and contractile recovery of the heart during ischemia-reperfusion. How ROS balance is affected by electron transport rate during oxidative phosphorylation and changes in mitochondrial membrane potential ($\Delta\Psi_m$) is still controversial. Here, we investigate the effect of $\Delta\Psi_m$ uncoupling on ROS balance in isolated mitochondria and in mitochondria in intact cardiomyocytes in forward electron transport mode. Opposite effects of the protonophore FCCP on ROS balance were observed when either intact cardiomyocytes or isolated mitochondria from guinea pig hearts were subjected to increasing (10-50nM) FCCP concentrations while monitoring mitochondrial $\Delta\Psi_m$, NADH, and ROS ($O_2^{\cdot-}$; and H_2O_2). Low FCCP concentrations increased both $O_2^{\cdot-}$ and H_2O_2 in intact cardiomyocytes, whereas it decreased their levels in 5mM glutamate/malate energized isolated mitochondria. In cardiomyocytes imaged with two-photon laser scanning fluorescence microscopy, a faster accumulation of both $O_2^{\cdot-}$ and H_2O_2 (indicated by MitoSOX or CM-DCF, respectively) was noted for FCCP concentrations up to 20nM: further increases of protonophore elicited either slower ROS production or hypercontracture and death. In isolated mitochondria, ROS levels decreased by $\approx$60% in parallel with $\Delta\Psi_m$ and NADH, at FCCP concentrations similar to those utilized in intact cells. In cells, the effects of FCCP on ROS balance could be prevented by preincubation with dithiothreitol, indicating that oxidation of the thiol pool was involved. In isolated mitochondria, the ROS signals were increased significantly with exogenous H_2O_2 exposure, or depleting the GSH pool with monochlorobimane. The findings highlight the important role played by the redox environment, particularly with respect to GSH levels, in determining the net effect on mitochondrial ROS balance in response to uncoupling oxidative phosphorylation.

1948-Pos
Mitochondrial Superoxide Flashes in Skeletal Muscle are Linked to Metabolism

Sandrine Pouvreau.
CNRS, Villeurbanne, France.

Reactive Oxygen Species (ROS) constitute important intracellular signalling molecules. Mitochondria are a well known source of ROS production, especially through the electron transport chain. In the present work, the Ca^{2+} biosensor mt-pericam, kindly provided by Pr Miyawaki (RIKEN, Saitama, Japan) was used as a mitochondria-targeted specific superoxide biosensor, by appropriate choice of the excitation wavelength. Mt-pericam was transfected *in vivo* into mouse *flexor digitorum brevis* adult muscles. Fibers were isolated and studied by confocal microscopy. Targeting of the biosensor was specific to the mitochondrial network with little, if any, cytosolic contamination. Fluorescence flashes were detected using excitation at 477 nm which was isosbestic for calcium. Flashes corresponded to superoxide production as shown from simultaneous records of either Mitosox (a mitochondrial superoxide probe) or Rhod-2 fluorescence signals. In addition, the superoxide scavenger Tiron decreased the flash frequency by 85%. On average, flashes have a 20 sec duration, and a F/F0 amplitude of 2. Flashes were recorded in subsarcolemmal, and intermyofibrillar mitochondria. Intermyofibrillar flashes presented three different spatial patterns: longitudinal, transversal or patch-shaped. Flash frequency was increased by application of glucose/pyruvate and decreased by inhibition of the electron transport chain with antimycin A. This is strong evidence for quantal superoxide production being intimately linked to mitochondrial metabolism. Superoxide flashes were also found to cause a decrease of the mitochondrial -potential and -free calcium, as shown by simultaneous measurements of TMRM and Rhod-2/X-Rhod-1, respectively. Together, my results show that superoxide flashes are a physiological phenomenon linked to mitochondrial metabolism that occurs in all subcellular populations of mitochondria in adult skeletal muscle fibers.

1949-Pos
Mitochondria Function in Arterial Smooth Muscle Cells

Guiling Zhao, W. Jonathan Lederer.
University of Maryland Biotechnology Institute, Baltimore, MD, USA.

Mitochondria are organelles that play a central role in the cellular metabolic regulation of diverse cells including vascular smooth muscle cells. Reactive oxygen species (ROS) produced from mitochondria was reported to activate Ca^{2+} sparks in arterial smooth muscle cells, but the underlying mechanisms are still unclear. This work was designed to investigate the ROS production, mitochondria organization, and the interplay of cellular Ca^{2+} ($[Ca^{2+}]_i$) and mitochondrial Ca^{2+} ($[Ca^{2+}]_{mito}$) with the mitochondrial membrane potential, $\Delta\Psi_{mito}$. Tetra methyl rhodamine methyl ester (TMRM) was used to identify mitochondria in both single arterial smooth muscle cells and intact artery to track $\Delta\Psi_{mito}$, and Di-8-ANNEPS was used as a plasma membrane marker. ROS was monitored by transfecting cpYFP into intact cerebral arteries, and mitochondria Ca^{2+} was tracked using Rhod-2. The spatial organization of the arterial smooth muscle mitochondria in isolated cells and intact perfused arteries have been examined (Figure). In cannulated cerebral arteries, we have monitored the $\Delta\Psi_{mito}$ with TMRM and local and global Ca^{2+} with fluo 4 simultaneously (Figure). The interaction of ROS, $\Delta\Psi_{mito}$, $[Ca^{2+}]_i$ and $[Ca^{2+}]_{mito}$ will be discussed.

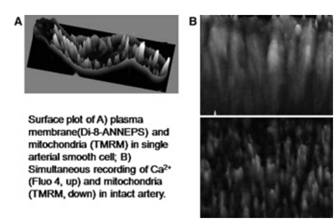

Surface plot of A) plasma membrane(Di-8-ANNEPS) and mitochondria (TMRM) in single arterial smooth cell; B) Simultaneous recording of Ca^{2+} (Fluo 4, up) and mitochondria (TMRM, down) in intact artery.

1950-Pos
Methylglyoxal Increases Mitochondrial Superoxide Production in Rat Colony-Forming Endothelial Progenitor Cells (cf-EPCs)

Caronda Moore, Chun-Hong Shao, Cyrus DeSouza, Keshore Bidasee.
University of Nebraska Medical Center, Omaha, NE, USA.

Endothelial progenitor cells (EPC) play an important role in replenishing the vasculature and its inability will lead to endothelial dysfunction. It is known that endothelium becomes dysfunctional during diabetes and that production of reactive carbonyl species (RCS) increases. What remains undefined is the impact RCS have on the function of EPC. This study was designed to determine effects of the potent RCS methylglyoxal (MGO) on EPC function and viability. Colony-forming EPCs (cf-EPC) were isolated from whole blood of male Sprague-Dawley rats using Ficoll density gradient centrifugation and RT-PCR was used to confirm the presence of cf-EPC markers. After 7 days in culture, cf-EPC (10,000 cells per well) from controls were incubated with MGO for 24 hr at 37°C. Thereafter mitochondrial dehydrogenase activities were determined using the MTT assay. Cf-EPC were isolated from rats overexpressing glyoxalase 1 (AAV2/9-Glo1), the enzyme that degrades MGO. Changes in cytoplasmic Ca^{2+} and mitochondrial superoxide were determined using Fluo-3 and MitoSOX with confocal microscopy. Approximately 2-2.5 million cells were isolated per mL of rat blood. MGO induced a dose-dependent decrease in mitochondrial dehydrogenase activities in control cf-EPC. In cf-EPC from rats overexpressing glyoxalase 1, low concentrations of MGO (5-20 μM) enhanced mitochondrial dehydrogenase activities. Higher

concentrations (30-500 μM) inhibited this activity. Acute exposure of control cf-EPC to 100 μM MGO increased basal cytoplasmic Ca^{2+} and this was followed by an increased production of mitochondrial superoxide. These new data suggest that MGO whose production is increased shortly after the onset of hyperglycemia is inducing cf-EPC demise by mechanisms that involve perturbations in intracellular calcium homeostasis and increased production of mitochondrial superoxide. Overexpression of glyoxalase 1 minimizes the effects of MGO. This work was funded in part by NIH HL085061 and the Nebraska Redox Biology Center.

1951-Pos
Effect of Transient and Permanent Permeability Transition Pore Opening on NAD(P)H Localization in Intact Cells

Eric Fontaine.
Joseph Fourier University, Grenoble, France.

In order to study the effect of mitochondrial Permeability Transition Pore (PTP) opening on NAD(P)H localization, intact cells were exposed to the Ca2+ ionophore A23187. PTP opening, mitochondrial membrane potential, mitochondrial volume and NAD(P)H localization were assessed by time-lapse laser confocal microscopy using the calcein-cobalt technique, TMRM, MitoTracker and NAD(P)H autofluorescence respectively. Concomitant with PTP opening, NAD(P)H fluorescence increased outside mitochondria. These events occurred in all cells and were prevented by cyclosporin A. Mitochondrial membrane potential was not systematically collapsed while mitochondrial volume did not change, confirming that A23187 induced transient PTP opening in a subpopulation of cells, and suggesting that mitochondrial swelling did not immediately occur after PTP opening in intact cells. NAD(P)H autofluorescence remained elevated after PTP opening, particularly after membrane potential had been collapsed by an uncoupler. Extraction of nucleotide for NAD(P)H quantification confirmed that PTP opening led to an increase in NAD(P)H content. Because the oxygen consumption rate decreased while the lactate/pyruvate ratio increased after PTP opening in intact cells, we conclude that PTP opening inhibits respiration and dramatically affects the cytosolic redox potential in intact cells.

1952-Pos
mtDNA T8993G-Augmented Mitochondrial Stresses Upon Mca^{2+} Overload and its Protection by Melatonin in a Narp Cybrid

Mei-Jie Jou.
Chang Gung University, Tao-Yuan, Taiwan.

Mitochondrial DNA (mtDNA) T8993G mutation inhibits specifically mitochondrial F1F0-ATPase (complex V) for severe ATP deficiency and is clinically associated with neurological muscle weakness, ataxia, and retinitis pigmentosa so called NARP mutation. At present, detail T8993G-associated mitochondrial mechanisms as well as its therapeutic strategies are limited. Using time-lapse laser scanning dual fluorescence imaging microscopy, this study investigated T8993G-altered apoptotic mitochondrial pathology particular upon mCa2+ stress and protection by melatonin, previously reported to protect mCa2+ stress-mediated apoptosis (Hsu et al., 2009 JPR in press). In comparison to its parental osteosarcoma 143B and mtDNA less (ρ^0) cells, T8993G induced significant hyperpolarization of mitochondrial membrane potential ($\Delta\Psi$m) and potentiated greatly ionomycin-induced mCa2+ stress. T8993G-augmented mCa2+ stress subsequently elicited rigorously generation of mitochondrial oxygen species (mROS), depletion of cardiolipin (CL) and activation of the mitochondrial permeability transition (MPT). In contract, ρ^0 cells, with much depolarized $\Delta\Psi$m, suffered less mCa2+ stress, mROS formation, CL depletion and the MPT opening. Interestingly, melatonin reduced significantly peak amplitude of the ionomycin-induced mCa2+ transient and antagonized efficiently mCa2+-augmented mROS generation for a reduced depletion of CL and activation of the MPT. In addition, melatonin prevented ''oxidation free mCa2+''-mediated MPT suggesting its direct targeting on the MPT. Melatonin-enhanced tail amplitude of mCa2+ transient possibly due to the reduced MPT-dependent depolarization of $\Delta\Psi$m, however, did not enhance mCa2+ stress-mediated pathology in NARP cybrids possibly as melatonin-elevated mCa2+ improved mitochondrial respiratory. Thus, the administration of melatonin may provide potential improvement for the treatment of mtDNA T8993G-associated NARP syndromes and diseases.

1953-Pos
Visualization of Melatonin's Multiple Mitochondrial Levels of Protection Against Mitochondrial Ca^{2+}-Mediated Permeability Transition and Beyond in Rat Brain Astrocytes

Mei-Jie Jou[1], Tsung-I Peng[2].
[1]Chang Gung University, Tao-Yuan, Taiwan, [2]Chang Gung Memorail Hospital, Kee-lung Meidcal Center, Taiwan.

Melatonin protects cells against oxidative stress-induced apoptosis due primarily to its ability to effectively scavenge pathological condition-augmented generation of mitochondrial reactive oxygen species (mROS). Once produced, mROS in addition to indiscriminately damage mitochondrial components they crucially activate directly the mitochondrial permeability transition (MPT), one of the critical mechanisms for initiating post mitochondrial apoptotic signaling. Whether or not melatonin targets directly the MPT, however, remains inconclusive, particularly during oxidative stress. Thus, we investigated this possibility of an ''oxidation free Ca^{2+} stress'' in the presence of vitamin E after ionomycin exposure as a sole Ca^{2+}-mediated MPT in order to exclude melatonin's primary antioxidative effects as well as Ca^{2+}-mediated oxidative stress. With the application of laser scanning fluorescence imaging microscopy, we visualized for the first time multiple mitochondrial protections provided by melatonin during Ca^{2+} stress in cultured rat brain astrocytes RBA-1. Melatonin, due to its primary antioxidative actions, completely prevented mCa^{2+}-induced mROS formation for a reduced mROS-activated MPT during ionomycin exposure. In the presence of vitamin E, melatonin, significantly reduced cyclosporin A (CsA) sensitive mitochondrial depolarization and MPT during ionomycin exposure suggesting its direct targeting of the MPT. Moreover, when the MPT was inhibited by CsA, melatonin reduced further MPT-independent mitochondrial depolarization and apoptosis suggesting its targeting beyond the MPT. As astrocytes play active role in regulating neuronal pathophysiology, these multiple mitochondrial protections provided by melatonin against mCa^{2+}- and/or mROS-mediated apoptosis may thus be crucial for the future therapeutic prevention and treatment of astrocyte-mediated neurodegeneration in the CNS.

1954-Pos
High-Frequency Photoconductive Stimulation Reveals Central Role of Mitochondrial Permeability Transition Pore in Activity-Driven Neuronal Cell Death

Evgeny Pavlov, R. Carolina Gutiérrez, Yuan Zhang, Audrey C. Kertesz, Ferdinand Joseph Espina, **Michael A. Colicos**.
University of Calgary, Calgary, AB, Canada.

Loss of the ability to regulate calcium is a central event leading to neuronal cell death during a wide range of pathological conditions including stroke and seizure. Here we present a new dissociated hippocampal cell culture model of acute electrical activity which incorporates the photoconductive stimulation of neuronal networks grown on silicon wafers. This technology allows precise modeling of user defined neuronal activity patterns, and the study of their effect on neuronal physiology. Here, seizure-like conditions were created by continuous stimulation, causing hundreds of neurons to fire synchronously at 50 Hz for 4 minutes. This stimulation protocol induced cell death as monitored by propidium iodide staining. The number of dead cells per stimulation region increased from 3.6 $\pm$ 2.1 preceding stimulation to 81 $\pm$ 21 30 minutes following stimulation. Excitotoxicity primarily affected excitatory rather than inhibitory neurons, and was preceded by an increase in intracellular calcium as well as changes in the mitochondrial morphology and membrane potential as measured by a tetramethylrhodamine methyl ester (TMRM) assay. Cyclosporin A (CsA), a mitochondrial permeability transition pore (PTP) blocker, was effective in preventing cell death. We propose that photoconductive stimulation is a useful tool for investigating the pathogenesis of excitotoxicity in vitro.

1955-Pos
Aging Results in Downregulation of Putative Components of mPTP in Human Atria

Anu Gupta[1], Claudia Preston[1], Sulaiman Sultan[1], Viqar Maria[1], Arshad Jahangir[2].
[1]Mayo Clinic, Rochester, MN, USA, [2]Mayo Clinic Arizona, Scottsdale, AZ, USA.

Cardiac vulnerability to injury is increased with aging and is associated with enhanced susceptibility to opening of mitochondrial permeability transition pore (mPTP), a nonspecific high conductance channel in the inner mitochondrial membrane, however the basis for this is not fully understood. The effect of aging on the expression of putative components of mPTP in human myocardium was determined in atrial tissue obtained from elderly (76 $\pm$ 6 yrs) and adult (49 $\pm$ 5 yrs) patients undergoing coronary artery bypass surgery using microarray, Quantitative RT-PCR and Western blot. Aging was associated with a significant reduction in the expression of genes coding for the voltage-dependent anion channel isoforms, *VDAC1*, *VDAC2* and *VDAC3* ,adenine nucleotide translocase (ANT) and Cyclophilin-D (*PPID*) in atria from the elderly patients (Fig A, p<0.01). The expression of

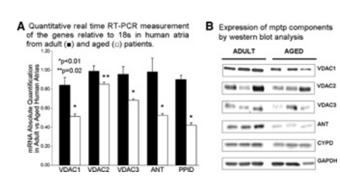

VDAC1 and ANT proteins was significantly reduced ($p<0.05$), while VDAC2, VDAC3 and cyclophillin D were not significantly altered at protein level (Fig B). Downregulation of VDAC1 and ANT expression in the aging human heart may underlie the increased predisposition of the atria to injury during stress.

1956-Pos
Ranolazine Reduces Mitochondrial Tyrosine Nitration During Cardiac Ischemia and Reperfusion Injury
Meiying Yang, Ashish K. Gadicherla, David F. Stowe,
Martin Bienengraeber, Bassam Wakim, Amadou K.S. Camara.
Medical College of Wisconsin, Milwaukee, WI, USA.
Excess superoxide ($O_2^{\bullet-}$) and nitric oxide ($NO^{\bullet}$) generate peroxynitrite ($OONO^-$) during cardiac ischemia-reperfusion (IR) injury. $NO^{\bullet}$ alone may be cardioprotective whereas $OONO^-$ has deleterious effects. Tyrosine nitration by $OONO^-$ may lead to dysfunctional mitochondrial proteins. Ranolazine (RAN), a slow Na^+ channel blocker and anti-ischemic drug, may also attenuate mitochondrial complex I respiratory activity. We tested if the tyrosine nitration of mitochondrial proteins that occurred during IR was reduced when RAN was given just before ischemia. **Method:** Guinea pig hearts were perfused with Krebs -Ringer solution and subjected to one of six treatments: (i) control (no ischemia), (ii) 30 min global ischemia alone, (iii) 30 min ischemia + 10 min reperfusion, (iv) ischemia reperfusion plus RAN given for 10 min before, but not during ischemia, (v) ischemia plus RAN (no reperfusion), (vi) RAN control perfusion (no ischemia). Mitochondria were isolated immediately after each treatment. Tyrosine nitration was measured by Western blotting using 3nitro-tyrosine (3-NT) antibody. **Result:** RAN markedly improved cardiac function. Two bands positioned at about 25 kDa and 15 kDa were 3-NT immunopositive in all experiment groups. Compared to the control, mitochondria after ischemia reperfusion displayed increased 3-NT immunopositivity at the 25 kDa and 15 kDa positions by approximately 100% and 28%, respectively. Treating hearts with RAN before ischemia reperfusion decreased the 3-NT immunopositive 25 kDa band density to non-ischemia levels and the 15 kDa band density to 10% of the ischemia reperfusion alone level. The nitrated proteins require further identification. **Conclusion:** Cardiac injury increases the tyrosine nitration of selected mitochondrial proteins. Inhibition of complex I may underlie the cardiac injury-induced increase in mitochondrial protein tyrosine nitration. This reduction in mitochondrial protein nitration may correlate with the improved cardiac function we observed previously with RAN.

1957-Pos
Modulation of the Mitochondrial Permeability Transition Pore of Cardiac Myocytes by Inorganic Polyphosphate
Lea Seidlmayer[1], Bob Winkfein[2], Lothar A. Blatter[1], Evgeny Pavlov[3],
Elena N. Dedkova[1].
[1]Rush University Medical Center, Chicago, IL, USA, [2]University of Calgary, Calgary, AB, Canada, [3]Dalhousie University, Halifax, NS, Canada.
Background: Inorganic polyphosphate (polyP) is a long polymer made of up to several hundred orthophosphates linked together by phosphoanhydride bonds.Previously we found that polyP of rat liver mitochondria participates in formation of a channel with properties similar to the mitochondrial permeability transition pore (mPTP) suggesting a possible role in pathophysiology. The aim of this study was to investigate the role of polyP in the regulation of mitochondrial Ca homeostasis and Ca-induced opening of mPTP in cardiac myocytes. **Methods:** We used primary cultures of adult rabbit ventricular myocytes with enzymatically reduced levels of mitochondrial polyP achieved by adenoviral expression of polyP hydrolyzing enzyme from yeast (scPPX). Cytosolic Ca ($[Ca]_i$), mitochondrial Ca ($[Ca]_m$), mitochondrial membrane potential, and mPTP activity were measured using the fluorescent dyes indo-1, rhod-2, TMRM, or calcein red, respectively. **Results:** 1) No difference was detected in amplitude, rise and decay time of $[Ca]_i$ transients induced by electrical field stimulation (1 Hz) in control and scPPX expressing intact myocytes. 2) In permeabilized cells under conditions of mitochondrial Ca overload, mitochondrial Ca uptake in control cells was followed by fast Ca release which was prevented by the mPTP inhibitor cyclosporine A. The rate of mitochondrial Ca release was significantly slower in scPPX cells. 3) Similar levels of basal mitochondrial membrane potential were observed in both cell types, however Ca-induced mitochondrial membrane depolarization was more pronounced in control cells. 4) Mitochondria of permeabilized myocytes expressing scPPX were less sensitive to Ca-induced mPTP opening as estimated by the kinetics of calcein red release and the degree of Ca-induced mitochondrial membrane depolarization. **Conclusion:** Our data indicate that reducing of the mitochondrial polyP levels decreases Ca-induced opening of the mPTP in cardiac myocytes.

1958-Pos
Hydroxide Ion Channel Controls Uncoupling and Thermogenesis of Brown Fat Mitochondria
Andriy Fedorenko, Polina Lishko, Yuriy Kirichok.
University of California, San Francisco, CA, USA.
Uncoupling proteins (UCP1- UCP5) are six-transmembrane-domain transport proteins of the inner mitochondrial membrane (IMM). They increase electrical conductance of the IMM, thus dissipating the electrochemical proton gradient across this membrane and uncoupling mitochondrial respiration and ATP synthesis. By controlling mitochondrial membrane potential, UCPs can affect many aspects of mitochondrial function and have been implicated in regulation of body's energy efficiency, reducing fat depositions, thermogenesis, diabetes, and protecting the cell against oxidative damage and ageing. The founding member of the family, UCP1, is specifically expressed in brown adipose tissue (BAT) and is responsible for adaptive thermogenesis mediated by this tissue. Due to its unusually high level of expression, upon activation UCP1 completely uncouples BAT mitochondria and converts the energy of the substrate oxidation into heat. Since UCP1 can dissipate large amounts of energy, it has attracted attention as a potential target to treat obesity. In spite of their physiological and therapeutic significance, the mechanism of operation of uncoupling proteins including their ionic selectivity has long remained unknown due to the lack of direct methods to study their activity in their native membrane environment. Here, by applying the patch-clamp technique to the whole inner membrane of BAT mitochondria and for the first time directly measuring transmembrane currents produced by UCP1, we show that UCP1 is a ligand-gated hydroxide (OH-) ion channel activated by fatty acids. UCP1 is the only hydroxide ion channel reported to date. Thus, BAT thermogenesis involves the outward transport of protons by the electron transport chain along with the outward transport of OH- by UCP1, thereby amounting to cycling of water across the IMM and not to futile cycling of protons as was largely considered before.

1959-Pos
Characterization of an Anion Channel on the Inner Membrane of Heart Mitochondria
Yifan Zhou, Wai-Meng Kwok.
Medical College of Wisconsin, Milwaukee, WI, USA.
Preconditioning is a powerful form of cardioprotection whereby a brief ischemic episode, or a brief exposure to drugs such as volatile anesthetics, can protect the myocardium from a subsequent prolonged ischemia. It triggers an intracellular signaling cascade that leads to the delay in the opening of the mitochondrial permeability transition pore (mPTP). Depolarization of the inner membrane of mitochondria (IMM) can delay mPTP opening. Ion channels have been identified on the IMM that may play key roles in this depolarization. Yet their molecular identities and detailed electrophysiological characterizations have been elusive. In the present study, we recorded ion channel activities on the IMM isolated from guinea pig hearts. Mitoplasts (mitochondria sans the outer membrane) were formed by incubating mitochondria in a hypotonic buffer. The inside-out configuration of the patch clamp technique was utilized. We have identified a channel with a primary conductance of 109 ± 5 pS (n=9) in equimolar 150 mM KCl. The channel exhibited voltage-dependent behavior, with activity being more prominent at positive membrane potentials. When the 150 mM KCl bath solution that corresponded to the mitochondrial matrix side was replaced with 150 mM K-glutamate, channel activity was abolished. When TEA-Cl substituted for KCl, channel activity was not significantly affected. These results suggested an anion channel permeable to chloride. This was confirmed by DIDS (100 μM), a chloride channel blocker, which abolished channel activity. However, bongkrekic acid (100 nM), a specific inhibitor of the mitochondrial adenine nucleotide translocase, failed to inhibit channel activity. In addition, the presence of 2 mM $Mg2+$ in the buffer solution, a concentration that blocks IMAC, the inner membrane anion channel, did not prevent channel opening. Experiments are currently underway to further characterize and identify this anion channel on the IMM.

1960-Pos
Upregulation Leads Bcl2 to Behave as a Mitochondrial Decoy Receptor for Bax
Oscar Teijido Hermida, Laurent Dejean.
New York University, New York, NY, USA.
Cytochrome c release, the commitment step of apoptosis, is regulated at the mitochondria through protein-protein interactions between the Bcl2 family proteins. An imbalance of this interaction network due to the upregulation of the proto-oncogene *Bcl2* leads to a resistance to apoptosis and is associated with tumor formation. Bcl2 overexpression inhibits BAX oligomerization and mitochondrial outer membrane (MOM) permeabilization. However, the molecular

mechanisms through which upregulation of Bcl2 affects earlier steps of BAX-mediated apoptosis are not fully understood. We found that BAX insertion into the MOM was the earliest apoptotic step inhibited by Bcl2 overexpression. Paradoxically, we also found that BAX translocation to the mitochondria was not inhibited but rather spontaneously increased in this same genetic context. This increase in mitochondrial associated BAX required a physical interaction between BAX and Bcl2. We therefore propose that, at least when upregulated, Bcl2 behaves as a 'decoy receptor' which sequestrates BAX at the mitochondria but inhibits its insertion into the MOM, committing the cell to survive.
Supported by NYU Research challenge Funds to LD.

1961-Pos

Compartmentalization of BCL2 Family Proteins Mediated by Organelle Lipid Membranes

Rebecca J. Boohaker, Ge Zhang, Adina Loosley, Kathleen Nemec, Annette R. Khaled.
University of Central Florida, Orlando, FL, USA.

Cancer is defined by a pronounced inhibition of cell death. The BCL2 family of proteins tightly regulates the delicate balance between life and death. One method of regulation is the compartmentalization of antagonistic members. For example, Bax, a pro-apoptotic member of this family, acts as the penultimate factor in the apoptotic cascade by releasing apoptogenic factors such as Cytochrome C from the mitochondrial lumen. The normally cytosolic protein translocates from one internal compartment to another through an elusive mechanism. Individual organelles are defined not only by function (mediated by specific membrane bound proteins), but by the unique composition of their phospholipid membranes. In this work, we have evaluated the contribution of organelle lipids to the localization of of BCL2 proteins.

1962-Pos

In Search of the Structure of MAC in the Mitochondrial Outer Membrane

Pablo M. Peixoto[1], Christian Renken[2], Shefali Haldar[3], Carmen Mannella[2], Kathleen W. Kinnally[1].
[1]New York University College of Dentistry, New York, NY, USA,
[2]Wadsworth Center, Albany, NY, USA, [3]Academy of the Holy Names, Albany, NY, USA.

Several groups have tried to determine the structure of the channel (MAC) formed in mitochondrial outer membranes (OM) of apoptotic cells or in synthetic membranes by Bax and related proteins/peptides, using electron microscopy (EM), atomic force microscopy and x-ray diffraction. Here, pore-like structures ~3-10 nm were handpicked from transmission EM images of uranyl-acetate-stained OMs isolated from control and apoptotic (IL3-deprived) FL5.12 cells. These ''candidate pores'' were aligned by correlation procedures, and class averages defined by principal component and K-means analyses. Main differences in the class averages were (1) the presence of one or more dark (stain-filled) pores, and (2) the nature of white (stain excluding) features around the pores. A class average consisting of a single 3-nm pore with pronounced white rim was rotationally averaged and used as a reference for cross-correlation searches of 50 OM images from control and apoptotic cells. Searches using this 3-nm ''donut'' motif and the same motif doubled in size (6-nm ''donut'') yielded thousands of ''hits'' in both control and apoptotic membranes, which were subsequently aligned and classified as before. The predominant stain-filled structures found with both motifs were not circular but elongated (up to ~4x6 nm), extending away from stain-excluding crescent-shaped features. The radial anisotropy ruled out reference bias and was inconsistent with pores formed by rings of evenly spaced protein subunits. We hypothesize that the different classes of structures detected represent stages in formation of MAC as an increasingly large membrane bilayer defect (or ''cleft'') induced by successive aggregation or clustering of Bax/Bak molecules. A progressive assembly mechanism for MAC has been recently suggested by real-time monitoring of MAC conductances in isolated mitochondria by patch clamping (Martinez-Caballero et al. J Biol Chem 284: 12235-45). Supported by NIH grant GM57249.

1963-Pos

Effects of MAC Formation on Mitochondrial Morphology

Pablo M. Peixoto, Shin-Young Ryu, Robert Range, Kathleen W. Kinnally.
New York University College of Dentistry, New York, NY, USA.

Accumulating literature associate mitochondrial dynamics with apoptosis, since regulation of either process has reciprocal effects. These processes seem to converge in formation of the mitochondrial apoptosis induced channel, MAC, which releases cytochrome c and triggers the degradation phase of apoptosis. While Bax and Bak, core components of MAC, were shown to interact with fusion and fission proteins, some studies also suggest proteins from the intermembrane space could leak to the cytosol and further promote mitochondrial fission during apoptosis. The temporal relationship between apoptosis induction, MAC formation and mitochondrial fragmentation was investigated by time lapse microscopy. MAC function was induced through staurosporine treatment and microinjection of tBid or cytochrome c. MAC formation and mitochondrial dynamics under these conditions were monitored in Hela cells (clone 10) that stably express low levels of GFP-Bax and were transiently transfected with a pDsRed-2 plasmid. GFP-Bax relocation to mitochondria only during apoptosis signals MAC formation, while pDsRed-2 expression shows mitochondrial structure as red fluorescence. Treatment with staurosporine and microinjection with tBid or cytochrome c induced relocation of Bax and collapse of the mitochondrial network. The temporal relationship between these two events was further analyzed. Interestingly, pretreatment with iMAC2, a specific MAC blocker, protected against cell death and prevented mitochondrial fragmentation after tBid injection. Our results suggest a link exists between MAC formation and collapse of the mitochondrial network during apoptosis.
Supported by NIH grant GM57249.

1964-Pos

Mechanism of the Mitochondrial Cytochrome C Release Wave in Bid-Induced Apoptosis

Soumya Sinha Roy, Cecilia Garcia-Perez, Erika Davies, Xuena Lin, György Hajnóczky.
Thomas Jefferson University, Philadelphia, PA, USA.

Bid, a BH3-only Bcl2 family protein, plays a central role in apoptosis. Bid is cleaved by caspase-8 and other enzymes forming tBid that induce mitochondrial outer membrane (OMM) permeabilization and cytochrome c (cyto-c) release. However a mystery remains how Bid synchronizes the function of a large number of discrete organelles, particularly in mitochondria-rich liver or muscle cells. Here we showed that tBid (0.5-50nM) elicited progressive OMM permeabilization and complete cyto-c release with a dose-dependent lag time and rate in H9c2 cell populations. Once started, the OMM permeabilization was not prevented by tBid washout. In contrast, the dose-response for digitonin-induced OMM permeabilization displayed quantal behavior. In single cell imaging studies, permeabilized H9c2 and primary human cardiac cells transfected with cyto-c-GFP showed complete tBid-induced cyto-c-GFP release closely followed by mitochondrial depolarization. The cyto-c-GFP release started at discrete sites and propagated through the mitochondria with a constant velocity and a relatively stable kinetic of release in each organelle. Similar tBid-induced cyto-c-GFP release wave was documented in intact H9c2 cells transfected with tBid. The waves were not dependent on Ca^{2+}, caspase activation or permeability transition pore opening. However, treatment with MnTMPyP, a ROS scavenger or overexpression of mitochondrial superoxide dismutase suppressed the coordinated cyto-c release and also inhibited tBid-induced cell death. On the other hand, both superoxide and hydrogen peroxide sensitized mitochondria to the tBid-induced permeabilization. Thus, tBid engages a ROS-dependent inter-mitochondrial signaling mechanism for spatial amplification of the apoptotic signal by mitochondrial waves.

1965-Pos

Role of Milton Domains in the Calcium-Dependent Regulation of Mitochondrial Motility

Sudipto Das, Gyorgy Hajnoczky.
Thomas Jefferson University, Philadelphia, PA, USA.

The mammalian GRIF1 and OIP106, and the drosophila Milton are kinesin-binding proteins that form a complex with the Miro GTPase, an outer mitochondrial membrane EF-hand protein, to support the movement of mitochondria along the microtubules. Our study demonstrates that in H9c2 cells overexpressing OIP106 or GRIF1, the basal motility of mitochondria is increased, whereas the sensitivity to calcium-induced movement inhibition is decreased. To dissect the interaction between Milton, kinesin and Miro, three different Milton constructs were tested: Milton (1-450), the soluble domain of Milton; Milton (750-1116), lacking the kinesin heavy chain binding site and Milton (847-1116) that lacks additional ~100 amino acid presumably containing part of the Miro binding site. Immunohistochemistry revealed that the overexpressed Milton (1-450) was cytoplasmic, whereas the other two Milton constructs showed mitochondrial localization. The basal mitochondrial motility was increased by Milton (750-1116) but was not altered by Milton (847-1116) or Milton (1-450). A plot of mitochondrial motility against slowly rising cytoplasmic [Ca2+] induced by thapsigargin (2μM), shows that overexpression of Milton (750-1116) significantly reduced the calcium sensitivity of mitochondrial motility reminiscent of OIP106 and GRIF1. By contrast, Milton (847-1116) or Milton (1-450) did not have any effect. The thapsigargin-induced cytoplasmic calcium signal was not affected by any of the Milton constructs. These data indicate that

the C terminus of Milton is an important regulator of the mitochondria associated motors and is involved in conferring the calcium sensitivity from Miro to the motors. Milton 847-1116 is sufficient for the mitochondrial binding, whereas the 750-847 amino acids are critical for the control of calcium sensitivity of mitochondrial motility.

1966-Pos
Biophysical Properties of Mitochondria Undergoing Fusion
Xingguo Liu[1], Orian Shirihai[2], Gyorgy Hajnoczky[1].
[1]Thomas Jefferson University, Philadelphia, PA, USA, [2]Boston University, Boston, MA, USA.
Emerging evidence shows the importance of genes controlling mitochondrial fusion in physiology and their deregulation in neurodegenerative and metabolic disorders. However, apart from $\Delta\Psi_m$, the biophysical properties of the fusion-competent mitochondria remain elusive. To evaluate the conditions of contact formation and fusion, we used organelle-targeted fluorescent proteins, including photoactivatable GFP, which allow tracking of individual mitochondria. In H9c2 cells, almost every mitochondrion is aligned with microtubules that provide the primary tracks for mitochondrial movement. Our results show that ~90% of fusion events involve moving mitochondria. However, fusion occurs irrespective of mitochondrial speed. Furthermore, ~80% of fusion events involve the tip portion of the mitochondrion, whereas only ~50% of these events involve organelle side. Nocodazol, a microtubule disrupting agent that inhibits mitochondrial movements decreases the fusion frequency and changes mitochondrial fusion sites. Strikingly, 80-90% of the physical contacts between adjacent mitochondria did not result in fusion events. To evaluate whether the fusion efficacy depends on the spacing between the outer and inner mitochondrial membranes we used drugs that alter the matrix volume. Valinomycin, a K^+ ionophore that induces matrix swelling evoked a decrease in mitochondrial motility leading to fewer contacts among mitochondria but the number of fusion events was maintained, indicating an increase in fusion efficacy. This change occurred at a low valinomycin concentration (0.25nM) that did not affect $\Delta\Psi_m$ or Opa1 cleavage. Nigericin (0.5μM), a K^+/H^+ ionophore that induces shrinkage of the matrix elicited fusion inhibition and mitochondrial aggregation. Importantly, no motility inhibition or Opa1 cleavage occurred at the same time and the $\Delta\Psi_m$ was increased. These results suggest that mitochondrial fusion is facilitated by mitochondrial motility, the key determinant of the inter-mitochondrial encounter numbers and preferentially involves the front-tip of the moving organelle. In addition, fusion efficacy depends on the mitochondrial matrix volume.

1967-Pos
Mitochondrial Fusion Dynamics in Human Skeletal Muscle-Derived Cells
Veronica Eisner, Gyorgy Hajnoczky.
Thomas Jefferson University, Philadelphia, PA, USA.
Mitochondria have a fundamental role in both muscle physiology and pathology. Mitochondrial fusion and fission are important for energy metabolism, calcium homeostasis and cell death. However, the mechanisms underlying mitochondrial dynamics are poorly understood, especially in physiological models such as skeletal muscle. Here we evaluated mitochondrial fusion dynamics in human skeletal muscle cells (HUSMC). Skeletal muscle satellite cells were isolated from human muscle biopsies and were maintained and differentiated in cell culture. Mitochondrial fusion events were evaluated by confocal imaging of cells expressing mitochondria matrix targeted DsRed and matrix targeted or outer mitochondrial membrane (OMM) targeted photoactivatable-GFP. When we tagged the mitochondria in ~20% of total cellular area with photoactivated-GFP, we found those mitochondria undergoing matrix fusion with a frequency of 1.3 $\pm$ 0.1 events/min/cell (n=70). Among the fusion events, 40% led to complete fusion and only 10% was followed by separation at the apparent fusion site within 20 to 40 seconds. Both complete and transient fusion events resulted mostly from longitudinal mergers, involving end to end interaction or from mergers of adjacent mitochondria in side to side orientation. Furthermore, we found that OMM and matrix fusion are sequential and separable steps, displaying 5.8 $\pm$ 1 seconds gap (n=10). Finally, we evaluated the mitochondrial fusion dynamics in HUSMC derived from both normal and malignant hyperthermia susceptible individuals. At resting state, no significant differences were found in the number of events or in their characteristics. Thus, mitochondrial fusion commonly occurs in HUSMC, and enables mixing of both soluble and integral membrane factors. This process would help to maintain the stability of mitochondrial metabolism. The relatively low frequency of the transient fusion is probably due to the parallel organization of the cytoskeletal tracks for mitochondria and to the limited mitochondrial motility.

1968-Pos
Imaging Interorganelle Contacts and Local Calcium Dynamics at the ER-Mitochondrial Interface
György Csordás[1], Péter Várnai[2], Tünde Golenár[1], Swati Roy[1], George Purkins[1], Tamás Balla[3], György Hajnóczky[1].
[1]Thomas Jefferson University, Philadelphia, PA, USA, [2]Semmelweis University, Budapest, Hungary, [3]National Institutes of Child Health and Human Development, Bethesda, MD, USA.
The local coupling between ER and mitochondria is essential for proper cell function. A main role of the ER-mitochondrial junctions is to provide a local calcium signaling domain that is important both for keeping energy production in line with demand and for the control of apoptotic mechanisms. So far it has not been possible to visualize the tiny ER-mitochondrial contact points in living cells or to monitor the localized $[Ca^{2+}]$ changes in the narrow space between ER and mitochondria ($[Ca^{2+}]_{ER\text{-}mt}$).
Here, we exploited rapamycin-mediated heterodimerization of FKBP12 and FRB domains of fluorescent protein constructs respectively targeted to the outer mitochondrial membrane and the ER as drug-inducible inter-organelle linkers to identify ER-mitochondrial contacts and to measure the $[Ca^{2+}]_{ER\text{-}mt}$. High-resolution fluorescence imaging and 3D reconstruction revealed rapamycin-induced clustering of the ER-targeted fluorescent linker-half to the contact areas with the mitochondria without major changes in the spatial arrangement of the ER. Essentially all mitochondria displayed contacts with the ER in both RBL-2H3 and H9c2 cells. Plasma membrane-mitochondrial contacts were less frequent with ER stacks being inserted between the two organelles. Single mitochondria display discrete patches of ER contacts as well as continuous associations. Cytoplasmic and mitochondrial matrix $[Ca^{2+}]$ showed robust ER-mitochondrial Ca^{2+} transfer with considerable heterogeneity even among adjacent mitochondria. Pericam-containing linkers revealed IP_3-induced $[Ca^{2+}]_{ER\text{-}mt}$ signals that were resistant to buffering bulk cytosolic $[Ca^{2+}]_c$ increases and exceeded 9 uM. The largest $[Ca^{2+}]_{ER\text{-}mt}$ signals did not occur at the tightest associations, indicating space requirements for the Ca^{2+} transfer machinery and functional diversity among ER-mitochondrial junctions.
These studies provide direct evidence for the existence of high Ca^{2+} microdomains between the ER and mitochondria in living cells, and open new possibilities to probe the functional importance of this specialized compartment.

1969-Pos
Dependence of ER-Mitochondria Calcium Transfer on Different IP3 Receptor Isoforms
Tunde Golenar[1], Szava Bansaghi[1], Gyorgy Csordas[1], David I. Yule[2], Suresh K. Joseph[1], Gyorgy Hajnoczky[1].
[1]Thomas Jefferson University, Philadelphia, PA, USA, [2]University of Rochester Medical Center, Rochester, NY, USA.
IP3 receptors (IP3Rs) release Ca2+ from the ER, which is locally relayed to the mitochondria to control several aspects of mitochondrial function. Recent studies have suggested that type 3 IP3Rs (IP3R3) are particularly important for mediating the Ca2+ transfer at the ER-mitochondrial interface. We set out to systematically evaluate the respective role of each IP3R isoform in chicken DT40 cell lines that express only one IP3R isoform (double-knockout, DKO1, DKO2 and DKO3) or provide a null-background (triple-knockout, TKO) for analysis of mammalian IP3Rs and their mutants.
Simultaneous imaging of cytoplasmic and mitochondrial matrix [Ca2+] ([Ca2+]c and [Ca2+]m) was performed in either permeabilized cells challenged with IP3 or in muscarinic receptor overexpressing intact cells stimulated with carbachol (Cch), an IP3-linked agonist. Saturating IP3 evoked complete discharge of ER calcium and resulted in comparable [Ca2+]m increases in each DKO. Furthermore, the Cch-induced [Ca2+]c spike was closely followed by a [Ca2+]m rise in each DKO. When TKO cells were rescued with rat IP3R1 or IP3R3, the latter mediated a larger [Ca2+]c transient but the [Ca2+]m increases were very similar for both isoforms. The relationship between the [Ca2+]c peak and the corresponding [Ca2+]m response was also very similar for IP3R1 and IP3R3. To assess the impact of the release kinetic through IP3R1 in the mitochondrial Ca2+ transfer we used two point mutants of the IP3R1, which display either enhanced inhibition by Ca2+ (D426N) or are relatively insensitive to Ca2+ inhibition (D442N). D426N showed dampened [Ca2+]m signal and [Ca2+]m vs. [Ca2+]c relationship, whereas D442N displayed a steeper [Ca2+]m vs. [Ca2+]c relationship than the wild type IP3R1. Thus, each IP3R isoform can support local ER-mitochondrial Ca2+ transfer and their competence to activate mitochondrial Ca2+ uptake depends on their deactivation kinetic.

1970-Pos
Mimicking Mitochondrial Cristae Dynamics and the Amyloid - beta (1- 42) Induced Failure of Mitochondrial Cristae. A Study Involving Model Lipid Membranes

Nada Khalifat[1], Nicolas Puff[2], Mariam Dliaa[1], **Miglena I. Angelova[2]**.
[1]Université Paris 6, CDR St Antoine, 75012 Paris, France, [2]Université Paris 6, Matière et Systèmes Complexes CNRS UMR 7057, Université Paris 7, 75205 Paris, France.

Number of studies showed, in the case of Alzheimer's disease, abnormalities in the oxidative metabolism of mitochondria, reduced ATP production, and, mitochondrial damage (broken *cristae*), which were related, amongst others, to the excessive presence of Amyloid-beta peptide in mitochondrial *cristae*. Surprisingly, the mechanisms relating the accumulation of Amyloid-beta in the *cristae* with the large number of mitochondria with broken *cristae* was even not evoked, never mind that it is widely recognized now that mitochondria function and morphology are coupled. In our previous work (Khalifat *et al*., 2008, Biophys J 95:4924), using giant unilamellar vesicles (GUVs) for modeling mitochondrial inner membrane, we offered some original insights into the factors that determine the dynamical tubular structures of the mitochondrial inner membrane *cristae*. Furthermore, we suggested a theoretical model (Fournier *et al*., 2009, Phys Rev Lett 102:018102) for elucidating the physical background of a particular membrane instability - membrane tubule formation, triggered by modulation of local pH. In the present work, using GUVs in a similar manner, we show directly (using video-microscopy) that Amyloid-beta might itself cause brutal rupturing of the model lipid membrane and make cristae-like morphology fail. Using large unilamellar vesicles we showed as well that the Amyloid-beta induces membrane dehydration and rise of membrane viscosity. Our hypothesis is: the failure of mitochondrial inner membrane morphology might be due to very basic and purely physical mechanism - the deterioration of mechanical (visco-elastic) properties of the lipid membrane. Thereby, the local strain created during *cristae* formation could provoke the inner membrane rupture. In other words, the Amyloid-beta (1-42) could induce the lipid bilayer incapacity to support the dynamics of shape changes underlying (and inherent to) mitochondrial inner membrane normal functioning.

1971-Pos
Mitochondria Structure and Function Matures During Mammalian Cardiac Development

Jennifer Hom, Quintanilla Rodrigo, Bentley Karen, George A. Porter Jr.
University of Rochester Medical Center, Rochester, NY, USA.

The adult heart requires a precise coupling between oxidative metabolism, excitation and contraction to provide sufficient energy for each heart beat. In contrast, the early embryo, due to the hypoxic environment in utero, generates energy mainly through anaerobic glycolysis. Although the heart is the first organ to become functional in the embryo, ensuring effective circulation and embryonic survival by the mid-embryonic period, little is known about mitochondria as the embryonic heart matures. To investigate the role of energetics and mitochondrial biogenesis during murine cardiac development, we examined mitochondrial structure and function in whole hearts and cultured myocytes harvested throughout the embryonic period. Primary culture of embryonic ventricular myocytes at embryonic day (E) 9.5 displayed less mitochondrial mass and mitochondria that were shorter in length and less organized, as they did not associate closely with the contractile apparatus and resided primarily around the nucleus and cell periphery. Compared to E9.5, E13.5 ventricular myocytes displayed greater mitochondrial mass, and mitochondria that were longer, branched, networked, and more closely associated with the contractile apparatus. Data from whole hearts using multiphoton and electron microscopy confirmed these findings. Functional measurements indicated that mitochondrial membrane potential was higher at E13.5 than at E9.5, suggesting higher mitochondrial activity at later stages of development. Taken together, these data suggest that mitochondrial biogenesis and function may be important in the differentiation of early cardiac myocytes and the maturation of the heart.

1972-Pos
Cyclophilin D Modulates Mitochondrial F_OF_1 ATP Synthase by Interacting with the Lateral Stalk of the Complex

Valentina Giorgio[1], Maria Eugenia Soriano[1], Elena Bisetto[2], Federica Dabbeni-Sala[1], Emy Basso[1], Valeria Petronilli[1], Michael A. Forte[3], Giovanna Lippe[2], **Paolo Bernardi[1]**.
[1]University of Padova, Padova, Italy, [2]University of Udine, Udine, Italy, [3]Oregon Health and Sciences University, Padova, OR, USA.

Blue-native gel electrophoresis purification and immunoprecipitation of F_OF_1 ATP synthase from bovine heart mitochondria revealed that cyclophilin (CyP) D associates to the complex. Treatment of intact mitochondria with the membrane-permeable bifunctional reagent dimethyl 3,3-dithiobis-propionimidate crosslinked CyPD with the lateral stalk of ATP synthase, while no interactions with F_1 sector subunits, the ATP synthase natural inhibitor protein IF1 and the ATP/ADP carrier were observed. The ATP synthase-CyPD interactions have functional consequences on enzyme catalysis, and are modulated by phosphate (increased CyPD binding and decreased enzyme activity) and cyclosporin (Cs) A (decreased CyPD binding and increased enzyme activity). Treatment of MgATP submitochondrial particles or intact mitochondria with CsA displaced CyPD from membranes, and activated both hydrolysis and synthesis of ATP sustained by the enzyme. No effect of CsA was detected in CyPD-null mitochondria, which displayed a higher specific activity of the ATP synthase than wild-type mitochondria. Modulation by CyPD binding appears to be independent of IF1, whose association to ATP synthase was not affected by CsA treatment. These findings demonstrate that CyPD association to the lateral stalk of ATP synthase modulates the activity of the complex.

1973-Pos
PINK1 Deficiency and Mitochondrial Dysfunction in Neurons and Skeletal Myocytes

Zhi Yao, Sonia Gandhi, Helene Plun-Favreau, Nicholas W. Wood, **Andrey Y. Abramov**.
UCL Institute of Neurology, London, United Kingdom.

Mutations in the mitochondrial kinase PINK1 cause a recessive form of Parkinson's disease. Recent studies suggest that PINK1 is important for long term cell survival and mitochondrial function in midbrain neurons by regulating mitochondrial respiration, calcium homeostasis and oxidative stress. We used live fluorescence imaging to examine the effect of PINK1 deficiency on cell metabolism in primary midbrain neurons and skeletal myotubes. We found that basal mitochondrial membrane potential ($\Delta\psi$m) was decreased in PINK1 KO neurons (to $63.7 \pm 4.2\%$, $p<0.001$) compared to wild type (WT). In contrast, the $\Delta\psi$m was increased by $98.7 \pm 40.5\%$ ($p<0.001$) in PINK1 KO myocytes compared to WT. Despite the difference in the level of $\Delta\psi$m, in both PINK1 KO neurons and myocytes, application of oligomycin induced mitochondrial depolarisation, suggesting that $\Delta\psi$m is partially maintained by the hydrolysis of ATP by F_1F_0-ATPases, rather than solely by respiration. Using the luciferin/luciferase assay, we showed that the ATP level was 14.6 ± 2.3 ($p<0.05$) fold higher in the muscle compared to the midbrain, which may explain the selective vulnerability of PINK1 midbrain neurons to disease. Furthermore, the ATP level was 1.8 ± 0.1 ($p<0.05$) fold higher in PINK1 KO muscle compared to WT. We have also assessed the ATP metabolism in PINK1 KO neurons and myocytes, using an indirect measurement of ATP by Mag-fura and confirmed that both the PINK1 KO and WT myocytes exhibit more glycolytic activity than neurons. This accounts for the differences in $\Delta\psi$m between neurons and myocytes, which ultimately contributes to alterations in calcium buffering and cell survival between different cell types. Our results demonstrate that PINK1 deficiency leads to impaired mitochondrial function not only in neurons but also in myocytes. Investigation of different responses in these tissues may lead to further understanding of PINK1 function and Parkinson's disease pathogenesis.

1974-Pos
Thermodynamic Analysis of Protein-Membrane Interactions: The case of Octameric Mitochondrial Creatine Kinase

Malgorzata Tokarska-Schlattner[1], **Uwe Schlattner[1,2]**.
[1]University Joseph Fourier - Grenoble 1, Grenoble, France, [2]ETH Zurich, Zurich, Switzerland.

Mitochondrial creatine kinase (MtCK) is a key enzyme for bioenergetics, membrane topology and possibly also for general organelle morphology. X-ray structural analysis (1), EM (2) and mutational studies with SPR (3,4) revealed that the large MtCK octamers bind to and ''cross-link'' mitochondrial membranes by their two identical top or bottom faces (5). These expose expose four C-terminal basic interaction motifs that interact mainly with acidic cardiolipin (4). This interaction induces cardiolipin-rich domains in the membrane (5,6). However, earlier data point to additional hydrophobic interactions (7,8). Using SPR, we have performed a thermodynamic analysis of the MtCK binding process. Main results were: (i) Affinity of the MtCK-cardiolipin interaction increases with temperature, pointing to a participation of hydrophobic interactions. (ii) Rate constants of two MtCK binding sites identified earlier differed in temperature-dependence. (iii) Thermodynamic parameters revealed that the gain in free energy of MtCK binding mainly depends on the contribution of entropy, possibly due to charge neutralization and release of bound water. These data are consistent with a two-phase model of rapid electrostatic docking of MtCK to cardiolipin, and slower anchoring via a C-terminal hydrophobic MtCK stretch. This would reinforce MtCK membrane interaction, allow integration of this bulky enzyme into the narrow mitochondrial intermembrane space, and contribute to its functional coupling with adenine nucleotide translocator.

1. Eder M et al (2000) Proteins 39, 216.
2. Schlattner et al (2000) Biol Chem 381, 1063.
3. Schlattner et al (2000) J Biol Chem 275, 17314.
4. Schlattner et al (2004) J Biol Chem 279, 24334.
5. Schlattner et al (2009) Biochim Biophys Acta 1788, 2032.
6. Epand et al (2007) J Mol Biol 365, 968.
7. Rojo et al (1991) FEBS Lett 281, 123.
8. Granjon et al (2001) Biochemistry 40, 6016.

1975-Pos
Differential Sensitivity of Sarcomeric and Ubiquitous Isoenzymes of Mitochondrial Creatine Kinase to Oxidative Inactivation
Malgorzata Tokarska-Schlattner, Uwe Schlattner.
University Joseph Fourier - Grenoble 1, Grenoble, France.
Oxidative modifications of creatine kinase (CK) isoenzymes are thought to play a critical role during pathologies involving oxidative stress. Reactive oxygen and nitrogen species (ROS, RNS) not only induce enzymatic inactivation, which occurs with all CK isoenzymes, but also specific damage to the mitochondrial CK isoforms, namely interference with their oligomeric state and membrane binding capacity. Using purified recombinant proteins, cell homogenates and mitochondria isolated from rat heart and brain, we have compared the two isoforms of mitochondrial CK (sarcomeric sMtCK expressed in heart and skeletal muscle, ubiquitous uMtCK expressed in other tissues) in respect to their sensitivity to oxidative inactivation induced by the drug doxorubicin or occurring spontaneously after extraction under non-reducing condition. We confirmed that sarcomeric sMtCK shows significantly higher sensitivity to oxidation and that the loss of total CK activity in heart extracts upon storage under non-reducing condition is mainly due to the inactivation of sMtCK. We could also show that the sMtCK dimer is particularly easily inactivated and that solubilization of sMtCK from membrane (promoting dimerization) makes the protein an especially vulnerable substrate for inactivation. The differential susceptibility of the two MtCK isoenzymes has been related to some differences in their molecular structures (e.g. number and surface exposure of cysteine residues).

Cryo-Electron Microscopy & Reconstruction

1976-Pos
The *Trypanosoma Brucei* Flagellum Reveals Unique and Dynamic Structures of a Nanomachine
Alexey Y. Koyfman[1], Michael F. Schmid[1], Ladan Gheiratmand[2], Htet A. Khant[1], Caroline J. Fu[1], Cynthia Y. He[2], Wah Chiu[1].
[1]Baylor College of Medicine, Houston, TX, USA, [2]National University of Singapore, Singapore, Singapore.
The *Trypanosoma brucei* flagellum is vital for the organism's locomotion, pathogenesis and cell division. It contains a microtubular axoneme, a paraflagellar rod (PFR), and connecting proteins bridging these two structures. Our investigation by cryo-electron tomography revealed a characteristic arrangement of the axoneme internal features: the 9+2 arrangement of microtubule doublets displayed radial spoke spacing not found in other organisms. We have determined that the PFR is a quasi-crystal with a unit cell that repeats every 55 nm along the length of the axoneme. Connecting proteins are attached at 55 nm intervals (the spacing of a PFR repeat) along two of the nine doublets. During flagellar bending, the PFR unit cell axial lengths remain constant while the interaxial angles vary to accommodate the quasi-crystal's expansion and compression. RNAi silencing of one of the major PFR proteins completely abolished the assembly of the PFR, and resulted in defective cell motility. Our tomographic data of this mutated flagellum also showed that the microtubule doublets are not properly arranged within the axoneme. Thus the PFR simultaneously provides structural organization to the axoneme and the flexibility and regulation required for productive locomotion.
Acknowledgements: This research has been supported by NIH grants (P41RR02250, training grant in molecular virology T32AI07471) and Singapore National Research Foundation Fellowship to CYH.

1977-Pos
A Uniique Density at the Portal Vertex of HSV Virions Revealed by Asymmetric Averaging of Subtomograms
Michael F. Schmid[1], Wah Chiu[1], David Bhella[2], Frazer Rixon[2].
[1]Baylor College of Medicine, Houston, TX, USA, [2]MRC Virology Inst., Inst. of Virology, Glasgow, United Kingdom.
The best characterized herpesvirus is the important human pathogen, herpes simplex virus type 1 (HSV-1). The HSV-1 virion comprises 1) an icosahedral capsid which encloses the genome, 2) a surrounding variable proteinaceous layer called the tegument and 3) an enclosing lipid envelope with glycoprotein spikes. The capsid shell has the form of a T=16 icosahedron and has been studied extensively both as an isolated capsid and as the core of the virion. Several proteins have been described as minor capsid components, prominent among which is pUL6. A dodecameric ring of pUL6 proteins forms the portal, which replaces a penton at one capsid vertex. The portal has a central channel and by analogy with tailed bacteriophage, is believed to form the route for transit of the DNA into and out of the capsid. Here we describe a cryo-ET reconstruction of the intact HSV-1 virion that identifies the portal vertex and reveals a previously unsuspected structure that spans the tegument, linking the capsid to the envelope, which we term the ''tegument cylinder''. The position and nature of this structure suggests possible roles in virus assembly or transport.

1978-Pos
Electron Tomography and Molecular Modeling Study of Chemoreceptor Organization
Xiongwu Wu, Peijun Zhang, Cezar M. Khursigara, Sriram Subramaniam, Bernard R. Brooks.
National institutes of Health, Bethesda, MD, USA.
The movement of bacteria in response to external stimuli represents a paradigm of broad general interest for the understanding of mechanisms underlying signal transduction across cell membranes. Bacterial chemoreceptors respond to changes in concentration of extracellular ligands by undergoing conformational changes that initiate a series of signaling events, leading ultimately to regulation of flagellar motor rotation. Atomic structures for several domains of chemoreceptors, including the periplasmic ligand-binding domain, the cytoplasmic signaling domain and the HAMP domain are available, but the molecular architectures of an intact receptor dimer, or the functionally relevant trimer-of-dimer configuration have remained elusive. Here, we have used cryo-electron tomography combined with 3D averaging to determine the *in situ* 3D structure of receptor assemblies in bacterial cells that have been engineered to overproduce only the receptor for serine chemotaxis, Tsr, and lacking all other chemotaxis receptors and signaling components. We identified two major conformations of the chemotaxis receptors. Through comparative modeling and map-constrained molecular dynamics simulations, we obtained the assembly structures of tsr organized in a two dimensional array. We show that receptors are organized in trimer-of-dimer conformations with peripasmic domain, HAMP domain, and signal traction domain transiting between conformations. It is suggested that the position of the ligand binding domain and the HAMP domain play a pivotal role in mediating signal transduction across the cell membrane.

1979-Pos
Combined Approach Towards Automatic Identification of Protein Secondary Structure Elements in Volumetric Data Sets
Zbigniew A. Starosolski, Stefan Birmanns.
University of Texas Health Science Center at Houston, Houston, TX, USA.
Single particle cryo-electron microscopy studies, but also data from tomographic experiments, often result in volumetric 3D reconstructions of low- to intermediate resolution. Although a direct atomic interpretation is not feasible at these levels of detail, one may be able to extract structural information that describes the overall conformation of the molecular system. Especially a detection of secondary structure elements, would aid in a further description of large macromolecular complexes.
On the other hand, the limited resolution often prohibits a clear visual identification of those elements.
We therefore propose a novel algorithmic tool, which is able to annotate automatically volumetric reconstructions and determines the secondary structure elements inside the maps. Our technique is based on a multi-stage analysis: In a first step, a spatial digital path filtering technique is applied, which is able to enhance local features that may characterize helices or sheets.
In a second step those features are extracted by combining the voxel information and modeling the likelihood of the presence of a secondary structure element at the specific location. To evaluate the performance of our algorithm, we have tested it using both, synthetic and experimental maps. The results show that our software is able to successfully annotate even intermediate-resolution maps. In addition, we have combined the before-mentioned algorithmic technique with our visualization system Sculptor. Sculptor provides a user-friendly environment, which enables not only an interactive pre-processing of the volume data, but also an intuitive exploration of the results.
This work was supported by NIH grant R01GM62968, by a grant from the Gillson Longenbaugh Foundation, and by startup funds of the University of Texas Health Science Center at Houston.

1980-Pos

Simultaneous Multicomponent Registration of High-Resolution X-Ray Structures into Electron Microscopy Maps

Mirabela Rusu, Stefan Birmanns.
University of Texas Health Science Center at Houston, Houston, TX, USA.

A structural characterization of multicomponent cellular assemblies is essential to explain the mechanisms governing biological function. Macromolecular architectures may be revealed by integrating spatial information collected from various biophysical sources. For instance, low-resolution electron cryomicroscopy (cryo-EM) reconstructions of entire assemblies can be interpreted in relation with the crystal structures of the constituent fragments. A simultaneous registration of these multiple components is beneficial when building atomic models as it introduces additional spatial constraints to facilitate the native placement inside the map. The high-dimensional nature of such a search problem prevents the exhaustive exploration of all possible solutions. Here we introduce MOSAEC (Multi-Object Simultaneous Alignment by Evolutionary Computing), a method based on genetic algorithms, for the efficient exploration of the multi-body registration search space. MOSAEC employs principles inspired by biological evolution to iteratively optimize a population of candidate solutions. The classic scheme of a genetic algorithm was enhanced with new genetic operations, tabu search and parallel computing strategies and validated on a benchmark of synthetic and experimental cryo-EM datasets. Even at very low level of detail, MOSAEC successfully registered multiple component biomolecules, measuring accuracies within one order of magnitude of the nominal resolutions of the maps, for example 35-40 A.

The present work was supported by NIH grant R01GM62968, a grant from the Gillson-Longenbaugh Foundation, and startup funds from the University of Texas at Houston.

1981-Pos

Integrative Structural Bioinformatics: The Sculptor Modeling Software

Stefan Birmanns.
University of Texas Health Science Center, Houston, TX, USA.

Integrative modeling techniques promise to deliver new insight by fusing data from multiple sources. Especially the docking of atomic models into low- to intermediate resolution volumetric data from cryo-electron microscopy has grown into an established technique over the last decade. In recent years the field has expanded and targets now also macromolecular systems that undergo large-scale conformational changes and models those also using data from various biophysical sources.

Although the results reported so far indicate a wide-spread applicability, the development of integrative modeling techniques on the other hand also leads to new challenges. The size and complexity of the multi-scale data sets is extremely diverse and demands novel strategies not only for the modeling approaches but also regarding pre- and post-processing and visualization. We propose a series of new modeling and analysis techniques, tailored towards handling of heteroneous data sets - heterogeneous in size, level of detail, resolution and conformation. To overcome the challenges, an interactive peak search approach is presented, coarse graining is employed to efficiently model conformational differences, and new programmable graphics cards are used to efficiently render the resulting, time-varying atomic models. The new methods are embedded in an interactive visualization tool termed Sculptor, forming together a flexible, robust and versatile interactive modeling tool. The present report highlights also the overall concept and implementation of Sculptor. Sculptor is freely available from http://sculptor.biomachina.org and can be downloaded as package for Linux, Windows and MacOSX.

This work was supported by NIH grant R01GM62968, by a grant from the Gillson Longenbaugh Foundation, and by startup funds of the University of Texas Health Science Center at Houston.

1982-Pos

Calcium Gating by the DHPR-RyR1 Pair

Montserrat Samso.
Brigham & Women's Hospital/Harvard Medical School, Boston, MA, USA.

In skeletal muscle the L-type voltage-gated calcium channel (DHPR) in the t-tubule coexists in a tight functional interaction with the sarcoplasmic reticulum calcium release channel (RyR1). By means of this interaction a depolarization-induced conformational change in the DHPR is translated into RyR1's opening, and a massive calcium release from intracellular stores. We are performing structural studies on purified DHPRs and RyRs to understand structural details involved in the gating mechanism.

The DHPR is a heteropentamer with total molecular weight of ~450 kDa. Up to now he best structural knowledge has been gained by electron microscopy, although its relative small size has limited the resolution obtained to date. Our new 25Å resolution 3D reconstruction shows two distinct parts: a main body shaped like an irregular pentagon with distinct corners, and a hook-shaped feature. Consistent with the considerable conservation of membrane topology among voltage-gated channels, a good part of the main body can be closely fitted with an atomic structure of a full-length potassium channel, and this in turn is helping to locate the RyR1-interacting domains identified using biochemistry and molecular biology techniques.

The RyR is a large homotetramer of 2.2 MDa, which has facilitated its structural study by 3D cryo-electron microscopy. Its reproducible 3D structure consists of a large cytoplasmic domain and a smaller transmembrane domain. Our 3D reconstructions of RyR1 in the open and closed states at 10 Å resolution show that the ion pathway consists of two right-handed bundles converging into a constriction (putative ion gate) that changes its diameter by ~4Å upon gating. Although the molecular distance between the putative ion gate and the closest site of proximity to the DHPR is very large (>130 Å), the conformational changes associated with gating are generalized, suggesting long-range allosteric pathways connecting these distant domains.

1983-Pos

Ultrastructural Organization of Budding Yeast Septin Filaments Both *in vitro* and *in situ*, Analyzed by Electron Microscopy

Aurelie Bertin, Michael McMurray, Luong Thai, Galo Garcia,
Jeremy Thorner, Eva Nogales.
UC Berkeley, Berkeley, CA, USA.

Septins have been discovered more than 30 years ago as temperature sensitive mutants in budding yeast *Saccharomyces Cerevisiae*. Septins make an hourglass shaped structure of filaments bound to the inner cell membrane. Mitotic budding yeasts express five septins: Cdc3, Cdc10, Cdc11, Cdc12, and Shs1/Sep7. All, but Shs1, are essential for cell division.

Using electron microscopy of negatively-stained samples, *in vitro*, we have observed that the Cdc3-Cdc10-Cdc11-Cdc12 septin complex self-assemble into octameric rods in high salt. At lower ionic strength, septins polymerize into paired filaments. The position and identity of each subunit in the rod has been determined. This analysis revealed a symmetric organization where the different subunits are arranged in the following order: Cdc11-Cdc12-Cdc3-Cdc10-Cdc10-Cdc3-Cdc12-Cdc11. We have also shown that the subunit-subunit interfaces alternate between so called N-C and G interfaces.

To get more insight into septin organization *in situ* we have studied septin-lipid interaction using a lipid monolayer model assay. We have seen that budding yeast septins interact specifically with ($PI(4,5)P_2$). This interaction promotes filament formation and organization, even for mutants or under conditions where septins do not polymerize in solution. This interaction appears to be specifically mediated through Cdc10 and Cdc3.

We have been also analyzed the organization of septin filaments *in situ*, using electron tomography to visualized dividing budding yeast cells. 3D reconstructions of yeast sections were obtained by electron tomography using either freeze substituted samples or cryo-sections (Cemovis). Surprisingly, an array of two sets of perpendicular filaments is present at the bud neck. Cells displaying different types of septin mutations are now being analyzed.

1984-Pos

The Molecular Architecture of Human Low Density Lipoprotein and Bound Receptor Revealed by Electron Cryo-Microscopy

Gang Ren[1], Gabby Rudenko[2], Steven J. Ludtke[3], Johann Deisenhofer[4],
Henry J. Pownall[3], Wah Chiu[3].
[1]University of California, San Francisco, San Francisco, CA, USA,
[2]University of Michigan, Ann Arbor, MI, USA, [3]Baylor College of Medicine,
Houston, TX, USA, [4]The University of Texas Southwestern Medical Center
at Dallas, Dallas, TX, USA.

An elevated plasma level of low density lipoprotein (LDL)-cholesterol is a well-documented risk factor for cardiovascular disease. LDL transfers cholesterol from plasma to liver cells via the LDL receptor (LDLr). LDL is heterogeneous in composition, shape, size, density and charge and is difficult for structural study by X-ray crystallization and NMR. Here, we used electron cryo-microscopy (Cryo-EM) and image analysis to study the structures of LDL and LDL•LDLr complex. We found 1) the reconstructed LDL embedded in vitreous ice is approximated a flattened ellipsoid with planar opposing faces. 2) The reconstructed map of the LDL•LDLr complex was similar to that of LDL in shape and size, but with a ~35-45 Å protrusion attached on the surface. The protrusion matched in size to the LDL receptor beta-propeller domain. 3) The internal density distribution of LDL showed a liquid crystalline core containing three similarly sized internal high density ''isthmi''. 4) The LDL high-density regions that correspond to the apo B-100 appear as a pair of paddles connected at one end of the particle by a linker region with three separate long semicircular ''fingers'' extending from each edge of the linker region to wrap around the particle. These results allowed us to propose an architecture

model of LDL, in which the core CE molecules arranged in stacks with their sterol moieties side-by-side in the higher density regions and the fatty acyl chains extending from either side. These stacks of acyl chains in the CE core are directed outward towards the amphipathic beta-sheet domains on the top and bottom faces of the particle and are surrounded by a semicircle of flexible amphipathic alpha-helix rich domains, which is important to maintaining the structural integrity, and thus functionality, of normal LDL.

1985-Pos
Statistical Analysis and Deblurring of Class Averages in Single-Particle Electron Microscopy
Wooram Park[1], Dean R. Madden[2], Daniel N. Rockmore[3], Gregory S. Chirikjian[1].
[1]Department of Mechanical Engineering, Johns Hopkins University, Baltimore, MD, USA, [2]Department of Biochemistry, Dartmouth Medical School, Hanover, NH, USA, [3]Departments of Mathematics and Computer Science, Dartmouth College, Hanover, NH, USA.
In single-particle electron microscopy, the electron dose is limited to avoid damaging the specimen. This results in images with low signal-to-noise ratios (SNR). Class averaging techniques are used to enhance the low-SNR electron micrograph images. A class is defined as a collection of projection images taken along nominally identical projection directions. The images in each class are aligned and averaged in order to cancel or reduce the background noise. The class-averaged images with high-SNR can be used for more accurate three-dimensional reconstruction in single-particle electron microscopy. However, errors in the alignment process are inevitable due to noise in electron micrographs. This error results in blurry averaged images. Using the mean and variance of the background noise that is assumed to be Gaussian, we derive equations for the mean and variance of translational and rotational misalignments in the class averaging process. Furthermore, the blurring function representing the distribution of the misalignments is estimated using a Gaussian with the computed mean and variance of the misalignments. The blurring process in class averaging is formulated as convolution of an underlying clear image with the blurring function. We propose a deconvolution method to estimate the underlying image using the Fourier analysis in the appropriate domain. This deconvolution method is applied to artificial and experimental electron micrographs. The deburred class averages are assessed quantitatively and qualitatively.
This work was supported by NIH Grant R01GM075310 ''Group-Theoretic Methods in Protein Structure Determination.''

1986-Pos
Determining Orientation in Cryoem Single Particle Analysis
Regis A. James, Steven J. Ludtke.
Baylor College of Medicine, Houston, TX, USA.
In CryoEM single particle analysis, images are recorded of individual molecules or macromolecular assemblies in the 10-100 nm size range embedded in vitreous ice. These images approximately represent a projection of the electron density of the specimen. Due to dose limitations, these images are extremely noisy, with spectral signal-to-noise ratios generally peaking at less than 1. To perform a 3D reconstruction from such images, the orientations of all of the thousands of particle images must be accurately determined. The most common strategy for accomplishing this task is iterative projection matching, meaning that the accuracy and resolution of the structure are limited by the similarity metric used to assess the similarity of each particle image vs. a set of projection references. A wide range of metrics has been used for this purpose, such as correlation coefficient, phase residual and Fourier ring correlation, with variants in application of each. Each of these methods represent a tradeoff in sharpening the orientation vs. decreasing the probability of making a noise-based, rather than a data-based decision. We present a thorough comparison of a number of different similarity metrics when applied to particles with varying noise levels and symmetries.

1987-Pos
High-Throughput, High-Resolution Cryoem Structural Analysis of Helical Assemblies of Biological Macromolecules Toward Atomic Resolution
Takashi Fujii, Takayuki Kato, Keiichi Namba.
Graduate School of Frontier Biosciences, Osaka University, Suita, Japan.
We report structures of helical assemblies of biological macromolecules at near atomic resolution obtained by electron cryomicroscopy. These structural analyses were completed within a week. One of the factors that enabled such high-throughput, high-resolution analyses is the use of a CCD detector instead of film. Since the modulation transfer functions of CCD detectors are significantly worse than those of films, high-resolution image data are too poor to attain atomic resolution if conventional magnifications are used. The resolution of 3D image reconstructions from data collected at a magnification of 88000 was limited to ~7 Å. However, the higher magnification of 170000 solved this problem. We have reached 3.8 Å resolution for the stacked disk aggregate of TMV coat protein. The density map clearly shows the main chain and large side chains. The only disadvantage with high-magnification imaging is a small image area of CCD, making the data collection efficiency lower. However, CCD imaging is still fast enough to allow high-throughput analysis. The other factors include the thickness of vitreous ice film embedding specimen particles and the specimen temperature, both of which affect image contrast. We improved the quick-freezing method to optimize ice thickness. We also found that images recorded at ~50 K have ~1.6 times higher contrast than those at 4 K. By improving these factors in further technical development, we believe we should be able to achieve atomic resolution within a week from data collection to image analysis.

1988-Pos
SONICC: A Novel Nonlinear Optical Detection Technique for 2D Celluar Crystallography
Fei Guo, Ellen Gualtieri, Garth Simpson, Wen Jiang.
Purdue University, West Lafayette, IN, USA.
2D crystallization is one of the most powerful methods to study the structure and function of membrane proteins in their native lipid bilayer environment, yet obtaining high resolution diffraction protein crystals is the most difficult and time consuming step. Traditional techniques for protein crystal detection mostly depend on optical microscopy and the birefringence property of crystals. This situation becomes even more difficult for 2D crystallization because a negative stain check on electron microscope is required which makes it nearly impossible for high-throughput screening. Recently, UV spectroscopy has also been applied to distinguish protein crystals from salt ones. However, all these methods has detection limit which depends on the crystal size and crystallization condition. The Second Order Nonlinear Imaging of Chiral Crystals (SONICC) therefore is developed to overcome this difficulty. SONICC could selectively detect large or small non-centrosymmetric 2D and 3D protein crystals (<1um) with high signal noise ratio. Using this method, we successfully detected purple membrane (ie 2-D crystal of bacteriohrodopsin). We could even detect the crystal patch in a single living H. Salinarium R1 cell. By removing retinals from purple membrane, the signal dramatically decreased (~5 fold) due to the distortion of the crystalline order and the absence of pigment. Considering the difficulty of growing 2D membrane crystals, SONICC not only solved the current detection limitation, but also provided a new opportunity for direct detection membrane crystals in situ formed naturally or artificially by overexpression.

Molecular Dynamics I

1989-Pos
Membrane Diffusion of Tethered DPPC and Tethered PIP3-Bound Protein Systems
Michael G. Lerner, Richard W. Pastor.
NIH/NHLBI, Rockville, MD, USA.
We have used molecular dynamics simulations to investigate the diffusion of tethered proteins in lipid bilayers. Coarse-grained (CG) models of DPPC dimers were simulated in a DPPC bilayer with the MARTINI model, and single-lipid diffusion constants compared to those obtained for dimers at various tether lengths. The ratio of diffusion constants matches well with both experimental results and theoretical predictions of a simple bead model. CG models of pleckstrin homology domain (PH) bound to a lipid with a PIP_3 (phosphatidylinositol (3,4,5)-trisphosphate) head group were then constructed and compared for the monomer, tethered dimer, and tethered trimer cases.

1990-Pos
Quantifying Correlations Between Allosteric Sites in Thermodynamic Ensembles
Christopher L. McClendon[1], Gregory Friedland[2], Matthew P. Jacobson[1].
[1]University of California San Francisco, San Francisco, CA, USA, [2]Sandia National Laboratories, Joint Bioenergy Institute, Emeryville, CA, USA.
Allostery describes altered protein function at one site due to a perturbation at another site. One mechanism of allostery involves correlated motions, which can occur even in the absence of substantial conformational change. We present a novel method, ''MutInf'', to identify statistically significant correlated motions from equilibrium molecular dynamics simulations. We quantify correlated motions using a mutual information metric, which we extend to incorporate data from multiple short simulations and to filter out correlations that are not statistically significant. Applying our approach to uncover mechanisms of allostery in human interleukin-2 and other proteins, we identify clusters of correlated residues from 50 ns of molecular dynamics simulations (see figure). In

interleukin-2, two of the clusters with the strongest correlations highlight known cooperative small-molecule binding sites and show substantial correlations between these sites. We also present a newer approach based on the Kullback-Leibler divergence, an information-theory metric that quantifies population shifts and perturbations to the free energy landscape. Since these approaches identify pairs of residues with correlated conformations in an unbiased, statistically robust manner, they should be useful tools for finding novel or ''orphan'' allosteric sites in proteins of biological and therapeutic importance.

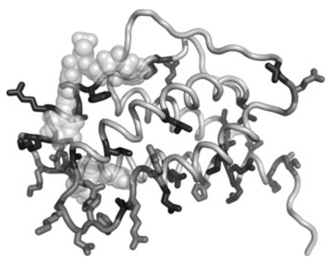

1991-Pos
Influence of Organic Solvents on the Structure and Enzymatic Activity of Haloalkane Dehalogenase DhaA
Morteza Khabiri.
Institute of systems biology and ecology, Nove Hrady, Czech Republic.
Organisms with the ability to degrade anthropogenic chemicals are using for this purpose haloalkane dehalogenases. Hereby, a active site nucleophile attacks a carbon atom of the halogenated substrate, leading to cleavage of the carbon-halogen bond, displacement of a halide and formation of a covalent alkyl-enzyme intermediate that is subsequently hydrolyzed. The haloalkane dehalogenase DhaA from Rhodococcus rhodochrous NCIMB13064 is enzymatically active for a broad range of halogenated substrates including 1,2,3-trichloropropane (TCP) (2) and sulphur mustard (3), some of them with high hydrophobicity and low solubility in water. Improving the solubility by addition of water miscible co-solvents like dimethyl sulfoxide (DMSO) to the reaction mixture could be a way to enhance the range of potential applications for these enzymes. Therefore, in the present study we investigate effects of DMSO on structure and dynamics of DhaA using molecular dynamics (MD) simulations demonstrating that the DMSO molecules penetrate to the active site of protein and compete with the halogentaed substrate for the catalytic site histidine272. On the other hand, histidine 272 traps DMSO and thus prevents further progress of DMSO deeper into the active site. With respect to protein solubility, interactions of DMSO with the protein surface decrease the solvation energy of the protein compared to protein in pure water. However, the enzyme is clearly stable in up to 42% DMSO and we can conclude that the enzyme activity is expected to be less than in pure water, however retained.

1992-Pos
Characterizing Structure and Activity of Subtilisin Enzyme in Nonaqueous Media with Molecular Dynamics Simulations
Eugene Auh, Sihyun Ham.
Sookmyung Women's University, Seoul, Republic of Korea.
Structural and dynamical behaviors of enzyme are critical for determining its catalytic activity. Knowing that the enzyme activity may vary with different solvent polarity due to the changes in enzyme structure and flexibility, Subtilisin Carlsberg enzyme was subjected to investigate the structural variation upon different solvent systems by using molecular dynamics simulation with explicit solvents. Characterization of the structure and activity focusing on the hydration of the active site will be discussed with the effects of crystallographic water bound to the active site of this enzyme and with the solvent effects.

1993-Pos
Influence of dsDNA Architecture on Diffusion Properties in Networks
Renat N. Khaliullin[1], **Jay D. Schieber[1]**, Jorge A. Iniguez-Lluhi[2].
[1]Illinois Institute of Technology, Chicago, IL, USA, [2]University of Michigan Medical School, Ann Arbor, MI, USA.
DNA is an essential element for genetic disease treatments. Its application depends on the diffusive properties of DNA through tissues. Although, there are works on linear DNA diffusion in a network environment, the dependence of the diffusion coefficient on chain architecture is not completely understood.
In this work we study dsDNA molecule behavior in a network with the discrete slip-link model. We show dependence of the diffusion coefficient on the chain molecular weight and network mesh size. We compare theoretical predictions with experimental measurements of linear dsDNA thermal diffusion in agarose gels. To analyze the influence of the architecture of the DNA molecule on its diffusion properties, the theory can be applied to star-shaped molecules. However, to obtain experimental data it requires to synthesize a well characterized star-shaped dsDNA molecule.

1994-Pos
Electric Field Effects on Water and Water-Vacuum Interfaces in Molecular Dynamics Simulations
Jane HyoJin Lee[1], Zachary A. Levine[2,3], P. Thomas Vernier[4,3], Mayya Tokman[1], Michael E. Colvin[1].
[1]School of Natural Sciences, University of California, Merced, Merced, CA, USA, [2]Department of Physics and Astronomy, University of Southern California, Los Angeles, CA, USA, [3]MOSIS, Information Sciences Institute, Viterbi School of Engineering, University of Southern California, Marina del Rey, CA, USA, [4]Ming Hsieh Department of Electrical Engineering, Viterbi School of Engineering, University of Southern California, Los Angeles, CA, USA.
Understanding the behavior of water in atomic-scale detail is essential to explaining the microscopic dynamics of such phenomena as electroporation, electrospinning, electrospraying, and electric-field-driven evaporation. In this study we employ molecular dynamics simulations to investigate water-vacuum systems under the influence of an externally imposed electric field. SPC and SPC/E water models are used to describe nanodroplets and interlaced water-vacuum slab configurations. The dynamics of these systems is studied in detail with respect to the strength of the applied electric field, and we note the importance of a proper representation of long-range electrostatics in the simulations. Water behavior is analyzed from both structural and energetic points of view. We discuss how such characteristics as the system geometry, local water density, and water molecular dipole orientation change as the electric field is increased. These changes are described in the context of interplay between pressure, surface tension, and electrodynamic dipole-field and dipole-dipole interactions. For example, we find that for nanodroplets containing ~900 water molecules there is a critical electric field strength above which there is a jump in the alignment between the water dipole and the field. Concomitant with the dipole alignment is a distortion of the droplet shape from a sphere to a prolate ellipsoid oriented along the electric field. We also study formation of small-scale structures at the water-vacuum interface in both droplet and slabs configurations and investigate the relationship between these structures and a subsequent creation of pore-like bridges between the water slabs in the water-vacuum-water systems.

1995-Pos
A Molecular Dynamics Simulation Study of the 9_25-11 Dnazyme
Walter R. Scott, Jason Thomas, David M. Perrin.
University of British Columbia, Vancoiver, BC, Canada.
DNAzymes (catalytic DNA) have recently attracted increased research interest with an eye towards applications as therapeutic agents and biosensors, among others. Advantages over proteins include an increased resistance to hydrolysis and cost-effective production.
Most DNAzymes recruit divalent metal ions as cofactors, however D.M. Perrin and coworkers have recently synthesised a M2+-independent, multiple turnover DNAzyme (Dz9(25)-11 by the inclusion of two kinds of modified nucleotides (8-histaminyl-dA and aminoallyl-dU in place of dA and dT, respectively) which afford enhanced catalytic rates that are attributed to the roles of electrostatic (cationic amine) catalysis as well as both general base and general acid catalysis (imidazoles). In this regard, Dz9(25)-11 functions as a sequence specific RNaseA mimic.
The use of DNAzymes in a number of applications notwithstanding, structural and dynamic information about DNAzymes in general is scarce compared to proteins. Moreover there is no X-ray structure of Dz9(25)-11, however, D.M. Perrin and coworkers have conducted a site-directed chemical study from which proximity information between specific nucleotides can be inferred.
Here, this information is incorporated into an atomistic, fully solvated model of Dz9(25)-11using the GROMOS96 biomolecular simulation package. The structure, dynamics and putative function of the DNAzyme is discussed in light of the simulation results.

1996-Pos
Oxidative Damage in Lipid Bilayers: A Reactive Molecular Dynamics Study
Joseph Fogarty, Sagar Pandit.
Univeristy of South Florida, Tampa, FL, USA.
Current simulations of lipid bilayers focus on their structural and compositional properties. Chemical reactivity between cell membranes and extra cellular species is an unexplored field for molecular dynamics. To explore this new area of research, we have simulated a lipid bilayer composed of 200 POPC lipids (along with 50 waters per lipid) and its reaction with a simple peroxide for 8 ns using Reactive Molecular Dynamics (Purdue Reax). The specific chemical pathways of oxidative damage can be determined from these simulations and a greater insight into the process can be achieved.

1997-Pos
Life Cycle of an Electropore: A Molecular Dynamics Investigation of the Electroporation of Heterogeneous Lipid Bilayers (PC:PS) In the Presence of Calcium Ions
Zachary A. Levine[1,2], Matthew J. Ziegler[3,2], P. Thomas Vernier[4,2].
[1]Department of Physics and Astronomy, University of Southern California, Los Angeles, CA, USA, [2]MOSIS, Information Sciences Institute, Viterbi School of Engineering, University of Southern California, Marina del Rey, CA, USA, [3]Mork Family Department of Chemical Engineering and Materials Science, Viterbi School of Engineering, University of Southern California, Los Angeles, CA, USA, [4]Ming Hsieh Department of Electrical Engineering, Viterbi School of Engineering, University of Southern California, Los Angeles, CA, USA.
To aid in understanding the mechanism of electric field-driven pore formation in lipid bilayers, we propose a scheme for characterizing the life cycle of a transient membrane electropore, from the formation of the initial defect to the restoration of the intact bilayer. We apply this analysis to heterogeneous phospholipid bilayers (phosphatidylcholine:phosphatidylserine, PC:PS) in the presence of calcium ions. Previous reports of molecular dynamics (MD) simulations of similar PC:PS systems containing $Ca2+$ [1,2] are consistent with experimental observations [3]. In this study we assembled systems containing varying amount of PC, PS, and $Ca2+$ and observed how long it took each bilayer to porate after the application of an electric field. We also measured the effect of $Ca2+$ on pore lifetime (the time it takes to restore the porated bilayer after removal of the electric field). We find that systems containing $Ca2+$ are more difficult to electroporate, and that this effect is magnified in systems containing PS. We also observe that $Ca2+$ has little effect on pore lifetime, but that PC:PS systems have shorter lifetimes than pure PC systems. Finally, we report binding isotherms for $Ca2+$ and PC:PS bilayers, an additional metric for the validity of phospholipid bilayer simulations containing calcium.
[1] Bockmann, R. A., and H. Grubmuller. 2004. Multistep binding of divalent cations to phospholipid bilayers: A molecular dynamics study. Angewandte Chemie-International Edition 43:1021-1024.
[2] Vernier, P. T., M. J. Ziegler, and R. Dimova. 2009. Calcium binding and head group dipole angle in phosphatidylserine-phosphatidylcholine bilayers. Langmuir 25:1020-1027.
[3] Sinn, C. G., M. Antonietti, and R. Dimova. 2006. Binding of calcium to phosphatidylcholine-phosphatidylserine membranes. Colloids and Surfaces A-Physicochemical and Engineering Aspects 282:410-419.

1998-Pos
Molecular Dynamics Study of the Interaction of HHC-10 with the Mixed POPG/POPE Membrane
Mostafa NateghолEslam[1], Bryan Holland[1], Bruno Tomberli[2], Chris G. Gray[1].
[1]University of Guelph, Guelph, ON, Canada, [2]Brandon University, Brandon, MB, Canada.
The documented selectivity [A.Cherkasov et al, ACS Chem. Biol., 4, 65, (2009)] for disrupting bacterial membranes as opposed to mammalian membranes exhibited by many cationic antimicrobial peptides (CAPs) is poorly understood. Molecular dynamics simulations are a useful tool for exploring the underlying molecular mechanisms for this selectivity [I. Tolokh et al, 80, 031911, (2009).]. The interaction of the cationic peptide HHC-10, a novel antimicrobial peptide recently designed through a neural network investigations of large families of antimicrobial peptides, is studied when in the vicinity of a pure POPC (mammalian model) membrane and mixed POPG/POPE (bacterial model) membrane. Non-equilibrium methods are used for performing the molecular dynamics simulations and for obtaining the PMF of the interaction along the reaction coordinate of interest, namely the distance from the center of the mass of HHC-10 peptide with the outer leaflet of the membrane.

Computational Methods I

1999-Pos
Multiscale Modeling of PCNA - Ubiquitin Interactions
Ivaylo Ivanov[1], Adam Van Wynsberghe[2], John A. Tainer[3], J. Andrew McCammon[4].
[1]Georgia State University, Atlanta, GA, USA, [2]Hamilton College, Clinton, NY, USA, [3]The Scripps Research Institute, La Jolla, CA, USA, [4]University of California, San Diego, La Jolla, CA, USA.
Covalent attachment of ubiquitin (Ub) to proliferating cell nuclear antigen (PCNA) plays a crucial role in translesion synthesis (TLS). However, structural knowledge of the complex between Ub and PCNA is currently lacking. The problem is important from a biological perspective since ubiquitinated PCNA is involved in the recruitment of specialized lesion bypass polymerases. A loss of regulation of TLS and other damage-avoidance pathways can lead to a variety of cell fates including apoptosis and uncontrolled cell growth. We have modeled the Ub-PCNA complex using a combination of tethered Brownian dynamics (TBD), protein-protein docking with RosettaDock, flexible loop modeling with ModLoop, and molecular dynamics(MD). The TBD simulations were used to generate a large ensemble of electrostatically and geometrically favorable configurations, subsequently used as a starting point for local docking searches. The final models were refined with all-atom explicit solvent MD simulations. Ubiquitin was found to bind in a groove on the PCNA surface directly above the PCNA subunit interface. A mutation originally identified in genetics screens (pol30-113) and known to interfere with TLS, is positioned directly beneath the bound ubiquitin in our models. Thus, the results provide unexpected insight into previously unexplained biological observations.

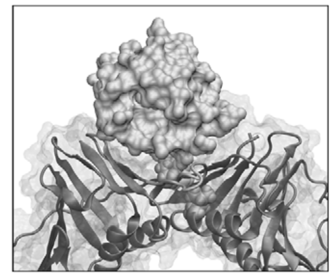

2000-Pos
Adaptive Anisotropic Kernels for Nonparametric Estimation of Absolute Configurational Entropies in High-Dimensional Configuration Spaces
Ulf Hensen[1], Helmut Grubmüller[1], Oliver F. Lange[2].
[1]Max-Planck-Institute for Biophysical Chemistry, Goettingen, Germany, [2]Department of Biochemistry, University of Washington, WA, USA.
The quasiharmonic approximation is the most widely used estimate for the configurational entropy of macromolecules from configurational ensembles generated from atomistic simulations. This method, however, rests on two assumptions that severely limit its applicability (i) that a principal component analysis yields sufficiently uncorrelated modes an (ii) that configurational densities can be well approximated by Gaussian functions. In this paper we introduce a nonparametric density estimation method which rests on adaptive anisotropic kernels. It is shown that this method provides accurate configurational entropies for up to 45 dimensions thus improving on the quasiharmonic approximation. When embedded in the minimally coupled subspace framework, large macromolecules of biological interest become accessible, as demonstrated for the 67-residue coldshock protein.

2001-Pos
Construction of Energy Based Protein Structure Networks: Application in the Comparative Analysis of Thermophiles and Mesophiles
Mahalingam S. Vijayabaskar, Saraswathi Vishveshwara.
Indian Institute of Science, Bangalore, India.
Thermophilic proteins sustain themselves and function at higher temperatures. Despite their structural and functional similarities with their mesophilic homologues, they show enhanced stability. Various comparative studies at genomic, protein sequence and structure levels, and experimental works highlight the different factors and dominant interacting forces contributing to this increased stability. In this comparative structure based study, we have used interaction energies between amino acids, to generate structure networks called as Protein Energy Networks (PENs). The interaction energy is the averaged sum of the Lennard-Jones and the Coulombic energies, over an equilibrium ensemble of conformations. The PENs are used to compute network parameters like largest connected component, clusters, cliques, communities and hubs. These parameters are then compared between the thermophile-mesophile homologues. The results show an increased number of clusters and low energy cliques in thermophiles as the main contributing factors for their enhanced stability. Further more, we see an increase in the number of hubs in thermophiles. We also observe no community of electrostatic cliques forming in PENs of both thermophiles and mesophiles. In summary, we have developed protein structure networks based on non-covalent interaction energies between amino acids. These networks are then exploited to identify the factors responsible for enhanced stability of thermophilic proteins, by comparative analysis. We were able to point out that the sub-graph parameters are the prominent contributing factors and also that the thermophilic proteins have a better packed hydrophobic core. We have also discussed how thermophilic proteins, although increasing stability through higher connectivity, retain conformational flexibility, from a cliques and communities perspective.

2002-Pos
A New, Fundamental Multiscale Modeling Framework Based on the Relative Entropy
M. Scott Shell, Aviel Chaimovich.
University of California Santa Barbara, Santa Barbara, CA, USA.
Our understanding of biology stems from models at many resolutions, as we seek from detailed atomic-scale interactions simpler emergent physical principles to support our understanding and to produce useful theoretical reductions and tractable simulations. In particular, multiscale methods coupling coarse-grained and atomic models are essential to modeling, predicting, and understanding the basic driving forces that operate across many biomolecular length and time scales. Yet, though coarse-graining strategies exist, it has been challenging to identify universal approaches to the multiscale problem that build systematic, quantitative connections between atomic interactions and reduced models.
We have created a powerful, rigorous theoretical framework that addresses this problem. Its focus is the relative entropy, an information-theoretic and statistical-thermodynamic quantity that measures the information lost when moving from a detailed to coarse-grained description of a system. We postulate that the most descriptive physical principles and simple models are those that minimize this quantity, hence minimizing the physical information lost when atomic detail is removed. Importantly, we show that this concept unifies and broadens a number of established statistical-mechanical principles. For the first time, the relative entropy provides a general, systematic framework for multiscale modeling.
A practical benefit is that the relative entropy suggests how to transform atomistic models into reduced ones that capture the same physics, enabling seamless integration of models spanning scales. We describe a family of algorithms that optimize coarse-grained molecular models by minimizing the relative entropy numerically. These coarse-graining algorithms are general to arbitrary models and the first to offer a universal metric for model quality. We describe the application of these algorithms to the development of simple models of water for modeling large-scale association processes driven by hydrophobic interactions, and to models of peptides for interrogating early steps in aggregation.

2003-Pos
Using Statistically Significant Correlated Motions of Residues in a MD Based Approach to Investigate Allostery in Ubiquitin Conjugating Protein
Salma B. Rafi, Christopher L. McClendon, Matthew P. Jacobson.
University of California at San Francisco, San Francisco, CA, USA.
Ubiquitin conjugating proteins (E2s) are an important component of the ubiquitin proteasome pathway. E2s interact with ubiquitin activating enzyme (E1) and ubiquitin ligases (E3s) to transfer ubiquitin to target proteins to mark them for degradation. In some E3s, RING domains act as scaffolds to bind E2s and target proteins so that the ubiquitin can be directly transferred from the E2 to the target protein. This ubiquitin transfer has been shown to be allosterically regulated: E3 RING domain binding to E2 at one site promotes ubiquitin release from the active site cysteine (~15Å distance) without substantial conformational change in E2. Previous studies used statistical coupling analysis (SCA) to identify clusters of residues that might transmit information. Here, we use a novel information-theory approach to identify residues with statistically significant correlated conformations in a set of equilibrium molecular dynamics simulations. From the matrix of correlations between residues, we observed substantial coupling between an E2's active site and its E3 RING domain binding site. However, in the I88A mutant, the pattern of correlations is disrupted, consistent with the experimental observation that this I88A mutation abrogates the allostery in the E2s. Thus, our approach is sensitive enough to identify effects of single point mutations in the protein. Unlike SCA, which infers couplings from many protein sequences, our approach identifies couplings between residues in individual proteins, some of which coincide with residues identified by SCA. As our approach is general and sensitive to small physical-chemical differences in sequence, structure, and dynamics, we can apply our approach to study similarities and differences in the allosteric networks of different E2s in order to better understand how protein degradation is regulated, also providing a mechanistic insight of the process.

2004-Pos
Toward Accurate Simulations of Cu+ - Protein Binding: Computational Studies of Model Systems with a Polarizable Force Field
George Kaminski.
Worcester Polytechnic Institute, Worcester, MA, USA.
Cu+ binding and transport plays an important role in biological processes. It would be advantageous to have the ability to accurately determine their binding affinities via computational means. At the same time, simulation of ions presents a number of fundamental and practical difficulties. We have compared energetic and structural properties of the Cu+ ion complexes with small model molecules. While these simulations without explicit treatment of electrostatic polarization have in some cases lead to more than three-fold errors in the magnitudes of the binding energies, similar calculating with a polarizable force field produced results in good agreement with the available experimental and high-level quantum mechanical data. We believe that this work (a) demonstrates the importance of explicit treatment of the electrostatic polarization in ion-transport and binding simulations and (b) opens a road to accurate *in silico* determination of Cu+ and other ions binding affinities with proteins.

2005-Pos
Simulation Studies of a TRI-PEDAL, Protein-Based Artificial Molecular Motor
Nathan J. Kuwada[1], Gerhard A. Blab[2], Martin J. Zuckermann[2], Paul M.G. Curmi[3], Elizabeth H.C. Bromley[4], Roberta Davies[3], Derek N. Woolfson[4], Nancy R. Forde[2], Heiner Linke[5].
[1]University of Oregon, Eugene, OR, USA, [2]Simon Fraser University, Burnaby, BC, Canada, [3]University of New South Wales, Sydney, Australia, [4]University of Bristol, Bristol, United Kingdom, [5]Lund University, Lund, Sweden.
Though the biological function of many natural molecular motors is fairly well established, many structure-function details responsible for motor performance remain vague or unknown completely. Recently, we have undertaken a new bottom-up approach to understanding biological molecular motors by designing and building an artificial, protein-based molecular motor dubbed the Tumbleweed (TW). The TW is a purely diffusive motor construct consisting of three DNA-binding proteins attached to a designed, protein-based central hub, where directional stepping along a DNA track is maintained by a temporally periodic external chemical supply. To better understand important design and performance characteristics of the TW, coarse-grained Langevin Dynamics (LD) simulations and numerical solutions to the Master Equation (ME) were carried out. The LD approach, which is a single motor simulation, is particularly suitable for exploring the diffusional behavior of the system, where the ME approach, which models an ensemble of motor states, is best suited for statistically exploring the parameter space of the system and the interaction of processes at different time scales. We present results from these two theoretical approaches that illuminate not only important design and experimental considerations, such as motor geometry and track spacing, but also produce unexpected diffusional behavior. Of particular interest is that the addition of certain internal symmetric potentials can increase motor performance. For example, the addition of a non-specific binding potential, symmetric about the DNA track, can double motor speed by replacing some of the 3D diffusional search by a relatively fast 1D diffusional slide along the DNA. This, and other symmetric potential inputs that increase motor performance by subtly amplifying asymmetries in the system, are not only fundamentally interesting but also may be applicable to any molecular motor that incorporates a diffusional search in its stepping cycle.

2006-Pos
Thermodynamic Efficiency Out of Equilibrium
David A. Sivak, Gavin E. Crooks.
Lawrence Berkeley National Laboratory, Berkeley, CA, USA.
Equilibrium thermodynamics satisfactorily explains the efficiency of macroscopic machines, whose operation is posited as a quasi-static, infinite time, zero power process exemplified by the Carnot heat engine. Microscopic biomolecular motors differ markedly from their macroscopic counterparts, as they are subject to large fluctuations, operate far from equilibrium, and by necessity accomplish their tasks in finite time with non-zero power. They thus demand novel non-equilibrium frameworks. We explore thermodynamic length as an analytic framework for understanding the physical limits on biomolecular motors. Thermodynamic length defines the length of a non-equilibrium transformation as the root-mean squared fluctuations of the variables conjugate to the control parameters. It is a natural measure of distance between equilibrium thermodynamic states, but unlike the free energy change explicitly depends on the path taken through thermodynamic state space. Thermodynamic length equips thermodynamic state space with a Riemannian metric and thus facilitates the discovery of minimum thermodynamic length paths, which minimize the dissipation for slow, but finite time, transformations. We derive analytic expressions for Fisher information (related to the derivative of thermodynamic length) in simple bistable energy landscapes, finding that it can vary by several orders of magnitude across a given energy landscape. Our novel dynamic programming approach allows more detailed analysis of these model landscapes, establishing that thermodynamic length analysis accurately predicts the instantaneous dissipation of

far-from-equilibrium processes across the entire energy landscape. We also derive thermodynamic length as a special case of linear response theory, a standard non-equilibrium framework. Thermodynamic length analysis should prove useful in the further analysis of molecular motors, as it gives access to non-equilibrium properties (dissipation) through equilibrium properties (Fisher information and relaxation time).

2007-Pos
A Webserver for Generating Stereochemically-Acceptable Protein Pathways and Movies
Daniel W. Farrell, Kirill Speranskiy, Michael F. Thorpe.
Arizona State University, Tempe, AZ, USA.
We introduce a new, quick method for generating stereochemically-acceptable pathways in proteins, The method, called geometric targeting, is an alternative to the computationally-intensive targeted molecular dynamics approach. Geometric targeting takes as input two distinct protein conformations and produces an all atom pathway between the two states, guided by geometric considerations that will be described. We also present our new webserver for protein pathways. The user submits two protein structures to the webserver, and the geometric targeting method is run automatically to generate a pathway. The webserver also includes tools for visualization of the pathway and downloading of pathway movie files for use in presentations. The strategy behind the geometric targeting method is to take random steps while gradually decreasing the RMSD to the target, and while imposing various geometric constraints to make sure that each snapshot has good stereochemistry. The pathways maintain good covalent bond distances and angles, keep backbone dihedral angles in allowed Ramachandran regions, avoid eclipsed side-chain torsion angles, avoid non-bonded overlap, and maintain a set of hydrogen bonds and hydrophobic contacts. The method does not necessarily produce the optimal pathway, but rather a stereochemically-acceptable pathway. By running multiple times, a collection of random pathways between the two states can be generated. These pathways will be useful for further quantitative analysis, such as to study free energy changes or search for transition states.

2008-Pos
B Cell Affinity Discrimination Requires Kinetic Proofreading
Philippos Tsourkas, Subhadip Raychaudhuri.
UC Davis, Davis, CA, USA.
B cells signaling in response to antigen is proportional to antigen affinity, a process known as affinity discrimination. Recent research suggests that B cells can acquire antigen in membrane-bound form on the surface of antigen-presenting cells (APCs), with signaling being initiated within a few seconds of B cell/APC contact. During the earliest stages of B cell/APC contact, B cell receptors (BCRs) on protrusions of the B cell surface bind to antigen on the APC surface and form micro-clusters of 10-100 BCR/Antigen complexes. In this study, we use computational modeling to show that B cell affinity discrimination at the level of BCR-antigen micro-clusters requires a threshold antigen binding time, in a manner similar to kinetic proofreading. We find that if BCR molecules become signaling-capable immediately upon binding antigen, the loss in serial engagement due to the increase in bond lifetime as affinity increases results in a considerable decrease in signaling with increasing affinity. Adding a threshold antigen binding time for BCR to become signaling-capable favors high affinity BCR-antigen bonds, as these long-lived bonds can better fulfill the threshold time requirement than low-affinity bonds. A threshold antigen binding time of ~10 seconds for BCR to become signaling-capable results in monotonically increasing signaling with affinity, replicating the affinity discrimination pattern observed in B cell activation experiments. This time matches well (within order of magnitude) with the experimentally observed time (~ 20 seconds) required for the BCR signaling domains to undergo antigen and lipid raft-mediated conformational changes that lead to association with Syk.

2009-Pos
Study of the Role of Factor VII in Venous Thrombus Formation Using Combination of a Multiscale Model and Experiment
Mark Alber[1], Zhiliang Xu[1], Joshua Lioi[1], Malgorzata Kamocka[2], Xiaomin Liu[1], Jian Mu[1], Danny Chen[1], Elliot Rosen[2].
[1]University of Notre Dame, Notre Dame, IN, USA, [2]Indiana University School of Medicine, Indianapolis, IN, USA.
To prevent the loss of blood following a break in blood vessels, components in blood and the vessel wall interact rapidly to form a venous thrombus to limit hemorrhage. Combination of extended multiscale model, new image processing algorithms and biological experiments is used for studying the role of Factor VII (FVII) in venous thrombus formation. A detailed sub-model of the tissue factor (TF) pathway of blood coagulation is introduced within the framework of the multiscale model to provide detailed description of coagulation cascade. Macro scale dynamics of the blood flow is described by the continuum Navier-Stokes equations. Micro scale interactions between activated platelets, platelets and fibrin(ogen) and platelets and vessel wall are modeled using an extended stochastic discrete model. The novelty of the approach is in representing each platelet as an extended object with a boundary and modeling in detail the production of thrombin by each individual platelet. Also, clot is treated as a porous medium. Surface reactions of the extrinsic coagulation pathway on membranes of platelets are studied under different flow conditions. It is shown that low levels of FVII in blood result in a significant delay in thrombin production leading to changes in the surface composition of developing thrombi. The changes likely alter the mechanism and dynamics of thrombus stabilization which we are now studying in computational and experimental models.
Xu, Z., Chen, N., Shadden, S., Marsden, J.E., Kamocka, M.M., Rosen, E.D., and M.S. Alber [2009], Study of Blood Flow Impact on Growth of Thrombi Using a Multiscale Model, Soft Matter 5, 769-779.
Xu, Z., Chen, N., , Kamocka, M.M., Rosen, E.D., and M.S. Alber [2008], Multiscale Model of Thrombus Development, Journal of the Royal Society Interface 5 705-722.

2010-Pos
Multiscale Modelling of Membrane Systems
Jonathan W. Essex[1], Mario Orsi[1], George Chellapa[1], Wendy E. Sanderson[2], Massimo G. Noro[3].
[1]University of Southampton, Southampton, United Kingdom, [2]Johnson & Johnson PRD, Beerse, Belgium, [3]Unilever R&D, Port Sunlight, United Kingdom.
We have developed both 10- and 2-site molecular dynamics simulation models of biological membranes, tested their ability to model various lipid phases, and to reproduce important membrane physical properties, particularly the lateral pressure profile which is critical in determining the phases adopted in lipid systems [1]. The novelty in these models lies predominantly in the way they capture shape anisotropy, and the realistic way in which electrostatic interactions are incorporated. Furthermore, through careful design, the 10-site model in particular is compatible with atomistic models, allowing multiscale simulations of membrane systems [2].
In this presentation, the design philosophy and parameterisation procedures for these models will be described, together with their validation, with a particular focus on their lateral pressure profiles and phase behaviour. The application of these models in the context of multiscale simulations will then be considered. First, their use to calculate the permeability coefficients of small molecules through phospholipid bilayers, by combining molecular dynamics simulations with constraints, will be outlined [3]. Second, the effect of small molecules on membrane properties will be discussed, focusing particularly on antibacterials, which, it is postulated, may work through modifying the underlying physics of the membrane.
[1] M. Orsi, D. Y. Haubertin, W. E. Sanderson and J. W. Essex, J. Phys. Chem. B, 2008, 112, 802-815.
[2] J. Michel, M. Orsi and J. W. Essex, J. Phys. Chem. B, 2008, 112, 657-660.
[3] M. Orsi, W.E. Sanderson and J.W. Essex, J. Phys. Chem. B, 2009, 113, 12019-12029.

2011-Pos
Techniques for Modeling the Electrostatic Field of Large Biomolecules
Apostol Gramada, Philip E. Bourne.
University of California San Diego, La Jolla, CA, USA.
Electrostatic interactions play an essential role in many molecular processes within living organisms. However, for the large biological macromolecules typically involved in such processes, the accurate representation of the electrostatic potential is difficult to achieve in simple and, at the same time, computationally efficient ways: coarse-graining the electrostatic interactions becomes therefore necessary for any meaningful computational simulation of these processes. Multipole expansions offer a natural approach to coarse-graining due to their ability to capture directional variation of the interacting fields. Yet, the dependence of the multipole moments on the center of expansion and their limitations in accuracy near the molecular surface makes their application to large molecules unreliable. We present strategies in which we combine our Rankwise Distributed Multipole Analysis (RWDMA) method with partitioning schemes to overcome these limitations and develop relatively simple electrostatic models for large molecules. We illustrate the method with models of the electrostatic potentials of the histone core of a nucleosome complex and of the Arc repressor protein.

2012-Pos
Capturing the Roles of Attraction and Shape in Nonpolar Solvation
Christopher J. Fennell, Charlie Kehoe, Ken A. Dill.
UCSF, San Francisco, CA, USA.
We present a new approach to computer modeling of solvation free energies of oil in water. Informed by the behavior of TIP3P waters around simple Lennard-Jones spheres, Semi-Explicit assembly is a fast implicit approach for computing the nonpolar solvation properties of arbitrary solutes. By summing interactions from whole regions of the solute molecule, this method solves problems that appear as nonadditivities in traditional γ A approaches. Semi-Explicit assembly involves little parameter fitting because the solute and water properties come from existing force fields. We test the predictions on alkanes, alkynes, linear and planar polyaromatic hydrocarbons, and on a general set of 504 molecules previously explored by explicit solvent simulations. We find that not all hydrocarbons are the same. Hydrocarbons have ‘hot spots’, places where first-shell waters interact more strongly with the molecule than at other locations. By accounting for these ‘hot spots’, Semi-Explicit assembly attains the physical accuracies of explicit solvent models, but because of the pre-computations and the regional additivities, it is nearly as fast to compute as γ A methods.

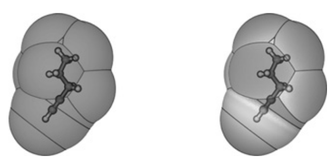

2013-Pos
Image Processing Techniques for Assessing Contractility in Isolated Adult and Neonatal Cardiac Myocytes
Carlos Bazan, David Torres-Barba, Peter Blomgren,
Esteban Vazquez-Hidalgo, Paul Paolini.
San Diego State University, San Diego, CA, USA.
We propose two computational frameworks for the assessment of contractile responses of enzymatically dissociated adult and neonatal cardiac myocytes. The proposed methodologies are variants of mathematically sound and computationally robust algorithms very well established in the image processing community. The computational pipeline for assessing contractility in adult cardiocytes comprises the following stages: digital video recording of the contracting cell, edge preserving total variation-based image smoothing, segmentation of the smoothed images, contour extraction from the segmented images, shape representation by Fourier descriptors, and contractility assessment. For assessing contractility of neonatal cardiocytes, the stages in the computational framework consist of digital video recording of the contracting cell, signal masking, representation by polar Fourier descriptors, and contractility assessment.
The physiologic applications of the methodologies are evaluated by assessing the contractions in isolated adult and neonatal rat cardiocytes. Our results demonstrate the effectiveness of the proposed approaches in characterizing the contraction process of the cardiocytes. The proposed methods provide a more comprehensive assessment of the myocyte contraction processes. Furthermore, adult contractility assessment method is suitable for determining myocyte contraction in cells that usually bend or move during contraction, e.g., atrial myocytes and isolated smooth muscle cells, or in cardiac myocytes which develop spatially nonuniform oscillatory contractile activity induced by intracellular calcium fluctuations. More importantly, the proposed methods can be utilized to evaluate changes in contractile behavior resulting from drug intervention, disease modeling, transgeneity, or other common applications to mammalian cardiocytes.

2014-Pos
Development of a High-Throughput Computational Protocol, AESOP, and its Application to the Electrostatic Analysis of the SUMO-1:SENP2 Complex
Chris A. Kieslich, Jiayu Liao, Dimitrios Morikis.
University of California, Riverside, Riverside, CA, USA.
Sumoylation of cellular proteins by the ubiquitin-like protein, SUMO, has been found to be one of the essential regulation mechanisms in signal transduction and genome integrity. SENP2, an endopeptidase, is responsible for both maturation of SUMO-1 into its conjugatable form, and the deconjugation of SUMO-1 containing species. Due to the excessive charge of SUMO-1 and SENP2, it has been proposed that electrostatics is important for the association of SUMO-1 and SENP2. In the current study we have used computational methods to investigate the possible role of electrostatics in the formation of the SUMO-1:SENP2 complex. Here we introduce a newly developed computational protocol, AESOP (Analysis of Electrostatic Similarities Of Proteins), which provides a systematic analysis of the contributions of each ionizable residue to the spatial distribution of electrostatic potential and their implied role in protein association. The AESOP protocol performs computational alanine scans, by mutating each ionizable residue within a protein or protein complex to alanine, one at a time. AESOP utilizes Poisson-Boltzmann electrostatic calculations to obtain the spatial distributions of electrostatic potential of proteins or protein mutants at atomic resolution. Electrostatic free energies of association, electrostatic similarity indices, and clustering methods then provide a quantitative comparison of the effects of each alanine mutation, leading to the prediction of key residues in protein association. The data of the current study provide a comprehensive comparison of several electrostatic clustering schemes that have been incorporated into the AESOP protocol. The data also depict important interactions for both SUMO1:SENP2 binding and the stability of the individual components of the complex. The produced predictions provide physicochemical insight into the mechanism of SUMO-1:SENP2 binding and will be used to guide mutagenesis experiments.

2015-Pos
Cardiomyopathy Mutations in Actomyosin: A Tertiary Structure Dynamics Approach within an in Silico Optical Trap Experiment
Steven Kreuzer[1], Jun Zhou[1], Joel Marquez[1], Dennis Liu[1],
Esfandiar Khatiblou[1], Tess Moon[1,2].
[1]University of Texas at Austin, Austin, TX, USA, [2]Texas Materials Institute, Austin, TX, USA.
Despite great success in simulating protein energetics, molecular dynamics approaches are currently too computationally intensive for use in studying supramolecular actomyosin assemblies. Here tertiary structure coarsegraining strategies are developed to create low-dimension potential functions (Tertiary Structure Models, or TSM) from MD-generated statistical potentials. The effect of domain selection is probed through comparison of successively finer coarsening, beginning with a 4-domain (lever-arm + converter, upper 50k, lower 50k, and n-terminal) TSM. In an attempt to discern and reproduce the basic characteristics of the power stroke the TSM is parameterized for the pre- and post-powerstroke states based on the scallop crystal structures 1qvi and 2ovk, respectively.
A first implementation of this approach to study the mechanical effect of mutations in the myosin actin-binding regions is presented in a rigid-body dynamics simulation of domain motion within an in silico optical trap experiment. Both the S532P and R403Q mutations to the myosin S1 are known to cause cardiomyopathy. It is known that the S532P mutation in the lower 50k domain decreases step size from wild-type while the R403Q mutation shows no difference with wild-type within the optical trap experiment. The differential effect of two mutations both occurring in the actin-binding regions is probed within simulation through alterations to the binding parameters of the upper 50k and lower 50k domains with actin. The ability of the TSM model to capture these fundamental results is used as a validation of the approach.

2016-Pos
Can a Reduced Dimension Interface Model be More Computationally Effective than a Docking Algorithm?
Chia-Cheng Liu[1], Esfandiar A. Khatiblou[1], Jun Zhou[1], Steven M. Kreuzer[1],
Joel D. Marquez[1], Tess J. Moon[1,2].
[1]The University of Texas at Austin, Austin, TX, USA, [2]Texas Materials Institute, Austin, TX, USA.
Actomyosin dynamics are central to elemental cellular processes, yet the precise molecular mechanisms by which actin and myosin transform ATP’s chemical energy into mechanical work remain a mystery. Further advances in understanding the actomyosin machine require computational, molecular-level models of the structural dynamics of myosin and its actin complexes, which correlate multi-domain structural changes with force/movement measurements and biochemical kinetics, to serve as adjuncts to molecular-level experiments. Existing modeling approaches, e.g., molecular dynamics which provides atomic-scale simulations of crystal structures, statistical mechanics which provides molecule-size extrapolations of experimental results, lack either the computational speed or the structural resolution necessary to capture the details necessary to reveal critical dynamics of supramolecular assemblies like actomyosin. Novel modeling approaches using targeted coarse-graining of high-resolution crystal structures and interaction potential fields may offer unified, mechanically rigorous, yet computationally efficient method to model supramolecular assemblies, as well as to develop model adjuncts for experiments.
While a core component in any such model is adequately depicting protein-protein binding-domain dynamics, key structural transitions cannot be defined by static crystal structures, as they involve dynamically disordered states. As a result, development of reasonable, inter-molecular potential functions requires estimations of protein-protein interactions, which could be and typically are obtained from docking algorithms like ZDOCK/RDOCK or AutoDock that, depending on the specific proteins, can be computationally expensive. In this work, the conjecture that a Reduced Dimension Interface Model (RDIM), which is constructed using multipole potential expansions, is sufficiently

accurate, yet computationally more efficient_and perhaps even better suited for supramolecular assembly dynamics modeling_than standard docking algorithms. Here, the relative efficacy, merits and demerits of RDIMs for estimating protein-protein interactions examined in the context of two key binding domains, namely myosin:actin and G-actin:G-actin.

2017-Pos
Automated Protein-Insertion into Membranes for Molecular Dynamics Simulation Set-Up Using Taragrid
René Staritzbichler, Lucy R. Forrest, José Faraldo-Gómez.
Max Planck Institute for Biophysics, Frankfurt, Germany.
Given a known membrane protein structure, a crucial and non-trivial preparation step in order to perform simulations of the protein in a lipid bilayer is the creation of the equilibrated bilayer-protein system. TaraGrid links an implicit protein force field with standard MD packages to automate this process. In the initial steps TaraGrid places the protein into the membrane and carves any water molecules out of the protein volume. It also erases as many lipids as necessary to conserve the bilayer density. In the main optimization phase TaraGrid calculates intermolecular forces between the protein and the molecules of the bilayer-solution system. Molecules that are within the protein volume are assigned a force that pushes them out of that volume. Molecules outside of the protein surface are assigned a linear combination of electrostatic and van-der-Waals forces. These forces are passed to a subsequent MD step carried out with a standard MD package, to obtain new peptide and water positions. This procedure enables creation of realistic and reproducible starting conformations for membrane-protein simulations within a reasonable time and with minimal intervention. Presently TaraGrid is tested to interact with NAMD and GROMACS, but as a standalone tool it is designed to work with any existing MD package.

2018-Pos
Coarse-Graining Electrostatics in Multiscale Molecular Simulations of Proteins
Davide Alemani[1], Francesca Collu[2], Michele Cascella[2], **Matteo Dal Peraro[1]**.
[1]Swiss Federal Institute of Technology Lausanne - EPFL, Lausanne, Switzerland, [2]University of Bern, Bern, Switzerland.
All-atom molecular dynamics (MD) simulations are a powerful tool to investigate the structure and function of biomolecular systems. Nonetheless, within the atomistic framework it remains computationally unaffordable to thoroughly sample size and time scales that are critical to most of the biological processes both in vitro and in vivo. Coarse-grained (CG) schemes have been introduced to overcome these limitations; nonetheless, many issues, such as the lack of universality and transferability, still afflict CG models and limit in turn their general applicability to a vast class of relevant biological problems.
We introduce a reliable and robust scheme to account for the intrinsic non-radial nature of backbone-backbone interactions in CG molecular dynamics simulations of proteins. Specifically, we define a new CG potential term, which, mimicking the backbone dipole-dipole interactions, is able to naturally stabilize elementary secondary structure motifs, such as α-helices and β-sheets, and to modulate basilar transitions to super-secondary structure assemblies. Moreover, the scheme can properly describe the long-range electrostatic contributions in a multiscale MD framework, contributing to an accurate description of protein-ligand and protein-protein recognition. Thus, this novel scheme represents a promising step towards the development of a CG force field able to take into account intrinsic anisotropy of protein structures, leading to an improved description of the structural and dynamic properties of protein assemblies and networks.

2019-Pos
Polymer Translocation Through a Nanopore in an Interacting Membrane
Wen-Qin Lu.
Department of Physics, Zhejiang University, Hangzhou, China.
The translocation of polymers through nanopores in membranes occurs in many biological processes, such as proteins transporting through membrane channels, DNA and RNA translocating across nuclear pores, and drug delivery. The mechanism of the translocations has attracted a lot of attention from experiments, analytical theories and computer simulations. In a recent simulation study, the influence of pore-polymer interaction on the polymer translocations was discussed. Some experiments implied that the interaction between polymers and membranes might play an important role in the polymer translocation through membranes. In the present work, we use dynamic Monte Carlo simulations to study the effects of interaction between polymer segments and the membrane on the translocation of polymer chains through an interacting membrane from *cis* side (high concentration of chains) to *trans* side (zero concentration). Results show that there is a critical adsorption point ϵ_c of the interaction strength ϵ . We find the translocation timeτ is almost independent from ϵ for$\epsilon < \epsilon_c$ and $\tau = f(exp(\epsilon), n)$ for $\epsilon > \epsilon_c$, where n is the length of polymer chains. We estimate the value of the critical adsorption point ϵ_c is about -0.3, which is in good agreement with previous results in many literatures studying the adsorptions of polymers on surfaces.

2020-Pos
Conservative Algorithm for an Adaptive Change of Resolution in Mixed Atomistic / Coarse-Grained Multiscale Simulations
Andreas Heyden.
University of South Carolina, Columbia, SC, USA.
Understanding complex materials often requires investigating multiple, tightly coupled time and length scales. Neither atomistic nor coarse-grained simulations are often able to adequately capture all the relevant scales. To combine the efficiency of coarse-grained models with the accuracy of atomistic models for systems that require atomistic resolution only locally, for example at an interface, mixed-resolution models have been developed. These models use a coarse-grained description for the part of the system distant from an active site and atomistic description for the active site and its direct environment. Since the active zone may diffuse during a simulation, the simulation algorithm needs to permit an on-the-fly reclassication of atoms as they transition between the high- and low-resolution regimes. In this paper, we derive a conservative Hamiltonian and present an explicit symplectic integrator for mixed-resolution systems that allows for such a change in resolution of selected groups of atoms during a MD simulation.

2021-Pos
Hydrogen-Bonding Strengths in Pyrrolidinyl Peptide Nucleic Acid and DNA Base Pairs: A Density Functional Theory (DFT) Study
Chinapong Kritayakornupong[1], Arthitaya Meeprasert[1,2],
Ladawan Leelasatiankun[1].
[1]King Mongkut's University of Technology Thonburi, Bangkok, Thailand,
[2]Chulalongkorn University, Bangkok, Thailand.
The H-bond strengths of the single base pair formed from Pyrrolidinyl Peptide Nucleic Acid (PNA) and charged as well as neutral Deoxyribonucleic Acid (DNA) were studied using the density functional theory. The B3LYP/6-31+G(d,p) level of theory was employed for evaluating the binding energies and structural parameters of heterogeneous and homogeneous base pairs. The strongest H-bond strengths were obtained from the heterogeneous base pairs, yielding the binding energies of -29.9 and -18.9 kcal/mol for the PNA-GC-DNA and PNA-AT-DNA base pairs, respectively. In contrast, a dramatic change on the H-bond strengths was observed from the charged homogenous base pairs with the binding energies of -6.2 and $+10.2$ kcal/mol for the DNA-GC-DNA and DNA-AT-DNA base pairs, respectively. With the neutralization of negative charges in the DNA backbone, the corresponding values of -29.1 and -11.7 kcal/mol were elucidated from the Na-DNA-GC-DNA-Na and Na-DNA-AT-DNA-Na base pairs, respectively, proving that the repulsion between two negative charges in the phosphate backbone plays a significant role to the H-bond interactions in base pairs. In addition, a high specificity and preferential binding between the pyrrolidinyl PNA and DNA base pairs were also observed.

2022-Pos
Protein Classification Based on Physicochemical Descriptors
Tim Meyer, Ulf Hensen, Rene Rex, Helmut Grubmueller.
MPI Biophysical Chemistry, Goettingen, Germany.
ystematic and efficient analysis of proteins on the proteome scale requires their classification into meaningful sub groups. Approaches to the problem are either top-down, following the evolutionary pathways (SCOP, CATH) and bottom-up, where structures are compared pairwise and aggregated to clusters (DALI). Here we present a novel way of protein classification based on physicochemical descriptors. Atomistic structures are for classification purpose overly rich in information and we distilled biologically relevant features by projecting from the structure space into a lower dimensional descriptor space. Chosen descriptors fall into three groups, sequence dependent, topology, and overall structure and consist of amino acid distribution, charge, hydrophobicity, average path length, cluster coefficient, helix content, sheet content, solvent accessible surface area, radius of gyration, besides others. All descriptors were corrected for chain length and normalized by the standard deviation.
Over 3000 representative and non-redundant structures from the pdb Cluster90 were mapped to descriptor space and clustered. The identified clusters coincide to large extend with those from existing classification methods. Our method provides, unlike others, a direct measure for the distance between any two proteins and is easily expandable by for instance descriptors for molecular dynamics.

Nothing about protein structure classification makes sense except in the light of evolution.
Valas, R.B., Yang S., and Bourne P.E. Curr Opin Struct Biol 2009 19:329-34
Multipolar representation of protein structure.
Gramada, A. Bourne P.E. BMC Bioinformatics 2006 7:242

2023-Pos
BIBEE: a Rigorous and Computationally Efficient Approximation to Continuum Electrostatics
Jaydeep P. Bardhan.
Rush University Medical Center, Chicago, IL, USA.
The computational costs associated with modeling biomolecular electrostatics using continuum theory have motivated numerous approximations, such as Generalized-Born (GB) models, that can be computed in much less time. Unfortunately, most of these approximate models abandon physics in favor of computational efficiency. On the other hand, a new approximation method for molecular electrostatics, called BIBEE (boundary-integral-based electrostatics estimation), retains the underlying physics of continuum theory, but is nearly as efficient as Generalized-Born models. The BIBEE approach derives from well-known results in potential theory and the theory of boundary-integral equations. Three main results demonstrate the value BIBEE may hold for biomolecular analysis and design. First, the integral-equation theory clarifies the origin of accuracy of the Coulomb-field approximation (CFA). Second, BIBEE models offer significantly better accuracy for individual pairwise interactions, relative to GB methods. Third, BIBEE readily provides provable upper and lower bounds to the electrostatic solvation free energy of the original (exact) continuum-theory problem.

2024-Pos
Evaluating Empirical Force Fields Through Combined QM/MM Computations of the Vibrational Stark Effect
Ashley L. Ringer, Alexander D. MacKerell, Jr.
University of Maryland Baltimore, School of Pharmacy, Baltimore, MD, USA.
The proper description of the electric environment of the interior of macromolecular structures is a critical challenge for force field methods. To test and validate the CHARMM force field's ability to describe this electric environment, combined QM/MM calculations have been used to calculate the vibrational Stark effect (VSE). The Stark effect refers to the characteristic shift of a specific vibrational frequency upon the introduction of an electric field. In this work, we calculate the Stark shift of several experimentally characterized Stark effect probes (5-cyanoindole, methyl thiocyanate, and fluorobenzene) in several solvents. The solvent environment around the probe is sampled through 20 ns molecular dynamics simulations of each molecule surrounded by several hundred explicit solvent molecules. From these simulations, two hundred snapshots of the solvent environment are collected for the QM/MM analysis. The QM/MM computation uses correlated electronic structure methods to calculate the vibrational spectrum of the VSE probe in the field created by the solvent molecules, which are treated as MM atoms with the CHARMM force field. From these computations, an average Stark shift is determined for each probe molecule and compared to experimental measurements. This information can be directly related to the electric field surrounding the probe molecule, and therefore may be used as a direct test of the ability of a force field to reproduce the electric field around those functional groups. Information from these calculations will act as the basis for additional optimization of the force field to more accurately represent the electric fields in macromolecules.

2025-Pos
Weighted Ensemble Path Sampling for Efficient Calculation of Steady State Properties
Divesh Bhatt, Andrew A. Petersen, Daniel M. Zuckerman.
University of Pittsburgh, Pittsburgh, PA, USA.
Steady states are common in biological processes, most famously in enzymatic catalysis. We present a rigorous path sampling procedure, generalizing the ''weighted ensemble'' (WE) method, to attain a steady state (SS) efficiently. We apply this procedure to several different systems, from toy models to the folding of the atomistic Trp cage mini-protein. For systems without significant intermediates, we find that the SS-WE procedure is able to attain steady state fairly efficiently. However, for systems with significant intermediates, we develop an enhanced version of SS-WE that shifts probability to speed-up the establishment of a steady state, without perturbing the system's natural dynamics. The enhanced SS-WE approach is able to attain a steady state in significantly less time for systems with significant intermediates, and gives correct results for the steady state rates and probability distribution. First-passage rates are also obtained simultaneously.

2026-Pos
Simulations of Binding Free Energy of Targeted Nanocarriers to Cell Surfaces: the Effects of Antigen Flexural Rigidity, Glycocalyx Resistance, and Shear Flow
Jin Liu, Neeraj J. Agrawal, Portonovo S. Ayyaswamy, David M. Eckmann, Ravi Radhakrishnan.
University of Pennsylvania, Philadelphia, PA, USA.
We develop an equilibrium mesoscale model to study the binding free energy of functionalized nanocarriers (NC) to cell surfaces, which plays a central role in targeted drug delivery. Our model is parametrized to mimic interactions between intercellular adhesion molecule 1 (ICAM-1) on cell surface and anti-ICAM (antibody) on NCs and accounts for ICAM-1 diffusion and flexure, bond stiffness, effect of glycocalyx, and shear flow; parameters are chosen from several independent literature experiments. Using umbrella sampling in conjunction with Monte Carlo simulations, we compute the potential of mean force (PMF) as a function of distance between the NC and the cell surface. Our results show that the PMF landscape is rugged along the distance of the NC from the cell surface with multiple equilibrium points separated by free energy barriers of comparable magnitudes. Calculations reveal: (1) a significant effect of the antigen flexural rigidity, namely with decreasing flexural rigidity, even though the multivalency of binding increases, we record decrease in the binding free energy due to increasing entropic penalty; (2) The presence of glycocalyx does not alter multivalency, but significantly reduces the binding free energy; (3) Hydrodynamic shear stress plays a central role in mediating the binding conformations and alters the PMF landscape. Our results provide quantitative assessments of the effects of tunable/controllable properties on the binding of NCs to cell surfaces. Our model provides a rational and unique approach to bridge single molecule and biophysical measurements at the molecular scale with microscopy and flow experiments at the micro and macroscales. This integrative step will enhance optimization of delivery vehicles for use in targeted therapeutics.
This work is supported by NIH through Grant 1R01EB006818.

2027-Pos
Multi-Body Knowledge-Based Potentials for Protein Structure Prediction Evaluation
Yaping Feng, Robert L. Jernigan, **Andrzej Kloczkowski**.
Iowa State University, Ames, IA, USA.
Knowledge-based potentials have been widely used in the last 20 years for fold recognition, evaluation of protein structure predictions from amino acid sequences, ligand binding, protein design, and many other purposes. The most commonly known are two-body residue-level contact potentials, especially those first introduced by Miyazawa and Jernigan in 1985, and then rederived using an updated, larger protein dataset in 1996. Dense packing of residues in globular proteins is one of their characteristic features. Because of such dense packing cooperative multi-body interactions, especially in protein cores are important. The four-body contact potentials and short-range interaction potentials have been derived by considering different aspects of protein structures than those used to derive pair-contact potentials. The four-body contact potentials are appropriate for representing the cooperative parts of the protein folding process, and we have shown that they are quite successful for recognizing the native structures among hundreds or even thousands of decoys from the Decoys'R'Us database. Short-range interaction energies allow us to estimate free energies from the statistical distribution of local conformational descriptors. We developed two types of four-body potentials: sequential and non-sequential ones. We have found that combining the former ones with short-range interactions yields excellent results for threadings, that significantly outperforms all other methods for coarse-grained models of proteins. We have developed also our knowledge-based potential server http://gor.bb.iastate.edu/potential for coarse-grained protein energy estimations that uses two types of four-body potentials, short-range potentials, and 23 different two-body potentials.

2028-Pos
Prediction of Calcium Binding Site in the RCK1 Domain of BK_{Ca} Channel Using Multisite Cation Model
Akansha Saxena[1], David Sept[2].
[1]Washington University, St Louis, MO, USA, [2]University of Michigan, Ann Arbor, MI, USA.
Calcium plays a major role in controlling the opening and closing of the large conductance BK_{Ca} channels. Two high affinity binding sites have been identified in the channel structure and one of these sites is the DRDD loop in the N-terminus of the RCK1 domain. Mutation of the first aspartate in this conserved DRDD motif significantly reduces Ca^{2+} sensitivity and hence this residue has been implicated as a coordinating group in the binding site. Here we present results on the prediction of the Ca^{2+} binding site based on a series of detailed computational studies. We use a novel multisite cation model for calcium ion to accurately simulate the ion-coordination. The basic protocol involves multiple

iterations of random ion placement, implicit solvent molecular dynamics simulations and statistical analysis. Our resulting model matches very well with existing mutagenesis data, and subsequent explicit solvent molecular dynamics simulations have been performed using this Ca^{2+} bound structure. Comparison of the dynamics and conformations of the Ca^{2+} bound and unbound simulations reveal a concerted conformational change in the structure and suggest a potential mechanism for calcium dependent activation of these channels.

Imaging & Optical Microscopy II

2029-Pos

Characterization of the Use of Far-Red Dyes for Localization Microscopy of Biological Samples

Sabrina Rossberger[1,2], David Baddeley[1], Mark B. Cannell[1], Christoph Cremer[2], Christian Soeller[1].
[1]University of Auckland, Auckland, New Zealand, [2]University of Heidelberg, Heidelberg, Germany.

Recently it has been shown that conventional fluorescent dyes can be used to achieve super-resolution by single-molecule localization. The use of conventional fluorochromes for this new approach, termed ‘localization microscopy’, depends critically on the observation of rapid on-off blinking of these dyes in certain chemical environments. Here we characterize the photophysical behavior of several commercially available far-red dyes that have similar properties to the cyanine dye Cy5 and use them to visualize the distribution of proteins in fixed cardiac cells.

To obtain super-resolution images several thousand individual ‘blinking’-events, which arise from dye molecules that briefly enter a bright (fluorescent) state, were analyzed and the molecular positions determined by a fitting algorithm. We tested far-red Alexa dyes (647,680,700,750) linked to secondary antibodies for use in immuno-labeling super-resolution microscopy. The dyes were observed in mounting media of various refractive indices containing oxygen scavengers and triplet quenching compounds that favors fluorochrome ‘blinking’. Under these conditions typically over 1000 photons per ‘blinking’-event were detected and a localization accuracy of ~30 nm (full width at half maximum) was readily achieved with Alexa 680. These accuracies are in good agreement with theoretical calculations when the background present in labeled cellular preparations (largely arising from out-of-focus fluorescence) is taken into account.

For practical super-resolution imaging of immuno-stained preparations, several advantages are provided by these dyes, for example, as compared to blue/green excited fluorochromes less autofluorescence is generally caused by organelles and fixation. We investigate the possibility to use a combination of these dyes for simultaneous localization imaging of multi-labeled preparations excited with a single laser line. This is illustrated using fixed ventricular myocytes that were labeled for β-tubulin, caveolin-3 and ryanodine receptors.

2030-Pos

Synthetic Chromophore Maturation by Split Green Fluorescent Protein (GFP)

Luke M. Oltrogge, Kevin P. Kent, Steven G. Boxer.
Stanford University, Stanford, CA, USA.

Green fluorescent protein (GFP) undergoes a self-catalyzed cyclization, dehydration, oxidation reaction sequence to form a fluorescent chromophore in the protein’s interior. We have developed a system for studying chromophore maturation and the photophysical properties of novel chromophores *in vitro*. Intact GFPs, circularly permutated to locate the interior α-helix at the N-terminus, were expressed with a flexible proteolytic loop inserted on the C-terminal side of the chromophore-containing helix. With trypsin, the helix was severed and subsequently removed by size exclusion chromatography after denaturation. The split GFP was then renatured in the presence of a synthetic peptide which underwent chromophore maturation to acquire fluorescence. Since the complementary helix peptide is fully synthetic we have unprecedented control through specific incorporation of multiple unnatural amino acids. We are studying these effects with a range of spectroscopic techniques including steady state fluorescence, time-correlated and upconversion time-resolved fluorescence in order to better understand the process of chromophore maturation, the photochemistry of the protein, and the kinetics and efficiency of fluorescence reconstitution to inform the strategies for producing more robust *in vivo* probes.

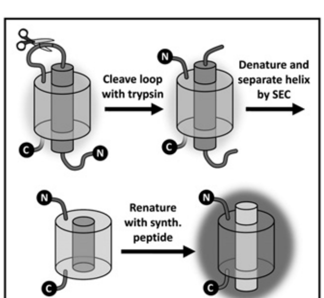

2031-Pos

Dynamics of Individual BK_{Ca} Channels in Live Cells Monitored by Site-Specific Labeling Using Quantum Dots

Hae-Deun Kim, **Sehoon Won**, Chul-Seung Park.
GIST, Gwangju, Republic of Korea.

In order to monitor the movement of individual large-conductance Ca^{2+}-activated K^{+} channels (BK_{Ca} channels) in live cells at real-time, we co-expressed the BK_{Ca} channel tagged at its extracellular N-terminus with the ‘acceptor peptide (AP)’ for biotin and a genetically modified *E. coli* biotin ligase in various mammalian cells. Using the quantum dots (QDs) coated with streptavidin, we were able to visualize individual BK_{Ca} channels that had been biotinylated intracellularly and then expressed on to the surface of the cells. The channels were determined to be labeled by two QDs in average, based on the levels of quantized fluctuations of fluorescence intensity, known as ‘photo-blinkings’. We monitored the movements of BK_{Ca} channels in both live mammalian cell-lines and primary hippocampal neurons using time-lapse imaging. Depending on the type of cells and the location where the channels were expressed within a cell, BK_{Ca} channels showed different patterns and speeds in their movements. We are currently quantifying the movement of individual channels and investigating those protein motifs affecting the channel dynamics. We wish to understand the molecular mechanism of BK_{Ca} channel trafficking and the cellular players involved in.

2032-Pos

Counting Pictures of Cell that Count: A Biotiff-Based Strategy for Indexing Cell Images and Associated Metadata in Large Series of Digital Microscopy-Based Biophysical Result

Peter S. Pennefather, West Suhanic.
University of Toronto, Toronto, ON, Canada.

Last year we described how BioTIFF code (www.biotiff.org) enables all metadata needed to interpret a given digital image region to be embedded within the same file structure used to store that image (Biophys J. 96: 30a). Here we show how that metadata can then be indexed so that Google-like queries can be performed on any set of BioTIFF files. Indexing can be done either on a single local set of BioTIFF images or a distributed set by using a distributed file system. This then creates a distributed index that has many interesting applications for exploring image relationships across different subsets of images within large sets. For example, single cell (or single molecule) responses measured using digital microscopy-based biophysical methods that relate cellular mechanism to light-based surrogate measures can then be linked to a specific cell in a specific field-of-view of a specific sample. The replication of such results over time in the same lab or in a distributed manner by multiple labs can allow for collaborative replicable science to anchor the evolution of shared understanding of cell physiology mechanisms. We will demonstrate how the approach can be implemented using a plurality of commodity gear meeting certain minimum standards and open source imaging, indexing and search software. This level of transparency and annotation of experimental detail allows for differences in experimental conditions between experiments and labs to be accommodated in open collaborative interpretation of biophysical data.

2033-Pos

Site-Specific, Orthogonal Two Color Labeling of Different Proteins with Flash and Reash in Living Cells

Alexander Zürn, Christpoh Klenk, Ulrike Zabel, Martin J. Lohse, Carsten Hoffmann.
Institute of Pharmacology and Toxicology Würzburg, Würzburg, Germany.

Multiparameter imaging of independent cellular functions is limited by the lack of distinct molecular probes that would specifically label two different proteins. Here we report a strategy to simultaneously label two different proteins in living cells with two different fluorophores, FlAsH and ReAsH.

Recently, tetracysteine binding motifs have been improved to selectively bind to FlAsH or ReAsH respectively. We compared the six amino acid motif CCPGCC and the twelve amino acid motif FLNCCPGCCMEP with respect to their affinities for FlAsH and ReAsH. Both fluorophores showed higher affinity for the FLNCCPGCCMEP motif. For both target sequences, FlAsH showed more stable interactions than ReAsH. Using a new labelling protocol we selectively labeled different proteins in the same cell. Our target proteins were localized in different cellular compartments, a plasmamembrane localized G protein-coupled receptor for PTH (PTH-receptor) and the cytosolic β-arrestin2- protein. Our protocol allowed selective labelling of PTH-receptor with ReAsH at a C-terminal FLNCCPGCCMEP motif, while the cytosolic β-arrestin-2 protein was C-terminally modified with the CCPGCC motif and specificly labeled with FlAsH. Both proteins were simultaneously visualized in intact cells, and their interaction was determined by colocalization and fluorescence resonance energy transfer (FRET).

Taken together, our data demonstrate that FlAsH and ReAsH can be used for orthogonal labeling of different target proteins in living cells.

2034-Pos
Quantum Dot Sensors and Nanoactuators in Living Cells
Guillermo Menendez[1], M. Julia Roberti[1], Maria H. Etchehon[1], Thomas M. Jovin[2,3], **Elizabeth A. Jares-Erijman**[1].
[1]University of Buenos Aires, Buenos Aires, Argentina, [2]Max Planck Institute for Biophysical Chemistry, Goettingen, Germany, [3]Laboratory of Cellular Dynamics, University of Buenos Aires, Buenos Aires, Argentina.
Quantum dots (QDs) are unique probes due to their special properties (brightness, photostability, narrowband emission and broadband absorption), and excellent bio(chemical)compatibility for imaging structures and functions of living cells. When functionalized with ligands, they enable the recognition of specific targets and the tracking of dynamic processes for extended periods of time, detecting biomolecules with a sensitivity extending to the single molecule level. Here we present nanosensors and nanoactuators based on QDs in which the multivalency of the particle plays an essential role in determining the functionality and sensing characteristics of the nanodevices. Two examples are discussed:
(i) luminescent pH nanosensing QDs calibrated and measured by FLIM (Fig. A). The underlying process is bidirectional (a novel feature) FRET between the QD and the conjugated sensor with pH-sensitive spectral properties[1].
(ii) nanoactuators consisting of strepatividin QD to which biotinylated alpha-synuclein (AS) has been conjugated (Fig. B). These constructs are very efficient intiators and sensors of AS aggregation *in vitro* and in live cells[2] .

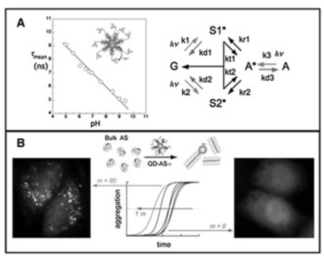

[1] G. Menendez, in preparation.
[2] M. J. Roberti, M. Morgan, L. I. Pietrasanta, T. M. Jovin, E. A. Jares-Erijman, *J. Am. Chem. Soc*. (2009) 131: 8102-8107; in preparation.

2035-Pos
Nonlinear Structured-Illumination Microscopy Using Photo-Switchable Labels
Hesper Rego.
UCSF and Janelia Farm Research Institute, Ashburn, VA, USA.
Periodically structured illumination light can extend the resolution of a light microscope beyond the classical limit by an amount equal to the spatial frequency, k1, of the illumination structure [1]. The wavelength and the laws of physics limit the set of frequencies that can be physically generated in a light intensity field in the same way as the set of frequencies that can be observed. Consequently, k_1 cannot be much greater than the classic resolution limit itself, and therefore the resolution extension cannot exceed a factor of two.
However, dramatically greater resolution extension is possible if the emission rate is made to be nonlinear with the incoming illumination intensity. This nonlinearity can cause the effective excitation to contain harmonics at multiples of k_1, with correspondingly multiplied resolution-enhancing ability [3].
Photo-switching of fluorophores is a nearly ideal source of such nonlinearity. This phenomenon has produced modest resolution improvements when applied on one dimension and analyzed with real-space methods [4]. We are using it to develop high-resolution microscopy of 2D samples based on our frequency-space-based approach to nonlinear structured-illumination microscopy. Here we describe recent progress toward multidimensional super-resolution of biological samples using this technique.
[1] M.G.L. Gustafsson, ''Surpassing the lateral resolution limit by a factor of two using structured illumination microscopy,'' *J. Microsc.***198**, (2000).
[2] R. Heintzmann, T.M. Jovin, and C. Cremer, ''Saturated Patterned Excitation Microscopy - a Concept for Optical Resolution Improvement,'' *J. Opt. Soc. Am. A*. **19**, (2002).
[3] M.G.L. Gustafsson, ''Nonlinear structured-illumination microscopy: wide-field fluorescence imaging with theoretically unlimited resolution,'' *Proc. Nat. Acad. Sci. USA* **102**, (2005).
[4] M. A. Schwentker, H. Bock, M. Hofmann, S. Jakobs, J. Bewersdorf, C. Eggeling, and S.W. Hell, ''Wide-Field Subdiffraction RESOLFT Microscopy Using Fluorescent Protein Photoswitching'', Microscopy Res. & Techn. **70**, (2007).

2036-Pos
Reversibly Switchable Fluorescent Proteins
André C. Stiel, Martin Andresen, Tanja Brakemann, Tim Grotjohann, Stefan W. Hell, Stefan Jakobs.
Max Planck Institute for Biophysical Chemistry, Göttingen, Germany.
Recently, reversibly switchable fluorescent proteins (RSFPs) have become a new branch of the green fluorescent protein (GFP) like family. RSFPs may be reversibly switched between a fluorescent and a non-fluorescent state by irradiation with light of distinct wavelengths; the key structural event of this switch is a cis / trans isomerization of the chromophore which is accompanied by changes in the protonation state of the chromophore. These proteins may be applied in sub-diffraction resolution microscopy as well as in novel protein tracking schemes or even as data storage elements.
Consequently, the creation of novel RSFPs with unique characteristics for the respective applications is of great importance. To this end, the combination of rational and random mutagenesis together with an automated screening system allowed us to create several new RSFPs. These include rsCherryRev, Padron and bsDronpa. rsCherryRev, the first red fluorescent monomeric RSFP, was successfully applied in a live cell sub-diffraction resolution microscopy experiment to visualize the movement of the endoplasmic reticulum. Padron, a green RSFP with reversed switching behavior, in combination with the RSFP rsFastLime allowed for multilabel single detection color microscopy, while bsDronpa, a Dronpa variant with a broad excitation spectrum, was used for two-color sub-diffraction resolution microscopy.

2037-Pos
Photoswitching Mechanism of Cyanine Dyes
Graham T. Dempsey[1], Mark Bates[1], Walter E. Kowtoniuk[1], David R. Liu[1], Roger Y. Tsien[2], Xiaowei Zhuang[1].
[1]Harvard University, Cambridge, MA, USA, [2]University of California, San Diego, La Jolla, CA, USA.
Photoswitchable fluorescent probes have been used in recent years to enable super-resolution fluorescence microscopy by single-molecule imaging. Among these probes are red cyanine dyes, which can be reversibly photoconverted between a fluorescent and a dark state for hundreds of cycles before permanently photobleaching, yielding several thousand detected photons per switching cycle. While these properties make them excellent probes for super-resolution imaging, the photochemical mechanism by which switching occurs has yet to be elucidated. In this study we determine the mechanism of photoswitching by characterizing the kinetics of dark state formation, and the spectral and structural properties of the dark state. The rate of switching to the dark state depends on the concentration of the primary thiol in solution and the solution pH, in a manner quantitatively consistent with the formation of an encounter complex between the cyanine dye and ionized thiol prior to their conjugation. Using mass spectrometry, we identify the photoconversion product as a thiol-cyanine adduct in which covalent attachment of the thiol to the polymethine bridge disrupts the original conjugated pi electron system of the dye. Such an understanding could prove useful for creating new photoswitchable probes with improved properties.

2038-Pos
Fluorescence Enchancement from Single Molecules Confined in SiO2 Nanochannels
Fredrik Westerlund[1], Fredrik Persson[1], Anders Kristensen[2], Jonas Tegenfeldt[1].
[1]University of Gothenburg, Gothenburg, Sweden, [2]Technical University of Denmark, Kongens Lyngby, Denmark.
A large challenge in biophysics when studying single molecules using fluorescence microscopy is to obtain a signal that is clearly detectable above the background noise. Ways to improve or optimize the fluorescence signal is therefore of great interest. We here study DNA extended in 320 nm deep funnel-shaped SiO2 nanochannels with a width ranging from 40nm to 600nm. The DNA is stained with a fluorescent dye (YOYO-1) and we show that the total emission from the DNA varies significantly with the dimensions of the channels and has a peak intensity at half the wavelength of the emitted light. Measurements at varying salt concentrations, where the same confinement leads to different extension of the DNA, confirm that it is solely the geometry of the channel that governs the enhancement effect, ruling out alternative explanations, such as self-quenching. By using polarizers on the emission side we can investigate the light polarized parallel and perpendicular to the channel separately and we see that they show vastly different behavior with the peak in emission only detected in the light polarized parallel to the channels. We will discuss how our data may be explained by cavity-resonance effects when the lateral dimensions of the channels coincide with half the wavelength of the emitted light. Our results suggest that it is possible to fine-tune the size and shape of the nanochannels to maximize the number of photons collected from the molecule under study, for example when studying DNA interacting with single DNA-binding proteins where maximizing the photon budget is paramount.

2039-Pos

Probing the Interaction between a Nanopipette and a Soft Surface Using Scanning Ion Conductance Microscopy (SICM)

Owen Richards[1], Nick Johson[1], Chao Li[1], Pavel Novak[2], Richard Clarke[1], Yuri Korchev[2], David Klenerman[1].
[1]The University of Cambridge, Cambridge, United Kingdom, [2]Imperial College London, London, United Kingdom.

Imaging cell topography to high spatial and temporal resolution is key for many areas of biological research. SICM, based on the scanned nanopipette, is a technique ideally suited to this and works by regulation of the ion current flowing through the tip opening.1 SICM is a noncontact method and works under physiological conditions making it an excellent method for high resolution imaging of cells. Previously this technique has been used to image numerous cell types2-5.

We have performed a detailed study of the small forces that are exerted on model oil droplet surfaces of known surface tension by the tip of a nanopipette. By varying salt concentration and applied voltage we can quantify the force. This force under our normal SICM imaging conditions is found to be very small but increases as the pipette approaches the surface. This allows non-contact cell imaging at high resolution while applying small forces of set magnitude, and has been used to image the underlying cytoskeleton of Osteoblast and Stem Cells.

1. Hansma, P. K., Drake, B., Marti, O., Gould, S. A. C. & Prater, C. B. Science 243, 641-643 (1989).
2. Zhang, Y. J. et al. Kidney International 68, 1071-1077 (2005).
3. Shevchuik, A. I. et al Angewandte Chemie-International Edition 45, 2212-2216 (2006).
4. Novak, P. et al. Nature Methods 6, 279-281 (2009).
5. Mann, S. A., Hoffmann, G., Hengstenberg, A., Schuhmann, W. & Dietzel, I. D. Journal of Neuroscience Methods 116, 113-117 (2002).

2040-Pos

Surface Charge Mapping Based on Scanning Ion Conductance Microscopy

Louis Burkinshaw[1], Richard Clarke[1], Pavel Novak[2], Yuri Korchev[2], David Klenerman[1].
[1]University of Cambridge, Cambridge, United Kingdom, [2]Imperial College, London, United Kingdom.

Scanning Ion Conductance Microscopy (SICM) is capable of high resolution, non-contact topographic imaging of live biological cells under physiological conditions(1, 2). The technique uses the ion current flowing through a nanopipette as a feedback signal to control the pipette probe over the surface. SICM has successfully been combined with a number of other techniques to study live cells. For example, SICM topographic imaging has been performed simultaneously with both patch clamping(3) and confocal microscopy(4). The integration of a surface charge mapping technique with SICM imaging is currently being developed.

The charge mapping technique has successfully been used to detect charge arranged in three-dimensions, such as in cationic and anionic polymer brushes. The next stage is to optimise the detection of two-dimensional charge distributions. The technique has the potential for efficient and reliable characterisation of surface charge throughout a biological membrane. Knowledge of membrane surface charge is important because membrane electrostatics affect the conformation and function of many biomolecules and also play a role in intracellular and intercellular recognition and transport(5).

(1) Shevchuk, A. I., Frolenkov, G. I. *et al*. *Angew. Chem. Int. Ed.* **45**, 2212 (2006).
(2) Novak, P., Li, C. *et al*. *Nature Methods* **6**, 279 (2009).
(3) Korchev, Y. E., Negulyaev, Y. A. *et al*. *Nature Cell Biology* **2**, 616 (2000).
(4) Gorelik, J., Shevchuk, A. I. *et al*. *PNAS* **99**, 16018 (2002).
(5) Cevc, G. *Biochim. Biophys. Acta* **1031**, 311 (1990).

2041-Pos

Optimizing Protein-Based Optical Voltage Sensitive Probes: A Systematic Study

Zhou Han[1], Lei Jin[2], Bradley Baker[2], Lawrence Cohen[2], Thomas Hughes[3], Vincent Pieribone[1].
[1]The John B. Pierce Laboratory, New Haven, CT, USA, [2]Dept. of Molecular and Cellular Physiology, Yale University, New Haven, CT, USA, [3]Cell Biology & Neuroscience, Montana State University, Bozeman, MT, USA.

Replacement of the phosphatase domain of the *Ciona intestinalis* voltage sensitive phosphatase (CiVSP) with fluorescence protein (FP) FRET pairs generates chimeric proteins that respond to voltage fluctuations with changes in FRET efficiency. VSFP 2.1 and Mermaid represent two different CiVSP-based voltage probes. We have developed a single FP-based, CiVSP-based probe (pKF215). These probes have different FPs and linker domains. As these constructs represent the most promising probes developed to date, we have undertaken a structure/function analysis of these constructs by: i) altering the inserted FPs and ii) replacing the VSD with species orthologs. The goal is to produce probes with a larger and faster $\Delta F/F$ response. We have created a matrix of 33 different constructs replacing the FPs of the original constructs with a range of red-shifted FPs (mCherry, mStrawberry, mTangerine, mOrange, tdTomato and TagRFP). We have also replaced the inserts with the two currently most viable FRET pairs (CFP/YFP and the Mermaid FRET pair). Finally we have chosen three other FPs which we have previously identified as 'modulatable' (mCerulean, PHluorin and eGFP). As the S1 to S4 domain of CiVSP has produced the most successful fluorescent voltage sensing constructs, we sought orthologs of Ciona VSD that might perform better. We identified VSPs orthologs from a variety of different species. We cloned the VSP orthologs from chicken, mouse, human, *Xenopus laevis*, *Xenopus tropicalis*, and zebra fish. To test these VSDs, we have created VSFP 2.1-like constructs from these cDNAs by inserting the CFP/YFP FRET pairs at homologous positions in the orthologous sequence. The constructs are being tested for membrane expression and voltage-dependent fluorescence changes in HEK293 cells.

2042-Pos

Solvatochromic Polarity-Sensitive Probes for Live Cell Imaging

Giovanni Signore[1], Riccardo Nifosì[2], Barbara Storti[1,2], Lorenzo Albertazzi[1,2], Ranieri Bizzarri[1,2].
[1]IIT@NEST, Center for Nanotechnology Innovation, Pisa, Italy, [2]NEST, Scuola Normale Superiore and CNR-INFM, Pisa, Italy.

Polarity-dependent fluorescent probes are attracting increasing interest for high-resolution cell imaging. A notable example is that of solvatochromic dyes located in a domain where polarity changes occurring upon binding lead to the enhancement of the fluorescence signal. This can yield a very sensitive detection of molecular recognition events that is applicable even in the case of non-overexpressed proteins.[1] We shall present a toolbox of new solvatochromic coumarin derivatives that are suitable for *in vivo* imaging applications.

Following a preliminary screening by computational methods of a set of candidate-structures selected on the basis of their spectral properties, we designed a synthetic protocol allowing a broad range of substitution patterns. We shall present experimental data on several probes showing excellent fluorescence quantum yields (up to 0.95), high molar-extinction coefficients (up to 46,000 $M^{-1}cm^{-1}$), and large Stokes shifts. Notably, our molecules display marked solvatochromism: they are virtually non emissive in water, but intensely fluorescent in less polar media (we shall show up to 780-fold fluorescence enhancement).

We shall also report on probe suitability for *in vivo* experiments. When tested on cultured cells, these coumarins proved not harmful and their photophysical properties were unchanged compared to data in solution. Owing to both their strong solvatochromic properties and their lipophilic character, the coumarins fluoresce only in the most lipophilic environments of the cell. In particular, colocalization experiments with organelle markers indicate that our coumarins locate in ER, membranes and lysosomes, depending on their chemical structure. Finally, one compound shows monoexponential decay of fluorescence with a lifetime which is linearly dependent on solvent polarity. We shall discuss how this feature promotes its use as ratiometric indicator of cell polarity at the nanoscale level.

1) Nalbant, P.; Hodgson, L.; Kraynov, V.; Toutchkine, A.; Hahn, K. M. *Science* **2004**, *305*, 1615-1619.

2043-Pos

Determination of Stoichiometry and Geometry of G Protein Coupled Receptor Homo-Oligomers in Living Cells Using Spectrally Resolved FRET

Michael R. Stoneman[1], Deo R. Singh[1], Arron Sullivan[1], **Valerica Raicu**[2].
[1]University of Wisconsin-Milwaukee, Department of Physics, Milwaukee, WI, USA, [2]University of Wisconsin-Milwaukee, Department of Physics, Department of Biological Sciences, Milwaukee, WI, USA.

Förster Resonance Energy Transfer (FRET) between donor and acceptor molecules is widely used for detection of molecular interactions. When donor and acceptor tags are fused to proteins of interest, FRET may be used to probe whether the tagged proteins form functional complexes in living cells. Typically, the cell under study is scanned at several times in order to accumulate enough spectral information to determine the FRET efficiency for each region of interest within the cell. However, diffusion as well as biochemical reactions may cause the molecular make-up of the regions of interest to change during the course of data acquisition. For a long time, this has dramatically limited the information content of FRET imaging. Advances in theory and optical instrumentation recently lead to the development of a FRET technique that avoids the problems caused by molecular diffusion and enabled us to determine the stoichiometry, structure, and localization in living cells of membrane protein complexes (Raicu et al., Nature Photonics, **3**, 2009). This presentation will review the results obtained from our recent studies of oligomeric complexes of some G protein-coupled receptors (GPCRs) in vivo, both, in the presence and in the absence of natural as well synthetic ligands.

2044-Pos
Fab Fragments Versus Full IgGs in Stimulated Emission Depletion (STED) Nanoscopy
Pit Bingen[1], Jakub Chojnacki[2], Thorsten Staudt[1], Johann Engelhardt[1], Hans-Georg Kräusslich[2], Stefan Hell[1,3].
[1]German Cancer Research Center, Heidelberg, Germany, [2]Department of Virology, University Hospital of Heidelberg, Heidelberg, Germany, [3]Max-Plank Institute for Biophysical Chemistry, Göttingen, Germany.
STED microscopy is an optical far-field microscopy technique which breaks the diffraction limit by quenching excited fluorophores into the dark state and thus reducing the effective (excitation) point spread function. The state of the art STED microscopes achieve resolution below 20 nm.
Standard labelling techniques use full IgG antibodies to tag specific proteins, an interaction similar to a lock and key, by two antigen binding sites. On a single protein scale IgGs therefore can potentially induce protein clustering, falsifying the results with respect to the cell or particle's natural environment. This effect is not observable in the standard confocal microscopy. However, in STED and other nanoscopic techniques protein clustering will lead to artifacts, which must be considered in an image interpretation.
In contrast Fab fragments have only one antigen binding site and clustering doesn't have to be taken into account.
We show the difference between full IgGs and Fab fragments on the nanoscopic scale by analyzing Env molecules on the surface of HIV particles and CD4 on the surface of JC53 cells. We demonstrate that Fab fragments result in images closer to the true structure of biological samples.

2045-Pos
Long-Term Super-Resolution Imaging of Actin Cytoeskeleton in Dendritic Spines Using a Low-Affinity Photoactivatable Probe
Ignacio Izeddin[1], Christian G. Specht[1], Mickaël Lelek[2], Christophe Zimmer[2], Antoine Triller[1], Xavier Darzacq[1], Maxime Dahan[1].
[1]École Normale Supérieure, Paris, France, [2]Institut Pasteur, Paris, France.
The transmission of signals across synapses requires the precise interaction of a large number of different synaptic proteins such as neurotransmitter receptors, adhesion, scaffold, signaling and cytoskeletal proteins. In small central excitatory synapses, this molecular machinery is contained in specialized cellular compartments called dendritic spines. Plastic changes in the strength of synaptic neurotransmission include alterations of the spine morphology. The shape of dendritic spines is determined by the actin cytoskeleton and is highly dynamic. Rearrangements of the actin network occur in response to synaptic activity. Thus, actin plays an important role in morphological aspects of synaptic plasticity.
The visualization of the precise spine morphology has been hampered by the limited spatial resolution of conventional wide field optical microscopy (typically in the range of 300 nm). The recent development of nanoscopic imaging methods makes it now possible to achieve a spatial resolution below the diffraction limit of light. Here, we have implemented photoactivated localization microscopy (PALM) to study the organization of the actin cytoskeleton within dendritic spines at 25 nm resolution.
To this aim we have generated a low affinity actin probe that consists of an actin-binding peptide (ABP) fused to a tandem Eos photoconvertible fluorescent protein (tdEos). ABP-tdEos was expressed in hippocampal neurons, where it binds reversibly to actin, thus allowing for long-term live imaging of the spine cytoskeleton at a spatial resolution beyond the diffraction limit of light. By reconstructing super-resolution images we have quantified morphological parameters of dendritic spines. Furthermore, we have studied dynamic changes of dendritic spine morphology over 30 minutes at a temporal resolution of 50 s. Using this approach we determined changes in the actin distribution within spines in response to pharmacologically induced synaptic activity.

2046-Pos
Photounbinding of Fluorescent Proteins
Klaus G. Neumüller[1], Kareem Elsayad[1], M. Neal Waxham[2], **Katrin G. Heinze**[1].
[1]Research Institute of Molecular Pathology (IMP), Vienna, Austria, [2]Department of Neurobiology and Anatomy, University of Texas Health Science Center, Houston, TX, USA.
Fluorescent probes are commonly used in biological experiments. Despite their great success story over the last century, fluorescent conjugates can not only visualize but also influence the properties of the molecules under study.
Recent studies have shown that fluorescently labeled antibodies can be dissociated from their antigen by illumination with laser light; the same has been observed for protein-peptide binding, including toxins. The mechanism responsible for the photounbinding effect however remains elusive. Here, we give insights into the mechanism of photounbinding and discuss bio (medical) applications of photounbinding.
We present studies of the photounbinding of labeled calmodulin (CaM) from a set of CaM-binding peptides with different affinities to CaM. Our results suggest that photounbinding is linked to photobleaching and a 'radiative' process requiring a fluorescent label. Interestingly, the photounbinding effect becomes stronger with increasing binding affinity, however, does not induce breakage of covalent bonds. We show that by writing a simple rate law for the dissociation process that takes into account the effective concentration of the fluorescent molecule, the affinity of binding and the laser intensity, it becomes possible to describe the intensity dependence of the photounbinding of our data. The proposed model assumes that an intermediate (transitional) complex is formed before the unbinding occurs and is consistent with the labeled-protein undergoing a conformational change resulting in a distinct dissociation constant which is in turn responsible for the unbinding.
We believe that detailed knowledge about the molecular processes involved in photounbinding will not only allow a systematic improvement of quantitative fluorescent studies, but also open the door to inducing or inhibiting molecular interactions by light and thus the development of novel tools, such as drug activation or delivery.

2047-Pos
3D Nanoscopic Optical Imaging of Subcellular Protein Organization and Neuronal Dendritic Morphology
Jianyong Tang, Jasper Akerboom, Alipasha Vaziri, Loren L. Looger, Charles V. Shank.
Janelia Farm Research Campus, Howard Hughes Medical Institute, Ashburn, VA, USA.
Single molecule localization microscopy enables biological samples to be optically observed with sub-diffraction resolution. Here we report new progress in 3D nanoscopic imaging of cellular and subcellular structures by our newly developed virtual volume photoactivated localization microscopy (VVPALM), in which a tilted mirror is used to generate side view of biological samples in addition to the front view, therefore providing precise single molecule localization in three dimensions. VVPALM brings advantages including high efficiency to use detected photons, minimum vulnerability to optical aberration, and simplicity of implementation. VVPALM is ideally compatible with weak chromophores, such as fluorescent proteins. We have used VVPALM to probe the localization and organization of various bacterial proteins, which are fused with photoactivatable proteins, inside or on the membrane of single *Escherichia coli* cells with sub-100 nm resolution in 3D. We have also combined VVPALM with label-free PAINT (points accumulation for imaging in nanoscale topography) technique to measure the nanoscale morphology of rat neuronal dendrites. Advances in multi-color nanoscopic imaging for protein 3D colocalization will also be presented.

2048-Pos
Photoactivation Localization Microscopy (PALM) on Orai1 Channels
Daniel Bergmair, Josef Madl, Julian Weghuber, Irene Frischauf, Christoph Romanin, Gerhard J. Schuetz.
Institut für Biophysik, JKU Linz, Linz, Austria.
Store Operated Calcium Entry (SOCE) is a crucial mechanism for many cellular signalling processes. The two major proteins involved in SOCE are Orai1 (located in the plasma membrane) and STIM1 (located in the membrane of the endoplasmatic reticulum (ER)). Upon depletion of the calcium stores in the ER, the STIM1 co-clusters with the Orai1 in the plasma membrane which results in a calcium influx into the cell.
In order to investigate the distribution of the Orai1 in the plasma membrane we used Photoactivation Localization Microscopy (PALM). PALM is a technique that allows overcoming the diffraction limit by photo-activating only a small subset of fluorophores with a laser pulse. At shallow illumination conditions, the active fluorophores are spatially well separated and can be localized with a precision of a few ten nm. Sequential activation, readout and photobleaching allows for recording a complete image of the sample. The Orai1 subunits were fused to photoactivatable GFP (paGFP) and expressed in Chinese hamster ovary cells. PALM revealed submicrometer clusters of Orai1, which show a high degree of colocalization with STIM1-mCherry, as confirmed by two-color microscopy.

2049-Pos
Using Ab-Space to Remove Background Components from Images in Systems of Multiple Fluorophores
Andrew H.A. Clayton[1], Noga Kozer[1], **Quentin Hanley**[2].
[1]Ludwig Institute for Cancer Research, Melbourne, Australia, [2]Nottingham Trent University, Nottingham, United Kingdom.
The linearization of the mixing of fluorescence intensity afforded by the AB-space formalism, simplifies a number of Frequency domain lifetime imaging

tasks. Biological systems often consist of multiple components due to the a presence of Donor, Donor-Acceptor complex, and fluorescent background. Tools allowing a third component to be removed from lifetime imaging data would represent a significant advance. We will describe a simplified treatment for resolving binary mixtures and a novel approach to ternary and higher mixtures using frequency domain procedures. For binary and ternary mixtures there is no requirement for single exponential decay, meaning that each component can represent a multi-fluorophore mix. For many applications in biology, resolution of the fractional fluorescence contributions from the donor and donor-acceptor components is desirable as this allows activation and related parameters to be observed. From frequency domain data, this can be done in a straightforward fashion without computing lifetimes by using the linear mixing characteristics of the AB-coordinate system. We present the theory and demonstrate the approach using solutions and apply it to a simple biological system. Ternary mixtures work well using the technique, however, the advantages of additional frequencies is limited. We have applied the formalism to A431 cells labelled with quantum dots (QDs) which have three components: QDs, cellular autofluorescence and plate background. The method allowed us to strip the autofluoresence and plate background image leaving only the QDs.

2050-Pos

Using Phasors in Interpreting One- and Two-Photon Fluorescence Lifetime Images of Fruit and Polymer Interfaces

M. vandeVen.
Hasselt University, Diepenbeek, Belgium.

Phasors prove to be an elegant way of characterizing time-resolved fluorescence images, (Digman et al., Biophys. J., 94, 1483-96, 2008). Fast Flim micro- and macro imaging (Biophys. J., 82, 502a) was applied to: 1. the pre-symptom and early detection of biotic and abiotic stress as well as surface defects and physiological disorders in fruit tissue using photosystem II Chlorophyll a fluorescence and 2. the characterization of conjugated polymer film produced under various conditions for biosensor development. Both Olympus and Zeiss imaging systems were used in conjunction with one photon 488 nm and 80 MHz, typically 15 mW two-photon illumination. For comparison overview color or transmission images were also collected. Several spots spread over the surfaces were used. Images have been analysed using phasors with Globals for Images, aka. SimFCS (LFD, UCI, CA, USA). The potential of the phasor approach as analysis tool for detection of both ageing and physiological stress progression (biological surfaces) and the influence of bleaching and preparation methods (polymer interfaces) is discussed.

2051-Pos

Investigation of the Lipid Metabolism during *Drosophila* Larva Development by Coherent Anti-Stokes Raman Scattering (CARS) Microscopy

Cheng-Hao Chien[1,2], Wei-Wen Chen[1,2], Meng-Ju Tsai[1,2], Ta-Chau Chang*[1,2].
[1]Institute of Biophotonics, National Yang-Ming University, Taipei, Taiwan, [2]Institute of Atomic and Molecular Sciences, Academia Sinica, Taipei, Taiwan.

Drosophila melanogaster is one of the most valuable model organisms in studying genetics and developmental biology. The *Drosophila* fat body stores lipids that act as an energy source for the developing animal during its larval stages. Studies on lipid metabolism of the fat body allow us to better understand human energy metabolism and related illnesses.

Coherent anti-Stokes Raman Scattering (CARS) microscopy is a nonlinear optical (NLO) technique which gives three-dimensional imaging based on chemically-selective vibrational scattering signals without any labeling agent. It has been widely used in the imaging of lipids in biological samples due to the strong CARS signal from carbon-hydrogen (C-H) bonds. Here we used CARS microscopy to image the distribution of the fat body in *Drosophila* larva *in vivo* with minimal invasion. Combined with two-photon excitation (TPE) and second harmonic generation (SHG), we could also obtain images of internal organs from autofluorescence and collagen/muscular tissues from SHG simultaneously in the same NLO platform. This study allowed us to visualize the three-dimensional structures of the *Drosophila* larva under the most natural living condition which cannot be achieved by conventional biochemical staining and labeling system. We further investigated the development of the fat body during different larval stages and under various conditions through long-term *in vivo* observations.

To our knowledge, this is the first demonstration on *in vivo* imaging of unstained/label-free *Drosophila* fat body to get new insights into the lipid metabolism during *Drosophila* larva development by using multimodal NLO microscopy.

2052-Pos

Diffusion Measurements of Lipophilic Fluorescent Probes in Fixed Tissue and Living Cells

Jeff Tonniges[1], Maria Hansen[1], Jeremy Duncan[2], Bernd Fritzsch[2], Brian Gray[3], Arunkumar Easwaran[3], Michael G. Nichols[1].
[1]Creighton University, Omaha, NE, USA, [2]University of Iowa, Iowa City, IA, USA, [3]Molecular Targeting Technologies, Inc., West Chester, PA, USA.

By diffusing laterally along cell membranes, lipophilic fluorescent dyes delineate the neural pathways of both wild-type and mutant models. Multicolor imaging studies using a spectrally distinct set of diffusion-matched dyes are needed to further develop our understanding of complex neuronal connections. Previously, a set of dyes with fluorescence emission ranging from the UV to NIR was characterized and used to demonstrate six-color neuronal tracing. Using FRAP and relative distance measurements, transcellular diffusion in fixed tissue was shown to depend on the fluorescent head group. Now to compensate for this head-group-dependent diffusion, the influence of the hydrocarbon chain length has been characterized. Time-scaling exponents and diffusion coefficients within peripheral nerve tissue were compared to measurements in living cell culture. Surprisingly, it was found that the diffusion rates along the nerve increased with increasing hydrocarbon chain length. To elucidate the mechanism of lipid diffusion between cells, additional relative diffusion measurements in cultured living cells were performed by labeling a single cell within an interconnected network and measuring the spread of the fluorescent probe into surrounding cells. Taken together, these studies provide a systematic approach for the design of spectrally-discrete and diffusion-matched fluorescence probes for neurotracing.

2053-Pos

Real Time Monitoring of Endogenous Messenger RNA Using Linear Antisense Probe

Kohki Okabe[1], Yoshie Harada[2], Takashi Funatsu[1].
[1]University of Tokyo, Tokyo, Japan, [2]Kyoto University, Kyoto, Japan.

In eukaryotic cells mRNA plays a key role in gene regulation. However, the function of mRNA is not fully understood because direct analysis of endogenous mRNAs in living cells has been difficult. We developed a method for the observation of endogenous mRNA in living cells using two fluorescently labeled linear antisense 2′*O*-methyl RNA oligonucleotides. When those two antisense probes, each is labeled with different fluorescent dyes, are hybridized to an adjacent sequence of the target mRNA, the distance between two fluorophores becomes close and FRET occurs.

Here we applied linear antisense probes to the real time monitoring of endogenous mRNA, which will be useful in understanding the function of mRNA as well as the intracellular localization. First, two kinds of linear antisense probes were microinjected into the cytoplasm of living COS7 cells and the FRET signal from cells was recorded over time to examine the kinetics of the hybridization reaction with c-*fos* mRNA. The hybridization reaction of linear antisense probes proceeded quickly and time constants of linear antisense probe was estimated to be less than one minute. When using Molecular Beacon, the conventional probe for endogenous mRNAs, it took more than one hour to complete the hybridization. Next, the induction of c-*fos* mRNA in the cytoplasm of COS7 cells was investigated in real time using linear antisense probes. As a result, the elevation of c-*fos* mRNA expressed in the cytoplasm was observed within one hour after the stimulation with PMA (phorbol 12-myristate 13-acetate). In conclusion, we showed the linear antisense probes are advantageous in monitoring of mRNAs due to their prominent kinetics in hybridizing with target mRNAs in living cells.

2054-Pos

3D-Frap of PAGFP Reveals Inhomogeneity in Cytoplasmic Structures between the Major Rod Photoreceptor Compartments

Mehdi Najafi, Peter D. Calvert.
SUNY Upstate Medical University, Syracuse, NY, USA.

Introduction: Diffusion of signaling proteins is thought to be essential for photoreceptor physiology, allowing, for example, regulation of the photoresponse through dynamic sequestration of key transduction proteins in either of the two major photoreceptor compartments, the inner and outer segments (IS and OS, respectively). The influence of the physical nature of the cytoplasm in these compartments on protein mobility is not known, but is essential for understanding photoreceptor function. We have thus developed a novel approach to quantifying protein mobility in 3D in live photoreceptors.

Methods: Transgenic *Xenopus laevis* expressing the photoactivatable variant of GFP, PAGFP, exclusively in rod photoreceptors were generated using established methods. Live retinal slices were imaged with a custom-built

multiphoton/confocal microscope. A source of photoactivated PAGFP was generated within selected compartments using multiphoton excitation at 820nm and its dissipation was monitored with 488nm confocal scanning. Images were compared with the output of a 3D diffusion model to estimate effective radial and axial diffusion coefficients.
Results: PAGFP diffusion in the IS was isotropic and faster than in the OS, $D_{IS} = 5.2\ \mu m^2\ s^{-1}$. In the OS PAGFP diffusion was anisotropic, with faster radial diffusion, $D_{OS\text{-}radial} = 3.5\ \mu m^2\ s^{-1}$, and slower axial diffusion, $D_{OS\text{-}axial} = 0.19\ \mu m^2\ s^{-1}$.
Conclusion: PAGFP diffusion in both compartments was substantially retarded relative to aqueous solution, $D_{aq,PAGFP} \sim 90\ \mu m^2\ s^{-1}$, and cultured Chinese hamster ovary (CHO) cell cytoplasm, $D_{CHO,PAGFP} \sim 20\ \mu m^2\ s^{-1}$. Moreover, axial diffusion of PAGFP in the OS was hindered to a larger extent than expected from the geometry of disc membranes that span the compartment orthogonal to the cylinder axis. These results suggest that the photoreceptor cytoplasm possess higher density of cytoskeleton and/or macromolecules.

2055-Pos
Lipopolysaccharide Regulation of Dendritic Cells Activation and Life Cycle: in vitro and in vivo Studies Towards Antitumor Immunoactivity
Maddalena Collini, Ivan Zanoni, Renato Ostuni, Michele Caccia, Laura D'Alfonso, Giuseppe Chirico, Laura Sironi, Tatiana Gorletta, Marco Di Gioia, Francesca Granucci.
università di milano-bicocca, milano, Italy.
Dendritic cells (DCs) are key regulators of innate and adaptive immune responses that can be exploited in the immunological treatment of many type of cancers. Recently, we have demonstrated that lipopolysaccharide (LPS) is able to regulate DC life cycle through the activation of a CD14-dependet pathway [1]. Once activated with LPS, DCs become also able to prime Natural Killer (NK) cells to exert their anti-tumoral activity as demonstrated both *in-vitro* and *in-vivo* using mouse models in which melanoma tumors were sub-cute implanted. Using two-photon microscopy, we are currently extending these experiments to the direct investigation of the interaction of LPS-activated DCs with NK cells in *in vivo* condition at the level of peripheral lymph nodes.
DCs and NK cells,labeled with different fluorescent markers, are tracked continuously in the lymph nodes while the structure of the lymph node is monitored by second harmonic generation microscopy. The analysis of the traces and the comparison of the experimental results to statistical and simulative models of the lymphocytes motion allows to elucidate their dynamic behavior at different times after the activation of the DCs shedding new light on the DCs - NK cells interaction.
[1] Zanoni, I.; Ostuni, R.; Capuano, G.; Collini, M.; Caccia, M.; Ronchi, A.E.;Rocchetti, M.; Mingozzi, F.; Foti, M.; Chirico, G.; Costa, B.;Zaza, A.; Ricciardi-Castagnoli, P.; Granucci, F. (2009) CD14 regulates the dendritic cell life cycle after LPS exposure through NFAT activation. ***Nature,*** 460:264-269.

2056-Pos
Growing Lung A549 Epithelial Cells on Metallic Surfaces
Irina Akopova[1], Ryszard Grygorczyk[2], Myoung Kim[1], Harlan Jones[1], Rafal Luchowski[1], Julian Borejdo[1], Ignacy Gryczynski[1], Zygmunt Gryczynski[1].
[1]UNT HSC, Fort Worth, TX, USA, [2]University of Montreal, Montreal, QC, Canada.
Fluorescence can be greatly enhanced near metal surfaces due to many-fold increased brightness and photostability of fluorophores located near metallic nanoparticles or nanostructures. Further more, fluorophores deposited on a plane of a 50 nm thick silver or gold mirrors, show directional fluorescence in a form of hollow cone. These favorable properties of fluorophore-plasmonic interaction can be utilized in high-sensitivity imaging of cellular processes. However, the cell growth strongly depends on the nature of the substrate and is often very difficult on bare metal surfaces. In our study we examined suitability of different metal surface coatings for growing lung A549 epithelial cells. Six different surfaces were tested - glass, silver mirror, silver mirror coated with SiO_2, gold mirror, gold mirror coated with SiO_2 and silver fractals on glass. The glass coverslips with five different metallic surface coatings and one control were placed in a tissue culture plates containing DMEM-High Glucose media. Suspension of 0.5×10^6 cells/plate was deposited on the slides and the cell cultures were placed in 37°C, 5%CO_2 incubator. Cell growth was monitored every 24 hours. No substantial differences in cell morphology were found whether they were on the regular microscopic glass slide or slide covered with metals, but cells initially grew significantly slower on fractals compared to other ''smooth'' surfaces. The findings demonstrate feasibility of growing A549 cells on metal-coated glass surfaces and opens the opportunity for imaging live A549 cells using metal enhanced fluorescence.
Supported by the Canadian Institutes of Health Research and the Canadian Cystic Fibrosis Foundation (R.G), and Emerging Technologies Fund Grant Texas (Z.G.).

2057-Pos
Fluorinated Voltage Sensitive Dyes for SHG and Multiphoton Microscopy
Stacy A. Wilson, Ping Yan, Leslie M. Loew.
University of Connecticut Health Center, Farmington, CT, USA.
Dyes based on hemicyanine chromophores have high membrane affinities and the ability to report on local membrane environment and act as sensors of membrane voltage. Laser-scanning second harmonic generation (SHG) microscopy utilizing such voltage sensitive dyes has shown considerable promise as an imaging modality, possessing several advantages over fluorescence for the optical mapping of membrane potentials. The addition of electronegative fluorine atoms to the chromophore is intended to lower both the ground and excited state energies, so as to make dyes less susceptible to photobleaching. Improved photostability will allow extension of the duration of optical recording measurements, permit the use of more intense laser excitation, and minimize photodamage to the biological sample. The effect of fluorination on photostability and dye performance has been systematically investigated for a series of newly synthesized dyes and found to depend critically on the location of the substituent within the chromophore. Voltage-clamped neuroblastoma cells stained with these dyes were imaged with 1064nm excitation, allowing sensitivities and response kinetics of SHG and two-photon fluorescence to be determined simultaneously for several fluorinated dyes. Our results suggest that voltage sensitive dyes can be developed which have large SHG signal changes, sufficient photostability, and the requisite speed for use as a practical tool for measuring electrical activity in biological systems.
(Supported by NIH grant EB001963)

2058-Pos
High Throughput Screening of Biosensor Domains: Visualizing Dynamic Activation of Src Kinases in Live Cells
Akash Gulyani[1], Eric Vitriol[1], Dmitriy Gremyachinskiy[1], Brian J. Dewar[1], Alan Nguyen[1], Lee M. Graves[1], Brian K. Kay[2], Klaus M. Hahn[1].
[1]University of North Carolina, Chapel Hill, NC, USA, [2]University of Illinois, Chicago, IL, USA.
Biosensors that report activation of native, unmodified proteins can help delineate complex cellular processes with minimal perturbation of normal behavior. However, sensors for endogenous proteins are rare, in part due to the absence of readily available binding reagents that are selective for the active form of the targeted molecule. To address this issue we combined high throughput screening of engineered state-specific binding elements with a fluorescence-based reporting system that turns these elements into biosensors. We have targeted Src family kinases (SFKs) since they are key signaling nodes that control numerous cellular functions, including migration and adhesion. Also, the multiple roles performed by Src kinases and their involvement in several signaling networks suggest spatio-temporally regulated pools of SFK activities. Phage display screening was used to generate fibronectin domain III (FN3) binders that selectively bind SH3 domains from Src family kinases. Pull down experiments demonstrated that an FN3 binds selectively to active Src kinases. Using merocyanine dyes developed in our lab for live cell imaging, we have converted this FN3 into a sensitive fluorescence-based biosensor for activation of Src family kinases. The new sensors reveals patterns of Src activation in migrating cells and in cells stimulated with growth factors. In migrating cells, a distinct band of Src activation was observed at the leading edge. This transient activation coincided with protrusion. We also observed precisely timed Src activation in linear and circular dorsal ruffles. In keeping with our overall aim of developing a generally applicable strategy of sensor design, we have generated multiple binders using HT screening and are developing biosensors specific to individual Src family kinases.

EPR Spectroscopy

2059-Pos
Alignment Studies Employing the Rigid TOAC Spin Label Utilizing Electron Paramagnetic Resonance (EPR)
Daniel J. Mayo, You Zhou, Gary A. Lorigan.
Miami University, Oxford, OH, USA.
For electron paramagnetic resonance (EPR) spectroscopic studies, the TOAC spin label offers the unique advantage over other conventional labels in that it reports accurate backbone motion and peptide dynamics due to its rigid nature. This label has become extremely important in EPR studies to study membrane protein topology and their associated dynamics. Additionally, some researches have also developed spectroscopic techniques using magnetically aligned (bicelles) and mechanically aligned (glass plates) lipid samples to extract additional information directly related to structural topology with respect to the membrane. Based upon the samples orientation, other anisotropic spectral parameters can also be determined. EPR spectroscopy offers a unique solution due to the fact it has a much higher sensitivity and also a different frequency domain than other conventional techniques. Thus, we have performed EPR alignment studies on two-model peptides magainin-2 and the M2δ subunit of the acetylcholine receptor. Both of these peptides have been well characterized and are 23 amino acids in length.

2060-Pos
Peldor Beyond Distances
Olav Schiemann.
Centre for Biomolecular Sciences, St Andrews, United Kingdom.
Structural Biology is engaging ever larger assemblies of biomacromolecules either isolated, embedded in membranes or in whole cells. Thus, biophysical methods are needed that access these architectures on the critical nanometer length scale in these environments. Electron Paramagnetic Resonance provides several tools to precisely and reliably measuring such these distance in the nanometer range in particular a method called Pulsed Electron-Electron Double Resonance (PELDOR).[1] In this presentation, it will be shown that PELDOR yields not only distances and distance distribution but also full information about label orientation,[2] coupling mechanisms[3] and that it can be used to count the monomers in aggregates.[4] Examples will include covalently and non-covalently labelled duplex DNAs/RNAs, complex folds of RNAs and the 320 kDa membrane channel Wza[5].
1. O. Schiemann, T.F. Prisner *Quart. Rev. Biophys.* **2007**, 40, 1.
2. O. Schiemann, P. Cekan, D. Margraf, T. F. Prisner, S.T. Sigurdsson, *Angew. Chem. Int. Ed. Engl.* **2009**, 121, 3342.
3. D Margraf, P. Cekan, T.F. Prisner, S.Th. Sigurdsson, O. Schiemann *PCCP* **2009**, 11, 6708.
4. B.E Bode, D. Margraf, J. Plackmeyer, G. Durner, T.F. Prisner, O. Schiemann *J. Am. Chem. Soc.* **2007**, 129, 6736.
5. G. Hagelueken, W.J. Ingledew, H. Huang, B. Petrovic-Stojanovska, C. Whitfield, H. ElMkami, O. Schiemann, J.H. Naismith *Angew. Chem. Int. Ed.* **2009**, 121, 2948.

2061-Pos
Increased Sensitivity and Range of Distance Measurements in Spin Labeled Membrane Proteins
Hassane S. Mchaourab, Ping Zou.
Vanderbilt University, Nashville, TN, USA.
We report a significant methodological advance in the application of double electron-electron resonance (DEER) to spin-labeled membrane proteins. DEER is an unparalleled tool in structural biology yielding long range distance restraints that can be used to model protein folds, to define the nature of conformational changes and determine their amplitudes. Distances are obtained in native-like environments in the absence of conformational selectivity imposed by the crystal lattice and regardless of the molecular mass. However, the realization of these advantages in proteolipsomes has so far lead to significant reduction in the distance range and loss of sensitivity compromising experimental throughput. In the two-dimensional environment of a liposome, the background of intermolecular dipolar spin coupling leads to a strong decay that can obscure the contribution of intramolecular coupling rendering the DEER signals uninterpretable. We found that the combination of two emerging technologies, Q-band pulsed electron paramagnetic resonance and Nanodiscs phospholipid bilayers, overcome the factors limiting DEER sensitivity and distance range. Spin labeled mutants of the ABC transporter MsbA were functionally reconstituted into Nanodiscs at a ratio of one dimer per lipid bilayer. In comparison to proteolisposmes, DEER data from Nanodiscs have a linear baseline reflecting the three dimensional spatial distribution of MsbA. The order of magnitude increase in absolute sensitivity at Q-band microwave frequency is critical given limited sample quantities and working concentrations in the 10-30 μM range. We took advantage of the higher throughput to demonstrate that the magnitude of the distance changes in the ATP hydrolysis cycle is not affected by the lipid headgroup. The advances described here set the stage for the use of DEER spectroscopy to analyze the conformational dynamics of eukaryotic membrane proteins.

2062-Pos
Novel Approaches for Distance Determination by EPR: Large Anisotropy, Fast Relaxing Paramagnetic Centres, Such as Fe(III), as Markers
Sergey Milikisyants[1], Francesco Scarpelli[1], Michelina G. Finiguerra[1], Marcellus Ubbink[2], Edgar J.J. Groenen[1], **Martina Huber[1]**.
[1]Leiden University, Leiden, Netherlands, [2]Department of Chemistry, Leiden University, Leiden, Netherlands.
Recent advances in structure determination of biomacromolecules have been achieved by pulsed EPR methods, such as double electron electron paramagnetic resonance (DEER or PELDOR), by which distances in the nano-meter range between two nitroxide spin labels or low-anisotropy paramagnetic metal ions are accessible. Ways to extend the existing methods are presented: One of them is a new pulse sequence improving the orientation selectivity of the method (os-DEER), which could be a step towards measuring shorter distances (Milikisyants et al., JMR 2008). High-anisotropy, fast relaxing paramagnetic centres had been off-limits for DEER. We show that distances between nitroxide spin labels and high-anisotropy paramagnetic centres are accessible with RIDME (Kulik et al. JMR 2002), if dead-time is avoided (Milikisyants JMR 2009). We show that thereby the distance between the low-spin Fe(III)-ion and a nitroxide in a mutant of cytochrome f can be measured (see Fig.).

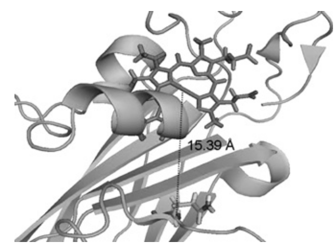

Given the prevalence of high-anisotropy, fast relaxing centres in bio-macromolecules the method proposed extends the range of systems that can be accessed greatly, including protein-protein and protein-ligand interactions.

2063-Pos
EPR Spectroscopic Studies on the Structural and Dynamic Properties of Human KCNE1 Membrane Protein in Lipid Bilayers
Thusitha S. Gunasekera[1], Aaron T. Coey[1], Congbao Kang[2], Richard Welch[2], Carlos G. Vanoye[2], Charles R. Sanders[2], Gary A. Lorigan[1].
[1]Miami University, 45056, OH, USA, [2]Vanderbilt University, 37322, TN, USA.
The KCNE1 membrane protein regulates KCNQ1, which forms the voltage-gated potassium channel in the human heart. Mutations in these genes are responsible for the human genetic disease, long QT syndrome. However, the structure of KCNE1 in a lipid bilayer and biophysical basis for KCNE1's modulation of KCNQ1 are not completely understood. Recent research from Sanders group using solution NMR indicates the transmembrane domain of KCNE1 is a curved alpha-helix and is flanked by intra- and extracellular domains comprised of alpha-helices joined by flexible linkers (Kang et al., Biochemistry 2008 47:7999-8006). Site-directed spin labeling (SDSL) electron paramagnetic resonance (EPR) spectroscopy has emerged as a well-established method to study the structural properties of membrane proteins. Our objective is to use advanced EPR spectroscopic techniques including CW and pulsed EPR spectroscopy to obtain structural parameters of the KCNE1 protein in a bilayer. To date, we have successfully over-expressed KCNE1 in E. coli and reconstituted the protein into POPG/POPC lipid bilayers. Electrophysiological experiments confirm KCNE1 can co-assemble with the channel protein, KCNQ1 and are fully functional. Electrophysiological experiments further confirm that KCNE1 is inserted correctly into the lipid-bilayers. Additionally we have also demonstrated potential use of DEER (Double Electron-Electron Resonance) and CW-EPR power saturation experiments for distance and depth measurements of KCNE1 in lipid bilayers, respectively.

2064-Pos
Structure and Dynamics of the Calcium Binding Domains of the Na/Ca Exchanger (NCX1.1) Determined by Site Directed Spin Labeling
Mrinalini Dixit, Sunghoon Kim, Eric J. Hustedt, Charles E. Cobb, Albert H. Beth.
Vanderbilt University, Nashville, TN, USA.
The cardiac Na^{+}/Ca^{2+} exchanger (NCX1.1) serves as the primary means of Ca^{2+} extrusion from cardiomyocytes following the rise in intracellular Ca^{2+}

during contraction. The exchanger is regulated by binding of Ca^{2+} to the intracellular domain. This domain is composed of an α-catenin-like domain (CLD) that connects two structurally homologous Ca^{2+} binding domains (CBD1 and CBD2) to the transmembrane domain of the exchanger. NMR and X-ray crystallographic studies have provided structures for the isolated CBD1 and CBD2 domains and have suggested how Ca^{2+} binding alters their structures and motional dynamics. It remains unknown how Ca^{2+} binding to the intact Ca^{2+} sensor signals the transmembrane domain to regulate exchanger activity. We have used site directed spin labeling to address this question. Conventional EPR experiments have shown that: 1) residues in, or near, the Ca^{2+} binding loops of CBD1 and CBD2 show decreased mobility upon Ca^{2+} binding; and 2) residues in the β-sandwich regions are insensitive to Ca^{2+} binding. Double Electron Electron Resonance (DEER) measurements on doubly labeled constructs revealed that: 1) the structure of the β-sandwich domains of CBD1 and CBD2 are not altered upon Ca^{2+} binding; 2) CBD1 and CBD2 do not lie lengthwise antiparallel in close proximity but rather residues in the distal ends that connect to the CLD are greater than 60 Å apart; and 3) residues nearer to the apex of the Ca^{2+} sensor are in close enough proximity to be measured by DEER and these distances are sensitive to Ca^{2+} binding. These studies support recent SAXS studies by Hilge et al. (PNAS 106:14333-8, 2009) and provide additional insight into a structural rearrangement of the intact Ca^{2+} sensor that may be involved in regulation of Na^{+}/Ca^{2+} exchange.

2065-Pos
Structure of the CDB3 - ankD34 Complex from Site - Directed Spin - Labeling Studies
Sunghoon Kim, Eric J. Hustedt, Suzanne Brandon, Charles E. Cobb, Christopher W. Moth, Christian S. Parry, Terry P. Lybrand, Albert H. Beth.
Vanderbilt University, Nashville, TN, USA.
The association between the cytoplasmic domain of band 3 (CDB3) and ankyrinR forms a critical link between the lipid bilayer of the erythrocyte membrane and its underlying spectrin cytoskeleton. This interaction is responsible for the remarkable mechanical stability of the erythrocyte membrane that is essential for the durability of the erythrocyte. While the structures of CDB3 [1] and ankD34 (repeats 13-24 from full length ankyrinR) [2] have been determined by X-ray crystallography, the structure of the CDB3-ankD34 complex has not been established. Using distance constraints from site-directed spin labeling (SDSL) and DEER spectroscopy, we propose a new structural model of CDB3-ankD34 complex modeled assuming rigid-body docking between the two proteins combined with rigorous modeling of the spin label. Unexpectedly, the new model generated by Rosetta docking calculations and filtered through multiple DEER distance constraints shows features which are quite different from the previously proposed docking model. The binding interface of CDB3 is widely scattered over its peripheral surface but the β6-β7 hairpin loop makes no direct contact with ankD34. Second, the binding interface of ankD34 resides on the opposite side of β-hairpin loops from the concave groove. The validity of our current model is also supported by a series of SDSL and cross-linking experiments where the binding interface of ankD34 was mapped by the model-guided scanning of a series of surface sites on ankD34. Supported by NIH P01 GM080513.
[1] D. Zhang et al., *Blood*, 96, 2925 (2000)
[2] P. Michaely et al., *EMBO J.*, 21, 6387 (2002)

2066-Pos
Structural Origins of Nitroxide EPR Spectra in a β-Barrel Membrane Protein
Daniel M. Freed, David S. Cafiso.
University of Virginia, Charlottesville, VA, USA.
Site-directed spin labeling is a powerful tool for studying structure and dynamics in proteins, due to its ability to bypass several fundamental limitations suffered by methodologies such as NMR and x-ray crystallography. The utility of this technique, however, hinges on our ability to reliably interpret EPR lineshapes of spin-labeled proteins, so that spectral features may be unambiguously associated with their structural origins. In the present work, X-ray crystallography has been combined with mutagenesis and a quantitative analysis of EPR spectra to examine for the first time the origins of spectra from a β-barrel membrane protein, BtuB. The hydrocarbon-exposed residue T156C was spin-labeled and gave rise to a two-component EPR spectrum, corresponding to two conformers of the spin-labeled side chain. Quantitative lineshape analysis revealed a dominant population of highly (spatially) ordered yet mobile nitroxide, and a second population of weakly ordered yet immobile nitroxide. EPR spectra show that single mutations to nearest-neighbor residues affect the ordering and or equilibrium of label rotamers, however these changes are small in each case. In the 2.6Å crystal structure of spin-labeled BtuB, the likely source of weak pairwise interaction with nearest-neighbors is attributed to the extent of barrel curvature, β-strand twist, and direction of strand tilt. It is postulated that residues Q158, L160 (periplasmic loop), V166, and L168 (hydrogen-bonded neighbor) may cooperatively stabilize the nitroxide spin label by forming a hydrophobic pocket. This approach is being applied to an additional hydrocarbon-exposed site on BtuB which exhibits a different degree of strand tilt and twist.

2067-Pos
Characterization of the L511P and D512G Mutations in the MsbA Lipid Flippase
Kathryn M. Westfahl, Jacqueline Merten, Candice S. Klug.
Medical College of Wisconsin, Milwaukee, WI, USA.
MsbA is a 65kDa lipid flippase found in the inner membrane of Gram-negative bacteria such as E. coli and S. typhimurium. As a member of the ABC transporter superfamily, MsbA contains two nucleotide binding domains and two transmembrane domains, one from each of its two monomers. ABC transporters transport a diverse group of substrates from lipids to antibiotics and their dysfunction contributes to a number of human pathologies including cystic fibrosis. As an essential protein in E. coli, the deletion or dysfunction of MsbA results in the toxic accumulation of lipid A in the inner membrane resulting in membrane instability and cell death. The L511P and D512G mutations have been previously identified through mutational analysis as dysfunctional nucleotide binding domain mutations specific to MsbA and were suggested to have a lower affinity for ATP. To further understand the cause of dysfunction in these point mutations, in vivo growth assays, in vitro ATPase activity assays, DEER and CW EPR spectroscopy studies throughout the ATP hydrolysis cycle were conducted. L511P and D512G were each paired with nine different reporter residues, each in or near an important conserved nucleotide binding domain motif and compared to the reporter residues alone. To identify the stage in the ATP hydrolysis cycle in which the L511P and D512G mutations are dysfunctional, the local tertiary interactions before, during, and after ATP hydrolysis were monitored by EPR spectroscopy at each stage of the ATP hydrolysis cycle.

2068-Pos
Free Radical Generation and Electron Flux in Mitochondrial Fe-S Centers During Cardiac Injury; Changes with Mitochondrial Protective Drug Ranolazine
Ashish K. Gadicherla, William E. Antholine, Amadou K.S. Camara, James S. Heisner, Mohammed Aldakkak, Age D. Boelens, David F. Stowe.
Medical College of Wisconsin, Milwaukee, WI, USA.
Some TCA cycle enzymes, like aconitase, are more susceptible to ischemia reperfusion (IR) injury. Ranolazine (RAN) is cardioprotective against IR injury. It is a late Na^{+} current blocker that may also limit lipid peroxidation and complex I activity. It is unknown if RAN alters the redox state of Fe-S clusters or free radical generation (FRG) to underlie its protection. Here we examined how IR injury affects FRG and Fe-S clusters of aconitase and succinate dehydrogenase, using electron paramagnetic resonance (EPR), and if RAN alters these effects. Guinea pig hearts (n=8) were isolated and perfused with Krebs Ringer buffer and exposed to: a) control, b) 30 min global ischemia, c) 10 μM RAN for 10 min just before ischemia, or d) ischemia and 10 min reperfusion. Hearts were immediately ground in liquid N_2 and packed into EPR tubes. We examined changes in signal intensity in liquid He (10°K) of assigned g=2.016 (aconitase 3Fe-4S), g=1.93 (succinate dehydrogenase 2Fe-2S), g=2.006 (free radical), and g=6.0 (Fe group of cytochrome *c*). Versus time control (100%), the signal for aconitase Fe-S at the end of ischemia was 46%, suggesting oxidative damage; this was partially restored by 10 min reperfusion to 91% and after I+RAN treatment to 55% of control. Signal intensity for succinate dehydrogenase was unaltered by IR or RAN+IR. The presumptive ubisemiquinone radical signal increased 19% after ischemia, suggesting increased FRG, but only by 4% at 10 min reperfusion. I+RAN treatment decreased the signal by 19%. The signal for cytochrome *c* (g=6.0) increased 730% after IR, but was only 81% after I+RAN. These data suggest that RAN treatment partially restores electron flow through some Fe-S centers and reduces FRG, which may partially underlie its cardioprotective effects.

2069-Pos
Structural Analysis of the Membrane Docking Geometry of PI(3,4,5)P3-Specific GRP1-PH Domain Via Site-Directed Spin Labeling
Zachary J. Owens, Kyle E. Landgraf, John A. Corbin, Danielle C. Dukellis, Joseph J. Falke.
University of Colorado Boulder, Boulder, CO, USA.
Peripheral membrane binding proteins play critical roles in dynamic cell signaling processes that occur at membrane surfaces. Many of these signaling proteins contain membrane targeting domains that act to mediate signal dependent membrane localization for proper enzyme function. Phosphoinositide-specific

pleckstrin homology (PH) domains are an important class of membrane targeting domains that specifically bind target phosphoinositides present at the surface of inner cell membranes. Aside from target lipid headgrouprecognition, the other protein-lipid interactions that occurduring membrane docking are not well defined. Currently, high-resolution structural characterization of protein-membrane interfaces is difficult to achieve while this information is crucial to a physical chemical understanding of reversible protein-membrane binding. In this study, site-directed spin-labeling and electron paramagnetic resonance (EPR) power saturation measurements were employed to determine membrane depth parameters for the PI(3,4,5)P3-specific GRP1-PH domain docked to synthetic bilayer membranes. A library of nitroxide spin-labeled PH domain mutants was generated using site-directed cysteine mutagenesis and disulfide coupling to a methanethiosulfonate spin label (MTSSL). Subsequently, membrane depth parameters were determined for each spin-labeled position in the membrane-docked state. The depth parameters were then used as constraints to model the angular orientation and depth of penetration that describes the membrane docking geometry. Our preliminary structural model identifies the membrane binding surface of GRP1-PH and characterizes its partitioning into the membrane bilayer. Ultimately, the results of this study will aid in understanding the molecular determinants of the electrostatic search mechanism this PH domain uses to rapidly find its rare target lipid on the plasma membrane surface. Supported by NIH GM063235 (J.J.F.).

2070-Pos
Sequence-Specific Stereomeric Environment in a DNA Duplex Revealed by a Nucleotide-Independent Nitroxide Probe

Anna Popova, Peter Z. Qin.
University of Southern California, Los Angeles, CA, USA.

In site-directed spin labeling, structural and dynamic information on a parent macromolecule is obtained by monitoring a covalently linked nitroxide radical using electron paramagnetic resonance (EPR) spectroscopy. Our group have developed a method of attaching nitroxide species, such as 1-oxyl-4-bromo-2,2,5,5-tetramethylpyrroline (R5a), to a specific nucleotide position within a target DNA or RNA sequence. The method relies on site-specific introduction of a phosphorothiate during the solid phase chemical synthesis of nucleic acids, and at each given labeling site the nitroxide is attached to one of two phosphorothioate diastereomers (Rp or Sp) in an approximately 50/50 ratio. We have recently reported that variations in DNA structural and dynamic features at the level of an individual nucleotide can be detected using R5a attached to mixed phosphorothioate diastereomers, in which an observed EPR spectrum is presumably a sum of those obtained from either diastereomer (Popova et al., Biochemistry, 2009, 48, 8540-50). In this work, we report X-band EPR spectra of R5a attached to purified Rp and Sp diastereomers at different sites within a B-form DNA duplex. Results are compared to those obtained with mixed nitroxide diastereomers, and advantages and limitations are discussed regarding the necessity of diastereomer separation when probing DNA local environment. Our work is a further step forward in developing a SDSL methodology that may provide a mean for studying structure and dynamics in large DNA molecules.

Nano-Materials

2071-Pos
Analysis of Postphotoactivation Scanning Diffusion Profiles for Multiple Species with Distributed Diffusion Coefficients

Bonnie E. Lai, Jason A. Chen, S Munir Alam, David F. Katz.
Duke University, Durham, NC, USA.

Postphotoactivation scanning (PPS) is a method for quantifying diffusion coefficients of particles in simple and complex materials (e.g., hydrogels) over length scales ~100μm-mm (Geonnotti et al., 2008). Diffusing particles are labeled with caged fluorophore, and a slit-shaped region of sample is exposed to UV to generate a line of fluorescence. A high-resolution scanner quantifies intensity profiles as particles diffuse out from the fluorescent region over time; these are fit to the solution of the diffusion equation to obtain the diffusion coefficient. We use this technique to measure mobility of HIV-like liposomes. Here, we describe a novel method for analyzing PPS profiles for multiple diffusing species with a distribution (α) of diffusion coefficients (D). To determine $\alpha(D)$, we generated sets of diffusion profiles for a discretized range of D by numerically solving the diffusion equation using the experimental initial condition and assuming given D. We computed net diffusion profiles resulting from the sums of profiles with distribution α. We used an optimization scheme to deduce $\alpha(D)$ that minimized the squared difference of observed and computed profiles. The method was validated using simulated and experimental data. Experimental results for fluorescein diffusing in PBS (D=4.3×10^{-6} cm^2/s) are similar to literature values. We also measured diffusion coefficients of solutions of labeled ~100nm liposomes (D=$3.2\pm2\times10^{-8}$ cm^2/s, n=4). We were able to resolve 2 distinct peaks in α corresponding to the D of liposomes and of free label. Measured values for diffusion coefficients of liposomes are similar to those predicted by Stokes-Einstein (D=$3.9\pm1\times10^{-8}$ cm^2/s). We are using the technique to analyze interactions of HIV-like liposomes and anti-HIV antibodies. The method can be applied to describe diffusion of multiple species within complex materials. [Supported by Duke CFAR and NIH AI48103]

2072-Pos
Mucus Rheological Properties Altered by Functional Nanoparticles

Yung-Chen Wang, Eric Yi-Tong Chen, Chi-Shuo Chen, Albert Sun, Wei-Chun Chin.
University of Califronia, Merced, Merced, CA, USA.

Multi-functionalized nanoparticles (NPs) have recently been extensively explored for their potential in novel drug delivery and nanomedicine applications. Functionalized NPs based local drug delivery across the mucosal epithelia has gained much interest.

Despite reports confirming cellular nanotoxicity effects, possible health hazards resulted from mucus rheological disturbances induced by NPs are underexplored.

Accumulation of viscous, poorly dispersed and less transportable mucus that could result in improper mucus rheology and dysfunctional mucociliary clearance are typically found to associate with many respiratory diseases such as asthma, cystic fibrosis (CF) and COPD (chronic obstructive pulmonary disease). Whether functionalized NPs can alter mucus rheology and its operational mechanisms are not resolved. Here we show for the first time that positively-charged functionalized NPs can effectively induce mucin aggregation and hinder mucin gel hydration. These NPs significantly increase the size of aggregated mucin approximately 30 times within 24 hrs. EGTA (ethylene glycol tetraacetic acid, 2 mM) chelation of indigenous mucin crosslinkers (Ca^{2+} ions) was unable to effectively disperse NPs-induced aggregated mucins. We also found that positively-charged NPs can significantly reduce the swelling kinetics and hydration of newly released mucus. Our results have demonstrated that positively charged functionalized NPs can serve as effective crosslinkers hindering mucin disaggregation and dispersion resulting in potential dysfunctional mucociliary clearance and health problems. This report also highlights the unexpected health risk of NP-induced change in mucus rheology and possible mucociliary transport impairment on epithelial mucosa. In addition, our data can serve as a prospective guideline for designing nanocarriers specific for mucosal epithelia drug delivery applications.

(Supported by NSF CBET-0932404, NIH 1R15HL095039-01A1 and CITRIS #31 seed grant)

2073-Pos
Silica Nanoparticles Permeabilize Lipid Bilayers

Sara Aghdaei, Hywel Morgan, **Maurits R.R. de Planque**.
University of Southampton, Southampton, United Kingdom.

Potential toxic effects of synthetic nanoparticles are of great public concern. Presently, the impact of nanoparticles at a cellular level is assessed by adding nanoparticles to cell cultures and subsequent evaluation of particle uptake by confocal fluorescence microscopy and of cell viability by conventional (fluorescence) assays. Cytotoxic effects of nanoparticles have been reported but a correlation between nanoparticle properties (e.g. size, shape, surface chemistry) and cell viability remains elusive. However, cellular uptake of nanoparticles is almost universally observed. Membrane translocation of nanoparticles is generally considered to be an active process, requiring the presence of receptors that mediate encapsulation of the nanoparticles into an intracellular vesicle, from which the particles may or may not escape into the cytosol.

Using electrophysiological methods we have demonstrated that spherical silica nanoparticles, under development for intracellular drug delivery, are able to permeabilize protein-free lipid bilayers as a function of size and surface charge. Single channel-like conductances, similar to those induced by membrane-disrupting β-amyloid peptides, are observed for rigid sterol-containing bilayers. For more fluid bilayers of DOPC the conductance gradually increases until the bilayer disintegrates, which has also been observed for cytotoxic amyloid oligomers. The most disruptive nanospheres were shown by confocal fluorescence microscopy to accumulate at the bilayer surface, and we demonstrated that a fraction of these particles translocate across the lipid bilayer, suggesting that passive uptake of nanoparticles may contribute to cellular uptake.

Our combined electrophysiology and fluorescence microscopy approach is experimentally straightforward and enables rapid systematic investigation of the interactions between nanoparticles and the lipid components of the cell membrane. These model studies will aid in the rational design of safe nanoparticles -for drug delivery and subcellular labeling- that traverse the plasma membrane without adverse effects on membrane integrity.

2074-Pos
Surface Electrostatics and Lipid-Substrate Interactions of Nanopore-Confined Lipid Bilayers

Antonin Marek, Maxim A. Voinov, **Alex I. Smirnov**.
North Carolina State University, Raleigh, NC, USA.

Substrate-supported lipid bilayers serve many purposes: from acting as versatile models of cellular membranes to biotechnological applications including substrate functionalization and stabilizing membrane proteins in functional conformations. While adsorption and subsequent reorganization of phospholipid vesicles on solid substrates were studied in the past, the exact nature of physicochemical interactions between the lipids and substrate surfaces remain largely unknown. Here we employed recently synthesized pH-sensitive spin-labeled phospholipids - derivatives of 1,2-dipalmitoyl-*sn*-glycero-3-phosphothioethanol (PTE) with pH-reporting nitroxides that are covalently attached to the lipid's headgroup - to investigate surface electrostatics of nanotubular lipid bilayers confined in cylindrical nanopores. The lipid nanotubes were formed by self-assembling phospholipids inside ordered nanochannels of anodic aluminum oxide with pore diameters from 60 to 170 nm and diameter-to-pore length ratio of up to 1:1000. ^{31}P NMR confirmed formation of macroscopically aligned lipid nanotubes with just 1-2° mosaic spread from zwitterionic DMPC, anionic DMPG, and their mixtures. Interfacial potentials were measured by carrying out titration experiments and observing the protonation state of the nitroxide tag by EPR. For nanopore-confined DMPC:DMPG (1:1) bilayers the protonation equilibrium was shifted to more acidic values: when the single lipid bilayer was deposited per nanopore the pK_a of the nitroxide probe was shifted by (-0.91 ± 0.05) pH units but only by (-0.34 ± 0.05) when three bilayers per nanopore were present. Notably, the nitrogen hyperfine coupling constant for non-protonated nitroxides remained the same in all the samples indicating essentially the same interfacial dielectric environment. Thus, these shifts in pK_a must come from changes in the lipid bialyer surface potential that was estimated to increase by 52 ± 3 mV. EPR data on the lipid-substrate interface were combined with differential scanning calorimetry to elucidate effects of pore curvature, surface modification, and binding of antibacterial peptides on lipid-substrate interactions. Supported by DE-FG02-02ER15354.

2075-Pos
Reconstitution of Nanosized HDL Bearing Anti-Amyloid Flavonoids for Targeted Drug Delivery

Panupon Khumsupan[1], Chris E. Manansala[1], Vasanthy Narayanaswami[1,2].
[1]California State University, Long Beach, Long Beach, CA, USA, [2]Center for the prevention of obesity, Cardiovascular Disease & Diabetes, Children's Hospital Oakland Research Institute, Oakland, CA, USA.

High-density lipoproteins (HDL) are lipid-protein particles that are involved in transport of plasma cholesterol from peripheral tissues to the liver, a process called reverse cholesterol transport. In humans a subclass of HDL contains apolipoprotein E (apoE), an anti-atherogenic protein. ApoE serves as a ligand for the low-density lipoprotein (LDL) receptor family of proteins. Our objective is to employ reconstituted HDL containing recombinant human apoE3 as a vehicle to transport and target curcumin, an anti-amyloid and anti-inflammatory flavonoid, to the cells lining the blood brain barrier. Curcumin metabolites are far less potent than curcumin; therefore it is important to deliver active curcumin at inflammatory or amyloid aggregation sites. To achieve this, HDL was prepared by reconstituting palmitoyloleoylphosphatidylcholine, cholesterol, and human apoE3. Non-denaturing polyacrylamide gel electrophoresis of the reconstituted HDL indicates the molecular mass and diameter of the particles to be ~600 kDa and ~17nm, respectively. Curcumin was incorporated by direct addition into reconstituted HDL particles by incubation at 37oC for 6 h. We exploited the inherent fluorescent property of curcumin to determine its presence within the reconstituted HDL. A dramatic shift of the wavelength of maximal fluorescence emission of curcumin was noted from ~550 nm in dimethylsulfoxide or aqueous buffer or Triton X-100 micelles to ~490 nm in HDL. In addition, an enormous enhancement in fluorescence emission intensity was noted in curcumin-containing HDL. These observations indicate that curcumin has partitioned efficiently into apoE3-containing HDL. Partitioning of curcumin does not significantly alter the particle integrity. In conclusion, we report that curcumin can be packaged into apoE containing HDL particles. Its presence in the context of a lipoprotein complex bearing apoE offers the potential for its delivery across the blood brain barrier in an active form for treatment of Alzheimer's disease.

2076-Pos
Identification of the Membrane Interactome Using Nanodisc Phospholipid Particles

Catherine S. Chan, Xiao X. Zhang, Huan Bao, Leonard J. Foster, Franck Duong.
University of British Columbia, Vancouver, BC, Canada.

Membrane proteins have mostly been excluded in proteomic and interactomic studies due to the inherent difficulties in dealing with their highly hydrophobic properties. Nanodiscs have aided in the study of membrane proteins by overcoming many disadvantages arising from the use of detergent micelles and liposomes. These nanoparticles consist of a phospholipid bilayer circumscribed by an amphipathic scaffold protein, generating a soluble yet near-native environment for biophysical and biochemical studies of inserted membrane proteins. Nanodisc particles in combination with SILAC (stable isotope labeling by amino acids in cell culture) were used to study the membrane interactome for both protein-protein and lipid-protein interactions. Cultures grown in media containing an essential amino acid (arginine) that is either 'heavy-C^{13}' or 'light-C^{12}' labeled were used as prey in pull down assays containing immobilized nanodiscs as bait, followed by LC/MS-MS analysis. A quantitative proteome fingerprint based on the ratio of heavy versus light peptides of identified proteins was used to separate true interactors from contaminants. The well-characterized bacterial SecYEG and SecYEGDFyajC complexes reconstituted in nanodiscs were used as model systems to study protein-protein interactions. For lipid-protein interactions, dioleoyl-*sn*-glycero-3-[phosphor-*rac*-(1-glycerol)] (DOPG) and *E. coli* total lipid-reconstituted empty nanodiscs were used to isolate and identify acidic lipid-binding proteins.

2077-Pos
Icosahedral DNA Nanocapsules by Modular Assembly

Shabana Mehtab, Dhiraj Bhatia, Yamuna Krishnan.
National Centre for Biological Sciences - TIFR, Bangalore, India.

The construction of well-defined 3D architectures is one of the greatest challenges of self-assembly. Nanofabrication through molecular self-assembly has resulted in the formation of DNA polyhedra with the connectivities of cubes,tetrahedra, octahedra,dodecahedra,and buckminsterfullerene. DNA polyhedra could also function as nanocapsules and thereby enable the targeted delivery of entities encapsulated from solution. Key to realizing this envisaged function is the construction of complex polyhedra that maximize encapsulation volumes while preserving small pore size. Polyhedra based on platonic solids are most promising in this regard, as they maximize encapsulation volumes. We therefore constructed the most complex DNA-based platonic solid, namely, an icosahedron, through a unique modular assembly strategy and demonstrated this functional aspect for DNA polyhedra by encapsulating gold nanoparticles from solution.

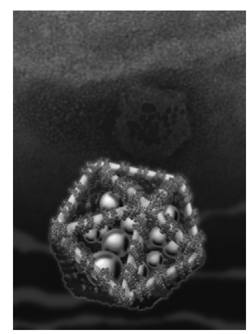

2078-Pos
Computational Design of an RNA Nanoparticle Consisting of a Three-Way Junction and pre-miRNAs

Shu-Yun Le, Taejin Kim, Bruce A. Shapiro.
NCI-Frederick, Frederick, MD, USA.

Recent research on RNA-based regulation, RNAi, and development of human diseases has shed light on the huge potential of miRNAs as novel therapeutic agents for medicine. It has been suggested that a successful tissue-targetable nucleic acid delivery system has to overcome the problem of poor stability of nucleic acids in biological media. To solve this problem we rationally designed a pre-miRNA-nanoparticle-mediated RNA delivery system by integrating computer modeling, miRNA regulatory function and RNA structure versatility. It has been well documented that the initial product of a miRNA, the pri-miRNA, is transcribed in the nucleus. It forms a highly stable stem-loop structure that is processed to form the pre-miRNA by the RNase III enzyme, Drosha. The stable pre-miRNA stem-loop structure of 60-70 nt is transported to the cytoplasm and is then processed into a short double stranded fragment by dicer. Finally the miRNA duplex is unwound to form a ~22-nt single stranded mature miRNA which is associated with the RISC complex. In this study, we present a computational design of a synthetic, highly stable superstructure made from an RNA junction that can accommodate multiple

pre-miRNAs. A three-way junction building block, which was obtained from the RNAjunction database, was attached to three human let-7 pre-miRNAs. This highly stable RNA nanoparticle is expected to enable the binding of the dicer protein for the efficient cleavage of the pre-miRNA in the cytoplasm. As a result, the mature let-7 miRNAs can enter into the targeted cell cytosol, and be protected from degrading interactions while performing its specific regulatory functions.

2079-Pos
Surface-Charge Influences Voltage-Dependent Pore Formation in Lipid Membranes by Quantum Dots
Srujan Kumar Dondapati[1], Gerhard Baaken[1,2], Ali Zulqurnain[3], Feng Zhang[3], Wolfgang J. Parak[3], Jan C. Behrends[1].
[1]Laboratory for Electrophysiology and Biotechnology, Department of Physiology, University of Freiburg, Freiburg, Germany, [2]Laboratory for Chemistry and Physics of Interfaces, Department of Microsystems Engineering, Freiburg, Germany, [3]Department of Physics, Philipps University of Marburg, Marburg, Germany.
Semiconductor nanocrystals, such as quantum dots (QDs) have many biomedical applications. It is of great interest to understand the mechanism by which these nanoparticles cross the cell membrane. Here, QDs, such as cadmium selenide / zinc sulfide core shell (CdSe/ZnS) nanoparticles are shown to interact with lipid bilayers painted on picoliter microelectrode cavities and to produce rapid current bursts with half widths in the range of tens of microseconds. These bursts are voltage dependent and are observed in both polarities. The voltage-dependence of the burst frequency is strongly influenced by external solution parameters like pH and salt valency, charge of the lipids, bilayer size and also nanoparticle size and charge. Correlating these findings with results of dynamic light scattering (zetasizer), we present evidence that electrostatic interactions play a pivotal role in generating the current bursts. Future experiments will focus on optical characterization in order to obtain more insight into the mechanism of interaction.

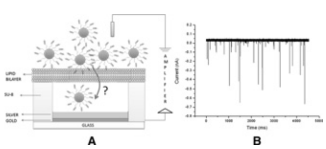

Figure 1. (A) Scheme of the measurement set up. (B) Current bursts measured across the bilayer formed over 10 um electrode in the presence of QDs at - 200 mV.

2080-Pos
Retrieval of a Metabolite from Cells with Polyelectrolyte Microcapsules
Deborah Studer[1,2], Raghavendra Palankar[1], Sebastian Springer[1], **Mathias Winterhalter**[1].
[1]Jacobs University Bremen, Bremen, Germany, [2]EPFL, Lausanne, Switzerland.
To monitor cellular processes in individual cells, it is an important goal to measure the concentrations of intracellular components in real time, and to retrieve them for analysis. We report here the use of functionalized polyelectrolyte microcapsules as intracellular sensors for in vivo reporting. When capsules were loaded with streptavidin and introduced into Vero fibroblasts by electroporation, they were initially inaccessible to cytosolic biotin-fluorescein (BF), but after several hours, they bound and accumulated BF. Our work demonstrates the utility of polyelectrolyte microcapsules for intracellular sensing and suggests that they can autonomously escape from an endocytic compartment, making them ideal carriers for intracellular investigations.

2081-Pos
Monofunctional Quantum Dot Probes for Single-Molecule Imaging
Samuel Clarke[1], Fabien Pinaud[1], Assa Sittner[1], Geraldine Gouzer[1], Oliver Beutel[2], Jacob Piehler[2], Maxime Dahan[1].
[1]ENS Paris, Paris, France, [2]Universität Osnabrück, Osnabrück, Germany.
Recently, it has been shown that the optical properties of quantum dot (QDs) nanoparticles enable novel experiments at the single molecule level in live cells, thereby opening new prospects for the understanding of cellular processes. One difficulty with these experiments is that the complex biological environment imposes stringent design requirements on QD probes, necessitating the development of smaller, low valency and more biocompatible QDs. In this work, we present our efforts towards minimizing the size and controlling the surface functionality of QDs. We show that an engineered peptide surface coating and a purification method based on gel electrophoresis are sufficient to produce compact monofunctional QDs covalently conjugated to streptavidin (SAV), biotin and antibodies. To prove the monofunctionality of the QD-SAV probes, we apply novel single-molecule assay following complexation of the QDs with a fluorescent dye biotin derivative. Counting the photobleaching steps of the fluorescent dye gives us direct access to the number of binding sites present on the QD surface. We then apply these QD probes to the targeting and tracking of individual biotinylated membrane proteins expressed in living HeLa cells. We analyze the diffusion properties of these membrane proteins and compare the measurements to those obtained using commercially available QD probes. Overall, these monofunctional QD probes should be useful for studying a wide-range of biophysical phenomena, down to the single molecule level in live cells.

2082-Pos
Quantification of Functional Binding Sites Per Quantum Dot
Holly N. Wolcott, Eric C. Greene.
Columbia University, New York, NY, USA.
Antibody conjugated quantum dots have become increasingly useful in the study of proteins both *in vitro* and *in vivo* and are particularly valuable in single molecule experiments due to their narrow emission spectra and photostability. Despite their wide range of uses, it has been difficult to determine the number of functional binding sites per quantum dot. Previous studies focused on the characterization the total number of antibodies conjugated to quantum dots rather than the quantification of functional antibodies per quantum dot. Understanding the later is especially important to interpretation of data obtained in single molecule experiments using quantum dot labeled proteins. Additionally, since the number of functional binding sites per quantum dot may vary depending on the antibody conjugation method and also between quantum dot preparations, it is necessary to develop a simple and rapid method to test this experimentally. In this study, we use a direct read-out from the protein itself to determine the average number of proteins bound per quantum dot. By using radio-labeled enhanced green fluorescent protein (EGFP) constructs conjugated to common affinity tags used for protein labeling, we will quantify the number of functional binding sites per quantum dot and the specificity of quantum dot labeling *in vitro*. This method will be extremely useful in the interpretation of data obtained using quantum dot labeled proteins.

2083-Pos
Quantitative Study of the Protein Corona on Engineered Nanoparticles
Xiue Jiang[1], Carlheinz Röcker[1], Feng Zhang[2], Wolfgang J. Parak[2], **G. Ulrich Nienhaus**[3,4].
[1]University of Ulm, Ulm, Germany, [2]University of Marburg, Marburg, Germany, [3]Karlsruhe Institute of Technology, Karlsruhe, Germany, [4]University of Illinois, Urbana-Champaign, IL, USA.
Nanoparticles are finding a rapidly expanding range of applications in research and technology, finally entering our daily life in medical, cosmetic or food products. Colloidal inorganic nanoparticles rendered water soluble by highly ordered organic shells hold great promise as powerful tools for applications in biotechnology and biomedicine. However, their ability to invade tissues, cells and even subcellular compartments may result in biological hazards if nanoparticle incorporation and migration within the body cannot be tightly controlled.
As yet, little known about the detailed mechanisms by which objects on the nanoscale interact with living organisms. Upon incorporation via the lung, gut or skin, nanoparticles become exposed to biological fluids containing dissolved biomolecules, especially proteins. Quantitative studies of the interactions between nanoparticles and biomolecules, which depend on the nature of the nanoparticle surface, are still scarce, and even less is known as to how such a ‘protein corona’ affects nanoparticle uptake by living cells.
Here we have employed fluorescence methods, especially FCS, to investigate the adsorption of human serum albumin and (apo-)transferrin on polymer-coated FePt nanoparticles of ~5 nm radius. Both proteins form a monolayer on the surface of these nanoparticles and bind with micromolar affinity. We have also studied the effect of the protein corona on the nanoparticle uptake behavior by HeLa cells (1, 2).
1. Röcker, C. et al., Nature Nanotechnology 4, 577-580 (2009).
2. Jiang, X. et al., J. R. Soc. Interface, published online, doi:10.1098/rsif.2009.0272.focus

2084-Pos
Nanocandles: Developing Optical Probes for the Cell Interior
Lindsey Hanson, Chong Xie, Yi Cui, Bianxiao Cui.
Stanford University, Stanford, CA, USA.
As knowledge of the bulk behavior of biological systems continues to grow, there is an increasing demand for knowledge of cellular processes at the single-molecule level. This presents a unique challenge, a combination of the dynamic nature of the system and the inability to modulate the concentration of

the target species. A significant limitation of previous low-penetration methods arises from the very character that provides their utility: the low penetration depth also means they can only probe molecular events very close to the substrate surface. We have fabricated vertical silicon dioxide nanopillars which, at a height of up to one micron, carry that low penetration depth up into the cell environment where the relevant molecular processes occur. The pillars can also be specifically functionalized with molecules of interest for either delivery into the local environment or study while tethered in the observation volume. With single molecule detection at biologically-relevant concentrations and biologically-applicable locations, these nanopillars provide a template on which to study a multitude of biological processes in a controlled, dynamic, and localized fashion.

2085-Pos
Evaluation of Photophysical Properties of Methylene Blue Incorporated within ZMOF Framework
Jaroslava Miksovska, Kathryn Perez.
Florida International University, Miami, FL, USA.
Zeolite-like metal organic frameworks (ZMOF) are of particular interest due to their application as gas storage material, drug delivery vehicles, and sensors. Stability, relatively straightforward synthesis and large internal cavities allow us to explore the possibility using of ZMOF material as a nanoreactors for various chemical and photochemical reactions. Here we present a synthesis and photophysical characterization of the ZMOF framework functionalized by encapsulation of a photosensitizer, methylene blue. Our data show that encapsulation of methylene blue within the ZMOF framework facilitates fluorophore self-aggregation as evident from the red-shift of methylene blue emission spectra, anisotropy increase, and decrease of the fluorescence lifetime. Interestingly, the fluorescent properties of methylene blue incorporated within zeolite-like methyl organic framework differ significantly from those reported previously for methylene blue aggregates in aqueous medium indicating strong interactions between the fluorophore and the framework.

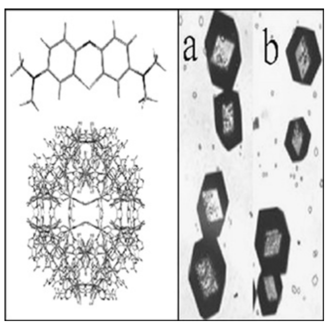

Biotechnology & Bioengineering I

2086-Pos
Intracellular Effects of Nanosecond, High Field Electrical Pulses
Yu-Hsuan Wu[1], Tina Batista-Napotnik[2], Martin A. Gundersen[3], Damijan Miklavcic[4], P. Thomas Vernier[3,5].
[1]Mork Family Department of Chemical Engineering and Materials Science, Viterbi School of Engineering, University of Southern CaliforniaUniversity of Southern California, Los Angeles, CA, USA, [2]Laboratory of Biocybernetics, Faculty of Electrical Engineering, University of Ljubljana,, Ljubljana, Slovenia, [3]Ming Hsieh Department of Electrical Engineering, University of Southern California, Los Angeles, CA, USA, [4]Laboratory of Biocybernetics, Faculty of Electrical Engineering, University of Ljubljana, Ljubljana, Slovenia, [5]MOSIS, Information Sciences Institute, USC, Marina Del Rey, CA, USA.
Mitochondria, which play a crucial role in apoptosis, release several apoptosis-inducing factors into the cytoplasm, presumably through the mitochondrial permeability transition pore (MTP). Under certain conditions, nanoelectropulses can manipulate mitochondrial structure and permeabilize the mitochondrial membrane without permanent damage to the plasma membrane. In this work we investigate the effects of nanoelectropulses on mitochondrial membrane permeabilization, assess changes in mitochondrial transmembrane potential, and monitor plasma membrane integrity under the same pulse conditions. 4 ns electrical pulses were applied to living human Jurkat T lymphoblasts in an electrode microchamber on a microscope slide. Changes in mitochondrial transmembrane potential were evaluated with rhodamine 123 (R123), a lipophilic cationic fluorescent dye that is accumulated within mitochondria. For assessing MTP opening, a calcein-cobalt quenching method was used. Calcein-AM is an anionic fluorochrome that enters cells freely and labels cytoplasmic as well as mitochondrial regions following esterase removal of the acetoxymethyl group. Because cobalt ions do not readily pass through mitochondrial membrane, mitochondria can be specifically identified by the cobalt quenching of cytoplasmic, not mitochondrial, calcein fluorescence, and MTP opening can be recognized by the decrease of calcein fluorescence within mitochondria. Finally, cell membrane integrity was evaluated with propidium iodide (PI), which is excluded from the cell interior by intact cell membranes. When the cell membrane is permeabilized, PI enters the cell, binds to double-stranded nucleic-acid molecules, and exhibits red fluorescence. The effects of different pulse amplitudes and pulse numbers on mitochondrial membrane permeability will be reported, providing a framework for an analysis of pulse doses and exposure conditions which lead to mitochondrial modifications while minimizing effects on the plasma membrane. We will also discuss the interpretation of data from fluorescence microscopic imaging analysis using R123 and cobalt-quenched intracellular calcein fluorescence intensity and the influx of PI.

2087-Pos
Hydrodynamic Trap for Single Cells and Particles
Melikhan Tanyeri, Charles M. Schoeder.
University of Illinois at Urbana Champaign, Urbana, IL, USA.
Particle trapping and micromanipulation techniques have revolutionized biological sciences during the last two decades. Proteins, enzymes and cells have been studied extensively through manipulation methods based on optical, magnetic and electric fields. In this work, we present an alternative trapping method called the hydrodynamic trap which is based solely on hydrodynamic forces generated in a microfluidic device. The hydrodynamic trap is based on a purely extensional flow field created at the junction of two perpendicular microchannels where opposing laminar flow streams converge. The flow field in the vicinity of the microchannel junction can be described as a potential flow with a semi-stable potential well and a stagnation point. We implement an automated feedback-control mechanism to adjust the location of the stagnation point, thereby actively trapping arbitrary particles in free solution. Using the hydrodynamic trap, we successfully demonstrate trapping and manipulation of single cells and single particles with micron and sub-micron dimensions for arbitrarily long observation times. Brownian dynamics simulations show that the trap stiffness is comparable to alternative trapping techniques including magnetic traps. Overall, this new technique offers a venue for observation of biological materials without surface immobilization, eliminates potentially perturbative optical, magnetic and electric fields, and enables the ability to vary the surrounding medium conditions of the trapped object in real-time.

2088-Pos
Atomic and Photonic Force Microscope: from Nanonewton to Piconewton
B. Torre, F. Di Fato, A. Diaspro.
Italian Institute of technology, Genoa, Italy.
Cell differentiation and organization is influenced from chemical and mechanical characteristics of the extracellular matrix which determine its fate. Cellular compartmentalization can be explained as mechanical equilibrium of tensed and compressed cables which is continuously changing during cell motility, intracellular transport and cell division. Chemical composition of subcellular compartments determine the function they accomplish in the cell. Change in the chemical composition of subcellular structure produce not only change in their function but create also a change in their mechanical properties.
Dynamic behavior of the cell is obtained by continuous modulation of chemical composition and local recruitment of molecules in cell compartments: cell membrane vary its stiffness during endocytosis and exocytosis, cell refractive index change during cell division, actin and tubulin persistence length is modulate by assembly proteins during cell protrusions formation. Moreover single molecule mechanical characterization is becoming an important tool to study the molecule properties in different condition.
On the other side during pathologies cell mechanical characteristics change too: Brownian motion of trapped healthy cell is different from malignant one, membrane elasticity is changed in cell presenting abnormal organization of cytoskeleton.
Cell mechanics is becoming an emerging field to understand cell organization in healthy state and represent an additional way to analyze the onset of pathologies. Therefore we are developing a setup which combine AFM and Photonic force microscope to apply force spectroscopy measurement either in the piconewton and nanonewton range.

2089-Pos
Mechanotransductive Engineering of Neural Stem Cell Behavior
Albert J. Keung, Elena M. de Juan-Pardo, David V. Schaffer, Sanjay Kumar.
UC Berkeley, Berkeley, CA, USA.
Neural stem cells (NSCs) play important roles in learning and memory in the adult mammalian brain and may also serve as a source of cells in cell

replacement therapies to treat neurodegenerative diseases. Therefore, investigating how NSC behavior is regulated is crucial to understanding the fundamental biology of the brain as well as in engineering biomedical therapies. Towards these ends, an increasing wealth of knowledge in the NSC field describes a complex picture of biochemical and genetic regulation of NSC self-renewal and differentiation. However, little is known about the biophysical control of NSC behavior by the extracellular matrix (ECM). Here we demonstrate that ECM-derived mechanical signals can act with Rho GTPases to regulate NSC stiffness and differentiation. Culturing NSCs on increasingly stiff ECMs suppresses neurogenesis and enhances gliogenesis, even in the absence of exogenous differentiating agents. This shift is accompanied by enhanced RhoA and Cdc42 activation and increased cellular stiffness. Direct manipulation of RhoA and Cdc42 activity disrupts the ability of NSCs to sense ECM stiffness and tips the balance between neurogenesis and gliogenesis in the presence and absence of exogenous differentiation cues. Inhibitors of a downstream effector of RhoA, Rho kinase, as well as inhibition of myosin II contractility rescues neuronal differentiation of NSCs cultured on stiff substrates as well as for NSCs expressing CA RhoA and CA Cdc42, suggesting that NSC stiffness/contractility regulates NSC differentiation. These results establish Rho GTPase-based mechanotransduction and cellular stiffness as novel regulators of NSC behavior.

2090-Pos

Biophysical and Biochemical Tunable Environments for Controlled Cell Adhesion and Differentiation

Tobias Wolfram[1,2], Ilia Louban[1,2], Joachim P. Spatz[1,2].
[1]Max-Planck Institute Stuttgart, Stuttgart, Germany, [2]University of Heidelberg, Heidelberg, Germany.

In the present study, we used a nanoengineered gold particle array on elastic polyethylene glycol (PEG) hydrogels and biofunctionalized the particles with different peptides. This experimental setup was used to investigate neural cell adhesion, neurite outgrowth, and cell binding in co-culture systems.
Nanostructured hydrogels were generated with interparticle distances of 50 nm and 100 nm measured by cryo-sem. In order to quantify the mechanical properties of PEG-DA hydrogels (Young's modulus EY) we performed AFM indentation measurements based on the Hertz model and adjusted for conical-shaped tips with a semi-vertical opening angle α. PEG-hydrogels were used in this work with EY <1kPa to 6MPa.
Cell adhesion on nanostructured gels were visualized and analyzed with cryo-sem and static adhesion assays. On substrates with 50 nm interparticle distances, cell adhesion was observed for up to two weeks for neural cell lines as well as for fibroblasts. Fibrolast cell lines (REF-52 and NIH3T3) adhere around two times better to RGD PEG-hydrogels in mono-cell culture when compared to neuroblastoma cell lines. For IKVAV decorated PEG-hydrogels neuroblastoma cell adhesion was increased to a comparable level of fibroblast adhesion on similar substrates. In co-culture systems a significant lower amount of fibroblast cells adhere to IKVAV substrates and vice versa a higher number of N2a cells (2,5fold) were detected on the surface. Lower elasticity (<1kPa) increased the neural cell number to around 5fold over fibroblasts. Neurite length was increased on substrates with lower elasticities independently from functionalization. Neurite initiation was independent from substrate elasticity but 4fold more cells with neurites were observed on IKVAV functionalized hydrogels.
In conclusion, neural cell adhesion and neurite formation depends on substrate elasticity as well as biofunctionalization and particle density. Substrates can be tuned to direct the adhesion of specific cell types.

2091-Pos

Control of Cardiomyocyte Adhesion and Organization by Microscale Topographical Cues

Anuj A. Patel[1], Matthew G. Chown[2], Rahul G. Thakar[3], Tejal A. Desai[1,3], Sanjay Kumar[1].
[1]UCSF/UCB Joint Graduate Group in Bioengineering, Berkeley, CA, USA,
[2]Department of Bioengineering, UC Berkeley, Berkeley, CA, USA,
[3]Department of Physiology, Division of Bioengineering, UC San Francisco, San Francisco, CA, USA.

Regeneration of myocardial tissue through the use of synthetic scaffolds requires strategies to promote cardiomyocyte attachment and organization. Our previous studies and others have demonstrated that a synthetic platform consisting of an array of microscale polydimethylsiloxane (PDMS)-based pillars (''micropegs'') can accomplish this, yet the mechanism through which this occurs remains a mystery. Here we test the hypothesis that the micropegs serve as organizational centers for cardiomyocytes, enhancing adhesion and clustering of cells via cell-ECM and cell-cell junction proteins. Our studies utilize HL-1 cardiomyocytes, a continuous cell line of atrial origin that retains several defining molecular markers and functional properties of primary cardiomyocytes. We show that ECM-coated PDMS surfaces can support the growth of HL-1 cardiomyocytes and that these cells maintain the ability to beat and express cardiac-specific myosin. Furthermore, adhesion of cardiomyocytes to micropegs alters nuclear positioning within the cell, as well as expression of several cell-ECM and cell-cell junction proteins. Interestingly, adhesion to micropegs does not appear to significantly alter cellular compliance as measured by atomic force microscopy. These findings support a model in which micropegs act as topological and spatial cues for the cardiomyocytes, and suggest potential value in incorporating such cues into myocardial tissue engineering scaffolds.

2092-Pos

Monitoring Gene Expression Via Novel Nucleic Acid and Delivery Methods

Konstantinos Lymperopoulos[1], Christina Spassova[1], Anne Seefeld[1], Harendra S. Parekh[2], Dirk P. Herten[1].
[1]University of Heidelberg, Heidelberg, Germany, [2]University of Queensland, Queensland, Australia.

Application of single-molecule and high-resolution fluorescence methods to monitor gene expression in living cells increase the demand on novel probes and delivery methods. They require fluorophores with high photostability and quantum yield and highly-efficient delivery methods that ensure the minimum interference with cell processes such as metabolism and signal transduction.
Here, we use a novel class of dendrimers (Parekh et al., Bioorgan Med Chem 2006, 14: 4775) with varying generations and branching factors and different number of positive charges due to different moieties and functional groups. These different properties were tested for their efficiency to transfect eukaryotic cell lines with oligodeoxynucleotides (ODNs) labelled with fluorophores. Different parameters (temperature, concentration of dendrimers, ratio of dendrimers and ODNs) were evaluated and optimised. We utilised these established optimal conditions to deliver a modified concept of SmartProbes (Stöhr et al., Anal Chem 2005, 77 (22):7195) to mammalian cells targeting endogenous mRNAs involved in signal pathways. We tested different mRNA targets and we optimised the fluorescence signal by varying a range of parameters, namely the fluorescent label and the intrinsic properties of the SmartProbe (length of the loop and stem, conformation and number of guanosines). In the near future, we plan to use these probes for monitoring gene expression levels using Diffusion Imaging Microscopy (DIFIM).

2093-Pos

Raster Image Correlation Spectroscopy for Anti-Cancer Drug Screening Based on the Identification of Molecular Dynamics

Sungmin Hong[1], Harinibytaraya Sreenivasappa[1], Hirohito Yamaguchi[2], Ying-Nai Wang[2], Chao-kai Chou[2], Mien-Chie Hung[2], Jun Kameoka[1].
[1]Texas A&M University, College Station, TX, USA, [2]University of Texas, M.D.Anderson Cancer Center, Houston, TX, USA.

Analysis of protein-protein or protein-DNA interaction in cells is indispensable for current basic cancer research and anti-cancer drug screening. However, it usually performed by conventional biochemical approaches, which require long process time and a large amount of samples. In this presentation, we will show the new application of Raster image Correlation spectroscopy (RICS) that can detect protein-protein, or protein-DNA interactions directly without the time-consuming biochemical process. As a result, this technique significantly reduces the analysis time from a few days to a few hours. As a proof of the concept, we investigated the effects of anti-cancer drugs, cisplatin and etoposide, on tumor-suppressor p53 protein dynamics in Hela cells. We measured the fast diffusion of GFP-tagged p53 in living Hela cells treated or untreated with each anti-cancer drug by RICS. After the drug treatment, the significant reductions of p53 mobility were observed compared to the one without drug treatment. Both cisplatin and etoposide induce DNA damage, and it has been shown that DNA damage stabilizes and activates p53, resulting in the formation of the DNA-p53 complex. Therefore, data obtained by RICS perfectly explain the status of p53 inside the cells. Together, these results suggest that RICS approach is a powerful tool to measure protein-protein or protein-DNA interactions in living cells. Since the small molecules disrupt specific protein-protein interactions are considered as promising drugs for targeted cancer therapy, our novel RICS system may serve as a powerful tool for future drug screening.

2094-Pos

Microscale Colocalization of CD3 and CD28 is Required for Activation of Human CD4+ T Cells

Jones Tsai[1], Keyue Shen[1], Michael L. Dustin[2], Michael Milone[3], Lance C. Kam[1].
[1]Columbia University, New York, NY, USA, [2]New York University School of Medicine, New York, NY, USA, [3]University of Pennsylvania School of Medicine, Philadephia, PA, USA.

It is increasingly recognized that intracellular cell signaling is dependent on the spatial organization of signaling molecules. We previously introduced a platform for investigating spatially-dependent signaling, in the context of the immune synapse, a small (~70 square micrometer) region of contact between T cells and Antigen Presenting Cells. Multiple rounds of microcontact printing are combined to produce glass surfaces with independently defined, microscale patterns of antibodies to CD3 (part of the TCR complex) and CD28 (a major costimulatory signal), surrounded by ICAM-1; antibodies locally engage and activate their respective ligands, organizing signaling complexes in cells on these substrates. We demonstrated that Il-2 secretion by naïve mouse CD4+ T cells is sensitive to the position of CD28 signaling within the region of cell-substrate contact, analogous to the immune synapse. Mouse T cell activation is less sensitive to the organization of CD3 both within the cell-substrate interface and with respect to the location of CD28. In sharp contrast, we demonstrate here that Il-2 secretion by human CD4+ T cells requires colocalization of CD3 and CD28 signaling. All patterns we examined in which antibodies to CD3 and CD28 are separated by micrometer-scale distances were ineffective in inducing Il-2 secretion. Immunohistochemcial staining using phospho-specific antibodies after 15 and 60 minutes following cell-substrate binding revealed that colocalized patterns are more effective than segregated counterparts in maintaining Lck phosphorylation at Y394, a site associated with full activation of this kinase. No differences in Zap70, PI3K, or PKC-theta were observed as a function of pattern geometry. Together, these results identify a dramatic difference between mouse and human T cell physiology, and suggest that Lck may be responsible for spatial integration of CD3 and CD28 signaling.

2095-Pos

Monte Carlo Study of B-Cell Receptor Clustering by Antigen Cross-Linking

Srinivas R. Alla, Subhadip Raychaudhuri.
University of California-Davis, Davis, CA, USA.

B cell signaling is triggered by the recognition of antigens by the surface proteins of the cell known as B-cell receptors (BCRs). It is known from experiments that, in the presence of soluble antigens BCRs assemble into small micro clusters and then structure into a macro cluster. However the underlying mechanisms of the antigen interaction with the BCRs and their cluster formation remain unclear. In our recent effort we have investigated, using Monte Carlo simulations, the mechanism of BCR clustering which would arise due to the intrinsic attractions among them. Such mutual attraction between two adjacent BCR molecules could arise, among other possibilities, due to cross-linking by bivalent soluble antigens. Recently, we have developed and studied a Monte Carlo model of B cell receptor clustering caused by binding and cross-linking of soluble antigens. The results of our study demonstrate the formation of small micro-clusters of BCR molecules (typically of size 2-10 molecules). But antigen cross-linking only is not adequate enough for the formation of large macro-clusters. A simple model of biased diffusion where BCR molecules experience a biased directed motion towards the largest cluster is then applied, which results in a single macro cluster of receptor molecules. The types of receptor clusters formed are analyzed using various network-based metrics such as the average distance between any pairs of receptors and number of adjacent pairs. The effect of BCR and antigen concentrations on the receptor clustering, the stability of the formed clusters over the time, and size of BCR-antigen cross-linked chains are all analyzed using suitable network-based metrics.

2096-Pos

Amplification & Analysis of the Synechococcus Os-B' Crispr Region from Single Cells

Eric Hall[1], Samuel Kim[1], Michelle Davis[2], Huibin Wei[3], Devaki Bhaya[2], Richard N. Zare[1].
[1]Stanford University, Stanford, CA, USA, [2]Carnegie Institute of Washington, Stanford, CA, USA, [3]Tsinghua University, Beijing, China.

The Octopus Hot Spring at Yellowstone National Park, which can reach near-boiling temperatures at its surface, is home to a microbial mat that has been found to be a good model for microbial diversity [90]. Among the many species of prokaryotes found in the hot spring mat are thermophilic strains of *Synechococcus*, which can be found in the photic zone at locations that correspond to a wide range of temperatures [2]. Fluorescence measurements of vertical mat slices have revealed a large degree of heterogeneity in the *Synechococcus* populations [3].

Conventional methods of genetic analysis require axenic cultures of bacteria, but less than 1% of bacteria species can be cultured in such a fashion [4]. To examine the genetics related to the aforementioned heterogeneity at the single-cell level, we have utilized and adapted a microfluidic chip for multiple displacement amplification (MDA) of DNA, which can amplify the DNA of a single cell for off-chip PCR and subsequent analysis [5,6]. Specifically, we are interested in examining the variation of the clustered regularly interspaced short palindromic repeats (CRISPR) region of the *Synechococcus* species found in the mat.

1. Ward, D. M., Ferris, M. J., Nold, S. C., Bateson, M. M. *Microbiol. Micro. Biol. Rev.* **62**, 1353 (1998).
2. Stenou, A. S. et al, *Proc. Natl. Acad. Sci. U. S. A.* **103**, 2398 (2006).
3. Ramsing, N. B., Ferris, M. J., Ward, M. D. *Appl. Environ. Microbiol.* **66**, 1038 (2000).
4. Rappe, M. S., Giovannoni, S. J. *Annu. Rev. Microbiol.* **57**, 369 (2003).
5. Marcy, Y. et al. *PLoS Genet.* **3**, 1702 (2007).
6. Marcy, Y. et al. *Proc. Natl. Acad. Sci. U. S. A.* **104**, 11889 (2007).

2097-Pos

Cavitation Bubble Based Measurement of Red Blood Cell Elasticity

Claus-Dieter Ohl, Pedro Antonio Quinto-Su, Claudia Kuss, Peter Rainer Preiser.
Nanyang Technological University, Singapore, Singapore.

We present a novel technique to measure the red blood cell's (RBC) elasticity by exposing RBCs to an impulsive and transient flow. The flow is created from a rapidly expanding laser-induced cavitation bubble. The expanding bubble leads to a stretching deformation of cells close by. The fast flow lasts for approximately 20 microseconds and quickly ceases afterwards. Thereafter the RBCs relax back to their original shape, however on a much slower timescale. This relaxation is studied with high-speed photography and analyzed with digital image processing. In particular we determine the relaxation of the RBC's major and minor axis and find excellent agreement with a power law over several decades.

We compare findings on the elasticity of RBCs treated with neuraminidase and confirm the results from the common but much more laborious aspiration method. The figure above depicts the measured strain in linear and logarithmic scaling of treated and untreated RBCs, and a typical relaxation process of a single cell as a function of time.

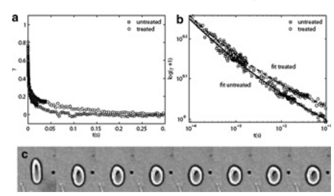

The advantages of this novel technique are its simple implementation and the study of many cells simultaneously.

2098-Pos

Mechanical Properties of Desmin in Skinned Fibers from Normal and *desmin-Null* Mice

Karla Paola Garcia-Pelagio[1,2], Robert J. Bloch[3], Robert Wimmer[4], Hugo Gonzales-Serratos[1,2].
[1]Universidad Nacional Autonoma de Mexico, Mexico, Mexico, [2]University of Maryland at Baltimore, Baltimore, MD, USA, [3]University of Maryland at Baltimore, Baltimore, MD, USA, [4]University of Maryland at Baltimore, USA, MD, USA.

Biomechanical properties of desmin, an intermediate filament protein, and its links through costameres to the contractile apparatus and the subsarcolemal cytoskeleton in single mammalian myofibers of *Extensor digitorum longus* single myofibers isolated from wild (**WT**) and desmin-null (**des-/-**) mice were measured. Suction pressures (**P**) applied through a pipette to the sarcolemma generated a bleb, the height of which increased with increasing **P**. At large **P**s, the connections between the sarcolemma and myofibrils broke; eventually the sarcolemma itself burst. We determined the values of **P** at which these changes occurred, and used these to determine the tensions and stiffness of the system and its individual elements. Tensions of the whole system and the maximal tension sustained by the costameres were (1.6-fold) lower in **des-/-** muscles than in **WT**. Separation and bursting **P**s, as well as the stiffness of the whole system and the isolated sarcolemma were ~1.4-fold lower in **des-/-** than in **WT**. The viscoelastic parameters of the entire system and costameres were also reduced in desmin-null myofibers. Our results indicate that the absence of desmin reduces muscle stiffness, increases sarcolemmal elasticity, and compromises the mechanical stability of costameres and their connections

to nearby myofibrils as desmin act as scaffold around the Z disk. We develop an elastic model of the sarcolemma and its links through costameres to the contractile apparatus based on our results.

2099-Pos
Spatial Correlation of Speckle Fluctuations Reveals Thickness and Features of the Ocular Surface Tear Film
Kaveh Azartash, Enrico Gratton.
University of California Irvine, Irvine, CA, USA.
Here we present Fluctuation Analysis of Spatial Image Correlation (FASIC), a non-invasive method for evaluating the complex dynamics of the tear film surface by spatial correlation analysis. Tear film stability and its interaction with the corneal surface play an important role in maintaining ocular surface integrity and quality of vision. Dry Eye Syndrome (DES) refers to abnormalities of tear film secretion and/or stability diagnosed by conventional methods such as the Schirmer test and tear break-up time (TBUT). Several different physical methods have been developed to measure non-invasively the structure and function of the tear film including high-speed videokeratography and dynamic wavefront aberrometry. Interferometry and optical coherence tomography are amongst new proposed methods to measure tear film thickness that have remained in research phase.
With FASIC, a series of images are obtained using a laser illumination and a cMOS camera. The spatial correlation is calculated for every frame. A sinusoidal background due to interference of the tear film appears in this spatial correlation together with other features. We have developed a mathematical model to obtain the thickness of the tear film from this sinusoidal background. The model includes the macroscopic dynamics of small lipid droplets in the tear film. Consistent data with live animal model and human clinical study has been obtained. The authors gratefully thank the support from NIH grant numbers: PHS-5P41-RR003155 and P50-GM076516.

2100-Pos
A Bluetooth Device for Wireless Communication of in vivo Data from Freely Moving Research Animals
Alycia S. Gailey, Khajak Berberian, Brian N. Kim, Manfred Lindau.
Cornell University, Ithaca, NY, USA.
Collecting neurophysiological data through electrodes can impact behavior when the animal is connected to wires and less able to move. In Parkinson's disease there is a clear link between reduction in dopamine availability and Parkinson's symptoms, which include tremor, slowness of movement and postural alterations. To better study the link between dopamine release in the basal ganglia and motor behavior, we are developing the implementation of a Bluetooth wireless technology for the measurement of neurotransmitter release. Data of dopamine release can be collected by means of fast scan cyclic voltammetry in which voltage ramps between -450 mV and $+1000$ mV are applied at a rate of ~300 V/s to a carbon fiber electrode (CFE) implanted in the striatum. The oxidation and reduction currents can be converted to cyclic voltammograms to identify the dopamine signal. The voltage ramp signals are wirelessly delivered to a remote unit connected to the implanted CFE and the resulting currents are amplified and sampled at 44.1 kHz at the remote unit. Using stereo headset protocol to transmit the data back to the computer, a recording bandwidth of ~1.3 kHz has been achieved. As usual, the voltammetric current collected before dopamine release is subtracted from the voltammetric signal collected after dopamine release within the computer to extract the net oxidation and reduction currents due to dopamine release alone and to generate the cyclic voltammogram. We anticipate that this technology will be useful for the study of the mechanisms of Parkinson's disease and possibly other electrophysiological recordings from freely moving research animals.

2101-Pos
Modeling the Relative Effects of Biofouling, Fibrous Encapsulation and Microvessel Density on Implanted Glucose Sensor Performance
Matthew T. Novak, Fan Yuan, William M. Reichert.
Duke University, Durham, NC, USA.
The formation of a foreign body capsule around implanted sensors is purported as a key contributor to sensor failure. A number of different processes during the wound healing sequence not only decrease the vascular density proximal to sensor but also provide diffusive and bioactive barriers to the transport of analytes from the few remaining vessels that are near the implanted sensor. While a number of surface treatments have mediated this response, the relative contributions of the different stages of wound healing to the attenuation of sensor response have yet to be elucidated. A 1D partial differential equation model was constructed to examine glucose transport through the interstitium and assess the effects that different results of the inflammatory and wound healing processes will have on glucose transport to the sensor surface. By incorporating the effects of biofouling, macrophage adhesion, and fibrous encapsulation, we have been able to recreate subcutaneous glucose traces with attenuated signals and delayed responses that mimic those seen in previous experiments. Such a tool will allow us to probe the characteristic traits of the foreign body capsule (avascularity, dense fibrous matrix, inflammatory cell presence, etc.) to gain a better understanding of what aspects of the wound healing process contribute most to sensor failure. With a more thorough knowledge of the relative contributions of the wound healing process to the decrease of sensor effectiveness, researchers can more rationally address issues of biocompatibility in the design of subcutaneous sensors.

2102-Pos
Jet-Fluid Effects on the Stented-Flow Structure in the Cavity of Cerebral Aneurysm
Miki Hirabayashi[1], Makoto Ohta[2], Hiroaki Kojima[1], Kazuhiro Oiwa[1], Daniel A. Rüfenacht[3], Bastien Chopard[4].
[1]Kobe Advanced ICT Research Center, National Institute of Information and Communications Technology, Kobe, Japan, [2]Institute of Fluid Science, Tohoku University, Sendai, Japan, [3]Neuroradiology, Neuro Center, Hirslanden Clinic, Zurich, Switzerland, [4]Department d'Informatique, University of Geneva, Geneva, Switzerland.
The endovascular treatment of cerebral aneurysms using coils and stents, which are metal mesh cylinders, provides a promising alternative to open surgery. Although various analyses on the property of stented flow have been presented [1,2], the flow reduction mechanisms are not completely understood.
Our numerical simulation indicates that the jet flow through stent struts can reduce near the aneurysm mouth but increases the flow speed far from the mouth (Fig. 1). In this work, based on this observation, we reveal the effect of the phenomenon that the pulsed jet flow drives the fluid with different velocity on the flow structure in the aneurysm cavity. As a result, we found a possibility that the shape of aneurysm may induce the self-oscillation of jet flow. We expect that our findings introduce new strategies in stent development and improve the endovascular treatment of cerebral aneurysms.

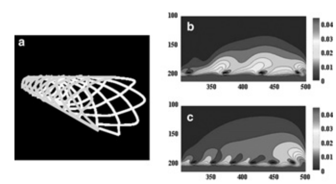

(a) Stent image. (b,c) Velocity distribution of stented flow.

[1] Biondi, A., et al., Neurosurgery, 61, 460-468 (2007)
[2] Appanaboyina, S., et al., Int. J. Numer. Meth. Fluids, 57, 475-493 (2008)

2103-Pos
Development of Non-Viral Gene Delivery Carriers for Ischemic Heart Disease (IHD)
Malavosklish Bikram[1], Mohamed Ismail Nounou[1], Dongling Li[1], Guilherme V. Silva[2], **Bradley K. McConnell**[1].
[1]University of Houston, Houston, TX, USA, [2]Texas Heart Institute, Houston, TX, USA.
Ischemic heart disease (IHD) or coronary artery disease (CAD) is a leading cause of death in the United States resulting in a major financial burden to the health care system and is projected to be one of the main contributors to disability by 2020. The poor prognosis of IHD is directly related to a build-up of atherosclerotic plaque that produces narrowing of the coronary artery lumen. The rupture of the artery and/or narrowing of the artery lumen results in myocardial ischemia, which can lead to myocardial infarction or death of the heart muscle tissue. Current treatments include bypass surgery, angioplasty, stent implantation, and pharmacotherapy but unfortunately many patients with IHD remain refractory to pharmacological treatments and are unsuitable candidates for surgical interventions. Also, restenosis of the vessel lumen due to neointimal hyperplasia is a recurrent problem. Gene therapy is a promising alternative to traditional treatment strategies since the delivery of angiogenic cytokines can stimulate neovascularisation in a process known as therapeutic angiogenesis. To this end, we have designed, synthesized, and characterized novel biodegradable polymeric carrier systems for the delivery of therapeutic angiogenic plasmids. The polymers were found to have a MW of ~3.2 kDa. A gel retardation assay showed condensation of DNA at N/P ratios higher than 20/1. The particle sizes of the polymer/DNA complexes were 100-231 nm with surface charges of 0.8-20 mV. Preliminary data with the reporter gene luciferase showed that the complexes produced significantly higher transfection efficiencies and lower cytotoxicities in several cell lines as compared to

the control. Thus, these novel nonviral carriers are very efficient, versatile, and biocompatible polymers for nonviral gene delivery.

2104-Pos

Measurement of Linear Compressibility in Transpalpebral Tonometry

Gordon Thomas[1], Robert D. Fechtner[2], Irene Nwosuh[3], Stephanie Milczarski[1].
[1]NJIT, Newark, NJ, USA, [2]UMDNJ, Newark, NJ, USA, [3]WSSC, Winston-Salem, NC, USA.

We have measured the force required to depress the palpebrum over the center of the cornea in human patients and found that the curve is linear to within the accuracy of our measurements (R-value=0.9991). The motivation of this measurement is its clinical relevance to the development of a device to measure the intra ocular pressure in patients at risk for glaucoma without touching the cornea. This class of device has promise for patient-operated tonometry, including glaucoma monitoring in third-world counties. We find that non-linearity in the compressibility develops proportional to the distance of the center of the point of application of force from the center of the cornea. We show that this non-linearity can give rise to uncertainty in determination of the compressibility, with values up to 30% as compared to the well-aligned case with values typically 4%. We show that the compressibility value varies from subject to subject because of its three sources: the palpebrum, the cornea supported by the intra ocular pressure and the retropulsive structures. We find that the linearity of the compressibility of the compound structure and therefore of each of its constituents is intrinsic. We conclude that the understanding of the linearity of the compressibility indicates feasibility of this class of tonometer for glaucoma monitoring.

2105-Pos

Concentration and Removal of Waterborne Bacteria for Easy Detection

Audrey L. Buttice, Peter G. Stroot, Norma A. Alcantar.
University of South Florida, Tampa, FL, USA.

In the past decade a significant amount of research and development has been geared towards water treatment and distribution, especially in low income areas. Large fractions of this research have focused on waterborne contaminant removal, such as filters and flocculation agents, and biosensors designed to detect waterborne threats. In low income areas many of the currently used treatment methods are not suitable as they commonly are more expensive and difficult to maintain. Problems have also been observed with biosensors including a very low sensitivity, making it difficult to get accurate readings when low bacteria concentrations are present. In an attempt to address both of these problems in conjunction with one another, we have been studying the effects of a natural compound extracted from the Opuntia ficus-indica cactus as a flocculation and concentration agent for bacteria suspended in water. This material, known as mucilage, has proven to be an effective tool for aggregating and removing the sediment kaolin, and has also demonstrated flocculation of E. coli, B. cereus and B. subtilis. In bacteria treated columns thus far, the response in mucilage treated columns was almost immediate and large flocs were observed to form both with the naked eye and using a light microscope. Removal rates of up to 97% were also observed. Current tests with B. anthracis (fully attenuated) also demonstrate a great potential for mucilage in the fields of water treatment and biosensors. The aggregated bacteria that are formed within the column settle to the bottom forming a compact pellet that can then be removed for testing with biosensors. This type of flocculating agent has the potential to be very valuable in both of these fields because it is inexpensive, sustainable and easy to process and use.

2106-Pos

Size Distributions of Quantum Dots and Colloidal Gold Nanoparticles Using Analytical Ultracentrifugation

Patrick H. Brown.
NIBIB, Bethesda, MD, USA.

Colloidal gold and quantum dot nanoparticles are currently an area of significant interest in the biomedical field with important applications in the diagnosis and treatment of human disease. The hydrodynamic diameter of nanoparticles is a critical parameter in the development of potential diagnostic and therapeutic agents. Electron microscopy and light scattering methods have been used predominantly in the past to determine particle sizes, but analytical ultracentrifugation sedimentation velocity is a technique that has been gaining more attention as it provides significantly higher resolution particle size distributions. Here, we apply the sedimentation velocity technique to commercially-available stocks of colloidal gold and quantum dot nanoparticles. The size-distributions obtained from this method are compared to those obtained from dynamic light scattering measurements conducted in parallel. Further, comparison of changes in particle sedimentation rate affected by increasing solution density was employed as an alternative method to densimetry in order to determine the particle partial specific volume- a parameter requisite for determining molecular weights. This work demonstrates the utility of the sedimentation velocity technique for the characterization of nanoparticles.

2107-Pos

Magnetic and Fluorescence Detection of Hybridized DNA Assemblies Immobilized onto a Hall Device

Steven M. Hira, Khaled Khaled Aledealat, Kansheng Chen, Peng Xiong, Stephan von Molnar, P. Bryant Chase, Geoffrey F. Strouse.
Florida State University, Tallahassee, FL, USA.

The development of a dual detection platform to probe and discriminate nucleic acid base-pairing events through a combination of fluorescent and magnetic signatures may significantly impact the performance and dimensions of biomedical sensing devices. Toward this aim, investigations on the selective and controlled assembly of DNA duplex formation onto a micro-scale Hall device will be addressed. The biological assembly is composed of three distinct components. The first component is a streptavidin-coated magnetic nanobead (350 nm mean diameter) pre-conjugated with both biotinylated and fluorescently labeled ssDNA. The second component is thiolated ssDNA that was selectively immobilized onto photolithography prepared Au patterns on a fabricated Hall sensor. The third component is the label free target ssDNA sequence for detection, which is complementary to both the biotinylated and thiolated DNA sequences. The device readout consists of a decrease in voltage across the Hall junction due to the biologically assembled magnetic nanobead, as well as a redundant fluorescence signature. The Hall device sensitivity is approaching single nanobead bead detection. Support: NIH NIGMS GM079592.

2108-Pos

Refractometry Measurements for Industrial Quality Control

Christopher E. Bassey, Cynthia A. Siguenza.
Azusa Pacific University, Azusa, CA, USA.

A knowledge of the optical properties of liquid substances is useful in enhancing the understanding of their unique characteristics. Properties such as refractive index, refractivity, and phase velocity have been used to assess the purity of liquids. We utilized measurements from a Digital Refractometer to detect and quantify the contamination of liquids such as drinking water, wine, and other beverages. We used antifreeze, ethylene glycol, and propylene glycol as contaminants. Results show that the level of contamination increases linearly with refractive index and that a contamination level of 1 % is detectable. The application of this technique in industrial settings will improve the detection of contamination of beverages.

2109-Pos

Dielectric Relaxation Spectroscopy and Dark-Field Imaging Based Quantification of Amyloid-Beta Fibrillization Via Transparent Nanogap Electrodes

Yeonho Choi, Luke P. Lee.
University of California at Berkeley, Berkeley, CA, USA.

Since the precise role of amyloid-β aggregates in causing the neurodegenerative diseases is still unknown, understanding of amyloid-β fibrillization is a focus of interest for the development of innovative therapeutic and diagnostic applications. The fibrillization of amyloid-β has similar growth characteristics of polymeric nanoparticles and current monitoring methods show only qualitative or static information. Here we describe a non-invasive real-time monitoring of nanoscale amyloid-β fibrillization by simultaneous Dielectric Relaxation Spectroscopy and label-free dark-field imaging. First, the hydrodynamic radius is characterized by DRS, which can reflect the averaged radius of fibrilized amyloid-β, and we observe an increase from 19 to 21 nm during 48 hours. Second, scattering intensity from DF imaging allowed us to visualize and quantify the fibrillization with respect to the incubation time of amyloid-β. The total intensities were consistently increased and this change showed a good agreement with the change of hydrodynamic radii. Consequently, real-time observation and quantification of changes in

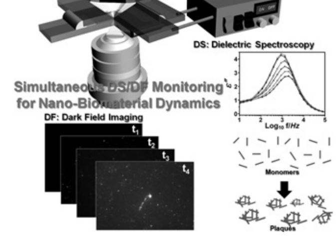

both hydrodynamic radii and optical properties were performed simultaneously. Such a dual-mode technique may prove valuable for elucidating the mechanism of amyloid fibrillization and ultimately for designing possible diagnostic methods.

Biophysics Education

2110-Pos
Strategies for Successful Diversity Participation in Biophysics Research
Virginia M. Ayres, Theodore D. Caldwell.
Michigan State University, East Lansing, MI, USA.
In the summers of 2008 and 2009, two individual students from the Michigan Louis Stokes Alliance for Minority Participation (MI-LSAMP) Summer Undergraduate Research Academy (SURA) program joined the Ayres' Electronic and Biological Nanostructures Laboratory for an 8-week 40 hours per week research experience. As their tasks were essentially the same as those of the resident students, an expedited learning curve was essential for productivity. Both students, even in the time-limited circumstances, produced outstanding and viable research contributions. The SURA08 student quickly developed authentic skills in atomic force microscopy that enabled him to produce clear images of growth-factor derivatized nanofibers within a central nervous system prosthetic that are, as far as we know, the first of their kind to be reported. The SURA09 student contributed specialized expertise in Nuclear Magnetic Resonance spectroscopy that has enabled a new series of complementary NMR experiments that enhance the scanning probe investigations. The work contributed by both students has been published or accepted in high impact referred journals. In this presentation, we explore the strategies of the MI-LSAMP Summer Undergraduate Research Academy program that resulted in the observed successes. These include:
- Selection criteria for both students and faculty mentors. The students are screened for evidence of high motivation as well as good academics during the application process. The faculty mentors are screened for evidence of a direct interaction approach as well as an active research program. The importance of biophysics/bioengineering/biomedical research as a motivating force is discussed.
- An immersion experience that includes support at many levels. The SURA program requires 8-week dormitory residence at the research host university. SURA program personnel invest approximately 40 hours per week in providing classroom support for meeting professional research expectations, and evening social support for friendship and teaming.

2111-Pos
Advanced Undergraduate Laboratory in Biological Physics
Nancy R. Forde.
Simon Fraser University, Burnaby, BC, Canada.
We have developed a new one-semester senior laboratory course as part of our undergraduate Biological Physics stream at Simon Fraser University. This course, designed for students with either a Physics or Biology background, comprises two parts. The first half of the course entails modules to give the students hands-on experience with basic molecular and cell biology and leading-edge biophysical techniques: DNA electrophoresis and topology-dependence of mobility; cell growth; light scattering and spectroscopy; microscopy and cell motility; optical tweezers; and fluorescence correlation spectroscopy (FCS). The experimental goals and learning outcomes of these modules will be presented. In the second half of the course, students propose and carry out independent research projects that include biological and quantitative measurement components. The experiences of the students and their feedback will also be presented.

2112-Pos
Disappearance of Tumors by the Action of Sound
Vinicio N. Lanza.
Centro Medico Herbel, Puerto Ordaz -Estado Bolivar, Venezuela, Bolivarian Republic of.
Background: Starting with observations of tumours which had disappeared following treatment with alternative therapies, the main objective of this work was to discover the underlying physical phenomenon that occurs in such instances. **Method**: Patients with tumours were treated with sound therapy. The methods included a newly developed technique using the Tibetan bowl and the Tibetan bell. **Results**: The tumours disappeared totally in the majority of patients. **Conclusions**: The only phenomenon that could explain such tumour disappearances is the *annihilation of pairs.* These results challenge the following: a) The concept of the physical constitution of living matter and, b) the real constitution of the human being.

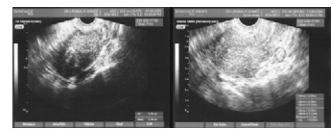

2113-Pos
Teaching Basic Electrophysiology with the Aid of a Computer Program
Jose L. Puglisi, Donald M. Bers.
University of California, Davis, Davis, CA, USA.
Objective: Understanding the basis of electrophysiology is essential to the formation of a student of biological sciences. A solid base on the fundamental concepts paves the way for a better comprehension of more complex phenomena. We implemented a computer program (LabAXON) that simulates the electrical activity of an axon in a user friendly format. This program helps the student to understand the generation of the action potential and the effects of extracellular ionic concentration and stimuli waveform.
Methods: This program was based on the classical Hodgkin and Huxley formalism. LabAXON allows the students to reproduce the basic experiment these Nobel prize-winning scientists performed on the squid giant axon. Important concepts such as Cronaxia curve, Current-Voltage relationship and Ion Reversal Potential can be explored in an interactive way. A user-friendly interface permits a rapid change of parameters and the ability to see the effects on-line. Also we created a workbook with a list of exercises that covers the essential points of the lecture.
Conclusions: The processes that take place at the membrane set the stage for several concepts that will come out in the following years of the student's education: how drugs interact with channels, effect of ionic imbalance, refractoriness of the membrane, to name a few. Computer simulations help to reinforce those topics in the student in a self paced manner. It constitutes an excellent aid for the medical educator. LabAXON and the companion workbook are freely available on our departmental website.

Symposium 11: DNA Nanomachines in Vitro and Inside Living Cells

2114-Symp
Self-Assembly of DNA into Nanoscale Three-Dimensional Shapes
William Shih.
Harvard Med Sch, Boston, MA, USA.
I will present a general method for solving a key challenge for nanotechnology: programmable self-assembly of complex, three-dimensional nanostructures. Previously, scaffolded DNA origami had been used to build arbitrary flat shapes 100 nm in diameter and almost twice the mass of a ribosome. We have succeeded in building custom three-dimensional structures that can be conceived as stacks of nearly flat layers of DNA. Successful extension from two-dimensions to three-dimensions in this way depended critically on calibration of folding conditions. We also have explored how targeted insertions and deletions of base pairs can cause our DNA bundles to develop twist of either handedness or to curve. The degree of curvature could be quantitatively controlled, and a radius of curvature as tight as 6 nanometers was achieved. This general capability for building complex, three-dimensional nanostructures will pave the way for the manufacture of sophisticated devices bearing features on the nanometer scale.

2115-Symp
The I-Switch: a DNA Nanomachine that Maps Spatiotemporal pH Changes in Living Systems
Yamuna Krishnan.
TIFR, National Ctr Biol Sci, Bangalore, India.
Thus far, directed DNA assembly has relied on Watson-Crick base pairing, and this has been a powerful and preferred approach in structural DNA nanotechnology.[1] We have been interested in developing non-Watson-Crick based building blocks to make functional assemblies in structural DNA nanotechnology.[2] I will describe how one can use a four-stranded DNA motif called the i-tetraplex[3] to build a pH triggered conformational switch. We demonstrate the first intracellular application of DNA nanoswitches by mapping spatiotemporal pH changes associated with endosome maturation in living cells.[5] I will also describe our recent developments of this system that improve the temporal resolution, tune pH sensitivity to desirable pH regimes suited to measuring pH in various cellular compartments.
Figure 1. DNA nanomachine maps spatiotemporal pH changes in living cell endosome maturation.
References
1. S. Pitchiaya, **Y. Krishnan**, *Chem. Soc. Rev.*, 2006, **35**, 1111-1121.
2. a) S. Modi, A. H. Wani, **Y. Krishnan**, *Nucleic Acids Res.* 2006, **34**, 4354-4363. b) S. Chakraborty, S. Modi, **Y. Krishnan,** *Chem Commun.* 2008, 70-72. c) A. Paul, P. Sengupta, **Y. Krishnan**, S. Ladame, *Chem. Eur. J.* 2008, **14**, 8682-8689. d) H. B. Ghodke, R. Krishnan, K. Vignesh, G. V. P. Kumar, C. Narayana, **Y. Krishnan*,** *Angew. Chem. Int. Ed.* 2007, **46**, 2646-2649. e) S. Chakraborty, S. Sharma, P.K. Maiti, **Y.Krishnan** *, *Nucleic Acids Res.* 2009*,* **37**, 2810-2817.
3. K. Gehring, J.-L. Leroy, M. Gúeron, *Nature*, 1993, **363**, 561-564.
4. S. Modi, M. G. Swetha, D. Goswami, G. Gupta, S. Mayor, **Y. Krishnan*,** *Nature Nanotechnology*, 2009, **4**, 325-330.
www.zingconferences.com

2116-Symp
Single Molecule Cut and Paste by DNA-Hybridization and AFM-Positioning
Hermann Gaub.
Ludwig Maximilians Univ, Muenchen, Germany.
Molecule by molecule assembly of functional units promises a wide range of new applications in different fields of nanotechnology. In this lecture a new method for the bottom-up assembly of biomolecular structures is introduced, which combines the precision of the atomic force microscope with the selectivity of DNA hybridization. Functional units coupled to DNA oligomers were picked up from a depot using a complementary DNA strand bound to an AFM tip. These units were transferred to and deposited on a target area. Each of these cut and paste events were characterized by single molecule force spectroscopy. Using this technique basic geometrical structures were assembled from units with different functions. The precision of the assembly and the accuracy of the quantification by force spectroscopy were confirmed by single molecule fluorescence microscopy using TIRF excitation. We demonstrated the reproducibility and robustness of this new technique through the transport and deposition of more than 5000 units without significant loss in transfer efficiency. This technology was furthermore used to write ligand pattern for the assisted self assembly of nanoparticles. Pattern of DNA-Hybrids with different length and composition were furthermore employed as force sensors in a parallel label free format to sense various analytes like peptides and transcription factors. Aptamer sequences were employed for small molecule detection in such force based differential assays.
Kufer, S.K., E.M. Puchner, H. Gumpp, T. Liedl, and H.E. Gaub, Single-molecule cut-and-paste surface assembly. Science, 2008. 319(5863): p. 594-
Kufer, S.K., M. Strackharn, S.W. Stahl, H. Gumpp, E.M. Puchner, and H.E. Gaub, Optically monitoring the mechanical assembly of single molecules. NatureNanotechnology, 2009. 4(1): p. 45-
Ho, D., K. Falter, P. Severin, and H.E. Gaub, DNA as a Force Sensor in an Aptamer-Based Biochip for Adenosine. AnalyticalChemistry, 2009. 81(8): p. 3159-

2117-Symp
Designer DNA Architectures for Nanobiotechnology
Hao Yan.
Arizona State Univ, Tempe, AZ, USA.
Naturally existing biological systems, from the simplest unicellular diatom to the most sophisticated organ such as human brain, are functional self-assembled architectures. Scientists have long been dreaming about building artificial nanostructures that can mimic such elegance in nature. Structural DNA nanotechnology, which uses DNA as blueprint and building material to organize matter with nanometer precision, represents an appealing solution to this challenge. Based on the knowledge of helical DNA structure and Watson-Crick base pairing rules, we are now able to construct DNA nanoarchitectures with a large variety of geometries, topologies and periodicities with considerably high yields. Modified by functional groups, those DNA nanostructures can serve as scaffolds to control the positioning of other molecular species, which opens opportunities to study inter-molecular synergies, such as protein-protein interactions, as well as to build artificial multi-component nano-machines. In this talk, I will introduce the principle of DNA self-assembly, describe our recent progress in designing and implementing designer DNA architectures for directed self-assembly, biosensing and molecular robotics and discuss some potential applications of structural DNA nanotechnology.

Symposium 12: Target Structure-Guided Drug Design

2118-Symp
Histone Acetylation: Inhibition, Regulation, and Mimicry
Philip Cole.
Johns Hopkins Univ, Baltimore, MD, USA.
Histone acetyltransferases (HATs) catalyze the targeted acetylation of lysine residues in histones and other proteins. Through reversible protein acetylation, they modulate gene expression, cell growth, and development. Among the HATs, the paralogs p300 and CBP appear to have major roles in many pathways related to metabolism, immune regulation, cardiac development, and cancer. We have taken a design approach to generate synthetic HAT inhibitors with selectivity against p300/CBP and are applying these compounds in mechanistic analyses. In addition, we have found that autoacetylation of p300 and its yeast structural homolog Rtt109 can contribute to the regulation of these enzymes. Finally, we have recently developed a chemical approach to install an acetyl-Lys mimic into proteins at sites of acetylation and will describe this new method.

2119-Symp
Chemical Genetic Approaches for Dissecting Signaling Cascades
Kavita Shah.
Purdue Univ, West Lafayette, IN, USA.
Our laboratory focuses on the development of chemically based tools to dissect signaling pathways in cancer and Alzheimer's disease. Recently we developed a chemical genetic approach for specific activation or inhibition of G Proteins. G proteins are a large family of proteins comprising approximately 0.5% of mammalian genomes. To date, there exists a lack of small-molecule modulators that could contribute to their functional study. We used H-Ras to develop a system that answers this need. Small molecules that allow for the highly specific inhibition or activation of the engineered G protein were developed. The rational design preserved binding of the natural substrates to the G protein, and the mutations were functionally innocuous in a cellular context. This tool can be used for isolating specific G protein effectors. We demonstrate the feasibility of this approach by identifying Nol1 as a putative novel effector of H-Ras. Nol1 is overexpressed in a variety of tumors, including lung adenocarcinoma, prostate adenocarcinoma, breast cancer, oral carcinoma, follicular lymphoma, and human gliomas, and this overexpression is correlated with poor prognosis and shorter patient survival. Identification of Nol1 as a downstream effector of Ras might thus suggest a novel mechanism by which Ras may influence malignancy. Finally, to ensure the transferability of this approach to other G proteins

of interest, we demonstrated a straightforward transfer to Rap1B. As understanding the precise functions of closely related family members is a current frontier in Ras research, this specific control over the activity of a given member is of particular interest. More importantly, successful sensitization of a different G protein to the compounds controlling the activity of the previously engineered H-Ras demonstrates the potential breadth of application of this approach.

2120-Symp

Protein Structure Prediction by Golbal Optimization and its Applications

Jooyoung Lee.

Korea Inst Advanced Study, Seoul, Republic of Korea.

One of the fundamental goals of modern sciences is to understand the nature of life, and deciphering the protein structure and its working mechanism lies at the very heart of this agenda. Due to the tremendous success of many genome projects, the number of available protein sequences reached over 5.3 million as of 2007, but less than 1% of these protein structures are known. Reliable and accurate protein structure prediction using only the sequence information is greatly in demand, but it remains as an unsolved problem even after many years of efforts. We intend to establish a successful protein modeling method that is solely based on direct application of principles excluding human interference in modeling steps. This should be contrasted to the common conception in the field that human expertise accumulated by many years of protein modeling is the most important asset for accurate protein structure prediction. In this talk we will discuss recent progresses of our efforts in protein structure prediction. It appears that our newly proposed method, which is based on the direct and rigorous optimization of relevant score functions, can provide significantly improvement for 3D modeling of proteins in the category of High-Accuracy Template-Based Modeling. Applications of highly accurate proteins 3D models to various biological systems will be discussed.

2121-Symp

Finding Small Molecule Ligands for Protein-Protein Interactions and Other "undruggable" Targets

Michelle Arkin.

Univ California San Francisco, San Francisco, CA, USA.

The central tenant of chemical biology and small-molecule drug discovery is that biology can be manipulated using small, organic compounds. Nevertheless, the known drugs act on only ~1% of the proteome, and the realm of undrugged targets is vast. Protein complexes occupy much of this realm, yet are widely considered ‘‘undruggable’’ or, at best, ‘‘challenging.’’ Thus, there is an opportunity to greatly expand the range of chemical tools and drugs if we can identify which protein-protein interactions are most amenable to small-molecule interference, and what small-molecule discovery approaches are most likely to yield potent and selective modulators. This presentation will describe some of the outstanding issues and promising advances in tackling protein-protein interactions. For example, we note that many protein interfaces are structurally adaptive, and therefore could have low-energy conformations that are amenable to binding small ligands. Additionally, many enzymes are allosterically regulated by protein complexation, and these protein-protein interfaces are also targets for unconventional enzyme inhibitors.

Platform AC: Cardiac Electrophysiology

2122-Plat

Diverse Effects of a Familial Atrial Fibrillation (FAF)-Related KCNE2 Mutation, R27C, on Cardiac Voltage-Gated Potassium (Kv) Channels

Yu-Hong Wang, Min Jiang, Mei Zhang, Gea-Ny Tseng.

Virginia Commonwealth University, richmond, VA, USA.

Background: KCNE2 (E2) is expressed in human heart and can potentially associate with all major cardiac Kv channels to modulate their current amplitude and/or gating kinetics. An E2-R27C mutation was identified in fAF patients, and shown to have a gain-of-function effect on E2/(KCN)Q1 channel complex. However, it is not clear whether/how E2-R27C affects E2 modulation of other cardiac Kv channels, and the biophysical nature of its gain-of-function phenotype when associated with Q1. **Methods**: We express E2-WT or E2-R27C with partner Kv channel α-subunits (E2:α-subunit = 3:1), and record currents using TEVC. **Results**: Coexpressing E2-WT with Kv4.3 (pore-forming subunit of I_{to} channels) reduces peak current amplitude and induces a depolarizing shift in $V_{0.5}$ of inactivation (from −45+5 to −37+5 mV). Relative to E2-WT/Kv4.3, E2-R27C reduces the current-suppressing effect and shifts $V_{0.5}$ of inactivation in the hyperpolarizing direction (to −41+5 mV). Relative to E2-WT/hERG (pore-forming subunit of I_{Kr} channels), E2-R27C induces a modest current suppressing effect along with a hyperpolarizing shift in $V_{0.5}$ of activation (from 10+4 to −8+1 mV). Relative to E2-WT/Q1 (pore-forming subunit of I_{Ks} channels), E2-R27C markedly increases the estimated fully-available current amplitude and induces a hyperpolarizing shift in $V_{0.5}$ of activation (from −7+2 to to −41+5 mV). **Conclusion**: E2-R27C affects how E2 modulates the current amplitude and voltage-dependence of gating of Kv4.3 and hERG channels. The net results can be gain-of-function or loss-of-function, depending on the resting membrane potential (RMP, depolarizing RMP exacerbates Kv4.3 inactivation by E2-R27C) and action potential plateau voltage (APPV, loss of APPV favors currents through E2-R27C/hERG channels). E2-R27C exerts a strong gain-of-function effect on E2/Q1 channels by 2 mechanisms: increasing the fully-available current amplitude and shifting the voltage range of activation in the hyperpolarizing direction.

2123-Plat

Simulation of the Impact of Elevated Cytosolic Na+ on Ca2+ Handling, Mitochondrial Energetics and Cellular Electrophysiology in Guinea Pig Myocytes

Lufang Zhou, An-Chi Wei, Ting Liu, Sonia Cortassa, Raimond Winslow, Brian O’Rourke.

Johns Hopkins University, Baltimore, MD, USA.

Chronic heart failure is one of the leading causes of morbidity and mortality in the United States. One of the classical strategies for treating heart failure is to inhibit sarcolemmal Na+/K+-ATPase (NKA). Blocking NKA can result in dramatic elevation of [Na+]i, increasing the sarcoplasmic reticulum (SR) Ca2+ load by acting on the plasmalemmal Na+/Ca2+ exchanger (NCX). Whether and how change of [Na+]i affects mitochondrial Ca2+ dynamics and energetics is still under investigation. Since intracellular Na+ is regulated by a complex system involving multiple ions, channels, exchangers and membrane potentials, unraveling its effect on cell physiology and function requires an integrative view of cardiomyocyte physiology. In the present study we developed a mathematical model of cardiomyocyte that incorporates mitochondrial energetics, ion channels and exchangers, and E-C coupling. Using this model, we simulated the effect of elevated cytosolic Na+ on Ca2+ handling, mitochondrial energetics and reactive oxygen species (ROS) generation. Model simulations show that inhibition of NKA (50%) dramatically increased [Na+] in both the cytosol and mitochondria, which consequently caused Ca2+ overload in the cytoplasm during increased workload. Elevated Na+ also decreased ATP concentration and increased mitochondrial ROS production. Concomitant inhibition of mitochondrial Na+/Ca2+ exchanger (mNCE) ameliorated these effects by attenuating cellular Ca2+ overload and increasing [Ca2+]m. Furthermore, inhibiting mNCE also prevented the [ATP]i drop and decreased ROS production. The findings indicate that increasing cytosolic Na+ has an adverse effect on mitochondrial energetics that can be attenuated by simultaneous inhibition of mNCE.

2124-Plat

Biexcitability and Early Afterdepolarization-Mediated Cardiac Arrhythmias

Daisuke Sato, Alan Garfinkel, James N. Weiss, Zhilin Qu.

University of California, Los Angeles, CA, USA.

Under normal conditions in ventricular tissue, both planar wave propagation and spiral wave reentry are mediated by Na current (I_{Na})-mediated depolarization. Under diseased conditions in which repolarization reserve is reduced, however, secondary depolarizations can occur in the plateau or repolarizing phase of the action potential (AP) due to reactivation of the L-type calcium current ($I_{Ca,L}$), known as early afterdepolarizations (EADs). Under these conditions, we observed a novel behavior in which both I_{Na}-mediated spiral wave reentry and $I_{Ca,L}$-mediated spiral wave reentry coexisted in the same homogeneous tissue. I_{Na}-mediated spiral waves were similar to those observed under normal condition, with high rotation frequency (~10 Hz) and nearly full repolarization between beats. $I_{Ca,L}$-mediated spiral waves, however, rotated much slower (2-3 Hz) with membrane voltage remaining above −40 mV, at which I_{Na} is inactivated. We call this novel property of an excitable medium ***biexcitability***. In heterogeneous tissue with transmural AP gradients, pause-induced EADs initiated $I_{Ca,L}$-mediated rotors from the M-cell region. The resulting arrhythmia was characterized by co-existing $I_{Ca,L}$- and I_{Na}-mediated wavefronts, with a frequency and electrocardiographic appearance resembling Torsades de Pointes. The arrhythmia either terminated spontaneously or degenerated to ventricular fibrillation. We propose biexcitability as a novel mechanism of Torsades de Pointes in long QT syndromes.

2125-Plat

B-Type Natriuretic Peptide (BNP) Prolongs Action Potential Duration through Suppressing Transient Outward Potassium Current in Rat Hearts

Junping Sun, Yutao Xi, Geru Wu, Justin Wang, Jie Cheng.

Texas Heart Institute/St.Luke’s Episcopal Hospital and Baylor College of Medicine, Houston, TX, USA.

Background: Nesiritide (B-type natriuretic peptide) improves hemodynamic function and heart failure status for patients with decompensated congestive heart failure. However, studies associated the use of nesiritide with an increased risk of sudden death, to date, little is known of the underlying mechanisms. In this study, the effect of BNP on action potential duration and underlying electrophysiologic mechanisms were investigated in rat hearts.
Method: Wistar rats were anesthetized with sodium pentobarbital (40mg/kg) and injected with BNP-32 (12μg/kg) from abdominal vena cava. EKG was recorded using electrodes inserted into the subcutaneous layer of the paws. Action potentials from 8 rat left ventricles were recorded by a high-resolution optical mapping with voltage-sensitive dye RH237 in Langendoff perfusion system. Transient outward potassium current of rat ventricular myocytes was recorded by the whole cell configuration of patch clamp technique.
Results: BNP-32, at a clinically relevant concentration, prolonged corrected QT interval ($QTc = QT / \sqrt{RR}$) obviously in adult rats, whereas heart rate was comparable during and after BNP-32 treatment. BNP-32 (0.1μM) increased action potential duration at 50% (APD_{50}) repolarization (45.62 ± 4.45ms, $P<0.01$) and this effect persisted after 15 min of washout (57.71 ± 12.62ms, $P<0.05$) compared to baseline (BL: 41.22 ± 2.88ms). In control group of 6 rat hearts, APD_{50} had no obvious changes over the same time period without BNP perfusion. The peak transient outward potassium current at +60mV was significantly reduced (7.11 ± 4.97 to 2.85 ± 3.30 pA/pF, n=6; $P<0.05$) by 0.01μM BNP-32, and then partially recovered to 5.85 ± 4.12 pA/pF (n=6, $P<0.05$) after washout of BNP-32.
Conclusion: BNP prolongs action potential duration and reduces transient outward potassium current in rat hearts, which might contribute to BNP-induced increase of death risk in decompensated heart failure patients.

2126-Plat
The Mitochondrial Bioenergetic Phenotype for Protection from Ischemia in Sur2-Mutant Mice
Nitin Aggarwal[1], Danijel Pravdic[2], Elizabeth M. Mcnally[3], Zeljko J. Bosnjak[2], Nian-Qing Shi[1], Jonathan C. Makielski[1].
[1]Univ. Of Wisconsin, Madison, Madison, WI, USA, [2]Medical College of Wisconsin, Milwaukee, WI, USA, [3]Uni. of Chicago, Chicago, IL, USA.
ATP-sensitive potassium channels (K_{ATP}) in mitochondria are postulated to play a key role to protect mitochondria and myocytes from cardiac ischemic insult. The sulfonylurea receptor-2 (SUR2) is a subunit of K_{ATP} in sarcolemma, although its role in mitochondrial physiology is unclear. Mice where the SUR2 gene was disrupted (SUR2 mutant) have been shown to be constitutively protected from ischemic injury.
We characterized the bioenergetic phenotype of mitochondria in SUR2 mutant mice to gain insight into mechanisms of protection from ischemia.
Membrane potential ($\Delta\Psi_m$), Ca^{2+} uptake, and reactive oxygen species (ROS) generation were studied in the isolated mitochondria by fluorescence based assays and K^+-influx was studied by volume measurements. Mitochondrial respiration was studied in normoxia and after hypoxia-reoxygenation. Myocyte protection against metabolic inhibition was also investigated. $\Delta\Psi_m$ was depolarized (53.37 ± 1.5 vs 48.4 ± 1.8 %), tolerance to Ca^{2+} loading was increased (163 ± 26 vs 116 ± 23 μM), and ROS generation was increased (9.3 ± 0.4 vs 7.4 ± 0.6 FU/sec) in the SUR2 mutant mitochondria compared to wild type (Wt). SUR2 mutant mitochondria had greater swelling (30.2 ± 3.1%) compared with Wt (14.5 ± 0.6%) indicating greater K^+ influx. SUR2 mutant mitochondria recovered better from post hypoxia-reoxygenation than Wt as measured by the respiration control index (RCI). Finally, the SUR2 mutant myocytes viability was better protected against metabolic inhibition.
We concluded that SUR2 plays a key role in mitochondrial mechanisms of protection from ischemia by altering a potassium conductance consistent with a mitochondrial K_{ATP} and causing a protected mitochondrial phenotype.

2127-Plat
Multiple Mechanisms of hERG Liability: K^+ Current Inhibition, Disruption of Protein Trafficking, and Apoptosis Induced by Amoxapine
Sabrina Obers[1], Ingo Staudacher[1], Ramona Bloehs[1], Eckhard Ficker[2], Adrienne Dennis[2], Jana Kisselbach[1], Patrick Schweizer[1], Ioana Baldea[1], Hugo Katus[1], **Dierk Thomas**[1].
[1]University of Heidelberg, Heidelberg, Germany, [2]Case Western Reserve University, MetroHealth Medical Center, Cleveland, OH, USA.
The antidepressant amoxapine has been linked to QT prolongation, acute heart failure, and sudden death. Drug binding to cardiac hERG (Kv11.1) potassium channels causes prolonged repolarization and induces apoptosis. This study was designed to investigate amoxapine effects on hERG currents, hERG protein trafficking, and hERG-associated apoptosis in order to elucidate molecular mechanisms underlying cardiac side effects of the drug. hERG channels were expressed in *Xenopuslaevis* oocytes and HEK 293 cells, and potassium currents were recorded using patch clamp and two-electrode voltage clamp electrophysiology. Protein trafficking was evaluated in HEK 293 cells by Western blot analysis, and cell viability was assessed by immunocytochemistry and colorimetric MTT assay. Amoxapine caused acute hERG blockade in oocytes ($IC_{50} = 21.6$ μM) and in HEK 293 cells ($IC_{50} = 5.1$ μM). Mutation of residues Y652 and F656 attenuated hERG blockade, suggesting drug binding to a receptor inside the channel pore. Channels were mainly blocked in open and inactivated states, and voltage-dependence was observed with reduced inhibition at positive potentials. Amoxapine block was reverse frequency-dependent and resulted in accelerated and leftward-shifted inactivation. Furthermore, amoxapine caused chronic reduction of hERG trafficking into the cell surface membrane ($IC_{50} = 15.3$ μM). Finally, the antidepressant drug triggered apoptosis in cells expressing hERG channels. Triple mechanisms of hERG liability associated with a single compound, are revealed. Amoxapine causes direct hERG current inhibition and disruption of hERG protein trafficking. Furthermore, the drug induces apoptosis of cells expressing hERG potassium channels.

2128-Plat
Cardiac Glycoside Chronotropic and Arrhythmogenic Effects in Sinoatrial Nodal Pacemaker Cells (SANC) Occur Along a Continuum of Electrochemical Gradients of Na^+ (E_{Na}) and Ca^{2+} (E_{Ca})
Syevda Sirenko[1,2], Dan Yaeger[1], Tatiana M. Vinogradova[1], Yue Li[1], Yael Vaniv[1], Ihor Zahanich[1], Harold Spurgeon[1], Victor Maltsev[1], Edward.G. Lakatta[1].
[1]Laboratory of Cardiovascular Science, National Institute on Aging, NIH, Baltimore, MD, USA, [2]MedStar Research Institute, Baltimore, MD, USA.
Cardiac glycosides reduce E_{Na} and E_{Ca} (due to an increase of Na^+_i via Na-K pump inhibition, and of Ca^{2+}_i, due to a secondary reduction in Ca efflux for Na influx via NaCa exchange). Here we show that exposure of single rabbit SANC to the cardiac glycoside, digoxigenin (10-20μM) results in a continuum of time-dependent effects. Within 30s to 1 min, the rate of rhythmic spontaneous action potentials (AP) increases by 20% (n=3) and this is associated with an earlier occurrence (reduced period) of local sub-membrane Ca^{2+} releases (LCR's) during diastolic depolarization, detected by confocal Ca^{2+} imaging. Approximately 1-3 minutes following AP rate acceleration, LCR period lengthens by 40%, accompanied by a similar reduction in the rhythmic AP rate. The changes in LCR period during the biphsic changes in rhythmic AP firing rate increase are highly correlated with the changes in AP cycle length (R^2=0.98). A progressive increase in the steady level of diastolic Ca^{2+} beneath the surface membrane then ensues usually within 4 to 6 additional minutes, LCR's became undetectable, and dysrhythmic and chaotic AP firing occurs. Numerical model simulations (Maltsev-Lakatta model, AJP 2009) in which Na_i was increased progressively 5-15mM during glycoside exposure reproduced the experimental results. That rate and rhythm regulation of SANC AP firing during cardiac glycoside exposure occurs along a continuum of E_{Na}/E_{Ca} is in agreement with repeated observations over the last decade, showing that the SANC spontaneous AP firing rate is critically dependent on the timing of acute changes in sub-membrane E_{Ca} during DD caused by LCR occurrence (LCR period) that accelerates DD by activation of an inward Na/Ca exchange current.

2129-Plat
Calcium Currents in Chronically Dysfunctional Pig Myocardium
Derek L. Beahm, Ki-Hyuk Yoo, Glenna C.L. Bett, John M. Canty, James A. Fallavollita, **Randall L. Rasmusson**.
SUNY Buffalo, Buffalo, NY, USA.
Chronic reduction in coronary artery blood flow due to stenosis results in reduced myocardial contractile function, termed ‘‘hibernating’’ myocardium. This change involves electrical remodeling and a propensity for sudden cardiac death in the absence of infarction. We used a pig model of chronic left anterior descending artery stenosis to study calcium currents associated with the hibernating myocardium. We developed a cell isolation technique from punch biopsies of the left ventricle. This yields calcium-tolerant isolated myocytes with brick shaped morphology and clear striation patterns. Myocyte length from hibernating myocardium averaged 145 ± 7.7 (n=15) vs. 124 ± 4.8 μm (n=42) for control, suggesting cellular hypertrophy. The cell shortening of hibernating cells was also reduced compared to the remote region from 6.4 ± 1% (n=21) to 4.45 ± 1% (n=11) suggesting that the reduced contractility seen in the hibernating region was preserved in the isolated myocytes. Furthermore, cells isolated from hibernating myocardium had significantly higher numbers of premature contractions 4/15 for hibernating vs. 0/19 for control suggesting a cellular propensity for arrhythmias. The L-type calcium channel current ($I_{Ca,L}$) in myocytes from hibernating myocardium (1.35 ± 0.08 pA/pF, n=22) was reduced compared to normal myocardium (1.96 ± 0.07 pA/pF, n=33; $P<0.01$). The voltage dependence of steady state activation and inactivation were nearly

identical. Isoproterenol (100 nM) shifted the activation curves nearly identically for both groups, but the ability of isoproterenol to enhance the current was decreased from a 4.1 $\pm$ 0.48 fold increase to a 2.64 $\pm$ 0.37 ($p < 0.05$). Finally, the recovery rate for calcium current was reduced by hibernation, reflecting an approximate 20 mV shift. These changes in L-type calcium current and isoproterenol response may explain the reduced contractility of hibernating myocytes and the increased the likelihood of sudden cardiac arrhythmias.

Platform AD: Fluorescence Spectroscopy

2130-Plat

Proton Transfer and Hydrogen-Bond Interactions Determine the Fluorescence Quantum Yield of Bacteriophytochrome, a Novel Deep-Tissue Fluorescent Probe

K.C. Toh[1], Emina Stojkovic[2], Ivo H.M. van Stokkum[1], Keith Moffat[2], **John T. Kennis[1]**.
[1]Vrije Universteit, Amsterdam, Netherlands, [2]University of Chicago, Chicago, IL, USA.

Phytochromes are red-light photoreceptors that regulate a variety of responses and cellular processes. The phytochrome light activation mechanism involves isomerization around the C15=C16 double bond of an open-chain tetrapyrrole chromophore, resulting in a flip of its D-ring. In an important new development, bacteriophytochrome (Bph) has been engineered for use as a fluorescent marker in mammalian tissues (Shu et al. Science 2009). Bph fluoresces at ~720 nm, a wavelength less prone to scattering that can penetrate more deeply into tissue than light emitted by GFP-derived fluorescent proteins. The Bph chromophore biliverdin is a naturally occurring cofactor in mammalian tissue that covalently binds to a conserved cysteine in Bph, and hence BPhs can readily be genetically encoded. BPh photochemistry is thus of considerable significance for biomedical technology. Here we report that an unusual Bph, P3 from Rps. palustris, is highly fluorescent. We identify the factors that determine the fluorescence and isomerization quantum yields of P3 through the application of ultrafast spectroscopy to wild-type and mutants of P3 and a classical Bph, P2. The excited-state lifetime of biliverdin in P3 was significantly longer at 330 - 500 ps than in P2, and accompanied by a significantly reduced isomerization quantum yield. H/D exchange reduces the rate of decay from the biliverdin excite state by a factor of 1.4 and increases the isomerization quantum yield. Comparison of the properties of the P2 and P3 variants in relation to X-ray structures shows that the quantum yields of fluorescence and isomerization are determined by excited-state deprotonation of biliverdin at the pyrrole rings, in competition with hydrogen-bond rupture between the biliverdin D-ring and the apoprotein. This work provides a basis for structure-based conversion of BPh into an efficient near-IR fluorescent marker.

2131-Plat

Fine Tuning the Optical Properties of Green to Red Photoconvertible Fluorescent Proteins

Karin Nienhaus[1], Virgile Adam[2], Dominique Bourgeois[2], G. Ulrich Nienhaus[1].
[1]Karlsruhe Institute of Technology, Karlsruhe, Germany, [2]European Synchrotron Radiation Facility, Grenoble, France.

Dendra2 is an engineered, monomeric GFP-like protein that belongs to a subclass of fluorescent proteins undergoing irreversible photoconversion from a green- to a red-emitting state upon exposure to purple-blue light. We have measured the X-ray structure of the green species of Dendra2 and performed a comprehensive characterization of the optical absorption and fluorescence properties of the protein in both its green and red forms. The structure, which is very similar to those reported for the closely related proteins EosFP and Kaede, revealed a local structural change next to the chromophore, involving mainly Arg66 and a water molecule. We propose that this structural change explains the blue shift of the absorption and emission bands, as well as the markedly higher pKs of the hydroxyphenyl moiety of the chromophore, which were determined as 7.1 and 7.5 for the green and red species, respectively. The 20-fold enhancement of the neutral species in Dendra2 at physiological pH accounts for the observed higher photoconversion yield of this protein in comparison to EosFP.

2132-Plat

Color Hues in Fluorescent Proteins with the Same Chromophore are due to Internal Quadratic Stark Effect

Mikhail Drobizhev, Shane Tillo, Nikolay S. Makarov, Aleksander Rebane, Thomas Hughes.
Montana State Univ, Bozeman, MT, USA.

Intrinsically fluorescent proteins (FPs) exhibit broad variations of absorption and emission colors and are available for different imaging applications. The physical cause of the absorption wavelength change in series of mutants with the same chromophore structure, but different surrounding, is however not understood. Here we study the FP series with acylimine-containing red chromophore, in which the absorption maximum varies from 540 nm to 590 nm, and a series of green FPs with phenolate chromophore, where the absorption peak shifts from 450 to 500 nm. We use two-photon absorption spectroscopy to show that the different colors in each series can be explained by quadratic Stark effect due to variations of the strong local electric field within the beta barrel. The model allows us to experimentally access the chromophore parameters, such as vacuum transition frequency (ν_0) and vacuum changes of permanent dipole moment ($\Delta\mu_0$) and polarizability ($\Delta\alpha_0$) upon excitation. Using this purely experimental and all-optical approach, we estimate, for the first time to our knowledge, the amplitudes of the internal electric field (namely its projection on $\Delta\mu_0$) in a protein. These values amount 10 to 100 MV/cm in the mFruits series. Although these fields appear to be very large, they fall well in the range previously estimated theoretically for different other proteins, and are still 1 $-$2 orders of magnitude smaller than the fields required to ionize the chromophore. Our model brings simplicity to a bewildering diversity of fluorescent protein properties, and it suggests a new way to sense electrical fields in biological systems. On the other hand, it opens up the way to create two-photon brighter FP probes by tuning internal electric field with smart mutagenesis around the chromophore.

2133-Plat

TIRF-Based FRET with One Base-Pair Resolution

Seamus J. Holden, Stephan Uphoff, David Yadin, Johannes Hohlbein, Ludovic Le Reste, Oliver J. Britton, Achillefs N. Kapanidis.
University of Oxford, Oxford, United Kingdom.

Single-molecule FRET (smFRET) is commonly used as a ‘‘nanoscale ruler’’ for the measurement of biomolecular distances and distance changes. However, the limits of FRET resolution for measurements on surface-immobilized molecules have not been rigorously explored. Using total-internal reflection fluorescence (TIRF) microscopy on a set of DNA standards and advanced image analysis software, we have quantified and extended the limits of FRET resolution associated with the use of electron-multiplying CCD (EMCCD) cameras. For such measurements, we derived a novel theoretical description of the major sources of noise (photon shot noise, background, CCD noise and pixelation effects); we find excellent agreement between our experimental results and predictions from theory and Monte Carlo simulations. For FRET measurements on a truly single-molecule basis (as opposed to measurements on an ensemble of single molecules), analysis of the experimental noise allows us to predict a resolution of 4% FRET within the linear FRET range (20-80%), sufficient to directly observe a distance difference equivalent to one DNA base-pair separation (3.4 Å). For FRET distributions obtained from an ensemble of single molecules (which exhibits broadening due to presence of static heterogeneity), we demonstrate the ability to distinguish between distances differing by as little as 2 base pairs (~7Å). Current work focuses on real-time observation of single-base-pair translocation steps of Escherichia coli RNA polymerase within single early transcription-elongation complexes; such observations are crucial for understanding the mechanisms of DNA and RNA polymerases.
Our work paves the way for ultra-high resolution studies of processes involving conformational changes and protein translocation on nucleic acids.

2134-Plat

Single-Molecule STED with Photostable Fluorophores

Robert Kasper.
Bielefeld University, Bielefeld, Germany.

With recent advantage in the development of far-field super-resolution microscopy, further development depends crucially on improved fluorescent probes. We combined STED microscopy with fluorophore stabilization through a reducing and oxidizing system (ROXS) and demonstrate significant improvement of photostability. We show that this improvement can be exploited either for repetitive measurements necessary for 3D or dynamic STED imaging or for resolution enhancement through the application of higher STED beam intensities. Accordingly, a lateral resolution below 30 nm is demonstrated for single organic fluorophores immobilized in aqueous buffer.

2135-Plat

Fluorescence Correlation Spectroscopy Elucidates the Pathway of RNA Interference

Jörg Mütze[1], Thomas Ohrt[2], Wolfgang Staroske[1], Lasse Weinmann[3], Julia Höck[3], Gunter Meister[3], Petra Schwille[1].
[1]TU Dresden, Dresden, Germany, [2]MPI for Biophysical Chemistry, Göttingen, Germany, [3]MPI for Biochemistry, Munich, Germany.

Short double-stranded RNA molecules have recently emerged as important regulators of gene expression. These small RNAs associate with a member of the Argonaute protein family in an assembly known as RNA-induced silencing complex (RISC).
Here we elucidate the pathway of RNA Interference (RNAi) in vivo by applying fluorescence correlation and cross-correlation spectroscopy (FCS/FCCS).
We show that two distinct RISC exist: a large ~3 MDa complex in the cytoplasm and a 20-fold smaller complex in the nucleus. Nuclear RISC, consisting only of Ago2 and a short RNA, is loaded in the cytoplasm and imported into the nucleus. The import of Ago2 into the nucleus is mediated by the import receptor Impotin8.
We further demonstrate that FCCS can be used to study the interaction of different members of the Argonaute protein family with short double-stranded RNAs and their target mRNA molecules.

2136-Plat

G-Quadruplex Folding Observed by two Photon Fluorescence Correlation Spectroscopy and Dual Time Scale

Tilman Rosales[1], Xiuyi Liu[2], Yasemin Kopkalli[2], Lesley Davenport[2], Mary Hawkins[3], Jay R. Knutson[1].
[1]NIH, NHLBI, LMB, OSS, Bethesda, MD, USA, [2]Brooklyn College of CUNY, Dept. of Chemistry, Brooklyn, NY, USA, [3]NIH, NCI, POB, Bethesda, MD, USA.

G-rich DNA sequences are known to fold upon addition of salt into a stacked well defined configuration called a quadruplex. A fluorescently labeled 5′-FAM −24-mer G-quadruplex sequence was used to explore the variation of diffusion coefficients at extremely low, low and high KCl concentrations. We found a shift in the diffusion coefficient of about 10μm2/sec toward faster diffusion from extremely low to high KCl concentrations. This shift can be related to the compact structure formed by the G-quadruplex. We have also used a fluorescent guanosine analog, 6MI, to label a 24mer that has shown folding behavior at high KCl concentrations. To explore this further, we have added in excess a sequence that complements the G-rich region to deter the formation of the G-quadruplex. The diffusion coefficient also increased from the unfolded, low KCl concentration to the high salt, G-quadruplex structure. We have constructed a dual-time-scale (ps TCSPC and uS-mS FCS) photon correlation system and we are using it to explore linked changes in the fluorophores' lifetimes and the translational diffusion coefficients as they move between low and high salt environments. Part of this work was supported by NIH SCORE Grant S06 GM 060654.

2137-Plat

Observing Nuclear Receptor / Coactivator Interactions in Live Cells by Hetero-Species Partition Analysis

Joachim Mueller[1], Bin Wu[2], Yan Chen[1].
[1]University of Minnesota, Minneapolis, MN, USA, [2]Albert Einstein College of Medicine, New York, NY, USA.

Measuring the binding curve and stoichiometry of protein complexes in living cells is a prerequisite for quantitative modeling of cellular processes. Dual-color fluorescence fluctuation spectroscopy provides a general framework for detecting protein interactions. However, quantitative characterization of protein hetero-interactions remains a difficult task. To address this challenge we introduce hetero-species partition (HSP) analysis for measuring protein hetero-interactions of the type D + nA -> DA_n. HSP directly identifies the hetero-interacting species from the sample mixture and determines the binding curve and stoichiometry in the cellular environment. The method is applied to measure the ligand-dependent binding curve of the nuclear receptor retinoic X receptor to the coactivator transcription intermediate factor 2. The binding stoichiometry of this protein system has not been directly measured yet. A previous study using protein fragments observed a higher binding stoichiometry than biologically expected. We address this difference in stoichiometry by measuring the binding curves of the full-length proteins in living cells. This study provides proof-of-principle experiments that illustrate the potential of HSP as a general and robust analysis tool for the quantitative characterization of protein hetero-interactions in living cells.

Platform AE: Muscle Regulation

2138-Plat

Determining Mechanism of Phosphorylation of Smooth Muscle Myosin by Calmodulin-Myosin Light Chain Kinase Using an in vitro Model System

Feng Hong, Brain D. Haldeman, Shaowei Ni, Nick Ruana, Del R. Jackson, Josh E. Baker, Christine R. Cremo.
University of Nevada, Reno, School of Medicine, Reno, NV, USA.

We have shown that MLCK and calmodulin (CaM) co-purify with unphosphorylated SMM (up-SMM) from chicken gizzard, suggesting that they are tightly bound. Although the MLCK:SMM molar ratio in SMM preparations was well below stoichiometric (1:73 ± 9), the ratio was ~ 23-37% of that in gizzard tissue. Fifteen to 30% of MLCK was associated with CaM at ~1 nM free [Ca^{2+}]. There were two MLCK pools that bound up-SMM with Kd ~10 μM and 0.2 μM and phosphorylated SMM with a Kd ~ 20 μM and 0.2 μM. Using motility assays, co-sedimentation assays, and on-coverslip ELISA assays, we provide strong evidence that most of the MLCK is bound directly to SMM through the telokin domain. The bound MLCK can phosphorylate SMM in a Ca^{2+}-dependent manner with a pCa_{50} ~ 6 as measured by in vitro motility, similar to in vivo results. After activation of SMM-bound MLCK/CaM with Ca^{2+} and ATP, both motility (0.5 μm/sec) and phosphorylation (>15%) of SMM reach a maximum after ~15-30 min, inconsistent with a free diffusion mechanism. Actin movement over the SMM is not required for this phosphorylation process. Experiments are underway to test the idea that SMM heads proximal to the MLCK-SMM become phosphorylated by a tethered diffusion mechanism.

2139-Plat

The Crystal Structure of the N-terminal 15 Heptads of Smooth Muscle Myosin Rod Offers Insights into the Inhibited State of Myosin

Usha B. Nair, Patricia M. Fagnant, Susan Lowey, Mark A. Rould, Kathleen M. Trybus.
University of Vermont, Burlington, VT, USA.

The coiled coil rod of smooth muscle myosin is important both for regulation of activity and optimal mechanical performance. Myosin with a phosphorylated light chain is active, while in the inhibited, dephosphorylated state the two heads form an asymmetric intramolecular interaction. The minimal myosin that can attain an ''off'' state has two heads and 15 heptads of coiled coil rod, a length approximately equal to that of the myosin head. This observation implies that there may be head-rod interactions in the inhibited state. Here we have determined the crystal structure of this region of the rod. Despite being a parallel, coiled coil dimer, the core arrangement is asymmetric. We propose that this asymmetry is wired into its sequence and crucial to its function. The core of the S2 segment is loosely packed in stretches and the two helical segments are locally off-register or staggered relative to one another. Staggered regions are centered on non-canonical core residues. This relative staggering causes three prominent bends in the coiled coil. Significant deviations from two-fold symmetry are observed in our structure, and to a lesser extent in equivalent crystal structures of S2 fragments from cardiac myosin. The larger variations in stagger and bend angles in the rods of smooth versus striated muscle myosins may explain in part why asymmetric head-head interactions are more prevalent in the thick filament regulated myosins.

2140-Plat

Electron Microscopy and Molecular Dynamics on a D137L Mutant of Tropomyosin

Jasmine Nirody[1], Xiaochuan Li[1], Duncan Sousa[1], John Sumida[1], Stefan Fischer[2], Sherwin S. Lehrer[3], William Lehman[1].
[1]Boston University School Medicine, Boston, MA, USA, [2]University Heidelberg, Heidelberg, Germany, [3]Boston Biomedical Research Institute, Watertown, MA, USA.

It is generally agreed that constraints on the curvature and flexibility of tropomyosin are necessary both for the binding and regulatory movements of tropomyosin on actin filaments. It follows that mutagenesis of residues that may affect curvature and/or flexibility is commonly used as an analytical tool. The tropomyosin coiled-coil is stabilized by hydrophobic residues in the "a" and "d" positions of its heptad repeat. However, a highly conserved Asp137 places a negative charge on each chain in a position typically occupied by hydrophobic residues. Substituting a canonical Leu for Asp137 suggested that Asp137 destabilizes tropomyosin and imparts flexibility (Sumida et al., 2008). The D137L mutant does retain F-actin binding properties. We have now assessed changes of curvature and flexibility by EM and Molecular Dynamics (MD) on the Leu137 mutant. Contrary to expectation, rotary shadowed D137L tropomyosin is more curved, not straighter, than control tropomyosin. Moreover, overall the average MD shape of the molecule is extremely bent and, unlike wild type tropomyosin, does not match the contours of the F-actin helix at all. We find that the persistence length of D137L is half that of wild-type tropomyosin (measured either on EM images or on MD frames), indicating that the mutant is more curved and more flexible than the wild type is. MD shows that there is a modest decrease in curvature in the surrounds of residue 137 in the D137L mutant, but it is accompanied by a large unexpected increase in curvature near residue 175. Thus we find that mutation at one site on tropomyosin leads to an unexpected delocalized change at another site along the molecule.

2141-Plat
Troponin Regulatory Function and Dynamics Revealed by H/D Exchange-Mass Spectrometry
Devanand Kowlessur, **Larry S. Tobacman**.
University of Illinois at Chicago, Chicago, IL, USA.
Troponin is the thin filament protein that confers tight, Ca^{2+}-dependent control over muscle contraction. The mechanism of this regulation was investigated by detailed mapping of the dynamic properties of cardiac troponin, using amide hydrogen exchange-mass spectrometry, in the presence of either saturation or non-saturation of the regulatory Ca^{2+} binding site in the NH_2-domain of subunit TnC. Troponin was found to be highly dynamic, with 60% of amides exchanging H for D within seconds of exposure to D_2O. In contrast, portions of the TnT-TnI coiled-coil exhibited high protection from exchange, more than six hours, identifying the most stable portion of the trimeric troponin complex. Regulatory site Ca^{2+} binding altered dynamic properties (i.e., H/D exchange protection) locally, near the binding site and in the TnI switch helix that attaches to the Ca^{2+}-saturated TnC NH_2-domain. More notably, Ca^{2+} also altered the dynamic properties of other parts of troponin: the TnI inhibitory peptide region that binds to actin, the TnT-TnI coiled-coil, and the TnC COOH-domain that contains the regulatory Ca^{2+} sites in many invertebrate as opposed to vertebrate troponins. Mapping of these affected regions onto troponin's highly extended structure indicates contacts important in conformational change: in the low Ca^{2+} state the TnI region that effects inhibition bends back and interacts with the end of the TnT-TnI coiled-coil, as previously suggested by intermediate resolution X-ray data of skeletal muscle troponin. Thus, troponin-mediated Ca^{2+} sensitive regulation of muscle contraction consists of Ca^{2+}-triggered switching between alternative sets of intra-troponin interactions.

2142-Plat
Magnesium Stabilizes the Closed Conformation of the C-Domain of Troponin C
Sarah S. Learman, Rishabh Khandelwal, Franklin Fuchs, Zenon Grabarek.
Boston Biomedical Research Institute, Watertown, MA, USA.
Activation of the thin filament in striated muscles requires both the binding of Ca^{2+} to the N-domain of troponin C (TnC) and the binding of myosin cross-bridges to actin, which has been shown to alter the C-domain conformation. Here we have evaluated the structural and functional consequences of divalent cation exchange in skeletal and cardiac TnC (sTnC and cTnC). We have used intrinsic tyrosine fluorescence, circular dichrosim (CD), and the fluorescent nonspecific hydrophobic probe bis-ANS to monitor changes in domain conformation in response to Ca^{2+} and Mg^{2+} binding in the sTnC, cTnC, and in a cTnC mutant in which the invariant Glu residue at the 12th position of the calcium binding loops III and IV were substituted with Asp (cTnCDD). Ca^{2+} binding causes an increase in Tyr fluorescence and α-helical content in sTnC and cTnC, but not in cTnCDD. Ca^{2+} induced C-domain opening characteristic of sTnC and cTnC was also greatly reduced in cTnCDD, as measured by bis-ANS fluorescence. Thus the Asp to Glu substitutions appear to prevent the C-domain from opening. Bis-ANS Ca^{2+} titrations also showed that high Ca^{2+} concentrations may be sufficient to open the N-domain of cTnC, which was reported to remain in the closed conformation in the Ca^{2+}-bound state. Lastly, bis-ANS Mg^{2+} titrations indicate that Mg^{2+} does not cause domain opening in either cTnC or cTnCDD. The closed conformation of the Mg^{2+}-bound C-domain of TnC implies a different mechanism of interaction with TnI than that in the presence of Ca^{2+} and suggests that the Mg^{2+}-Ca^{2+}exchange in TnC may contribute to the thin filament activation of muscle contraction. This conclusion is consistent with our observation that physiological concentrations of Mg^{2+} significantly lower the Ca^{2+}-sensitivity of reconstituted cardiac thin filaments.

2143-Plat
Phosphomimetic Substitutions in One or Both Ser43/45 Residues of Cardiac Troponin I Produces Comparable Changes in Contractile Performance
Tamara Stevenson, Sarah Kampert, Justin Steggerda, Gail Romanchuk, **Margaret Westfall**.
University of Michigan, Ann Arbor, MI, USA.
Cardiac troponin I (cTnI) is phosphorylated on three clusters of residues in response to protein kinase C (PKC) activation. Previously, studies on the cTnISer43/45 cluster showed phosphomimetic Asp substitution reduced peak shortening and accelerated re-lengthening in adult cardiac myocytes. The goal of the present study is to determine whether one or both Ser residues contribute to the functional response observed with cTnISer43/45Asp. We studied adult rat cardiac myocytes 2 and 4 days after viral-mediated gene transfer of cTnIFLAG, cTnISer43Asp or cTnISer45Asp (+FLAG). Western analysis indicated similar levels of cTnI replacement developed for all groups, and extensive replacement with cTnIFLAG ($71 \pm 9\%$, n= 6), and FLAG-tagged epitopes of cTnIS43D ($72 \pm 3\%$, n=8) and cTnIS45D ($70 \pm 5\%$, n=8) within 4 days. Further analysis showed no significant change in cTnI stoichiometry and confocal analysis confirmed a sarcomeric incorporation pattern for each mutant. In functional studies, shortening amplitude decreased significantly in chronically paced myocytes expressing non-tagged Ser43Asp and/or Ser45Asp compared to controls (Control = 0.149 ± 0.008 μm, n=36; cTnISer43/45Asp = 0.110 ± 0.006 μm; n=32*; cTnISer43Asp = 0.095 ± 0.007, n=44*; cTnISer45-Asp = 0.108 ± 0.007*, n=50; *$p<0.05$ vs control) 4 days after gene transfer. An accelerated re-lengthening accompanied this reduced shortening (Time to 75% relaxation = $TTR_{75\%}$ (ms): Control = 79 ± 4; cTnISer43/45Asp = 62 ± 4*; cTnISer43Asp = 63 ± 4*, cTnISer45Asp = 65 ± 3*; *$p<0.05$ vs control). Interestingly, each single mutant also accelerated the time to peak shortening (TTP (ms): Control = 83 ± 5; cTnISer43Asp = 68 ± 3*; cTnISer45Asp = 67 ± 2*; *$p<0.05$ vs control) while cTnISer43/45Asp did not (84 ± 5). These initial results provide evidence that each Ser residue in the Ser43/45 cluster is capable of altering cTnI function in response to phosphorylation by PKC, yet phosphorylation of both residues does not produce an additive response.

2144-Plat
Effect of Troponin Ca^{2+} Binding Properties on the Kinetics of Myofibril Force Initiation and Relaxation
Nicoletta Piroddi[1], Kareen L. Kreutziger[2], Beatrice Scellini[1], Scott Lundy[2], Cecilia Ferrantini[1], Chiara Tesi[1], Michael Regnier[2], Corrado Poggesi[1].
[1]Università di Firenze, Firenze, Italy, [2]University of Washington, Seattle, WA, USA.
We have engineered the Ca^{2+} binding properties of troponin C (TnC) to study the role of increased (I60Q sTnC) and decreased (M80Q $sTnC^{F27W}$) Ca^{2+} dissociation rate (k_{off}) on activation and relaxation of skeletal muscle. Previously we reported that myofibril force development kinetics (k_{ACT}) are not influenced by decreasing k_{off} from Tn, but are slowed by an increase in k_{off} (Kreutziger et al. 2008 JPhsiol. 586;3683-3700) at low $[P_i]$ (5 μm). The time to initiation of force ($k_A$lag) following a rapid (~10ms) switch from pCa 9.0 to pCa 3.5 provides information about thin filament activation rate and our preliminary data suggest this rate may also be sensitive to k_{off}. In rabbit psoas myofibrils (15°C) $k_A$lag (~20 ms for native or WT sTnC) is almost eliminated for M80Q $sTnC^{F27W}$ and increased by I60Q sTnC (~40-50 ms). Additionally, though k_{ACT} is similar for force increases from either full or partial activation to full activation, $k_A$lag disappears when starting from partial activation. We have also reported that fast and slow phase rates of relaxation are not affected by k_{off}, but that duration of the slow phase is affected in skeletal myofibrils. Here we report that lag prior to initiation of the slow phase ($k_R$lag) may be also influenced by k_{off}. Opposite to $k_A$lag, $k_R$lag (~20 ms for WT or native sTnC) was increased (~40-50 ms) by decreased k_{off} (M80Q $sTnC^{F27W}$) and almost eliminated by increased k_{off} (I60QsTnC). These experiments demonstrate a potential approach to study thin filament activation/deactivation kinetics without the need for fluorescent probes attached to thin filament proteins that can affect their function. Supported by Telethon GGP07133, MIUR (CP, CT), NIH-HL65497 (MR).

2145-Plat
Nebulin Alters Crossbridge Cycling Kineticis and Increases Thin Filament Activation - a Novel Mechanism for Increasing Tension and Reducing Tension Cost
Coen Ottenheijm[1], Murali Chandra[2], R. Mamidi[2], Steven Ford[2], Carlos Hidalgo[3], Christian Witt[4], Ger Stienen[1], Siegfried Labeit[4], Alan Beggs[5], Henk Granzier[3].
[1]VU University medical center, Amsterdam, Netherlands, [2]Washington State University, Pullman, WA, USA, [3]University of Arizona, Tucson, AZ, USA, [4]University Hospital Mannheim, Mannheim, Germany, [5]Harvard Medical School, Boston, MA, USA.
Nebulin is a giant filamentous F-actin binding protein that binds along the thin filament of the skeletal muscle sarcomere. Although nebulin is usually viewed as a structural protein, here we investigated whether nebulin plays a role in muscle contraction by using skinned muscle fiber bundles from a nebulin knockout (NEB KO) mouse model. We measured force-pCa and force-ATPase relations, as well as the rate of tension redevelopment (k_{tr}) in tibialis cranialis fibers. To rule out any alterations in troponin (Tn) isoform expression and/or status of Tn phosphorylation, we studied fibers that had been reconstituted with fast skeletal muscle recombinant Tn. We also performed a detailed analysis of myosin heavy chain, myosin light chain (MLC) and MLC2

phosphorylation, and found no significant differences between NEB KO and wt muscle. Our mechanical studies revealed that NEB KO fibers had increased tension cost (5.9 vs. 4.4 pmol mN^{-1} mm^{-1} s^{-1}) and reductions in k_{tr} (4.7 vs. 7.3 s^{-1}), calcium sensitivity (pCa_{50} 5.74 vs. 5.90), and cooperativity of activation (n_H 3.64 vs. 4.38). Our findings indicate that in skeletal muscle (1) nebulin increases thin-filament activation, and (2) that through altering crossbridge cycling kinetics, nebulin increases force and efficiency of contraction. In addition to nebulin deficient murine muscle, we also studied nebulin-deficient muscle fibers from patients with Nemaline Myopathy (NM). We found increased tension cost, and reductions in k_{tr} and calcium sensitivity in NM fibers when compared to human control fibers, consistent with the findings from nebulin-deficient murine muscle. This novel role of nebulin in regulating muscle contraction adds a new level of understanding to skeletal muscle function, and might provide a mechanism for the muscle weakness in patients with nebulin-based Nemaline Myopathy.

Platform AF: Bacterial Motility

2146-Plat

High Resolution, Long Term Characterization of Bacterial Motility Using Optical Tweezers

Taejin L. Min, Patrick J. Mears, Lon M. Chubiz, Christopher V. Rao, Ido Golding, Yann R. Chemla.
University of Illinois at Urbana-Champaign, Urbana, IL, USA.

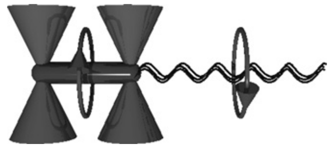

We present a single-cell motility assay[1], which allows the quantification of bacterial swimming in a well-controlled environment, for durations of up to an hour and with a temporal resolution greater than the flagellar rotation rates of ~100 Hz. The assay is based on an instrument combining optical tweezers, light and fluorescence microscopy, and a microfluidic chamber. Using this device we characterized the long-term statistics of the run-tumble time series in individual *Escherichia coli* cells. We also quantified higher-order features of bacterial swimming, such as changes in velocity and reversals of swimming direction.

[1] Min, T.L., Mears, P.J., Chubiz, L.M., Rao, C.V., Golding, I. & Chemla, Y.R. (2009) High-resolution, long-term characterization of bacterial motility using optical tweezers. *Nature Methods* (in press)

2147-Plat

Impact of Microscopic Motility Schemes on the Overall Swimming Behavior of Parasites

Sravanti Uppaluri[1], Jan Nagler[1,2], Eric Stellamanns[1], Niko Heddergott[3], Markus Engstler[3], Thomas Pfohl[1,4].
[1]Max Planck Insitute for Dynamics and Self Organization, Goettingen, Germany, [2]University of Goettingen, Goettingen, Germany, [3]University of Würzburg, Würzburg, Germany, [4]University of Basel, Basel, Switzerland.

In recent work, Engstler et al. showed that the motility of the trypanosomes, causative agents of African sleeping sickness, is essential in their evasion of the host immune response. Our studies reveal that the trypanosome travels in one of three distinct motility modes: random walk, directional persistence, and an intermediate class in which they exhibit a combination of both. To further elucidate the parasite's motility we utilize high-speed videomicroscopy to uncover the microscopic origin of the macroscopic motility modes. Trypanosome swimming is facilitated by a flagellum that runs along the cell body with only a small 'free' segment at the anterior end of the cell. We use a straightforward parameter, namely the distance between the anterior and posterior ends of the cell to characterize trypanosome swimming. Remarkably this parameter is sufficient for extraction of relevant time scales for classification of the motility modes. Further, we find not only that these different motility modes correspond to distinct physical movements but also that a stiffer cell body gives rise to directional persistence.

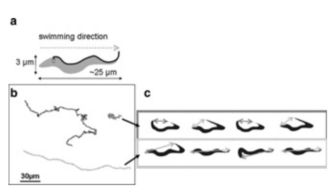

Figure 1. a) schematic of cell body b) typical swimming trajectories c) directionally persistent cells are 'stretched'

2148-Plat

A Model for Bacterial Motility Utilizing Helical Cytoskeleton Filaments and Ion-Driven Motors

Jing Chen, Beiyan Nan, John Neu, David R. Zusman, George Oster.
UC Berkeley, Berkeley, CA, USA.

The bacterial cytoskeleton determines cell shape and mediates cell division. Recent work indicates that the cytoskeleton mediates cell motility as well. Adventurous (A) motility in Myxococcus xanthus requires actin-like MreB filaments. During the motility, a double helix structure – possibly consisting of MreB – rotates in the cell's cytoplasm. Proteins localized along the helical structure are associated with proton transporting protein complexes homologous to the MotA-MotB stator that drives rotation of the bacterial flagellar motor. These observations suggest an entirely new model for bacterial motility in which motors driven by ion motive force move along the helical cytoskeleton to generate propulsive forces. This mechanism may be widespread in bacteria, since both MreB homologs and MotA-MotB homologs are common across a variety of bacterial species, including species that move in the absence of flagella. We have constructed a biophysical model to test the feasibility of this motility mechanism. Our model explains many intriguing observations in Myxococcus motility, including rotation of the helical cytoskeleton, periodic reversals of cells, and clustering of motility-related proteins at the cell poles and the substrate interface. Previous models assumed that periodic cell reversals are attributed to biochemical oscillators in the cell. This model, in contrast, proposes that reversals result from a mechanical oscillator intrinsic to a system with transmembrane motors traveling on a closed helical track. According to this mechanism, mechanical interactions play an important role in signal transduction.

2149-Plat

Direct Evidences of a Motility Motors in Myxococcus Xanthus

Mingzhai Sun[1], Adrien Ducret[2], Tam Mignot[2], Joshua Shaevitz[1,3].
[1]Lewis-Sigler Institute for integrative genomics, Princeton University, Princeton, NJ, USA, [2]Institut de Microbiologie de la Méditerranée, CNRS UPR, Marseille, France, [3]Physics Department, Princeton University, Princeton, NJ, USA.

Myxococcus xanthus, a gram-negative soil bacterium, glides over solid surfaces with two independent motility mechanisms termed social (S) and adventurous (A) motility. S-motility has been shown to be powered by the extrusion, adhesion and retraction of type IV pili. A-motility, however, is much less well understood. Two main models have been proposed to explain A-motility. The first, the ''slime gun'' model, implicates the secretion of polyelectrolyte slime from the cell pole, pushing a cell forward. More recently, we proposed a second model that involves lateral force generation at focal adhesion sites between the cell and substrate. In this model, unknown motors drive cells forward by moving along a filament inside the cell. To date, however, there has been no direct evidence for lateral force generation or the presence of motor proteins in Myxococcus.

We have developed an optical trapping bead assay, which enables us to adhere polystyrene beads to the surface of Myxococcus cells. We find that beads are moved along the cell surface with speeds comparable with those of gliding cells. Beads move in a helical pattern along the cell surface with a pitch size of a few microns. Multiple beads on the same cell can move in the different directions, indicating that beads are carried by individual motors instead of by a global movement of the cell envelope. We also show that in mutant cells lacking key A-motility regulatory genes, beads move in a less coordinated fashion.

2150-Plat

Morphogenesis and Cell Division of E. Coli Under Mechanical Confinement

Jaan Mannik, Peter Galajda, Juan E. Keymer, Cees Dekker.
Delft University of Technology, Delft, Netherlands.

Bacteria have characteristic shapes and sizes which are conserved by an elaborate cytoskeletal machinery. Surprisingly, these well-defined shapes are strongly modified in E. coli bacteria in narrow nanofabricated channels. Growth in constrictions where bacteria are squeezed to about twice thinner than their typical diameter leads to flattened cells that laterally are much wider (up to 5 micron) than regular E. coli [1]. We will report on the cell growth, spatial structure and dynamics of cytoskeletal proteins and the nucleoid in this unusual bacterial phenotype. While the physical confinement has a profound effect on the cell shape and the pattern of cell division, it has only a limited effect on the replication rate of the cells. In most cases, broad (multinucleate) cells are still able to segregate chromosomes in roughly equal amounts to two daughter cells. This process typically starts with the formation of a chromosome-free area in the middle of the cell, which propagates asymmetrically to the perimeter of cell.

From this asymmetric location, the cell wall starts to constrict and a septum forms. Our results show that the cellular structure of bacteria has a high degree of plasticity in coping with lateral stress and confinement.

[1] Bacterial growth and motility in sub-micron constrictions, J. Männik, R. Driessen, P. Galajda, J.E. Keymer and C. Dekker, Proc. Natl. Acad. Sci. U. S. A. 106 (2009) 14861.

2151-Plat
Morphology, Growth and Size Limit of Bacteria

Hongyuan Jiang, Sean X. Sun.
Johns Hopkins University, Baltimore, MD, USA.

Bacterial cell wall is the main structure to maintain a specific cell shape and to resist the osmotic pressure of several atmospheres. Despite many research, some basic questions remain unsolved: Out of many possibilities, why do bacteria only have several defined shapes? What is the relation between growth and morphology of a bacteria? How do rod-like bacteria select and maintain a specific radius, but grow in the axial direction? Is there any size limit for bacteria? What factors determine the size limit if it exists? In this paper, we set up a general growth model for bacterial cell wall and try to answer the previous questions. We found the growth modes and the size limits for coccus, bacillus, vibrio and spirillum, which are consistent with the experiments well.

2152-Plat
Structure and Assembly of CFA/I pili from Enterotoxigenic Escherichia Coli That Cause Traveler's Diarrhea

Di Xia[1], Stephen J. Savarino[2], Esther Bullitt[3].
[1]National Cancer Institute, Bethesda, MD, USA, [2]Naval Medical Research Center, Silver Spring, MD, USA, [3]Boston University, Boston, MA, USA.

Enterotoxigenic Escherichia coli (ETEC) bacteria that cause traveler's diarrhea utilize pili to initiate infection via pilus binding to epithelial cells in the small intestine. According to the World Health Organization, ETEC cause the largest number of recorded community-acquired cases of childhood diarrhea in the developing world, and are the most common cause of Traveler's diarrhea. Through a multi-disciplinary approach that includes x-ray crystallography, electron microscopy, site-directed mutagenesis, and genetic sequence analysis we elucidate the structure and assembly of CFA/I pili expressed on ETEC. We show that the distinction between Class I pili from the chaperone/usher pathway (e.g., P-pili from uropathogenic bacteria) and Class 5 pili from the alternate chaperone pathway (e.g., CFA/I pili), which was based on the lack of genetic sequence homology, does not correlate with any major structural or functional differences between these classes of pili. Pilin subunits transit the outer membrane through an usher that can accommodate single subunits, but not the assembled helical filament. We identify a proline residue in the major pilin, CfaB, that appears to isomerize from the trans to the cis conformation, producing the conformational change required for assembly of the mature pilus filament comprising about 1,000 subunits. Lastly, analysis of genetic variability among clinical strains representative of the eight discrete Class 5 fimbrial subtypes, in combination with structural data, show that each bacterial strain presents a distinct outer surface of CfaB, while the interior and protein-protein interface residues are more highly conserved. These data suggest that protein surface variability facilitates evasion of the immune system by ETEC.

2153-Plat
Force Generation by Type IV pili of *Neisseria Gonorrhoeae*

Dirk Opitz, Martin Clausen, Berenike Maier.
University of Muenster, Muenster, Germany.

Type IV pili are major bacterial virulence factors supporting adhesion, surface motility, and gene transfer. During infection they mediate attachment to mammalian host cells and elicit downstream signals. The polymeric pilus fiber is a highly dynamic molecular machine that switches between elongation and retraction. We used laser tweezers to investigate the dynamics of individual pili of the human pathogen *Neisseria gonorrheae*. We found that the retraction velocity of bacteria adhered to an abiotic surface is bimodal and that the bimodality depends on force and on the concentration of the putative motor protein PilT [1]. When adhered to host cells the bimodality persisted at higher forces compared to an abiotic environment. This increase in average velocity is consistent with an up-regulation of PilT due to interaction with host cells. Bacteria generated considerable force during infection but the maximum force was reduced from (120 ± 40)pN on abiotic surfaces to (70 ± 20)pN on host cells, most likely due to elastic effects. Velocity and maximum force of pilus retraction were independent of the infection period within 1h and 24h post infection [2]. Thus the force generated by type IV pili during infection is high enough to induce cytoskeletal rearrangements in the host cell.

[1] M. Clausen, M. Koomey and B. Maier, Biophys. J. 2009, 96, 1169-1177
[2] D. Opitz, M. Clausen and B. Maier, ChemPhysChem 2009, 10, 1614-1618

Platform AG: Membrane Protein Structure I

2154-Plat
Molecular Modeling and Simulations of the Transmembrane Domain of Human Growth Hormone Receptor

Ritesh Kumar[1], Shahir S. Rizk[2], Anthony A. Kossiakoff[2], Wonpil Im[1].
[1]University of Kansas, Lawrence, KS, USA, [2]University of Chicago, Chicago, IL, USA.

How transmembrane (TM) domains of membrane proteins transmit the signal across the cell membrane has long been a subject of keen interest in biology. There is a recent paradigm shift in the mechanism of activation for the cytokine receptor superfamily. The role of cytokine hormone binding to the extracellular domain is now recognized as an ''inducer'' of the conformational change of pre-dimerized TM domains that triggers subsequent intracellular responses. This is drastically different from its traditional role as an ''organizer'' whose sole function was to initiate the receptor TM dimer formation. Toward quantitative understanding of the mechanisms and accompanying energetics of TM-induced signaling of various single-pass TM receptors, we have generated TM homodimer models of human growth hormone receptor (hGHR) from primary sequence information using the GBSW implicit membrane model and replica-exchange molecular dynamics (REX-MD) simulations. The conformational clustering shows that hGHR forms right-handed TM dimers with two different interfacial motifs, i.e., LFFQ and GxxG. To test such prediction, we first carried out TOXCAT experiments of two hGHR TM mutants: Gly256Ile and Gly259Ile. Mutation of either position to isoleucine disrupts dimer formation. These results suggest the involvement of the glycine residues in the TM helix interaction through the GxxG motif, although we need more extensive experiments to examine the involvement of other residues in the TM dimer interface, or the existence of an alternate dimerization point. In addition, we have performed MD simulations of various hGHR dimer models extracted from GBSW REX-MD in explicit POPC membranes. The stability and orientational changes of hGHR TM dimers as well as various helix-lipid interactions will be also presented and discussed.

2155-Plat
Molecular Dynamics Simulations of the Dimerization of Transmembrane α-Helices

Emi Psachoulia, Beatrice Nikolaidi, David Marshall, **Mark S.P. Sansom**.
University of Oxford, Oxford, United Kingdom.

The lateral association of transmembrane (TM) α-helices within a lipid bilayer environment is a key stage in the folding of membrane proteins. It may also play a role in signalling across cell membranes. Dimerization of TM helices provides a simple example of such lateral association. Direct atomistic (AT) resolution MD simulation of self-assembly of a TM helix bundle remains challenging. AT-MD may be complemented by coarse-grained (CG) simulations. We demonstrate how CG-MD may be used to simulate formation of dimers of TM helices. We also show how a serial combination of CG and AT simulation provides a *multi-scale* approach for generating and refining models of TM helix dimers. This approach has been applied to a number of examples, including the glycophorin TM helix dimer (a paradigm for helix/helix packing) [1], and the TM domain of the syndecan-2 receptor protein, which contains a GxxxG motif comparable to that of glycophorin. The multi-scale approach has also been applied to a more complex system, the heterodimeric αIIb/β3 integrin TM helix dimer.

[1] Psachoulia, E., P. J. Bond, P. W. Fowler, and M. S. P. Sansom. 2008. Helix-helix interactions in membrane proteins: coarse grained simulations of glycophorin helix dimerization. Biochem. 47:10503-105012.

2156-Plat
Aromatic Interfaces between Transmembrane Helices M1/M4 and M3/M4 Play a Key Role in Cys-loop Receptor Assembly

Svenja Haeger[1], Dmitry Kuzmin[2], Silvia Detro-Dassen[1], Niklas Lang[1], Michael Kilb[3], Victor Tsetlin[2], Heinrich Betz[4], Bodo Laube[3], **Gunther Schmalzing**[1].
[1]RWTH Aachen University, Aachen, Germany, [2]Russian Academy of Sciences, Moscow, Russian Federation, [3]Technical University Darmstadt, Darmstadt, Germany, [4]Max-Planck-Institute for Brain Research, Frankfurt am Main, Germany.

Cys-loop receptors, also designated pentameric ligand-gated ion channels (pLGICs) include nicotinic acetylcholine receptors (nAChRs), serotonin type 3 receptors ($5HT_3Rs$), γ-amino butyric acid type-A receptors ($GABA_ARs$) and glycine receptors (GlyRs). pLGICs function as obligate pentamers linked by non-covalent interactions between the N-terminal extracellular domains of identical or homologous subunits. Here we show that expression of GlyR $\alpha 1$ or $5HT_3A$ subunits in two separate fragments (one containing the ectodomain

and transmembrane domains M1-M3, and the other the fourth transmembrane domain M4) results in the assembly of functional pLGICs indistinguishable in their electrophysiological properties from wt pLGICs assembled from contiguous subunits. Alanine scanning of M1, M3 and M4 of the GlyR α1 subunit identified a total of 12 aromatic residues as important or crucial for pentameric assembly. The assembly-relevant aromatic residues cluster in one face of each helix. Homology modelling based on crystal structures (Hilf & Dutzler 2008; Bocquet et al 2008) predicted π- π interactions between the aromatic face of the M4 helix and three or two aromatic residues located in the M1 helix (Tyr228, Trp239, and Phe242) and the M3 helix (Trp286, Phe293), respectively . The loss of homopentamer formation and function seen upon alanine replacement of any of these contact residues strongly supports the existence of a membrane-embedded network of pairwisely interacting aromatic side chains that compacts and stabilizes the membrane core region of the GlyR. We infer from these results that a precise geometric arrangement of transmembrane helices defined by the tri-helical aromatic network is a prerequisite to allow the circular arrangement of the subunits stabilized essentially by earlier occurring random subunit interactions between the ectodomains.

2157-Plat

Conformational Changes in GPCR Surface and Core Probed by [^{13}C]-Methyl NMR Spectroscopy

Michael P. Bokoch[1], Rie Nygaard[1], Yaozhong Zou[1],
Soren G. F. Rasmussen[1], Leonardo Pardo[2], R. Scott Prosser[3],
Luciano Mueller[4], Brian K. Kobilka[1].
[1]Stanford University, Stanford, CA, USA, [2]Universitat Autonoma de Barcelona, Barcelona, Spain, [3]University of Toronto - Mississauga, Mississauga, ON, Canada, [4]Bristol-Myers Squibb, Princeton, NJ, USA.

Recent crystal structures reveal the inactive states of non-rhodopsin G-protein coupled receptors (GPCRs) in beautiful detail. Solution NMR spectroscopy is ideally suited to contribute dynamic information regarding GPCR activation. However, these eukaryotically-expressed membrane proteins remain challenging NMR targets. We apply selective labeling with [^{13}C]methyl probes and two-dimensional NMR to analyze ligand-induced conformational changes in beta2-adrenergic receptor (b2AR).
Lysine side chains were labeled with [^{13}C]dimethyl probes to explore conformational changes in the b2AR extracellular surface. Lys305 forms a salt bridge connecting the extracellular end of transmembrane (TM) helix 7 with extracellular loop 2. The Lys305 NMR resonances are sensitive to conformational changes in the receptor extracellular surface. Using NMR, we observe disruption of the Lys305 salt bridge upon receptor activation by agonist. Computational modeling suggests that a lateral displacement of TM7 occurs in concert with an inward motion at the extracellular end of TM6 (thus extending the ''global toggle switch'' model of Schwartz (2006) *Annu. Rev. Pharmacol. Toxicol.*) Different conformational changes occur upon inverse agonist binding. Molecular dynamics simulations suggest that a conserved phenylalanine (Phe193) in the orthosteric ligand binding site is key for inverse agonism. Taken as a whole, these results demonstrate conformational coupling between the GPCR extracellular surface and orthosteric ligand binding site within the transmembrane domains (Ahuja (2009) *Nat. Struct. Mol. Biol.*) This provides rationale for developing allosteric pharmaceuticals targeting the GPCR extracellular surface.
Conformational changes within the b2AR transmembrane core are also observed by NMR using selective epsilon-[$^{13}CH_3$] labeling of methionines. While assignments are pending, clear conformational changes are seen with activation or inverse agonist binding. [^{13}C]methyl NMR spectroscopy, in combination with crystal structures and molecular dynamics simulation, provides a dynamic view of the conformational changes intrinsic to GPCR function.

2158-Plat

Observation of Structural Changes on Activation of the NTS1 G-Protein-Coupled Receptor on DNA-Templated Protein Arrays by cryo-EM

Daniele N. Selmi[1], Helen Attrill[2], Anthony Watts[2], Robert J.C. Gilbert[3], Andrew J. Turberfield[1].
[1]University of Oxford, Department of Physics, Clarendon Laboratory, Parks Road, Oxford OX1 3PU, United Kingdom, [2]University of Oxford, Department of Biochemistry, South Parks Road, Oxford OX1 3QU, United Kingdom, [3]University of Oxford, Division of Structural Biology, Wellcome Trust Centre for Human Genetics, Roosevelt Drive, Oxford OX3 7BN, United Kingdom.

We report the use of self-assembled DNA templates to create dense, orientationally disordered protein arrays that are optimized for single-particle cryo-EM. The nanostructure templates dramatically simplify data collection and have allowed us to obtain the first structures of a wild-type, neuropeptide-binding GPCR, the rat neurotensin receptor type 1 (NTS1), in both its ligand-free and liganded forms. Resolution better than 7Å allows clear identification of the 7 trans-membrane (TM) alpha-helices. Comparison of the structures provides the first direct observations and measurements of helix excursions during the conformational changes associated with activation of a ligand-binding GPCR. Conformational changes in the TM helices are observed upon ligand binding, namely shifts in TM1 and TM2 at the extracellular side of the membrane and pronounced shifts in TM5 and TM6 on the intracellular, G-protein interacting side that are the hallmark of the GPCR-activated state. Our results suggest a mechanism for ligand activation of a class A GPCR.
This is the highest resolution achieved to date by single-particle cryo-EM of a membrane protein, and NTS1 (43kDa) is an order of magnitude smaller than the nearest similar existing reconstruction of an asymmetric protein at comparable resolution. Our results suggest that the use of DNA-templated protein arrays has the potential to make high-resolution structure determination for small, asymmetric and hard-to-crystallize proteins routinely achievable.

2159-Plat

The Structure and Transport Mechanism of AdiC - an Arginine/agmatine Antiporter

Yiling Fang, Tania Shane, Fang Wu, Carole Williams, Christopher Miller.
Brandeis University, Waltham, MA, USA.

AdiC transports arginine and agmatine (the decarboxylation product of arginine) across the membrane of certain enteric bacteria including *E. coli*, as well as pathognic organisms such as *Salmonella*. It belongs to the APC (amino acids, polyamines and organic cations) superfamily. Its major role is to maintain the internal pH of the cell in the acidic environment (such as stomach) by functioning as a virtual proton pump - transporting arginine (+1 charge) into and agmatine (decarboxylated arginine, +2 charge) out of the cell, resulting in export of 1 proton out during each turnover.
We recently solved the crystal structure of AdiC with a Fab fragment at 3.2 Å. The protein is captured in an outward-open, substrate-free conformation. Both structure and functional data have shown that some aromatic residues (Y93, W293 and Y365) are important for the substrate binding and transport, yet we don't have the direct picture of the structure in the presence of either arginine or agmatine. Therefore, our current work is focused on obtaining the conformation with substrate-bound. One approach is to design pair wise cysteines that can crosslink and mimic the conformation with substrate. Comparing the structure of AdiC and several other proteins with similar fold, we are targeting TM2 and TM8 for the cysteine crosslinking now. A second approach, based on our experience with Fab production, is to find another Fab that can stabilize the substrate-bound conformation. Currently we have twelve more monoclonal antibodies that bind AdiC and need to be tested.

2160-Plat

Crystal Structure of the Membrane Fusion Protein CusB from Escherichia Coli

Edward Yu.
Iowa State University, Ames, IA, USA.

Gram-negative bacteria, such as Escherichia coli, frequently utilize tripartite efflux complexes belonging to the resistance-nodulation-division family to expel diverse toxic compounds from the cell. These systems contain a periplasmic membrane fusion protein that is critical for substrate transport. We here present the x-ray structures of the CusB membrane fusion protein from the copper/silver efflux system of E. coli. This is the first structure of any membrane fusion proteins associated with heavy-metal efflux transporters. CusB bridges the inner membrane efflux pump CusA and outer membrane channel CusC to mediate resistance to Cu+ and Ag+ ions. Two distinct structures of the elongated molecules of CusB were found in the asymmetric unit of a single crystal, which suggests the flexible nature of this protein. Each protomer of CusB can be divided into four different domains, whereby the first three domains are mostly β-strands and the last domain adopts an entirely helical architecture. Unlike other known structures of membrane fusion proteins, the α-helical domain of CusB is folded into a three-helix bundle. This three-helix bundle presumably interacts with the periplasmic domain of CusC. The N and C-termini of CusB form the first β-strand domain, which is found to interact with the periplasmic domain of the CusA efflux pump. Atomic details of how this efflux protein binds Cu+ and Ag+ were revealed by the crystals of the CusB-Cu(I) and CusB-Ag(I) complexes. The structures indicate that CusB consists of multiple binding sites for these metal ions. These findings reveal novel structural features of a membrane fusion protein in the resistance-nodulation-division efflux system, and provide direct evidence that this protein specifically interacts with transported substrates.

2161-Plat
A Novel Photosynthetic Strategy for Adaptation to Low Iron Environments
Petra Fromme[1], Devendra Chauhan[1], Mihaela Folea[2], Craig Jolley[3], Roman Kouřil[2], Carolyn E. Lubner[4], Su Lin[1], Dorota Kolber[5], Felisa Wolfe-Simon[6], John H. Golbeck[4], Egbert J. Boekema[2].
[1]Arizona State University, Tempe, AZ, USA, [2]University of Groningen, Groningen, Netherlands, [3]Montana State University, Bozeman, MT, USA, [4]Pennsylvania State University, University Park, PA, USA, [5]Monterey Bay Aquarium Research Institute, Moss Landing, CA, USA, [6]Harvard University, Cambridge, MA, USA.
Iron availability is a major limiting factor for photosynthesis and hence for life in most of the aquatic environments on earth. . Cyanobacteria are important primary producers and prevail over Fe- deficiency by de-repressing the *isiAB* operon, which codes for the antenna protein IsiA and flavodoxin. We demonstrate that under nanomolar iron concentrations, a giant IsiA-Photosystem I supercomplex is formed, consisting of a Photosystem I trimer encircled by two complete IsiA rings with 18 and 25 copies in the inner ring and outer ring, respectively. The IsiA-Photosystem I supercomplex contains more than 850 chlorophylls and has a mass of 3.2 MDa, making it the most complex membrane protein that has been isolated to date. Ultrafast fluorescence spectroscopic results show fast and efficient excitation transfer and trapping in the supercomplex. The electron transfer throughput of Photosystem I is increased by 300%, an evolutionary adaptation that has allowed cyanobacteria to avoid oxidative stress. This adaptation of the photosynthetic apparatus confers an enormous, as-yet unrecognized, evolutionary advantage to cyanobacteria living under conditions of severe Fe stress and thereby have adapted to the modern low iron concentration in aquatic environments.
1. Eldridge, M. et al. Aquatic Microbial Ecology 35, 79-91 (2004).
2. Martin, J. & Fitzwater, S. Nature 331, 341-343 (1988).
3. Wilhelm, S. Aquatic Microbial Ecology 9, 295-303 (1995).
4. Bibby, T. S., Nield, J. & Barber, J. Nature 412, 743-5 (2001).
5. Boekema, E. J. et al. Nature 412, 745-8 (2001).
6. Singh, A., McIntyre, L. & Sherman, L. Plant Physiology 132, 1825 (2003).

Platform AH: Membrane Receptors & Signal Transduction

2162-Plat
A Novel Method to Probe Membrane Protein Topology Using Unnatural Amino Acid Mutagenesis and Antibody Epitope Tagging
Saranga Naganathan, Shixin Ye, Terence Duarte, Thomas Huber, Pallavi Sachdev, Thomas P. Sakmar.
www.sakmarlab.org, The Rockefeller University, New York, NY, USA.
We have developed a novel strategy to probe the topology of membrane proteins in their native bilayer environment. Our technique relies on unnatural amino acid mutagenesis to incorporate *p*-azido-L-phenlyalanine at a specific site in the expressed target protein. The reactive azido moiety facilitates Staudinger-Bertozzi ligation chemistry to introduce a monoclonal antibody (mAb) epitope-tagged phosphine derivative. This site-specific labeling method allows the flexibility and precision of single codon scanning, and appears to be superior to current biochemical approaches that rely on chemical modifications and/or introduction of epitope tags by mutagenesis. Our approach can be used to identify gross topological determinants for transmembrane proteins of unknown topology as well as to elucidate secondary structural elements with chemical precision. We demonstrate the experimental feasibility of our technique on human C-C chemokine receptor 5 (CCR5), a heptahelical transmembrane G protein-coupled receptor (GPCR) of known topology. CCR5 is a major co-receptor for HIV-1 entry into host cells. We labeled CCR5 in membranes with FLAG peptide epitope-phosphine at various sites on the receptor's intra- and extracellular surfaces. The differential reactivity of the FLAG epitope-phosphine reagent for the azido group on the various CCR5 mutants correlated to the known topology of CCR5 and defined specific helical boundaries. We further applied the new label/probe technology to mammalian cells in culture in order to label extracellular sites on surface-expressed CCR5. Our new method appears to be satisfactory to probe membrane protein topology in polytopic membrane proteins and has potential applications in the study of receptor signaling mechanisms in live cells.

2163-Plat
Large-Scale MD Simulations Reveal Structural Elements of the Activated State in the 5-HT2a Receptor and their Relation to Cholesterol Dynamics
Jufang Shan, George Khelashvili, Harel Weinstein.
Weill Medical College of Cornell University, New York, NY, USA.
The 5-HT_{2A} Serotonin receptor (5-HT_{2A}R) is a G-protein coupled receptor (GPCR) targeted by therapeutic drugs as well as hallucinogens such as LSD. We have previously shown that different modes of receptor activation and distinct cellular signaling are produced by hallucinogens and nonhallucinogenic congeners acting on the 5-HT_{2A}R (Weinstein, 2006). We characterize the ligand-dependent states of 5-HT_{2A}R from MD simulations of an experimentally-validated homology model based on rhodopsin and β_2AR structures complemented by cognate information about other GPCRs. At different stages of 0.3 μs simulations of 5-HT-bound 5-HT_{2A}R we observe sequential conformational changes that produce structural characteristics of receptor activation: (*1*) the extracellular part of TM6 moves inwards; (*2*) the toggle switch W6.48 flips to become parallel to the membrane; (*3*) the intracellular part of TM6 moves outwards and (*4*) the ionic lock in the DRY motif breaks. In the parallel simulations of 5-HT_{2A}R with LSD (currently at 0.12 μs), only some of the same active-like components are observed (e.g., TM7 moving away from TM2, and the breaking of the ionic lock). Comparing the dynamics of 5-HT_{2A}R complexed with LSD and 5-HT, we found that H8 of the LSD-bound receptor undergoes less rearrangement during the same time period, and that the interaction of extracellular loop 2 with LSD is stronger than with 5-HT, but that local distortions in TMs (e.g., proline kinks) are similar in the two systems. Interestingly, correlation analysis indicates that some of the local changes in 5-HT_{2A}R relate to the dynamics of cholesterol in the membrane, at a series of preferred sites of interaction with the receptor, in a manner similar to those reported previously from μs rhodopsin simulations (Grossfield et al., 2006; Khelashvili et al., 2009).

2164-Plat
Molecular Model of the Opsin-G-Protein Complex
Parag Mukhopadhyay, Thomas P. Sakmar, Thomas Huber.
www.sakmarlab.org, Rockefeller University, New York, NY, USA.
A recent highlight in the structural biology of G-protein-coupled receptors includes the structural elucidation of opsin in an active-state conformation (Ops*). We modeled the complex of opsin with the heterotrimeric G-protein transducin (Ops*-$G_t\alpha\beta\gamma$, figure below), using the NMR structure of an 11-residues peptide from the C-terminus of the alpha-subunit of transducin ($G_t\alpha$CT) and the crystal structures of opsin in its G-protein interacting conformation (Ops*-$G_t\alpha CT_{K341L}$), of rhodopsin in an inactive state, and of transducin ($G_t\alpha\beta\gamma\bullet$GDP). We reconstructed the C-terminal α5 helix of $G_t\alpha$ and docked it to the open binding site in Ops*. It has been proposed that a 40°-tilt of $G_t\alpha\beta\gamma$ relative to the α5 helix is necessary to avoid steric clashes between $G_t\beta\gamma$ and the membrane. We propose an alternative model without these massive changes in α5 helix packing. With an alternative conformation of the intra-cellular loop connecting helix 5 and helix 6 in Ops* it is possible to obtain a model that maintains the Ops*-induced α_L-type C-capping conformation of Gt_αCT and its key interactions with Ops*. The model will be used for detailed MD simulations of the complex in the membrane and to design cross-linking experiments for biochemical validation.

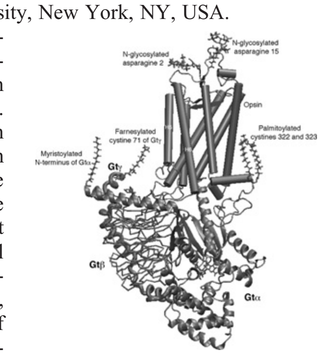

2165-Plat
Insights into G-Protein Coupled Receptors Activation from All-Atom Molecular Dynamics Simulations
Stefano Vanni, Marilisa Neri, Ivano Tavernelli, Ursula Rothlisberger.
EPFL, Lausanne, Switzerland.
G protein coupled receptors (GPCRs) are a large family of integral membrane proteins involved in many signal transduction pathways. The recently crystallized structures of two engineered adrenergic receptors (ARs)[1,2] and of ligand-free opsin bound to a G-protein peptide[3] have opened new avenues for the understanding of the molecular mechanisms of action of GPCRs, but they also generated some controversy on the proposed mechanism of GPCR activation.
To understand the molecular details of GPCR activation, we carried out submicrosecond molecular dynamics simulations of wild type β1AR and β2AR and of rhodopsin dimer in explicit lipid bilayer under physiological conditions.
Our simulations showed that the equilibrated structures of ARs recover all the previously suggested features of inactive GPCRs, including formation of a crucial salt bridge between the cytoplasmatic moieties of helices III and VI (''ionic-lock'') that is absent in the crystal structures[4].
We found that cooperation between a number of highly conserved residues is a key component in the early steps of the activation mechanism of diffusible

ligand class A GPCRs and that ''ionic-lock'' formation in ARs is directly correlated with the protonation state of a highly conserved aspartic acid, even though the two sites are located more than 20Å away from each other[5].
Additionally, following the real time evolution of the rhodopsin dimer up to microseconds after photoexcitation, we propose a tandem mechanism for signal transduction where one monomer is responsible for light detection while the other one serves as G-protein coupling site[6]. This interface-mediated pathway suggests oligomerization-aided signal transduction as a crucial biological mechanism to enhance activation of GPCRs.

[1] Cherezov et al, Science, 2007.
[2] Warne et al, Nature, 2008.
[3] Scheerer et al. Nature, 2008.
[4] Vanni et al. Biochemistry, 2009.
[5] Vanni et al. Submitted.
[6] Neri et al. Submitted.

2166-Plat

Dynamics of Gq Protein Interactions with PLCβ3 Studied by TIRF Microscopy

Thomas Pollinger[1], Markus Milde[1], Monika Frank[1], Moritz Bünemann[2].
[1]University of Würzburg, Würzburg, Germany, [2]University of Marburg, Marburg, Germany.

G protein-mediated activation of phospholipase Cβ (PLCβ) represents a primary mechanism to regulate many physiological events such induce smooth muscle contraction, secretion and modulation of synaptic transmission. Both Gαq- and Gβγ-subunits are known to interact and activate PLCβ enzymes, however little is known about the dynamics of this interactions and the relative contribution of the G protein subunits in intact cells. Using fluorescence resonance energy transfer- (FRET-) based assays in single intact cells we studies kinetics of receptor-induced interactions between Gβγ- and Gαq-subunits, interactions of both Gαq and Gβγ with PLCβ3 as well as interactions of regulator of G proteins signalling 2 (RGS2) with Gαq- and Gβγ-subunits. In order to restrict the protein/protein interaction studies to the cell membrane we applied total internal reflection (TIRF) microscopy. High temporal resolution ratiometric FRET imaging uncovered a markedly faster dissociation of Gαq and PLC upon withdrawal of purinergic agonists compared to the deactivation of Gq proteins in the absence of PLCβ3. This apparent difference in kinetics could be contributed to the GTPase-activating property of PLCβ3 in living cells. Furthermore we found that PLCβ3 modulated Gq protein kinetics to a similar extent compared to RGS2, which in vitro is about 100 fold more efficient in activating Gq-GTPase activity. We observed that both Gαq subunits and Gq-derived Gβγ-subunits interact with PLCβ3 in response to receptor stimulation. In the absence of receptor stimulation we did neither detect any specific FRET signals between Gq protein subunits and PLCβ3 nor did we detect any interactions between RGS2 and Gαq subunits. Finally we could not detect agonist- dependent FRET between RGS2 and Gβγ-subunits. Taken together, ratiometric FRET-imaging under conditions of TIRF allowed new insights into dynamics and interaction patterns within the Gq signalling pathway.

2167-Plat

Role of Plasma Membrane Structuring on Interferon Receptor Assembly & Signaling

Anna Pezzarossa[1], Jacob Piehler[2], Thomas Schmidt[1].
[1]Leiden University, Leiden, Netherlands, [2]Osnabruck university, Osnabruck, Germany.

Signaling in cells is mediated through multi-protein complexes, and is triggered by recognition of a chemical molecule, the ligand, to membrane receptors at the extracellular side. Binding in turn leads to activation of intracellular signaling. Understanding of the dynamical behavior of receptors and its nanometric organization in the membrane is fundamental to understand the processes of cell signaling. We are studying type I interferon (IFN) receptor, a member of the cytokine family, which plays a key role in early innate and adaptive immune responses upon infection by pathogens. It is puzzling how different members of the ligand type-1 IFN family elicit differential responses while binding to only one surface receptor. The latter comprises of two proteins ifnar1 and ifnar2, present at very low surface concentration of 100-1000 molecules/cell. Upon ligand binding a ternary complex is formed and downstream signaling pathways activated. Cells quickly and effectively respond, despite the very low amount of receptor present. Using single-molecule wide-field fluorescence microscopy we follow individual receptor in the plasma membrane of living HeLa cells. Receptor subunits were labeled post-translationally with synthetic dyes, or with fluorescent proteins. Each of the receptor subunit was transfected and expressed, separately and simultaneously, allowing measurements on single component as well as on the ternary complex formed upon IFN binding. Through correlative analysis of Ifnar1 and Ifnar2 mobility we visualized association/dissociation events of the ternary complex upon stimulation, and obtained information on receptor's diffusion constants. We observed a switching in between fast and slow motility and vice versa, and a confinement of receptor components in domains. Upon stimulation an increase of cross-correlation between the components was observed as well as a change in mobility. Our findings suggest a role for membrane nanostructure as platform for differential cell signaling.

2168-Plat

Involvement of Transmembrane Helix Dimerization and Rotation in Signaling by the Thrombopoietin Receptor

Damien Thévenin[1], Erin E. Matthews[1], Julia M. Rogers[1], Ming An[1], Lisa Gotow[2], Paul D. Lira[2], Lawrence A. Reiter[2], William H. Brissette[2], Donald M. Engelman[1].
[1]Yale University, New Haven, CT, USA, [2]Pfizer Global Research and Development, Groton, CT, USA.

In this study, we investigate the role of the transmembrane (TM) domain in the activation of one member of the cytokine receptor family: the thrombopoietin receptor (TpoR). The TM domain is thought to play a key role in the activation by facilitating receptor homodimerization and by transmitting the ligand-induced re-orientation of the extracellular domain to the cytoplasmic domain through conformational changes. However, the precise mechanisms underlying these events are not fully understood. Here, we considered several unanswered questions: Is the homodimerization of TpoR TM domain important in receptor activation? Which TM residues are involved in stabilizing receptor interactions? Additionally, we investigated the role of a constitutively activating mutation (S505N) and the mechanism of action of a piperidine-4-carboxylic acid TpoR agonist (Compound 2). We show that the TM domain of the human TpoR dimerizes strongly and that the full-length receptors exist as homodimers on the surface of mammalian cells in the absence of ligand. Our results indicate that TpoR can adopt two different conformations involving two different sets of residues. One of the contact interfaces mimics an inactive unliganded TpoR dimer and the other corresponds to an active conformation that is compatible with the constitutive signaling induced by the S505N mutation. We also show that Compound 2 interacts specifically with the N-terminus portion of the active dimer conformation. Overall, our results give new insight into the role of the TM domain in the activation mechanism of TpoR and provide a more detailed model of cytokine receptor activation and modulation by small molecule agonists.

2169-Plat

Spatio-Temporal Patterns of Reactive Oxygen Species Production in PDGF Signaling Revealed by Nanoparticle Imaging in Living Cells

Cedric I. Bouzigues, Thanh-Liem Nguyên, Didier Casanova, Rivo Ramodiharilafy, Thierry Gacoin, Jean-Pierre Boilot, Antigoni Alexandrou.
Ecole polytechnique, Palaiseau, France.

Signaling by PDGF (Platelet Derived Growth Factor) is involved in cell migration, for metastasis formation or reparation of vascular lesions. Hydrogen peroxide (H2O2) is a known second messenger in this pathway and its intracellular concentration regulates the cell response. However, conventional methods are unable to measure quantitatively its temporal evolution. Here, we propose a new approach based on the imaging of YVO4:Eu nanoparticles. Their luminescence is indeed modulated by the oxidation state of doping europium ions. After photoinduced reduction, their chemical oxidation by H2O2 can be monitored by the nanoparticle imaging. We demonstrated in vitro that these particles are efficient probes to dynamically and quantitatively measure H2O2 concentration. By internalizing these nanoparticles in mamallian cells, we measured the oxidant response to a PDGF stimulation. We revealed the temporal pattern of H2O2 production and determined the effective affinity of PDGF receptors for their ligand. We thus proved that a persistent stimulation was necessary to trigger a significant H2O2 production: this intrinsic filtering could be of major physiological interest for understanding reliable cell migration. This response implies transactivation of EGF receptors, which we proved to be dominant at short times. The comparison of normal and tumoral cells revealed a faster and more important H2O2 production in tumoral cells. This likely relies on the different expression levels of proteins of the signaling cascade and points to the potential role of signal transduction dynamics for the regulation of metastasis formation.
This work proposes the first quantitative measurements of the oxidant signaling in cells by the use of new nanoprobes. It more generally opens new perspectives for the study of the spatio-temporal organization of the cell response and its physiological importance.